BEILSTEIN JOURNAL OF ORGANIC CHEMISTRY

Multicomponent reactions IV

Edited by Thomas J. J. Müller and Valentyn A. Chebanov

Generated on 05 December 2025, 20:28

Imprint

Beilstein Journal of Organic Chemistry
www.bjoc.org
ISSN 1860-5397
Email: journals-support@beilstein-institut.de

The *Beilstein Journal of Organic Chemistry* is published by the Beilstein-Institut zur Förderung der Chemischen Wissenschaften.

Beilstein-Institut zur Förderung der Chemischen Wissenschaften
Trakehner Straße 7–9
60487 Frankfurt am Main
Germany
www.beilstein-institut.de

The copyright to this document as a whole, which is published in the *Beilstein Journal of Organic Chemistry*, is held by the Beilstein-Institut zur Förderung der Chemischen Wissenschaften. The copyright to the individual articles in this document is held by the respective authors, subject to a Creative Commons Attribution license.

BEILSTEIN JOURNAL OF ORGANIC CHEMISTRY

Multicomponent reactions IV

Thomas J. J. Müller*[1] and Valentyn A. Chebanov*[2,3]

Editorial

Open Access

Address:
[1]Heinrich-Heine-Universität Düsseldorf, Institut für Organische Chemie und Makromolekulare Chemie, Universitätsstraße 1, D-40225 Düsseldorf, Germany, [2]Institute of Functional Materials Chemistry, State Scientific Institution “Institute for Single Crystals” of National Academy of Sciences of Ukraine, Nauky Av. 60, 61072 Kharkiv, Ukraine, and [3]Faculty of Chemistry, V. N. Karazin Kharkiv National University, Svobody Sq. 4, 61077 Kharkiv, Ukraine

Email:
Thomas J. J. Müller* - tjm@hhu.de; Valentyn A. Chebanov* - chebanov@isc.kh.ua

* Corresponding author

Keywords:
multicomponent reactions

Beilstein J. Org. Chem. **2025,** *21,* 2082–2084.
https://doi.org/10.3762/bjoc.21.163

Received: 05 September 2025
Accepted: 01 October 2025
Published: 14 October 2025

This article is part of the thematic issue "Multicomponent reactions IV".

Associate Editor: T. J. J. Müller; Guest Editor: V. A. Chebanov

© 2025 Müller and Chebanov; licensee Beilstein-Institut.
License and terms: see end of document.

The synthesis of complex molecules is a cornerstone of modern science. Chemistry is not only concerned with understanding and modifying chemical bonds but also with creating enabling technologies that help to address challenges at the interface of materials science and the life sciences. The growing need to provide substance libraries for the identification and optimization of promising lead structures has therefore inspired the development of powerful synthetic strategies. A glance at Web of Science reveals that one-pot methods and multicomponent reactions (MCRs) [1] have attracted steadily increasing attention within the scientific community over the past 25 years (Figure 1).

According to a quick Web of Science [2] keyword search of "multicomponent reaction" and "one-pot reaction" (Figure 1A) and "multicomponent reaction" (Figure 1B) filtered by publication year, the impressive sum of 136,658 publications on multicomponent (Figure 1A) and one-pot reactions and 24,369 publications on MCRs alone (Figure 1B) clearly underline the central importance and topicality of the MCR concept. In sensu stricto, MCRs involve the reaction of three or more components in a single vessel, proceeding under domino, sequential, or consecutive control without the need for intermediate purification, work-up, or solvent exchange. Domino processes [3] are characterized by the simultaneous presence of all reactants from the outset, whereas sequential reactions permit the controlled addition of components while maintaining the same reaction conditions. Consecutive processes, in turn, even allow changes in conditions from one step to the next. In essence, MCRs embody a reactivity-driven concept [4] within the broader family of one-pot methodologies.

This thematic issue on multicomponent reactions continues the previously published editions from 2011 [5], 2014 [6], and 2019 [7] and is guest-edited by Thomas J. J. Müller (Heinrich Heine University Düsseldorf, Germany) together with Valentyn A. Chebanov (State Scientific Institution “Institute for Single Crystals” of the National Academy of Sciences of Ukraine, Kharkiv, Ukraine). The 30 contributions collected in this thematic issue (1 Letter, 22 Full Research Papers, and 7 Reviews) reflect the broad spectrum of MCR chemistry worldwide.

Among the Full Research Papers, isocyanide-based multicomponent reactions still constitute the relative majority. Ugi and

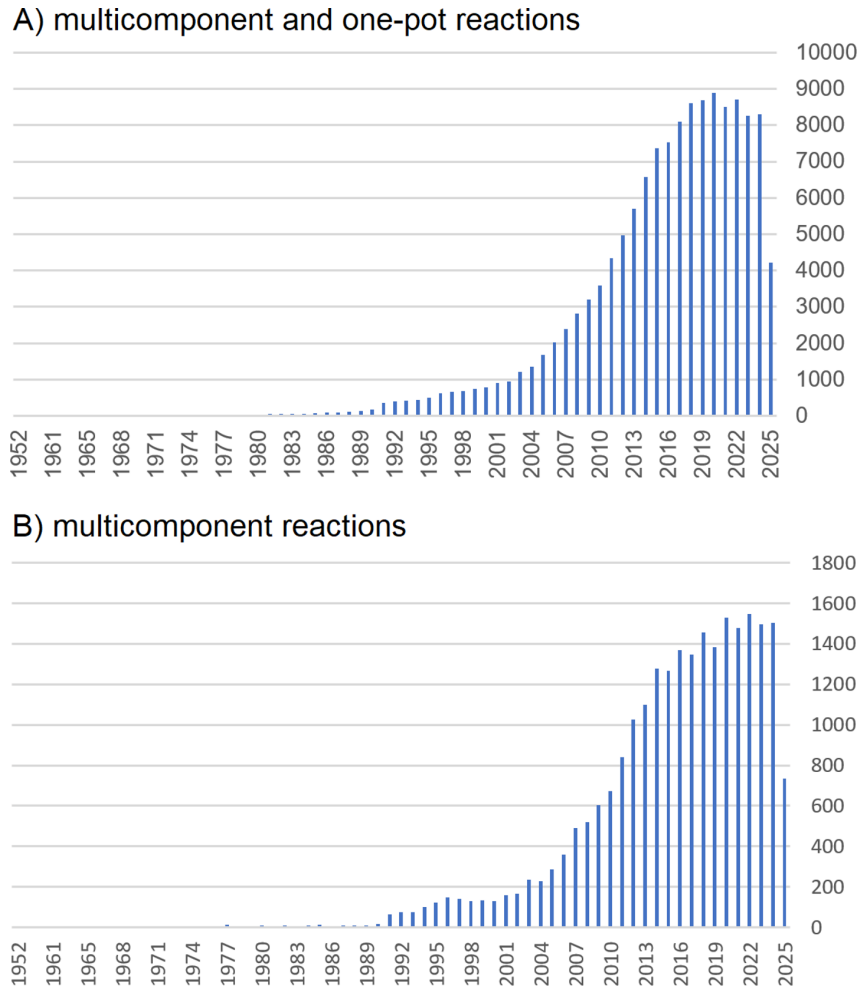

Figure 1: Number of publications by year on multicomponent and one-pot reactions (A) and multicomponent reactions alone (B) accessed by Web of Science on June 16, 2025.

co-workers' groundbreaking discovery of the four-component reaction between an aldehyde, an amine, a carboxylic acid, and an isonitrile in 1959 [8], which marked the beginning of modern MCR chemistry, continues to attract undiminished attention. It has since been applied in manifold ways, from breathtaking reaction sequences and post-Ugi transformations to the generation of countless molecules, spanning small compounds to microstructures. The amphiphilic reactivity of isonitriles appears virtually limitless, extending well beyond classical Ugi-type reactions into other MCR contexts. At the same time, MCRs not based on isonitriles are gaining increasing momentum, with a strong emphasis on heterocycle synthesis. Beyond traditional condensation-based approaches, mechanistically innovative crossovers – linking metal catalysis with radical chemistry and, more recently, with photo(redox) catalysis – are opening entirely new avenues for MCR development. Finally, seven focused Reviews on heterocycles, reactivity patterns, and the role of MCRs as enabling tools at the interface with biosciences underscore the timeliness and enduring elegance of this powerful and concise concept in molecular synthesis.

As the guest editors of this thematic issue, we would like to thank all the authors – dedicated and outstanding scientists – for sharing their exciting findings. We are especially grateful to the staff of the Beilstein-Institut for their excellent support and professional execution of this project.

Thomas J. J. Müller and Valentyn A. Chebanov

Düsseldorf and Kharkiv, September 2025

ORCID® iDs

Thomas J. J. Müller - https://orcid.org/0000-0001-9809-724X
Valentyn A. Chebanov - https://orcid.org/0000-0001-7564-778X

Data Availability Statement

Data sharing is not applicable as no new data was generated or analyzed in this study.

References

1. Zhu, J.; Wang, Q.; Wang, M., Eds. *Multicomponent Reactions in Organic Synthesis;* Wiley-VCH: Weinheim, Germany, 2014. doi:10.1002/9783527678174
2. Web of Science. https://www.webofscience.com (accessed June 6, 2025).
3. Tietze, L. F., Ed. *Domino Reactions: Concepts for Efficient Organic Synthesis;* Wiley-VCH: Weinheim, Germany, 2014. doi:10.1002/9783527671304
4. Relative Reactivities of Functional Groups as the Key to Multicomponent Reactions. In *Multicomponent Reactions, Volume 1;* Müller, T. J. J., Ed.; Science of Synthesis; Georg Thieme Verlag: Stuttgart, Germany, 2014; pp 5–27. doi:10.1055/sos-sd-210-00002
5. Müller, T. J. J. *Beilstein J. Org. Chem.* **2011,** *7,* 960–961. doi:10.3762/bjoc.7.107
6. Müller, T. J. J. *Beilstein J. Org. Chem.* **2014,** *10,* 115–116. doi:10.3762/bjoc.10.7
7. Müller, T. J. J. *Beilstein J. Org. Chem.* **2019,** *15,* 1974–1975. doi:10.3762/bjoc.15.192
8. Ugi, I.; Meyr, R.; Fetzer, U.; Steinbrückner, C. *Angew. Chem.* **1959,** *71,* 386. doi:10.1002/ange.19590711110

License and Terms

This is an open access article licensed under the terms of the Beilstein-Institut Open Access License Agreement (https://www.beilstein-journals.org/bjoc/terms), which is identical to the Creative Commons Attribution 4.0 International License (https://creativecommons.org/licenses/by/4.0). The reuse of material under this license requires that the author(s), source and license are credited. Third-party material in this article could be subject to other licenses (typically indicated in the credit line), and in this case, users are required to obtain permission from the license holder to reuse the material.

The definitive version of this article is the electronic one which can be found at:
https://doi.org/10.3762/bjoc.21.163

BEILSTEIN JOURNAL OF ORGANIC CHEMISTRY

HPW-Catalyzed environmentally benign approach to imidazo[1,2-*a*]pyridines

Luan A. Martinho and Carlos Kleber Z. Andrade*

Full Research Paper

Open Access

Address:
Instituto de Química, Laboratório de Química Metodológica e Orgânica Sintética (LaQMOS), Universidade de Brasília, 70904-970, Brasília, DF, Brazil

Email:
Carlos Kleber Z. Andrade* - ckleber@unb.br

* Corresponding author

Keywords:
GBB-3CR; imidazo[1,2-*a*]pyridine; microwave; phosphotungstic acid

Beilstein J. Org. Chem. **2024,** *20,* 628–637.
https://doi.org/10.3762/bjoc.20.55

Received: 07 December 2023
Accepted: 05 March 2024
Published: 19 March 2024

This article is part of the thematic issue "Multicomponent reactions IV".

Associate Editor: T. J. J. Müller

© 2024 Martinho and Andrade; licensee Beilstein-Institut.
License and terms: see end of document.

Abstract

The imidazo[1,2-*a*]pyridine moiety is present in drugs with several biological activities. The most direct way of obtaining this nucleus is the Groebke–Blackburn–Bienaymé three-component reaction (GBB-3CR) between aminopyridines, aldehydes, and isocyanides under both Lewis and Brønsted acid catalysis. However, several catalysts for this reaction have major drawbacks such as being expensive, extremely dangerous, strong oxidizing, and even explosive. In this scenario, heteropolyacids emerge as greener and safer alternatives due to their very strong Brønsted acidity. In particular, phosphotungstic acid (HPW) is an economical and green attractive catalyst for being cheap, non-toxic, and is known for its chemical and thermal stability. Herein, we report a straightforward approach to the GBB-3CR using HPW as catalyst in ethanol under microwave (μw) heating. This convenient environmentally benign methodology is broad in scope, provides the heterobicyclic products in high yields (up to 99%), with a low catalyst loading (2 mol %) in only 30 minutes, and allows the successful use of aliphatic aldehydes, substrates not so frequently explored with most usual catalysts for this reaction. Furthermore, the aforementioned advantages make this methodology very attractive and superior to the existing ones.

Introduction

Imidazo[1,2-*a*]pyridine is a privileged structure that plays an important role in organic synthesis and in the pharmaceutical industry. This scaffold is present in drugs with several biological activities, such as antiviral [1], anticonvulsant [2], antibacterial [3], antipyretic [4], antituberculosis [5], anticancer [6], anthelmintic [5], antifungal [7], analgesic [8], antiulcer [9], antiprotozoal [10], antitumor [11], and anti-inflammatory [12]. Examples of commercial drugs are depicted in Figure 1 [13] and include alpidem (anxiety disorders), minodronic acid (osteoporosis), miroprofen (non-steroidal anti-inflammatory drug,

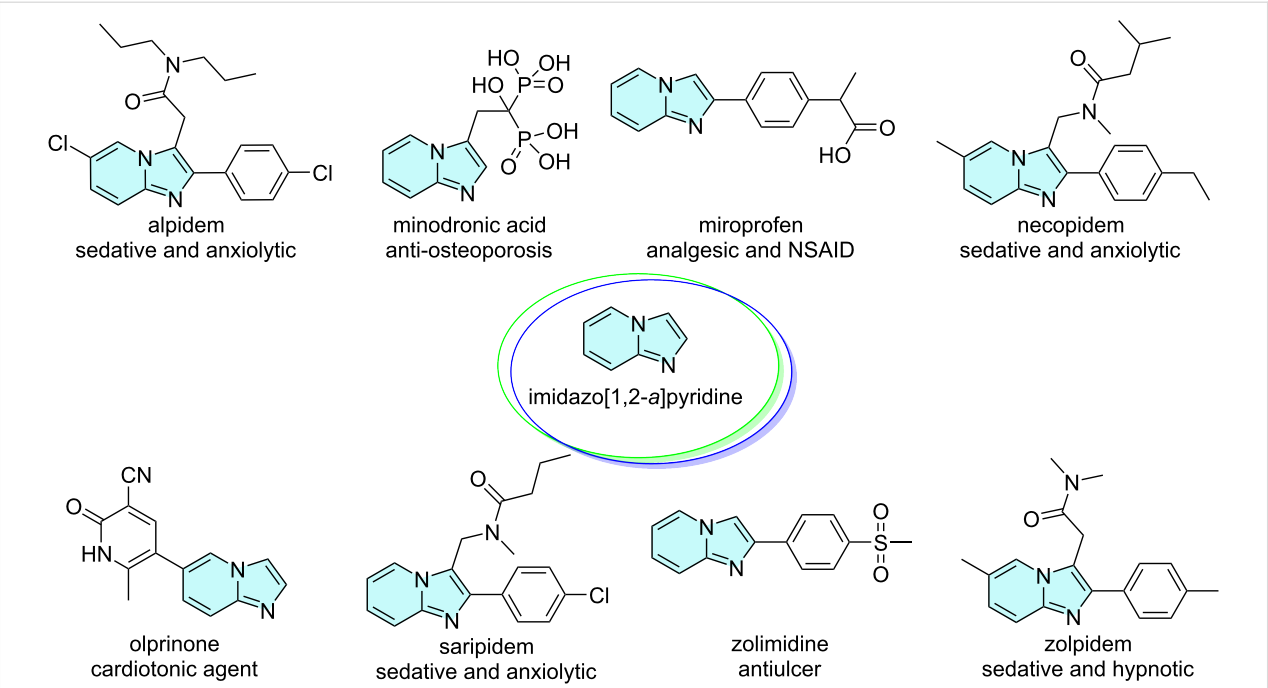

Figure 1: Selected examples of commercial drugs containing the imidazo[1,2-*a*]pyridine core [13].

NSAID), necopidem (insomnia), olprinone (acute heart failure), saripidem (type A GABA receptor agonist), zolimidine (gastroesophageal reflux disease), and zolpidem (insomnia).

Some recent synthetic approaches to imidazo[1,2-*a*]pyridine scaffolds include synthetic pathways of transition metal-catalyzed reactions [14], cyclization [15], condensation [16], heteroannular [17], and photocatalytic reactions [18]. These approaches usually involve non-trivial reaction conditions and the employment of relatively complex starting materials [19]. A more efficient way of obtaining this nucleus is through the Groebke–Blackburn–Bienaymé three-component reaction (GBB-3CR) between amidines (aminoazoles), aldehydes, and isocyanides under both Lewis and Brønsted acid catalysis [20-22]. Multicomponent reactions (MCRs) provide one-pot reactions, simple synthetic procedures, less waste being produced, fewer purification steps, and a high atom economy [23].

The GBB three-component reaction is carried out in the presence of Lewis or Brønsted acid catalysis to increase the reactivity of the imine formation [24]. The most common catalysts are those derived from triflate salts such as $Sc(OTf)_3$ [25], $Yb(OTf)_3$ [26], $In(OTf)_3$ [27] and $Gd(OTf)_3$ [28], and inorganic Brønsted or Lewis acids like $HClO_4$ [29], $ZrCl_4$ [30], $InCl_3$ [31], $BiCl_3$ [32], $RuCl_3$ [33], NH_4Cl [34], HCl [35], $LaCl_3{\cdot}7H_2O$ [36], and $ZnCl_2$ [37], or organic acids such as *p*-toluenesulfonic acid (PTSA) [38], TFA [39], and AcOH [40], etc. Nonetheless, most of these acids have major drawbacks such as being expensive, dangerous, strong oxidizing, or even potentially explosive, with long reaction times being required.

In contrast, heteropolyacids (HPAs) have been reported as greener catalysts not only for being a safer alternative to toxic catalysts [41] but also for providing easy recovery and reuse linked to high selectivity [42]. An example of HPA is phosphotungstic acid, $H_3PW_{12}O_{40}$ (HPW), an inexpensive, non-toxic, and green catalyst with greater chemical and thermal stability in comparison to other heteropolyacids [43]. HPW has been shown to catalyze MCRs in the synthesis of heterocyclic compounds with high efficiency and chemoselectivity (Figure 2), including functionalized benzo[*c*]chromeno[2,3-*a*]phenazine [44], pyrazolo-fused benzophenazines [45], 4,5-dioxopyrrolidines [46], 1,2-dihydropyridine (1,2-DHPs) [47], pyrimido[4,5-*b*]quinoline-tetraones [48], tetrahydrobenzo[*b*]pyrans and indazolo[2,1-*b*]phthalazinetriones [49]. Herein, we report the synthesis of imidazo[1,2-*a*]pyridines via the GBB-3CR using HPW as catalyst in ethanol under microwave (μw) heating. This convenient environmentally benign methodology is broad in scope, provides the heterobicyclic products in high yields (up to 99%), with a low catalyst loading (2 mol %) in only 30 minutes.

Results and Discussion

A search in the literature revealed a single report on the use of a heteropolyacid (phosphomolybdic acid) in the GBB reaction but for a limited number of examples (Scheme 1a) [50]. That

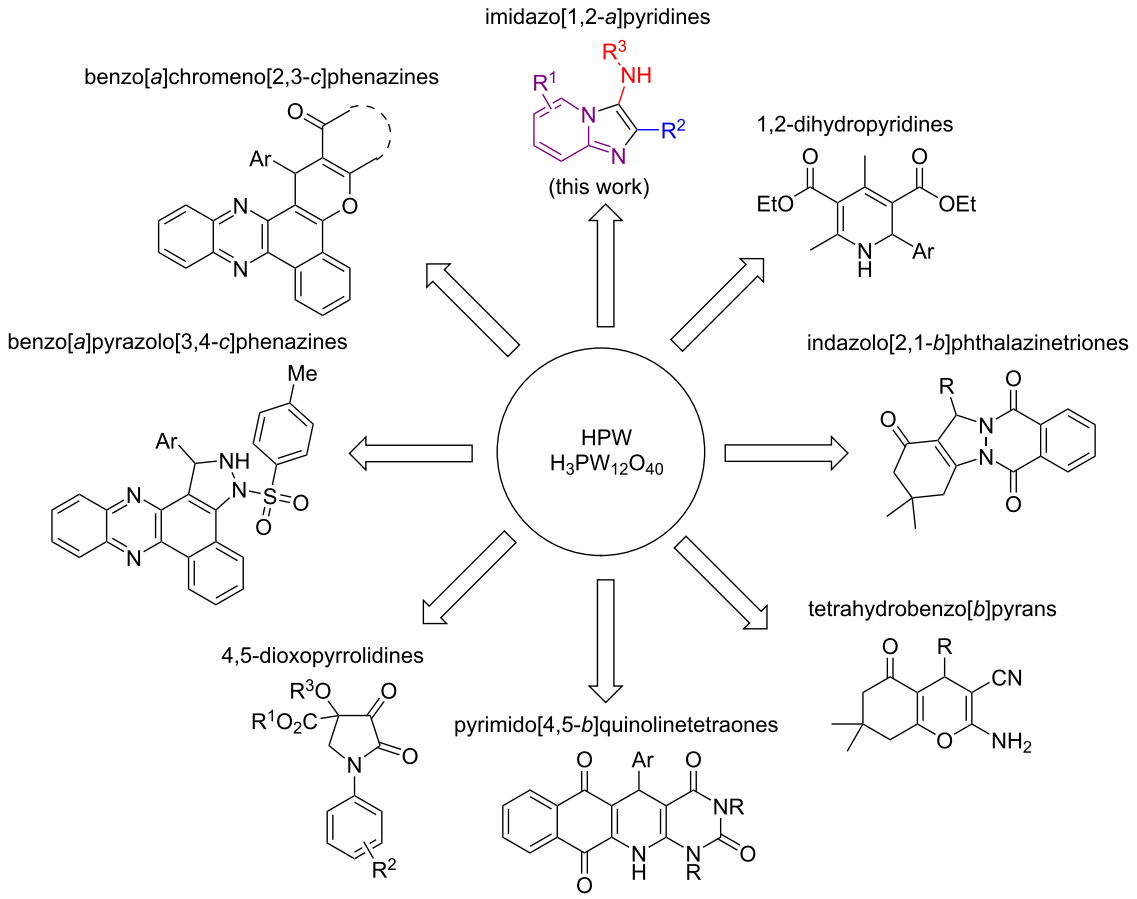

Figure 2: Examples of application of HPW as catalyst in the synthesis of heterocyclic compounds through multicomponent reaction approaches.

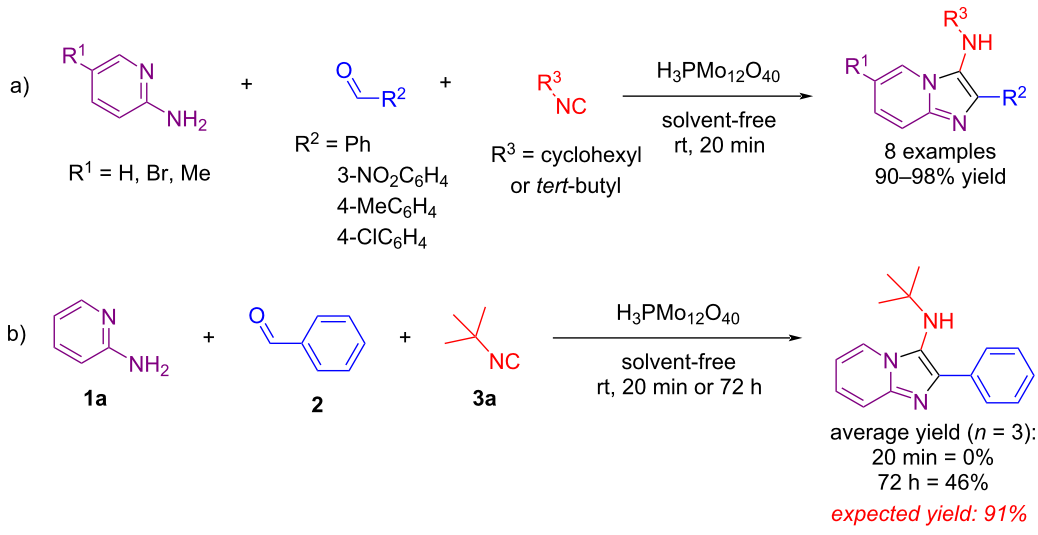

Scheme 1: a) Reported phosphomolybdic acid-catalyzed synthesis of imidazo[1,2-*a*]pyridines via GBB-3CR. b) Attempts to reproduce the results reported in (a).

caught our attention for being the only example so far of a room temperature GBB reaction carried out in less than an 18-hour period. However, at least in our hands, when we tried to reproduce the reaction between 2-aminopyridine (**1a**), benzaldehyde (**2**), and *tert*-butyl isocyanide (**3a**), following in detail the reported protocol using exactly the same reaction conditions, the reaction failed completely in 20 minutes (followed by TLC) and after 72 h only 46% yield (compared to the expected 91% yield) was obtained (Scheme 1b). This reaction was carried out in triplicate with the same outcome. Therefore, the search for a broader and more reliable methodology to obtain imidazo[1,2-*a*]pyridines using heteropolyacids became necessary.

Due to its already mentioned attractive intrinsic properties, HPW was used in our initial studies to find the best reaction conditions. Additionally, knowing that a higher temperature is crucial for faster GBB reactions, μw heating was used, taking into account our experience over the years on the μw-mediated MCRs [51-53]. 2-Aminopyridine (**1a**), 4-nitrobenzaldehyde (**2a**), and *tert*-butyl isocyanide (**3a**) were chosen as model substrates and different conditions were screened (Table 1). Glycerol, a green and sustainable solvent, was tried first, but unfortunately, the expected intense orange solid product **4a** was obtained in low yields (Table 1, entries 1 and 2).

Significantly better yields were obtained using methanol, which is the most common solvent for this reaction, especially at 120 °C (Table 1, entries 3–12). Interestingly, the yield was also better for a lower catalyst loading (Table 1, entry 7). Further changes either in the temperature or in the reaction time were checked, however, with no benefit in the yields (Table 1, entries 9–12). Accordingly, with the established optimal conditions of 2 mol % of HPW, 120 °C, and 30 min, other solvents were tested, and ethanol was found to give similar results (Table 1, entry 13). For being much greener as compared to methanol, it was chosen as the solvent to study the reaction scope. The use of water or solvent-free conditions resulted in much lower reaction yields (Table 1, entries 14–16).

Next, the scope of the reaction was investigated with a range of 2-aminopyridines/2-aminothiazoles **1**, aromatic/heteroaromatic aldehydes **2**, and isocyanides **3** to obtain the imidazo[1,2-*a*]pyridine derivatives **4** (Scheme 2). In general, the efficiency of the HPW-catalyzed GBB reaction is very dependent upon the type

Table 1: Optimization of the reaction conditions.[a]

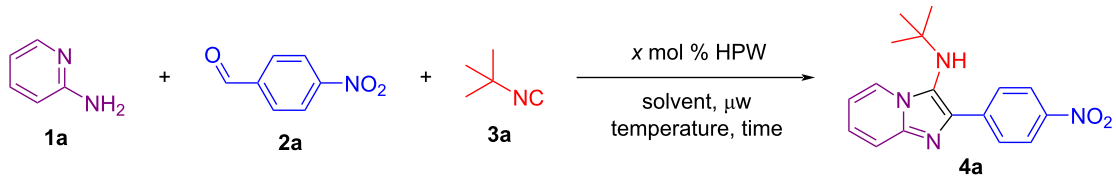

Entry	HPW (mol %)	Solvent	Temp. (°C)	Time (min)	Yield (%)[b]
1	10	glycerol	100	5	25
2	10	glycerol	100	30	29
3	10	MeOH	100	5	54
4	10	MeOH	120	30	76
5	5	MeOH	120	30	86
6	2	MeOH	100	30	77
7	2	MeOH	120	30	87
8	1	MeOH	120	30	81
9	2	MeOH	100	30	77
10	2	MeOH	150	30	86
11	2	MeOH	120	5	68
12	2	MeOH	120	15	81
13	**2**	**EtOH**	**120**	**30**	**87**
14	2	H_2O	120	30	17
15	2	EtOH/H_2O 1:1	120	30	25
16	2	solvent-free	120	30	24

[a]Reaction conditions: 2-aminopyridine (0.50 mmol), 4-nitrobenzaldehyde (0.50 mmol), and *tert*-butyl isocyanide (0.50 mmol) in 0.5 mL of the specified solvent. [b]Isolated yields after column chromatography.

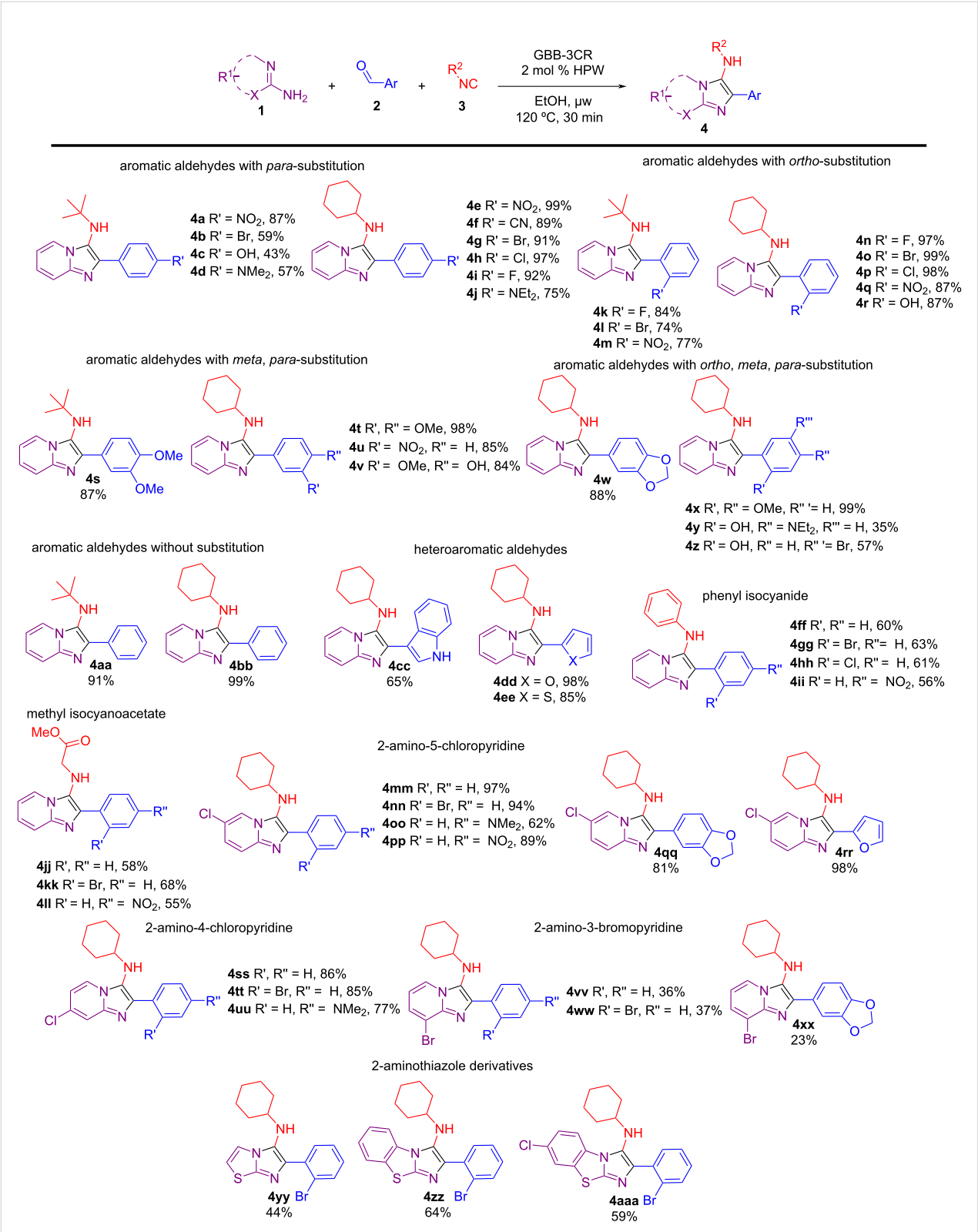

Scheme 2: Substrate scope of the HPW-catalyzed GBB reactions using a range of aromatic/heteroaromatic aldehydes. Reaction conditions: 2-aminopyridine/2-aminothiazole (0.50 mmol), aromatic/heteroaromatic aldehyde (0.50 mmol), isocyanide (0.50 mmol), and HPW (0.01 mmol, 2 mol %) in EtOH (0.5 mL), under μw heating. The yields refer to isolated yields after column chromatography and the structures were confirmed by FTIR, NMR, and HRMS.

of 2-aminopyridine or isocyanide compound used, and not influenced by different substituents at the aromatic aldehydes (both electron-withdrawing and electron-donating groups can be successfully used). The use of *para*-substituted aromatic aldehydes gave the corresponding products **4a–j** in moderate to excellent yields (up to 99%). Aromatic aldehydes with electron-donating groups at the *para*-position gave moderate product yields (**4c** and **4d**). Furthermore, cyclohexyl isocyanide gave higher yields compared to *tert*-butyl isocyanide. *Ortho*-substituted aromatic aldehydes were very efficient, regardless the type of substituents used, and good to excellent yields (74–99%) of products **4k–r** were obtained. *Meta*,*para*-substituted aromatic aldehydes showed a high reactivity with yields greater than 84% for products **4s–w**. Notably, the use of trisubstituted aromatic aldehydes gave imidazo[1,2-*a*]pyridines **4x–z** in moderate to excellent yields (35–99%), though the hydroxy substituent at the *ortho* position made the aldehyde less reactive. The use of non-substituted aromatic aldehydes also provided the expected products (**4aa** and **4bb**) in excellent yields (up to 99%). Heteroaromatic aldehydes gave the respective products **4cc–ee** in moderate to excellent yields (65–98%). However, the use of phenyl isocyanide and methyl isocyanoacetate furnished the desired products (**4ff–ii** and **4jj–ll**, respectively) in moderate yields (55–68%), possibly due to the lower reactivity of these isocyanides compared to *tert*-butyl and cyclohexyl isocyanides [54]. In the latter cases, transesterification of the ester group with ethanol was not observed. 2-Aminopyridines containing a chlorine atom in positions 4 or 5 provided the products **4mm–uu** in excellent yields (up to 97%). Nonetheless, with 2-amino-3-bromopyridine, low product yields were observed for **4vv–xx**, which may be due to the high hindrance of that substrate to imine formation, essential for the GBB-3CR mechanism. Moderate yields were obtained with the use of 2-aminothiazole derivatives (**4yy–aaa**). These lower yields did not change using MeOH as a solvent or increasing the amount of HPW used.

The use of aliphatic aldehydes in the GBB multicomponent reaction for the synthesis of imidazo[1,2-*a*]pyridines is not as usual, given that Schiff bases from aliphatic aldehydes are found to be less stable and readily polymerize in comparison to stable Schiff bases of aromatic aldehydes. Nonetheless, our protocol for the HPW-catalyzed GBB multicomponent reaction proved to be very effective for aliphatic aldehydes (Scheme 3). For instance, isovaleraldehyde proved to be quite reactive for a range of isocyanides (**5a–e**), furnishing the products in good to excellent yields (83–99%). Phenylacetaldehyde provided the expected product **5f** in a moderate yield. The imidazo[1,2-*a*]pyridines **5g–l** were obtained in good to excellent yields (74–99%) when isobutyraldehyde and cyclohexanecarboxaldehyde were used. Notably, even the less reactive isocyanides phenyl isocyanide and methyl isocyanoacetate reacted well and gave high product yields. Besides, the longer chain aldehyde heptaldehyde also furnished good results for the HPW-catalyzed GBB-3CR with yields greater than 63% (**5m–o**).

It is always important to point out the limitations of a given method and in our case, we did have some. Purification by column chromatography became necessary since product isolation by precipitation was not effective. The catalyst was impregnated in the isolated crude product, and its removal through a recrystallization step was not successful. The use of a liquid–liquid extraction work-up step proved less effective compared to column chromatography purification. Moreover, attempts to recover the catalyst were not reproducible. Unsuccessful substrates for these reactions were also detected (Scheme 4). The use of 2-amino-3-hydroxypyridine provided a complex mixture of products (^{1}H and ^{13}C NMR analysis). When 6-amino-2-thiouracil was used, only the starting materials were recovered. Regarding the aldehyde component, the use of glyoxals did not provide the desired products. Instead, the respective starting materials were almost quantitatively recovered from the column chromatography purification step. The use of very reactive aldehydes such as formaldehyde and crotonaldehyde also did not provide the GBB adduct, probably due to decomposition by the high temperature used in the protocol. Furthermore, the use of the less reactive TosMIC as isocyanide did not furnish the expected product; only the formamide product was isolated from the chromatographic column, which may be due to the lower nucleophilicity of this substrate.

The present HPW-catalyzed GBB reaction also worked very well when a 10-fold increase (5.0 mmol) in scale was applied (Scheme 5). In this case, the reaction was carried out using 5.0 mmol of each substrate and the product was obtained in gram scale in excellent yield (98%).

Based on a previous report from the literature [24] a plausible reaction mechanism is shown in Scheme 6. It involves the nucleophilic attack of the aminopyridine **1** to the HPW-activated carbonyl compound **2**, followed by iminium ion formation (iii) and [4 + 1] cycloaddition with the isocyanide. A 1,3-hydrogen shift yields the final products.

Our HPW-catalyzed GBB reaction has some advantages compared to several procedures reported in the literature for GBB reactions under μw and conventional heating conditions (Table 2), such as the use of a relatively inexpensive catalyst and a short reaction time. Furthermore, our protocol was applied to a broader range of aromatic/heteroaromatic

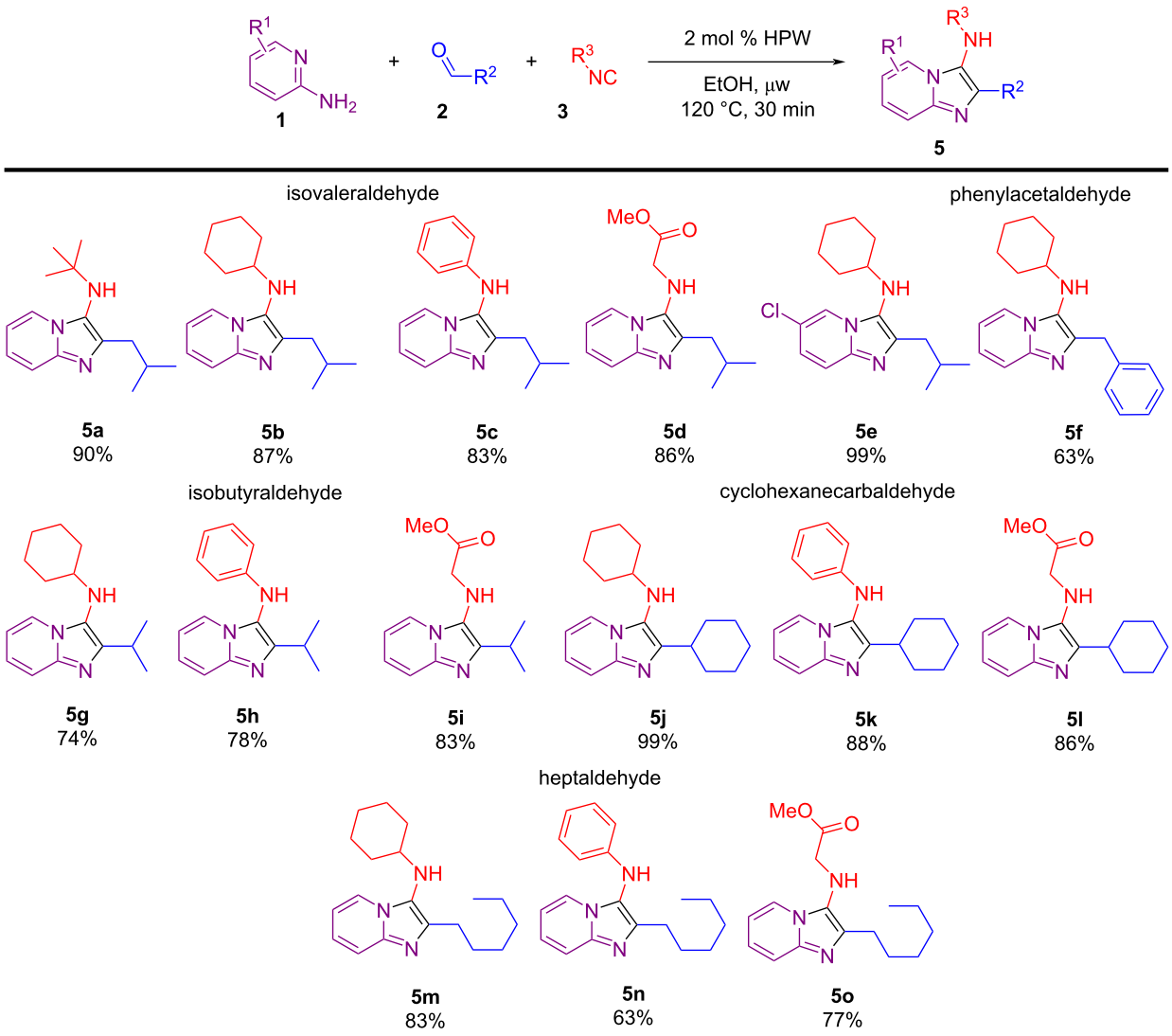

Scheme 3: Substrate scope of the HPW-catalyzed GBB reaction using aliphatic aldehydes. Reaction conditions: 2-aminopyridine (0.50 mmol), aliphatic aldehyde (0.50 mmol), isocyanide (0.50 mmol), and HPW (0.01 mmol, 2 mol %) in EtOH (0.5 mL), under μw heating. The yields refer to isolated yields after column chromatography and the structures were confirmed by FTIR, NMR, and HRMS.

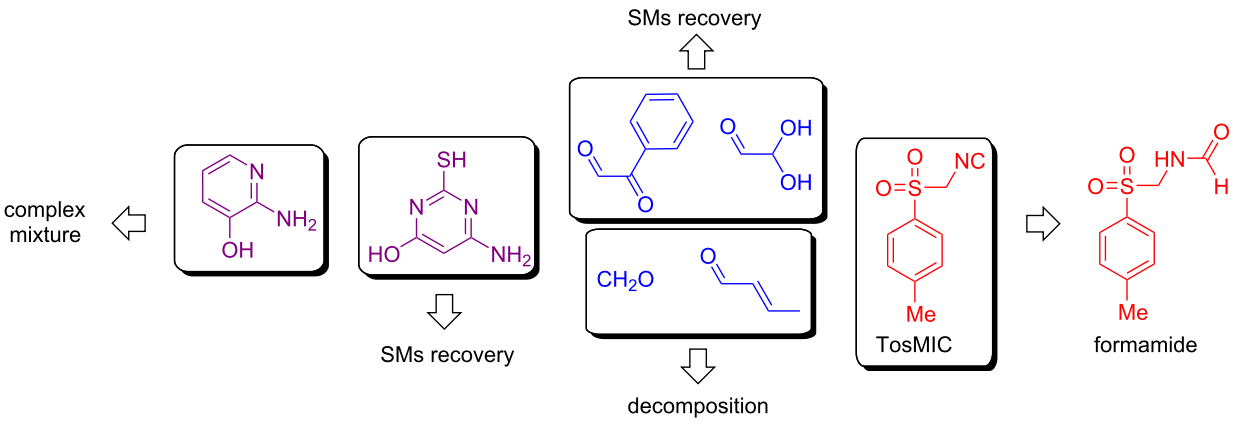

Scheme 4: Unsuccessful substrates for the HPW-catalyzed GBB-3CR for the synthesis of imidazo[1,2-*a*]pyridines.

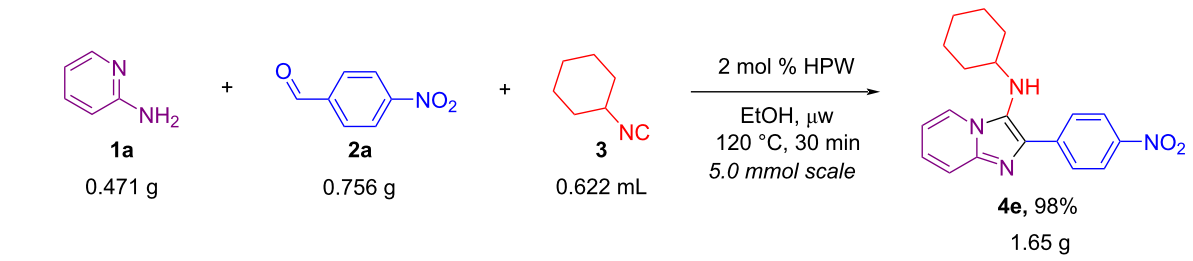

Scheme 5: 10-Fold scale-up of the HPW-catalyzed GBB reaction (5.0 mmol) between 2-aminopyridine (**1a**), 4-nitrobenzaldehyde (**2a**) and cyclohexyl isocyanide (**3**) in EtOH under μw heating.

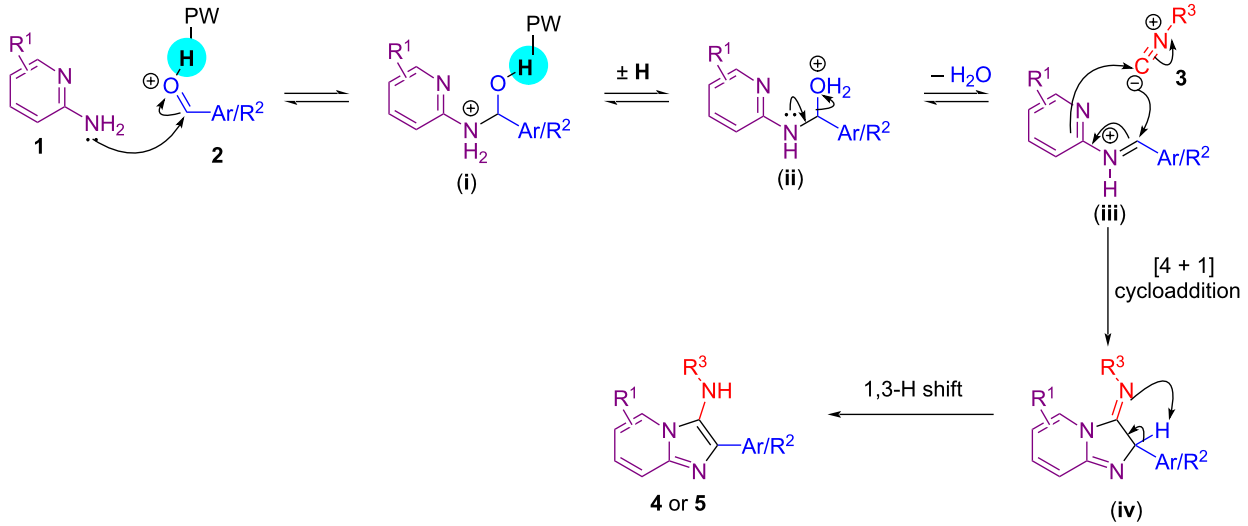

Scheme 6: Plausible reaction mechanism for the HPW-catalyzed GBB reaction.

Table 2: Comparison of reaction conditions and Green Chemistry metrics for the GBB reactions under μw and conventional heating conditions.[a]

Entry	Reaction conditions	Time (min)	Examples	Yields (%)[a]	E-factor[b]	Mass intensity	Ref.
1	CALB, EtOH, rt	18 h	11	0–91	12.79	10.75	[55]
2	20 mol % AgOAc, EG, 90 °C	120	23	72–92	11.01	12.01	[56]
3	5 mol % $Gd(OTf)_3$, MeOH, μw, 150 °C	30	23	54–94	8.79	9.79	[28]
4	5 mol % $ZnCl_2$, 1,4-dioxane, μw or reflux	60 or 300	17	9–78	7.21	8.21	[37]
5	10 mol % $ZrCl_4$, PEG-400, μw, 140 °C	7	28	72–97	4.09	5.09	[30]
6	2 mol % HPW, EtOH, μw, 120 °C	30	68	23–99	2.61	3.61	this work

[a]Isolated yield. [b]Excluding work-up and purification processes (extraction, column chromatography and/or recrystallization).

or aliphatic aldehydes, 2-aminopyridines/2-aminothiazoles and isocyanides. Regarding some Green Chemistry metrics, our methodology proved superior at least considering E-factor and mass intensity. As can be seen in entry 6 of Table 2, our protocol showed a lower E-factor by far, which makes it a cleaner and environmentally friendly process. Through the mass

intensity parameter, our procedure also showed a lower mass loss compared to the total raw material used to produce a given mass of product. The calculations of these parameters can be found in Supporting Information File 1.

Conclusion

In summary, we have developed a straightforward approach to the GBB reaction using HPW as a cheap catalyst in ethanol under μw heating for the synthesis of imidazo[1,2-*a*]pyridines. Although some minor limitations exist, this convenient environmentally benign methodology is broad in scope (68 products were obtained, many of them not previously reported), provides the heterobicyclic products in moderate to excellent yields (23–99%), with a low catalyst loading (2 mol %). The reactions are fast, and the method can be applied to a wide range of aromatic/heteroaromatic and aliphatic aldehydes. Furthermore, the isolation process is simple and there is no need for liquid–liquid extraction. In addition, our methodology showed superior Green Chemistry metrics as compared to some already reported methodologies.

Supporting Information

Supporting Information File 1

Typical experimental procedures, FTIR, NMR and mass spectra of all compounds and GC metrics calculations.
[https://www.beilstein-journals.org/bjoc/content/supplementary/1860-5397-20-55-S1.pdf]

Funding

The authors thank the Universidade de Brasília, FAPDF (project number 00.193.00001027/2021-04) and CAPES for financial support.

Author Contributions

Luan A. Martinho: conceptualization; investigation; methodology; validation; visualization; writing – original draft. Carlos Kleber Z. Andrade: conceptualization; funding acquisition; methodology; project administration; resources; supervision; validation; writing – review & editing.

ORCID® iDs

Luan A. Martinho - https://orcid.org/0000-0001-6658-5847
Carlos Kleber Z. Andrade - https://orcid.org/0000-0003-0798-9133

Data Availability Statement

All data that supports the findings of this study is available in the published article and/or the supporting information to this article.

References

1. Gudmundsson, K. S.; Johns, B. A. *Bioorg. Med. Chem. Lett.* **2007,** *17,* 2735–2739. doi:10.1016/j.bmcl.2007.02.079
2. Ulloora, S.; Shabaraya, R.; Adhikari, A. V. *Med. Chem. Res.* **2014,** *23,* 3019–3028. doi:10.1007/s00044-013-0887-7
3. Sapegin, A.; Rogacheva, E.; Kraeva, L.; Gureev, M.; Dogonadze, M.; Vinogradova, T.; Yablonsky, P.; Balalaie, S.; Baykov, S. V.; Krasavin, M. *Biomedicines* **2022,** *10,* 2203. doi:10.3390/biomedicines10092203
4. Almirante, L.; Polo, L.; Mugnaini, A.; Provinciali, E.; Rugarli, P.; Biancotti, A.; Gamba, A.; Murmann, W. *J. Med. Chem.* **1965,** *8,* 305–312. doi:10.1021/jm00327a007
5. N'Guessan, J.-P. D. U.; Delaye, P.-O.; Pénichon, M.; Charvet, C. L.; Neveu, C.; Ouattara, M.; Enguehard-Gueiffier, C.; Gueiffier, A.; Allouchi, H. *Bioorg. Med. Chem.* **2017,** *25,* 6695–6706. doi:10.1016/j.bmc.2017.11.012
6. Gomes, G. B.; Zubieta, C. S.; Guilhermi, J. d. S.; Toffoli-Kadri, M. C.; Beatriz, A.; Rafique, J.; Parisotto, E. B.; Saba, S.; Perdomo, R. T. *Pharmaceuticals* **2023,** *16,* 814. doi:10.3390/ph16060814
7. Shukla, P.; Deswal, D.; Pandit, M.; Latha, N.; Mahajan, D.; Srivastava, T.; Narula, A. K. *Drug Dev. Res.* **2022,** *83,* 525–543. doi:10.1002/ddr.21883
8. Lacerda, R. B.; de Lima, C. K. F.; da Silva, L. L.; Romeiro, N. C.; Miranda, A. L. P.; Barreiro, E. J.; Fraga, C. A. M. *Bioorg. Med. Chem.* **2009,** *17,* 74–84. doi:10.1016/j.bmc.2008.11.018
9. Sonawane, R. S.; Shirsat, M.; Patil, S. R.; Hundiwale, J. C.; Patil, A. V. *Asian J. Chem.* **2020,** *32,* 2685–2692. doi:10.14233/ajchem.2020.22697
10. Biftu, T.; Feng, D.; Fisher, M.; Liang, G.-B.; Qian, X.; Scribner, A.; Dennis, R.; Lee, S.; Liberator, P. A.; Brown, C.; Gurnett, A.; Leavitt, P. S.; Thompson, D.; Mathew, J.; Misura, A.; Samaras, S.; Tamas, T.; Sina, J. F.; McNulty, K. A.; McKnight, C. G.; Schmatz, D. M.; Wyvratt, M. *Bioorg. Med. Chem. Lett.* **2006,** *16,* 2479–2483. doi:10.1016/j.bmcl.2006.01.092
11. Yu, Y.; Li, Y.; Yang, X.; Deng, Q.; Xu, B.; Cao, H.; Mao, J. *Anti-Cancer Agents Med. Chem.* **2022,** *22,* 1102–1110. doi:10.2174/1871520621666210805130925
12. Movahed, M. A.; Abbasi, F. K.; Rajabi, M.; Abedi, N.; Naderi, N.; Daraei, B.; Zarghi, A. *Med. Chem. Res.* **2023,** *32,* 856–868. doi:10.1007/s00044-023-03041-x
13. Mishra, N. P.; Mohapatra, S.; Das, T.; Nayak, S. *J. Heterocycl. Chem.* **2022,** *59,* 2051–2075. doi:10.1002/jhet.4534
14. Babu, S. A.; P. V, V.; Poulose, S.; Varughese, S.; John, J. *J. Org. Chem.* **2023,** *88,* 10027–10039. doi:10.1021/acs.joc.3c00849
15. Régnier, S.; Bechara, W. S.; Charette, A. B. *J. Org. Chem.* **2016,** *81,* 10348–10356. doi:10.1021/acs.joc.6b01324
16. Huo, C.; Tang, J.; Xie, H.; Wang, Y.; Dong, J. *Org. Lett.* **2016,** *18,* 1016–1019. doi:10.1021/acs.orglett.6b00137
17. Tan, J.; Ni, P.; Huang, H.; Deng, G.-J. *Org. Biomol. Chem.* **2018,** *16,* 4227–4230. doi:10.1039/c8ob00981c
18. Filippov, I. P.; Agafonova, A. V.; Titov, G. D.; Smetanin, I. A.; Rostovskii, N. V.; Khlebnikov, A. F.; Novikov, M. S. *J. Org. Chem.* **2022,** *87,* 6514–6519. doi:10.1021/acs.joc.2c00514
19. Panda, J.; Raiguru, B. P.; Mishra, M.; Mohapatra, S.; Nayak, S. *ChemistrySelect* **2022,** *7,* e202103987. doi:10.1002/slct.202103987
20. Groebke, K.; Weber, L.; Mehlin, F. *Synlett* **1998,** 661–663. doi:10.1055/s-1998-1721

21. Blackburn, C.; Guan, B.; Fleming, P.; Shiosaki, K.; Tsai, S. *Tetrahedron Lett.* **1998,** *39,* 3635–3638. doi:10.1016/s0040-4039(98)00653-4
22. Bienaymé, H.; Bouzid, K. *Angew. Chem., Int. Ed.* **1998,** *37,* 2234–2237. doi:10.1002/(sici)1521-3773(19980904)37:16<2234::aid-anie2234>3.0.co;2-r
23. Carvalho, M.; Amarante, G.; de Castro, P. *J. Braz. Chem. Soc.* **2023,** *34,* 1041–1070. doi:10.21577/0103-5053.20230082
24. Boltjes, A.; Dömling, A. *Eur. J. Org. Chem.* **2019,** 7007–7049. doi:10.1002/ejoc.201901124
25. Burchak, O. N.; Mugherli, L.; Ostuni, M.; Lacapère, J. J.; Balakirev, M. Y. *J. Am. Chem. Soc.* **2011,** *133,* 10058–10061. doi:10.1021/ja204016e
26. Ansari, A. J.; Sharma, S.; Pathare, R. S.; Gopal, K.; Sawant, D. M.; Pardasani, R. T. *ChemistrySelect* **2016,** *1,* 1016–1021. doi:10.1002/slct.201600241
27. Devi, N.; Singh, D.; Sunkaria, R. K.; Malakar, C. C.; Mehra, S.; Rawal, R. K.; Singh, V. *ChemistrySelect* **2016,** *1,* 4696–4703. doi:10.1002/slct.201601133
28. Santos, G. F. D.; Anjos, N. S.; Gibeli, M. M.; Silva, G. A.; Fernandes, P. C. S.; Fiorentino, E. S. C.; Longo, L. S., Jr. *J. Braz. Chem. Soc.* **2020,** *31,* 1434–1444. doi:10.21577/0103-5053.20200028
29. Arnould, M.; Hiebel, M.-A.; Massip, S.; Léger, J. M.; Jarry, C.; Berteina-Raboin, S.; Guillaumet, G. *Chem. – Eur. J.* **2013,** *19,* 12249–12253. doi:10.1002/chem.201300961
30. Guchhait, S. K.; Madaan, C.; Thakkar, B. S. *Synthesis* **2009,** 3293–3300. doi:10.1055/s-0029-1216916
31. Kishore, K. G.; Basavanag, U. M. V.; Islas-Jácome, A.; Gámez-Montaño, R. *Tetrahedron Lett.* **2015,** *56,* 155–158. doi:10.1016/j.tetlet.2014.11.047
32. Shahrisa, A.; Safa, K. D.; Esmati, S. *Spectrochim. Acta, Part A* **2014,** *117,* 614–621. doi:10.1016/j.saa.2013.09.056
33. Rostamnia, S.; Hassankhani, A. *RSC Adv.* **2013,** *3,* 18626–18629. doi:10.1039/c3ra42752h
34. Dianat, S.; Mahdavi, M.; Moghimi, S.; Mouradzadegun, A.; Shafiee, A.; Foroumadi, A. *Mol. Diversity* **2015,** *19,* 797–805. doi:10.1007/s11030-015-9622-2
35. Tazeem; Han, X.; Zhou, Q.; Wei, J.; Tien, P.; Yang, G.; Wu, S.; Dong, C. *RSC Adv.* **2016,** *6,* 95177–95188. doi:10.1039/c6ra17656a
36. Shinde, A. H.; Srilaxmi, M.; Satpathi, B.; Sharada, D. S. *Tetrahedron Lett.* **2014,** *55,* 5915–5920. doi:10.1016/j.tetlet.2014.08.126
37. Rousseau, A. L.; Matlaba, P.; Parkinson, C. J. *Tetrahedron Lett.* **2007,** *48,* 4079–4082. doi:10.1016/j.tetlet.2007.04.008
38. Jalani, H. B.; Jeong, J.-H. *J. Heterocycl. Chem.* **2022,** *59,* 1266–1271. doi:10.1002/jhet.4456
39. Vázquez-Romero, A.; Kielland, N.; Arévalo, M. J.; Preciado, S.; Mellanby, R. J.; Feng, Y.; Lavilla, R.; Vendrell, M. *J. Am. Chem. Soc.* **2013,** *135,* 16018–16021. doi:10.1021/ja408093p
40. Manvar, P.; Shaikh, F.; Kakadiya, R.; Mehariya, K.; Khunt, R.; Pandey, B.; Shah, A. *Tetrahedron* **2016,** *72,* 1293–1300. doi:10.1016/j.tet.2016.01.023
41. Heravi, M. M.; Bamoharram, F. F. Heteropoly Acids: An Overview. In *Heteropolyacids as Highly Efficient and Green Catalysts Applied in Organic Transformations;* Torok, B.; Dransfield, T., Eds.; Advances in Green and Sustainable Chemistry; Elsevier: Amsterdam, Netherlands, 2022. doi:10.1016/b978-0-323-88441-9.00002-8
42. Escobar, A. M.; Blustein, G.; Luque, R.; Romanelli, G. P. *Catalysts* **2021,** *11,* 291. doi:10.3390/catal11020291
43. Mokhtar, M.; Saleh, T. S.; Narasimharao, K.; Al-Mutairi, E. *Catal. Today* **2022,** *397–399,* 484–496. doi:10.1016/j.cattod.2021.07.006
44. Rajeswari, M.; Khanna, G.; Chaudhary, A.; Khurana, J. M. *Synth. Commun.* **2015,** *45,* 1426–1432. doi:10.1080/00397911.2015.1024324
45. Mohebat, R.; Dehgan, P.; Yazdani-Elah-Abadi, A. *J. Chin. Chem. Soc.* **2018,** *65,* 1259–1265. doi:10.1002/jccs.201800071
46. Basu, S.; Ghosh, T.; Maity, S.; Ghosh, P.; Mukhopadhyay, C. *ChemistrySelect* **2019,** *4,* 5763–5767. doi:10.1002/slct.201901011
47. Bosica, G.; Demanuele, K.; Padrón, J. M.; Puerta, A. *Beilstein J. Org. Chem.* **2020,** *16,* 2862–2869. doi:10.3762/bjoc.16.235
48. Safari, J.; Tavakoli, M.; Ghasemzadeh, M. A. *Polyhedron* **2020,** *182,* 114459. doi:10.1016/j.poly.2020.114459
49. Mozafari, R.; Heidarizadeh, F. *Polyhedron* **2019,** *162,* 263–276. doi:10.1016/j.poly.2019.01.065
50. Oskooie, H. A.; Amini, M.; Heravi, M. M.; Bamoharram, F. F. *Chin. J. Chem.* **2010,** *28,* 299–302. doi:10.1002/cjoc.201090070
51. Barreto, A. F. S.; Vercillo, O. E.; Andrade, C. K. Z. *J. Braz. Chem. Soc.* **2011,** *22,* 462–467. doi:10.1590/s0103-50532011000300008
52. Barreto, A. F. S.; Andrade, C. K. Z. *Tetrahedron* **2018,** *74,* 6861–6865. doi:10.1016/j.tet.2018.10.018
53. Martinho, L. A.; Rosalba, T. P. F.; Sousa, G. G.; Gatto, C. C.; Politi, J. R. S.; Andrade, C. K. Z. *Mol. Diversity* **2024,** *28,* 111–123. doi:10.1007/s11030-023-10618-6
54. Mironov, M. A. General Aspects of Isocyanide Reactivity. In *Isocyanide Chemistry;* Nenajdenko, V. G., Ed.; Wiley-VCH: Weinheim, Germany, 2012; pp 35–73. doi:10.1002/9783527652532.ch2
55. Budhiraja, M.; Kondabala, R.; Ali, A.; Tyagi, V. *Tetrahedron* **2020,** *76,* 131643. doi:10.1016/j.tet.2020.131643
56. Hussain, M.; Liu, J.; Fu, L.; Hasan, M. *J. Heterocycl. Chem.* **2020,** *57,* 955–964. doi:10.1002/jhet.3746

License and Terms

This is an open access article licensed under the terms of the Beilstein-Institut Open Access License Agreement (https://www.beilstein-journals.org/bjoc/terms), which is identical to the Creative Commons Attribution 4.0 International License (https://creativecommons.org/licenses/by/4.0). The reuse of material under this license requires that the author(s), source and license are credited. Third-party material in this article could be subject to other licenses (typically indicated in the credit line), and in this case, users are required to obtain permission from the license holder to reuse the material.

The definitive version of this article is the electronic one which can be found at:
https://doi.org/10.3762/bjoc.20.55

BEILSTEIN JOURNAL OF ORGANIC CHEMISTRY

Palladium-catalyzed three-component radical-polar crossover carboamination of 1,3-dienes or allenes with diazo esters and amines

Geng-Xin Liu‡, Xiao-Ting Jie‡, Ge-Jun Niu, Li-Sheng Yang, Xing-Lin Li, Jian Luo and Wen-Hao Hu*

Full Research Paper

Open Access

Address:
Guangdong Key Laboratory of Chiral Molecule and Drug Discovery, School of Pharmaceutical Sciences, Sun Yat-sen University, Guangzhou, Guangdong 510006, China

Email:
Wen-Hao Hu* - huwh9@mail.sysu.edu.cn

* Corresponding author ‡ Equal contributors

Keywords:
carboamination; diazo chemistry; palladium catalysis; radical-polar crossover; three-component reaction

Beilstein J. Org. Chem. **2024,** *20,* 661–671.
https://doi.org/10.3762/bjoc.20.59

Received: 11 December 2023
Accepted: 13 March 2024
Published: 27 March 2024

This article is part of the thematic issue "Multicomponent reactions IV".

Associate Editor: T. J. J. Müller

© 2024 Liu et al.; licensee Beilstein-Institut.
License and terms: see end of document.

Abstract

Herein, we report a visible-light-mediated palladium-catalyzed three-component radical-polar crossover carboamination of 1,3-dienes or allenes with diazo esters and amines, affording unsaturated γ- and ε-amino acid derivatives with diverse structures. In this methodology, the diazo compound readily transforms into a hybrid α-ester alkylpalladium radical with the release of dinitrogen. The radical intermediate selectively adds to the double bond of a 1,3-diene or allene, followed by the allylpalladium radical-polar crossover path and selective allylic substitution with the amine substrate, thereby leading to a single unsaturated γ- or ε-amino acid derivative. This approach proceeds under mild and simple reaction conditions and shows high functional group tolerance, especially in the incorporation of various bioactive molecules. The studies on scale-up reactions and diverse derivatizations highlight the practical utility of this multicomponent reaction protocol.

Introduction

Since the discovery of the existence of non-canonical amino acids (AAs) in organisms, such structural motifs have attracted considerable attention owing to their wide applications in medicinal chemistry [1-5]. γ- and ε-AA derivatives are widely distributed in peptide natural products, bioactive molecules, and drugs, such as pregabalin, baclofen, ε-aminocaproic acid and lysine (Scheme 1a) [6-12]. The number of reported synthetic methods for γ- and ε-AA derivatives is much lower than those of α-AA derivatives [13,14]. Although synthetic strategies of γ- and ε-AA derivatives have been developed [15-20], acquiring

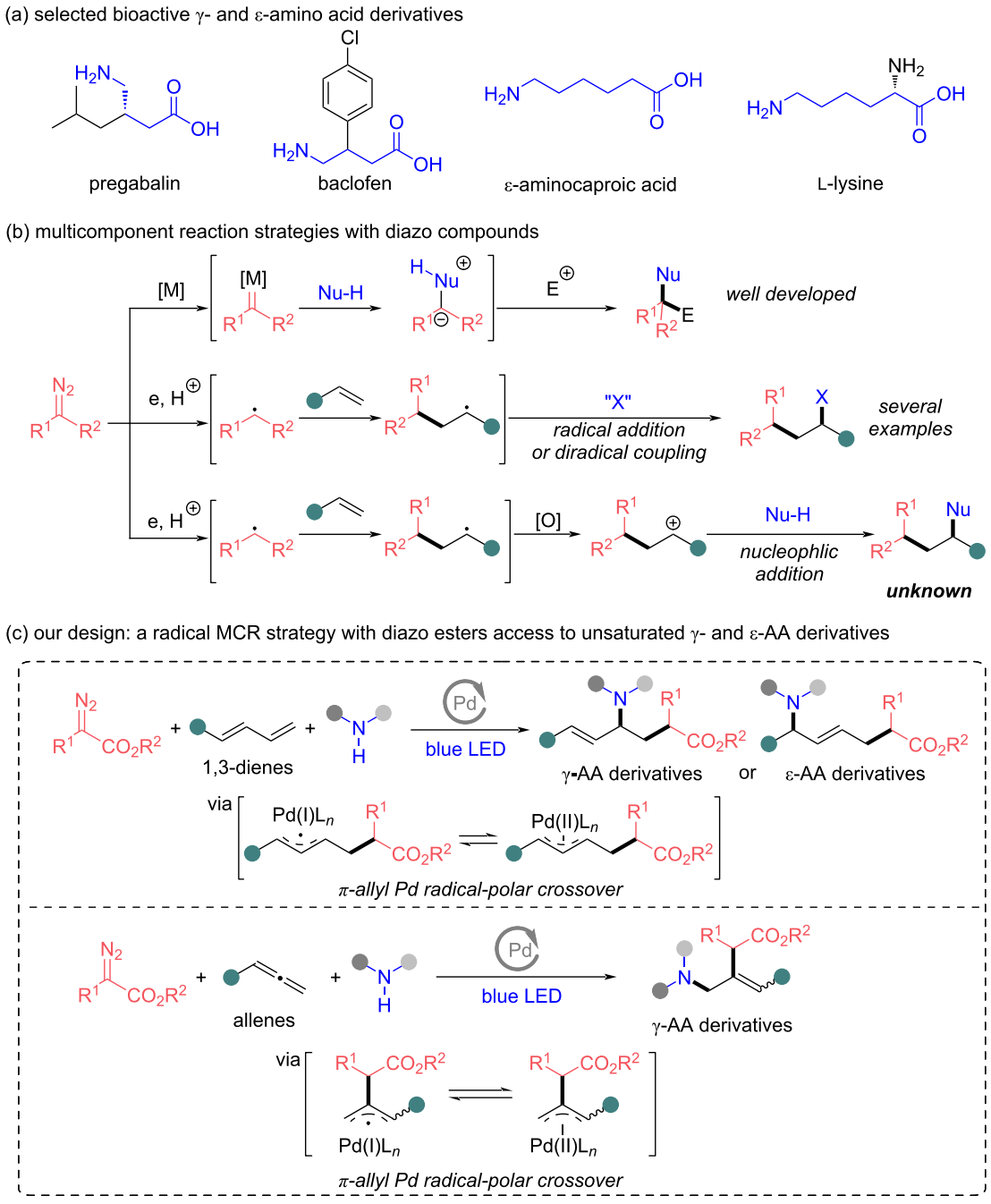

Scheme 1: Background (a and b) and proposed carboamination MCR with diazo esters (c). a) Selected bioactive γ- and ε-amino acid derivatives. b) Multicomponent reaction strategies with diazo compounds. c) Our design: a radical MCR strategy with diazo esters to access unsaturated γ- and ε-AA derivatives.

complex γ- and ε-AA derivatives with simple starting materials in a one-step reaction remains a challenge. In addition, many studies show that unsaturated AAs exhibit a variety of unique biological activities [21-24]. Accordingly, the development of efficient methods to synthesize unsaturated γ- and ε-AA derivatives is a highly sought-after target to enrich non-natural AA chemistry.

Multicomponent reactions (MCRs) by virtue of high efficiency for the construction of complex chemicals, have shown the superiority in high step and atom economy in organic synthesis [25-27]. Over the past two decades, our group and others have developed a transition-metal-catalyzed MCR strategy involving electrophilic trapping of onium ylides generated from metal carbenes with nucleophiles, providing an ingenious difunction-

alization strategy for diazo compounds to access structurally complex and diverse molecules (Scheme 1b, top) [28,29]. In recent years, radical-mediated MCRs with diazo compounds have become a highly emerging area of research and exhibit complementary reactivity to those well-developed carbene-mediated MCRs [30-42]. In the radical-mediated difunctionalization of alkenes, the carbon-centered radical species from a diazo compound can add to diverse alkenes followed by a diradical coupling or radical addition process to achieve the difunctionalization (Scheme 1b, middle) [32-37]. However, to the best of our knowledge, the methodology involving the addition of a carbon radical from a diazo compound onto the double bond of an alkene followed by a nucleophilic addition, is unknown (Scheme 1b, bottom).

The radical-polar crossover strategy has been steadily emerging in synthetic organic chemistry during the last few years [43-46]. This strategy allows complex chemicals to be assembled with high step economy that would be difficult to achieve using either radical or polar chemistry alone. In recent years, Gevorgyan, Glorius, Huang and their co-workers reported elegant examples of the carboamination of 1,3-dienes with unactivated alkyl halides and amines under photoinduced palladium catalysis via a radical-polar crossover process [47-50]. However, activated alkyl halides are not suitable for these carboamination reactions due to the direct nucleophilic substitution of activated alkyl halides with nucleophilic reagents under the necessary alkaline conditions [51]. Recently, a Pd-catalyzed alkyl Heck reaction of diazo compounds mediated by visible light has been reported by the group of Gevorgyan, which achieves the monofunctionalization of alkenes [52]. Inspired by these collective studies, we considered diazo compounds could be a competent activated alkyl halide equivalent to overcome the synthetic limitation of the photoinduced palladium-catalyzed carboamination reactions and the radical-mediated difunctionalization of alkenes with diazo compounds. We envisioned an interesting MCR strategy with mild conditions to access unsaturated γ- and ε-AA derivatives via a π-allyl Pd radical-polar crossover process (Scheme 1c). In this process, the hybrid α-ester alkylpalladium radical species from diazo ester adds to the double bond of 1,3-dienes or allenes, followed by the allylpalladium radical-polar crossover path. As with the classical Tsuji–Trost reaction, a subsequent nucleophilic attack of an amine toward the allylpalladium species would afford the desired unsaturated γ- and ε-AA derivatives. This methodology would represent the first reaction mode for the difunctionalization of alkenes with diazo compounds via a radical-polar crossover process.

Results and Discussion

As summarized in Table 1, we started our studies with the palladium-catalyzed MCR of ethyl diazoacetate (**1a**), 1,3-butadiene (**2a**), and 1-phenylpiperazine (**3a**) in the presence of 5 mol % $Pd(OAc)_2$ and 10 mol % Xantphos as ligand. To our delight, after irradiation with blue LED light in dimethylformamide (DMF) for 12 h at room temperature (rt), the desired unsaturated ε-AA derivative **4a** was obtained in 75% isolated yield (Table 1, entry 1). Isolation and NMR analysis demonstrated that this model reaction provided amino acid **4a** with good *E*-selectivity and excellent regioselectivity (*E*/*Z* = 91:9, 1,4-/1,2-addition >20:1). Control experiments indicated that ligand, palladium, light and argon atmosphere were necessary for this transformation (Table 1, entries 2–5). Heating conditions could not facilitate the reaction instead of light conditions (Table 1, entry 6). The efficiency was maintained with another Pd(II) catalyst $Pd(PPh_3)_2Cl_2$ (Table 1, entry 7), whereas only low yields of **4a** were observed with Pd(0) catalysts $Pd(PPh_3)_4$ and $Pd_2(dba)_3$ (Table 1, entries 8 and 9). Moreover, adding potassium carbonate as additive failed to furnish **4a**, demonstrating that the trace amount of acid from the Pd(II) catalyst may facilitate the formation of the hybrid α-ester alkylpalladium radical generated from the diazo ester (Table 1, entry 10) [53]. Replacing Xantphos with *rac*-BINAP or DPEphos gave very low product formation, indicating that the type of ligand was crucial for this transformation (Table 1, entries 11 and 12). Changing the reactant ratio produced the desired product **4a** in 84% yield as optimal conditions for this protocol (Table 1, entry 13).

With the optimized conditions obtained, we examined the generality of our palladium-catalyzed regioselective carboamination of 1,3-dienes with diazo esters and amines (Scheme 2). First, different alkylamines with various functional groups were evaluated under the optimized conditions, successfully delivering the corresponding 1,4-difunctionalized products in moderate to excellent yields (**4a**–**k**, 35–84%) with high regioselectivity. Some simple secondary amines including cyclic amines **3a**, **3c** and linear amine **3b** were found to readily participate in this protocol, furnishing the corresponding products **4a**–**c** in 61–84% yields. To our delight, this MCR strategy was compatible with a wide variety of complex bioactive molecules, including tetrahydropapaverine, (*R*)-duloxetine, sertraline, amoxapine, an ibrutinib derivative, *N*-desmethyl sildenafil, silodosin, and lapatinib (**4d**–**k**, 35–67%). The late-stage modification of these drug agents and their derivatives in this MCR underlined the synthetic value and high functional group tolerance (e.g., aromatic amine, amide, alcohol, heterocycle).

We next turned to evaluate the scope of 1,3-dienes. Although the regioselectivity control of allylic substitution can be attributed to many factors, it is agreed that steric hindrance generally is the primary factor affecting the regioselectivity of nucleo-

Table 1: Optimization of conditions and control experiments.[a]

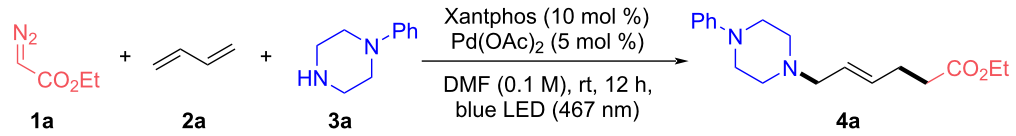

1a **2a** **3a** **4a**

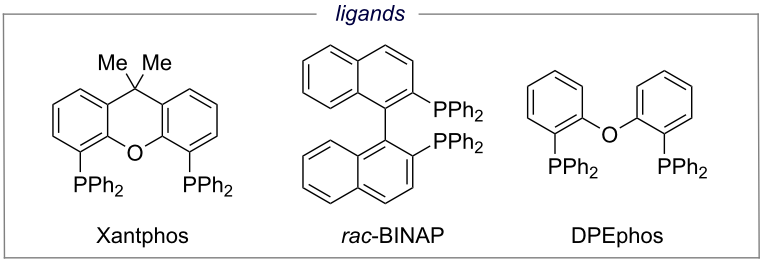

Entry	Variations	**4a** (%)[b,c]
1	none	75[c]
2	without Xantphos	0
3	without $Pd(OAc)_2$	0
4	without blue LED ligt	0
5	without argon protection	0
6	100 °C instead of blue LED light	0
7	$Pd(PPh_3)_2Cl_2$ instead of $Pd(OAc)_2$	70
8	$Pd(PPh_3)_4$ instead of $Pd(OAc)_2$	20
9	$Pd_2(dba)_3$ instead of $Pd(OAc)_2$	24
10	add K_2CO_3 (1.5 equiv)	0
11	*rac*-BINAP instead of Xantphos	<5
12	DPEphos instead of Xantphos	6
13	**1a**/**2a**/**3a** = 0.15:0.2:0.1 mmol	84

[a]Reactions (**1a**/**2a**/**3a**/$Pd(OAc)_2$/Xantphos = 0.12:0.12:0.1:0.005:0.01 mmol) were irradiated with blue LED light (467 nm) in 1.0 mL DMF at rt for 12 h under argon. [b]Yields of compound **4a** were determined by ^{1}H NMR spectroscopic analyses of the reaction mixture using 1,3,5-trimethoxybenzene as the internal standard or detected by LC–MS. [c]The crude NMR yield was consistent with the isolated yield (for more details, see the Supporting Information File 1).

philic attack [54-57]. Monoalkyl-substituted dienes **2b** and **2c** were suitable for this MCR, affording the 1,4-addition products **4l** and **4m** albeit with moderate regioselectivity (1,4-/1,2-addition = 2:1). To our delight, the reactions with 2,3-disubstituted diene **2d** and 1,4-disubstituted diene **2e** also readily provided products **4n** and **4o**. In the case of 1,3-cyclohexadiene **2e**, the amine was expected to attack the π-allyl palladium from the exo side. Considering that substituent effects might affect the regioselectivity in this MCR, we further investigated the 1,4-/1,2-addition selectivity with 1-phenyl-substituted 1,3-dienes **2f**–**i**. Interestingly, the corresponding 1,2-addition products **4p**–**t** were formed with high selectivity (*E*/*Z* > 20:1, 1,2-/1,4-addition >20:1), presumably due to steric hindrance by the phenyl group. Furthermore, the 1,3-diene bearing a 1-furan group with smaller steric hindrance afforded product **4u** with moderate chemoselectivity (1,2-/1,4-addition = 4:1).

Diazo esters suitable for this transformation were examined next. The MCRs with diazo substrates equipped with different substitution patterns were accommodated under the mild photocatalytic conditions to generate the desired 1,4-addition products in moderate to good yields (**4v**–**ab**, 51–77%). α-Diazo esters with benzyl, cyclobutanemethyl, and adamantyl groups could be transformed smoothly to the products **4v**, **4w**, and **4x** in 64%, 69% and 77% yields, respectively. Gratifyingly, except for acceptor-substituted diazo esters, donor/acceptor-substituted diazo compounds were also compatible with these mild conditions (**4y**–**aa**, 51–72%). Additionally, the diazo derivative of epiandrosterone was reactive in this protocol, giving the product **4ab** in 59% yield.

Delightedly, this procedure was successfully applied to aromatic amine (*N*-methylaniline), primary amine (aniline) and diazo-

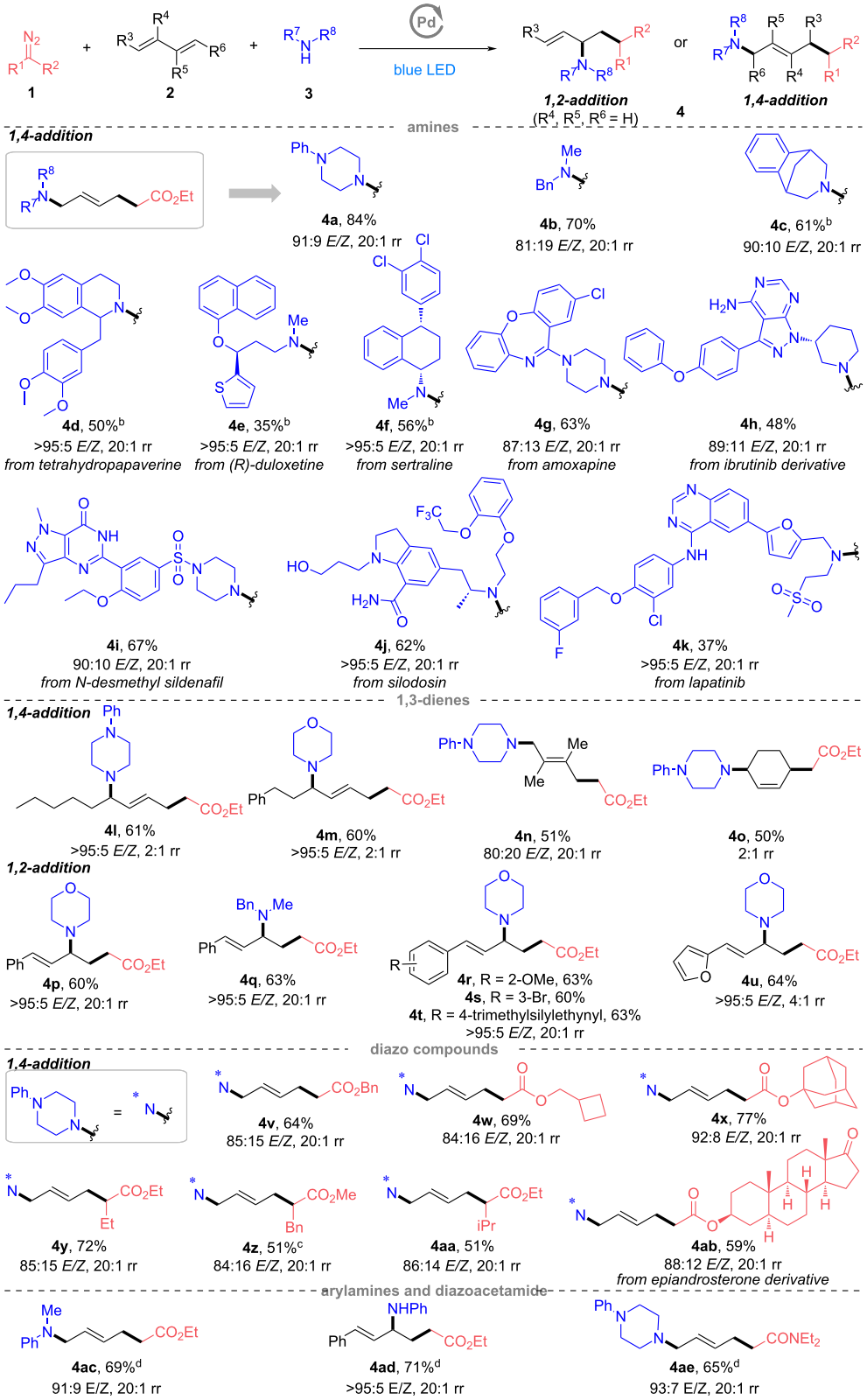

Scheme 2: Substrate scope of diazo compounds, 1,3-dienes and amines. [a]Reactions (**1**/**2**/**3**/$Pd(OAc)_2$/Xantphos = 0.3:0.4:0.2:0.01:0.02 mmol) were irradiated with blue LED light (467 nm) in 2.0 mL DMF at rt for 12 h under argon. Isolated yields. [b]Amine hydrochloride and Et_3N (1.5 equiv) were used. [c]Diazo compound (0.4 mmol) was used. [d]$Pd(Ph_3P)_2Cl_2$ was used. For more experimental details, see Supporting Information File 1.

acetamide, affording the corresponding products **4ac**, **4ad**, and **4ae** in high yields with $Pd(PPh_3)_2Cl_2$ (69%, 71% and 65%, respectively).

With a reliable set of conditions for the carboamination of 1,3-dienes with diazo esters and amines, we wondered whether this three-component reaction could be applied to allenes that were never used as substrates in interrupted radical Heck/allylic substitution reactions. As summarized in Scheme 3, unsaturated γ-AA derivatives were observed in this reaction albeit with poor stereoselectivity. Linear amines containing alkyl, hydroxy, and terminal alkenyl groups were reactive under the photocatalytic conditions, providing the corresponding 1,2-adducts **6a**, **6b**, and **6c** smoothly in 73%, 93% and 34% yields, respectively. Commercially available amines with a broad range of heterocyclic rings (e.g., morpholine, piperazine, pyrrolidine, homopiperazine) also readily participated in this MCR, affording the products in moderate to good yields (**6d–k**, 43–73%).

Then, the investigations of the scope of allenes demonstrated that the substrates possessing substituents at *para*-, *meta*-, and *ortho*-positions of the aromatic ring were also tolerated under our catalysis conditions. *Para*-(methoxy, chloro, *n*-propyl), *meta*-fluoro, *ortho*-methyl and β-naphthyl-substituted allenes delivered the 1,2-adducts **6l–q** in 58–70% yields, indicating a weak influence of different electronic groups on the aromatic ring.

We further assessed the reaction applicability with respect to diazo esters. 1,2-Adducts could be produced fluently with diazo substrates containing alkyl-substituted esters. Benzyl- (**6r**, 57%), cyclobutanemethyl- (**6s**, 81%), methoxyethyl- (**6t**, 66%), and adamantyl- (**6u**, 82%) substituted diazo esters underwent this photoinitiated radical reaction well. The donor/acceptor-substituted diazo compounds with benzyl- and ester groups were also compatible with this MCR system (**6v**, 78%). Furthermore, the successful transformation of the diazo compounds derived from epiandrosterone (**6w**, 84%) and testosterone (**6x**, 56%) highlighted the general utility of this reaction in the modification of pharmaceutical scaffolds.

Naturally, we were eager to acquire detailed mechanistic insights into this protocol. To validate the radical nature of this transformation, both model reactions of 1,3-diene **2a** and allene **5a** were terminated completely with 2.5 equiv 2,2,6,6-tetramethylpiperidinyloxyl (TEMPO) and the corresponding radical-trapping product **A** could be confirmed by HRMS of both reaction mixtures, unambiguously supporting radical mechanisms (Scheme 4a). The reaction with styrene was conducted under standard conditions, but no product **X** could be detected, indicating the cationic intermediate **B** should be ruled out from this methodology (Scheme 4b). The product *Z*-**6i** was subjected to the standard conditions, but *Z*-**6i** was obtained in 100% recovery yield. Therefore, the *E/Z* selectivity of the MCRs with allenes could be determined by the allylic substitution process (Scheme 4c). Using $HPd(PPh_3)_2Cl$ as catalyst, the model reaction also afforded the corresponding product **4a** in 31% yield, demonstrating the H–Pd(II)–X species could be a possible catalytic species (Scheme 4d). According to the UV–visible spectra, the only absorbing species at 467 nm consists in the pre-catalytic system $Pd(OAc)_2$ and Xantphos (Scheme 4e). In addition, deuterium labeling experiments were conducted to investigate the H-source of this transformation (for more details, see Supporting Information Information File 1). The isotopic-labeling experiments suggested that both types of protons from the N–H bond of the amine and the traces amount of water in this reaction system may serve as proton sources for the formation of hybrid α-ester alkylpalladium radical.

On the basis of above mechanistic studies and previous reports [47-50,52,58], the following plausible mechanisms are proposed for the palladium-catalyzed carboamination of 1,3-dienes (Scheme 5, lower left) or allenes (Scheme 5, lower right) with diazo esters. There are two possible paths to generate the hybrid α-ester alkylpalladium radical **I**. Path a undergoes an oxidative addition of HX with $Pd(0)L_n$, followed by the formation of Pd–carbene species, hydride shift process, and photoinduced homolytic cleavage of the C–Pd bond, furnishing hybrid α-ester alkylpalladium radical **I**. In path b, upon irradiation with blue light, photoexcited $Pd(0)L_n$* reduces ethyl diazoacetate (**1a**) to Pd-radical species **I** by a proton-coupled electron transfer (PCET) process [32-37,59-62], upon the loss of dinitrogen. The radical **I** further adds to the terminal position of 1,3-butadiene (**2a**) to produce hybrid allylPd radical **II**, which would exist in equilibrium with π-allyl complex **III**. Following the classical Tsuji–Trost reaction mechanism, a subsequent attack of amine **3** at the latter stage would afford the unsaturated ε-AA derivative **4** and regenerates the $Pd(0)L_n$ to close the catalytic cycle. Different from the reactive site of 1,3-diene, the hybrid alkylPd radical **I** selectively adds to the central position of the allenyl group of allene **5a**, providing another type of hybrid allylPd radical **IV**. After the equilibrium shifting to the π-allyl complex **V**, the unsaturated γ-AA derivative **6** would be obtained with the nucleophilic attack of amine **3**.

The utility of this protocol was further highlighted by scale-up reactions and diverse derivatizations of products **4a** and **6a** (Scheme 6). Both model reactions with diene **2a** and allene **5a** were proven to be easily scalable without further conditions optimization, delivering unsaturated γ- and ε-AA derivatives **4a** and **6a** in good yields. Starting from the unsaturated ε-AA derivative **4a**, unsaturated ζ-amino alcohols **7** and **8** were pro-

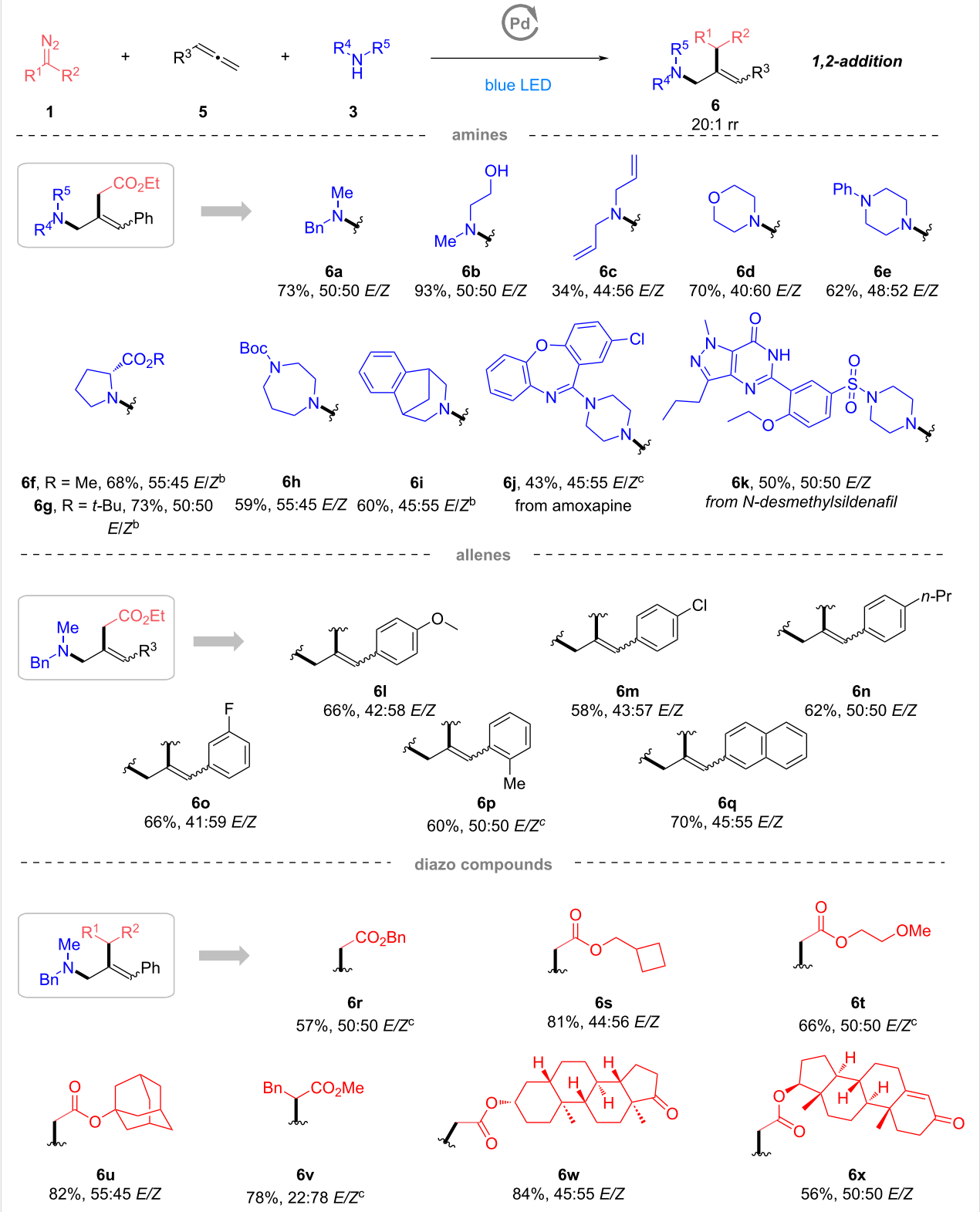

Scheme 3: Substrate scope of diazo compounds, allenes and amines. [a]Reactions (**1**/**5**/**3**/$Pd(OAc)_2$/Xantphos = 0.3.0.4:0.2:0.01:0.02 mmol) were irradiated with blue LED light (467 nm) in 2.0 mL DMF at rt for 12 h under argon. Isolated yields. [b]Amine hydrochloride and Et_3N (1.5 equiv) were used. [c]Diazo compound (0.4 mmol) was used. For more experimental details, see Supporting Information Information File 1.

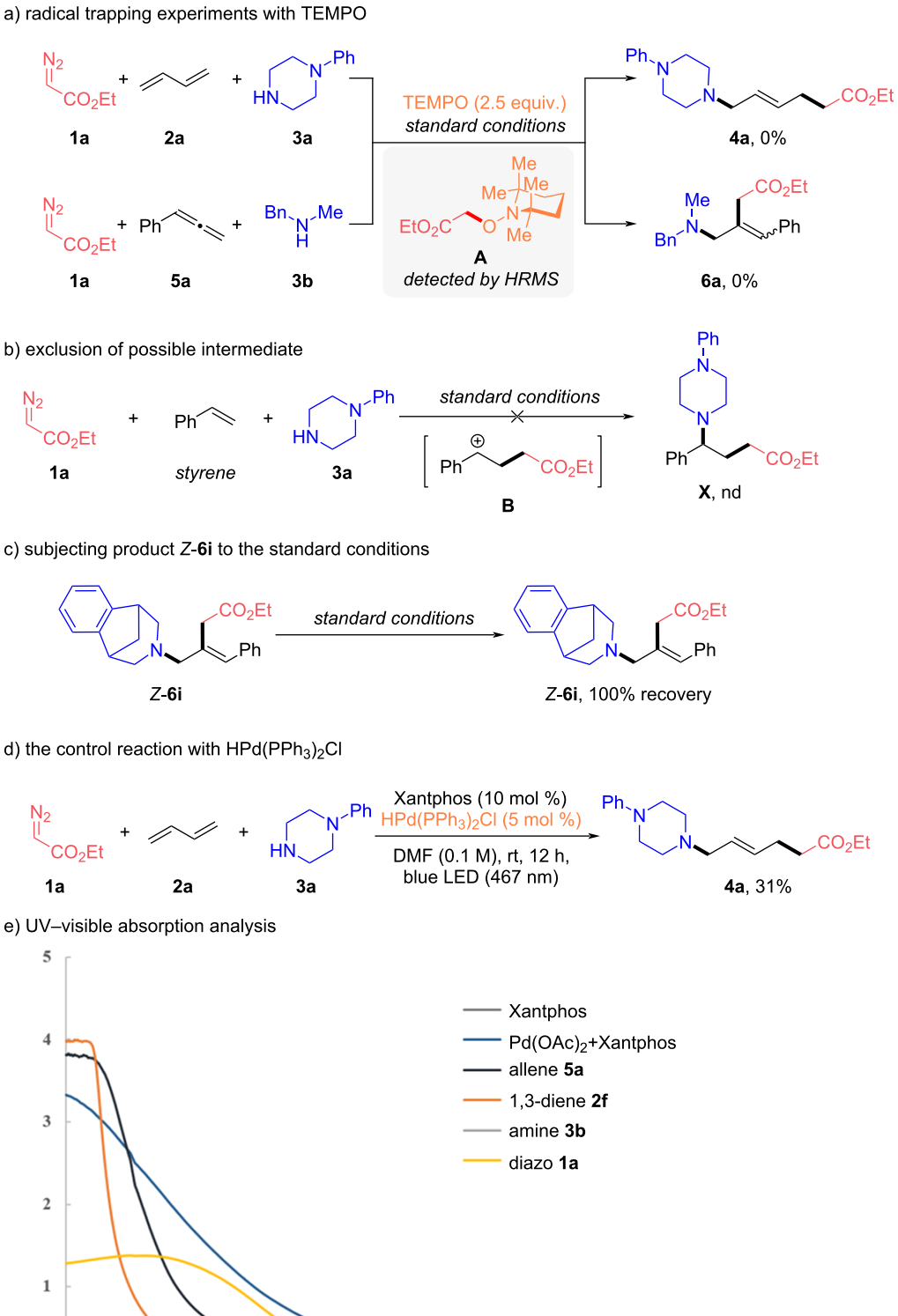

Scheme 4: Mechanistic experiments. a) Radical trapping experiments with TEMPO. b) Exclusion of possible intermediate. c) Subjecting the product *Z*-**6i** to the standard conditions. d) The control reaction with $HPd(PPh_3)_2Cl$. e) UV–visible absorption analysis.

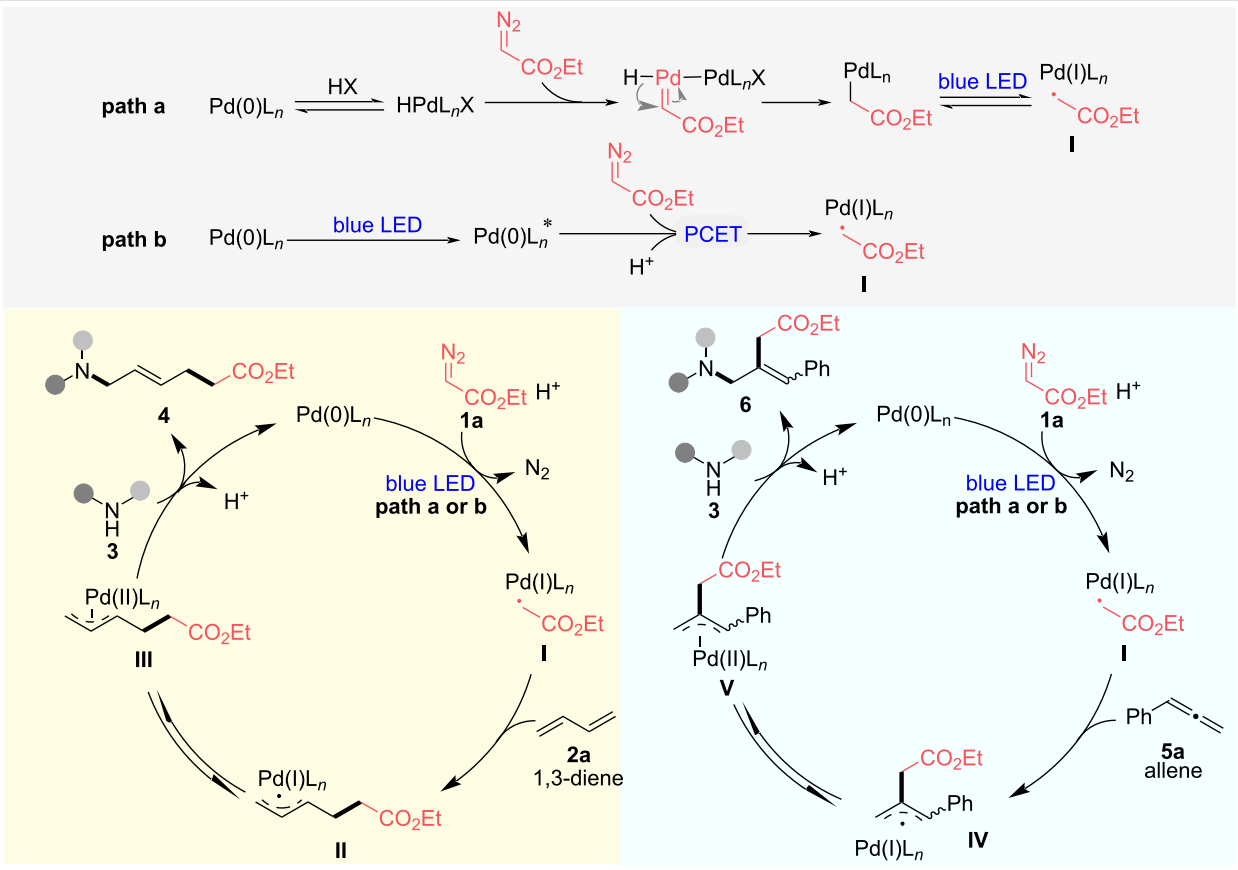

Scheme 5: Proposed mechanisms for the carboamination of 1,3-dienes or allenes with diazo esters and amines.

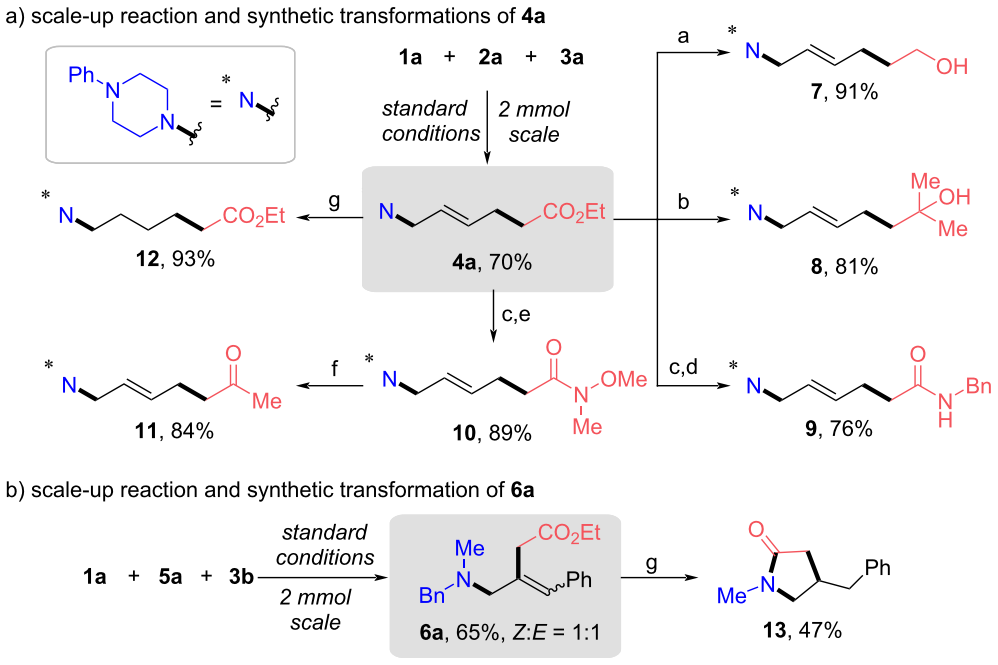

Scheme 6: Scale-up reactions and synthetic transformations. Reaction conditions: a) $LiAlH_4$, THF, 0 °C; b) MeMgBr, THF, rt to reflux; c) NaOH, MeOH, 60 °C, d) EDCI, DMAP, $BnNH_2$, DCM, rt; e) EDCI, DMAP, Et_3N, HN(OMe)(Me)·HCl, DCM, rt; f) MeMgBr, THF, 0 °C to rt; g) Pd/C, HCO_2NH_4, 65 °C. For more details, see Supporting Information File 1.

duced in high yields through $LiAlH_4$ conditions or nucleophilic addition of methylmagnesium bromide. Moreover, product **4a** could be easily transformed to unsaturated ε-amino amide **9** in total 76% yield. Likewise, Weinreb amide **10** was produced and further transformed into ketone **11** in 84% yield. Compound **4a** could be hydrogenated to the corresponding reduction product **12** using Pd/C and ammonium formate conditions (Scheme 6a). Notably, as shown in Scheme 6b, treatment of the unsaturated γ-AA derivative **6a** with Pd/C and ammonium formate led to a cyclization reaction, furnishing γ-lactam **13** in a moderate yield.

Conclusion

In summary, we have developed a visible-light-mediated palladium-catalyzed carboamination reaction of 1,3-dienes or allenes with diazo esters and amines, providing a broad array of synthetically valuable unsaturated γ- and ε-AA derivatives. This methodology represents the first reaction mode for a difunctionalization of alkenes with diazo compounds via a radical-polar crossover process. This synthetic transformation proceeds under mild reaction conditions and shows high functional group tolerance. The studies on late-stage functionalization, scale-up reactions, and diverse derivatizations further highlight the practical utility of this MCR protocol.

Supporting Information

Supporting Information File 1

Full experimental details, analytical data and NMR spetra.
[https://www.beilstein-journals.org/bjoc/content/supplementary/1860-5397-20-59-S1.pdf]

Funding

Financial support from the National Natural Science Foundation of China (92256301,92056201,22171294,81973176), the Natural Science Foundation of Guangdong Province, China (2021A1515010401), Key-Area Research and Development Program of Guangdong Province (2022B1111050003) is gratefully acknowledged.

Author Contributions

Geng-Xin Liu: conceptualization; data curation; formal analysis; investigation; methodology; visualization; writing – original draft. Xiao-Ting Jie: data curation; formal analysis; investigation. Ge-Jun Niu: investigation. Li-Sheng Yang: investigation. Xing-Lin Li: investigation; validation. Jian Luo: validation. Wen-Hao Hu: funding acquisition; project administration; supervision; writing – review & editing.

ORCID® iDs

Geng-Xin Liu - https://orcid.org/0000-0003-1378-6359

Data Availability Statement

All data that supports the findings of this study is available in the published article and/or the supporting information to this article.

References

1. Gentilucci, L.; De Marco, R.; Cerisoli, L. *Curr. Pharm. Des.* **2010,** *16,* 3185–3203. doi:10.2174/138161210793292555
2. Hendrickson, T. L.; Crécy-Lagard, V. d.; Schimmel, P. *Annu. Rev. Biochem.* **2004,** *73,* 147–176. doi:10.1146/annurev.biochem.73.012803.092429
3. Hohsaka, T.; Sisido, M. *Curr. Opin. Chem. Biol.* **2002,** *6,* 809–815. doi:10.1016/s1367-5931(02)00376-9
4. de Graaf, A. J.; Kooijman, M.; Hennink, W. E.; Mastrobattista, E. *Bioconjugate Chem.* **2009,** *20,* 1281–1295. doi:10.1021/bc800294a
5. Hodgson, D. R. W.; Sanderson, J. M. *Chem. Soc. Rev.* **2004,** *33,* 422–430. doi:10.1039/b312953p
6. Fromm, G. H.; Terrence, C. F.; Chattha, A. S.; Glass, J. D. *Arch. Neurol. (Chicago)* **1980,** *37,* 768–771. doi:10.1001/archneur.1980.00500610048007
7. Silverman, R. B. *Angew. Chem., Int. Ed.* **2008,** *47,* 3500–3504. doi:10.1002/anie.200704280
8. Lapin, I. *CNS Drug Rev.* **2001,** *7,* 471–481. doi:10.1111/j.1527-3458.2001.tb00211.x
9. Griebel, G.; Holmes, A. *Nat. Rev. Drug Discovery* **2013,** *12,* 667–687. doi:10.1038/nrd4075
10. Conti, P.; Tamborini, L.; Pinto, A.; Blondel, A.; Minoprio, P.; Mozzarelli, A.; De Micheli, C. *Chem. Rev.* **2011,** *111,* 6919–6946. doi:10.1021/cr2000702
11. Pettinger, J.; Jones, K.; Cheeseman, M. D. *Angew. Chem., Int. Ed.* **2017,** *56,* 15200–15209. doi:10.1002/anie.201707630
12. Mukhopadhyay, D.; Riezman, H. *Science* **2007,** *315,* 201–205. doi:10.1126/science.1127085
13. Wang, J.; Liu, X.; Feng, X. *Chem. Rev.* **2011,** *111,* 6947–6983. doi:10.1021/cr200057t
14. Mita, T.; Sato, Y. *Chem. – Asian J.* **2019,** *14,* 2038–2047. doi:10.1002/asia.201900379
15. Ooi, T.; Fujioka, S.; Maruoka, K. *J. Am. Chem. Soc.* **2004,** *126,* 11790–11791. doi:10.1021/ja047047v
16. Magauer, T.; Smaltz, D. J.; Myers, A. G. *Nat. Chem.* **2013,** *5,* 886–893. doi:10.1038/nchem.1746
17. Pipaliya, B. V.; Trofimova, D. N.; Grange, R. L.; Aeluri, M.; Deng, X.; Shah, K.; Craig, A. W.; Allingham, J. S.; Evans, P. A. *J. Am. Chem. Soc.* **2021,** *143,* 6847–6854. doi:10.1021/jacs.0c12404
18. Meng, L.; Yang, J.; Duan, M.; Wang, Y.; Zhu, S. *Angew. Chem., Int. Ed.* **2021,** *60,* 23584–23589. doi:10.1002/anie.202109881
19. Das, S.; Mitschke, B.; De, C. K.; Harden, I.; Bistoni, G.; List, B. *Nat. Catal.* **2021,** *4,* 1043–1049. doi:10.1038/s41929-021-00714-x
20. Chen, L.; Qu, Q.; Ran, C.-K.; Wang, W.; Zhang, W.; He, Y.; Liao, L.-L.; Ye, J.-H.; Yu, D.-G. *Angew. Chem., Int. Ed.* **2023,** *62,* e202217918. doi:10.1002/anie.202217918
21. Katagiri, K.; Tori, K.; Kimura, Y.; Yoshida, T.; Nagasaki, T.; Minato, H. *J. Med. Chem.* **1967,** *10,* 1149–1154. doi:10.1021/jm00318a035
22. Rando, R. R. *Nature* **1974,** *250,* 586–587. doi:10.1038/250586a0

23. Fisher, S. K.; Davies, W. E. *Biochem. Pharmacol.* **1976,** *25,* 1881–1885. doi:10.1016/0006-2952(76)90193-3
24. Roblin, G.; Laduranty, J.; Bonmort, J.; Aidene, M.; Chollet, J.-F. *Plant Physiol. Biochem.* **2016,** *107,* 67–74. doi:10.1016/j.plaphy.2016.05.025
25. Ruijter, E.; Scheffelaar, R.; Orru, R. V. A. *Angew. Chem., Int. Ed.* **2011,** *50,* 6234–6246. doi:10.1002/anie.201006515
26. Graebin, C. S.; Ribeiro, F. V.; Rogério, K. R.; Kümmerle, A. E. *Curr. Org. Synth.* **2019,** *16,* 855–899. doi:10.2174/1570179416666190718153703
27. John, S. E.; Gulati, S.; Shankaraiah, N. *Org. Chem. Front.* **2021,** *8,* 4237–4287. doi:10.1039/d0qo01480j
28. Guo, X.; Hu, W. *Acc. Chem. Res.* **2013,** *46,* 2427–2440. doi:10.1021/ar300340k
29. Zhang, D.; Hu, W. *Chem. Rec.* **2017,** *17,* 739–753. doi:10.1002/tcr.201600124
30. Ciszewski, Ł. W.; Rybicka-Jasińska, K.; Gryko, D. *Org. Biomol. Chem.* **2019,** *17,* 432–448. doi:10.1039/c8ob02703j
31. Durka, J.; Turkowska, J.; Gryko, D. *ACS Sustainable Chem. Eng.* **2021,** *9,* 8895–8918. doi:10.1021/acssuschemeng.1c01976
32. Su, Y.-L.; Liu, G.-X.; Liu, J.-W.; Tram, L.; Qiu, H.; Doyle, M. P. *J. Am. Chem. Soc.* **2020,** *142,* 13846–13855. doi:10.1021/jacs.0c05183
33. Ma, N.; Guo, L.; Qi, D.; Gao, F.; Yang, C.; Xia, W. *Org. Lett.* **2021,** *23,* 6278–6282. doi:10.1021/acs.orglett.1c02071
34. Zhang, B.; Qi, J.-Q.; Liu, Y.; Li, Z.; Wang, J. *Org. Lett.* **2022,** *24,* 279–283. doi:10.1021/acs.orglett.1c03941
35. Su, Y.-L.; Liu, G.-X.; De Angelis, L.; He, R.; Al-Sayyed, A.; Schanze, K. S.; Hu, W.-H.; Qiu, H.; Doyle, M. P. *ACS Catal.* **2022,** *12,* 1357–1363. doi:10.1021/acscatal.1c05611
36. Gao, Y.; Zheng, Z.; Zhu, Y.; Xu, W.; Zhou, Y.; Yu, C.; Jiang, X. *Green Chem.* **2023,** *25,* 3909–3915. doi:10.1039/d3gc00643c
37. Liu, G.-X.; Liang, H.-C.; Fu, X.; Tang, J.; Hu, W.-H.; Qiu, H. *Org. Lett.* **2022,** *24,* 4908–4913. doi:10.1021/acs.orglett.2c01751
38. Ma, M.; Hao, W.; Ma, L.; Zheng, Y.; Lian, P.; Wan, X. *Org. Lett.* **2018,** *20,* 5799–5802. doi:10.1021/acs.orglett.8b02487
39. Zhao, P.; Wang, L.; Guo, X.; Chen, J.; Liu, Y.; Wang, L.; Ma, Y. *Org. Lett.* **2023,** *25,* 3314–3318. doi:10.1021/acs.orglett.3c01145
40. Wang, X.; Tong, W.-Y.; Huang, B.; Cao, S.; Li, Y.; Jiao, J.; Huang, H.; Yi, Q.; Qu, S.; Wang, X. *J. Am. Chem. Soc.* **2022,** *144,* 4952–4965. doi:10.1021/jacs.1c12874
41. Shou, J.-Y.; Qing, F.-L. *Angew. Chem., Int. Ed.* **2022,** *61,* e202208860. doi:10.1002/anie.202208860
42. Liu, G.-X.; Jie, X.-T.; Li, X.-l.; Yang, L.-S.; Qiu, H.; Hu, W.-H. *ACS Catal.* **2023,** *13,* 5307–5314. doi:10.1021/acscatal.3c00619
43. Sharma, S.; Singh, J.; Sharma, A. *Adv. Synth. Catal.* **2021,** *363,* 3146–3169. doi:10.1002/adsc.202100205
44. Wiles, R. J.; Molander, G. A. *Isr. J. Chem.* **2020,** *60,* 281–293. doi:10.1002/ijch.201900166
45. Lang, S. B.; O'Nele, K. M.; Douglas, J. T.; Tunge, J. A. *Chem. – Eur. J.* **2015,** *21,* 18589–18593. doi:10.1002/chem.201503644
46. Lang, S. B.; O'Nele, K. M.; Tunge, J. A. *J. Am. Chem. Soc.* **2014,** *136,* 13606–13609. doi:10.1021/ja508317j
47. Cheung, K. P. S.; Kurandina, D.; Yata, T.; Gevorgyan, V. *J. Am. Chem. Soc.* **2020,** *142,* 9932–9937. doi:10.1021/jacs.0c03993
48. Huang, H.-M.; Bellotti, P.; Pflüger, P. M.; Schwarz, J. L.; Heidrich, B.; Glorius, F. *J. Am. Chem. Soc.* **2020,** *142,* 10173–10183. doi:10.1021/jacs.0c03239
49. Huang, H.-M.; Koy, M.; Serrano, E.; Pflüger, P. M.; Schwarz, J. L.; Glorius, F. *Nat. Catal.* **2020,** *3,* 393–400. doi:10.1038/s41929-020-0434-0
50. Huang, H.-M.; Bellotti, P.; Kim, S.; Zhang, X.; Glorius, F. *Nat. Synth.* **2022,** *1,* 464–474. doi:10.1038/s44160-022-00085-6
51. See the mechanistic experiment (5) in Supporting Information File 1 for more details.
52. Zhang, Z.; Kvasovs, N.; Dubrovina, A.; Gevorgyan, V. *Angew. Chem., Int. Ed.* **2022,** *61,* e202110924. doi:10.1002/anie.202110924
53. Fors, B. P.; Krattiger, P.; Strieter, E.; Buchwald, S. L. *Org. Lett.* **2008,** *10,* 3505–3508. doi:10.1021/ol801285g
54. Trost, B. M.; Strege, P. E. *J. Am. Chem. Soc.* **1975,** *97,* 2534–2535. doi:10.1021/ja00842a036
55. Trost, B. M.; Van Vranken, D. L. *Chem. Rev.* **1996,** *96,* 395–422. doi:10.1021/cr9409804
56. Trost, B. M.; Crawley, M. L. *Chem. Rev.* **2003,** *103,* 2921–2944. doi:10.1021/cr020027w
57. Kazmaier, U.; Stolz, D.; Krämer, K.; Zumpe, F. L. *Chem. – Eur. J.* **2008,** *14,* 1322–1329. doi:10.1002/chem.200701332
58. Kurandina, D.; Parasram, M.; Gevorgyan, V. *Angew. Chem., Int. Ed.* **2017,** *56,* 14212–14216. doi:10.1002/anie.201706554
59. Mayer, J. M. *J. Phys. Chem. Lett.* **2011,** *2,* 1481–1489. doi:10.1021/jz200021y
60. Mayer, J. M. *Acc. Chem. Res.* **2011,** *44,* 36–46. doi:10.1021/ar100093z
61. Gentry, E. C.; Knowles, R. R. *Acc. Chem. Res.* **2016,** *49,* 1546–1556. doi:10.1021/acs.accounts.6b00272
62. Miller, D. C.; Tarantino, K. T.; Knowles, R. R. *Top. Curr. Chem.* **2016,** *374,* 30. doi:10.1007/s41061-016-0030-6

License and Terms

This is an open access article licensed under the terms of the Beilstein-Institut Open Access License Agreement (https://www.beilstein-journals.org/bjoc/terms), which is identical to the Creative Commons Attribution 4.0 International License (https://creativecommons.org/licenses/by/4.0). The reuse of material under this license requires that the author(s), source and license are credited. Third-party material in this article could be subject to other licenses (typically indicated in the credit line), and in this case, users are required to obtain permission from the license holder to reuse the material.

The definitive version of this article is the electronic one which can be found at:
https://doi.org/10.3762/bjoc.20.59

BEILSTEIN JOURNAL OF ORGANIC CHEMISTRY

Synthesis and properties of 6-alkynyl-5-aryluracils

Ruben Manuel Figueira de Abreu[1], Till Brockmann[1], Alexander Villinger[1], Peter Ehlers[1] and Peter Langer[*1,2,§]

Full Research Paper

Open Access

Address:
[1]Universität Rostock, Institut für Chemie, A.-Einstein-Str.3a, 18059 Rostock, Germany and [2]Leibniz Institut für Katalyse an der Universität Rostock, A.-Einstein-Str.29a, 18059 Rostock, Germany

Email:
Peter Langer[*] - peter.langer@uni-rostock.de

* Corresponding author
§ Tel.: +49 381 498 6410, Fax: +49 381 498 6412

Keywords:
catalysis; cross-coupling; fluorescence; heterocycles; regioselectivity

Beilstein J. Org. Chem. **2024,** *20,* 898–911.
https://doi.org/10.3762/bjoc.20.80

Received: 25 January 2024
Accepted: 09 April 2024
Published: 22 April 2024

This article is part of the thematic issue "Multicomponent reactions IV".

Associate Editor: T. J. J. Müller

© 2024 de Abreu et al.; licensee Beilstein-Institut.
License and terms: see end of document.

Abstract

The development of a new and straightforward chemoselective method for the synthesis of uracil-based structures by combining Suzuki–Miyaura and Sonogashira–Hagihara cross-coupling is reported. The methodology was applied to synthesize a series of novel compounds. The tolerance of the combination of different functional groups was tested. The influence of different functional groups on the physical properties was studied by ultraviolet–visible (UV–vis) and fluorescence spectroscopy, providing new insights into the potential applications of uracil-based structures.

Introduction

Organic life is a complex interplay of many different building blocks. One of these building blocks is uracil. Discovered for the first time in 1901 by Alberto Ascoli, it is now known to be one of the four nucleobases of RNA [1]. It therefore plays a very important role in many vital biological processes in the human body and other life forms. Uracil is rarely found in DNA, due to its lower stability and mutagenic properties when mismatched with guanine [2-5]. This fact can be used to differentiate between RNA and DNA-dependent targets, making uracil very interesting for medical applications. The first modification of uracil was already synthesized in 1906 [6]. However, the medical potential of uracil was not discovered until 40 years later. One of the first antibacterial studies was carried out in 1945. The first anticarcinogenic studies followed in 1953 [7,8]. Since then, uracil has played an important role in the development of antiviral and anticarcinogenic agents against various targets [9-16].

5-Fluorouracil is one of the best-known anticancer drugs and is used to treat a variety of cancers, including pancreatic, breast, and cervical cancers. Zidovudine is effective against retroviruses and is still used today for the prevention and treatment of HIV/AIDS infections. Brivudine is one of the most potent antiviral agents against herpes zoster virus infections (Figure 1) [17-20].

Given the proven medical potential of uracil, further investigation was carried out to fully utilize the synthetic possibilities

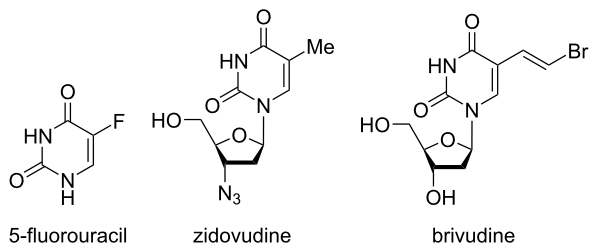

Figure 1: Uracil derivatives in drugs.

uracil has to offer and to synthesize new drugs against existing or hitherto unknown targets. Moreover, studies have even shown that a sugar moiety is not always required to act against a targeted enzyme [21-23]. One of these focus areas was the synthesis of alkyne-linked derivatives. The first alkyne-linked compound was already published in 1976, accompanied by new synthesis methods in the following years [24-27]. With the discovery of potential antiviral properties and other synthetic opportunities, alkyne-linked derivatives remained an integral part of research to the present day [28-35]. However, the main methods known so far are to substitute uracil either only at position 6 or at position 5 [26-28,34-47]. The remaining known methods use only both positions to induce cyclization [25,31-33,48-56]. Therefore, to the best of our knowledge, there are no known methods that allow the selective reaction of both positions of uracil (Figure 2).

In this work, we report a new chemoselective method for the synthesis of a series of hitherto unknown uracil-based compounds by combining Suzuki–Miyaura and Sonogashira–Hagihara cross-coupling [60,61]. The method is designed to be flexible and could also be used to synthesize other structural motifs. Applications and tolerance to a wide range of functional groups have been tested. Furthermore, their physical properties were analyzed by ultraviolet–visible and fluorescence spectroscopy.

Results and Discussion

Synthesis

The synthetic strategy for the desired compounds is based on a four-step sequence starting with commercially available 6-chloro-1,2-dimethyluracil (**1**), as depicted in Scheme 1. Subsequently, 5-bromo-6-chloro-1,3-dimethyluracil (**2**) was synthesized by brominating the starting material. The single Sonogashira–Hagihara cross-coupling afforded **3a**–**j** and, by a two-fold approach, **4a**–**h** could be obtained. Compounds **3a**–**j** were subsequently transformed to **5a**–**t** by Suzuki–Miyaura cross-coupling.

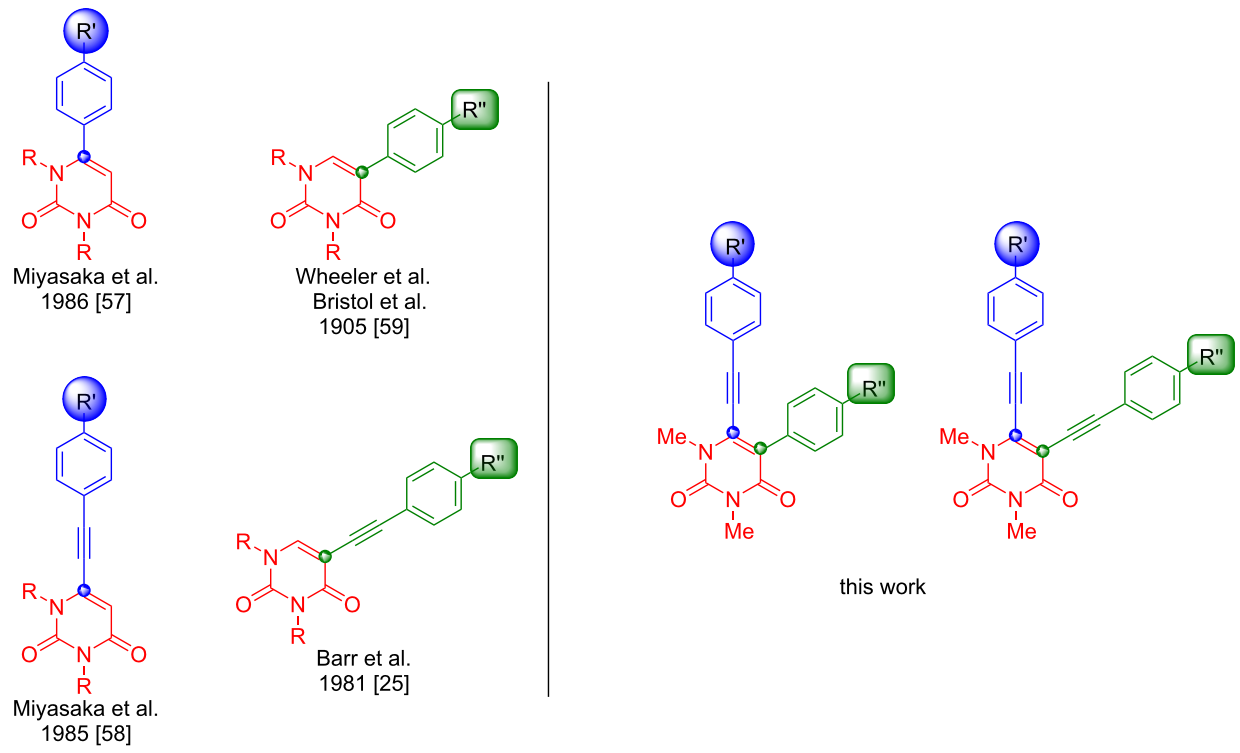

Figure 2: Present work as compared to previous studies [25,57-59].

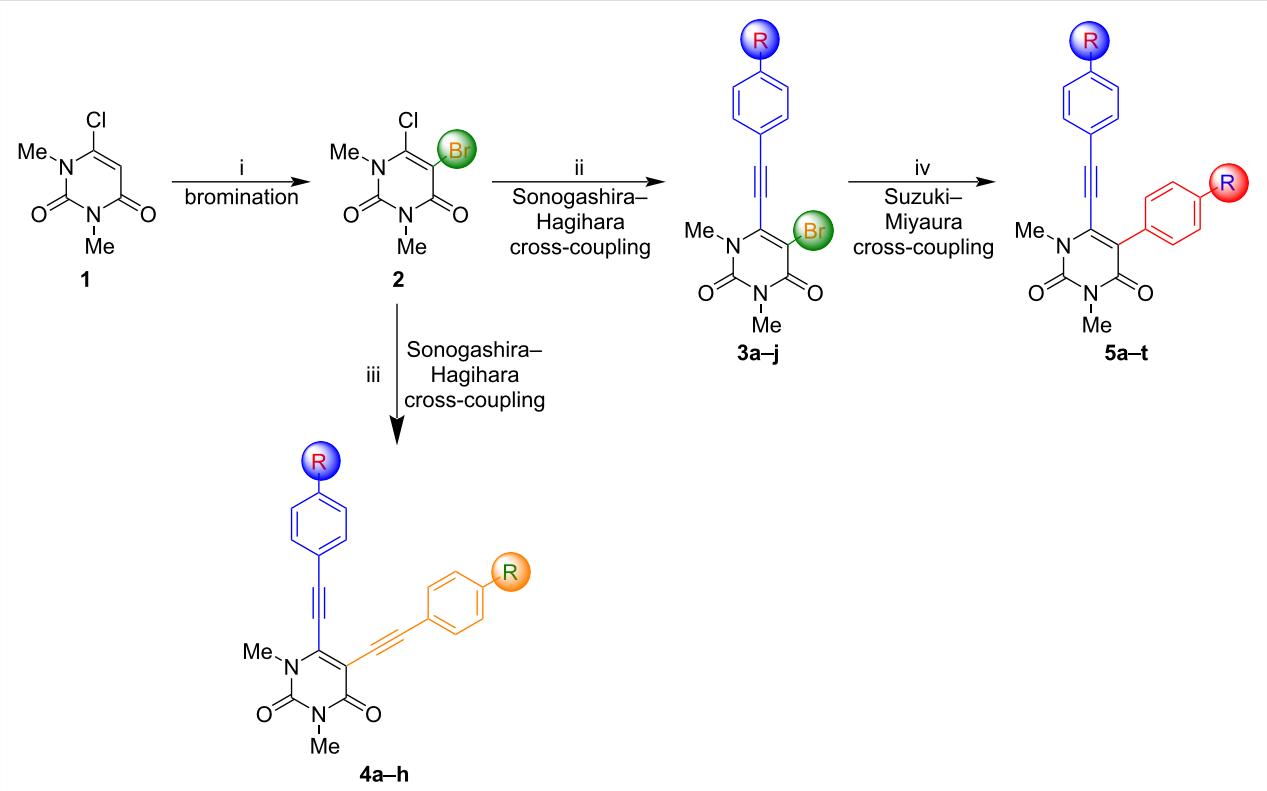

Scheme 1: Synthesis of 1,3-dimethly-5-[2-(aryl)ethynyl]-6-[2-(aryl)ethynyl]uracils **4** and 1,3-dimethyl-5-aryl-6-[2-(aryl)ethynyl]uracils **5**. Conditions: i) Br_2 (1.0 equiv), Ac_2O (1.5 equiv), AcOH, 25 °C, 1 h [62]; ii) $Pd(PPh_3)Cl_2$ (5 mol %), CuI (5 mol %), NEt_3 (10 equiv), DMSO, 25 °C, 6 h; iii) $Pd(CH_3CN)_2Cl_2$ (5 mol %), CuI (5 mol %), NEt_3 (10 equiv), 1,4-dioxane, 100 °C, 6 h; iv) $Pd(PPh_3)_4$ (10 mol %), NaOH (3 equiv), 1,4-dioxane/water 5:1, 100 °C, 1 h.

The bromination of **1** was performed by using Br_2 (1 equiv), Ac_2O (1.5 equiv), AcOH (25 °C, 1 h) and yielded the desired product in 52% [62]. With the starting material in hand, initial Sonogashira–Hagihara cross-coupling was carried out using $Pd(PPh_3)_4$ as catalyst with K_3PO_4 as base in toluene as solvent which gave a mixture of different products. Further investigation revealed the presence of the two-fold Sonogashira–Hagihara product, starting material **2**, and the desired product **3**. Hence, starting material **2** and product **3** show similar reactivity under the employed reaction conditions. Therefore, the reaction had to be optimized to overcome this competition and to achieve a higher yield and selectivity for the desired product (Supporting Information File 1, Table S1). Finally, the transformation was realized by using $Pd(PPh_3)Cl_2$ (5 mol %), CuI (5 mol %), NEt_3 (10 equiv), DMSO, at 25 °C for 6 h as reaction conditions with excellent yield and selectivity. With the optimized conditions in hand, the next step was to investigate the scope and afford **3a**–**j**. The corresponding results are depicted in Scheme 2.

The scope resulted in the synthesis of products **3a**–**j** with very good to good yields and was performed with a high tolerance towards different functional groups, allowing for a wide range of applications. However, lower yields were observed when a strong electron-withdrawing or pushing group was used. This effect can be observed for **3e**, **3f** and **3i**. Furthermore, the separation of these products has proven to be more challenging than other compounds with higher yields. In the reaction with 3-pyridylacetylene no product **3g** could be obtained. The reaction at 50 °C was found to be chemoselective, giving only the 6-substituted product. This behavior has also been observed in previous studies [63]. It was expected that there would be a low chemoselectivity, due to the availability of two halogenated positions in the starting material. However, the 5-substituted product was not observed. At higher temperatures, only the double-substituted product could be found. No reaction was observed when the reaction temperature was lowered to 0 °C. This could be due to the double activation of the 5-position, despite the fact that bromine is a better leaving group than chlorine. Both positions might be influenced by the functional groups adjacent to them, due to withdrawing effects. Chlorine has a stronger electron-withdrawing effect than bromine, so the electrophilic character of the 6-position should be higher than that of the 5-position. However, it is unlikely to be the only reason for the formation of just one intermediate. A second effect appears to play a more important role and could be related to the structure of the

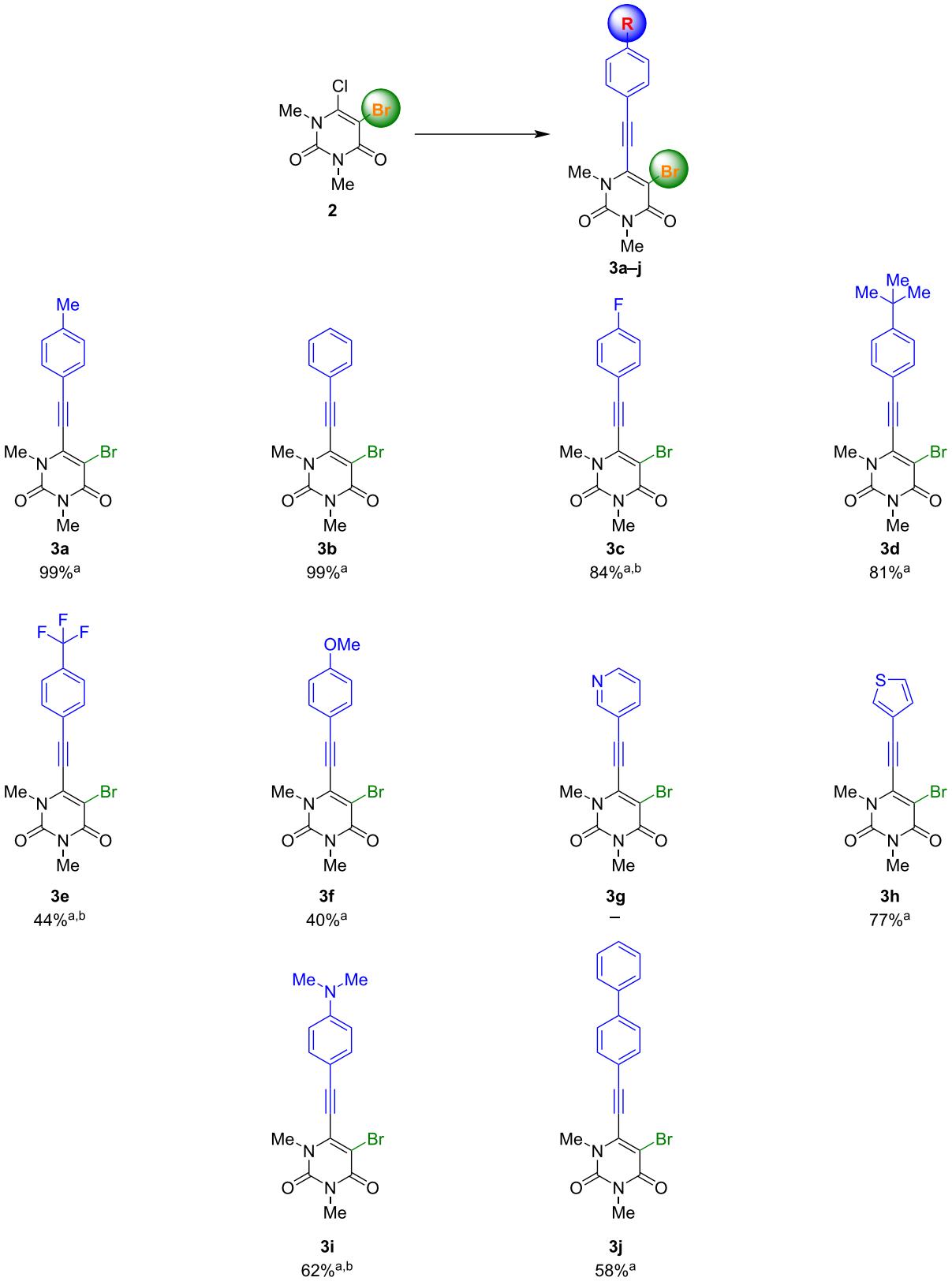

Scheme 2: Synthesis of 5-bromo-1,3-dimethyl-6-[2-(aryl)ethynyl]uracils **3a–j**. Reaction conditions: **2** (1.0 equiv), arylacetylene (1.2 equiv), $Pd(PPh_3)Cl_2$ (5 mol %), CuI (5 mol %), NEt_3 (10 equiv), DMSO, 25 °C, 6 h. [a]Yields of isolated products. [b]Reaction temperature: 50 °C.

starting material. The 6-position is part of an enamine and an α,β-unsaturated carbonyl structure, as depicted in Scheme 3. According to the mesomeric structure of the enamine, the 6-position could be activated, and the 5-position deactivated for the nucleophilic attack that occurs during the oxidative addition of the metal catalyst. This may explain the formation of only the 6-substituted product during the Sonogashira reaction.

As mentioned above, new reaction conditions had to be chosen to synthesize the desired product **4** and to avoid a mixture. A different catalyst and a higher temperature were chosen to obtain the desired products in higher yields. With the optimized conditions in hand ($Pd(CH_3CN)_2Cl_2$ (5 mol %), CuI (5 mol %), NEt_3 (10 equiv), dioxane, 100 °C, 6 h), the scope was investigated next and allowed for the synthesis of compounds **4a**–**h** (Scheme 4).

The formation of compounds **4a**–**h** was achieved over two steps with very good to good yields and a high tolerance towards different functional groups was observed. Similarly to the monoalkynylated products, lower yields were obtained with stronger electron-withdrawing groups, as can be seen in case of product **4d**. The yield of **4b** was comparatively lower, which may be due to the higher steric hindrance of the used arylacetylene. Product **4f** could not be synthesized, due to decomposition during the reaction.

Furthermore, no precursor could be isolated. This could be due to instabilities caused by two strong electron-withdrawing groups. As a prove of concept, a sequential reaction set-up was used to realize the formation of product **4h** containing differentially functionalized arylalkynes.

Subsequently, the formation of the desired product **5** was carried out by application of the Suzuki–Miyaura cross-coupling. The optimization was carried out with **3a** as the model compound (Table 1).

The starting material **3a** is a sterically hindered system in which the bromine is only partially accessible, due to the large residue. This could be the reason for the low yield of the first approach. Replacing the catalyst and increasing the temperature or the amount of boronic acid proved to be unsuccessful. With entry 6 (Table 1) it was shown that similar yields could be obtained by removing the ligand and using higher amounts of catalyst. Therefore, no additional ligand was used in the next attempts.

Additionally, it was observed that by replacing the less polar solvent by a mixture of a more polar solvent and water in a 5:1 ratio, yields could be significantly improved. Therefore, sodium hydroxide was used as the water-soluble base, which also proved to be beneficial to the yield. Finally, by monitoring the reaction time, it was discovered that reducing the reaction time to 1 h further improved the yield to 62%. Finally, using the optimized conditions (Table 1, entry13), the scope was carried out and afforded the desired products **5a**–**t** (Scheme 5).

The products **5a**–**t** were obtained in 95 to 25% yields, with an average yield of 56%. Furthermore, the method was shown to be highly tolerant towards different functional groups and their combinations. A higher yield tended to be observed when a donor group was located on the arylalkyne at the 6-position (**5k**, **5l, 5r**). However, this effect seems to be neutralized when using an electron-rich arylboronic acid (**5m**). Lower yields are obtained when an acceptor group is present on the arylalkyne (**5p**, **5q**). This leads to the suggestion that an electron-donor group activates and an electron-withdrawing group deactivates the compound for the subsequent Suzuki reaction. Furthermore, lower yields were generally observed when a strong electron-donor or -acceptor was attached to the phenyl group at position 5. Higher yields could be obtained by reducing the steric hindrance at position 5 by introducing a 5-membered ring instead of a benzene moiety. This was demonstrated by the introduction of thiophene (**5r**) and furan (**5t**) to the uracil structure. The molecules **5n** and **5o** could not be obtained, due to decomposition during the reaction.

The structure of **5a** was confirmed by X-ray crystallographic analysis. Crystals were obtained by slow evaporation of the solvent from a mixture of the compound in dichloromethane and heptane at room temperature (Figure 3).

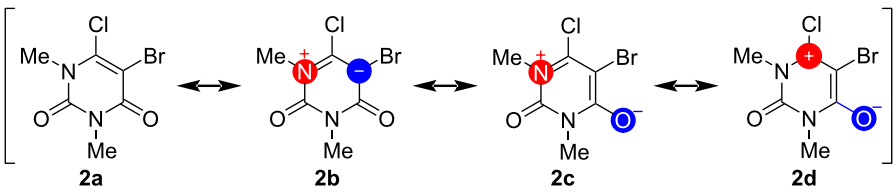

Scheme 3: Structure of the starting material **2** with its possible mesomeric structures.

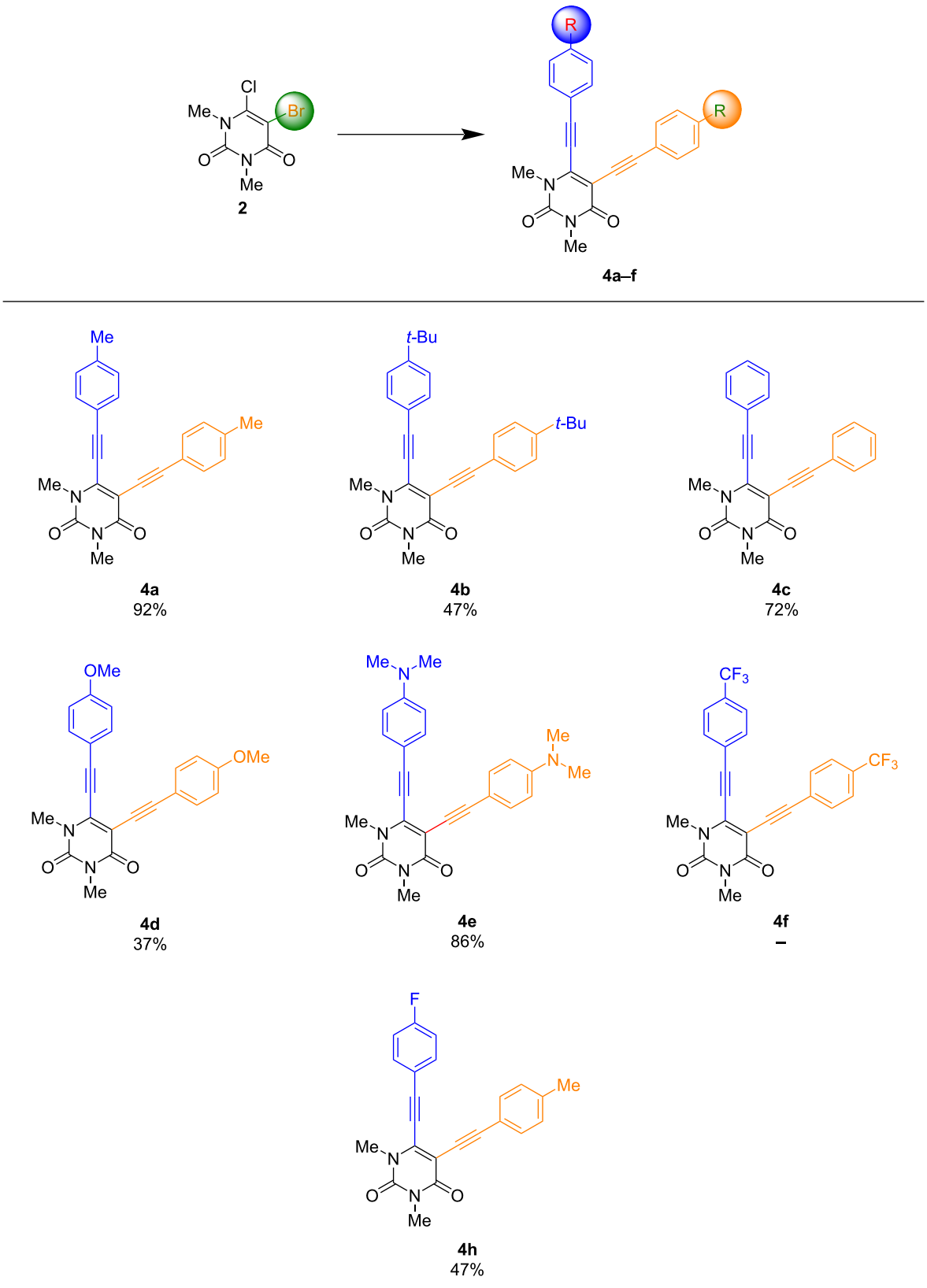

Scheme 4: Synthesis of 1,3-dimethyl-5-[2-(aryl)ethynyl]-6-[2-(aryl)ethynyl]uracils **4a–h**. Reaction conditions: **2** (1 equiv), arylacetylene (2.2 equiv), $Pd(CH_3CN)_2Cl_2$ (5 mol %), CuI (5 mol %), NEt_3 (10 equiv), dioxane, 100 °C, 6 h. Yields of isolated products.

Table 1: Optimization of the reaction conditions for the synthesis of **5a**.

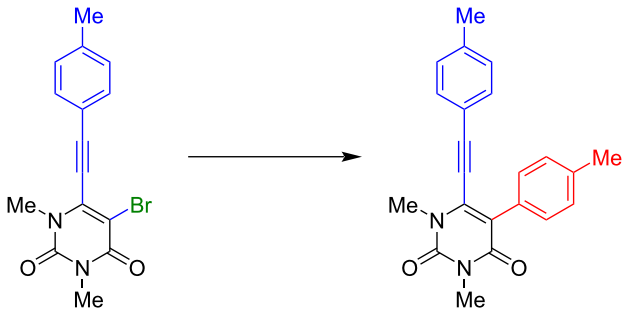

Entry	Boronic acid (equiv)	Cat. (mol %)	Ligand (mol %)	Base (equiv)	Solvent (mixture)	Temp (°C)	Time (h)	Yield (%)
1	1.2	$Pd(CH_3CN)_2Cl_2$ (5)	SPhos (10)	Na_2CO_3 (3)	toluene	100	16	27
2	1.2	$Pd(CH_3CN)_2Cl_2$ (5)	SPhos (10)	Na_2CO_3 (3)	DMA	150	16	–
3	2.5	$Pd(CH_3CN)_2Cl_2$ (5)	SPhos (10)	Na_2CO_3 (3)	toluene	100	16	34
4	1.2	$Pd(PPh_3)_2Cl_2$ (5)	SPhos (10)	Na_2CO_3 (3)	toluene	100	16	–
5	1.2	$Pd(PPh_3)_4$ (5)	SPhos (10)	Na_2CO_3 (3)	toluene	100	16	31
6	1.2	$Pd(PPh_3)_4$ (10)	–	Na_2CO_3 (3)	toluene	100	16	27
7	1.2	$Pd(PPh_3)_4$ (10)	–	K_3PO_4 (3)	toluene	100	16	24
8	1.2	$Pd(PPh_3)_4$ (10)	–	KO*t*-Bu (3)	toluene	100	16	–
9	1.2	$Pd(PPh_3)_4$ (10)	–	KO*t*-Bu (3)	dioxane	100	16	–
10	1.2	$Pd(PPh_3)_4$ (10)	–	NaOH (3)	dioxane	100	16	44
11	1.2	$Pd(PPh_3)_4$ (10)	–	NaOH (3)	dioxane/water 5:1	100	16	55
12	1.2	$Pd(PPh_3)_4$ (10)	–	NaOH (3)	dioxane/water 5:1	100	6	53
13	1.2	$Pd(PPh_3)_4$ (10)	–	NaOH (3)	dioxane/water 5:1	100	1	62

Crystal structure analysis revealed that **5a** crystallizes in a base-centered monoclinic system with the *P*21/*c* space group. The structure is mostly planar, except for the 5-phenyl group, which is twisted out of the plane with a dihedral angle of φ = 70.3°. Furthermore, it could be observed that the 6-[2-(phenyl)ethynyl] group is slightly curved, due to the dihedral angle of the alkyne group (174.5 ° and 176.7 °).

Analysis of the lattice structure of **5a** revealed that the distance between the molecules within the unit cell is higher than the distance between the unit cells. In addition, the molecules are arranged parallel-displaced to each other, which is considered to be more stable than the sandwich arrangement [64-68]. Consequently, the distance between the layers varies periodically between 3.373 Å and 3.662 Å. This results in different interactions between the layers, as depicted in Figure 3. Furthermore, the layers are arranged in an anti-parallel face-to-face order to reduce the steric hindrance. Within the shorter distance layers (3.373 Å), π–π interactions between the alkyne groups can be observed. Moreover, the alkyne phenyl group interacts mainly with molecules between different layers in the vertical direction, while the phenyl group interacts vertically and horizontally with different molecules.

The two-fold Suzuki reaction was also investigated, but no desired product could be obtained. In fact, starting material **2** appears to be too unreactive to undergo a Suzuki reaction. Reversing the reaction steps gave the desired intermediate 5-bromo-6-phenyl-1,3-dimehtyluracil, which turned out to be unstable. This could be the reason why the desired product could not be synthesized at the first attempt. Therefore, the synthesis of the desired product from starting material **2** appears to be unlikely. It is reasonable to assume that this finding is due to the instability of the intermediate formed, as the desired product has been synthesized by other methods and the single Suzuki reaction on uracil is well studied [42,69-71].

Physical properties

The photophysical properties of selected derivatives were investigated by steady-state absorption and photoluminescence spectroscopy. The influence of the substitution pattern on the photophysical properties is displayed in Figure 4. Corresponding photophysical data and quantum yields are described in Table 2.

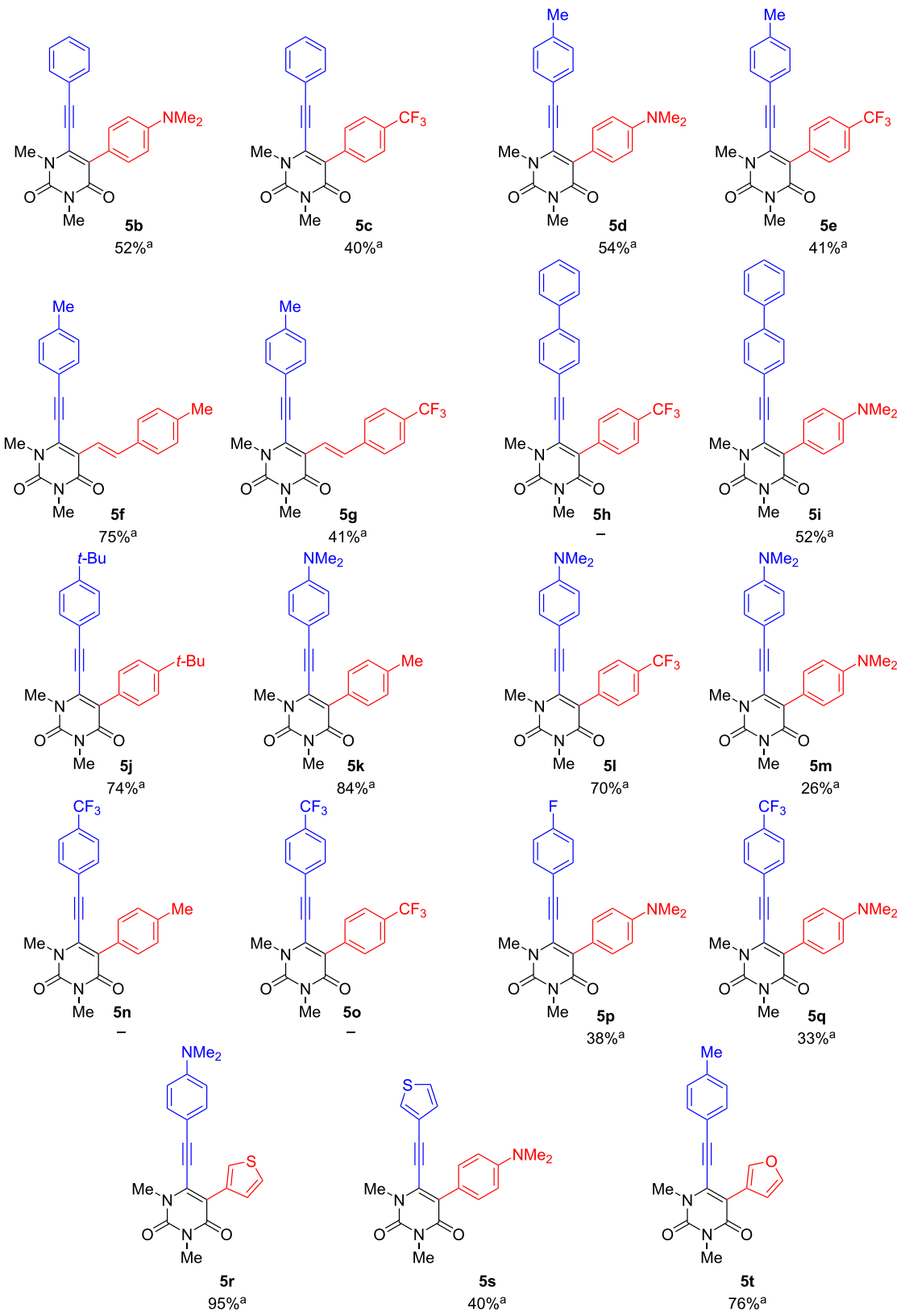

Scheme 5: Synthesis of 1,3-dimethyl-5-aryl-6-[2-(aryl)ethynyl]uracils **5a–t**. Reaction conditions: **3** (1 equiv), boronic acid (1.2 equiv), $Pd(PPh_3)_4$ (5 mol %), NaOH (3 equiv), dioxane/water 5:1, 100 °C, 1 h. [a]Yields of isolated products.

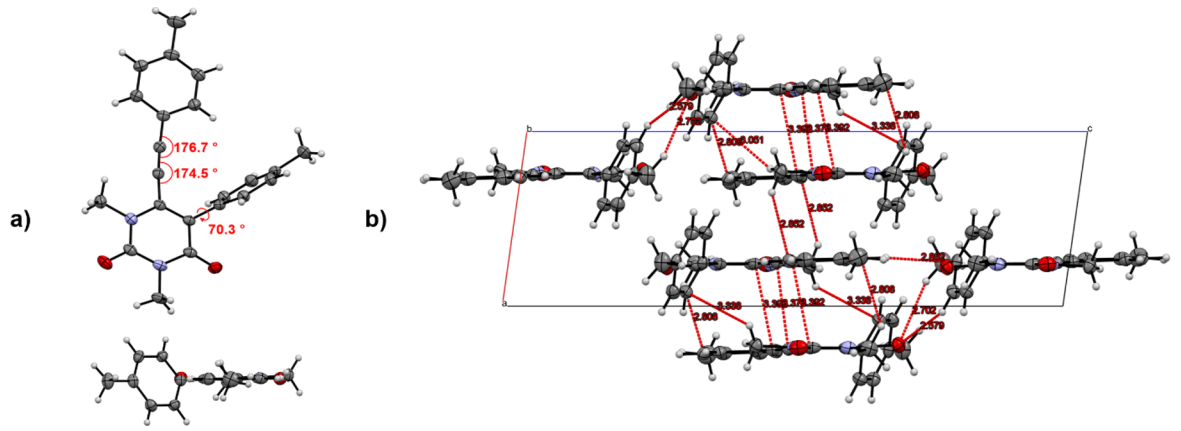

Figure 3: ORTEP diagram of **5a** front view (a) and side view (b). a) Interactions of the molecules within and between a layer with two molecules at the top and the bottom of the unit cell. b) Determined from X-ray structural analysis at 123 K. Element color: carbon (grey), hydrogen (white), oxygen (red) and nitrogen (blue). The thermal ellipsoids are drawn at the 50% probability level.

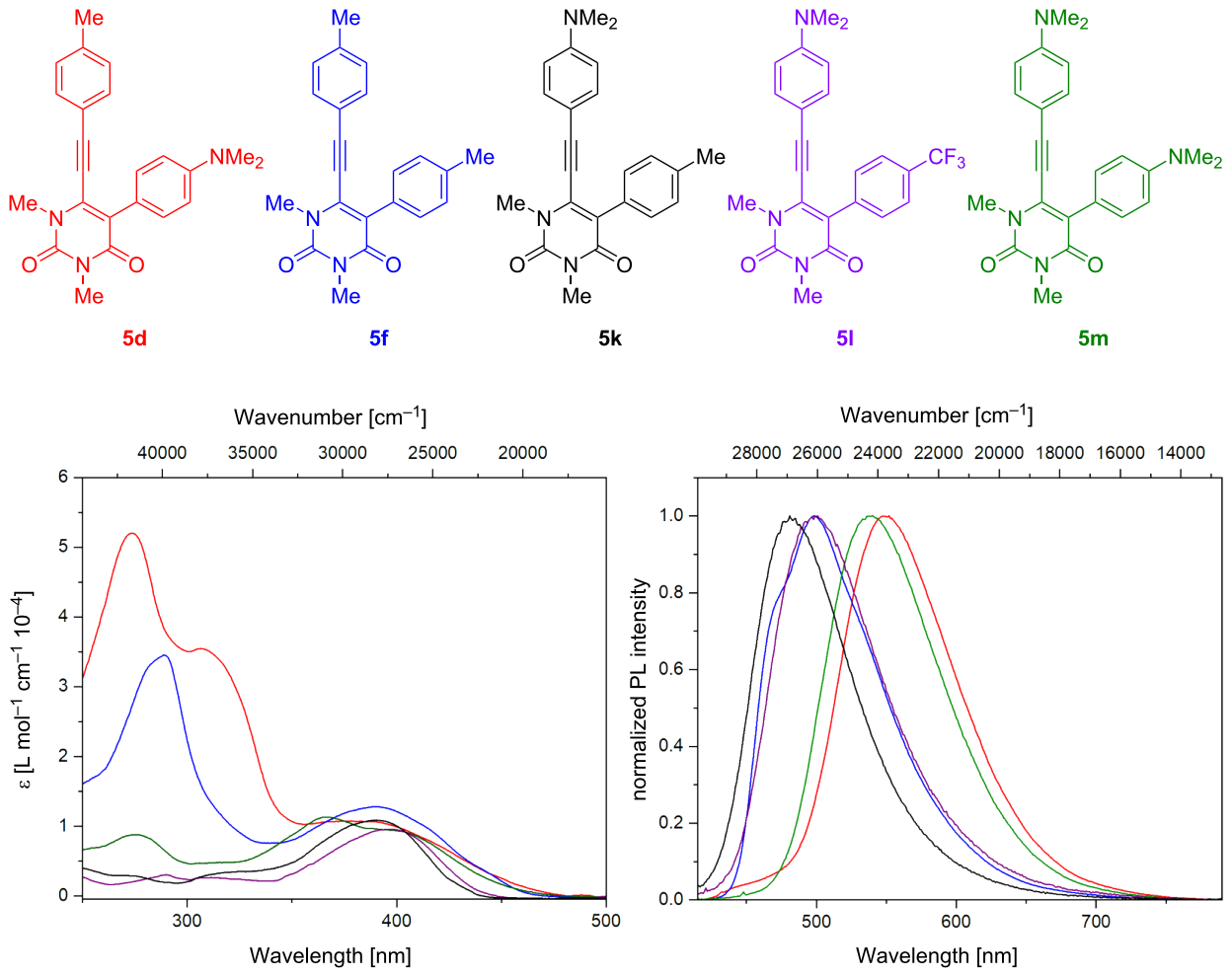

Figure 4: UV–vis absorption (left) and emission (right, λ_{ex} = 400 nm) spectra of 1,3-dimethyl-5-phenyl-6-[2-(phenyl)ethynyl]uracil derivatives **5d**, **5f**, **5k**, **5l**, and **5m** in dichloromethane (c = 1·10^{-5} M).

Table 2: Photophysical data of selected 1,3-dimethyl-5-phenyl-6-[2-(phenyl)ethynyl]uracil derivatives **5d**, **5f**, **5k**, **5l**, and **5m** in dichloromethane (c = 1·10^{-5} M) at 20 °C.

	5d	5f	5k	5l	5m
$\lambda_{1,abs}$ (nm)	273	289	324	289	274
$\varepsilon_{\lambda1}$ (M^{-1} cm^{-1})	52015	35001	3470	3008	8766
$\lambda_{2,abs}$ (nm)	306	389	390	396	368
$\varepsilon_{\lambda2}$ (M^{-1} cm^{-1})	35462	13267	10846	9548	11283
$\lambda_{3,abs}$ (nm)	387				402
$\varepsilon_{\lambda3}$ (M^{-1} cm^{-1})	10644				9259
$\lambda_{1,em}^{400}$ (nm)	548	473[a]	480	498	537
$\lambda_{2,em}^{400}$ (nm)		497			
$\Phi^{b,c}$	13%	23%	2%	9%	

[a]Shoulder in the spectrum. [b]For the excitation wavelength λ_{ex} = 400 nm. [c]Fluorescence standards: coumarin153 in ethanol (Φ = 0.38) [72,73].

The analysis of the absorption spectra revealed that the spectra can be divided into a short-wave and long-wave region. In the long wavelength region (350–500 nm) all measured compounds show a very similar absorption band, indicating that the first transition state ($S_0 \rightarrow S_1$) does not seem to be affected by the substitution pattern. Furthermore, all compounds show broadened absorption bands and no major differences in the first absorption band were observed. The greatest difference was observed in the short wavelength region (250–350 nm). Interestingly, compounds with a π-donor group on the 5-phenyl group were found to have the highest absorption intensity (**5d**, **5f**, and **5m**) in the short wavelength region. Particularly noteworthy is compound **5d**, where the highest intensity could be observed with an absorption band at 273 nm and a shoulder at 306 nm. The second highest peak was observed for **5f**, followed by **5m**. Only one broadened peak was observed in both cases.

The influence of the substitution pattern could be revealed by comparing the two regioisomers **5d** and **5k**. As a result, the overall absorption intensity in the short-wavelength region was drastically reduced. This leads to the assumption that this absorption band is highly influenced by the dimethylamino group on the 5-phenyl group, even though the phenyl ring is twisted out of the plane. Interaction between the two π-systems is rather unlikely due to the twisted position of the phenyl ring. It is therefore reasonable to assume that this behavior is more likely to be related to a possible interaction of the dimethylamino group with the rest of the system.

However, the combination of two dimethylamino groups appears to have the opposite effect, as **5m** demonstrates. Although it was expected that this would result in a higher absorption intensity, a drastic reduction in the intensity was observed. The extinction coefficient of **5m** (8766 M^{-1} cm^{-1}) was rather low compared to **5d**. Furthermore, the substitution of a π-donor group by a π-acceptor group led to a reduction of the absorption intensity until it almost disappeared. This behavior can be observed in the spectra of **5l**. As the spectra of **5k** and **5l** indicate, the spectral influence of a *p*-substituted alkyne-linked phenyl group appears to be negligible. However, this negligible influence could also be explained by the distance between the functional group and the core system.

Compound **5f** is extended by a double bond between the uracil entity and the phenyl group. In addition, it is not influenced by groups other than methyl. Interestingly, it has the second-highest overall absorption intensity after **5d** and a similar absorption peak can be observed. The similarity could be due to the double bond and its ability to interact with the system as a π-donor group. Consequently, the double bond could similarly influence the system as the dimethylamino group. As already discussed for **5d**, this again reinforces the assumption that this phenomenon could be caused by a π-donor at 5-position, regardless of its structure. Further investigation is required, but if confirmed, this could be used to create specific desired absorption behaviors.

Subsequently, the emission spectra were investigated. As explained in the previous section, a similar behavior was observed in the emission spectra with respect to the substitution pattern. In general, a bathochromic shift of the emission was observed in the presence of a dimethylamino group at the 5-position. The bathochromic shift of **5d** compared to its regioisomer **5k** is 68 nm. This underlines the spectral effect of the π-donor on the 5- or 6-position and the dependence of the distance between the functional group and the uracil core system.

In the spectra of **5m**, a combination of both situations can be observed. The bathochromic shift of **5m** is 57 nm and lies between the two emission peaks of **5d** and **5k**. Therefore, it can be concluded that combining the two substitution patterns leads to this intermediate behavior. Substitution of the 5-π-donor with a π-acceptor group reduced the bathochromic shift from 57 nm to

18 nm, which may indicate that the influence of the π-acceptor group is higher than that of a methyl group, but much weaker than that of a π-donor group (**5l**). Similar findings were also observed in the absorption behavior.

In the emission spectra of **5f**, no significant difference regarding the shift could be observed, despite the presence of the π-donor group at the same position. However, a shoulder on the emission peak was observed, which may indicate the influence of the double bond.

Finally, the quantum yields of all compounds were determined and compared. Compound **5f** afforded the highest quantum yield with 23% and **5k** the lowest with 2%. The second highest quantum yield was obtained with **5d** closely followed by **5m**. With regard to the previously discussed data, this could also be due to the influence of a π-donor group directly connected to the core system. This again shows the influence of the substitution pattern on the phenyl groups and that the properties can be modulated by the choice of substituents.

Conclusion

In summary, we have developed a new, straightforward method for the synthesis of a series of new and hitherto unknown uracil derivatives. Different structural motifs could be obtained based on the same starting material. Furthermore, we could demonstrate a high tolerance towards different functional groups and their combinations. The physical properties of selected derivatives were investigated by steady-state absorption and photoluminescence spectroscopy. The corresponding data gives first insights into the optical properties. It was observed that the photophysical properties could be partially modulated by the chosen substituents.

Experimental

General information

Nuclear magnetic resonance spectra ($^{1}H/^{13}C/^{19}F$ NMR) were recorded on a Bruker AVANCE 300 III, 250II, or 500. The analyzed chemical shifts δ are referenced to the residual solvent signals of the deuterated solvents $CDCl_3$ (δ = 7.26 ppm/77.16 ppm). Multiplicities due to spin–spin correlation are reported as follows: s = singlet, d = doublet, dd = double doublet, m = multiplet; they are further described by their coupling constants *J*. Infrared spectra (IR) were measured as attenuated total reflection (ATR) experiments using a Nicolet 380 FT-IR spectrometer. The signals were characterized by their wavenumbers and corresponding absorption as very strong (vs), strong (s), medium (m), weak (w) or very weak (vw). UV–vis spectra were recorded on a Cary 60 UV–vis spectrophotometer and emission spectra were recorded on an Agilent Cary Eclipse fluorescence spectrophotometer. Basic and high-resolution mass spectra (MS/HRMS) were measured on instruments coupled to a preceding gas chromatograph (GC) or liquid chromatograph (LC). Samples were ionized by electron impact ionization (EI) on an Agilent 6890/5973 or Agilent 7890/5977 GC–MS equipped with a HP-5 capillary column using helium carrier gas or by electron spray ionization (ESI) on an Agilent 1200/6210 time-of-flight (TOF) LC–MS. X-ray single-crystal structure analysis was performed on a Bruker Apex Kappa-II CCD diffractometer. The solvents used, dimethyl sulfoxide and 1,4-dioxane, were purchased as dry solvents and applied without further purification. Other reagents, catalysts, ligands, acids, and bases were used as purchased from commercial suppliers. Column chromatography was performed on Merck Silica gel 60 (particle size 63–200 μm). Solvents for extraction and column chromatography were distilled prior employment.

Representative method for the preparation of starting materials

5-Bromo-6-chloro-1,3-dimethyluracil (2). Uracil **1** (22.9 mmol; 4.00 g) was dissolved in glacial acetic acid (60 mL) and after 5 min acetic anhydride (3 mL) was added. The reaction mixture was stirred for 10 min. Then, bromine (1 equiv; 23.4 mmol; 1.2 mL) was slowly added dropwise. After 1 hour, the reaction was stopped by adding water (25 mL) and cooling to 4 °C for 30 minutes. The precipitate was then filtered and dried.

Representative procedure A for the synthesis of 3a–j. A mixture of **2** (1.99 mmol; 0.504 mg), $Pd(PPh_3)Cl_2$ (5 mol %; 98.3 μmol; 6.9 mg), CuI (5 mol %; 98.7 μmol; 18.8 mg) was dissolved in DMSO (5 mL) and stirred for 5 min under an argon atmosphere. NEt_3 (11 equiv; 21.5 mmol; 3 mL) was added and the emulsion was stirred for 10 min at room temperature. The corresponding arylacetylene (*p*-tolylacetylene, 2.20 mmol, 0.28 mL) was slowly added dropwise to the reaction mixture and stirred for 6 hours at room temperature. The reaction was monitored by TLC until the reaction was complete. The reaction was neutralized with an HCl solution (1 M) and diluted with water (40 mL). The phases were separated, and the aqueous layer was extracted with dichloromethane (3 × 30 mL). The combined organic layers were dried over Na_2SO_4, concentrated under reduced pressure, and purified by column chromatography (heptane/ethyl acetate).

Representative procedure B for the synthesis of 4a–j. A mixture of **2** (402 μmol; 102 mg), $Pd(CH_3CN)_2Cl_2$ (5 mol %; 23 μmol; 6 mg), CuI (5 mol %; 21 μmol; 4 mg) was dissolved in 1,4-dioxane (5 mL) and stirred for 5 min under an argon atmosphere. NEt_3 (11 equiv; 4.30 mmol; 0.6 mL) was added and the reaction mixture was heated to 100 °C. The corresponding arylacetylene (*p*-tolylacetylene, 2.2 equiv; 946 μmol; 0.12 mL)

was slowly added dropwise to the reaction mixture and stirred for 6 hours at 100 °C. The reaction was monitored by TLC until the reaction was complete. The reaction was neutralized with an HCl solution (1 M) and diluted with water (40 mL). The phases were separated, and the aqueous layer was extracted with dichloromethane (3 × 30 mL). The combined organic layers were dried over Na_2SO_4, concentrated under reduced pressure, and purified by column chromatography (heptane/ethyl acetate).

Representative procedure C for the synthesis of 4h. A mixture of **2** (400 µmol; 100 mg), $Pd(CH_3CN)_2Cl_2$ (5 mol %; 23 µmol; 6 mg), CuI (5 mol %; 21 µmol; 4 mg) was dissolved in 1,4-dioxane (5 mL) and stirred for 5 min under an argon atmosphere. NEt_3 (11 equiv; 4.30 mmol; 0.6 mL) was added and the reaction mixture was heated to 50 °C. The corresponding arylacetylene (*p*-tolylacetylene, 1.1 equiv; 473 µmol; 0.06 mL) was slowly added dropwise to the reaction mixture and stirred for 6 hours at 50 °C. After 6 hours, the second corresponding arylacetylene (4-fluorophenylacetylene, 1.1 equiv; 460 µmol; 0.06 mL) was slowly added dropwise to the reaction mixture and heated at 100 °C. The reaction was stirred at 100 °C for a further 6 h. The reaction was monitored by TLC until the reaction was complete. The reaction was neutralized with an HCl solution (1 M) and diluted with water (40 mL). The phases were separated, and the aqueous layer was extracted with dichloromethane (3 × 30 mL). The combined organic layers were dried over Na_2SO_4, concentrated under reduced pressure, and purified by column chromatography (heptane/ethyl acetate).

Representative procedure D for the synthesis of 5a–t. A mixture of **3a** (303 µmol; 109 mg), $Pd(PPh_3)_4$ (10 mol %; 369 µmol; 5 mg), NaOH (3.0 equiv; 933 µmol; 37 mg) and the corresponding boronic acid (4-tolylboronic acid, 1.2 equiv; 369 µmol; 5 mg) was dissolved in a mixture of 1,4-dioxane and water 5:1. The reaction mixture was heated to 100 °C and stirred for 1 hour. The reaction was monitored by TLC until the reaction was complete. The reaction was neutralized with an HCl solution (1 M) and diluted with water (40 mL). The phases were separated, and the aqueous layer was extracted with dichloromethane (3 × 30 mL). The combined organic layers were dried over Na_2SO_4, concentrated under reduced pressure, and purified by column chromatography (heptane/ethyl acetate).

Supporting Information

Supporting Information File 1

Experimental data and copies of spectra.
[https://www.beilstein-journals.org/bjoc/content/supplementary/1860-5397-20-80-S1.pdf]

Acknowledgements

We are grateful for the technical and analytical support of the University of Rostock (Germany).

Funding

We are grateful for the financial support of the State of Mecklenburg-Western Pomerania (Germany).

Conflict of Interest

There are no conflicts or financial interests to declare.

Author Contributions

Ruben Manuel Figueira de Abreu: data curation; formal analysis; investigation; validation; visualization; writing – original draft. Till Brockmann: investigation. Alexander Villinger: data curation; investigation; methodology; visualization. Peter Ehlers: conceptualization; data curation; methodology; supervision; validation; writing – original draft; writing – review & editing. Peter Langer: conceptualization; funding acquisition; methodology; project administration; resources; supervision; visualization; writing – review & editing.

ORCID® iDs

Alexander Villinger - https://orcid.org/0000-0002-0868-9987
Peter Ehlers - https://orcid.org/0000-0001-6444-7563

Data Availability Statement

All data that supports the findings of this study is available in the published article and/or the supporting information to this article.

References

1. Ascoli., A. *Hoppe-Seyler's Z. Physiol. Chem.* **1901,** *31,* 161–214. doi:10.1515/bchm2.1901.31.1-2.161
2. Visnes, T.; Doseth, B.; Pettersen, H. S.; Hagen, L.; Sousa, M. M. L.; Akbari, M.; Otterlei, M.; Kavli, B.; Slupphaug, G.; Krokan, H. E. *Philos. Trans. R. Soc., B* **2009,** *364,* 563–568. doi:10.1098/rstb.2008.0186
3. Krokan, H. E.; Drabløs, F.; Slupphaug, G. *Oncogene* **2002,** *21,* 8935–8948. doi:10.1038/sj.onc.1205996
4. Krokan, H. E.; Standal, R.; Slupphaug, G. *Biochem. J.* **1997,** *325,* 1–16. doi:10.1042/bj3250001
5. Nilsen, H.; Otterlei, M.; Haug, T.; Solum, K.; Nagelhus, T. A.; Skorpen, F.; Krokan, H. E. *Nucleic Acids Res.* **1997,** *25,* 750–755. doi:10.1093/nar/25.4.750
6. Johnson, T. B.; Johns, C. O. *J. Biol. Chem.* **1906,** *1,* 305–320. doi:10.1016/s0021-9258(17)46068-6
7. Hitchings, G. H.; Falco, E. A.; Sherwood, M. B. *Science* **1945,** *102,* 251–252. doi:10.1126/science.102.2645.251
8. Prusoff, W. H.; Holmes, W. L.; Welch, A. D. *Cancer Res.* **1953,** *13,* 221–225.

9. Fischl, M. A.; Richman, D. D.; Grieco, M. H.; Gottlieb, M. S.; Volberding, P. A.; Laskin, O. L.; Leedom, J. M.; Groopman, J. E.; Mildvan, D.; Schooley, R. T.; Jackson, G. G.; Durack, D. T.; King, D.; The AZT Collaborative Working Group. *N. Engl. J. Med.* **1987,** *317,* 185–191. doi:10.1056/nejm198707233170401
10. Horwitz, J. P.; Chua, J.; Noel, M. *J. Org. Chem.* **1964,** *29,* 2076–2078. doi:10.1021/jo01030a546
11. Bergmann, W.; Burke, D. C. *J. Org. Chem.* **1956,** *21,* 226–228. doi:10.1021/jo01108a020
12. Bergmann, W.; Feeney, R. J. *J. Am. Chem. Soc.* **1950,** *72,* 2809–2810. doi:10.1021/ja01162a543
13. Prusoff, W. H. *Biochim. Biophys. Acta* **1959,** *32,* 295–296. doi:10.1016/0006-3002(59)90597-9
14. Ramesh, D.; Vijayakumar, B. G.; Kannan, T. *Eur. J. Med. Chem.* **2020,** *207,* 112801. doi:10.1016/j.ejmech.2020.112801
15. Geisman, A. N.; Valuev-Elliston, V. T.; Ozerov, A. A.; Khandazhinskaya, A. L.; Chizhov, A. O.; Kochetkov, S. N.; Pannecouque, C.; Naesens, L.; Seley-Radtke, K. L.; Novikov, M. S. *Bioorg. Med. Chem.* **2016,** *24,* 2476–2485. doi:10.1016/j.bmc.2016.04.010
16. Tănase, C. I.; Drăghici, C.; Cojocaru, A.; Galochkina, A. V.; Orshanskaya, J. R.; Zarubaev, V. V.; Shova, S.; Enache, C.; Maganu, M. *Bioorg. Med. Chem.* **2015,** *23,* 6346–6354. doi:10.1016/j.bmc.2015.08.033
17. Sneader, W. *Drug Discovery: A History;* John Wiley & Sons: Chichester, UK, 2005. doi:10.1002/0470015535
18. de Clercq, E. *Adv. Virus Res.* **2009,** *73,* 1–53. doi:10.1016/s0065-3527(09)73001-5
19. de Clercq, E. *Acta Pharm. Sin. B* **2012,** *2,* 535–548. doi:10.1016/j.apsb.2012.10.001
20. Sidwell, R. W.; Allen, L. B.; Huffman, J. H.; Witkowski, J. T.; Cook, P. T.; Tolman, R. L.; Revankar, G. R.; Simon, L. N.; Robins, R. K. The Potential of Nucleosides as Antiviral Agents. *Parasites, Fungi, and Viruses;* Springer: New York, NY, USA, 1976; Vol. 6, pp 279–294. doi:10.1007/978-1-4684-3129-2_41
21. Schaeffer, H. J.; Gurwara, S.; Vince, R.; Bittner, S. *J. Med. Chem.* **1971,** *14,* 367–369. doi:10.1021/jm00286a024
22. Elion, G. B.; Furman, P. A.; Fyfe, J. A.; de Miranda, P.; Beauchamp, L.; Schaeffer, H. J. *Proc. Natl. Acad. Sci. U. S. A.* **1977,** *74,* 5716–5720. doi:10.1073/pnas.74.12.5716
23. Schaeffer, H. J.; Beauchamp, L.; de Miranda, P.; Elion, G. B.; Bauer, D. J.; Collins, P. *Nature* **1978,** *272,* 583–585. doi:10.1038/272583a0
24. Hirota, K.; Kitade, Y.; Isobe, Y.; Maki, Y. *Heterocycles* **1987,** *26,* 355–358. doi:10.3987/r-1987-02-0355
25. Robins, M. J.; Barr, P. J. *Tetrahedron Lett.* **1981,** *22,* 421–424. doi:10.1016/0040-4039(81)80115-3
26. Perman, J.; Sharma, R. A.; Bobek, M. *Tetrahedron Lett.* **1976,** *17,* 2427–2430. doi:10.1016/0040-4039(76)90010-1
27. Farina, V.; Hauck, S. I. *Synlett* **1991,** 157–159. doi:10.1055/s-1991-20661
28. Rahim, S. G.; Trivedi, N.; Bogunovic-Batchelor, M. V.; Hardy, G. W.; Mills, G.; Selway, J. W. T.; Snowden, W.; Littler, E.; Coe, P. L.; Basnak, I.; Whale, R. F.; Walker, R. T. *J. Med. Chem.* **1996,** *39,* 789–795. doi:10.1021/jm950029r
29. Neitz, H.; Bessi, I.; Kuper, J.; Kisker, C.; Höbartner, C. *J. Am. Chem. Soc.* **2023,** *145,* 9428–9433. doi:10.1021/jacs.3c01611
30. Brenske, K.-O.; Emondts, M.; Hörnig, S. T.; Panitz, S.; Pieper, M. I.; Ligori, A.; Schacht, A.; Henkel, J.; Klankermayer, J.; Herrmann, A. *Angew. Chem., Int. Ed.* **2023,** *62,* e202300531. doi:10.1002/anie.202300531
31. Kraljević, T. G.; Bistrović, A.; Dedić, M.; Pavelić, S. K.; Sedić, M.; Raić-Malić, S. *Tetrahedron Lett.* **2012,** *53,* 5144–5147. doi:10.1016/j.tetlet.2012.07.068
32. Srivastav, N. C.; Rai, D.; Tse, C.; Agrawal, B.; Kunimoto, D. Y.; Kumar, R. *J. Med. Chem.* **2010,** *53,* 6180–6187. doi:10.1021/jm100568q
33. Hudson, R. H. E.; Moszynski, J. M. *Synlett* **2006,** 2997–3000. doi:10.1055/s-2006-948176
34. Platonova, Y. B.; Volov, A. N.; Tomilova, L. G. *Bioorg. Med. Chem. Lett.* **2020,** *30,* 127351. doi:10.1016/j.bmcl.2020.127351
35. Stevenson, T. M.; Crouse, B. A.; Thieu, T. V.; Gebreysus, C.; Finkelstein, B. L.; Sethuraman, M. R.; Dubas-Cordery, C. M.; Piotrowski, D. L. *J. Heterocycl. Chem.* **2005,** *42,* 427–435. doi:10.1002/jhet.5570420310
36. Roh, K. R.; Kim, J. Y.; Kim, Y. H. *Tetrahedron Lett.* **1999,** *40,* 1903–1906. doi:10.1016/s0040-4039(98)02491-5
37. De Clercq, E.; Desgranges, C.; Herdewijn, P.; Sim, I. S.; Jones, A. S.; McLean, M. J.; Walker, R. T. *J. Med. Chem.* **1986,** *29,* 213–217. doi:10.1021/jm00152a008
38. De Clercq, E.; Descamps, J.; De Somer, P.; Barr, P. J.; Jones, A. S.; Walker, R. T. *Proc. Natl. Acad. Sci. U. S. A.* **1979,** *76,* 2947–2951. doi:10.1073/pnas.76.6.2947
39. Lin, T. S.; Guo, J. Y.; Schinazi, R. F.; Chu, C. K.; Xiang, J. N.; Prusoff, W. H. *J. Med. Chem.* **1988,** *31,* 336–340. doi:10.1021/jm00397a011
40. Hudson, R. H. E.; Li, G.; Tse, J. *Tetrahedron Lett.* **2002,** *43,* 1381–1386. doi:10.1016/s0040-4039(02)00024-2
41. Sharma, R. A.; Bobek, M. *J. Org. Chem.* **1975,** *40,* 2377–2379. doi:10.1021/jo00904a025
42. Shih, Y.-C.; Chien, T.-C. *Tetrahedron* **2011,** *67,* 3915–3923. doi:10.1016/j.tet.2011.03.051
43. Fang, W.-P.; Cheng, Y.-T.; Cheng, Y.-R.; Cherng, Y.-J. *Tetrahedron* **2005,** *61,* 3107–3113. doi:10.1016/j.tet.2005.01.085
44. Cho, Y.-M.; Johnson, F. *Tetrahedron Lett.* **1994,** *35,* 1149–1152. doi:10.1016/0040-4039(94)88009-3
45. Tanaka, H.; Hayakawa, H.; Shibata, S.; Haraguchi, K.; Miyasaka, T.; Hirota, K. *Nucleosides Nucleotides* **1992,** *11,* 319–328. doi:10.1080/07328319208021706
46. Palmisano, G.; Santagostino, M. *Tetrahedron* **1993,** *49,* 2533–2542. doi:10.1016/s0040-4020(01)86332-8
47. Nencka, R.; Sinnaeve, D.; Karalic, I.; Martins, J. C.; Van Calenbergh, S. *Org. Biomol. Chem.* **2010,** *8,* 5234–5246. doi:10.1039/c0ob00061b
48. Youssefyeh, R. D.; Weisz, M. *Tetrahedron Lett.* **1973,** *14,* 4317–4318. doi:10.1016/s0040-4039(01)87209-9
49. Senda, S.; Hirota, K.; Takahasi, M. *J. Chem. Soc., Perkin Trans. 1* **1975,** 503–507. doi:10.1039/p19750000503
50. Majumdar, K. C.; Sinha, B.; Maji, P. K.; Chattopadhyay, S. K. *Tetrahedron* **2009,** *65,* 2751–2756. doi:10.1016/j.tet.2009.01.107
51. Dudkin, S.; Iaroshenko, V. O.; Sosnovskikh, V. Y.; Tolmachev, A. A.; Villinger, A.; Langer, P. *Org. Biomol. Chem.* **2013,** *11,* 5351–5361. doi:10.1039/c3ob26837c
52. Petricci, E.; Radi, M.; Corelli, F.; Botta, M. *Tetrahedron Lett.* **2003,** *44,* 9181–9184. doi:10.1016/j.tetlet.2003.10.028

53. Sun, G.; Fecko, C. J.; Nicewonger, R. B.; Webb, W. W.; Begley, T. P. *Org. Lett.* **2006,** *8,* 681–683. doi:10.1021/ol052876m
54. Van Tinh, D.; Fischer, M.; Stadlbauer, W. *J. Heterocycl. Chem.* **1996,** *33,* 905–910. doi:10.1002/jhet.5570330358
55. Nishigaki, S.; Sato, J.; Shimizu, K.; Furukawa, K.; Senga, K.; Yoneda, F. *Chem. Pharm. Bull.* **1980,** *28,* 142–149. doi:10.1248/cpb.28.142
56. Sako, M.; Ichioka, T.; Totani, R.; Hirota, K. *J. Org. Chem.* **1995,** *60,* 8115–8116. doi:10.1021/jo00129a068
57. Satoh, K.; Tanaka, H.; Andoh, A.; Miyasaka, T. *Nucleosides Nucleotides* **1986,** *5,* 461–469. doi:10.1080/07328318608068688
58. Tanaka, H.; Haraguchi, K.; Koizumi, Y.; Fukui, M.; Miyasaka, T. *Can. J. Chem.* **1986,** *64,* 1560–1563. doi:10.1139/v86-257
59. Wheeler, H. L.; Bristol, H. S. *Am. Chem. J.* **1905,** *33,* 437–447.
60. Sonogashira, K.; Tohda, Y.; Hagihara, N. *Tetrahedron Lett.* **1975,** *16,* 4467–4470. doi:10.1016/s0040-4039(00)91094-3
61. Miyaura, N.; Yamada, K.; Suzuki, A. *Tetrahedron Lett.* **1979,** *20,* 3437–3440. doi:10.1016/s0040-4039(01)95429-2
62. Pfleiderer, W.; Deiss, H. *Isr. J. Chem.* **1968,** *6,* 603–614. doi:10.1002/ijch.196800078
63. Nencka, R.; Votruba, I.; Hřebabecký, H.; Tloušťová, E.; Horská, K.; Masojídková, M.; Holý, A. *Bioorg. Med. Chem. Lett.* **2006,** *16,* 1335–1337. doi:10.1016/j.bmcl.2005.11.050
64. Sinnokrot, M. O.; Valeev, E. F.; Sherrill, C. D. *J. Am. Chem. Soc.* **2002,** *124,* 10887–10893. doi:10.1021/ja025896h
65. Pitoňák, M.; Neogrády, P.; Rezáč, J.; Jurečka, P.; Urban, M.; Hobza, P. *J. Chem. Theory Comput.* **2008,** *4,* 1829–1834. doi:10.1021/ct800229h
66. Park, Y. C.; Lee, J. S. *J. Phys. Chem. A* **2006,** *110,* 5091–5095. doi:10.1021/jp0582888
67. Lutz, P. B.; Bayse, C. A. *Phys. Chem. Chem. Phys.* **2013,** *15,* 9397–9406. doi:10.1039/c3cp51077h
68. Špirko, V.; Engkvist, O.; Soldán, P.; Selzle, H. L.; Schlag, E. W.; Hobza, P. *J. Chem. Phys.* **1999,** *111,* 572–582. doi:10.1063/1.479338
69. Capuano, L.; Fischer, W.; Scheidt, H.; Schneider, M. *Chem. Ber.* **1978,** *111,* 2497–2509. doi:10.1002/cber.19781110704
70. Youssefyeh, R. D.; Lichtenberg, L. *J. Chem. Soc., Perkin Trans. 1* **1974,** 2649–2654. doi:10.1039/p19740002649
71. Cheng, C.; Shih, Y.-C.; Chen, H.-T.; Chien, T.-C. *Tetrahedron* **2013,** *69,* 1387–1396. doi:10.1016/j.tet.2012.11.001
72. Jones, G., II; Jackson, W. R.; Choi, C. Y.; Bergmark, W. R. *J. Phys. Chem.* **1985,** *89,* 294–300. doi:10.1021/j100248a024
73. Meech, S. R.; Phillips, D. *J. Photochem.* **1983,** *23,* 193–217. doi:10.1016/0047-2670(83)80061-6

License and Terms

This is an open access article licensed under the terms of the Beilstein-Institut Open Access License Agreement (https://www.beilstein-journals.org/bjoc/terms), which is identical to the Creative Commons Attribution 4.0 International License (https://creativecommons.org/licenses/by/4.0). The reuse of material under this license requires that the author(s), source and license are credited. Third-party material in this article could be subject to other licenses (typically indicated in the credit line), and in this case, users are required to obtain permission from the license holder to reuse the material.

The definitive version of this article is the electronic one which can be found at:
https://doi.org/10.3762/bjoc.20.80

BEILSTEIN JOURNAL OF ORGANIC CHEMISTRY

One-pot Ugi-azide and Heck reactions for the synthesis of heterocyclic systems containing tetrazole and 1,2,3,4-tetrahydroisoquinoline

Jiawei Niu[‡1], Yuhui Wang[‡1], Shenghu Yan[1], Yue Zhang[1], Xiaoming Ma[*1], Qiang Zhang[*2] and Wei Zhang[*3]

Full Research Paper

Open Access

Address:
[1]School of Pharmacy, Changzhou University, 1 Gehu Road, Changzhou 213164, China, [2]School of Chemistry and Life Sciences, Suzhou University of Science and Technology, 99 Xuefu Road, Suzhou 215009, China and [3]Department of Chemistry and Center for Green Chemistry, University of Massachusetts Boston, 100 Morrissey Blvd, Boston, MA 02125, USA

Email:
Xiaoming Ma[*] - mxm.wuxi@cczu.edu.cn; Qiang Zhang[*] - qzhang@mail.usts.edu.cn; Wei Zhang[*] - wei2.zhang@umb.edu

* Corresponding author ‡ Equal contributors

Keywords:
Heck reaction; one-pot; tetrahydroisoquinoline; tetrazolo-pyrazino[2,1-*a*]isoquinolin-6(5*H*)-ones; tetrazole; Ugi-azide reaction

Beilstein J. Org. Chem. **2024,** *20,* 912–920.
https://doi.org/10.3762/bjoc.20.81

Received: 17 January 2024
Accepted: 11 April 2024
Published: 23 April 2024

This article is part of the thematic issue "Multicomponent reactions IV".

Associate Editor: T. J. J. Müller

© 2024 Niu et al.; licensee Beilstein-Institut.
License and terms: see end of document.

Abstract

A new method for the synthesis of heterocyclic systems containing tetrazole and tetrahydroisoquinoline is developed via the performance of one-pot Ugi-azide and Heck cyclization reactions. The integration of the multicomponent and post-condensation reactions in one-pot maximizes the pot-, atom-, and step-economy (PASE).

Introduction

Tetrazole is a privileged heterocycle existing in a range of biological and medicinally interesting compounds [1,2] with antifungal [3,4], antibacterial [5], anticancer [6,7], antiparasitic [8], and antihypertensive properties [9] including FDA approved drugs such as valsartan and cefmetazole [10,11] (Figure 1). The tetrazole ring can also be found in functional materials for photography, imaging, and military applications [12-17]. The hydroisoquinoline core, such as 1,2,3,4-tetrahydroisoquinoline and pyrazino[2,1-*a*]isoquinolinone, is also a privileged heterocycle which can be found in natural products and synthetic compounds with antitumor, anti-HIV, antibiotic, antifungal, antivirus, and anti-inflammatory activities [18-21]. The antischistosomal drug praziquantel (PZQ), a tetrahydroisoquinoline derivative, is a commercialized drug for the treatment of schis-

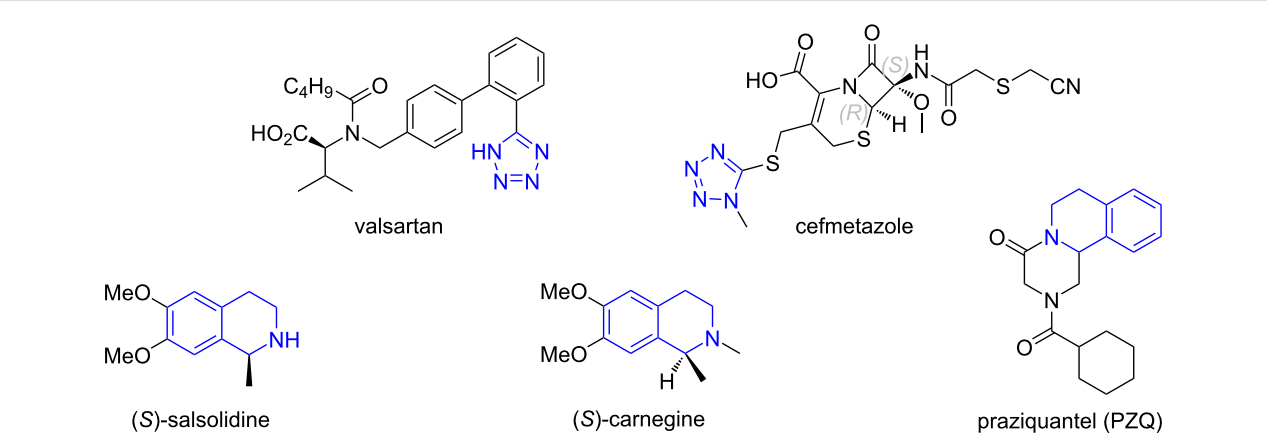

Figure 1: Representative bioactive tetrazole- and tetrahydroisoquinoline-containing compounds.

tosomiasis [22-25]. The combination of the privileged heterocycles tetrazole and tetrahydroisoquinoline in one molecule generates new molecules which could have biological activities.

A standard Ugi four-component reaction (Ugi-4CR) of an aldehyde, amine, isocyanide, and a carboxylic acid produces highly diverse peptidic structures **A** with up to four points of substitution (Scheme 1) [26,27]. By replacing the carboxylic acid with a nucleophilic azide reagent XN_3 (generally $TMSN_3$), the Ugi-azide four-component reaction (UA-4CR) of an aldehyde, amine, isocyanide, and azide gives 1,5-disubstituted 1*H*-tetrazoles (1,5-DS-1*H*-Ts) **B**. The performance of post-condensation reactions of UA-4CR adducts has resulted in various 1,5-DS-1*H*-Ts containing heterocyclic compounds [28-32], such as bis-heterocyclic lactam-tetrazoles [33,34], 2-tetrazolylmethyl-2,3,4,9-tetrahydro-1*H*-β-carbolines [35], ketopiperazinetetrazoles [36], imidazotetrazolodiazepinones [37], tetracyclic tetrazolylpyridoimidazoquinolines [38], bis-heterocyclic 1,5-disubstituted tetrazoleindolizines [39] and (*E*)-12-tetrazolyl-5*H*-quinazolino[3,2-*a*]quinazolines [40]. Among them, the Hulme group reported a UA-4CR/post-condensation sequence to give fused imidazotetrazolodiazepinones (Scheme 2A) [37]. The Gámez-Montaño group introduced a one-pot synthesis of Ugi-azide/*N*-acylation/Diels–Alder/dehydration reactions for isoindolin-1-one and 1,5-DS-T in a linked manner (Scheme 2B) [41]. The Ding group developed sequential Ugi-azide/Ag-catalyzed oxidative cycloisomerization reactions for the synthesis of 2-tetrazolyl-substituted 3-acylpyrroles (Scheme 2C) [42]. The Ding group also reported sequential Ugi-azide/Staudinger/aza-Wittig/addition/Ag-catalyzed cyclization reactions for obtaining 12-tetrazolyl-substituted (*E*)-5*H*-quinazolino[3,2-*a*]quinazolines (Scheme 2D) [40].

There are numbers of Ugi and subsequential Heck (or reductive Heck) reactions that have been developed for the synthesis of poly-heterocyclic compounds [43-51]. Reported in this paper is a one-pot Ugi-azide reaction followed by an intramolecular Heck reaction for the synthesis of tetrazolyl-1,2,3,4-tetrahydroisoquinoline scaffolds **6** and **8** (Scheme 3). The first step is the Ugi-azide reaction of a 2-bromobenzoaldehyde **1**, allylamine hydrochloride (**2**), azidotrimethylsilane ($TMSN_3$, **3**), and an isocyanide **4** affording tetrazoles **5**. If ethyl isocyanoacetate is used as the isocyanide source, the Ugi-azide reaction gives rise to ring-fused tetrazolo[1,5-*a*]pyrazin-6(5*H*)-one adducts **5**. The subsequent Pd-catalyzed intramolecular Heck reaction of compounds **5** or **7** then affords 1,2,3,4-tetrohydroisoquinolines **6** and **8**, respectively.

Results and Discussion

Following the reported procedures [41], the Ugi-azide reaction of 2-bromobenzaldehyde (**1a**, 1 mmol), allylamine hydrochloride (**2**, 1 mmol), trimethylsilyl azide (**3**, 1 mmol) and *tert*-

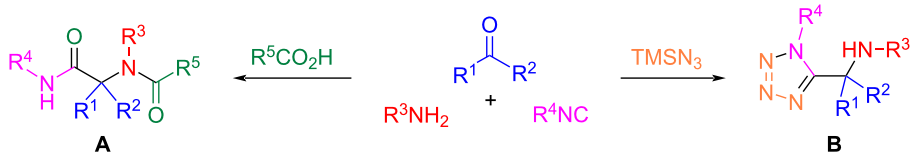

Scheme 1: The Ugi and Ugi-azide reactions.

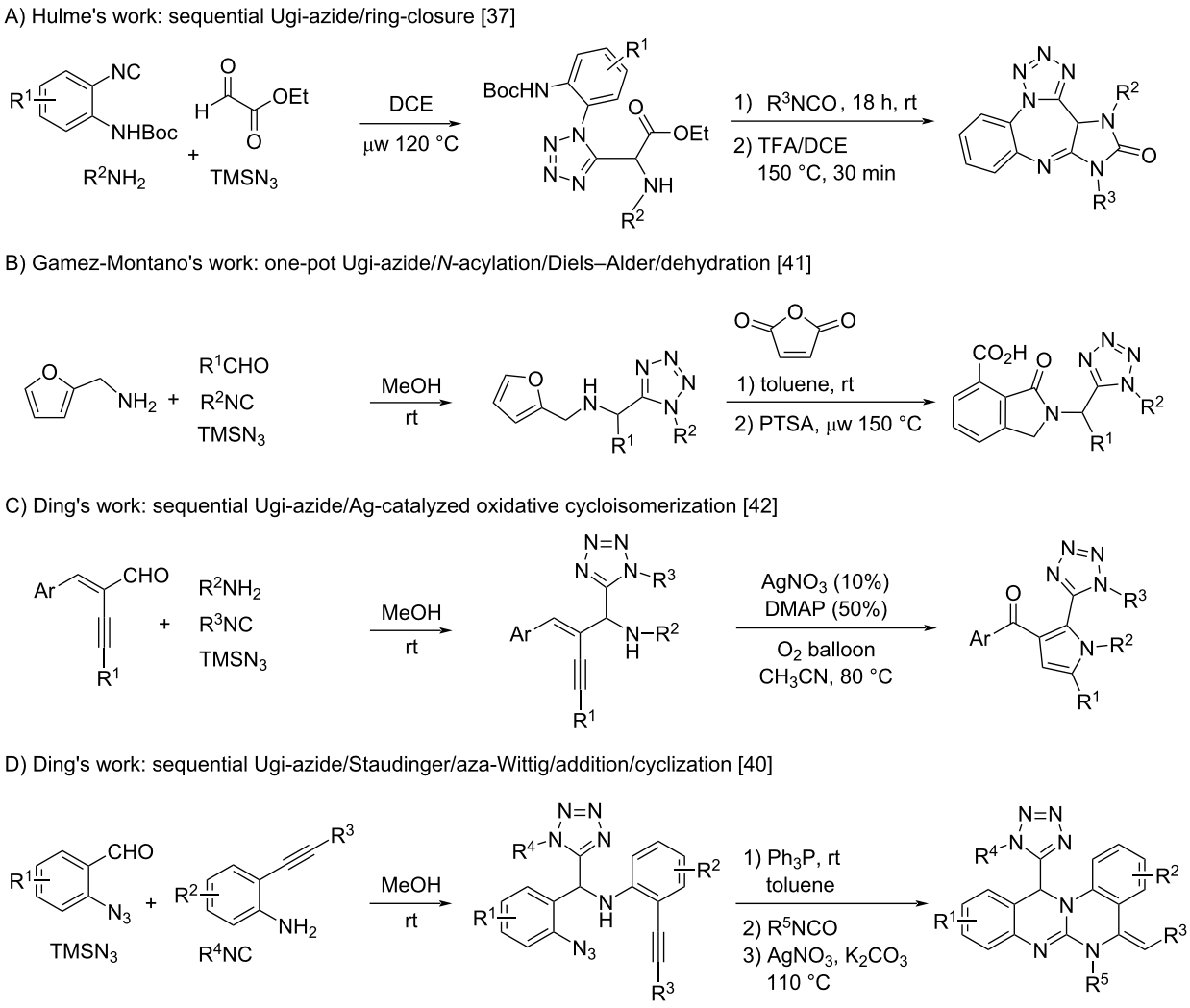

Scheme 2: Ugi-azide and post-condensation reactions for the synthesis of various heterocyclic scaffolds.

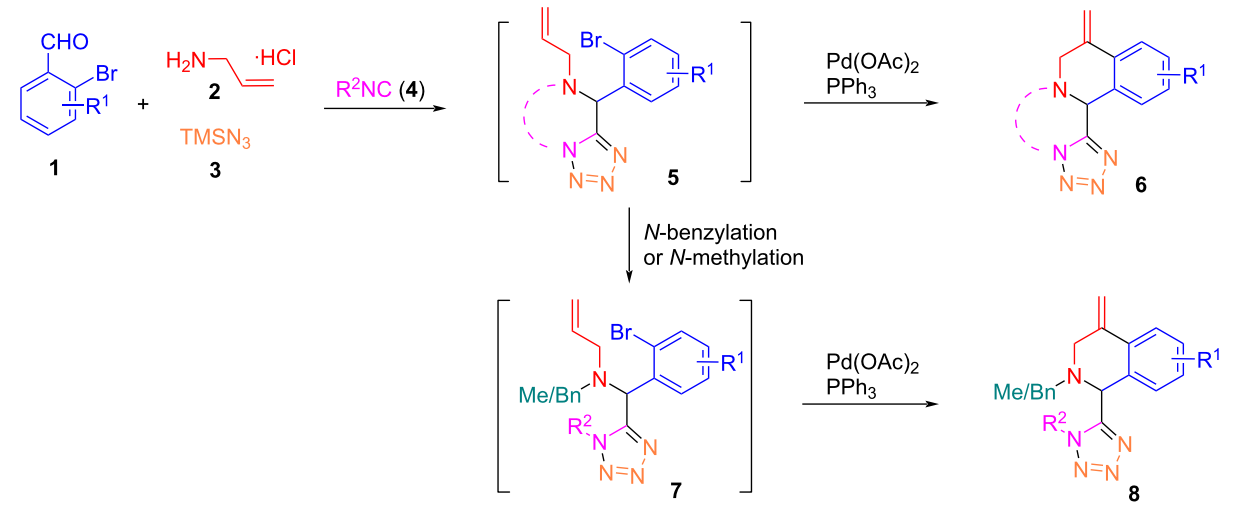

Scheme 3: One-pot synthesis of tetrazolyl-1,2,3,4-tetrahydroisoquinoline.

butyl isocyanide (**4a**, 1 mmol) in MeOH at 40 °C for 24 h afforded 1,5-DS-1*H*-T **5a** in 92% yield after chromatography purification. Our effort was then focused on the optimization of the intramolecular Heck reaction of **5a** for making 1,2,3,4-tetrahydroisoquinoline **6a**. A systematic evaluation of different catalysts and ligands, solvents, bases, as well as reaction temperatures and times was conducted (Table 1). The Heck reaction of **5a** was first examined by using 10 mol % $Pd(OAc)_2$, 20 mol % PPh_3, 2 equiv of Et_3N in CH_3CN or DMF at 105 °C for 24 h under N_2 atmosphere. However, the reactions failed under these conditions (Table 1, entries 1 and 2). When K_2CO_3 was used as a base to replace Et_3N, the reactions in either CH_3CN or DMF for 3 h both gave cyclized product **6a** in 70% yield (Table 1, entries 3 and 4). An increase of the reaction time to 12 h did not improve the yield (Table 1, entry 5). The reaction was further evaluated in the absence of ligand which afforded the product in 35% yield (Table 1, entry 6). Screening of ligands, e.g., PCy_3 and $P(o\text{-tol})_3$ reduced the yield of the desired product **6a** (Table 1, entries 7 and 8). Lowering the amount of $Pd(OAc)_2$ or changing the reaction temperatures resulted low yields of **6a** (Table 1, entries 9–11). Similar results were observed from the reactions using other bases, such as K_3PO_4, NaOAc, and Cs_2CO_3 (Table 1, entries 12–14). Investigating other Pd catalysts, suche as $PdCl_2$ and $Pd(dba)_2$ also gave low yields (Table 1, entries 15 and 16). Since CH_3CN is a more favorable solvent than DMF in green chemistry consideration [52,53], the optimal reaction conditions for the Heck reaction were to use 1 mmol of **5a** with 10 mol % $Pd(OAc)_2$ and 20 mol % PPh_3, 2 equiv of K_2CO_3 in 3 mL CH_3CN at 105 °C for 3 h under N_2 atmosphere which afforded product **6a** in 70% yield (Table 1, entry 3).

The combination of an initial multicomponent reaction with post-condensation reactions in one-pot is a good strategy to develop high pot, atom and step economy (PASE) syntheses [54-58]. We then made the effort to integrate the Ugi and Heck

Table 1: Conditions for one-pot Ugi-azide and Heck reactions.[a]

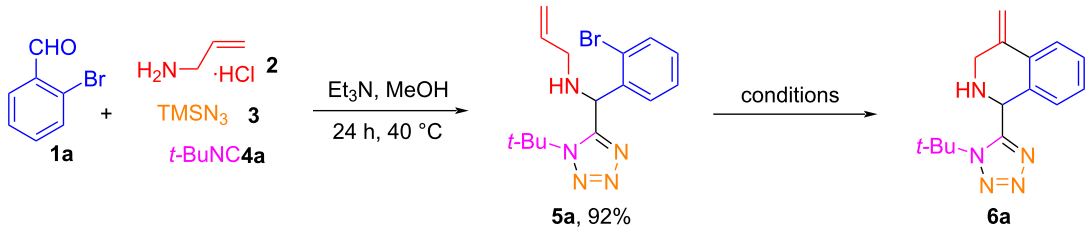

Entry	Catalyst	Ligand	Solvent	Base	Temp (°C)	Time (h)	Yield (%)[b]
1	$Pd(OAc)_2$	PPh_3	MeCN	Et_3N	105	24	–
2	$Pd(OAc)_2$	PPh_3	DMF	Et_3N	105	24	–
3	$Pd(OAc)_2$	PPh_3	MeCN	K_2CO_3	105	3	70
4	$Pd(OAc)_2$	PPh_3	DMF	K_2CO_3	105	3	70
5	$Pd(OAc)_2$	PPh_3	MeCN	K_2CO_3	105	12	65
6	$Pd(OAc)_2$	–	MeCN	K_2CO_3	105	6	35
7	$Pd(OAc)_2$	PCy_3	MeCN	K_2CO_3	105	6	46
8	$Pd(OAc)_2$	$P(o\text{-tol})_3$	MeCN	K_2CO_3	105	6	56
9[c]	$Pd(OAc)_2$	PPh_3	MeCN	K_2CO_3	105	3	58
10	$Pd(OAc)_2$	PPh_3	MeCN	K_2CO_3	70	8	60
11	$Pd(OAc)_2$	PPh_3	MeCN	K_2CO_3	120	3	62
12	$Pd(OAc)_2$	PPh_3	MeCN	K_3PO_4	105	3	39
13	$Pd(OAc)_2$	PPh_3	MeCN	NaOAc	105	3	62
14	$Pd(OAc)_2$	PPh_3	MeCN	Cs_2CO_3	105	3	56
15	$PdCl_2$	PPh_3	MeCN	K_2CO_3	105	5	53
16	$Pd(dba)_2$	PPh_3	MeCN	K_2CO_3	105	6	61
17[d]	**$Pd(OAc)_2$**	**PPh_3**	**MeCN**	**K_2CO_3**	**105**	**3**	**60**

[a]Reaction conditions: Ugi-azide step, 2-bromobenzaldehyde (**1a**, 1 mmol), allylamine hydrochloride (**2**, 1 mmol), trimethylsilyl azide (**3**, 1 mmol) and *tert*-butyl isocyanide (**4a**, 1 mmol), Et_3N (1.2 mmol) in 5 mL MeOH, 40 °C for 24 h. Heck reaction step, catalyst (10 mol %), ligand (20 mol %), solvent (3 mL), base (2 equiv), nitrogen atmosphere. [b]Isolated yield. [c]$Pd(OAc)_2$ 5 mol %, PPh_3 10 mol %. [d]Reaction was carried out in one-pot, starting compound is **1a** (1 mmol), first Ugi-azide reaction followed by the Heck reaction.

reactions in one-pot for making tetrazolyl-1,2,3,4-tetrahydroisoquinolines **6**. Thus, a mixture of 2-bromobenzaldehyde (**1a**, 1 mmol), allylamine hydrochloride (**2**, 1 mmol), trimethylsilyl azide (**3**, 1 mmol), and *tert*-butyl isocyanide (**4a**, 1 mmol) was stirred in MeOH at 40 °C for 24 h, and after the reaction was completed, the solvent was evaporated under vacuum to give crude Ugi adduct **5a** which was used for the intramolecular Heck reaction without further purification. Thus, to the solution of crude **5a** dissolved in MeCN (3 mL) were added 10 mol % of $Pd(OAc)_2$, 20 mol % of PPh_3, and 2 equiv of K_2CO_3 and the mixture stirred for 3 h at 105 °C under N_2 atmosphere to give the desired product **6a** in 60% isolated yield (entry 17 in Table 1).

With the optimized one-pot reactions in hands, we next evaluated the substrate scope by synthesizing 11 derivatives (Scheme 4) using nine benzaldehydes **1**, two isonitriles or ethyl isocyanoacetate **4**, allylamine hydrochloride (**2**), and trimethylsilyl azide (**3**) for the initial Ugi-azide reaction. Among them, products **6a** and **6b** from the reaction of isonitriles were synthesized in moderate yields (58–60%). For the Ugi reaction involving isocyanoacetate, lactamination occurred spontaneously to provide the ring-fused tetrazolo[1,5-*a*]pyrazin-6(5*H*)-one adducts **5** which after intramolecular Heck reaction gave functionalized tetracyclic tetrazolo-pyrazino[2,1-*a*]isoquinolin-6(5*H*)-ones **6c**–**k** in 73–79% yields. The presence of electron-donating or electron-withdrawing groups on the aromatic ring did not show significant effects on the Heck reaction.

Products **6c**–**k** were obtained in higher yields than products **6a**,**b**. We believe that the secondary amine in the Ugi reaction products **5** could affect the yield of the Heck reaction. To address the issue, compounds **5** were *N*-alkylated to afford intermediates **7** which were used in the subsequent Heck reac-

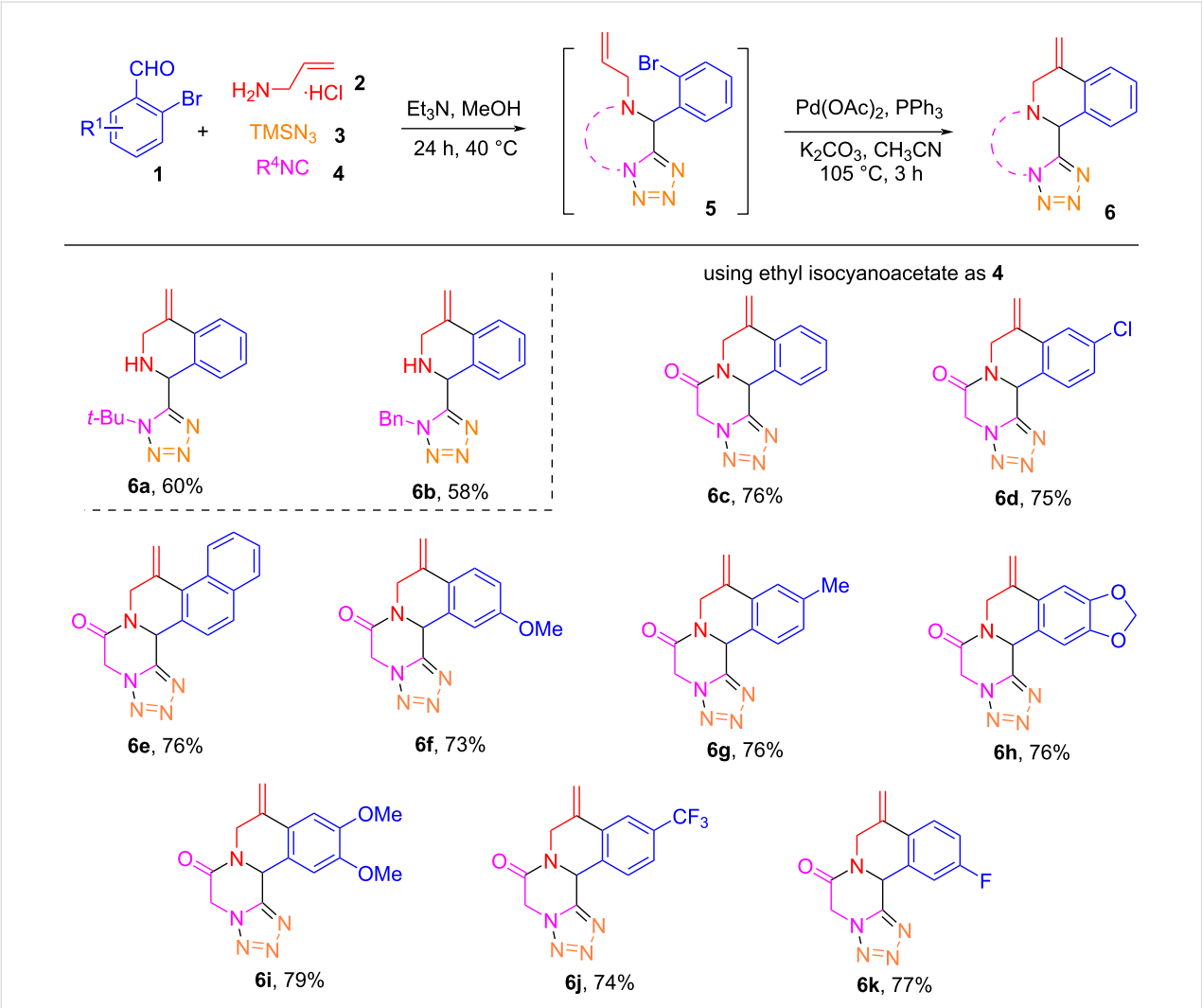

Scheme 4: One-pot synthesis of tetrazolo-pyrazino[2,1-*a*]isoquinolin-6(5*H*)-ones **6**.

tion step. Thus, an alternative one-pot Ugi-azide/*N*-alkylation/Heck reaction procedure was developed (Scheme 5). A mixture of 2-bromobenzaldehyde (**1a**, 1 mmol), allylamine hydrochloride (**2**, 1 mmol), trimethylsilyl azide (**3**, 1 mmol) and benzyl isocyanide (1 mmol) in MeOH was reacted at 40 °C for 24 h. After evaporating the solvent, 3 mL CH_3CN were added to the crude 1,5-DS-1*H*-T **5a** followed by the addition of 1 equiv of benzyl bromide and 2 equiv of K_2CO_3 for the alkylation reaction at 80 °C for 3 h to give *N*-benzylated compound **7a**. Finally, 10 mol % of $Pd(OAc)_2$, 20 mol % of PPh_3, 2 equiv of K_2CO_3 were added to the reaction mixture for the Heck reaction at 105 °C for 3 h under N_2 atmosphere to afford tetrazolyl-1,2,3,4-tetrahydroisoquinoline **8a** in 74% isolated yield which is higher than the one-pot Ugi/Hecke reaction to give product **6b** (58%). Under the alternative one-pot reaction conditions involving an *N*-alkylation step, the substrate scope was explored by the preparation of 10 derivatives **8a–j** (Scheme 5) using seven benzaldehydes **1**, two isonitriles **4**, and allylamine hydrochloride (**2**) with trimethylsilyl azide (**3**) for the Ugi-azide reaction. The *N*-alkylations were conducted using benzyl bromide and iodomethane, respectively. The final products **8b–j** were obtained in 66–74% yields.

To evaluate the scalability of the two-step one-pot reaction protocol, we performed the synthesis of tetracyclic tetrazolopyrazino[2,1-*a*]isoquinolin-6(5*H*)-one **6c** in gram quantity from 10 mmol of **1a** which led to the formation of product **6c** in a satisfactory yield 77% (Scheme 6).

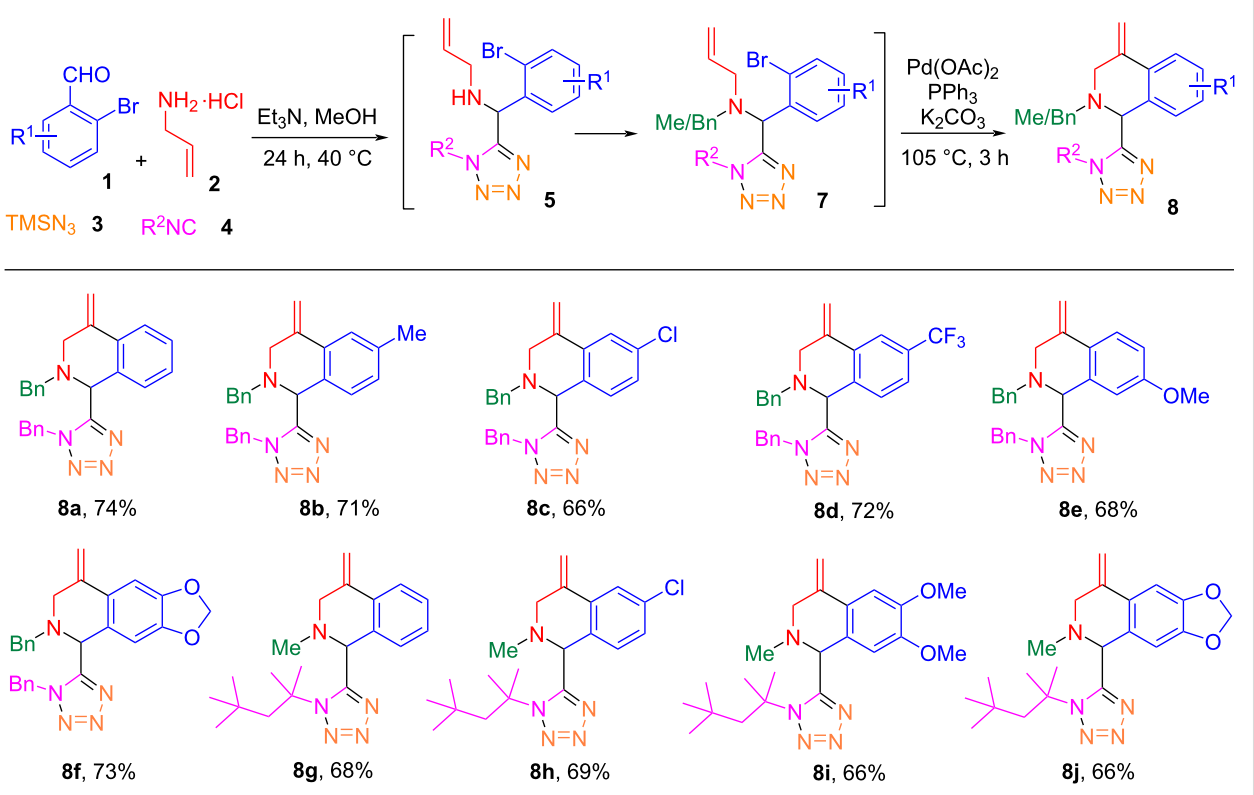

Scheme 5: One-pot synthesis for tetrazolyl-1,2,3,4-tetrahydroisoquinolines **8**.

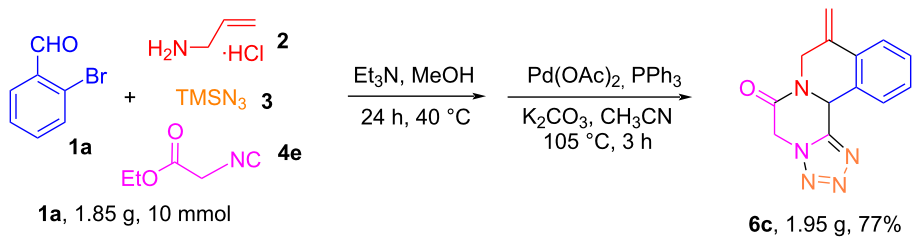

Scheme 6: Gram-scale two-step one-pot synthesis of **6c**.

The products **6** and **8** were characterized by ^{1}H and ^{13}C NMR, and HRMS analysis. In addition, single crystals of compound **6d** and **8c** were obtained for X-ray analysis to confirm the structures (Figure 2).

Conclusion

In conclusion, we have developed a one-pot synthesis with two or three steps for making tetrazolo-pyrazino[2,1-*a*]isoquinolin-6(5*H*)-ones. The initial Ugi-azide four-component reaction constructs the tetrazole motif while the subsequent intramolecular Heck reaction assembles the tetrahydroisoquinoline. The one-pot reaction avoids the intermediate purification which has favorable PASE in the synthesis of heterocyclic compounds.

Experimental

General procedure for the synthesis of Ugi-azide adduct 5a

A solution of 2-bromobenzaldehyde **1** (1 mmol, 1 equiv), allylamine hydrochloride (**2**, 1 mmol, 1 equiv), trimethylsilyl azide (**3**, 1 mmol, 1 equiv) and *tert*-butyl isocyanide **4a** (1 mmol, 1 equiv) in MeOH (5 mL) with Et_3N (1.5 mmol) was heated at 40 °C for 24 h in a sealed vial. Upon completion of the reaction, the reaction mixture was filtered and evaporated under vacuum to give crude products **5a**. Further purification was conducted by flash chromatography with 1:6 petroleum ether/EtOAc to afford **5a** in 92% yields. The adduct was confirmed by NMR.

General procedure for the Heck reaction; synthesis of product 6a

A mixture of Ugi-azide adduct **5a** (1 mmol), $Pd(OAc)_2$ (0.1 mmol), PPh_3 (0.2 mmol), K_2CO_3 (2 mmol) or NaOAc (2 mmol) in MeCN (3 mL) was stirred at 105 °C for 3 h under nitrogen atmosphere. After aqueous work-up, the crude product was purified by flash chromatography with 1:4 ethyl acetate/petroleum ether to afford product **6a**.

General procedure for the one-pot synthesis of tetrazole-containing 1,2,3,4-tetrahydroisoquinolines 6

A mixture of 2-bromobenzaldehyde **1** (1 mmol), allylamine hydrochloride (**2**, 1 mmol), trimethylsilyl azide (**3**, 1 mmol) and isocyanide **4** (1 mmol) in MeOH was stirred at 40 °C for 24 h. After the reaction was complete, the solvent was evaporated under vacuum to give the crude Ugi adduct **5**, which was used in the Heck reaction without further purification. To a solution of the crude intermediate **5** in MeCN (3 mL) was added 10 mol % of $Pd(OAc)_2$, 20 mol % of PPh_3, 2 equiv of K_2CO_3 and the mixture stirred for 3 h at 105 °C under N_2 atmosphere. After aqueous work-up, the crude product was purified by flash chromatography with 1:3 ethyl acetate/petroleum ether to afford products **6**.

General procedure for the one-pot synthesis of tetrazolyl-1,2,3,4-tetrahydroisoquinolines 8

A mixture of 2-bromobenzaldehyde **1** (1 mmol), allylamine hydrochloride (**2**, 1 mmol), trimethylsilyl azide (**3**, 1 mmol) and isocyanide **4** (1 mmol) in MeOH was reacted at 40 °C for 24 h. After evaporating the solvent, 3 mL CH_3CN were added to the crude 1,5-DS-1*H*-T **5** followed by the addition of 1 equiv of benzyl bromide or iodomethane and 2 equiv of K_2CO_3 for the alkylation reaction at 80 °C for 3 h to give *N*-alkylated compounds **7**. Finally, 10 mol % of $Pd(OAc)_2$, 20 mol % of PPh_3, 2 equiv of K_2CO_3 were added to the reaction mixture for the Heck reaction at 105 °C for 3 h under N_2 atmosphere. After aqueous work-up, the crude products were purified by flash

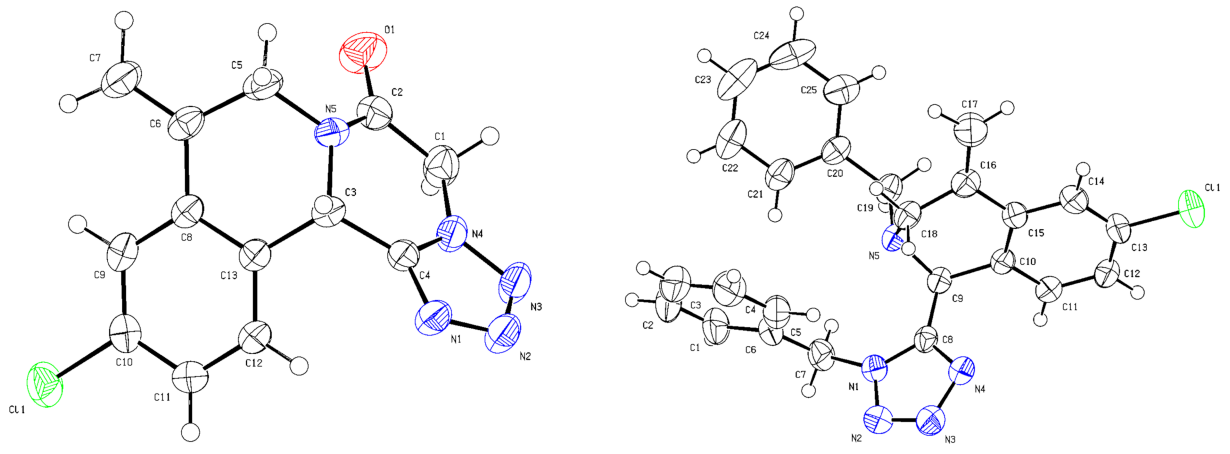

Figure 2: ORTEP diagrams of compound **6d** (left) [CCDC: 2164364] and **8c** (right) [CCDC: 2321622].

chromatography with 1:4 ethyl acetate/petroleum ether to afford products **8**.

Supporting Information

Supporting Information File 1

General reaction procedures, compound characterization data, and copies of NMR spectra.
[https://www.beilstein-journals.org/bjoc/content/supplementary/1860-5397-20-81-S1.pdf]

Supporting Information File 2

Crystallographic information file for compound **6d**.
[https://www.beilstein-journals.org/bjoc/content/supplementary/1860-5397-20-81-S2.cif]

Supporting Information File 3

Crystallographic information file for compound **8c**.
[https://www.beilstein-journals.org/bjoc/content/supplementary/1860-5397-20-81-S3.cif]

Acknowledgements

We acknowledge Shaodong Jiang's early work on this project.

Author Contributions

Jiawei Niu: investigation; methodology. Yuhui Wang: investigation; methodology. Shenghu Yan: investigation; methodology. Yue Zhang: investigation; methodology. Xiaoming Ma: conceptualization; data curation; supervision; validation; writing – original draft. Qiang Zhang: data curation; supervision; validation. Wei Zhang: conceptualization; supervision; writing – review & editing.

ORCID® iDs

Xiaoming Ma - https://orcid.org/0000-0003-1358-428X
Qiang Zhang - https://orcid.org/0000-0002-8173-8722
Wei Zhang - https://orcid.org/0000-0002-6097-2763

Data Availability Statement

All data that supports the findings of this study is available in the published article and/or the supporting information to this article. Data generated and analyzed during this study is openly available in CCDC. The data of CCDC-2164364 can be obtained free of charge at doi: https://doi.org/10.5517/ccdc.csd.cc2bn66f; the data of CCDC- 2321622: can be obtained free of charge at doi: https://doi.org/10.5517/ccdc.csd.cc2hxv1b.

Preprint

A non-peer-reviewed version of this article has been previously published as a preprint: https://doi.org/10.3762/bxiv.2024.2.v1

References

1. Neochoritis, C. G.; Zhao, T.; Dömling, A. *Chem. Rev.* **2019,** *119,* 1970–2042. doi:10.1021/acs.chemrev.8b00564
2. Ostrovskii, V. A.; Popova, E. A.; Trifonov, R. E. Tetrazoles. In *Comprehensive Heterocyclic Chemistry IV;* StC. Black, D.; Cossy, J.; Stevens, C. V., Eds.; Elsevier: Amsterdam, Netherlands, 2022; Vol. 6, pp 182–232. doi:10.1016/b978-0-12-818655-8.00131-1
3. Vandecruys, P.; Baldewijns, S.; Sillen, M.; Van Genechten, W.; Van Dijck, P. *Expert Rev. Anti-Infect. Ther.* **2023,** *21,* 799–812. doi:10.1080/14787210.2023.2233696
4. Staniszewska, M.; Zdrojewski, T.; Gizińska, M.; Rogalska, M.; Kuryk, Ł.; Kowalkowska, A.; Łukowska-Chojnacka, E. *Eur. J. Med. Chem.* **2022,** *230,* 114060. doi:10.1016/j.ejmech.2021.114060
5. Kritchenkov, A. S.; Lipkan, N. A.; Kurliuk, A. V.; Shakola, T. V.; Egorov, A. R.; Volkova, O. V.; Meledina, T. V.; Suchkova, E. P.; Zabodalova, L. A.; Dysin, A. P. *Pharm. Chem. J.* **2020,** *54,* 138–141. doi:10.1007/s11094-020-02180-4
6. Cortes-García, C. J.; Islas-Jácome, A.; Rentería-Gómez, A.; Gámez-Montaño, R. *Monatsh. Chem.* **2016,** *147,* 1277–1290. doi:10.1007/s00706-016-1686-x
7. Vanam, N. R.; Anireddy, J. S. *Chem. Data Collect.* **2023,** *48,* 101092. doi:10.1016/j.cdc.2023.101092
8. Cano, P. A.; Islas-Jácome, A.; González-Marrero, J.; Yépez-Mulia, L.; Calzada, F.; Gámez-Montaño, R. *Bioorg. Med. Chem.* **2014,** *22,* 1370–1376. doi:10.1016/j.bmc.2013.12.069
9. Toplak Časar, R.; Časar, Z. *Bioorg. Med. Chem.* **2018,** *26,* 4348–4359. doi:10.1016/j.bmc.2018.06.036
10. Prieto, C.; Evtoski, Z.; Pardo-Figuerez, M.; Hrakovsky, J.; Lagaron, J. M. *Mol. Pharmaceutics* **2021,** *18,* 2947–2958. doi:10.1021/acs.molpharmaceut.1c00098
11. Li, L.-H.; Yen, M.-Y.; Ho, C.-C.; Wu, P.; Wang, C.-C.; Maurya, P. K.; Chen, P.-S.; Chen, W.; Hsieh, W.-Y.; Chen, H.-W. *PLoS One* **2013,** *8,* e64794. doi:10.1371/journal.pone.0064794
12. Wei, C.-X.; Bian, M.; Gong, G.-H. *Molecules* **2015,** *20,* 5528–5553. doi:10.3390/molecules20045528
13. Frija, L. M. T.; Ismael, A.; Cristiano, M. L. S. *Molecules* **2010,** *15,* 3757–3774. doi:10.3390/molecules15053757
14. Myznikov, L. V.; Hrabalek, A.; Koldobskii, G. I. *Chem. Heterocycl. Compd. (N. Y., NY, U. S.)* **2007,** *43,* 1–9. doi:10.1007/s10593-007-0001-5
15. Lv, F.; Liu, Y.; Zou, J.; Zhang, D.; Yao, Z. *Dyes Pigm.* **2006,** *68,* 211–216. doi:10.1016/j.dyepig.2004.07.017
16. Song, W.; Wang, Y.; Qu, J.; Madden, M. M.; Lin, Q. *Angew. Chem., Int. Ed.* **2008,** *47,* 2832–2835. doi:10.1002/anie.200705805
17. Shmatova, O. I.; Nenajdenko, V. G. *J. Org. Chem.* **2013,** *78,* 9214–9222. doi:10.1021/jo401428q
18. Shang, X.-F.; Yang, C.-J.; Morris-Natschke, S. L.; Li, J.-C.; Yin, X.-D.; Liu, Y.-Q.; Guo, X.; Peng, J.-W.; Goto, M.; Zhang, J.-Y.; Lee, K.-H. *Med. Res. Rev.* **2020,** *40,* 2212–2289. doi:10.1002/med.21703
19. Li, D.-D.; Yu, P.; Xiao, W.; Wang, Z.-Z.; Zhao, L.-G. *Curr. Top. Med. Chem.* **2020,** *20,* 2634–2647. doi:10.2174/1568026620666200908165913
20. Qing, Z.-X.; Yang, P.; Tang, Q.; Cheng, P.; Liu, X.-B.; Zheng, Y.-J.; Liu, Y.-S.; Zeng, J.-G. *Curr. Org. Chem.* **2017,** *21,* 1920–1934. doi:10.2174/1385272821666170207114214
21. Maiti, M.; Kumar, G. S. *J. Nucleic Acids* **2010,** *2010,* 593408. doi:10.4061/2010/593408

22. Wang, Z.-x.; Chen, J.-l.; Qiao, C. *Chem. Biol. Drug Des.* **2013,** *82,* 216–225. doi:10.1111/cbdd.12153
23. Liu, H.; William, S.; Herdtweck, E.; Botros, S.; Dömling, A. *Chem. Biol. Drug Des.* **2012,** *79,* 470–477. doi:10.1111/j.1747-0285.2011.01288.x
24. Dömling, A.; Khoury, K. *ChemMedChem* **2010,** *5,* 1420–1434. doi:10.1002/cmdc.201000202
25. Waechtler, A.; Cezanne, B.; Maillard, D.; Sun, R.; Wang, S.; Wang, J.; Harder, A. *ChemMedChem* **2023,** *18,* e202300154. doi:10.1002/cmdc.202300154
26. Dömling, A.; Ugi, I. *Angew. Chem., Int. Ed.* **2000,** *39,* 3168–3210. doi:10.1002/1521-3773(20000915)39:18<3168::aid-anie3168>3.0.co;2-u
27. Hooshmand, S. E.; Zhang, W. *Molecules* **2023,** *28,* 1642. doi:10.3390/molecules28041642
28. Maleki, A.; Sarvary, A. *RSC Adv.* **2015,** *5,* 60938–60955. doi:10.1039/c5ra11531k
29. Mohammadkhani, L.; Heravi, M. M. *Mol. Diversity* **2020,** *24,* 841–853. doi:10.1007/s11030-019-09972-1
30. Barreto, A. d. F. S.; Santos, V. A. d.; Andrade, C. K. Z. *Beilstein J. Org. Chem.* **2017,** *13,* 2596–2602. doi:10.3762/bjoc.13.256
31. Foley, C.; Shaw, A.; Hulme, C. *Org. Lett.* **2018,** *20,* 1275–1278. doi:10.1021/acs.orglett.7b03977
32. Wang, Y.; Patil, P.; Kurpiewska, K.; Kalinowska-Tluscik, J.; Dömling, A. *Org. Lett.* **2019,** *21,* 3533–3537. doi:10.1021/acs.orglett.9b00778
33. Gunawan, S.; Petit, J.; Hulme, C. *ACS Comb. Sci.* **2012,** *14,* 160–163. doi:10.1021/co200209a
34. Gunawan, S.; Hulme, C. *Org. Biomol. Chem.* **2013,** *11,* 6036. doi:10.1039/c3ob40900g
35. Cárdenas-Galindo, L. E.; Islas-Jácome, A.; Alvarez-Rodríguez, N. V.; El Kaim, L.; Gámez-Montaño, R. *Synthesis* **2014,** *46,* 49–56. doi:10.1055/s-0033-1340051
36. Zarganes-Tzitzikas, T.; Patil, P.; Khoury, K.; Herdtweck, E.; Dömling, A. *Eur. J. Org. Chem.* **2015,** 51–55. doi:10.1002/ejoc.201403401
37. Medda, F.; Martinez-Ariza, G.; Hulme, C. *Tetrahedron Lett.* **2015,** *56,* 5295–5298. doi:10.1016/j.tetlet.2015.07.083
38. Saha, D.; Kharbanda, A.; Essien, N.; Zhang, L.; Cooper, R.; Basak, D.; Kendrick, S.; Frett, B.; Li, H.-y. *Org. Chem. Front.* **2019,** *6,* 2234–2239. doi:10.1039/c9qo00389d
39. Niño-Pantoja, I.; Gallardo-Alfonzo, A.; Solis-Santos, M.; Ordoñez, M.; Contreras-Celedón, C.; Islas-Jácome, A.; Chacón-García, L.; Cortés-García, C. J. *Eur. J. Org. Chem.* **2022,** e202200230. doi:10.1002/ejoc.202200230
40. Yang, M.-L.; Zhao, L.; Chen, H.-R.; Ding, M.-W. *J. Org. Chem.* **2023,** *88,* 1898–1906. doi:10.1021/acs.joc.2c02621
41. Rentería-Gómez, A.; Islas-Jácome, A.; Cruz-Jiménez, A. E.; Manzano-Velázquez, J. C.; Rojas-Lima, S.; Jiménez-Halla, J. O. C.; Gámez-Montaño, R. *ACS Omega* **2016,** *1,* 943–951. doi:10.1021/acsomega.6b00281
42. Kong, H.-H.; Pan, H.-L.; Ding, M.-W. *J. Org. Chem.* **2018,** *83,* 12921–12930. doi:10.1021/acs.joc.8b01984
43. Amador-Sánchez, Y. A.; Hernández-Vázquez, E.; González-Mojica, N.; Ramírez-Apan, M. T.; Miranda, L. D. *Tetrahedron* **2020,** *76,* 131383. doi:10.1016/j.tet.2020.131383
44. Janatian Ghazvini, H.; Müller, T. J. J.; Rominger, F.; Balalaie, S. *J. Org. Chem.* **2019,** *84,* 10740–10748. doi:10.1021/acs.joc.9b01269
45. García-González, M. C.; Hernández-Vázquez, E.; Vengochea-Gómez, F. A.; Miranda, L. D. *Tetrahedron Lett.* **2018,** *59,* 848–852. doi:10.1016/j.tetlet.2018.01.058
46. Balalaie, S.; Ramezani Kejani, R.; Ghabraie, E.; Darvish, F.; Rominger, F.; Hamdan, F.; Bijanzadeh, H. R. *J. Org. Chem.* **2017,** *82,* 12141–12152. doi:10.1021/acs.joc.7b01855
47. Hernández-Vázquez, E.; Miranda, L. D. *Org. Biomol. Chem.* **2016,** *14,* 4875–4884. doi:10.1039/c6ob00431h
48. Vachhani, D. D.; Butani, H. H.; Sharma, N.; Bhoya, U. C.; Shah, A. K.; Van der Eycken, E. V. *Chem. Commun.* **2015,** *51,* 14862–14865. doi:10.1039/c5cc05193b
49. Moni, L.; Denißen, M.; Valentini, G.; Müller, T. J. J.; Riva, R. *Chem. – Eur. J.* **2015,** *21,* 753–762. doi:10.1002/chem.201404209
50. Rasouli, M. A.; Miri, S.; Rashidi Ranjbar, P. *J. Heterocycl. Chem.* **2015,** *52,* 1864–1870. doi:10.1002/jhet.2270
51. Peshkov, A. A.; Peshkov, V. A.; Pereshivko, O. P.; Van der Eycken, E. V. *Tetrahedron* **2015,** *71,* 3863–3871. doi:10.1016/j.tet.2015.04.022
52. Alfonsi, K.; Colberg, J.; Dunn, P. J.; Fevig, T.; Jennings, S.; Johnson, T. A.; Kleine, H. P.; Knight, C.; Nagy, M. A.; Perry, D. A.; Stefaniak, M. *Green Chem.* **2008,** *10,* 31–36. doi:10.1039/b711717e
53. Prat, D.; Wells, A.; Hayler, J.; Sneddon, H.; McElroy, C. R.; Abou-Shehada, S.; Dunn, P. J. *Green Chem.* **2016,** *18,* 288–296. doi:10.1039/c5gc01008j
54. Zhang, W.; Yi, W.-B. *Pot, Atom, and Step Economy (PASE) Synthesis; SpringerBriefs in Molecular Science*; Springer International Publishing: Cham, Switzerland, 2019. doi:10.1007/978-3-030-22596-4
55. Ma, X.; Zhang, W. *iScience* **2022,** *25,* 105005. doi:10.1016/j.isci.2022.105005
56. Hayashi, Y. *Chem. Sci.* **2016,** *7,* 866–880. doi:10.1039/c5sc02913a
57. Hayashi, Y. *Acc. Chem. Res.* **2021,** *54,* 1385–1398. doi:10.1021/acs.accounts.0c00803
58. Biesen, L.; Müller, T. J. J. *Adv. Synth. Catal.* **2021,** *363,* 980–1006. doi:10.1002/adsc.202001219

License and Terms

This is an open access article licensed under the terms of the Beilstein-Institut Open Access License Agreement (https://www.beilstein-journals.org/bjoc/terms), which is identical to the Creative Commons Attribution 4.0 International License (https://creativecommons.org/licenses/by/4.0). The reuse of material under this license requires that the author(s), source and license are credited. Third-party material in this article could be subject to other licenses (typically indicated in the credit line), and in this case, users are required to obtain permission from the license holder to reuse the material.

The definitive version of this article is the electronic one which can be found at:
https://doi.org/10.3762/bjoc.20.81

BEILSTEIN JOURNAL OF ORGANIC CHEMISTRY

Innovative synthesis of drug-like molecules using tetrazole as core building blocks

Jingyao Li[‡1], Ajay L. Chandgude[‡1], Qiang Zheng[1] and Alexander Dömling[*1,2]

Full Research Paper

Open Access

Address:
[1]Department of Drug Design, University of Groningen, A. Deusinglaan 1, 9713 AV Groningen, The Netherlands and [2]Institute of Molecular and Translational Medicine, Faculty of Medicine and Dentistry and Czech Advanced Technology and Research Institute, Palackỳ University in Olomouc, Olomouc, Czech Republic

Email:
Alexander Dömling[*] - alexander.domling@upol.cz

* Corresponding author ‡ Equal contributors

Keywords:
building blocks; green chemistry; multicomponent reaction; Passerini tetrazole reaction; tetrazole; Ugi reaction

Beilstein J. Org. Chem. **2024,** *20,* 950–958.
https://doi.org/10.3762/bjoc.20.85

Received: 02 February 2024
Accepted: 12 April 2024
Published: 29 April 2024

This article is part of the thematic issue "Multicomponent reactions IV".

Associate Editor: T. J. J. Müller

© 2024 Li et al.; licensee Beilstein-Institut.
License and terms: see end of document.

Abstract

Tetrazole is widely utilized as a bioisostere for carboxylic acid in the field of medicinal chemistry and drug development, enhancing the drug-like characteristics of various molecules. Typically, tetrazoles are introduced from their nitrile precursors through late-stage functionalization. In this work, we propose a novel strategy involving the use of diversely protected, unprecedented tetrazole aldehydes as building blocks. This approach facilitates the incorporation of the tetrazole group into multicomponent reactions or other chemistries, aiding in the creation of a variety of complex, drug-like molecules. These innovative tetrazole building blocks are efficiently and directly synthesized using a Passerini three-component reaction (PT-3CR), employing cost-effective and readily available materials. We further showcase the versatility of these new tetrazole building blocks by integrating the tetrazole moiety into various multicomponent reactions (MCRs), which are already significantly employed in drug discovery. This technique represents a unique and complementary method to existing tetrazole synthesis processes. It aims to meet the growing demand for tetrazole-based compound libraries and novel scaffolds, which are challenging to synthesize through other methods.

Introduction

The efficient synthetic accessibility of drug-like molecules is of key importance. Interestingly, over the years the complexity of molecules entering the market is steadily increasing, supposedly due to the increasing complexity of contemporary molecular targets. A major Swiss API CRO reported that the complexity of chemical synthesis towards novel drugs has almost doubled from eight chemical steps to an average of 14 in 2021 [1]. Therefore, the need for robust reactions compatible with many functional groups in complex molecules is an integral part in contemporary medicinal chemistry and drug development. During preclinical research large screening libraries are integral part of the structure-based drug design and high-throughput

screening and facile, efficient synthetic methods to explore diverse chemical spaces are of great help [2-4]. However, due to the vastness of chemical space, generation of ready-to-screen drug-like molecules remains a key challenge in the medicinal chemistry field [5,6].

Tetrazole is considered as a privileged scaffold in pharmaceutical and medicinal chemistry, used as a carboxylic acid bioisostere and a *cis*-amide mimic contributing to improvements in lipophilicity, metabolic stability, conformational rigidity, and potency [7-9]. Recently, the use of the tetrazole moiety in drug development has been increased and exhibited prevalent occurrence in bioactive compounds; being present in more than 20 marketed drugs with a very broad range of biological activities such as anticancer, antitubercular, antibacterial, antiviral, antimalarial, antiallergic, and antihypertensive (Figure 1a) [7,10]. In addition, tetrazoles constitute a diverse range of industrial applications and are extensively used in materials, agriculture, explosives and photography [11,12].

Due to the high synthetic value, significant efforts have been devoted to developing methods for the preparation of the tetrazole scaffolds, in particular recently through multicomponent reactions (MCRs) and mostly Ugi and Passerini reactions [7-9].

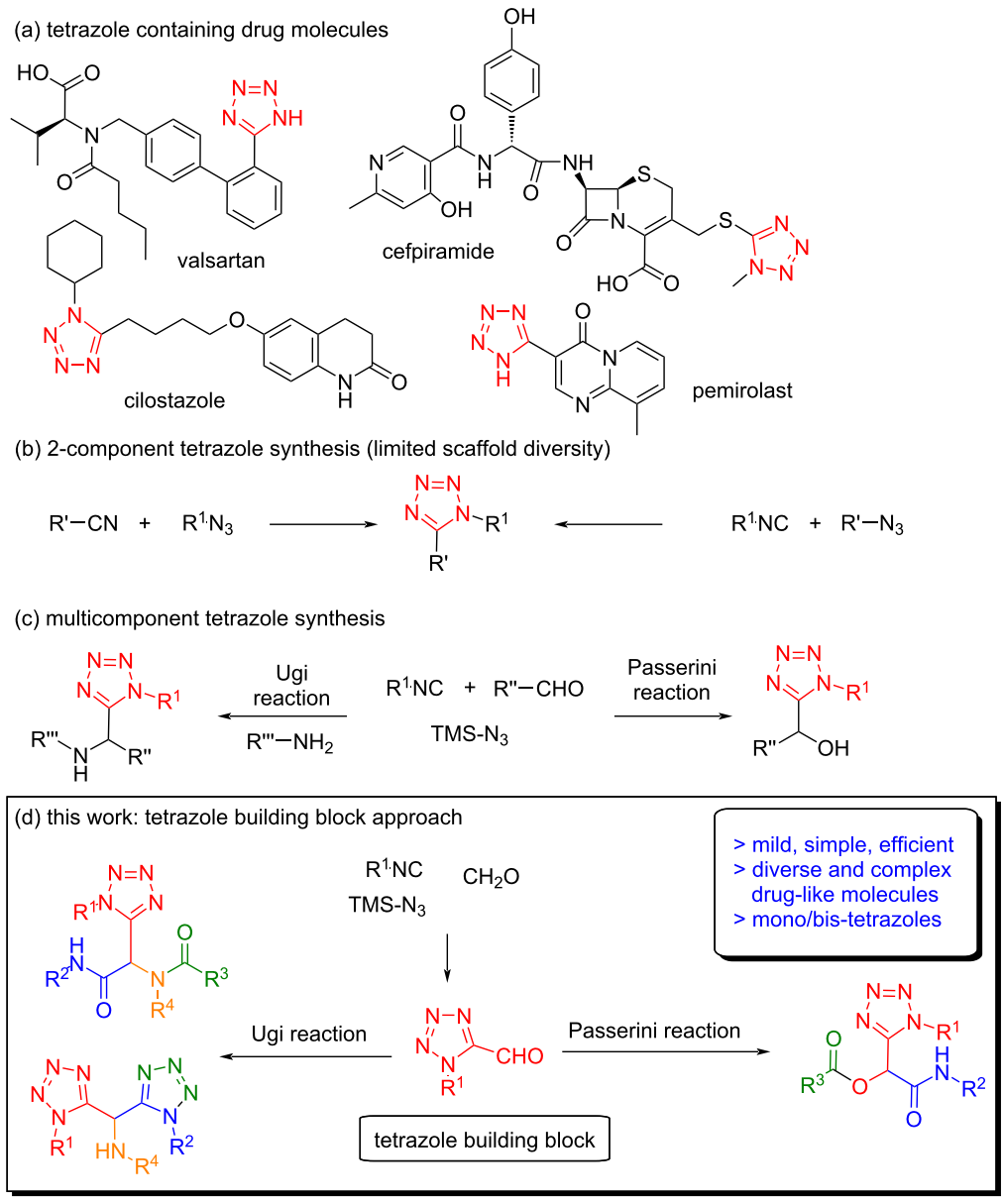

Figure 1: Tetrazole drugs, current assembly strategies, and novel building block strategy.

Traditionally, due to its charged nature the tetrazole moiety is introduced in a late-stage-modification approach, mostly from nitriles or isocyanides (Figure 1b) [13]. On the other hand, accessing diverse tetrazole scaffolds from MCRs, typically involves first de novo construction of the tetrazole scaffold and subsequent post-modifications (Figure 1c) [14]. In stark contrast, a method for the synthesis of drug-like tetrazole compound libraries involving a building block approach have remained elusive, with success being reported thus far only with the tetrazole amine [14,15]. The use of a tetrazole building block in MCRs would have all the advantages of the de novo approach and furthermore provides an extra efficiency, complexity and diversity in the same number of steps (Figure S1, Supporting Information File 1). Also, it offers a flexibility of placement of the tetrazole moiety in the scaffold and enables additional facile post-modifications due to the protected nature of the tetrazol. Additionally, inclusion of a strategically placed tetrazole and bioisostere replacement of MCR substrate with tetrazole may give rise to molecules with improved drug-like characteristics with nominal weight or size difference. This tetrazole building block approach will allow direct access to ready to screen molecular scaffolds for medicinal chemistry programs to investigate different biological activities [16-18].

Motivated by the shortcomings of current methodologies and the absence of a tetrazole building block approach, we have pursued and report herein the development of a rapid synthetic approach to generate libraries in which the tetrazole ring is conveniently introduced in a scaffold rather than built up de novo for each molecule. We report the synthesis of diverse tetrazole building blocks, which were readily prepared and their unprecedented use in MCRs to access diverse molecular scaffolds. To do that, we first developed an efficient and scalable MCR-based route of the building blocks, in order to provide useful quantities by utilizing diverse isocyanides, azide and paraformaldehyde. Then, this novel tetrazole building block was used in the Passerini and Ugi reactions amenable to convenient, efficient, simple, and fast synthesis of diverse scaffolds library to afford variously functionalized tetrazole-based drug-like molecules.

In order to achieve the synthesis of novel tetrazole building blocks and their use in organic synthesis we envisioned the use of multicomponent reactions in both steps. The use of MCRs provides the benefits of simplicity, speed, complexity, and diversity with the minimum number of steps and with an environmentally friendly nature. First, we focused on the use of the Passerini-tetrazole reaction for the synthesis of tetrazole building blocks which provides the handle of alcohol functionality and further oxidation serves as an oxo component in subsequent MCRs (Figure 1d). The synthesis of oxo-tetrazoles was targeted because of the prevalence of the aldehyde substrate in MCRs and their use in medicinal chemistry literature.

Results and Discussion

First, we planned to provide a number of orthogonally protected tetrazole carbaldehyde building blocks. This should be accomplished by synthesizing the hydroxymethyl precursors by a Passerini-tetrazole synthesis, followed by oxidation to the aldehyde (Figure 1d). Based on our recently reported highly improved α-hydroxylmethyltetrazole synthesis under mild and save conditions we started to explore the utility of the Passerini-tetrazole reaction with cost-efficient and readily available paraformaldehyde (powder form) [19]. However, paraformaldehyde can sometimes be a challenging substrate for MCRs and this was also the case for the synthesis of oxo-tetrazoles via a Passerini tetrazole reaction [19]. In a model reaction, we investigated benzyl isocyanide (1 equiv), paraformaldehyde (2 equiv) and trimethylsilyl azide (1 equiv) as easily available substrates. Trimethylsilyl azide is considered as a safe replacement of metal azides. We started the solvent optimization with MeOH and H_2O as solvent system at room temperature, however, it did not yield any product even after 3 days (Table 1, entry 1). The use of DMF to improve the solubility of the paraformaldehyde solid was also unsuccessful to increase the product yield. The increased use of microwave conditions in organic synthesis [20] and our previous promising studies on microwave-assisted MCRs [21], motivated us to use microwave conditions for further optimization. Accordingly, we investigated several sets of reaction conditions with or without solvents at low or high temperature under microwave irradiation and the results are summarized in Table 1. Notably, the reaction with water as a solvent provided a promising yield of 52%, whereas other solvents and conditions resulted only in trace product formation. Combining water with different co-solvents such as MeOH, DCM, CH_3CN and THF provided products generally with low to moderate yields of 29–69% (Table 1, entries 9–14). The low yield of the desired product is either due to the formation of 1-benzyl-1*H*-tetrazole as side product or low conversion and the oxo-tetrazole component remaining unreacted. To our delight, the use of toluene/water (9:1) as a biphasic solvent system provided quantitative product formation with 90% isolated yield (Table 1, entry 15). Upon trying to reduce the reaction time and performing the reactions at higher temperature, the product yields were significantly reduced. Noteworthy, the synthesis of tetrazole building blocks under the optimized conditions could be easily scaled up to gram amounts.

After establishing the optimized conditions, we next examined the substrate scope of the Passerini-tetrazole reaction by varying the isocyanide component (Scheme 1). Aliphatic isocyanides, such as *tert*-octyl and *tert*-butyl isocyanide (**1b** and **1c**) were

Table 1: Optimization of reaction conditions.

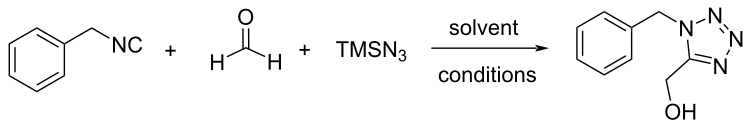

1a

entry	solvent	conditions	temp	time (min)	yield (%)[a]
1	MeOH/H_2O (9:1)	rt	rt	3 days	0
2	DMF	rt	rt	3 days	0
3	DCM	mw	60 °C	60	<5
4	MeOH	mw	80 °C	40	<5
5	MeOH	mw	100 °C	20	<5
6	–	mw	100 °C	10	<5
7	H_2O	mw	100 °C	60	52
8	toluene	mw	150 °C	60	<5
9	MeOH/H_2O (9:1)	mw	100 °C	60	29
10	MeOH/H_2O (1:9)	mw	100 °C	60	50
11	DCM/H_2O (9:1)	mw	80 °C	70	57
12	DCM/H_2O(9:1)	mw	80 °C	80	69
13	CH_3CN/H_2O(9:1)	mw	100 °C	120	51
14	THF/H_2O(9:1)	mw	100 °C	80	56
15	**toluene/H_2O (9:1)**	**mw**	**80 °C**	**60**	**90**
16	toluene/H_2O (9:1)	mw	100 °C	60	80
17	toluene/H_2O (9:1)	mw	150 °C	60	77

[a]Isolated yields. mw = microwave.

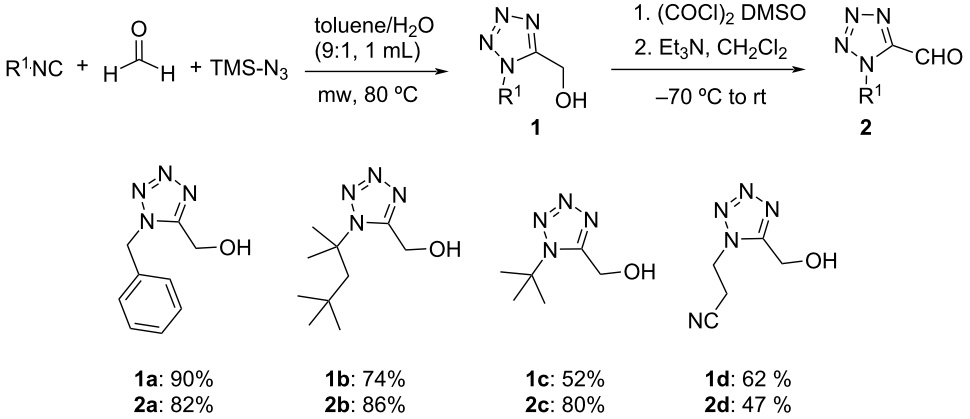

Scheme 1: Synthesis of tetrazole building blocks. Isolated yields.

well-tolerated in the Passerini-tetrazole reaction, leading to the corresponding tetrazole products in moderate to good yields of 74% and 52%, respectively. β-Cyanoethyl isocyanide (**1d**) was also well tolerated providing a good yield (62%). The tolerability of different isocyanides, and the possibility to remove the cleavable isocyanides under different reaction conditions (acidic for the *tert*-octyl and *tert*-butyl isocyanide, basic for β-cyanoethyl isocyanide, or reductive for the benzyl isocyanide) in the developed methodology provides multiple opportunities for various further chemical manipulations, easy access of 1*H*-tetrazole moieties, and great orthogonal functional group compatibility.

First, the tetrazole building blocks were prepared on a multi-gram scale to access the free alcohol Passerini-tetrazole product. Then, the Swern oxidation [22-24], which is widely exploited and has a wide tolerance of functional groups, was used to convert the tetrazole containing alcohols to aldehydes, in particular for derivatives bearing convertible isocyanides. Most building blocks were well tolerated in Swern oxidation providing moderate to excellent yields of the target aldehydes, except cyclohexyl isocyanide, which decreased the reaction yield and only gave trace amount of product. Importantly, the synthetized carboxaldehyde-tetrazole building blocks are bench stable and can be easily and efficiently scaled-up to gram scale. Noteworthy, 1-substituted tetrazole-5-carbaldehydes are almost elusive from chemical literature [25-29]. Moreover, all synthesis routes described so far are lengthy and involve dangerous chemicals. The 4-step procedure of Sun et al. starts from anilines and involves the hazardous chemicals NaN_3, DIBAL-H, and CCl_4 [25]. Moderhack described the synthesis of 1-substituted tetrazole-5-carbaldehyde through a Kröhnke reaction involving lengthy to access 5-chloromethyltetrazole and the well-known carcinogen *p*-nitrosodimethylaniline [27]. Also Ugi described the synthesis of 5-hydroxymethyltetrazoles through a Passerini reaction, however, in low yields, with very long reaction times, and using hazardous aluminum azide [30]. Clearly our novel access to this elusive substance class of 1-substituted tetrazole-5-carbaldehyde outperforms all hitherto described synthetic pathways in terms of economy, sustainability, generalizability, step-count, reaction simplicity, and yields.

With these tetrazole building blocks in hand, we next aimed to investigate the scope and limitations by assembling smaller compound libraries with a high degree of complexity and skeletal diversity. The well described, excellent functional group compatibility and versatility of MCRs along with their promising impact on medicinal chemistry and drug discovery for the library generation prompted us to further use the tetrazole building blocks in MCRs [31,32]. Building on our previous interest in the Passerini reaction involving atypical substrates, we aimed to investigate the unprecedented use of the tetrazole building block as an oxo component in the Passerini reaction to build a library that would possess drug-like molecules and could be easily screened for biological activity and establishment of structure–activity relationships [33]. We envision that the use of tetrazole oxo component in the Passerini reaction will provide more diversity and complexity in the same number of steps and conditions and at the same time provide a simple means to introduce the bioisosteric tetrazole group (Figure S1, Supporting Information File 1).

Thus, we examined the ability of the Passerini reaction to incorporate an oxo-tetrazole group with a diverse panel of isocyanide and acid derivatives. Various aliphatic and aromatic acid derivatives are well tolerated leading to the corresponding tetrazole products **3a**–**j** (Scheme 2) in moderate to good yields when the reactions were conducted in DCM at room temperature for 24 hours. Both aliphatic and aromatic substituents on the tetrazole ring of the oxo component were equally well tolerated. Aliphatic aldehydes with aliphatic and aromatic groups reacted smoothly and provided moderate to excellent yields of 58–83%. Among this, the *tert*-octyl-substituted aldehyde exhibited excellent product transformation with a yield of 83% of **3e**. Various isocyanides such as benzyl, phenylethyl, *tert*-octyl and *tert*-butyl isocyanides participated in the reaction with moderate to good yields, mainly lower yields were obtained with β-cyanoethyl isocyanide (e.g., **3g**). In addition, good substrate tolerance was also achieved for the acid component with both aliphatic, aromatic, and heterocyclic acids.

The excellent overall performance of these tetrazole-aldehyde building blocks in Passerini reactions reflected the commendable feasibility of our strategy. These results pave the way to the development of a tetrazole building block approach for other MCRs and can furnish a synthetically important tetrazole-based scaffold.

To even further demonstrate the utility of the developed building block approach, we decided to incorporate an oxo-tetrazole into an Ugi four-component reaction, the most studied and versatile MCR in organic synthesis and drug discovery [31,32]. Despite tremendous exploration, finding novel substrates or bioisosteres as a starting material in the Ugi reaction remains a highly challenging and desired research area [34-36].

The use of these atypical oxo-tetrazole building blocks in the Ugi reaction can be a direct and effective way to further explore the tetrazole-based vast chemical space, importantly their use in Ugi reactions can create molecules with diversity and complexity with minor effect on the molecular weight (Figure S1, Supporting Information File 1). The oxo-tetrazole scaffold proved to be successful in the incorporation of the Ugi reaction generating a diverse range of molecules having both mono and ditetrazole scaffolds (Scheme 3). This method is applicable to different amines, isocyanide and acid components including Ugi-4-component and Ugi-tetrazole reactions proving the desired products with low to moderate yields. The Ugi reactions were performed in MeOH at room temperature for 24 hours and without any further optimization. As this oxo-tetrazole building block is a challenging substrate to incorporate in Ugi reactions, it remained mostly intact during the reaction and ultimately provides lower yields as compared to Passerini reactions (Scheme 2).

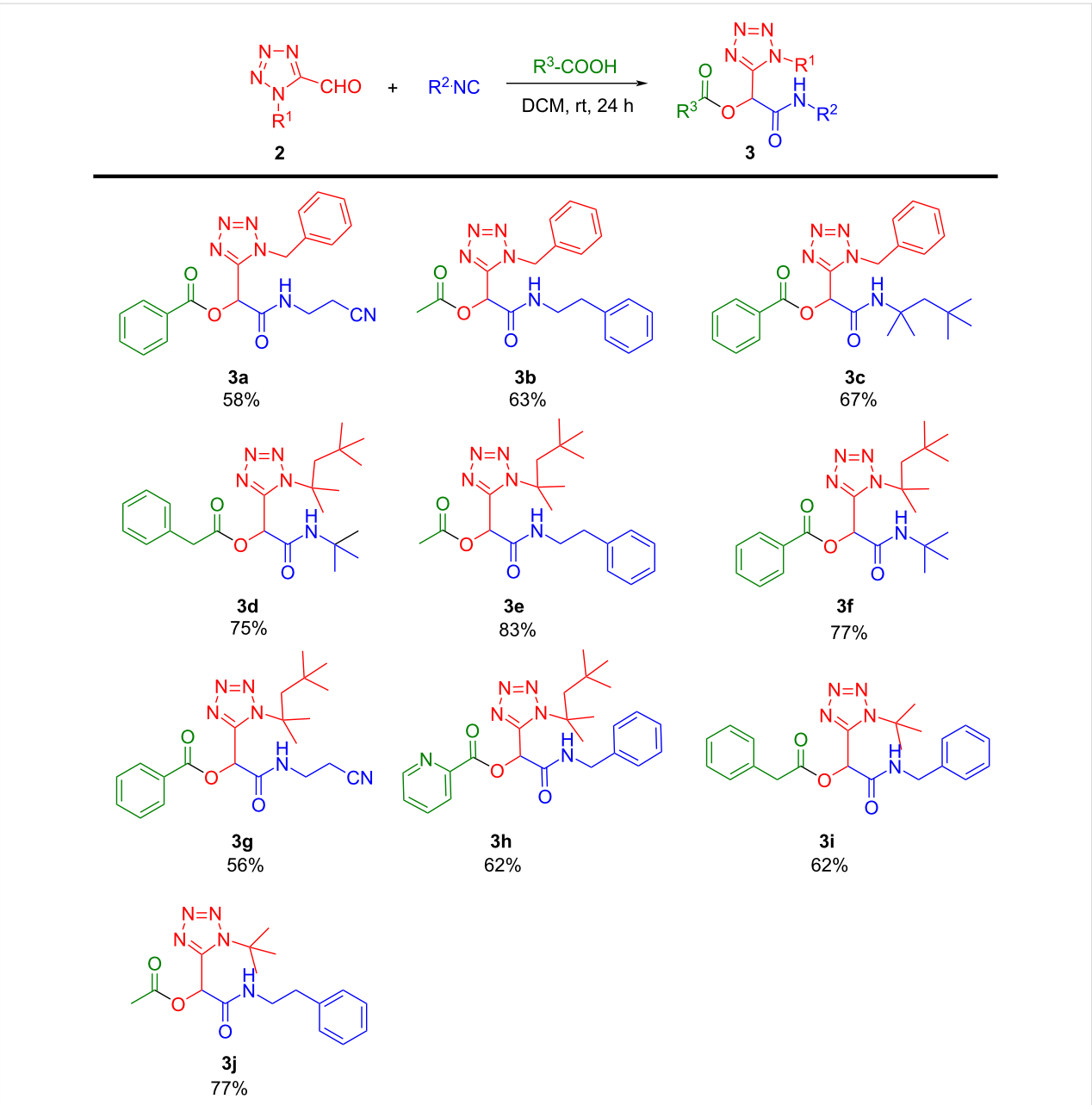

Scheme 2: Substrate scope of Passerini products **3**. Isolated yields.

Although yields for the Ugi reactions are modest with this unusual and unprecedented substrate, this simple and powerful method offers unique tetrazole-based products in a single step that could not be easily obtained by alternative procedures. These low yields could be further improved with the optimization of individual substrates and reaction conditions such as solvent, temperature or assisting techniques such as sonication or microwave. Collectively, this building block strategy opens a new avenue to screen acid bioisostere or amide bioisostere compound libraries to revisit or investigate novel drug targets. The diverse scaffold generation from this method also provides multiple opportunities for various further chemical manipulations which may allow the discovery of novel bioactive small molecule tools.

Recently, the fragment-based drug discovery (FBDD) approach has been emerged as a promising starting point for the new drug discovery, which typically involves the screening of small fragments followed by building the lead molecules by combining active fragments or elaborating the molecules on this fragment. We became interested in investigating the new, easy and direct access to the commercially unavailable 1*H*-oxo-tetrazole frag-

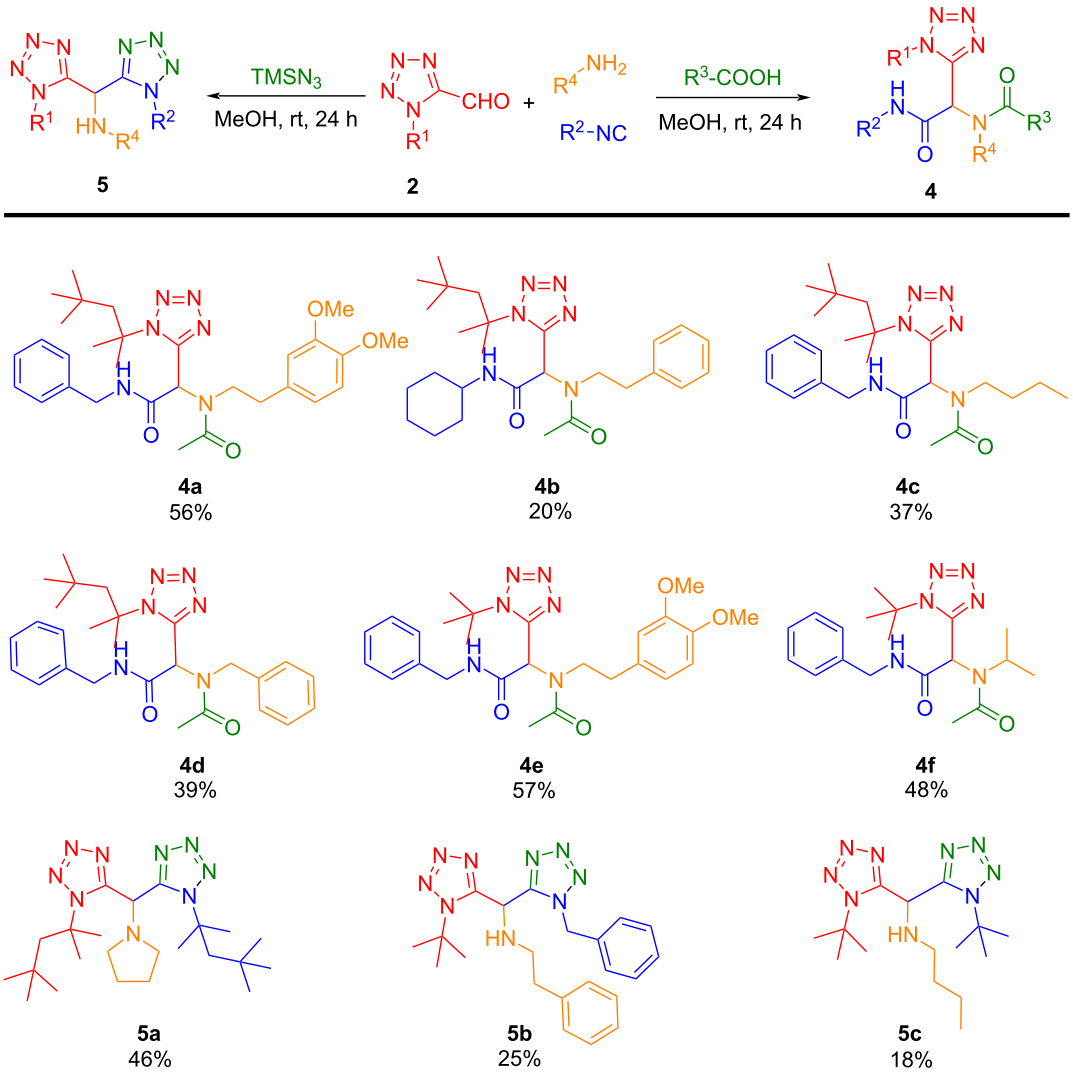

Scheme 3: Substrate scope of Ugi products **4** and **5**. Isolated yields.

ment. We envisioned the use of tetrazole building blocks having cleavable isocyanide moieties for the synthesis of 5-substitued 1*H*-tetrazoles (Scheme 4). Commercially available *tert*-octyl isocyanide, which has an excellent performance in each step of this strategy, was utilized as a model substrate and further treated with 1.15 M HCl in EtOH under refluxing overnight conditions which provides the desired 1*H*-tetrazole with an acceptable yield of 31%. Noteworthy, only two syntheses of **6** are described in the literature [28,29]. Both methods use dangerous, explosive and toxic hydrazoic acid in a sequential multistep synthesis. In contrast our easy, short and direct method towards **6** provides further opportunities to use this fragment in FBDD or as building block for organic synthesis.

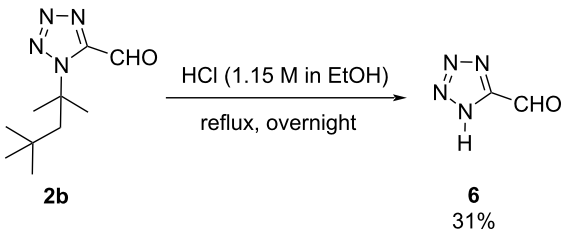

Scheme 4: Synthesis of tetrazole building block **6**. Isolated yield.

Conclusion

Our study presented herein comprise a significant advancement in the field of medicinal chemistry and drug development. The introduction of 1*H*-tetrazole as a bioisostere for carboxylic acid has long been recognized for its potential in enhancing drug-like properties [37]. Predominantly, tetrazoles are currently

introduced by a late-stage-functionalization approach from their nitrile precursors. This work, however, takes an additional step forward by employing novel 1*H*-protected tetrazole aldehydes as versatile building blocks, a strategy not previously explored. A key innovation of this research lies in the synthesis of these tetrazole building blocks. The use of the Passerini three-component reaction (PT-3CR) utilizing cost-effective and readily available materials not only simplifies the process but also opens up avenues for gram-scale production. This method stands out for its efficiency, simplicity, and environmental friendliness, in contrast to previous syntheses. The incorporation of these tetrazole building blocks into various multicomponent reactions (MCRs) is an additional aspect of our work. This approach significantly expands the chemical space available for drug discovery, offering a means to create complex, drug-like molecules with high skeletal diversity. The study demonstrates that these tetrazole building blocks can be effectively integrated into both Passerini and Ugi reactions, indicating their broad applicability in synthesizing a wide range of molecular scaffolds. Additionally, it is conceivable that the aldehyde group can be introduced in all commonly used chemistries of oxo groups. The potential future applications of this work are vast. The diverse scaffolds prepared can be further diversified, allowing the exploration of new compounds with potential pharmaceutical applications. This opens up exciting possibilities in the development of novel treatments for various diseases of unmet medical needs. Furthermore, the versatility of these tetrazole building blocks could extend beyond medicinal chemistry, finding utility in organic and materials applications. In conclusion, this research represents a significant step forward in the synthesis of drug-like molecules using tetrazole building blocks. Its implications for future drug discovery and development are profound, with the potential to streamline the process of creating new and effective pharmaceuticals. We hope the methodologies and findings described herein will inspire further research and innovation. As the exploration of the synthetic utility of this tetrazole scaffold continues, particularly in other MCRs and post-modification processes, we anticipate more applications in the near future. Investigation of these drug-like molecules for the targets PD-1/PDL-1, caspase-1, and IL-17A are currently in progress in our laboratory.

Supporting Information

Supporting Information File 1

Experimental procedures, compound characterizations, and NMR spectra.
[https://www.beilstein-journals.org/bjoc/content/supplementary/1860-5397-20-85-S1.pdf]

Acknowledgements

We acknowledge the contribution from the Ph.D. thesis of co-author Jingyao Li, https://research.rug.nl/en/publications/substrate-exploitation-of-multicomponent-reactions-toward-diverse, doi:10.33612/diss.150511881

Funding

Jingyao Li and Qiang Zheng acknowledge the China Scholarship Council for financial support. The Erasmus Mundus Scholarship "Svaagata" is acknowledged for a fellowship to A. L. Chandgude. This research has been also supported (AD) through the ERA Chair grant ACCELERATOR (101087318). This study was supported by the National Institute for Cancer Research–Programme EXCELES (ID Project No. LX22NPO5102), funded by the Cancer Research Czech Republic.

Author Contributions

Jingyao Li: conceptualization; formal analysis; investigation; methodology; writing – original draft. Ajay L. Chandgude: conceptualization; formal analysis; investigation; methodology. Qiang Zheng: formal analysis; investigation; methodology. Alexander Dömling: conceptualization; funding acquisition; investigation; methodology; project administration; validation; visualization; writing – review & editing.

ORCID® iDs

Jingyao Li - https://orcid.org/0000-0002-9357-9896
Ajay L. Chandgude - https://orcid.org/0000-0001-8236-9626
Qiang Zheng - https://orcid.org/0000-0002-8800-924X
Alexander Dömling - https://orcid.org/0000-0002-9923-8873

Data Availability Statement

All data that supports the findings of this study is available in the published article and/or the supporting information to this article.

Preprint

A non-peer-reviewed version of this article has been previously published as a preprint: https://doi.org/10.3762/bxiv.2024.7.v1

References

1. Small molecule trends to follow in 2023 "An executive at Lonza weighs in on what to expect from complex small molecules". https://www.drugdiscoverytrends.com/small-molecule-trends-to-follow-in-2023/ (accessed Jan 3, 2023).
2. Blakemore, D. C.; Castro, L.; Churcher, I.; Rees, D. C.; Thomas, A. W.; Wilson, D. M.; Wood, A. *Nat. Chem.* **2018,** *10,* 383–394. doi:10.1038/s41557-018-0021-z
3. Kutchukian, P. S.; Dropinski, J. F.; Dykstra, K. D.; Li, B.; DiRocco, D. A.; Streckfuss, E. C.; Campeau, L.-C.; Cernak, T.; Vachal, P.; Davies, I. W.; Krska, S. W.; Dreher, S. D. *Chem. Sci.* **2016,** *7,* 2604–2613. doi:10.1039/c5sc04751j

4. Lovering, F.; Bikker, J.; Humblet, C. *J. Med. Chem.* **2009,** *52,* 6752–6756. doi:10.1021/jm901241e
5. Leeson, P. D.; Springthorpe, B. *Nat. Rev. Drug Discovery* **2007,** *6,* 881–890. doi:10.1038/nrd2445
6. Kortagere, S.; Krasowski, M. D.; Ekins, S. *Trends Pharmacol. Sci.* **2009,** *30,* 138–147. doi:10.1016/j.tips.2008.12.001
7. Neochoritis, C. G.; Zhao, T.; Dömling, A. *Chem. Rev.* **2019,** *119,* 1970–2042. doi:10.1021/acs.chemrev.8b00564
8. Sarvary, A.; Maleki, A. *Mol. Diversity* **2015,** *19,* 189–212. doi:10.1007/s11030-014-9553-3
9. Maleki, A.; Sarvary, A. *RSC Adv.* **2015,** *5,* 60938–60955. doi:10.1039/c5ra11531k
10. Herr, R. J. *Bioorg. Med. Chem.* **2002,** *10,* 3379–3393. doi:10.1016/s0968-0896(02)00239-0
11. Lv, F.; Liu, Y.; Zou, J.; Zhang, D.; Yao, Z. *Dyes Pigm.* **2006,** *68,* 211–216. doi:10.1016/j.dyepig.2004.07.017
12. Shmatova, O. I.; Nenajdenko, V. G. *J. Org. Chem.* **2013,** *78,* 9214–9222. doi:10.1021/jo401428q
13. Wang, Y.; Patil, P.; Dömling, A. *Synthesis* **2016,** *48,* 3701–3712. doi:10.1055/s-0035-1562435
14. Zarganes-Tzitzikas, T.; Patil, P.; Khoury, K.; Herdtweck, E.; Dömling, A. *Eur. J. Org. Chem.* **2015,** 51–55. doi:10.1002/ejoc.201403401
15. Liao, G. P.; Abdelraheem, E. M. M.; Neochoritis, C. G.; Kurpiewska, K.; Kalinowska-Tłuścik, J.; McGowan, D. C.; Dömling, A. *Org. Lett.* **2015,** *17,* 4980–4983. doi:10.1021/acs.orglett.5b02419
16. Yamamoto, K.; Suzuki, T.; Imamura, R.; Nagano, T.; Okabe, T.; Miyachi, H. *Bioorg. Med. Chem. Lett.* **2017,** *27,* 2567–2570. doi:10.1016/j.bmcl.2017.03.083
17. Małecki, P. H.; Rüger, N.; Roatsch, M.; Krylova, O.; Link, A.; Jung, M.; Heinemann, U.; Weiss, M. S. *ChemMedChem* **2019,** *14,* 1828–1839. doi:10.1002/cmdc.201900441
18. Schaffert, E. S.; Höfner, G.; Wanner, K. T. *Bioorg. Med. Chem.* **2011,** *19,* 6492–6504. doi:10.1016/j.bmc.2011.08.039
19. Chandgude, A. L.; Dömling, A. *Green Chem.* **2016,** *18,* 3718–3721. doi:10.1039/c6gc00910g
20. Kappe, C. O. *Angew. Chem., Int. Ed.* **2004,** *43,* 6250–6284. doi:10.1002/anie.200400655
21. Chandgude, A. L.; Dömling, A. *Eur. J. Org. Chem.* **2016,** 2383–2387. doi:10.1002/ejoc.201600317
22. Mancuso, A. J.; Brownfain, D. S.; Swern, D. *J. Org. Chem.* **1979,** *44,* 4148–4150. doi:10.1021/jo01337a028
23. Mancuso, A. J.; Huang, S.-L.; Swern, D. *J. Org. Chem.* **1978,** *43,* 2480–2482. doi:10.1021/jo00406a041
24. Dondoni, A.; Perrone, D. *Org. Synth.* **2004,** *10,* 64–77. doi:10.15227/orgsyn.077.0064
25. Sun, Y.; Wang, Z.; Yang, H.; Zhu, X.; Wu, H.; Ma, L.; Xu, F.; Hong, W.; Wang, H. *Int. J. Mol. Sci.* **2019,** *20,* 3840. doi:10.3390/ijms20153840
26. Zinner, G.; Moderhack, D.; Hantelmann, O.; Bock, W. *Chem. Ber.* **1974,** *107,* 2947–2955. doi:10.1002/cber.19741070918
27. Moderhack, D. *Justus Liebigs Ann. Chem.* **1972,** *758,* 29–42. doi:10.1002/jlac.19727580104
28. Prieto, A.; Halland, N.; Jørgensen, K. A. *Org. Lett.* **2005,** *7,* 3897–3900. doi:10.1021/ol051301m
29. Moderhack, D. *J. Prakt. Chem.* **1998,** *340,* 687–709. doi:10.1002/prac.19983400802
30. Ugi, I.; Meyr, R. *Chem. Ber.* **1961,** *94,* 2229–2233. doi:10.1002/cber.19610940844
31. Zarganes-Tzitzikas, T.; Chandgude, A. L.; Dömling, A. *Chem. Rec.* **2015,** *15,* 981–996. doi:10.1002/tcr.201500201
32. Dömling, A.; Wang, W.; Wang, K. *Chem. Rev.* **2012,** *112,* 3083–3135. doi:10.1021/cr100233r
33. Chandgude, A. L.; Dömling, A. *Org. Lett.* **2016,** *18,* 6396–6399. doi:10.1021/acs.orglett.6b03293
34. Ugi, I. *Angew. Chem., Int. Ed. Engl.* **1962,** *1,* 8–21. doi:10.1002/anie.196200081
35. El Kaïm, L.; Grimaud, L.; Oble, J. *Angew. Chem., Int. Ed.* **2005,** *44,* 7961–7964. doi:10.1002/anie.200502636
36. Chandgude, A. L.; Dömling, A. *Org. Lett.* **2017,** *19,* 1228–1231. doi:10.1021/acs.orglett.7b00205
37. Murray, C. W.; Rees, D. C. *Nat. Chem.* **2009,** *1,* 187–192. doi:10.1038/nchem.217

License and Terms

This is an open access article licensed under the terms of the Beilstein-Institut Open Access License Agreement (https://www.beilstein-journals.org/bjoc/terms), which is identical to the Creative Commons Attribution 4.0 International License (https://creativecommons.org/licenses/by/4.0). The reuse of material under this license requires that the author(s), source and license are credited. Third-party material in this article could be subject to other licenses (typically indicated in the credit line), and in this case, users are required to obtain permission from the license holder to reuse the material.

The definitive version of this article is the electronic one which can be found at:
https://doi.org/10.3762/bjoc.20.85

BEILSTEIN JOURNAL OF ORGANIC CHEMISTRY

Carbonylative synthesis and functionalization of indoles

Alex De Salvo[1,2], Raffaella Mancuso[*1] and Xiao-Feng Wu[*2,3]

Review

Open Access

Address:
[1]Laboratory of Industrial and Synthetic Organic Chemistry (LISOC), Department of Chemistry and Chemical Technologies, University of Calabria, Via Pietro Bucci 12/C, 87036 Arcavacata di Rende (CS), Italy, [2]Leibniz-Institut für Katalyse e.V., Albert-Einstein-Str. 29a, 18059 Rostock, Germany and [3]Dalian National Laboratory for Clean Energy, Dalian Institute of Chemical Physics, Chinese Academy of Sciences, 116023 Liaoning, China

Email:
Raffaella Mancuso[*] - raffaella.mancuso@unical.it; Xiao-Feng Wu[*] - xwu2020@dicp.ac.cn

* Corresponding author

Keywords:
carbonylation; functionalization; indole; metal catalyst; organometallic chemistry

Beilstein J. Org. Chem. **2024,** *20,* 973–1000.
https://doi.org/10.3762/bjoc.20.87

Received: 21 February 2024
Accepted: 19 April 2024
Published: 30 April 2024

This article is part of the thematic issue "Multicomponent reactions IV".

Associate Editor: T. J. J. Müller

© 2024 De Salvo et al.; licensee Beilstein-Institut.
License and terms: see end of document.

Abstract

Carbonylation processes have become widely recognized as a versatile, convenient, and low-cost method for the synthesis of high-value compounds. Given the great importance of heterocyclic compounds, the carbonylative approach has become increasingly important for their synthesis. In this mini-review, as a class of benzo-fused nitrogen-containing heterocyclic compounds, we summarized and discussed the recent achievements on the synthesis and functionalization of indole derivatives via carbonylative approaches.

Introduction

Indole is a heterocyclic compound consisting of a benzene ring fused with a pyrrole ring. It was discovered in 1866 by Baeyer and Knop as the basic structure of the natural dye indigo, from which it is derived [1]. The indole ring is a common structural element found in both natural and synthetic products, including pharmaceuticals, agrochemicals, dyes, herbicides, and materials [2-4]. The indole core is particularly noteworthy for its role in various biologically active compounds and drugs, such as antihypertensives, anti-inflammatories, antimycotics, antimigrants, anticancer drugs, and many others [5-7]. The first synthesis of indole has been introduced by Fischer in 1883 and involves its synthesis from phenylhydrazine and an aldehyde or ketone using an appropriate acid catalyst [8]. In the following years, new processes were developed for the synthesis of indole such as the Castro, Bischler, and Larock synthesis etc. [2,9,10]. Carbonylation reactions represent a powerful method for the introduction of a C1 building block into organic substrates using carbon monoxide, its surrogates, or compounds able to act as carbon monoxide sources [11]. In recent years, many groups have used the carbonylation approach for the synthesis and functionalization of indoles, which is what we are discussing in this mini-review.

Review

Carbonylative synthesis of indoles

Synthesis of indoles by Pd(0)-catalyzed carbonylation reaction of halide compounds

Processes using organic halides as their starting materials involving the oxidative addition of Pd(0) to C–X bonds to give Ar–Pd^{II}–X complexes are important for the synthesis of heterocyclic and non-heterocyclic compounds. In 2009, Arthuis and co-workers developed a new process for the synthesis of 2-aroylindoles and 2-heteroaroylindoles by a one-pot palladium-catalyzed domino reaction that involves an initial C,N-coupling followed by carbon monoxide insertion, and Suzuki–Miyaura coupling reaction, from 2-*gem*-dibromovinylaniline [12]. In the presence of $Pd(PPh_3)_4$ (5 mol %) as catalyst, 5 equivalents of base (K_2CO_3), an aryl- or heteroarylboronic ester (1.1 equivalents), CO (12 bar), in dioxane at 100 °C after 16 h the indole derivatives were isolated with good yields (Scheme 1).

Instead, in the Senadi et al. approach, 1-(3-amino)-1*H*-indol-2-yl)-1-ketones were obtained through a Pd(0)-catalyzed cascade process consisting of isonitrile insertion as carbon monoxide surrogate and a C–H cross-coupling [13]. The reaction took place in the presence of K_2CO_3 (3 equiv) as base, an isonitrile (1.2 equiv), and $Pd(OAc)_2$ (10 mol %) which in situ undergoes a reduction to Pd(0) (Scheme 2). Another example was published by Wu's group, who carried out the synthesis of 1-(1*H*-indol-1-yl)-2-arylethan-1-one derivatives by promoting the formation of amides from 2-alkynylanilines by using TFBen (benzene-1,3,5-triyl triformate) as a CO source, $Pd(OAc)_2$, DPEPhos (bis[(2-diphenylphosphino)phenyl] ether), and DIPEA (*N*,*N*-diisopropylethylamine) in MeCN. After 24 h,

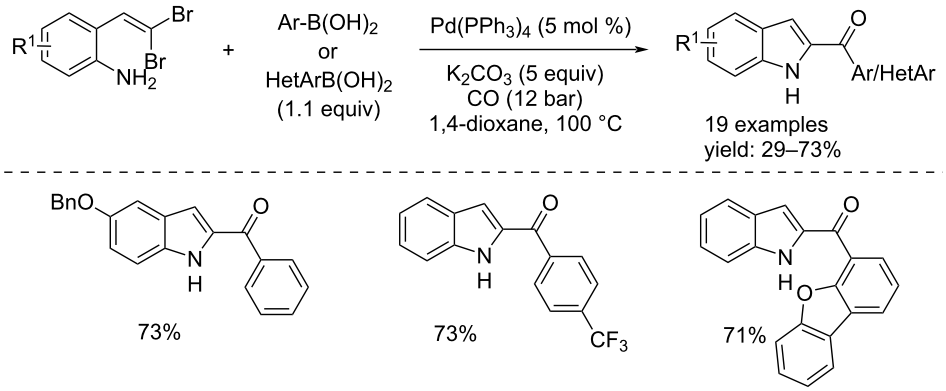

Scheme 1: Pd(0)-catalyzed domino C,N-coupling/carbonylation/Suzuki coupling reaction for the synthesis of 2-aroylindoles and 2-heteroaroylindoles.

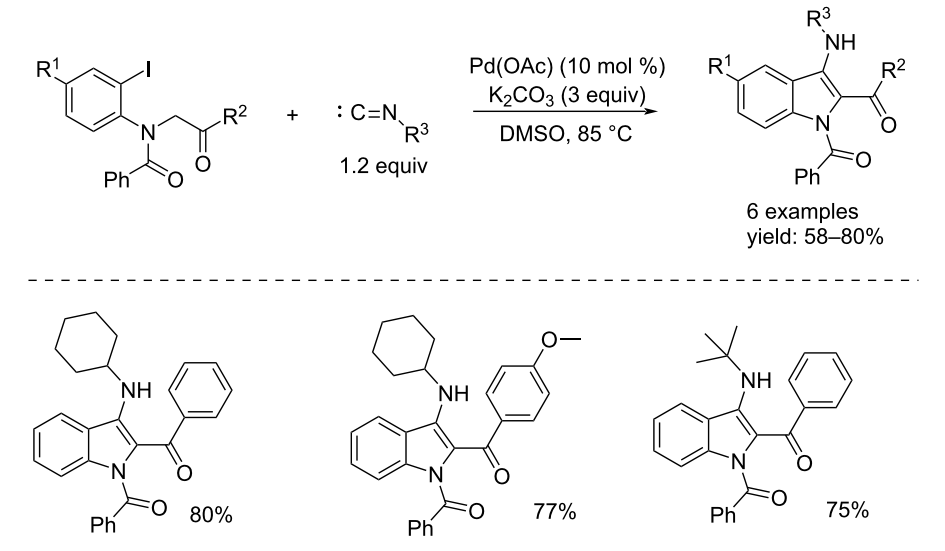

Scheme 2: Pd(0)-catalyzed single isonitrile insertion: synthesis of 1-(3-amino)-1*H*-indol-2-yl)-1-ketones.

$Pd(OAc)_2$ and $AlCl_3$ were added to promote a selective cyclization reaction [14]. The reaction mechanism proceeds with an initial reduction of Pd(II) to Pd(0) followed by oxidative addition on the $ArCH_2$–Cl bond to form the $ArCH_2$–Pd^{II}–Cl complex. Then, insertion of CO, from TFBen, takes place followed by nucleophilic displacement and reductive elimination. The obtained compound undergoes selective cyclization to the indole derivative in the presence of $Pd(OAc)_2$ and $AlCl_3$. A variety of indole derivatives were synthetized in good isolated yields (Scheme 3).

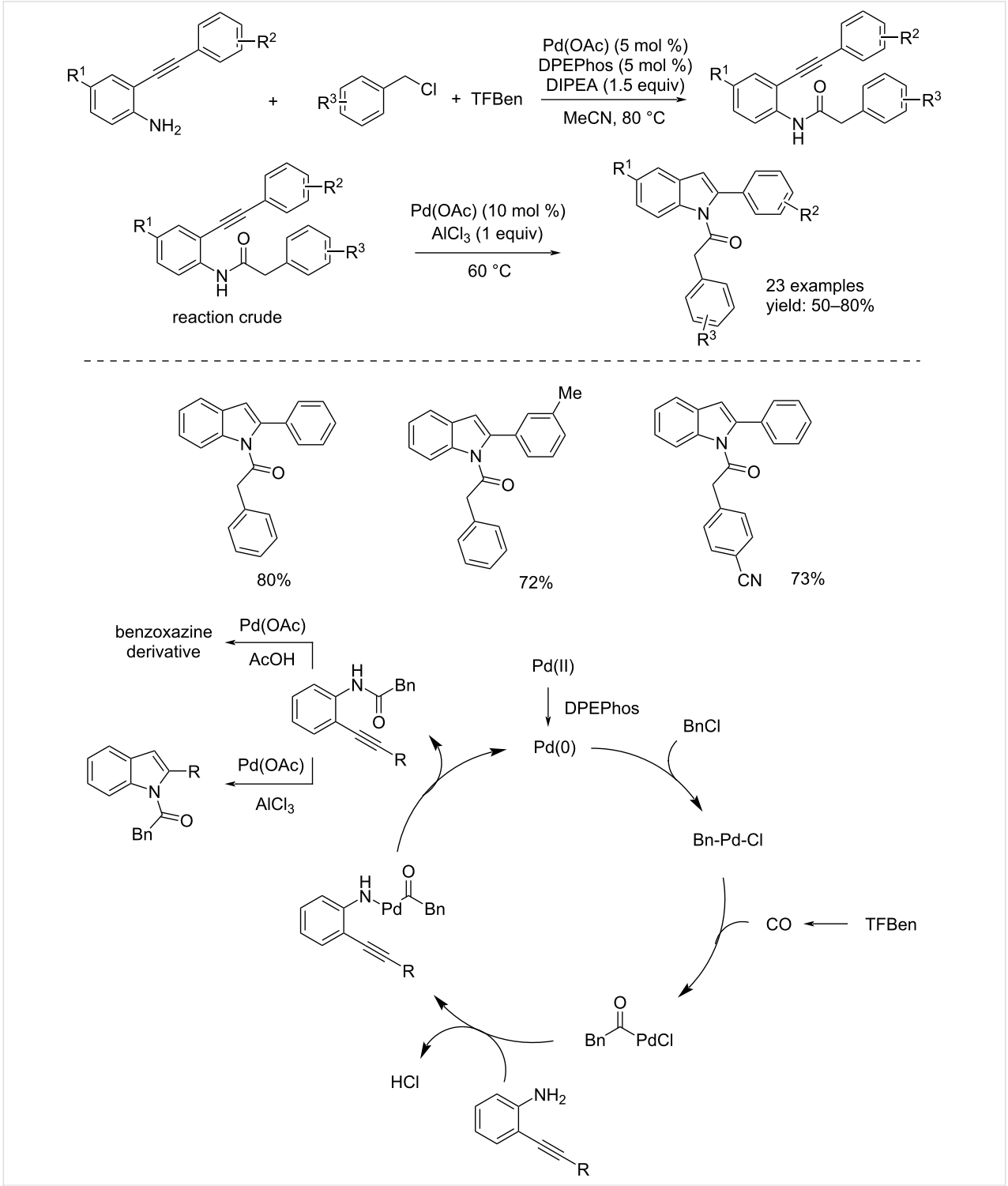

Scheme 3: Pd(0)-catalyzed gas-free carbonylation of 2-alkynylanilines to 1-(1*H*-indol-1-yl)-2-arylethan-1-ones.

Synthesis of indoles by Pd(II)-catalyzed carbonylation reaction

Oxidative carbonylation reactions, as well as all other types of carbonylation reactions, represent a simple and more environmentally friendly method for the synthesis of important organic compounds. Since the development of the Wacker process, the study of oxidative carbonylations has made enormous progress by investigating even the possibility of catalyzing carbonylative heterocyclization reactions by exploiting the electrophilic character of Pd(II) species. Starting from substrates bearing a triple bond and a nucleophile in the appropriate position, a versatile process of heterocyclization can be initiated, resulting in indole derivatives with important properties. Gabriele et al., in two different periods, reported two paradigmatic examples for indole syntheses. In 2010, they developed the synthesis of 1-(alkoxyarylmethyl)indole-3-carboxylic esters from 2-alkynylaniline imines by using PdI_2/KI as catalyst system and oxygen as oxidant [15]. In particular, the reaction was carried out using 2 mol % of PdI_2, 20 mol % of KI and 40 bar of a 4:1 mixture of CO–air, in methanol or ethanol in the presence of an *ortho*-ester (1:3 mixture) as solvent to prevent hydrolysis of the substrate. After 15 hours at 80 °C the indoles derivatives were isolated in good yields (Scheme 4).

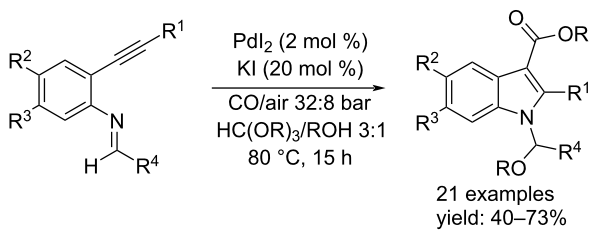

Scheme 4: Pd(II)-catalyzed heterocyclization/alkoxycarbonylation of 2-alkynylaniline imines.

Two years later, they performed, using the same catalytic and oxidative conditions, another oxidative heterocyclization/alkoxycarbonylation process for the synthesis of *N*-substituted indole-3-carboxylic esters and N–H free indole-3-carboxylic esters from *N*-substituted 2-alkynylanilines and 2-alkynylanilines bearing a secondary amino group and an internal triple bond [16]. In the same research group, it has been demonstrated that with a terminal alkynyl group, the reactivity is completely different leading to the formation of dihydroindol-2-one derivatives [17]. The process was versatile and efficient towards the formation of *N*-substituted indole derivatives from *N*-substituted anilines. The direct PdI_2/KI oxidative carbonylation of 2-alkynylanilines does not lead to the formation of indole-3-carboxylic esters but to the formation of acyclic carbamates. For this reason, they performed the reaction in the presence of trimethyl orthoformate to transform, in situ, the primary amino group into a secondary amino group with an easy-to-remove substituent thus performing a not direct synthesis process. Indeed, the desired N–H-free product was obtained by acidic treatment of the reaction crude. In both cases, the targeted products were isolated in good yields (Scheme 5).

In 2014, Shen and co-workers developed a selective synthesis for methyl 1-benzyl-1*H*-indole-3-carboxylates and bis(1-benzyl-1*H*-indol-3-yl)methanones [18] starting from the same kind of substrates used by Gabriele's group two years before. The first indole derivatives were obtained by catalyzing the reaction with 5 mol % of $Pd(tfa)_2$ (palladium(II) trifluoroacetate) and 1.5 equivalents of *p*-benzoquinone as oxidant in a 1:5 DMSO/MeOH solvent mixture at a temperature between 0 °C and 15 °C and, for a time between 48 and 120 hours depending on the substrate. In the second case the reaction was catalyzed under the same conditions except for changing the solvent to iPrOH and the catalyst to [$Pd(tfa)_2$L] (Scheme 5).

Furthermore, Gabriele and co-workers developed the oxidative carbonylation of 1-(2-aminoaryl)-2-yn-1-ols to quinoline-3-carboxylic esters. Meanwhile, they also discovered that by conducting the reaction under non-oxidative conditions the reaction mechanism changed, leading to the formation of indol-2-acetic esters via the H–Pd^{II}–I species formed in situ [19]. The reaction was performed in the presence of PdI_2 and KI (2 mol % and 20 mol %, respectively) in methanol under 90 bar of CO at 100 °C for two hours (Scheme 6).

As already seen, triple bonds can be activated by Pd(II) catalysts towards the addition of nucleophiles in the right position, leading to heterocyclization reactions. Taking advantage of this possibility, in the Della Cá group, a carbonylative double cyclization process was developed obtaining 3,4-dihydro-1*H*-furo[3,4-*b*]indol-1-ones from suitably functionalized 2-alkynylanilines [20]. The reaction occurs in the presence of PdI_2 (1 mol %) as catalyst and KI (10 mol %) as co-catalyst in MeCN at 120 °C for 24 h. At the end of the process the catalyst undergoes reduction, therefore, rather using only CO, a mixture of CO–air (12:48 bar) was used with the aim of oxidizing the Pd(0) species in order to restore the catalyst able to catalyze the process again. The reaction mechanism proceeds with an initial interaction between the Pd(II) species and the triple bond that promotes an intramolecular nucleophilic attack of the amino group giving a indolcyclopalladium species. This is followed by CO insertion and intramolecular nucleophilic displacement by the hydroxy group to give the indole–Pd^{II}-cycle derivate. The reaction ends with a reductive elimination and the generated Pd(0) species gets oxidated by the oxygen to the active Pd(II) species (Scheme 7).

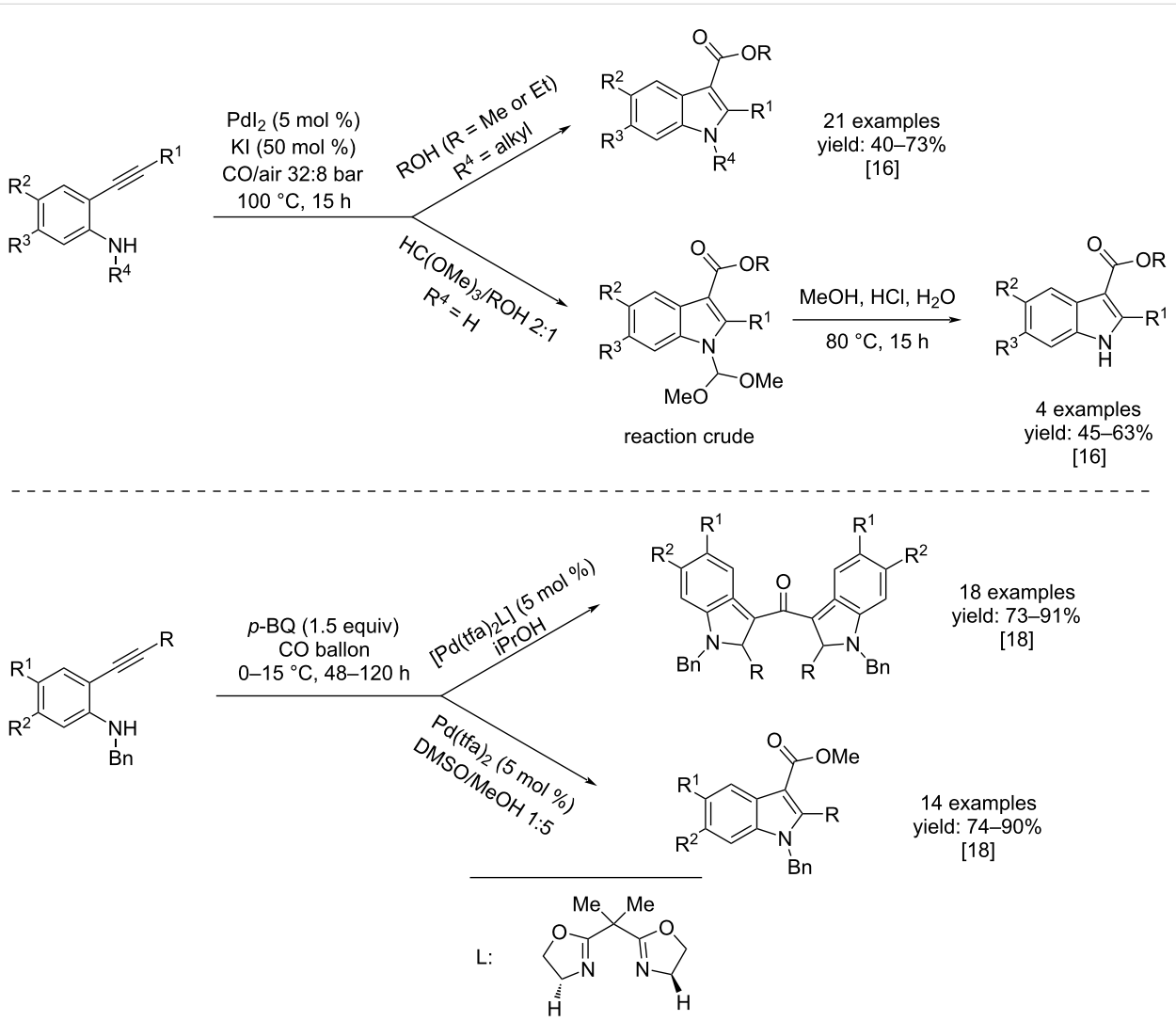

Scheme 5: Pd(II)-catalyzed heterocyclization/alkoxycarbonylation of 2-alkynylanilines to *N*-substituted indole-3-carboxylic esters and indole-3-carboxylic esters (top). Pd(II)-catalyzed selective carbonylation of 2-alkynylaniline to methyl 1-benzyl-1*H*-indole-3-carboxylates and bis(1-benzyl-1*H*-indol-3-yl)methanones (bottom).

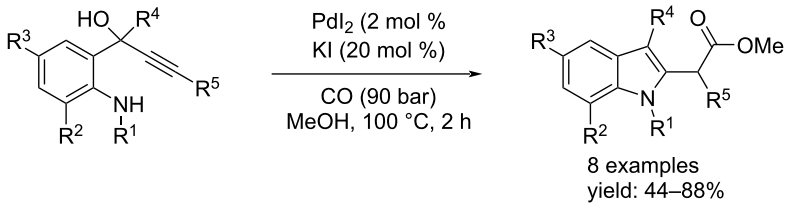

Scheme 6: Synthesis of indol-2-acetic esters by Pd(II)-catalyzed carbonylation of 1-(2-aminoaryl)-2-yn-1-ols.

Synthesis of indoles by metal-catalyzed reductive cyclization reaction of organic nitro compounds with carbon monoxide as reductant

In the last 60 years, the metal-catalyzed carbonylative reduction approach of organic nitro compounds has been used for the synthesis of important industrial and pharmaceutical compounds such as indoles. In 1986, Cenini et al. reported a new synthetic method for indoles that involved 2-nitrostyrene derivatives. The reaction took place under drastic conditions (200 °C and 80 bar CO) for 5 hours in the presence of catalysts such as

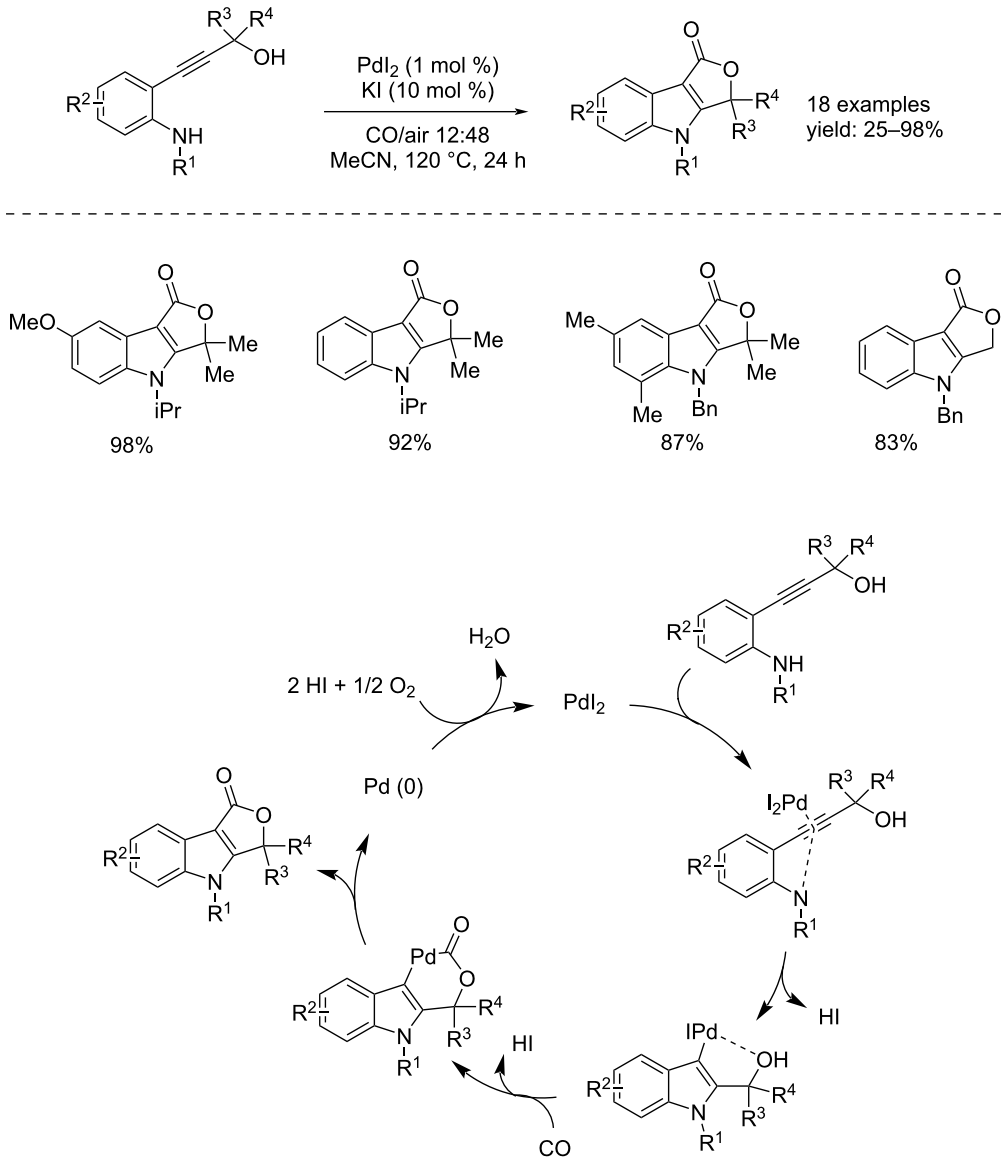

Scheme 7: Pd(II)-catalyzed carbonylative double cyclization of suitably functionalized 2-alkynylanilines to 3,4-dihydro-1*H*-furo[3,4-*b*]indol-1-ones.

$Fe(CO)_5$, $Ru_3(CO)_{12}$, or $Rh_6(CO)_{16}$ [21]. The process was not selective because aniline derivatives and other byproducts were also formed; moreover, the substrate conversion, in some cases, was not complete (Scheme 8).

In subsequent years, this kind of synthesis was investigated by other groups. Watanabe's group improved the process by studying the reactivity of $Pd(PPh_3)_2/SnCl_2$ as a new catalyst system [22]. This made it possible to conduct the reaction under milder conditions, making the process less expensive and more environmentally friendly. Indeed, the reaction was carried out under 20 bar of CO at 100 °C for 16 h. The indole derivatives were obtained in moderate to good yields and complete conversion of the substrates was observed (Scheme 9).

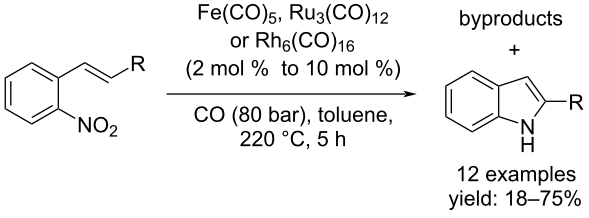

Scheme 8: Indole synthesis by deoxygenation reactions of nitro compounds reported by Cenini et al. [21].

In 1997, Söderberg and co-workers reported a more sustainable procedure. In this protocol the use of a Lewis base such as $SnCl_2$ was not required and the reaction took place under milder

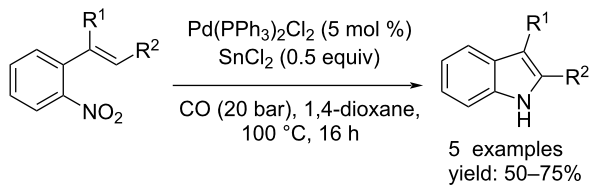

Scheme 9: Indole synthesis by reduction of nitro compounds: approach reported by Watanabe et al. [22].

conditions using $Pd(OAc)_2$ as catalyst and PPh_3 as ligand. The reaction was performed at 70 °C for 15–48 hours, under 4 bar of CO in a DMF/MeOH 2:1 mixture giving the indole derivatives without obvious byproducts (Scheme 10) [23].

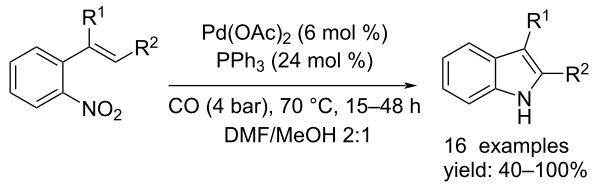

Scheme 10: Indole synthesis from *o*-nitrostyrene compounds as reported by Söderberg and co-workers [23].

Two years later they developed two Pd-catalyzed reductive *N*-heteroannulations for the synthesis of fused indoles [24] and indoles isolated from two species of *European Basidiomycetes* [25] starting from suitably functionalized nitro compounds. Both in the first case and in the second case the reactions were catalyzed by 6 mol % of $Pd(OAc)_2$ and carried out under 4 bar of CO. The fused indoles were obtained when adding 24 mol % of dppp (1,3-bis(diphenylphosphino)propane) at 120 °C for 70 hours in DMF. Instead, in the other case, PPh_3 was used as ligand at 70 °C for 17–46 hours in CH_3CN (Scheme 11).

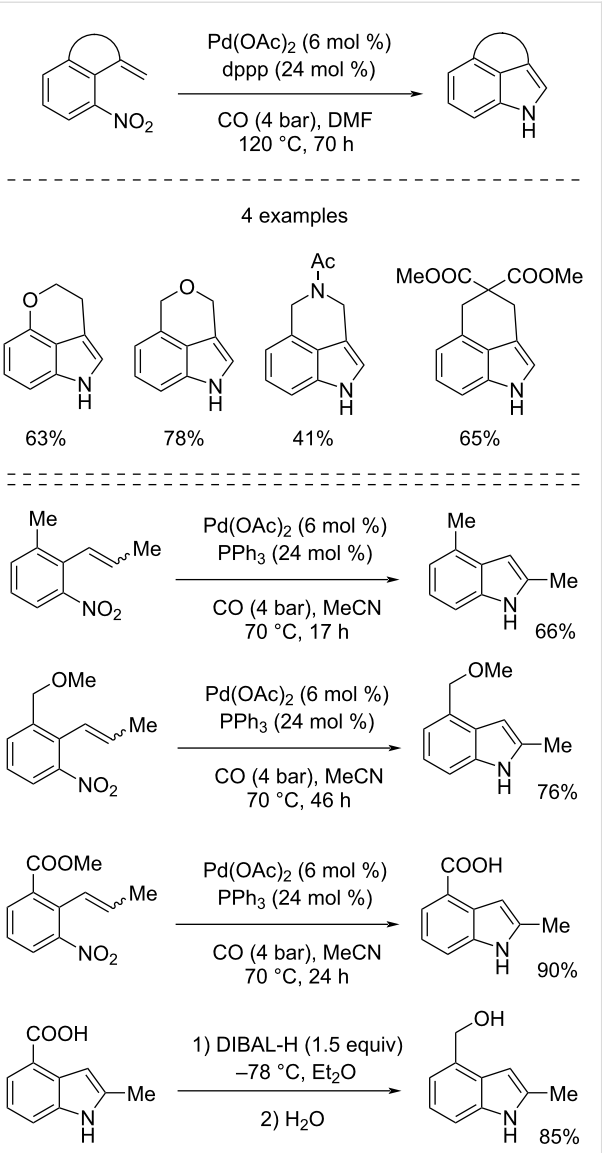

Scheme 11: Synthesis of fused indoles (top) and natural indoles present in two species of *European Basidiomycetes* (bottom) by reductive *N*-heteroannulation of suitably functionalized nitro compounds.

Another interesting example concerns the synthesis of 1,2-dihydro-4(3*H*)-carbazolones by a Pd(0)-catalyzed *N*-heteroannulation of functionalized 2-nitrostyrenes [26]. $Pd(dba)_2$ was able to catalyze the reaction because a five-membered Pd(II)-cyclic species could be formed, favored by the oxidation of the catalyst. The reaction proceeded with dppp and 1,10-phenantroline (12 mol % each) under 6 bar of CO at 80 °C in DMF for 22–96 hours depending on the substrate. After the required reaction time, seven carbazolones were isolated with good yields of up to 89% (Scheme 12).

In 2005, Davies et al. published a paper presenting a new method for the synthesis of indoles from *o*-nitrostyrenes by using a different catalyst system and performing the reaction under mild conditions [27]. At first they decided to change the catalytic system applied by Söderberg using 1,10-phen instead of PPh_3 as ligand, because it was already known that catalysts derived from palladium(II) salts and bidentate nitrogen ligands were highly reactive systems for the reduction of *o*-nitrostyrenes [28-30]. The catalytic system $Pd(OAc)_2$/1,10-phen worked better than Söderberg´s one ($Pd(OAc)_2/PPh_3$) under mild conditions. In addition, $Pd(phen)_2(BF_4)_2$ and $Pd(tfa)_2$ in conjunction with tertramethyl-1,10-phenanthroline (tm-phen) reactivity were investigated. The process was generalized: by using $Pd(OAc)_2$ (1–1.5 mol %) and 1,10-phen (2–3 mol %) to catalyze the reaction of some substrates and $Pd(tfa)_2$ (0.1–1 mol %) and tm-phen (0.7–2 mol %) for others, 14 indole derivatives were isolated with yields of up to 100%. Among the

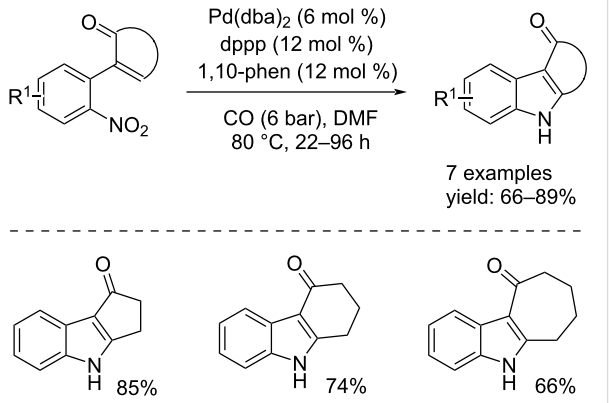

Scheme 12: Synthesis of 1,2-dihydro-4(3*H*)-carbazolones through *N*-heteroannulation of functionalized 2-nitrostyrenes in the presence of the $Pd(dba)_2$/dppp/1,10-phen catalyst system.

14 examples is a more soluble derivative of a KDR kinase inhibitor identified by researchers from Merck for blocking tumor-induced angiogenesis [31] (Scheme 13).

An interesting synthesis of 3-arylindoles by reductive carbonylation of unfunctionalized nitroarenes in the presence of arylalkynes and $Pd(phen)_2(BF_4)_2$ as catalyst has been demonstrated by Cenini's group. The reaction was regioselective, with no detection of 2-arylindole byproducts. No prefunctionalization of the *ortho* position of the nitroarene is required for the reaction [32]. When $Pd(phen)_2(BF_4)_2$ was used in conjunction with $Ru_3(CO)_{12}$ the yield of the indole products increased. Additionally, when 4-fluorophenylacetylene and nitrobenzene were used as substrates the indole skeleton of fluvastatin and other pharmaceutically active compounds was obtained in one step [33].

Clawson et al. showed that it was possible to achieve the synthesis of substituted 3-alkoxyindoles via the palladium-catalyzed reductive *N*-heteroannulation of 1-(2-nitrophenyl)-1-alkoxyalkenes. Only in one case 2-(1-ethoxyvinyl)-3-nitropyridine was used [34]. The reactions were catalyzed through $Pd(dba)_2$, dppp, 1,10-phenantroline under 6 bar of CO at 120 °C in DMF and the products were obtained within 48–96 hours. All

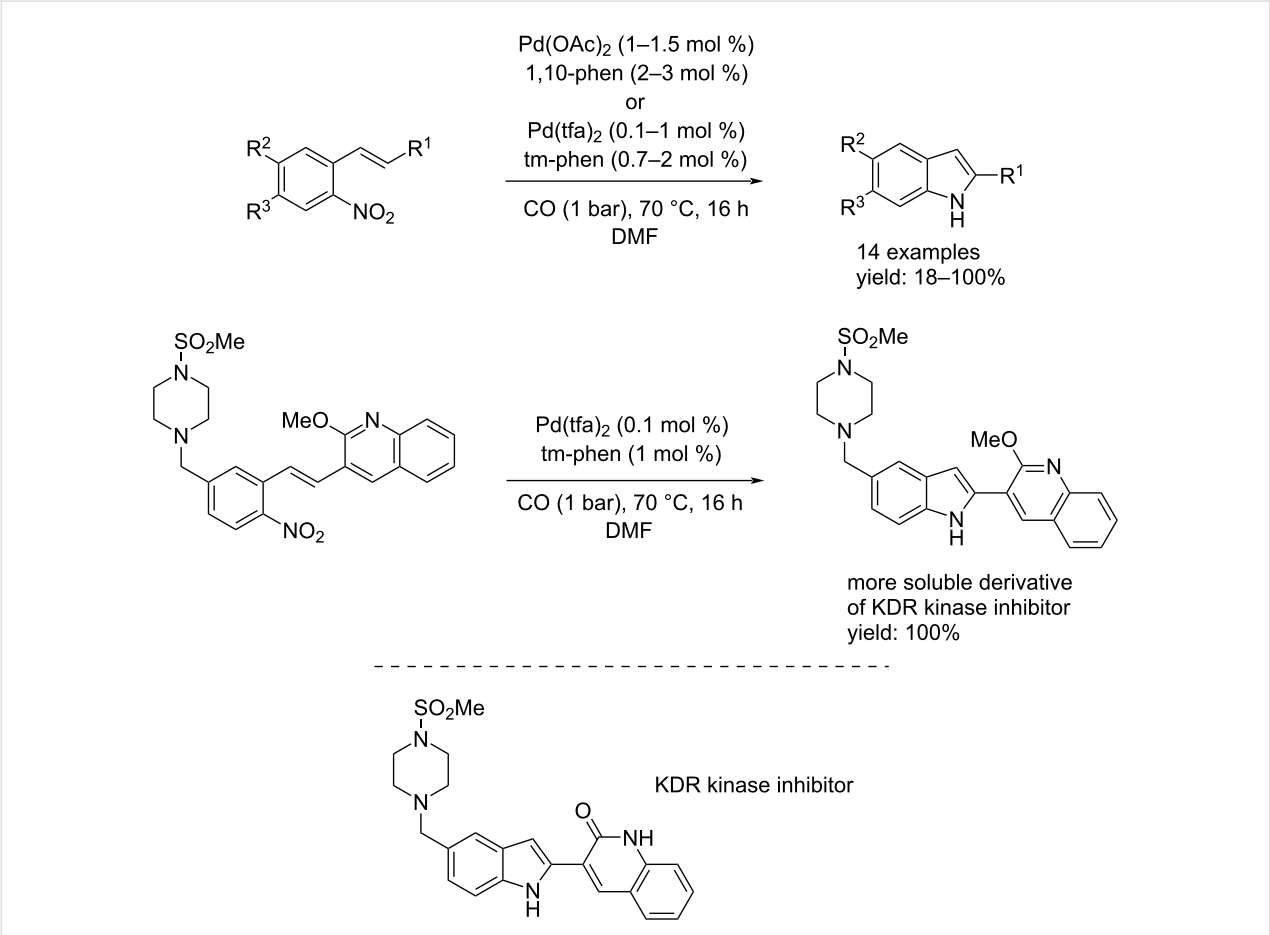

Scheme 13: Synthesis of indoles from *o*-nitrostyrenes by using $Pd(OAc)_2$ and $Pd(tfa)_2$ in conjunction with bidentate nitrogen ligands: 1,10-phen (1,10-phenanthroline) and tm-phen (3,4,7,8-tetramethyl-1,10-phenanthroline).

products were isolated with good yields except the pyranindole because it decomposed; it could only be isolated after complete oxidation in air. The isolated product was an indol-3-one derivative (Scheme 14).

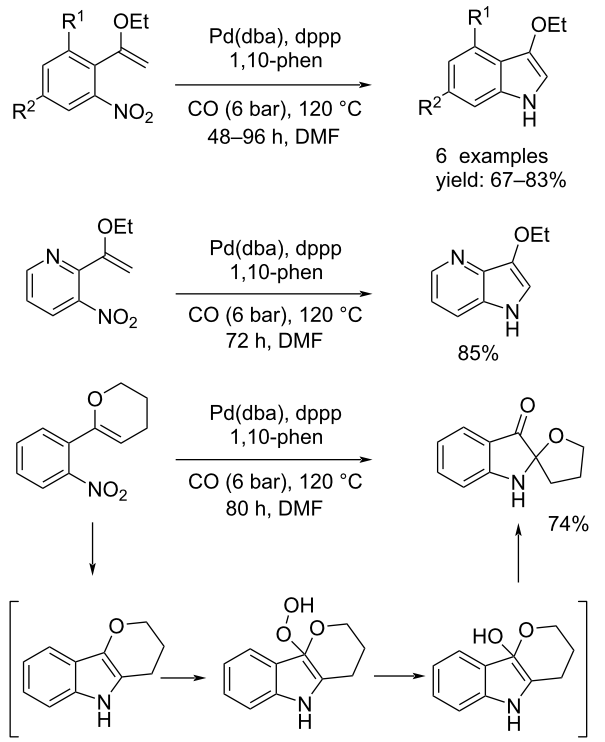

Scheme 14: Synthesis of substituted 3-alkoxyindoles via palladium-catalyzed reductive *N*-heteroannulation.

Another example for the synthesis of 3-substituted indoles was described by Hsieh and Dong [35]. They synthesized 3-arylindoles by palladium-catalyzed C–H bond amination via reduction of nitroalkenes using carbon monoxide as reducing agent. The reaction took place in the presence of $Pd(OAc)_2$ (2 mol %), 1,10-phenantroline (4 mol %) under 1 bar of CO at 110 °C in DMF. After the right time, six products were isolated, while, in three cases, when the benzene ring was *meta*-substituted, a regioisomeric mixture was obtained. The regioselectivity was determined by ^{1}H NMR spectroscopy (Scheme 15).

More recently, in 2016, still in Söderberg's group, the synthesis of 2,2′-bi-1*H*-indoles, 2,3′-bi-1*H*-indoles, 3,3′-bi-1*H*-indoles, indolo[3,2-*b*]indoles, and indolo[2,3-*b*]indoles via reductive cyclization Pd-catalyzed was developed [36]. The reaction was possible starting from nitro compounds with one or two double bonds in the suitable position. The process has been generalized using nitro compounds substituted on the aromatic ring with electron-donating and electron-withdrawing groups. Also the synthesis of 4,4′-diaza-3,3′-bi-1*H*-indole from 2,2'-(buta-1,3-diene-2,3-diyl)bis(3-nitropyridine) was performed. All reactions were carried out in the presence of $Pd(dba)_2$ as catalyst, dppp and 1,10-phen as ligands under 6 bar of CO at 120 °C for the appropriate time. The processes to 2,2′-bi-1*H*-indoles, 2,3′-bi-1*H*-indoles, and 3,3′-bi-1*H*-indoles were selective leading to product formation with good to excellent isolated yields (Scheme 16). On the other hand, the synthesis of indolo[3,2-*b*]indoles and indolo[2,3-*b*]indoles were not selective leading to byproducts such as 5,7-dihydro-6*H*-indolo[2,3-*c*]quinolin-6-one, 5,11-dihydro-6*H*-indolo[3,2-*c*]quinolin-6-one, and indolo[1,2-*c*]quinazolin-6(5*H*)-one derivatives. Finally, starting

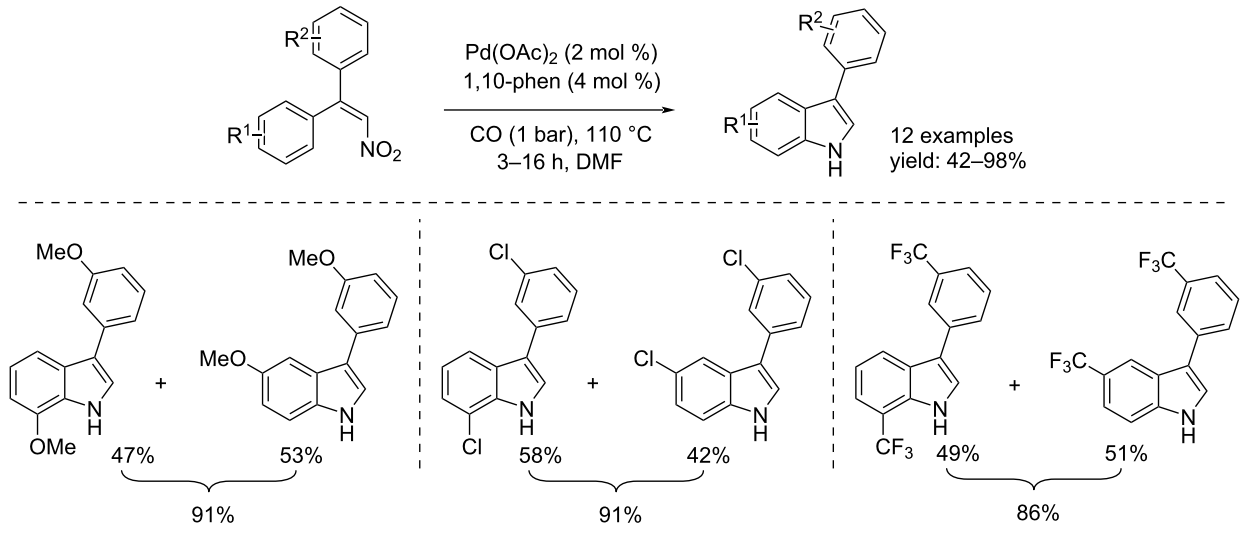

Scheme 15: Synthesis of 3-arylindoles by palladium-catalyzed C–H bond amination via reduction of nitroalkenes.

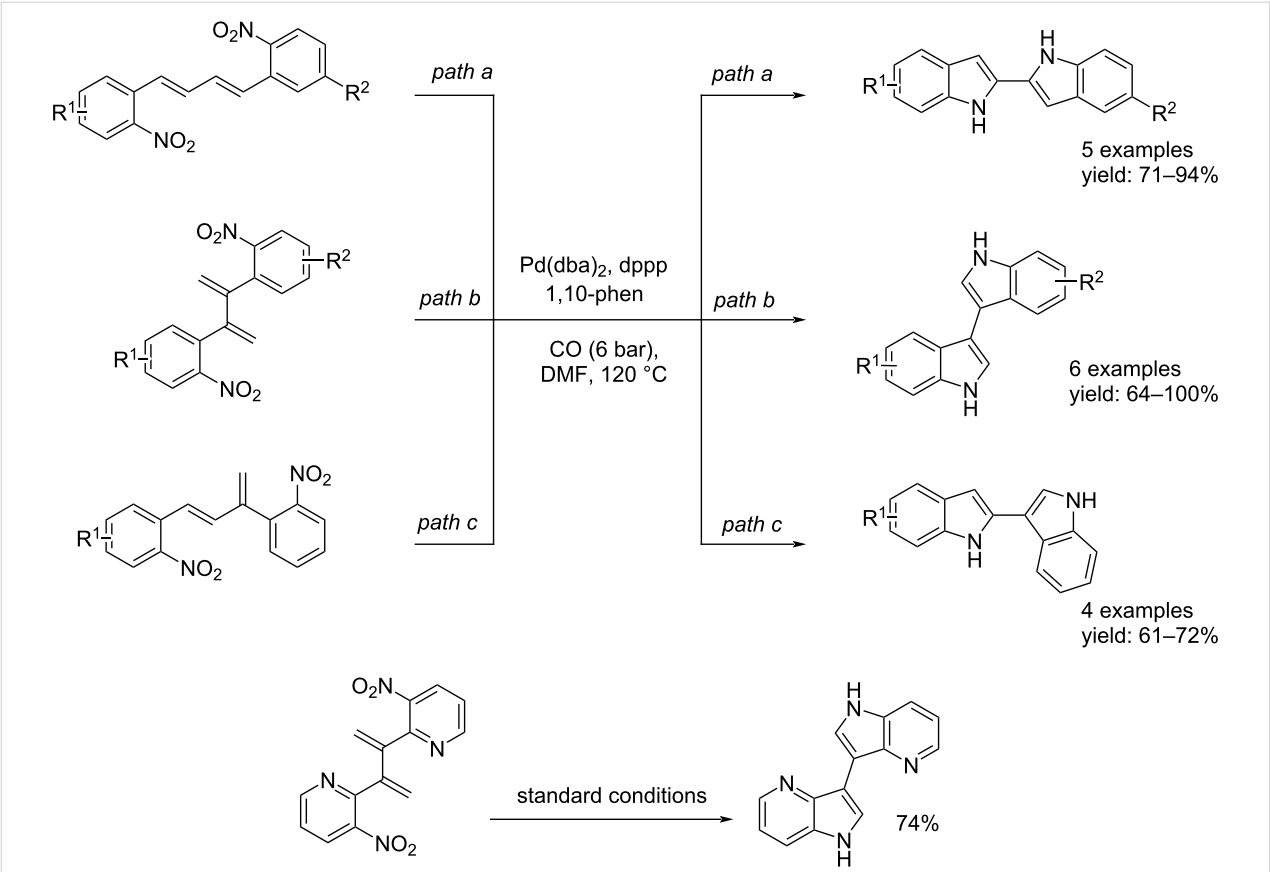

Scheme 16: Synthesis of 2,2′-bi-1*H*-indoles, 2,3′-bi-1*H*-indoles, 3,3′-bi-1*H*-indoles, indolo[3,2-*b*]indoles, indolo[2,3-*b*]indoles, and 4,4′-diaza-3,3′-bi-1*H*-indole.

from 1,2-bis(2-nitrophenyl)ethene and 1-methoxy-2-nitro-3-(2-nitrostyryl)benzene the related indolo[3,2-*b*]indoles were not observed (Scheme 17).

One year later, by using continuous flow technology, Gutmann, Kappe and colleagues developed a palladium-catalyzed transformation of *o*-vinylnitrobenzenes and *o*-nitrostilbenes with carbon monoxide as the reductant to give indoles after cyclization [37]. In the presence of 1–2 mol % of $Pd(OAc)_2$, 1,10-phen (4 mol %) and tributylamine (40 mol %), the desired products were formed in good to excellent yields in CH_3CN under 10–20 bar of CO at 140 °C within 15–30 min and with carbon dioxide as the side-product (Scheme 18).

Carbon monoxide is a cheap gas but its use requires safe and controlled environments and systems because it is highly toxic to human. In addition, reactions in which carbon monoxide is used as a gas require suitable equipment to withstand the high pressures such as autoclaves. The use of compounds able to generate carbon monoxide in situ is a convenient, less dangerous and effective method to perform carbonylation reactions using less complex apparatus. In recent years, many syntheses via carbonylation reactions, without the use of carbon monoxide, have been demonstrated. Regarding the synthesis of indoles, Zhou et al. discovered that the combination of $Mo(CO)_6$, $Pd(OAc)_2$ and 1,10-phen, was suitable to afford 3*H*-indoles from variously substituted nitrostyrenes [38]. CO is generated by heating 1 equiv of $Mo(CO)_6$ at 100 °C in DMF in a sealed glass chamber (chamber 1). Afterwards, the gas passes into another sealed glass chamber (chamber 2) containing the substrate, $Pd(OAc)_2$ (5 mol %), tm-phen (10 mol %) and DMF at the same temperature (Scheme 19).

Ragaini and co-workers, in 2018, 2022 and 2023, developed three procedures for the synthesis of substituted indoles from functionalized nitro compounds by using, in the first two cases phenyl formate as CO source [39,40] and, in the third case formic acid [41]. All of three processes allow the use of inexpensive reactors, in fact, the reactions were carried out in heavy borosilicate tubes. In the first two works, $Pd(MeCN)_2Cl_2$ in conjunction with 1,10-phen were used to catalyze the reactions. In addition, Et_3N was added to the reaction mixture in order to favor the catalyst´s reduction to Pd(0). In the work published in 2022, some substrates led to a non-selective reaction

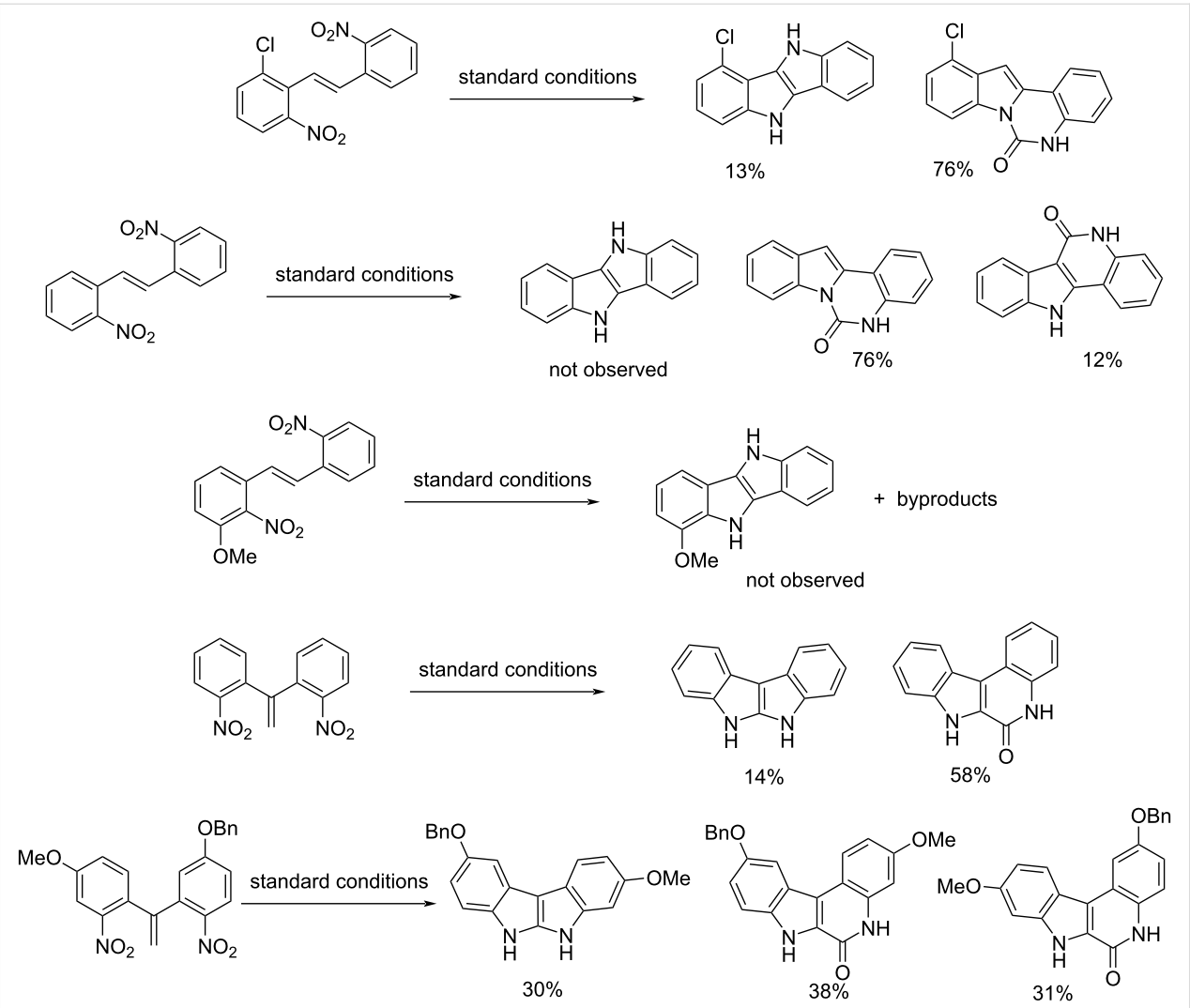

Scheme 17: Pd-catalyzed reductive cyclization of 1,2-bis(2-nitrophenyl)ethene and 1,1-bis(2-nitrophenyl)ethene derivatives.

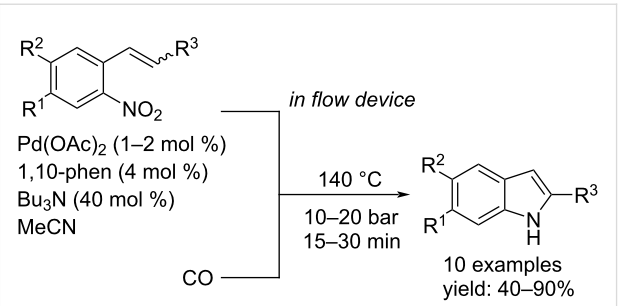

Scheme 18: Flow synthesis of 2-substituted indoles by reductive carbonylation.

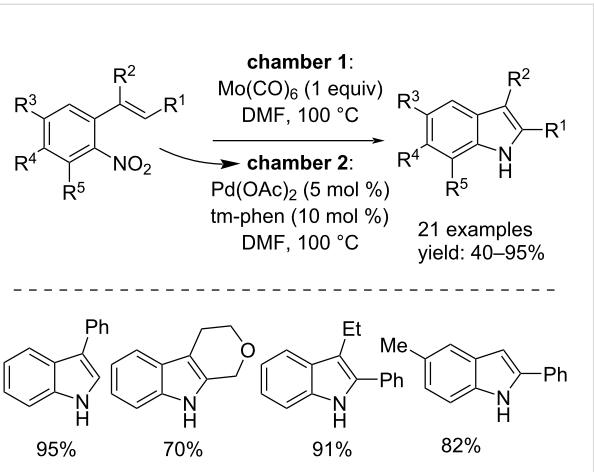

Scheme 19: Pd-catalyzed synthesis of variously substituted 3*H*-indoles from nitrostyrenes by using $Mo(CO)_6$ as CO source.

(Scheme 20). On the other hand, in the approach in which formic acid was used, the catalyst system was $Pd(acac)_2$/1,10-phen. Also, in this case the addition of Et_3N favored the reaction, moreover, Ac_2O was added as additive (Scheme 21).

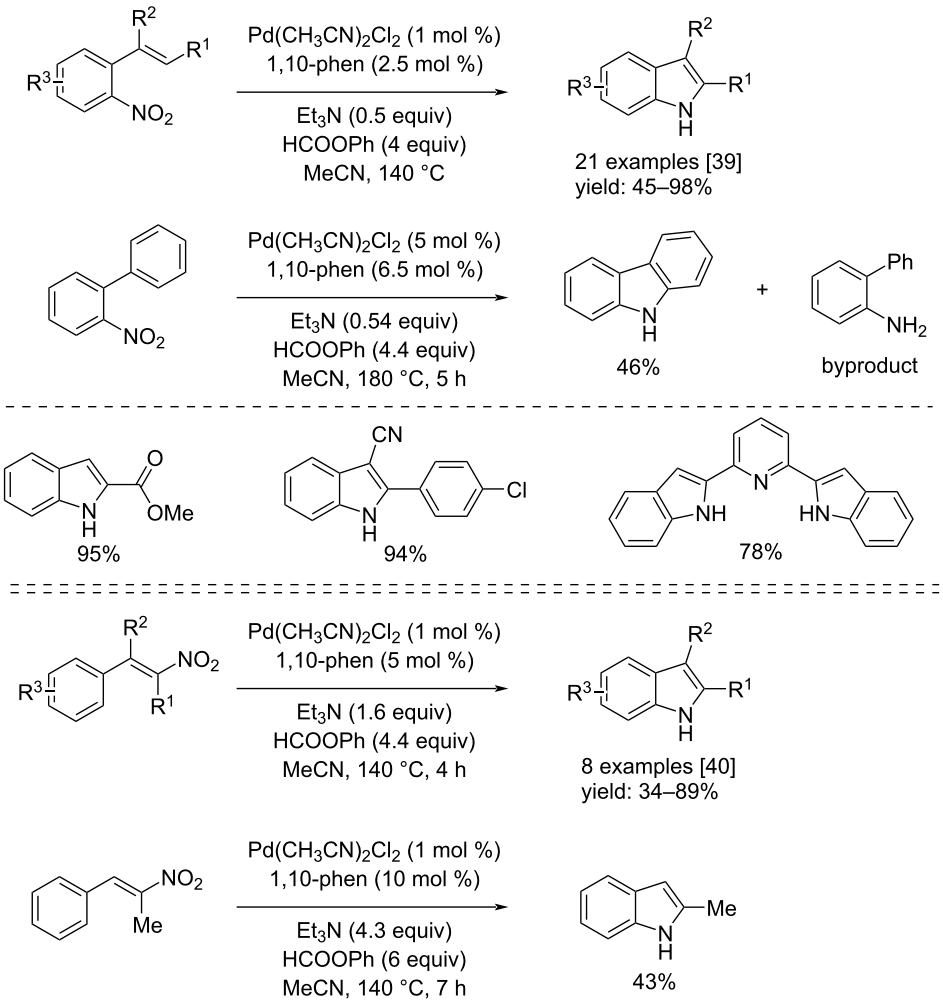

Scheme 20: Synthesis of indoles from substituted 2-nitrostyrenes (top) and ω-nitrostyrenes (bottom) via reductive cyclization with phenyl formate as the carbon monoxide source.

At the same time, Wu and co-workers contributed to the introduction of two new syntheses of *N*-aroylindole derivatives by means of nickel catalysis. In 2021, they reported a nickel-catalyzed carbonylative cyclization of 2-nitroalkynes and aryl iodides with $Co_2(CO)_8$ as the CO source. The reaction was performed in the presence of Ni(dme)Cl_2 (a nickel(II) chloride ethylene glycol dimethyl ether complex), dtbbpy (4,4-di-*tert*-butyl-2,2-dipyridyl), Zn(0) and ZnI_2 in DMF at 120 °C [42] (Scheme 22). The nickel catalyst catalyzed the oxidative addition and CO insertion on aryl iodide compounds, while the Zn/ZnI_2 couple catalyzed the reduction of the nitro group with CO as reductant. The last step is an *N*-cyclization toward the 2-aroylindole formation with moderate to high isolated yields. In the other example, reported one year later, the same kind of compounds was obtained from 2-nitroalkynes and arylboronic pinacol esters [43]. The reaction took place in the presence of Ni(OTf)$_2$, dtbbpy, Zn(0), and TMSCl (trimethylsilyl chloride) in DMF at 130 °C (Scheme 22). The Ni(OTf)$_2$ catalyzed the

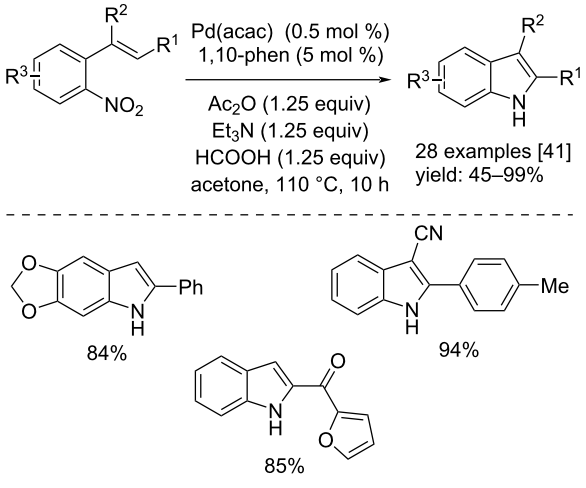

Scheme 21: Synthesis of indoles from substituted 2-nitrostyrenes with formic acid as CO source.

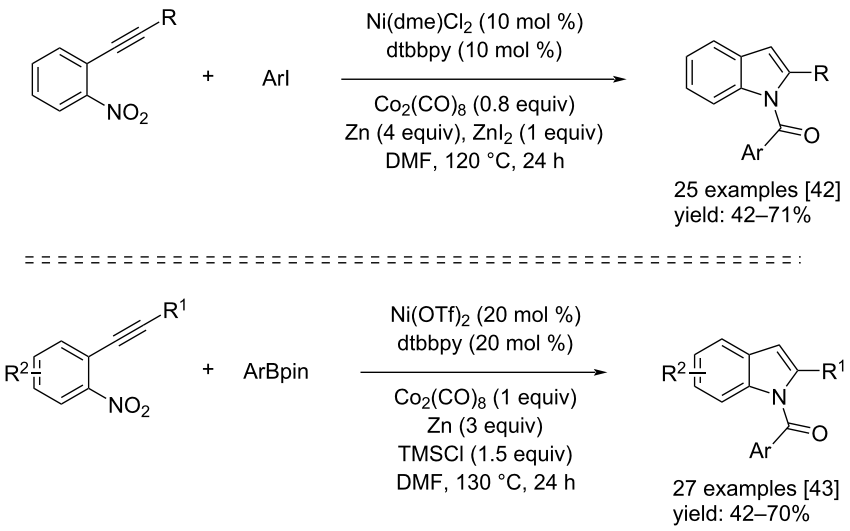

Scheme 22: Ni-catalyzed carbonylative cyclization of 2-nitroalkynes and aryl iodides (top) and the Ni-catalyzed carbonylative cyclization of 2-nitroalkynes and arylboronic pinacol esters (bottom) reported by Wu and co-workers [42,43].

transmetallation reaction with Ar-Bpin and subsequent insertion of CO. The reduction of the nitro group is catalyzed by Zn(0)/TMSCl in the presence of CO. The reaction, again, ends with an *N*-cyclization giving the *N*-aroylindoles with fair to good isolated yields. The reaction mechanisms are reported in Scheme 23.

Synthesis of indoles by Rh-catalyzed carbonylation reactions

In the past, Tang and co-workers, demonstrated that vinyl propargylic esters could be employed as five-carbon atom building blocks in [5 + 2] cycloadditions with alkynes or alkenes by carbene intermediates. Starting from those results they envisaged the benzannulation of heteroaryl propargylic esters favored by CO [44]. The process led to the desired result with some effort because a dearomatization, followed by aromatization, was necessary to achieve the goal. With $[Rh(CO)_2Cl]_2$ or $[Rh(COD)_2]BF_4$ as the catalyst under atmospheric pressure of CO (1 bar), good yields of the desired products were obtained (Scheme 24).

Carbonylative functionalization of indoles

Metal-catalyzed cyclocarbonylative coupling reaction of indoles to 6*H*-isoindolo[2,1-*a*]indol-6-one scaffolds

Substituted 6*H*-isoindolo[2,1-*a*]indol-6-ones are important structural components of many naturally occurring and pharmacologically active compounds [45-51]. They are also relevant intermediates in organic synthesis [52,53]. Therefore, the significance of 6*H*-isoindolo[2,1-*a*]indol-6-ones has led to a long-standing interest in the development of efficient and versatile methods for their synthesis. In 2016, four independent studies reported the first successful application of a metal-catalyzed cyclocarbonylation in an efficient synthetic pathway towards 6*H*-isoindolo[2,1-*a*]indol-6-ones. In three of these, the products were obtained through Pd-catalyzed cyclization of 2-(2-haloaryl)indoles: Yoo et al. reported the synthesis by using various 2-(2-bromophenyl)-1*H*-indoles, $PdCl_2/PPh_3$ as catalyst system in the presence of a base (Et_3N) in toluene at 110 °C for 5 hours under 10 bar of CO [54]. Guo et al. developed the synthesis from substrates of the same chemical nature but using $Pd(OAc)_2/BuPAd_2$ as the catalyst system. In their approach, DABCO was also added to the reaction mixture in DMSO and the reaction was carried out at 120 °C for 12 hours under a low pressure of CO (1 bar) [55]. Another version was reported by Han and co-workers, who synthesized the desired products starting from 2-(2-iodophenyl)-1*H*-indoles, catalyzing the reaction with $Pd(OAc)_2$, PPh_3, and K_2CO_3. The reaction was run in toluene at 100 °C for 24 h under 20 bar of CO [56] (Scheme 25).

The other example, however, accomplished the synthesis through Rh-catalysis from substrates without halogens in their structure. This synthesis was published by Huang et al. who obtained good results by using $[(Cp^*RhCl_2)_2]$ as catalyst to achieve an NH-indole–C–H carbonylation [57]. A base was added to improve the efficiency of the process and an oxidant to restore the catalytic active species. The reaction was carried out under a low pressure of CO (1 bar) at 110 °C in xylene for 24 hours (Scheme 26).

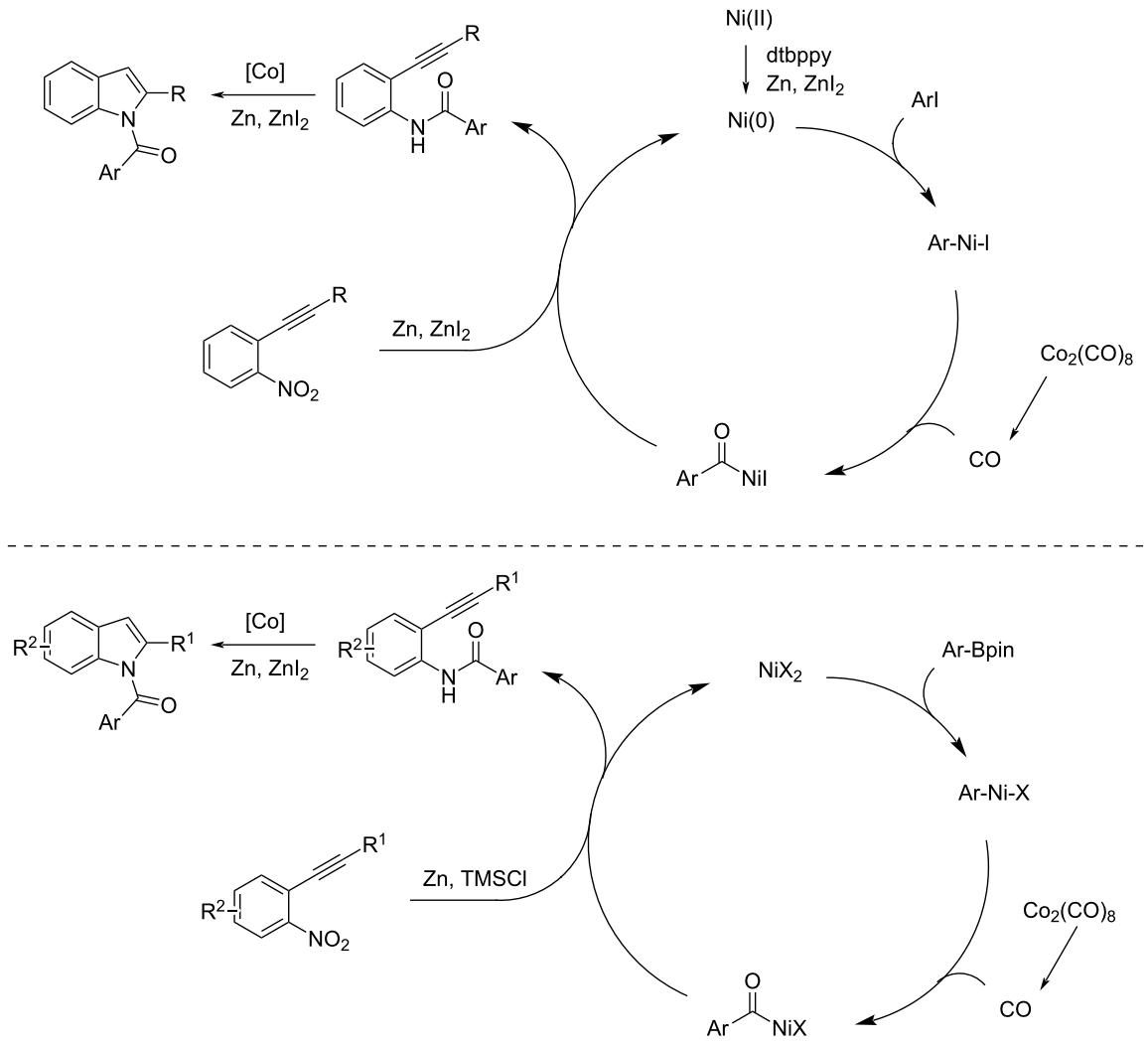

Scheme 23: Mechanism of the Ni-catalyzed carbonylative cyclization of 2-nitroalkynes and aryl iodides (top) and Ni-catalyzed carbonylative cyclization of 2-nitroalkynes and arylboronic pinacol esters (bottom).

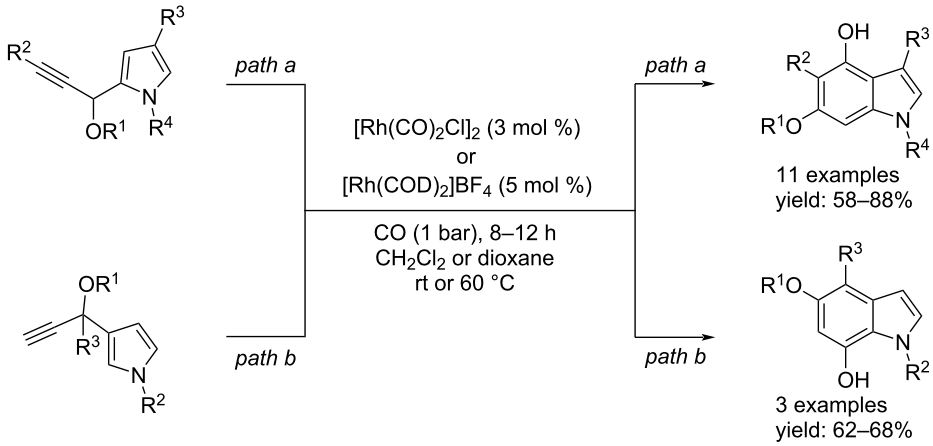

Scheme 24: Route to indole derivatives through Rh-catalyzed benzannulation of heteroaryl propargylic esters favoured by CO.

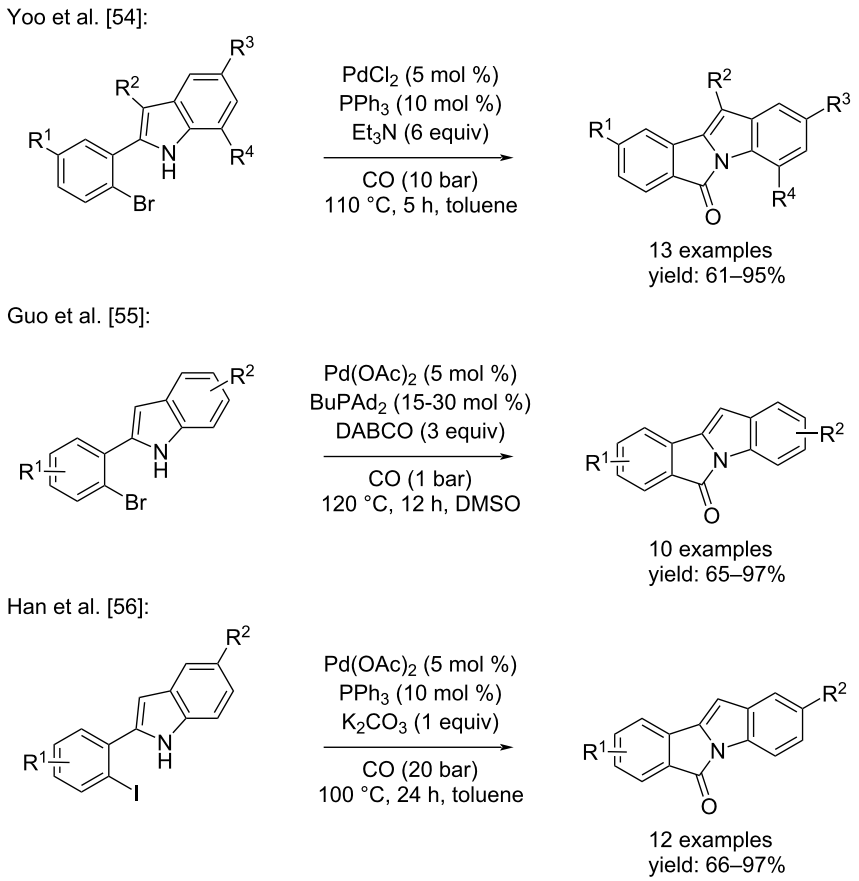

Scheme 25: Pd-catalyzed cyclization of 2-(2-haloaryl)indoles reported by Yoo and co-workers [54], Guo and co-workers [55], and Han and co-workers [56] for the synthesis of 6*H*-isoindolo[2,1-*a*]indol-6-ones.

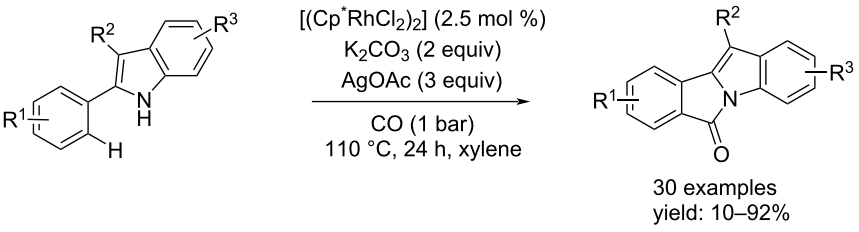

Scheme 26: Approach for the synthesis of 6*H*-isoindolo[2,1-*a*]indol-6-ones reported by Huang and co-workers [57].

In 2018, the Zhou et al. proposed the synthesis of 2-(1*H*-indol-2-yl)phenyl tosylates via a Pd-catalyzed cycloaminocarbonylation reaction [58]. In this approach $Pd(TFA)_2$/dppp was the catalyst system and able to catalyze the reaction in the best way. Also in this case a base was added to improve the reaction under 10 bar of CO, in CH_3CN at 160 °C. By this route, 29 examples were synthesized with isolated yields up to 91% (Scheme 27).

One year later, Čarný and co-workers described a facile construction of the isoindolo[2,1-*a*]indol-6-one structure via a Pd-catalyzed aminocarbonylation and C–H activation reaction starting from indoles and *o*-dibromoarenes as substrates [59]. In this tandem reaction, various symmetrical bromoarenes were utilized to eliminate the problem with regioselectivity. Two tests by using 2-bromo-5-methoxyphenyl triflate and 2-bromo-4-methoxyphenyl triflate were performed to evaluate the regio-

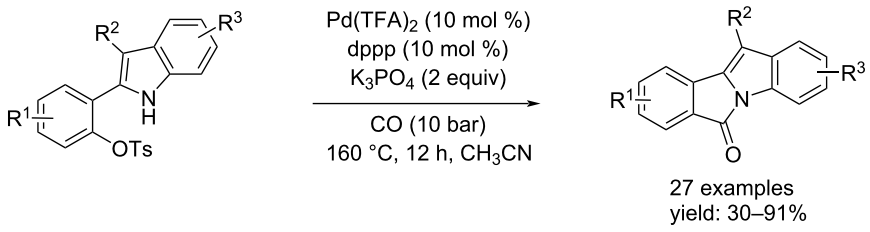

Scheme 27: Zhou group's method for the synthesis of 6*H*-isoindolo[2,1-a]indol-6-ones.

selectivity of the process. The regioselectivity was good with a regioisomeric ratio of 95:5. All reactions took place in the presence of $Pd(OAc)_2$ as catalyst, cataCXium as ligand, and K_2CO_3 as base. Besides, the authors proposed glyoxylic acid monohydrate as an environmentally friendly CO surrogate (Scheme 28).

Metal-catalyzed carbonylative cyclization reaction of indole derivatives

In 2016, Guo and co-workers, in the same work in which different examples of 6*H*-isoindolo[2,1-*a*]indol-6-ones were reported, performed the synthesis of indeno[1,2-*b*]indol-10(5*H*)-ones from 2-(2-bromophenyl)-1-alkyl-1*H*-indoles [55] under the same conditions as mentioned in Scheme 25. The presence of an alkyl group on the indole nitrogen led to a Heck cyclization instead of a cycloaminocarbonylation (Scheme 29).

In 2019, two different groups independently reported a carbonylative cyclization of *o*-indolylarylamines. In particular, Xu and co-workers used tertiary amines for achieving the reaction through a Pd/Cu co-catalysis [60]. The 17 examples were

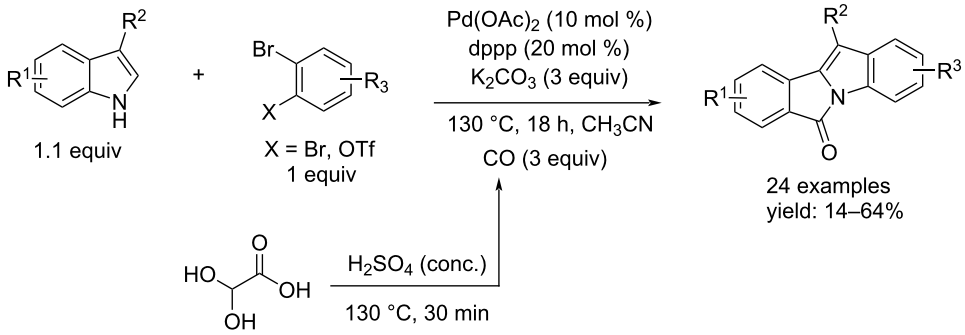

Scheme 28: Synthesis of 6*H*-isoindolo[2,1-*a*]indol-6-ones from *o*-1,2-dibromobenzene and indole derivatives by using glyoxylic acid monohydrate as CO surrogate.

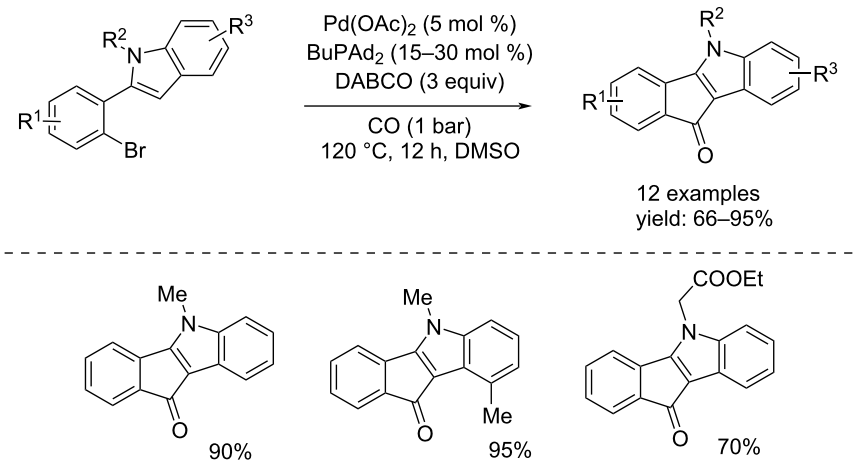

Scheme 29: $Pd(OAc)_2$-catalyzed Heck cyclization of 2-(2-bromophenyl)-1-alkyl-1*H*-indoles reported by Guo et al. [55].

obtained by using $PdCl_2$ (10 mol %) as catalyst and $Cu(TFA)_2{\cdot}H_2O$ (30 mol %) as co-catalyst. At the end of the process the catalyst underwent reduction, and therefore, in order to make the process catalytic, the reaction was performed in the presence of O_2. Furthermore, the addition of 1 equivalent of PivOH led to an improved isolated yield. A mixture of dioxane/DMA was the best solution to carry out the reaction that has been performed at 100 °C for 48 h (Scheme 30).

On the other hand, Chandrasekhar and Sankararaman reported the same process starting from secondary amines instead of tertiary amines [61]. In this case, the catalyst system was $Pd(OCOCF_3)_2$ (10 mol %) and the oxidant $Cu(OAc)_2$ (2 equiv) and oxygen. The reaction was carried out in toluene at 80 °C for 24 h and, in terms of gas pressure, took place under mild conditions comparable to the ones reported by Xu et al. (Scheme 31). Chandrasekhar and Sankararaman also tested primary amines under the conditions outlined in Scheme 31, however, the reaction gave the annulated products (as the secondary amines) and the corresponding urea derivatives as byproducts.

In the middle of the same year, Wu's group succeeded in using *N*-(2-bromobenzoyl)indoles in the reaction with alcohols and anilines to achieve a Pd-catalyzed diasteroselective carbonylative cyclodearomatization [62]. The synthesis proceeded best when the reaction was performed in the presence of 10 mol % of $Pd(OAc)_2$ and dppp as catalyst system, $Na_2WO_4{\cdot}2H_2O$ (1 or 2 equiv) as base and an excess of nucleophile (alcohols or anilines) in toluene as reaction solvent under 5 bar of CO at 100 °C. Also, 20 mol % of LiBr were added as additive when alcohols were used as the nucleophiles (Scheme 32).

About three years later, the same group developed a simple and efficient method to access CO-linked heterocyclic scaffolds by a Pd-catalyzed carbonylative cyclization of alkene–indole derivatives with 2-alkynylanilines and 2-alkynylphenols, in the presence of TFBen as CO source [63]. The reaction proceeded to heterocyclic compounds in the presence of 10 mol % of $Pd(TFA)_2$ and dppb (1,4-bis(diphenylphosphino)butane), 3 equivalents of TFBen, 2 equivalents of Na_2CO_3 in dioxane at 100 °C. The products were obtained in very good isolated yields (Scheme 33). The proposed mechanism, shown in Scheme 34, suggested that the process proceeded through a Pd(0) catalysis proceeding through first an intramolecular Heck reaction, followed by CO insertion, *N*-cyclization (anilines) or *O*-cyclization (phenols) and final reductive elimination.

Carbonylative functionalization of indoles to 3-substituted indoles

Functionalization through direct C–H alkoxycarbonylation

The transition-metal-catalyzed carbonylation of aryl halides, triflates, and tosylates with carbon monoxide and an alcohol was first pioneered by Heck and co-workers in 1974 [64,65].

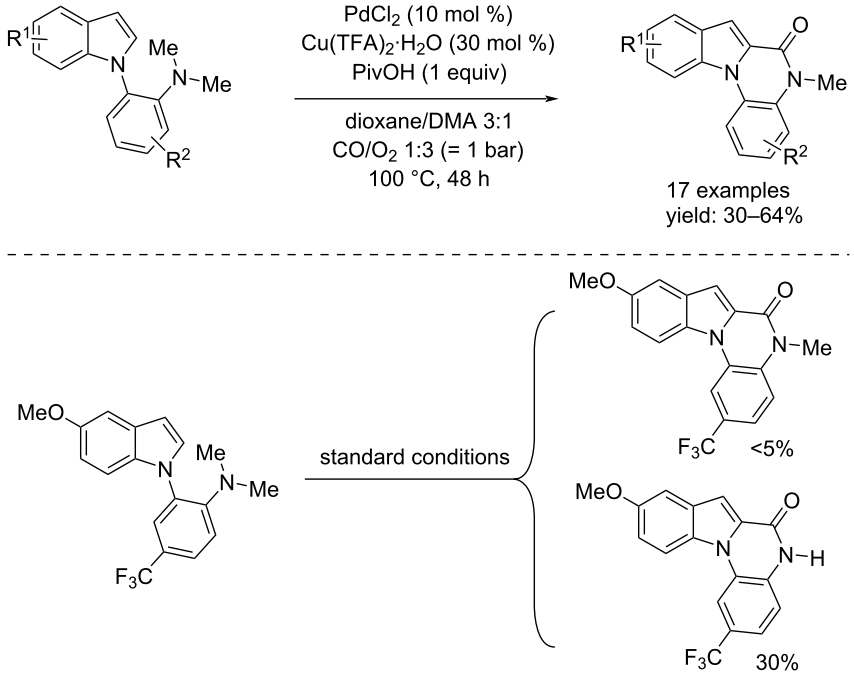

Scheme 30: Synthesis of indolo[1,2-*a*]quinoxalinone derivatives through Pd/Cu co-catalyzed carbonylative cyclization from *o*-indolyl-*N*,*N*-dimethylarylamines.

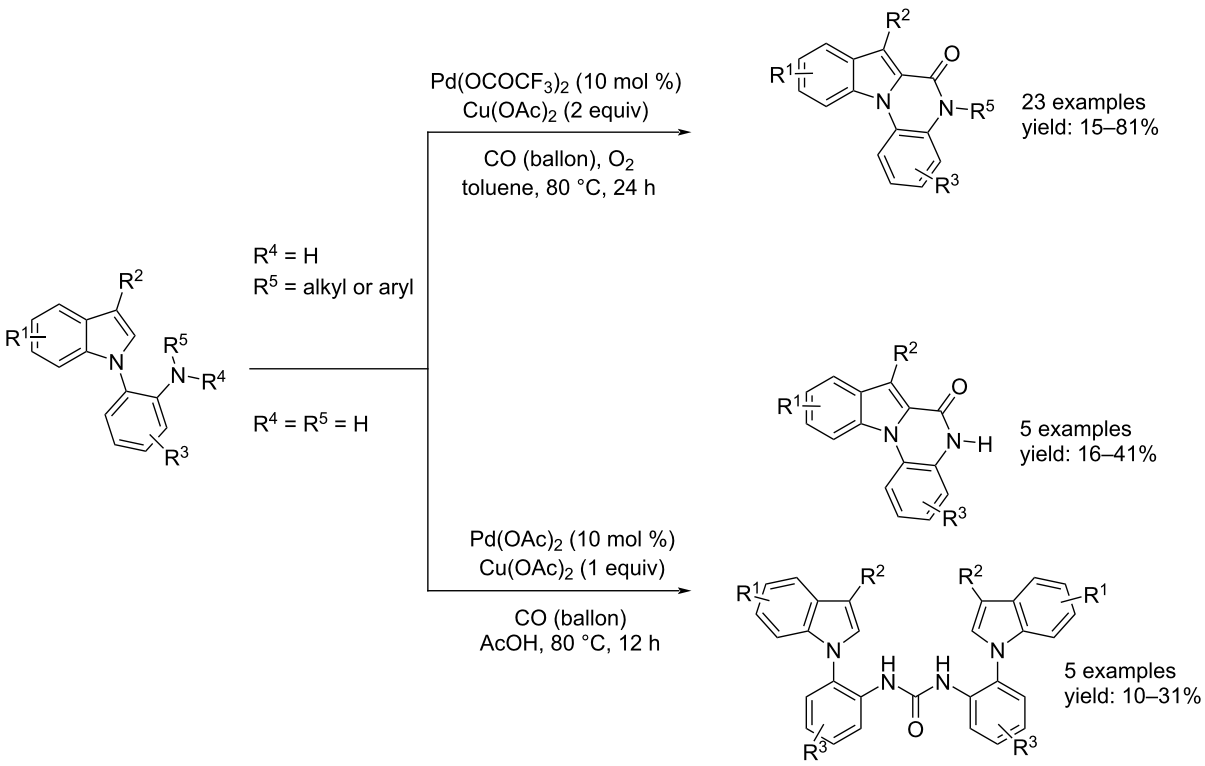

Scheme 31: Pd-catalyzed carbonylative cyclization of *o*-indolylarylamines and *N*-monosubstituted *o*-indolylarylamines reported by Chandrasekhar and Sankararaman [61].

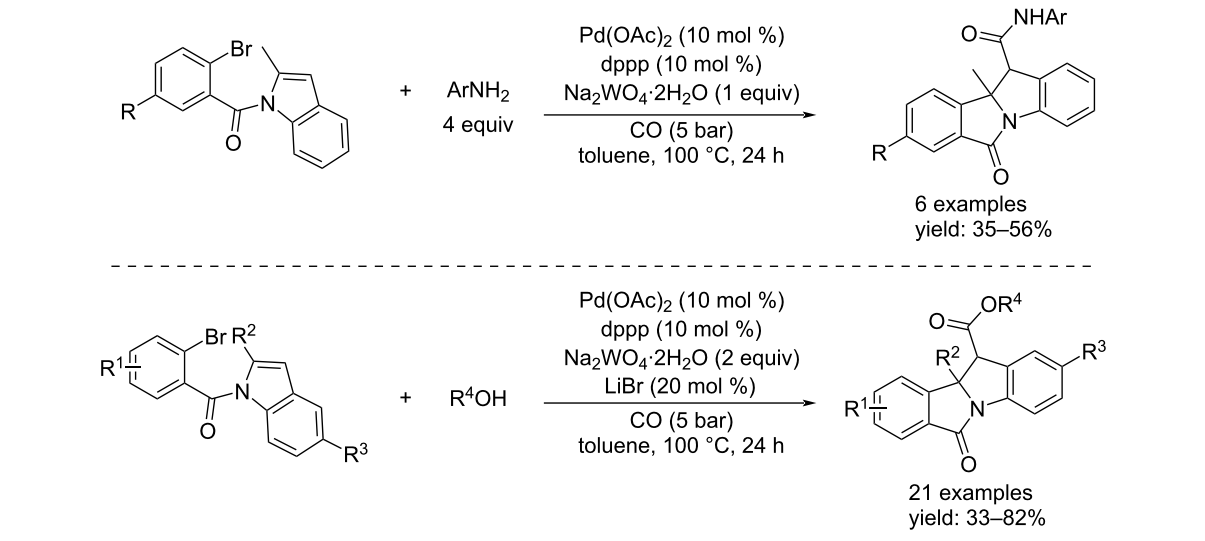

Scheme 32: Pd-catalyzed diasteroselective carbonylative cyclodearomatization of *N*-(2-bromobenzoyl)indoles with anilines (top) and alcohols (bottom).

Since then, this method has been well-developed and is considered one of the most straightforward ways to access carboxylic esters. In later years, other compounds were studied as substrates for alkoxycarbonylation processes. In fact, aromatic C–H functionalizations have been increasingly used for the synthesis of organic building blocks and pharmaceutical compounds. In this context, given the importance of indoles, in 2011, the groups by Lei and Li independently reported the C–H alkoxy-

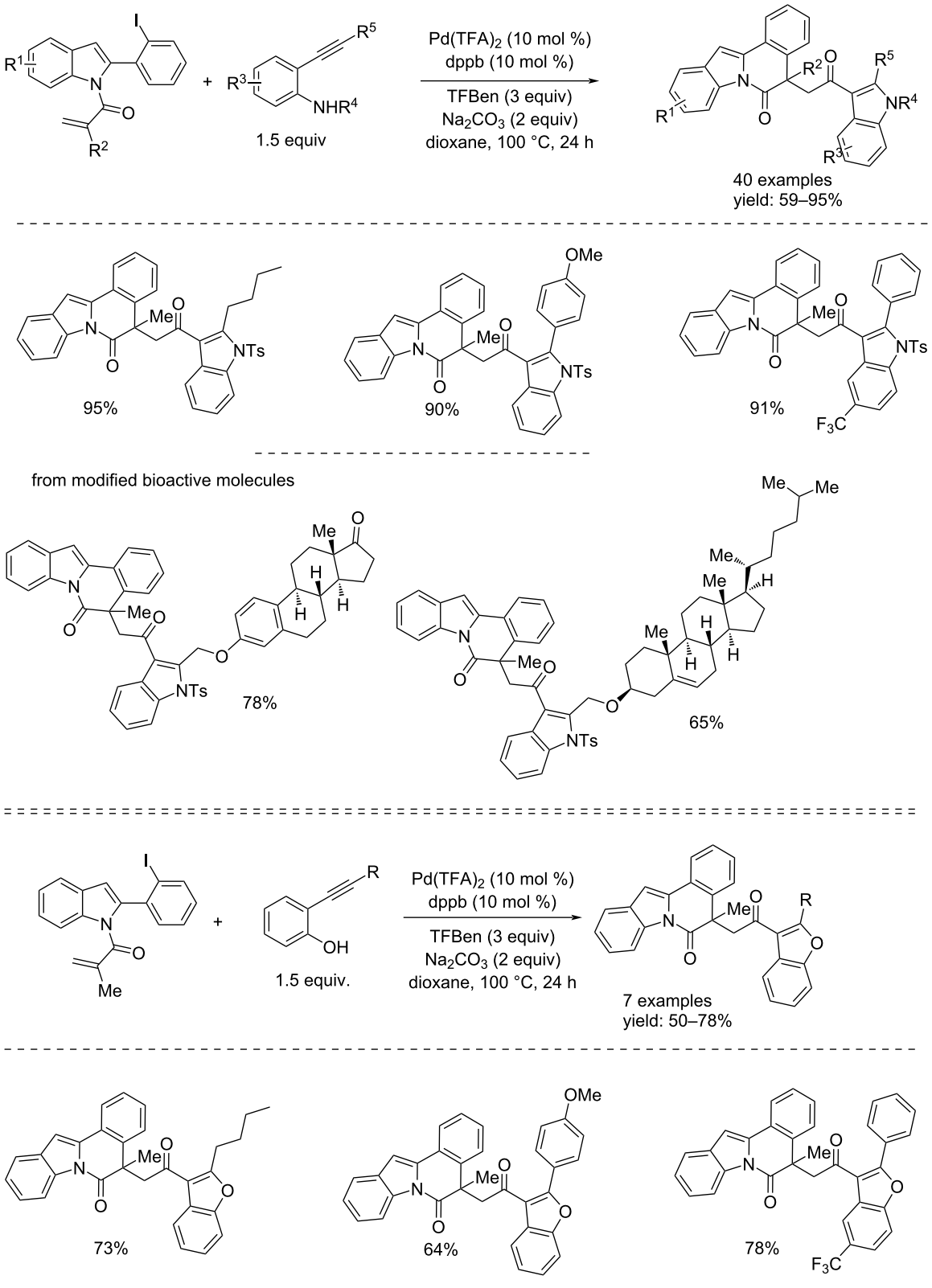

Scheme 33: Pd(0)-catalyzed synthesis of CO-linked heterocyclic scaffolds from alkene-indole derivatives and 2-alkynylanilines (top) and 2-alkynylphenols (bottom).

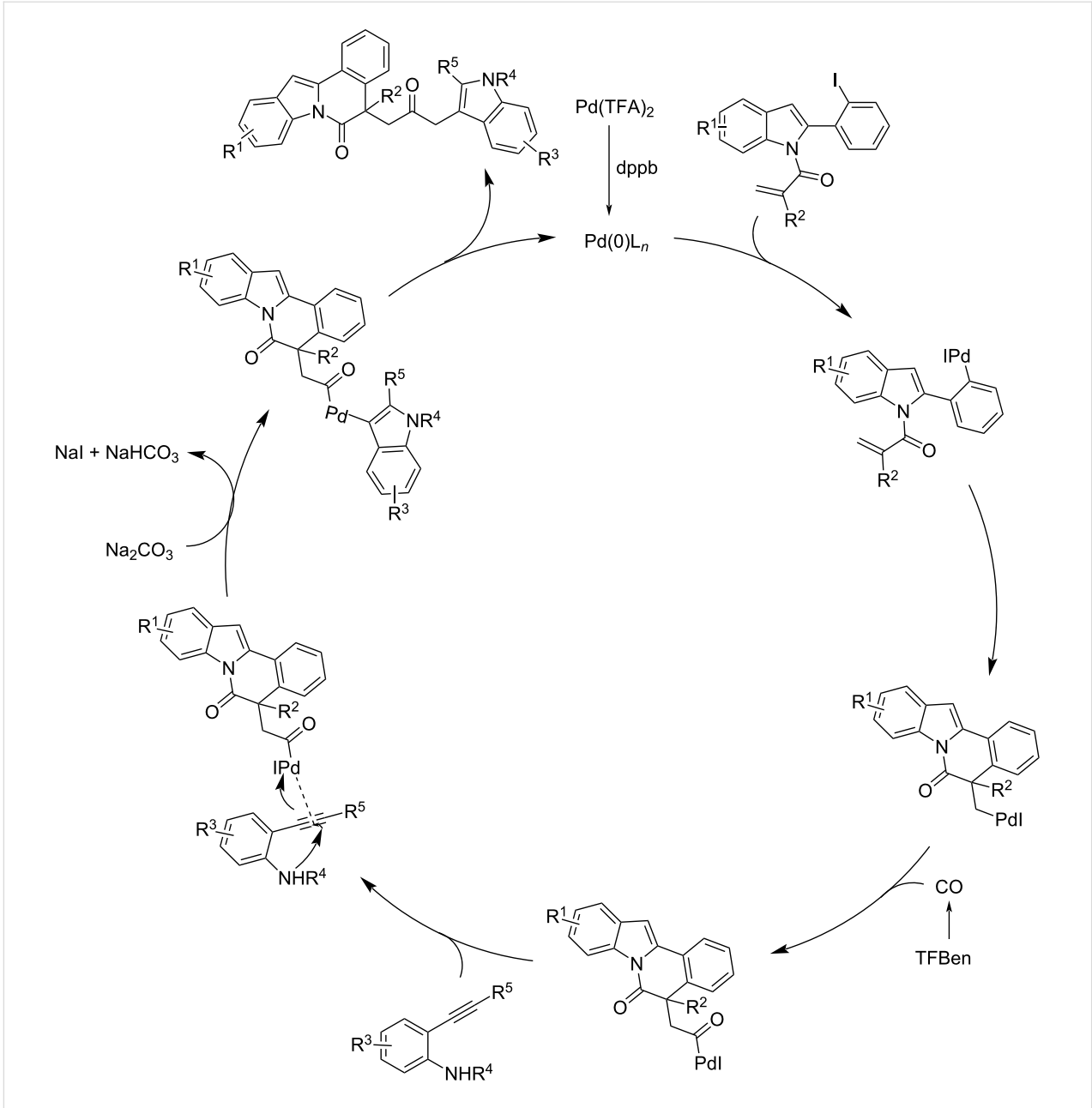

Scheme 34: Proposed mechanism for the Pd(0)-catalyzed synthesis of CO-linked heterocyclic scaffolds.

carbonylation of indole derivatives [66,67]. In addition, Lei and co-workers also reported the N–H alkoxycarbonylation [66]. Both processes took place in a Schlenk tube loaded with 2.5 mol % of $Pd(PPh_3)_2Cl_2$ as catalyst, 10 mol % of $Cu(OAc)_2$ as co-catalyst, 5 mol % of PPh_3 as ligand under a mixture of CO/air 7:1 in toluene/DMSO as solvent at 100 °C for 36 h. The desired products were isolated in yields up to 98% (Scheme 35).

Unlike what we have just written, Li's group performed the reaction by a Rh-catalysis using $[Rh(COD)Cl]_2$ and re-oxidizing it with $K_2S_2O_8$. The reactions led to the products in toluene after 24–48 hours at 110 °C under 1 bar of CO (Scheme 36).

Another example to obtain indole-3-carboxylates, was again reported by Li et al. [68]. The process occurred under mild conditions (such as the approaches seen above) under 1 bar of CO, in DMF or CH_3CN, at 80–100 °C for 24–48 h. In addition to 5 mol % of $Pd(OAc)_2$, 3 equiv of K_2CO_3 and 2.5 equiv of I_2 were added. The reactions were carried out by using both aliphatic alcohols and phenols (Scheme 37) and good isolated yields were achieved.

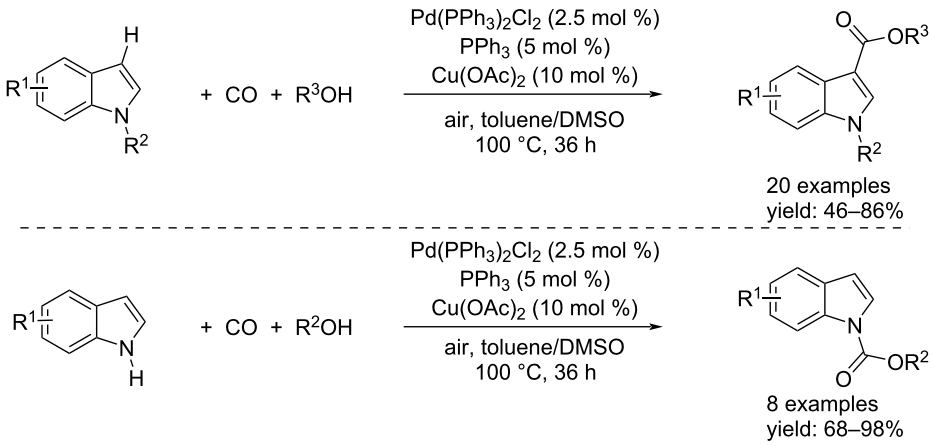

Scheme 35: Pd-catalyzed C–H and N–H alkoxycarbonylation of indole derivatives to indole-3-carboxylates and indole-*N*-carboxylates reported by Lei et al. [66].

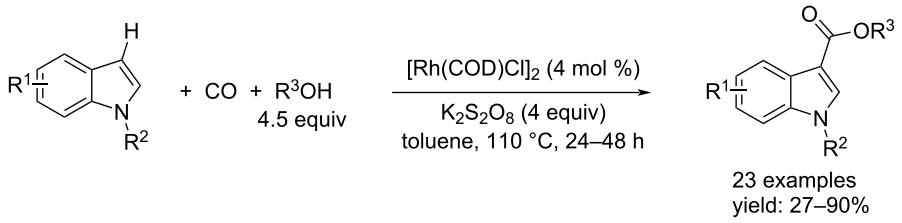

Scheme 36: Rh-catalyzed C–H alcoxycarbonylation of indole derivatives to indole-3-carboxylates reported by Li et al. [67].

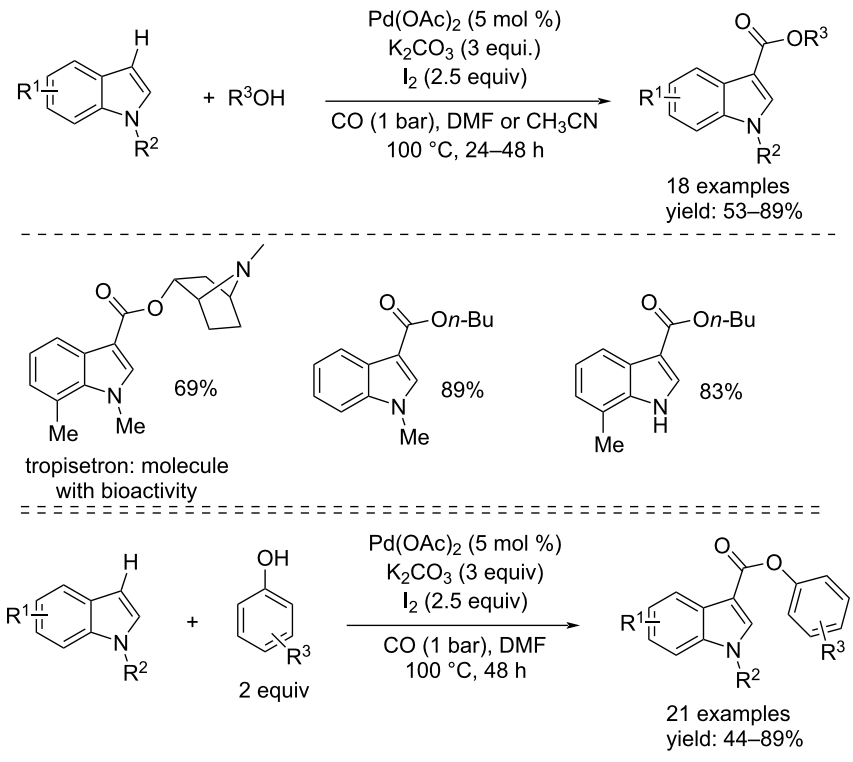

Scheme 37: Pd-catalyzed C–H alkoxycarbonylation of indole derivatives with alcohols and phenols to indole-3-carboxylates.

In 2021, Peng and co-workers published a more environmentally friendly alkoxycarbonylation approach with phenols, from *N*-methylindoles, to synthesize *N*-methylndole-3-carboxylates without using of noble metal catalysts [69]. The process was catalyzed by visible light in the presence of $Mo(CO)_6$ (1 equiv) as CO source, I_2 (2 equiv), and K_2CO_3 (3 equiv) at 120 °C in an inert reaction environment (N_2) and in DMSO as solvent (Scheme 38).

Functionalization through direct C–H carbonylations

The direct functionalization of indoles via C–C bond formation has received great interest due to the broad applications of functionalized indole derivatives. In this context, many groups developed different routes to 3-substituted indoles. In this minireview, we just show the carbonylative approaches.

Xing and co-workers presented a controllable and regioselective synthesis of indol-3-α-ketoamides and indol-3-amides via the direct double- and monoaminocarbonylation of indole derivatives by using secondary amines [70]. They used $Pd(dppf)Cl_2$ as catalyst system. The indol-3-α-ketoamides were synthesized by adding dppf as ligand, CuI as co-catalyst, and LiCl as additive under 40 bar of CO. To make the process regioselective towards indol-3-amides, dppf as ligand, the base (K_2CO_3), and I_2 were added, and the reaction run under a low pressure of CO (1 bar), in addition to the catalyst. Both processes took place well in THF (Scheme 39).

In 2013, the Li's group and Zeng and Alper developed two different methods for carrying out a direct carbonylation of indoles with alkynes. Li's group reported the direct Sonogashira carbonylation coupling reaction of indoles and alkynes cata-

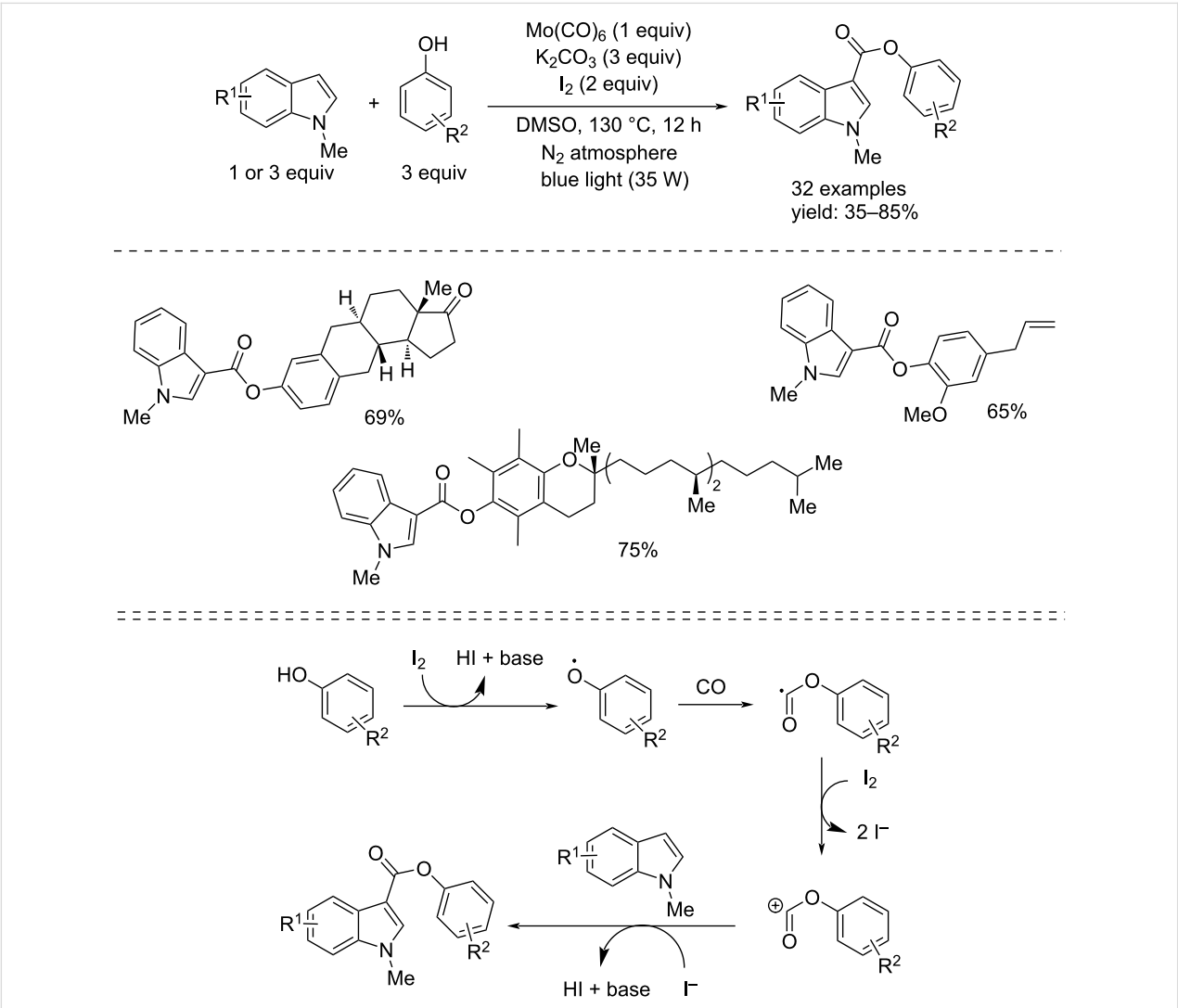

Scheme 38: Synthesis of *N*-methylindole-3-carboxylates from *N*-methylindoles and phenols through metal-catalyst-free reaction (top) and its hypothesized mechanism (bottom).

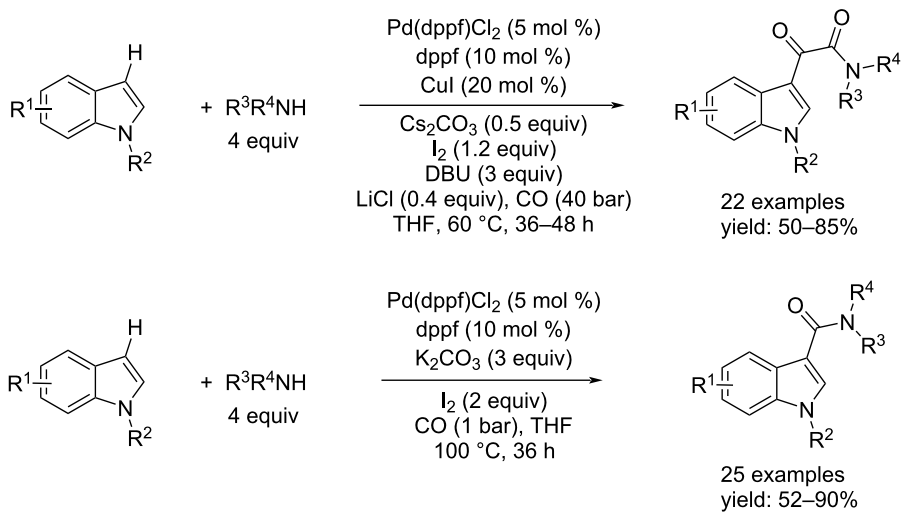

Scheme 39: Synthesis of indol-3-α-ketoamides (top) and indol-3-amides (bottom) via direct double- and monoaminocarbonylation of indole derivatives with secondary amines.

lyzed by Pd/CuI in the presence of iodine as oxidant [71]. The catalyst system was $Pd(OAc)_2$/CuI, in addition, a base (K_2CO_3) was added in DMF as solvent. Performing the reactions at 90 °C for 24 hours led to 38 products with isolated yields up to 94% (Scheme 40).

Instead, Zeng and Alper presented a new regioselective and chemoselective method for the direct coupling of indoles/CO/alkynes (alkynylcarboxylates) towards linear α,β-unsaturated ketones [72]. The reactions occurred in the presence of $Pd(CH_3CN)_4(BF_4)_2$/Xantphos as catalyst system under 20.7 bar of CO at 105 °C in THF. After 15 h, each reaction led selectively to the desired products (Scheme 40).

More recently, Zhao and co-workers published a novel synthesis of indole-3-yl aryl ketones by a Pd-catalyzed direct carbonylation of the corresponding indoles with boronic acids [73]. The best catalyst was $Pd(OAc)_2$ which catalyzed the reaction well in

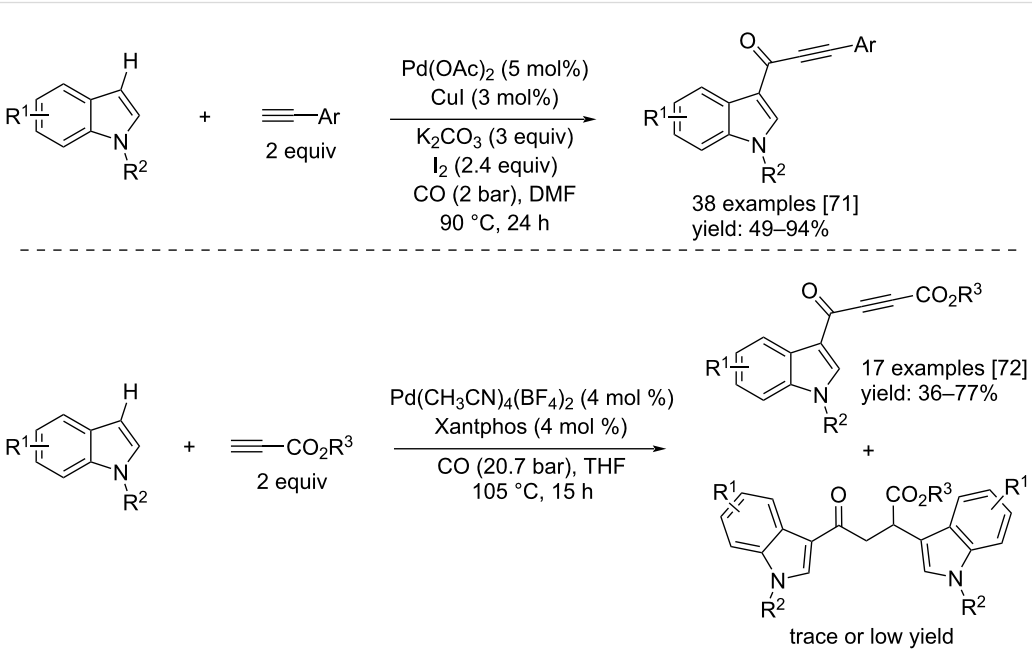

Scheme 40: The direct Sonogashira carbonylation coupling reaction of indoles and alkynes via Pd/CuI catalysis reported by Li et al. [71] (top). The Pd-catalyzed regio- and chemoselective direct coupling of indoles/CO/alkynyl carboxylates developed by Zeng and Alper [72] (bottom).

the presence of a base, such as KOH, in toluene as solvent and by adding pyridine and CsF as additives. By this route the products were obtained under mild reaction conditions applying low pressure of CO, temperature of 80 °C for 12 h. A stoichiometric amount of I_2 was necessary to restore the catalyst that underwent a possible reduction (Scheme 41).

Another interesting method toward indole-3-yl aryl ketones was reported by Zhang et al. Considering the ability of the aryldiazonium salts to act as aryl radical source, in presence of the suitable metal catalyst or taking advantage of photocatalysis, they decided to perform a direct carbonylation of indoles with that kind of chemicals [74]. The reaction was cheap because it took place by irradiation with green light (5 W) in the presence of eosin Y as photocatalyst, under 70 bar of CO, in CH_3CN at room temperature (Scheme 41).

In 2018, Wu et al. published two papers about the functionalization of indoles. In the first one, based on the known bioactivity displayed by bis(indolyl)methane (BIM) compounds, they reported the Pd-catalyzed carbonylative synthesis of the target compounds from aryl iodides and *N*-substituted and NH-free indoles in the presence of TFBen as the CO source [75]. A wide range of bis(indolyl)methane compounds were isolated in moderate and excellent yields after 24 hours in DMSO, Et_3N and formic acid as additives and, $Pd(PPh_3)_2Cl_2$/P(*o*-tolyl)$_3$ as catalyst system. The reaction conditions and some important BIMs synthesized are shown in Scheme 42.

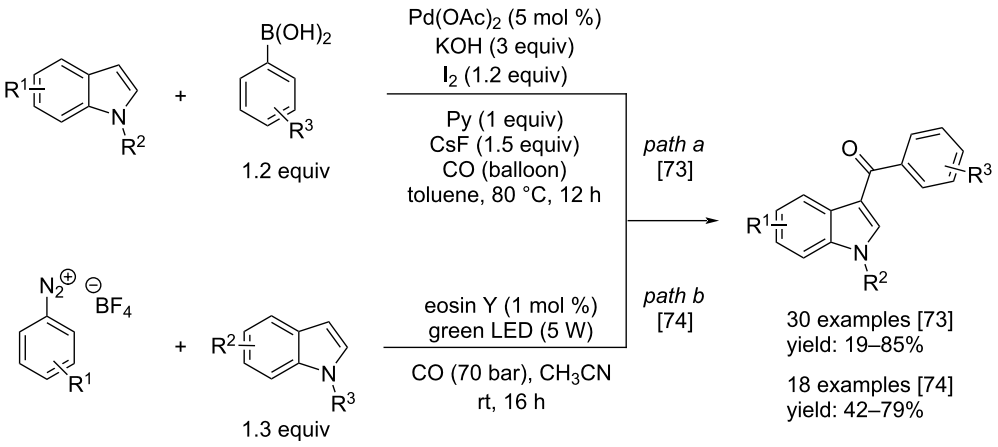

Scheme 41: Synthesis of indole-3-yl aryl ketones reported by Zhao and co-workers [73] (path a) and Zhang and co-workers [74] (path b).

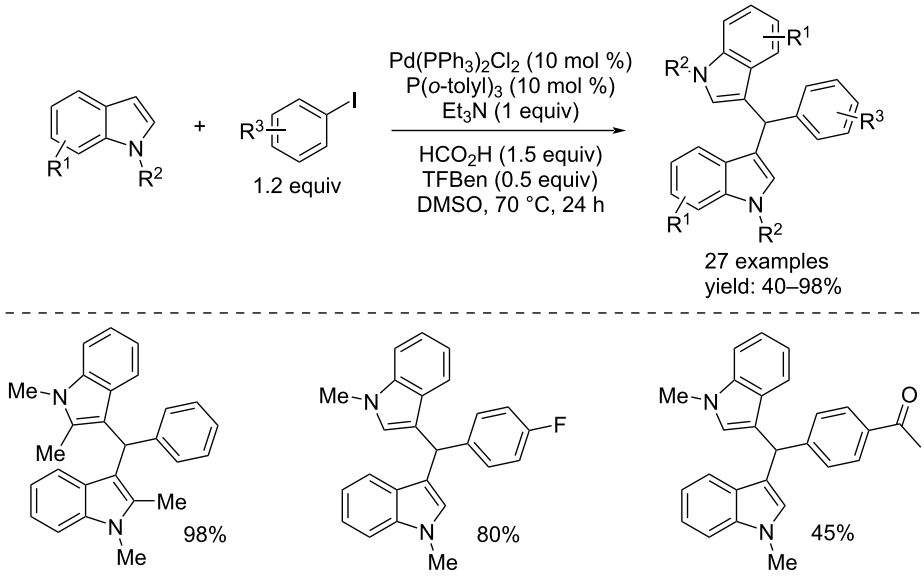

Scheme 42: Pd-catalyzed carbonylative synthesis of BIMs from aryl iodides and *N*-substituted and NH-free indoles with of TFBen as CO source.

In the second paper they used hexaketocyclohexane octahydrate as the CO source again. This cyclic hexaketone is a non-toxic stable solid and therefore, it is simple and safe to use unlike of carbon monoxide. It was used as reagent to obtain indol-α-ketoesters by the Cu-catalyzed direct double-carbonylation of indoles and alcohols [76]. The authors demonstrated that by adding Ag_2CO_3 in addition to $CuBr(Me_2S)$ as catalyst, 1-10-phen as ligand, and TFA as additive in CH_3CN, the process led to the direct double-carbonylation products. Furthermore, they showed, through an example, that carrying out the reaction under the standard conditions but by changing the solvent (PhCl instead of CH_3CN) and further increasing the temperature to 130 °C, the reaction took another pathway toward the direct monocarbonylation product, i.e. an indolester (Scheme 43).

Carbonylative functionalization of indoles to 2-substituted indoles

As illustrated above, the metal-catalyzed direct C–H carbonylation of indoles is an effective and straightforward approach to synthesize indole derivatives containing a carbonyl function in position 3. On the other hand, only a few examples to synthesize indole-2-carbonyl derivatives have been realized.

One example is the regioselective Ru-catalyzed direct carbonylative arylation of heterocycles developed by Beller et al. in 2014 [77]. In this paper various heterocycles were investigated including five examples of indoles.

Another example was reported by Driver an co-workers, who developed the Pd-catalyzed direct aryl C–H aminocarbonylation with nitroarenes as nitrogen source [78]. In this case just one example of indole functionalization was reported.

In 2019, Zhao and co-workers, reported an interesting method to synthesize indole-2-carboxylates through a Rh-catalyzed direct C–H alkoxycarbonylation of indoles [79]. The reaction took place under only 1 bar of CO and in the presence of $RhCl_3·3H_2O$ as catalyst and 2 equivalents of $Cu(OAc)_2$ as oxidant. 44 examples were obtained in good to excellent isolated yields (Scheme 44). Nevertheless, the approaches by Zhao et al. and the other examples, have in common the use of expensive catalysts. Therefore, Wu's group developed the direct C–H aminocarbonylation of indoles by using cheaper $Co(OAc)_2·4H_2O$ as catalyst [80] which allowed the reaction to proceed well when used in conjunction of Ag_2CO_3 as oxidant and a further addition of PivONa as additive. The presence of CO as reagent was guaranteed by the addition of TFBen. The reaction conditions are reported in Scheme 44.

Carbonylative functionalization of indoles toward 4 to 7-substituted indoles

In 2004, Beller and co-workers evaluated the possibility of synthesizing indole carboxylic amides from 4 to 7-haloindoles through a Pd-catalyzed carbonylation reaction [81]. Initially it was assumed that the presence of the halide and the NH group

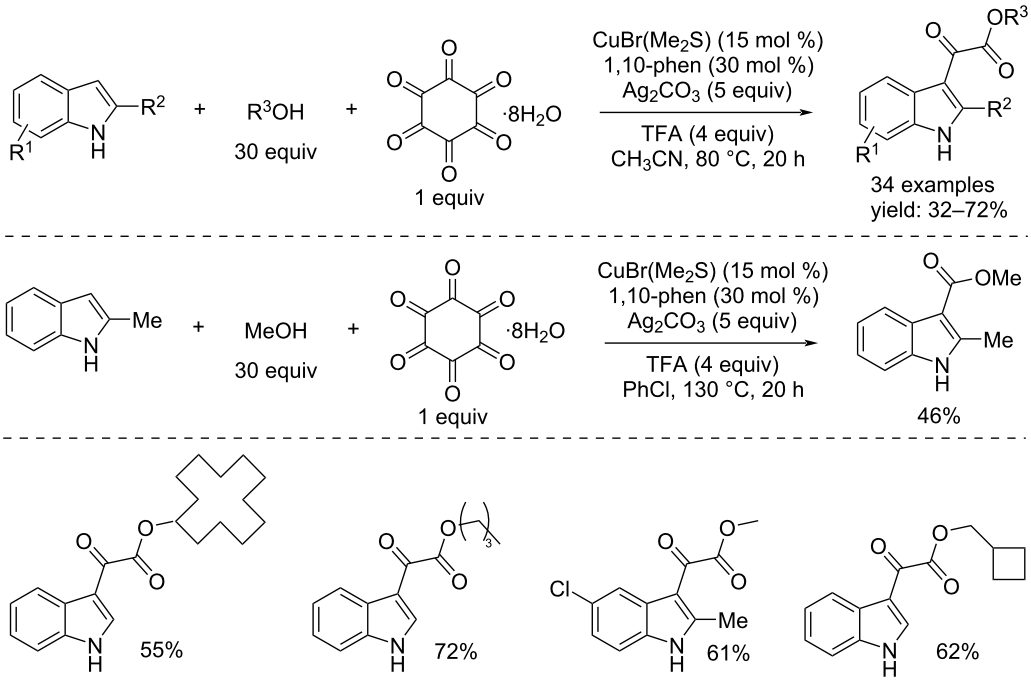

Scheme 43: Cu-catalyzed direct double-carbonylation and monocarbonylation of indoles and alcohols with hexaketocyclohexane octahydrate as CO source.

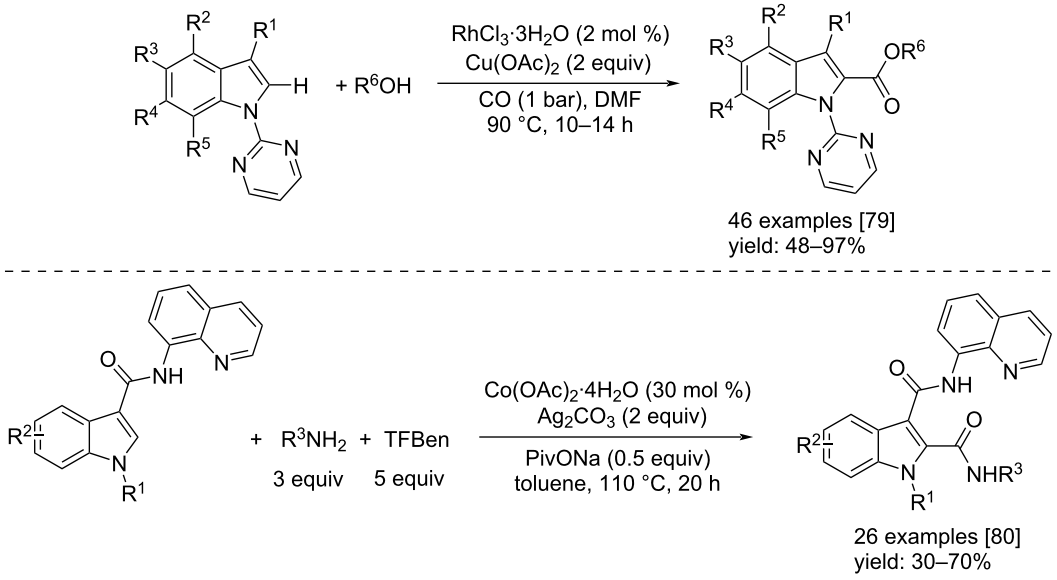

Scheme 44: Rh-catalyzed direct C–H alkoxycarbonylation of indoles to indole-2-carboxylates [79] (top) and Co-catalyzed direct C–H aminocarbonylation of indoles to indole-2-amides [80] (below).

could lead to an oligomerization or polymerization reaction, but carrying out the reaction with $Pd(CH_3CN)_2Cl_2$/dppf as catalyst system and Et_3N as the base at 130 °C under 25 bar of CO, they succeeded in the synthesis of a set of 12 desired products. These included an ethyl ester and a carboxylic acid, and were all obtained in good yields of up to 99% (Scheme 45).

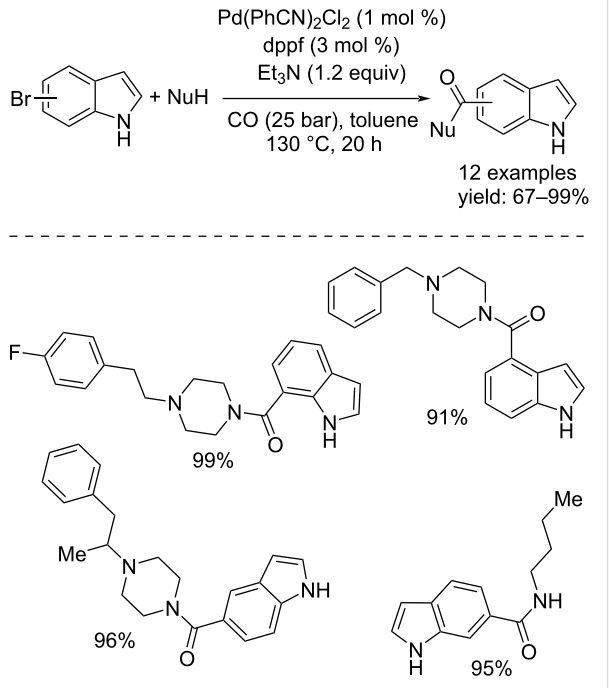

Scheme 45: Pd-catalyzed carbonylation of NH free-haloindoles.

Conclusion

We have summarized the importance of carbon monoxide as C1 building block to promote different kinds of transformations to synthesize and functionalize indole scaffolds. We have seen different approaches in which high catalyst efficiencies, mild conditions and the use of low-toxic chemicals as CO source, that do not require the use of autoclaves, have been successfully applied. Furthermore, in some cases, "green" oxidants such as air were used making the process more environmentally friendly especially if we think about them in the industrial field. Clearly, the research in this field is ongoing and it will continue, and more active catalysts and new "green" synthetic approaches will be developed.

Funding

We appreciate the financial support provided by the National Key R&D Program of China (2023YFA1507500).

Author Contributions

Alex De Salvo: writing – original draft. Raffaella Mancuso: funding acquisition; supervision; writing – original draft; writing – review & editing. Xiao-Feng Wu: conceptualization; funding acquisition; project administration; supervision; writing – original draft; writing – review & editing.

ORCID® iDs

Alex De Salvo - https://orcid.org/0000-0001-5657-4394
Raffaella Mancuso - https://orcid.org/0000-0001-7514-6096
Xiao-Feng Wu - https://orcid.org/0000-0001-6622-3328

Data Availability Statement

Data sharing is not applicable as no new data was generated or analyzed in this study.

References

1. Higasio, Y. S.; Shoji, T. *Appl. Catal., A* **2001,** *221,* 197–207. doi:10.1016/s0926-860x(01)00815-8
2. Vicente, R. *Org. Biomol. Chem.* **2011,** *9,* 6469. doi:10.1039/c1ob05750b
3. Gribble, G. W. *Indole Ring Synthesis. From Natural Products to Drug Discovery;* John Wiley & Sons: Chichester, UK, 2016. doi:10.1002/9781118695692
4. Amaral, A. A.; Willig, J. C. M.; Olguin, C. F. A.; Oliveira, I. M.; Stefani, H. A.; Botteselle, G. V.; Manarin, F. *J. Braz. Chem. Soc.* **2023,** *34,* 1464–1473. doi:10.21577/0103-5053.20230058
5. Kaushik, N. K.; Kaushik, N.; Attri, P.; Kumar, N.; Kim, C. H.; Verma, A. K.; Choi, E. H. *Molecules* **2013,** *18,* 6620–6662. doi:10.3390/molecules18066620
6. Kumari, A.; Singh, R. K. *Bioorg. Chem.* **2019,** *89,* 103021. doi:10.1016/j.bioorg.2019.103021
7. Chadha, N.; Silakari, O. *Eur. J. Med. Chem.* **2017,** *134,* 159–184. doi:10.1016/j.ejmech.2017.04.003
8. Fischer, E.; Jourdan, F. *Ber. Dtsch. Chem. Ges.* **1883,** *16,* 2241–2245. doi:10.1002/cber.188301602141
9. Chauhan, M.; Saxena, A.; Saha, B. *Eur. J. Med. Chem.* **2021,** *218,* 113400. doi:10.1016/j.ejmech.2021.113400
10. Bugaenko, D. I.; Karchava, A. V.; Yurovskaya, M. A. *Russ. Chem. Rev.* **2019,** *88,* 99–159. doi:10.1070/rcr4844
11. Gabriele, B., Ed. *Carbon Monoxide in Organic Synthesis: Carbonylation Chemistry;* Wiley-VCH: Weinheim, Germany, 2021. doi:10.1002/9783527829354
12. Arthuis, M.; Pontikis, R.; Florent, J.-C. *Org. Lett.* **2009,** *11,* 4608–4611. doi:10.1021/ol901875z
13. Senadi, G. C.; Hu, W.-P.; Boominathan, S. S. K.; Wang, J.-J. *Chem. – Eur. J.* **2015,** *21,* 998–1003. doi:10.1002/chem.201405933
14. Wang, Q.; Yao, L.; Wang, J.-S.; Ying, J.; Wu, X.-F. *J. Org. Chem.* **2022,** *87,* 3874–3882. doi:10.1021/acs.joc.2c00006
15. Gabriele, B.; Veltri, L.; Salerno, G.; Mancuso, R.; Costa, M. *Adv. Synth. Catal.* **2010,** *352,* 3355–3363. doi:10.1002/adsc.201000642
16. Gabriele, B.; Veltri, L.; Mancuso, R.; Salerno, G.; Costa, M. *Eur. J. Org. Chem.* **2012,** 2549–2559. doi:10.1002/ejoc.201200120
17. Gabriele, B.; Salerno, G.; Veltri, L.; Costa, M.; Massera, C. *Eur. J. Org. Chem.* **2001,** 4607–4613. doi:10.1002/1099-0690(200112)2001:24<4607::aid-ejoc4607>3.0.co;2-d
18. Shen, R.; Kusakabe, T.; Takahashi, K.; Kato, K. *Org. Biomol. Chem.* **2014,** *12,* 4602–4609. doi:10.1039/c4ob00714j
19. Gabriele, B.; Mancuso, R.; Salerno, G.; Lupinacci, E.; Ruffolo, G.; Costa, M. *J. Org. Chem.* **2008,** *73,* 4971–4977. doi:10.1021/jo8006495
20. Acerbi, A.; Carfagna, C.; Costa, M.; Mancuso, R.; Gabriele, B.; Della Ca', N. *Chem. – Eur. J.* **2018,** *24,* 4835–4840. doi:10.1002/chem.201706067
21. Crotti, C.; Cenini, S.; Rindone, B.; Tollari, S.; Demartin, F. *J. Chem. Soc., Chem. Commun.* **1986,** 784. doi:10.1039/c39860000784
22. Akazome, M.; Kondo, T.; Watanabe, Y. *J. Org. Chem.* **1994,** *59,* 3375–3380. doi:10.1021/jo00091a026
23. Söderberg, B. C.; Shriver, J. A. *J. Org. Chem.* **1997,** *62,* 5838–5845. doi:10.1021/jo970516+
24. Söderberg, B. C.; Rector, S. R.; O'Neil, S. N. *Tetrahedron Lett.* **1999,** *40,* 3657–3660. doi:10.1016/s0040-4039(99)00552-3
25. Söderberg, B. C.; Chisnell, A. C.; O'Neil, S. N.; Shriver, J. A. *J. Org. Chem.* **1999,** *64,* 9731–9734. doi:10.1021/jo991208+
26. Scott, T. L.; Söderberg, B. C. G. *Tetrahedron Lett.* **2002,** *43,* 1621–1624. doi:10.1016/s0040-4039(02)00072-2
27. Davies, I. W.; Smitrovich, J. H.; Sidler, R.; Qu, C.; Gresham, V.; Bazaral, C. *Tetrahedron* **2005,** *61,* 6425–6437. doi:10.1016/j.tet.2005.03.142
28. Tollari, S.; Cenini, S.; Crotti, C.; Gianella, E. *J. Mol. Catal.* **1994,** *87,* 203–214. doi:10.1016/0304-5102(93)e0228-9
29. Ragaini, F.; Sportiello, P.; Cenini, S. *J. Organomet. Chem.* **1999,** *577,* 283–291. doi:10.1016/s0022-328x(98)01076-6
30. Tollari, S.; Penoni, A.; Cenini, S. *J. Mol. Catal. A: Chem.* **2000,** *152,* 47–54. doi:10.1016/s1381-1169(99)00267-8
31. Fraley, M. E.; Hoffman, W. F.; Arrington, K. L.; Hungate, R. W.; Hartman, G. D.; McFall, R. C.; Coll, K. E.; Rickert, K.; Thomas, K. A.; McGaughey, G. B. *Curr. Med. Chem.* **2004,** *11,* 709–719. doi:10.2174/0929867043455729
32. Ragaini, F.; Rapetti, A.; Visentin, E.; Monzani, M.; Caselli, A.; Cenini, S. *J. Org. Chem.* **2006,** *71,* 3748–3753. doi:10.1021/jo060073m
33. Ragaini, F.; Ventriglia, F.; Hagar, M.; Fantauzzi, S.; Cenini, S. *Eur. J. Org. Chem.* **2009,** 2185–2189. doi:10.1002/ejoc.200801274
34. Clawson, R. W., Jr.; Deavers, R. E., III; Akhmedov, N. G.; Söderberg, B. C. G. *Tetrahedron* **2006,** *62,* 10829–10834. doi:10.1016/j.tet.2006.08.101
35. Hsieh, T. H. H.; Dong, V. M. *Tetrahedron* **2009,** *65,* 3062–3068. doi:10.1016/j.tet.2008.11.034
36. Ansari, N. H.; Dacko, C. A.; Akhmedov, N. G.; Söderberg, B. C. G. *J. Org. Chem.* **2016,** *81,* 9337–9349. doi:10.1021/acs.joc.6b01987
37. Glotz, G.; Gutmann, B.; Hanselmann, P.; Kulesza, A.; Roberge, D.; Kappe, C. O. *RSC Adv.* **2017,** *7,* 10469–10478. doi:10.1039/c7ra01087g
38. Zhou, F.; Wang, D.-S.; Driver, T. G. *Adv. Synth. Catal.* **2015,** *357,* 3463–3468. doi:10.1002/adsc.201500700
39. Formenti, D.; Ferretti, F.; Ragaini, F. *ChemCatChem* **2018,** *10,* 148–152. doi:10.1002/cctc.201701214
40. Ferretti, F.; Fouad, M. A.; Ragaini, F. *Catalysts* **2022,** *12,* 106. doi:10.3390/catal12010106
41. Fouad, M. A.; Ferretti, F.; Ragaini, F. *J. Org. Chem.* **2023,** *88,* 5108–5117. doi:10.1021/acs.joc.2c02613
42. Yao, L.; Ying, J.; Wu, X.-F. *Org. Chem. Front.* **2021,** *8,* 6541–6545. doi:10.1039/d1qo01284c
43. Yao, L.; Wei, P.; Ying, J.; Wu, X.-F. *Org. Chem. Front.* **2022,** *9,* 2685–2689. doi:10.1039/d2qo00112h
44. Li, X.; Xie, H.; Fu, X.; Liu, J.-t.; Wang, H.-y.; Xi, B.-m.; Liu, P.; Xu, X.; Tang, W. *Chem. – Eur. J.* **2016,** *22,* 10410–10414. doi:10.1002/chem.201602088
45. Kadam, H. K.; Tilve, S. G. *ARKIVOC* **2015,** No. vi, 524–539. doi:10.3998/ark.5550190.p009.316
46. Nirogi, R. V. S.; Kambhampati, R.; Kothmirkar, P.; Konda, J.; Bandyala, T. R.; Gudla, P.; Arepalli, S.; Gangadasari, N. P.; Shinde, A. K.; Deshpande, A. D.; Dwarampudi, A.; Chindhe, A. K.; Dubey, P. K. *J. Enzyme Inhib. Med. Chem.* **2012,** *27,* 443–450. doi:10.3109/14756366.2011.595713
47. Guillaumel, J.; Léonce, S.; Pierré, A.; Renard, P.; Pfeiffer, B.; Arimondo, P. B.; Monneret, C. *Eur. J. Med. Chem.* **2006,** *41,* 379–386. doi:10.1016/j.ejmech.2005.10.008

48. Guillaumel, J.; Léonce, S.; Pierré, A.; Renard, P.; Pfeiffer, B.; Peruchon, L.; Arimondo, P. B.; Monneret, C. *Oncol. Res.* **2003,** *13,* 537–549. doi:10.3727/000000003108748063
49. Nallapati, S. B.; Adepu, R.; Ashfaq, M. A.; Sreenivas, B. Y.; Mukkanti, K.; Pal, M. *RSC Adv.* **2015,** *5,* 88686–88691. doi:10.1039/c5ra17908d
50. Boussard, M.-F.; Truche, S.; Rousseau-Rojas, A.; Briss, S.; Descamps, S.; Droual, M.; Wierzbicki, M.; Ferry, G.; Audinot, V.; Delagrange, P.; Boutin, J. A. *Eur. J. Med. Chem.* **2006,** *41,* 306–320. doi:10.1016/j.ejmech.2005.12.002
51. Jasti, V.; Ramakrishna, V. S. N.; Kambhampati, R. S.; Battula, S. R.; Rao, V. S. V. V. Novel Tetracyclic Arylcarbonyl Indoles Having Serotonin Receptor Affinity Useful as Therapeutic Agents, Process for their Preparation and Pharmaceutical Compositions Containing them. WO Pat. Appl. WO2004/000205A2, Dec 31, 2003.
52. Laha, J. K.; Dayal, N.; Jethava, K. P.; Prajapati, D. V. *Org. Lett.* **2015,** *17,* 1296–1299. doi:10.1021/acs.orglett.5b00290
53. Dai, C.; Draganov, A. B.; Wang, B. *Heterocycl. Commun.* **2010,** *16,* 245–247. doi:10.1515/hc.2010.007
54. Yoo, J. M.; Ho, S. L.; Cho, C. S. *Synlett* **2016,** *27,* 1383–1386. doi:10.1055/s-0035-1561560
55. Guo, S.; Tao, L.; Wang, F.; Fan, X. *Chem. – Asian J.* **2016,** *11,* 3090–3096. doi:10.1002/asia.201601067
56. Han, Q.; Fu, S.; Zhang, X.; Lin, S.; Huang, Q. *Tetrahedron Lett.* **2016,** *57,* 4165–4169. doi:10.1016/j.tetlet.2016.07.108
57. Huang, Q.; Han, Q.; Fu, S.; Yao, Z.; Su, L.; Zhang, X.; Lin, S.; Xiang, S. *J. Org. Chem.* **2016,** *81,* 12135–12142. doi:10.1021/acs.joc.6b01200
58. Liu, B.; Lai, C.; Zhang, C.; Zhou, X. *Tetrahedron* **2018,** *74,* 752–757. doi:10.1016/j.tet.2017.12.058
59. Čarný, T.; Markovič, M.; Gracza, T.; Kóóš, P. *J. Org. Chem.* **2019,** *84,* 12499–12507. doi:10.1021/acs.joc.9b02008
60. Mu, Q.-C.; Nie, Y.-X.; Bai, X.-F.; Chen, J.; Yang, L.; Xu, Z.; Li, L.; Xia, C.-G.; Xu, L.-W. *Chem. Sci.* **2019,** *10,* 9292–9301. doi:10.1039/c9sc03081f
61. Chandrasekhar, A.; Sankararaman, S. *Org. Biomol. Chem.* **2020,** *18,* 1612–1622. doi:10.1039/c9ob02703c
62. Wang, H.; Wu, X.-F. *Org. Lett.* **2019,** *21,* 5264–5268. doi:10.1021/acs.orglett.9b01868
63. Wang, J.-S.; Zhang, J.; Wang, S.; Ying, J.; Li, C.-Y.; Wu, X.-F. *J. Catal.* **2022,** *414,* 313–318. doi:10.1016/j.jcat.2022.09.023
64. Schoenberg, A.; Bartoletti, I.; Heck, R. F. *J. Org. Chem.* **1974,** *39,* 3318–3326. doi:10.1021/jo00937a003
65. Schoenberg, A.; Heck, R. F. *J. Org. Chem.* **1974,** *39,* 3327–3331. doi:10.1021/jo00937a004
66. Zhang, H.; Liu, D.; Chen, C.; Liu, C.; Lei, A. *Chem. – Eur. J.* **2011,** *17,* 9581–9585. doi:10.1002/chem.201101300
67. Lang, R.; Wu, J.; Shi, L.; Xia, C.; Li, F. *Chem. Commun.* **2011,** *47,* 12553–12555. doi:10.1039/c1cc15143f
68. Lang, R.; Shi, L.; Li, D.; Xia, C.; Li, F. *Org. Lett.* **2012,** *14,* 4130–4133. doi:10.1021/ol3017726
69. Qi, Z.; Li, L.; Liang, Y.-K.; Ma, A.-J.; Zhang, X.-Z.; Peng, J.-B. *Org. Lett.* **2021,** *23,* 4769–4773. doi:10.1021/acs.orglett.1c01494
70. Xing, Q.; Shi, L.; Lang, R.; Xia, C.; Li, F. *Chem. Commun.* **2012,** *48,* 11023–11025. doi:10.1039/c2cc36341k
71. Li, D.; Shan, S.; Shi, L.; Lang, R.; Xia, C.; Li, F. *Chin. J. Catal.* **2013,** *34,* 185–192. doi:10.1016/s1872-2067(11)60491-9
72. Zeng, F.; Alper, H. *Org. Lett.* **2013,** *15,* 2034–2037. doi:10.1021/ol400722h
73. Zhao, M.-N.; Ran, L.; Chen, M.; Ren, Z.-H.; Wang, Y.-Y.; Guan, Z.-H. *ACS Catal.* **2015,** *5,* 1210–1213. doi:10.1021/cs5019106
74. Zhang, H.-T.; Gu, L.-J.; Huang, X.-Z.; Wang, R.; Jin, C.; Li, G.-P. *Chin. Chem. Lett.* **2016,** *27,* 256–260. doi:10.1016/j.cclet.2015.10.012
75. Qi, X.; Ai, H.-J.; Zhang, N.; Peng, J.-B.; Ying, J.; Wu, X.-F. *J. Catal.* **2018,** *362,* 74–77. doi:10.1016/j.jcat.2018.03.028
76. Wang, Z.; Yin, Z.; Wu, X.-F. *Chem. Commun.* **2018,** *54,* 4798–4801. doi:10.1039/c8cc01784k
77. Pospech, J.; Tlili, A.; Spannenberg, A.; Neumannn, H.; Beller, M. *Chem. – Eur. J.* **2014,** *20,* 3135–3141. doi:10.1002/chem.201304314
78. Zhou, F.; Wang, D.-S.; Guan, X.; Driver, T. G. *Angew. Chem., Int. Ed.* **2017,** *56,* 4530–4534. doi:10.1002/anie.201612324
79. Zhao, K.; Du, R.; Wang, B.; Liu, J.; Xia, C.; Yang, L. *ACS Catal.* **2019,** *9,* 5545–5551. doi:10.1021/acscatal.9b01193
80. Wei, P.; Ying, J.; Wu, X.-F. *Org. Lett.* **2023,** *25,* 7700–7704. doi:10.1021/acs.orglett.3c03034
81. Kumar, K.; Zapf, A.; Michalik, D.; Tillack, A.; Heinrich, T.; Böttcher, H.; Arlt, M.; Beller, M. *Org. Lett.* **2004,** *6,* 7–10. doi:10.1021/ol035988r

License and Terms

This is an open access article licensed under the terms of the Beilstein-Institut Open Access License Agreement (https://www.beilstein-journals.org/bjoc/terms), which is identical to the Creative Commons Attribution 4.0 International License (https://creativecommons.org/licenses/by/4.0). The reuse of material under this license requires that the author(s), source and license are credited. Third-party material in this article could be subject to other licenses (typically indicated in the credit line), and in this case, users are required to obtain permission from the license holder to reuse the material.

The definitive version of this article is the electronic one which can be found at:
https://doi.org/10.3762/bjoc.20.87

BEILSTEIN JOURNAL OF ORGANIC CHEMISTRY

Synthesis and optical properties of bis- and tris-alkynyl-2-trifluoromethylquinolines

Stefan Jopp[1], Franziska Spruner von Mertz[1], Peter Ehlers[1,2], Alexander Villinger[1] and Peter Langer[*1,2]

Full Research Paper

Open Access

Address:
[1]Universität Rostock, Institut für Chemie, Albert-Einstein-Str. 3a, 18059 Rostock, Germany and [2]Leibniz-Institut für Katalyse e.V. an der Universität Rostock, Albert-Einstein-Str. 29a, 18059 Rostock, Germany

Email:
Peter Langer[*] - peter.langer@uni-rostock.de

* Corresponding author

Keywords:
alkynes; catalysis; fluorescence; heterocycles; palladium

Beilstein J. Org. Chem. **2024,** *20,* 1246–1255.
https://doi.org/10.3762/bjoc.20.107

Received: 12 January 2024
Accepted: 23 April 2024
Published: 29 May 2024

This article is part of the thematic issue "Multicomponent reactions IV".

Associate Editor: T. J. J. Müller

© 2024 Jopp et al.; licensee Beilstein-Institut.
License and terms: see end of document.

Abstract

Three bis- or tris-brominated 2-trifluoromethylquinolines have been successfully applied in palladium-catalysed Sonogashira reactions, leading to several examples of alkynylated quinolines in good to excellent yields. Optical properties of selected products have been studied by steady state absorption and fluorescence spectroscopy which give insights of the influence of the substitution pattern and of the type of substituents on the optical properties.

Introduction

Quinoline is a well-known core structure which can be found in several natural and synthetic products and many of them show interesting pharmacological properties [1-3]. Quinine, for example, is a widely known natural product which was first isolated from the cinchona tree besides many other quinoline-containing cinchona alkaloids [4]. It is applied as antimalarial agent and furthermore as a bitter flavour component. Mefloquin [5] and ciprofloxacin [6], on the other hand, are synthetic compounds containing a fluorinated quinoline and quinolone core structure and are used as antimalarial and antibacterial agents, respectively (Figure 1). Fluorine-containing quinolines and quinolinones are of particular interest, since fluorine atoms are known to enhance the pharmacological properties of organic molecules [7-15]. Fluorine atoms act as bioisosteres of hydrogen atoms, while CF_3 groups are bioisosteres of hydroxy and methyl groups and are known to protect from metabolic oxidation [16]. Fluorine-containing arenes are metabolically more stable as compared to non-fluorinated arenes and they show a higher lipophilicity.

Known synthetic approaches towards 2-trifluoromethylquinolines include the cyclisation of anilines with trifluoroacetoacetate [17], the synthesis from enaminoketones [18] and the gold-catalysed cyclisation of propargylanilines [19].

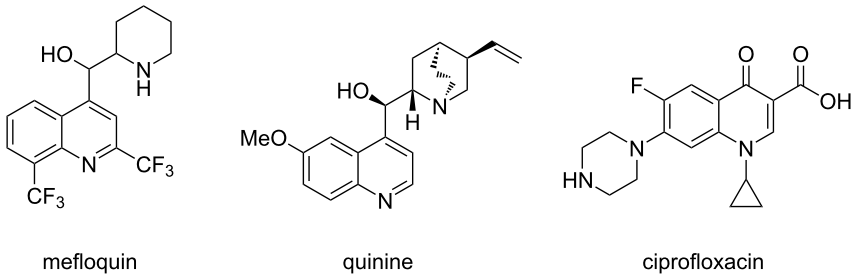

Figure 1: Natural and synthetic compounds containing a quinoline or quinolone core-structure.

Aside from its pharmaceutical significance quinoline compounds have been reported as strongly fluorescent with applications as electroluminescence materials [20-23], dyes, preservatives and as ligands in complex chemistry [24-27].

In the context of our interest in the application of cross-coupling reactions to polyhalogenated heterocycles [28-31], we studied Sonogashira reactions of brominated 2-trifluoromethylquinolines. The optical properties of selected products, bis- and tris-alkynylated quinolines, were studied to gain insights into how the substitution pattern at different positions may alter the optical properties.

Results and Discussion

The starting material, 4,8-dibromo-2-(trifluoromethyl)quinoline (**4**), was synthesized from 2-bromoaniline (**1a**) and ethyl trifluoroacetoacetate (**2**), adapting a known procedure from Schlosser and Marull (Scheme 1) [17]. The cyclization of **1a** with **2a** chemoselectively afforded 8-bromo-2-trifluoromethyl-4-quinolone (**3**) rather than 8-bromo-4-trifluoromethyl-2-quinolone. Bromination of **3** with phosphoryl bromide gave **4**.

With quinoline **4** in hand, we studied palladium-catalysed Sonogashira reactions with phenylacetylene (**5a**). Gratifyingly, our initial test reaction, using $Pd(OAc)_2$ as catalyst with XPhos as ligand, gave bis-alkynylated product **6a** in quantitative yield. Reducing the catalyst loading from 5 to 2.5 mol % or switching to more simple $Pd(PPh_3)_4$ still achieved quantitative yields. Less catalyst led to a reduced yield (Table 1). Consequently, we chose 2.5 mol % $Pd(PPh_3)_4$ for all further reactions.

Table 1: Optimization of the Sonogashira reaction.[a]

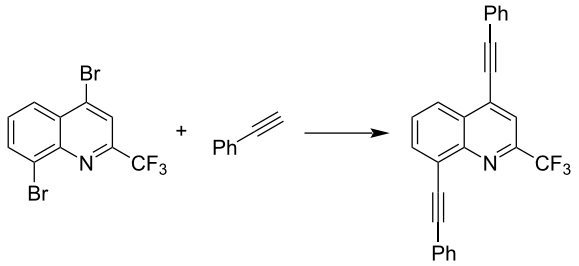

Pd-catalyst (mol %)	Ligand (mol %)	Cu-catalyst (mol %)	Yield (%)
$Pd(OAc)_2$ (5)	XPhos (10)	CuI (10)	99
$Pd(OAc)_2$ (2.5)	XPhos (5)	CuI (5)	99
$Pd(PPh_3)_4$ (5)	–	CuI (10)	99
$Pd(PPh_3)_4$ (2.5)	–	CuI (5)	99
$Pd(PPh_3)_4$ (1.75)	–	CuI (3.5)	93
$Pd(PPh_3)_4$ (1)	–	CuI (2)	90

[a]Reaction conditions: Pd catalyst, ligand, Cu catalyst, phenylacetylene (3.0 equiv), dioxane, NEt_3, 100 °C, 6 h.

As a next step, we analysed the scope of our methodology (Scheme 2). The optimized conditions allow cross-coupling reactions of various acetylenes containing electron-rich and electron-withdrawing functional groups, like methoxy or cyano, as well as thienyl and cyclopropyl groups. In general, all products were achieved in very good yields, ranging from 71 to 99%. Only product **6h**, containing a TMS group, could not be

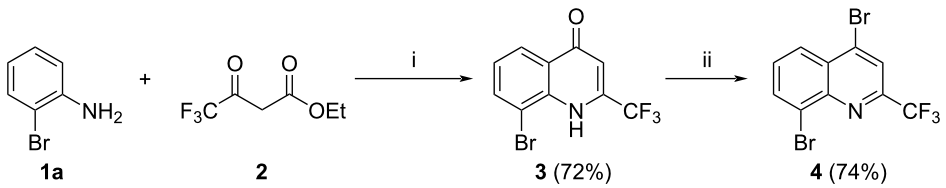

Scheme 1: Synthesis of **4**. Reaction conditions: i: polyphosphoric acid, 150 °C, 2 h; ii: $POBr_3$ (1.1 equiv), 150 °C, 2 h.

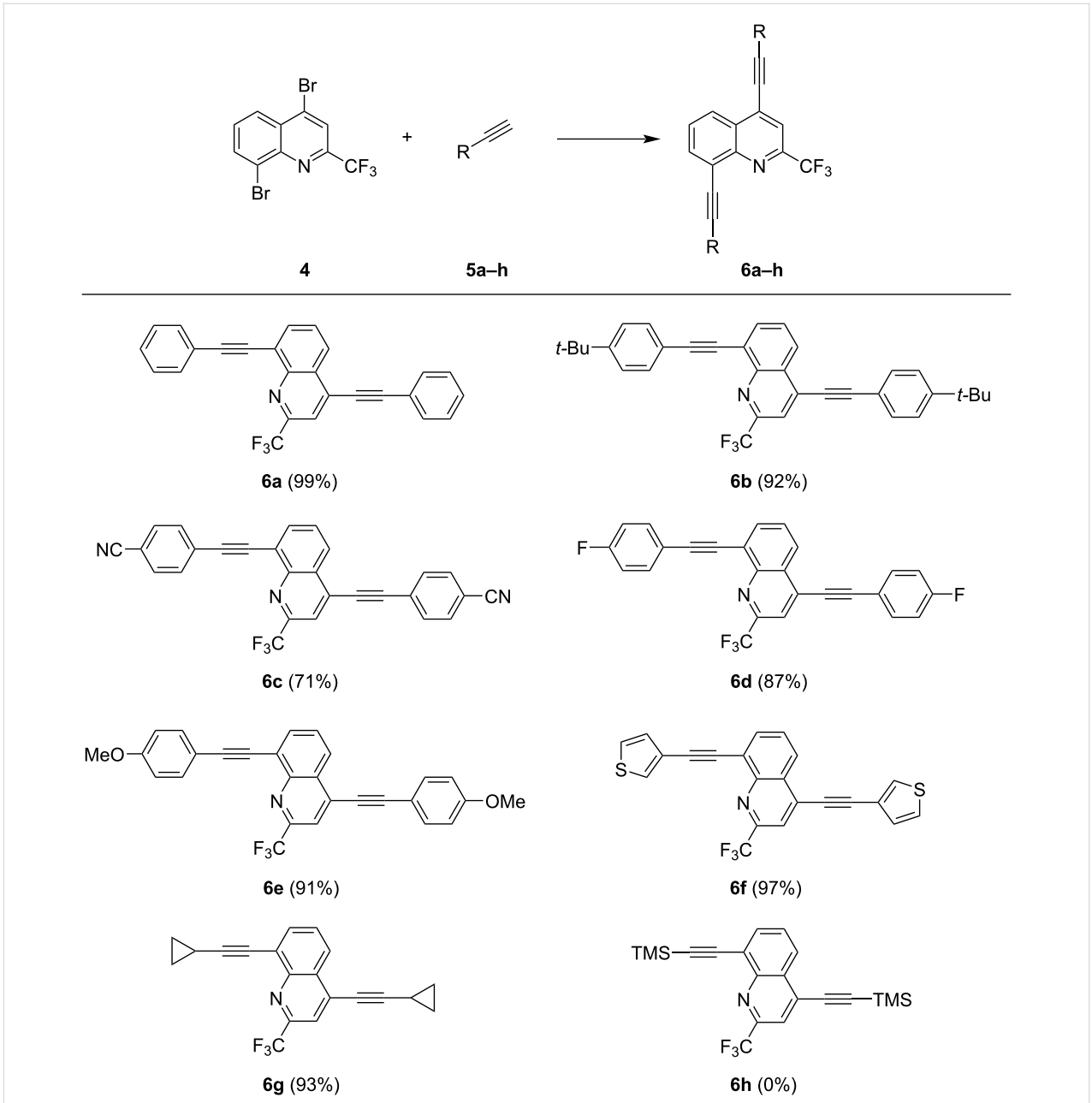

Scheme 2: Synthesis of compounds **6a–h**. Reaction conditions: $Pd(PPh_3)_4$ (2.5 mol %), CuI (5 mol %), acetylene (3.0 equiv), dioxane, NEt_3, 100 °C, 6 h; isolated yields.

isolated at all, since the reaction resulted in an inseparable mixture of several products.

The structure of **6b** could be independently confirmed by X-ray crystallography (Figure 2). Both phenyl rings are found to be twisted in an angle of approximately 45° from the quinoline core.

As a next step of our synthetic studies, we synthesized 4,6-dibromo-2-trifluoromethylquinoline (**8**) [32], an isomer of **4**, using 4-bromoaniline (**1b**) instead of **1a** (Scheme 3). Afterwards, we studied the scope of the twofold Sonogashira reaction, using the same reaction conditions as before (Scheme 4).

All 2,6-bis-alkynylated quinolines **9** were obtained in good yields of 77–85%, except for **9c** containing a cyano group (20%), most likely due to its low solubility. The yields are generally lower as compared to isomeric 2,8-bis-alkynylated products **6a–g**, which might be due to a slightly lower reactivity of the 6-position in comparison to the 8-position.

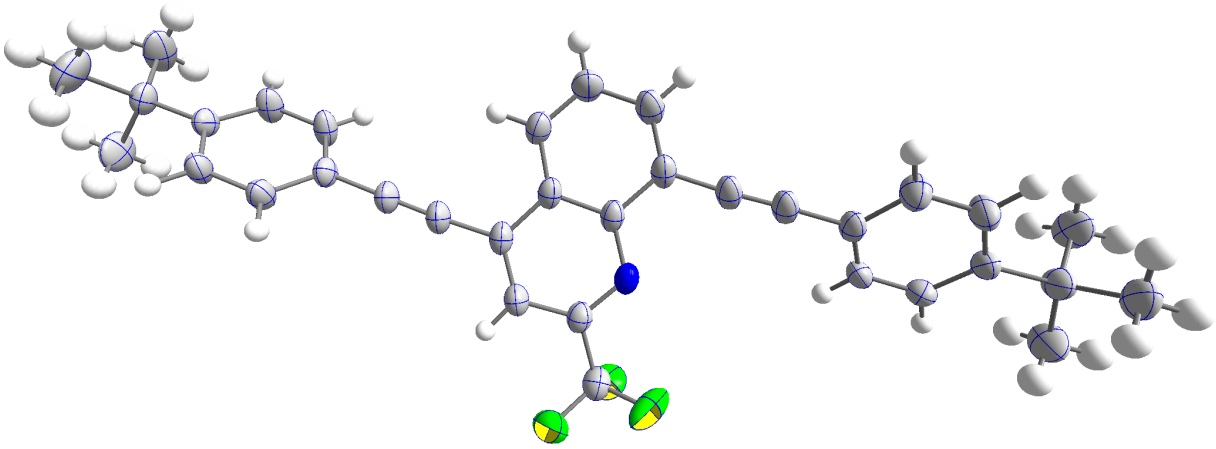

Figure 2: ORTEP of **6b** (CCDC 2322985).

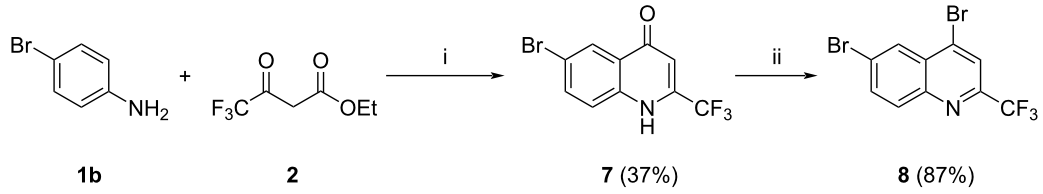

Scheme 3: Synthesis of **8**. Reaction conditions: i: polyphosphoric acid, 150 °C, 2 h [33]; ii: $POBr_3$ (1.1 equiv), 150 °C, 2 h.

The structure of product **9f** was confirmed by X-ray crystallography (Figure 3). The thiophene ring in 4-position is in plane with the quinoline core, while the other ring is twisted in an angle of approximately 85°. This might be explained by an electronic push–pull interaction of the thiophene and the quinoline moieties via the alkyne.

Finally, we focussed on the synthesis of tris-alkynylated quinolines starting from 3,4,8-tribromo-2-(trifluoromethyl)quinoline (**11**). Starting material **11** was synthesized in very good yield from quinolone **3** by bromination in position 3, followed by treatment of brominated intermediate **10** with phosphoryl bromide (Scheme 5) [34].

To our delight, the optimized conditions for the synthesis of alkynylated quinolines **6** could be applied also to the three-fold Sonogashira reaction of **11**. However, the reaction time had to be prolonged from 6 to 24 h and the amount of acetylene was increased. Thus, tris-alkynylated quinolines **12a–g** were prepared in good 64–75% yields (Scheme 6). The yields of products **12a–g** were lower as compared to bis-alkynylated products **6a–g** which were, in fact, found as major side-products, due to dehalogenation at position 3. In particular, the side-product **6b** was isolated in 25% yield during the purification of **12b**. The structure of product **12d** was proven by X-ray crystallography (Figure 4). All three phenyl rings are found to be nearly in plane with the quinoline core, showing only a slight twist of 5–10°.

Optical properties

Steady-state absorption and fluorescence measurements were carried out. Compounds **6a**, **9a**, and **12a** were selected to study the impact of the position of the alkynyl group on the optical properties. Comparison of the absorption and emission features of **12a**, **12b** and **12c** gives first insights on how the optical properties can be fine-tuned by the substitution pattern of the arylalkyne. The key optical properties are summarized in Table 2.

All molecules display relatively high quantum yields (QYs) with the highest being 0.66 for **6a** and the lowest 0.54 for **12a**. This is in accordance with similar poly-alkynylated molecules from the literature [31,36]. Differences in the absorption and photoluminescence spectra of **6a**, **9a** and **12a** can be explained by the different positions of the alkyne moieties (Figure 5). All absorption spectra exhibit a broad first absorption band with different fine structures. However, TD-DFT calculations using the long-range correlated CAM-B3LYP/6-311G(d,p) level of

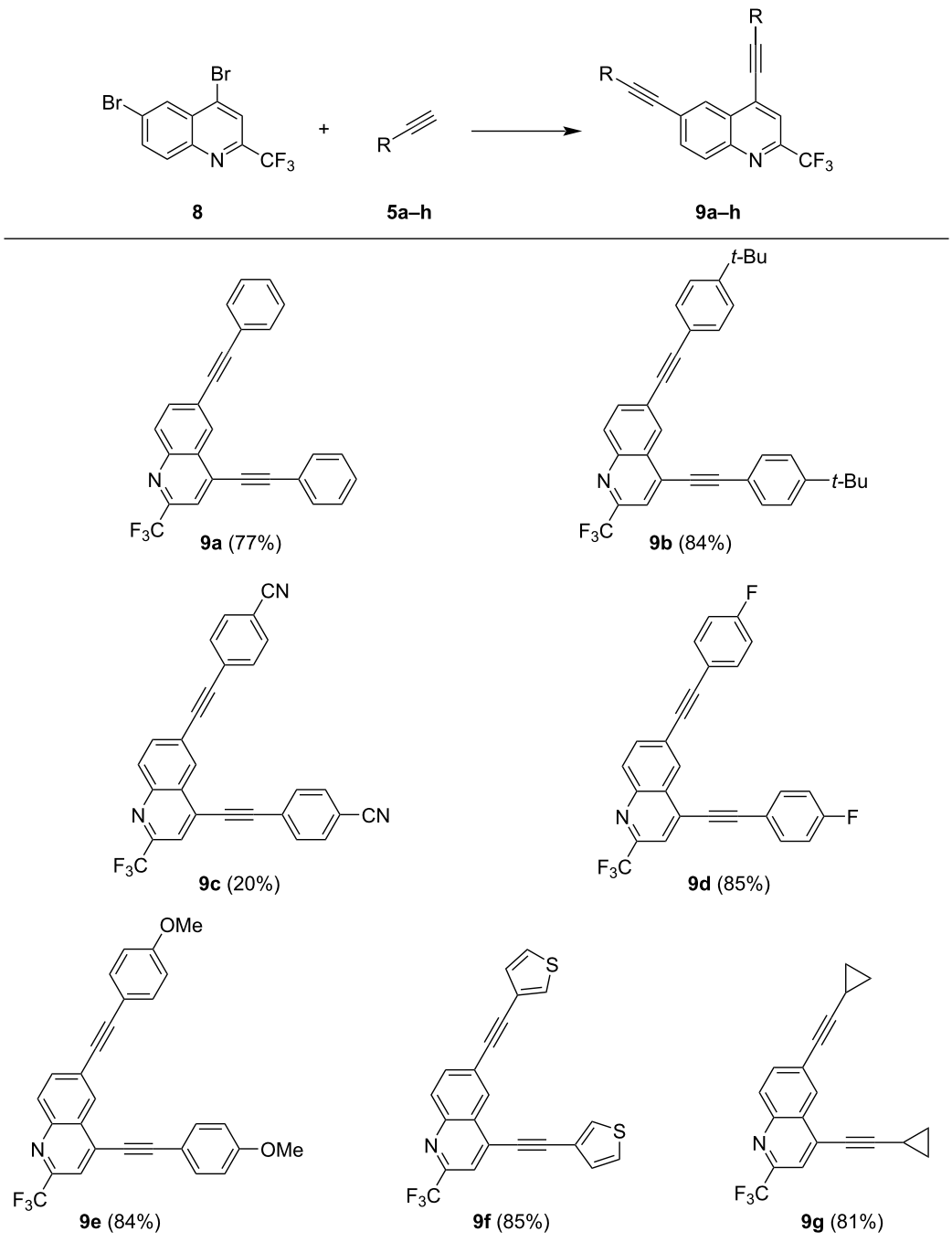

Scheme 4: Synthesis of compounds **9a–g**: Reaction conditions: $Pd(PPh_3)_4$ (2.5 mol %), CuI (5 mol %), acetylene (3.0 equiv), dioxane, NEt_3, 100 °C, 6 h, isolated yields.

theory reveal that the lowest energy band for all three derivatives **6a**, **9a** and **12a** originate mainly from a HOMO→LUMO transition with some admixture of HOMO−1→LUMO+1 and HOMO−1→LUMO, respectively. A bathochromic shift is observed from **9a** over **6a** to **12a** in the first absorption maximum with a total of 0.29 eV. This trend can be observed in the emission spectrum as well. All three emission spectra are characterized by a single broad emission peak which is almost identical for **6a** and **12a** and is redshifted by 0.26 eV compared to **9a**. Thus, the position of the substituent at the quinoline core has a significant impact on the optical properties of the molecules. An alkynyl group located at the 8-position seems to have a greater impact on the properties than one at the 3-position, since **6a** and **12a** are almost identical in their emission.

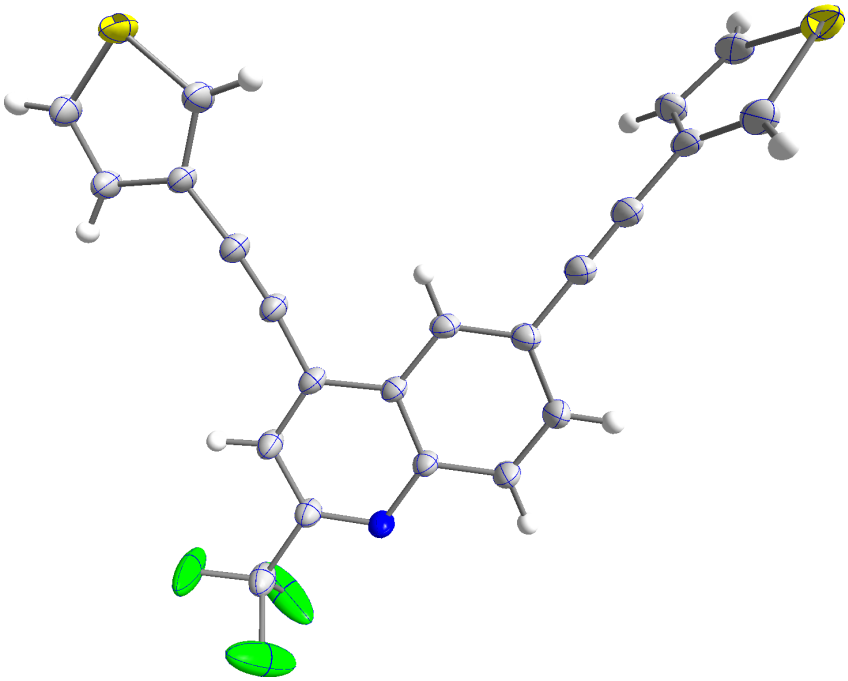

Figure 3: ORTEP of **9f** (CCDC 2322983).

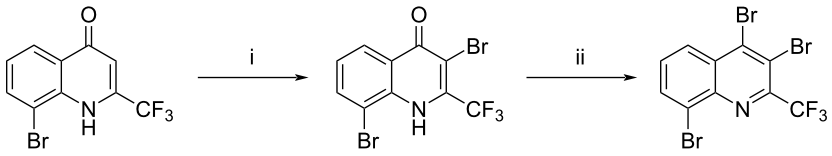

Scheme 5: Synthesis of starting material **11**. Reaction conditions: i: AcOH, Br_2 (1.1 equiv), reflux, 24 h; ii: $POBr_3$ (1.1 equiv), 150 °C, 2 h.

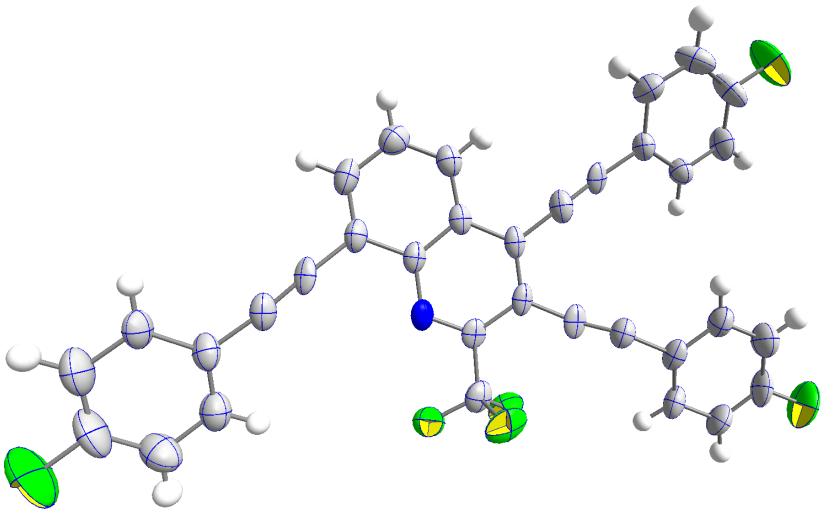

Figure 4: ORTEP of **12d** (CCDC 2322984).

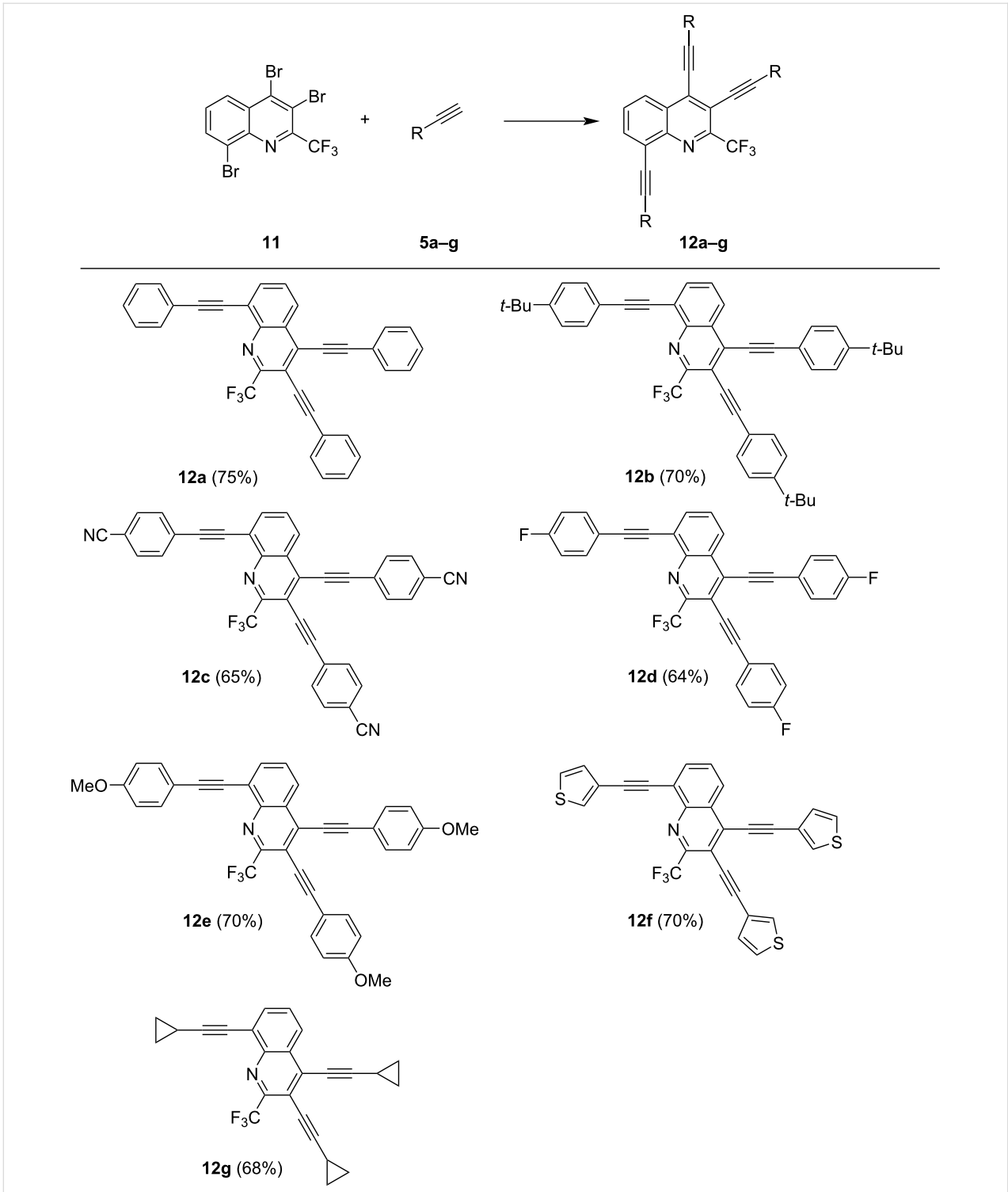

Scheme 6: Synthesis of compounds **12a–g**. Reaction conditions: $Pd(PPh_3)_4$ (2.5 mol %), CuI (5 mol %), acetylene (4.0 equiv), dioxane, NEt_3, 100 °C, 24 h; isolated yields.

The influence of the type of substituent located at the alkyne moieties of **12a**, **12c**, and **12e** was also studied. The intensity increases from **12a** to **12e** and a bathochromic shift of the absorption maxima can be observed. Interestingly, the emission spectra of **12a** and **12c** are identical which suggests that the strong acceptor groups of **12c** do not have an impact on the emission. On the other hand, the strong donor groups of **12e** cause a redshift of 0.20 eV as compared to the simple phenyl-substi-

Table 2: Spectroscopic data of **6a**, **9a**, **12a**, **12c**, and **12e** in dichloromethane (10^{-5} M) at 20 °C (λ_{ex} = 380 nm).

	6a	**9a**	**12a**	**12c**	**12e**
$\lambda_{1,abs}$ (nm)	280	267	279	298	276
$\varepsilon_{\lambda1}$ ($M^{-1}cm^{-1}$)	17200	36600	36600	53900	77600
$\lambda_{2,abs}$ (nm)	295	282	308	318	292[a]
$\varepsilon_{\lambda2}$ ($M^{-1}cm^{-1}$)	17900	39600	42700	55400	64000
$\lambda_{3,abs}$ (nm)	331	293	315	330[b]	303
$\varepsilon_{\lambda3}$ ($M^{-1}cm^{-1}$)	17400	43200	43600	51100	56100
$\lambda_{4,abs}$ (nm)	337	347	377	378	335
$\varepsilon_{\lambda4}$ ($M^{-1}cm^{-1}$)	17100	20500	17500	21100	75700
$\lambda_{5,abs}$ (nm)	365	362[a]	395[a]	397[a]	395
$\varepsilon_{\lambda5}$ ($M^{-1}cm^{-1}$)	18800	17500	14300	15800	37400
$\lambda_{6,abs}$ (nm)					416[a]
$\varepsilon_{\lambda6}$ ($M^{-1}cm^{-1}$)					32089
$\lambda_{1,em}^{380}$ (nm)	457	419	459	458	494
Φ^{b}	0.66	0.63	0.54	0.56	0.59

[a]Shoulder; [b]fluorescence standard: perylene in cyclohexane (Φ = 0.94) [35].

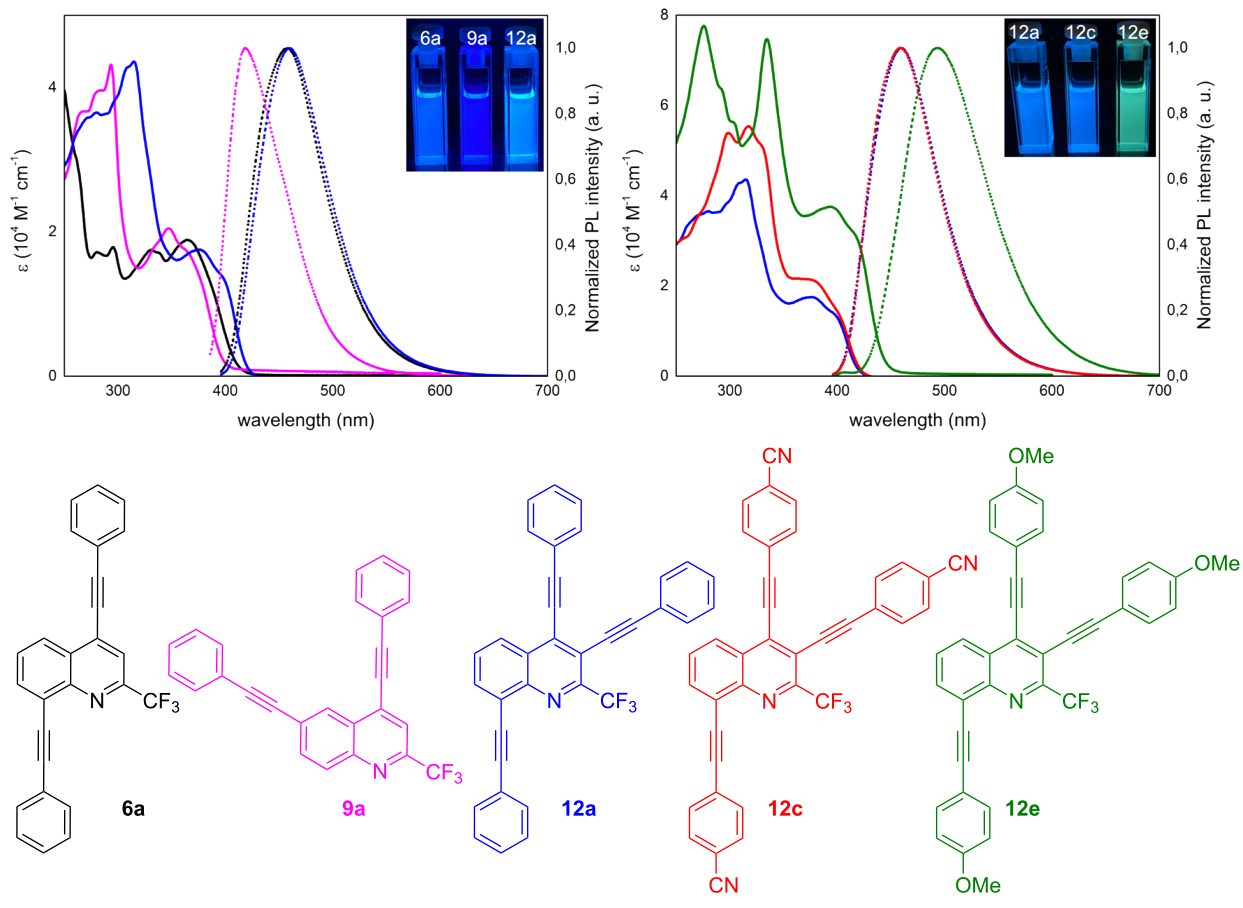

Figure 5: UV–vis and emission spectra of **6a**, **9a** and **12a** (left) and **12a**, **12c**, and **12e** (right, λ_{ex} = 380 nm) in DCM (c = 10^{-5} M) at 20 °C.

tuted molecule. Electron-acceptor groups usually have a slighter impact on the emission than electron-donating groups [36]. These findings show that by varying the position and the substituents of the alkynyl groups the properties of the products can be tuned effectively.

Conclusion

Three different brominated 2-trifluoromethylquinolines have been synthesized and applied to palladium-catalysed Sonogashira reactions. Optimised reaction conditions allow the synthesis of various bis- or tris-alkynylated products in one step. Products were generally obtained in high yields and intensive fluorescence. The photophysical properties of selected compounds were investigated via steady-state absorption and fluorescence spectroscopy and gives first insights into the structure–optical property relationship of polyalkynylated quinolines. In particular, high fluorescence quantum yields have been determined for all studied compounds. Variation of the substitution pattern on the quinoline scaffold and on the arylalkyne moiety permits the fine tuning of the optical properties.

Supporting Information

Supporting Information File 1

Experimental part.
[https://www.beilstein-journals.org/bjoc/content/supplementary/1860-5397-20-107-S1.pdf]

Author Contributions

Stefan Jopp: data curation; formal analysis; investigation; validation; visualization; writing – original draft. Franziska Spruner von Mertz: formal analysis; investigation; validation; writing – original draft. Peter Ehlers: project administration; supervision; validation; visualization; writing – review & editing. Alexander Villinger: data curation; formal analysis; investigation; validation. Peter Langer: conceptualization; funding acquisition; project administration; resources; supervision; visualization; writing – review & editing.

ORCID® iDs

Stefan Jopp - https://orcid.org/0000-0003-2148-7914
Peter Ehlers - https://orcid.org/0000-0001-6444-7563
Alexander Villinger - https://orcid.org/0000-0002-0868-9987

Data Availability Statement

All data that supports the findings of this study is available in the published article and/or the supporting information to this article.

References

1. Cannon, J. G. *J. Med. Chem.* **1997,** *40,* 4165–4166. doi:10.1021/jm9706123
2. Michael, J. P. *Nat. Prod. Rep.* **2008,** *25,* 166–187. doi:10.1039/b612168n
3. Taylor, J. B.; Triggle, D. J. *Comprehensive medicinal chemistry II;* Elsevier: Amsterdam, Netherlands, 2007.
4. Willcox, M.; Bodeker, G.; Rasoanaivo, P.; Addae-Kyereme, J., Eds. *Traditional Medicinal Plants and Malaria;* CRC Press: Boca Raton, FL, USA, 2004. doi:10.1201/9780203502327
5. Ohnmacht, C. J.; Patel, A. R.; Lutz, R. E. *J. Med. Chem.* **1971,** *14,* 926–928. doi:10.1021/jm00292a008
6. Grohe, K.; Zeiler, H.-J.; Metzger, K. 1-Cyclopropyl-6-fluor-1,4-dihydro-4-oxo-7-piperazino-chinolin-3-carbon säuren, Verfahren zu ihrer Herstellung. Ger. Pat. Appl. DE3142854A1, Oct 29, 1981.
7. Baraznenok, I. L.; Nenajdenko, V. G.; Balenkova, E. S. *Eur. J. Org. Chem.* **1999,** 937–941. doi:10.1002/(sici)1099-0690(199904)1999:4<937::aid-ejoc937>3.0.co;2-3
8. Crousse, B.; Bégué, J.-P.; Bonnet-Delpon, D. *J. Org. Chem.* **2000,** *65,* 5009–5013. doi:10.1021/jo9918807
9. Takaya, J.; Kagoshima, H.; Akiyama, T. *Org. Lett.* **2000,** *2,* 1577–1579. doi:10.1021/ol005812e
10. Fuchigami, T.; Ichikawa, S. *J. Org. Chem.* **1994,** *59,* 607–615. doi:10.1021/jo00082a018
11. Schlosser, M.; Keller, H.; Sumida, S.-i.; Yang, J. *Tetrahedron Lett.* **1997,** *38,* 8523–8526. doi:10.1016/s0040-4039(97)10304-5
12. Latham, E. J.; Murphy, S. M.; Stanforth, S. P. *Tetrahedron Lett.* **1994,** *35,* 3395–3396. doi:10.1016/s0040-4039(00)76917-6
13. Strekowski, L.; Lin, S.-Y.; Lee, H.; Zhang, Z.-Q.; Mason, J. C. *Tetrahedron* **1998,** *54,* 7947–7954. doi:10.1016/s0040-4020(98)00440-2
14. Xie, H.; Zhu, J.; Chen, Z.; Li, S.; Wu, Y. *Synlett* **2010,** 2659–2663. doi:10.1055/s-0030-1258770
15. Strekowski, L.; Czarny, A.; Lee, H. *J. Fluorine Chem.* **2000,** *104,* 281–284. doi:10.1016/s0022-1139(00)00252-9
16. Patani, G. A.; LaVoie, E. J. *Chem. Rev.* **1996,** *96,* 3147–3176. doi:10.1021/cr950066q
17. Marull, M.; Schlosser, M. *Eur. J. Org. Chem.* **2003,** 1576–1588. doi:10.1002/ejoc.200390217
18. El Kharrat, S.; Laurent, P.; Blancou, H. *Tetrahedron* **2014,** *70,* 1252–1266. doi:10.1016/j.tet.2013.12.073
19. Zhu, M.; Fu, W.; Zou, G.; Xun, C.; Deng, D.; Ji, B. *J. Fluorine Chem.* **2012,** *135,* 195–199. doi:10.1016/j.jfluchem.2011.11.002
20. Całus, S.; Gondek, E.; Danel, A.; Jarosz, B.; Kityk, A. V. *Opt. Commun.* **2007,** *271,* 16–23. doi:10.1016/j.optcom.2006.10.010
21. Całus, S.; Gondek, E.; Danel, A.; Jarosz, B.; Pokładko, M.; Kityk, A. V. *Mater. Lett.* **2007,** *61,* 3292–3295. doi:10.1016/j.matlet.2006.11.055
22. Gondek, E.; Danel, A.; Nizioł, J.; Armatys, P.; Kityk, I. V.; Szlachcic, P.; Karelus, M.; Uchacz, T.; Chwast, J.; Lakshminarayana, G. *J. Lumin.* **2010,** *130,* 2093–2099. doi:10.1016/j.jlumin.2010.05.033
23. Gondek, E.; Danel, A.; Kityk, I. V. *Philos. Mag.* **2010,** *90,* 2677–2685. doi:10.1080/14786431003685490
24. Kappaun, S.; Slugovc, C.; List, E. J. W. *Int. J. Mol. Sci.* **2008,** *9,* 1527–1547. doi:10.3390/ijms9081527

25. Park, J.; Park, J. S.; Park, Y. G.; Lee, J. Y.; Kang, J. W.; Liu, J.; Dai, L.; Jin, S.-H. *Org. Electron.* **2013,** *14,* 2114–2123. doi:10.1016/j.orgel.2013.05.013
26. Li, J.; Wang, R.; Yang, R.; Zhou, W.; Wang, X. *J. Mater. Chem. C* **2013,** *1,* 4171. doi:10.1039/c3tc30586d
27. Tonzola, C. J.; Alam, M. M.; Kaminsky, W.; Jenekhe, S. A. *J. Am. Chem. Soc.* **2003,** *125,* 13548–13558. doi:10.1021/ja036314e
28. Reimann, S.; Ehlers, P.; Ohlendorf, L.; Langer, P. *Org. Biomol. Chem.* **2017,** *15,* 1510–1520. doi:10.1039/c6ob02264b
29. Miliutina, M.; Ivanov, A.; Ejaz, S. A.; Iqbal, J.; Villinger, A.; Iaroshenko, V. O.; Langer, P. *RSC Adv.* **2015,** *5,* 60054–60078. doi:10.1039/c5ra10948e
30. Parpart, S.; Petrosyan, A.; Ali Shah, S. J.; Adewale, R. A.; Ehlers, P.; Grigoryan, T.; Mkrtchyan, A. F.; Mardiyan, Z. Z.; Karapetyan, A. J.; Tsaturyan, A. H.; Saghyan, A. S.; Iqbal, J.; Langer, P. *RSC Adv.* **2015,** *5,* 107400–107412. doi:10.1039/c5ra22407a
31. Petrosyan, A.; Ehlers, P.; Surkus, A.-E.; Ghochikyan, T. V.; Saghyan, A. S.; Lochbrunner, S.; Langer, P. *Org. Biomol. Chem.* **2016,** *14,* 1442–1449. doi:10.1039/c5ob02083b
32. Upadhayaya, R. S.; Dixit, S. S.; Földesi, A.; Chattopadhyaya, J. *Bioorg. Med. Chem. Lett.* **2013,** *23,* 2750–2758. doi:10.1016/j.bmcl.2013.02.054
33. da Silva, E. T.; de Andrade, G. F.; da Araújo, A. S.; Lourenço, M. C. S.; de Souza, M. V. N. *Eur. J. Pharm. Sci.* **2021,** *157,* 105596. doi:10.1016/j.ejps.2020.105596
34. Kuhrt, D.; Ejaz, S. A.; Afzal, S.; Khan, S. U.; Lecka, J.; Sévigny, J.; Ehlers, P.; Spannenberg, A.; Iqbal, J.; Langer, P. *Eur. J. Med. Chem.* **2017,** *138,* 816–829. doi:10.1016/j.ejmech.2017.07.017
35. Brouwer, A. M. *Pure Appl. Chem.* **2011,** *83,* 2213–2228. doi:10.1351/pac-rep-10-09-31
36. Ehlers, P.; Neubauer, A.; Lochbrunner, S.; Villinger, A.; Langer, P. *Org. Lett.* **2011,** *13,* 1618–1621. doi:10.1021/ol2000183

License and Terms

This is an open access article licensed under the terms of the Beilstein-Institut Open Access License Agreement (https://www.beilstein-journals.org/bjoc/terms), which is identical to the Creative Commons Attribution 4.0 International License (https://creativecommons.org/licenses/by/4.0). The reuse of material under this license requires that the author(s), source and license are credited. Third-party material in this article could be subject to other licenses (typically indicated in the credit line), and in this case, users are required to obtain permission from the license holder to reuse the material.

The definitive version of this article is the electronic one which can be found at:
https://doi.org/10.3762/bjoc.20.107

BEILSTEIN JOURNAL OF ORGANIC CHEMISTRY

Domino reactions of chromones with activated carbonyl compounds

Peter Langer[1,2,§]

Review

Open Access

Address:
[1]Institut für Chemie, Universität Rostock, Albert-Einstein-Str. 3a, 18059 Rostock, Germany and [2]Leibniz-Institut für Katalyse e. V. an der Universität Rostock, Albert-Einstein-Str. 29a, 18059 Rostock, Germany

Email:
Peter Langer - peter.langer@uni-rostock.de

§ Fax: +49 381 4986412

Keywords:
cyclizations; 1,3-dicarbonyl compounds; domino reactions; heterocycles; regioselectivity; silyl enol ethers

Beilstein J. Org. Chem. **2024,** *20,* 1256–1269.
https://doi.org/10.3762/bjoc.20.108

Received: 27 February 2024
Accepted: 08 May 2024
Published: 29 May 2024

This article is part of the thematic issue "Multicomponent reactions IV".

Associate Editor: T. J. J. Müller

© 2024 Langer; licensee Beilstein-Institut.
License and terms: see end of document.

Abstract

Domino reactions of chromones with activated carbonyl compounds, such as dimethyl acetone-1,3-dicarboxylate and 1,3-diphenylacetone, and with 1,3-bis(silyloxy)-1,3-butadienes, electroneutral equivalents of 1,3-dicarbonyl dianions, allow for a convenient synthesis of a great variety of products. The regioselectivity and course of the reaction depends of the substituent located at carbon C3 of the chromone moiety and also on the type of nucleophile employed.

Introduction

Domino reactions (also called cascade or tandem reactions) allow for the synthesis of complex products with formation of several bonds in only one step [1-5]. In contrast to non-activated acetone (**1a**), methylene-active compounds, such as 1,3-dicarbonyl compounds, are of considerable relevance as building blocks in domino reactions (Scheme 1). For example, methyl acetoacetate (**2a**) possesses one CH-acidic methylene carbon which can be deprotonated in equilibrium by weak organic bases, such as triethylamine, piperidine or DBU, under thermodynamic conditions. Dimethyl acetone-1,3-dicarboxylate (**3a**) contains even two reactive methylene groups which can undergo cyclization reactions under mild conditions. In case of 1,3-diphenylacetone (**4a**) some activation of the methylene group is observed as well, because of benzylic stabilization.

Dianions of 1,3-dicarbonyl compounds follow a different regioselectivity as compared to simple monoanions [6-12]. For example, **2** can be transformed to its dianion **7** by action of two equivalents of LDA or by sequential addition of sodium hydride and *n*-butyllithium (Scheme 1). In contrast to **2**, dianion **7** reacts with electrophiles at its terminal carbon atom. 1,3-Bis(silyloxy)-1,3-butadienes, containing two silyl enol ether moieties, can be regarded as masked dianions or electroneutral equivalents of 1,3-dicarbonyl dianions and react with the same regioselectivi-

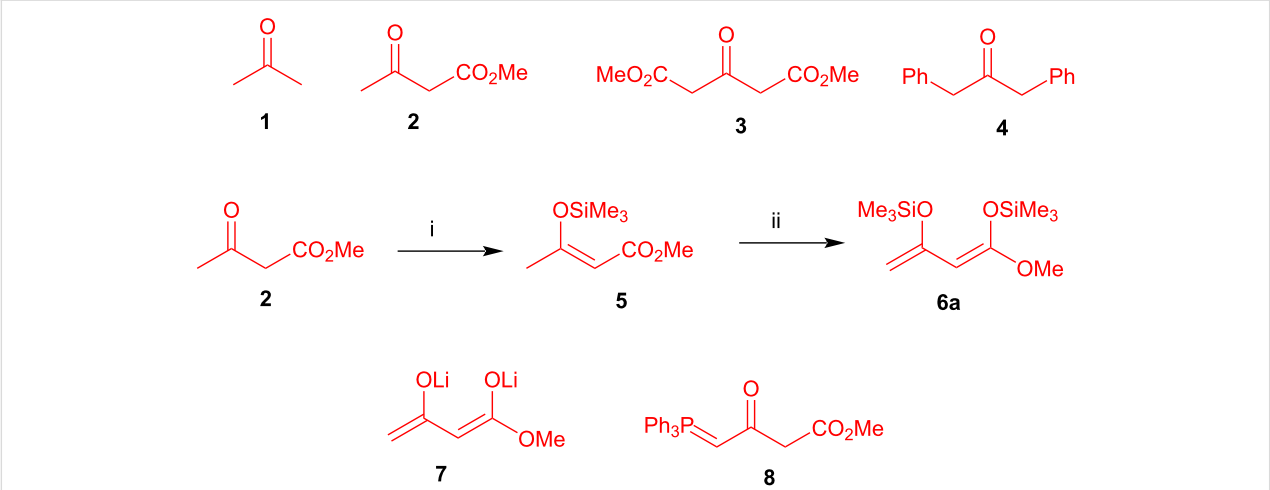

Scheme 1: Structures of carbonyl compounds **1**, **2, 3,** and **4**, dianion **7**, phosphorane **8** and synthesis of 1,3-bis(silyloxy)-1,3-butadiene **6a** via **5**. Conditions: i, Me_3SiCl, toluene, NEt_3, 24 h; ii, 1) LDA, THF, –78 °C, 1 h; 2) Me_3SiCl, –78 to 20 °C, 12 h.

ty [13-22]. Both free and masked dianions were studied extensively in my group for many years. 1,3-Bis(silyloxy)-1,3-butadienes are highly moisture sensitive compounds which can be prepared from the corresponding 1,3-dicarbonyl dianions in two steps. For example, diene **6a** is available by silylation of **2** to give silyl enol ether **5** which is subsequently deprotonated by LDA and treated with trimethylchlorosilane. A direct preparation of **6a** by reaction of dianion **7** with trimethylchlorosilane is not possible, because the silylation occurs at the terminal carbon atom of the dianion. (2,4-Dioxobutylidene)phosphorane **8** also represents a synthetic equivalent of dianion **7** [23]. However, reactions of such phosphoranes were less studied in my group.

Chromones are oxygen heterocycles which are of pharmacological interest and represent versatile synthetic building blocks which can undergo various types of domino reactions [24-28]. In 2001, Nehad N. R. Saleh in my group developed a new synthesis of benzocoumarines by reaction of 1,3-bis(silyloxy)-1,3-butadiene **6a** with parent 2,3-unsubstituted chromone (**9a**). This marked the starting point of chromone chemistry in my group. In the following years, we studied reactions of various types of chromones with 1,3-bis(silyloxy)-1,3-butadienes [29]. Starting in 2010, we studied also cyclization reactions of chromones with heterocyclic enamines [30,31]. The present review aims to provide a personalized account of our work related to domino reactions of various types of chromones with carbonyl compounds, such as **3** and **4**, and with 1,3-bis(silyloxy)-1,3-butadienes, such as **6a**. These studies include various types of chromones, including 2,3-unsubstituted chromone (**9a**), 3-formylchromone (**10a**), 3-acetylchromone, 3-(methoxalyl)chromone (**11a**), 3-benzoylchromone (**12a**), 3-(2-nitrobenzoyl)chromone (**13a**), 3-trifluoroacetylchromone (**14a**), 3-perfluoroalkanoylchromones, 3-bromochromone (**15a**), 3-chloro- and 3-iodochromone, and 3-cyanochromone (**16a**) (Scheme 2). Depending on the type of chromone and nucleophile, the reactions follow a different regioselectivity.

Review

2,3-Unsubstituted chromones

Dimethyl acetone-1,3-dicarboxylate

The base-mediated reaction of dimethyl acetone-1,3-dicarboxylate (**3**) with 2,3-unsubstituted parent chromone (**9a**) afforded benzocoumarine **17** in 56% yield (Scheme 3) [32]. The formation of the product can be explained by 1,4-addition of **3** to the chromone to give intermediate **A** and ring cleavage to give intermediate **B**. Subsequent Knoevenagel reaction by attack of the methylene carbon to the carbonyl group gave intermediate **C** which underwent lactonization to give the final product.

1,3-Bis(silyloxy)-1,3-butadienes

The reaction of chromones **9a–j** with 1,3-bis(silyloxy)-1,3-butadienes **6a–h**, carried out in the presence of Me_3SiOTf, and subsequent treatment with triethylamine in methanol afforded benzocoumarines **18a–ac** (Scheme 4) [33,34]. The formation of the product, which was obtained in a two-step one-pot reaction, can be explained by a mechanism similar to the one discussed for the formation of **17**. 1,4-Addition gave intermediate **D** which was isolated, but used in crude form for the next step. Treatment of the latter with triethylamine in methanol resulted in ring-cleavage to give intermediate **E**. Subsequent base-mediated Knoevenagel reaction with extrusion of water gave intermediate **F** which underwent lactonization and resulted in the formation of the final product. The reaction proved to be rather general and various dienes and chromones were successfully employed to give the corresponding benzozocoumarines in

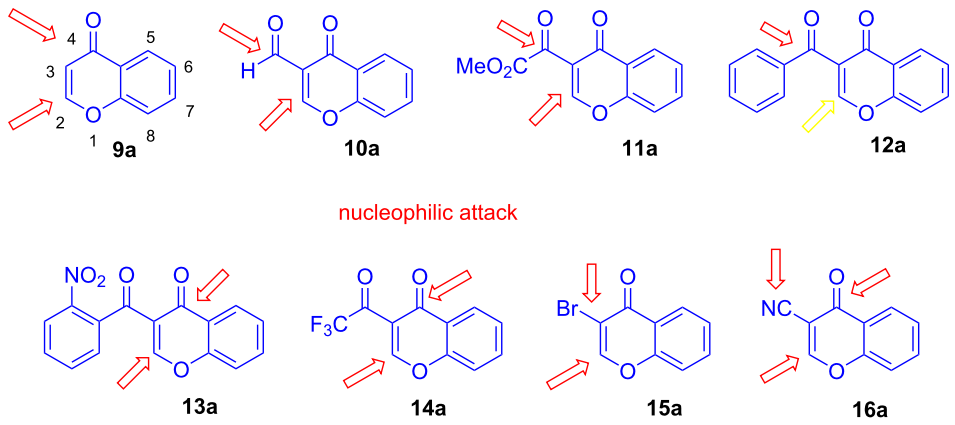

Scheme 2: Structures of chromones with different substituents located at carbon C-3 and atom numbering scheme exemplified for **9a**.

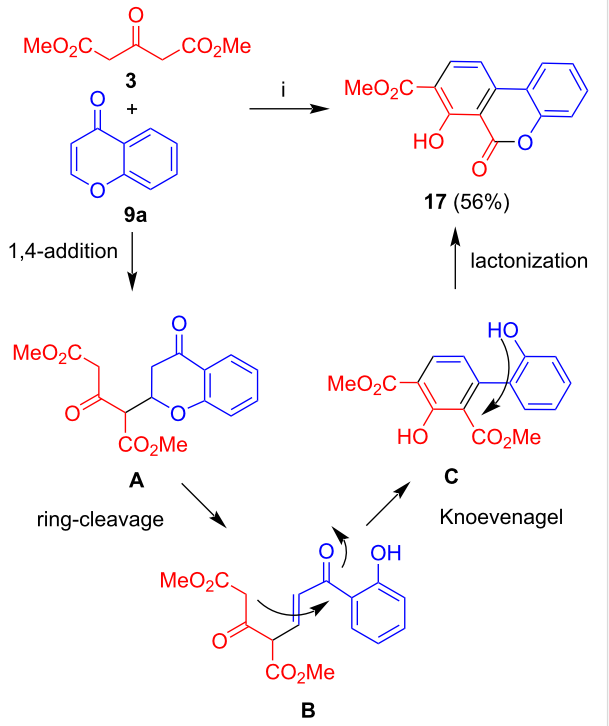

Scheme 3: Synthesis of **17**. Conditions: i, DBU (1.3 equiv), THF, 20 °C, 12 h.

good yields. The yields were in most of the cases in the range of 42 to 65% (over two steps) and did not depend much on the substituents attached to the chromone and at carbon C-4 of the diene. However, in case of a benzyl and a benzyloxy group located at carbon C-4 of the diene, the overall yields were rather low (20%). This might be explained by steric effects. One of the best yields was obtained for the reaction of diene **6a** with unsubstituted chromone **9a** and for the diene containing a methoxy group (R^4 = OMe). The products proved to be interesting, due to their blue fluorescence.

3-Formylchromones

Dimethyl acetone-1,3-dicarboxylate

The reaction of **3** with 3-formylchromones **10a–d** afforded benzophenones **19a–d** in moderate to good yields (Scheme 5) [32]. The formation of the products can be explained by Michael reaction (1,4-addition) of **3** to the chromone and ring cleavage to give intermediate **G**. Subsequent Knoevenagel reaction by attack of the methylene carbon to the aldehyde resulted in the formation of the final products. The regioselective cyclization can be explained by the higher electrophilicity of the aldehyde as compared to the ketone. The yields were in general quite good (51–65%). Relatively low yields (51–52%) were obtained for chromones containing methyl substituents, presumably due to the lower electrophilicity of the chromone based on the electron-donating effect of the methyl groups. Good yields were obtained for parent 3-formylchromone (**10a**) and for chlorine-substituted chromones, because of the higher electrophilicity of the chromone based on the electron-withdrawing effect of the methyl groups.

1,3-Bis(silyloxy)-1,3-butadienes

The reaction of 3-formyl- and 3-acetylchromones **10a–i** with 1,3-bis(silyloxy)-1,3-butadienes **6a–h**, catalysed by Me_3SiOTf, afforded hydroxylated benzophenones **20a–ag** (Scheme 6) [35,36]. The products are formed by a mechanism related to the one discussed for the formation of products **19a–d**. The same type of product is formed in the reaction of 3-formylchromones with (2,4-dioxobutylidene)phosphoranes [37]. The yields were in a range of 33 to 82%. No clear trend was observed for the yields depending on the structure of the diene and the chromone. Similar to unsubstituted diene **6a**, dienes containing a substituent R^5 located at carbon C-4 gave good yields, except for methoxy and benzyloxy which did not work at all. Dienes derived from 1,3-diketones (R^6 = Me, Ph) gave similar yields to those obtained from dienes derived form β-ketoesters, although

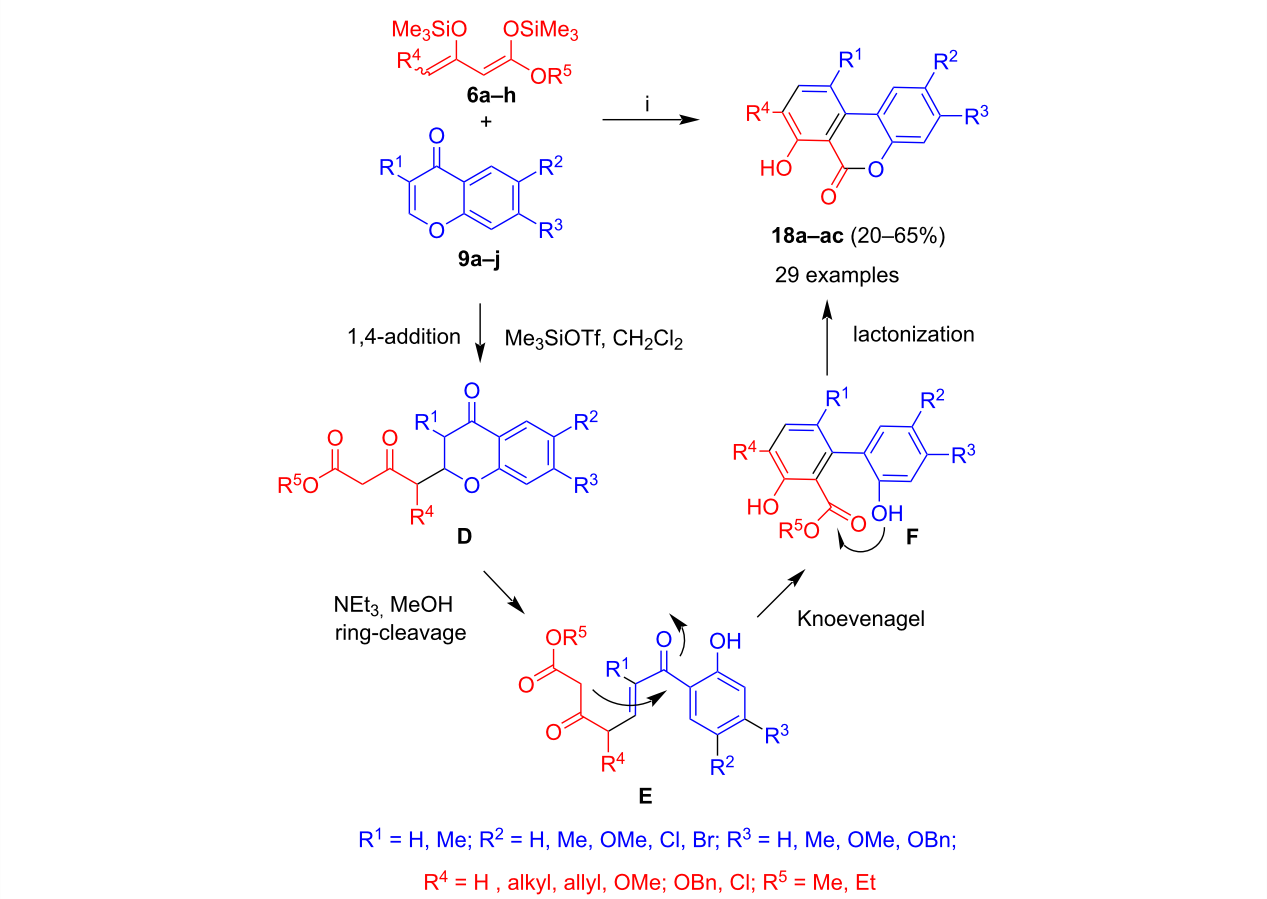

Scheme 4: Synthesis of **18a–ac**. Conditions: i, 1) **9a–j**, Me_3SiOTf (1.3 equiv), 20 °C, 1 h; 2) **6a–h** (1.3 equiv), CH_2Cl_2, 0 → 20 °C, 12 h; 3) HCl (10%); 4) NEt_3 (2.0 equiv), EtOH, 20 °C, 12 h.

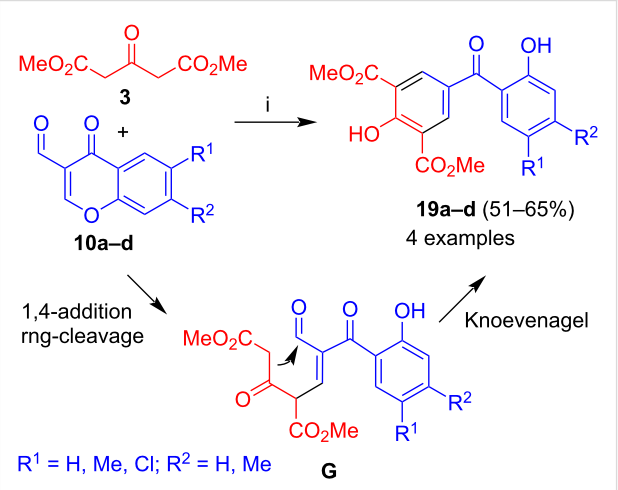

Scheme 5: Synthesis of **19a–d**. Conditions: i, DBU (1.3 equiv), THF, 20 °C, 12 h.

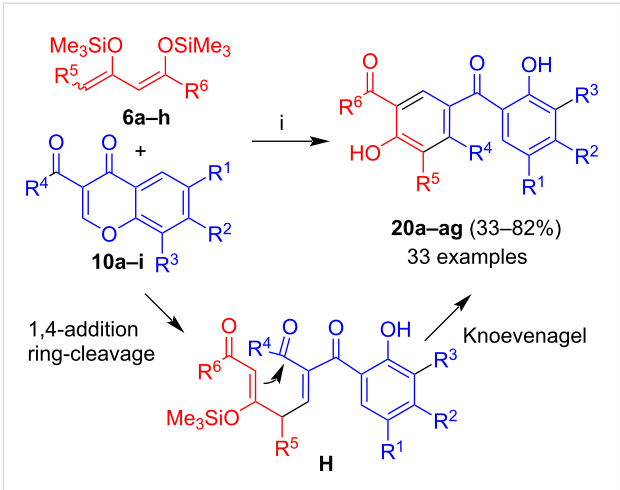

Scheme 6: Synthesis of **20a–ag**. Conditions: i, 1) **10a–i**, Me_3SiOTf (0.3 equiv), 20 °C, 10 min; 2) **6a–h** (1.3 equiv), CH_2Cl_2, 0 → 20 °C, 12 h; 3) HCl (10%).

yields were slightly lower in case of R^6 = Me. The best yield was obtained for the cyclization of unsubstituted diene **6a** with a chlorine-substituted chromone, presumably because of the

electron-withdrawing character of the chlorine atoms and, thus, higher electrophilicity of the chromone.

3-(Methoxalyl)chromones

Dimethyl acetone-1,3-dicarboxylate

The reaction of dimethyl acetone-1,3-dicarboxylate (**3**) with 3-(methoxalyl)chromones **11a–g**, a new type of chromone developed in our group, afforded benzophenones **21a–g** in moderate to very good yields (Scheme 7) [38]. The formation of the products can be explained by Michael reaction (1,4-addition) of **3** to the chromone and ring cleavage to give intermediate **I**. Subsequent Knoevenagel reaction by attack of the methylene carbon to the carbonyl group adjacent to the ester group resulted in the formation of the final products. The regioselective cyclization can be explained by the higher electrophilicity of the carbonyl group adjacent to the ester, due to the electron-withdrawing effect of the latter. The yields were generally good to very good and no trend was observed depending on the structure of the chromones.

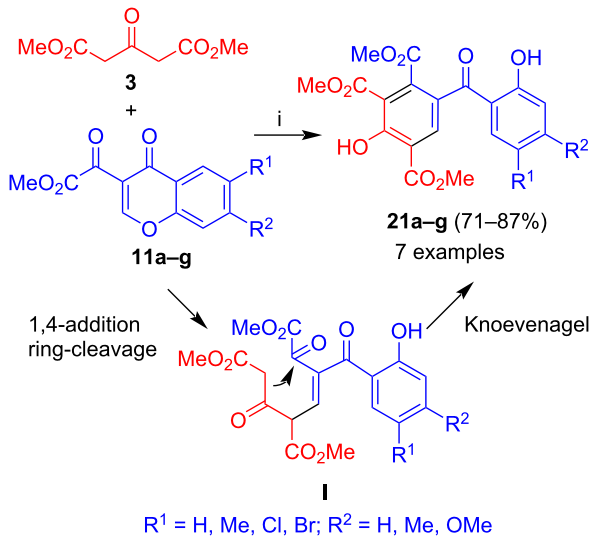

Scheme 7: Synthesis of **21a–g**. Conditions: i, DBU (1.3 equiv), dioxane, 20 °C, 12 h.

1,3-Diphenylacetone

Similarly, reaction of 1,3-diphenylacetone (**4**) with **11a**,**d** afforded benzophenones **22a**,**b** in moderate yields (Scheme 8) [38]. Again, no trend was observed depending on the structure of the chromones.

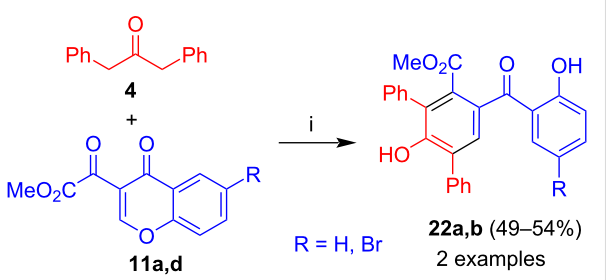

Scheme 8: Synthesis of **22a,b**. Conditions: i, DBU (1.3 equiv), dioxane, 20 °C, 12 h.

1,3-Bis(silyloxy)-1,3-butadienes

The reaction of **11a–c** with 1,3-bis(silyloxy)-1,3-butadienes **6a–h**, catalyzed by Me_3SiOTf, afforded products **23a–j** with excellent diastereoselectivity (Scheme 9) [39]. The formation of the products can be explained by 1,4-addition of the terminal carbon of the diene to the chromone to give intermediate **J** and subsequent attack of the central carbon atom of the 1,3-dicarbonyl unit (aldol reaction). No aromatization and extrusion of the hydroxy group was observed under these conditions, because the electron-withdrawing character of the additional ester group which destabilizes formation of a cation at the neighboring position. The yields were in most cases moderate (42–54%). Two products were obtained in higher yields (71 and 80%). However, no clear trend was observed for the yields depending on the substitution pattern. Instead, the individual purity and quality of the dienes played an important role.

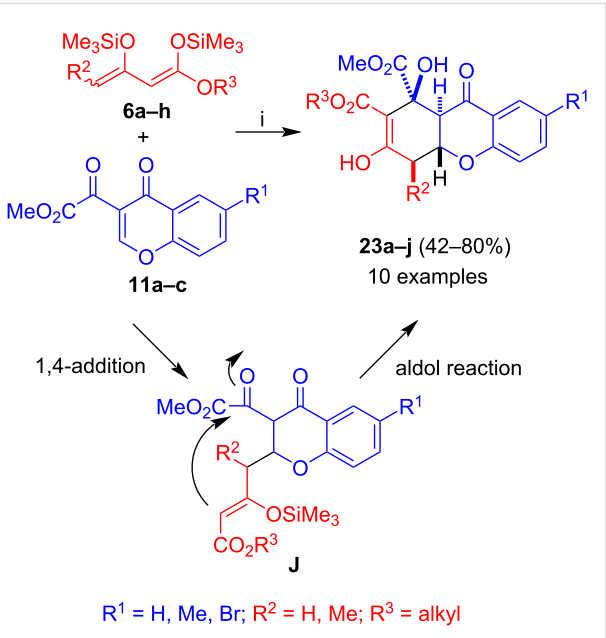

Scheme 9: Synthesis of **23a–j**. Conditions: i, 1) **11a–c**, Me_3SiOTf (0.3 equiv), 20 °C, 1 h; 2) **6a–h** (1.3 equiv), CH_2Cl_2, 0 → 20 °C, 12 h; 3) HCl (10%).

Reflux of an EtOH solution of **23a** in the presence of PTSA (*para*-toluenesulfonic acid) afforded benzophenone **24a** in 50% yield. The reaction of **6a–r** with **13a–c**, following the conditions discussed above for the synthesis of **23a–j**, and subse-

quent treatment with PTSA afforded benzophenones **24a–w** in a two-step on-pot procedure (Scheme 10) [39]. The formation of the products can be explained by 1,4-addition and subsequent aldol reaction to give products **24** and subsequent acid-catalyzed ring-cleavage and Knoevenagel reaction, similar to the formation of products **21** and **22**. The products were formed in 54–84% yields. Again, no systematic trend was observed for the yields. Good yields were observed for dienes containing various substituents located at carbon C-4 and for chromones containing a hydrogen, methyl or bromide at carbon C-6 of the chromone.

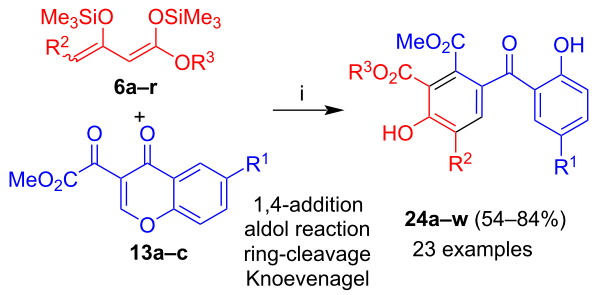

Scheme 10: Synthesis of **24a–w**. Conditions: i, 1) **13a–c**, Me_3SiOTf (0.3 equiv), 20 °C, 1 h; 2) **6a–r** (1.3 equiv), CH_2Cl_2, 0 → 20 °C, 12 h; 3) HCl (10%); 4) EtOH, *p*-TsOH (3 mol %), reflux, 5–10 h.

3-(Benzoyl)chromones

Dimethyl acetone-1,3-dicarboxylate

The reaction of dimethyl acetone-1,3-dicarboxylate (**3**) with 3-aroylchromones **12a–f** afforded benzophenones **25a–f** (Scheme 11) [38]. A variety of aryl groups were tolerated, including 3- and 4-nitrophenyl and 3,5-dinitrophenyl. The formation of the product proceeds analogously to the reaction leading to benzophenones **19** and **21**. The yields were in most cases moderate to good. A poor yield (7%) was obtained from the chromone substituted by a 2-thienyl group which might be explained by the electron-rich nature of the thiophene and, thus, a reduced electrophilicity of the neighboring carbonyl group. Likewise, a poor yield (23%) was observed for a 2-fluorophenyl group, presumably due to steric hindrance because of the *ortho*-substituent. Excellent yields (70 and 83%) were obtained for a 3-nitro- and a 3,5-dinitrophenyl group, presumably due to the electron-withdrawing character of the nitro groups and an enhanced electrophilicity. A moderate yield (49%) was obtained for the phenyl derivative.

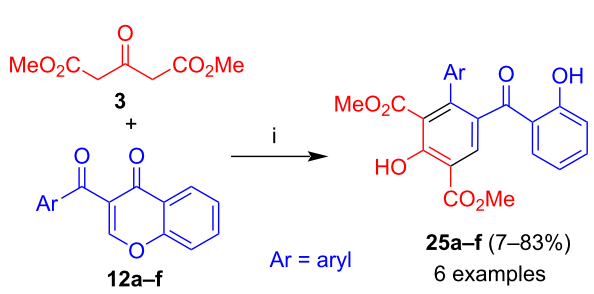

Scheme 11: Synthesis of **25a–f**. Conditions: i, DBU (1.3 equiv), dioxane, 20 °C, 12 h.

1,3-Diphenylacetone

Similarly, reaction of 1,3-diphenylacetone (**4**) with **12a–e** afforded benzophenones **26a–e** in moderate to good yields (Scheme 12) [38]. Similar to products **25**, a relatively low yield (29%) was observed for the chromone substituted by a 2-thienyl group. A low yield (32%) was also obtained for the phenyl derivative. Similar to products **25**, good yields (up to 74%) were obtained for products containing nitro groups.

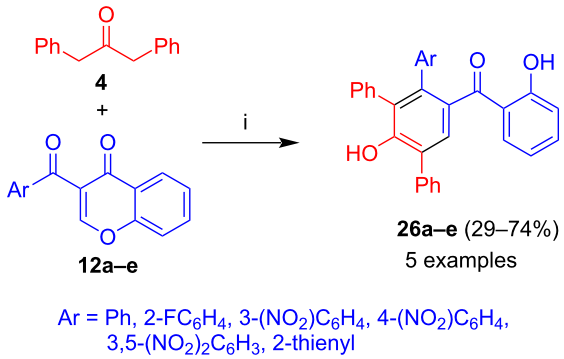

Scheme 12: Synthesis of **26a–e**. Conditions: i, DBU (1.3 equiv), dioxane, 20 °C, 12 h.

3-(2-Nitrobenzoyl)chromones

Dimethyl acetone-1,3-dicarboxylate

A completely different result was obtained when chromones containing a 2-nitrobenzoyl group were employed. The reaction of dimethyl acetone-1,3-dicarboxylate (**3**) with 3-(2-nitrobenzoyl)chromones **13a–c** afforded benzocoumarines **27a–c** in good yields (Scheme 13) [38]. The formation of the products can be explained by 1,4-addition of **3** to the chromone and ring cleavage to give intermediate **K**. Subsequent Knoevenagel reaction by attack of the methylene carbon to the carbonyl group adjacent to the phenol moiety resulted in formation of intermediate **L** and lactonization gave the final products. The regioselectivity of the cyclization can be explained by steric hindrance of the carbonyl group adjacent to the 2-nitrophenyl moiety containing an *ortho*-substituent. Interestingly, in case of a 2-fluorophenyl group, the regioselectivity was different and product **26** was obtained (see Scheme 12). The yields were, in general, very good. The best yield (84%) was obtained for the

reaction of 6-methyl-substituted 3-(2-nitrobenzoyl)chromone **13b**, presumably due to a better solubility of the product. However, the yields were in a similar range (72–84%).

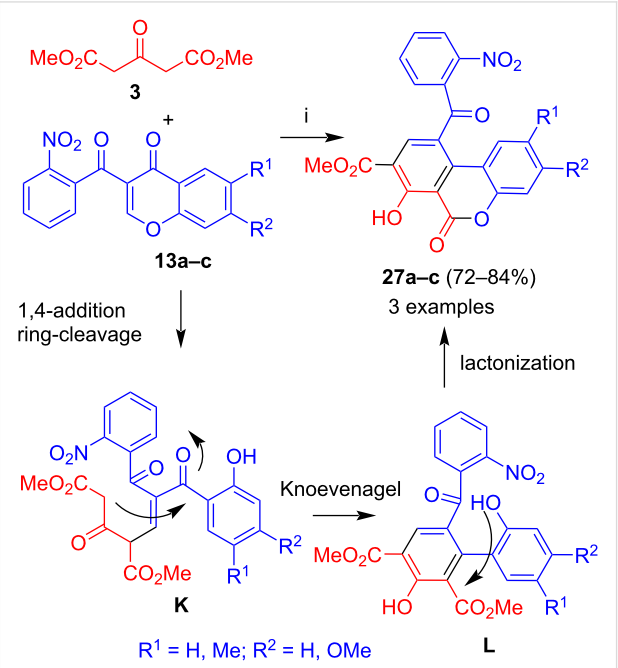

Scheme 13: Synthesis of **27a–c**. Conditions: i, DBU (1.3 equiv), dioxane, 20 °C, 12 h.

1,3-Diphenylacetone

The reaction of 1,3-diphenylacetone (**4**) with **13a–c** afforded biaryls **28a–c** (Scheme 14) [38]. Due to the absence of an ester group in starting material **4**, a lactonization in the final step was not possible. Similarly to products **27**, the best yield (73%) was obtained for the reaction of 6-methyl-substituted 3-(2-nitrobenzoyl)chromone **13b**. The yield of the product derived from unsubstituted 3-(2-nitrobenzoyl)chromone **13a** was slightly lower (59%).

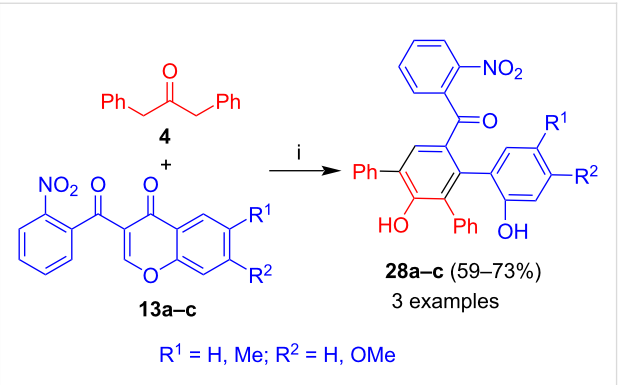

Scheme 14: Synthesis of **28a–c**. Conditions: i, DBU (1.3 equiv), dioxane, 20 °C, 12 h.

3-(Perfluoroalkanoyl)chromones

Dimethyl acetone-1,3-dicarboxylate

The reaction of dimethyl acetone-1,3-dicarboxylate (**3**) with 3-trifluoroacetyl- and 3-(perfluoroalkanoyl)chromones **14a–n** afforded hemiacetals **29a–n** in moderate to good yields (Scheme 15) [38]. The first step is again a 1,4-addition with subsequent ring cleavage of the chromone (intermediate **M**). Similar to the formation of products **27**, the cyclization proceeded by attack of the methylene carbon to the carbonyl group adjacent to the phenol moiety (intermediate **N**). This might be explained by the fact that the carbonyl adjacent to the perfluoroalkyl group exists as a hydrate which reduces significantly its electrophilicity. The products are finally generated by intramolecular formation of a semi-acetal. The yields were generally good (56–78%). The yields for pentafluoroethyl- and heptafluoropropyl-substituted derivatives were slightly better than the yields of trifluoromethyl-substituted derivatives which might be explained by a better solubility. For the other substituents of the chromone, no clear trend was observed. Product **29c** underwent cleavage of the perfluoroalkyl group upon treatment with potassium hydroxide in methanol to give benzocoumarine **30**.

1,3-Bis(silyloxy)-1,3-butadienes

The reaction of 3-(trifluoroacetyl)chromone (**14a**) with 1,3-bis(silyloxy)-1,3-butadienes proved not to be successful in our hands. However, reaction of 3-(trifluoroacetyl)thiochromone (**31**) with 1,3-bis(silyloxy)-1,3-butadienes **6a**,**b**, in the presence of Me_3SiOTf, afforded products **32a**,**b** with excellent diastereoselectivity (Scheme 16) [40]. The formation of the products can be explained by 1,4-addition of the terminal carbon of the diene to the chromone to give intermediate **O** and subsequent attack of the central carbon atom of the 1,3-dicarbonyl unit (aldol reaction). No aromatization and extrusion of the hydroxy group was observed, because the electron-withdrawing character of the CF_3 group which destabilizes the formation of a cation at the neighboring position. In addition, the carbon–sulfur bond was not cleaved, due to the lower leaving group ability of sulfur as compared to oxygen. The yields of the two products were moderate.

3-Halochromones

Dimethyl acetone-1,3-dicarboxylate

The reaction of dimethyl acetone-1,3-dicarboxylate (**3**) with 3-bromochromone (**15a**) afforded product **33** (Scheme 17) [32]. The first step is again a 1,4-addition to give intermediate **P**. Subsequent cyclization by intramolecular nucleophilic attack of the oxygen atom to the bromide afforded intermediate **Q** which underwent ring cleavage to give intermediate **R**. Subsequent 1,4-addition of the methylene carbon to a second molecule of **15a** gave intermediate **S** which underwent cyclization by attack

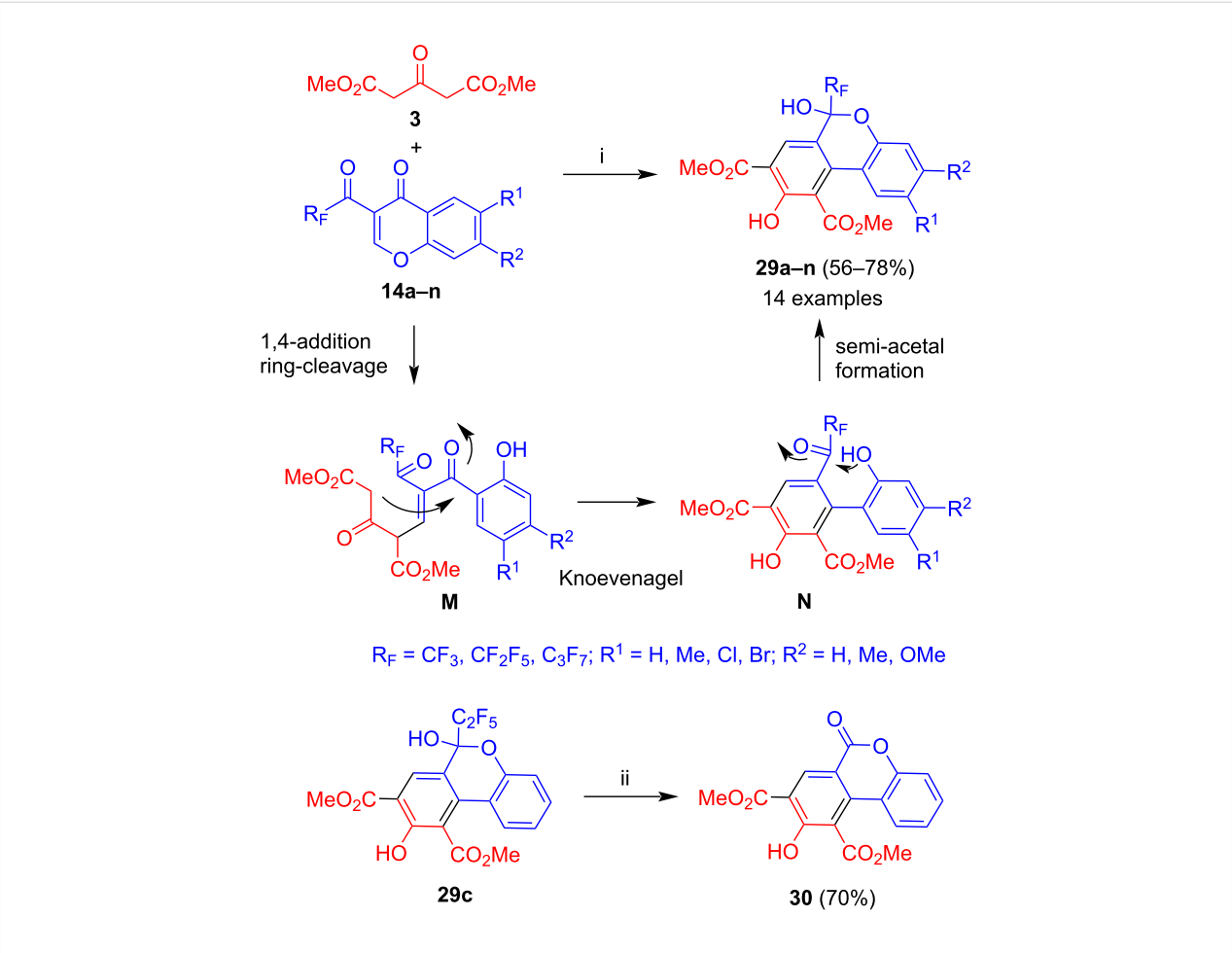

Scheme 15: Synthesis of **29a–n** and **30**. Conditions: i, DBU (1.3 equiv), dioxane, 20 °C, 12 h; ii, 1) KOH, MeOH; 2) HCl (30%).

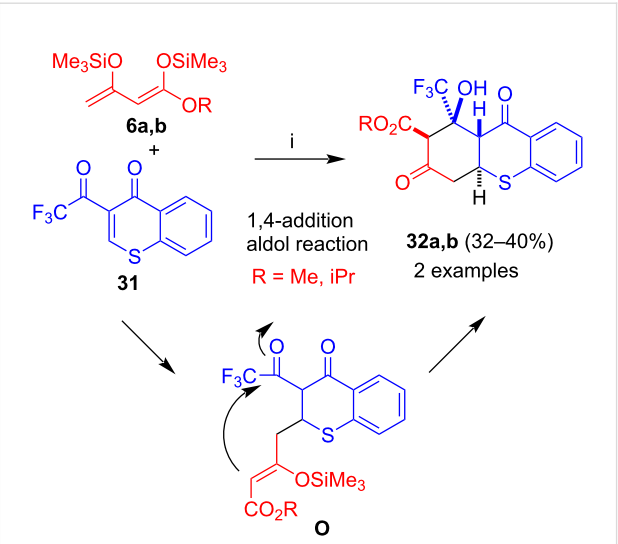

Scheme 16: Synthesis of **32a**,**b**. Conditions: i, 1) **31**, Me_3SiOTf (2.0 equiv), 20 °C, 1 h; 2) **6a**,**b** (3.0 equiv), CH_2Cl_2, 0 → 20 °C, 12 h; 3) HCl (10%).

of the methylene carbon to the bromide to give cyclopropane **33**.

3-Ketoamides

The reaction of 3-ketoamides **34a–f** with 3-halochromones **15a–g** afforded 2-(salicyloyl)furans **35a–x** in mostly good to excellent yields (Scheme 18) [41]. The reaction proceeds by 1,4-addition of the methylene carbon of **34** to the chromone to give intermediate **T**, cyclization by regioselective intramolecular nucleophilic attack of the oxygen to the halide to give intermediate **U** and subsequent ring-cleavage. The reaction of 3-ketoamide **34a** (R^3 = Me, R^4 = Ph) with 3-chloro-, 3-bromo-, and 3-iodochromone showed that the yields strongly depend on the type of halogen atom located at position 3 of the chromone. During the optimization of the conditions, the best yields were in many cases obtained when chloride was employed as the leaving group. However, for some other products the yields were slightly better in case of employment of 3-bromochromone. Most of the yields were higher than 70%, in several cases excellent (higher than 90%). Only in a few cases, the

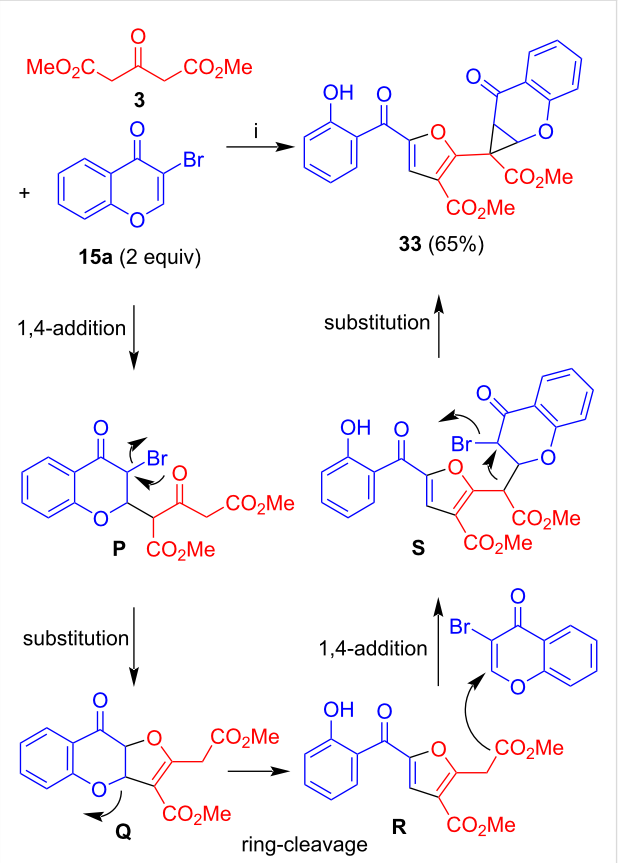

Scheme 17: Synthesis of **33**. Conditions: i, DBU (1.3 equiv), THF, 20 °C, 12 h.

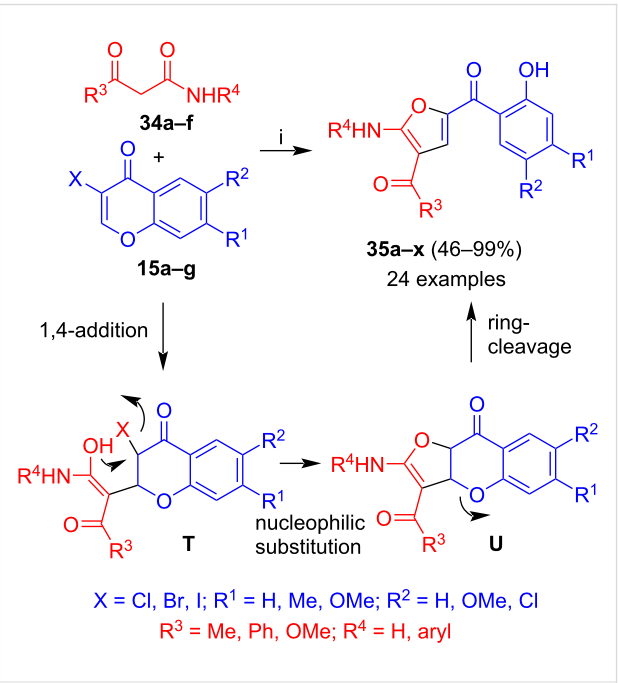

Scheme 18: Synthesis of **35a–x**. Conditions: i, DBU (1.3 equiv), 1,4-dioxane, 20 °C, 12 h.

yields were moderate (46–53%). However, no clear trend was observed for the yields depending on the substituents. The reaction of 7-methoxy-substituted 3-halochromones were in most cases lower as compared to unsubstituted or chloro-substituted chromones, presumably due to the electron-donating character of the methoxy group and the lower electrophilicity of the chromone. But this trend was also not general. Similar yields were obtained for ketones (R^3 = Me, Ph) or esters (R^3 = OMe).

Treatment of 2-(salicyloyl)furan **35a** with iodine in the presence of DBU afforded furo[3,2-*b*]chromen-9-one **36a** in 32% yield. Based on this observation, the two-step one-pot reaction of ketoamides **34a–f** with 3-halochromones **15a–c** was studied which afforded furo[3,2-*b*]chromen-9-ones **36a–f**, albeit, in only low to moderate yields (Scheme 19) [41]. The formation of these products can be explained by initial formation of the corresponding 2-(salicyloyl)furans **V**. Iodination of the latter afforded iodonium salt **W** which underwent cyclization by attack of the salicylate hydroxy group to give intermediate **X**. Extrusion of hydrogen iodide afforded the final product. Similarly to products **35**, relatively low yields were observed for reactions of methoxy-substituted 3-halochromones.

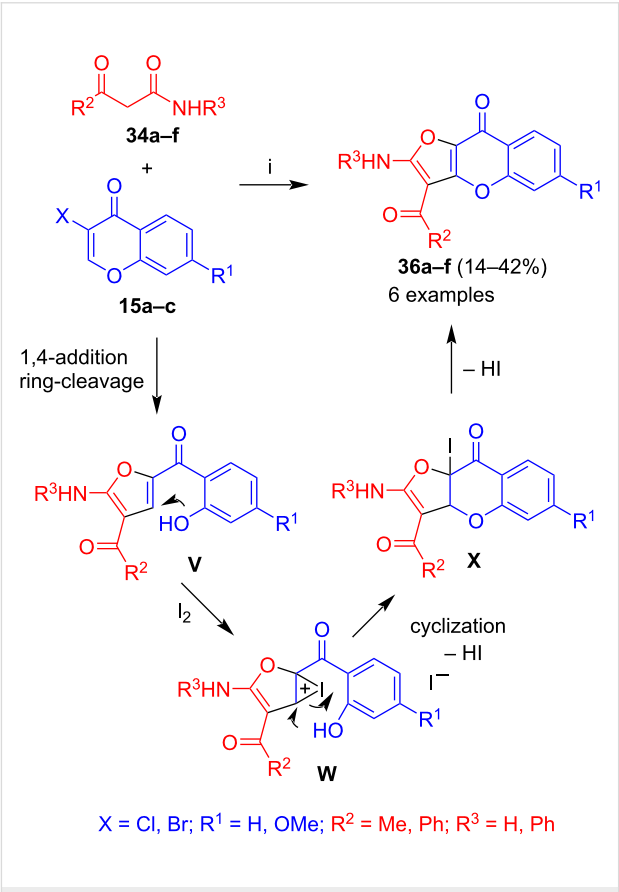

Scheme 19: Synthesis of **36a–f**. Conditions: i, 1) DBU (1.3 equiv), 1,4-dioxane, 20 °C, 12 h; 2) I_2 (2 equiv), DBU (3 equiv), MeCN or DMF.

The two-step one-pot reaction of *N*-unsubstituted ketoamide **33a** with 3-halochromones **29a** and **31a** afforded spirocycles **36a**,**b**, albeit, in only moderate yields (Scheme 20) [41]. The formation of these products can be explained, similarly to the formation of **35a–f**, by generation of intermediate **Y** which afforded iodonium salt **Z** upon addition of iodine. Cyclization by attack of the salicylate hydroxy group to carbon C5 gave intermediate **AB**. Hydrolysis of the iodide upon aqueous work-up to give an alcohol and oxidation of the latter resulted in formation of the final product. The reason for the change of the regioselectivity of cyclization, as compared to the formation of products **36**, remains unclear at present.

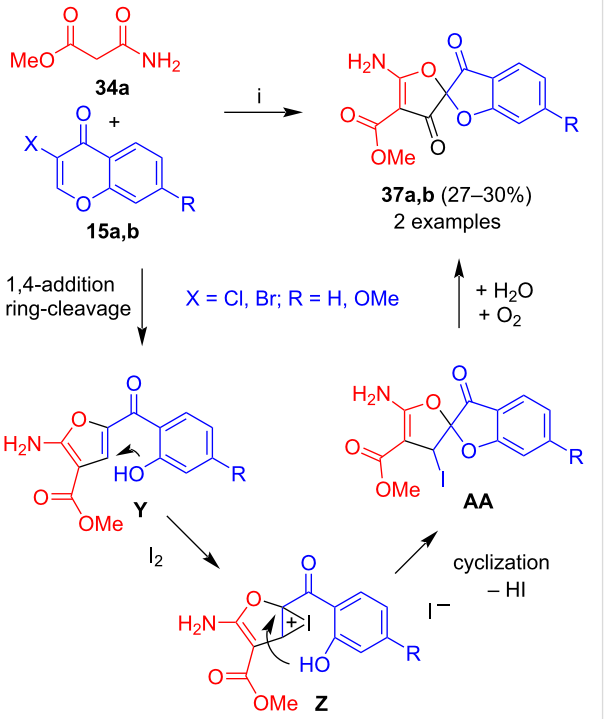

Scheme 20: Synthesis of **37a**,**b**. Conditions: i, 1) DBU (1.3 equiv), 1,4-dioxane, 20 °C, 12 h; 2) I_2 (2 equiv), DBU (3 equiv), MeCN or DMF. Then aqueous work-up at the air.

The reaction of 3-halochromones with 3*H*-indole-2-thiones (thiooxindoles) **38a–c** afforded 2-salicyloyl-8*H*-thieno[2,3-*b*]indoles **39a–i** in mostly moderate to good yields (Scheme 21) [41]. The formation of these products can be explained, similarly to the formation of products **35**, by 1,4-addition of the carbon atom of **38** to the chromone to give intermediate **AB**, cyclization by nucleophilic attack of the sulfur to the bromide (intermediate **AC**) and subsequent ring-cleavage. In most reactions, DBU was employed as the base. In case of products derived from *N*-unsubstitituted 3*H*-indole-2-thiones (R^3 = H), employment of potassium carbonate proved to be advantageous. Similarly to the formation of products **35**, the use of 3-chlorochromones gave the best yields. Likewise, the presence of a methoxy group located at the chromone moiety, resulted in a decrease of the yield, due to the electron-donating effect of the methoxy group.

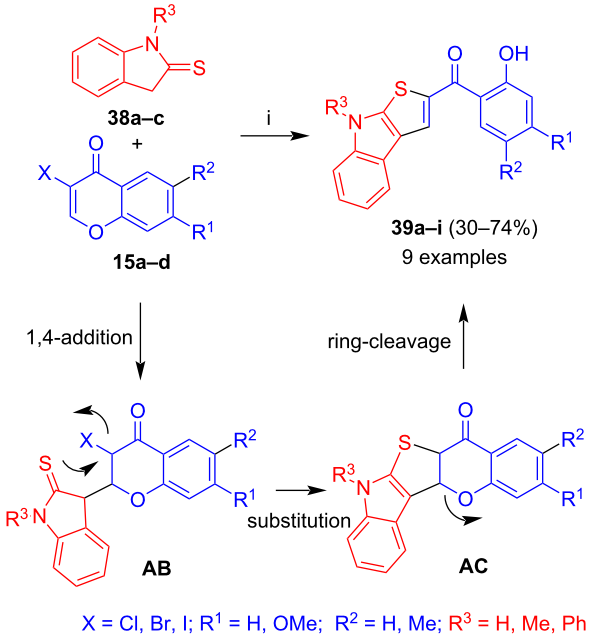

Scheme 21: Synthesis of **39a–i**. Conditions: i, method A: DBU (1.3 equiv), 1,4-dioxane, 20 °C; method B: K_2CO_3 (4 equiv), DMF, 20 °C.

3-Cyanochromones

Dimethyl acetone-1,3-dicarboxylate

The reaction of dimethyl acetone-1,3-dicarboxylate (**3**) with 3-cyanochromone (**16a**) afforded azaxanthone **40** in 49% yield (Scheme 22) [42-44]. The reaction again proceeds by 1,4-addition with subsequent ring cleavage of the chromone (intermediate **AD**). Subsequent attack of the methylene carbon to the nitrile gave intermediate **AE**. Attack of the imine to the carbonyl group and subsequent extrusion of water afforded product **40**. The reaction proved to be rather general and a variety of substituted 3-cyanochromones were successfully employed.

1,3-Bis(silyloxy)-1,3-butadienes

The two-step reaction of 3-cyanochromones **16a–h** with 1,3-bis(silyloxy)-1,3-butadienes **6a–z** afforded azaxanthones **41a–am** (Scheme 23) [45,46]. The formation of the products can be explained by the mechanism discussed for the formation of azaxanthone **40** that involves intermediates **AF** and **AG**. For most products, the yields were in the range of 30 to 66%. Employment of dienes derived from 1,3-diketones (R^3 = Me, Ph) proved to be unsuccessful, presumably due to the lower nucleophilicity of these dienes as compared to those derived

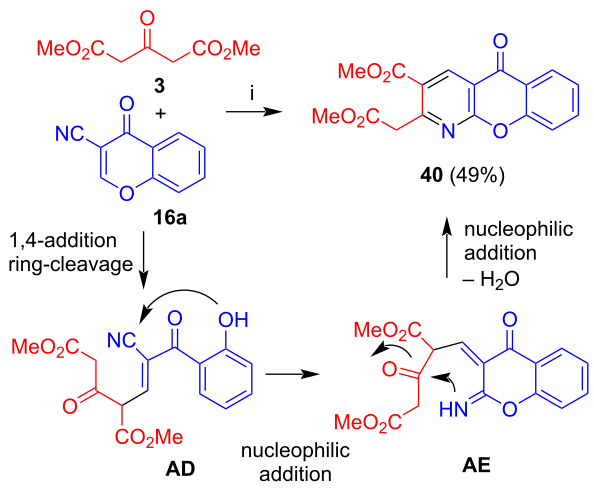

Scheme 22: Synthesis of **40**. Conditions: i, piperidine, MeOH, $CHCl_3$, reflux, 3 h.

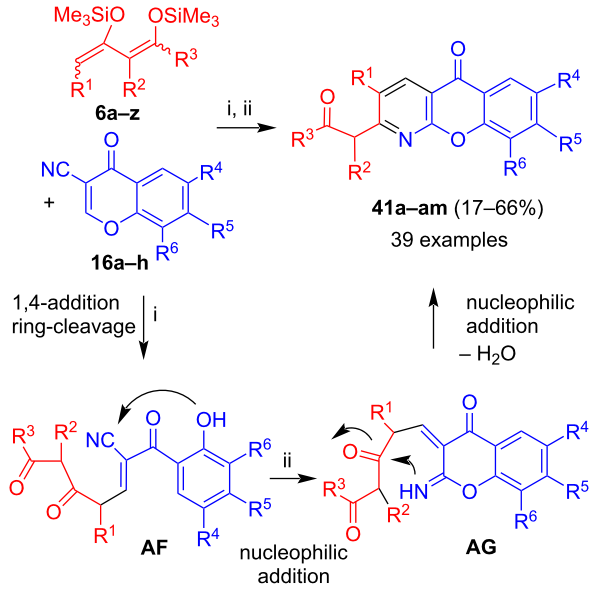

Scheme 23: Synthesis of **41a–am**. Conditions: i, Me_3SiOTf, CH_2Cl_2, 20 °C, 12 h, then: HCl (10%); ii, NEt_3, EtOH or MeOH, 20 °C, 12 h, then: HCl (1 M).

from β-ketoesters (R^3 = Oalkyl). Substituents located at carbon C-4 of the diene (R^1) were generally tolerated as well. In fact, the best yield (66%) was obtained for the product derived from unsubstituted 3-cyanochromone (**16a**) and a diene containing a phenoxy group located at carbon C-4 (R^1 = OPh). But in other cases, the yields were less. In fact, in some cases, cyano-substituted benzocoumarines, similar to products **18**, were formed as byproducts. Substituents located at carbon C-2 of the diene (R^2) were tolerated, but the yields were lower, presumably due to the instability of these dienes [13]. In summary, no clear trend was observed for the influence of the substituents on the yields.

The reaction of 3-cyanochromones **16a–h** with 2-fluoro-1,3-bis(silyloxy)-1,3-butadienes **42a–z** afforded separable mixtures of azaxanthones **43a–aa** and biphenyls **44a–ac** (Scheme 24) [47]. In case of 4-unsubstituted 2-fluoro-1,3-bis(silyloxy)-1,3-butadienes, azaxanthones **43** were exclusively formed in 33–56% yields. A similar result was obtained for the corresponding 2-chloro-1,3-bis(silyloxy)-1,3-butadiene [48]. In case of 4-alkyl-2-fluoro-1,3-bis(silyloxy)-1,3-butadienes, biphenyls **44** were formed as the major products in 63–79% yields. In some cases, these products were exclusively formed. In other cases, azaxanthones **43** were isolated as minor products as well

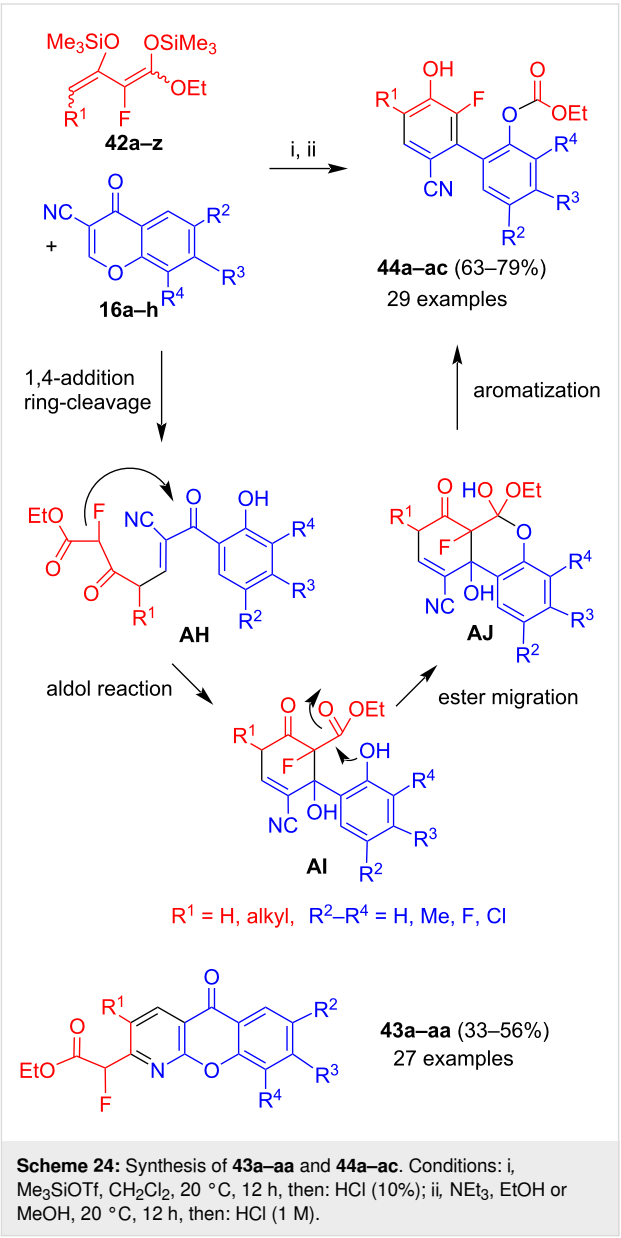

Scheme 24: Synthesis of **43a–aa** and **44a–ac**. Conditions: i, Me_3SiOTf, CH_2Cl_2, 20 °C, 12 h, then: HCl (10%); ii, NEt_3, EtOH or MeOH, 20 °C, 12 h, then: HCl (1 M).

(7–20% yields). The formation of biphenyls **44** can be explained by 1,4-addition and ring-cleavage to give intermediate **AH**, aldol reaction (intermediate **AI**), migration of the ester group from the quaternary carbon to the phenolic oxygen atom (intermediate **AJ**) and aromatization. The steric influence of the fluorine atom and of the substituent R^1 might have an influence on the conformation which facilitates the intramolecular aldol reaction at the expense of the nitrile addition. In the case of formation of biphenyls **44**, these products were generally obtained in good yields (63–79%). While the presence of a substituent located at carbon C-4 was mandatory, the exact type of substituent was not decisive for the yield. The substituents located at the chromone moiety also did not have a great impact on the yield.

Conclusion

The present review highlighted reactions of chromones with 1,3-dicarbonyl compounds and 1,3-bis(silyloxy)-1,3-butadienes which can be regarded as electroneutral equivalents of dianions of 1,3-dicarbonyl compounds. The regioselectivity of these reactions depends mainly on the type of chromone. 2,3-Unsubstituted chromones undergo initial 1,4-addition and subsequent Knoevenagel condensation via the carbonyl group. In contrast, in case of 3-formylchromones the cyclization proceeds via the formyl group, due to its higher electrophilicity. The same regioselectivity was observed for 3-(methoxalyl)- and 3-benzoylchromones. In contrast, a cyclization via the carbonyl group of the chromone moiety was observed for 3-(2-nitrobenzoyl)chromone, presumably due to steric hindrance. The same selectivity was observed also for 3-trifluorochromone and 3-perfluoroalkanoylchromones which might be explained by the fact that the carbonyl adjacent to the perfluoroalkyl group exists as a hydrate which reduces significantly its electrophilicity. In case of 3-halochromones, the halide acts as a leaving group during the reaction. For 3-cyanochromones, a nucleophilic attack of chromone-derived hydroxy group to the nitrile was observed in most cases. However, a different reaction was observed for long chained 2-fluoro-1,3-bis(silyloxy)-1,3-butadienes. In conclusion, the interaction of activated carbonyl compounds with chromones offer a great variety of different reaction pathways leading to various types of products with potential applications in materials science and medicinal chemistry.

The domino reactions presented, which involve mostly the combination of 1,4-additions of the carbonyl compounds to the chromone moiety with ring cleavage reactions, allow for the synthesis of products which are not readily available by other methods. The benefit for the employment of chromones as building blocks is their dense functionalization in combination with their (commercial) availability. On the other hand, highly substituted or functionalized chromones have to be prepared in multi-step syntheses. In general, the substitution pattern of the chromone does not seem to have a great influence on the yields which is beneficial for studies related to the scope and the synthesis of compound libraries. The use of dimethyl acetone-1,3-dicarboxylate as a starting material has the advantage that it is commercially available, stable and easy to handle. The use of 1,3-bis(silyloxy)-1,3-butadienes is, on the other hand, significantly more difficult and usually requires the use of the Schlenck technique to avoid hydrolysis of the moisture sensitive compounds. The handling of these reagents, which have to be stored at low temperature, requires some experience. In fact, the synthesis of the dienes has to proceed with full conversion and in high yield as the they cannot be purified by chromatography. Distillation is also problematic, as dienes containing substituents located at carbon atom C-2 readily undergo isomerization reactions. The reactions of 1,3-bis(silyloxy)-1,3-butadienes with chromones requires the action of trimethylsilyl trifluoromethanesulfonate (TMSOTf) which is a relatively expensive reagent.

In future studies, especially the chemistry of 3-methoxalyl- and 3-nitrochromones should be further explored. In case of the methoxalyl derivatives, so far not many synthetic applications have been developed. In the future, it will be interesting also to study reactions of 3-nitrochromone with carbonyl compounds. In this context, biological properties of the products will be interesting, as the nitro group can be transformed to the biologically important amino group.

Acknowledgements

I am grateful to my co-workers who contributed to the work included in this account article. These are (in alphabetical order): Drs Uwe Albrecht, Bettina Appel, Alina Bunescu, Friedrich Erben, Edith Holtz, Muhammad Farooq Ibad, Ilia Freifeld, Viktor O. Iaroshenko, Abid Obaid-ur-Rahman, Muhammad A. Rashid, Nasir Rasool, Stefanie Reim, Sven Rotzoll, Nehad N. R. Saleh and Iryna Savych.

Data Availability Statement

Data sharing is not applicable as no new data was generated or analyzed in this study.

References

1. Tietze, L. F.; Beifuss, U. *Angew. Chem., Int. Ed. Engl.* **1993,** *32,* 131–163. doi:10.1002/anie.199301313
2. Padwa, A.; Bur, S. K. *Tetrahedron* **2007,** *63,* 5341–5378. doi:10.1016/j.tet.2007.03.158
3. Pellissier, H. *Tetrahedron* **2006,** *62,* 1619–1665. doi:10.1016/j.tet.2005.10.040
4. Nicolaou, K. C.; Edmonds, D. J.; Bulger, P. G. *Angew. Chem., Int. Ed.* **2006,** *45,* 7134–7186. doi:10.1002/anie.200601872

5. Tietze, L. F. *Chem. Rev.* **1996,** *96,* 115–136. doi:10.1021/cr950027e
6. Langer, P.; Döring, M. *Eur. J. Org. Chem.* **2002,** 221–234. doi:10.1002/1099-0690(20021)2002:2<221::aid-ejoc221>3.0.co;2-m
   See for cyclizations of dianions; other dinucleophiles with oxalic acid-bis(imidoyl)dichlorides.
7. Langer, P.; Freiberg, W. *Chem. Rev.* **2004,** *104,* 4125–4150. doi:10.1021/cr010203l
   See for cyclizations of free dianions with dielectrophiles in general.
8. Bellur, E.; Feist, H.; Langer, P. *Tetrahedron* **2007,** *63,* 10865–10888. doi:10.1016/j.tet.2007.08.046
   See for the synthesis of 2-(alkylidene)tetrahydrofurans.
9. Dang, T. T.; Dang, T. T.; Langer, P. *Synlett* **2011,** 2633–2642. doi:10.1055/s-0031-1289550
   See for cyclizations of oxime; hydrazine dianions.
10. Langer, P. *Synlett* **2023,** *34,* 414–422. doi:10.1055/s-0042-1753200
    See for reactions of the dianion of 1;1-diphenylacetone.
11. Langer, P. *Synlett* **2023,** *34,* 1765–1776. doi:10.1055/s-0042-1751430
    See for applications in the field of cyclopropanes.
12. Langer, P. *Synlett* **2023,** *34,* 1953–1960. doi:10.1055/s-0042-1751438
    See for applications in the field of epihalohydrins.
13. Langer, P. *Synthesis* **2002,** 441–459. doi:10.1055/s-2002-20954
    See for 1,3-bis(trimethylsilyloxy)-1;3-butadienes in general.
14. Langer, P. *Synlett* **2006,** 3369–3381. doi:10.1055/s-2006-958416
    See for cyclizations with oxalyl chloride.
15. Feist, H.; Langer, P. *Synthesis* **2007,** 327–347. doi:10.1055/s-2006-958958
    See for formal [3 + 3] cyclizations.
16. Langer, P. *Eur. J. Org. Chem.* **2007,** 2233–2238. doi:10.1002/ejoc.200601040
    See for cyclizations with iminium salts.
17. Langer, P. *Synlett* **2009,** 2205–2216. doi:10.1055/s-0029-1217554
    See for fluorine-containing products.
18. Nawaz, M.; Sher, M.; Langer, P. *Synlett* **2010,** 2383–2391. doi:10.1055/s-0030-1258559
    See for sulfur-containing products.
19. Karapetyan, G.; Dang, T. T.; Sher, M.; Ghochikyan, T. V.; Saghyan, A.; Langer, P. *Curr. Org. Chem.* **2012,** *16,* 557–565. doi:10.2174/138527212799859372
    See for cyclizations with 3-alkoxy-2-en-1-ones.
20. Dang, T. T.; Kelzhanova, N. K.; Abilov, Z. A.; Turmukhanova, M. Z.; Langer, P. *Synlett* **2012,** *23,* 1283–1290. doi:10.1055/s-0031-1290490
    See for cyclizations of 1,1-bis(trimethylsilyloxy)ketene acetals.
21. Hassan, Z.; Langer, P. *Synlett* **2019,** *30,* 665–673. doi:10.1055/s-0037-1609660
    See for chlorine-containing products.
22. Langer, P. *Synlett* **2021,** *32,* 2036–2045. doi:10.1055/s-0037-1610780
    See for cyclizations with acid chlorides.
23. Feist, H.; Langer, P. *Synthesis* **2008,** 3877–3902. doi:10.1055/s-0028-1083256
    See for (2,4-dioxobutylidene)phosphoranes.
24. Madhav, H.; Jameel, E.; Rehan, M.; Hoda, N. *RSC Med. Chem.* **2022,** *13,* 258–279. doi:10.1039/d1md00394a
    See for a review of pharmacological applications of chromones.
25. Fu, L.; Wan, J.-P. *Asian J. Org. Chem.* **2019,** *8,* 767–776. doi:10.1002/ajoc.201900196
    See for a review on the synthesis of 3-substituted chromones.
26. Keri, R. S.; Budagumpi, S.; Pai, R. K.; Balakrishna, R. G. *Eur. J. Med. Chem.* **2014,** *78,* 340–374. doi:10.1016/j.ejmech.2014.03.047
27. Gaspar, A.; Matos, M. J.; Garrido, J.; Uriarte, E.; Borges, F. *Chem. Rev.* **2014,** *114,* 4960–4992. doi:10.1021/cr400265z
28. Sharma, S. K.; Kumar, S.; Chand, K.; Kathuria, A.; Gupta, A.; Jain, R. *Curr. Med. Chem.* **2011,** *18,* 3825–3852. doi:10.2174/092986711803414359
29. Langer, P. *Synlett* **2007,** 1016–1025. doi:10.1055/s-2007-973894
30. Langer, P. *Synlett* **2022,** *33,* 207–223. doi:10.1055/s-0040-1719830
    See for cyclizations of heterocyclic enamines with chromones.
31. Langer, P. *Synlett* **2022,** *33,* 440–457. doi:10.1055/s-0040-1719845
    See for cyclizations with other 1;3-dielectrophiles.
32. Terzidis, M. A.; Tsoleridis, C. A.; Stephanidou-Stephanatou, J.; Terzis, A.; Raptopoulou, C. P.; Psycharis, V. *Tetrahedron* **2008,** *64,* 11611–11617. doi:10.1016/j.tet.2008.10.023
33. Langer, P.; Saleh, N. N. R.; Freifeld, I. *Chem. Commun.* **2002,** 168–169. doi:10.1039/b110236m
34. Appel, B.; Saleh, N. N. R.; Langer, P. *Chem. – Eur. J.* **2006,** *12,* 1221–1236. doi:10.1002/chem.200501024
35. Appel, B.; Rotzoll, S.; Kranich, R.; Reinke, H.; Langer, P. *Eur. J. Org. Chem.* **2006,** 3638–3644. doi:10.1002/ejoc.200600082
36. Wolf, V.; Adeel, M.; Reim, S.; Villinger, A.; Fischer, C.; Langer, P. *Eur. J. Org. Chem.* **2009,** 5854–5867. doi:10.1002/ejoc.200900816
37. Holtz, E.; Albrecht, U.; Langer, P. *Tetrahedron* **2007,** *63,* 3293–3301. doi:10.1016/j.tet.2007.02.062
38. Iaroshenko, V. O.; Savych, I.; Villinger, A.; Sosnovskikh, V. Y.; Langer, P. *Org. Biomol. Chem.* **2012,** *10,* 9344–9348. doi:10.1039/c2ob07020k
39. Iaroshenko, V. O.; Bunescu, A.; Spannenberg, A.; Supe, L.; Milyutina, M.; Langer, P. *Org. Biomol. Chem.* **2011,** *9,* 7554–7558. doi:10.1039/c1ob05931a
40. Iaroshenko, V. O.; Bunescu, A.; Sevenard, D. V.; Sosnovskikh, V. Y.; Langer, P. *Russ. Chem. Bull.* **2015,** *64,* 470–472. doi:10.1007/s11172-015-0889-3
41. Savych, I.; Gläsel, T.; Villinger, A.; Sosnovskikh, V. Y.; Iaroshenko, V. O.; Langer, P. *Org. Biomol. Chem.* **2015,** *13,* 729–750. doi:10.1039/c4ob01730g
42. Ghosh, C.; SinhaRoy, D. K.; Mukhopadhyay, K. K. *J. Chem. Soc., Perkin Trans. 1* **1979,** 1964. doi:10.1039/p19790001964
43. Kubo, K.; Ukawa, K.; Kuzuna, S.; Nohara, A. *Chem. Pharm. Bull.* **1986,** *34,* 1108–1117. doi:10.1248/cpb.34.1108
44. Zheng, H.; Lin, G.; Weng, L. L. *Indian J. Chem.* **1998,** *37B,* 933.
45. Langer, P.; Appel, B. *Tetrahedron Lett.* **2003,** *44,* 5133–5135. doi:10.1016/s0040-4039(03)01030-x
46. Rashid, M. A.; Rasool, N.; Appel, B.; Adeel, M.; Karapetyan, V.; Mkrtchyan, S.; Reinke, H.; Fischer, C.; Langer, P. *Tetrahedron* **2008,** *64,* 5416–5425. doi:10.1016/j.tet.2008.02.105
47. Ibad, M. F.; Abid, O.-u.-R.; Adeel, M.; Nawaz, M.; Wolf, V.; Villinger, A.; Langer, P. *J. Org. Chem.* **2010,** *75,* 8315–8318. doi:10.1021/jo1018443
48. Reim, S.; Adeel, M.; Hussain, I.; Yawer, M. A.; Ahmed, Z.; Villinger, A.; Langer, P. *Tetrahedron Lett.* **2008,** *49,* 4901–4904. doi:10.1016/j.tetlet.2008.05.151

License and Terms

This is an open access article licensed under the terms of the Beilstein-Institut Open Access License Agreement (https://www.beilstein-journals.org/bjoc/terms), which is identical to the Creative Commons Attribution 4.0 International License (https://creativecommons.org/licenses/by/4.0). The reuse of material under this license requires that the author(s), source and license are credited. Third-party material in this article could be subject to other licenses (typically indicated in the credit line), and in this case, users are required to obtain permission from the license holder to reuse the material.

The definitive version of this article is the electronic one which can be found at:
https://doi.org/10.3762/bjoc.20.108

BEILSTEIN JOURNAL OF ORGANIC CHEMISTRY

Rapid construction of tricyclic tetrahydrocyclopenta[4,5]pyrrolo[2,3-*b*]pyridine via isocyanide-based multicomponent reaction

Xiu-Yu Chen, Ying Han, Jing Sun and Chao-Guo Yan*

Full Research Paper

Open Access

Address:
College of Chemistry & Chemical Engineering, Yangzhou University, Jiangsu, Yangzhou 225002, China

Email:
Chao-Guo Yan* - cgyan@yzu.edu.cn

* Corresponding author

Keywords:
[3 + 2] cycloaddition; cyclopenta-1,3-diene; cyclopenta[4,5]pyrrolo[2,3-*b*]pyridine; 1,4-dihydropyridine; electron-deficient alkyne; isocyanide

Beilstein J. Org. Chem. **2024,** *20,* 1436–1443.
https://doi.org/10.3762/bjoc.20.126

Received: 15 April 2024
Accepted: 18 June 2024
Published: 28 June 2024

This article is part of the thematic issue "Multicomponent reactions IV".

Associate Editor: T. J. J. Müller

© 2024 Chen et al.; licensee Beilstein-Institut.
License and terms: see end of document.

Abstract

An efficient protocol for the synthesis of polyfunctionalized tetrahydrocyclopenta[4,5]pyrrolo[2,3-*b*]pyridine-3,4b,5,6,7(1*H*)-pentacarboxylates was developed by a three-component reaction. In the absence of any catalyst, the three-component reaction of alkyl isocyanides, dialkyl but-2-ynedioates and 5,6-unsubstituted 1,4-dihydropyridines in refluxing acetonitrile afforded polyfunctionalized tetrahydrocyclopenta[4,5]pyrrolo[2,3-*b*]pyridine-3,4b,5,6,7(1*H*)-pentacarboxylates in high yields and with high diastereoselectivity. The reaction was finished by in situ generation of activated 5-(alkylimino)cyclopenta-1,3-dienes from addition of alkyl isocyanide to two molecules of but-2-ynedioates and sequential formal [3 + 2] cycloaddition reaction with 5,6-unsubstituted 1,4-dihydropyridine.

Introduction

Isocyanide is a unique and attractive functional group in organic chemistry. The carbon atom of isocyanide has both a lone electron pair and empty orbitals, so it has outstanding electrophilic and nucleophilic reactivity. At the same time, isocyanide also has good coordination ability to coordinate with metals to form diverse metal complexes [1-3]. Therefore, isocyanides have been known as indispensable building blocks in modern organic chemistry. Many isocyanide-based carbon–carbon and carbon–heteroatom bond forming reactions have been developed in fascinating ways over the past decades [4-6]. The famous multicomponent reactions such as Passerini reaction, Ugi reaction, Orru reaction and Van Leusen reaction, in which isocyanides were employed as key substrates have become the most powerful tools for rapid construction of various nitrogen-containing organic compounds [7-14]. On the other hand, the reactive Huisgen' 1,4-dipoles can be in situ generated by addition reaction of isocyanides to electron-deficient alkynes, which were sequentially trapped by various electrophiles and nucleophiles to give versatile acyclic and heterocyclic compounds [15-26]. In recent years, many multicomponent reactions based on

alkyl isocyanides, electron-deficient alkynes and other reagents have been successfully developed for the synthesis of various carbocyclic and heterocyclic compounds [27-35].

The 5,6-unsubstituted 1,4-dihydropyridine is one of special kinds of 1,4-dihydropyridines. It can act as an activated enamino unit and electron-rich dienophile to take part in some synthetic reactions [36-39]. In recent years, 5,6-unsubstituted 1,4-dihydropyridines have been recognized as the reactive electron-rich dienophiles, which proceeded several Povarov reactions with various 1-aza-1,3-butadienes [40-44]. Recently, we have found that the three-component reaction of isoquinolines, dialkyl but-2-ynediaotes and 5,6-unsubstituted 1,4-dihydropyridines afforded functionalized isoquinolino[1,2-*f*][1,6]naphthyridines in good yields and with high diastereoselectivity via a [4 + 2] cycloaddition process [45]. Very recently, we also found that base-promoted [4 + 2] cycloaddition of salicyl *N*-tosylimines and 5,6-unsubstituted 1,4-dihydropyridines resulted in novel tetrahydrochromeno[3,2-*b*]pyridine derivatives in satisfactory yields [46]. Inspired by these efficient synthetic protocols and in continuation of our aim to develop isocyanide-based multicomponent reactions for construction of diverse nitrogen-containing heterocyclic compounds [47-58], herein we wish to report the mutlicomponent reaction of alkyl isocyanides, dialkyl but-2-ynedioates and 5,6-unsubstituted dihydropyridines for the efficient synthesis of polyfunctionalized tetrahydrocyclopenta[4,5]pyrrolo[2,3-*b*]pyridine-3,4b,5,6,7(1*H*)-pentacarboxylates.

Results and Discussion

Initially, the reaction conditions were examined by employing cyclohexyl isocyanide (**1a**), dimethyl but-2-ynedioate (**2a**) and 5,6-unsubstituted dihydropyridine **3a** as standard reaction. The main results are summarized in Table 1. The expected product

Table 1: Optimizing reaction conditions[a].

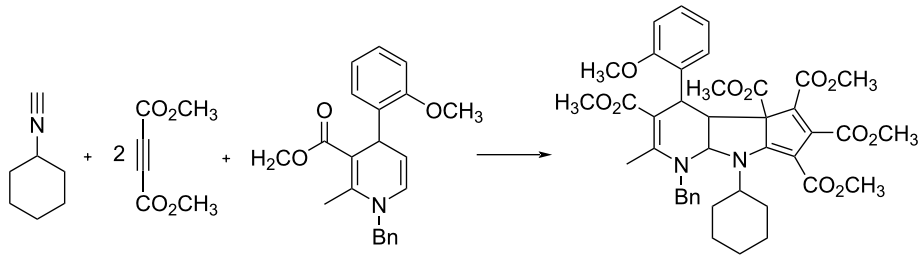

1a **2a** **3a** **4a**

Entry	Base	Ratio of **1a**/**2a**/**3a**	Solvent	Temp (°C)	Time (h)	Yield (%)[b]
1		1.5:3:1	MeOH	rt	6	–
2		1.5:3:1	EtOH	rt	6	–
3		1.5:3:1	THF	rt	6	–
4		1.5:3:1	PhMe	rt	1	12
5		1.5:3:1	CH_2Cl_2	rt	1	13
6		1.5:3:1	MeCN	rt	1	18
7		1.5:3:1	CH_2Cl_2	reflux	1	29
8		1.5:3:1	PhMe	reflux	1	45
9		1.5:3:1	MeCN	40 °C	1	27
10		1.5:3:1	MeCN	60 °C	1	40
11		1.5:3:1	MeCN	reflux	1	47
12		1:2:1	MeCN	reflux	1	52
13		1:3:1	MeCN	reflux	1	62
14		1:4:1	MeCN	reflux	1	71
15		**1:5:1**	**MeCN**	**reflux**	1	**89**
16	DABCO	1:5:1	MeCN	reflux	1	27
17	Et_3N	1:5:1	MeCN	reflux	1	70
18	DMAP	1:5:1	MeCN	reflux	1	39
19		1:5:1	MeCN	reflux	3	87

[a]Reaction conditions: cyclohexyl isocyanide (0.1 mmol), dialkyl but-2-ynedioate, 1,4-dihydropyridine, acetonitrile (5.0 mL); [b]isolated yields.

was not observed when the three-component reaction was carried out in methanol, ethanol or tetrahydrofuran at room temperature (Table 1, entries 1–3). The reaction in toluene, methylene dichloride or acetonitrile at room temperature afforded an unexpected tricyclic compound **4a** in 12–18% yields (Table 1, entries 4–6). ^{1}H NMR spectra clearly indicated that two molecules of dimethyl but-2-ynedioates took part in the reaction. The yields of the product **4a** slightly increased to 29–45% yields when the reaction was carried out at elevated temperature in toluene, methylene dichloride or acetonitrile (Table 1, entries 7–10). When the reaction was carried out in refluxing acetonitrile, the tricyclic compound **4a** can be obtained in 47% yield (Table 1, entry 11). Then, the stoichiometry of dimethyl but-2-ynedioate was examined (Table 1, entries 12–15). The highest yield of **4a** (89%) was obtained by employing five equiv of dimethyl but-2-ynedioate in the reaction (Table 1, entry 15). It can be found that the reaction can be finished in less than one hour. In the presence of DABCO as base catalyst, the yield of **4a** decreased to 27% (Table 1, entry 16). Other common bases such as Et_3N and DMAP were also employed in the reaction, they did no gave the product **4a** in higher yields than that in the absence of any base, which showed that the reaction does not need any base promotor (Table 1, entry 17 and 18). It was also found that the yield of product **4a** cannot be increased when the reaction time was prolonged to three hours (Table 1, entry 19). Thus, the optimized reaction conditions for this multicomponent reaction were successfully established.

Under the optimized reaction conditions, the scope of the reaction was developed by using various substrates. The results are summarized in Table 2. At first, several alkyl isocyanides such as cyclohexyl, *tert*-butyl and benzyl isocyanide have been successfully employed in the reaction. Dimethyl but-2-ynedioate usually gave the expected tricyclic products in good yields. However, the reaction with diethyl but-2-ynedioate afforded products **4p**, **4r** and **4t** in moderate to lower yields. The 5,6- un-

Table 2: The synthesis of the tricyclic compounds **4a–t**[a].

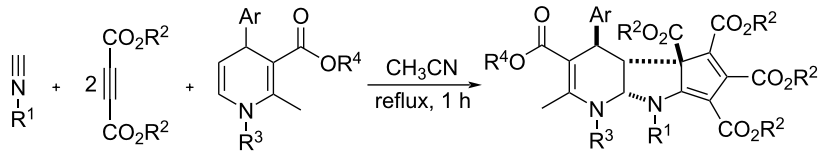

1 **2** **3** **4a–t**

Entry	Compound	R^1	R^2	Ar	R^3	R^4	Yield (%)[b]
1	**4a**	cyclohexyl	CH_3	*o*-$CH_3OC_6H_4$	Bn	CH_3	89
2	**4b**	cyclohexyl	CH_3	*p*-$NO_2C_6H_4$	Bn	CH_3	84
3	**4c**	cyclohexyl	CH_3	*p*-$CH_3C_6H_4$	Bn	CH_3	81
4	**4d**	cyclohexyl	CH_3	*o*-$CH_3OC_6H_4$	*p*-$CH_3OC_6H_4CH_2$	CH_3	84
5	**4e**	cyclohexyl	CH_3	C_6H_5	*p*-$ClC_6H_4CH_2$	CH_3	82
6	**4f**	cyclohexyl	CH_3	C_6H_5	Bn	CH_3	90
7	**4g**	cyclohexyl	CH_3	C_6H_5	*o*-$CH_3C_6H_4CH_2$	CH_3	81
8	**4h**	cyclohexyl	CH_3	C_6H_5	*o*-$ClC_6H_4CH_2$	CH_3	80
9	**4i**	cyclohexyl	CH_3	C_6H_5	*m*-$CH_3OC_6H_4CH_2$	CH_3	80
10	**4j**	cyclohexyl	CH_3	C_6H_5	*p*-$CH_3OC_6H_4$	CH_3	87
11	**4k**	cyclohexyl	CH_3	C_6H_5	*p*-BrC_6H_4	CH_3	93
12	**4l**	cyclohexyl	CH_3	C_6H_5	*m*-ClC_6H_4	CH_3	92
13	**4m**	cyclohexyl	CH_3	*o*-$CH_3OC_6H_4$	*o*-$CH_3C_6H_4$	CH_3	93
14	**4n**	cyclohexyl	CH_3	C_6H_5	*n*-Bu	CH_3	80
15	**4o**	cyclohexyl	CH_3	C_6H_5	Bn	CH_2CH_3	79
16	**4p**	cyclohexyl	CH_2CH_3	C_6H_5	Bn	CH_3	72
17	**4q**	*t*-Bu	CH_3	C_6H_5	Bn	CH_3	66
18	**4r**	*t*-Bu	CH_2CH_3	C_6H_5	Bn	CH_3	58
19	**4s**	Bn	CH_3	C_6H_5	Bn	CH_3	54
20	**4t**	Bn	CH_2CH_3	C_6H_5	Bn	CH_3	30

[a]Reaction conditions: cyclohexyl isocyanide (0.1 mmol), dialkyl but-2-ynedioate (0.5 mmol), 1,4-dihydropyridine (0.1 mmol), acetonitrile (5.0 mL), reflux, 1 h; [b]isolated yields.

substituted dihydropyridines with various substituents showed marginal effects on the yields. These results clearly showed that this reaction has a wide scope of substrates. The obtained compounds **4a–t** have four chiral carbon atoms. The multicomponent reaction might result in several diastereomers. On the basis of TLC analysis and ^{1}H NMR spectra of the crude products, only one relative stereochemistry was produced in the reaction, while the other diastereomers were not detected. In order to elucidate the relative configuration of the obtained compounds, the molecular structure of the compound **4a** was determined by single crystal X-ray diffraction (Figure 1). From Figure 1, it can be seen that the fused dihydropyridine ring connects with the pyrrolidine ring in *cis*-position. The 4-aryl group exists on the *trans*-position to the 2,3-pyrrolidine ring. The methoxycarbonyl group in the ring of the cyclopentadiene stretches to the *cis*-position of the 4-aryl group in the dihydropyridine ring. Thus, it can be assigned that all tricyclic compounds have this kind of relative configuration on the basis of NMR spectra and single crystal structure.

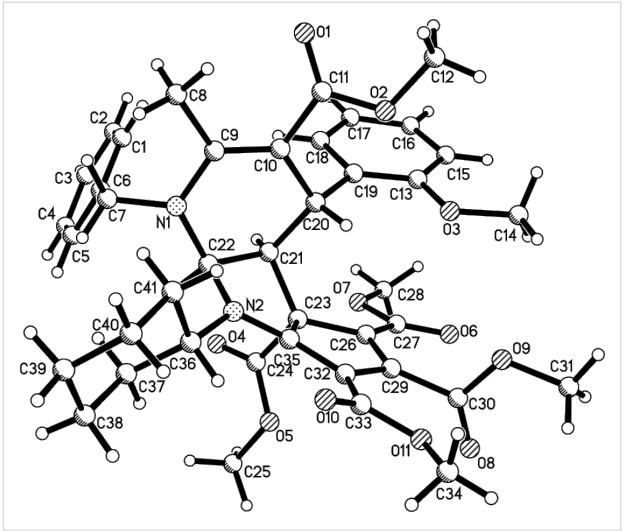

Figure 1: Molecular structure of compound **4a**.

In order to develop the scope of the reaction, another kind of 5,6-unsubstituted 1,4-dihydropyridines **5** were also employed in the reaction, which were previously prepared from the three-component reaction of methyl propiolate, cinnamaldehyde and arylamines. The results are summarized in Table 3. It should be pointed out that TLC analysis and ^{1}H NMR spectra of the crude products usually indicated that only one diastereomer was predominately produced in the reaction even though there are four chiral carbon atoms in the products. It can be found that all reactions proceeded smoothly to give the expected polycyclic compounds **6a–k** in satisfactory yields. The substituents on the three components showed very little effect on the yields. These results showed that this reaction can be performed with a wide variety of substrates. The molecular structure of the compound **6g** was determined by single crystal X-ray diffraction method (Figure 2). The *o*-methoxyphenyl group exists on the *trans*-po-

Table 3: The synthesis of the tricyclic compounds **6a–k**[a].

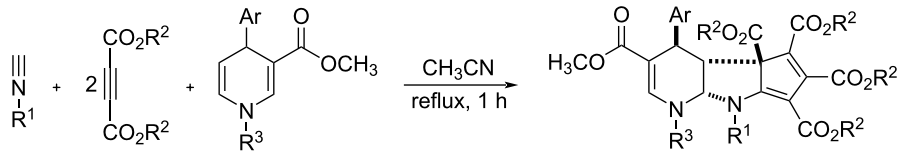

1 **2** **5** **6a–k**

Entry	Compd	R^1	R^2	Ar	R^3	Yield (%)[b]
1	**6a**	cyclohexyl	CH_3	C_6H_5	Bn	92
2	**6b**	cyclohexyl	CH_3	C_6H_5	*m*-$CH_3OC_6H_4CH_2$	82
3	**6c**	cyclohexyl	CH_3	C_6H_5	*o*-$CH_3C_6H_4CH_2$	83
4	**6d**	cyclohexyl	CH_3	C_6H_5	*p*-$CH_3C_6H_4$	83
5	**6e**	cyclohexyl	CH_3	C_6H_5	*m*-ClC_6H_4	84
6	**6f**	cyclohexyl	CH_3	C_6H_5	*o*-$CH_3C_6H_4$	81
7	**6g**	cyclohexyl	CH_3	*o*-$CH_3OC_6H_4$	*p*-BrC_6H_4	88
8	**6h**	cyclohexyl	CH_3	*p*-$NO_2C_6H_4$	*p*-BrC_6H_4	82
9	**6i**	cyclohexyl	CH_2CH_3	C_6H_5	Bn	77
10	**6j**	*t*-Bu	CH_3	C_6H_5	Bn	70
11	**6k**	Bn	CH_3	C_6H_5	Bn	58

[a]Reaction conditions: cyclohexyl isocyanide (0.1 mmol), dialkyl but-2-ynedioate (0.5 mmol), 1,4-dihydropyridine (0.1 mmol), acetonitrile (5.0 mL), reflux, 1 h; [b]Isolated yields.

sition of the fused pyrrolidine unit. The methoxycarbonyl group also exists on the *cis*-position of the *o*-methoxyphenyl group. Therefore, compound **6g** has the same relative configuration to that of the above mentioned product **3a**, which also indicated that this reaction has same steric controlling effect.

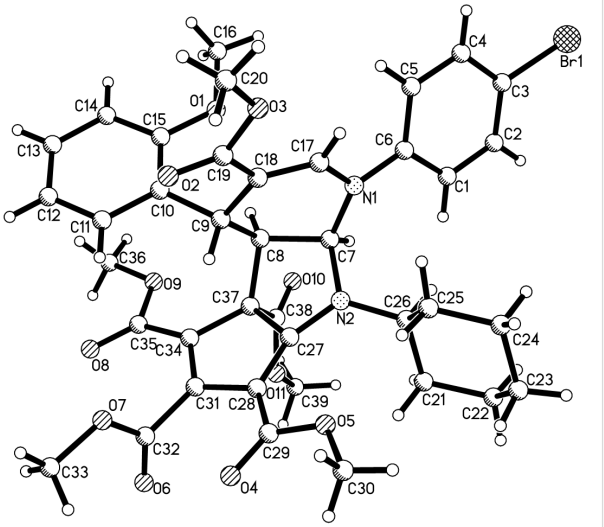

Figure 2: Molecular structure of compound **6g**.

A plausible reaction mechanism is proposed in Scheme 1 to explain the formation of the polycyclic compounds. At first, the nucleophilic addition of alkyl isocyanide to dialkyl but-2-ynedioate afforded the expected Huisgen's 1,4-dipolar intermediate **A**. Secondly, the sequential addition of the Huisgen's 1,4-dipole **A** to the second molecular dialkyl but-2-ynedioate resulted in a 1,5-dipolar intermediate **B**. Thirdly, the intramolecular coupling of the positive charge and the negative charge in intermediate **B** resulted in the formation of polysubstituted 5-(alkylimino)cyclopenta-1,3-diene intermediate **C**, which has been described in several papers about the reaction of alkyl isocyanides and electron-deficient alkynes [59-63]. The in situ generated cyclic intermediate **C** has a resonance hybrid **C'**. Then, the further nucleophilic addition of the electron-rich enamino unit to 5-(alkylimino)cyclopenta-1,3-diene intermediate **C** gave intermediate **D**. At last, the coupling of the iminium cation with the amide anion in intermediate **D** afforded the final product **4** or **6**. On the other hand, the final product **4** or **6** might be directly produced by dipolar cycloaddition reaction of 5-(alkylimino)cyclopenta-1,3-diene intermediate **C** with 5,6-unsaturated dihydropyridine. In consideration of the high diastereoselectivity of the reaction, the concerted addition process is much more likely. However, it is difficult to distinguish between these two reaction processes at present.

Conclusion

In summary, we investigated the three-component reaction of alkyl isocyanides, dialkyl but-2-ynedioates and 5,6-unsubstituted 1,4-dihydropyridines in refluxing acetonitrile. This reaction provided an efficient synthetic protocol for the polyfunctionalized tetrahydrocyclopenta[4,5]pyrrolo[2,3-*b*]pyridine-3,4b,5,6,7(1*H*)-pentacarboxylates in high yields and with high diastereoselectivity. A novel example of an activated intermediate derived from the reaction of alkyl isocyanide and two molecules of but-2-ynedioate was successfully explored in the reaction. This reaction has the advantages of using readily available reagents, simple reaction conditions, high atomic convergence and atomic economy, which might be found potential applications in heterocyclic chemistry.

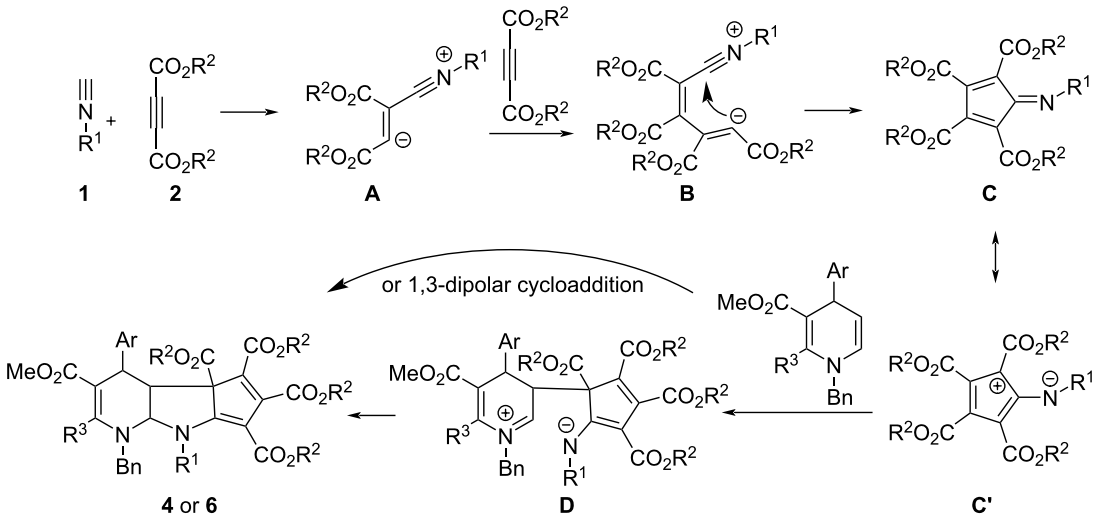

Scheme 1: Proposed reaction mechanism.

Experimental

General procedure for the multicomponent reaction

To a round flask was added alkyl isocyanide (0.1 mmol), dialkyl but-2-ynedioate (0.5 mmol), 5,6-unsubstitued 1,4-dihydropyridine (0.1 mmol) and acetonitrile (5.0 mL). The solution was stirred at reflux temperature for nearly one hour. After removing the solvent by rotatory evaporation at reduced pressure, the residue was subjected to column chromatography with a mixture of ethyl acetate and petroleum ether (v/v = 1:4) as eluent to give the pure product for analysis.

Pentamethyl *rel*-(4*R*,4a*R*,4b*S*,8a*S*)-1-benzyl-8-cyclohexyl-4-(2-methoxyphenyl)-2-methyl-4,4a,8,8a-tetrahydrocyclopenta[4,5]pyrrolo[2,3-*b*]pyridine-3,4b,5,6,7(1*H*)-pentacarboxylate (4a): yellow solid, 89%, mp 209–211 °C; ^{1}H NMR (400 MHz, $CDCl_3$) δ 7.49 (d, *J* = 8.0 Hz, 1H, ArH), 7.47–7.44 (m, 3H, ArH), 7.41–7.38 (m, 1H, ArH), 7.02–6.97 (m, 1H, ArH), 6.68–6.62 (m, 3H, ArH), 5.76 (d, *J* = 3.6 Hz, 1H, CH), 4.96–4.90 (m, 1H, CH), 4.84 (d, *J* = 16.0 Hz, 1H, CH_2), 4.36 (d, *J* = 15.6 Hz, 1H, CH_2), 3.95 (s, 3H, OCH_3), 3.74 (s, 3H, OCH_3), 3.65–3.63 (m, 1H, CH), 3.61 (s, 3H, OCH_3), 3.58 (s, 3H, OCH_3), 3.38 (d, *J* = 8.4 Hz, 1H, CH), 3.21 (s, 3H, OCH_3), 2.96 (s, 3H, OCH_3), 2.28 (s, 3H, CH_3), 1.89–1.86 (m, 2H, CH_2), 1.80–1.68 (m, 4H, CH_2), 1.55–1.33 (m, 3H, CH_2), 1.20–1.13 (m, 1H, CH_2) ppm; ^{13}C NMR (100 MHz, $CDCl_3$) δ 170.1, 168.3, 167.8, 166.5, 162.5, 161.9, 157.2, 157.0, 144.7, 137.6, 131.4, 130.9, 129.1, 128.0, 127.9, 127.1, 112.0, 113.6, 111.0, 110.2, 98.9, 84.0, 72.2, 58.2, 56.7, 55.2, 53.3, 52.2, 51.3, 50.4, 50.2, 32.4, 31.5, 31.2, 26.2, 25.7, 25.6, 18.2 ppm; IR (KBr) ν: 3435, 2931, 2862, 2360, 1737, 1698, 1587, 1547, 1435, 1385, 1335, 1251, 1204, 1125, 1092, 1001, 977, 895, 853, 792 cm^{-1}; HRESIMS (*m*/*z*): $[M + Na]^+$ calcd. for $C_{41}H_{46}NaN_2O_{11}$, 765.2994; found, 765.2993.

Supporting Information

The crystallographic data of the compounds **4a** (CCDC 2346135) and **6g** (CCDC 2346136) have been deposited at the Cambridge Crystallographic Database Center (http://www.ccdc.cam.ac.uk).

Supporting Information File 1

Characterization data and ^{1}H NMR, ^{13}C NMR, and HRMS spectra of compounds.
[https://www.beilstein-journals.org/bjoc/content/supplementary/1860-5397-20-126-S1.pdf]

Funding

This work was financially supported by the National Natural Science Foundation of China (Nos. 21572196, 21871227).

Author Contributions

Xiu-Yu Chen: investigation. Ying Han: methodology. Jing Sun: data curation; formal analysis. Chao-Guo Yan: conceptualization; project administration; supervision; writing – review & editing.

ORCID® iDs

Ying Han - https://orcid.org/0000-0002-2424-5163
Chao-Guo Yan - https://orcid.org/0000-0002-2777-9582

Data Availability Statement

All data that supports the findings of this study is available in the published article and/or the supporting information to this article.

References

1. Zhu, J. *Eur. J. Org. Chem.* **2003,** 1133–1144. doi:10.1002/ejoc.200390167
2. Lygin, A. V.; de Meijere, A. *Angew. Chem., Int. Ed.* **2010,** *49,* 9094–9124. doi:10.1002/anie.201000723
3. Gulevich, A. V.; Zhdanko, A. G.; Orru, R. V. A.; Nenajdenko, V. G. *Chem. Rev.* **2010,** *110,* 5235–5331. doi:10.1021/cr900411f
4. Dömling, A.; Huang, Y. *Synthesis* **2010,** 2859–2883. doi:10.1055/s-0030-1257906
5. Dömling, A.; Ugi, I. *Angew. Chem., Int. Ed.* **2000,** *39,* 3168–3210. doi:10.1002/1521-3773(20000915)39:18<3168::aid-anie3168>3.0.co;2-u
6. Wang, W.; Dömling, A. *J. Comb. Chem.* **2009,** *11,* 403–409. doi:10.1021/cc9000136
7. Nair, V.; Rajesh, C.; Vinod, A. U.; Bindu, S.; Sreekanth, A. R.; Mathen, J. S.; Balagopal, L. *Acc. Chem. Res.* **2003,** *36,* 899–907. doi:10.1021/ar020258p
8. Qiu, G.; Ding, Q.; Wu, J. *Chem. Soc. Rev.* **2013,** *42,* 5257–5269. doi:10.1039/c3cs35507a
9. Estévez, V.; Villacampa, M.; Menéndez, J. C. *Chem. Soc. Rev.* **2014,** *43,* 4633–4657. doi:10.1039/c3cs60015g
10. Wan, J.-P.; Liu, Y. *RSC Adv.* **2012,** *2,* 9763–9777. doi:10.1039/c2ra21406g
11. Sadjadi, S.; Heravi, M. M.; Nazari, N. *RSC Adv.* **2016,** *6,* 53203–53272. doi:10.1039/c6ra02143c
12. Khan, I.; Zaib, S.; Ibrar, A. *Org. Chem. Front.* **2020,** *7,* 3734–3791. doi:10.1039/d0qo00698j
13. Safaei, H. R.; Dehbozorgi, F. *RSC Adv.* **2016,** *6,* 26783–26790. doi:10.1039/c5ra22293a
14. Wang, H.-Y.; Bao, M.; Jiang, B.; Li, L. *RSC Adv.* **2016,** *6,* 6459–6466. doi:10.1039/c5ra25408f
15. Rostamnia, S. *RSC Adv.* **2015,** *5,* 97044–97065. doi:10.1039/c5ra20455k
16. Gao, Q.; Hao, W.-J.; Liu, F.; Tu, S.-J.; Wang, S.-L.; Li, G.; Jiang, B. *Chem. Commun.* **2016,** *52,* 900–903. doi:10.1039/c5cc08071a
17. Terzidis, M. A.; Zarganes-Tzitzikas, T.; Tsimenidis, C.; Stephanidou-Stephanatou, J.; Tsoleridis, C. A.; Kostakis, G. E. *J. Org. Chem.* **2012,** *77,* 9018–9028. doi:10.1021/jo3014947

18. Fu, W.; Dong, L.; Shi, J.; Tong, B.; Cai, Z.; Zhi, J.; Dong, Y. *Polym. Chem.* **2018,** *9,* 5543–5550. doi:10.1039/c8py01336e
19. Yavari, I.; Sheikhi, S.; Taheri, Z. *Mol. Diversity* **2024,** *28,* 143–157. doi:10.1007/s11030-023-10635-5
20. Nazeri, M. T.; Ghasemi, M.; Ahmadi, M.; Shaabani, A.; Notash, B. *J. Org. Chem.* **2023,** *88,* 13504–13519. doi:10.1021/acs.joc.3c01013
21. Nazeri, M. T.; Ahmadi, M.; Ghasemi, M.; Shaabani, A.; Notash, B. *Org. Biomol. Chem.* **2023,** *21,* 4095–4108. doi:10.1039/d3ob00250k
22. Yavari, I.; Ravaghi, P.; Safaei, M. *Synthesis* **2022,** *54,* 1870–1876. doi:10.1055/s-0041-1737817
23. Li, Y.; Kopcha, W. P.; Emge, T. J.; Sun, Y.; Zhang, J. *Org. Lett.* **2021,** *23,* 8867–8872. doi:10.1021/acs.orglett.1c03371
24. Bankura, A.; Saha, J.; Maity, R.; Das, I. *Adv. Synth. Catal.* **2021,** *363,* 1014–1021. doi:10.1002/adsc.202001376
25. Nazeri, M. T.; Shaabani, A.; Notash, B. *Org. Biomol. Chem.* **2021,** *19,* 3722–3734. doi:10.1039/d0ob02339f
26. Mohlala, R. L.; Coyanis, E. M.; Fernandes, M. A.; Bode, M. L. *Tetrahedron Lett.* **2020,** *61,* 151796. doi:10.1016/j.tetlet.2020.151796
27. Wang, C.-C.; Ma, Z.-W.; Qu, Y.-L.; Liu, Z.-J.; Chen, X.-P.; Zhou, J.; Chen, Y.-J. *Chem. – Asian J.* **2020,** *15,* 560–563. doi:10.1002/asia.201901780
28. Nazeri, M. T.; Mohammadian, R.; Farhid, H.; Shaabani, A.; Notash, B. *Tetrahedron Lett.* **2020,** *61,* 151408. doi:10.1016/j.tetlet.2019.151408
29. Alizadeh, A.; Amir Ashjaee Asalemi, K.; Halvagar, M. *Synthesis* **2019,** *51,* 2936–2944. doi:10.1055/s-0037-1612426
30. Krishna Swaroop, D.; Ravi Kumar, N.; Reddy, N. S.; Punna, N.; Jagadeesh Babu, N.; Narsaiah, B. *Eur. J. Org. Chem.* **2019,** 3654–3657. doi:10.1002/ejoc.201900482
31. Li, Z.; Huo, T.; Li, L.; Feng, S.; Wang, Q.; Zhang, Z.; Pang, S.; Zhang, Z.; Wang, P.; Zhang, Z. *Org. Lett.* **2018,** *20,* 7762–7766. doi:10.1021/acs.orglett.8b03115
32. Sabouri, N.; Mahdavinia, G. H.; Notash, B. *Chin. Chem. Lett.* **2016,** *27,* 1040–1043. doi:10.1016/j.cclet.2016.03.015
33. Song, P.; Zhao, L.; Ji, S. *Chin. J. Chem.* **2014,** *32,* 381–386. doi:10.1002/cjoc.201400155
34. Dimitriadou, E.; Stephanidou-Stephanatou, J.; Tsoleridis, C. A.; Hadjipavlou-Litina, D. J.; Kontogiorgis, C.; Kostakis, G. E. *Tetrahedron* **2014,** *70,* 2938–2943. doi:10.1016/j.tet.2014.03.031
35. Emtiazi, H.; Amrollahi, M. A. *Helv. Chim. Acta* **2014,** *97,* 1422–1426. doi:10.1002/hlca.201400002
36. Ghandi, M.; Ghomi, A.-T.; Kubicki, M. *J. Org. Chem.* **2013,** *78,* 2611–2616. doi:10.1021/jo302790y
37. Lavilla, R.; Carranco, I.; Díaz, J. L.; Bernabeu, M. C.; de la Rosa, G. *Mol. Diversity* **2003,** *6,* 171–175. doi:10.1023/b:modi.0000006756.83821.80
38. Vicente-García, E.; Catti, F.; Ramón, R.; Lavilla, R. *Org. Lett.* **2010,** *12,* 860–863. doi:10.1021/ol902913j
39. Vohra, R. K.; Bruneau, C.; Renaud, J.-L. *Adv. Synth. Catal.* **2006,** *348,* 2571–2574. doi:10.1002/adsc.200600343
40. Basu, S.; Chatterjee, S.; Ray, S.; Maity, S.; Ghosh, P.; Bhaumik, A.; Mukhopadhyay, C. *Beilstein J. Org. Chem.* **2022,** *18,* 133–142. doi:10.3762/bjoc.18.14
41. Lavilla, R.; Bernabeu, M. C.; Carranco, I.; Díaz, J. L. *Org. Lett.* **2003,** *5,* 717–720. doi:10.1021/ol027545d
42. Carranco, I.; Díaz, J. L.; Jiménez, O.; Vendrell, M.; Albericio, F.; Royo, M.; Lavilla, R. *J. Comb. Chem.* **2005,** *7,* 33–41. doi:10.1021/cc049877a
43. Maiti, S.; Sridharan, V.; Menéndez, J. C. *J. Comb. Chem.* **2010,** *12,* 713–722. doi:10.1021/cc100084b
44. Islam, K.; Das, D. K.; Akram, E.; Khan, A. T. *Synthesis* **2015,** *47,* 2745–2755. doi:10.1055/s-0034-1380431
45. Chen, X.-Y.; Zheng, H.; Han, Y.; Sun, J.; Yan, C.-G. *Beilstein J. Org. Chem.* **2023,** *19,* 982–990. doi:10.3762/bjoc.19.73
46. Liu, X.; Wang, D.; Sun, J.; Yan, C.-G. *J. Mol. Struct.* **2024,** *1304,* 137684. doi:10.1016/j.molstruc.2024.137684
47. Ma, W.; Han, Y.; Sun, J.; Yan, C. *Chin. J. Org. Chem.* **2021,** *41,* 3180–3191. doi:10.6023/cjoc202103034
48. He, Y.-W.; Ma, W.-Q.; Han, Y.; Sun, J.; Yan, C.-G. *J. Org. Chem.* **2023,** *88,* 14911–14927. doi:10.1021/acs.joc.3c01246
49. Liu, D.; Sun, J.; Han, Y.; Yan, C.-G. *J. Org. Chem.* **2023,** *88,* 17181–17196. doi:10.1021/acs.joc.3c02047
50. Zhu, L.-Y.; Sun, J.; Liu, D.; Yan, C.-G. *Org. Biomol. Chem.* **2023,** *21,* 9392–9397. doi:10.1039/d3ob01560b
51. Liu, X.; Shi, W.; Sun, J.; Yan, C.-G. *Beilstein J. Org. Chem.* **2023,** *19,* 1923–1932. doi:10.3762/bjoc.19.143
52. Xiao, Z.; Xu, F.; Sun, J.; Yan, C.-G. *Beilstein J. Org. Chem.* **2023,** *19,* 1234–1242. doi:10.3762/bjoc.19.91
53. Sun, J.; Liu, X.; Sun, Q.; Han, Y.; Yan, C.-G. *J. Org. Chem.* **2023,** *88,* 11562–11580. doi:10.1021/acs.joc.3c00887
54. Huang, L.; Han, Y.; Sun, J.; Sun, Q.; Yan, C.-G. *Org. Biomol. Chem.* **2023,** *21,* 6028–6033. doi:10.1039/d3ob00769c
55. Liu, D.; Sun, J.; Sun, Q.; Yan, C.-G. *Org. Chem. Front.* **2023,** *10,* 540–547. doi:10.1039/d2qo01771g
56. Sun, J.; Yan, C.; Sun, Q.; Han, Y.; Yan, C.-G. *New J. Chem.* **2023,** *47,* 6694–6699. doi:10.1039/d3nj00013c
57. Zhan, S.-C.; Sun, J.; Sun, Q.; Han, Y.; Yan, C.-G. *J. Org. Chem.* **2023,** *88,* 5440–5456. doi:10.1021/acs.joc.2c03094
58. Wang, D.; Tang, T.; Sun, J.; Han, Y.; Yan, C.-G. *Org. Lett.* **2024,** *26,* 4117–4121. doi:10.1021/acs.orglett.4c01236
59. Winterfeldt, E.; Schumann, D.; Dillinger, H.-J. *Chem. Ber.* **1969,** *102,* 1656–1664. doi:10.1002/cber.19691020530
60. Gougoutas, J. Z.; Saenger, W. *J. Org. Chem.* **1971,** *36,* 3632–3633. doi:10.1021/jo00822a041
61. Junjappa, H.; Saxena, M. K.; Ramaiah, D.; Loharay, B. B.; Rath, N. P.; George, M. V. *J. Org. Chem.* **1998,** *63,* 9801–9805. doi:10.1021/jo981427f
62. Cheng, F.-Y.; Sung, K.; Lee, G.-H.; Wang, Y. *J. Chin. Chem. Soc.* **2000,** *47,* 1295–1298. doi:10.1002/jccs.200000180
63. Zhao, L.-L.; Wang, S.-Y.; Xu, X.-P.; Ji, S.-J. *Chem. Commun.* **2013,** *49,* 2569–2571. doi:10.1039/c3cc38526d

License and Terms

This is an open access article licensed under the terms of the Beilstein-Institut Open Access License Agreement (https://www.beilstein-journals.org/bjoc/terms), which is identical to the Creative Commons Attribution 4.0 International License (https://creativecommons.org/licenses/by/4.0). The reuse of material under this license requires that the author(s), source and license are credited. Third-party material in this article could be subject to other licenses (typically indicated in the credit line), and in this case, users are required to obtain permission from the license holder to reuse the material.

The definitive version of this article is the electronic one which can be found at:
https://doi.org/10.3762/bjoc.20.126

BEILSTEIN JOURNAL OF ORGANIC CHEMISTRY

Generation of multimillion chemical space based on the parallel Groebke–Blackburn–Bienaymé reaction

Evgen V. Govor[1,2], Vasyl Naumchyk[1,2], Ihor Nestorak[1,3], Dmytro S. Radchenko[1], Dmytro Dudenko[1], Yurii S. Moroz[1,2], Olexiy D. Kachkovsky[3] and Oleksandr O. Grygorenko[*1,2]

Full Research Paper

Open Access

Address:
[1]Enamine Ltd., Winston Churchill Street 78, Kyïv 02094, Ukraine, [2]Taras Shevchenko National University of Kyiv, Volodymyrska Street 60, Kyïv 01601, Ukraine and [3]V. P. Kukhar Institute of Bioorganic Chemistry and Petrochemistry, Akademik Kukhar Street 1, Kyïv 02094, Ukraine

Email:
Oleksandr O. Grygorenko[*] - gregor@univ.kiev.ua

* Corresponding author

Keywords:
fused rings; heterocycles; imidazoles; isonitrile; multicomponent reactions

Beilstein J. Org. Chem. **2024,** *20,* 1604–1613.
https://doi.org/10.3762/bjoc.20.143

Received: 29 April 2024
Accepted: 03 July 2024
Published: 16 July 2024

This article is part of the thematic issue "Multicomponent reactions IV".

Associate Editor: T. J. J. Müller

© 2024 Govor et al.; licensee Beilstein-Institut.
License and terms: see end of document.

Abstract

Parallel Groebke–Blackburn–Bienaymé reaction was evaluated as a source of multimillion chemically accessible chemical space. Two most popular classical protocols involving the use of $Sc(OTf)_3$ and TsOH as the catalysts were tested on a broad substrate scope, and prevalence of the first method was clearly demonstrated. Furthermore, the scope and limitations of the procedure were established. A model 790-member library was obtained with 85% synthesis success rate. These results were used to generate a 271-Mln. readily accessible (REAL) heterocyclic chemical space mostly containing unique chemotypes, which was confirmed by comparative analysis with commercially available compound collections. Meanwhile, this chemical space contained 432 compounds that already showed biological activity according to the ChEMBL database.

Introduction

Multicomponent reactions are widely recognized as a powerful source of biologically active compounds, in particular, for drug discovery purposes [1-6]. Isonitrile-based multicomponent reactions, such as the Groebke–Blackburn–Bienaymé (GBB) reaction, is an important tool in chemical synthesis providing easy access to a huge compound diversity and complexity [7-17]. Essentially, the GBB reaction is a three-component condensation of an α-amino heterocycle (e.g., 2-aminopyridine) **1**, an aldehyde **2**, and an isonitrile **3** providing the corresponding fused imidazoles (e.g., imidazo[1,2-*a*]pyridines) of general formula **4** (Scheme 1) [18-21]. Imidazo[1,2-*a*]pyridines and related heterocycles can be considered as privileged chemotypes in drug discovery: their representatives include the sedative drug zolpidem, disease-modifying antirheumatic agent

upadacitinib, anticancer drug capmatinib, or risdiplam, a medication for spinal muscular atrophy (SMA) treatment (Figure 1) [22,23].

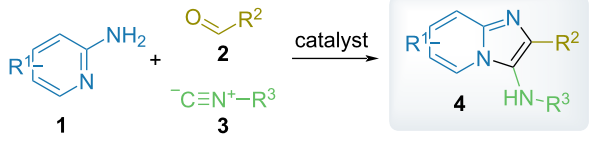

Scheme 1: Groebke–Blackburn–Bienaymé (GBB) reaction.

Over the last two decades, the GBB reaction has been studied in more than 200 research papers [21] and a number of works (including the original publication by Blackburn and coauthors [20]) described its parallel synthesis version [24-29]. Recently, we have shown that other (pseudo-)three-component reactions are very effective for the generation of synthetically tractable ultra-large chemical space [30-32]. Such virtual but readily accessible (REAL) compound libraries demonstrated excellent performance in early drug discovery programs when combined with modern computational tools such as high-throughput docking or machine learning [33-37]. In this work, we aimed at the implementation of the GBB reaction for the generation of such ultra-large chemical space, including experimental evaluation of the synthesis success rate (SSR, i.e., percentage of experiments that allowed obtaining the target library member in pure form) on a large set of starting materials.

Through the article, the compound numbering system common for the works on combinatorial chemistry was used: the starting materials used for the library generation were marked as **1**{*i*}, **2**{*j*}, and **3**{*k*}, whereas the corresponding library members were denoted as **4**{*i*,*j*,*k*}.

Results and Discussion

Library synthesis

Preliminary experiments on the parallel GBB reaction were performed with heterocyclic amines **1**{1–430}, aldehydes **2**{1–583}, and isonitriles **3**{1–73} available from our stock (based on our previous in-house experience on isonitrile-based parallel reactions, electron-poor (hetero)aromatic isonitriles were not included in the study). According to Boltjes and Dömling, the following three catalysts were applied most often to promote the title reaction [21]: $Sc(OTf)_3$ (described first in the original work by Blackburn and coauthors [20]), $HClO_4$, and TsOH. We wanted to avoid the use of $HClO_4$ in our parallel reaction set-up, so that only two remaining catalytic systems were evaluated. 580 library members were deliberately selected for both reaction conditions, and the corresponding experiments were performed (reactants at 1:1:1 ratio, 10 mol % of the catalyst, MeOH, rt, 16 h). It was found that TsOH, albeit being cheaper, demonstrated a poorer performance as the reaction promotor (62% SSR vs 67% for $Sc(OTf)_3$; 34% average yield in both cases). This is especially apparent if the product yields are compared for 24 library members that we attempted to obtain by both methods (Figure 2).

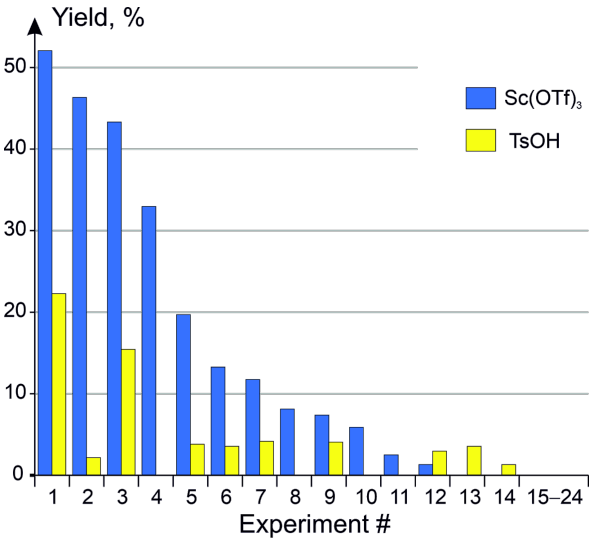

Figure 2: Yields of library members **4** synthesized using both $Sc(OTf)_3$ and TsOH as the catalysts.

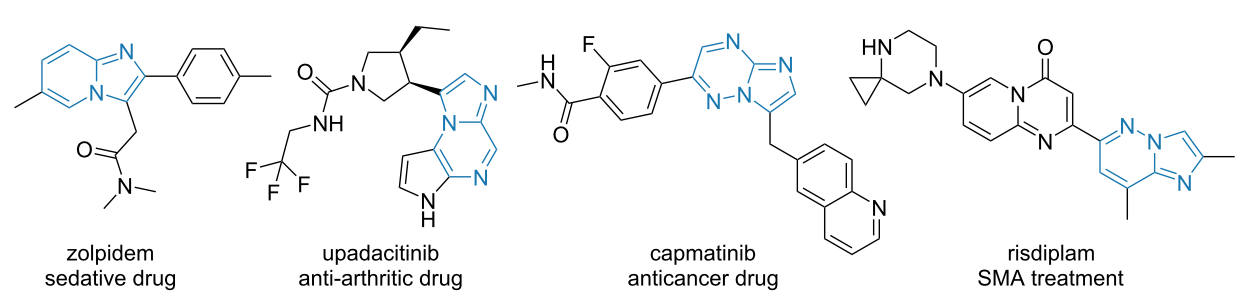

Figure 1: Marketed drugs comprising imidazo[1,2-*a*]azine scaffolds.

These preliminary experiments also allowed establishing the following limitations of the method and excluding the corresponding reactants from further studies (Figure 3):

- α-aminoazoles of varied electronic nature (e.g., 3-aminopyrazole (**1**{1}), 3-aminoisoxazole (**1**{2}), 2-aminothiazole (**1**{3}), 2-amino-1,3,4-thiadiazole (**1**{4}), or 2-aminotetrazole (**1**{5}) demonstrated poor conversion to the target products;
- 2-aminopyrimidines either gave isomeric mixtures (e.g., parent compound **1**{6}, alkyl-substituted derivatives **1**{7} and **1**{8}) or showed low conversion (halogenated derivatives **1**{9–11});
- 4-aminopyrimidines **1**{12–16} also demonstrated low conversion;
- pyridine derivatives with electron-withdrawing substituents (such as NO_2 at C-3 or C-5 positions, as well as CN, SO_2NH_2, or $C(O)NH_2$ at the C-3 atom) did not work (compounds **1**{17–21});
- for pyridazine or pyrazine derivatives, even the presence of halogen atoms was sufficient to deactivate the substrate (e.g., compounds **1**{22–24});
- a dialkylamino or alkoxy group at the C-6 position of pyridine derivatives also hampered the substrate's reactivity (e.g., compounds **1**{25–27}).

Some of these results (e.g., on the reactivity of aminopyrimidine derivatives) were in accordance with the previous literature data [21,29]. Meanwhile, electronic effects of the substituents in the amino heterocycle reported in the previous works were somewhat contradictory. Whereas for the NO_2 group, lowering the reactivity has been documented, other electron-withdrawing groups were reported to be generally compatible with the GBB reaction [21]. Interference of dialkylamino or alkoxy groups at the C-6 position was also mentioned previously [29].

In addition to that, it was found that electron-poor aromatic aldehydes (e.g., **2**{1–3}) did not work in the GBB reaction (Figure 4). This result is in accordance with the previous findings [21]. Notably, steric effects were not significant since *o*,*o*′-disubstituted aldehydes (e.g., **2**{4–6}) displayed usual efficiency. As might be expected from our previous experience, 4-fluoro- and 4-chloro-2-fluoro-1-isocyanobenzenes (**3**{1} and **3**{2}) showed poor performance and unsatisfactory results were also observed for isocyanocyclopropane (**3**{3}).

Using the guidelines described above, we have updated the reactant lists with additional representatives and excluded those demonstrating poor performance. Using the resulting sets of amino heterocycles **1**{22–485}, aldehydes **2**{4–867}, and isoni-

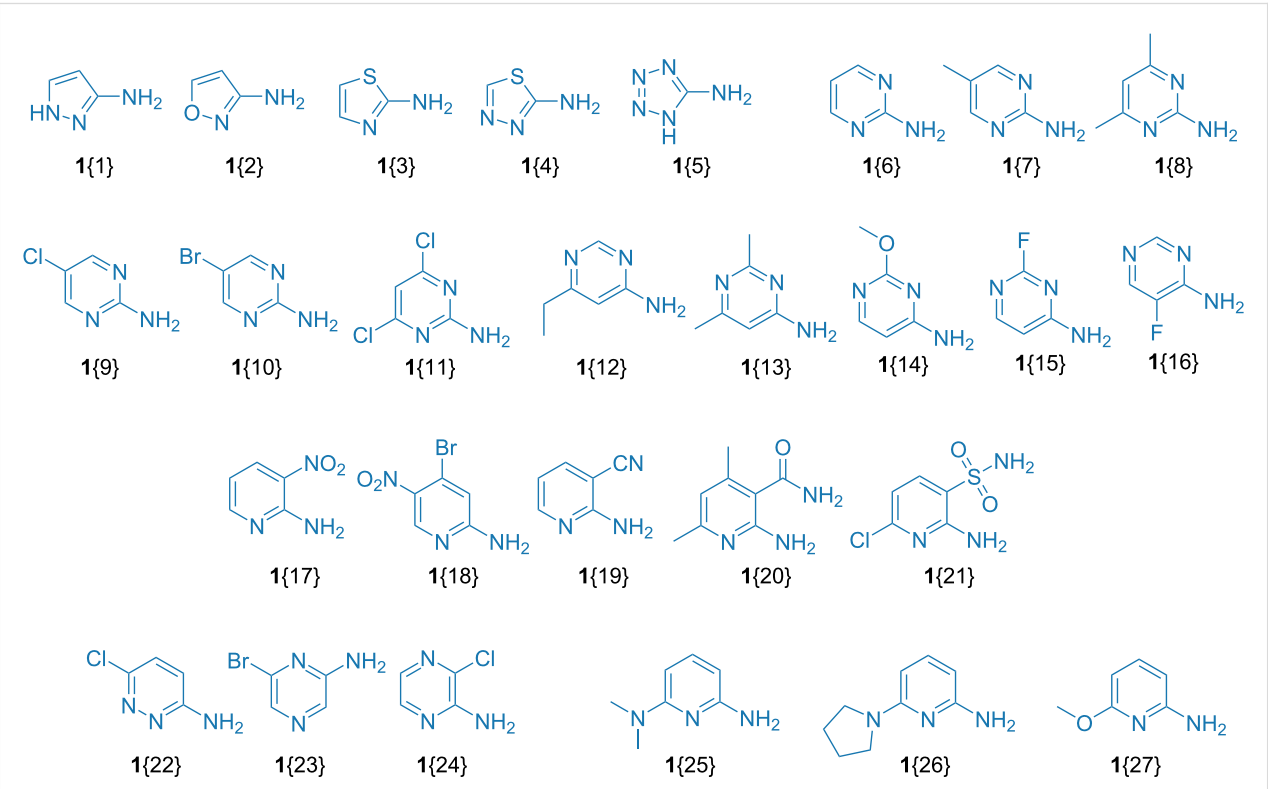

Figure 3: Amino heterocycles **1**{1–27} demonstrating poor performance in the parallel GBB reaction.

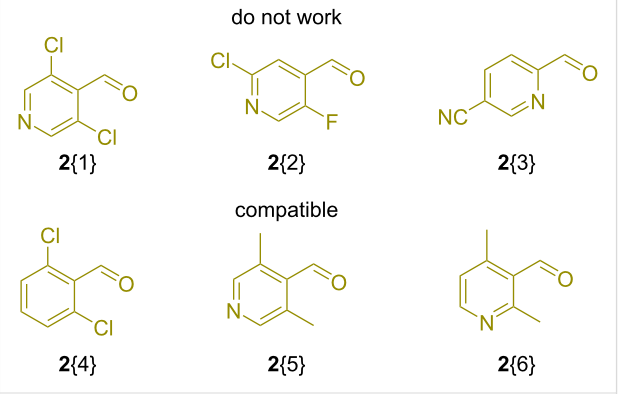

Figure 4: (Hetero)aromatic aldehydes **2**{1–6} illustrating electronic and steric effects on the parallel GBB reaction.

triles **3**{4–78}, 892 library members **4**{22–485,4–867,4–78} were deliberately selected and subjected to the parallel synthesis using the $Sc(OTf)_3$-based protocol. As a result, 790 library members were obtained successfully (SSR = 85%, average yield of 37%) (Scheme 2).

Chemical space generation

Since validation of the GBB reaction showed that it is compatible with the main readily accessible chemical space criteria (at least 80% synthesizability) [30], we have aimed at the generation of the corresponding REAL space. For this purpose, 686 amino heterocycles **1**, 3,927 aldehydes **2**, and 107 isonitriles **3** complying with our general in-house reactivity/availability filters were subjected to virtual coupling using the limitations mentioned above. Additionally, combinations providing compounds with more than two chiral centers were not included. This resulted in 271,026,660 library members with nearly 85% expected synthetic accessibility according to the model experiments described in the previous section.

Distributions of the resulting chemical space over molecular weight (MW), 1-octanol–water partition coefficient logarithm (log *P*), H-bond acceptor/donor count (HAcc/HDon), fraction of sp^3-hybrid carbon atoms ($F(sp^3)$), and rotatable bond count (RotB) are shown in Figure 5. It is apparent that the GBB chemical space contains many drug-like (69,043,101 molecules, 25%) and "beyond-Ro5" compounds (75%) [38]. Furthermore, although the proposed approach cannot be considered lead-oriented, it may provide 12,122,351 lead-like compounds compliant with the "rule-of-four" (MW < 400, log *P* < 4) [39], and 1,383,298 with the even stricter Churcher's rules (MW = 200–350, log *P* = −1 to 3) [40].

Next, we compared the GBB chemical space with common chemical databases (ChEMBL [42], PubChem [43], and

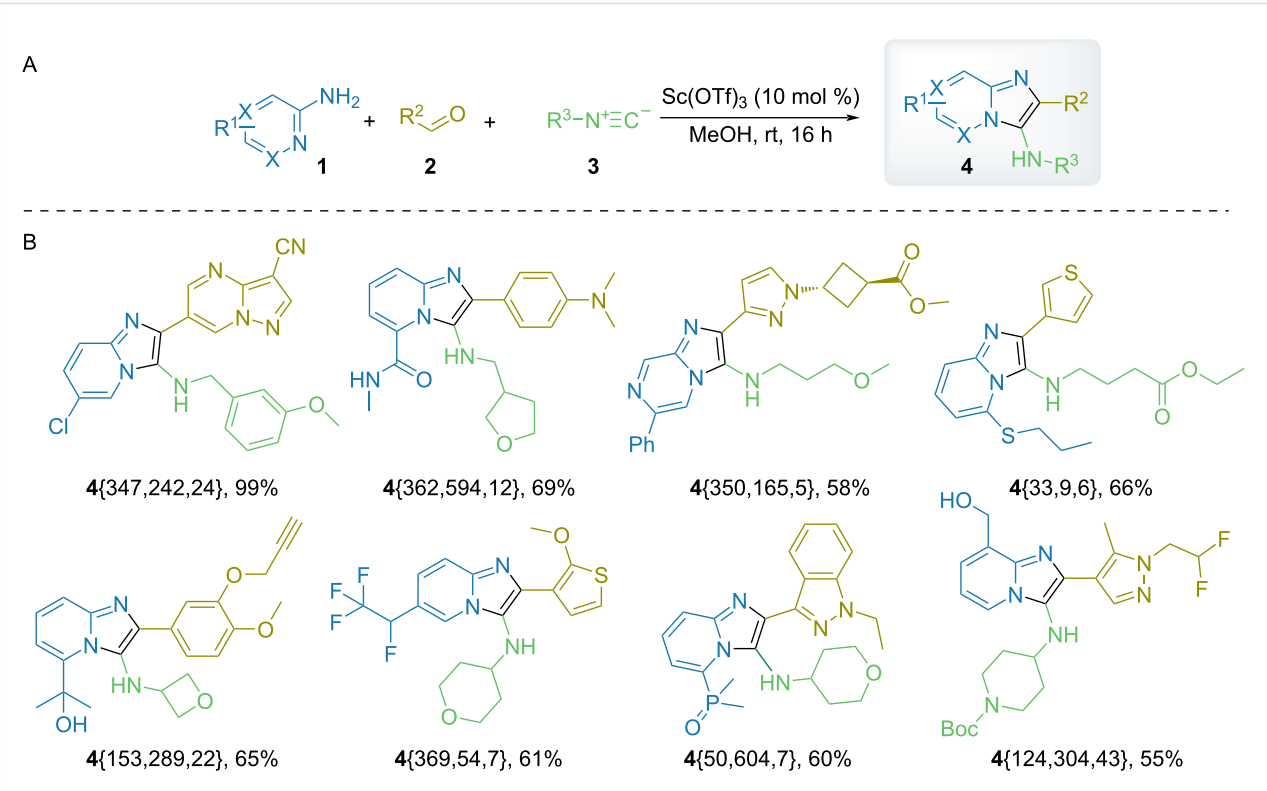

Scheme 2: A) Parallel GBB reaction and B) examples of library members **4** obtained (relative configurations are shown).

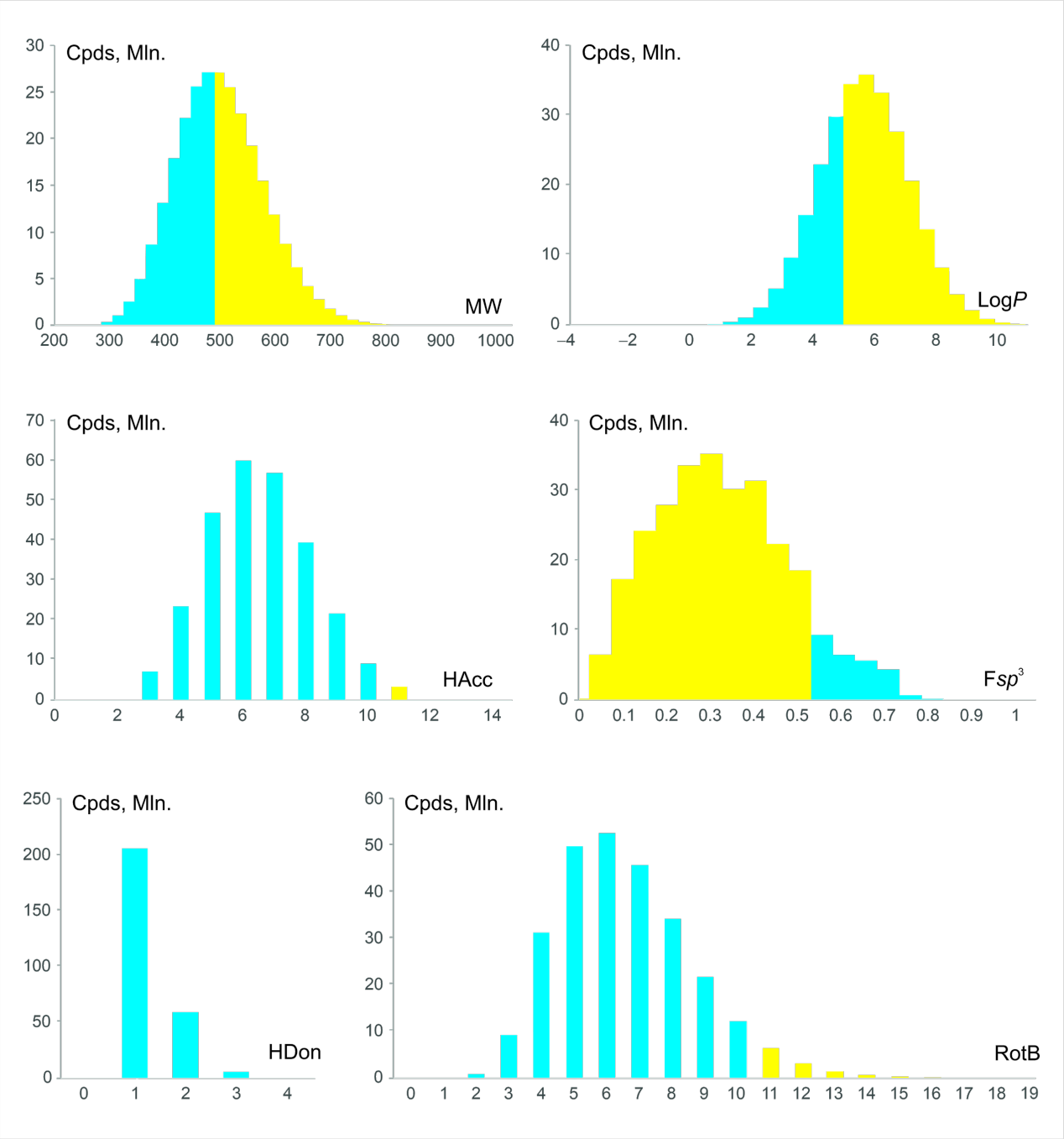

Figure 5: Physicochemical properties of the chemical space of 271 Mln. members obtained by virtual GBB reaction (MW – molecular weight; HAcc/HDon – H-bond acceptor/donor count; F(sp^3) – fraction of sp^3-hybrid carbon atoms; RotB – rotatable bond count); compounds complying with specific Lipinski/Veber rules (MW ≤ 500, log *P* ≤ 5, HDon ≤ 5, HAcc ≤ 10, RotB ≤ 10 [38,41]) as well as compounds with F(sp^3) > 0.5 are highlighted in blue, the rest of the compounds are shown in yellow.

ZINC15 [44]), as well as our stock screening compound collection [45]. Due to the enormous size of the databases, pairwise Tanimoto analysis was performed at the extended Bemis–Murcko scaffold level. First, extended Bemis–Murcko scaffolds were generated by cutting off the side chains of the molecules and retaining ring systems and linkers between them. After removal of duplicates, Tanimoto similarity coefficients were calculated for each pair of the molecules in the compared databases (T = 1 and 0 for similar and very dissimilar molecules, respectively). Average pairwise values for each molecule from the database of comparison are depicted in Figure 6. The mean values for all the databases were in the range of 0.44–0.45, which shows that despite there are some representatives that are similar to already known compounds, the gener-

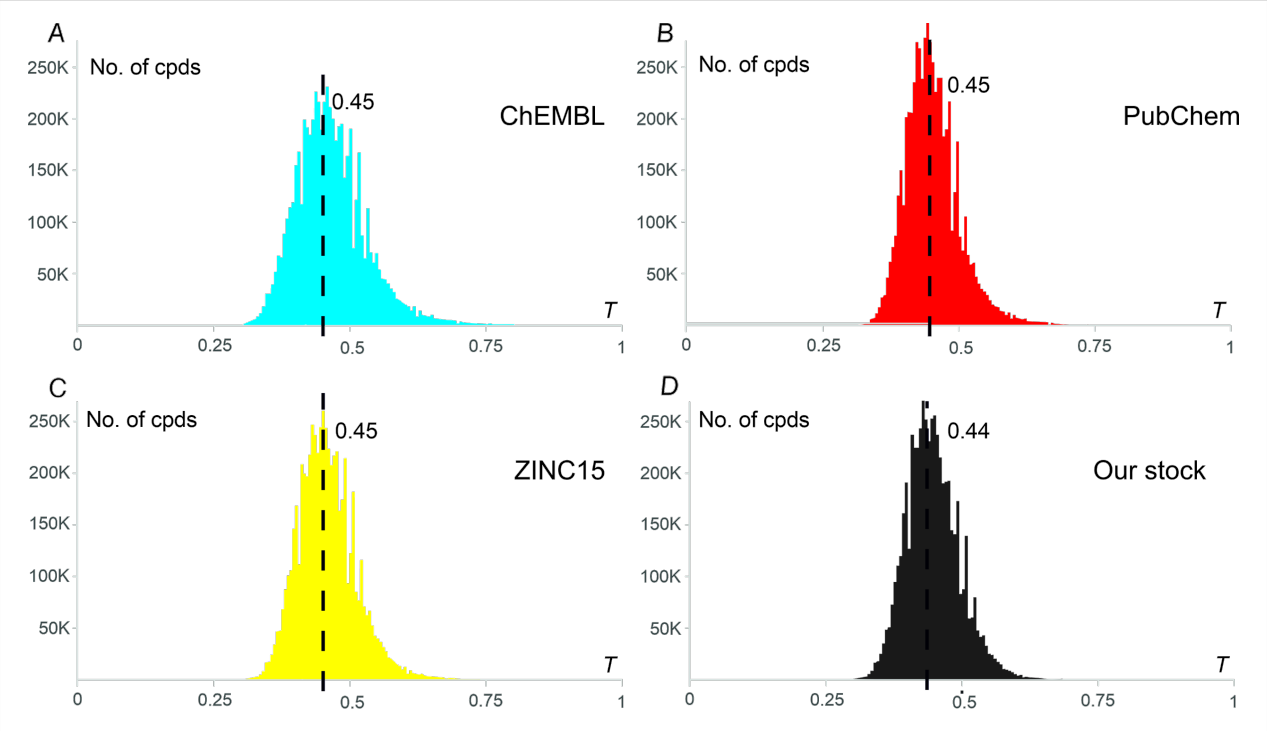

Figure 6: Distribution of maximal values among pairwise-calculated Tanimoto similarities *T* (MFP2 fingerprints [46]) of extended Bemis–Murcko scaffolds for the generated chemical space members (5.60 Mln. scaffolds) to the extended Bemis–Murcko scaffolds of A) ChEMBL compounds (v. 33); B) PubChem compounds (due to the large size of the dataset, a preliminary clusterization was performed to achieve ca. 5-fold size reduction); C) ZINC15 drug-like compounds, and D) enamine's stock screening collection. Average *T* values are shown by dotted lines.

ated GBB chemical space is unique as compared to the available compound collections.

This fact is even more apparent from the t-distributed stochastic neighbour embedding (t-SNE) analysis, a technique widely used for the dimension reduction in data visualization [47]. Due to the relatively high computational costs of this method, we randomly selected 50,000 compounds to represent each database. The dimension reduction algorithm uses molecular features as the starting inputs to generate a few coordinates (in this case, t-SNE1 and t-SNE2) reflecting the probability of the molecules to be similar. In this way, data visualization becomes possible since similar molecules will likely have close values of t-SNE1 and t-SNE2. As apparent from Figure 7, there is a small overlap between the GBB chemical space (yellow datapoints) with all four databases of comparison (blue data points), which is another confirmation of the GBB space uniqueness.

Notably, 432 members of the generated GBB chemical space were already present in the ChEMBL database [42]. Among them, potent nonacidic farnesoid X receptor (FXR) modulators [48], 5-lipooxygenase (5-LO) inhibitors [49], soluble epoxide hydrolase (sEH) inhibitors [50], HIV-1 non-nucleoside reverse transcriptase inhibitors [51], or potential agents against visceral leishmaniasis [52] were found (Figure 8).

Conclusion

The Groebke–Blackburn–Bienaymé (GBB) reaction, a three-component condensation of amino heterocycles, aldehydes, and isonitriles, is a powerful tool for the combinatorial synthesis of compound libraries. We have shown that the $Sc(OTf)_3$-catalyzed version of the reaction has a wide substrate applicability and established some limitations under the parallel synthesis conditions. In particular, while the method was applicable to a wide range of aminopyridines, pyrazines, and pyridazines, it worked poorly for aminoazoles, aminopyrimidines, substrates with strong electron-withdrawing groups, and substrates bearing additional dialkylamino or alkoxy substituents. The electronic nature was a major limiting factor for other two components of the reaction, the aldehyde and isonitrile, while the steric factor was found to be not significant. The protocol was used to prepare a 790-member compound library with 85% synthesis success rate. Furthermore, a readily available (REAL) chemical space comprising 271 Mln. members was generated. It was rich in both drug-like and "beyond rule-of-five" compounds and had considerable uniqueness as compared to the available collections (as was shown by Tanimoto similarity and t-distributed stochastic neighbor embedding (t-SNE) comparative analyses). Still, 432 members of the generated chemical space were found in the ChEMBL database, and some of them had high potency against various biological targets.

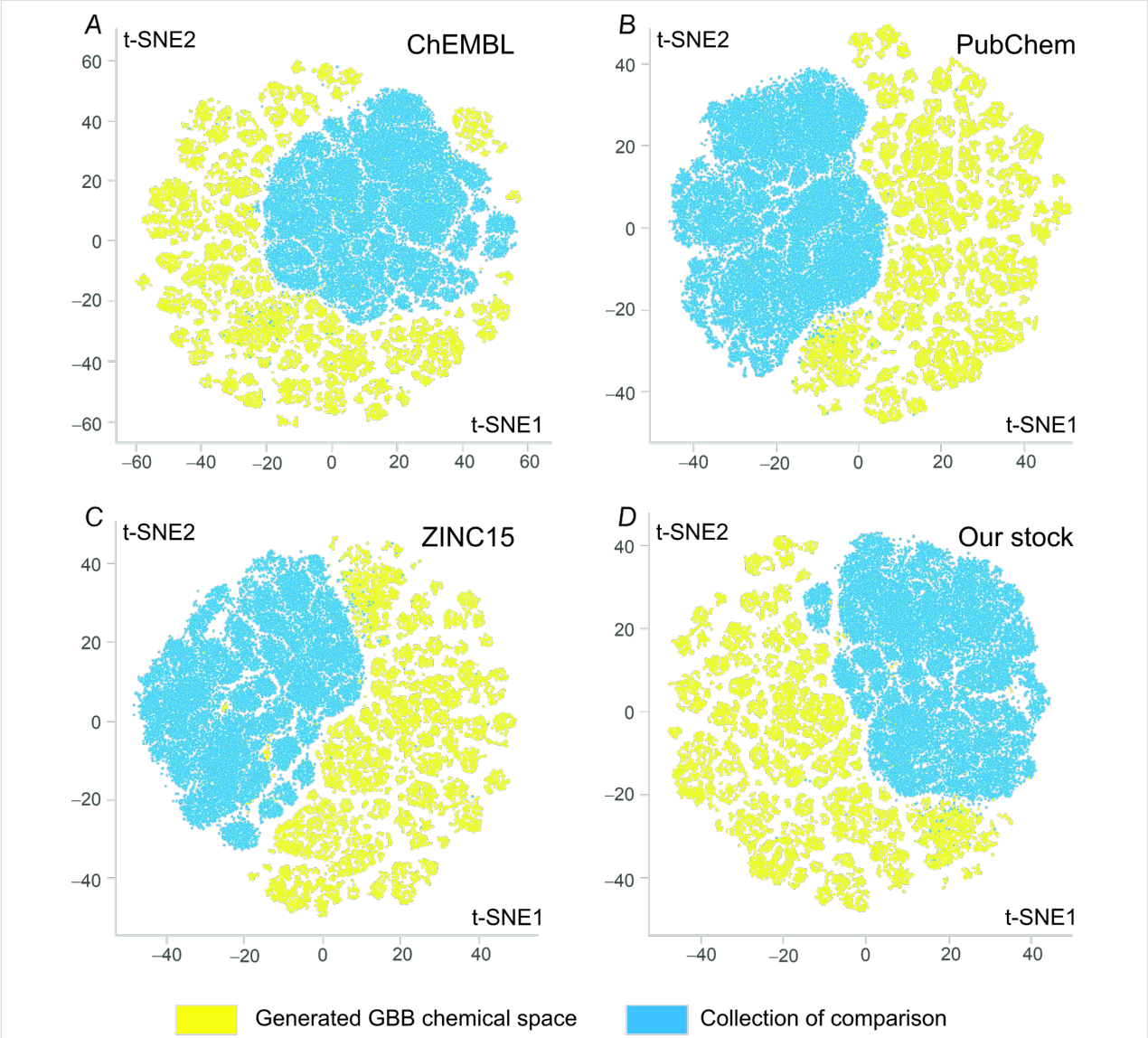

Figure 7: t-Distributed stochastic neighbor embedding (t-SNE) comparative analysis of 50,000 randomly selected molecules picked from the generated chemical space and A) ChEMBL compounds; B) PubChem compounds; C) ZINC15 compounds; and D) enamine's stock screening collection.

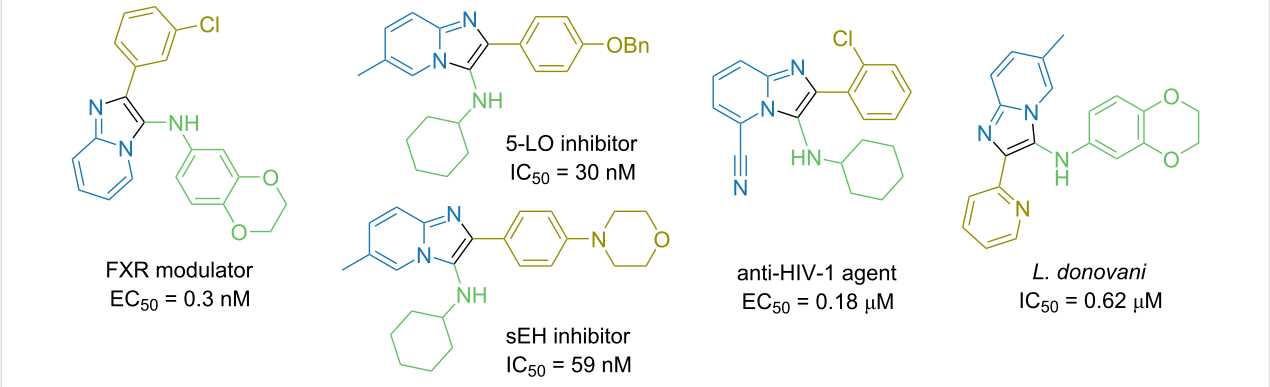

Figure 8: Some biologically active representatives of the generated GBB chemical space found in the ChEMBL database.

Supporting Information

The Supporting Information for this article contains structures of reactants **1**–**3**, experimental details on the parallel synthesis of compound library **4**, experimental section including compound characterization data, and copies of NMR spectra.

Supporting Information File 1

Structures of reactants **1**, **2**, and **3**.
[https://www.beilstein-journals.org/bjoc/content/supplementary/1860-5397-20-143-S1.zip]

Supporting Information File 2

Parallel synthesis of compound library **4**.
[https://www.beilstein-journals.org/bjoc/content/supplementary/1860-5397-20-143-S2.pdf]

Supporting Information File 3

Experimental part.
[https://www.beilstein-journals.org/bjoc/content/supplementary/1860-5397-20-143-S3.pdf]

Supporting Information File 4

Copies of NMR spectra.
[https://www.beilstein-journals.org/bjoc/content/supplementary/1860-5397-20-143-S4.pdf]

Acknowledgements

Dedicated to the memory of Kyrylo Burmagin and Yaroslav Mayboroda, students of Chemical Faculty at Taras Shevchenko National University of Kyiv, trainees at Enamine, and volunteer soldiers who died defending their country. The authors thank Mr. Oleksandr Liashuk and Dr. Anastasiia Hurieva for their help with manuscript preparation, Prof. Dr. Anrdiy A. Tolmachev for his encouragement and support, and all the brave people of Ukraine for making this publication possible.

Funding

The work was funded by Enamine Ltd. and NIH (Grant No. GM133836 to Prof. John Irwin and Y.S.M.). O.O.G. was also funded by Ministry of Education and Science of Ukraine (Grant No. 0122U001962 (22BF037-02)).

ORCID® iDs

Dmytro S. Radchenko - https://orcid.org/0000-0001-5444-7754
Yurii S. Moroz - https://orcid.org/0000-0001-6073-002X
Oleksandr O. Grygorenko - https://orcid.org/0000-0002-6036-5859

Data Availability Statement

Most data that supports the findings of this study is available in the published article and/or the supporting information to this article. Additional data cannot be shared due to restrictions that apply to availability.

References

1. Dömling, A.; Wang, W.; Wang, K. *Chem. Rev.* **2012,** *112,* 3083–3135. doi:10.1021/cr100233r
2. John, S. E.; Gulati, S.; Shankaraiah, N. *Org. Chem. Front.* **2021,** *8,* 4237–4287. doi:10.1039/d0qo01480j
3. Graebin, C. S.; Ribeiro, F. V.; Rogério, K. R.; Kümmerle, A. E. *Curr. Org. Synth.* **2019,** *16,* 855–899. doi:10.2174/1570179416666190718153703
4. Graziano, G.; Stefanachi, A.; Contino, M.; Prieto-Díaz, R.; Ligresti, A.; Kumar, P.; Scilimati, A.; Sotelo, E.; Leonetti, F. *Int. J. Mol. Sci.* **2023,** *24,* 6581. doi:10.3390/ijms24076581
5. Younus, H. A.; Al-Rashida, M.; Hameed, A.; Uroos, M.; Salar, U.; Rana, S.; Khan, K. M. *Expert Opin. Ther. Pat.* **2021,** *31,* 267–289. doi:10.1080/13543776.2021.1858797
6. Malinakova, H. C. *Rep. Org. Chem.* **2015,** *5,* 75–90. doi:10.2147/roc.s65115
7. Dömling, A. *Chem. Rev.* **2006,** *106,* 17–89. doi:10.1021/cr0505728
8. Rudick, J. G.; Shaabani, S.; Dömling, A. *Front. Chem. (Lausanne, Switz.)* **2020,** *7,* 918. doi:10.3389/fchem.2019.00918
9. Akritopoulou-Zanze, I. *Curr. Opin. Chem. Biol.* **2008,** *12,* 324–331. doi:10.1016/j.cbpa.2008.02.004
10. Russo, C.; Brunelli, F.; Cesare Tron, G.; Giustiniano, M. *Chem. – Eur. J.* **2023,** *29,* e202203150. doi:10.1002/chem.202203150
11. Divyavani, C.; Padmaja, P.; Reddy, P. N. *Curr. Org. Synth.* **2024,** *21,* 140–165. doi:10.2174/1570179420666230330170845
12. Mohlala, R. L.; Coyanis, E. M. *Phys. Sci. Rev.* **2024**. doi:10.1515/psr-2022-0206
13. Shaabani, A.; Hooshmand, S. E. *RSC Adv.* **2016,** *6,* 58142–58159. doi:10.1039/c6ra11701e
14. Hulme, C.; Lee, Y.-S. *Mol. Diversity* **2008,** *12,* 1–15. doi:10.1007/s11030-008-9072-1
15. Hulme, C.; Bienaymé, H.; Nixey, T.; Chenera, B.; Jones, W.; Tempest, P.; Smith, A. L. *Methods Enzymol.* **2003,** *369,* 469–496. doi:10.1016/s0076-6879(03)69024-5
16. Fragkiadakis, M.; Anastasiou, P.-K.; Volyrakis, I.; Pantousas, A.; Stoumpos, C. C.; Neochoritis, C. G. *Chem. Commun.* **2023,** *59,* 14411–14414. doi:10.1039/d3cc04597h
17. Fragkiadakis, M.; Anastasiou, P.-K.; Zingiridis, M.; Triantafyllou-Rundell, M. E.; Reyes Romero, A.; Stoumpos, C. C.; Neochoritis, C. G. *J. Org. Chem.* **2023,** *88,* 12709–12715. doi:10.1021/acs.joc.3c01379
18. Groebke, K.; Weber, L.; Mehlin, F. *Synlett* **1998,** 661–663. doi:10.1055/s-1998-1721
19. Bienaymé, H.; Bouzid, K. *Angew. Chem., Int. Ed.* **1998,** *37,* 2234–2237. doi:10.1002/(sici)1521-3773(19980904)37:16<2234::aid-anie2234>3.3.co;2-i
20. Blackburn, C.; Guan, B.; Fleming, P.; Shiosaki, K.; Tsai, S. *Tetrahedron Lett.* **1998,** *39,* 3635–3638. doi:10.1016/s0040-4039(98)00653-4
21. Boltjes, A.; Dömling, A. *Eur. J. Org. Chem.* **2019,** 7007–7049. doi:10.1002/ejoc.201901124

22. Wishart, D. S.; Feunang, Y. D.; Guo, A. C.; Lo, E. J.; Marcu, A.; Grant, J. R.; Sajed, T.; Johnson, D.; Li, C.; Sayeeda, Z.; Assempour, N.; Iynkkaran, I.; Liu, Y.; Maciejewski, A.; Gale, N.; Wilson, A.; Chin, L.; Cummings, R.; Le, D.; Pon, A.; Knox, C.; Wilson, M. *Nucleic Acids Res.* **2018,** *46,* D1074–D1082. doi:10.1093/nar/gkx1037
23. Wishart, D. S.; Knox, C.; Guo, A. C.; Shrivastava, S.; Hassanali, M.; Stothard, P.; Chang, Z.; Woolsey, J. *Nucleic Acids Res.* **2006,** *34,* D668–D672. doi:10.1093/nar/gkj067
24. An, Y.; Lee, J.; Seo, H.; Bae, S.; Kang, J.; Lee, J.; Kim, J.; Nam, M. H.; Song, M.; Hwang, G. T. *Org. Lett.* **2023,** *25,* 4445–4450. doi:10.1021/acs.orglett.3c01366
25. Baenziger, M.; Durantie, E.; Mathes, C. *Synthesis* **2017,** *49,* 2266–2274. doi:10.1055/s-0036-1588130
26. Shukla, N. M.; Salunke, D. B.; Yoo, E.; Mutz, C. A.; Balakrishna, R.; David, S. A. *Bioorg. Med. Chem.* **2012,** *20,* 5850–5863. doi:10.1016/j.bmc.2012.07.052
27. Kolomiiets, O. V.; Tsygankov, A. V.; Kornet, M. N.; Brazhko, A. A.; Musatov, V. I.; Chebanov, V. A. *Beilstein J. Org. Chem.* **2023,** *19,* 727–735. doi:10.3762/bjoc.19.53
28. Devi, N.; Rawal, R. K.; Singh, V. *Tetrahedron* **2015,** *71,* 183–232. doi:10.1016/j.tet.2014.10.032
29. Gao, K.; Shaabani, S.; Xu, R.; Zarganes-Tzitzikas, T.; Gao, L.; Ahmadianmoghaddam, M.; Groves, M. R.; Dömling, A. *RSC Med. Chem.* **2021,** *12,* 809–818. doi:10.1039/d1md00087j
30. Grygorenko, O. O.; Radchenko, D. S.; Dziuba, I.; Chuprina, A.; Gubina, K. E.; Moroz, Y. S. *iScience* **2020,** *23,* 101681. doi:10.1016/j.isci.2020.101681
31. Radchenko, D. S.; Naumchyk, V. S.; Dziuba, I.; Kyrylchuk, A. A.; Gubina, K. E.; Moroz, Y. S.; Grygorenko, O. O. *Mol. Diversity* **2022,** *26,* 993–1004. doi:10.1007/s11030-021-10218-2
32. Savych, O.; Kuchkovska, Y. O.; Bogolyubsky, A. V.; Konovets, A. I.; Gubina, K. E.; Pipko, S. E.; Zhemera, A. V.; Grishchenko, A. V.; Khomenko, D. N.; Brovarets, V. S.; Doroschuk, R.; Moroz, Y. S.; Grygorenko, O. O. *ACS Comb. Sci.* **2019,** *21,* 635–642. doi:10.1021/acscombsci.9b00120
33. Stein, R. M.; Kang, H. J.; McCorvy, J. D.; Glatfelter, G. C.; Jones, A. J.; Che, T.; Slocum, S.; Huang, X.-P.; Savych, O.; Moroz, Y. S.; Stauch, B.; Johansson, L. C.; Cherezov, V.; Kenakin, T.; Irwin, J. J.; Shoichet, B. K.; Roth, B. L.; Dubocovich, M. L. *Nature* **2020,** *579,* 609–614. doi:10.1038/s41586-020-2027-0
34. Sadybekov, A. A.; Sadybekov, A. V.; Liu, Y.; Iliopoulos-Tsoutsouvas, C.; Huang, X.-P.; Pickett, J.; Houser, B.; Patel, N.; Tran, N. K.; Tong, F.; Zvonok, N.; Jain, M. K.; Savych, O.; Radchenko, D. S.; Nikas, S. P.; Petasis, N. A.; Moroz, Y. S.; Roth, B. L.; Makriyannis, A.; Katritch, V. *Nature* **2022,** *601,* 452–459. doi:10.1038/s41586-021-04220-9
35. Gorgulla, C.; Boeszoermenyi, A.; Wang, Z.-F.; Fischer, P. D.; Coote, P. W.; Padmanabha Das, K. M.; Malets, Y. S.; Radchenko, D. S.; Moroz, Y. S.; Scott, D. A.; Fackeldey, K.; Hoffmann, M.; Iavniuk, I.; Wagner, G.; Arthanari, H. *Nature* **2020,** *580,* 663–668. doi:10.1038/s41586-020-2117-z
36. Tropsha, A.; Isayev, O.; Varnek, A.; Schneider, G.; Cherkasov, A. *Nat. Rev. Drug Discovery* **2024,** *23,* 141–155. doi:10.1038/s41573-023-00832-0
37. Gahbauer, S.; DeLeon, C.; Braz, J. M.; Craik, V.; Kang, H. J.; Wan, X.; Huang, X.-P.; Billesbølle, C. B.; Liu, Y.; Che, T.; Deshpande, I.; Jewell, M.; Fink, E. A.; Kondratov, I. S.; Moroz, Y. S.; Irwin, J. J.; Basbaum, A. I.; Roth, B. L.; Shoichet, B. K. *Nat. Commun.* **2023,** *14,* 8067. doi:10.1038/s41467-023-43506-6
38. Lipinski, C. A.; Lombardo, F.; Dominy, B. W.; Feeney, P. J. *Adv. Drug Delivery Rev.* **1997,** *23,* 3–25. doi:10.1016/s0169-409x(96)00423-1
39. Grygorenko, O. O.; Volochnyuk, D. M.; Ryabukhin, S. V.; Judd, D. B. *Chem. – Eur. J.* **2020,** *26,* 1196–1237. doi:10.1002/chem.201903232
40. Nadin, A.; Hattotuwagama, C.; Churcher, I. *Angew. Chem., Int. Ed.* **2012,** *51,* 1114–1122. doi:10.1002/anie.201105840
41. Veber, D. F.; Johnson, S. R.; Cheng, H.-Y.; Smith, B. R.; Ward, K. W.; Kopple, K. D. *J. Med. Chem.* **2002,** *45,* 2615–2623. doi:10.1021/jm020017n
42. Mendez, D.; Gaulton, A.; Bento, A. P.; Chambers, J.; De Veij, M.; Félix, E.; Magariños, M. P.; Mosquera, J. F.; Mutowo, P.; Nowotka, M.; Gordillo-Marañón, M.; Hunter, F.; Junco, L.; Mugumbate, G.; Rodriguez-Lopez, M.; Atkinson, F.; Bosc, N.; Radoux, C. J.; Segura-Cabrera, A.; Hersey, A.; Leach, A. R. *Nucleic Acids Res.* **2019,** *47,* D930–D940. doi:10.1093/nar/gky1075
43. Kim, S.; Chen, J.; Cheng, T.; Gindulyte, A.; He, J.; He, S.; Li, Q.; Shoemaker, B. A.; Thiessen, P. A.; Yu, B.; Zaslavsky, L.; Zhang, J.; Bolton, E. E. *Nucleic Acids Res.* **2021,** *49,* D1388–D1395. doi:10.1093/nar/gkaa971
44. Sterling, T.; Irwin, J. J. *J. Chem. Inf. Model.* **2015,** *55,* 2324–2337. doi:10.1021/acs.jcim.5b00559
45. Grygorenko, O. O. *Eur. J. Org. Chem.* **2021,** 6474–6477. doi:10.1002/ejoc.202101210
46. van der Maaten, L.; Hinton, G. *J. Mach. Learn. Res.* **2008,** *9,* 2579–2605.
47. Rogers, D.; Hahn, M. *J. Chem. Inf. Model.* **2010,** *50,* 742–754. doi:10.1021/ci100050t
48. Flesch, D.; Cheung, S.-Y.; Schmidt, J.; Gabler, M.; Heitel, P.; Kramer, J.; Kaiser, A.; Hartmann, M.; Lindner, M.; Lüddens-Dämgen, K.; Heering, J.; Lamers, C.; Lüddens, H.; Wurglics, M.; Proschak, E.; Schubert-Zsilavecz, M.; Merk, D. *J. Med. Chem.* **2017,** *60,* 7199–7205. doi:10.1021/acs.jmedchem.7b00903
49. Hieke, M.; Rödl, C. B.; Wisniewska, J. M.; la Buscató, E.; Stark, H.; Schubert-Zsilavecz, M.; Steinhilber, D.; Hofmann, B.; Proschak, E. *Bioorg. Med. Chem. Lett.* **2012,** *22,* 1969–1975. doi:10.1016/j.bmcl.2012.01.038
50. Meirer, K.; Rödl, C. B.; Wisniewska, J. M.; George, S.; Häfner, A.-K.; Buscató, E.; Klingler, F.-M.; Hahn, S.; Berressem, D.; Wittmann, S. K.; Steinhilber, D.; Hofmann, B.; Proschak, E. *J. Med. Chem.* **2013,** *56,* 1777–1781. doi:10.1021/jm301617j
51. Bode, M. L.; Gravestock, D.; Moleele, S. S.; van der Westhuyzen, C. W.; Pelly, S. C.; Steenkamp, P. A.; Hoppe, H. C.; Khan, T.; Nkabinde, L. A. *Bioorg. Med. Chem.* **2011,** *19,* 4227–4237. doi:10.1016/j.bmc.2011.05.062
52. Akao, Y.; Canan, S.; Cao, Y.; Condroski, K.; Engkvist, O.; Itono, S.; Kaki, R.; Kimura, C.; Kogej, T.; Nagaoka, K.; Naito, A.; Nakai, H.; Pairaudeau, G.; Radu, C.; Roberts, I.; Shimada, M.; Shum, D.; Watanabe, N.-a.; Xie, H.; Yonezawa, S.; Yoshida, O.; Yoshida, R.; Mowbray, C.; Perry, B. *RSC Med. Chem.* **2021,** *12,* 384–393. doi:10.1039/d0md00353k

License and Terms

This is an open access article licensed under the terms of the Beilstein-Institut Open Access License Agreement (https://www.beilstein-journals.org/bjoc/terms), which is identical to the Creative Commons Attribution 4.0 International License (https://creativecommons.org/licenses/by/4.0). The reuse of material under this license requires that the author(s), source and license are credited. Third-party material in this article could be subject to other licenses (typically indicated in the credit line), and in this case, users are required to obtain permission from the license holder to reuse the material.

The definitive version of this article is the electronic one which can be found at:
https://doi.org/10.3762/bjoc.20.143

BEILSTEIN JOURNAL OF ORGANIC CHEMISTRY

Harnessing unprotected deactivated amines and arylglyoxals in the Ugi reaction for the synthesis of fused complex nitrogen heterocycles

Javier Gómez-Ayuso‡, Pablo Pertejo‡, Tomás Hermosilla, Israel Carreira-Barral, Roberto Quesada and María García-Valverde*

Full Research Paper

Open Access

Address:
Departamento de Química, Universidad de Burgos, Burgos 09001, Spain

Email:
María García-Valverde* - magaval@ubu.es

* Corresponding author ‡ Equal contributors

Keywords:
arylglyoxals; deactivated amines; nitrogen heterocycles; Ugi reaction

Beilstein J. Org. Chem. **2024,** *20,* 1758–1766.
https://doi.org/10.3762/bjoc.20.154

Received: 14 May 2024
Accepted: 10 July 2024
Published: 25 July 2024

This article is part of the thematic issue "Multicomponent reactions IV".

Associate Editor: T. J. J. Müller

© 2024 Gómez-Ayuso et al.; licensee Beilstein-Institut.
License and terms: see end of document.

Abstract

Piperazines and diazepines are examples of nitrogen heterocycles present in many marketed drugs highlighting their importance in the discovery of novel bioactive compounds. However, their synthesis often faces challenges, including complex functionalization and lengthy reaction sequences. Multicomponent reactions, notably the Ugi reaction, have emerged as powerful tools to address these hurdles. Here, we have demonstrated the possibility of using the combination of arylglyoxals and carboxylic acids tethered to nonprotected deactivated amines as a powerful strategy for the synthesis of complex fused heterocycles. The limited nucleophilic character of the amino group of the anthranilic acid, indole-2-carboxylic acid, pyrrole-2-carboxylic acid or *N*-phenylglycine has allowed the use of these compounds in the Ugi reaction without triggering competitive reactions. The additional functional group present in the resulting Ugi adduct can be leveraged in different post-condensation strategies to easily generate multiple fused nitrogen heterocycles including benzodiazepinone and piperazinone cores.

Introduction

Nitrogen heterocycles such as piperazines or diazepines represent important systems in the search of new bioactive compounds, as evidenced by the fact that they are present in many marketed drugs [1,2]. These substructures are found fused with other heterocycles in many cases, as illustrated by the antineoplastic dibromophakellstatin [3-6], the CDK inhibitor trilaciclib [7] or the kinase inhibitor tinengotinib [8] (Figure 1). Despite the interest of these structures, several drawbacks are typically

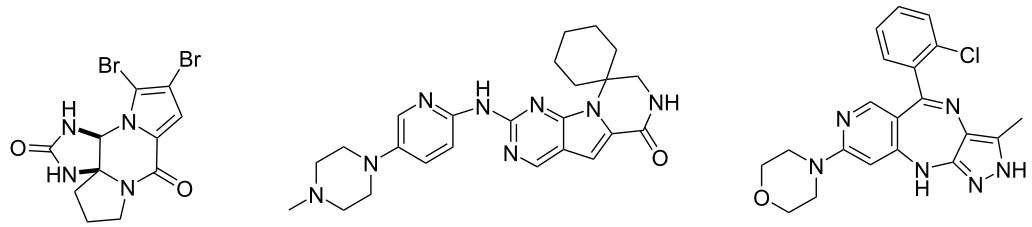

(–)-dibromophakellstatin trilaciclib tinengotinib

Figure 1: Fused heterocycles containing the piperazine and diazepine core.

found during their syntheses, for instance the difficulty in obtaining certain functionalizations or the need of long, elaborated reaction sequences.

In recent years, multicomponent reactions have become a useful tool for the synthesis of complex structures which overcome many of these problems, with the Ugi reaction leading these strategies. The scope of the Ugi reaction further increases when coupled with post-condensation reactions, which usually require the use of starting reagents that bear two functional groups. In order to avoid competitive reactions, these groups need to be compatible with the components of the Ugi reaction or the intermediates generated during the reaction. Thus, an amine can rarely be directly incorporated as an additional functional group, because of different competitive reactions triggered by it, such as the interrupted Ugi reaction resulting from the competitive addition over the nitrilium intermediate [9,10] or the split-Ugi reaction arising from a competitive *O*,*N*-acyl transference on the imidate intermediate, through a remote Mumm rearrangement [11].

Different strategies have been developed to avoid these competitive reactions, the most common ones being the use of protecting groups (Ugi/deprotection/cyclization strategy) [12-14] or of surrogates of amines [15]. However, direct incorporation of the second amine without derivatization is the most desirable strategy from the point-of view of sustainability. This has been achieved following two different approaches: the blockage of the amine group throughout the reaction by the incorporation of an additional group on the carbonyl component [16-18] or the use of amine groups with a limited reactivity, modulated by their substitution [19].

Results and Discussion

Synthesis of 3*H*-benzo[*e*][1,4]diazepin-5-ones

As part of our continued interest in developing new and efficient strategies for synthesizing complex fused nitrogen heterocycles, we decided to evaluate the use of amine groups with a reduced reactivity in the synthesis of 3*H*-benzo[*e*][1,4]diazepin-5-ones, heterocycles previously synthesized by our research group through Ugi/Staudinger/aza-Wittig and Ugi/reduction/cyclization sequences, using 2-azidobenzoic [20] and 2-nitrobenzoic [21] acids, respectively. The first methodology has several drawbacks, as the need to synthesise the 2-azidobenzoic acid from anthranilic acid and sodium azide, the requirement of anhydrous conditions to perform the Staudinger/aza-Wittig sequence or the generation of large quantities of triphenylphosphine oxide which needs to be removed by chromatography column, while the more eco-friendly second strategy needs an additional stage for the reduction of the nitro group on the Ugi adduct.

In order to find a more efficient synthesis, we thought that the second nitrogen in the diazepine nucleus could be incorporated without the need of surrogates or protecting groups, as the reduced nucleophilic character of the amino group of the anthranilic acid would prevent its participation in the Ugi reaction. In this way, the Ugi reaction was performed using arylglyoxals **1**, anthranilic acid derivatives **2**, amines **3** and isocyanides **4** following the most common procedure. Thus, initially the amine **3** (1 equiv) was added to a solution of the arylglyoxal **1** (1 equiv) in methanol and the mixture was stirred for 15 min. Then, the acid **2** (1 equiv) and the isocyanide **4** (1 equiv) were added and the reaction was stirred at room temperature for 24 h. Fortunately, after the workup the only product observed was the corresponding benzodiazepinone **5**, resulting from a spontaneous cyclization of the Ugi adduct, in a six-center four-component Ugi reaction (U-6C-4CR), which prevents the need of additional steps (Scheme 1, Table 1).

Due to the interest of these results and considering the diastereoselectivity observed when enantiopure (*S*)-α-methylbenzylamine was used as chiral component in the two-step syntheses from amine surrogates [22], we assayed our new strategy to achieve a one-pot diastereoselective synthesis of benzodiazepinones **6** (Scheme 2, Table 2). Interestingly, the reaction

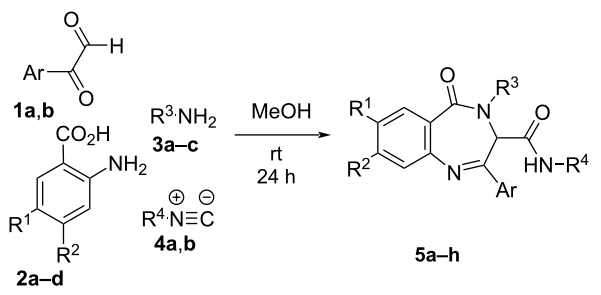

Scheme 1: Synthesis of benzodiazepinones **5** from anthranilic acid derivatives.

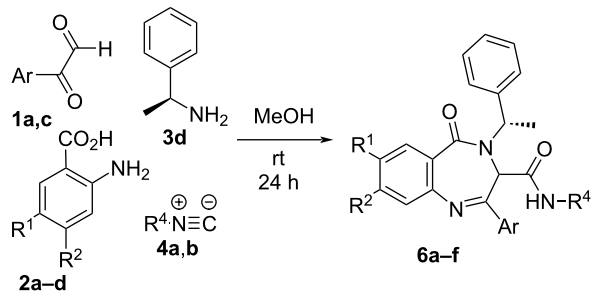

Scheme 2: Diastereoselective one-pot synthesis of benzodiazepinones **6**.

took place with a α,3-*like* relative configuration on the major diastereomer, similar to that obtained for the Ugi/Staudinger/aza-Wittig sequence and complementary to that observed for the Ugi/reduction/cyclization sequence (see Supporting Information File 1, Figure S2).

With the aim of building more complex systems, we explored post-condensation reactions on the 2-nitrobenzylamine and 3-bromopropylamine derivatives. Thus, we carried out the reduction of the nitro group on derivatives **5b** and **5h** employing tin(II) chloride and chlorhydric acid in boiling *n*-butanol (120 °C), conditions previously assayed in our group. Under these conditions, the bis-1,4-benzodiazepines **7** resulting from the reaction of the amino group with the imine on the benzodiazepine were obtained as a single diastereomer. On the basis of the preferred conformation for the 1,4-benzodiazepin-5-ones **5** and **6** [20,22], where the amide substituent in C3 is pseudoaxially oriented in an all-*trans* conformation, only the *unlike* attack would be allowed (Scheme 3).

On the other hand, when 3-bromopropanamine was used, the formation of the pyrrolobenzodiazepinone system **8** was ob-

Table 1: Results obtained in the synthesis of benzodiazepinones **5** from anthranilic acid derivatives.

Entry	**1** (Ar)	**2** (R^1, R^2)	**3** (R^3)	**4** (R^4)	**5** (%)[a]
1	**1a** (C_6H_5)	**2a** (H, H)	**3a** ($C_6H_5CH_2$)	**4a** (cC_6H_{11})	**5a** (66)[b]
2	**1a** (C_6H_5)	**2a** (H, H)	**3b** (2-$NO_2C_6H_4CH_2$)	**4a** (cC_6H_{11})	**5b** (80)
3	**1b** (4-$CH_3C_6H_4$)	**2a** (H, H)	**3c** ($CH_2CH_2CH_2Br$)	**4a** (cC_6H_{11})	**5c** (58)[c]
4	**1a** (C_6H_5)	**2a** (H, H)	**3a** ($C_6H_5CH_2$)	**4b** ($C_6H_5CH_2$)	**5d** (63)
5	**1a** (C_6H_5)	**2b** (H, NO_2)	**3a** ($C_6H_5CH_2$)	**4a** (cC_6H_{11})	**5e** (68)
6	**1a** (C_6H_5)	**2c** (NO_2, H)	**3a** ($C_6H_5CH_2$)	**4a** (cC_6H_{11})	**5f** (63)
7	**1a** (C_6H_5)	**2d** (I, H)	**3a** ($C_6H_5CH_2$)	**4a** (cC_6H_{11})	**5g** (67)
8	**1a** (C_6H_5)	**2d** (I, H)	**3b** (2-$NO_2C_6H_4CH_2$)	**4a** (cC_6H_{11})	**5h** (61)

[a]Yield after purification; [b]global yield for the synthesis of **5a** from Ugi/Staudinger/aza-Wittig sequence 42% [20], and from Ugi/reduction/cyclization sequence 55% [21]; [c]the formation of pyrrolobenzodiazepine **8** (35%) was observed (see Scheme 4).

Table 2: Results obtained in the diastereoselective one-pot synthesis of benzodiazepinones **6**.

Entry	**1** (Ar)	**2** (R^1, R^2)	**4** (R^4)	**6** (%)[a]	dr[b] (*l*:*u*)[c]
1	**1a** (C_6H_5)	**2a** (H, H)	**4a** (cC_6H_{11})	**6a** (66)	79:21
2	**1a** (C_6H_5)	**2a** (H, H)	**4b** ($C_6H_5CH_2$)	**6b** (80)	76:24
3	**1c** (4-FC_6H_4)	**2a** (H, H)	**4a** (cC_6H_{11})	**6c** (58)	74:26
4	**1a** (C_6H_5)	**2b** (H, NO_2)	**4a** (cC_6H_{11})	**6d** (63)	72:28
5	**1a** (C_6H_5)	**2c** (NO_2, H)	**4a** (cC_6H_{11})	**6e** (63)	68:32
6	**1a** (C_6H_5)	**2d** (I, H)	**4a** (cC_6H_{11})	**6f** (67)	76:24

[a]Yield referred to the major diastereomer after purification; [b]determined by ^{1}H NMR of the reaction mixture; [c]configuration *l*(α*S*,3*S*):*u*(α*S*,3*R*) [22].

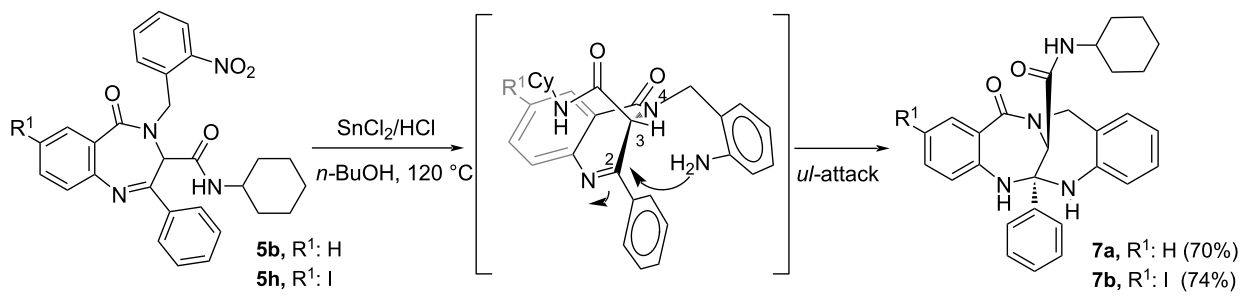

Scheme 3: Synthesis of bis-1,4-benzodiazepines **7**.

served albeit along with benzodiazepinone **5c** (Scheme 4). In order to improve the synthesis of this fused heterocycle, different strategies were tried, e.g., performing the Ugi reaction in different solvents (dichloromethane, ethyl acetate, methanol) to prevent the precipitation of benzodiazepine **5c**, conducting the Ugi reaction in boiling methanol or treating the benzodiazepine with different bases (caesium carbonate, sodium hydroxide). However, the complete cyclisation to the pyrrolobenzodiazepinone was not achieved, so the described three-step strategy starting from 2-nitrobenzoic acid (Ugi reaction/cyclization to pyrrolidine/reduction sequence) remains as a better choice [23].

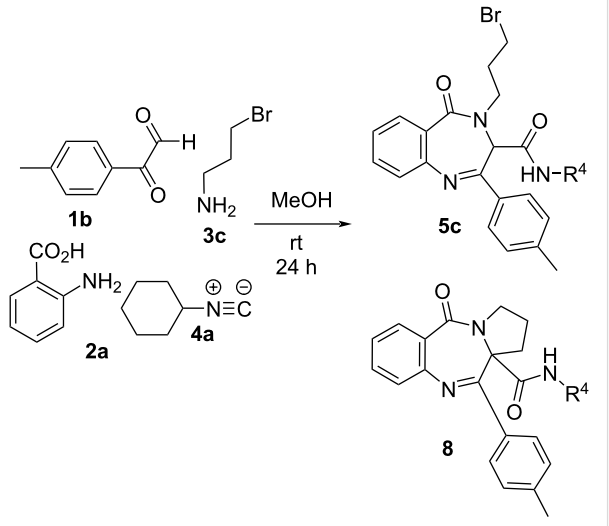

Scheme 4: Synthesis of benzodiazepinone **5c** and pyrrolobenzodiazepinone **8** from anthranilic acid and 3-bromopropanamine.

Synthesis of piperazinones

On the basis of these results, we planned to synthesise piperazinone derivatives following a similar strategy. Thus, we chose different deactivated 2-amino-substituted carboxylic acid derivatives such as the indole-2-carboxylic acid, recently used in a similar strategy with aromatic amines [24], pyrrole-2-carboxylic acid and *N*-phenylglycine, and carried out their reactions with arylglyoxals, alkylamines and isocyanides (Scheme 5). As we expected, the cyclization product **9** was observed, although the complete cyclization of the Ugi adduct, found as the enol tautomer, needed the addition of hydrochloric acid (1 equiv) in the case of the *tert*-butylamine derivatives. However, the nature of the cyclization product depended on the carboxylic acid employed in the Ugi reaction. Thus, the indole and pyrrole derivatives yielded the corresponding hemiaminal **9** as a single diastereomer (Scheme 5, Table 3), while *N*-phenylglycine afforded the enamine derivative **10** (Scheme 6, Table 4). Both structures were confirmed by single-crystal X-ray diffraction of compounds **9a** and **10a** (Figure 2). The diastereoselectivity ob-

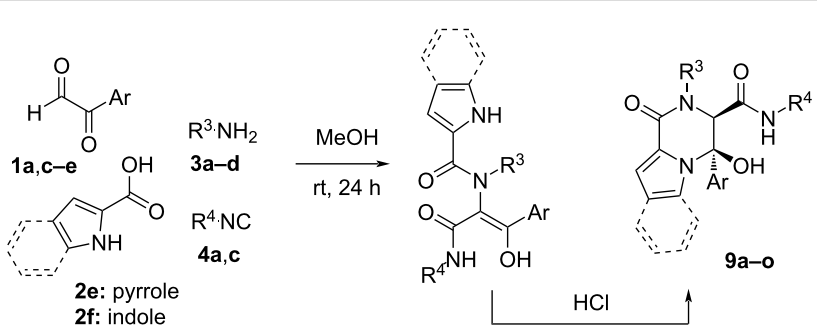

Scheme 5: Synthesis of pyrrolopiperazinones **9** from pyrrole and indole carboxylic acids.

Table 3: Results obtained in the synthesis of pyrrolopiperazinones **9** from pyrrole and indole carboxylic acids.

Entry	**1** (Ar)	**2**	**3** (R^3)	**4** (R^4)	**9** (%)[a,b]
1	**1a** (C_6H_5)	**2e**	**3a** ($C_6H_5CH_2$)	**4c** ($C(CH_3)_3$)	**9a** (61)[b]
2	**1a** (C_6H_5)	**2e**	**3d** ($C(CH_3)_3$)	**4a** (cC_6H_{11})	**9b** (52)[c]
3	**1a** (C_6H_5)	**2e**	**3c** ($CH_2CH_2CH_2Br$)	**4a** (cC_6H_{11})	**9c** (16)[d]
4	**1a** (C_6H_5)	**2e**	**3c** ($CH_2CH_2CH_2Br$)	**4a** ($C(CH_3)_3$)	**9d** (24)[d]
5	**1c** (4-FC_6H_4)	**2e**	**3c** ($CH_2CH_2CH_2Br$)	**4c** ($C(CH_3)_3$)	**9e** (22)[d]
6	**1a** (C_6H_5)	**2e**	**3b** (2-$NO_2C_6H_4CH_2$)	**4a** (cC_6H_{11})	**9f** (77)
7	**1d** (4-$CF_3C_6H_4$)	**2e**	**3b** (2-$NO_2C_6H_4CH_2$)	**4c** ($C(CH_3)_3$)	**9g** (69)
8	**1a** (C_6H_5)	**2f**	**3a** ($C_6H_5CH_2$)	**4a** (cC_6H_{11})	**9h** (49)
9	**1c** (4-FC_6H_4)	**2f**	**3a** ($C_6H_5CH_2$)	**4a** (cC_6H_{11})	**9i** (58)
10	**1a** (C_6H_5)	**2f**	**3d** ($C(CH_3)_3$)	**4c** ($C(CH_3)_3$)	**9j** (65)[c]
11	**1a** (C_6H_5)	**2f**	**3c** ($CH_2CH_2CH_2Br$)	**4c** ($C(CH_3)_3$)	**9k** (22)[d]
12	**1a** (C_6H_5)	**2f**	**3b** (2-$NO_2C_6H_4CH_2$)	**4a** (cC_6H_{11})	**9l** (72)
13	**1c** (4-FC_6H_4)	**2f**	**3b** (2-$NO_2C_6H_4CH_2$)	**4a** (cC_6H_{11})	**9m** (75)
14	**1e** (4-$CH_3OC_6H_4$)	**2f**	**3b** (2-$NO_2C_6H_4CH_2$)	**4c** ($C(CH_3)_3$)	**9n** (76)
15	**1d** (4-$CF_3C_6H_4$)	**2f**	**3b** (2-$NO_2C_6H_4CH_2$)	**4c** ($C(CH_3)_3$)	**9o** (71)

[a]Yield after purification; [b]the only diastereomer observed was the (3*R**,4*R**); [c]yield obtained after treatment of the reaction mixture with HCl (1 equiv) for 24 h; [d]the corresponding dipyrrolopiperazinone **12** resulting from a second cyclization was isolated from the reaction mixture (**12a** (32%), **12b** (7%), **12c** (13%), **12d** (15%)) (see Scheme 8).

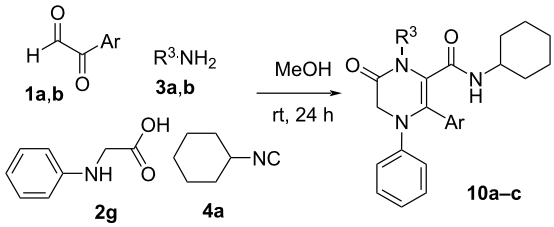

Scheme 6: Synthesis of pyrrolopiperazinones **10** from *N*-phenylglicine.

Table 4: Results obtained in the synthesis of pyrrolopiperazinones **10** from *N*-phenylglycine.

Entry	**1** (Ar)	**3** (R^3)	**10** (%)[a]
1	**1a** (C_6H_5)	**3a** ($C_6H_5CH_2$)	**10a** (54)
2	**1b** (4-FC_6H_4)	**3a** ($C_6H_5CH_2$)	**10b** (49)
3	**1a** (C_6H_5)	**3b** (2-$NO_2C_6H_4CH_2$)	**10c** (–)[b,c]

[a]Yield after purification; [b]unstable; [c]used in the following step without purification.

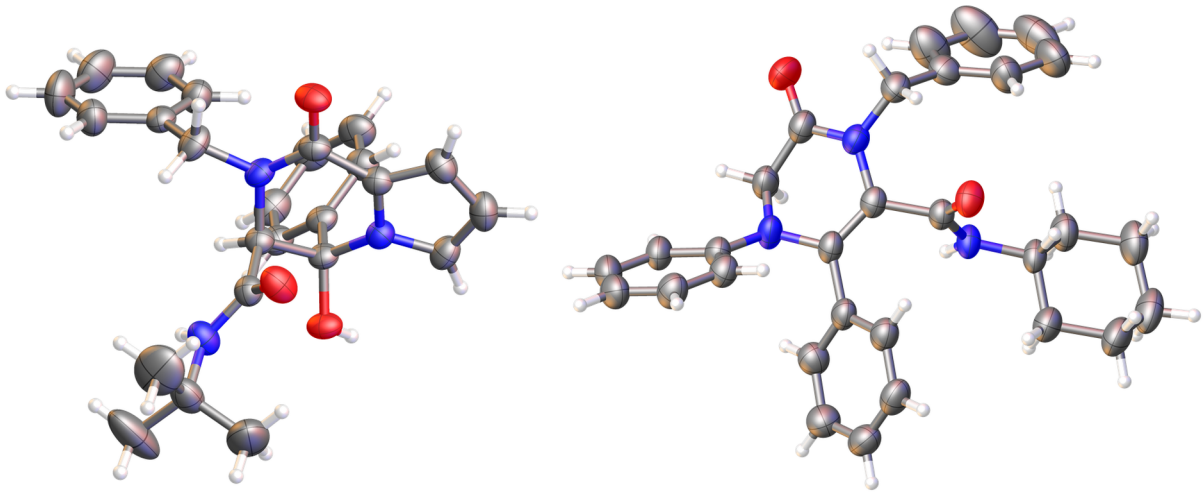

Figure 2: X-ray diffraction structures of pyrrolopiperazinones **9a** (left) and **10a** (right). The thermal ellipsoid plot (Olex2) is at the 40% probability level.

served in the hemiaminals and their stability can be explained by the intramolecular hydrogen bond formed between the hydroxy group and the carbamide substituent, which explains the high deshielding observed in the ^{1}H NMR spectra for the signal of the OH group (around 8.5 ppm).

As before, we also explored the stereochemical outcome in the synthesis of pyrrolopiperazinones when enantiopure (*S*)-α-methylbenzylamine was used as chiral component. In this case, although the relative configuration on C3,C4 remained unchanged ((3*R**,4*R**)), an equimolar mixture of diastereomers (2(1*S*),3*R*,4*R*) and (2(1*S*),3*S*,4*S*) was obtained (Scheme 7).

These results indicate that these reactions seem to take place through conjugated additions on the enol tautomer of the Ugi adduct. Indeed, the enolate intermediate would explain the stereochemical results, controlled by the configuration in the hemiaminal intermediate and not by the chiral information on the amine, unlike in the case of benzodiazepinones, where the protonation would be exclusively controlled by the chiral amine in the synthesis of **6**. Moreover, this proposed mechanism also explains the spontaneous cyclization in the absence of a base when 3-bromopropanamine was used (Scheme 8).

Moreover, we envisaged the possibility of obtaining piperazinoquinazoline derivatives, a core found in fungal metabolites [25,26], systems with promising antitumour activity [27], as well as dipyrrolopiperazinone derivatives, substructure found in some alkaloids such as dibromophakellin or the palau'amine [28], which possess immunosuppressive and cytotoxic properties [29], through post-condensation reactions.

Following the methodology previously described in our group [30], the reduction of the nitro group on indole and pyrrole derivatives **9f**,**g**,**l–o** (Scheme 9, Table 5) employing tin(II) chloride under acidic conditions in boiling *n*-butanol (120 °C) afforded the corresponding pyrrolopiperazinoquinazolines **13** with high yields. Interestingly, despite the acidic medium and high temperatures, the hemiaminal group was conserved, showing the high stability of these systems. On the other hand, the reduction of the *N*-phenylglycine derivative **10c**, used without purification after the Ugi/cyclization sequence, yielded the

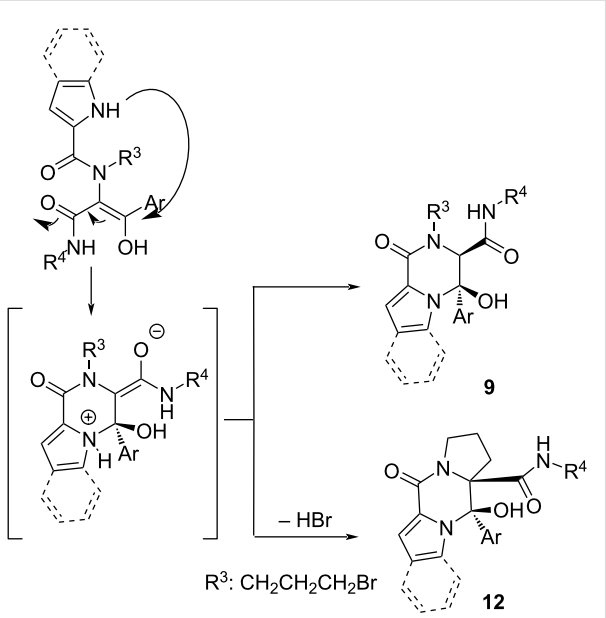

Scheme 8: Proposed mechanism in the spontaneous cyclization of Ugi adducts obtained from arylglyoxals and deactivated amines.

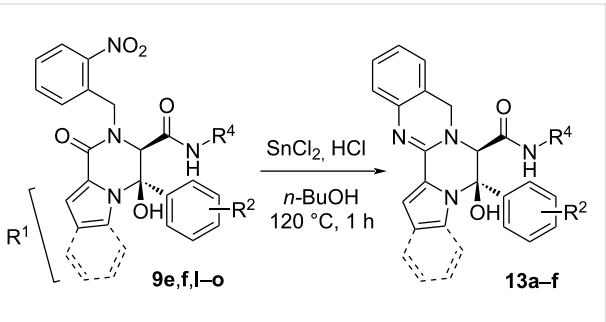

Scheme 9: Synthesis of pyrrolopiperazinoquinazolines **13**.

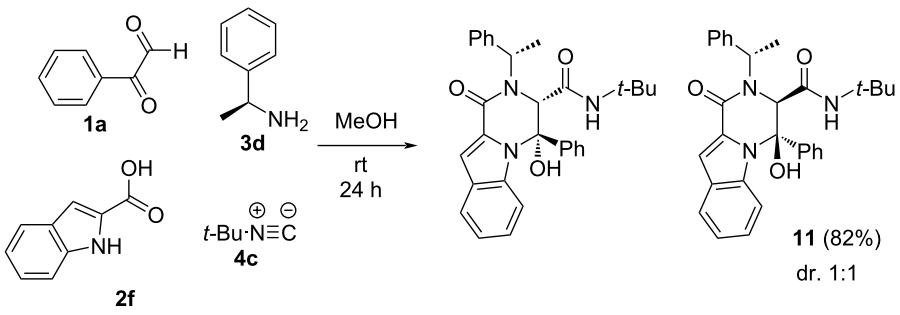

Scheme 7: Synthesis of pyrrolopiperazinone **11** using (*S*)-α-methylbenzylamine.

Table 5: Results obtained in the synthesis of pyrrolopiperazinoquinazolines **13**.

Entry	**9** (R^1, R^2, R^4)	**13** (%)[a,b]
1	**9f** (pyrrole, H, *c*C_6H_{11})	**13a** (70)
2	**9g** (pyrrole, 4-CF_3, $C(CH_3)_3$)	**13b** (70)
3	**9l** (indole, H, *c*C_6H_{11})	**13c** (72)
4	**9m** (indole, 4-F, *c*C_6H_{11})	**13d** (68)
5	**9n** (indole, 4-CH_3O, $C(CH_3)_3$)	**13e** (69)
6	**9o** (indole, 4-CF_3, $C(CH_3)_3$)	**13f** (68)

[a]Yield after purification; [b]the only diastereomer observed was the (3*R**,4*R**).

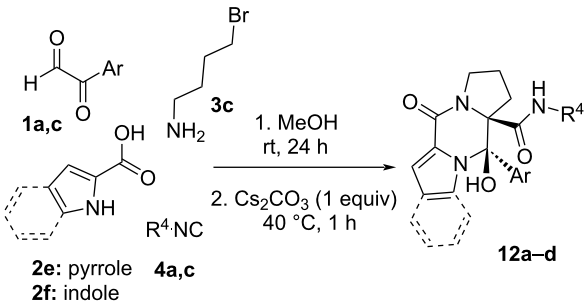

Scheme 11: Synthesis of dipyrrolopiperazinones **12**.

corresponding piperazinoquinazoline **14** with a high global yield (Scheme 10).

Moreover, the treatment of piperazinones **9c**–**e**,**k** derived from 3-bromopropanamine with caesium carbonate in boiling acetonitrile for 1 h afforded the corresponding dipyrrolopiperazinone **12** quantitatively. In view of the interest of these structures and the poor global yield obtained because of the purification in the first step, we tried the synthesis of these polycyclic systems in a one-pot sequence. In this way, after performing the Ugi reaction for 24 h, the reaction mixture, without purification, was treated with caesium carbonate (1 equiv) and heated to reflux for an hour. Gratefully, the dipyrrolopiperazinone derivatives **12** were obtained with high yields and complete diastereoselectivity in an efficient and simple way (Scheme 11, Table 6). The structure of these systems was further confirmed by single-crystal X-ray diffraction of compound **12c** (Figure 3).

Table 6: Results obtained in the synthesis of dipyrrolopiperazinones **12**.

Entry	**1** (Ar)	**2**	**4** (R^4)	**12** (%)[a,b]
1	**1a** (C_6H_5)	**2e**	**4a** (*c*C_6H_{11})	**12a** (93)
2	**1a** (C_6H_5)	**2e**	**4c** ($C(CH_3)_3$)	**12b** (74)
3	**1c** (4-FC_6H_4)	**2e**	**4c** ($C(CH_3)_3$)	**12c** (85)
4	**1a** (C_6H_5)	**2f**	**4c** ($C(CH_3)_3$)	**12d** (80)

[a]Yield after purification; [b]the only diastereomer observed was the (3*R**,4*R**).

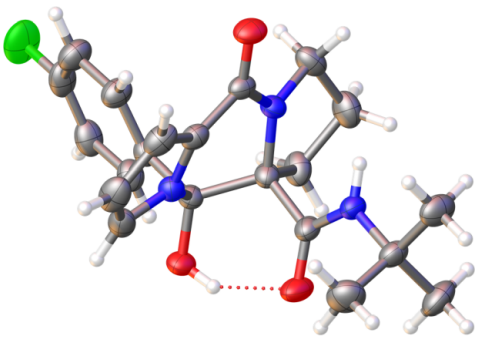

Figure 3: X-ray diffraction structure of dipyrrolopiperazinone **12c**. The thermal ellipsoid plot (Olex2) is at the 40 % probability level.

Conclusion

In this work, we have demonstrated the straightforward access to a variety of complex nitrogen heterocycles by using unprotected deactivated amines tethered to carboxylic acids combined with arylglyoxals in the Ugi reaction. The reduced nucleophilic character of the amino group of the anthranilic acid, indole-2-carboxylic acid, pyrrole-2-carboxylic acid or *N*-phenylglycine

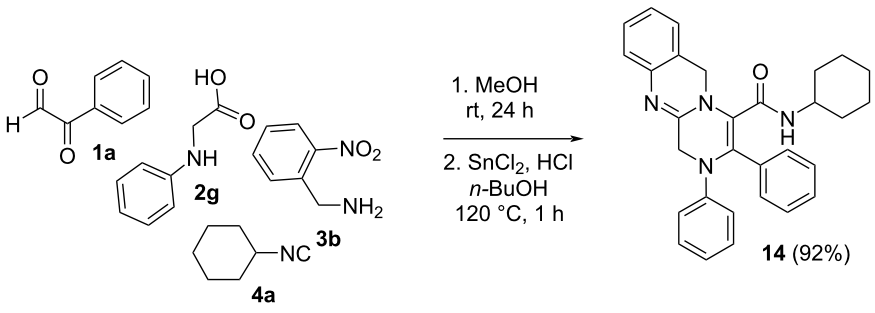

Scheme 10: Synthesis of piperazinoquinazoline **14**.

allowed the use of these compounds in this multicomponent reaction without triggering competitive reactions. The presence of an additional functional group in the resulting Ugi adduct can be exploited in different post-condensation strategies to generate multiple fused nitrogen heterocycles in an easy manner.

Supporting Information

Supporting Information File 1

General synthetic procedures and characterisation.
[https://www.beilstein-journals.org/bjoc/content/supplementary/1860-5397-20-154-S1.pdf]

Funding

Funding from MCIN/AEI/10.13039/501100011033 [grant PID2020-117610RB-I00] is gratefully acknowledged. J. G.-A. and I. C.-B. thank Consejería de Educación de la Junta de Castilla y León, European Social Fund (ESF) and ERDF for their predoctoral (J. G.-A.) and post-doctoral (I. C.-B.) contracts.

Author Contributions

Javier Gómez-Ayuso: investigation; methodology; writing – review & editing. Pablo Pertejo: investigation; methodology; writing – review & editing. Tomás Hermosilla: investigation; writing – review & editing. Israel Carreira-Barral: data curation; investigation; writing – review & editing. Roberto Quesada: funding acquisition; resources; writing – original draft; writing – review & editing. María García-Valverde: conceptualization; funding acquisition; methodology; project administration; resources; supervision; validation; visualization; writing – original draft; writing – review & editing.

ORCID® iDs

Javier Gómez-Ayuso - https://orcid.org/0000-0002-5238-3248
Israel Carreira-Barral - https://orcid.org/0000-0002-4835-8752
Roberto Quesada - https://orcid.org/0000-0003-2764-7157
María García-Valverde - https://orcid.org/0000-0002-3990-8388

Data Availability Statement

All data that supports the findings of this study is available in the published article and/or the supporting information to this article.

References

1. Vitaku, E.; Smith, D. T.; Njardarson, J. T. *J. Med. Chem.* **2014,** *57,* 10257–10274. doi:10.1021/jm501100b
2. Taylor, R. D.; MacCoss, M.; Lawson, A. D. G. *J. Med. Chem.* **2014,** *57,* 5845–5859. doi:10.1021/jm4017625
3. Burkholder, P. R.; Sharma, G. M. *Lloydia* **1969,** *32,* 466–483.
4. Sharma, G. M.; Burkholder, P. R. *J. Chem. Soc. D* **1971,** 151–152. doi:10.1039/c29710000151
5. Poullennec, K. G.; Romo, D. *J. Am. Chem. Soc.* **2003,** *125,* 6344–6345. doi:10.1021/ja034575i
6. Wang, S.; Romo, D. *Angew. Chem., Int. Ed.* **2008,** *47,* 1284–1286. doi:10.1002/anie.200703998
7. Dhillon, S. *Drugs* **2021,** *81,* 867–874. doi:10.1007/s40265-021-01508-y
8. Piha-Paul, S. A.; Xu, B.; Dumbrava, E. E.; Fu, S.; Karp, D. D.; Meric-Bernstam, F.; Hong, D. S.; Rodon, J. A.; Tsimberidou, A. M.; Raghav, K.; Ajani, J. A.; Conley, A. P.; Mott, F.; Fan, Y.; Fan, J.; Peng, P.; Wang, H.; Ni, S.; Sun, C.; Qiang, X.; Levin, W. J.; Ngo, B.; Ru, Q. C.; Wu, F.; Javle, M. M. *Oncologist* **2024,** *29,* e514–e525. doi:10.1093/oncolo/oyad338
9. Giustiniano, M.; Moni, L.; Sangaletti, L.; Pelliccia, S.; Basso, A.; Novellino, E.; Tron, C. G. *Synthesis* **2018,** *50,* 3549–3570. doi:10.1055/s-0037-1610193
10. Trudel, V.; Tien, C.-H.; Trofimova, A.; Yudin, A. K. *Nat. Rev. Chem.* **2021,** *5,* 604–623. doi:10.1038/s41570-021-00304-2
11. Giovenzana, G. B.; Tron, G. C.; Di Paola, S.; Menegotto, I. G.; Pirali, T. *Angew. Chem., Int. Ed.* **2006,** *45,* 1099–1102. doi:10.1002/anie.200503095
12. Hulme, C.; Peng, J.; Tang, S.-Y.; Burns, C. J.; Morize, I.; Labaudiniere, R. *J. Org. Chem.* **1998,** *63,* 8021–8023. doi:10.1021/jo980622r
13. Hulme, C.; Ma, L.; Romano, J.; Morrissette, M. *Tetrahedron Lett.* **1999,** *40,* 7925–7928. doi:10.1016/s0040-4039(99)01580-4
14. Xu, Z.; De Moliner, F.; Cappelli, A. P.; Ayaz, M.; Hulme, C. *Synlett* **2014,** *25,* 225–228. doi:10.1055/s-0033-1340219
15. Neo, A. G.; Ramiro, J. L.; García-Valverde, M.; Díaz, J.; Marcos, C. F. *Mol. Diversity* **2024,** *28,* 335–418. doi:10.1007/s11030-023-10641-7
16. Pertejo, P.; González-Saiz, B.; Quesada, R.; García-Valverde, M. *J. Org. Chem.* **2020,** *85,* 14240–14245. doi:10.1021/acs.joc.0c02103
17. v. Zychlinski, A.; Ugi, I. *Heterocycles* **1998,** *49,* 29–32. doi:10.3987/com-97-s2
18. Rossen, K.; Sager, J.; DiMichele, L. M. *Tetrahedron Lett.* **1997,** *38,* 3183–3186. doi:10.1016/s0040-4039(97)00607-2
19. Keating, T. A.; Armstrong, R. W. *J. Org. Chem.* **1996,** *61,* 8935–8939. doi:10.1021/jo961517p
20. Sañudo, M.; García-Valverde, M.; Marcaccini, S.; Delgado, J. J.; Rojo, J.; Torroba, T. *J. Org. Chem.* **2009,** *74,* 2189–2192. doi:10.1021/jo8025862
21. Pertejo, P.; García-Valverde, M.; Peña, P.; Cordero, N. A.; Torroba, T.; González-Ortega, A. *Org. Biomol. Chem.* **2014,** *12,* 4905–4916. doi:10.1039/c4ob00444b
22. Pertejo, P.; Corres, N.; Torroba, T.; García-Valverde, M. *Org. Lett.* **2015,** *17,* 612–615. doi:10.1021/ol503628r
23. Pertejo, P.; Carreira-Barral, I.; Peña-Calleja, P.; Quesada, R.; García-Valverde, M. *J. Org. Chem.* **2020,** *85,* 2291–2302. doi:10.1021/acs.joc.9b02995
24. Shourkaei, F. A.; Lish, A. B.; Talebi, M.; Abdoli, S.; Zare, N.; Amanlou, M.; Ranjbar, P. R.; mahdavi, M. *J. Mol. Struct.* **2024,** *1297,* 136939. doi:10.1016/j.molstruc.2023.136939
25. Resende, D. I. S. P.; Boonpothong, P.; Sousa, E.; Kijjoa, A.; Pinto, M. M. M. *Nat. Prod. Rep.* **2019,** *36,* 7–34. doi:10.1039/c8np00043c
26. Xin, Z. H.; Fang, Y.; Du, L.; Zhu, T.; Duan, L.; Chen, J.; Gu, Q.-Q.; Zhu, W.-M. *J. Nat. Prod.* **2007,** *70,* 853–855. doi:10.1021/np060516h

27. Wang, L.; Fang, K.; Cheng, J.; Li, Y.; Huang, Y.; Chen, S.; Dong, G.; Wu, S.; Sheng, C. *J. Med. Chem.* **2020,** *63,* 696–713. doi:10.1021/acs.jmedchem.9b01626
28. Lindel, T. Chemistry and biology of the pyrrole-imidazole alkaloids. In *The Alkaloids: Chemistry and Biology;* Knölker, H.-J., Ed.; Academic Press, 2017; Vol. 77, pp 117–219. doi:10.1016/bs.alkal.2016.12.001
29. Lansdell, T. A.; Hewlett, N. M.; Skoumbourdis, A. P.; Fodor, M. D.; Seiple, I. B.; Su, S.; Baran, P. S.; Feldman, K. S.; Tepe, J. J. *J. Nat. Prod.* **2012,** *75,* 980–985. doi:10.1021/np300231f
30. Pertejo, P.; Peña-Calleja, P.; Carreira-Barral, I.; Quesada, R.; Cordero, N. A.; Rodríguez, F. J.; García-Valverde, M. *Org. Biomol. Chem.* **2017,** *15,* 7549–7557. doi:10.1039/c7ob01807j

License and Terms

This is an open access article licensed under the terms of the Beilstein-Institut Open Access License Agreement (https://www.beilstein-journals.org/bjoc/terms), which is identical to the Creative Commons Attribution 4.0 International License (https://creativecommons.org/licenses/by/4.0). The reuse of material under this license requires that the author(s), source and license are credited. Third-party material in this article could be subject to other licenses (typically indicated in the credit line), and in this case, users are required to obtain permission from the license holder to reuse the material.

The definitive version of this article is the electronic one which can be found at:
https://doi.org/10.3762/bjoc.20.154

BEILSTEIN JOURNAL OF ORGANIC CHEMISTRY

Ugi bisamides based on pyrrolyl-β-chlorovinylaldehyde and their unusual transformations

Alexander V. Tsygankov[*1,2], Vladyslav O. Vereshchak[1,2], Tetiana O. Savluk[1,2], Serhiy M. Desenko[1], Valeriia V. Ananieva[1], Oleksandr V. Buravov[1,3], Yana I. Sakhno[1], Svitlana V. Shishkina[1,4] and Valentyn A. Chebanov[*1,4]

Full Research Paper

Open Access

Address:
[1]Institute of Functional Materials Chemistry, State Scientific Institution "Institute for Single Crystals" of National Academy of Sciences of Ukraine, Nauky Ave., 60, 61072, Kharkiv, Ukraine, [2]National Technical University "Kharkiv Polytechnic Institute", Kyrpychova st., 2, Kharkiv, 61002, Ukraine, [3]Enamine Ltd., Winston Churchill Street 78, Kyiv 02094, Ukraine and [4]Faculty of Chemistry, V. N. Karazin Kharkiv National University, Svobody sq., 4, 61022, Kharkiv, Ukraine

Email:
Alexander V. Tsygankov[*] - geminalsystemsn@gmail.com;
Valentyn A. Chebanov[*] - chebanov@isc.kh.ua

* Corresponding author

Keywords:
convertible isocyanides; multicomponent reaction; post-Ugi transformation; pyrrole derivative; Ugi reaction

Beilstein J. Org. Chem. **2024,** *20,* 1773–1784.
https://doi.org/10.3762/bjoc.20.156

Received: 26 April 2024
Accepted: 09 July 2024
Published: 26 July 2024

This article is part of the thematic issue "Multicomponent reactions IV".

Associate Editor: D. Spring

© 2024 Tsygankov et al.; licensee Beilstein-Institut.
License and terms: see end of document.

Abstract

By one-pot four- and three-component Ugi reactions involving convertible isocyanides and unexplored pyrrole-containing β-chlorovinylaldehyde, a small library of 20 bisamides with unusual behavior in post-Ugi transformations was prepared and characterized. Surprisingly, a well-documented approach to obtain peptide-containing carboxylic acids through acid hydrolysis of the convertible isocyanide moiety in the Ugi bisamides proceeded in an unexpected manner in our case, leading to the formation of derivatives of amides of heterylidenepyruvic acid. An optimized synthetic protocol for this transformation was elaborated and a plausible sequence involving the elimination of the 2-chloroacetamide moiety and the conversion of the β-chlorovinyl fragment into a vinyl one is provided.

Introduction

One of the keys to the development of mankind is the constant search for new substances and advanced materials. Today, we have powerful tools at our disposal that allow us to create entire libraries of structurally complex organic compounds [1-6] to expand and systematically explore the chemical space within the concepts of molecular diversity chemistry (diversity oriented synthesis) [6] and biologically oriented synthesis [7].

Among the multicomponent processes, the four-component Ugi reaction (Ugi-4CR) [8-13] is characterized by the greatest

versatility, through the variability of the starting components leading to a variety of possible products [12-17]. The Ugi-4CR has been used for the synthesis of numerous natural substances, e.g., bicyclomycin, furanomycin, penicillin, etc. [15,18]. Further, the application of reagents with additional functional groups in the Ugi reaction makes it possible to further increase the complexity of the product structures, also due to possible post-transformation reactions. For example, if an unsaturated bond is present in the aldehyde component, after the formation of the expected Ugi bisamide products, subsequent post-transformations allow the synthesis of products of intramolecular cyclization [19-22] and/or products of a tandem combination of several reactions (Scheme 1) [22-26].

At the same time, the use of so-called convertible isocyanides [27-36] in Ugi-4CR makes it possible to obtain carboxylic acids or esters after hydrolysis of the secondary amide group in the Ugi products (Scheme 2) [27-29,31,32,34-36]. Ugi bisamides modified in this way may be subsequently used as acid components in tandem combinations of various multicomponent pro-

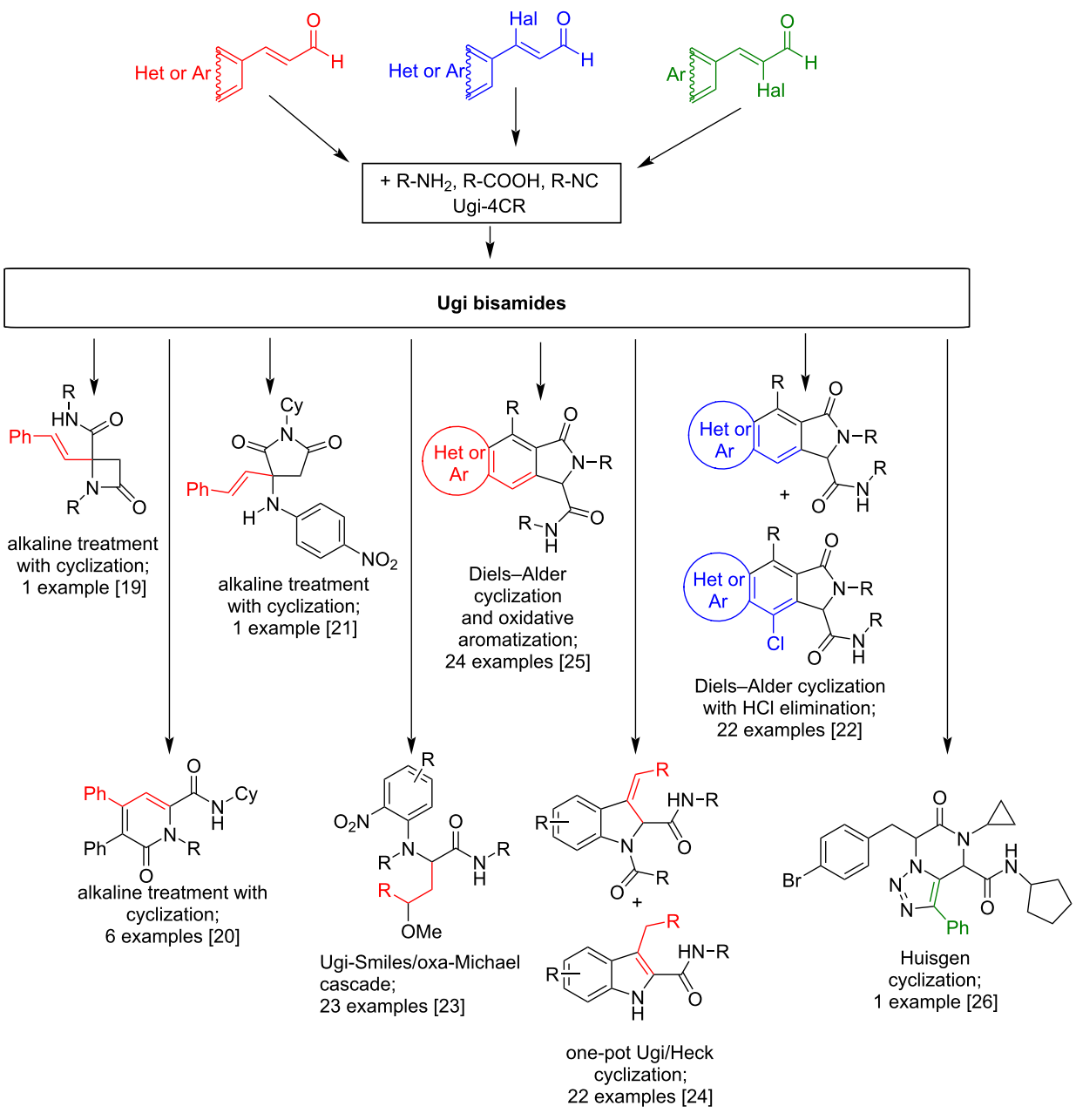

Scheme 1: The use of α,β-unsaturated aldehydes in the Ugi reaction.

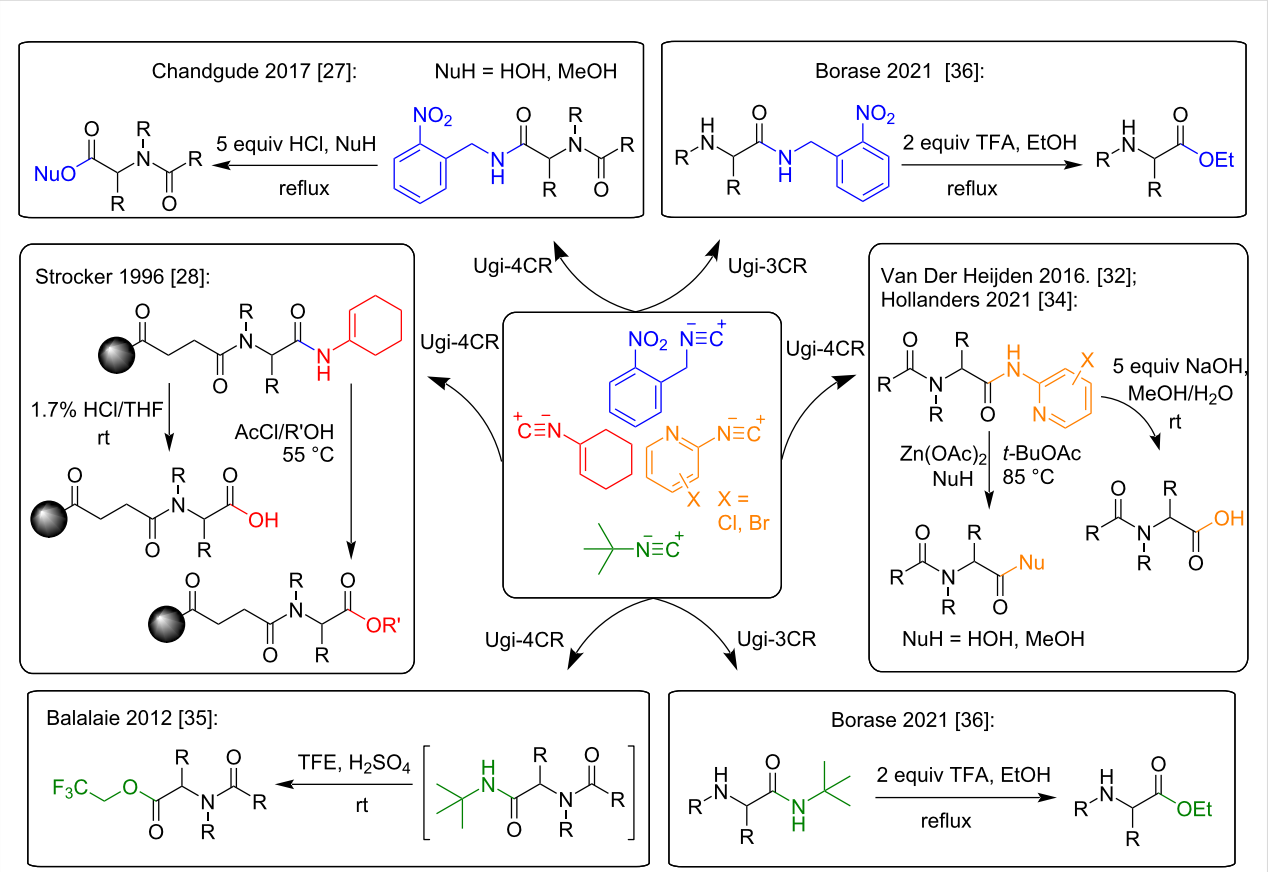

Scheme 2: Comparison of isocyanide conversion conditions.

cesses such as Ugi and Ugi, azido-Ugi and Ugi, Ugi and Passerini, Groebke–Blackburn–Bienaymé and Ugi, etc. [15,17,37,38].

The creation of hybrid molecules by using primary and post-modified Ugi products in combination with other isocyanide MCRs is effective and one promising direction to increase the diversity of new peptidomimetics is the use of, for example, α,β-unsaturated aldehydes including those containing a halogen atom in the β-position, in the Ugi-4CR reaction [1,39].

As our previous studies have shown, azomethines based on aromatic amines and substituted pyrrolecarbaldehyde [40] or pyrrolyl-β-chlorovinylaldehyde [39], contain several frequently encountered motifs in drugs and drug candidates – a pyrrole heterocycle and an azomethine C=N fragment (Figure 1) – and exhibit some biological activity. Thus, Ugi bisamides based on the same aldehydes and amines may also demonstrate biological activity.

In view of these facts, we decided to develop a new approach for the synthesis of hybrid molecules containing substituted

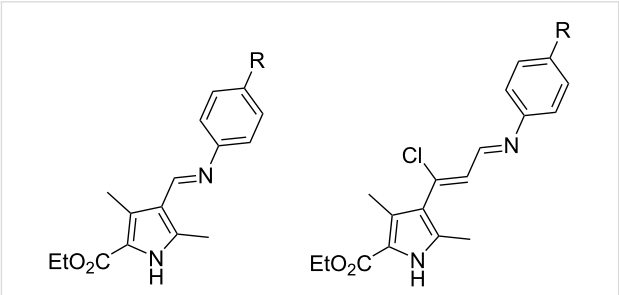

Figure 1: Azomethines based on ethyl 4-acetyl-3,5-dimethyl-1*H*-pyrrole-2-carboxylate and 4-[(*E*)-1-chloro-3-oxoprop-1-enyl]-3,5-dimethyl-1*H*-pyrrole-2-carboxylate.

heterocyclic and peptidomimetic moieties. The first stage of this approach was the preparation of Ugi bisamides based on pyrrole-containing β-chlorovinylaldehyde and convertible isocyanides. The subsequent post-transformation of the products by acidic hydrolysis conditions should then lead to an acidic component. However, due to the cascade nature of the multicomponent processes and the presence of several alternative reaction centers in the structure of our substances, we sometimes encountered unexpected and intriguing results.

Results and Discussion

Synthesis of Ugi bisamides

Four-component and three-component Ugi reactions

The combination of pyrrole-containing α,β-unsaturated aldehyde **1**, which contains a chlorine atom in the β-position, with convertible isocyanides **4a**–**d**, *para*-substituted anilines **2a**–**e** and monochloroacetic acid (**3**) as the smallest building blocks in a four-component reaction leads to the formation of the Ugi bisamides **5**–**8** (Table 1). Their structures offer several possibilities for subsequent post-transformation reactions.

The synthesis of the target Ugi bisamides **5**–**8** was carried out at room temperature in ethanol with stirring for 24–48 hours

Table 1: Library of Ugi bisamides **5**–**8** containing a β-chlorovinyl fragment.

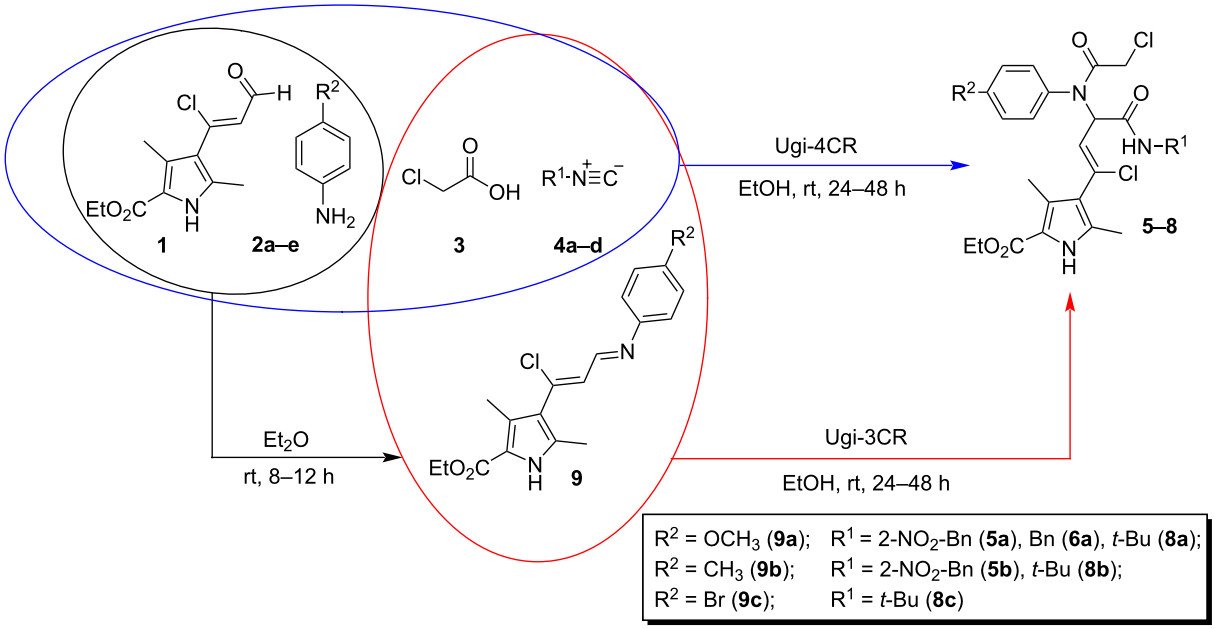

Bisamide	R^1	R^2	Yield 4CR[a]	Yield 3CR[a]
5a	2-NO_2-Bn	OMe	55	47
5b		Me	64	47
5c		Br	63	–
5d		CF_3	54	–
5e		Cl	50	–
6a	Bn	OMe	54[b]	26[b]
6b		Me	69	–
6c		Br	72	–
6d		CF_3	49[b]	–
6e		Cl	93	–
7a	Cy	OMe	59	–
7b		Me	87	–
7c		Br	64	–
7d		CF_3	79	–
7c		Cl	72	–
8a	*t*-Bu	OMe	65	27
8b		Me	69	66
8c		Br	79	53
8d		CF_3	64	–
8e		Cl	58	–

[a]Isolated, EtOH as a solvent; [b]the first precipitated compound was amide **10b**.

(depending on the type of starting material) with a yield of 54–93% (Table 1).

It is worth noting that the Ugi-4CR reaction also led to the formation of bisamides **5**–**8** when other solvents were used, e.g., methanol or acetonitrile. However, the yields of the targeted reaction products in methanol were generally lower than in ethanol, while the procedure in acetonitrile was not suitable for all reagents.

It is known that the Ugi-4CR proceeds through the formation of an azomethine (Schiff base) in the first stage [39,40]. Therefore, considering the results of our previous work [39] on the nature and properties of azomethines based on β-chlorovinylaldehyde **1** (Figure 1), we decided to study the possibility of using the three-component Ugi reaction (Ugi-3CR) with preliminary synthesis of azomethines **9a**–**c** (Table 1). In this case, the Ugi bisamides **5**, **6**, **8** were formed, however, it was found that the application of the Ugi-3CR approach had no significant effect on the yields of the target products. Considering the additional reaction step for the synthesis and purification of the starting azomethines **9**, we cannot propose the Ugi-3CR approach as more suitable compared to the Ugi-4CR approach.

The structure of the Ugi bisamides **5**–**8** were proved by X-ray diffraction study on the example of substance **8c** (Figure 2), according to which the *Z*-configuration of the chlorovinyl fragment was detected.

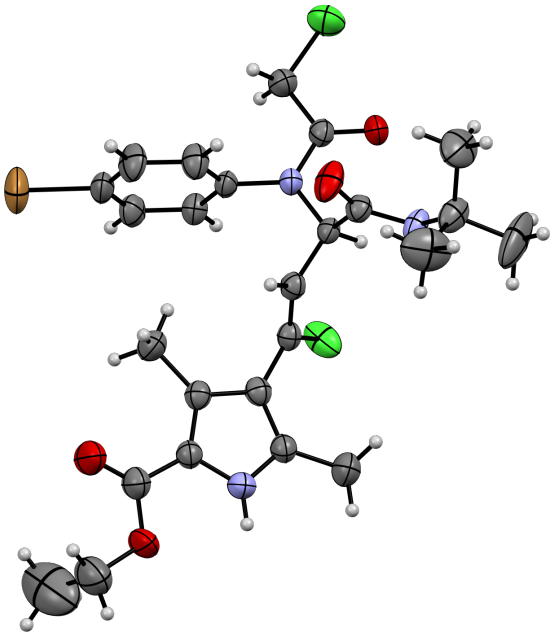

Figure 2: Molecular structure of ethyl (*Z*)-4-(3-(*N*-(4-bromophenyl)-2-chloroacetamido)-4-(*tert*-butylamino)-1-chloro-4-oxobut-1-en-1-yl)-3,5-dimethyl-1*H*-pyrrole-2-carboxylate (**8c**) according to the X-ray diffraction study. Non-hydrogen atoms are presented as thermal ellipsoids with 50% probability.

Post-Ugi transformations

As previously mentioned [32], the introduction of the convertible 2-bromo-6-isocyanopyridine into the Ugi bisamide structure allows the conversion of the newly formed amide into a carboxylic acid fragment after acid hydrolysis. Similar results were obtained by Dömling and co-workers [27], who used 2-nitrobenzyl isocyanide as a universal convertible isocyanide, and the amide group was also converted into a carboxylic acid under the conditions of acid hydrolysis (Scheme 2). Therefore, taking into account the experience of the authors [27,32], we tried to apply the described hydrolysis conditions (5 equiv HCl in MeOH) to our products (compounds **5**). As a model reaction, we heated a mixture of Ugi bisamide **5d** and an aqueous solution of HCl in methanol (glycerol bath, 80 °C) in a hermetically sealed vial with stirring for three hours (Scheme 3, conditions A).

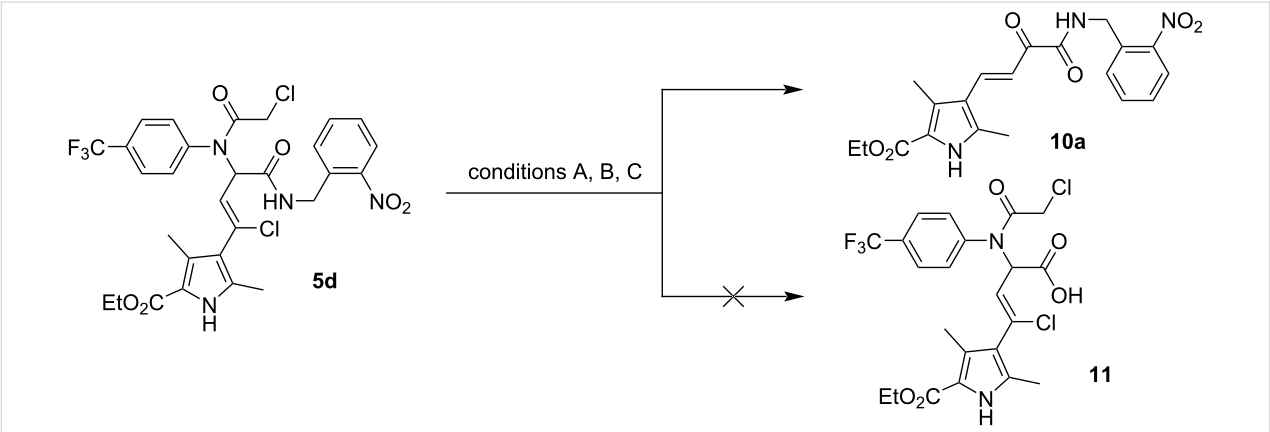

Scheme 3: Hydrolysis of Ugi bisamide **5d** in the presence of HCl. Conditions: (A) 5 equiv HCl, MeOH, 80 °C, 3 h; (B) 5 equiv HCl, EtOH, MW 120 °C, 15 min; (C) 5 equiv HCl, MeCN, MW 100 °C, 20 min.

However, the results of this attempted post-Ugi transformation were quite unexpected: Instead of acid **11**, we isolated the amide of the unsaturated derivative of pyruvic acid **10a** according to the ^{1}H and ^{13}C NMR spectra and mass spectrometry data. In order to drive the process towards the desired hydrolysis of the secondary amide group, we performed the post-Ugi transformation under MW activation in ethanol or acetonitrile (Scheme 3, conditions B or C). However, the application of MW irradiation did not change the course of the reaction, and as under conventional thermal heating, amide **10a** was isolated, albeit in a lower yield and accompanied with tar formation.

In addition to the ^{1}H, ^{13}C NMR spectra and mass spectrometry data, the structure of compound **10d** was established by X-ray diffraction analysis (Figure 3). It was also found that the substituents at the double bond are *trans* configured.

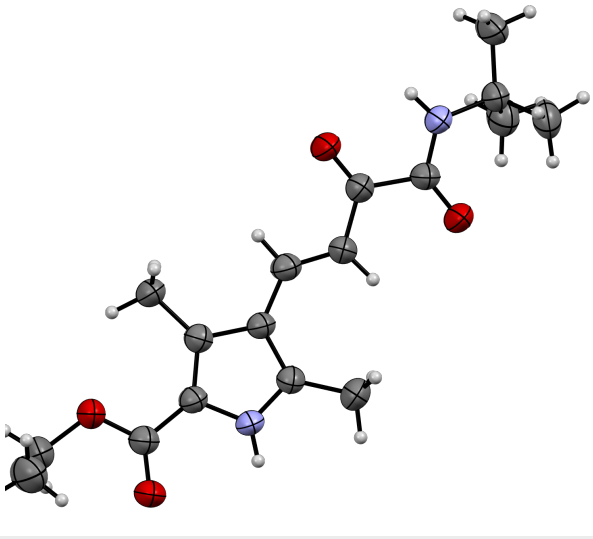

Figure 3: Molecular structure of ethyl (*E*)-4-(4-(*tert*-butylamino)-3,4-dioxobut-1-en-1-yl)-3,5-dimethyl-1*H*-pyrrole-2-carboxylate (**10d**) according to X-ray diffraction data. Non-hydrogen atoms are presented as thermal ellipsoids with 50% probability.

To find out the patterns of the new reaction, we applied different conditions to a wider range of starting bisamides **5**–**8** (Table 2). As in the model reaction (Scheme 3), the main products of the transformation were the corresponding amides **10a**–**d** (Table 2).

In the case of bisamides **5d**, **6a**, **6c**, **7b**, **8a**, and **8c** (Table 2), additional transformation products were also isolated from the reaction mixture. According to ^{1}H and ^{13}C NMR, MS, and X-ray diffraction studies these were the corresponding ketobisamides **12**, which are products of a nucleophilic substitution of the chlorine atom in the chlorovinyl fragment to the hydroxy group, probably under the influence of water (Figure 4).

It is worth noting that the synthesis of Ugi bisamides **5**–**8** (Table 1) yielded compounds **10** and ketobisamide **12** in some

Table 2: Post-Ugi transformations of bisamides **5–8** under different conditions.

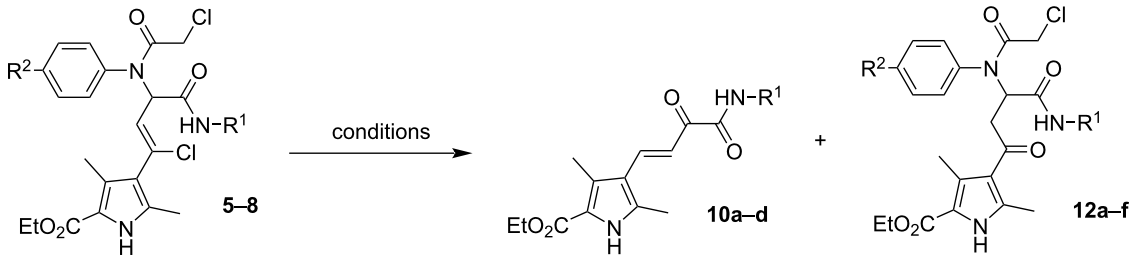

Entry	Bisamide			Conditions				Yield[a]	
	R^1	R^2	No.	solvent	cat	temperature[b], °C	time, h	amide **10**	ketobisamide **12**
1	2-NO_2-Bn	Br	**5c**	MeOH	HCl 5 equiv[c]	70	3	**10a**, 13	–
2		CF_3	**5d**	MeOH	HCl 5 equiv[c]	80	3	**10a**, 42	–
3		CF_3	**5d**	EtOH	–	80	3.5	**10a**, 44	**12a**, 19
4		CF_3	**5d**	EtOH	HCl 1 equiv[c]	80	3.5	**10a**, 47	**12a**, 20
5		CF_3	**5d**	MeOH	HCl 5 equiv[c]	85, MW	0.5	**10a**, 40	–
6		CF_3	**5d**	EtOH	HCl 5 equiv[c]	100, MW	0.5	**10a**, 39	–
7		CF_3	**5d**	EtOH	HCl 5 equiv[c]	120, MW	0.25	**10a**, 35	–
8		CH_3	**5b**	MeCN	HCl 5 equiv[c]	50	6	**10a**, 35	–
9		CF_3	**5d**	MeCN	HCl 5 equiv[c]	100, MW	0.5	**10a**, 26	–

Table 2: Post-Ugi transformations of bisamides **5–8** under different conditions. (continued)

10	Bn	Br	**6c**	EtOH	–	80	3	**10b**,42	–
11		Me	**6b**	EtOH	–	80	3	**10b**, 35	–
12		Cl	**6e**	EtOH	HCl 1 equiv[c]	50	168	**10b**, 20	–
13		Cl	**6e**	EtOH	HCl 1 equiv[c]	80	3	**10b**, 40	–
14		Br	**6c**	EtOH	HCl 1 equiv[c]	80	2.5	**10b**, 25	–
15		OMe	**6a**	EtOH	HCl 1 equiv[c]	80	3	**10b**, 39	**12b**, traces
16		Me	**6b**	EtOH	HCl 1 equiv[c]	80	3	**10b**, 38	–
17		Br	**6c**	MeCN	HCl 1 equiv[c]	25	216	**10b**, 20	**12c**, 9
18	Cy	Me	**7b**	EtOH	–	25	850	**10c**, 18	**12d**, 71
19		Me	**7b**	EtOH	HCl 5 equiv[c]	80	3	**10c**, 34	–
20		Br	**7c**	EtOH	HCl 5 equiv[c]	80	4.5	**10c**, 40	–
21		OMe	**7a**	EtOH	HCl 5 equiv[c]	80	3	**10c**, 38	–
23	*t*-Bu	Br	**8c**	EtOH	–	25	840	**10d**, 6	**12e**, 6
24		Br	**8c**	EtOH	–	80	3	**10d**, 56	**12e**, 15
25		Br	**8c**	EtOH	HCl 1 equiv[c]	25	850	**10d**, 14	**12e**, 5
26		Br	**8c**	EtOH	DIPEA 2 equiv	80	3	–	–
27		Br	**8c**	EtOH	Et_3N 2 equiv	80	3	–	–
28		Br	**8c**	EtOH	MCA 1 equiv	80	2	**10d**, 52	**12e**, 13
29		Br	**8c**	EtOH	HCl 0.5 equiv[c]	80	3	**10d**, 64	**12e**, 12
30		Br	**8c**	EtOH	HCl 1 equiv[c]	80	3	**10d**, 46	**12e**, 12
31		Br	**8c**	EtOH	HCl 2 equiv[c]	80	3	**10d**, 47	**12e**, 12
32		Br	**8c**	EtOH	HCl 5 equiv[c]	80	3	**10d**, 51	**12e**, 12
33		OMe	**8a**	EtOH	HCl 5 equiv[c]	80	3	**10d**, 62	**12f**, 21
34		Br	**8c**	MeCN	HCl 1 equiv[c]	25	72	**10d**, 34	**12e**, 46
35		Br	**8c**	MeCN	–	80	3	**10d**, 10	**12e**, 18

[a]Isolated yield; [b]the temperature in bath; [c]water 36% solution.

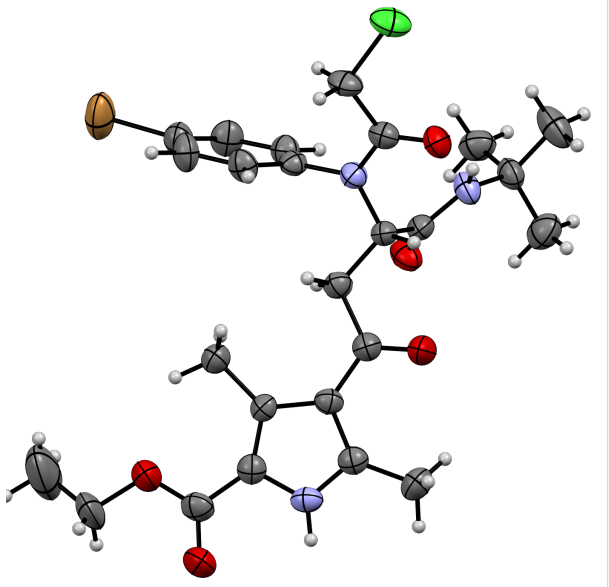

Figure 4: Molecular structure of ethyl 4-(3-(*N*-(4-bromophenyl)-2-chloroacetamido)-4-(*tert*-butylamino)-4-oxobutanoyl)-3,5-dimethyl-1*H*-pyrrole-2-carboxylate (**12e**) according to the X-ray diffraction data. Non-hydrogen atoms are presented as thermal ellipsoids with 50% probability.

cases. For example, in the Ugi reaction involving benzyl isocyanide (**4b**) and *p*-anisidine (**2a**), the product that precipitated first from the reaction mixture was 2-oxo-4-(1*H*-pyrrol-3-yl)but-3-enoic acid amide **10b** (Scheme 4; Table 1, footnote b). Pure Ugi bisamide **6a** could only be obtained when the reaction was carried out in MeCN or EtOH. The same was observed in the case of *p*-CF_3-substituted aniline when synthesizing bisamide **6d**. The yield of the amide **10c** was about 8% and it was also the first to precipitate.

In addition, it is worth mentioning that the corresponding amides **10** were observed in ^{1}H NMR spectra and LC–MS analysis in many mother liquors after filtration of the bisamides **6**–**8**. Moreover, traces of the ketobisamides **12** were also observed when the synthesis was carried out in 96% EtOH. The one-pot synthesis allows to combine two consecutive steps, the Ugi-4CR and the post-Ugi reaction, by keeping the mixture of starting materials **1**, **2c**, **3** and **4d** at 25 °C for two days and then heating the reaction mixture in a closed vessel at 80 °C for 3 hours (Scheme 5). This procedure led to the formation and isolation of the products **10d** and **12e** with yields which are similar to the tandem reaction.

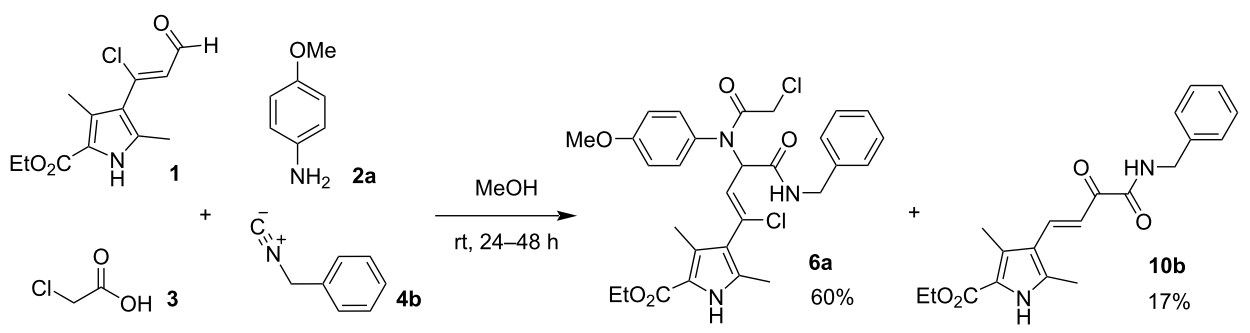

Scheme 4: The Ugi-4CR with the participation of *p*-anisidine and benzyl isocyanide.

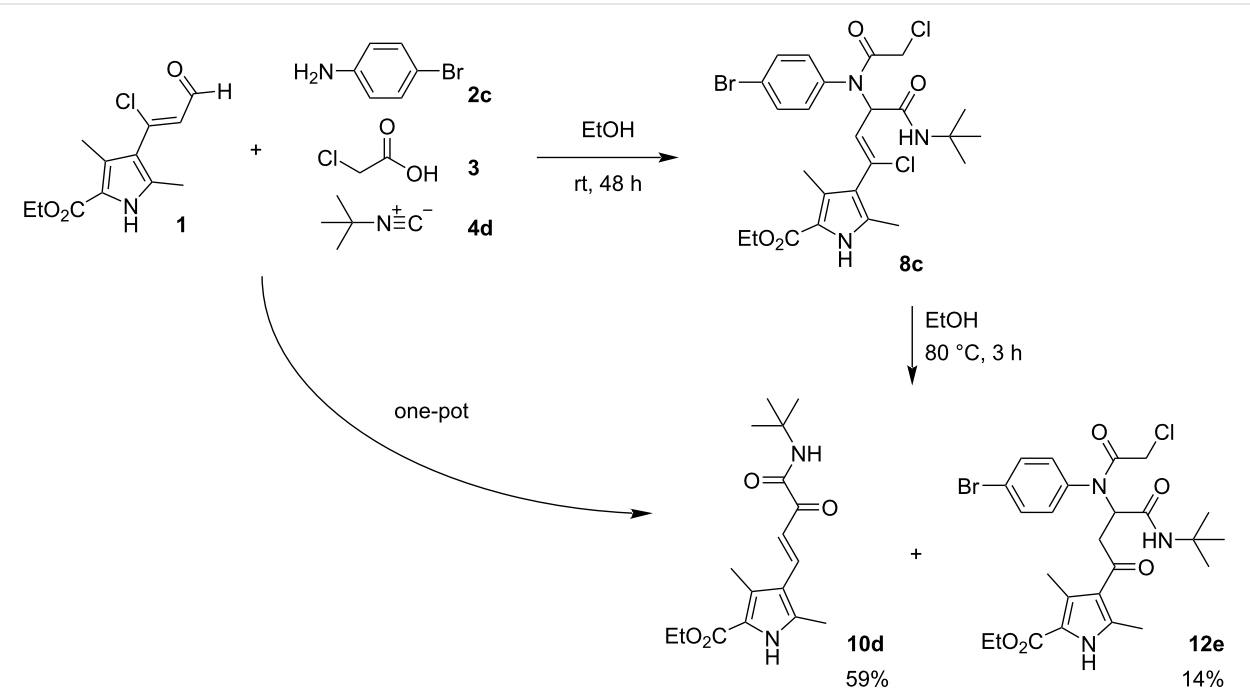

Scheme 5: Successful attempt at tandem one-pot coupling of the Ugi-4CR reaction and post-transformation of the corresponding bisamide **8c**.

Using the example of bisamide **8c**, it was found that changing the amount of HCl or replacing it with chloroacetic acid under otherwise identical conditions had no significant effect on the yields of products **10** and **12** (Table 2, entries 28–32). At the same time, decreasing the temperature of the post-Ugi transformation of bisamide **8c** in the presence of HCl to 25 °C significantly slowed down the reaction (Table 2, entry 25) and after 36 days a large amount of the starting bisamide remained unchanged in the reaction mixture, while the target amide **10d** and ketobisamide **12e** were observed in low yield. However, when the same reaction was carried out in MeCN, the bisamide **8c** completely disappeared within 3 days (Table 2, entry 34), and the amide **10d** and the ketobisamide **12e** were isolated from the reaction mixture in sufficiently higher yields than when the reaction was carried out in ethanol.

Moreover, the post-Ugi transformation of bisamides **6b**, **6c**, **7b**, and **8c** without addition of acid also led to the formation of amides **10b**–**d** as main products and the corresponding ketobisamides **12d**–**e** as minor products (Table 2, entries 10, 11, 18, 23, and 24). This can be explained by the formation of HCl in the reaction mixture due to the substitution of chlorine in the vinyl chloride moiety under the influence of water. The appearance of HCl in these cases was identified by the specific odor and detected by pH measurements. It is likely that this catalytic amount of HCl is enough for the conversion and formation of the amides **10**.

To confirm the influence of HCl and its necessity to initiate the formation of amide **10**, the post-Ugi transformation of bisamide **8c** was carried out in the presence of Et_3N or DIPEA (Table 2,

entries 26 and 27). The expected corresponding quaternary ammonium salts were isolated, and no trace of amide **10d** was observed.

It should also be noted that in the ^{1}H NMR spectra of the reaction mixtures and the various mother liquors, the signals of the 2-chloroacetamides **13a–d** (Scheme 6) [41] were clearly recognizable in many cases and were sometimes isolated individually. In addition, the hydrochlorides of the corresponding *para*-substituted anilines were identified. The amount of salt formed increased with increasing HCl excess, indicating that they were formed by the acidic hydrolysis of the corresponding 2-chloroacetamides **13a–e**. The amount of either 2-chloroacetamide or 2-chloroacetamide and ammonium salt together correlated well with the amount of the corresponding amide **10**.

The expected fact that the amides **10** could not be formed from the ketobisamides **12** (Table 3) was also confirmed; stirring the latter in MeCN or EtOH in the presence of HCl at room temperature or under heating did not lead to formation, not even to the appearance of traces of the amide **10d**.

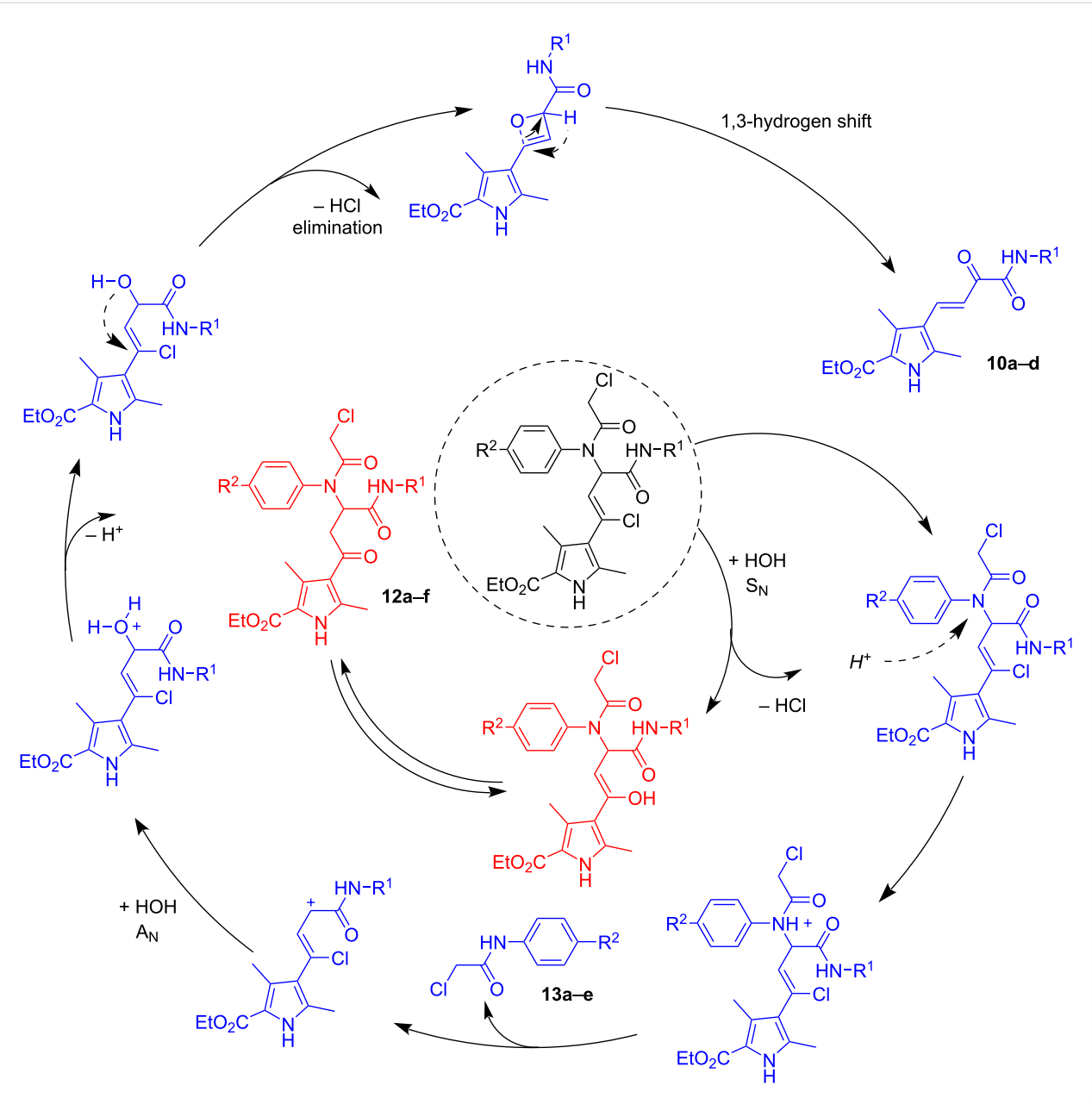

Scheme 6: Plausible transformation sequence of the formation of amides **10** and ketobisamides **12**.

Table 3: Hydrolysis of ketobisamide **12e**.

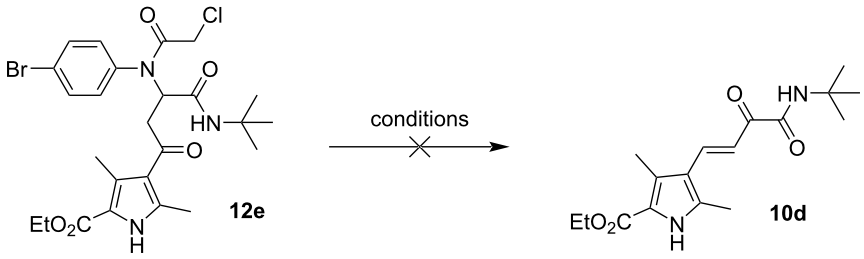

Entry	Conditions				residue of ketobisamide, **12e**, %	amide **10d**
	solvent	cat	temperature in bath, °C	time, h		
1	MeCN	HCl 1 equiv	25	168	95	not observed
2	MeCN	HCl 1 equiv	80	3	68	not observed
3	EtOH	HCl 2 equiv	80	3	70	not observed

Based on the above facts, we have proposed a plausible transformation sequence for the formation of amides **10** and ketobisamides **12** (Scheme 6).

Conclusion

Thus, in this work, the multicomponent reaction of pyrrole-containing β-chlorovinylaldehyde, *para*-substituted anilines, monochloroacetic acid, and different convertible isocyanides gives rise to products of the classic Ugi reaction, ethyl (*E*)-4-(4-(R^1-amino)-1-chloro-3-(2-chloro-*N*-(4-(R^2)phenyl)acetamido)-4-oxobut-1-en-1-yl)-3,5-dimethyl-1*H*-pyrrole-2-carboxylates, which, however, exhibit unusual behavior in *post*-Ugi transformations. The attempt to apply a well-documented approach for the subsequent synthesis of peptide-containing carboxylic acids by acid hydrolysis of the convertible isocyanide moiety in the Ugi bisamides proceeded in an unexpected manner: their treatment with acids led to elimination of the 2-chloroacetamide moiety and conversion of the β-chlorovinyl fragment into a vinyl fragment giving rise to ethyl (*E*)-4-(4-(R^1-amino)-3,4-dioxobut-1-en-1-yl)-3,5-dimethyl-1*H*-pyrrole-2-carboxylates. Another direction of the post-transformation was the replacement of the chlorine atom in the β-chlorovinyl group of the Ugi bisamides with a hydroxy group and the formation of a different type of peptidomimetic, namely ethyl 4-(3-(*N*-(4-R^2-phenyl)-2-chloroacetamido)-4-(R^1-amino))-4-oxobutanoyl)-3,5-dimethyl-1*H*-pyrrole-2-carboxylates. It was also found that these two unusual products of acidic transformation were observed as byproducts of the Ugi reaction. Optimized synthetic protocols were developed for all reactions and a plausible sequence of the post-Ugi transformation was provided.

Supporting Information

Supporting Information File 1

Experimental section, NMR and LC–MS spectra as well as X-ray data.
[https://www.beilstein-journals.org/bjoc/content/supplementary/1860-5397-20-156-S1.pdf]

Acknowledgements

The authors thank all brave defenders of Ukraine who allow us to continue our scientific work and prepare this publication. We also express our gratitude to the scientists who were not included in the main list of authors and took part in the initial stages of the work: Professor Olena I. Mikhedkina, Dr. Ihor I. Melnik, Dr. Anna I. Larina. Parts of the work were presented at the following conferences: International scientific and practical conferences MicroCAD 2022 and 2023, Kharkiv, Ukraine; XIX Scientific Conference Lviv Chemical Readings 2023, Lviv, Ukraine; Conferences XXIII and XXIV ”Advances in the Chemistry of Heteroorganic Compounds” 2023 and 2024, Lodz, Poland; VII International (XVII Ukrainian) Scientific Conference for Students and Young Scientists 2024, Vinnitsa, Ukraine; XVI All-Ukrainian Scientific conference of students and graduate students 2024 (HCC'24), Kharkiv, Ukraine.

Funding

The authors thank the National Academy of Sciences of Ukraine for financial support. Project of the national Academy of Sciences of Ukraine "Directed synthesis, chemical transfor-

mations and properties of new nitrogen-containing heterocyclic compounds" (0122U001857).

ORCID® iDs

Alexander V. Tsygankov - https://orcid.org/0000-0001-5298-8450
Vladyslav O. Vereshchak - https://orcid.org/0009-0007-2329-9411
Tetiana O. Savluk - https://orcid.org/0009-0001-1021-6249
Serhiy M. Desenko - https://orcid.org/0000-0001-8914-3232
Valeriia V. Ananieva - https://orcid.org/0000-0002-8059-5205
Oleksandr V. Buravov - https://orcid.org/0009-0008-8433-5524
Yana I. Sakhno - https://orcid.org/0000-0003-0561-635X
Svitlana V. Shishkina - https://orcid.org/0000-0002-3946-1061
Valentyn A. Chebanov - https://orcid.org/0000-0001-7564-778X

Data Availability Statement

The data that supports the findings of this study is available from the corresponding author upon reasonable request.

References

1. Koopmanschap, G.; Ruijter, E.; Orru, R. V. *Beilstein J. Org. Chem.* **2014,** *10,* 544–598. doi:10.3762/bjoc.10.50
2. Chebanov, V. A.; Desenko, S. M. *Chem. Heterocycl. Compd.* **2012,** *48,* 566–583. doi:10.1007/s10593-012-1030-2
3. Chebanov, V. A.; Desenko, S. M.; Lipson, V. V.; Gorobets, N. Y. Multicomponent-Switched Reactions in Synthesis of Heterocycles. In *Multicomponent Reactions towards Heterocycles: Concepts and Applications;* Van der Eycken, E. V.; Sharma, U. K., Eds.; Wiley-VCH: Weinheim, Germany, 2022; pp 287–338. doi:10.1002/9783527832439.ch8
4. Murlykina, M. V.; Morozova, A. D.; Zviagin, I. M.; Sakhno, Y. I.; Desenko, S. M.; Chebanov, V. A. *Front. Chem. (Lausanne, Switz.)* **2018,** *6,* 527. doi:10.3389/fchem.2018.00527
5. Desenko, S. M.; Gorobets, M. Y.; Lipson, V. V.; Sakhno, Y. I.; Chebanov, V. A. *Chem. Rec.* **2024,** *24,* e202300244. doi:10.1002/tcr.202300244
6. Schreiber, S. L. *Science* **2000,** *287,* 1964–1969. doi:10.1126/science.287.5460.1964
7. Nören-Müller, A.; Reis-Corrêa, I., Jr.; Prinz, H.; Rosenbaum, C.; Saxena, K.; Schwalbe, H. J.; Vestweber, D.; Cagna, G.; Schunk, S.; Schwarz, O.; Schiewe, H.; Waldmann, H. *Proc. Natl. Acad. Sci. U. S. A.* **2006,** *103,* 10606–10611. doi:10.1073/pnas.0601490103
8. Ugi, I.; Werner, B.; Dömling, A. *Molecules* **2003,** *8,* 53–66. doi:10.3390/80100053
9. Van der Eycken, E.; Sharma, U. K., Eds. *Multicomponent Reactions towards Heterocycles: Concepts and Applications;* Wiley-VCH: Weinheim, Germany, 2022. doi:10.1002/9783527832439
10. Hulme, C.; Gore, V. *Curr. Med. Chem.* **2003,** *10,* 51–80. doi:10.2174/0929867033368600
11. Váradi, A.; Palmer, T. C.; Dardashti, R. N.; Majumdar, S. *Molecules* **2016,** *21,* 19. doi:10.3390/molecules21010019
12. Dömling, A.; Ugi, I. *Angew. Chem., Int. Ed.* **2000,** *39,* 3168–3210. doi:10.1002/1521-3773(20000915)39:18<3168::aid-anie3168>3.0.co;2-u
13. Zhu, J.; Bienayme, H., Eds. *Multicomponent Reactions;* Wiley-VCH: Weinheim, Germany, 2005. doi:10.1002/3527605118
14. Bode, M. L.; Gravestock, D.; Rousseau, A. L. *Org. Prep. Proced. Int.* **2016,** *48,* 89–221. doi:10.1080/00304948.2016.1138072
15. Fouad, M. A.; Abdel-Hamid, H.; Ayoup, M. S. *RSC Adv.* **2020,** *10,* 42644–42681. doi:10.1039/d0ra07501a
16. Murlykina, M. V.; Kolomiets, O. V.; Kornet, M. M.; Sakhno, Y. I.; Desenko, S. M.; Dyakonenko, V. V.; Shishkina, S. V.; Brazhko, O. A.; Musatov, V. I.; Tsygankov, A. V.; Van der Eycken, E. V.; Chebanov, V. A. *Beilstein J. Org. Chem.* **2019,** *15,* 1281–1288. doi:10.3762/bjoc.15.126
17. Kolomiiets, O. V.; Tsygankov, A. V.; Kornet, M. N.; Brazhko, A. A.; Musatov, V. I.; Chebanov, V. A. *Beilstein J. Org. Chem.* **2023,** *19,* 727–735. doi:10.3762/bjoc.19.53
18. Ugi, I. *Angew. Chem., Int. Ed. Engl.* **1982,** *21,* 810–819. doi:10.1002/anie.198208101
19. Bossio, R.; Marcos, C. F.; Marcaccini, S.; Pepino, R. *Tetrahedron Lett.* **1997,** *38,* 2519–2520. doi:10.1016/s0040-4039(97)00389-4
20. Bossio, R.; Marcos, C. F.; Marcaccini, S.; Pepino, R. *Heterocycles* **1997,** *45,* 1589–1592. doi:10.3987/com-97-7855
21. Marcos, C. F.; Bossio, R.; Marcaccini, S.; Pepino, R. *J. Chem. Educ.* **2000,** *77,* 382–384. doi:10.1021/ed077p382
22. Huang, J.; Du, X.; Van Hecke, K.; Van der Eycken, E. V.; Pereshivko, O. P.; Peshkov, V. A. *Eur. J. Org. Chem.* **2017,** 4379–4388. doi:10.1002/ejoc.201700747
23. Thessing, A.; Ayres, R.; Jones, J.; Bauer, H.; Zangi, M.; Luesse, S. B. *Results Chem.* **2022,** *4,* 100416. doi:10.1016/j.rechem.2022.100416
24. Kalinski, C.; Umkehrer, M.; Schmidt, J.; Ross, G.; Kolb, J.; Burdack, C.; Hiller, W.; Hoffmann, S. D. *Tetrahedron Lett.* **2006,** *47,* 4683–4686. doi:10.1016/j.tetlet.2006.04.127
25. Lu, K.; Luo, T.; Xiang, Z.; You, Z.; Fathi, R.; Chen, J.; Yang, Z. *J. Comb. Chem.* **2005,** *7,* 958–967. doi:10.1021/cc050099b
26. Pokhodylo, N. T.; Tupychak, M. A.; Goreshnik, E. A.; Obushak, M. D. *Synthesis* **2023,** *55,* 977–988. doi:10.1055/s-0042-1751382
27. Chandgude, A. L.; Li, J.; Dömling, A. *Asian J. Org. Chem.* **2017,** *6,* 798–801. doi:10.1002/ajoc.201700177
28. Strocker, A. M.; Keating, T. A.; Tempest, P. A.; Armstrong, R. W. *Tetrahedron Lett.* **1996,** *37,* 1149–1152. doi:10.1016/0040-4039(96)00012-3
29. Keating, T. A.; Armstrong, R. W. *J. Am. Chem. Soc.* **1995,** *117,* 7842–7843. doi:10.1021/ja00134a044
30. Gilley, C. B.; Buller, M. J.; Kobayashi, Y. *Org. Lett.* **2007,** *9,* 3631–3634. doi:10.1021/ol701446y
31. Neves Filho, R. A. W.; Stark, S.; Morejon, M. C.; Westermann, B.; Wessjohann, L. A. *Tetrahedron Lett.* **2012,** *53,* 5360–5363. doi:10.1016/j.tetlet.2012.07.064
32. van der Heijden, G.; Jong, J. A. W.; Ruijter, E.; Orru, R. V. A. *Org. Lett.* **2016,** *18,* 984–987. doi:10.1021/acs.orglett.6b00091
33. Hulme, C.; Ma, L.; Cherrier, M.-P.; Romano, J. J.; Morton, G.; Duquenne, C.; Salvino, J.; Labaudiniere, R. *Tetrahedron Lett.* **2000,** *41,* 1883–1887. doi:10.1016/s0040-4039(00)00052-6
34. Hollanders, C.; Elsocht, M.; Van der Poorten, O.; Jida, M.; Renders, E.; Maes, B. U. W.; Ballet, S. *Chem. Commun.* **2021,** *57,* 6863–6866. doi:10.1039/d1cc01701b
35. Balalaie, S.; Motaghedi, H.; Tahmassebi, D.; Bararjanian, M.; Bijanzadeh, H. R. *Tetrahedron Lett.* **2012,** *53,* 6177–6181. doi:10.1016/j.tetlet.2012.08.096
36. Borase, B. B.; Godbole, H. M.; Singh, G. P.; Upadhyay, P. R.; Trivedi, A.; Bhat, V.; Shenoy, G. G. *J. Chem. Sci.* **2021,** *133,* 35. doi:10.1007/s12039-021-01892-8
37. Zhi, S.; Ma, X.; Zhang, W. *Org. Biomol. Chem.* **2019,** *17,* 7632–7650. doi:10.1039/c9ob00772e

38. Barreto, A. d. F. S.; Santos, V. A. d.; Andrade, C. K. Z. *Beilstein J. Org. Chem.* **2017,** *13,* 2596–2602. doi:10.3762/bjoc.13.256
39. Mikhedkina, E. I.; Ananieva, V. V.; Tsygankov, A. V.; Osolodchenko, T. P.; Ponomarenko, S. V.; Chebanov, V. A. *Funct. Mater.* **2021,** *28,* 587–596. doi:10.15407/fm28.03.587
40. Mikhedkina, O. I.; Ananieva, V. V.; Sakhno, Y. I.; Melnyk, I. I.; Vereshchak, V. O.; Osolodchenko, T. P.; Shishkina, S. V.; Tsygankov, A. V.; Chebanov, V. A. *Chem. Heterocycl. Compd.* **2023,** *59,* 449–455. doi:10.1007/s10593-023-03215-w
41. Peixoto, I. N.; Souza, H. D. S.; Lira, B. F.; Silva, D. F.; Lima, E. O.; José, B.-F.; Athayde-Filho, P. F. *J. Braz. Chem. Soc.* **2016,** *27,* 1807–1813. doi:10.5935/0103-5053.20160063

License and Terms

This is an open access article licensed under the terms of the Beilstein-Institut Open Access License Agreement (https://www.beilstein-journals.org/bjoc/terms), which is identical to the Creative Commons Attribution 4.0 International License (https://creativecommons.org/licenses/by/4.0). The reuse of material under this license requires that the author(s), source and license are credited. Third-party material in this article could be subject to other licenses (typically indicated in the credit line), and in this case, users are required to obtain permission from the license holder to reuse the material.

The definitive version of this article is the electronic one which can be found at:
https://doi.org/10.3762/bjoc.20.156

BEILSTEIN JOURNAL OF ORGANIC CHEMISTRY

A facile three-component route to powerful 5-aryldeazaalloxazine photocatalysts

Ivana Weisheitelová[‡1], Radek Cibulka[1], Marek Sikorski[2] and Tetiana Pavlovska[*,‡1]

Full Research Paper

Open Access

Address:
[1]Department of Organic Chemistry, University of Chemistry and Technology, Prague, Czech Republic and [2]Faculty of Chemistry, Adam Mickiewicz University, Poznań, Poland

Email:
Tetiana Pavlovska[*] - pavlovst@vscht.cz

* Corresponding author ‡ Equal contributors

Keywords:
catalysis; deazaalloxazine; flavin; multicomponent approach; one-pot reaction

Beilstein J. Org. Chem. **2024,** *20,* 1831–1838.
https://doi.org/10.3762/bjoc.20.161

Received: 21 May 2024
Accepted: 16 July 2024
Published: 31 July 2024

This article is part of the thematic issue "Multicomponent reactions IV".

Associate Editor: T. J. J. Müller

© 2024 Weisheitelová et al.; licensee Beilstein-Institut.
License and terms: see end of document.

Abstract

Functionalized 5-aryldeazaalloxazines have been successfully synthesised through a one-pot, three-component reaction involving *N,N*-dimethylbarbituric acid, an aromatic aldehyde and aniline. By utilizing readily available reagents, this approach opens up the opportunity for the efficient formation of a variety of 5-aryldeazaalloxazines bearing electron-donating or halogen groups. This practical method is characterised by atom economy and offers a direct route to the introduction of an aryl moiety into the C(5)-position of deazaalloxazines, thereby generating novel catalysts for photoredox catalysis without the need for subsequent purification. Thus, it significantly improves existing approaches.

Introduction

Heterocyclic compounds containing pyrimidine and quinoline motifs in their structure, both of natural and synthetic origin, find a wide set of applications in medicinal chemistry, chemosensors, polymers and catalysis [1-8]. Among them, flavins (Fl) are essential redox-active natural compounds that act as enzyme cofactors in numerous biochemical processes [9]. Structurally related to flavins are isomeric alloxazines (All) and also 5-deazaflavins (dFl) and 5-deazaalloxazines (dAll), where the N(5) atom of the isoalloxazine/alloxazine core is replaced by a C–H moiety (Figure 1A). In particular, 5-deazaflavins have generated considerable interest from scientists to study flavin-catalysed reactions in enzymatic and artificial systems. Additionally, 5-deazaflavins have emerged as prospective antitumor agents [9,10]. Surprisingly, among the broad family of flavin derivatives, 5-deazaalloxazines have received less attention regarding their photophysical properties, despite their close similarity to the above-mentioned 5-deazaflavins [11-13]. Recently, it has been discovered that both 5-deazaflavins **1** and 5-deazaalloxazines **2**, which have an aryl substituent in position C(5), form stable radicals that act as powerful reductive photocatalysts with a reducing power comparable to that of lithium [E^*(**1/1**$^{\bullet}$) = −3.3 V vs SCE, value for Ar = Ph] [14-18]

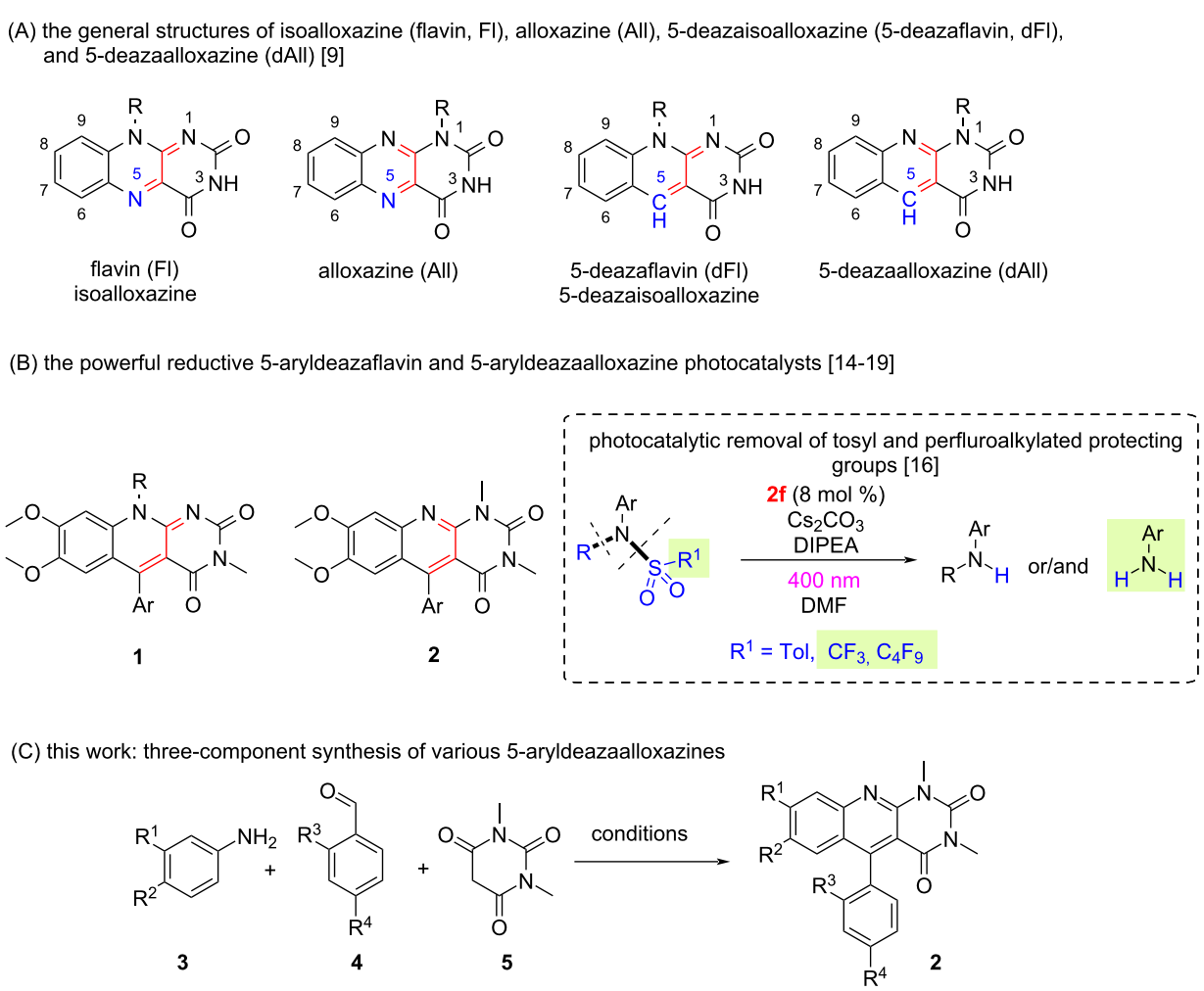

Figure 1: (A) The general structures of isoalloxazine (flavin, **Fl**), alloxazine (**All**), 5-deazaisoalloxazine (5-deazaflavin, **dFl**), and 5-deazaalloxazine (**dAll**). (B) The powerful reductive photocatalysts: 5-aryldeazaflavin (**1**) and 5-aryldeazaalloxazine (**2**). (C) This work, which describes an efficient three-component method for the synthesis of **2**.

(Figure 1B). 5-Aryldeazaalloxazines **2** have been found to be even more powerful reductants than **1** due to their more negative ground-state reduction potential by ca. 300 mV. Moreover, **2** exhibits higher photostability than **1**. Consequently, 5-aryldeazaalloxazine **2f** has been successfully applied as photoredox catalyst in the synthesis of secondary or primary anilines via light-dependent desulfonylation or desulfonylation/dealkylation procedures [19].

Thus, the design of novel and efficient routes for the synthesis of 5-aryldeazaalloxazines **2** has become a significant topic. Surprisingly, there has been limited information on 5-deazaalloxazines (dAll) synthesis [20-22]. Most known methods employ the cyclization of 6-(arylamino)uracils with one-carbon reagents such as triethyl orthoformate, dimethylformamide dimethylacetal, carbon disulfide, *N,N*-dimethyldichloromethyleniminium chloride and the Vilsmeier reagent, or condensations between *o*-aminobenzaldehydes and barbituric acid [20,21,23-27]. Neither of these methods allows for the introduction of an aryl substituent into C(5), which confers unique chemical and physical properties on 5-aryldeazaalloxazines **2**, as demonstrated in our previous studies with 5-aryldeazaflavins **1** [14-18].

Multicomponent reactions (MCRs) remain a powerful strategy in synthetic organic chemistry due to their widespread applications in drug discovery. By offering significant advantages over conventional, linear-type syntheses, MCRs have become helpful tools for more efficient preparation of chemical libraries with higher molecular diversity and complexity in fewer steps and less time [28,29].

Considering the limitations of existing methods, as well as the applications of 5-aryldeazaalloxazines **2**, and in the continua-

tion of our work on the synthesis of powerful photoredox flavins [14-19], we developed an efficient, general, one-pot domino method for the synthesis of a series of novel 5-aryldeazaalloxazines **2** from readily available substrates via a three-component fashion (Figure 1C).

Results and Discussion

Regarding the synthesis of 5-aryldeazaalloxazines **2** (5-arylpyrimido[4,5-*b*]quinoline-2,4(1*H*,3*H*)-diones), the data in the literature are quite limited, and the known methodology describes the dehydrogenation of initially formed 5,10-dihydro analogues (5-aryl-5,10-dihydropyrimido[4,5-*b*]quinoline-2,4(1*H*,3*H*)-dione) by refluxing with thionyl chloride [20,23]. However, the preparation of partially hydrogenated 5,10-dihydropyrimido[4,5-*b*]quinolinediones has been repeatedly reported by one-pot condensation of substituted anilines, aldehydes and barbituric acids, usually in protic solvents (alcohols, water), which has become a common method for the synthesis of these derivatives [3,22,25,30-33].

In our previous studies [14-19] we have shown that the 5-aryl and 7,8-substitutients of the pyrimido[4,5-*b*]quinoline core have a significant effect on the photocatalytic activity of photocatalysts by tuning their redox and photophysical properties. Thus, we successfully developed a one-pot, three-component synthetic method with those substituents in 5-aryldeazaflavins **1** on the deazaisoalloxazine core or on the phenyl ring by condensation of *N*-substituted anilines, aromatic aldehydes and *N*-methylbarbituric acid in AcOH/PPA (polyphosphoric acid). However, this method was not successful for the synthesis of 5-aryldeazaalloxazines **2**, and we never observed the formation of 5,10-dihydropyrimido[4,5-*b*]quinolinediones either. We noticed that the chemical nature of the solvent was highly important for the outcome of this reaction. Thus, we decided to significantly improve our approach by optimizing the reaction conditions of a three-component condensation of commercially available 3,4-dimethylaniline (**3a**, 1.0 mmol), benzaldehyde (**4a**, 1.0 mmol) and *N*,*N*-dimethylbarbituric acid (**5**, 1.0 mmol).

As illustrated in Table 1, DMSO was preferred as the optimal solvent, and 130 °C was chosen as the most suitable reaction temperature (Table 1, entry 1). Other solvents showed low yields, or the product was not isolated at all. However, we found that the yield of 5-phenyldeazaalloxazine **2a** was significantly enhanced when refluxing in DMF with a catalytic amount of $AlCl_3$ compared to the reaction in clear DMF (Table 1, entries 7–9). Other Lewis acids were not as effective, except for a combination of DMSO/TMSOTf (Table 1, entry 4). The application of AcOH/PPA for the synthesis of 5-aryldeazaflavins did not improve the result of the reaction

Table 1: Optimization of the reaction conditions for the synthesis of **2a**.

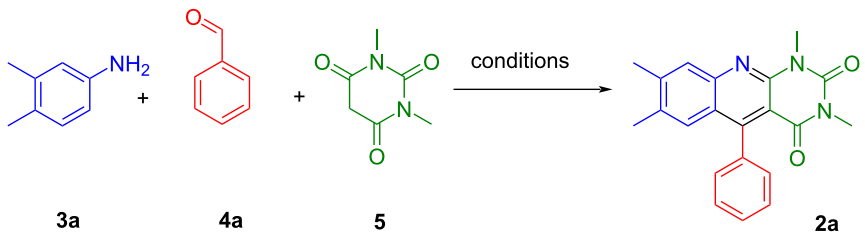

3a **4a** **5** **2a**

Entry	Solvent	Time (h)	Volume (mL)	Additive	Conditions	Yield[a] (%)
1	DMSO	15	**2**	–	CH	**57**
2	DMSO	15	**10**	–	CH	52
3	DMSO	15	2	**$AlCl_3$**	CH	**55**
4	DMSO	15	2	**TMSOTf**	CH	**48**
5	DMSO	1	2	–	**MW**	32
6	DMSO	1	2	$AlCl_3$	**MW**	39
7	DMF	15	2	–	CH	11
8	DMF	15	2	**$AlCl_3$**	CH	**41**
9	DMF	1	2	$AlCl_3$	**MW**	26
10	AcOH	15	2	PPA	CH	28
11	AcOH	15	2	H_2SO_4	CH	33
12	AcOH	1	2	H_2SO_4	MW	37[b]

[a]The isolated yields were calculated on the quantities of the starting materials **1–3**. [b]The product was contaminated with resinificated impurities.

(Table 1, entry 10). We also found that the yield of **2a** may be slightly affected by the volume of solvent, with increasing amounts of impurities in larger volumes.

We also tested the response of the **2a** formation to MW irradiation and under conventional heating conditions (CH). Syntheses were performed in DMSO, DMSO/$AlCl_3$, DMF/$AlCl_3$ and AcOH/H_2SO_4 at 110 °C (Table 1, entries 5, 6, 9, and 12). Under these conditions, the reaction time was significantly reduced to 1 hour from the usual 15 hours, however, the yields stayed in the range of 30%, and the reaction mixtures contained a large number of impurities.

In summary, standard heating conditions exhibited distinct advantages over MW, and the reaction performance in DMSO was the most effective. Moreover, DMSO is considered an environmentally friendly solvent (for detailed information on reaction condition optimisation, see Supporting Information File 1).

Under optimised reaction conditions (DMSO, 130 °C unless otherwise indicated, 15 h), a series of 5-aryldeazaalloxazines **2a**–**x** was synthesised in the 3.0 mmol scale with moderate to good yields (Scheme 1). Our protocol was successfully applied to various anilines and aromatic aldehydes with electron-donating groups or electron-withdrawing halogen atoms. However, the reaction yield was affected by the nature of the substituent on the aniline moiety. The results suggest that substrates bearing electron-donating groups on anilines have higher reactivity, thus giving higher yields than those bearing electron-withdrawing groups. The best reactivity was observed for 3,4-dimethylaniline (**3a**) and 3,4-dimethoxyaniline (**3b**) with the isolation of 5-aryldeazaalloxazines **2a**–**h,** with yields of 43–79%. Additionally, 5-aryldeazaalloxazines bearing methoxy substituents at positions 7 and 8 of the deazaalloxazine ring (see Figure 1 for numeration) showed the best reactivity as reductive photocatalysts. Such an outcome of MCR opens up the possibility of their production on a larger scale for commercial needs. However, the synthesis of the 7- and 8-methoxy derivatives, **2i**–**l** and **2m**–**p**, respectively, was accompanied by several complications, and the isolation of the products required precipitation with 2-propanol in several cases. The heating time was prolonged to two days for 8-methoxy derivatives **2m**–**p**, nevertheless giving moderate yields. For 7-methoxy derivatives **2i**–**k**, we changed the solvent to DMF/$AlCl_3$, which increased the yields to 41–45%. However, the 7-methoxy derivative **2l** with *o*-methyl substituent in the aldehyde moiety precipitated in DMSO after two days of reaction time. Interestingly, we observed only traces of another possible regioisomer **2m'** with a methoxy group in position C(6) in the ^{1}H NMR spectrum when using *m*-anisidine (**3c**) only with benzaldehyde (**4b**, for detailed information, see Supporting Information File 1). It should be mentioned that three-component condensation leading to the formation of 5-aryldeazaflavins **1** usually proceeds via Knoevenagel adduct formation as a first step, which may become a significant limitation of this reaction. However, we have never observed and isolated Knoevenagel adducts of aromatic aldehydes **4** and *N,N*-dimethylbarbituric acid (**5**) during the synthesis of 5-aryldeazaalloxazines **2a**–**x** in either of the described conditions.

The halogen groups on the anilines slightly decreased their reactivity, leading to the formation of products **2q**–**w** with lower yields. However, the 8-chlorine derivative **2u** with a *o*-tolyl aldehyde moiety was prepared with a yield of 37%. Aromatic aldehydes bearing bromine and methyl substituents were chosen to enhance the photophysical properties and photostability of the desired photocatalysts. It should be noted that our method encountered limitations when applying strongly deactivated anilines substituted with CF_3 or acetyl groups, with no formation of 5-aryldeazaalloxazines in any case. Finally, the unsubstituted derivative **2x** was formed with a yield of only 15% using DMF/$AlCl_3$.

The isolated products **2a**–**x** were characterized by ^{1}H, ^{13}C NMR and mass-spectral methods. The ^{1}H NMR spectra of 5-aryldeazaalloxazines **2a**–**x**, along with protons of aryl substituents of aldehyde moiety and pyrimido[4,5-*b*]quinoline core, contained singlets with 3H intensity of the N(1)–CH_3 and N(3)–CH_3 groups of the barbituric acid fragment at 3.20–3.56 ppm. The ^{13}C NMR spectra of 5-aryldeazaalloxazines **2a**–**x** were represented by groups of singlets at 27.9–57.2 and 100.0–160.5 ppm. The characteristic signals of the carbonyl atoms were seen as singlets at 155.6–160.5 ppm. Signals of the carbon atoms of the pyrimido[4,5-*b*]quinoline ring were located in the resonance region of the carbon atoms of the aryl substituents. Taken together, these data indicate the formation of the 5-arylpyrimido[4,5-*b*]quinoline-2,4(1*H*,3*H*)-dione cyclic system.

The absorption spectra of the methoxy derivatives **2f**, **2j** and **2n** in DMF provide interesting information on the effect of the position of the methoxy group in the core of deazaalloxazine on the absorption maxima (Figure 2). The 8-methoxydeazaalloxazine **2n** exhibited a characteristic band at 353 nm ($\varepsilon = 24.4 \times 10^3$ $M^{-1}\cdot cm^{-1}$), while it moved to 370 nm for 7,8-dimethoxydeazaalloxazine **2f** ($\varepsilon = 26.2 \times 10^3$ $M^{-1}\cdot cm^{-1}$) and even to 387 nm ($\varepsilon = 12.2 \times 10^3$ $M^{-1}\cdot cm^{-1}$) for 7-methoxydeazaalloxazine **2j**. This indicates that, besides the 7,8-dimethoxy derivatives usually studied in deazaflavin/alloxazine photoredox catalysis [9,14-19], 7-methoxyderivatives should also be considered due to their absorption closer to the visible light

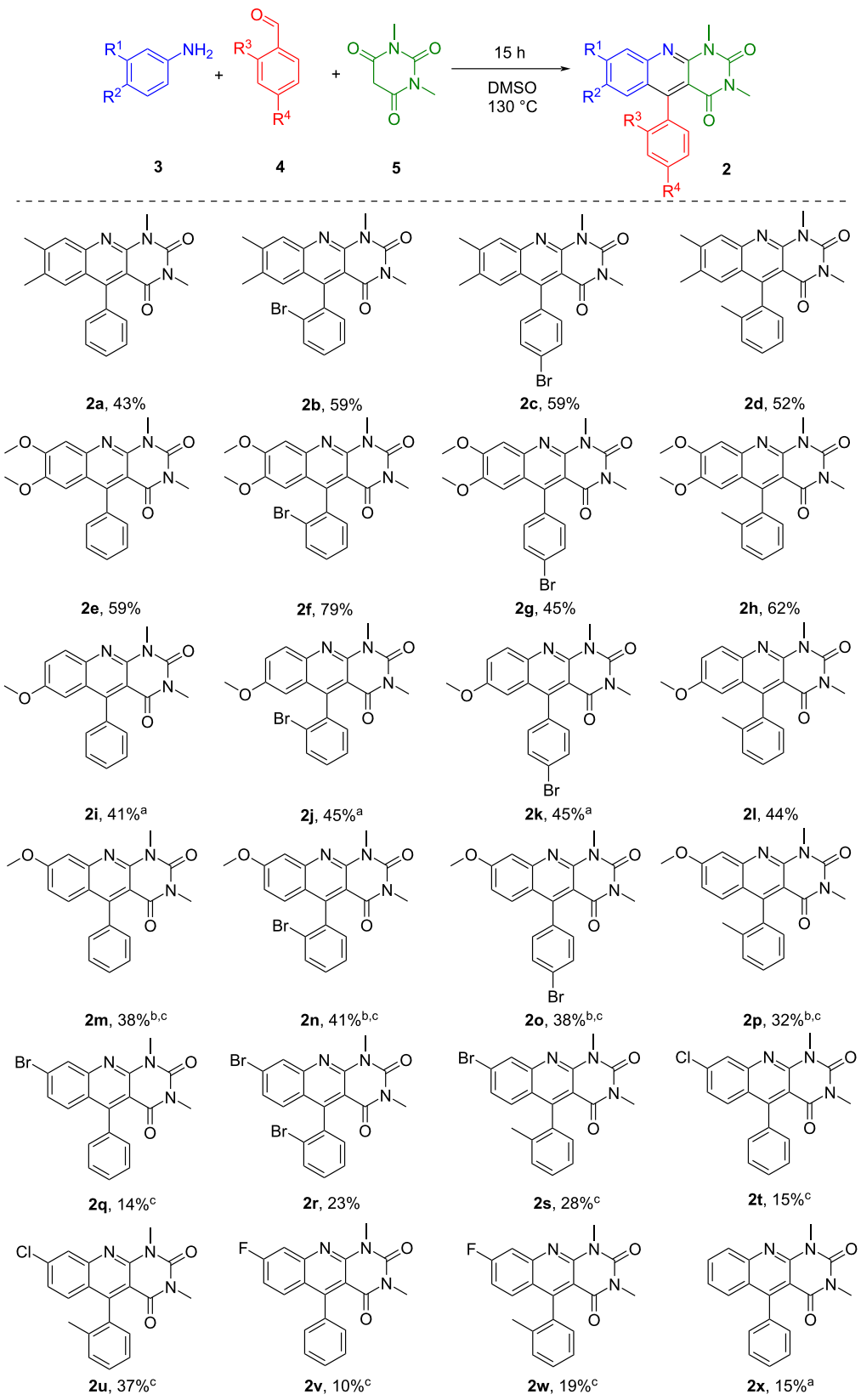

Scheme 1: Three-component condensation of anilines, aldehydes and *N*,*N*-dimethylbarbituric acid. [a]Reaction was done in DMF/$AlCl_3$. [b]Isolation requires precipitation with 2-propanol. [c]2 days.

region. This allows longer wavelength LEDs with lower energy photons to be applied, potentially contributing to avoiding undesired reactions [14-17,34].

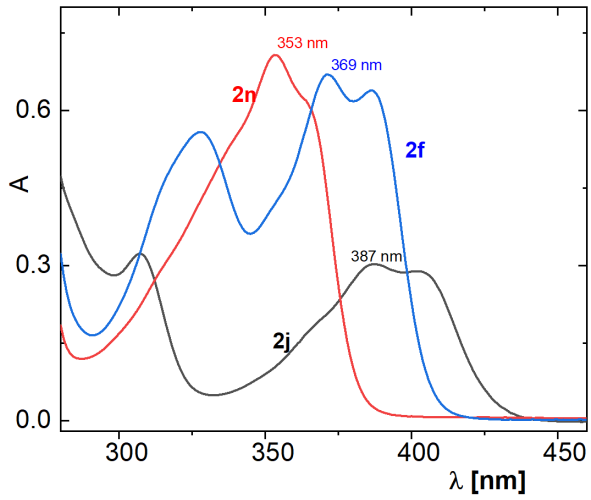

Figure 2: UV–vis absorption spectra of 5-arydeazaalloxazines **2f**, **2j** and **2n** in DMF (l = 1 cm, c = 2.50 × 10^{-5} mol·L^{-1}).

When investigating the possibility of the introduction of bulky aldehyde fragments (for example, with mesitaldehyde (**4e**)), we did not observe the formation of 5-aryldeazaalloxazine **2y**; however, we discovered the formation of 5-deazaalloxazine **6** with DMSO as a solvent (Scheme 2A). The unexpected structure of product **6** was confirmed by ^{1}H, ^{13}C NMR and mass spectrometry. The main feature of the ^{1}H NMR spectrum of compound **6** is the absence of the signals of the aromatic aldehyde moiety and the appearance of the singlet of the 5-CH methyne group at 9.56 ppm and the singlets of the protons of the benzene ring of the 5-deazaalloxazine core at 7.64 and 7.71 ppm. To support this theory, we conducted a control experiment between 3,4-dimethoxyaniline (**3b**) and *N*,*N*-dimethylbarbituric acid (**5**) in DMSO. To our delight, 5-deazaalloxazine **6** was formed (Scheme 2B). To prove that DMSO was the methylene source in this reaction, a deuterium labelling experiment was conducted (Scheme 2C). Indeed, the deazaalloxazine derivative **6-*d*** with quantitative incorporation of deuterium in C(5) position, was isolated and confirmed by ^{1}H NMR analysis and mass spectrometry (for more details on possible reaction mechanism, see Supporting Information File 1).

Such results with previous reports on DMSO acting as a methine source in the synthesis of heterocyclic compounds [35,36] are opening a new avenue for the green synthesis of non-substituted 5-deazaalloxazines in a pseudo MCR fashion.

Conclusion

In summary, we have developed a facile, efficient and environmentally friendly method for the synthesis of 5-aryldeazaalloxazine (5-arylpyrimido[4,5-*b*]quinoline-2,4(1*H*,3*H*)-dione) derivatives via three-component reactions in DMSO, with the possibility of varying reaction conditions. Although the yields of the

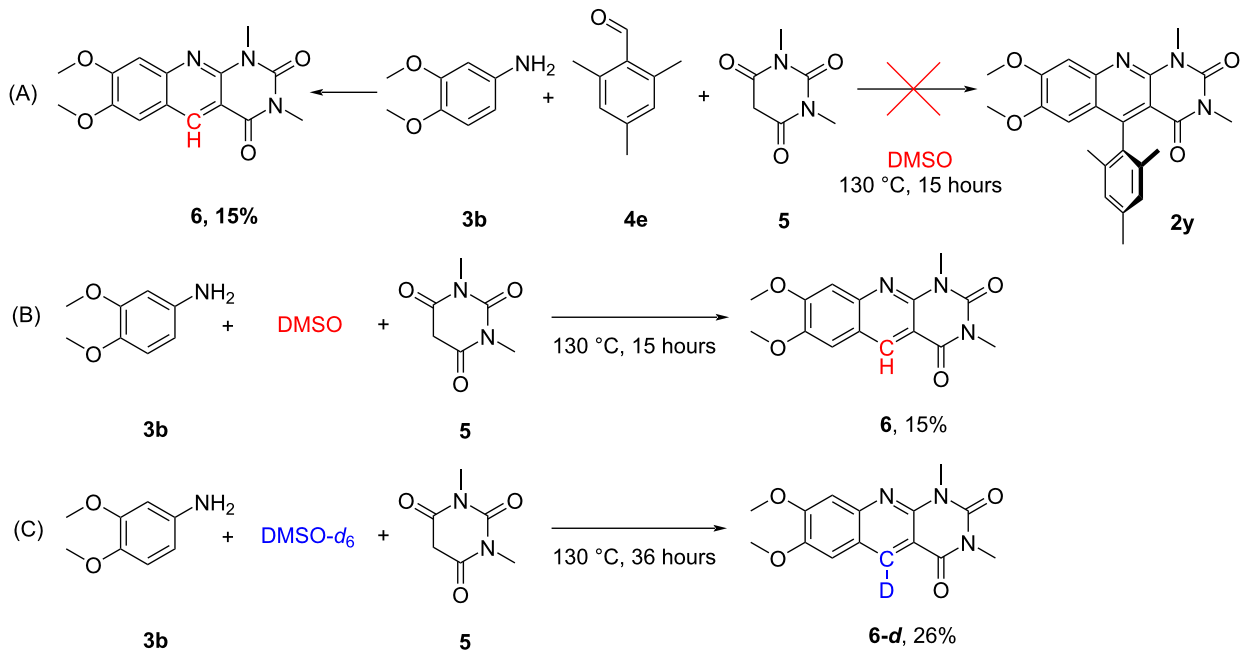

Scheme 2: Control experiments related to bulky substituted aldehydes.

reaction vary from low to moderate, the reaction starts from commercially available substances and leads to valuable compounds. The procedure is low cost and operationally easy with no need for further purification and opens a new route to the synthesis of powerful, phoredox, flavin-like catalysts, as well as potent, biologically active compounds. Interestingly, the introduction of a strong methoxy group at position 7 of the 5-aryldeazaalloxazine core led to a bathochromic shift in the absorption spectra of the synthesised molecules, making them more suitable for visible light photocatalysis.

Experimental

Reagents and analytics: Starting materials were purchased from Sigma-Aldrich and Fluorochem. The solvents were purified and dried using standard procedures. Commercially obtained reagents were used as received without further purification unless otherwise stated. The compound structures were drawn and named using ChemDraw. Nuclear magnetic resonance (NMR) spectra were recorded on an Agilent 400-MR DDR2 (399.94 MHz for ^{1}H, 100.58 MHz for ^{13}C, 376.50 MHz for ^{19}F) or on a JNM-ECZ500R NMR spectrometer, JEOL Resonance, (500.16 MHz for ^{1}H, 125.77 MHz for ^{13}C, 470.60 MHz for ^{19}F) at 298 K unless otherwise indicated. Data for ^{1}H NMR are reported as follows: chemical shift (δ ppm), multiplicity (s = singlet, d = doublet, t = triplet, q = quartet, m = multiplet, dd = doublet of doublets, dt = doublet of triplets, br = broad etc.), coupling constant (Hz), and integration. All NMR spectra were processed and assigned using MestreNova. High-resolution mass spectra were obtained on Q-Tof Micro (Waters), equipped with a quadrupole and time-of-flight (TOF) analyser and a multichannel plate (MCP) detector. The melting points were measured on a Boetilus melting point apparatus and are not corrected.

UV–vis spectra were recorded on Agilent Cary 8454 spectrophotometer at 25 °C in analytical-grade DMF. Absorption spectra were processed by using Microsoft Excel and Origin 2018 (OriginLab).

Typical procedure for the synthesis of 5-aryldeazaalloxazines 2: An equimolar mixture (3.0 mmol) of the corresponding aniline **3**, aromatic aldehyde **4**, and *N*,*N*-dimethylbarbituric acid (**5**) was dissolved in 6 mL DMSO or DMF/$AlCl_3$ (cat.) and heated at 130 °C until a precipitate was formed (ca. 15 h). After completion, the precipitated product was filtered, washed with 2-propanol and dried under vacuum. **2a**: white solid, 43%; mp 325–327 °C; ^{1}H NMR (400 MHz, DMSO-d_6) δ 7.82 (s, 1H), 7.55–7.46 (m, 3H), 7.23–7.17 (m, 2H), 6.97 (s, 1H), 3.71 (s, 3H), 3.17 (s, 3H), 2.44 (s, 3H), 2.23 (s, 3H); ^{13}C NMR (126 MHz, TFA-*d*) δ 166.0, 159.4, 153.7, 149.7, 146.5, 141.3, 136.1, 133.3, 129.8, 129.4, 128.5, 126.4, 124.1, 118.3, 106.9, 30.5, 28.8, 19.6, 18.1; HRMS (APCI$^+$) *m*/*z*: [M + H$^+$] calcd for $C_{21}H_{19}N_3O_2$, 346.1477; found, 346.1547.

Supporting Information

Supporting Information File 1

Spectroscopic and analytical data.
[https://www.beilstein-journals.org/bjoc/content/supplementary/1860-5397-20-161-S1.pdf]

Funding

This work was supported by the Czech Science Foundation (Grant No 21-14200K) and by the research grant CEUSUNISONO 2020/02/Y/ST4/00042, from The National Science Centre of Poland (NCN). I. W. thanks for support from Specific university research (reg. No. A2_FCHT_2023_025).

Author Contributions

Ivana Weisheitelová: conceptualization; data curation; formal analysis; funding acquisition; investigation; methodology; project administration; resources; validation; visualization; writing – original draft. Radek Cibulka: conceptualization; funding acquisition; project administration; resources; supervision; validation; writing – review & editing. Marek Sikorski: funding acquisition; project administration; resources; writing – review & editing. Tetiana Pavlovska: conceptualization; data curation; formal analysis; investigation; methodology; project administration; resources; supervision; validation; visualization; writing – original draft; writing – review & editing.

ORCID® iDs

Ivana Weisheitelová - https://orcid.org/0000-0002-3578-7582
Radek Cibulka - https://orcid.org/0000-0002-8584-7715
Marek Sikorski - https://orcid.org/0000-0002-9527-7322
Tetiana Pavlovska - https://orcid.org/0000-0002-3540-5863

Data Availability Statement

All data that supports the findings of this study is available in the published article and/or the supporting information to this article.

References

1. Singh, K.; Kaur, H.; Smith, P.; de Kock, C.; Chibale, K.; Balzarini, J. *J. Med. Chem.* **2014,** *57,* 435–448. doi:10.1021/jm4014778
2. Pretorius, S. I.; Breytenbach, W. J.; de Kock, C.; Smith, P. J.; N'Da, D. D. *Bioorg. Med. Chem.* **2013,** *21,* 269–277. doi:10.1016/j.bmc.2012.10.019
3. Panday, A. K.; Mishra, R.; Jana, A.; Parvin, T.; Choudhury, L. H. *J. Org. Chem.* **2018,** *83,* 3624–3632. doi:10.1021/acs.joc.7b03272
4. Tran, T. N.; Henary, M. *Molecules* **2022,** *27,* 2700. doi:10.3390/molecules27092700

5. Mal, K.; Naskar, B.; Chaudhuri, T.; Prodhan, C.; Goswami, S.; Chaudhuri, K.; Mukhopadhyay, C. *J. Photochem. Photobiol., A* **2020,** *389,* 112211. doi:10.1016/j.jphotochem.2019.112211
6. Hirota, K.; Maruhashi, K.; Asao, T.; Kitamura, N.; Maki, Y.; Senda, S. *Chem. Pharm. Bull.* **1983,** *31,* 3959–3966. doi:10.1248/cpb.31.3959
7. Chae, J. B.; Lee, H.; Kim, C. *J. Fluoresc.* **2020,** *30,* 347–356. doi:10.1007/s10895-020-02501-6
8. Yamamoto, T.; Lee, B.-L. *Macromolecules* **2002,** *35,* 2993–2999. doi:10.1021/ma011632o
9. Pavlovska, T.; Cibulka, R. Structure and Properties of Flavins. In *Flavin-Based Catalysis: Principles and Applications,* 1st ed.; Cibulka, R.; Fraaije, M., Eds.; Wiley-VCH: Weinheim, Germany, 2021; pp 1–27. doi:10.1002/9783527830138.ch1
10. Bedewy, W. A.; Mohamed, M. S.; Abdelhameed, A. M.; Elsawy, M. A.; Al-Muhur, M.; Ashida, N.; Abdalla, A. N.; Elwaie, T. A.; Nagamatsu, T.; Ali, H. I. *J. Enzyme Inhib. Med. Chem.* **2023,** *38,* 2220570. doi:10.1080/14756366.2023.2220570
11. Insińska-Rak, M.; Golczak, A.; Gierszewski, M.; Anwar, Z.; Cherkas, V.; Kwiatek, D.; Sikorska, E.; Khmelinskii, I.; Burdziński, G.; Cibulka, R.; Mrówczyńska, L.; Kolanowski, J. L.; Sikorski, M. *Photochem. Photobiol. Sci.* **2023,** *22,* 1655–1671. doi:10.1007/s43630-023-00401-9
12. Prukała, D.; Gierszewski, M.; Karolczak, J.; Sikorski, M. *Phys. Chem. Chem. Phys.* **2015,** *17,* 18729–18741. doi:10.1039/c5cp01566a
13. Prukała, D.; Taczkowska, M.; Gierszewski, M.; Pędziński, T.; Sikorski, M. *J. Fluoresc.* **2014,** *24,* 505–521. doi:10.1007/s10895-013-1320-9
14. Pavlovska, T.; Král Lesný, D.; Svobodová, E.; Hoskovcová, I.; Archipowa, N.; Kutta, R. J.; Cibulka, R. *Chem. – Eur. J.* **2022,** *28,* e202200768. doi:10.1002/chem.202200768
15. Pokluda, A.; Anwar, Z.; Boguschová, V.; Anusiewicz, I.; Skurski, P.; Sikorski, M.; Cibulka, R. *Adv. Synth. Catal.* **2021,** *363,* 4371–4379. doi:10.1002/adsc.202100024
16. Tolba, A. H.; Vávra, F.; Chudoba, J.; Cibulka, R. *Eur. J. Org. Chem.* **2020,** 1579–1585. doi:10.1002/ejoc.201901628
17. Obertík, R.; Chudoba, J.; Šturala, J.; Tarábek, J.; Ludvíková, L.; Slanina, T.; König, B.; Cibulka, R. *Chem. – Eur. J.* **2022,** *28,* e202202487. doi:10.1002/chem.202202487
18. Graml, A.; Neveselý, T.; Jan Kutta, R.; Cibulka, R.; König, B. *Nat. Commun.* **2020,** *11,* 3174. doi:10.1038/s41467-020-16909-y
19. Pavlovska, T.; Weisheitelová, I.; Pramthaisong, C.; Sikorski, M.; Jahn, U.; Cibulka, R. *Adv. Synth. Catal.* **2023,** *365,* 4662–4671. doi:10.1002/adsc.202300843
20. Nishigaki, S.; Sato, J.; Shimizu, K.; Furukawa, K.; Senga, K.; Yoneda, F. *Chem. Pharm. Bull.* **1980,** *28,* 142–149. doi:10.1248/cpb.28.142
21. Dudkin, S.; Iaroshenko, V. O.; Sosnovskikh, V. Ya.; Tolmachev, A. A.; Villinger, A.; Langer, P. *Org. Biomol. Chem.* **2013,** *11,* 5351–5361. doi:10.1039/c3ob26837c
22. Youssif, S. *Monatsh. Chem.* **1999,** *130,* 819–825. doi:10.1007/pl00010263
23. Yoneda, F.; Tsukuda, K.; Shinozuka, K.; Hirayama, F.; Uekama, K.; Koshiro, A. *Chem. Pharm. Bull.* **1980,** *28,* 3049–3056. doi:10.1248/cpb.28.3049
24. Kokel, B. *J. Heterocycl. Chem.* **1994,** *31,* 845–855. doi:10.1002/jhet.5570310427
25. Verma, C.; Olasunkanmi, L. O.; Obot, I. B.; Ebenso, E. E.; Quraishi, M. A. *RSC Adv.* **2016,** *6,* 15639–15654. doi:10.1039/c5ra27417f
26. Chandra, A.; Upadhyay, S.; Singh, B.; Sharma, N.; Singh, R. M. *Tetrahedron* **2011,** *67,* 9219–9224. doi:10.1016/j.tet.2011.09.032
27. Shen, Q.; Wang, L.; Yu, J.; Liu, M.; Qiu, J.; Fang, L.; Guo, F.; Tang, J. *Synthesis* **2012,** *44,* 389–392. doi:10.1055/s-0031-1289657
28. Graziano, G.; Stefanachi, A.; Contino, M.; Prieto-Díaz, R.; Ligresti, A.; Kumar, P.; Scilimati, A.; Sotelo, E.; Leonetti, F. *Int. J. Mol. Sci.* **2023,** *24,* 6581. doi:10.3390/ijms24076581
29. Cores, Á.; Clerigué, J.; Orocio-Rodríguez, E.; Menéndez, J. C. *Pharmaceuticals* **2022,** *15,* 1009. doi:10.3390/ph15081009
30. Khalafi-Nezhad, A.; Sarikhani, S.; Shahidzadeh, E. S.; Panahi, F. *Green Chem.* **2012,** *14,* 2876–2884. doi:10.1039/c2gc35765h
31. Mahmoud, S.; Samaha, D.; Mohamed, M. S.; Abou Taleb, N. A.; Elsawy, M. A.; Nagamatsu, T.; Ali, H. I. *Molecules* **2020,** *25,* 2518. doi:10.3390/molecules25112518
32. Pandey, A. M.; Digrawal, N. K.; Mohanta, N.; Jamdade, A. B.; Chaudhari, M. B.; Bisht, G. S.; Gnanaprakasam, B. *J. Org. Chem.* **2021,** *86,* 8805–8828. doi:10.1021/acs.joc.1c00714
33. Sharma, M.; Borah, P.; Bhuyan, P. J. *Synth. Commun.* **2015,** *45,* 1792–1798. doi:10.1080/00397911.2015.1045081
34. Marzo, L.; Pagire, S. K.; Reiser, O.; König, B. *Angew. Chem., Int. Ed.* **2018,** *57,* 10034–10072. doi:10.1002/anie.201709766
35. Yadav, P.; Awasthi, A.; Gokulnath, S.; Tiwari, D. K. *J. Org. Chem.* **2021,** *86,* 2658–2666. doi:10.1021/acs.joc.0c02696
36. Shi, X.; Zhang, Q.; Wang, A.; Jiang, T.-S. *Adv. Synth. Catal.* **2022,** *364,* 2086–2090. doi:10.1002/adsc.202200284

License and Terms

This is an open access article licensed under the terms of the Beilstein-Institut Open Access License Agreement (https://www.beilstein-journals.org/bjoc/terms), which is identical to the Creative Commons Attribution 4.0 International License (https://creativecommons.org/licenses/by/4.0). The reuse of material under this license requires that the author(s), source and license are credited. Third-party material in this article could be subject to other licenses (typically indicated in the credit line), and in this case, users are required to obtain permission from the license holder to reuse the material.

The definitive version of this article is the electronic one which can be found at:
https://doi.org/10.3762/bjoc.20.161

BEILSTEIN JOURNAL OF ORGANIC CHEMISTRY

The Groebke–Blackburn–Bienaymé reaction in its maturity: innovation and improvements since its 21st birthday (2019–2023)

Cristina Martini[1], Muhammad Idham Darussalam Mardjan[*2] and Andrea Basso[*1]

Review

Open Access

Address:
[1]Dipartimento di Chimica e Chimica Industriale, Università degli Studi di Genova, Via Dodecaneso 31, 16146 Genova, Italy and
[2]Department of Chemistry, Universitas Gadjah Mada, Bulaksumur, Sekip Utara, Yogyakarta 55281, Indonesia

Email:
Muhammad Idham Darussalam Mardjan[*] - idham.darussalam@ugm.ac.id; Andrea Basso[*] - andrea.basso@unige.it

* Corresponding author

Keywords:
Groebke–Blackburn–Bienaymé reaction; multicomponent reactions; heterocycles; imidazo[1,2-*a*]pyridines; isocyanides

Beilstein J. Org. Chem. **2024,** *20,* 1839–1879.
https://doi.org/10.3762/bjoc.20.162

Received: 06 May 2024
Accepted: 12 July 2024
Published: 01 August 2024

This article is part of the thematic issue "Multicomponent reactions IV".

Associate Editor: T. J. J. Müller

© 2024 Martini et al.; licensee Beilstein-Institut.
License and terms: see end of document.

Abstract

The Groebke–Blackburn–Bienaymé (GBB) three-component reaction, discovered in 1998, is a very efficient strategy to assemble imidazo[1,2-*a*]-heterocycles starting from amidines, aldehydes and isocyanides. This review aims to exhaustively describe innovative aspects of this reaction achieved during the last five years, and classifies them into five categories: synthetic methods, building blocks, scaffolds, biological activities and physical properties.

Introduction

The Groebke-Blackburn-Bienaymé (GBB) three-component reaction has been discovered in 1998 and during the course of the first two decades has emerged as one of the most exploited isocyanide-based MCRs, with more than 200 original publications reported and exhaustively reviewed by Boltjes and Dömling [1]. The GBB reaction turned 21 years old in 2019: the 21st birthday in many cultures is considered the attainment of maturity, and some traditions include that, upon reaching that age, the young person was given a key-pendant. The significance of this gesture was that the young person was considered old enough to be a key-holder to his family's home, and thus hold a symbolic 'senior' position in the family. Similarly, we can think of the GBB reaction in 2019 as having received the key-holder from the multicomponent reaction family, occupying now a senior position within it. The success encountered by the reaction until 2019 was far from being at its peak, in fact during the last 5 years about 70 new original works have been published, and it is therefore worth analyzing what are the new features of this, now, mature reaction.

Among isocyanide [2] based multicomponent reactions, the GBB reaction can be considered the third in importance after

Ugi [3] and Passerini [4] ones, and, as the two venerable reactions, is an α-addition of an electrophile and a nucleophile to an isocyanide, followed by a suitable rearrangement, as depicted in Scheme 1.

Compared with the Passerini and Ugi reactions, however, GBB has different features, either advantageous or not. Certainly, the most negative aspect of the GBB reaction is that, compared with the others, it usually requires more drastic reaction conditions. For this reason, many studies have been carried out aimed at the discovery of new catalysts to allow the reaction to take place under the mildest possible conditions. This search goes in parallel with the urge to use increasingly diverse and complex building blocks, up to and including DNA conjugates, which would be degraded under the classical conditions developed by Groebke, Blackburn and Bienaymé.

On the other hand, the GBB reaction, compared with the Ugi and Passerini reactions, has an undeniable advantage, namely, the possibility of obtaining cyclic, aromatic, and drug-like compounds, rather than linear structures. The immediate consequence of this fact is that there are numerous studies on biological activities or photophysical properties (i.e., fluorescence) of GBB adducts.

Another advantage is that, by replacing the amidine component (classically 2-aminopyridines) with other heterocycles, different scaffolds are obtained, and this is extremely efficient in diversity-oriented synthesis (DOS) where a single methodology should generate diverse scaffolds.

This comprehensive review focuses on all these aspects, and has been divided into five chapters, describing, respectively: a) efforts to develop new and milder reaction conditions; b) the use of new building blocks; c) the generation of new scaffolds by coupling the GBB reaction with other transformations; d) the study of the biological and pharmacological properties of these fused heterocycles; e) the study of the photophysical properties of the GBB adducts. At the end of this overview, conclusions will be drawn about the future perspectives of this reaction.

Review

1 Novel synthetic methods

The previously mentioned review, published in 2019 [1], had already highlighted how wide the variety of methods were used to conduct the GBB reaction: as much as 46 different catalytic systems had been reported in the literature at that time, along with some 30 solvents. The most widely used conditions, however, remained those originally discovered by Groebke, Blackburn and Bienaymé, namely the use of $Sc(OTf)_3$, perchloric acid or *p*-toluenesulfonic acid as catalysts, and methanol, ethanol or toluene as solvents, or under solvent-free conditions. Although some new metal or Brønsted acid catalysts have been reported in the last few years, the main innovations can be found in the use of organic catalysts, enzymes, and compartmentations. A few reports on the in situ generation of reactants and on the reaction conducted under flow conditions can also be found.

1.1 Metal and Brønsted acid catalysts

As previously mentioned, Sc triflate is the most widely used Lewis acid for the GBB reaction, generally exhibiting higher catalytic activity compared to other metal triflates, such as Yb, In or Bi. No extensive work had been done on rare earth (RE) triflates before the report by Longo et al. [5], who found La and Gd performing better than Eu and Yb, and similarly to Sc in a model reaction between 2-aminopyridine (**1**), benzaldehyde (**2**) and *tert*-butyl isocyanide to give **3** under microwave (MW) heating. However, when methyl isocyanoacetate replaced *tert*-butyl isocyanide, $Gd(OTf)_3$ was superior to $La(OTf)_3$, and again performed similarly to $Sc(OTf)_3$ (Scheme 2). With these results in hand, Longo et al. evaluated the scope and limitations of this lanthanide, obtaining good to excellent results in the synthesis of 23 different GBB adducts, using aliphatic and aromatic aldehydes, both with electron-donating (ED) and electron-withdrawing (EW) substituents. It is worth mentioning that Gd triflate is much cheaper than scandium triflate, and that in this study the so called “gadolinium break” phenomenon [6], a discontinuity in the lanthanide properties, was not observed.

In 2016, Sashidhara et al. reported the catalytic effect of Ag(OTf) on GBB reactions, postulating its role in activating the

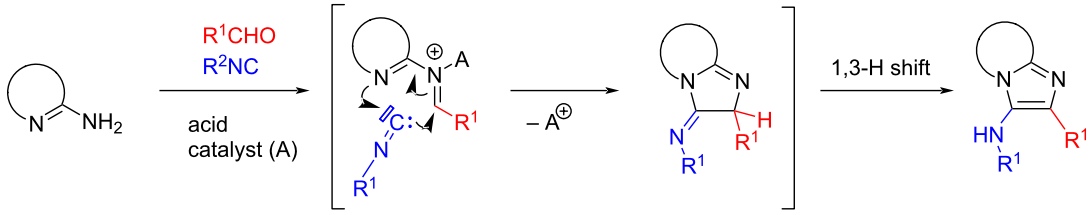

Scheme 1: Mechanism of the GBB reaction.

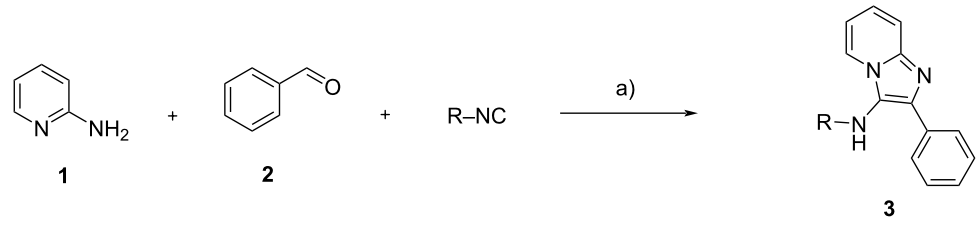

R	$Sc(OTf)_3$	$La(OTf)_3$	$Gd(OTf)_3$	$Eu(OTf)_3$	$Yb(OTf)_3$
$-C(CH_3)_3$	95%	90%	90%	72%	73%
$-CH_2CO_2CH_3$	76%	49%	70%	68%	65%

Scheme 2: Comparison of the performance of $Sc(OTf)_3$ with some $RE(OTf)_3$ in a model GBB reaction. Conditions: a) $M(OTf)_3$ (5 mol %), MeOH, 150 °C (MW, sealed tube), 0.5 h.

attack of the isocyanides onto the imine intermediates [7]; some years later Liu et al. reported a similar role of AgOAc [8]. Although the reaction was tested on different substrates, the conditions were similar: 20 mol % of the catalyst, ethanol as solvent at 80 °C in the first case, 30 mol % of catalyst, ethylene glycol at 90 °C in the second case; however, a striking difference appears when the reaction was carried out in the absence of silver catalyst. Sashidhara et al. reported no conversion, while Liu et al. reported a 58% yield of the GBB product, postulating the ability of ethylene glycol to function as an activator (through hydrogen bonding) and a facilitator of proton transfer. After this discovery, ethylene glycol has never been employed in GBB reactions, if we exclude a 96-member library of GBB adducts reported very recently by Dömling et al. [9]. In this case, however, $Sc(OTf)_3$ was used as the catalyst and the choice for ethylene glycol was dictated by the need to have a polar solvent with a high boiling temperature.

Shankar et al., however, reported that, by using hexafluoroisopropanol (HFIP) as the solvent, GBB adducts derived from glycal aldehydes could be isolated without additional catalysts in a few hours at 25–50 °C [10]. In this case, however, the role of the solvent as a Brønsted acid cannot be ruled out (this article will be discussed in more details in chapter 2).

Another recent article on the use of Brønsted acids has been reported by Vilapara et al., who employed for the first time etidronic acid (1-hydroxyethane-1,1-diphosphonic acid, HEDP) as a green catalyst. Reactions were efficient at room temperature [11]; although the catalyst was tested only with 5-aminopyrazole **4**, and no comparison with a "classic" GBB reaction can be made, the authors compared HEDP with other catalysts on the same substrates, demonstrating that HEDP in MeOH/water was superior for yields, mildness, and less hazardous conditions (Scheme 3).

Longo et al. prepared the Brønsted acid ionic liquid **7**, based on the 1-(butyl-4-sulfonic)-3-methylimidazolium cation, (Scheme 4) and tested it in the model reaction reported in Scheme 2 (R = *t*-Bu), obtaining a 71% yield using 20 mol % of

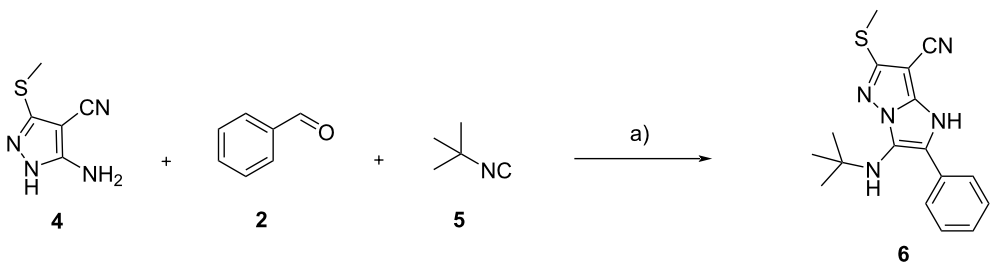

	–	HCl	H_2SO_4	PPA[a]	TFA	*p*TSA	HEDP	HEDP
yield (**6**)	–	62%	45%	44%	77%	74%	70%	83%
time	>24 h[b]	2 h[b]	2 h[b]	2 h[b]	2 h[c]	2 h[c]	2 h[b]	1 h[c]

Scheme 3: Comparison of the performance of various Brønsted acid catalysts in the synthesis of GBB adduct **6**. Conditions: a) catalyst (20 mol %), rt; [a]pyrophosphoric acid; [b]methanol as the solvent; [c]methanol/water 1:1 as the solvent.

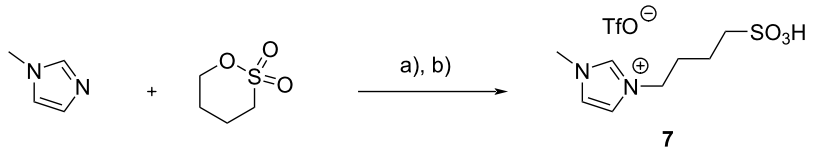

Scheme 4: Synthesis of Brønsted acidic ionic liquid catalyst **7**. Conditions: a) neat, 60 °C, 24 h; b) TfOH, DCM, 0 °C to rt, 24 h.

catalyst in ethanol as the solvent under reflux conditions. The yield could be raised up to 83% when the reaction was heated in a MW oven at 150 °C [12]. With the optimized conditions, 22 GBB adducts were assembled with yields ranging from 42–93%. It is worth noting that the catalyst in this case was recovered and reused four times without appreciable loss of activity.

1.2 Organic catalysts

Noncovalent organocatalysts display a few advantages compared to the traditional metal Lewis acids, such as lower environmental impact, higher stability to air and moisture, easier removal from the GBB products. In this regard, Bolotin et al. in 2022 have reported the high catalytic activity of diaryliodonium triflates such as **8** and **9** [13]. They studied a model reaction with 2-aminopyridine (**1**), *p*-tolualdehyde (**10**) and cyclohexyl isocyanide (**11**) both experimentally (by binding and kinetic studies) and theoretically (by density functional theory (DFT) calculations) (Scheme 5). Catalyst **8** was found to be significantly more active than **9**, owing to higher rigidity and the correct position of the *ortho* H atoms in close proximity to the σ-holes on the I atom. The authors demonstrated that hydrogen bonding between H in *ortho* position of **8** and both O atom of aldehyde and N atom of imine significantly increased the binding constants, leading to higher equilibrium concentrations of the electrophilically activated substrates. The H-bonds also increased the electrostatic potential on the σ-hole of the I atom, resulting in higher charge transfer values from the ligated species. Although no comparison was made with traditional metal catalysts, the authors synthetized 14 GBB adducts with yields ranging from 25% to 91% (compound **12** was obtained in 91% yield).

In the same year, the authors also reported aryl sulfonium and selenonium salts as alternatives to the previously described catalysts [14]. These compounds displayed an effective chalcogen bond donation to the substrates, in place of the halogen bonding previously described. Although their catalytic activity was reported to be lower than the one of aryl iodonium derivatives, this research contributed to the scarce number of publications on the catalytic activity of chalcogen-based noncovalent organocatalysts.

In 2023, Bolotin et al. published another article on the same subject [15], reporting a general improvement of electrophilic activation of carbonyl and imino groups by synergetic effect of aryl iodonium salts and silver cations. However, when similar conditions were tried in a GBB reaction, no cooperative effect was observed, but even a slight decrease in catalytic activity.

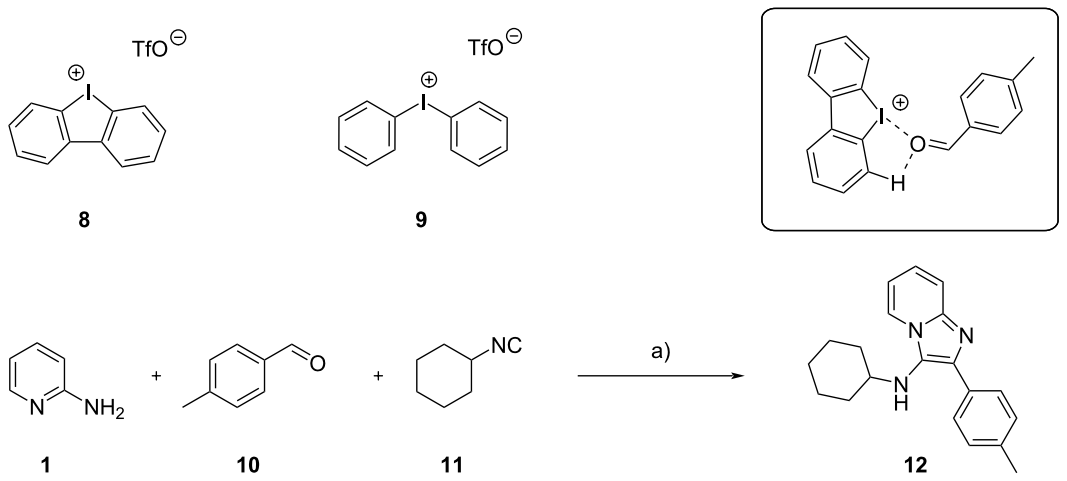

Scheme 5: Aryliodonium derivatives as organic catalysts in the GBB reaction. In the box the proposed binding mode between catalyst **8** and *p*-tolualdehyde **10** is shown. Conditions: a) **8** (10 mol %), $CHCl_3$/MeOH 95:5, 50 °C, 24 h.

The use of thiamine hydrochloride as organic catalyst was reported by Yamajala et al., who were able to obtain the GBB adduct depicted in Scheme 2 (**3**, R = *t*-Bu) in 97% under solvent-free conditions at room temperature for 2 h [16]. Although thiamine had already been reported to be effective in other chemical transformations and its role in carbonyl activation in vivo through its thiazole ring is well known, no mechanism of action in the GBB condensation was proposed by the authors.

1.3 Compartmented and enzyme-mediated reactions

Compartmentation of reaction media has already found many applications in chemistry. Amphiphilic molecules can associate in water to nanometer-sized micelles, above a certain critical concentration. Such micelles are characterized by a lipophilic core and a hydrophilic corona and can serve as heterogeneous systems for solubilizing hydrophobic chemicals in water. By concentrating reactants in nanometer-sized vessels, their reactivity is altered, and reaction rates are often accelerated. As a result, mild reaction conditions can be achieved.

Brunschweiger et al. employed the compartmentation strategy to overcome synthetic problems related to the preparation of a DNA-encoded GBB library [17]. DNA-encoded libraries (DELs) are widely used in screening projects, allowing the synthesis of a huge number of compounds as pools, and the identification of active ones by DNA sequencing. Great challenges, however, characterize the synthetic methodologies, since the chemistry must display a broad scope, be compatible with water and operationally simple, and preserve the genetic information (i.e., no harsh conditions, strongly acidic pHs, no oxidants or Lewis acids). In order to expand DELs to the GBB reaction, compartmentation was proposed to confine an acidic catalyst into the lipophilic core of micelles, inaccessible to water soluble DNA. Micelles were made of a sulfonic acid substituted, amphiphilic copolymer **13**. After reaction optimization, a narrow scope of 8 GBB adducts was obtained (Scheme 6).

Yamajala et al., in the last article discussed in the previous subchapter, also described the use of sodium dodecyl sulfate (SDS) as surfactant in GBB reactions performed in water, synthesizing 27 distinct imidazopyridines in 72–98% yield employing very mild conditions (10% SDS in water at rt with no added catalyst) [16].

Recently, the GBB reaction has also benefited from the use of inorganic nanocomposites and macromolecules, as demonstrated by the contributions of Rostamnia and Jung.

Rostamnia et al. intercalated, by ion exchange technique, Ni-based Keggin-type polyoxometalate α-$[SiW_9O_{37}\{Ni(H_2O)\}_3]$ into a Zn_3Al-based layered double hydroxide (LDH) [18]. Polyoxometalates are known for their tunable acidic (Brønsted/Lewis) properties, but also for their high solubility in polar solvents, therefore intercalation into a layered double hydroxide afforded a heterogeneous nanoreactor that could be employed in acid-catalyzed transformations. The GBB reactions were performed with 1 mol % catalyst at 35 °C under solvent-free condi-

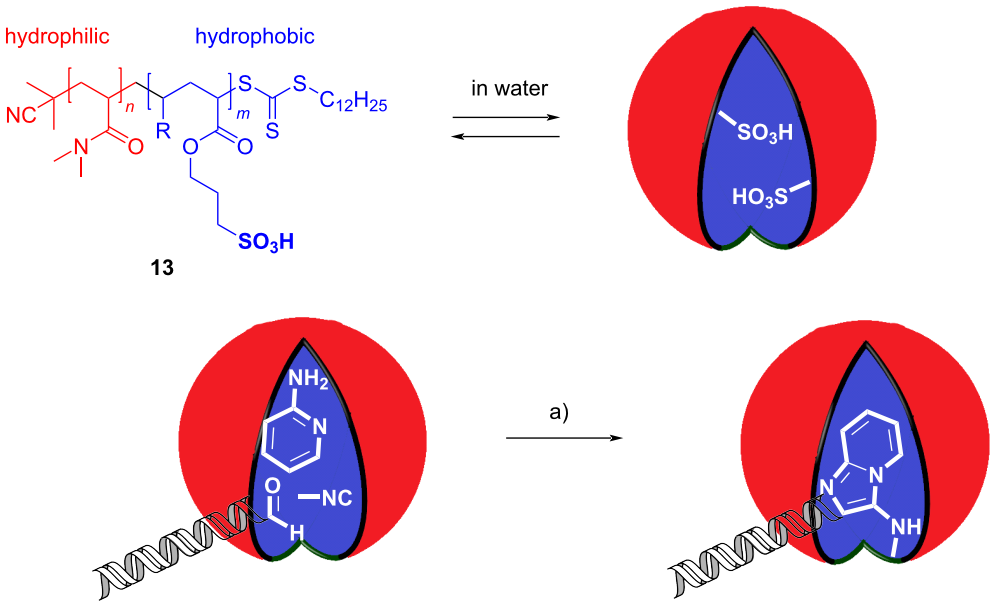

Scheme 6: DNA-encoded GBB reaction in micelles made of amphiphilic polymer **13**. Conditions: a) **13** (50 equiv), water, 40 °C, 54 h.

tions. A synergistic catalytic effect between polyoxometalate and LDH was evidenced by a higher catalytic activity of the composite compared to the individual constituents tested separately. Solvent-free conditions afforded better yields than traditional solvents (water, toluene, DCM, EtOH, MeOH) and 12 adducts were synthetized in 84–96% yield. Finally, the catalyst was recycled six times with a slight decrease in efficiency.

Jung and Shinde, on the other hand, synthetized a supramolecular acid catalyst **14** combining β-cyclodextrins with succinic acid and tested it in a GBB reaction between isatin (**15**), indazol-3-amine (**16**) and pentyl isocyanide (**17**), yielding, after a ring expansion triggered by a retro-aza-ene reaction via a [1,5]-H shift [19], indazolo[3',2':2,3]imidazo[1,5-*c*]quinazolin-6(5*H*)-one **18** (Scheme 7) [20]. The favorable host–guest interaction between **14** and the reactants (demonstrated by 2D NMR and FTIR spectroscopy as well as by scanning electron micrography), combined with the acidity of the succinyl derivatization, allowed the obtainment of **18** in high yield under relatively mild conditions, and was extended to the synthesis of 23 analogues, all in high yields (>86%). The catalyst could be recovered from the reaction medium by precipitation and reused up to five times without loss in activity.

In 2020, Tyagi et al. reported the first biocatalytic GBB reaction using lipase [21]. The model reaction depicted in Scheme 2 (R = *t*-Bu) was tested in ethanol at room temperature with various enzymes, where *Candida antarctica* lipase B (CALB) and *Aspergillus niger* gave best results, affording **3** in 63% and 64% yields, respectively. For further investigations, however, CALB was chosen due to its lower cost and easier availability. Optimization of enzyme loading and substrate ratios increased the yield up to 91%. Immobilization of the enzyme on silica particles was not detrimental to the yield, but allowed enzyme recycling, albeit with a slow but continuous deterioration of catalytic activity. Preliminary molecular docking and molecular dynamics simulation studies revealed that Thr40 and Ser105 residues played a crucial role in catalyzing the GBB reaction, forming hydrogen bonds with 2-aminopyridine substrate, increasing its nucleophilicity and improving its orientation. Furthermore, Ser105 formed a strong hydrogen bond also with benzaldehyde, making it a better electron acceptor. Interestingly, also the imine intermediate showed strong interaction with Thr40 and Ser105 residues, so becoming a good electrophile for the addition of *tert*-butyl isocyanide. On the other hand, the addition of *tert*-butyl isocyanide on the imine altered the orientation of adduct **19**, suppressing the interaction with Ser105 (Scheme 8).

Very recently, Tyagi et al. reported the double encapsulation of CALB and $Pd(PPh_3)_4$ within silica, obtaining an enzyme-metal biohybrid catalyst [22]. The authors tested it in a one-pot GBB reaction–Suzuki coupling, employing 5-bromo-2-aminopyridine (**20**), benzaldehyde (**2**), *tert*-butyl isocyanide (**5**) and phenylboronic acid (**21**). Compound **22** was obtained in 87% yield by performing the GBB reaction at room temperature and

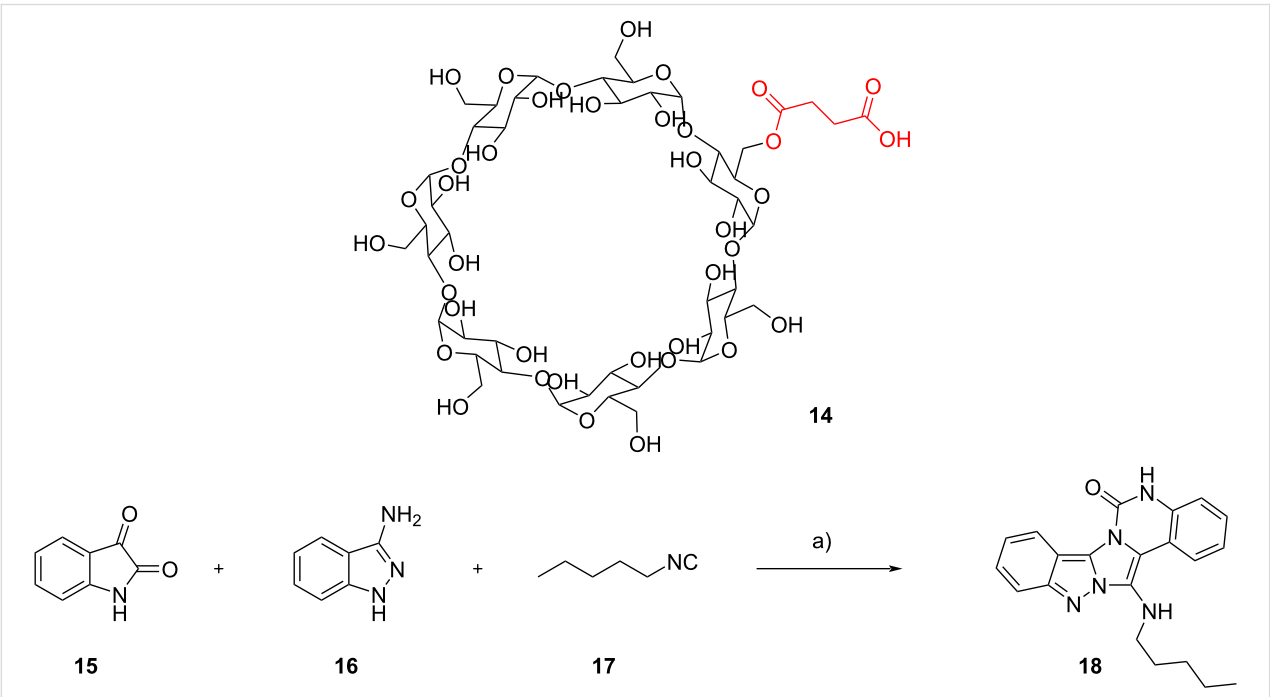

Scheme 7: GBB reaction catalyzed by cyclodextrin derivative **14**. Conditions: a) **14** (1 mol %), water, 100 °C, 45 min.

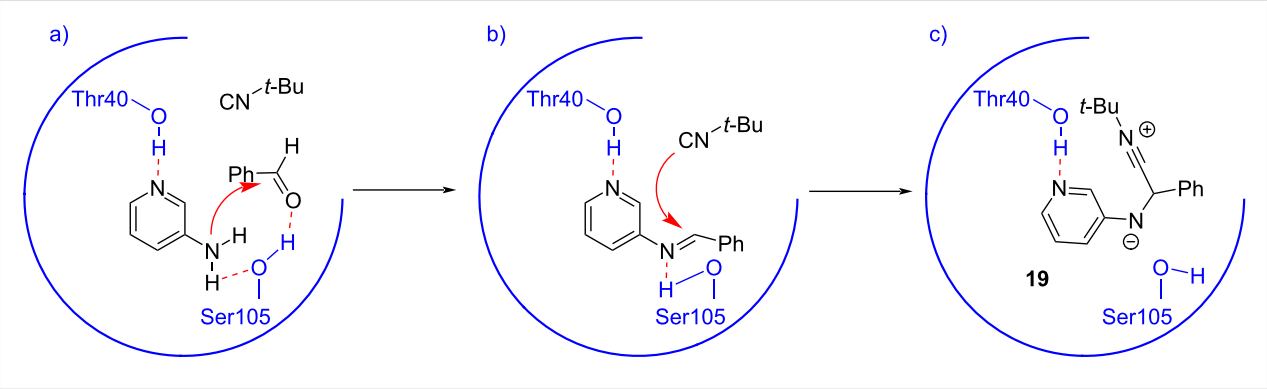

Scheme 8: Proposed mode of activation of CALB. a) activation of the substrates; b) activation of the imine; c) addition of the isocyanide.

then, upon addition of the boronic acid, heating at 60 °C (Scheme 9). Similar efficiencies were observed with a wide range of boronic acids (10 examples, 49–87% yield). The biohybrid was suitable also for gram-scale synthesis and for storage at room temperature under inert atmosphere, showing no loss of activity after 30 days. On the other hand, reusability seemed problematic, as significant decrement in yield was observed after the second cycle.

Kinetic target-guided synthesis (KTGS) has emerged as a promising strategy in drug discovery [24]. It relies on a drug target serving as a template, selecting the ligand building blocks with highest affinity and bringing them in proximity within the binding site. Building blocks are opportunely chosen to have complementary reactivity and therefore to react irreversibly within the binding site and assemble into the final ligand. Before the work described below, KTGS was applied to multicomponent reactions in limited cases [25]. Van der Veken et al. selected as template the protein urokinase plasminogen activator, a serine protease targeted in oncology and inhibited by imidazopyridines [26]. The main challenges of this project were the compatibility of the GBB reaction with typical KTGS conditions, such as aqueous solvent at near-physiological pH and high dilution, and the achievement of selective ligand amplification. First, molecular modeling studies were carried out to verify that building blocks and intermediates could bind the target protein in a manner comparable to the binding mode of known imidazopyridine inhibitors. Second, the possibility that reactants could covalently modify the enzyme was ruled out by analysis of the relevant literature. Finally, appropriate building blocks displaying additional functionalities capable of interactions with the target were synthetized. After optimization of the reaction medium and of the concentration of reactants, and after setting up an analytical method relying on UPLC with tandem quadrupole detector, the on-target KTGS experiments were conducted. In a first set of experiments, a single combination of reactants was studied, but a major hurdle was found to be the imine formation step in aqueous media. Consequently, imines were first prepared as metastable adducts (with benzotriazole or *p*-TSA as stabilizers) and then tested with isocyanides in the presence of the template protein, involving either a single combination of building blocks or competi-

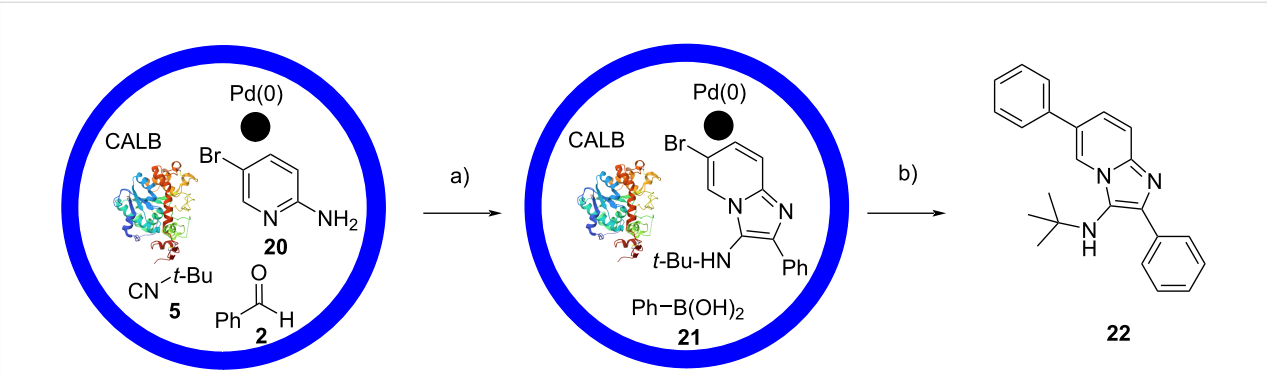

Scheme 9: One-pot GBB reaction–Suzuki coupling with a bifunctional hybrid biocatalyst. Conditions: a) Pd(0)-CALB@SiO_2, EtOH, rt; b) K_2CO_3, dioxane, 60 °C. The crystal structure of CALB from *Candida antarctica* (4K6G, doi:10.2210/pdb4K6G/pdb) was taken from RCSB Protein Data Bank [23].

tion between two of them. In both attempts, however, the results were not in line with expectations, as the enzyme proved to be unable to guide the synthesis of GBB adducts. The authors concluded, however, that this study, especially for the use of metastable imines, could serve as a starting point for the development of other TGS projects involving imine-based multicomponent reactions.

1.4 In situ generation of reactants and use of enabling technologies

Despite their high versatility, isocyanides have some drawbacks, such as their repellent smell (but only for most of unhindered small ones), their partial instability and their potential toxicity [27], thus in situ generation represents a sustainable alternative for their conventional use and this issue has been recently reviewed by Baht and Heravi [28]. In situ generation of isocyanides has been applied also to the GBB reaction in the past, as reported by Guchhait et al. in 2013 [29] and Dömling et al. in 2015 [30], however, in both cases an external acid was required for the multicomponent reaction to occur. The recent report by Salunke et al., instead, exploits the presence of in situ generated hydrogen iodide, deriving from the mixture of I_2, PPh_3 and Et_3N used for the dehydration of the formamide into isocyanide [31]. All substances are mixed from the very beginning, and the reaction could be carried out at room temperature for 12 h, or heated under MW at 60 °C for 30 min. Although this approach uses large excess of reagents and produces a lot of waste, the intrinsic operational simplicity and the reduced reaction times allowed its use in teaching labs at the undergraduate level. This represents one of the first examples of MCR demonstration for educational purposes [32].

Also, the aldehydic component has been generated in situ through Fe_3O_4-mediated aerobic oxidation of benzyl alcohols. Magnetic nanoparticles were supported by Shaabani and Farhid on spent coffee ground and served also as catalyst for the GBB reaction, although the role of coffee ground was not clearly explained [33].

In 2021, Poole et al. [34] reported the first GBB reaction performed under flow conditions. The method proved to be robust, efficient and scalable, and showed a broad functional group tolerance. A commercial apparatus was used and two stock solutions (the first consisting of the amines (1 equiv), the aldehydes (2 equiv) and mineral acid (HCl, 0.1 equiv) dissolved in ethanol, the second made of the isocyanides (2 equiv) dissolved in the same solvent) were pumped into the coil heated at 130 °C. Residence time was 50 min and the isolated yields (27 examples) ranged from 33% to 90%; noteworthy, the reaction performed under flow conditions afforded the desired product also when the corresponding batch reaction failed. The authors provided no comment on whether the imine could already be formed in the stock solution before pumping into the reaction coil. A multigram synthesis was also performed, affording a GBB adduct in more than 4 grams in a total time of 8 hours. The same amount was obtained in batch in a total time of 20 hours.

2 Novel building blocks

The scope and limitations of the GBB-3CR have been accurately delineated up to 2018, outlining a comprehensive understanding of its development, observing different combinations of starting materials and elucidating the effect of substituents on each of the partners [1].

Since 2019, research has been focused on broadening its scope with the aim of moving towards a more sustainable chemistry or to impart specific properties to the final products, therefore a series of novel building blocks, mainly carbonyl derivatives, have been used as starting materials.

2.1 Novel aldehydes

Carbonyl compounds are among the most common starting materials for multicomponent reactions: aldehydes play a central role also in the GBB-3CR. Several experiments have demonstrated the tolerability of a wide range of aldehydes, starting from one of the most used, benzaldehyde, passing through heteroaromatic and aliphatic structures with different substituents.

In this context, some examples where the aldehyde functionality is incorporated into sugar derivatives, natural compounds or molecules derived from biomass have been recently published. Due to the relatively drastic conditions of the GBB reaction and the inherent lability of these structurally complex building blocks, often specific reaction conditions have been developed to successfully obtain the multicomponent adducts.

An intriguing study is reported by Porcal et al. [35] in which they evaluate the use of 5-hydroxymethylfurfural (5-HMF, **23**). Nowadays, the need to move towards more sustainable protocols is impending and the emphasis on green chemistry and on the use of renewable carbon sources is huge. Indeed, the use of 5-HMF (**23**) [36], a renewable carbon source derived from biomass, responds to these requirements. This aldehyde displays additional functionalities useful for further modifications of the GBB adducts, but some optimization was necessary due to its intolerance to high temperatures and reaction conditions. The authors performed the optimization study using 5-HMF (**23**), 2-aminothiazole (**24**) and *tert*-butyl isocyanide (**5**, Scheme 10).

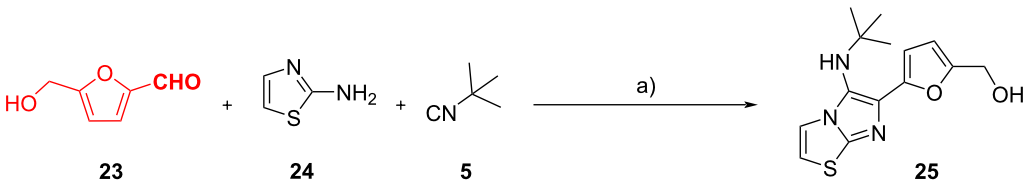

Scheme 10: GBB reaction employing 5-HMF (**23**) as carbonyl component. Conditions: a) TFA (20 mol %), EtOH, 60 °C, 2 h.

Inspired by a procedure reported by Demjén et al. [37], they found the best conditions using EtOH as a green solvent, trifluoroacetic acid (TFA, 20 mol %) or $Yb(OTf)_3$ (5 mol %) as acidic catalyst, and a non-microwave instant heating reactor, performing the reaction at 60 °C and obtaining **25** in 78% yield. Moving forward to investigate the scope of the reaction with different 2-aminoamidines and isocyanides, they obtained 18 different products with isolated yields up to 87%.

The use of sugar-derived building blocks has been reported by various authors. Prasad et al. studied the synthesis of 2-(β-D-glucopyranosyl)-3-*N*-alkylamino-1-azaindolizines **28** to get novel bioconjugates [38] and of 5-(3"-alkyl/arylamino-1"-azaindolizin-2"-yl)-2'-deoxyuridines **31** to obtain new fluorescent products [39]. Starting from perbenzylated β-C-glucopyranosyl aldehyde **26**, 2-aminopyridine (**1**) and cyclohexyl isocyanide (**11**), they synthesized C-glucoside **28** (Scheme 11). β-C-Glucopyranosyl aldehyde **26** was obtained from D-glucose following a procedure already established [40]. Aware of the trials made by Manvar et al. [41] with catalytic amount of acetic acid, the authors initially obtained **27** in moderate yield. Subsequently, testing different catalysts and solvents, they found out that performing the reaction in the presence of $InCl_3$ (20 mol %) in MeOH at 70 °C for 2–3 h was the best option (72%). With the optimized conditions in hand, they used different 2-aminopyridines and alkyl isocyanides, getting 14 distinct products with 56–88% yield. The reaction did not work with 2-aminopyridines with electron-withdrawing groups, and this was attributed to their reduced nucleophilicity.

In their second work about this topic, Prasad et al. synthesized 5-(3"-alkyl/arylamino-1"-azaindolizin-2"-yl)-2'-deoxyuridines **31** as new base-modified fluorescent nucleosides with high Stokes' shift, potentially useful for investigating nucleic acid structure and functions. The authors synthesized deoxyuridine-based aldehyde **29** starting from thymidine in 30% yield, according to a known procedure [42]. Then, they tested two different strategies: in the best one (depicted in Scheme 12) **29** was used in the GBB-3CR, then adduct **30** was deacetylated to afford the final product **31** in an overall yield of 83–95%. The second strategy, based on the deacetylation of **29** followed by the GBB-3CR, led to a lower overall yield of 21–23%. The reaction with different 2-aminopyridines and alkyl/aryl isocyanides afforded the intermediates **30** in 86 to 96% yield, and the subsequent deacetylation with potassium carbonate was almost quantitative (97–99% yield). It is worth mentioning that the GBB reaction starting from the deacetylated substrate also leads to good results (83–91% of yield), but the overall yield is lowered due to a sluggish deacetylation reaction of **29**.

Sugar-based aldehydes were employed also in the work reported by Shankar et al. [10], already mentioned in chapter 1. The authors established a solvent-catalyzed GBB-3CR to synthesize glycosylated imidazo[1,2-*a*]pyridines **33** starting from 1-formyl glycals **32**; using HFIP as the solvent, the addition of any metal catalyst was not needed (Scheme 13). Glycal aldehydes **32** were synthetized starting from D-glucose and D-galactose, following an established procedure [40]. The scope

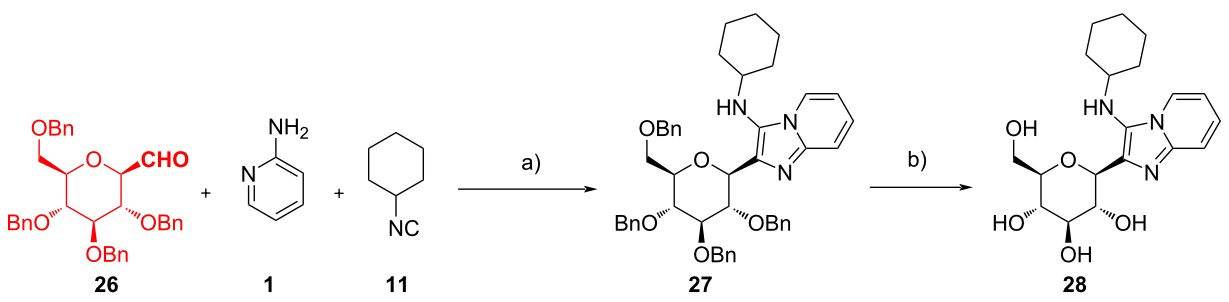

Scheme 11: GBB reaction with β-C-glucopyranosyl aldehyde **26**. Conditions: a) $InCl_3$ (20 mol %), MeOH, 70 °C, 2–3 h; b) Pd-C/H_2, MeOH, rt.

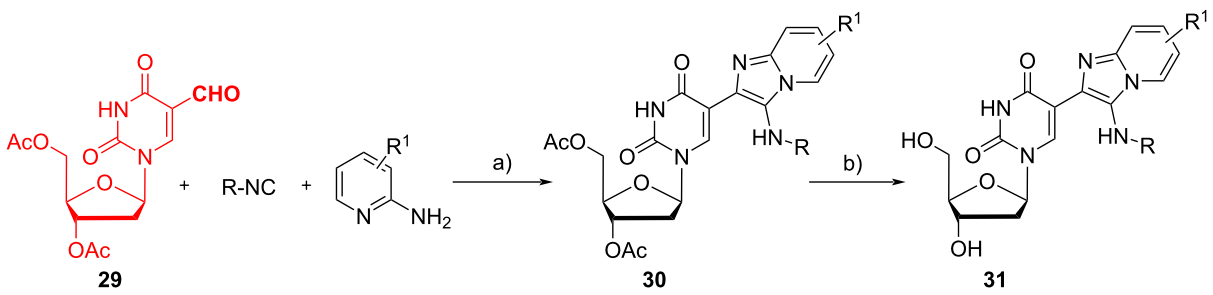

Scheme 12: GBB reaction with diacetylated 5-formyldeoxyuridine **29**, followed by deacetylation of GBB adduct **30**. Conditions: a) TFA (5 mol %), MeOH, 60 °C; b) K_2CO_3, MeOH/H_2O, 25 °C.

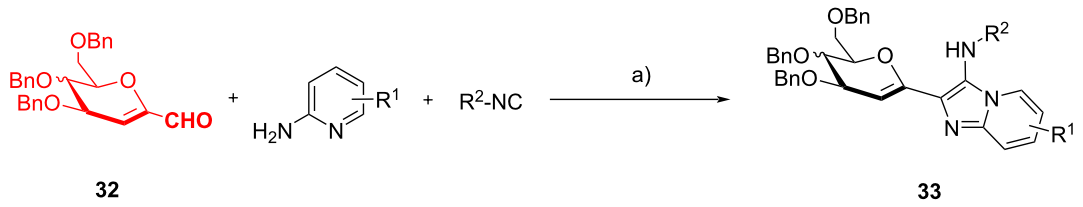

Scheme 13: GBB reaction with glycal aldehydes **32**. Conditions: a) HFIP, 25 °C, 2–4 h.

of the reaction was evaluated using differently substituted amidines, and 9 different 2-(β-D-glycal-1-yl-)-3-*N*-alkyl-amino-1-azaindolizines **33** were synthesized in excellent yields (71–89%).

Dömling et al. have used glyoxal dimethyl acetal as orthogonal bifunctional monoprotected aldehyde to synthetize GBB dimers as potential fluorophores. More details are given in chapter 5 [43].

The GBB reaction can be exploited also in the late-stage functionalization of natural molecules, with the possibility of generating pseudo-natural compound libraries: Cortés-García et al. [44] applied this strategy to vouacapane. The authors developed a two-step reaction for the synthesis of fused vouacapane-azoles **36**. Starting from the 6-β-acetoxyvouacapane (**34**), a natural product isolated from the dichloromethane extracts of the leaves of *Caesalpinia platyloba* by column chromatography, they performed a Vilsmeier–Haack formylation at the furan ring (Scheme 14) obtaining aldehyde **35** in 92% yield. This, in turn, was used as starting material in a GBB-3CR performed at room temperature to avoid opening of the furan ring. The authors explored the substrate scope by using different isocyanides and 2-aminoazines, obtaining 6 potentially bioactive pseudo natural products **35** in low to moderate yield (21–67%).

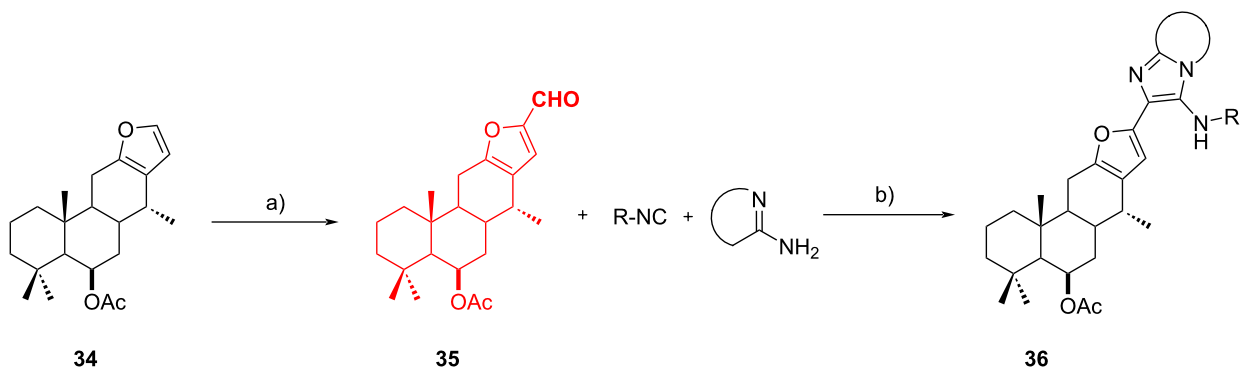

Scheme 14: Vilsmeier–Haack formylation of 6-β-acetoxyvouacapane (**34**) and subsequent GBB reaction. Conditions: a) $POCl_3$, DMF, 0 °C to rt; b) $Sc(OTf_3)$ (10 mol %), DCM/MeOH, rt.

Bräse et al. [45] reported the possibility of exploiting the GBB-3CR to synthesize a cyclophanyl-imidazole-based library of ligands. The synthesis of ligands based on the [2.2]paracyclophane (PCP) moiety, thanks to its structural features and inherent planar chirality upon selective substitution, has been recently reviewed by the same author [46]. Starting from 4-formylcyclophane **37**, a GBB-3CR with different isocyanides and amidines was exploited to synthesize PCP-based imidazo[1,2-*a*]pyridyl-substituted ligands **38** (Scheme 15). During the study of the scope, it was observed that 2-aminopyrazines afforded lower yields (12–48%) than 2-aminopyridines (42–87%), and this was attributed to their reduced nucleophilicity. Also the synthesis of a bis-imidazo[1,2-*a*]pyridine scaffold was achieved in 43% yield from the pseudo-*para*-substituted bis-aldehyde, using the same conditions, but longer reactions times (6 days). Following the same approach, the authors also developed a one-pot protocol for a GBB-3CR through an in situ generation of the cyclophanyl isocyanide. They synthesized the formamido[2.2]paracyclophane, and then, following the procedure reported by Dömling [30], dehydrated the formamide in situ and reacted the resulting isocyanide with 2-aminopyridine and an aldehyde. As a proof of concept, one of the GBB adducts was transformed into a *N*,*C*-palladacycle and was investigated as a potential catalyst for carbon–carbon bond-forming reactions. Furthermore, the authors studied in detail the fluorescence properties of the GBB adducts, that will be discussed in chapter 5.

As already discussed in section 1.3, Brunschweiger et al. [47] reported the synthesis of DNA–imidazole heterocyclic conjugates by the GBB-3CR. An alternative to the previously discussed encapsulated solution-phase synthesis is the solid-phase approach in which the DNA barcodes are synthesized on CPG (controlled pore glass). In this study they used a benzaldehyde unit conjugated to a hexathymidine oligonucleotide **39** and reacted it with various isocyanides and amidines to obtain a small collection (9 examples) of adducts **40** in yields ranging between 23% and 95%; large excess of reagent and a weak Brønsted acid were essential for the success of the reaction (Scheme 16). A cheminformatic analysis revealed that GBB-based encoded libraries could cover a diverse chemical space, different from the one covered by encoded libraries obtained with other isocyanide-based MCRs.

2.2 Novel heterocyclic amidines

Almost 90 different amidines had already been tested until 2018 [1], however, room for novel building blocks or old ones with novel reactivity is still available as demonstrated for example by Dömling et al. [48]. They focused on the use of 2,4-diaminopyrimidines **41** to synthetize diaminoimidazopyrimidines **43**. This substrate was already employed by Lavilla et al. [49] to obtain selectively imidazo[1,2-*a*]pyrimidin-7-amine derivatives, due to the higher reactivity of the amine in position 2. To uncover the reactivity of the amine in position 4, and thus obtain imidazo[1,2-*c*]pyrimidin-5-amines **43** instead, the

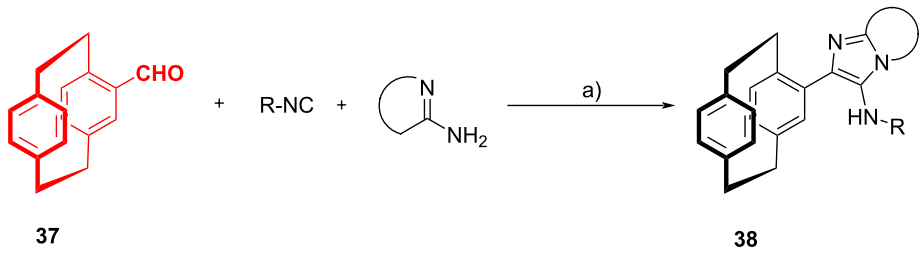

37 38

Scheme 15: GBB reaction of 4-formyl-PCP **37**. Conditions: a) HOAc or $HClO_4$, MeOH/DCM (2:3), rt, 3 d.

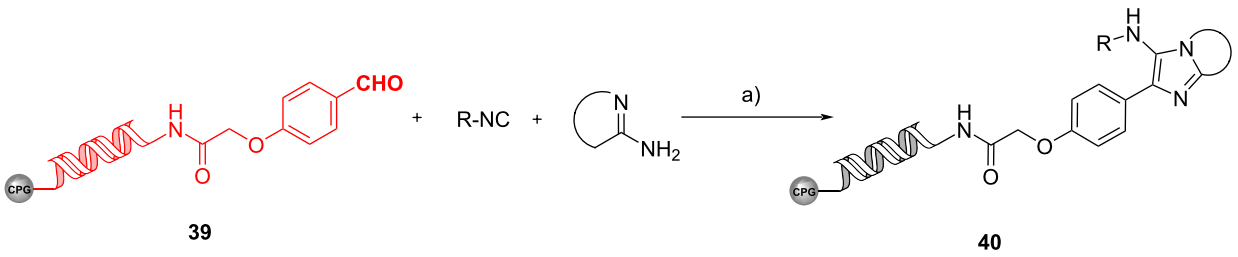

39 40

Scheme 16: GBB reaction with HexT-aldehyde **39**. Conditions: a) **39** (20 nmol) and amidine (20 μmol), MeOH, rt, 6 h, then isocyanide (20 μmol) and AcOH (1 mol %), rt, 16 h.

authors synthesized a series of 2-amino-protected compound **41** through an aromatic nucleophilic substitution on 2-chloropyrimidin-4-amines. Derivatives **41** were then reacted under the optimized conditions, leading to the formation of a series of GBB adducts **42**, finally deprotected with TFA to get **43** in an overall yield of 40–80% (Scheme 17). In this study, 14 distinct products were obtained, and the only limitation was observed using aliphatic aldehydes, due to the instability of the deprotected GBB adducts. Imidazopirimidines are a privileged scaffold incorporated in many bioactive compounds.

Dömling et al. [50] also reported the synthesis of *N*-edited guanine derivatives. Different drugs display the guanine motif, fundamental for its biological activity is a triad HBA–HBD–HBD (HBA = hydrogen bond acceptor, HBD = hydrogen bond donor) included in its structure. The authors propose a one-pot two-step procedure, combining the GBB-3CR and an acid-assisted deprotection reaction, to get a library of imidazo[2,1-*f*][1,2,4]triazin-4(3*H*)-ones **46**, characterized by a flat heterocyclic ring system displaying the essential triad. Guanine derivatives are typically synthesized through a sequential multistep procedure, however, by employing 3,6-diamino-1,2,4-triazin-5-one **44** as amidine derivative, **46** could be simply obtained through a GBB-3CR. The amino group in position 3 was opportunely protected to drive the GBB reaction to the selective formation of **45**. Microwave heating appeared to be beneficial compared to traditional heating for the outcome of the reaction (60% yield vs 49%). A consistent library of 22 compounds was prepared, in yields ranging from 21 to 75%, and the GBB adducts were finally deprotected under acid conditions. When TFA was used partial deprotection to **46** was achieved, while the use of triflic acid (TfOH) resulted also in the cleavage of the alkyl group derived from the isocyanide, with formation of **47** (Scheme 18).

Kanizsai et al. [51] have reported the synthesis of 4,5-disubstituted 2-amino-1*H*-imidazoles and their further modification through the GBB-3CR. The 2-aminoimidazole moiety can be found in different alkaloids isolated from sponges and exhibits useful bioactive properties. The methodology employed by the authors to assemble C4/C5-functionalized 2-aminoimidazoles **49** exploited a Mannich condensation followed by an iodoxybenzoic acid (IBX) and *N*-iodophthalimide (IPT)-mediated intramolecular oxidative annulation and a hydroxylamine-induced ring cleavage of intermediate **48**. With this one-pot sequential procedure they synthesized **49** in yields up to 95% (Scheme 19).

The subsequent GBB-3CR led to the unique 1*H*-imidazo[1,2-*a*]imidazole core **50** with 4 distinct diversification points. The

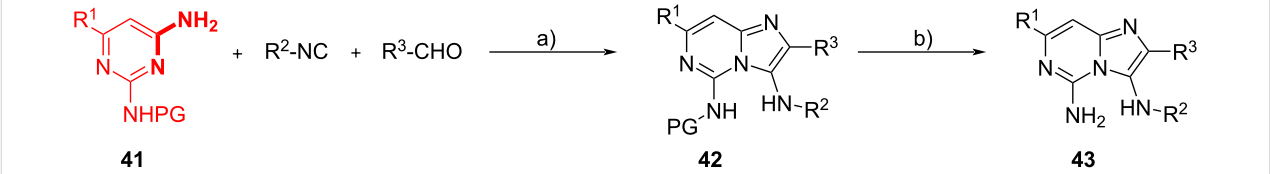

Scheme 17: GBB reaction of 2,4-diaminopirimidine **41**. Conditions: a) $Sc(OTf)_3$ (20 mol %), MeCN, 120 °C (MW), 1 h; b) TFA, reflux, overnight.

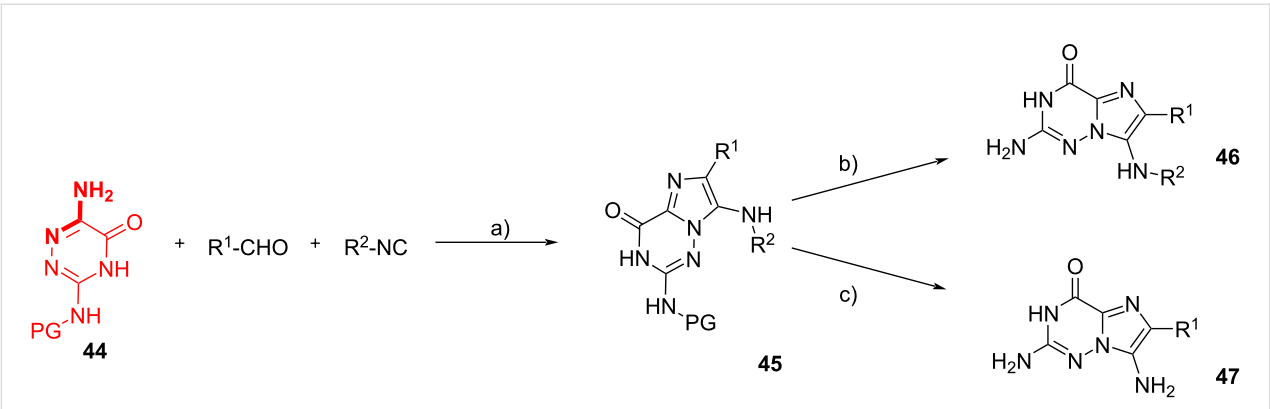

Scheme 18: Synthesis of *N*-edited guanine derivatives from 3,6-diamine-1,2,4-triazin-5-one **44**. Conditions: a) $Sc(OTf)_3$, MeOH, 100 °C; b) **45** (0.2–0.5 mmol), 0.1 M TFA, 80 °C, 12 h; c) **45** (0.1–0.5 mmol), 0.1 M TfOH, 55 °C, 4 h.

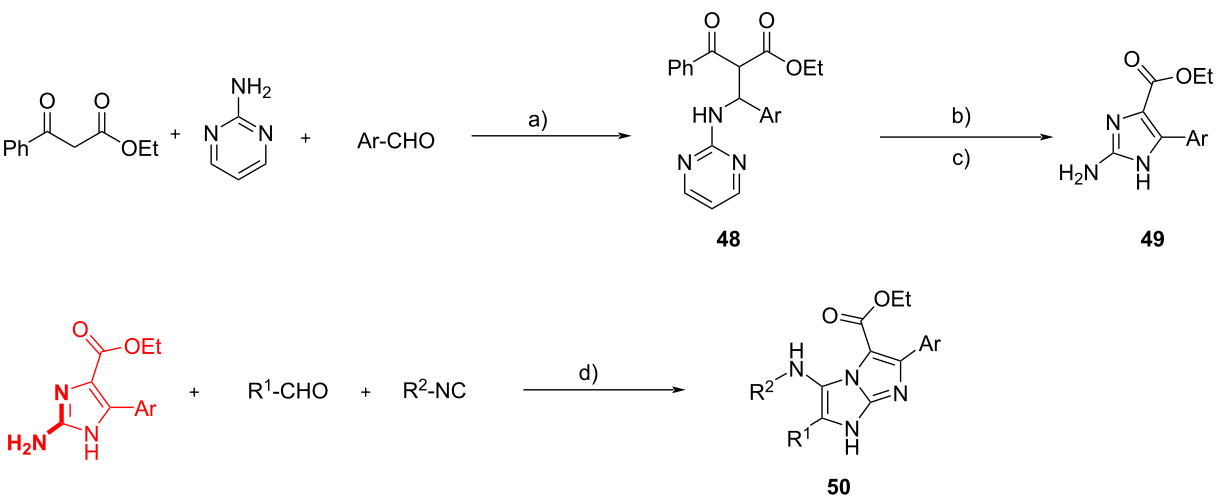

Scheme 19: Synthesis of 2-aminoimidazoles **49** by a Mannich-3CR followed by a one-pot intramolecular oxidative annulation/ring cleavage and subsequent GBB-3CR. Conditions: a) phosphotungstic acid (PTA) or TMSCl, MeCN or H_2O, 60 or 80 °C; b) IBX, IPT, DMA, 80 °C, 30 min; c) $NH_2OH{\cdot}HCl/Na_2CO_3$, DMA, 50 °C, 16 h; d) $HClO_4$ (20 mol %), MeCN, 60 °C, 24 h.

scope of the reaction was limited: alkyl aldehydes and aryl/benzyl isocyanides could not be used, and 4 distinct compounds were obtained in yields of 23–40%. Nevertheless, these results represent an improvement compared to previous studies where substitution on C4 of the 2-aminoimidazole scaffold prevented the GBB reaction to occur [52].

As it has already been described, DNA encoded GBB adducts can be effectively used in DEL screening techniques. Hwang et al. incorporated 2-amino-6-chloropyrimidine-4-carboxylic acid into a DNA sequence, reacted the resulting conjugate **51** through a Suzuki–Miyaura reaction and then subjected the adduct **52** to a GBB reaction with various aldehydes and isocyanides (Scheme 20) [53]. Focusing on the GBB part, the authors tested both Lewis acids ($Sc(OTf)_3$ or $Yb(OTf)_3$) and Brønsted acids (NH_4Cl or AcOH) and found that the best results could be obtained using 30 equiv of AcOH in DMA, with no damage of DNA observed. The GBB reaction, under these mild conditions, demonstrated a wide range of scope. Different aldehydes were tested: benzaldehydes with different substituents, heteroaromatic and bicyclic aromatic aldehydes, all giving good results. Only aliphatic aldehydes showed a higher variability (50–98%) and in some cases also the classic Ugi adducts were observed. Regarding the isocyanide, excellent yields were achieved for all tested reagents, such as aromatic, aliphatic, and sterically hindered ones. Problems were only observed using a morpholine derivative because the base properties of the reagent could hinder AcOH from catalyzing the reaction.

Smith et al. [54] explored the potential of acyclic amidines **54** in the synthesis of substituted-imidazoles via the GBB reaction under MW heating (Scheme 21). The resulting 5-aminoimida-

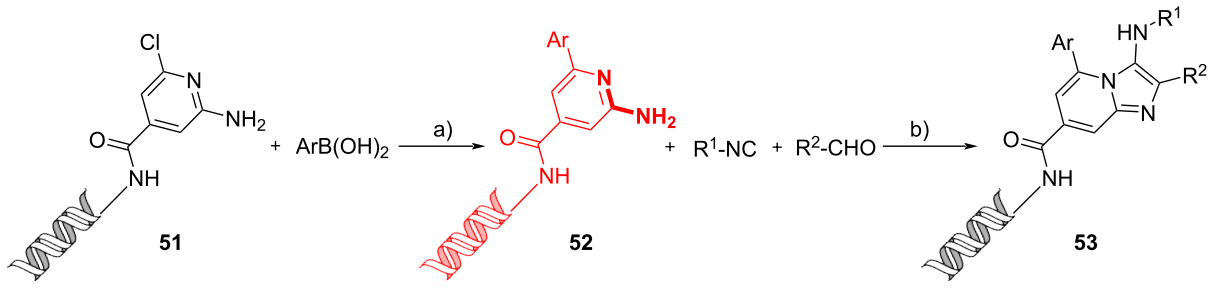

Scheme 20: On DNA Suzuki–Miyaura reaction followed by GBB reaction. Conditions: a) CsOH, sSPhos-Pd-G2; b) AcOH (30 equiv), H_2O/DMSO, 25 °C, 24 h.

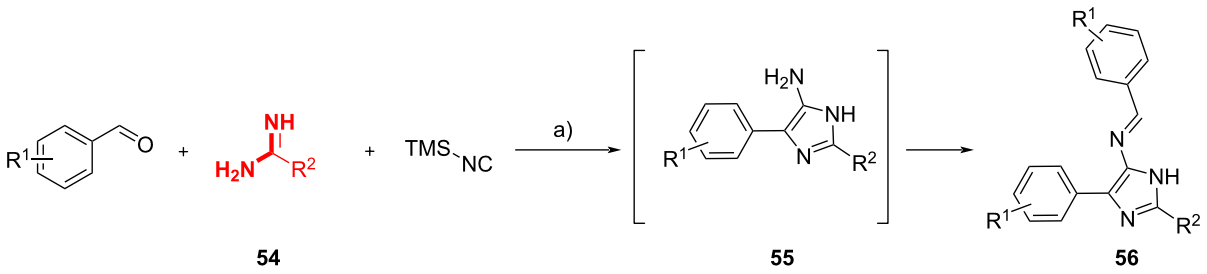

Scheme 21: One-pot cascade synthesis of 5-iminoimidazoles. Conditions: a) Na_2SO_4, DMF, 220 °C (MW).

zoles **55** were in situ-reacted with the aldehydes to yield 5-iminoimidazoles **56**. When benzamidine (**54**, R^2 = Ph) was used, aldehydes bearing electron-rich groups gave the products in higher yields compared to those with electron-poor groups. This study demonstrated that the GBB reaction could take place when acyclic amidines containing an aromatic ring or heteroatoms (**54**, R^2 = NHAc, NH_2) were used, while aliphatic amidines (**54**, R^2 = H, CH_3, CF_3) were unsuccessful, indicating that the resonance stabilization of the amidine was crucial to the reaction.

Finally, Guillaumet et al. [55] have proposed a simple way to synthesize the 2-substituted 1*H*-imidazo[1,5-*a*]imidazole scaffold. This scaffold has a significant relevance in drug synthesis and was not deeply studied yet. As depicted in Scheme 22, 5-amino-1*H*-imidazole-4-carbonitrile (**57**) was used as heterocyclic amidine, to obtain the desired bicyclic adducts **58**. The solvent choice was limited to methanol due to solubility problems, and $HClO_4$ was selected because other Brønsted acids caused amine deprotection. The GBB adducts **58** could be further elaborated through a Buchwald intramolecular nucleophilic substitution/cyclization, as it will be described in section 3.3.

3 Novel scaffolds

Owing to the flexibility for variation of the GBB reaction, it has been widely employed in combination with other reactions for the formation of novel scaffolds with high level of complexity. The general approach to generate complex architectures is the installation of functional groups on the GBB precursors which can be involved in further modifications. In addition, the GBB-like reactions can also be used to deliver other heterocyclic motifs.

3.1 One-pot synthesis

As an efficient approach in organic synthesis, one-pot synthesis has been exploited in the post-modification of GBB products. This approach offers several advantages since multiple bond formation, synthetic transformation and heterocyclic construction can be conducted in a single reactor [56]. Novel scaffolds derived from the GBB products have been successfully constructed through three types of one-pot synthesis, namely cascade/domino reaction, one-pot stepwise synthesis and multicomponent reaction.

In the one-pot cascade reaction, the complexity of heterocycles was achieved due to the presence of functional groups formed in the GBB reaction which allow further reactions to occur. In the case of one-pot stepwise synthesis, the GBB products were introduced to the subsequent reactions in the same pot without isolating them from the reaction mixture. In the one-pot multicomponent reaction, three substrates with di- or tri-functional groups were engaged in the GBB reaction to produce the heterocyclic polymers.

Panda and Ganesher [57] reported the one-pot cascade synthesis of indole-imidazo[1,2,*a*]pyridine hybrids **61** (Scheme 23). In this study, the convertible isocyanide 1-isocyano-2-(2,2-

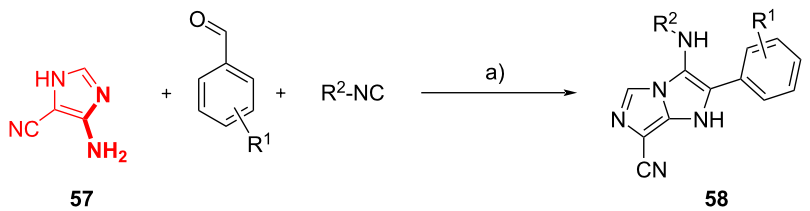

Scheme 22: GBB reaction of 5-amino-1*H*-imidazole-4-carbonile **57**. Conditions: a) $HClO_4$ (5 mol %), MeOH, rt, 24 h.

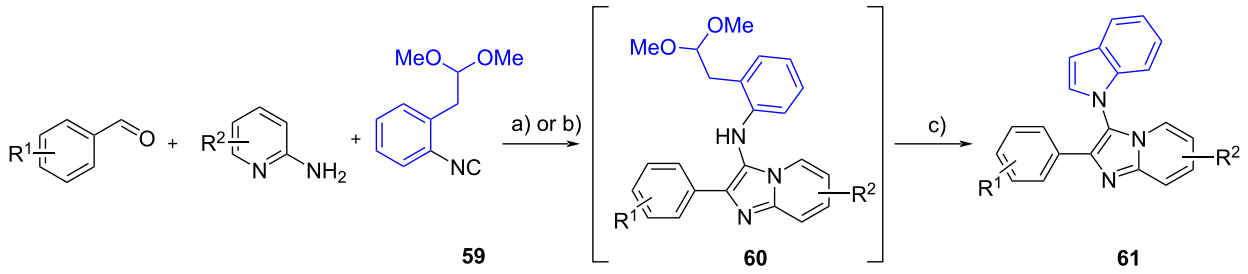

Scheme 23: One-pot cascade synthesis of indole-imidazo[1,2,*a*]pyridine hybrids. In blue the structural motif involved in the secondary transformation. Conditions: a) TFA (20 mol %), 1,4-dioxane, 110 °C, 2 h (Panda and Ganesher [57]); or b) $ZnCl_2$ (5 mol %), 1,4-dioxane, reflux, 5–6 h, c) DCM/TFA (1:1), rt, 4–5 h (Jain and Sen [58]).

dimethoxyethyl)benzene (**59**, Kobayashi–Wessjohann isocyanide) was utilized as one of the precursors in the GBB reaction. The acetal-substituted products **60** underwent TFA-promoted deprotection which triggered the intramolecular cyclization to furnish the indole moiety in the desired products **61**. A control experiment showed that the GBB product **60** was obtained as the sole product in the absence of acid catalyst.

Another group developed the same reaction via a two-step synthesis [58]. Initially, the three starting materials were subjected to the GBB reaction in the presence of a catalytic amount of $ZnCl_2$ to give the fused products **60**. Then, the cyclization was carried out using TFA to deliver **61** (14 examples) in yields ranging from 60% to 65%.

Lavilla et al. [59] explored the reactivity of indole carbaldehydes in the extended GBB multicomponent reaction. In this study, various fused-, linked- and bridged polyheterocycles were generated through different reaction pathways, depending on the type of indole carbaldehydes and the reaction conditions. The study was started by reacting 2-aminopyridines, indole-3-carbaldehyde **62** and ethyl isocyanoacetate (**63**) under open air in the presence of $Yb(OTf)_3$ catalyst (Scheme 24, conditions a). The results showed that fused polycyclic indoles **67** were ob-

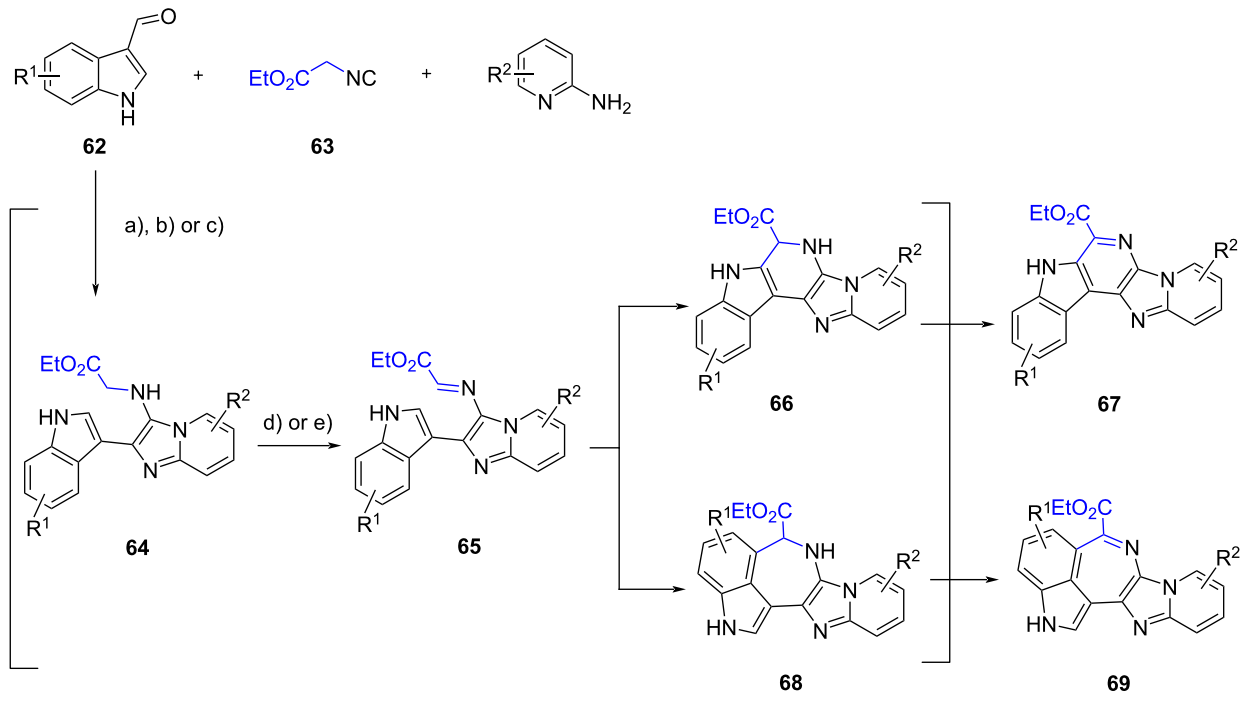

Scheme 24: One-pot cascade synthesis of fused polycyclic indoles **67** or **69** from indole-3-carbaldehyde. Conditions: a) $Yb(OTf)_3$ (20 mol %), O_2 (air), MeCN, 80 °C, 22 h, b) $Yb(OTf)_3$ (20 mol %), $CoBr_2$ (5 mol %), O_2 (air), MeCN, 80 °C, 22 h; c) $Yb(OTf)_3$ (20 mol %), MeCN, 80 °C (MW), 1 h; d) $CoBr_2$ (5 mol %), O_2 (air), MeCN, 80 °C, 22–60 h; e) I_2, MeCN, 80 °C, 48 h.

tained (albeit in lower yields, 25%) instead of the corresponding GBB products **64**. The authors proposed that adducts **64** were transformed into the intermediates **65** under atmospheric conditions which in turn underwent intramolecular Pictet–Spengler reaction through the addition of C-2 to the imine, to produce dihydropyridines **66**. Further oxidation converted **66** into pentacycles **67**. The same products were obtained when $CoBr_2$ was used as external oxidant in the one-pot cascade reaction (Scheme 24, conditions b). No substantial improvement in the yields of **67** and **69** was observed when the synthesis was carried out in two steps, performing the GBB reaction under inert atmosphere and oxidizing **64** in the presence of $CoBr_2$ (Scheme 24, conditions c and d; one-pot: 10–43%, two steps: 11–37% yields). Interestingly, polycycles **69** were formed when I_2 was employed as the oxidant (Scheme 24, conditions e), which was presumably due to the coordination between the oxidant and the nitrogen atom in imidazoles **65**. This interaction increased the steric hindrance around C-2 and allowed the Pictet–Spengler reaction to occur at position of C-4. Indole-4-carbaldehydes were also compatible with this transformation, while indole-2-carbaldehyde (**70**) surprisingly led to the formation of linked polyheterocycles **75**. The authors then decided to perform the reaction using 3 equiv of aldehyde **70** under acidic conditions (Scheme 25, conditions a). The presence of a nucleophilic indole in the GBB adducts **71** induced further additions towards the excess aldehydes **70**. The diols **73** underwent cyclization and dehydration to produce linked polyheterocyclic indoles **75**. The authors managed to prepare five adducts in 15–33% yield. Another mechanistic scenario occurred at higher temperature (Scheme 25, conditions b). The secondary amine of diol **73** substituted both secondary alcohols to provide the ammonium **77**. The intermediate **77** underwent Steven rearrangement to give a bridged polyheterocycle **78** in 28% yield.

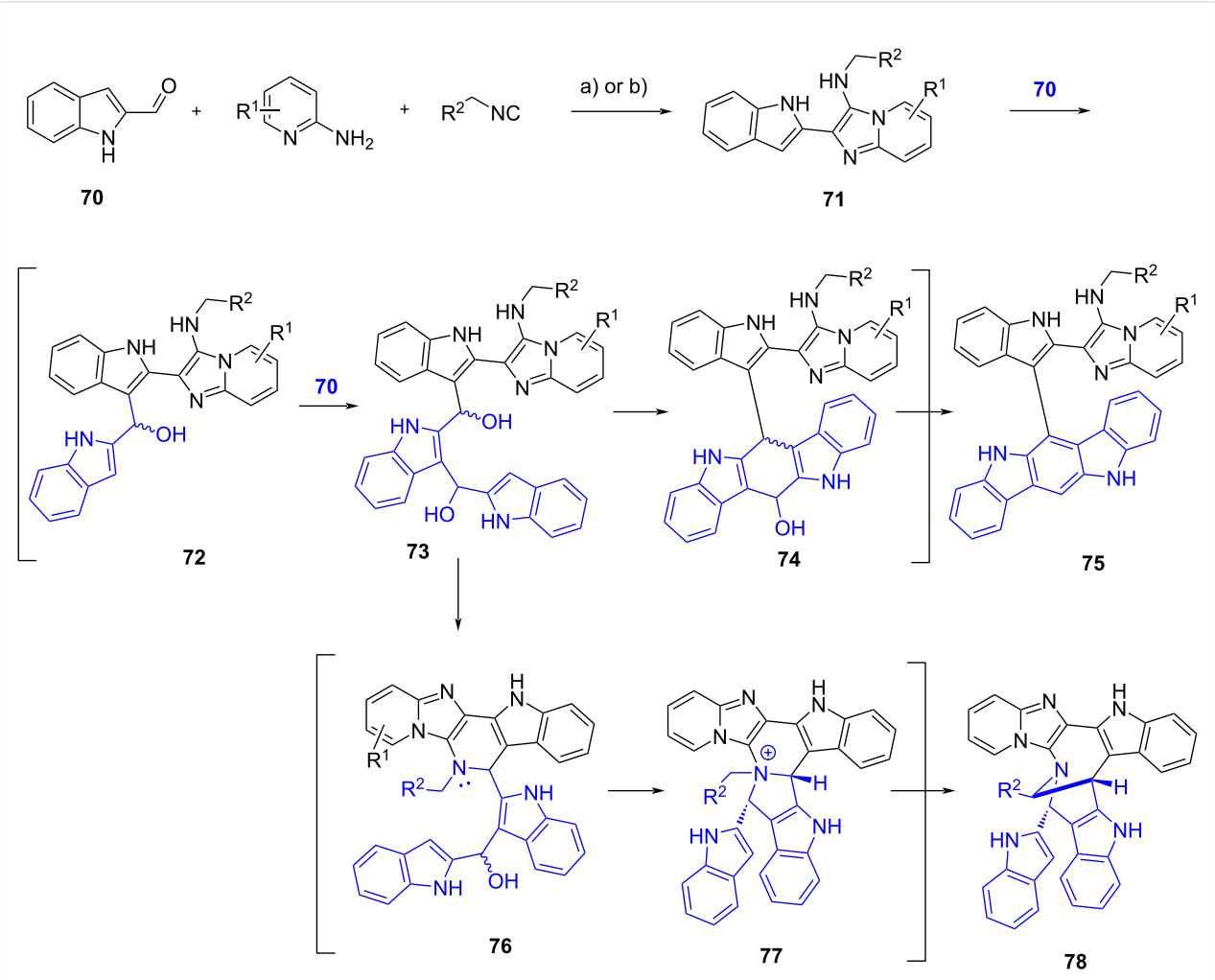

Scheme 25: One-pot cascade synthesis of linked- and bridged polycyclic indoles from indole-2-carbaldehyde (**70**). Conditions: a) for the synthesis of **75**: $Yb(OTf)_3$ (20 mol %), MeCN, rt, 48–72 h; b) for the synthesis of **78**: $Yb(OTf)_3$ (20 mol %), MeCN, 110 °C (MW), 90 min.

Unlike the previous examples, Jeong et al. [60] developed a cascade reaction by installing the additional ring prior to the GBB reaction (Scheme 26). The bifunctional 2-(2-bromoethyl)benzaldehyde **79** was utilized to form the highly reactive cyclic iminium intermediates **81** through the condensation with amidines **80**. The subsequent formal [4 + 1] cycloaddition with the isocyanide and the 1,3-*H*-shift occurred to afford pentacycles **82**. Performing the one-pot reaction under the optimized conditions allowed them to create a library comprising of 26 polyheterocycles **82** with yields ranging from 71 to 94%. This protocol was scaled up to 10 mmol scale without losing the performance of the GBB multicomponent reaction.

Recently, Xiong et al. [61] developed a one-pot stepwise synthesis comprising a GBB-3CR and a palladium-catalyzed azide-isocyanide coupling to generate imidazo[1,2-*a*]pyridine-fused 1,3-benzodiazepines **85** (Scheme 27). The GBB reaction smoothly proceeded using 2-azidobenzaldehydes **83**, 2-aminopyridines and isocyanides as the precursors. The in situ-generated azides **84** were then reacted with a different isocyanide (R^4–NC) in the presence of a palladium catalyst. The release of nitrogen from intermediates **I** resulted in nitrenes **II**, which in turn involved in the intramolecular transfer to yield species **III**. The carbodiimides **IV**, which were formed through reductive elimination of **III**, underwent intramolecular cyclization to deliver the desired products **85**. The scope of reaction showed that higher yield (57–90%) of **85** were obtained when benzaldehydes **83** were equipped with electron-donating groups (R^1) and when bulky groups, such as 1-adamantyl or *t*-Bu (R^4), were incorporated into the second isocyanides. The utility of this protocol was evaluated by conducting a gram-scale synthesis using 10 mmol of all precursors and there was no significant reduction in the yield of products.

Al-Tel et al. [62] developed a synthetic strategy where a Michael acceptor (a conjugated ester) was positioned in the aldehyde precursors **86** (Scheme 28). Various 2-aminothiazoles **87** and *tert*-butyl isocyanide (**5**) were reacted with **86** in the presence of $Yb(OTf)_3$, affording **88**. Addition of a new aliquot of $Yb(OTf)_3$ (30 mol %) allowed the new ring formation through a 7-*exo*-*trig* intramolecular aza-Michael addition, leading to the benzoxazepinium triflate salt **89**. To broaden the scope of the reaction, 2-aminopyrazine and 2-aminoquinoline were also introduced to the one-pot process, furnishing 6-7-5-6 and 6-7-5-6-6 polycycles, respectively (not shown).

Chen et al. [63] developed an interesting strategy for the construction of new tricyclic systems (Scheme 29). Adducts **92** were prepared from 3-phenylpropiolaldehyde (**90**), benzylisocyanides **91** and 2-aminopyridines via a $HClO_4$-promoted GBB reaction, then, under thermal conditions, in the presence of tetrabutylammonium bromide, an intramolecular nucleophilic addition of the secondary amines to the internal alkyne was expected to occur, forming a new pyrrole ring in **93** through a 5-*endo*-*dig* cyclization. Unexpectedly, they observed the generation of **95** with a new pyridine ring. The authors proposed that the benzylamine unit of **92** was oxidized to the corresponding imine **94** by oxygen in the air (as the cyclization did not proceed when the reaction was conducted under nitrogen atmosphere). The activation of the triple bond by tetrabutylammonium bromide regioselectively induced the 6-*endo*-*dig* cyclization to furnish **95** in moderate yields (41–67%).

Multicomponent polymerizations are simple and efficient methods to construct a library of polymers with great structural complexity and diversity, including fused-heterocyclic polymers[64]. Tang et al. [65] reported the transition-metal-free multicomponent polymerization of dialdehydes **96a–c** and diisocyanides **97a**,**b** in the presence of 2-aminopyridine (**1**, Scheme 30). The polymerization was carried out under mild conditions (in ethanol as the solvent and *p*-TsOH as the catalyst) and delivered six polymers featured with high yields (up to 98%), molecular weight (up to 41,700 g/mol), atom economy (water was the only byproduct) and thermal stability as well as remarkable fluorescence properties.

Multicomponent reaction can be also employed to prepare crystalline porous materials namely covalent organic frameworks (COFs). The structural diversity and functionality of COFs were assembled from organic monomers via a different type of

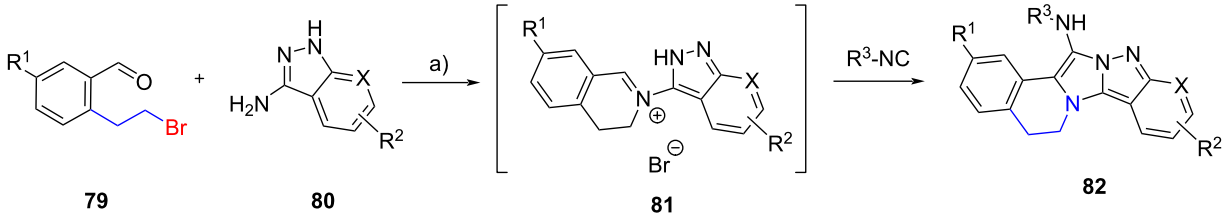

Scheme 26: One-pot cascade synthesis of pentacyclic dihydroisoquinolines (X = N or CH). In blue the structural motif involved in the secondary transformation, in red the leaving group that is not incorporated in the final product. Conditions: a) *p*-TsOH (20 mol %), EtOH, 78 °C, 1 h.

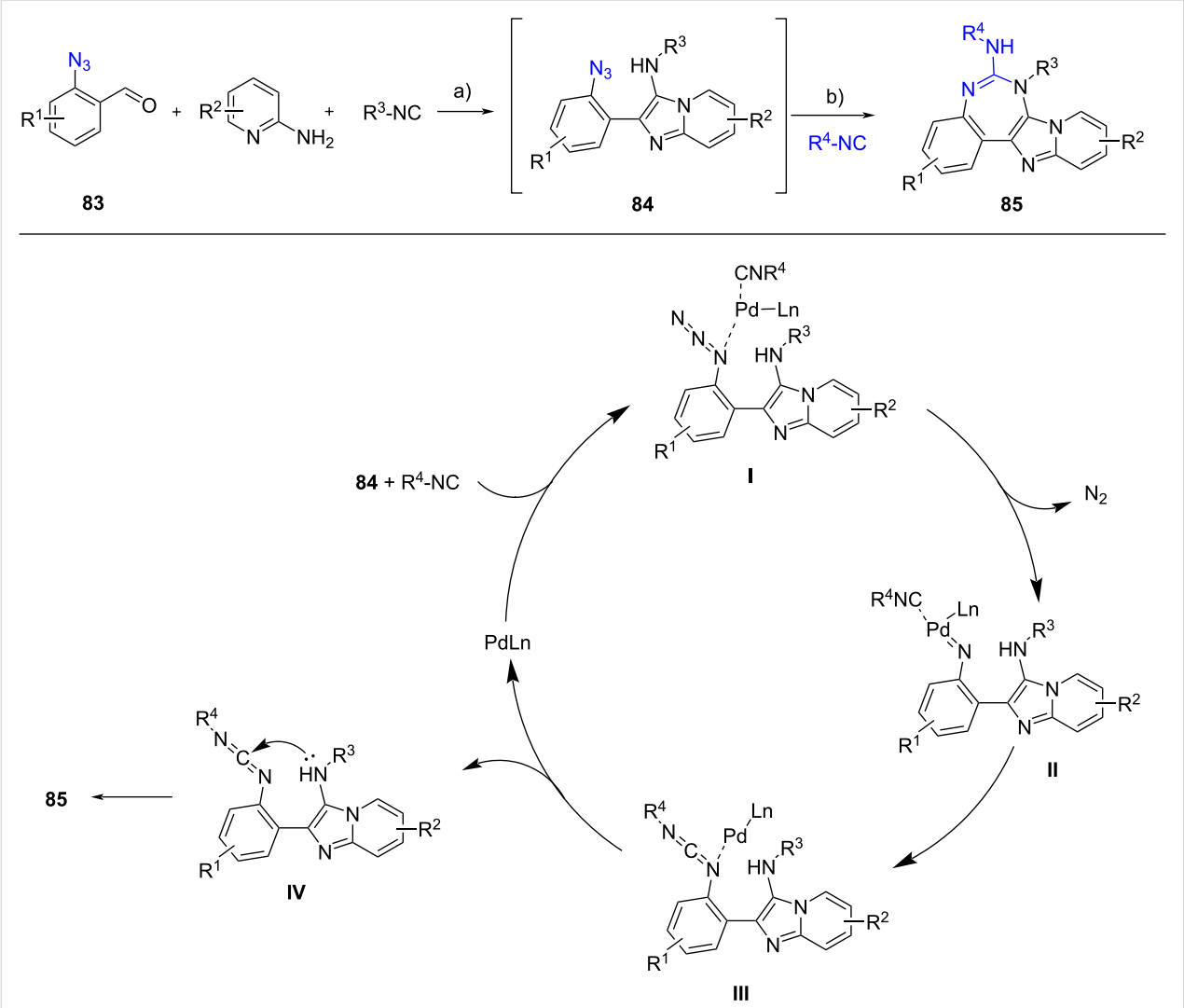

Scheme 27: One-pot stepwise synthesis of imidazopyridine-fused benzodiazepines **85**. Conditions: a) *p*-TsOH (20 mol %), MeOH, rt, 24 h; b) $Pd(OAc)_2$ (10 mol %), PhMe, 60 °C, 12 h.

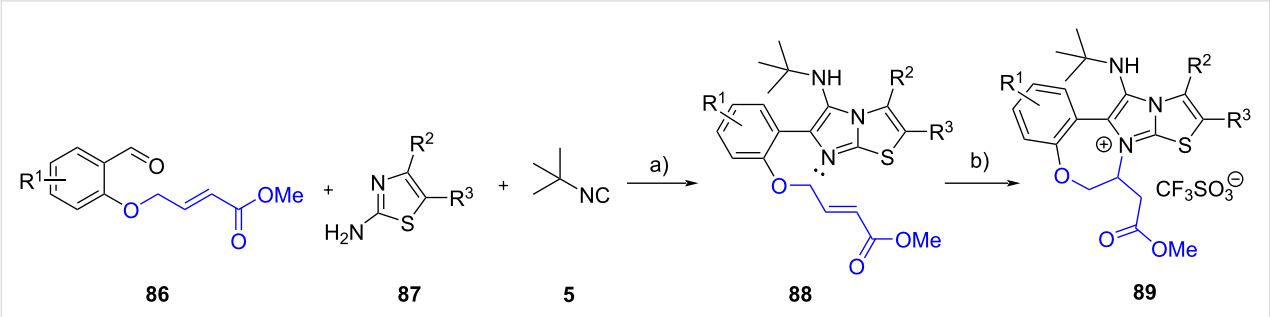

Scheme 28: One-pot stepwise synthesis of benzoxazepinium-fused imidazothiazoles **89**. Conditions: a) $Yb(OTf)_3$ (20 mol %), MeOH/DCM (3:1), rt, 12–15 h; b) $Yb(OTf)_3$ (30 mol %), 70 °C, 9–12 h.

organic reaction [66]. Wang et al. reported for the first time the synthesis of COFs via the GBB reaction [67]. In their study, 1,3,5-tris(3-fluoro-4-formylphenyl)benzene (**99**), 1,3,5-tris(4-isocyanophenyl)benzene (**100**) and 2-aminopyridines were engaged in the GBB reaction, furnishing COFs **101** (4 examples in 70–77% yield) in one-pot fashion. *p*-TsOH was utilized

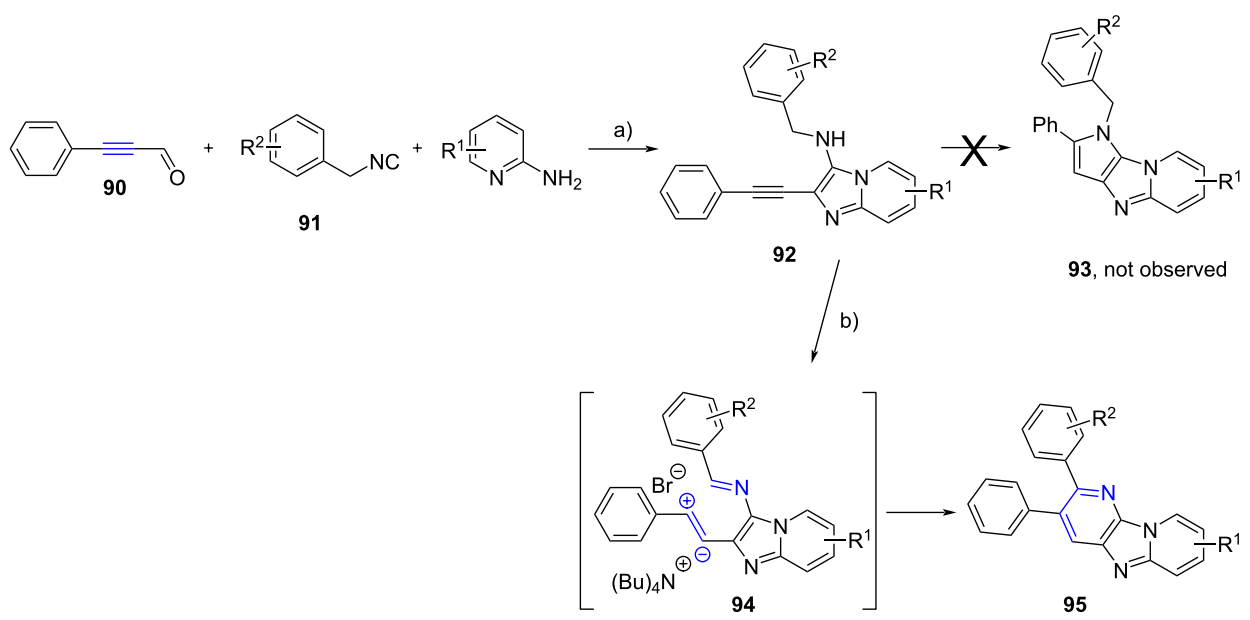

Scheme 29: One-pot stepwise synthesis of fused imidazo[4,5,*b*]pyridines **95**. Conditions: a) $HClO_4$, MeOH, rt, overnight; b) TBAB, DMF, 150 °C (MW), 30 min.

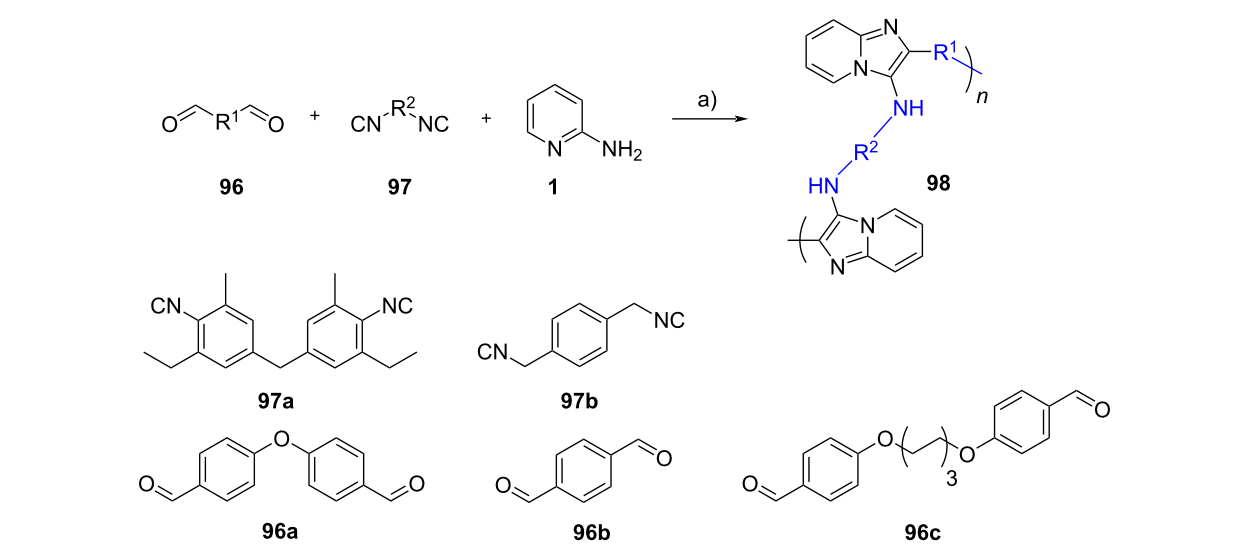

Scheme 30: Synthesis of heterocyclic polymers via the GBB reaction. Conditions: a) *p*-TsOH, EtOH, 70 °C, 24 h.

as the catalyst and the multicomponent reaction was conducted in ethanol/mesytilene at 120 °C. However, the reaction took 5 days to complete (Scheme 31).

The versatility of the GBB reaction in the synthesis of COFs was further demonstrated by employing the 1,4-diisocyanobenzene (**102**) monomer, leading to the generation of four COFs **103** in 71–88% yield. The results showed that the synthesized COFs displayed good chemical and thermal stability (Scheme 32).

3.2 GBB-like reactions

Basak et al. [68] reported a variation of the GBB reaction employing benzothiazole acetonitrile **104** (X = S) in place of the amidine component (Scheme 33). Knoevenagel condensation with an aldehyde in the presence of 2-(hydroxymethyl)pyrrolidinium acetate produced conjugated imines **105** as the reaction intermediates. Once generated, the intermediates **105** and isocyanides underwent formal [4 + 1] cycloaddition followed by tautomerization, affording benzothiazolpyrroles **106** (X = S) in moderate to good yields (52–82%). In addition, performing the

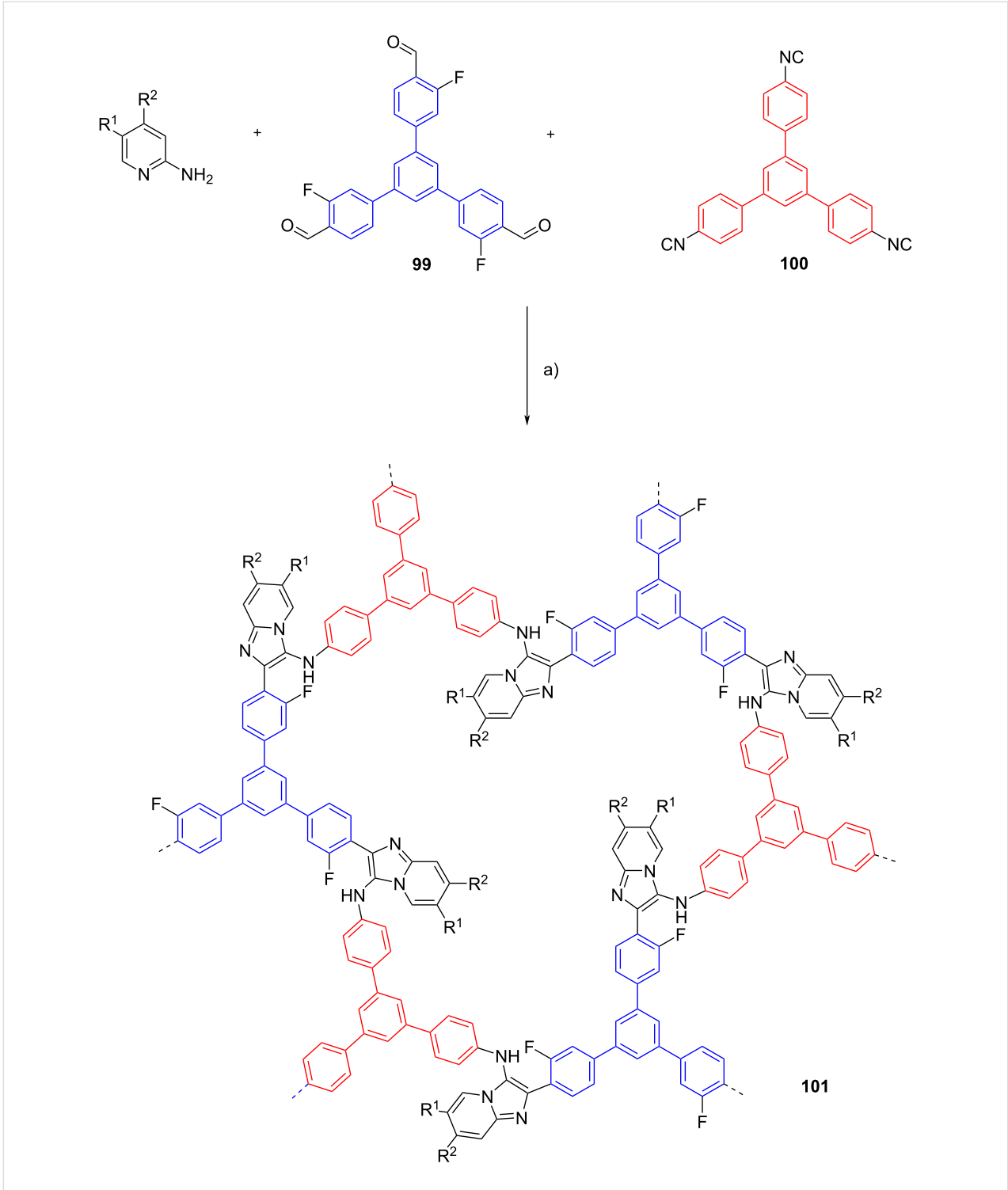

Scheme 31: One-pot multicomponent reaction towards the synthesis of covalent organic frameworks via the GBB reaction. Conditions: a) *p*-TsOH, ethanol/mesitylene (1:3), 120 °C, 5 d.

three-component reaction using benzoxazole acetonitrile **104** (X = O) or 2-pyridyl acetonitrile (not shown) led to the formation of benzoxazolpyrroles **106** (X = O) and indolizines (not shown), respectively.

The GBB reaction is a powerful tool for the construction of imidazo[1,2,*a*]pyridines. Khan et al. [69] envisioned an isocyanide-free protocol based on arylglyoxals **107**, 2-aminopyridines and aromatic amines (Scheme 34). The GBB-like multi-

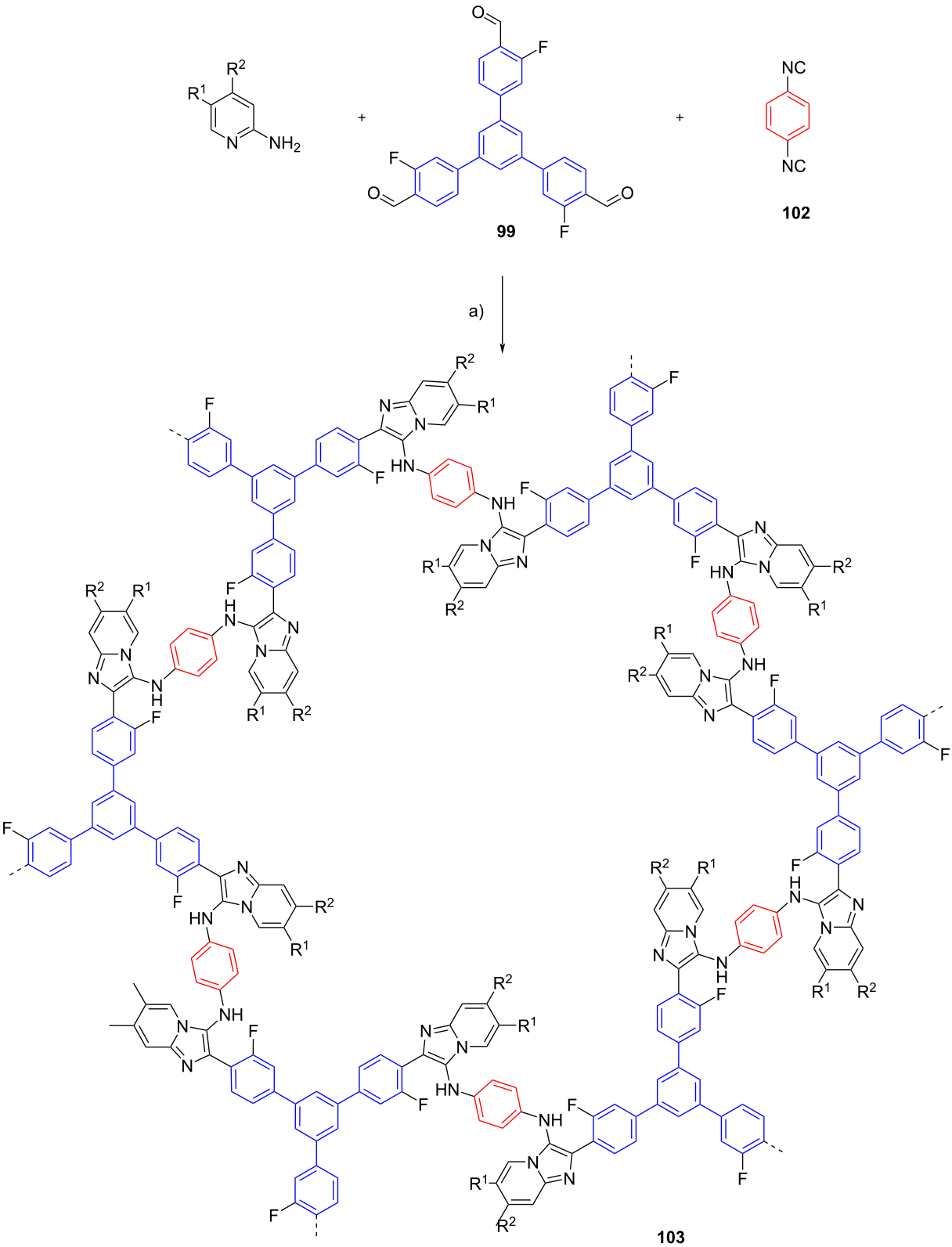

Scheme 32: One-pot multicomponent reaction towards the synthesis of covalent organic frameworks via the GBB reaction. Conditions: a) *p*-TsOH, ethanol/mesitylene (1:3), 120 °C, 5 d.

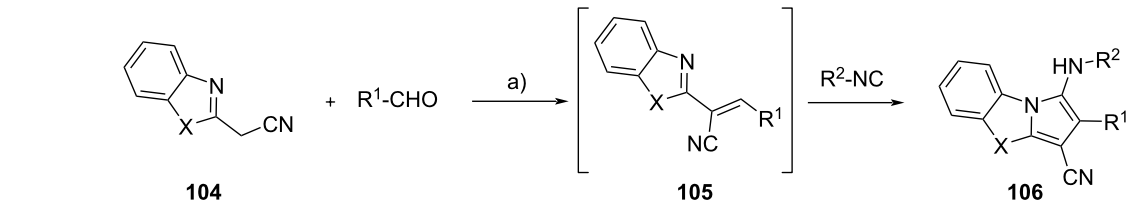

Scheme 33: GBB-like multicomponent reaction towards the synthesis of benzothiazolpyrroles (X = S) and benzoxazolpyrroles (X = O). Conditions: a) 2-(hydroxymethyl)pyrrolidinium acetate salt (10 mol %), PhMe, 80–130 °C, 3 h.

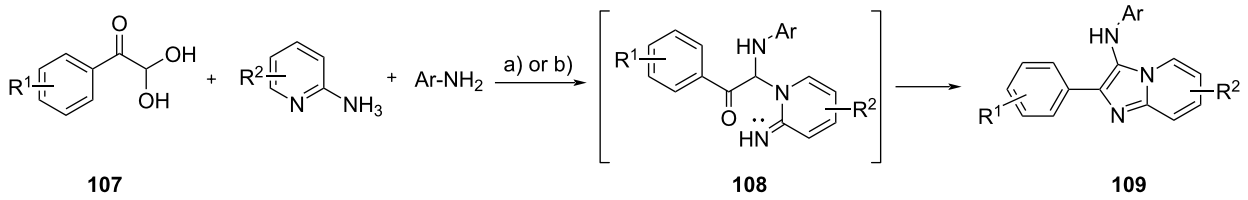

Scheme 34: GBB-like multicomponent reaction towards the formation of imidazo[1,2,*a*]pyridines. Conditions: a) I_2 (10 mol %), EtOH, 80 °C (MW), 45–300 min; or b) *p*-TsOH (20 mol %), EtOH, 55 °C, 1–1.5 h.

component reaction was carried out under MW heating. The initial condensation of the three precursors was catalyzed by I_2, providing electron deficient ketoimines **108**. The intermediates **108** underwent intramolecular heterocyclization to furnish the fused products **109**, formally derived from a GBB reaction with aromatic isocyanides and benzaldehydes. The same approach was used by Jalani and Jeong [70] where *p*-TsOH served as the catalyst for the one-pot reaction. A library of 21 examples of **109** were produced in 41–78% yields. Various functional groups were found to be compatible to the reaction conditions and a gram-scale synthesis was carried out to demonstrate the versatility of this methodology.

3.3 Post functionalization of GBB adducts

The structural complexity of the original scaffolds of the GBB adducts can be increased by decorating the structure of substrates (i.e., aldehydes or isocyanides) with additional functional groups for further modifications. Unlike the one-pot synthesis strategy, the adducts were isolated before being subjected to the post functionalization process.

Chebanov et al. [71] employed 2-(3-formylphenoxy)acetic acid (**110**), 2-amino-5-chloropyridine (**111**) and an isocyanide in a $HClO_4$-promoted GBB reaction (Scheme 35). The use of a benzaldehyde bearing a carboxylic acid enabled heterocycles **112** to undergo a Ugi four-component reaction with additional aldehydes, isocyanides and primary amines; the corresponding Ugi adducts (20 examples) **113** were obtained in 28–72% yields.

Mirza and Moghanlou [72] reported the solvent-free GBB reaction involving 4-(prop-2-yn-1-yloxy)benzaldehyde (**114**), 2-aminobenzimidazole (**115**) and isocyanides (Scheme 36). In this case, the additional alkyne group of **116** underwent a click [3 + 2] cycloaddition with the in situ-generated benzyl azides **117** to produce 15 examples of triazoles **118** in 63–88% yield.

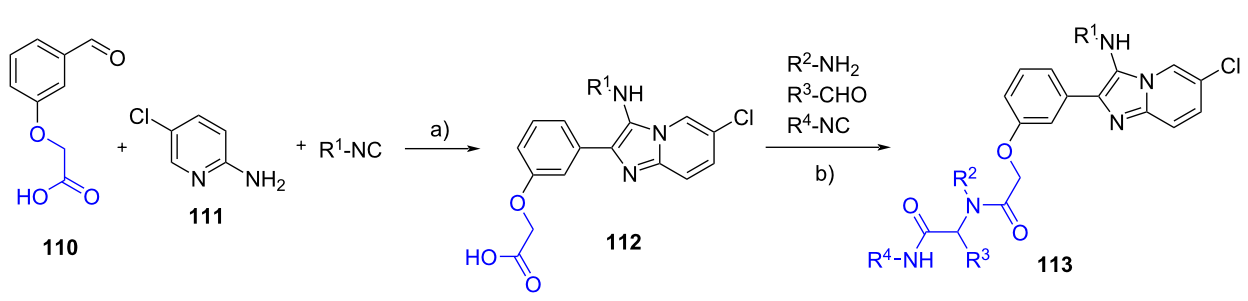

Scheme 35: Post-functionalization of GBB products via Ugi reaction. Conditions a) $HClO_4$, DMF, rt, 24 h; b) MeOH, 50 °C, 24–48 h.

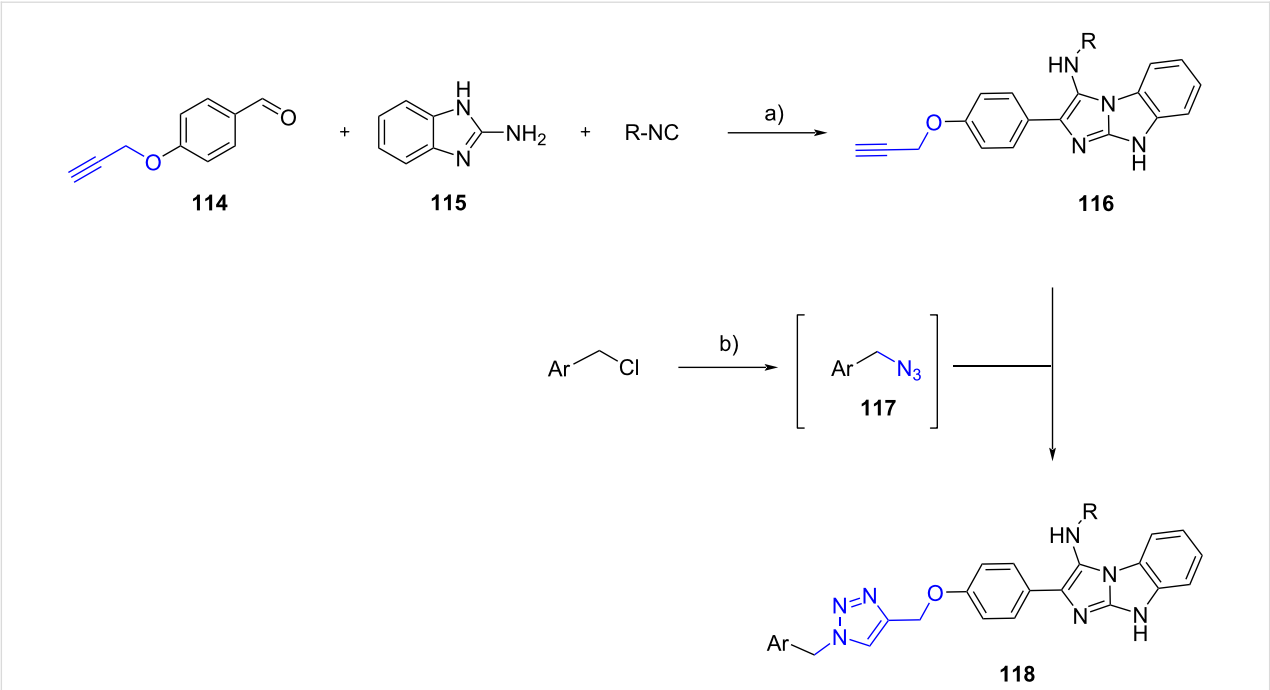

Scheme 36: Post-functionalization of GBB products via Click reaction. Conditions: a) solvent-free, 150 °C, 24 h; b) NaN_3, NEt_3, $CuSO_4$, sodium ascorbate, *t*-BuOH/H_2O (1:1), rt, 24 h.

Balalaie et al. [73] demonstrated a fascinating chemo- and regioselective post-functionalization of GBB products **120** by exploiting the reactivity of the triple bond of 2-(propargyloxy)benzaldehydes **119** (Scheme 37). They discovered the formation of unexpected spiro[chromene-imidazo[1,2,*a*]pyridine]-3'-imines **122** when the GBB precursors **120** were treated under basic conditions using 4 equivalents of KO*t*-Bu. They managed to create a small library of 15 spirocycles **122** in moderate to high yields (53–89% yields). The mechanism of spirocyclization reaction was studied using density functional theory (DFT). The DFT studies revealed that there were two possible mechanistic pathways. In the first scenario, the deprotonation of the propargyloxy group of **120** would trigger the alkyne–allene isomerization and the allene intermediates **121** were formed. The further treatment of allenes **121** using the excess KO*t*-Bu would induce the subsequent intramolecular nucleophilic *C*-addition (by imidazole carbon) or *N*-addition (by amine nitrogen) to allenes, leading to the generation of spirocycles **122** (via 6-*exo-dig* cyclization) or fused heterocycles **123** (via 8-*exo-dig* cyclization), respectively. In the second scenario, the treatment of the GBB products **120** using KO*t*-Bu could lead to the deprotonation of the secondary amine, generating nitrogen anionic intermediates **124**. Then, the spiro **125** and fused **126** products could be generated via the intramolecular nucleophilic *C*-addition or *N*-addition to the terminal alkynes. The DFT studies showed that the propargyloxy group displayed more thermodynamic acidity, whereas the amine showed more kinetic acidity. The potential energy surface can explain the selectivity of the reaction where the intramolecular nucleophilic addition was the rate-determining step in favor to the formation of spiro products **122** relatively to **123**, **125**, and **126**. Based on the calculation, the addition to allenes was more favorable than that to alkynes, as well as intramolecular nucleophilic *C*-addition compared to *N*-addition.

The combination of a GBB reaction with a Buchwald *N*-arylation was already reported by Guillamet et al. in 2012 [74], employing aminopyridines and aromatic aldehydes bearing a bromine atom in the *ortho*-position. In 2019, the same authors have reported an extension of the previous methodology using 5-amino-4-cyano-1*H*-imidazole (**56**) as amidine component (as described in the previous chapter), generating this time the imidazo[5′,1′:2,3]imidazo[4,5-*b*]indole scaffold **129** from adduct **128** (Scheme 38) [55]. The Buchwald reaction was found to be tolerant to both electron-donating (R = Me, 72% yield) and electron-withdrawing (R = F, 61% yield) groups displayed by aldehydes **127**, however, bromoheteroaryl aldehydes were unsuccessful.

The intramolecular *N*-arylation strategy could be extended through isocyanide insertion as demonstrated by Bräse et al. [75]. The authors proposed that the insertion of a second molecule of isocyanide on the GBB adduct **131**, derived from bromoaldehydes **127**, 2-aminopyridines **130** and *tert*-butyl

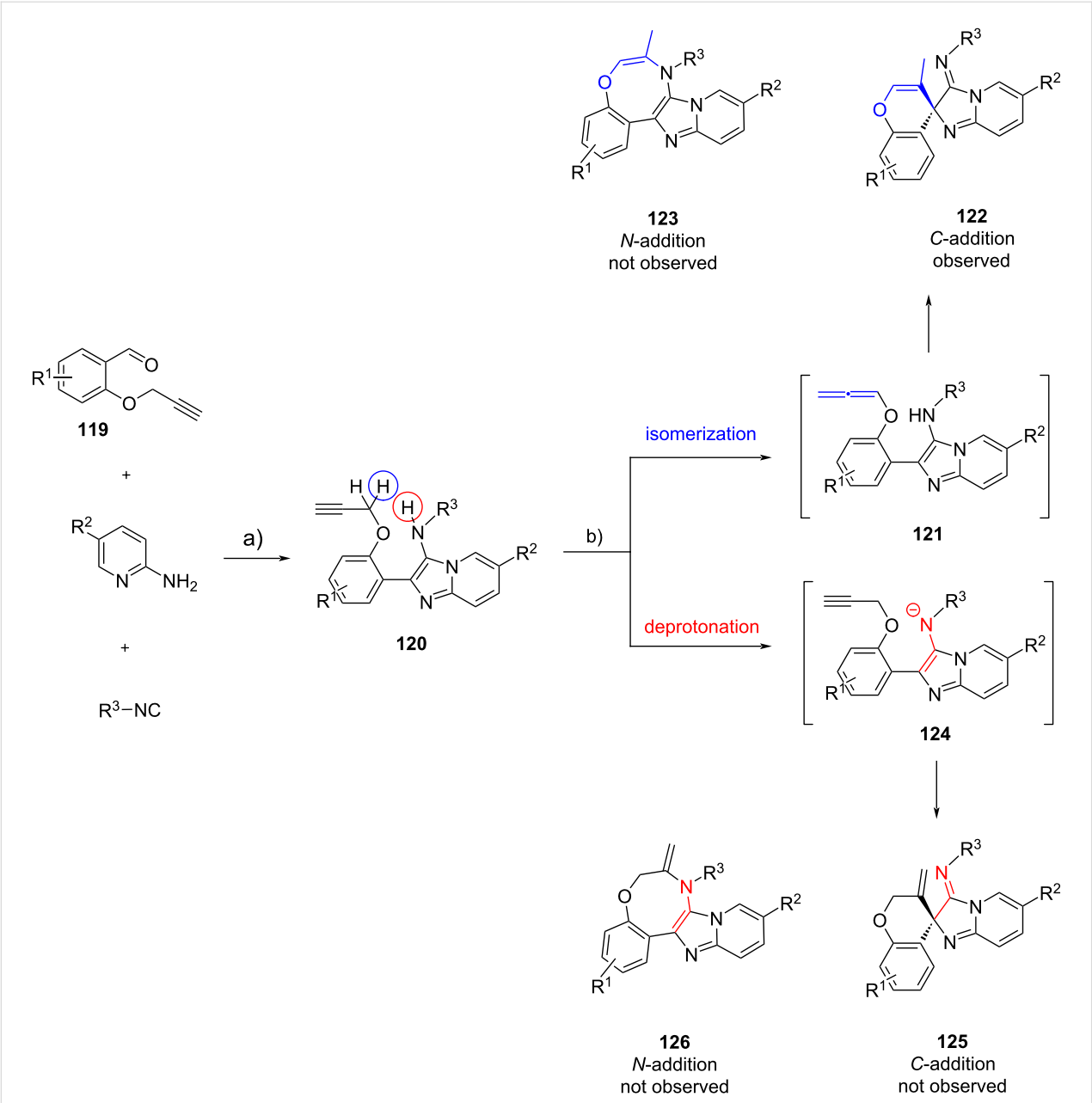

Scheme 37: Post-functionalization of GBB products via cascade alkyne–allene isomerization–intramolecular nucleophilic addition. Conditions: a) $InCl_3$ (10 mol %), MeOH, 55 °C, 12 h; b) KO*t*-Bu (4 equiv), DMSO, 55 °C, 4 h.

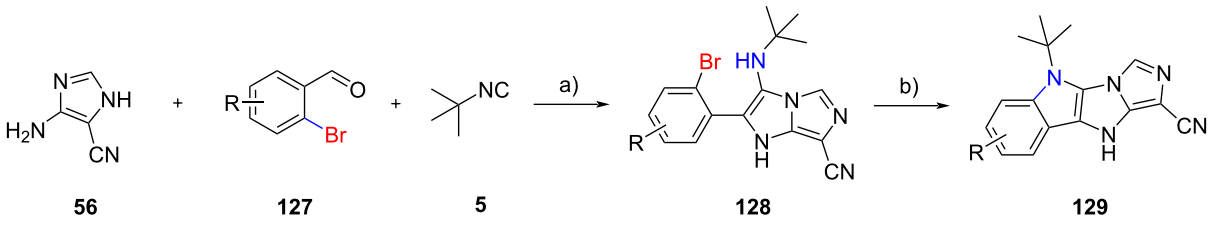

Scheme 38: Post-functionalization of GBB products via metal-catalyzed intramolecular *N*-arylation. In red and blue the functional groups involved in the Buchwald N-arylation. Conditions: a) $HClO_4$, MeOH, rt, 24 h; b) $Pd(OAc)_2$ (10 mol %), Xantphos, K_3PO_4, 1,4-dioxane, 120 °C, 2 h.

isocyanide (**5**), could take place between the secondary amine and the bromide, affording the imine intermediate **132** in the presence of a mild base like potassium acetate. The elimination of the *tert*-butyl group as isobutene gas, followed by tautomerization and aromatization, led to the generation of imidazo[4,5-*c*]isoquinolines **133** (Scheme 39). The use of a stronger base in the Buchwald reaction was not carried out since the *N*-arylation would be accelerated (compared to isocyanide insertion), yielding the corresponding five-membered ring as in Scheme 38. A small set of 13 polyheterocycles **133** was prepared with yields ranging from 20 to 94%.

Another strategy to access polyheterocyclic motif **133** was employed by Berteina-Raboin et al. [76] (Scheme 40). A series of GBB adducts **134** were initially prepared from 2-formylbenzonitriles, 2-aminopyridines and isocyanides under the reaction conditions optimized in their previous publication [77]. When R^3 = *t*-Bu, the treatment of the multicomponent products **134**

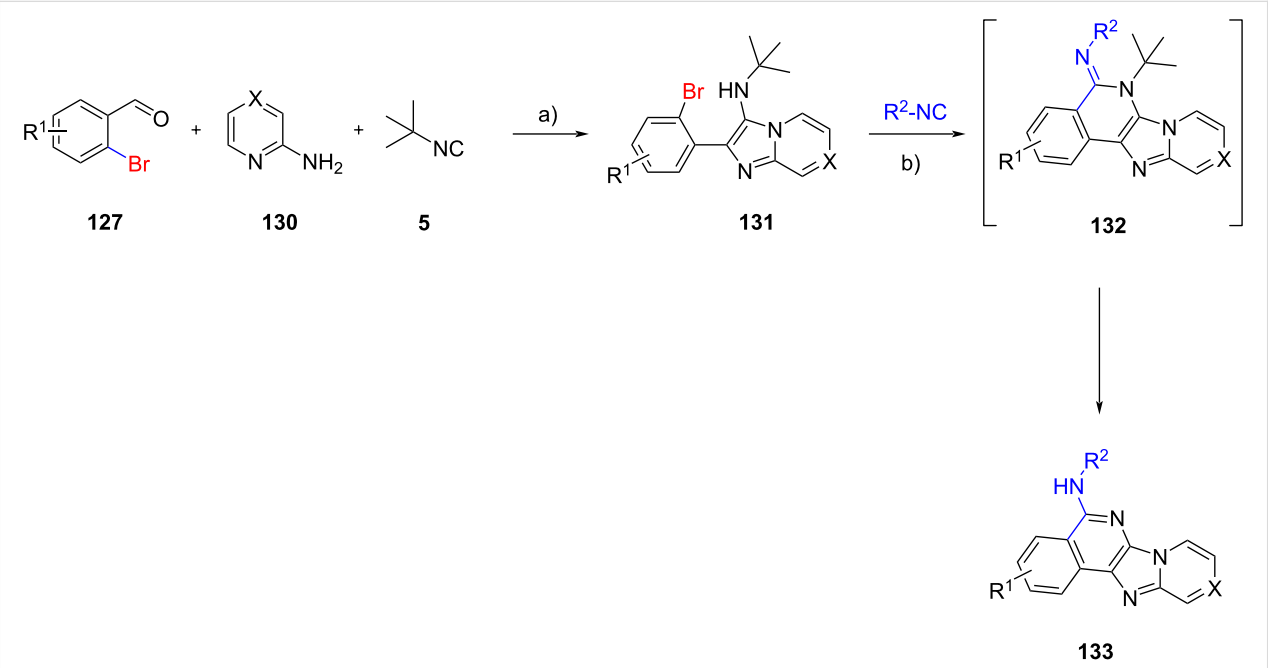

Scheme 39: Post-functionalization of GBB products via isocyanide insertion (X = N or CH). Conditions: a) $HClO_4$, MeOH, rt, 3 d; b) Pd-Peppsi, XPhos, KOAc, DMF, 120 °C, 24 h.

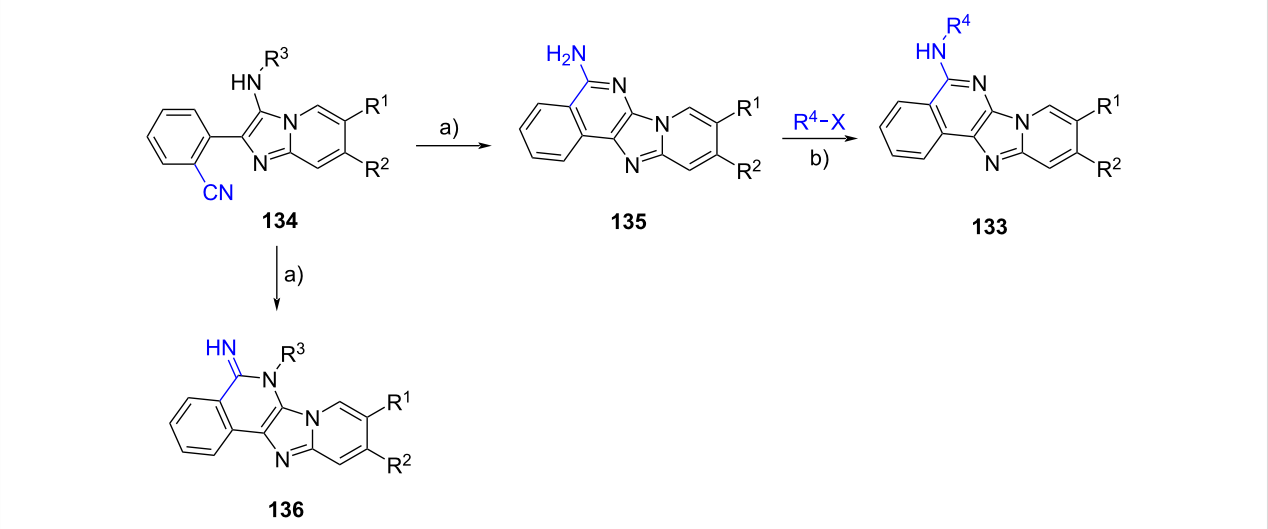

Scheme 40: Post-functionalization of GBB products via intramolecular nucleophilic addition to nitriles. Conditions: a) TFA/DCM (1:1), rt; b) $Pd(OAc)_2$, Xantphos, Cs_2CO_3, PhMe, 120 °C.

with TFA/DCM (1:1) facilitated the removal of the *t*-Bu group and the activation of the nitrile, leading to the formation of ten primary amines **135** with yields ranging from 65 to 92%. The primary amines **135** were then engaged with various aryl halides via Buchwald–Hartwig cross coupling reaction to generate the substituted polyheterocycles **133**. When cyclohexyl- and benzyl-tagged amines **134** (R^3 = Cy and Bn) were subjected to the intramolecular cyclization under acidic conditions, imines **136** were obtained in 80% and 78% yields, respectively.

The isocyanide-derived amino group of the GBB adducts can be involved also in a Pictet–Spengler reaction, as reported by Salunke et al. (Scheme 41) [78]. In this study, electron-rich aromatic aldehydes **137** were used as GBB substrates together with 2-aminopyridines and 1,1,3,3-tetramethylbutyl isocyanide (**138**). Upon completion of the multicomponent condensation, the *tert*-octyl group of **139** was removed by TFA, liberating primary amines **140**. *p*-TsOH-catalyzed Pictet–Spengler cyclization of primary amines **140** with other aromatic/aliphatic aldehydes (R^2-CHO) gave fused imidazo[4,5,*b*]pyridine derivatives **141**. By employing this protocol, the authors managed to produce 15 examples of polycyclic heterocycles **141** in 30–87% yields. The study of the reaction scope showed that the electronic effect on aromatic aldehydes (R^2–CHO) did not affect the cyclization reaction, however, lower yields were observed when aliphatic aldehydes were used as precursors, due to the instability of the Schiff base generated during the reaction.

In 2022, López et al. [79] prepared the hybrid compounds **145** by incorporating the furoxan moiety into the GBB adduct (Scheme 42). The multicomponent reaction was initially performed from 3-hydroxybenzaldehyde (**142**), 2-aminopyridine (**1**) and *tert*-butyl isocyanide (**5**). In the second reaction, **143**

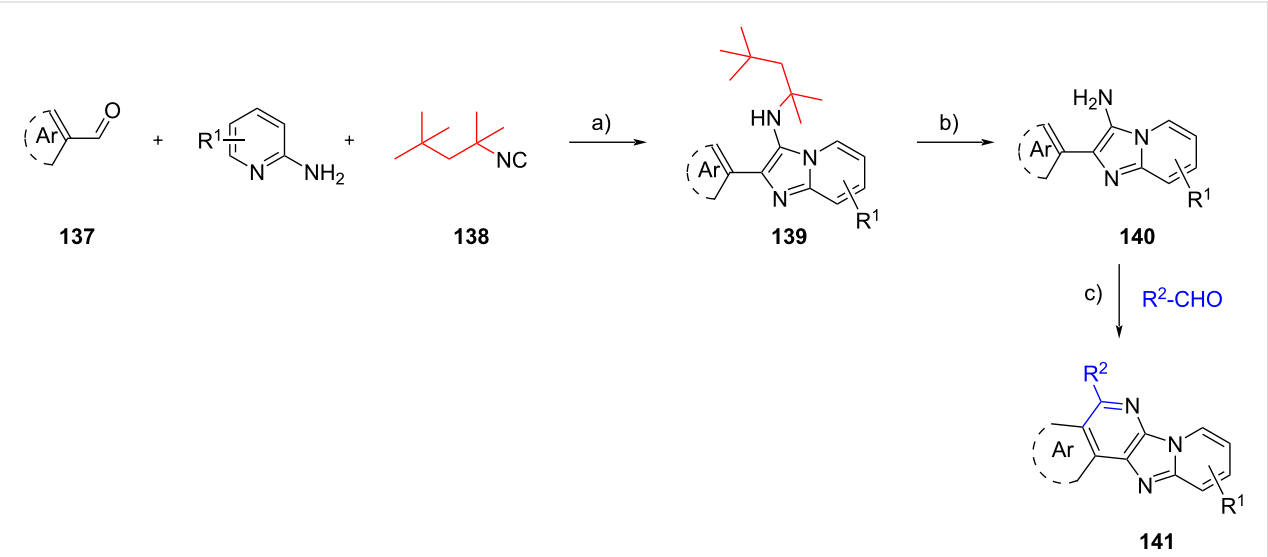

Scheme 41: Post-functionalization of GBB products via Pictet–Spengler cyclization. Conditions: a) 4 N HCl/dioxane, MeCN, 110 °C (MW), 20 min; b) TFA/DCM (1:1), rt, 25 min; c) *p*-TsOH, $PhNO_2$, 160 °C, 6 h.

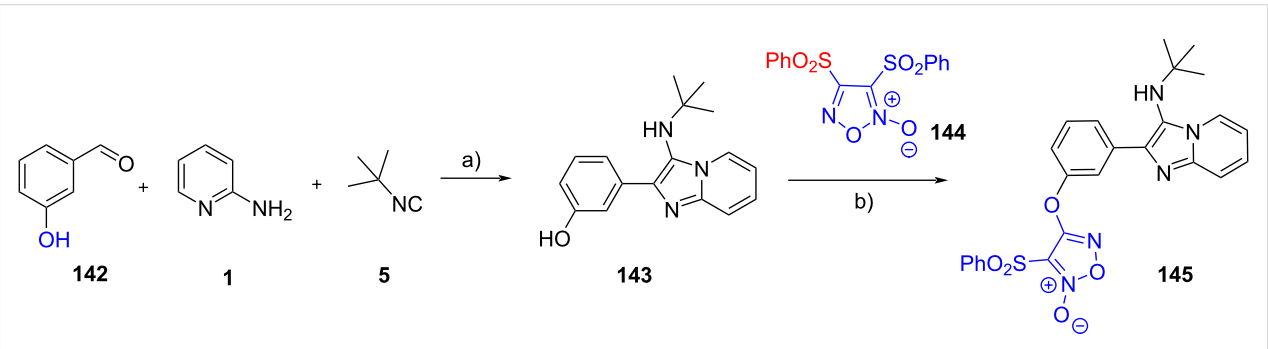

Scheme 42: Post-functionalization of GBB products via *O*-alkylation. Conditions: a) TFA (20 mol %), EtOH, 120 °C (MW), 20 min; b) NaOH, 2-MeTHF, rt. 24 h.

was then coupled with 3,4-bis(phenylsulfonyl)furoxan (**144**) under basic conditions to furnish GBB-furoxan hybrid **145**, albeit in low yield (23%).

Finally, Neochoritis et al. [80] exploited an intramolecular aliphatic nucleophilic substitution to obtain macrocycles. In this study, isocyanides were equipped with a tosylate leaving group. A range of substrates **147**, with different length and motif of the tethering groups, were prepared from the corresponding amino alcohols. Bifunctional derivatives **147** were then reacted with 2-hydroxybenzaldehydes **146** and 2-aminopyridines, affording adducts **148** in quantitative yields (Scheme 43). The subsequent treatment of **148** with DBU allowed the formation of 9-, 11-, and 13-membered macrocycles **149** with yields up to 69% (9 examples). The authors also demonstrated that 3-hydroxybenzaldehyde could be employed as the substrate for this transformation. Besides the GBB reaction, other multicomponent reactions such as Ugi–Smiles, classical Ugi four-component and tetrazole variation of Ugi reactions could be combined with the macrocyclization step to deliver numerous novel macrocyclic scaffolds.

4 Novel biological activities

Many GBB adducts displayed a variety of biological activities. In recent years, the researchers have evaluated their pharmacological properties by performing in vitro assays, such as antimicrobial (against bacteria and virus), anticancer (inhibition against cancer cell lines, tumor cells and proteins responsible for mechanisms of action) and anti-inflammatory. In some reports, the in silico studies (through molecular docking), ADMET predictions and structure–activity relationships were also carried out to evaluate the therapeutic potentials of the GBB products in drug development.

4.1 Antimicrobial activity

In 2023, Chebanov et al. [71] tested 9 compounds **113**, derived from the combination of GBB and Ugi type reactions (see Scheme 35), as antibacterial agents. There were four bacteria strains used in this study including Gram-negative of *Escherichia coli* strain 1257 and *Pseudomonas aeruginosa* strain 1111 as well as Gram-positive of *Bacillus subtilis* strain 1211 and *Staphylococcus aureus* strain 2231. Nitroxoline was employed as positive standard. Some of the synthesized adducts showed weak inhibition to the growth of four bacteria strains. Product **113a** (Figure 1) displayed bacteriostatic activity against *B. subtilis* at a concentration of 125 mg/L. It inhibited the growth of *S. aureus* and *E. coli* with MICs of 250 and 500 mg/L, respectively. The strain of *P. aeruginosa* was found to be resistant to most of adducts **113**.

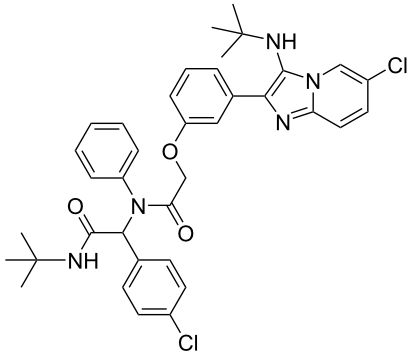

113a

MIC *Escherichia coli*, 500 mg/L
MIC *Pseudomonas aeruginosa*, –
MIC *Bacillus subtilis*, 125 mg/L
MIC *Staphylococcus aureus*, 250 mg/L

Figure 1: Antibacterial activity of GBB-Ugi adducts **113** on both Gram-negative and Gram-positive strains.

Molecular modification is an important strategy in drug discovery and development, in which the structure of known drug molecules is chemically altered to improve their physicochemical and pharmacodynamic/pharmacokinetic properties [81,82]. Lavilla et al. [83] developed antimicrobial agents by modifying the structure of trimethoprim (TMP, **150**), an antibiotic used to treat diseases due to bacterial infection such as bladder or middle ear infections and acute diarrhea. By taking advantage of the 2-aminopyrimidine group, TMP (**150**) along

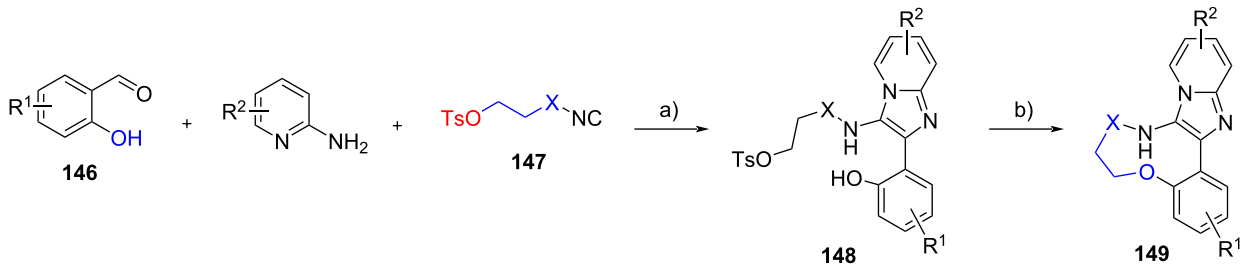

Scheme 43: Post-functionalization of GBB products via macrocyclization (X = -CH_2CH_2O-, -CH_2-, -$(CH_2)_4$-). Conditions: a) $Sc(OTf)_3$ (20 mol %), MeOH, rt, 24 h; b) DBU, DMF, 80 °C, 15–18 h.

with various aldehydes and isocyanides were introduced into the multicomponent reaction to generate the GBB adducts **151** with yields ranging from 6 to 59% (Scheme 44). Then, 15 compounds were evaluated for their antibacterial activity against *Escherichia coli* ATCC 25922, *Pseudomonas aeruginosa* PAO1 and *Staphylococcus aureus* ATCC 29213. The biological assay demonstrated that several GBB adducts (**151a**–**e**) were as potent as the marketed antibiotic TMP, where all tested compounds were more active against *E. coli* than *S. aureus*. The results indicated that the molecular modification strategy did not affect the synthesized compounds to penetrate the outer membrane of Gram-negative bacteria. However, *P. aeruginosa* was resistant to all GBB adducts and TMP standard. In addition, the synergistic effect was observed when all compounds **151a**–**e** were combined with sulfamethoxazole (1:20) in the in vitro assay against *E. coli* and *S. aureus*. The latter was found to be more sensitive to the drug combination than the individual compound. The drug synergism of all adducts **151a**–**e** with sulfamethoxazole was also effective to inhibit several clinical methicillin-resistant *Staphylococcus aureus* (MRSA) isolates, such as *S. aureus* 8125304770, 8139265926, 8125255044 and 8124825998 (not shown). Unfortunately, the drug combination with sulfamethoxazole showed no effect against *P. aeruginosa.*

Todd et al. [84] investigated the potential of 147 heterocycles containing fused imidazole scaffolds (where some of them (i.e., **152b**) were prepared through GBB multicomponent reaction) as antibacterials against methicillin-resistant *Staphylococcus aureus* (MRSA). A structure–activity relationship (SAR) study was carried out through the diversification of a bicyclic imidazole moiety with two (hetero)aryl substituents (in Figure 2 representative examples **152a**–**d** are reported). The in vitro assay revealed that 43 examples (including **152a**, **152b**, **152c**) showed promising antibacterial potency against MRSA with MIC ≤ 8 μg/mL. While 11 examples displayed moderate activity (MIC = 16 μg/mL), 88 examples were inactive (MIC > 32 μg/mL). Some products were also tested against vancomycin-resistant enterococcus (VRE), where **152b** displayed a low MIC value of 4 μg/mL.

The ADME prediction was then performed to evaluate the pharmacodynamics and pharmacokinetic properties of **152**, including thermodynamic aqueous solubility (≥10 μM), $logD_{7.4}$ value (<2), human PPB (≤95%), human liver intrinsic clearance (HLM CL_{int} < 9.0 mL/min/mg protein), and rat hepatocyte intrinsic clearance (rat hep CL_{int} < 5 mL/min/106 cells). The toxicity of the tested compounds was also carried out against the human lung fibroblast cell line MRC-5_{SV2} and primary mouse macrophages (PMM). The selectivity indices (SI, ratio of TC_{50} to MRSA MIC) were then calculated to evaluate the mammalian toxicity of the fused imidazole derivatives. Evaluation of MIC values, physicochemical properties and selectivity indices showed that compound **152c** could be a promising antibacterial agent against MRSA.

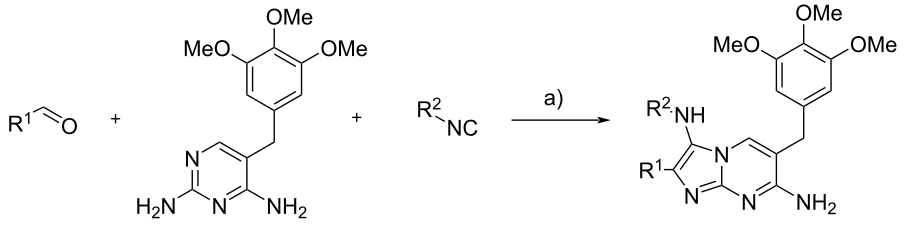

150

151a, R^1 = iPr, R^2 = *t*-Bu
151b, R^1 = Me, R^2 = *t*-Bu
151c, R^1 = 2-thienyl, R^2 = *t*-Bu
151d, R^1 = 3-pyridyl, R^2 = Cy
151e, R^1 = 4-pyridyl, R^2 = Cy

	MIC[a] (μM)			MIC[b] (μM)		
	E. coli	*S. aureus*	*P. aerug.*	*E. coli*	*S. aureus*	*P. aerug.*
151a	1.17	18.7	>74	1.17	4.68	37.4
151b	1.25	80.1	>82	0.63	5.01	40.0
151c	2.14	>68	>68	0.27	2.14	34.2
151d	1.02	65.5	>65	0.13	2.05	32.7
151e	2.05	65.5	>65	0.26	2.05	32.7

Scheme 44: GBB multicomponent reaction using trimethoprim as the precursor. Conditions: a) $Yb(OTf)_3$ or $Y(OTf)_3$ (20 mol %), MeCN, 80 °C. The table reports the antibacterial activity of the synthesized compounds against various bacteria strains. [a]Minimum inhibitory concentration (MIC, μM) of the GBB products; [b]minimum inhibitory concentration (MIC, μM) of the GBB products in combination with sulfamethoxazole (1:20).

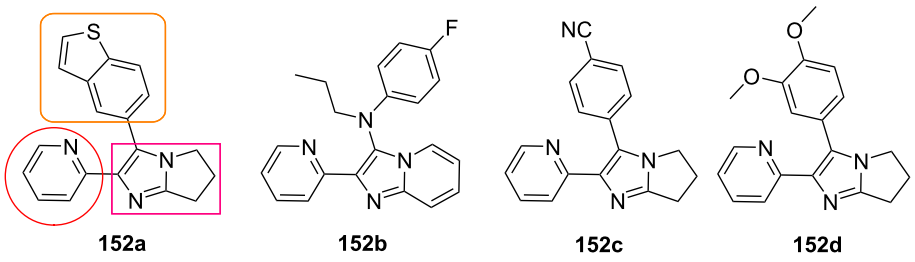

	152a	152b	152c	152d
MRSA MIC (μg/mL)	2	2	4	>32
VRE MIC (μg/mL)	8	4	16	NA
aq. sol (μM)	3	3	38	NA
$logD_{7.4}$	2.9	3.6	1.9	NA
PPB (%)	97.7	99.3	71	NA
HLM CLint (mL/min/mg protein)	61.5	61.8	99.1	NA
rat Hep CLint (mL/min/106 cells)	>300	108	7.99	NA
MRC5 TC_{50} (μg/mL)	0.5	1.5	7.5	NA
PMM TC_{50} (μg/mL)	0.6	0.7	18.3	NA
SI MRC5/MRSA	<0	1	2	NA
SI PMM/MRSA	<0	<0	5	NA

Figure 2: Antibacterial activity of GBB adducts **152** against MRSA and VRE; NA = not available.

A kinase target selectivity study was then applied to HEK293 cell lysates to comprehend the mechanism of action. In this case, the active (**152a**) and inactive (**152d**) compounds were used as the representative examples. The results demonstrated that the potential mammalian target for the tested compounds could be TGF-β1.

Salunke et al. [85] have created a library of 28 imidazo[1,2-*a*]pyrimidines and evaluated their in vitro antileishmanial activity against *Leishmania amazonensis* promastigotes and amastigotes. Among them, the GBB adduct **153** (Figure 3) displayed significant inhibition to the growth of promastigotes (IC_{50} = 8.41 μM) and intracellular amastigotes (IC_{50} = 6.63 μM). The authors found that the presence of a *tert*-octyl group at the secondary amine unit was important for biological activity. Compound **153** exhibited better activity than the reference drug miltefosine and showed low toxicity to the macrophages host cell (CC_{50} = 82.02 μM and SI macrophages/amastigotes = 12.37) as well as human-origin cancer cell lines of MCF-7, MDA-MB-231 and HEP-G2.

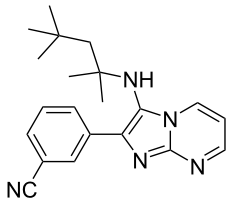

153

macrophages CC_{50} = 82.02 μM
promastigotes IC_{50} = 8.41 μM
amastigotes IC_{50} = 6.63 μM
SI macrophages/amastigotes = 12.37

Figure 3: Antibacterial activity of GBB adduct **153** against *Leishmania amazonensis* promastigotes and amastigotes, determined through growth inhibition assays.

The in silico study showed that compound **153** followed the Lipinski's rule of five, indicating that it displayed excellent bioavailability. Based on ADMET prediction, it is an inhibitor of several CYP450 enzymes and could be used through topical or oral administration.

ATP synthase is an essential enzyme for the growth of *Mycobacterium tuberculosis* and has been considered as potential target for antitubercular drugs [86]. Jain and Sen [58] investigated the potential of indole-substituted-imidazo[1,2-*a*]pyridines **61** (Scheme 23) as antitubercular agents. A series of 14 indole-substituted-imidazo[1,2-*a*]pyridines **61** were subjected to the ATP synthase inhibition assay. All compounds agreed the parameters of the Lipinski's rule of five. However, they showed a low level inhibition of ATP synthase.

Alsfouk et al. [87] have prepared fused imidazo[1,2-*a*]pyrazines **154** via GBB multicomponent reaction and evaluated their potential antiviral and anticancer activities (Figure 4). Among 4 tested compounds, adduct **154a** exhibited good antiviral activ-

154a

IC_{50} human coronavirus = 56.96 μM
CC_{50} = 406.86 μM
SI CC_{50}/IC_{50} = 7.14

154b

IC_{50} CDK9 = 0.16 μM
IC_{50} MCF7 = 8.59 μM; SI FHC/MCF7 = 11.31
IC_{50} HCT116 = 7.96 μM; SI FHC/HCT116 = 12.21
IC_{50} K652 = 4.45 μM; SI FHC/K652 = 21.84
IC_{50} FHC = 97.19 μM

Figure 4: Antiviral and anticancer evaluation of the GBB adducts **154a** and **154b**. In vitro antiproliferative activity was determined against several cell lines using the MTT assay.

ity against human coronavirus 229E with the IC_{50} value of 56.96 μM and no cytotoxicity on the target cells at CC_{50} of 406.86 μM. Both antiviral activity and selectivity indices of **154a** were even better than those of the standard drug ribavirin. Compound **154a** was then docked into SARS-Cov-2 main protease. The molecular docking studies demonstrated the key hydrogen bond interactions between Cys44 and the *N*-pyridine unit of **154a** with a binding free energy of −7.6 kcal/mol.

4.2 Anticancer activity

Imidazo[1,2-*a*]pyrazines **154** described above [87] have been tested by the same authors against cyclin-dependent kinase-9 (CDK9), a molecular target for the treatment of various malignant cancers, responsible for the cell cycle control and the promotion of cancer initiation as well as progression [88]. Derivative **154b** (Figure 4) exhibited promising inhibition potency on CDK9 with an IC_{50} of 0.16 μM. The in vitro antiproliferative activity of **154** was determined using the MTT (3-[4,5-dimethylthiazol-2-yl]-2,5 diphenyltetrazolium bromide) assay against several cancer cell lines including breast cancer (MCF7), colorectal myelogenous leukemia (K652) and colorectal cancer (HCT116). It was found that there was a correlation between cytotoxicity of **154** and their inhibitory activity against CDK9, indicating that the inhibition of CDK9 was the mechanism of action. Derivative **154b** was the most potent compound and superior to standard staurosporine. Moreover, it was more selective on cancer cell lines than on normal non-cancerous FHC cells. Molecular docking studies were performed into the ATP binding site of CDK9 and revealed a key interaction with Ile25 with a docking score of −8.3 kcal/mol. Based on in silico prediction, **154b** showed good drug-likeliness and displayed good oral bioavailability.

The anticancer activity against bladder cancer (T24) and prostate cancer (LNCaP) of previously described (Scheme 42) GBB-furoxan hybrids **145** was carried out by López et al. [79] by using the sulforhodamine B method. The results (Figure 5) demonstrated that hybrids **145b**, **145c**, and **145d** were more cytotoxic towards T24 and LNCaP cell lines than the reference compound cisplatin (GI_{50} T24 = 3.28 μM and GI_{50} LNCaP = 20.30 μM). Precursor **143**, lacking the furoxan scaffold (Scheme 42) showed no activity (GI_{50} > 100 μM) on both T24 and LNCaP cell lines, demonstrating the importance of the furoxan group. The antiproliferative activity of **145** against non-cancer cells (HaCaT cells, human keratinocyte) was then performed to determine the cytotoxic selectivity (SI = GI_{50} HaCaT/GI_{50} cell lines). While all compounds were selective toward T24 cancerous cells, showing better selectivity than the reference compound cisplatin, no selectivity was observed concerning the LNCaP cell line.

To elaborate the possible anticancer mechanisms of GBB-furoxan hybrids **145**, the authors carried out a nitric oxide (NO) release assessment [89]. The results showed that various levels of NO were produced in both T24 and LNCaP cancer cell lines by most of the compounds, however, there was no direct correlation between the antiproliferative activity and the amount of NO released.

Li et al. have synthetized 13 GBB-gossypol conjugates and evaluated them as anticancer agents [90]. Methylated gossypol **155**, 2-aminopyridines and isocyanides were transformed into double GBB adducts **156**, which in turn underwent demethylation to **157** with yields ranging from 78 to 94% yields (Scheme 45).

The antiproliferative assay on **157** was carried out against 7 cancer cell lines including HCT116, PC-3, A549, H23, U251, ACHN and H460. According to their previous study [91], hydrophobic groups embedded into the gossypol structure im-

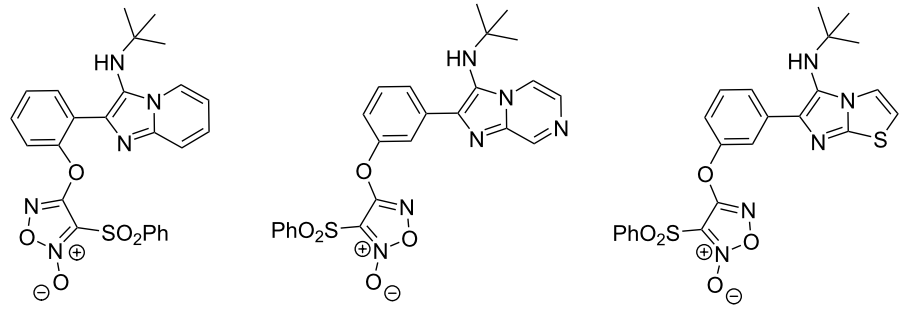

145b 145c 145d

	145b	145c	145d	cisplatin
GI_{50} T24 (μM)	0.85	2.72	0.83	3.28
GI_{50} LNCaP (μM)	7.70	8.13	16.53	20.3
GI_{50} HaCaT (μM)	3.11	9.86	9.01	2.51
SI HaCaT/T24	3.7	3.6	10.8	0.8
SI HaCaT/ LNCaP	0.4	1.2	0.2	0.1

Figure 5: Anticancer activity of the GBB-furoxan hybrids **145b**, **145c** and **145d** determined through antiproliferative assays on various cell lines.

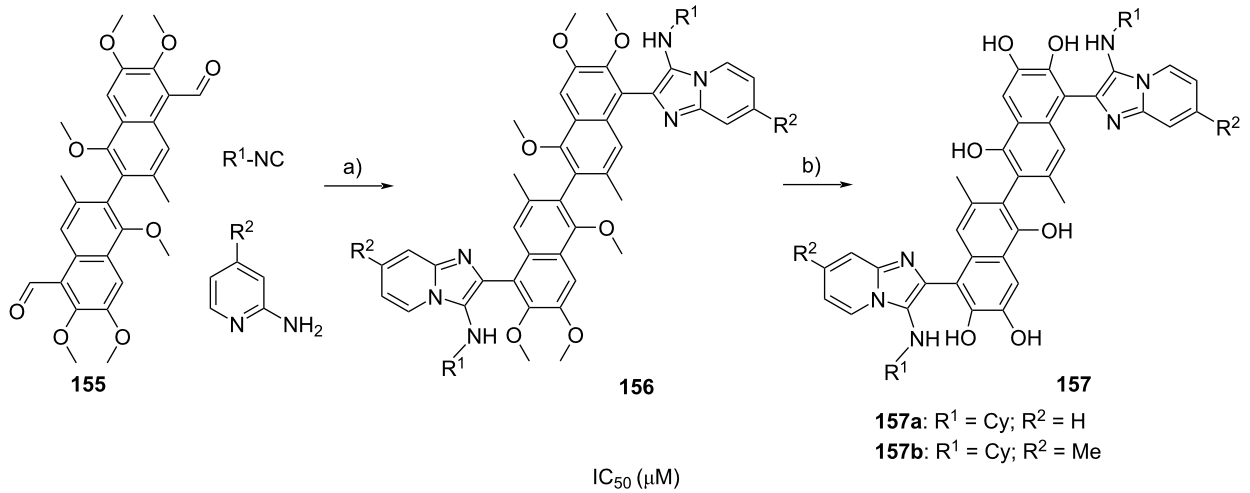

155 156 157

157a: R^1 = Cy; R^2 = H
157b: R^1 = Cy; R^2 = Me

IC_{50} (μM)

	HCT116	PC-3	A549	H23	U251	ACHN	H460
157a	0.79	4.55	0.31	2.61	0.41	0.79	2.73
157b	1.57	1.35	0.49	0.62	0.33	0.35	1.70

Scheme 45: Synthesis and anticancer activity of the GBB-gossypol conjugates. Conditions: a) $Sc(OTf)_3$ (10 mol %), DCM/MeOH (2:1), rt; b) BBr_3 (25 equiv), DCM, rt, then diluted HCl. Antiproliferative assays were carried out against 7 different cell lines.

proved the antiproliferative activity: GBB conjugates **157a** and **157b**, bearing a cyclohexyl group, were the most potent, compared to the conjugates bearing other alkyl or aromatic hydrophobic groups. The average IC_{50} on 7 cancer cells of **157a** was 1.74 μM. The cancer inhibition was enhanced when electron-donating groups were installed on the imidazopyridine unit (**157b**, R^2 = Me, average IC_{50} value of 0.91 μM). The mechanism of action, based on molecular modelling analyses and binding assays, demonstrated a possible interaction with anti-apoptotic proteins of the Bcl-2 family.

Previously described pyrido[2',1':2,3]imidazo[4,5-*c*]isoquinolin-5-amines **133** and pyrido[2',1':2,3]imidazo[4,5-*c*]isoquinolin-5(6*H*)-imines **136** (Scheme 40) have been tested for their anticancer activity against pediatric solid tumor neuroblastoma (SH-SY5Y cells) [76]. Derivatives **133a** and **136a**

exhibited antiproliferative activity below 10 μM in clonogenic assays (Figure 6). The apoptotic effects of **133a** and **136a** were validated through the upregulation of apoptotic proteins of cleaved caspase-3, cleaved PARP-1 and Bax.

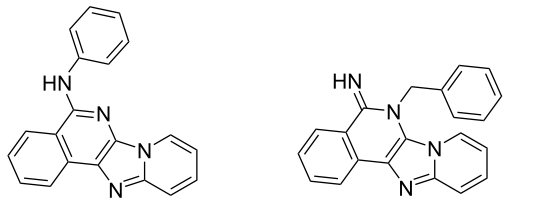

133a
IC_{50} neuroblastoma = 9.68 μM

136a
IC_{50} neuroblastoma = 1.68 μM

Figure 6: Anticancer activity of polyheterocycles **133a** and **136a** against human neuroblastoma. Clonogenic assays were carried out to determine the antiproliferative activity.

The molecular docking analysis was conducted using **133a** and **136a** as ligands and pro-apoptotic Bax protein as the target. The protein active site was positioned around the α1 and α2 helices. Compounds **133a** and **136a** showed docking scores of −6.7 and −6.9 kcal/mol, respectively. Both ligands generated important interactions with amino acid residues of Pro49, Pro51 and Leu25. Derivative **136a** also exhibited additional π-donor H-bond interactions with Gln52 and Asp53. The modelling study also showed that the interaction with the ligands could trigger the transformation of the α1–α2 loop from the closed conformation to the open one and this change of conformation could initiate the Bax activation, leading to the death of neuroblastoma cells.

Programmed death-1 (PD-1) is a co-inhibitory receptor which suppresses the activity of T-cells through the regulation of the TCR signaling. High expression of programmed death ligand-1 (PD-L1) in the microenvironment of tumors is frequently detected in various types of cancer. The binding of PD-L1 to PD-1 leads to T-cell disfunction, therefore blockage of the PD-L1/PD-1 interactions is a promising strategy in the development of anticancer agents [92,93]. Dömling et al. have designed, synthesized and evaluated 11 imidazo[1,2-*a*]pyridines **158** as PD-1/PD-L1 antagonists [94]. The design was conducted by incorporating a biphenyl, a methanamine and an amino group into the bicyclic heterocycle. The homogeneous time-resolved fluorescence (HTRF) assay against PD-1 and PD-L1 proteins showed that the compounds were able to disrupt PD-L1/PD-1 interactions. The presence of a dioxane moiety on the biphenyl unit and of a methyl group on the bicyclic ring lowered the IC_{50} values. The compounds with most promising PD-L1 inhibitory activity were **158a** and **158b** (Figure 7).

The use of topoisomerase (TOP1) poisons can kill cancer cells through the trapping of TOP1 on DNA, leading to lethal DNA double-strand breaks. A mechanism employed by cancer cells to resist killing by TOP1 poisons is the overexpression of enzymes capable to repair TOP1-DNA breaks, such as tyrosyl-DNA-phosphodiesterase 1 (TDP1). Therefore, the combination of TDP1 inhibitors and TOP1 poisons could synergistically be more effective for the treatment of cancer [95,96].

Burke, Jr. et al. have developed various imidazo[1,2-*a*]pyridine- and imidazo[1,2-*a*]pyrazine-based TDP1 inhibitors. In a first study [97] they exploited the small molecule microarray (SMM) method to identify new leads possessing TDP1 inhibition; a library of 21,000 compounds was screened generating 37 lead compounds, and among them imidazo[1,2-*a*]pyrazine derivative **159** exhibited micromolar TDP1 inhibition (Figure 8A).

Based on these findings, the authors synthesized a set of 23 imidazo[1,2-*a*]pyridines and imidazo[1,2-*a*]pyrazines via GBB reaction and evaluated their TDP1 inhibitory potency. The structure–activity relationship demonstrated that the presence of carboxylic groups at positions 1, 2 and 5 (Figure 8A) was important for TDP1 inhibition, while a carboxylic acid at position 4, as well as proton donors (such as CO_2H SO_3H and OH) at position 3, resulted in loss of inhibitory activity. On the other hand, introducing non-proton donor groups (such as CH_3, OBn,

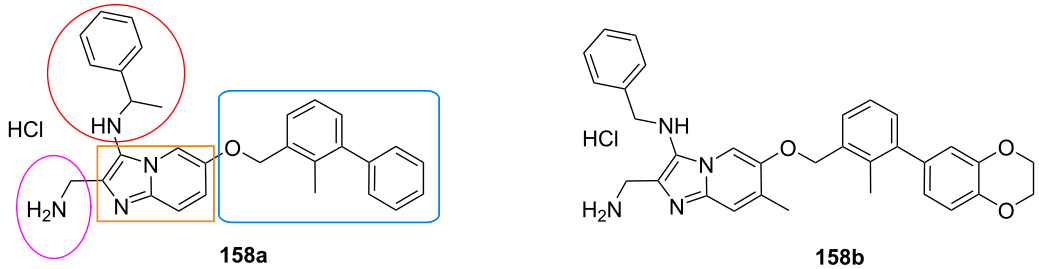

158a
IC_{50} PD-L1= 9.33 μM

158b
IC_{50} PD-L1 = 1.83 μM

Figure 7: Development of GBB-adducts **158a** and **158b** as PD-L1 antagonists. HTRF assays were carried out against PD-1 and PD-L1 proteins.

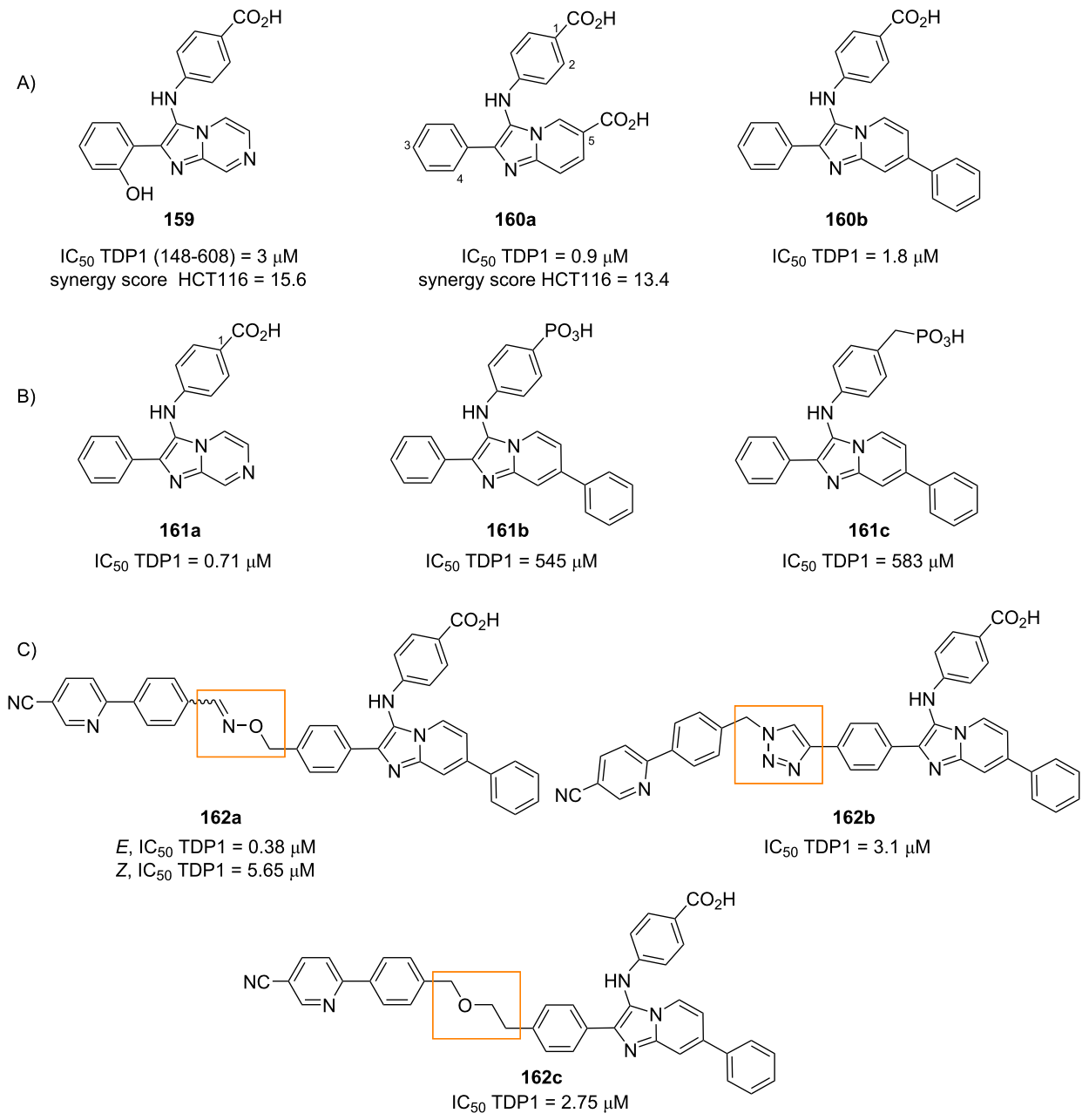

Figure 8: Development of imidazo[1,2-*a*]pyridines and imidazo[1,2-*a*]pyrazines as TDP1 inhibitors. The SMM method was used to identify new leads possessing TDP1 inhibition, determined through in vitro gel-based fluorescence assays.

CF_3 and NO_2) at position 3 was found beneficial. Moreover, the authors demonstrated that their TDP1 inhibitors synergistically acted with TOP1 poison camptotechin (CPT) in human colon cancer (HCT116) cell line, with synergy scores larger than 10.

As a continuation of their research, Burke, Jr. et al. designed phosphonic acid-containing variants of their previously reported inhibitors. X-ray crystal structures of phenylphosphonic acid- and benzylphosphonic acid-containing compounds **161b** and **162c** (Figure 8B) revealed that the phosphonic acid headgroup had different binding modes compared to the bioisosteric carboxyphenyl motif previously studied. Although an in vitro gel-based TDP1 assay demonstrated reduced TDP1 inhibitory potency compared to imidazo[1,2-*a*]pyrazine **161a**, having a carboxyl group at C-1 position, this work reported the first phosphonic acid-containing small molecule ligands capable of accessing the catalytic pocket of TDP [98].

Recently, Burke, Jr. et al. have modified compounds **160** introducing an oxime linker [99]. The GBB adducts bearing an

aminooxy group were initially reacted with 250 aldehydes in microtiter format and nearly 500 oximes were subjected to preliminary in vitro gel-based fluorescence assays. The promising oxime derivatives were further purified and tested for their TDP1 inhibitory activity (Figure 8C). Interestingly, the (*E*)-isomer of oxime **162a** exhibited greater inhibitory potency (IC_{50} = 0.38 μM) compared to (*Z*)-**162a** (5.65 μM). The oxime linker was then replaced with an isosteric triazole (**162b**) or ether (**162c**), obtaining however a slight decrease in TDP1 inhibitory activity. Additionally, the loss of inhibitory potency was observed when the length of the linker was increased. Compounds (*E*)-**162a**, **162b** and **162c** displayed great TDP1 selectivity over TDP2 and showed synergistic effect with TOP1 poison CPT against HCT116 cell lines.

Selective inhibition of histone deacetylases (HDACs) is a promising strategy in the discovery of anticancer agents. There are 18 human HDAC isoforms which can be classified into two different families and four distinct classes based on their structural properties, homology and cellular localization [100]. The first family is composed of zinc-dependent metalloproteins, divided into class I (HADC1, HADC2, HADC3 and HADC8), class IIa (HADC4, HADC5, HADC7, HADC9), class IIb (HADC6, HADC10) and class IV (HADC11); the second family is composed of NAD^+-dependent proteins and includes class III (Sirt1-7). Al-Tel et al. have developed anticancer agents through selective HDACs inhibition [101]. The HDAC inhibitors were designed based on the FDA-approved HDAC inhibitors for hematologic and solid malignancies treatment, such as vorinostat (SAHA) **163** (Figure 9). Key features were i) a zinc binding moiety (a trifluoromethyloxadiazole (TFMO) or a fluoro-aniline), ii) a cap group able to interact with the amino acid residues outside the hydrophobic pocket of HDACs (a GBB-derived imidazopyridine) and iii) a linker between them: to reduce the flexibility observed in vorinostat, a phenylbenzimidazole (**164a**) a phenyl (**164b**) or a benzamide spacer (**164c**) were investigated. The in vitro HDAC inhibition assay demonstrated that the derivatives bearing the TFMO unit **164a** and **164b** were selective toward HDAC5 while derivative **164c** displayed inhibitory activity against HDAC3 and HDAC9. The cytotoxic assay of adducts **164** and vorinostat **163** against breast (MCF7) and lung (A549) cancer cell lines showed that compound **164c** was active against MCF7 cancer cell lines and exhibited non-significant activity on A549 cells, while compounds **164a**, **164b** and **163** were inactive towards both cell lines. To further elucidate the mechanisms of action of compounds **164**, studies on apoptosis and cell cycle progression markers were performed. The activity could be correlated with the downregulation of the antiapoptotic biomarkers such as NF-kB, BCL2, BCL3 and C-MCY as well as the upregulation

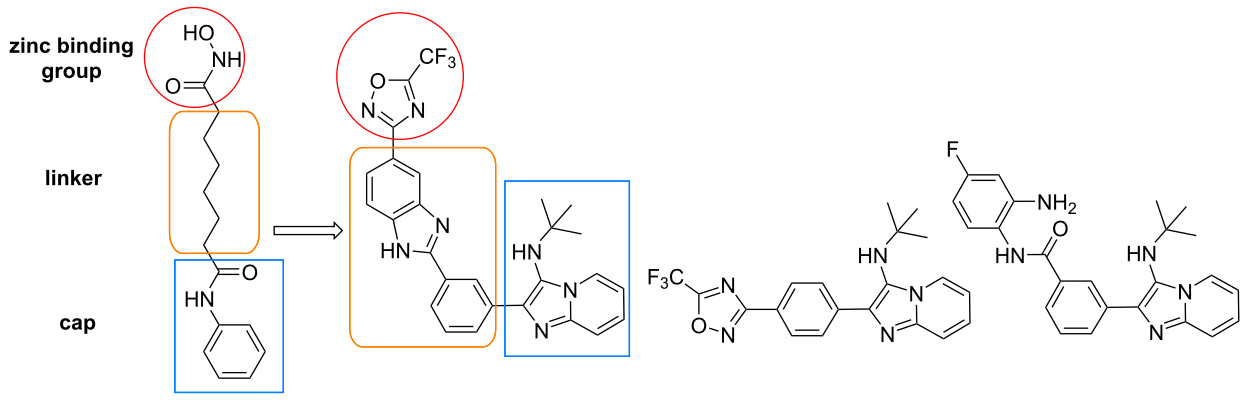

163 **164a** **164b** **164c**

	IC_{50} (μM)								
	HDAC1	HDAC2	HDAC3	HDAC4	HDAC5	HDAC7	HDAC9	MCF7	A549
164a	>10	>10	>10	1.646	0.31	4.851	0.818	>10	>10
164b	>10	>10	>10	3.584	0.8121	6.898	2.311	>10	>10
164c	>10	>10	2.12	>10	12.40	6.10	1.30	0.7	>10
163	0.010	0.013	0.019	>10	>10	>10	>10	>10	>10

Figure 9: GBB adducts **164a–c** as anticancer through in vitro HDACs inhibition assays. Additional cytotoxic assays were conducted against MCF7 and A549 cell lines.

of proapoptotic proteins such as caspases 3 and 7. Moreover, the expression of cell cycle progression of E2F1, RB1, CDK1, CDK2, CDK4 and CDK6 proteins was downregulated showing that the HDAC inhibitors **164** arrested the cell cycles. Based on the results, the authors concluded that the designed compounds **164** should be effective for the treatment of solid malignancies, such as MCF7.

Dömling et al. reported the synthesis of a 1536 member library of GBB adducts on nanomole scale: 71 isocyanides, 53 aldehydes and 38 cyclic amidines were dispensed in the wells of a 1536 plate using an innovative acoustic dispensing technology (only a subspace of the theoretical 142,994 compounds was synthetized). Although only in 21% of cases the multicomponent adduct was the major product (as determined by MS analysis), the unpurified GBB adducts were screened against the oncogenic protein–protein interaction menin–MLL (Mixed Lineage Leukemia) gene using differential scanning fluorimetry analysis, and several library members were found to be able to bind menin at μM concentrations [102]. This approach has been proposed as an alternative to high throughput screening (HTS) methods. Furthermore, the structural basis of the interactions between the ligands and menin was elucidated by co-crystal structure analysis, highlighting the ability of the imidazopyridine moiety to fit into the binding pocket, generating T-shaped π–π interactions.

4.3 Anti-inflammatory activity

Histone deacetylase 6 (HDAC6) has been associated with the activation of NLRP3 inflammasome, a target for anti-inflammatory therapy. This activation leads to the release of pro-inflammatory cytokines like interleukin IL1B, therefore HDAC6 inhibitors can be potentially used to treat chronic inflammatory diseases [103]. Hansen et al. have prepared 13 imidazo[1,2-*a*]pyridines **166** based on the structure of MAIP-032 **165** [104] and screened their anti-inflammatory activity through the inhibition of the HDAC6 enzyme [105]. Similarly to what reported in Figure 9, the imidazopyridine scaffold served as a cap group, while an hydroxamic acid was used this time as zinc binding group.

Molecular docking studies showed that derivatives **166** used their hydroxamic unit to bind Zn^{2+} ions and the secondary amine group to form a hydrogen bond with the serine residue (S531) at the L2-loop. The in vitro assay performed against human HDAC1 and HDAC6 additionally showed that the inhibitory activity against HDAC6 was improved when the C-1 position was decorated with a short or branched alkyl chain while introduction of an alkyl group into the C-2 position increased the inhibition of HDAC1 instead of HDAC6. Introduction of a fluorine atom in position C-3 of the linker improved both HDAC6 inhibitory activity and selectivity towards HDAC1. The results obtained by the most promising candidates **166a** and **166b** are shown in Figure 10.

The antiproliferative assay against glioblastoma U-87 MG cell line revealed that **166a** (IC_{50} = 19.5 μM) and **166b** (IC_{50} = 16.1 μM) were less potent than reference compound vorinostat (IC_{50} = 4.60 μM). In addition, both compounds inhibited the LPS-induced IL1B mRNA expression and TNF release by

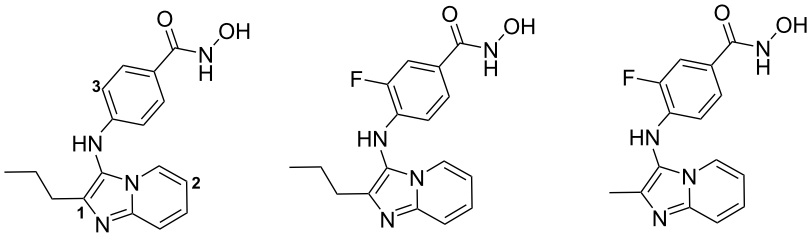

165 **166a** **166b**

	165	**166a**	**166b**
IC_{50} HDAC1 (μM)	2.20	5.87	3.07
IC_{50} HDAC6 (μM)	0.058	0.024	0.026
SI HDAC1/ HDAC6	38	245	118
IC_{50} U-87 MG (μM)	NA	19.5	16.1
IC_{50} TNF release (μM)	4.96	19.6	15.8

Figure 10: GBB adducts **165**, **166a** and **166b** as anti-inflammatory agents through HDAC6 inhibition; NA = not available. Additional antiproliferative assays against U-87 MG cell lines were carried out.

THP-1 macrophages. The results suggested that **166a** and **166b** could be developed for the treatment of inflammatory diseases driven by NLRP3 inflammasome.

5 Novel photophysical properties

It is widely recognized that the GBB-3CR leads to particularly fascinating products in terms of bioactive compounds. However, it is also important to underline that this multicomponent reaction allows a single-step synthesis of complex structures with a significant level of conjugation, hence compounds with potentially interesting photophysical properties, i.e., fluorescence [106]. Despite the evident advantages of this scaffold, examples of fluorescent GBB adducts published before 2019 and used for bio-imaging are limited, if we exclude for example the work by Lavilla et al. [49].

Gámez-Montaño et al. reported the synthesis of a series of potentially fluorescent imidazo[1,2-*a*]pyridine-3-amines **168** starting from triphenylamine aldehyde **167**, with a protocol that involved MW heating and NH_4Cl as catalyst; 16 different compounds have been synthesized in good yields (80–92%) (Scheme 46) [107]. Thanks to an intramolecular charge transfer (ICT) process between the strong electron-donor (triphenylamine) and the acceptor (imidazopyridine), demonstrated by time dependent DFT calculations, the products showed a fluorescence emission from blue to green, achieving a fluorescence quantum yield of 66.2% and a large Stokes shift (6780–9011 cm^{-1}). Substitution on the imidazole ring as well as on the 3-amino group could affect the quantum yield and both steric and electronic effects were evaluated, the latter having the greater influence. To prove that these compounds were suitable for bio-imaging applications, they tested compound **168a**, displaying the best quantum yield, as a fluorescent probe in HEK293 and Hela cells (epithelial from human kidney embryo and cervix carcinoma), observing nuclear-specific fluorescence imaging in both cell lines.

In bio-imaging, tuning the absorption and fluorescence emission of probes to higher wavelength is becoming increasingly important as demonstrated by Hulme et al., who published a work about the full spectrum tuning of fluorescent molecules synthesized through MCRs [108]. Specifically, they proposed the synthesis of pyrido[2′,1′:2,3]imidazo[4,5-*c*]isoquinolines and substituted imidazo[1,2-*a*]pyridin-3-amines via the GBB reaction. They studied the tuning of these compounds (achieving emission spectra from 400 to 700+ nm), the structure–photophysical property relationship (SPPR), the solvent effect and they also performed time-dependent DFT (TD-DFT) computations. The syntheses, shown in Scheme 47, involved either a trimethylsilyl cyanide (TMSCN) modified GBB-3CR or, using two equiv of aldehydes, a TMSCN-modified GBB-3CR combined with a one-pot aza-Friedel–Crafts/intramolecular cyclization/oxidation (AFCICO) step. They obtained respectively imidazo[1,2-*a*]pyridin-3-amines **169** and pyrido[2′,1′:2,3]imidazo[4,5-*c*]isoquinolines **170**. Fluorescent analysis showed that better results, in terms of quantum yields and increased wavelength, were obtained with primary amines **169**. It was observed that the most relevant effect for increasing the wavelengths of excitation and fluorescence was the introduction of an electron-withdrawing group on the *para* position of 2-aminopyridine, while electron-donating groups on the aldehyde consistently increased the quantum yield without affecting the fluorescence wavelength: compound **169a** showed an emission maximum above 700 nm, with a quantum yield close to 10% in MeOH. Thanks to TD-DFT computations, these effects were correlated to differing characters of the natural transition orbitals (NTOs).

In the work published by Dömling et al., already cited in chapter 2, the GBB-3CR is exploited to obtain imidazo-fused heterocycle dimers. Starting from a new building block, the glyoxal dimethyl acetal, an orthogonal bifunctional monoprotected reactant, they synthesized different structures **172** that have proven to be color-tunable fluorophores [43]. They used the optimized conditions, reported in Scheme 48, to synthesize 37 symmetric GBB dimers **172** and 6 unsymmetric ones (not shown). Investigating the luminescence properties of the obtained compounds, they observed how changing the substituents the emission could be tuned from blue to green and yellow. Exciting at 365 or 370 nm in THF at 25 °C, products **172** with

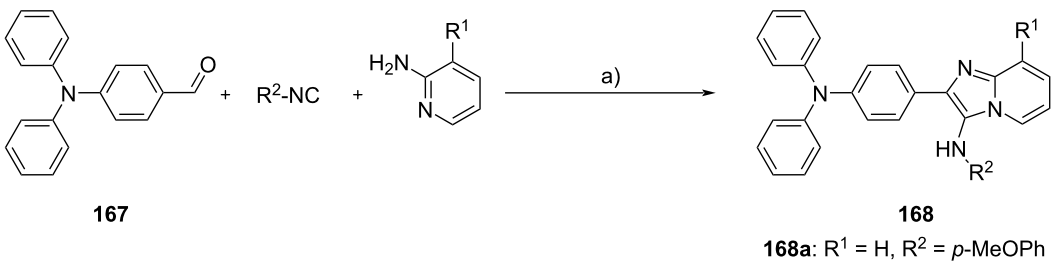

Scheme 46: GBB reaction of triphenylamine **167**. Conditions: a) NH_4Cl (10 mol %), MeOH, 80 °C (MW), 1 h.

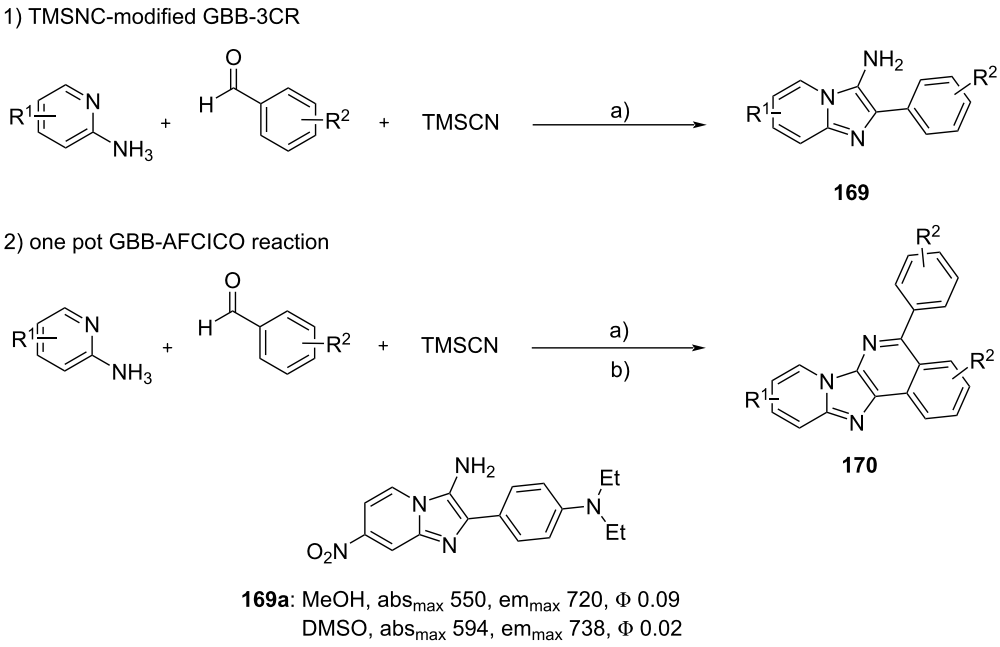

Scheme 47: 1) Modified GBB-3CR. Conditions: a) TMSCN (1.0 equiv), $Sc(OTf)_3$ (0.2 equiv), MeOH, 140 °C (MW), 20 min. 2) One pot synthesis. Conditions: a) TMSCN (1.0 equiv), $Sc(OTf)_3$ (0.2 equiv), MeOH, 140 °C (MW), 20 min; b) H_2SO_4 (50 equiv), MeOH, 140 °C (MW), 20 min.

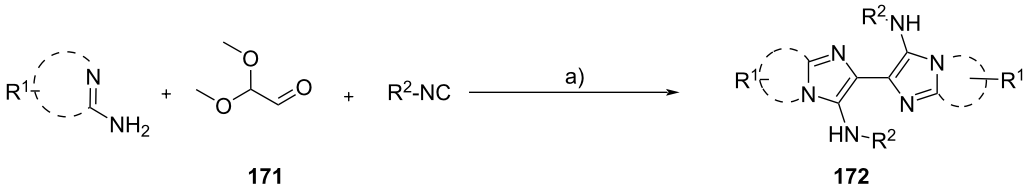

Scheme 48: GBB reaction to assemble imidazo-fused heterocycle dimers **172**. Conditions: a) $Sc(OTf)_3$ (20 mol %), MeOH, 100 °C (MW), 1 h.

an aromatic amine residue, emitted at 455 nm (blue), while compounds functionalized with alkylamino substituents (*tert*-butylamino or cyclohexylamino groups) shown a red-shifted emission spectrum (respectively 460 and 500 nm). It was also observed that the addition of an electron-donating group on the pyridine, such as a methyl group, led to a slight blue shift (490 nm vs 500 nm). By adding an electron-withdrawing group such as -Br or -CF_3 on the aromatic amidine, a red shift in the emission spectrum was observed, but associated to a decrease of fluorescence intensity.

A work that deserves to be mentioned also in this chapter is the one of Prasad et al., already reported in chapter 2, for the use of novel sugar-derived building blocks **31** (Scheme 12) [39]. Novel base-modified fluorescent nucleosides are essential to get a deep understanding of structure and function of nucleic acids. Products **31** exhibit fluorescence emission and a good Stokes shift (59–126 nm), therefore seem potentially useful for such applications. Due to the extensive conjugation provided by the imidazopyridine nucleus, these compounds have higher absorption and emission bands compared to parent thymidine.

Other two remarkable works, already presented in previous chapters, are the one presented by Bräse at al. [45] and by Tang et al. [65].

In the first one, the authors synthesized PCP-based imidazo[1,2-*a*]pyridyl-substituted ligands **38** (Scheme 15). These products can be potentially used as spatially-oriented through-space conjugated TADF (thermally activated delayed fluorescence) emitters. Checking their fluorescence properties, it was observed that they are strongly blue fluorescent both in solid state and solution. Changing the partners in the GBB-3CR, the fluorescence could be tuned. The amidine component influenced only slightly the Stokes shift, while strong electron-donating isocyanides could produce a decrease of the Stokes shift and a blue shift. The dimeric PCP adduct, also synthetized in the same study, did not lead to remarkable changes. Fluorescence proper-

ties could be modified also by inserting various π-extended or substituted components. A pH-dependency analysis was also carried out, and it was observed that fluorescence decreased in acidic solution, probably due to protonation of the nitrogen atom of the imidazole ring, while an increase of fluorescence and an hypsochromic shift was found in basic solution, possibly due to a destabilization of the excited state.

Tang et al. reported the synthesis of a series of polymers **98** through a transition-metal-free multicomponent polymerization (Scheme 30). These polymers showed acid/base-triggered reversible fluorescence response in solution. In fact, by increasing the amount of HCl, the emission intensity was gradually quenched, while absorption did not drastically change, but, by addition of NaOH, initial fluorescence properties were recovered. This proved that no structure decomposition occurred upon the addition of acid and also that the fluorescence of the polymer could be switched between the "off" state (when an excess amount of HCl was added) and the "on" state (when an equal amount of NaOH was added). The mechanism of fluorescence suppression was revealed by proton NMR studies of model compounds **173** and **174** (Figure 11) in the presence of increasing amounts of HCl in DMSO-d_6: the addition of acid led to the protonation of both the nitrogen atoms of the imidazo[1,2-*a*]pyridine scaffold and the amine moiety, generating a strongly electron-deficient center, resulting in an intramolecular photoinduced electron-transfer (PET) process that quenched the emission [109].

Conclusion

As demonstrated by the large number and diversity of articles reported in this review, the GBB reaction has now assumed considerable importance in the landscape of multicomponent reactions. As foretold by Dömling et al. in the review published five years ago, new fields of application, bioactive compounds and technologies have been developed in recent years. The use of the GBB reaction in the synthesis of DNA encoded libraries, the first example of a biocatalytic GBB reaction, the exploitation of enabling technologies such as flow chemistry, the preparation of covalent organic frameworks, and the synthesis of tunable bio-imaging agents are just some of the examples discussed in this review. Alongside these more innovative and interdisciplinary features, which make the GBB reaction extremely appealing in emerging fields of application, the incessant search for new catalysts, building blocks and scaffolds confirm the robustness of this reaction in the landscape of organic synthesis. At the same time, the constant search for increasingly potent and selective pharmacologically relevant compounds and the recent interest in the photophysical properties demonstrate the broad spectrum of applicability of GBB adducts. Resuming what was written in the introduction, the GBB reaction undoubtedly occupies a senior position in the family of multicomponent reactions, and the impression of the authors is that, compared with its older relatives, it has much more space for new future developments.

Author Contributions

Cristina Martini: conceptualization; writing – original draft; writing – review & editing. Muhammad Idham Darussalam Mardjan: conceptualization; writing – original draft; writing – review & editing. Andrea Basso: conceptualization; writing – original draft; writing – review & editing.

ORCID® iDs

Cristina Martini - https://orcid.org/0009-0008-8188-6208
Muhammad Idham Darussalam Mardjan - https://orcid.org/0000-0001-7282-1279
Andrea Basso - https://orcid.org/0000-0002-4700-1823

Data Availability Statement

Data sharing is not applicable as no new data was generated or analyzed in this study.

References

1. Boltjes, A.; Dömling, A. *Eur. J. Org. Chem.* **2019,** 7007–7049. doi:10.1002/ejoc.201901124
2. Giustiniano, M.; Basso, A.; Mercalli, V.; Massarotti, A.; Novellino, E.; Tron, G. C.; Zhu, J. *Chem. Soc. Rev.* **2017,** *46,* 1295–1357. doi:10.1039/c6cs00444j
3. Fouad, M. A.; Abdel-Hamid, H.; Ayoup, M. S. *RSC Adv.* **2020,** *10,* 42644–42681. doi:10.1039/d0ra07501a
4. Banfi, L.; Basso, A.; Lambruschini, C.; Moni, L.; Riva, R. *Chem. Sci.* **2021,** *12,* 15445–15472. doi:10.1039/d1sc03810a

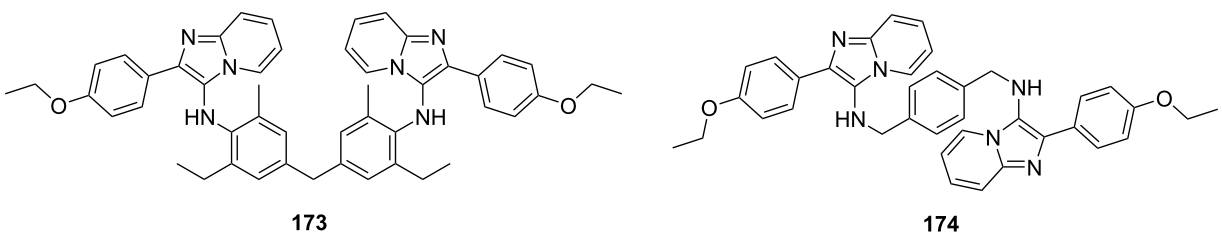

Figure 11: Model compounds **173** and **174**, used to study the acid/base-triggered reversible fluorescence response of polymers **98**.

5. Santos, G. F. D.; Anjos, N. S.; Gibeli, M. M.; Silva, G. A.; Fernandes, P. C. S.; Fiorentino, E. S. C.; Longo, L. S., Jr. *J. Braz. Chem. Soc.* **2020,** *31,* 1434–1444. doi:10.21577/0103-5053.20200028
6. Fortuna, C. G.; Musumarra, G.; Nardi, M.; Procopio, A.; Sindona, G.; Scirè, S. *J. Chemom.* **2006,** *20,* 418–424. doi:10.1002/cem.1016
7. Sashidhara, K. V.; Singh, L. R.; Choudhary, D.; Arun, A.; Gupta, S.; Adhikary, S.; Palnati, G. R.; Konwar, R.; Trivedi, R. *RSC Adv.* **2016,** *6,* 80037–80048. doi:10.1039/c6ra15674f
8. Hussain, M.; Liu, J.; Fu, L.; Hasan, M. *J. Heterocycl. Chem.* **2020,** *57,* 955–964. doi:10.1002/jhet.3746
9. Gao, L.; Shaabani, S.; Reyes Romero, A.; Xu, R.; Ahmadianmoghaddam, M.; Dömling, A. *Green Chem.* **2023,** *25,* 1380–1394. doi:10.1039/d2gc04312b
10. Shankar, B.; Kumar, B.; Kumar, S.; Arora, A.; Kavita; Tomar, R.; Singh, B. K. *Carbohydr. Res.* **2023,** *534,* 108974. doi:10.1016/j.carres.2023.108974
11. Vilapara, K. V.; Gami, S. P.; Gadara, S. A.; Naliapara, Y. T. *ChemistrySelect* **2019,** *4,* 11235–11238. doi:10.1002/slct.201902997
12. Anjos, N. S.; Chapina, A. I.; Santos, A. R.; Licence, P.; Longo, L. S., Jr. *Eur. J. Org. Chem.* **2022,** e202200615. doi:10.1002/ejoc.202200615
13. Il'in, M. V.; Sysoeva, A. A.; Novikov, A. S.; Bolotin, D. S. *J. Org. Chem.* **2022,** *87,* 4569–4579. doi:10.1021/acs.joc.1c02885
14. Il'in, M. V.; Novikov, A. S.; Bolotin, D. S. *J. Org. Chem.* **2022,** *87,* 10199–10207. doi:10.1021/acs.joc.2c01141
15. Il'in, M. V.; Polonnikov, D. A.; Novikov, A. S.; Sysoeva, A. A.; Safinskaya, Y. V.; Bolotin, D. S. *ChemPlusChem* **2023,** *88,* e202300304. doi:10.1002/cplu.202300304
16. Mathavan, S.; Yamajala, R. B. R. D. *ChemistrySelect* **2020,** *5,* 10637–10642. doi:10.1002/slct.202002894
17. Škopić, M. K.; Götte, K.; Gramse, C.; Dieter, M.; Pospich, S.; Raunser, S.; Weberskirch, R.; Brunschweiger, A. *J. Am. Chem. Soc.* **2019,** *141,* 10546–10555. doi:10.1021/jacs.9b05696
18. Ghiasi Moaser, A.; Afkham, A. G.; Khoshnavazi, R.; Rostamnia, S. *Sci. Rep.* **2023,** *13,* 4114. doi:10.1038/s41598-023-31356-7
19. Yang, B.; Tao, C.; Shao, T.; Gong, J.; Che, C. *Beilstein J. Org. Chem.* **2016,** *12,* 1487–1492. doi:10.3762/bjoc.12.145
20. Shinde, V. V.; Jung, S. *Tetrahedron* **2019,** *75,* 778–783. doi:10.1016/j.tet.2018.12.059
21. Budhiraja, M.; Kondabala, R.; Ali, A.; Tyagi, V. *Tetrahedron* **2020,** *76,* 131643. doi:10.1016/j.tet.2020.131643
22. Budhiraja, M.; Ali, A.; Tyagi, V. *Eur. J. Org. Chem.* **2023,** *26,* e202201426. doi:10.1002/ejoc.202201426
23. Xie, Y.; An, J.; Yang, G.; Wu, G.; Zhang, Y.; Cui, L.; Feng, Y. *J. Biol. Chem.* **2014,** *289,* 7994–8006. doi:10.1074/jbc.m113.536045
24. Bosc, D.; Jakhlal, J.; Deprez, B.; Deprez-Poulain, R. *Future Med. Chem.* **2016,** *8,* 381–404. doi:10.4155/fmc-2015-0007
25. Wong, E. L.; Nawrotzky, E.; Arkona, C.; Kim, B. G.; Beligny, S.; Wang, X.; Wagner, S.; Lisurek, M.; Carstanjen, D.; Rademann, J. *Nat. Commun.* **2019,** *10,* 66. doi:10.1038/s41467-018-07923-2
26. Gladysz, R.; Vrijdag, J.; Van Rompaey, D.; Lambeir, A.-M.; Augustyns, K.; De Winter, H.; Van der Veken, P. *Chem. – Eur. J.* **2019,** *25,* 12380–12393. doi:10.1002/chem.201901917
27. Massarotti, A.; Brunelli, F.; Aprile, S.; Giustiniano, M.; Tron, G. C. *Chem. Rev.* **2021,** *121,* 10742–10788. doi:10.1021/acs.chemrev.1c00143
28. Bhat, S. I.; Kigga, M.; Heravi, M. M. *Chem. Heterocycl. Compd.* **2021,** *57,* 709–719. doi:10.1007/s10593-021-02972-w
29. Guchhait, S. K.; Priyadarshani, G.; Chaudhary, V.; Seladiya, D. R.; Shah, T. M.; Bhogayta, N. P. *RSC Adv.* **2013,** *3,* 10867–10874. doi:10.1039/c3ra40347e
30. Neochoritis, C. G.; Stotani, S.; Mishra, B.; Dömling, A. *Org. Lett.* **2015,** *17,* 2002–2005. doi:10.1021/acs.orglett.5b00759
31. Kaur, M.; Singh, R.; Patil, M. T.; Kumar, K.; Sahoo, S. C.; Singh, K. N.; Chaudhari, V. D.; Salunke, D. B. *J. Heterocycl. Chem.* **2022,** *59,* 319–328. doi:10.1002/jhet.4386
32. Neochoritis, C. G.; Zarganes-Tzitzikas, T.; Katsampoxaki-Hodgetts, K.; Dömling, A. *J. Chem. Educ.* **2020,** *97,* 3739–3745. doi:10.1021/acs.jchemed.0c00290
33. Farhid, H.; Shaabani, A. *J. Iran. Chem. Soc.* **2021,** *18,* 1199–1209. doi:10.1007/s13738-020-02102-x
34. Baker, B. J. M.; Kerr, W. J.; Lindsay, D. M.; Patel, V. K.; Poole, D. L. *Green Chem.* **2021,** *23,* 280–287. doi:10.1039/d0gc03675g
35. de la Sovera, V.; López, G. V.; Porcal, W. *Eur. J. Org. Chem.* **2022,** e202101369. doi:10.1002/ejoc.202101369
36. Rosatella, A. A.; Simeonov, S. P.; Frade, R. F. M.; Afonso, C. A. M. *Green Chem.* **2011,** *13,* 754–793. doi:10.1039/c0gc00401d
37. Demjén, A.; Gyuris, M.; Wölfling, J.; Puskás, L. G.; Kanizsai, I. *Beilstein J. Org. Chem.* **2014,** *10,* 2338–2344. doi:10.3762/bjoc.10.243
38. Kumar, B.; Shankar, B.; Kumar, S.; Maity, J.; Prasad, A. K. *Synth. Commun.* **2020,** *50,* 2853–2859. doi:10.1080/00397911.2020.1786586
39. Kumar, S.; Kumar, S.; Maity, J.; Kumar, B.; Bali Mehta, S.; Prasad, A. K. *New J. Chem.* **2021,** *45,* 16635–16647. doi:10.1039/d1nj02423j
40. Khatri, V.; Kumar, A.; Singh, B.; Malhotra, S.; Prasad, A. K. *J. Org. Chem.* **2015,** *80,* 11169–11174. doi:10.1021/acs.joc.5b01933
41. Manvar, P.; Shaikh, F.; Kakadiya, R.; Mehariya, K.; Khunt, R.; Pandey, B.; Shah, A. *Tetrahedron* **2016,** *72,* 1293–1300. doi:10.1016/j.tet.2016.01.023
42. Amer, A.; Senior, S.; Fan, X. *Nucleosides, Nucleotides Nucleic Acids* **2012,** *31,* 42–54. doi:10.1080/15257770.2011.641651
43. Zheng, Q.; Li, X.; Kurpiewska, K.; Dömling, A. *Org. Lett.* **2022,** *24,* 5014–5017. doi:10.1021/acs.orglett.2c01642
44. Servín-García, G.; Chacón-García, L.; Islas-Jácome, A.; Gómez-Hurtado, M. A.; Rodríguez-García, G.; del Río, R. E.; Cortés-García, C. J. *J. Heterocycl. Chem.* **2023,** *60,* 1903–1910. doi:10.1002/jhet.4710
45. Stahlberger, M.; Schwarz, N.; Zippel, C.; Hohmann, J.; Nieger, M.; Hassan, Z.; Bräse, S. *Chem. – Eur. J.* **2022,** *28,* e202103511. doi:10.1002/chem.202103511
46. Hassan, Z.; Spuling, E.; Knoll, D. M.; Lahann, J.; Bräse, S. *Chem. Soc. Rev.* **2018,** *47,* 6947–6963. doi:10.1039/c7cs00803a
47. Kunig, V. B. K.; Ehrt, C.; Dömling, A.; Brunschweiger, A. *Org. Lett.* **2019,** *21,* 7238–7243. doi:10.1021/acs.orglett.9b02448
48. Konstantinidou, M.; Boiarska, Z.; Butera, R.; Neochoritis, C. G.; Kurpiewska, K.; Kalinowska-Tłuscik, J.; Dömling, A. *Eur. J. Org. Chem.* **2020,** 5601–5605. doi:10.1002/ejoc.202000933
49. Ghashghaei, O.; Caputo, S.; Sintes, M.; Revés, M.; Kielland, N.; Estarellas, C.; Luque, F. J.; Aviñó, A.; Eritja, R.; Serna-Gallego, A.; Marrugal-Lorenzo, J. A.; Pachón, J.; Sánchez-Céspedes, J.; Treadwell, R.; de Moliner, F.; Vendrell, M.; Lavilla, R. *Chem. – Eur. J.* **2018,** *24,* 14513–14521. doi:10.1002/chem.201802877
50. Li, X.; Romero, M. D.; Tcaturian, S.; Kurpiewska, K.; Dömling, A. *J. Org. Chem.* **2023,** *88,* 9823–9834. doi:10.1021/acs.joc.3c00467
51. Makra, Z.; Bényei, A.; Puskás, L. G.; Kanizsai, I. *Eur. J. Org. Chem.* **2020,** 7184–7196. doi:10.1002/ejoc.202001253

52. Pereshivko, O.; Peshkov, V.; Ermolat'ev, D.; Van der Eycken, E. *Synlett* **2013,** *24,* 351–354. doi:10.1055/s-0032-1317986
53. An, Y.; Lee, J.; Seo, H.; Bae, S.; Kang, J.; Lee, J.; Kim, J.; Nam, M. H.; Song, M.; Hwang, G. T. *Org. Lett.* **2023,** *25,* 4445–4450. doi:10.1021/acs.orglett.3c01366
54. Smith, J.; Osunsanya, M.; Nwadike, I.; Tankeu, B. *Tetrahedron Lett.* **2022,** *100,* 153876. doi:10.1016/j.tetlet.2022.153876
55. Loubidi, M.; Lorion, M.; El Hakmaoui, A.; Bernard, P.; Akssira, M.; Guillaumet, G. *Synthesis* **2019,** *51,* 3973–3980. doi:10.1055/s-0039-1690182
56. Hayashi, Y. *Chem. Sci.* **2016,** *7,* 866–880. doi:10.1039/c5sc02913a
57. Ganesher, A.; Panda, G. *Tetrahedron Lett.* **2019,** *60,* 151317. doi:10.1016/j.tetlet.2019.151317
58. Jain, S.; Sen, D. J. *Indian J. Chem.* **2022,** *61,* 305–312. doi:10.56042/ijc.v61i3.61721
59. Ghashghaei, O.; Pedrola, M.; Seghetti, F.; Martin, V. V.; Zavarce, R.; Babiak, M.; Novacek, J.; Hartung, F.; Rolfes, K. M.; Haarmann-Stemmann, T.; Lavilla, R. *Angew. Chem., Int. Ed.* **2021,** *60,* 2603–2608. doi:10.1002/anie.202011253
60. Balwe, S. G.; Vagh, S. S.; Jeong, Y. T. *Tetrahedron Lett.* **2020,** *61,* 152101. doi:10.1016/j.tetlet.2020.152101
61. Zhong, C.-R.; Zhang, Y.-H.; Yao, G.; Zhu, H.-L.; Hu, Y.-D.; Zeng, Z.-G.; Liao, C.-Z.; He, H.-T.; Luo, Y.-T.; Xiong, J. *J. Org. Chem.* **2023,** *88,* 13125–13134. doi:10.1021/acs.joc.3c01341
62. Srinivasulu, V.; Al-Marzooq, F.; Hamad, M.; Khanfar, M. A.; Ramanathan, M.; Soares, N. C.; Al-Tel, T. H. *Synthesis* **2021,** *53,* 1911–1922. doi:10.1055/s-0040-1706006
63. Li, Y.; Huang, J.-H.; Wang, J.-L.; Song, G.-T.; Tang, D.-Y.; Yao, F.; Lin, H.-k.; Yan, W.; Li, H.-y.; Xu, Z.-G.; Chen, Z.-Z. *J. Org. Chem.* **2019,** *84,* 12632–12638. doi:10.1021/acs.joc.9b01385
64. Alsolami, E. S.; Alorfi, H. S.; Alamry, K. A.; Hussein, M. A. *RSC Adv.* **2024,** *14,* 1757–1781. doi:10.1039/d3ra07278a
65. Chen, T.; Ye, F.; Hu, R.; Tang, B. Z. *Macromolecules* **2022,** *55,* 8590–8598. doi:10.1021/acs.macromol.2c01136
66. Guan, Q.; Zhou, L.-L.; Dong, Y.-B. *J. Am. Chem. Soc.* **2023,** *145,* 1475–1496. doi:10.1021/jacs.2c11071
67. Liu, J.; Yang, T.; Wang, Z.-P.; Wang, P.-L.; Feng, J.; Ding, S.-Y.; Wang, W. *J. Am. Chem. Soc.* **2020,** *142,* 20956–20961. doi:10.1021/jacs.0c10919
68. Prajapati, A.; Saini, M. K.; Verma, S. K.; Korawat, H. S.; Basak, A. K. *New J. Chem.* **2023,** *47,* 4944–4948. doi:10.1039/d3nj00277b
69. Shareef, S.; Saigal; Khizr, M.; Sahoo, S. C.; Musawwer Khan, M. *Tetrahedron Lett.* **2021,** *84,* 153452. doi:10.1016/j.tetlet.2021.153452
70. Jalani, H. B.; Jeong, J.-H. *J. Heterocycl. Chem.* **2022,** *59,* 1266–1271. doi:10.1002/jhet.4456
71. Kolomiiets, O. V.; Tsygankov, A. V.; Kornet, M. N.; Brazhko, A. A.; Musatov, V. I.; Chebanov, V. A. *Beilstein J. Org. Chem.* **2023,** *19,* 727–735. doi:10.3762/bjoc.19.53
72. Moghanlou, M.; Mirza, B. *Polycyclic Aromat. Compd.* **2020,** *40,* 1036–1044. doi:10.1080/10406638.2018.1519515
73. Nayebzadeh, B.; Amiri, K.; Khosravi, H.; Mirzaei, S.; Rominger, F.; Dar'in, D.; Krasavin, M.; Bijanzadeh, H. R.; Balalaie, S. *J. Org. Chem.* **2021,** *86,* 13693–13701. doi:10.1021/acs.joc.1c01789
74. El Akkaoui, A.; Hiebel, M.-A.; Mouaddib, A.; Berteina-Raboin, S.; Guillaumet, G. *Tetrahedron* **2012,** *68,* 9131–9138. doi:10.1016/j.tet.2012.07.081
75. Stahlberger, M.; Steinlein, O.; Adam, C. R.; Rotter, M.; Hohmann, J.; Nieger, M.; Köberle, B.; Bräse, S. *Org. Biomol. Chem.* **2022,** *20,* 3598–3604. doi:10.1039/d2ob00372d
76. Tber, Z.; Loubidi, M.; Jouha, J.; Hdoufane, I.; Erdogan, M. A.; Saso, L.; Armagan, G.; Berteina-Raboin, S. *Pharmaceuticals* **2021,** *14,* 750. doi:10.3390/ph14080750
77. Tber, Z.; Hiebel, M.-A.; Allouchi, H.; El Hakmaoui, A.; Akssira, M.; Guillaumet, G.; Berteina-Raboin, S. *RSC Adv.* **2015,** *5,* 35201–35210. doi:10.1039/c5ra03703d
78. Singh, R.; Kumar, R.; Kaur, M.; Patil, M. T.; Sahoo, S. C.; Salunke, D. B. *J. Heterocycl. Chem.* **2022,** *59,* 1007–1015. doi:10.1002/jhet.4438
79. Ingold, M.; de la Sovera, V.; Dapueto, R.; Hernández, P.; Porcal, W.; López, G. V. *Molecules* **2022,** *27,* 1756. doi:10.3390/molecules27061756
80. Fragkiadakis, M.; Anastasiou, P.-K.; Zingiridis, M.; Triantafyllou-Rundell, M. E.; Reyes Romero, A.; Stoumpos, C. C.; Neochoritis, C. G. *J. Org. Chem.* **2023,** *88,* 12709–12715. doi:10.1021/acs.joc.3c01379
81. Lima, L. M.; Alves, M. A.; do Amaral, D. N. *Curr. Top. Med. Chem.* **2019,** *19,* 1734–1750. doi:10.2174/1568026619666190808145235
82. Nadendla, R.; Yemineni, G. *Biomed. J. Sci. Tech. Res.* **2023,** *52,* 43511–43522. doi:10.26717/bjstr.2023.52.008220
83. Pedrola, M.; Jorba, M.; Jardas, E.; Jardi, F.; Ghashghaei, O.; Viñas, M.; Lavilla, R. *Front. Chem. (Lausanne, Switz.)* **2019,** *7,* 475. doi:10.3389/fchem.2019.00475
84. Klug, D. M.; Tse, E. G.; Silva, D. G.; Cao, Y.; Charman, S. A.; Chauhan, J.; Crighton, E.; Dichiara, M.; Drake, C.; Drewry, D.; da Silva Emery, F.; Ferrins, L.; Graves, L.; Hopkins, E.; Kresina, T. A. C.; Lorente-Macías, Á.; Perry, B.; Phipps, R.; Quiroga, B.; Quotadamo, A.; Sabatino, G. N.; Sama, A.; Schätzlein, A.; Simpson, Q. J.; Steele, J.; Shanu-Wilson, J.; Sjö, P.; Stapleton, P.; Swain, C. J.; Vaideanu, A.; Xie, H.; Zuercher, W.; Todd, M. H. *ACS Infect. Dis.* **2023,** *9,* 2423–2435. doi:10.1021/acsinfecdis.3c00286
85. Kumar, R.; Singh, R.; das Chagas Almeida, A.; da Trindade Granato, J.; de Oliveira Lemos, A. S.; Kumar, K.; Patil, M. T.; da Silva, A. D.; Rode, A. B.; Coimbra, E. S.; Salunke, D. B. *ACS Omega* **2023,** *8,* 40613–40621. doi:10.1021/acsomega.3c05441
86. Kelam, L. M.; Wani, M. A.; Dhaked, D. K. *Prog. Biophys. Mol. Biol.* **2023,** *180–181,* 87–104. doi:10.1016/j.pbiomolbio.2023.04.009
87. Alsfouk, A. A.; Alshibl, H. M.; Alsfouk, B. A.; Altwaijry, N. A.; Al-Abdullah, E. S. *Pharmaceuticals* **2022,** *15,* 859. doi:10.3390/ph15070859
88. Franco, L. C.; Morales, F.; Boffo, S.; Giordano, A. *J. Cell. Biochem.* **2018,** *119,* 1273–1284. doi:10.1002/jcb.26293
89. Hays, E.; Bonavida, B. *Antioxidants* **2019,** *8,* 407. doi:10.3390/antiox8090407
90. Wang, W.; Lu, Y.; Chen, E.; Shen, K.; Li, J. *Bioorg. Chem.* **2021,** *114,* 105146. doi:10.1016/j.bioorg.2021.105146
91. Lu, Y.; Wu, S.; Yue, Y.; He, S.; Li, J.; Tang, J.; Wang, W.; Zhou, H.-B. *ACS Med. Chem. Lett.* **2016,** *7,* 1185–1190. doi:10.1021/acsmedchemlett.6b00302
92. Liu, C.; Seeram, N. P.; Ma, H. *Cancer Cell Int.* **2021,** *21,* 239. doi:10.1186/s12935-021-01946-4
93. Lipson, E. J.; Forde, P. M.; Hammers, H.-J.; Emens, L. A.; Taube, J. M.; Topalian, S. L. *Semin. Oncol.* **2015,** *42,* 587–600. doi:10.1053/j.seminoncol.2015.05.013

94. Butera, R.; Ważyńska, M.; Magiera-Mularz, K.; Plewka, J.; Musielak, B.; Surmiak, E.; Sala, D.; Kitel, R.; de Bruyn, M.; Nijman, H. W.; Elsinga, P. H.; Holak, T. A.; Dömling, A. *ACS Med. Chem. Lett.* **2021,** *12,* 768–773. doi:10.1021/acsmedchemlett.1c00033
95. Meisenberg, C. *J. Cancer Sci. Ther.* **2014,** *6,* 7. doi:10.4172/1948-5956.1000280
96. Huang, S.-y. N.; Pommier, Y.; Marchand, C. *Expert Opin. Ther. Pat.* **2011,** *21,* 1285–1292. doi:10.1517/13543776.2011.604314
97. Zhao, X. Z.; Kiselev, E.; Lountos, G. T.; Wang, W.; Tropea, J. E.; Needle, D.; Hilimire, T. A.; Schneekloth, J. S.; Waugh, D. S.; Pommier, Y.; Burke, T. R. *Chem. Sci.* **2021,** *12,* 3876–3884. doi:10.1039/d0sc05411a
98. Zhao, X. Z.; Wang, W.; Lountos, G. T.; Tropea, J. E.; Needle, D.; Pommier, Y.; Burke, T. R., Jr. *Front. Chem. (Lausanne, Switz.)* **2022,** *10,* 910953. doi:10.3389/fchem.2022.910953
99. Zhao, X. Z.; Wang, W.; Lountos, G. T.; Kiselev, E.; Tropea, J. E.; Needle, D.; Pommier, Y.; Burke, T. R. *RSC Chem. Biol.* **2023,** *4,* 334–343. doi:10.1039/d2cb00230b
100. Chessum, N.; Jones, K.; Pasqua, E.; Tucker, M. *Prog. Med. Chem.* **2015,** *54,* 1–63. doi:10.1016/bs.pmch.2014.11.002
101. El-Awady, R.; Saleh, E.; Hamoudi, R.; Ramadan, W. S.; Mazitschek, R.; Nael, M. A.; Elokely, K. M.; Abou-Gharbia, M.; Childers, W. E.; Srinivasulu, V.; Aloum, L.; Menon, V.; Al-Tel, T. H. *Bioorg. Med. Chem.* **2021,** *42,* 116251. doi:10.1016/j.bmc.2021.116251
102. Gao, K.; Shaabani, S.; Xu, R.; Zarganes-Tzitzikas, T.; Gao, L.; Ahmadianmoghaddam, M.; Groves, M. R.; Dömling, A. *RSC Med. Chem.* **2021,** *12,* 809–818. doi:10.1039/d1md00087j
103. Coll, R. C.; Schroder, K.; Pelegrín, P. *Trends Pharmacol. Sci.* **2022,** *43,* 653–668. doi:10.1016/j.tips.2022.04.003
104. Mackwitz, M. K. W.; Hamacher, A.; Osko, J. D.; Held, J.; Schöler, A.; Christianson, D. W.; Kassack, M. U.; Hansen, F. K. *Org. Lett.* **2018,** *20,* 3255–3258. doi:10.1021/acs.orglett.8b01118
105. Kraft, F. B.; Enns, J.; Honin, I.; Engelhardt, J.; Schöler, A.; Smith, S. T.; Meiler, J.; Schäker-Hübner, L.; Weindl, G.; Hansen, F. K. *Bioorg. Chem.* **2024,** *143,* 107072. doi:10.1016/j.bioorg.2023.107072
106. Shahrisa, A.; Safa, K. D.; Esmati, S. *Spectrochim. Acta, Part A* **2014,** *117,* 614–621. doi:10.1016/j.saa.2013.09.056
107. Kurva, M.; Claudio-Catalán, M. Á.; Rentería-Gómez, Á.; Jiménez-Halla, J. O. C.; González-García, G.; Velusamy, J.; Ramos-Ortíz, G.; Castaño-González, K.; Piazza, V.; Gámez-Montaño, R. *J. Mol. Struct.* **2023,** *1276,* 134797. doi:10.1016/j.molstruc.2022.134797
108. Bedard, N.; Coen, A. G.; Pekarske, S.; Sennett, A.; Davis, G. J.; Chavez, T.; Lichtenberger, D. L.; Hulme, C. *Tetrahedron Lett.* **2023,** *130,* 154748. doi:10.1016/j.tetlet.2023.154748
109. Sevinç, G.; Küçüköz, B.; Yılmaz, H.; Şirikçi, G.; Yaglioglu, H. G.; Hayvalı, M.; Elmali, A. *Sens. Actuators, B* **2014,** *193,* 737–744. doi:10.1016/j.snb.2013.12.043

License and Terms

This is an open access article licensed under the terms of the Beilstein-Institut Open Access License Agreement (https://www.beilstein-journals.org/bjoc/terms), which is identical to the Creative Commons Attribution 4.0 International License (https://creativecommons.org/licenses/by/4.0). The reuse of material under this license requires that the author(s), source and license are credited. Third-party material in this article could be subject to other licenses (typically indicated in the credit line), and in this case, users are required to obtain permission from the license holder to reuse the material.

The definitive version of this article is the electronic one which can be found at:
https://doi.org/10.3762/bjoc.20.162

BEILSTEIN JOURNAL OF ORGANIC CHEMISTRY

Multicomponent syntheses of pyrazoles via (3 + 2)-cyclocondensation and (3 + 2)-cycloaddition key steps

Ignaz Betcke[‡1], Alissa C. Götzinger[‡1], Maryna M. Kornet[1,2] and Thomas J. J. Müller[*1]

Review

Open Access

Address:
[1]Heinrich-Heine-Universität Düsseldorf, Math.-Nat. Fakultät, Institut für Organische Chemie und Makromolekulare Chemie, Universitätsstrasse 1, D-40225 Düsseldorf, Germany and [2]Zaporizhzhia National University, Faculty of Biology, Department of Chemistry, Zhukovskogo Street 66, 69600 Zaporizhzhia, Ukraine

Email:
Thomas J. J. Müller[*] - ThomasJJ.Mueller@hhu.de

* Corresponding author ‡ Equal contributors

Keywords:
cycloaddition; cyclocondensation; multicomponent reaction; one-pot reactions; pyrazole

Beilstein J. Org. Chem. **2024,** *20,* 2024–2077.
https://doi.org/10.3762/bjoc.20.178

Received: 26 April 2024
Accepted: 19 July 2024
Published: 16 August 2024

This article is part of the thematic issue "Multicomponent reactions IV" and is dedicated to Prof. Dr. Constantin Czekelius on the occasion of his 50th birthday.

Associate Editor: N. Yoshikai

© 2024 Betcke et al.; licensee Beilstein-Institut.
License and terms: see end of document.

Abstract

Pyrazoles are rarely found in nature but are traditionally used in the agrochemical and pharmaceutical industries, while other areas of use are also actively developing. However, they have also found numerous other applications. The search for new and efficient syntheses of these heterocycles is therefore highly relevant. The modular concept of multicomponent reactions (MCR) has paved a broad alley to heteroaromatics. The advantages over traditional methods are the broader scope and increased efficiency of these reactions. In particular, traditional multistep syntheses of pyrazoles have considerably been extended by MCR. Progress has been made in the cyclocondensation of 1,3-dielectrophiles that are generated in situ. Limitations in the regioselectivity of cyclocondensation with 1,3-dicarbonyls were overcome by the addition–cyclocondensation of α,β-unsaturated ketones. Embedding 1,3-dipolar cycloadditions into a one-pot process has additionally been developed for concise syntheses of pyrazoles. The MCR strategy also allows for concatenating classical condensation-based methodology with modern cross-coupling and radical chemistry, as well as providing versatile synthetic approaches to pyrazoles. This overview summarizes the most important MCR syntheses of pyrazoles based on ring-forming sequences in a flashlight fashion.

Introduction

Pyrazoles and 1,2-diazoles [1] have received considerable interest in the past years. Although they are rarely found in nature [2], their spectrum of biological activity is remarkably broad, leading to numerous applications in pharmaceutical chemistry [3-6]. For instance, pyrazoles serve as monoamine oxidase A and B inhibitors [7] and as COX-II inhibitors [8], making them valuable analgesics [9]. Furthermore, several blockbuster drugs, such as VIAGRA® [10], Celecoxib® [11],

and Rimonabant [12], contain pyrazole cores. In addition, extensive agrochemical uses of pyrazoles [13] include insecticides [14], herbicides [15], and fungicides [16]. Furthermore, they are widely applied for the assembly of supramolecular ensembles [17] and molecular systems capable of photoinduced electron transfer [18]. Due to their pertinent photophysical properties [19], pyrazoles also find applications in OLED technology [20] and optical brighteners [21] in the textile and laundry industry.

The ongoing quest for novel, potent, and efficient syntheses of pyrazoles prompts the search for the "ideal" synthesis [22,23], one that addresses all the synthetic challenges to meet the ecological and economic requirements. This "ideal" synthesis would commence with simple starting materials, progress through safe, catalytic, and quantitative conversions, and culminate in streamlined processes, all conducted within a single reaction vessel. Multicomponent reactions (MCR) closely approach this ideal, representing a reactivity-based concept where reactive functionalities are generated and consumed in each step [24]. MCR can be conducted in a domino, sequential, or consecutive fashion, offering a versatile approach to synthetic design by creating countless new sequences by concatenation of organic elementary steps in a one-pot fashion. Many reviews on general syntheses of pyrazoles have been published [25-38], as well as a few dedicated reviews on MCR synthesis of pyrazole derivatives [39-41]. In sensu stricto, multicomponent methodology demands that all sequences have to be performed in the same reaction vessel; neither intermediate work-up, filtration of byproducts, nor solvent exchange by evaporation falls within the scope of MCR. Therefore, this review aims to present and discuss the concepts of ring-forming MCR syntheses of pyrazoles. The review will primarily focus on two major categories: two-carbon and three-carbon building blocks as key intermediates, while other special cases will be summarized separately.

Review

(3 + 2)-Cyclocondensation – C_3-building blocks as key intermediates

The majority of the numerous pyrazole syntheses known in the literature are based on the condensation of 1,3-dielectrophiles and their synthesis equivalents as C_3-building blocks, along with hydrazines as N_2-building blocks [25-38]. Conceptually, the en route generation of these C_3-building blocks or their transformation with additional components besides hydrazines is a logical entry to MCR syntheses of pyrazoles. Therefore, 1,3-dielectrophiles encompass 1,3-dicarbonyl compounds and α,β-unsaturated carbonyl compounds, including alkenoyl and alkynoyl systems, across various oxidation states of the carbonyl groups and their derivatives.

1,3-Dicarbonyl compounds as key intermediates

The most common and classic synthesis of ring-forming pyrazoles is the cyclocondensation of 1,3-dicarbonyl compounds with hydrazines (Knorr synthesis) [42,43]. Therefore, the in situ generation of 1,3-dicarbonyl compounds and their one-pot transformation pave the way for MCR syntheses of pyrazoles.

1,3-Dicarbonyl compounds can, for example, be generated in situ from enolates and carboxylic acid chlorides. They can be converted to the corresponding pyrazoles **1** in a consecutive multicomponent reaction with hydrazines **3** (Scheme 1) [44]. It is important for a chemoselective synthesis that the 1,3-diketones **2** formed are not further acylated, which is prevented by using LiHMDS as a base. The method provides good to excellent yields and tolerates diverse functional groups. However, one limitation of the synthesis is that the reaction with methylhydrazine leads to two different regioisomers.

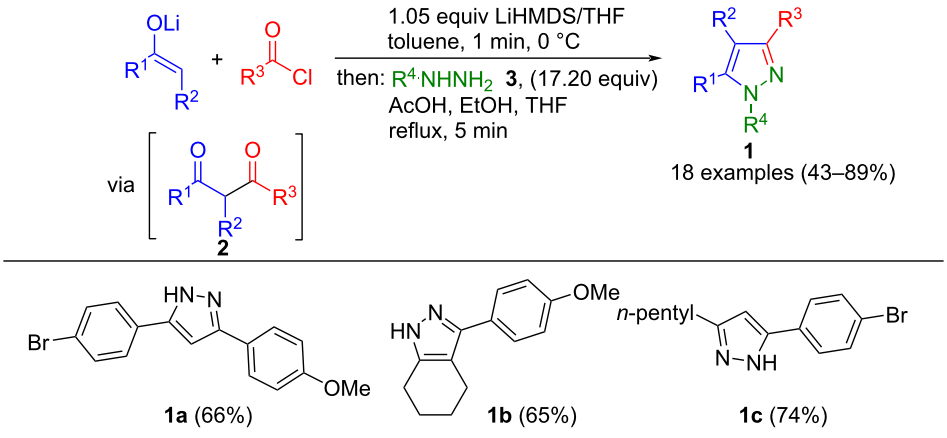

Scheme 1: Consecutive three-component synthesis of pyrazoles **1** via in situ-formed 1,3-diketones **2** [44].

Shen et al. used a concept developed by them for the C-acylation of β-ketoesters for the one-pot synthesis of pyrazoles. $SmCl_3$-catalyzed acylation of these yields the 1,3-diketones **4**, and after cyclization with hydrazine, 3,4,5-substituted pyrazoles **5** are formed (Scheme 2) [45]. The Lewis acid catalyst accelerates the reaction via participation in the formation of β-diketonate complexes.

Other carbonyl compounds suitable for pyrazole synthesis are 2,4-diketoesters **13**. These intermediates can be prepared from diethyl oxalate (**9**) and alkylphenones **10** through a sterically hindered Claisen condensation, producing a six-membered lithium enolate salt. Subsequent cyclocondensation with hydrazines concludes the formation of pyrazoles. However, this process could not be performed as a one-pot synthesis, as the solvent had to be exchanged after the Claisen step [46-50]. Gu et al. succeeded in adapting this concept for the one-pot synthesis of 1-(thiazol-2-yl)pyrazole-3-carboxylates **7** (Scheme 3) [51]. Starting from β-bromocarbonyl compounds **6** and 2-(propane-2-ylidene)thiosemicarbazide (**7**) thiazolylhydrazones **11** are formed via Hantzsch's thiazole synthesis. After acidic deprotection to thiazolylhydrazines **12**, these react with enolates of 2,4-diketoesters, which are intermediaries prepared in a separate reaction vessel, yielding the corresponding (thiazol-2-yl)pyrazoles **8**. However, hydrazines are not tolerated in this consecutive four-component reaction, as the 1,3,4-thiadiazine synthesis competes with the thiazole synthesis.

Salicylaldehydes **14** and 4-hydroxy-6-methyl-2*H*-pyran-2-one (**16**) can also be used to produce 1,3-dicarbonyl compounds **18** by Knoevenagel condensation and subsequent cyclization. This approach was also used to synthesize pyrazoles since the intermediary-formed diketone **18** forms the corresponding pyrazoles **17** in a Knorr reaction with 2-hydrazinyl-4-phenylthiazoles **15** in a one-pot process (Scheme 4) [52]. Piperidine was used as a catalyst for the Knoevenagel condensation. Remarkably, product **17a** shows cytotoxic activity against Hep G2 hepatocellular carcinoma and MCF-7 breast carcinoma cell lines.

The synthesis of 3,5-bis(arylamino)pyrazoles **21** involves the preparation of bisarylthioamides **22** via nucleophilic addition and double retro-Claisen condensation of isothiocyanates **19** and acetylacetonate **20**. Extension of the sequence by cyclization with hydrazine leads to the pyrazole products **21** (Scheme 5) [53]. The method works best with acetylacetonates, since deprotonation of other diketones with NaOEt leads to deactivation of the isothiocyanates. A limitation of the method is the formation of three different regioisomers when employing different isothiocyanates **19**. However, easy separation by LC–MS could be achieved, as demonstrated for one-pot process generated pyrazoles **21a–f**. The reaction demonstrates high tolerance to steric hindrance and electronic factors, enabling the synthesis of various 3,5-bis(arylamino)pyrazoles **21**.

In multicomponent syntheses, arylhydrazines were also presented in situ and could be cyclized with 1,3-dicarbonyl compounds in a one-pot process. This process yields *N*-functionalized pyrazoles, expanding the scope of available compounds. A common challenge in pyrazole synthesis is the synthetic accessibility of hydrazines. To circumvent this limitation, arylboronic acids can be coupled with Boc-protected diimide **23**

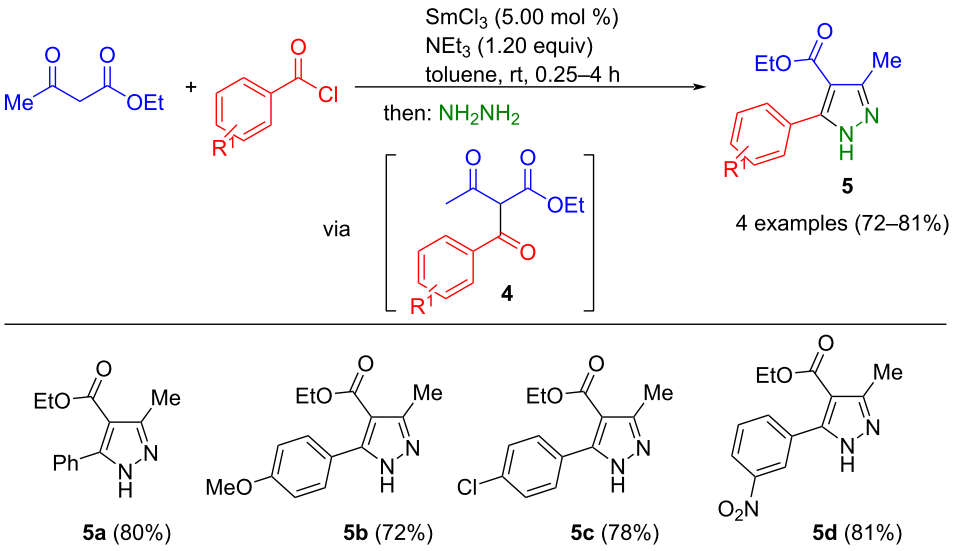

Scheme 2: Consecutive three-component synthesis of 4-ethoxycarbonylpyrazoles **5** via $SmCl_3$-catalyzed acylation of ethyl acetoacetate [45].

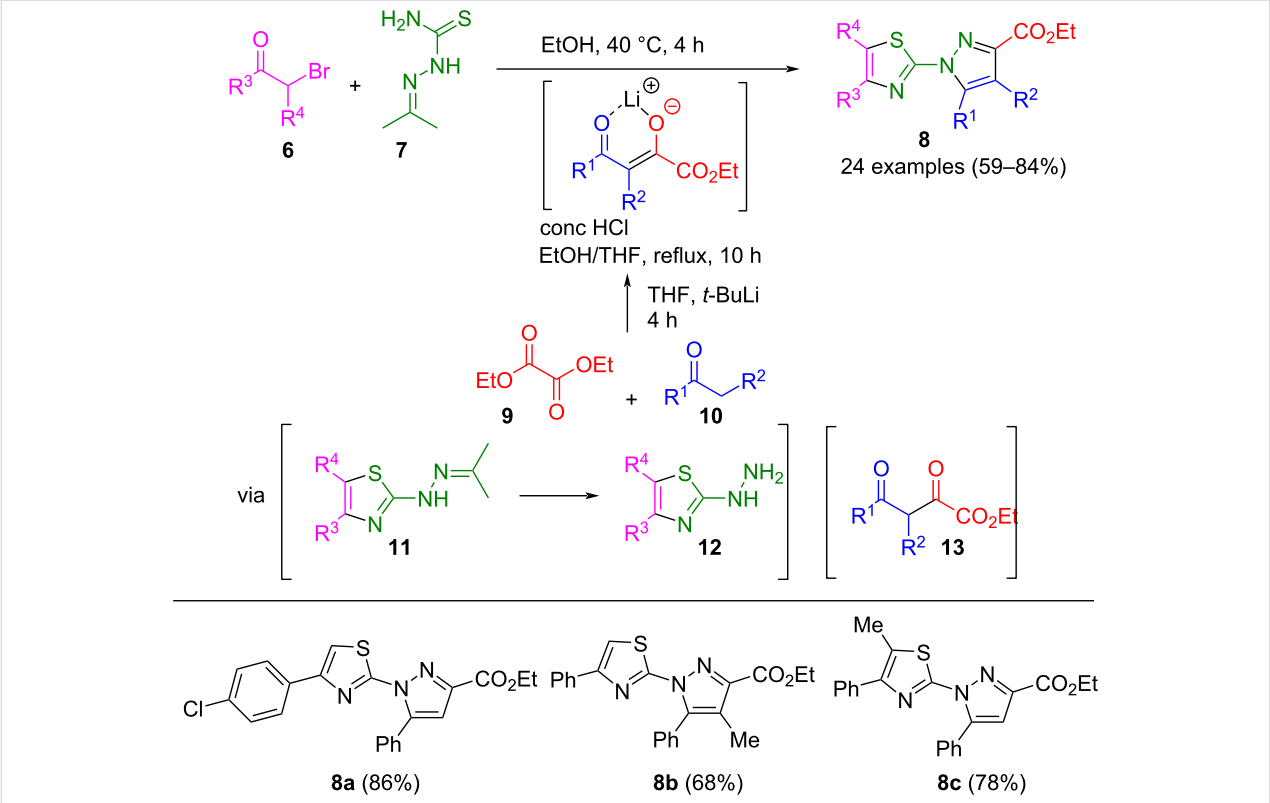

Scheme 3: Consecutive four-component synthesis of 1-(thiazol-2-yl)pyrazole-3-carboxylates **8** [51].

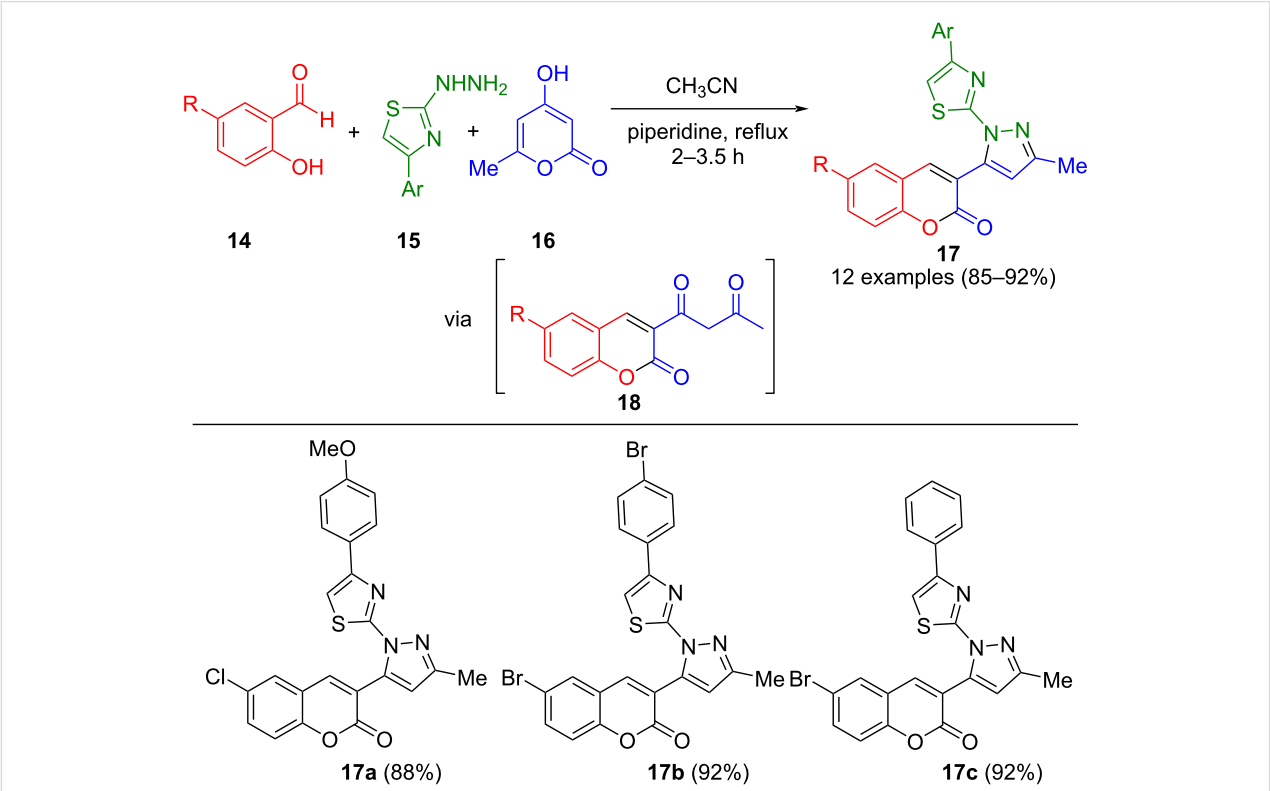

Scheme 4: Three-component synthesis of thiazolylpyrazoles **17** via in situ formation of acetoacetylcoumarins **18** [52].

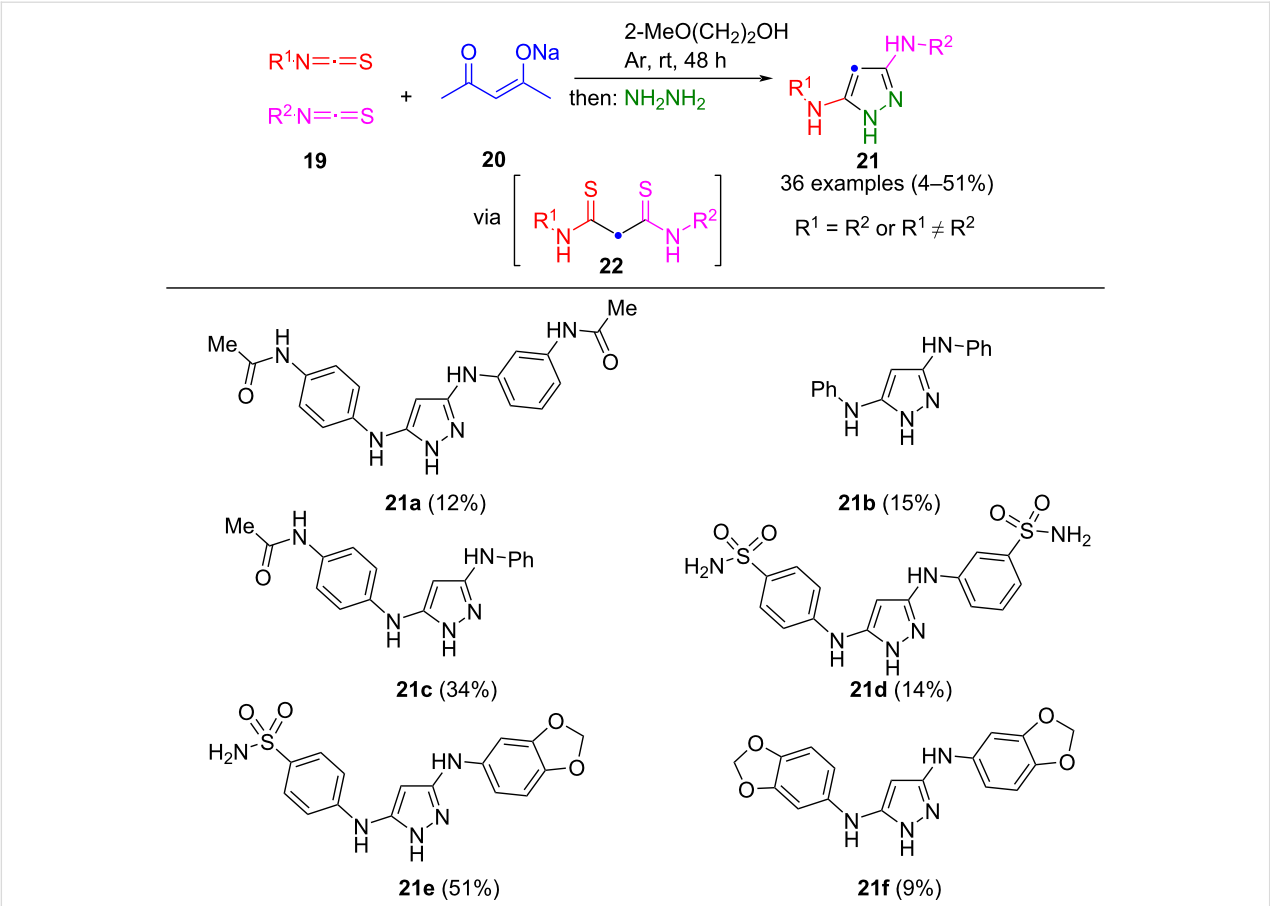

Scheme 5: Consecutive pseudo-four-component and four-component synthesis of pyrazoles **21** from sodium acetylacetonate (**20**), isothiocyanates **19**, and hydrazine [53].

under copper catalysis to form the hydrazine precursor in situ. Subsequent removal of the Boc groups and cyclocondensation with 1,3-dicarbonyl compounds leads to the formation of pyrazoles **24** in a one-pot process (Scheme 6) [54]. This versatile method enables the introduction of various functional groups at position 1 of the pyrazole ring. In addition, it can also be employed in synthesizing celecoxib, an active pharmaceutical ingredient.

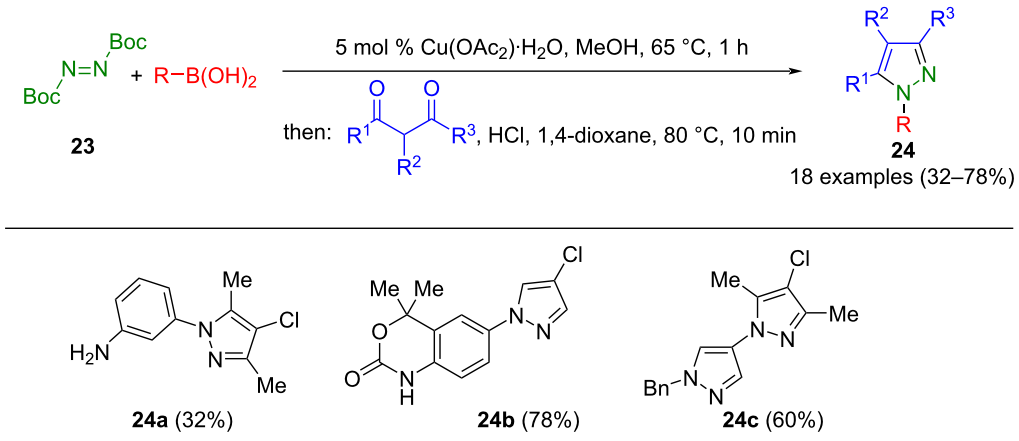

Scheme 6: Consecutive three-component synthesis of 1-substituted pyrazoles **24** from boronic acids, di(Boc)diimide **23**, and 1,3-dicarbonyl compounds [54].

Starting from di-*tert*-butyldiazocarboxylate (**23**), aryl-substituted di-Boc-hydrazines **26** were prepared by the addition of aryllithium species generated in situ by lithium-halogen exchange of aryl halides [55]. Gerstenberger et al. used this entry for the one-pot synthesis of *N*-arylpyrazoles **25,** as depicted in Scheme 7 [56].

In a consecutive process, after removing the protecting groups through acidic cleavage and cyclocondensation with 1,3-dicarbonyl compounds, the corresponding pyrazoles **25** were formed in a one-pot procedure. Interestingly, both β-aminoacrolein and β-aminovinylketones can also serve as substrates according to this method. However, attempts to carry out the reaction sequence with unprotected hydrazine were unsuccessful. Alternatively, Mitsunobu reagent **23** can be reacted with in situ generated benzyne (from *o*-(trimethylsilyl)phenyl triflate) to provide the hydrazides for the concomitant cyclocondensation with 1,3-dicarbonyl compounds [57].

In their program to synthesize regioselectively substituted pyrazoles, Raw and Turner established the one-pot preparation of triply substituted pyrazoles **27** and **28** via 1-formyl-1-methylhydrazine (**29**), generated in situ by reacting methylhydrazine and ethyl formate (Scheme 8) [58]. Upon reaction with β-ketoesters, hydrazone **30** is formed, which reacts via intramolecular Knoevenagel condensation to give the corresponding pyrazoles **27**. The method tolerates β-ketoesters with alkyl substituents and various ketoamides. In addition, an example could be synthesized starting from 3-aminocrotononitrile to yield pyrazole **28**. The authors explicitly mention that aryl ketones do not transform using this method.

Besides, the functionalization of 1,3-dicarbonyl compounds and their subsequent conversion into pyrazoles can be conducted in a one-pot fashion. For instance, oxidative allylation of 1,3-dicarbonyl compounds using allyltrimethylsilane (**31**) in the presence of ammonium cerium(IV) nitrate (CAN) provides access to allylated 1,3-dicarbonyl compounds **33** that are transformed with hydrazines to the corresponding pyrazoles **32** in a one-pot process (Scheme 9) [59]. CAN serves a dual role as a Lewis acid and an oxidizing agent. However, a significant limitation of the method is that it only tolerates aliphatic 1,3-dicarbonyl compounds, as the reaction with aromatic carbonyl compounds leads to very low yields. Improved yields for the latter can be achieved by isolating the functionalized 1,3-dicarbonyl compound **33** after the first step. Instead of allyl, a cyano group can also be introduced at position 2 of the 1,3-dicarbonyl compound using TsCN [60]. Cyclization of the intermediates leads to the corresponding 4-cyanopyrazoles.

Beyrati and Hasaninejad presented a microwave-assisted pseudo-five-component synthesis of tris(pyrazolyl)methanes **35**, where first β-ketoesters and hydrazines form pyrazolones **36**. One equivalent reacts in a Knoevenagel condensation with 4-formylpyrazole **34** to give pyrazolidine pyrazole **37**, while the second equivalent undergoes a Michael addition to form the corresponding trispyrazole **35** (Scheme 10) [61]. Similarly, aromatic aldehydes furnish the corresponding bispyrazolylmethanes either under ultrasound irradiation in low-boiling solvents [62] or under Ag/TiO_2 catalysis [63].

In addition to 1,3-dicarbonyl compounds, 1,3,5-tricarbonyl compounds **38** are also interesting building blocks in pyrazole

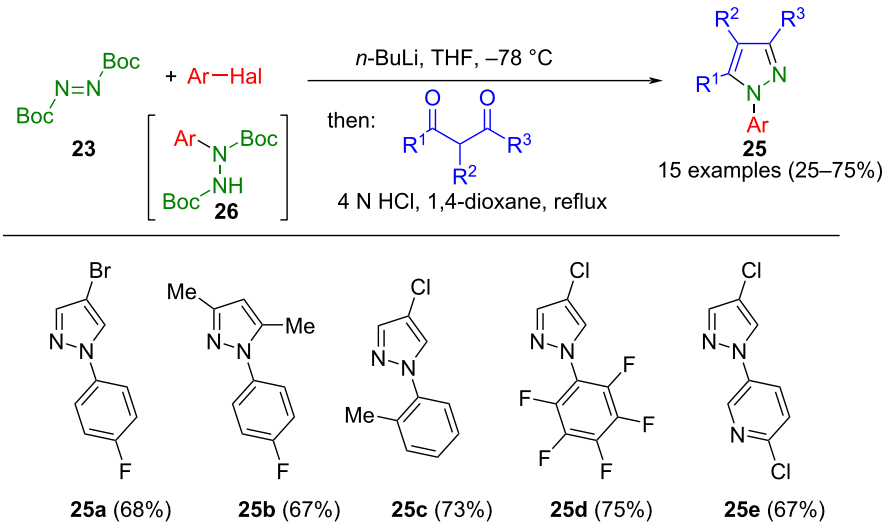

Scheme 7: Consecutive three-component synthesis of *N*-arylpyrazoles **25** via in situ formation of aryl-di(Boc)hydrazines **26** [56].

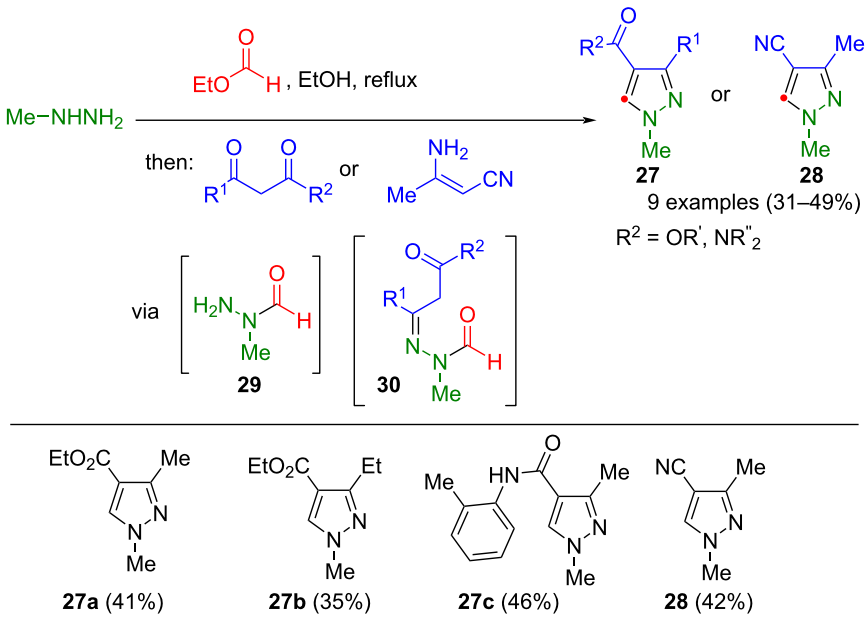

Scheme 8: Consecutive three-component synthesis of 1,3,4-substituted pyrazoles **27** and **28** from methylhydrazine, ethyl formate, and β-ketoesters, β-ketoamides or 3-aminocrotonitrile [58].

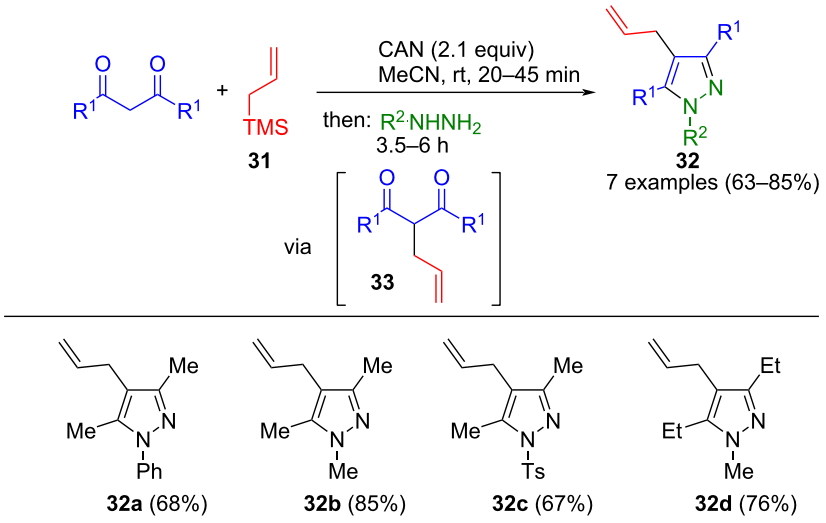

Scheme 9: Consecutive three-component synthesis of 4-allylpyrazoles **32** via oxidative allylation of 1,3-dicarbonyl compounds [59].

synthesis. Through the reaction of 1,5-diaryl-1,3,5-pentanetriones **38** with hydrazines, Knorr synthesis of pyrazoles and Fischer indole synthesis can be combined in a pseudo-three-component fashion to give 5-(indol-3-yl)pyrazoles **39** (Scheme 11) [64]. The reaction proceeds in moderate to good yields and can be conducted either consecutively or as a domino reaction. However, one limitation of the method is that the pyrazole formation is not regiospecific and leads to two isomers.

Functionalized hydrazines are versatile building blocks in organic synthesis. For instance, hydrazinecarbothioamide (**40**) can be used to synthesize bisheterocycles. Mohamed et al. were able to combine Hantzsch thiazole and Knorr pyrazole synthesis with this building block. Thiazolyl-pyrazolyl-chromenes **43** were synthesized in good yields from substituted 3-acetoacetylcoumarin **41**, 3-bromoacylpyran **42**, and semicarbazide **40** (Scheme 12) [65]. Alternatively, the corresponding chromenes

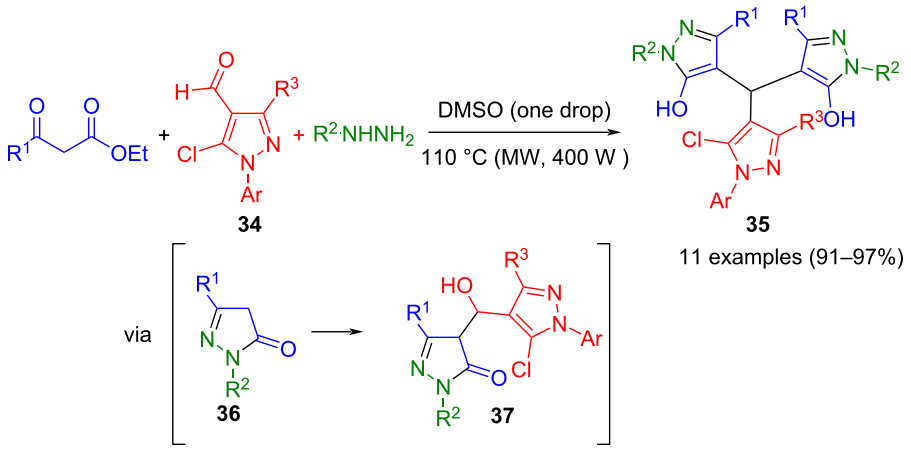

Scheme 10: Pseudo-five-component synthesis of tris(pyrazolyl)methanes **35** [61].

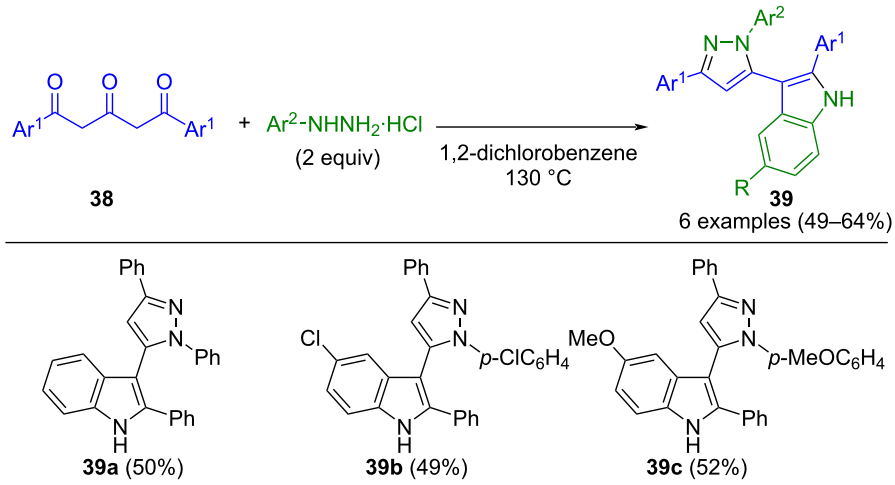

Scheme 11: Pseudo-three-component synthesis of 5-(indol-3-yl)pyrazoles **39** from 1,3,5-triketones **38** [64].

can replace the 3-bromoacylpyrans. A notable advantage of this process is its catalyst-free nature and the achievement of good regioselectivity. Due to the high heterocycle density, this method holds promise for the development of biologically active substances. In addition to acetoacetylcoumarins, the synthesis was also successfully conducted using acetylacetone [66].

Likewise, complex functionalized pyrazoles, such as triazolo[3,4-*b*]-1,3,4-thiadiazin-3-yl substituted 5-aminopyrazoles **47**, can be accessed from polyfunctional hydrazine derivatives via multicomponent reactions. For the preparation of pyrazoles **47**, 4-amino-5-hydrazinyl-4*H*-1,2,4-triazole-3-thiol (**44**), phenylacyl bromides **45**, and benzoylacetonitriles **46** were chosen as starting materials (Scheme 13) [67]. Thereby, benzoylacetonitrile and the hydrazinyl moiety constitute the pyrazole nucleus, while phenylacyl bromide condenses with the thiol and amino groups to form the thiadiazinyl moiety. In addition to bromoacetylchromenone, phenylacetyl bromide can also be used as an alternative starting material.

1,3-Dielectrophilic β-oxodithioesters **48** react with primary or cyclic aliphatic amines, resulting in the formation of β-oxothioamides **50**, which can then be directly converted into the corresponding 5-aminopyrazoles **49** with aromatic hydrazines in the presence of catalytic amounts of acetic acid (Scheme 14) [68]. The process exhibits regioselectivity, with 3,4-fused pyrazoles being accessible when cyclic β-oxodithioesters are employed as substrates. However, aromatic amines cannot be successfully employed in the sequence.

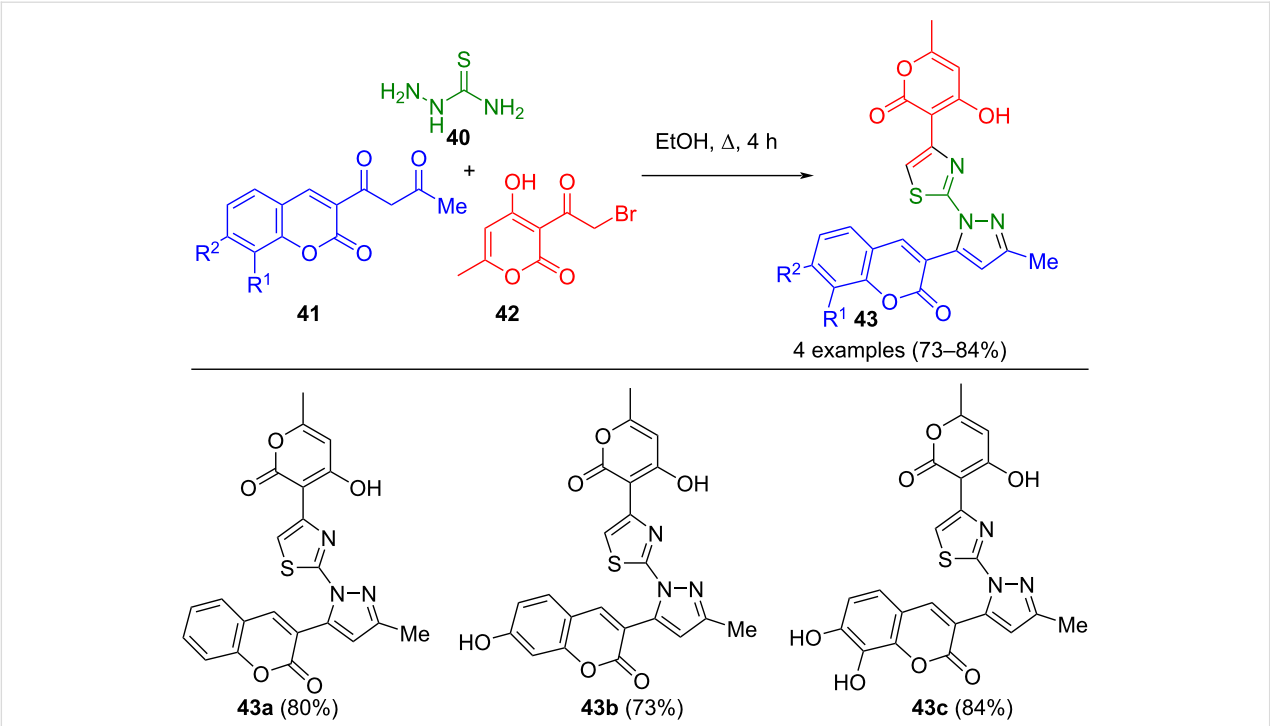

Scheme 12: Three-component synthesis of thiazolylpyrazoles **43** [65].

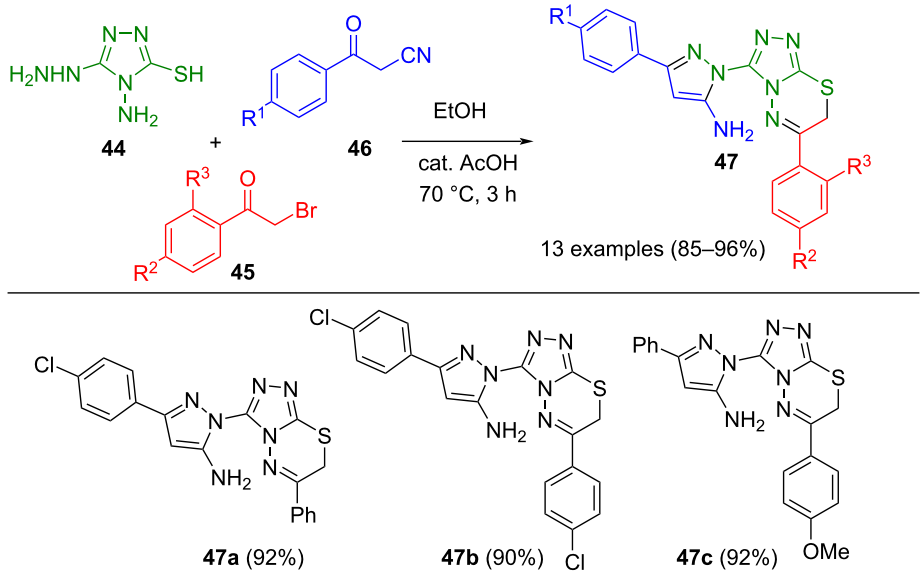

Scheme 13: Three-component synthesis of triazolo[3,4-*b*]-1,3,4-thiadiazin-3-yl substituted 5-aminopyrazoles **47** [67].

Alkenoyl derivatives as key intermediates

The Michael addition and cyclocondensation of hydrazines and α,β-unsaturated carbonyl compounds represent a standard approach for synthesizing pyrazolines, which readily oxidize to aromatic pyrazoles in the presence of ambient atmosphere. On the other hand, if good leaving groups are bound to the hydrazine, such as in tosylhydrazine, elimination directly yields aromatic pyrazoles. In cases where the α,β-unsaturated carbonyl compounds contain a heteroatom in the β-position, aromatization is triggered by elimination under redox-neutral conditions.

Tasch et al. successfully coupled aryl halides with α-bromocinnamaldehyde (**51**) using a Masuda borylation Suzuki cross-cou-

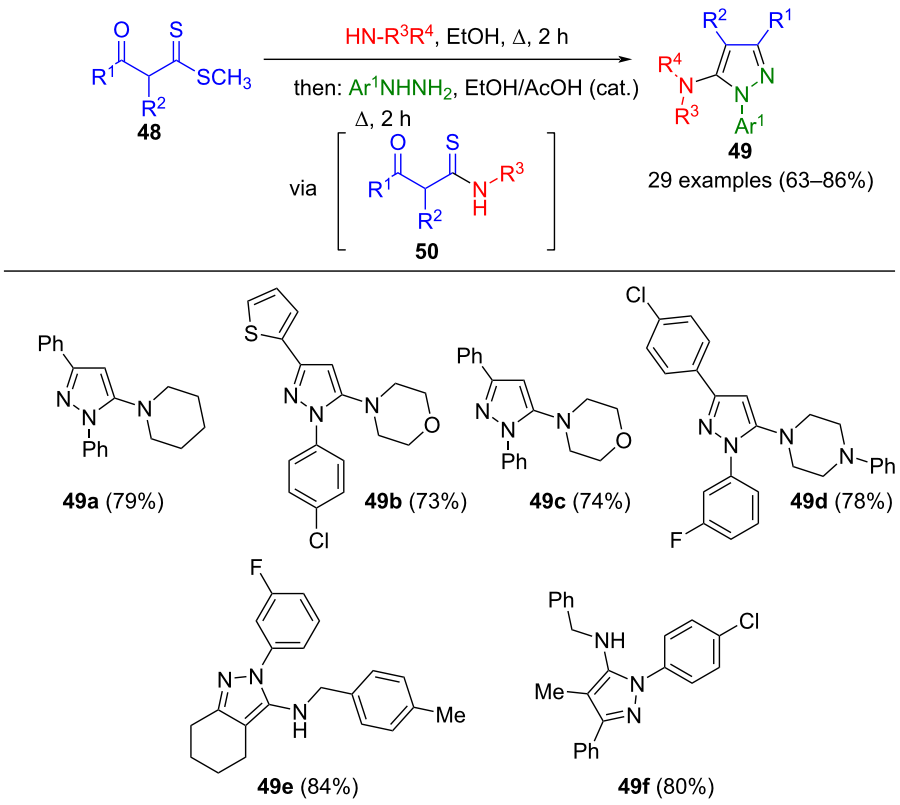

Scheme 14: Consecutive three-component synthesis of 5-aminopyrazoles **49** via formation of β-oxothioamides **50** [68].

pling (MBSC) [69] approach without reducing the reactivity of the Michael system. In this one-pot procedure, the borylation of aryl halides with pinacolborane gives aryl pinacolyl boronates **53**, which are then coupled with bromoenal **51** to generate the intermediary enal **54**. Subsequent cyclization with tosylhydrazine and elimination to give the corresponding pyrazoles **52** (Scheme 15) [70]. The cross-coupling introduced various aryl substituents at position 4. Furthermore, using 1,4-diiodobenzene as a starting material allows access to bispyrazole derivatives. According to Beller [71], using bisadamantyl-type phosphane ligands is crucial for the selectivity in this reaction.

Suzuki coupling can also serve for the functionalization of iodochromones **55**, which, as α,β-unsaturated ketones, undergo ring opening under the reaction conditions, followed by Michael addition–cyclocondensation. Xie et al. devised a method to synthesize 3,4-substituted pyrazoles **57** from iodochromones **55**, arylboronic acids **56**, and hydrazines (Scheme 16) [72]. During the Suzuki step, electronically and sterically diverse substituents were successfully coupled to chromones. Notably, a single regioisomer is formed when methylhydrazine is employed, likely due to the more electron-rich internal nitrogen atom reacting with the Michael system. When phenylhydrazine is used, an inverse reactivity is observed [73-75]. Remarkably, when hydroxyethylhydrazine is utilized, a mixture of regioisomers is formed, likely attributed to steric hindrances.

α,β-Unsaturated ketones embedded and tethered in chromene systems **58** were successfully employed in a pseudo-five-component reaction with hydrazine in boiling acetic acid to give the corresponding 4-acylpyrazolinylpyrazoles **59** (Scheme 17) [76]. The Michael addition–cyclocondensation of the α,β-unsaturated ketone with hydrazine and acetic acid forms a 1-acylpyrazoline, while the chromene moiety and hydrazine form the pyrazole nucleus by ring opening/ring closing cyclocondensation. Upon oxidation with DDQ, the pyrazolylpyrazoline products can be readily converted into the corresponding bispyrazoles.

The α,β-unsaturated carbonyl compounds **60** can undergo cyclization with tosylhydrazine in situ to form pyrazoles **61** under alkaline conditions, with the tosyl group acting as a leaving group. Upon deprotonation at position 1 by a base, followed by nucleophilic substitution of halides, *N*-functionalized pyrazoles **61** are accessible in a consecutive three-component fashion (Scheme 18) [77]. The reaction exhibits regioselectivity in many cases, attributed to steric influences.

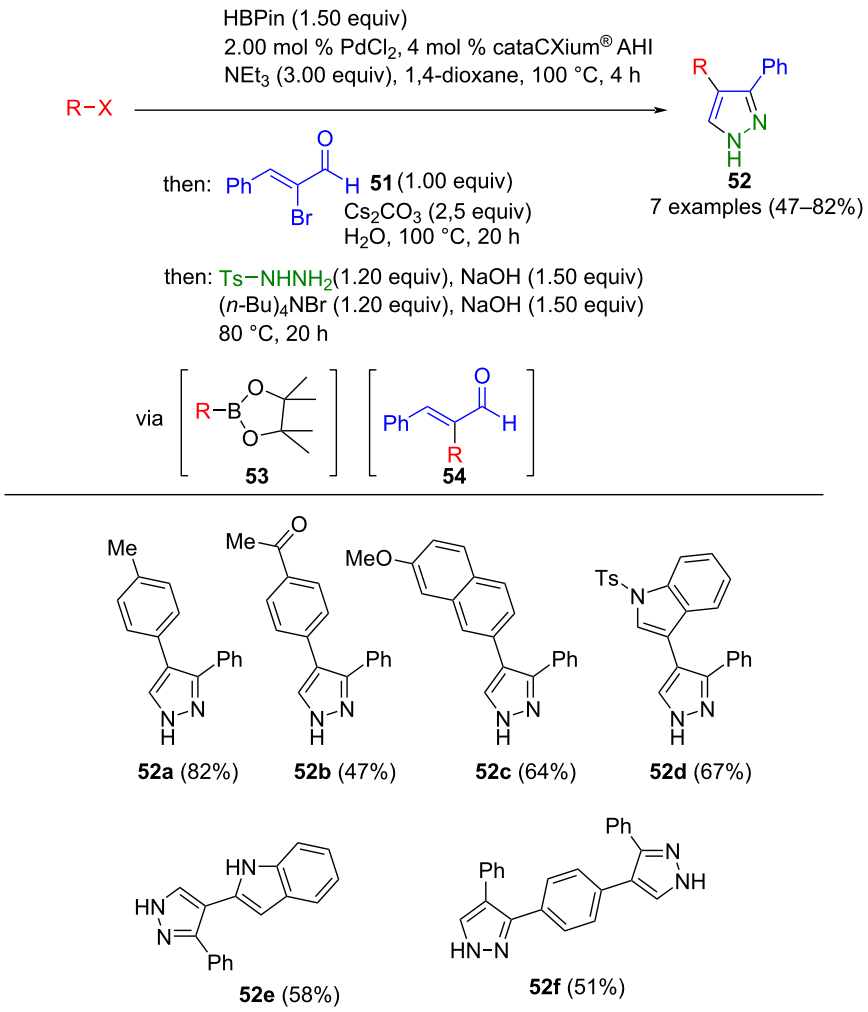

Scheme 15: Synthesis of 3,4-biarylpyrazoles **52** from aryl halides, α-bromocinnamaldehyde, and tosylhydrazine via MBSC/cyclocondensation-elimination sequence [70].

Aldehydes and nitriles with an activated methylene group, such as malononitrile, are well-known for being potent precursors of α,β-unsaturated cyano derivatives, which in turn can cyclocondense with hydrazines to furnish aminopyrazoles after oxidation. Hasanijedad and Firoozi developed a one-pot process for synthesizing 5-aminopyrazoles **62** in a three-component fashion (Scheme 19) [78]. Interestingly, hydrazine acts both as a Brønsted base in the Knoevenagel reaction and as a component for ring formation. Cyclization is completely regioselective when arylhydrazines are used; with methylhydrazine, the ratio is greater than 10:1. In addition to malononitrile, derivatives with reduced nucleophilicity (X = CO_2R) are also tolerated in the method. Starting from dialdehydes, bridged pyrazoles are accessible. However, one limitation of this strategy is the inability to use aliphatic aldehydes. Various modifications of the transformation using these substrates have been reported, where catalysts and/or conditions are varied. The one-pot process can be conducted in various solvents such as in PEG 400 [79], ionic liquids like 1-butyl-3-methylimidazolium hydroxide ((Bim)OH) [80], the nanoionic liquid 1-methylimidazolium trinitrocarbide ([[HMIM]C$(NO_2)_3$]) [81], *N*-methylpyridinium tosylate (NMPYT) [82], or glucose-based strong eutectic solvents (DES) [83]. Catalysis can also be achieved using molecular iodine [84], $AlCl_3$ [85], sodium ascorbate [86], and even solid-state and nanoparticle-mediated catalysts like CuO/ZrO_2 [87], Fe_3O_4@Si@MoO_2 [88], caspacin-cyclodextrin functionalized magnetite nanoparticles (CPS CD) [89], and Mg-Fe hydrolactite catalysts (C-Mg-Al HAT-3) [90].

With β-ketoesters, the method can be extended to a four-component synthesis. Initially, β-ketoesters react with hydrazine to form pyrazolones, while a Knoevenagel reaction between

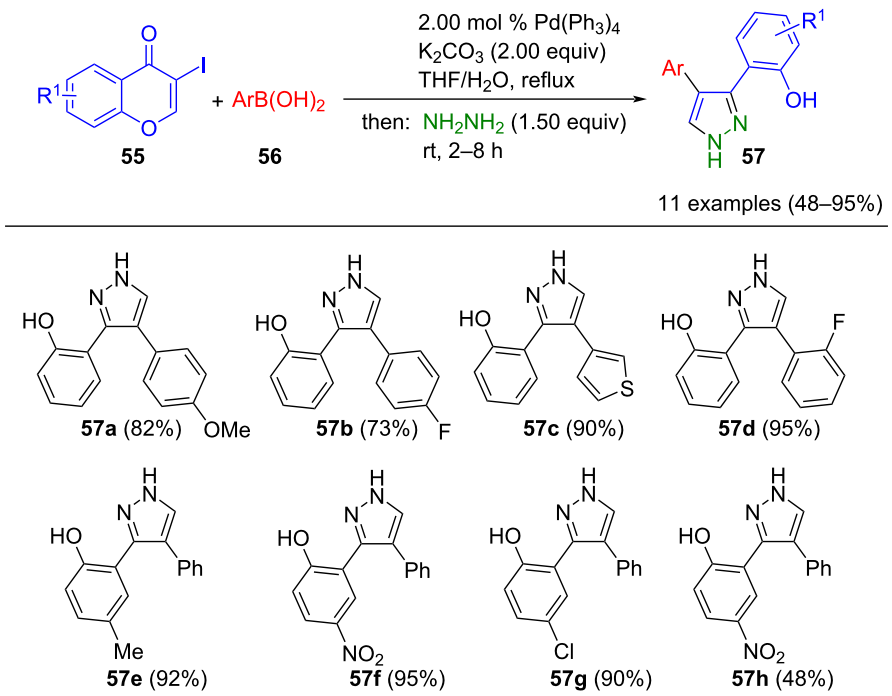

Scheme 16: Consecutive three-component synthesis of 3,4-substituted pyrazoles **57** from iodochromones **55** by Suzuki coupling and subsequent ring opening-ring closing cyclocondensation with hydrazine [72].

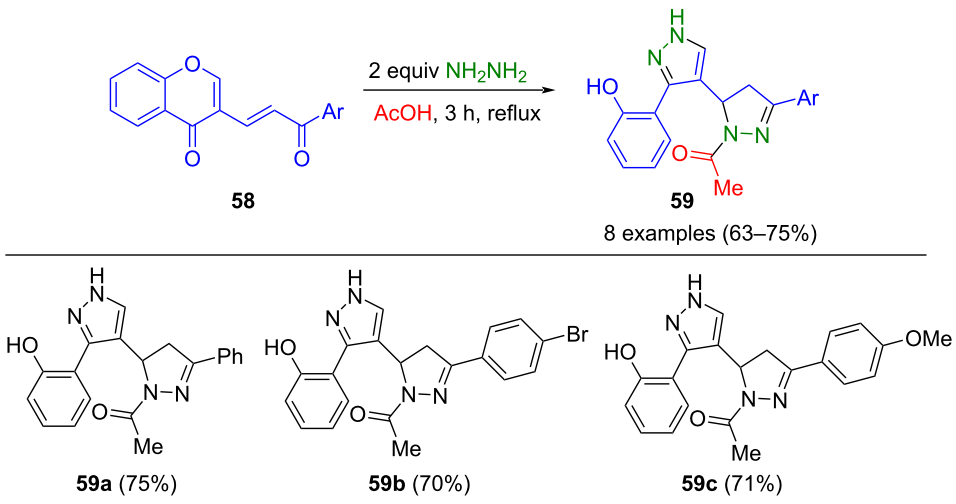

Scheme 17: Pseudo-four-component synthesis of pyrazolyl-2-pyrazolines **59** by ring opening/ring closing cyclocondensation with hydrazine [76].

malononitrile and aldehyde simultaneously generates a Michael system. Both intermediates undergo cyclization following a Michael addition to yield the corresponding pyrano[2,3-*c*]pyrazoles **63** (Scheme 20) [91]. Safaei-Ghomi et al. succeeded in isolating the intermediately formed pyrazole **64** [92]. Since pyrano[2,3-*c*]pyrazoles are fused heterocycles of interest, catalytic methods for their synthesis have been extensively reviewed [93].

When hydrazones undergo cyclization with β-ketoesters or ketones, the stability of the enol form of the carbonyl compounds plays a crucial role in the reaction. Recognizing this, a series of multicomponent reactions has been developed to synthesize pyrazole-4-carboxylates. Shen et al. used $Yb(PFO)_3$ (PFO: perfluorooctanoate), a mild and highly efficient catalyst shown to be effective in the Mannich reaction [94], to synthesize these pyrazoles **65** (Scheme 21) [95].

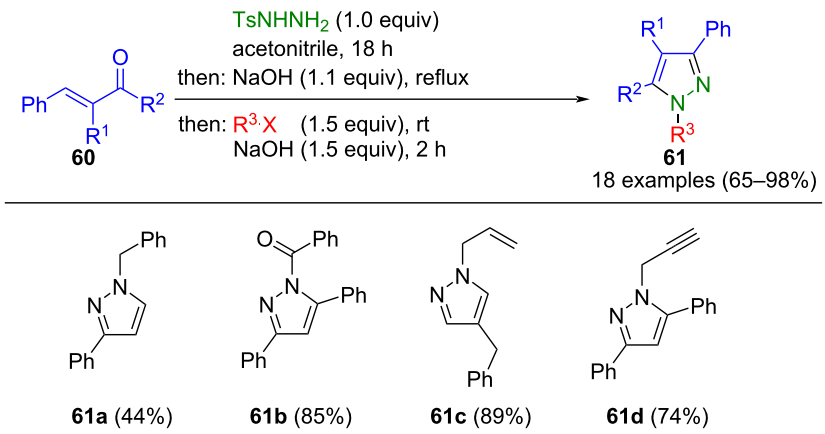

Scheme 18: Consecutive three-component synthesis of pyrazoles **61** [77].

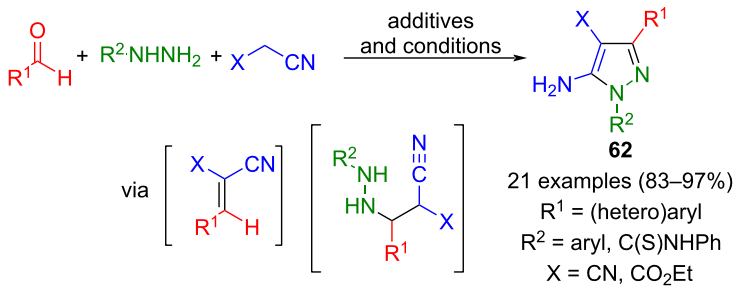

Scheme 19: Three-component synthesis of pyrazoles **62** from malononitrile, aldehydes, and hydrazines [78-90].

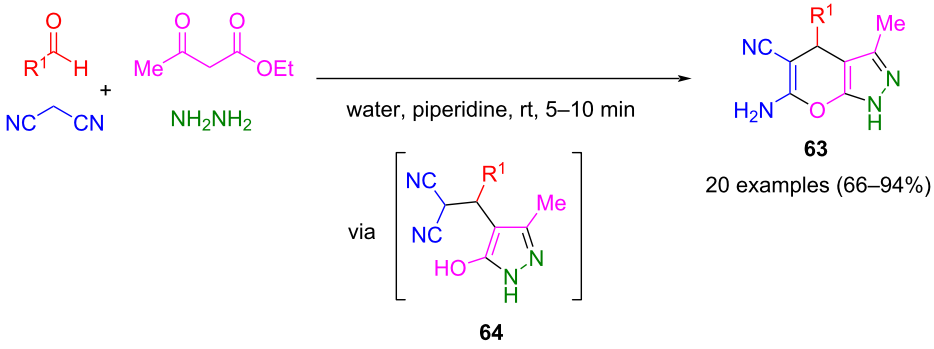

Scheme 20: Four-component synthesis of pyrano[2,3-*c*]pyrazoles **63** [91].

The Lewis acid catalyst activates and stabilizes the enol tautomer of β-ketoesters, facilitating their cyclization with intermediary formed hydrazones to yield 5-hydroxypyrazolines. After subsequent interaction with atmospheric oxygen, the product **65** is formed. This method exhibits a high degree of substituent tolerance, and aliphatic compounds generally lead to higher yields. A special feature of the method is the regioselectivity with asymmetric diketones. In addition to β-ketoesters, acetylacetone can be used in the concept. The same research group employed ethyl 4,4,4-trifluoroacetoacetate as a substrate in this method. The pyrazoline oxidation proved to be critical, and the addition of IBX ensured the completion of the reaction sequence [96]. A notable advantage of this method is the ability to reuse the catalyst multiple times. In addition to $Yb(PFO)_3$, zinc triflate can also serve as an effective catalyst for the synthesis of pyrazoles **65**. It also catalyzes the oxidation of pyrazoline, which leads to increased yields. In addition to fully substituted pyrazoles, bispyrazoles can also be synthesized [97].

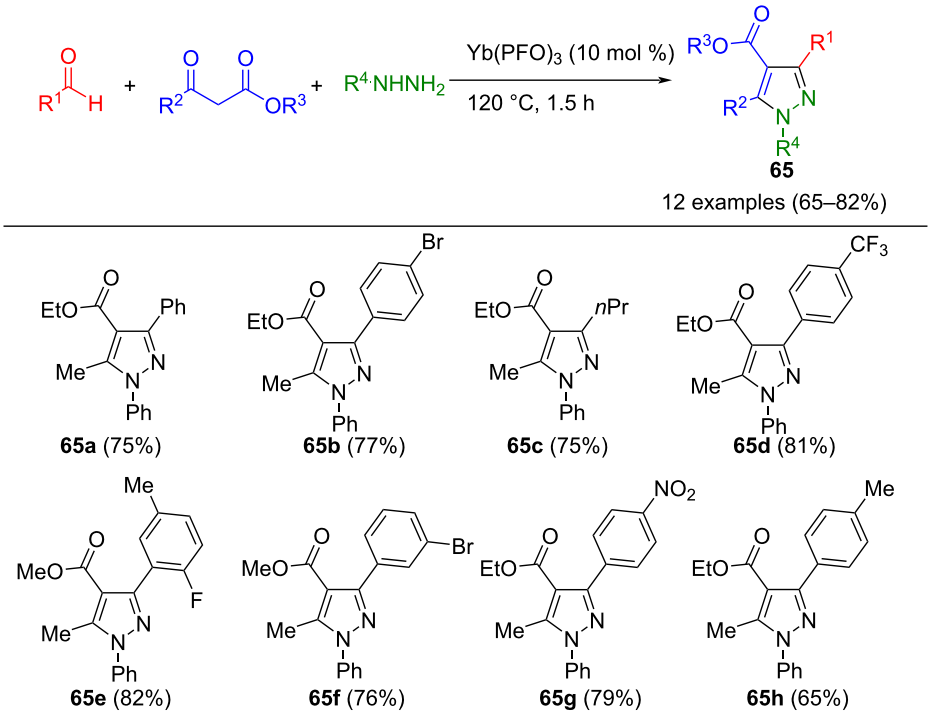

Scheme 21: Three-component synthesis of persubstituted pyrazoles **65** from aldehydes, β-ketoesters, and hydrazines [95].

Other Lewis acid catalysts employed in this method include chloride-functionalized silica gel (SiO_2Cl) [98] and $Sc(OTf)_3$ [99]. Importantly, all reactions of this method are conducted without solvent.

In a similar approach, Khan et al. succeeded in synthesizing pyrazole-4-carbodithioates **67**. The products are prepared from phenylhydrazine, aldehydes, and alkyl-3-oxo-3-arylpropane dithioates **66** catalyzed by iron sulfate (Scheme 22) [100]. In this method, aliphatic aldehydes as substrates also increase yields.

The ionic liquid [bmim][$InCl_4$] can be used as a catalyst for the one-pot synthesis of pyrazoles **68** from 1,3-diketones, aldehydes, and hydrazines (Scheme 23) [101]. The synergistic effect between anion and cation favors high regioselectivity, and high yields can be observed in the process for both electron-rich and electron-poor aldehydes. In addition to fully substituted

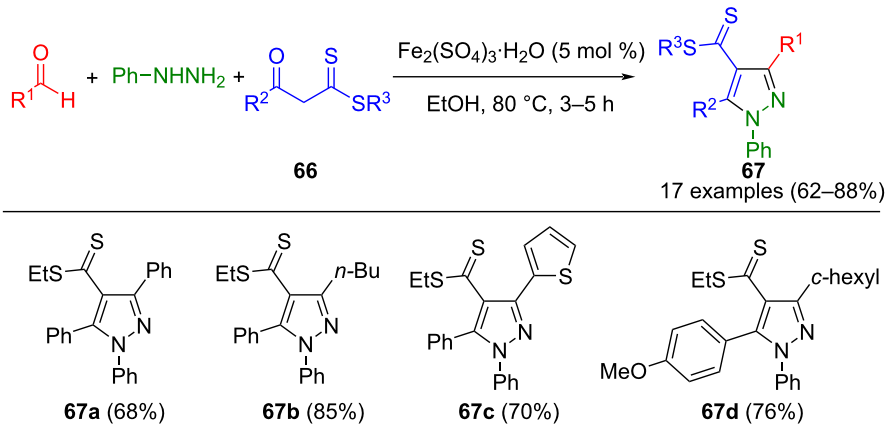

Scheme 22: Three-component synthesis of pyrazol-4-carbodithioates **67** [100].

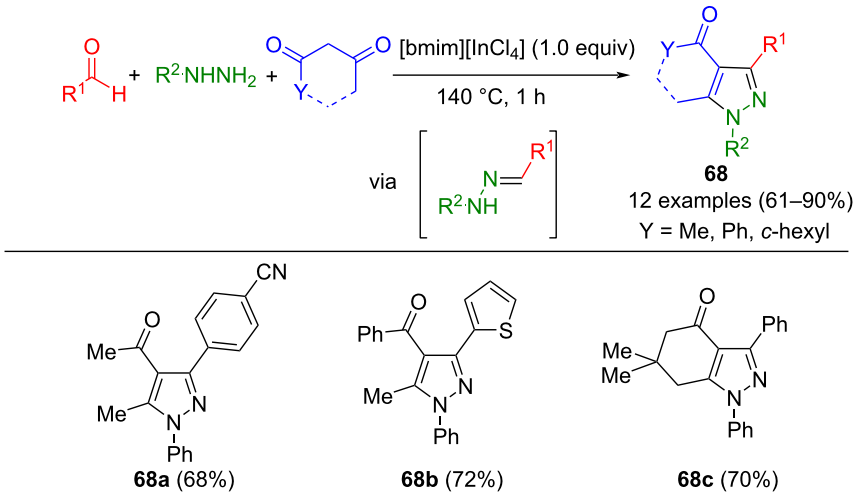

Scheme 23: Regioselective three-component synthesis of persubstituted pyrazoles **68** catalyzed by ionic liquid [bmim][$InCl_4$] [101].

pyrazoles, the method also provides access to anellated products.

Lellek's team has developed an alternative method for cyclizing hydrazones. In contrast to the previously mentioned method, intermediately generated hydrazones were cyclized with simple ketones to pyrazolines. The oxidation to the corresponding 4-halo-substituted pyrazoles **69** can be achieved in a one-pot fashion by halogenation with iodine chloride or elemental bromine (Scheme 24) [102]. When cyclic ketones are used, fused products **70** are formed. Notably, this process is compatible with both aromatic and aliphatic aldehydes.

Pyrazoles with fluorinated functionalities were synthesized via a three-component reaction utilizing trifluoroethanol both as a solvent and reactant. Gonçalves et al. developed a method whereby 1,1,1-trichloro-6-phenyl-2,4-hexanedione was generated in situ through acid hydrolysis of 1,1,1-trichloro-4-methoxy-6-phenyl-3-hexen-2-ones **71**. Subsequent cyclization with hydrazine hydrochloride followed by hydrolysis of the

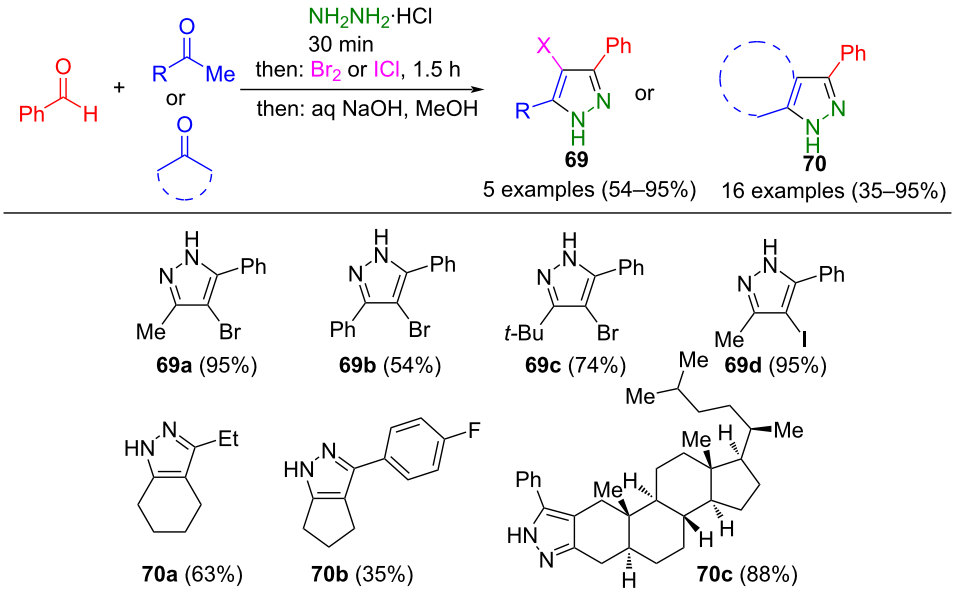

Scheme 24: Consecutive three-component synthesis of 4-halopyrazoles **69** and anellated pyrazoles **70** [102].

trichloromethyl group led to **73**. This intermediate was then reacted with 2,2,2-trifluoroethanol (TFE) as a solvent, yielding 2,2,2-trifluoroethyl pyrazole-5-carboxylates **72** (Scheme 25) [103]. A limitation of the method is that methanol formed in the first reaction step also reacts with the acid chloride to produce unwanted byproducts.

The carbonylative Heck coupling of aryl bromides with butyl vinyl ether enables the synthesis of 3-alkoxyalkenones **74**, presenting an elegant route. Subsequently, these compounds undergo a three-component reaction with various hydrazines, forming 1,3-substituted pyrazoles **75** (Scheme 26) [104]. However, one limitation is the formation of 1,5-substituted pyrazoles as byproducts in proportions of less than 10%.

Copper catalysis opens the unique opportunity to form C–N bonds, e.g., for N-functionalization of pyrazoles in a one-pot fashion. Raghunadh et al. developed a process for the synthesis of 1,3-substituted pyrazoles **76**, introducing aryl substituents at position 1. This protocol involves the utilization of enaminones, hydrazine, and various aryl halides as substrates, resulting in the formation of 1,3-substituted pyrazoles **76** (Scheme 27) [105].

Mechanistic studies have indicated that in this domino reaction, the initial formation of 3-substituted pyrazoles occurs through the cyclization of the hydrazine with the enaminone, followed by a Ullmann coupling with aryl halides to form the corresponding 1,3-substituted pyrazoles **76**. The method tolerates both sterically demanding and electronically versatile aryl moieties.

Enaminones embedded in dihydropyridines, specifically 3,5-acyl-1,4 dihydropyridines **77**, are well suited for undergoing ring opening-ring closing cyclocondensation with hydrazine in a pseudo-multicomponent reaction to give bis(pyrazol-yl)methanes **78** (Scheme 28) [106].

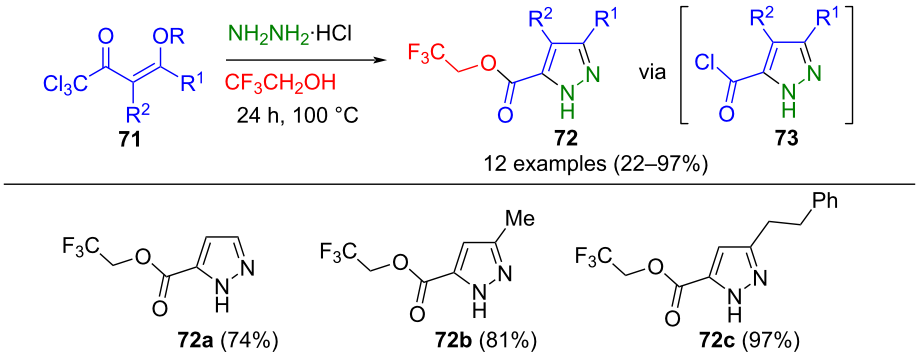

Scheme 25: Three-component synthesis of 2,2,2-trifluoroethyl pyrazole-5-carboxylates **72** [103].

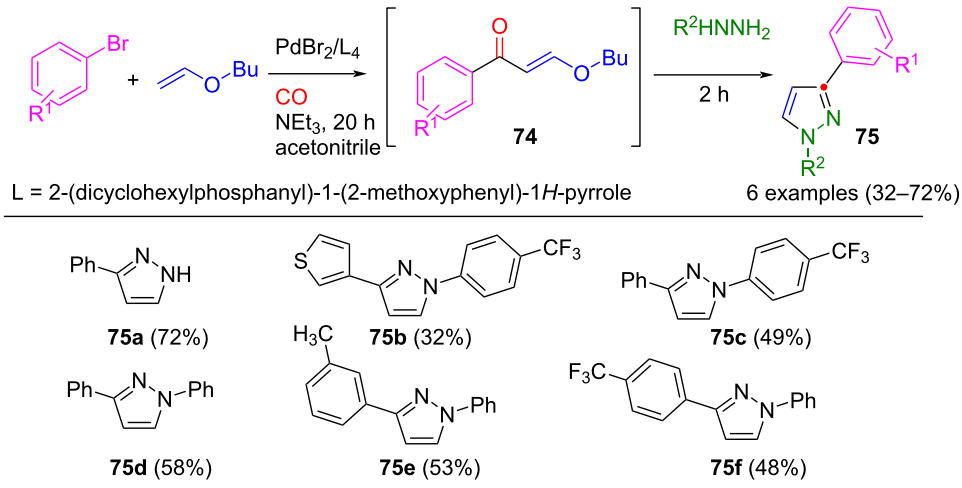

Scheme 26: Synthesis of pyrazoles **75** in a one-pot process via carbonylative Heck coupling and subsequent cyclization with hydrazines [104].

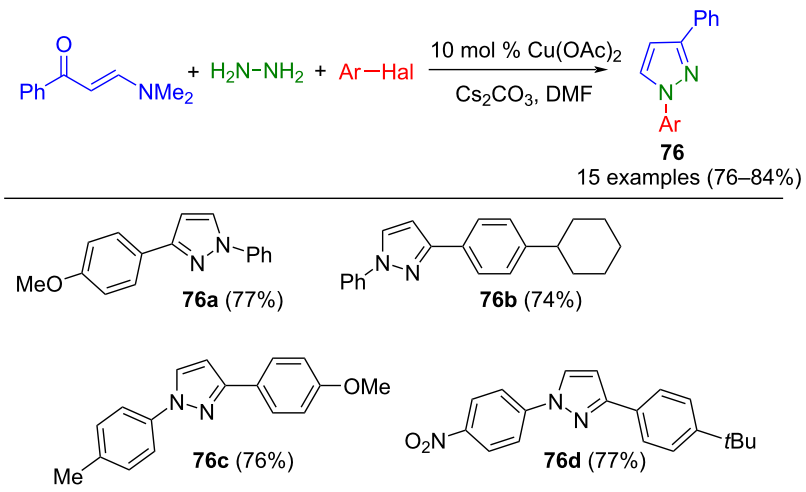

Scheme 27: Copper-catalyzed three-component synthesis of 1,3-substituted pyrazoles **76** [105].

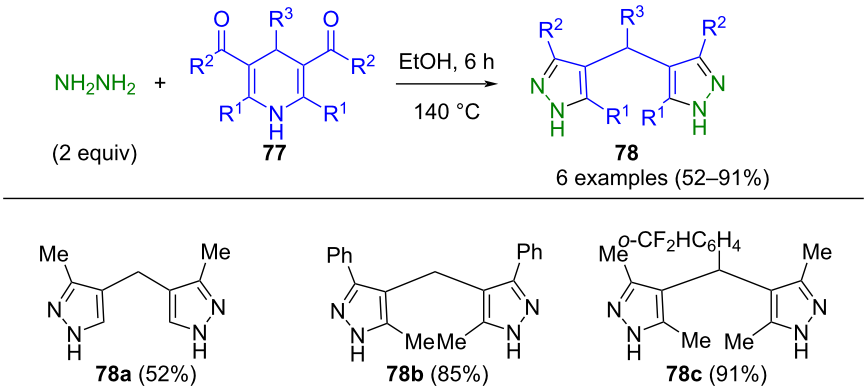

Scheme 28: Pseudo-three-component synthesis of bis(pyrazolyl)methanes **78** by ring opening-ring closing cyclocondensation with hydrazine [106].

Interestingly, the use of ester derivatives leads to the formation of the corresponding pyrazolone derivatives, thereby providing access to both bis(pyrazolyl) and bis(pyrazolonyl)methanes.

Enaminones **81** can be generated as intermediates by condensation of 1,3-dicarbonyl compounds and DMF-dimethylacetal (DMFDMA, **79**). The reaction is catalyzed by the solvent 2,2,2-trifluoroethanol, which coordinates with the carbonyl groups, and thereby stabilizing the enol form of the 1,3-dicarbonyl compounds. In the presence of hydrazines, cyclization furnishes the corresponding 1,4,5-substituted pyrazoles **80** in a one-pot process (Scheme 29) [107]. It is noteworthy that for arylhydrazines, all components can be initially present in the reaction vessel, whereas methylhydrazine is added dropwise to the enaminone to prevent the formation of regioisomers. The versatility of this method is highlighted by its tolerance towards both β-ketoesters and aliphatic 1,3-dicarbonyl compounds. Moreover, it can be performed under solvent-free conditions [108] and is applicable to the synthesis of anellated pyrazoles [109]. In addition, arylsulfonate-substituted pyrazoles can be accessed using this protocol [110].

Due to their significance in pharmaceutical chemistry [11], the formation of fluoropyrazoles from fluorinated 1,3-dielectrophiles represents a crucial synthetic pathway. For example, 1,1,2,2-tetrafluoro-*N*,*N*-dimethylethan-1-amine (TFEDMA) (**82**) can be activated using $BF_3{\cdot}OEt_2$ to generate an iminium salt **84** with increased electrophilicity. Subsequently, this intermediate reacts with various β-ketoesters to form enaminones **85**. The consecutive three-component reaction culminates in cyclization with substituted hydrazines, leading to the regioselective formation of 5-fluoroalkylpyrazoles **83** (Scheme 30) [111].

Following subsequent saponification, pyrazole-4-carboxylic acids can be obtained. The process tolerates various fluorinated

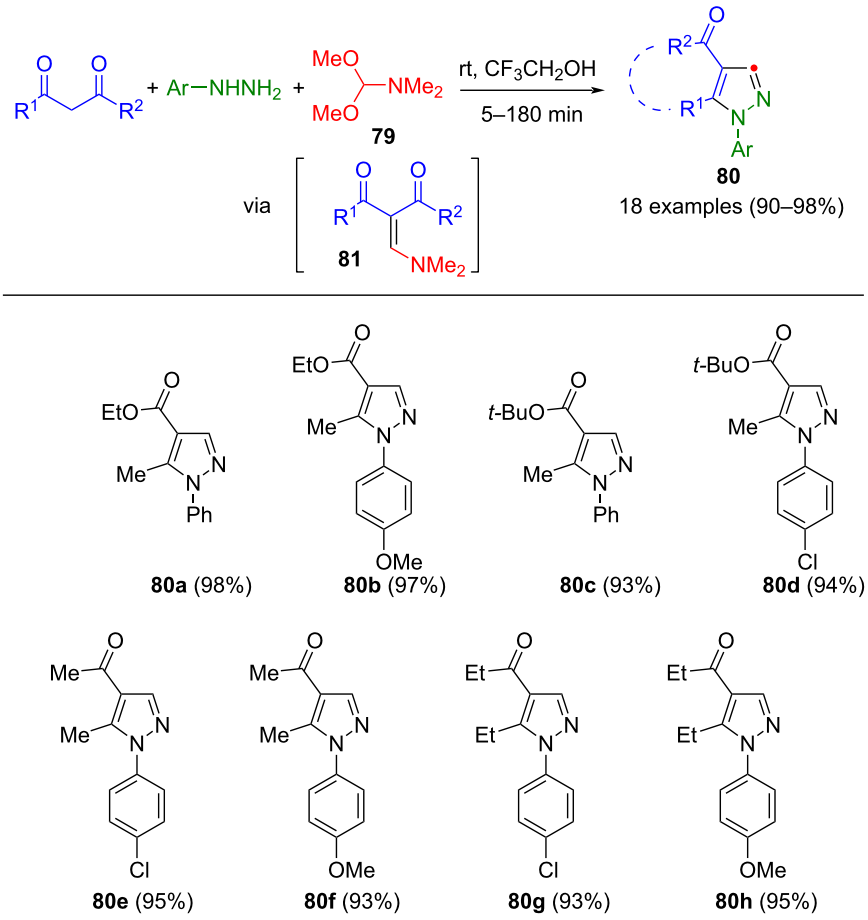

Scheme 29: Three-component synthesis of 1,4,5-substituted pyrazoles **80** [107].

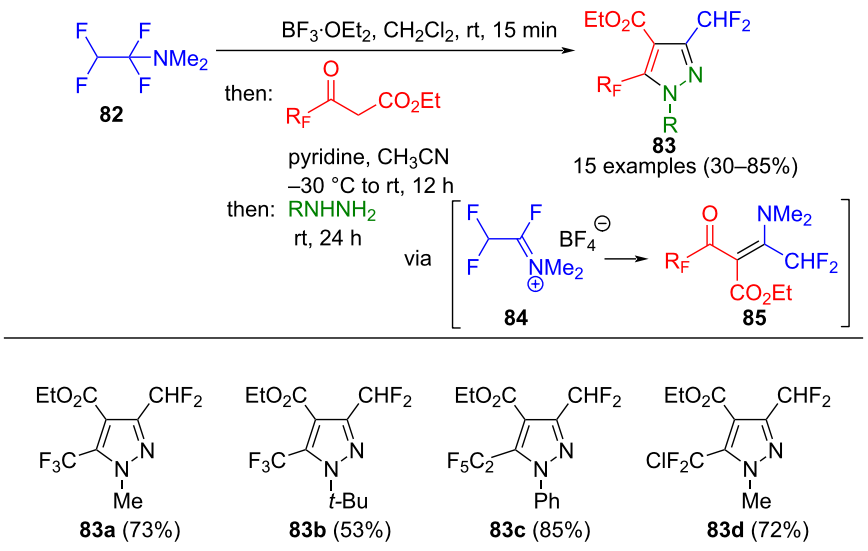

Scheme 30: Consecutive three-component synthesis of 3,5-bis(fluoroalkyl)pyrazoles **83** [111].

β-ketoesters. Moreover, both aliphatic and aromatic hydrazines can be used, with methyl and phenylhydrazines leading to increased yields. The one-pot synthesis of pyrazoles **83** can be carried out on a 100 g scale [112], and, in addition to β-ketoesters, enamino esters are tolerated in the method [113].

Starting from enaminone **86** functionalization, the hypervalent iodine compound **87** facilitates the introduction of a difluoromethanesulfonyl group in the copper(I) bromide-mediated consecutive three-component synthesis of difluoromethanesulfonyl-functionalized pyrazole **88** (Scheme 31) [114]. In addition to pyrazoles, functionalized pyrimidines can also be prepared in a one-pot process using this method.

In 2001, Bouillon et al. reported a one-pot process for synthesizing fluorinated pyrazoles. Initially, a lithium–halogen exchange was carried out on fluorinated iodoalkanes **89**. Subsequent reaction with acylsilanes **90** leads to alcohols, which react by Brook rearrangement to enoxysilanes and form the intermediate **92**. Following a Michael addition/cyclocondensation with methylhydrazine, 4-fluoropyrazoles **91** are regioselectively formed (Scheme 32) [115]. Bouillon hypothesized that the Michael addition occurs via the most nucleophilic nitrogen atom of the methylhydrazine at the β-fluorine atom of intermediate **92**. An excess of hydrazine is used in the method, as hydrofluoric acid is formed during the reaction.

Derivatives of α,β-unsaturated ketones, specifically 1,3-bis(hetero)aryl-3-(methylthio)-2-propenones **94**, are accessible through Claisen-type thioacylation of methylketones, followed by methylation. These intermediates serve as precursors for the concomitant cyclization with arylhydrazines in a consecutive multicomponent reaction to regioselectively give pyrazoles **93** (Scheme 33) [116]. The presence of two equivalents of sodium hydride deprotonates the acidic α-NH of arylhydrazine, thereby determining the regioselective attack in addition–elimination sequence furnishing a hydrazine enaminone intermediate, and ultimately leading to pyrazole **93** after cyclization. An advantage of this method for preparing 1,3,5-substituted pyrazoles is its tolerance towards a wide range of substituents.

Trimethyl phosphite can be added to acetylene dicarboxylates **95** to generate a zwitterion that readily reacts with electrophiles. This zwitterion undergoes a rearrangement similar to a Michaelis–Arbuzov reaction, yielding an α,β-unsaturated ketone **97**. The domino sequence concludes by cyclocondensation of intermediate **97** with phenylhydrazine, ultimately affording fully substituted pyrazoles **96** after the elimination of dimethyl phosphonate (Scheme 34) [117].

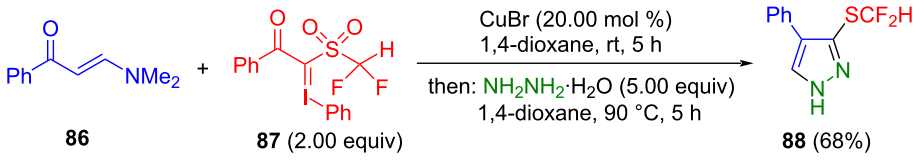

Scheme 31: Consecutive three-component synthesis of difluoromethanesulfonyl-functionalized pyrazole **88** [114].

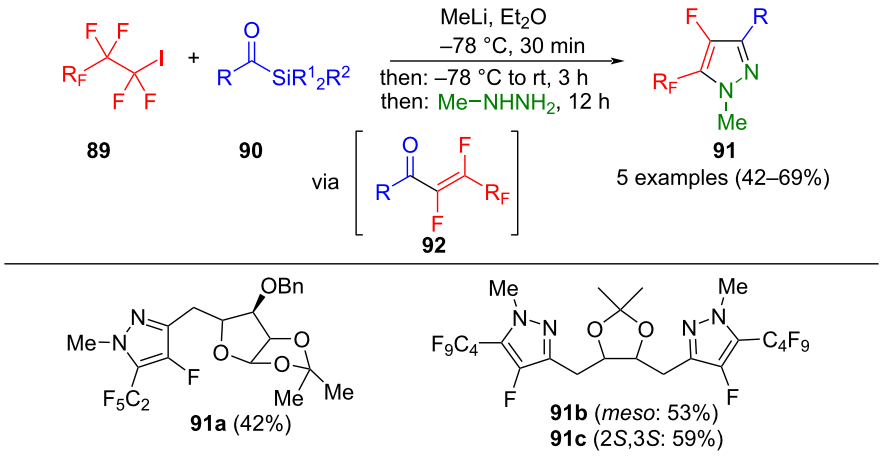

Scheme 32: Consecutive three-component synthesis of perfluoroalkyl-substituted fluoropyrazoles **91** [115].

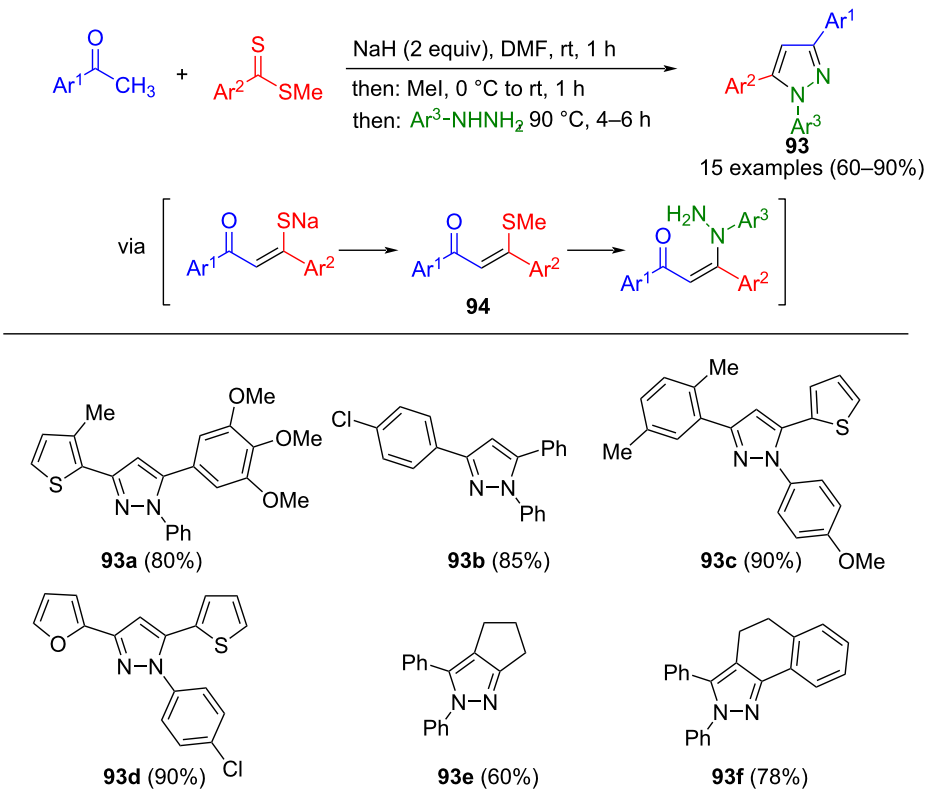

Scheme 33: Regioselective consecutive three-component synthesis of 1,3,5-substituted pyrazoles **93** [116].

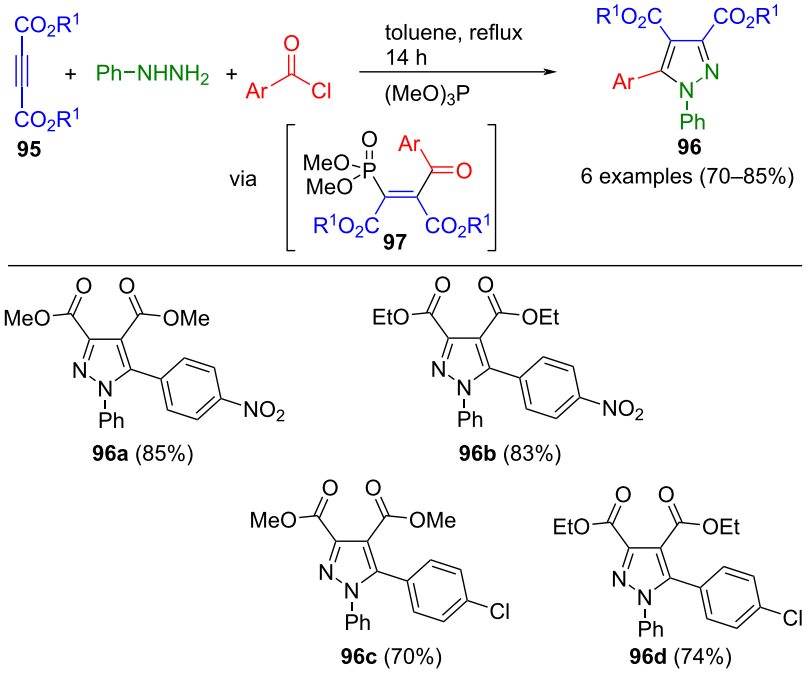

Scheme 34: Three-component synthesis of pyrazoles **96** mediated by trimethyl phosphite [117].

β-Thioalkyl-α,β-unsaturated ketones **98** are S,S-ketene acetals capable of undergoing Liebeskind–Srogl coupling with boronic acids and phenylhydrazine in a consecutive three-component reaction to give pyrazoles **99** (Scheme 35) [118].

Beltrán-Rodil et al. used a similar strategy to synthesize 1,3,5-substituted pyrazoles **101** by Suzuki coupling of β,β-dibromenones **100**, boronic acids, and 1,1-dimethylhydrazine in a three-component reaction (Scheme 36) [119]. The intermediary 5-bromopyrazoles formed by condensation/*N*-demethylation/cyclization sequence subsequently react by Suzuki–Miyaura cross-coupling in a one-pot fashion. The reaction is regioselective; however, methylhydrazine cannot be employed as a substrate.

Alkynoyl derivatives as key intermediates

Alkynones and alkynoyl derivatives also constitute a class of α,β-unsaturated carbonyl compounds, yet in a different oxidation state. Therefore, Michael addition and cyclocondensation with hydrazines proceed directly towards pyrazoles without oxidation. The formation of pyrazoles from alkynals and alkynones as three-carbon building blocks by cyclocondensation with hydrazine has been known for quite some time [120]. Recent advancements have sparked inquiries into whether three-carbon alkynoyl building blocks [121,122] could be generated catalytically [123], thereby facilitating reactions under mild reaction conditions and opening novel one-pot pathways for consecutive multicomponent syntheses of pyrazoles.

Sonogashira alkynylation of terminal alkynes and (hetero)aroyl chlorides furnishes alkynones **104** under mild reaction conditions [124,125]. Without isolation alkynones **104**, hydrazines react directly by Michael addition–cyclocondensation, affording 1,3,5-trisubstituted pyrazoles **102** and **103** with remarkable regioselectivity (Scheme 37) [126,127].

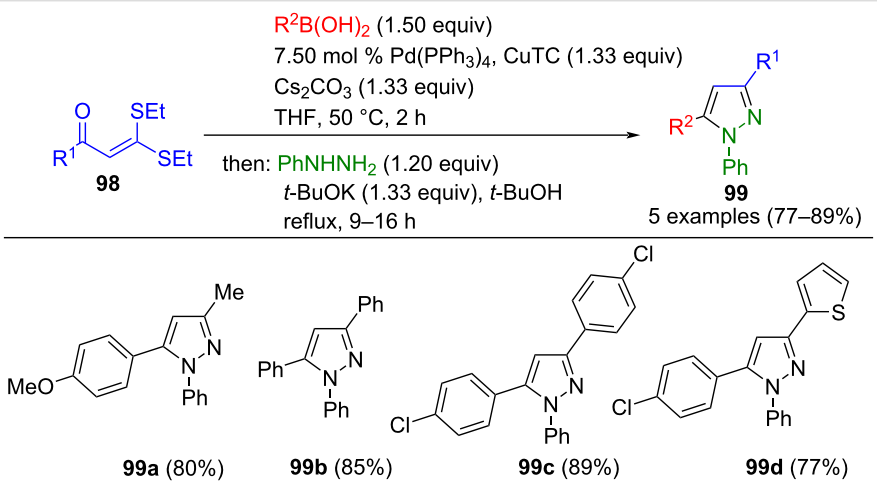

Scheme 35: One-pot synthesis of pyrazoles **99** via Liebeskind–Srogl cross-coupling/cyclocondensation [118].

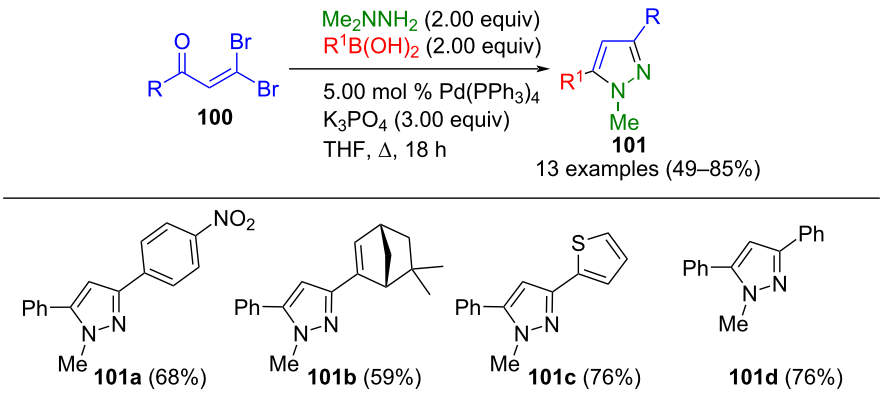

Scheme 36: Synthesis of 1,3,5-substituted pyrazoles **101** via domino condensation/Suzuki–Miyaura cross-coupling of β,β-dibromenones **100** and 1,1-dimethylhydrazine [119].

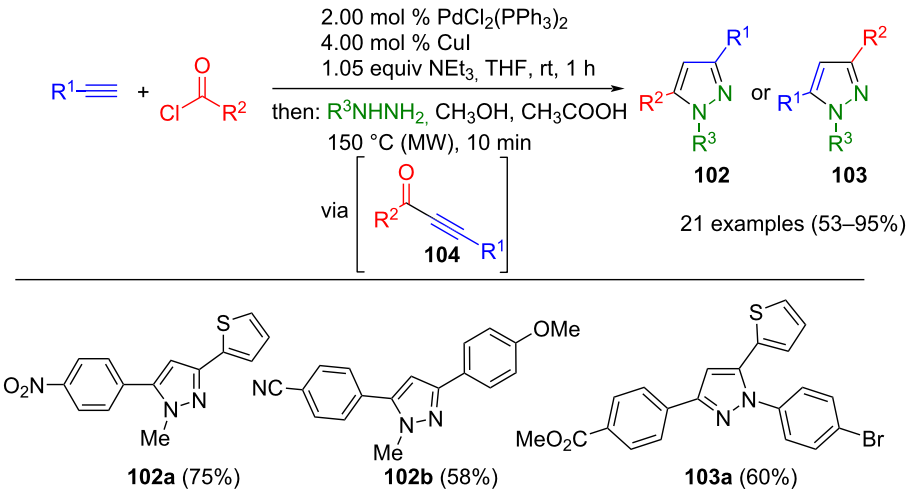

Scheme 37: Consecutive three-component synthesis of 1,3,5-trisubstituted pyrazoles **102** and **103** by Sonogashira alkynylation–cyclocondensation sequences from alkynes, (hetero)aroyl chlorides, and hydrazines [127].

The nucleophilicity of the attacking hydrazine nitrogen atom is essentially controlled by the regioselectivity. In the case of aliphatic hydrazines, the secondary nitrogen atom exhibits a higher electron density, thereby dictating the preferred formation of pyrazoles **102**. Conversely, for arylhydrazines, resonance stabilization of the secondary nitrogen atom attenuates the nucleophilicity on the secondary nitrogen, furnishing regioisomeric product **103**. This latter inverse regioselectivity is typical for arylhydrazines, and due to a lower overall nucleophilicity, often forcing conditions for the cyclocondensation are necessary [73].

Most advantageously, this methodology tolerates many polar functional groups and allows access to pyrazole libraries from simple starting materials (alkynes, acid chlorides, hydrazines) in good to excellent yield. Notably, pyrazoles **102** and **103** demonstrate intense luminescence both in solution and in the solid state [127]. Furthermore, even sugar-functionalized pyrazoles have been accessed by this approach [128], and it was readily implemented in a continuous flow reactor [129]. Besides traditional Sonogashira catalyst systems, highly reactive and reusable immobilized Pd-complexes, such as [MCM-41-2N-Pd(OAc)$_2$] [130] and Pd-SH-silica bound catalysts [131] have also been successfully employed in this three-component pyrazole synthesis. Interestingly, the latter catalyst system does not require a copper cocatalyst.

Tang's research group further extended polymer synthesis by using the consecutive three-component approach in a polymer analogous fashion with diynes **105**, terephthaloyl chloride (**106**), and hydrazines to synthesize high molecular weight pyrazole-based polymers **107** (Scheme 38) [132]. The materials **107**

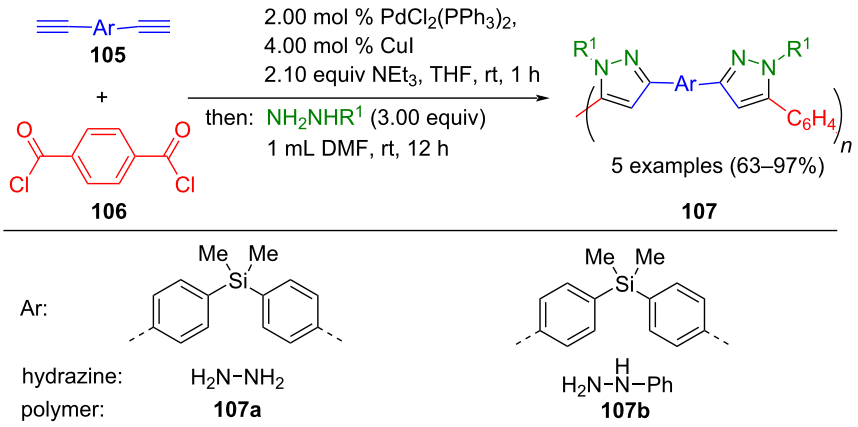

Scheme 38: Polymer analogous consecutive three-component synthesis of pyrazole-based polymers **107** [132].

fluoresce in THF solutions, form thin films, and possess high thermal stability and high optical refraction.

Functionalized alkynes can alternatively be prepared in situ by a Kumada coupling [133] of aryl iodides and ethynylmagnesium bromide [134]. The Pd catalyst is reused in the subsequent Sonogashira coupling for the synthesis of alkynones in the sense of sequential catalysis [135]. Following this, a one-pot process involving Michael addition/cyclocondensation with hydrazine derivatives leads to the corresponding pyrazoles. Since magnesium ions are formed during the Kumada coupling, the additive phenanthroline must be added during the cyclization step to prevent the coordination of the magnesium ions and subsequent hydrazine inactivation. The diversity-oriented nature of this consecutive four-component synthesis was used to synthesize 17 different donor/acceptor-substituted pyrazoles **108** in moderate to good yields (Scheme 39) [136]. The synthesis of bispyrazoles was also possible in a pseudo-seven-component reaction starting from 1,4-diiodobenzene. The product **108c** showed strong solvatochromism.

The synthesis of pyrazoles from terminal alkynes, acyl chlorides, and hydrazines [124,126] can be extended by subsequent halogenation at position 4 with *N*-halosuccinimide **109** (X = Cl, Br). The resulting 4-halopyrazoles **111** can either be isolated or undergo further Suzuki coupling with arylboronic acids. Both couplings use the Pd catalyst in a sequential fashion. To increase the yields, both cyclization and Suzuki coupling are carried out with microwave support. Some of the synthesized 4 halopyrazoles **111** and their Suzuki products **110** fluoresce blue in solution and have quantum yields of 29–72 % (Scheme 40) [137].

The Suzuki coupling can also be used for the functionalization of pyrazoles. For this purpose, *p*-bromo-substituted terminal alkynes **112**, acyl chlorides **114**, and arylhydrazines **116** are used as starting materials. The *p*-bromophenylpyrazoles presented in situ can be reacted with boronic acids or boronic acid esters in a sequentially Pd-catalyzed coupling towards biaryl-substituted pyrazoles **113**, **115**, and **117** (Scheme 41) [138]. Furthermore, a pseudo-five-component reaction pathway enables the synthesis of 3,5-bis(biphenyl)-1-methyl pyrazole. To stabilize the catalyst, additional triphenylphosphane is added as a ligand during the Suzuki coupling. The resulting products fluoresce blue, with the five biaryl-substituted derivatives **113** showing the highest quantum yields of up to 97%.

The Sonogashira coupling can also be effectively integrated with the CuAAC (copper-catalyzed azide–alkyne cycloaddition) reaction, offering a powerful tool for synthesizing diverse molecular architectures. In a consecutive multicomponent reaction, pyrazoles were first presented in a Sonogashira cyclization sequence from (triisopropylsilyl)butadiyne (**118**). Subsequent

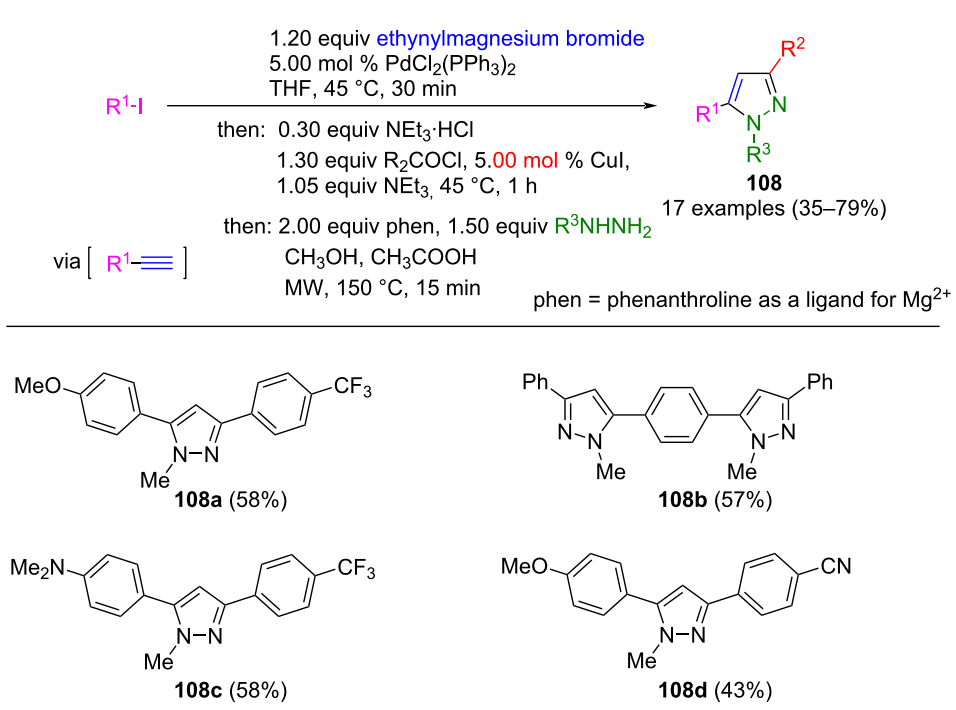

Scheme 39: Synthesis of 1,3,5-substituted pyrazoles **108** by sequentially Pd-catalyzed Kumada–Sonogashira cyclocondensation sequence [136].

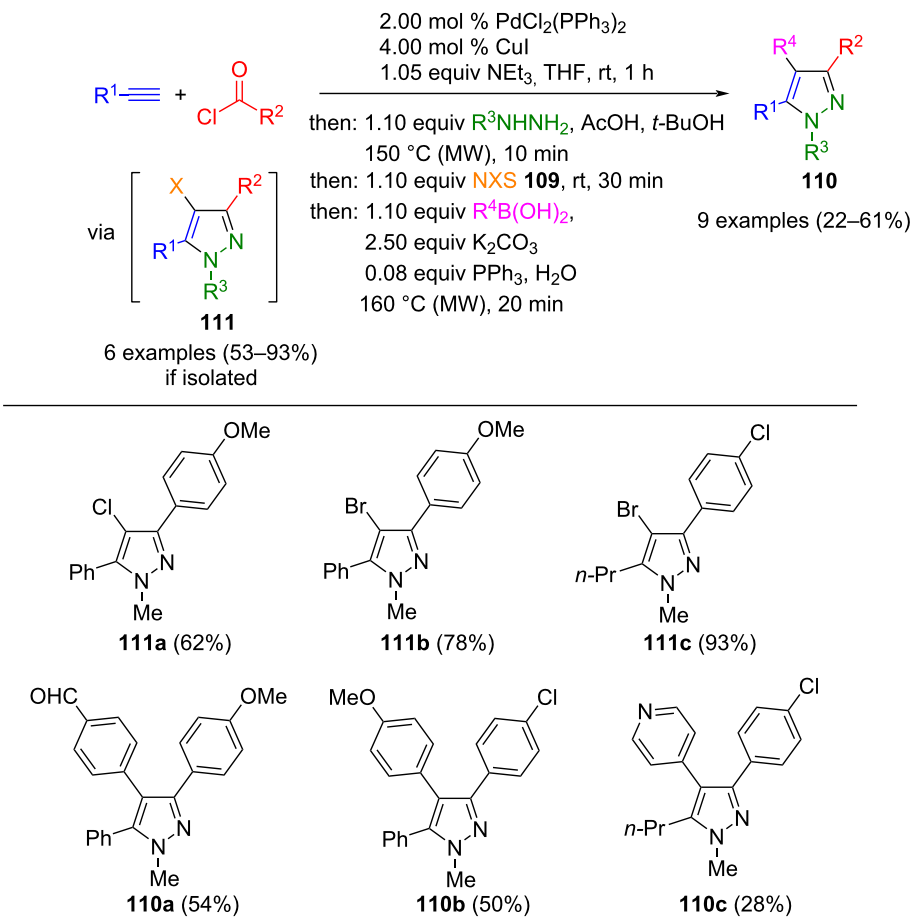

Scheme 40: Consecutive four-step one-pot synthesis of 1,3,4,5-substituted pyrazoles **110** [137].

immediate desilylation and Click reaction with organoazides lead to 4-pyrazolyl-1,2,3-triazoles **119** (Scheme 42) [139]. Notably, in some examples, it was even possible to synthesize the organoazides in situ from alkyl halides and cesium azide for the synthesis of compounds **120**. The choice of the hydrazine substituent represents a limitation, as no aromatic substituents are tolerated in the strategy due to the reduced reactivity. However, due to the building blocks' simplicity, various 4-pyrazolyl-1,2,3-triazoles are accessible.

Aryl iodides undergo conversion to the corresponding alkynones in aqueous ammonia through a palladium-catalyzed carbonylative coupling with terminal alkynes under 1 atm of carbon monoxide. Building upon this discovery, these intermediates were cyclized with hydrazines to give pyrazoles **121** in a one-pot process (Scheme 43) [140]. This alkynone generation fulfills two functions: on the one hand, it acts as an activating reagent in the coupling reaction and, on the other, as a ring-forming component. Notably, this process can only be carried out as a domino reaction. For the coupling of aliphatic alkynes, copper iodide is necessitated as a co-catalyst [141]. In addition to classic Sonogashira catalysts, phosphane-free palladium [Pd(NN)] chelate complexes can also be used, which promote excellent regioselectivity [142]. A variation of the reaction is possible with $Mo(CO)_6$ as a carbon monoxide source. This allows the use of phenylhydrazine, which is not tolerated under standard conditions. However, the synthesis of unsymmetric pyrazoles produces two regioisomers [143].

Recently, Tu et al. reported a similar method for the regioselective synthesis of trisubstituted pyrazoles via palladium-catalyzed oxidative carbonylative Sonogashira alkynylation and cyclocondensation with arylhydrazines [144].

In 2009, Müller and co-workers introduced an alternative approach for synthesizing alkynones through a one-pot process [145]. Azulen-3-ylalkynones **126**, obtained by glyoxylation of azulene (**122**) with oxalyl chloride (**123**) and a subsequent decarbonylating Sonogashira coupling of glyoxylchloride **125**, were transformed in the same reaction vessel with methylhydrazine afforded pyrazoles **124** in moderate yields (Scheme 44) [146].

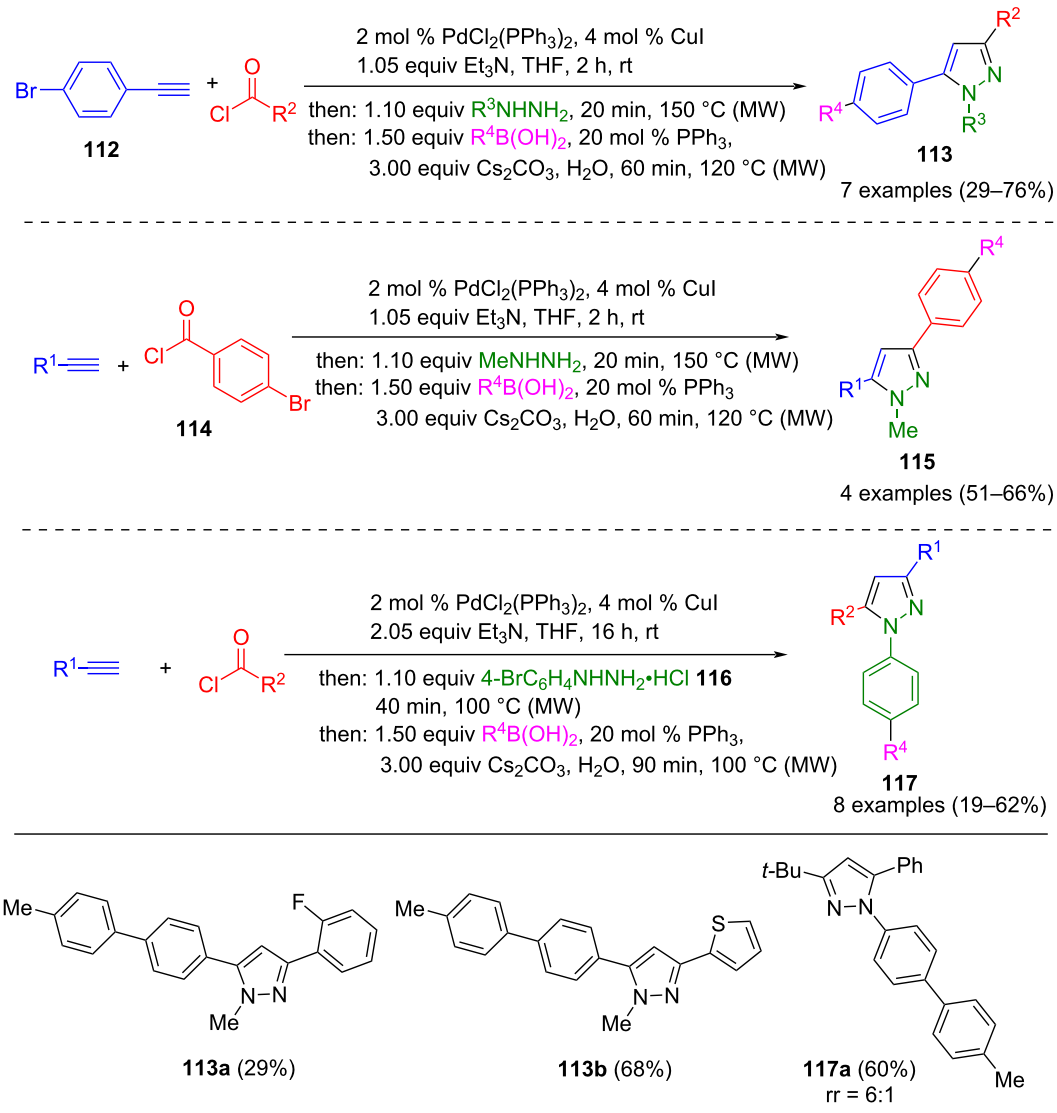

Scheme 41: Four-component synthesis of pyrazoles **113**, **115**, and **117** via Sonogashira coupling and subsequent Suzuki coupling [138].

Analogous to Bishop's observations [73], a single regioisomer was isolated. However, attempts to carry out the cyclization with phenylhydrazine, Boc-hydrazine, or hydrazine hydrate failed.

Alternatively, alkynylation can be achieved through copper catalysis. Glyoxylation of *N*-methylindole with oxalyl chloride and subsequent Stephens–Castro coupling with phenylacetylene gives access to polyfunctional ynedione **129** [147]. In contrast to Sonogashira alkynylation, where glyoxyl substrates furnish ynones with concomitant decarbonylation [145], Stephens–Castro alkynylation preserves the dicarbonyl functionality in the product [148]. Embedded within a consecutive four-component reaction, with a concluding cyclocondensation employing Boc hydrazine, 1,5-diacyl-5-hydroxypyrazoline **127** is formed, as later confirmed by isolation [149]. Upon alkaline workup, this gives 3-acylpyrazole **128** in good yield (Scheme 45) [147].

Ynediones are also accessible from α-ketocarboxylic acids **130** through chlorination and Stephens–Castro coupling [148]. With 1,4-dioxane as a solvent, chlorination yields could be increased by activation of oxalyl chloride to give glyoxyl chlorides **133**. The resulting ynediones **134** were cyclized in a consecutive three-component fashion with Boc-hydrazine to give 1,5-diacyl-5-hydroxypyrazolines **131**. Cleavage of the protecting group with potassium carbonate in methanol finally provides the corresponding 5-acyl NH-pyrazoles **132** (Scheme 46) [149].

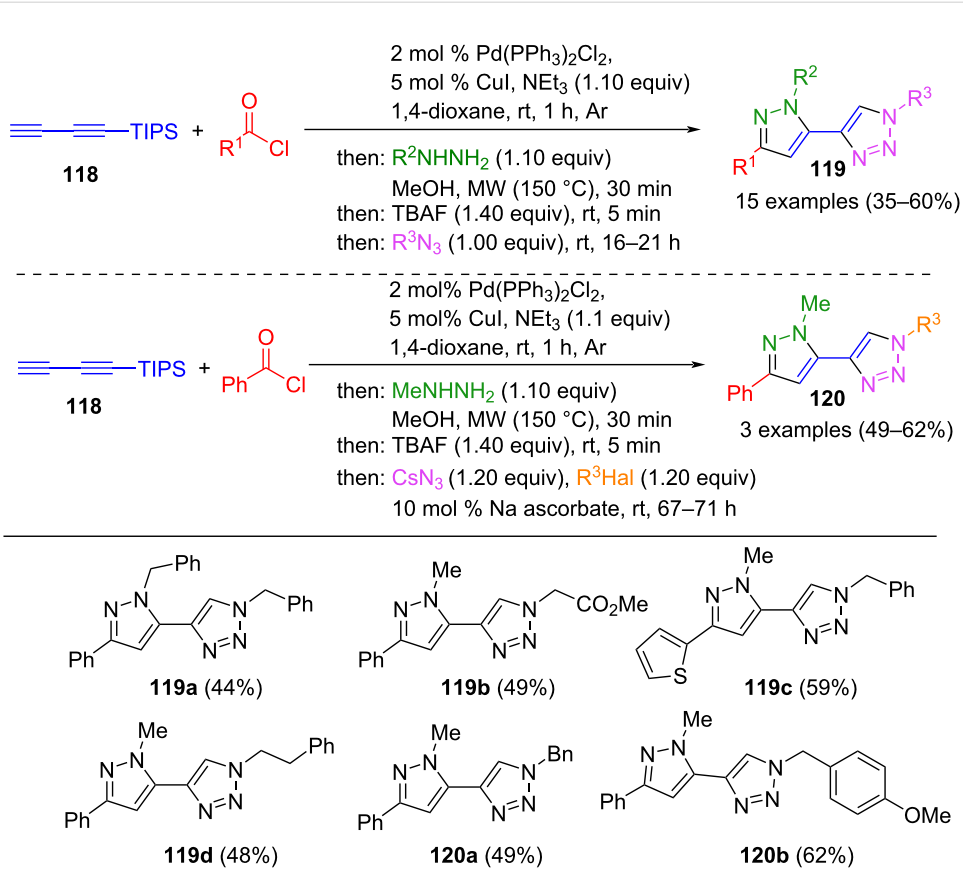

Scheme 42: Consecutive four- or five-component synthesis for the preparation of 4-pyrazoly-1,2,3-triazoles **119** and **120** [139].

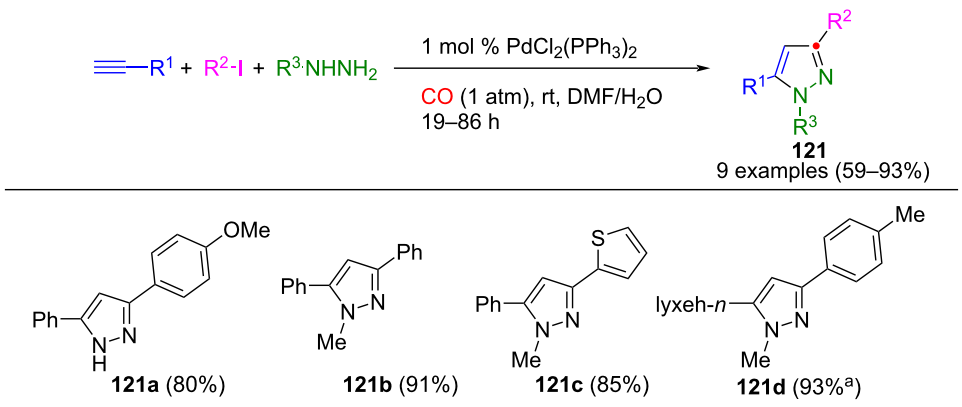

Scheme 43: Four-component synthesis of pyrazoles **121** via alkynone formation by carbonylative Pd-catalyzed coupling [140]. [a]5.00 mol % $PdCl_2(PPh_3)_2$, 2.00 mol % CuI.

A novel approach to synthesizing pyrazoles via the initial formation of isoxazoles **138** through (3 + 2)-cycloaddition of nitrile oxides **137**, generated in situ from hydroxyiminoyl chloride **135** and terminal alkynes, was proposed by Kovacs and Novak. Copper supported on iron serves as a catalyst and as a reagent for the reductive ring opening and leads to β-aminoenones **139**, which react in the consecutive one-pot process with hydrazine hydrate to give 3,5-substituted pyrazoles **136** (Scheme 47) [150]. Notably, nitro groups are reduced to amines due to the reductive conditions. Furthermore, neither aliphatic hydroxyiminoyl chlorides nor internal alkynes are competent substrates in this transformation.

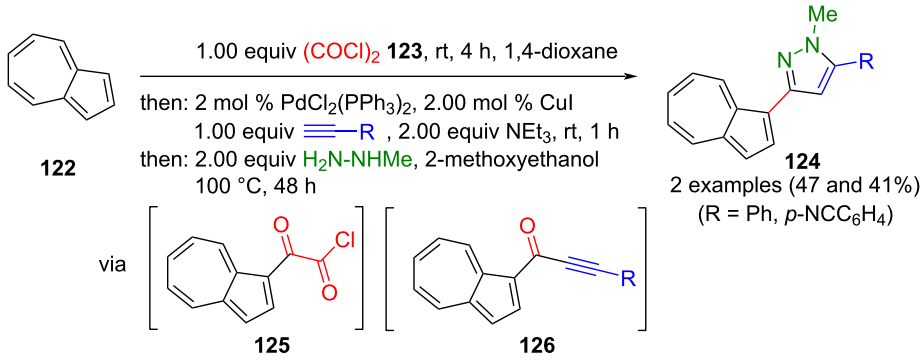

Scheme 44: Preparation of 3-azulenyl pyrazoles **124** by glyoxylation, decarbonylative Sonogashira coupling, and subsequent cyclization [146].

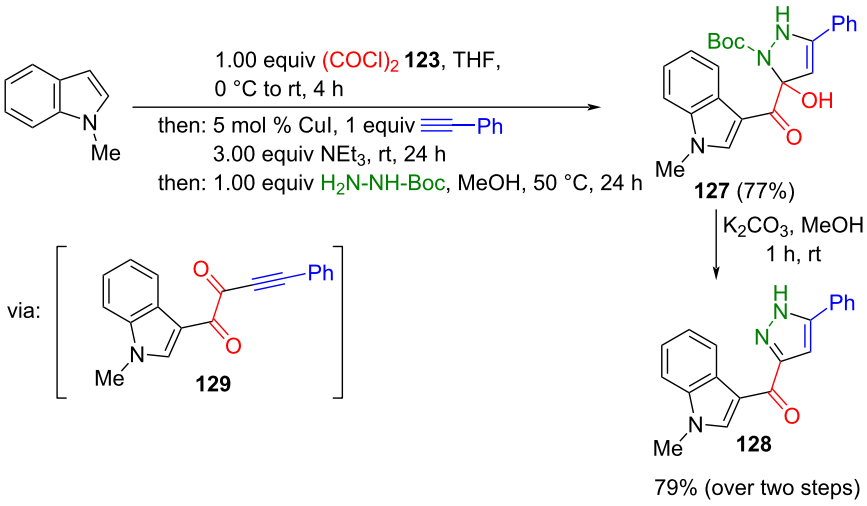

Scheme 45: Four-component synthesis of a 3-indoloylpyrazole **128** [147].

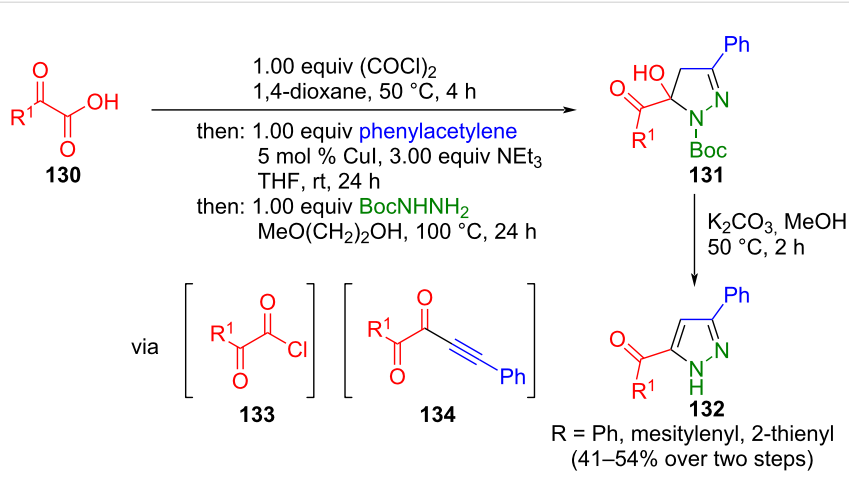

Scheme 46: Two-step synthesis of 5-acylpyrazoles **132** via glyoxylation-Stephen–Castro sequence and subsequent cyclization with Boc hydrazine [148,149].

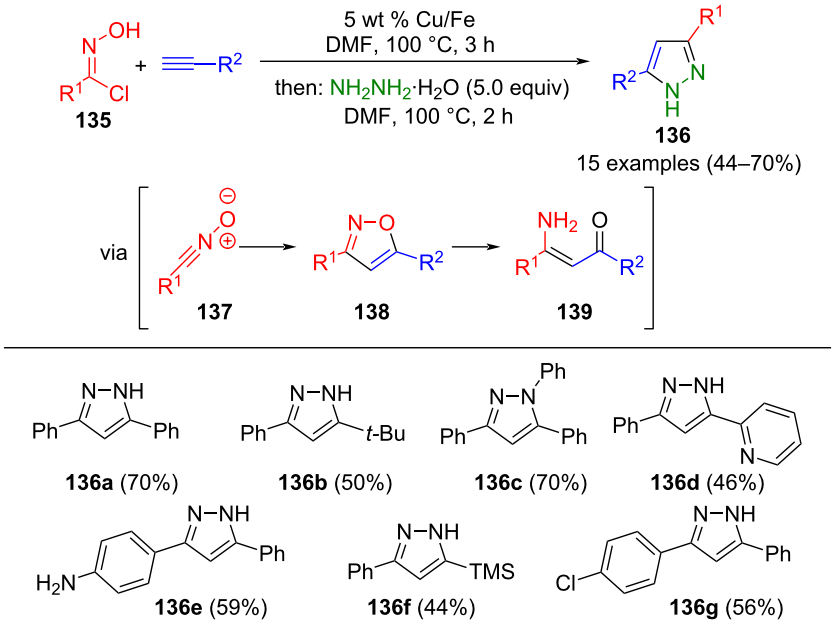

Scheme 47: Copper on iron mediated consecutive three-component synthesis of 3,5-substituted pyrazoles **136** [150].

Palladium catalysis not only enables the synthesis of alkynones, but also facilitates the introduction of protected alkynal moieties, which can be converted to pyrazoles in a one-pot fashion. Sonogashira coupling is particularly well-suited for this purpose. The alkynylation of propynal diethyl acetal (**140**) and (hetero)aryl iodides gives rise to 3-arylalkynyl acetals **142**. Since 3-arylpropynals are sensitive to oligo- and polymerization, it proved useful to perform acetal deprotection and cyclization with hydrazine hydrate in a one-pot procedure to give 3-substituted pyrazoles **141** (Scheme 48) [151]. Given that Sonogashira coupling is conducted under basic conditions, it is important to remove the protecting group with stoichiometric amounts of PTSA in this consecutive three-component synthesis. The process tolerates both electron-rich and electron-poor aryl substituents. However, it is not possible to introduce heteroaryls other than thiophene under standard conditions.

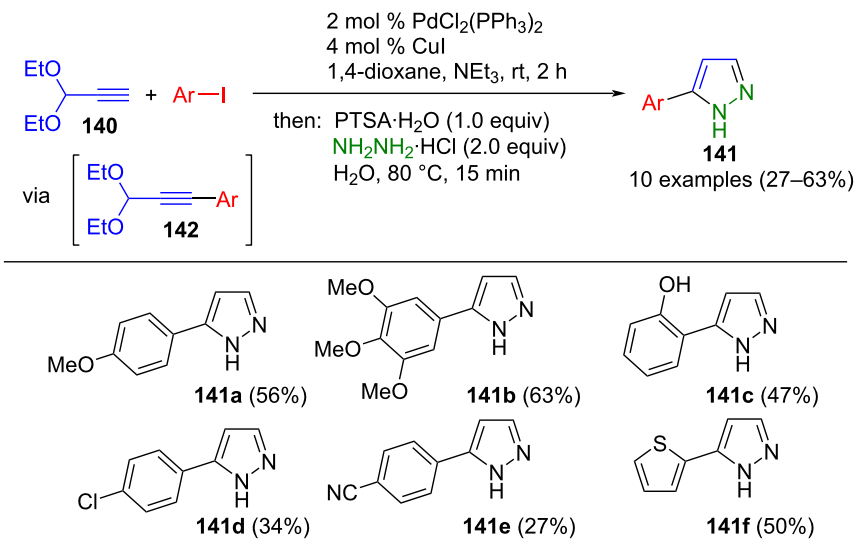

Scheme 48: Consecutive three-component synthesis of 3-substituted pyrazoles **141** by Sonogashira coupling and subsequent cyclization with hydrazine hydrate [151].

Schreiner et al. established a further protocol for the one-pot synthesis of pyrazoles, where the alkynoyl moiety is generated by copper-catalyzed carboxylation of terminal alkynes followed by alkylation with methyl iodide, forming propiolic acid methyl esters **144**. Subsequently, these esters are converted to various 3-hydroxypyrazoles **143** with hydrazine salts by microwave-assisted cyclization (Scheme 49) [152].

The method tolerates a large number of functional groups. In addition, X-ray structural analysis proved that the products are aromatic 3-hydroxypyrazoles **143** and not tautomeric 3-pyrazolones.

Alternative access to alkynones can be achieved by nucleophilic addition of lithiated alkynes to *N*-substituted phthalimides **145**, followed by ring opening to give, upon the addition of water, the corresponding 3-hydroxyindolines. These intermediates are in equilibrium with the ring-opened alkynones. The latter reacts in a one-pot fashion with hydrazines to give pyrazoles **146** (Scheme 50) [153,154]. Notably, due to steric reasons, the cyclocondensation proceeds regioconvergently with methylhydrazine and phenylhydrazine.

Harigae et al. have presented a consecutive three-component synthesis of 3,5-disubstituted pyrazoles. This synthesis is initiated by adding terminal acetylides to aldehydes, followed by oxidation to the ynone utilizing molecular iodine, and concludes through cyclocondensation with hydrazines [155].

In line with the discussion on the formation of alkenone intermediates, dialkyl acetylenedicarboxylates **147**, as alkynoyl derivatives, are transformed to pyrazolones **149** by Michael addition–cyclocondensation with phenylhydrazine. In a consecutive one-pot reaction, the latter intermediates undergo *O*-acylation with aryl chlorides to give *N*-phenyl-3,5-substituted pyrazoles **148** (Scheme 51) [156]. Efforts to synthesize bridged pyrazoles using fumaryl chloride proved unsuccessful, with only 3,5-substituted pyrazoles isolated. Nonetheless, the crystal structure of such a pyrazole was investigated [157].

In their study, Alizadeh et al. showed that ninhydrin (**150**), as an electrophile, reacts with the enol tautomeric form **153** of pyrazolone **152** to give ninhydrin-substituted pyrazoles **151** in a three-component reaction, as depicted in Scheme 52 [158].

The two-component formation of pyrazolone **156** from acetylenedicarboxylates and phenylhydrazine can be well embedded in en route formation of intermediate **157** from arylglyoxal and cyclic enaminone **154**. This transformation is catalyzed by acetic acid, ultimately yielding 4-(oxoindol)-1-phenylpyrazol-3-carboxylates **155** in the consecutive four-component process (Scheme 53) [159]. In this concept, the yields could be significantly increased by controlling the order of addition of reactants. It is noteworthy that both electron-rich and electron-poor arylglyoxals and enaminones lead to high yields in the reaction sequence.

Abid et al. developed a concise three-component synthesis method for pyrazole starting materials from isonitriles **158**, dialkyl acetylenedicarboxylate **147**, and hydrazine carboxamide **159**. The addition of the isonitrile to the Michael system yields a nitrilium-vinyl anion zwitterion **161**, that is protonated

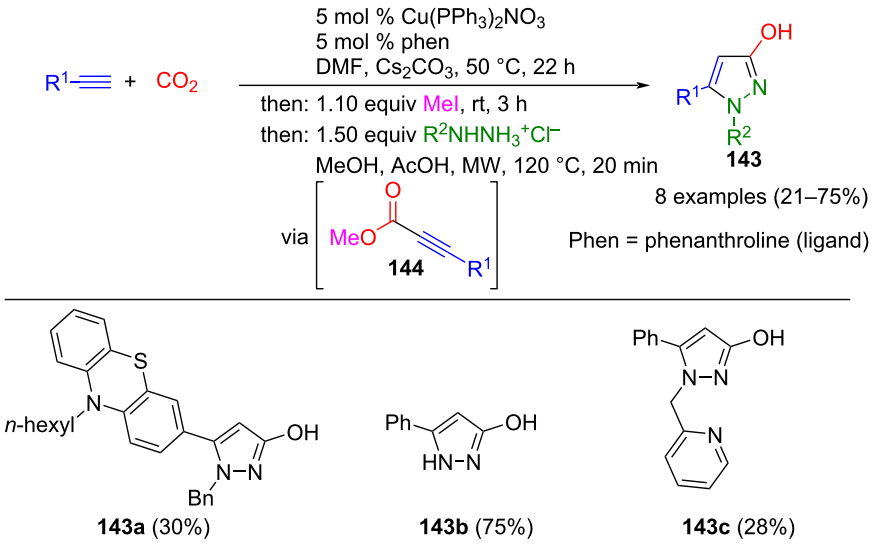

Scheme 49: Consecutive three-component synthesis of pyrazoles **143** initiated by Cu(I)-catalyzed carboxylation of terminal alkynes [152].

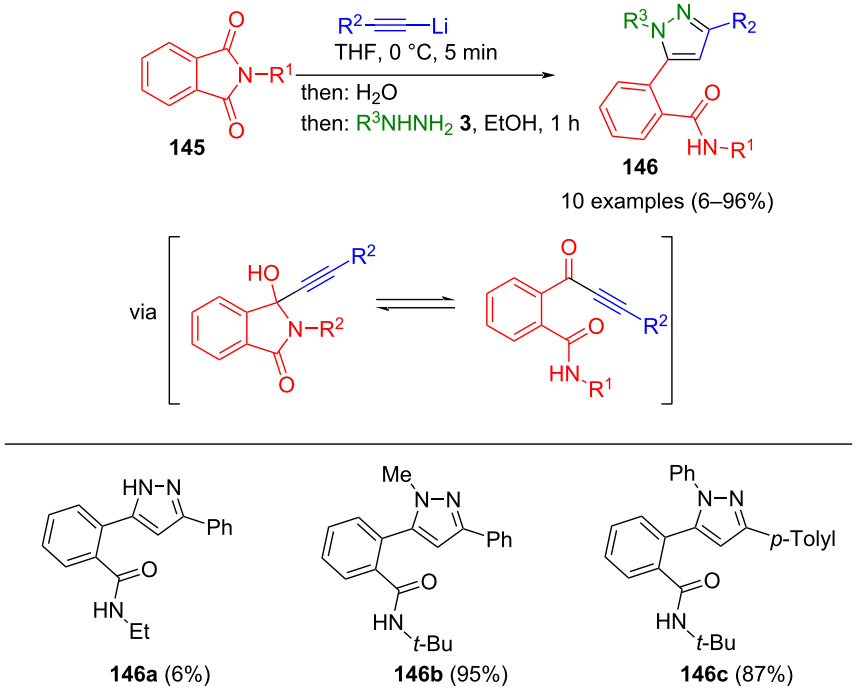

Scheme 50: Consecutive three-component synthesis of benzamide-substituted pyrazoles **146** starting from *N*-phthalimides and lithiated alkynes [153,154].

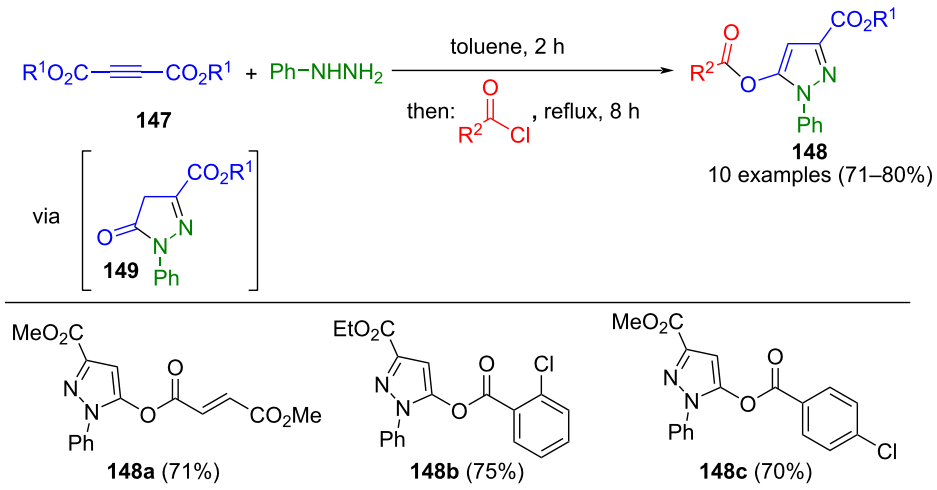

Scheme 51: Consecutive three-component synthesis of 1,3,5-substituted pyrazoles **148** [156].

by the hydrazine carboxamide, which undergoes addition to furnish the intermediary ketenimine **162**. The latter undergoes cyclization with elimination to form the corresponding pyrazoles **160** in a one-pot fashion (Scheme 54) [160]. The reaction can be extended by synthesizing hydrazone carboxamides in situ from hydrazine and isocyanates [161].

An unusual modification of alkynones is the use of aluminum alkynyl hydrazonides **166**, which are formed by nucleophilic displacement of hydrazonyl chlorides **163** with aluminum acetylides **164**. Subsequently, alkynyl hydrazonides **166** undergo metallacyclization to give aluminated pyrazoles **167**. These pyrazoles are then subjected to trapping with electro-

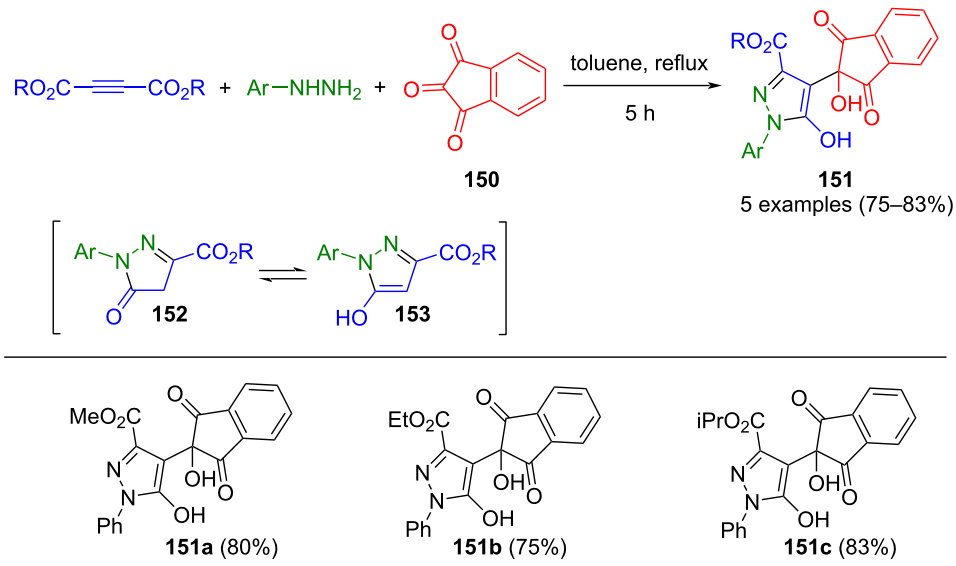

Scheme 52: Three-component synthesis of 4-ninhydrin-substituted pyrazoles **151** [158].

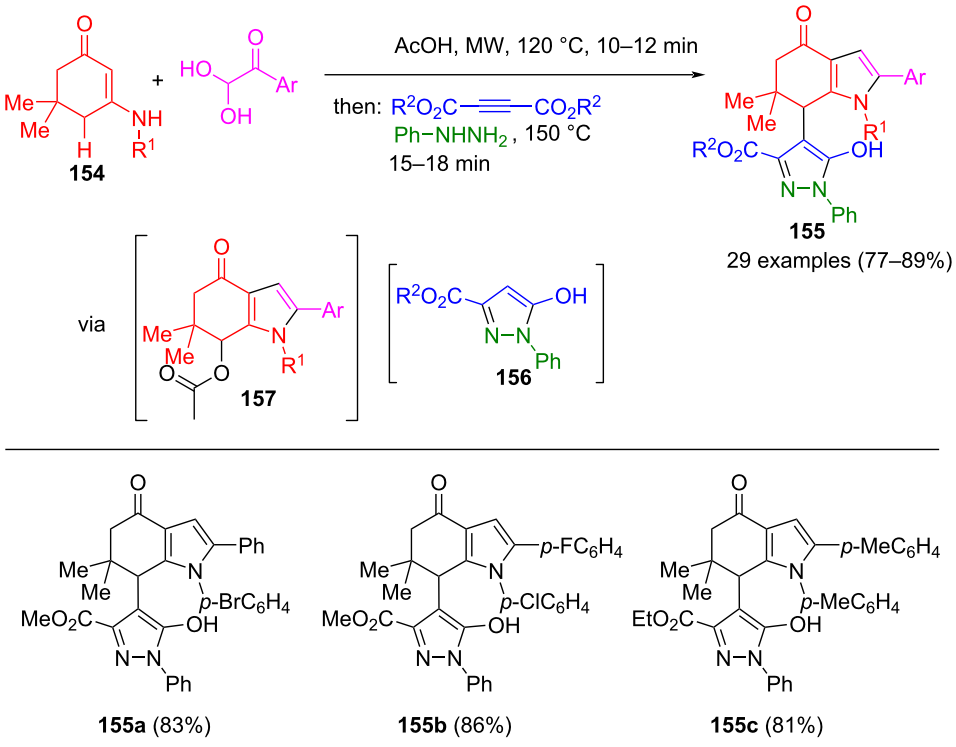

Scheme 53: Consecutive four-component synthesis of 4-(oxoindol)-1-phenylpyrazole-3-carboxylates **155** [159].

philes, such as deuteration or electrophilic chlorination using *N*-chlorosuccinimide, in this consecutive three-component synthesis to give persubstituted pyrazoles **165** (Scheme 55) [162].

(3 + 2)-Cycloaddition – C_2 building blocks as substrates

1,3-Dipolar cycloadditions are important reactions in heterocycle synthesis [163,164] and certainly also for substituted

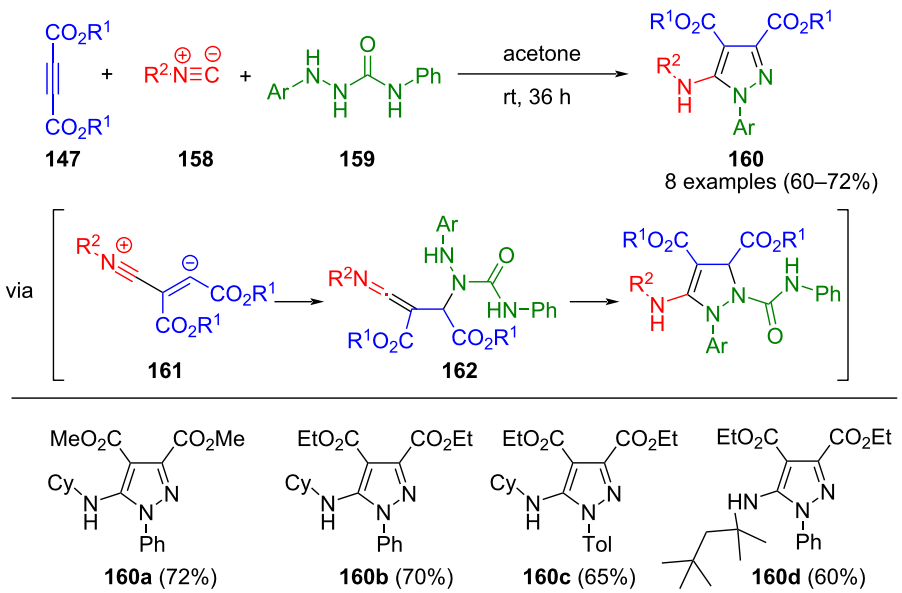

Scheme 54: Three-component synthesis of pyrazoles **160** [160].

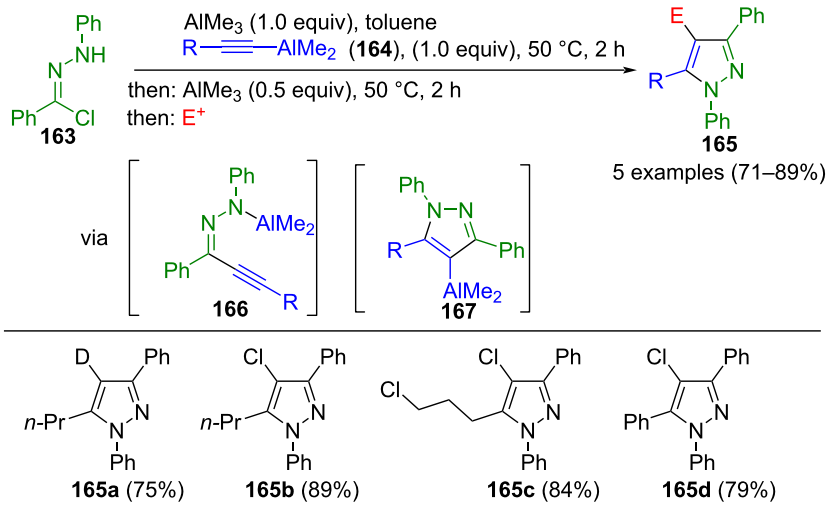

Scheme 55: Consecutive three-component synthesis of pyrazoles **165** [162].

pyrazoles. Four classes of 1,3-dipoles are considered as synthetic equivalents for the CN_2 synthon: diazo compounds [165], nitrilimines [166], sydnones [167], and azomethinimines [168]. These intermediates undergo (3 + 2) cycloadditions with alkenes or alkynes to form pyrazoles, also in the sense of MCR. Furthermore, while not strictly classified as pericyclic reactions, hydrazones are also recognized as CN_2 building blocks in pyrazole synthesis [169].

1,3-Dipoles as key intermediates

Various methods have been developed for the in situ preparation of diazo compounds, as the substances are difficult to handle and toxic [170]. Approaches such as nitrogen transfer with tosylhydrazones, use of the Bestmann–Ohira reagent, or transformation of primary amines or azides, among others, represent viable and practical options.

Diazo compounds can be formed by basic treatment of intermediary tosylhydrazones, known from the Bamford–Stevens reaction [171]. Based on this, Aggarwal et al. developed a consecutive three-component synthesis of 3-substituted and 3,5-disubstituted pyrazoles **168** and **169** (Scheme 56) [172]. Tosylhydrazones are formed in situ from aromatic aldehydes and tosylhydrazine. After basic treatment of these tosylhydrazones fol-

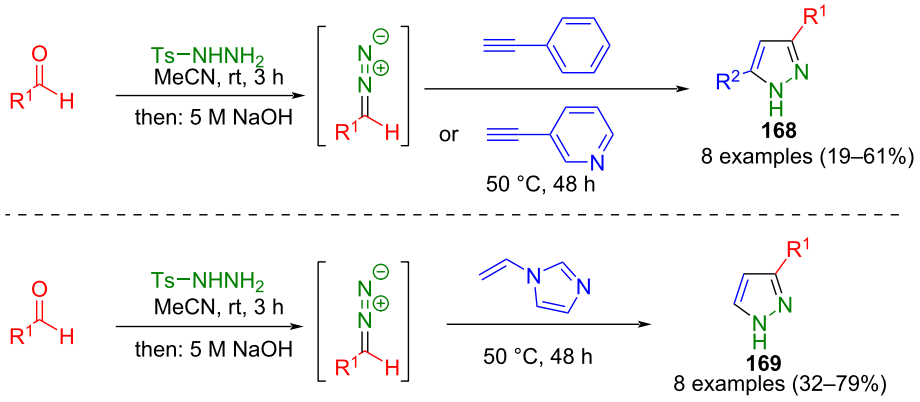

Scheme 56: Consecutive three-component synthesis of 3,5-disubstituted and 3-substituted pyrazoles **168** and **169** from in situ formed diazo compounds [172].

lowed by 1,3-dipolar cycloaddition with terminal alkynes, the corresponding pyrazoles **168** are obtained. The regioselectivity of this synthesis can be explained by steric causes and the favored HOMO (diazo compound)–LUMO (alkyne) interaction during the 1,3-dipolar cycloaddition [163], Wu et al. showed that electronic effects in this strategy do not influence the yield. In addition, sterically demanding reactants could be used in the method. Enhanced yields were achieved by using NaOEt and toluene [173]. *N*-Vinylimidazole, an alkene with a leaving group, was used to synthesize the 3-substituted pyrazoles **169** because, unlike acetylene, it is not gaseous and, therefore, easier to handle.

Instead of vinylimidazole, vinyl azides **170** can also be used as alkyne surrogates. After the 1,3-dipolar cycloaddition, the corresponding pyrazoles are formed by elimination of the azide group and subsequent tautomerization. Thus, the process enables access to 3,5- and 3,4,5-substituted pyrazoles **171** and also allows the synthesis of pyrazole 3-carboxylates (Scheme 57) [174]. An alternative method for the preparation of these pyrazoles involves the cycloaddition of diazo compounds generated in situ with (*Z*)-2-arylidene-2*H*-benzofuran-3-ones. This reaction yields intermediate spiropyrazolines, which react undergo 1,3-prototropic rearrangement to form the corresponding pyrazoles [175].

Aggarwal's method was also applied to synthesize 3,4,5-substituted pyrazoles **173** and **174** via 1,3-dipolar cycloaddition of in situ generated diazo compounds and vinylidenecyclopropane diesters **172**, which are synthetic equivalents of alkynes (Scheme 58) [176]. Notably, employing aromatic vinylidenecyclopropane diesters (R^2 = aryl) in the method regioisomers **174** are selectively formed, while unsubstituted diesters (R^2 = H) lead to pyrazoles **173** and **174** in a 1:2 ratio.

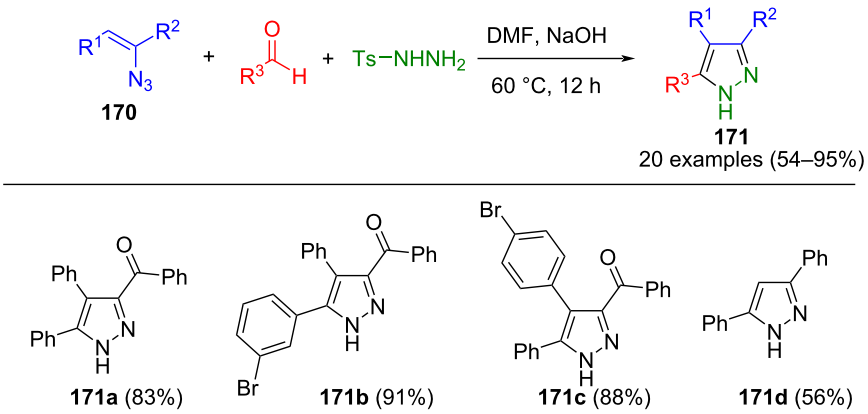

Scheme 57: Three-component synthesis of 3,4,5-substituted pyrazoles **171** via 1,3-dipolar cycloaddition of vinylazides and in situ formed diazo compounds [174].

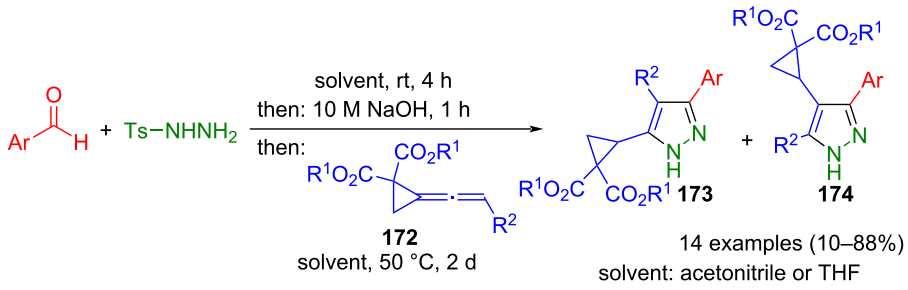

Scheme 58: Three-component synthesis of pyrazoles **173** and **174** from aldehydes, tosylhydrazine, and vinylidene cyclopropane diesters **172** [176].

The aforementioned method can be varied by generating β-diazoketones **176** from arylglyoxals and tosylhydrazine, thus making pyrazole 5-carboxylates accessible. Shu et al. used this for the regioselective one-pot synthesis of pyrazoles **175** by 1,3-dipolar cycloaddition with electron-deficient alkenes (Scheme 59) [177]. The reaction is carried out in air to oxidize an intermediary pyrazoline. It tolerates a large number of substituents without affecting the yields. Notably, the use of vinylamides does not lead to the corresponding products. In addition to electron-poor alkenes, quinones and coumarins can also be used as reactants.

However, aldehydes can also be reacted in a domino reaction with in situ generated β-diazoketones. Initially, they condense with tosylhydrazine to form an enol **178** after basic treatment with a further equivalent of aldehyde. This reacts with β-diazoketones, formed from tosylhydrazine and arylglyoxals, in a 1,3-dipolar cycloaddition to give the corresponding pyrazole **177** (Scheme 60) [178]. In addition to aldehydes, ketones can also be used in the reaction. Moreover, it was observed that neutral and halogenated substituents on the arylglyoxal moiety lead to increased yields. However, a notable limitation of this method is its incompatibility with aliphatic aldehydes, likely due to the instability of the intermediary diazo compounds formed.

Kamal et al. also developed a consecutive three-component reaction for the synthesis of pyrazole 5-carboxylates **179**

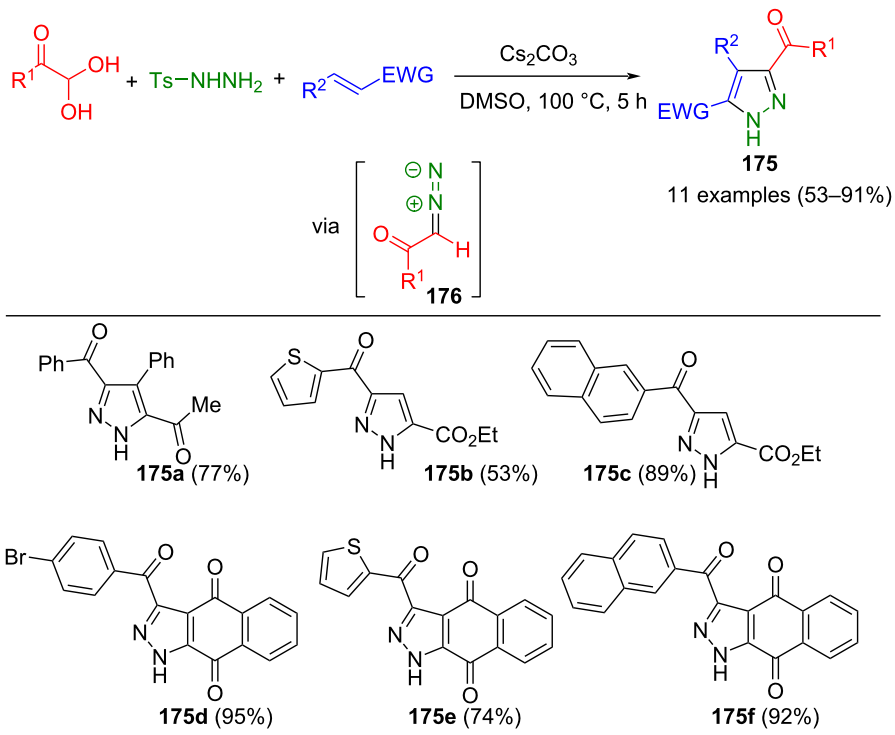

Scheme 59: Three-component synthesis of pyrazoles **175** from glyoxyl hydrates, tosylhydrazine, and electron-deficient alkenes [177].

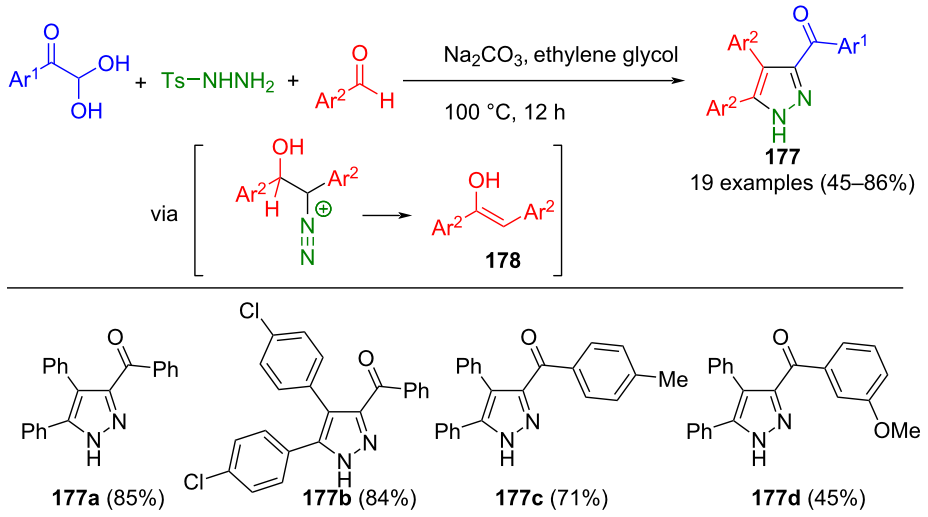

Scheme 60: Pseudo-four-component synthesis of pyrazoles **177** from glyoxyl hydrates, tosylhydrazine, and aldehydes [178].

(Scheme 61) [179]. In contrast to the previously mentioned methods, however, tosylhydrazones were directly employed. In the concept, unsaturated carbonyl compounds are initially formed via Koevenagel condensation between aldehydes and 1,3-carbonyl compounds. These intermediates then undergo reaction under basic conditions with tosylhydrazones to yield 3-diacylpyrazolines **180**. Subsequent elimination of the acyl group facilitated by water and potassium carbonate furnishes

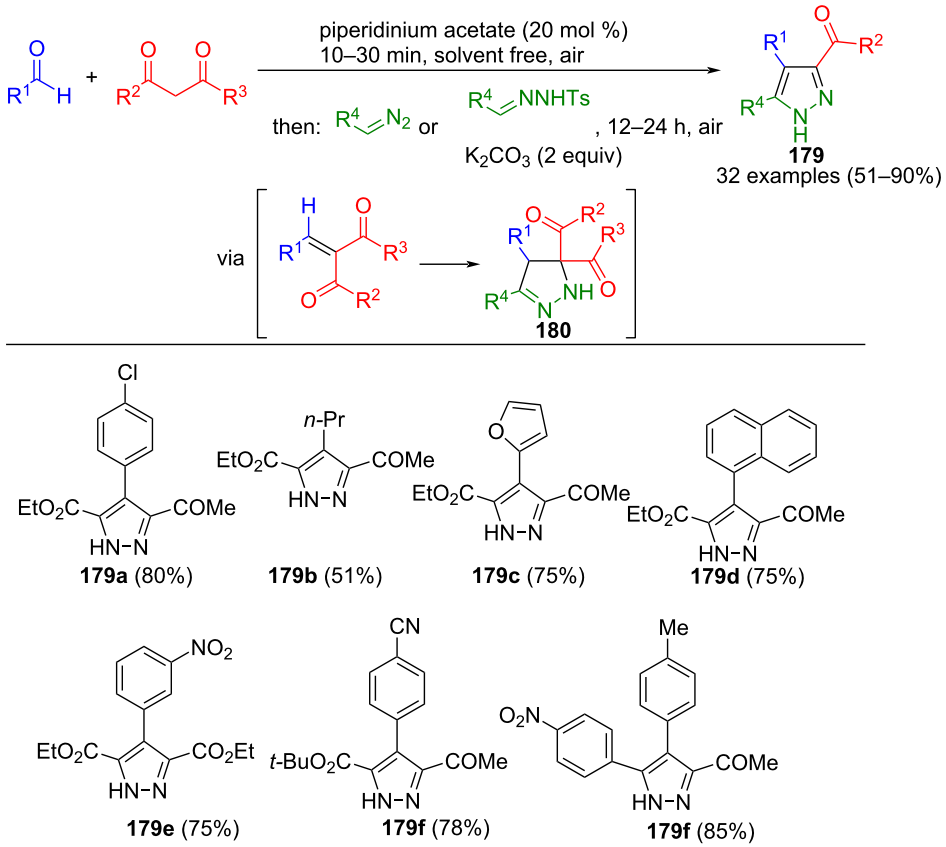

Scheme 61: Consecutive three-component synthesis of pyrazoles **179** via Knoevenagel-cycloaddition sequence [179].

the corresponding pyrazoles after aerobic aromatization. In the method, aromatic aldehydes with electron-withdrawing substituents demonstrate enhanced yields. In addition, both ketones and β-ketoesters are tolerated in the sequence. Aromatic hydrazones and β-carboxyhydrazones can be used as CN_2 building blocks. It was also shown that the process can be carried out on a gram scale and that diazoalkanes can also be used as starting materials in addition to tosylhydrazones.

Another potent source of diazoalkane is the Bestmann–Ohira reagent (**181**). Upon basic treatment, the Seyferth–Gilbert reagent is generated through acyl cleavage, which has been converted to pyrazoles via various reactions. In a domino three-component reaction, unsaturated nitriles **183** are initially produced from aldehydes and nitriles in a Knoevenagel reaction. These undergo a formal 1,3-dipolar cycloaddition with the intermediary Seyferth–Gilbert reagent (**184**), followed by the elimination of hydrogen cyanide to give 5-phosphonylpyrazoles **182** (Scheme 62) [180]. The reaction sequence tolerates a diverse range of substituents, and electronic effects have no influence on the yields. Only very weakly activated nitriles do not lead to the desired product. Remarkably, no homologation of the aldehyde to the alkyne takes place during the reaction due to the faster formation of the unsaturated nitriles, which supersedes possible side reaction. The present method can be extended to include a CuAAC reaction using alkyne-functionalized aldehydes, thus enabling the synthesis of interesting molecules pertinent to pharmaceutical and agrochemical applications.

The same research group also showed another way to prepare 5-phosphonylpyrazoles **185** (Scheme 63) [181]. Through a Claisen–Schmidt/1,3-dipolar cycloaddition/oxidation sequence, the aforementioned pyrazoles were obtained from methyl ketones, aldehydes, and the Bestmann–Ohira reagent (**181**). Both the use of aromatic aldehydes with electron-withdrawing substituents and electron-poor methyl ketones increase the yields. Steric effects play a crucial role in this method, as *ortho*-substituents lead to steric hindrance of the α,β-unsaturated ketone, thus impeding pyrazole formation. Nonetheless, a notable advantage of this process is that it can be combined with the CuAAC reaction.

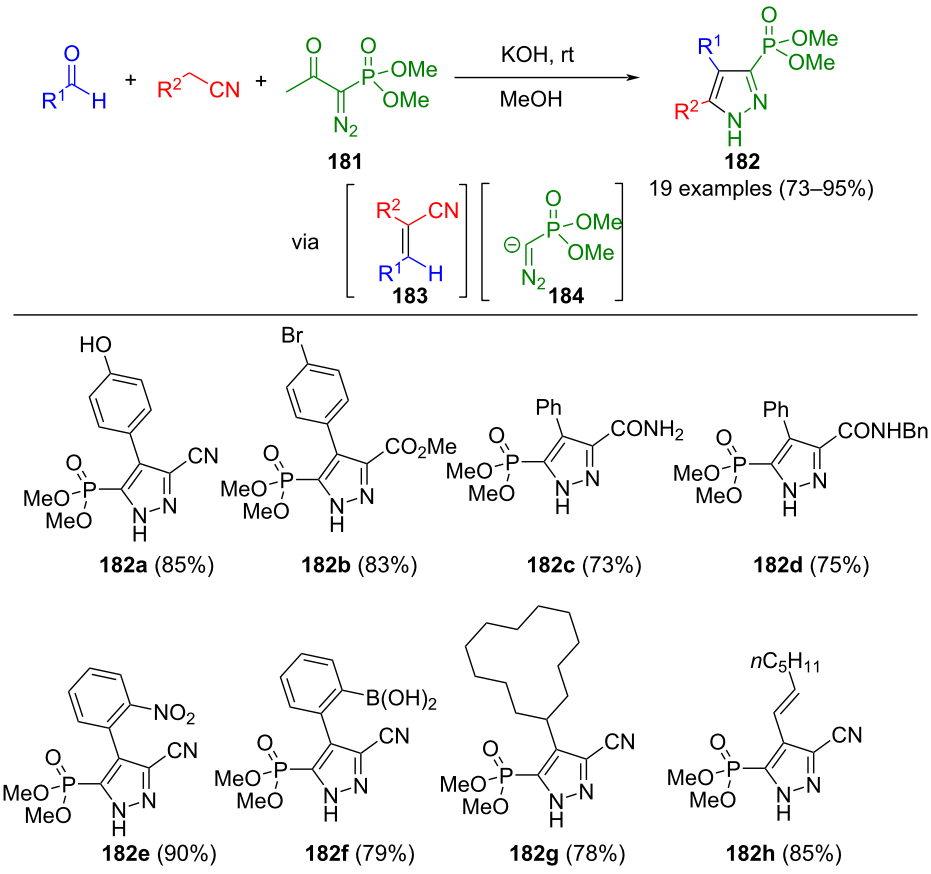

Scheme 62: Three-component synthesis of 5-dimethylphosphonate substituted pyrazoles **182** from aldehydes, the Bestmann–Ohira reagent (**181**), and nitriles [180].

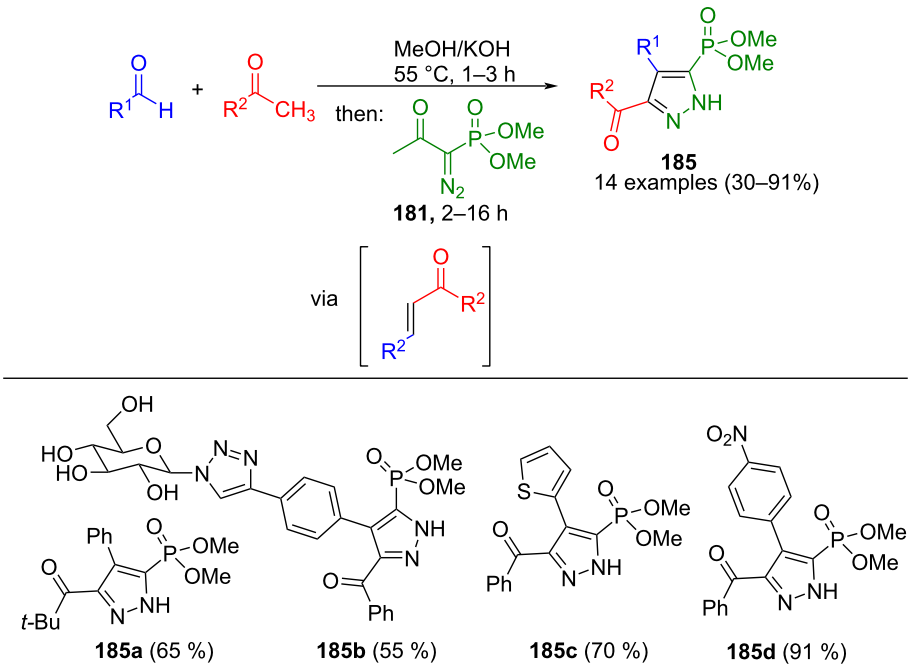

Scheme 63: Consecutive three-component synthesis of 5-(dimethyl phosphonate)-substituted pyrazoles **185** from aldehydes, methyl ketones, and the Bestmann–Ohira reagent (**181**) via Claisen–Schmidt/1,3-dipolar cycloaddition/oxidation sequence [181].

Another pyrazole synthesis using the Bestmann–Ohira reagent (**181**) was reported by Ahamad and co-workers. Enones can be synthesized in situ from β-ketophosphonates **186** and aldehydes by Horner–Emmons–Wadsworth olefination. These enones undergo cyclization with the Seyferth–Gilbert reagent, forming the corresponding pyrazole **187** upon oxidation. Notably, if the method is carried out as a domino reaction, the yields are higher than with a stepwise addition of the reactants (Scheme 64) [182]. In addition to the Bestmann–Ohira reagent, diazosulfones can also be used in the process. Here, 3,4-disubstituted pyrazoles are formed in a Horner–Emmons–Wadsworth/1,3 dipolar cycloaddition/desulfonation process [183].

The Bestmann–Ohira reagent (**181**) itself can also be used as a Horner–Emmons–Wadsworth reagent for the homologation of aldehydes to generate alkynes **188** in situ. Kumar et al. took advantage of this and also used the Bestmann–Ohira reagent as a cycloaddition partner. Pyrazoles **189** were obtained under basic conditions in a consecutive three-component reaction (Scheme 65) [184]. In the method, copper iodide must be added to activate the alkynes and the Seyferth–Gilbert reagent, as the intermediates are not sufficiently reactive. Moreover, by varying the starting materials, additionally, 5-sulfonylpyrazoles can be produced using this method.

In reactions involving α,β-unsaturated aldehydes, the Bestmann–Ohira reagent (**181**) can also take on a dual role. The Seyferth–Gilbert reagent generated from this engages in a cycloaddition with the vinyl unit, yielding a pyrazolinecarboxaldehyde **191**. Subsequent treatment with another equivalent of **181** homologates the intermediate's aldehyde moiety, giving the corresponding pyrazole **190** after 1,3-hydrogen shift and subse-

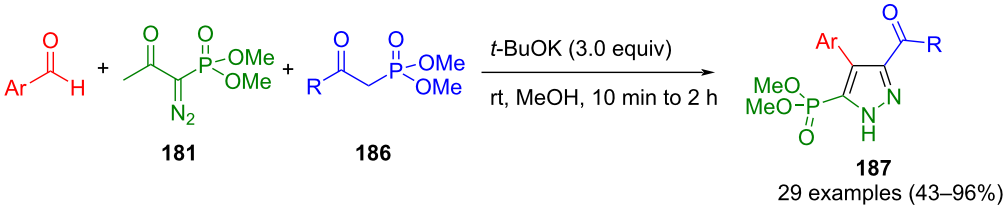

Scheme 64: Three-component synthesis of 5-(dimethyl phosphonate)-substituted pyrazoles **187** from aldehydes, the Bestmann–Ohira reagent (**181**), and β-keto phosphonates **186** [182].

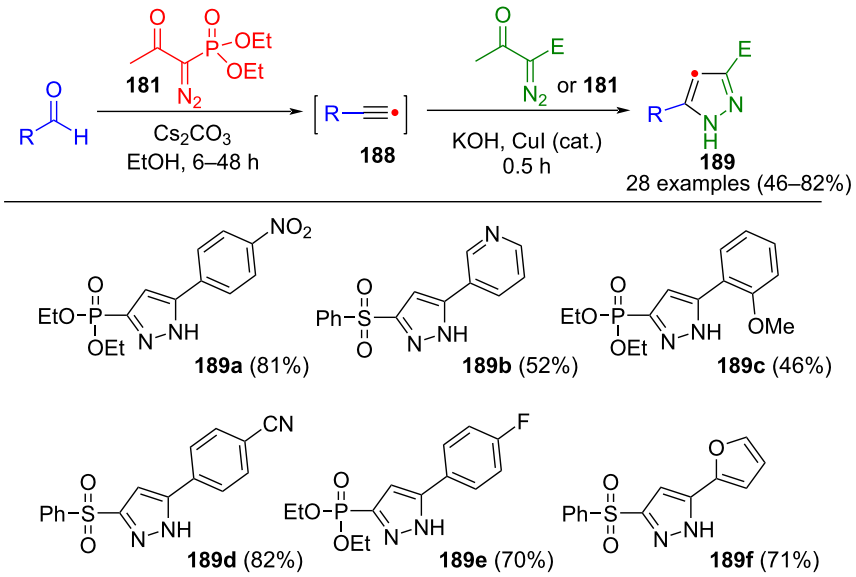

Scheme 65: Three-component synthesis of 5-diethylphosphonate/5-phenylsulfonyl substituted pyrazoles **189** from aldehydes, Bestmann–Ohira reagent (**181**), and α-diazo-β-keto esters [184].

quent aromatization (Scheme 66) [185]. The reaction proceeds independently of the substituents of the aldehyde and tolerates electron-withdrawing and electron-donating substituents.

Slobodyanyuk et al. developed a one-pot method for the synthesis of 3-trifluoromethylpyrazoles **193**, in which a diazo compound was synthesized in situ from sodium nitrite and $CF_3CH_2NH_2$·HCl **192** (Scheme 67) [186]. The reaction with alkynes with at least one electron-withdrawing substituent leads to the corresponding pyrazoles. Notably, the reaction is regioselective, and only 3,5-substituted pyrazoles are formed. However, internal alkynes can also partake in the reaction, provided that at least one electron-withdrawing group is present. If the second substituent is also electron-withdrawing, the reaction proceeds in excellent yields. The reaction time has to be extended for electron-rich substituents, whereas strongly electron-

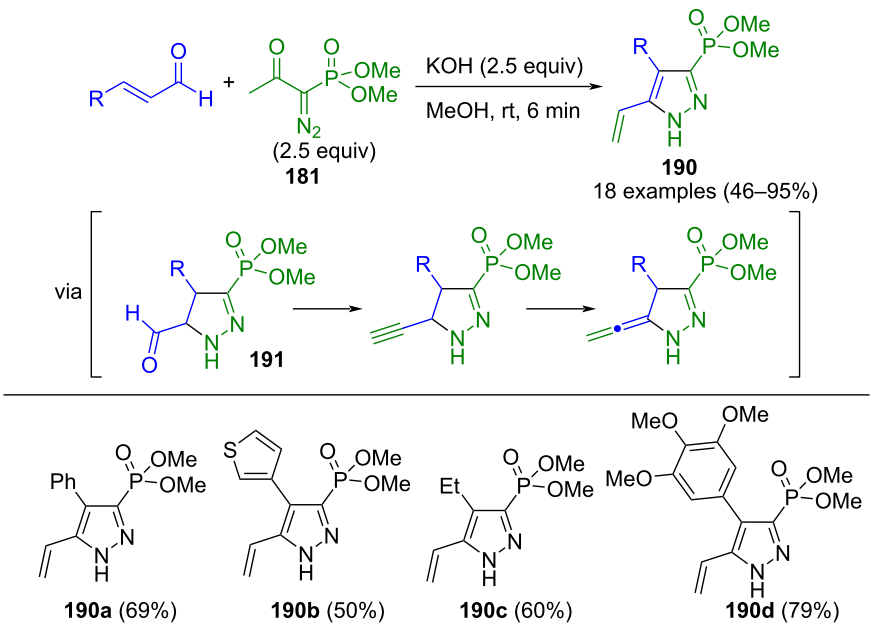

Scheme 66: Pseudo-three-component synthesis of 3-(dimethyl phosphonate)-substituted pyrazoles **190** [185].

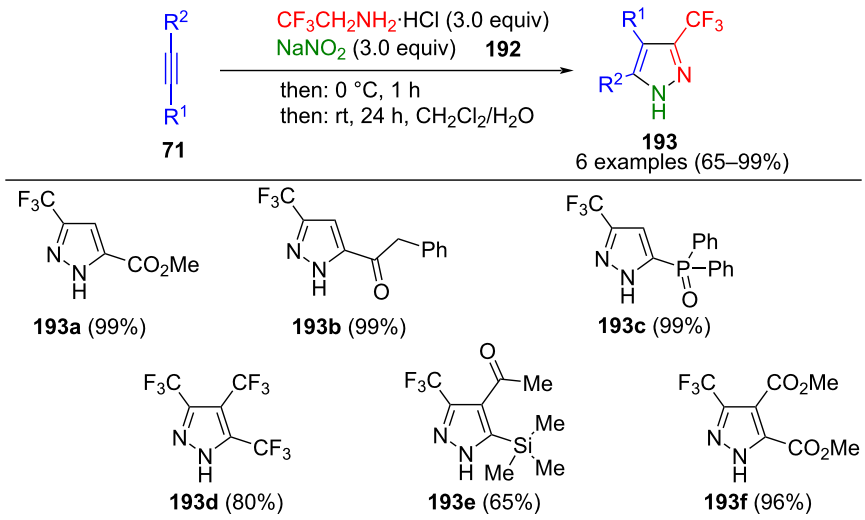

Scheme 67: Three-component synthesis of 3-trifluoromethylpyrazoles **193** [186].

releasing substituents fail to yield the desired product. Surprisingly, an inverse regioselectivity was observed for reaction of the diazoalkane with a TMS-substituted internal alkyne, presumably due to steric hindrance. Since the reactants only react in a specific order, they can all be present initially. In addition, the reaction can be scaled up to 100 g. The reaction of terminal alkynes can be catalyzed with Ag_2O [187]. In addition to alkynes, alkynones are also tolerated in this cycloaddition [188]. The process can also be carried out in a continuous flow reactor and can be extended by *N*-methylation, Chan–Lam–Evans coupling, or amidation of the corresponding substituents [189,190].

Hanamoto et al. succeeded in synthesizing 5-tributylstannyl-4-fluoropyrazole (**197**) using one-pot methodology. This compound was formed from diazomethane (**196**) and an in situ generated alkyne **198**. After treatment with butyllithium and reaction with chlorotributylstannane (**195**), 1,1-difluoroethene (**194**) was used as an intermediate to generate **198**. This alkyne immediately formed the corresponding pyrazole **197** in a 1,3-dipolar cycloaddition with diazomethane (Scheme 68) [191,192]. Notably, the synthesis of pyrazoles **197** is regioselective due to the HOMO–LUMO interaction of the 1,3-dipolar cycloaddition [163]. Additionally, the reaction can be alternatively conducted using chlorotrimethylsilane instead of chlorotributylstannane [193]. A variation with bis(tributyltin) oxide and 3,3,3-trifluoro-2-bromopropene is also possible [194].

3,5-Diacyl-4-arylpyrazoles **199** can be prepared from aromatic 1,3-dicarbonyl compounds in a pseudo-multicomponent reaction (Scheme 69) [195]. From 1,3-dicarbonyl compounds, α-aryldiazomethanes **200** were generated in situ by Regitz diazo transfer and concomitant acyl cleavage with methylamine. Sodium carbonate facilitates the enolate formation of the 1,3-dicarbonyl compound. One limitation of the method is that *ortho*-substituents lead to reduced yields and that strongly electron-withdrawing substituents are not tolerated.

Other important dipoles are nitrilimines **205**, which can be synthesized in situ by the basic treatment of hydrazonyl chlorides **202**. This concept was used by Gomha et al. in a domino reaction, wherein 4-acylpyrazoles **201** and DMF-dimethylacetal (**203**) initially form the corresponding enaminones, which subsequently engage in a cycloaddition with nitrilimines, giving bispyrazoles **204** (Scheme 70) [196]. The yields were increased

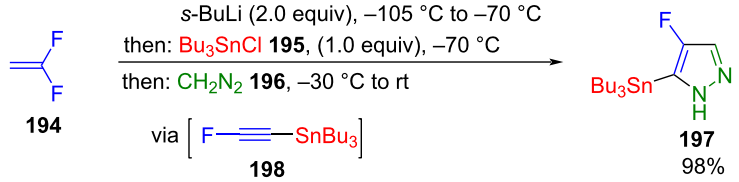

Scheme 68: Consecutive three-component synthesis of 5-stannyl-substituted 4-fluoropyrazole **197** [191,192].

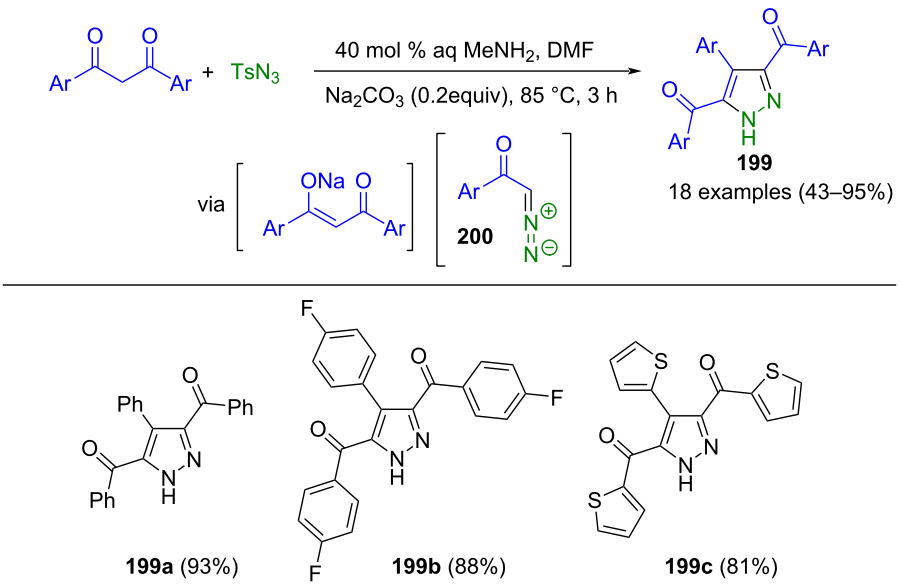

Scheme 69: Pseudo-three-component synthesis of 3,5-diacyl-4-arylpyrazoles **199** [195].

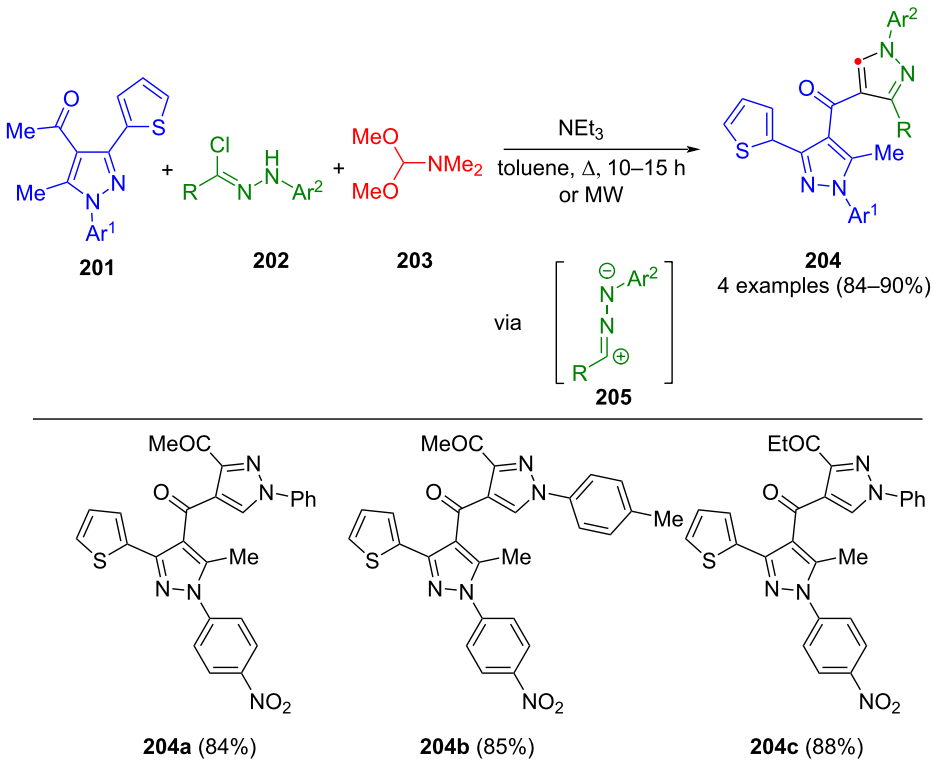

Scheme 70: Three-component synthesis of pyrazoles **204** via nitrilimines [196].

by dielectric heating. Interestingly, one of the products presented (**204a**) shows inhibitory activity against hepatocellular carcinoma (HepG-2).

Alizadeh et al. also used nitrilimines in a three-component reaction to synthesize 1,3-substituted 5-cyanopyrazoles **206** (Scheme 71) [197]. First, the reaction between 4-oxo-4*H*-

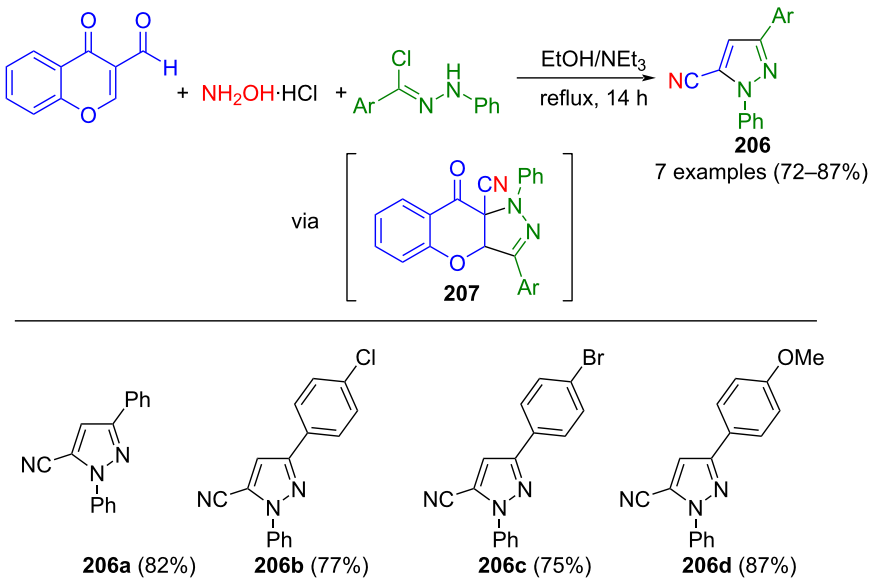

Scheme 71: Three-component synthesis of 1,3,5-substituted pyrazoles **206** via formation of nitrilimines and salicylate elimination [197].

chromene-3-carbaldehyde and hydroxylamine yielded 4-oxo-4*H*-chromene-3-cyanide. Subsequently, in a 1,3-dipolar cycloaddition with in situ-generated nitrilimines, intermediate **207** was formed. A nucleophilic attack by ethanol and concomitant elimination of ethyl salicylicate lead to pyrazoles **206**. In the method, both electron-rich and electron-poor arylhydrazonyl chlorides lead to excellent yields.

In an alternative approach, the same research team used acetylenedicarboxylates **147** as two-carbon building blocks for pyrazole synthesis. Initially, a domino reaction was employed to form 1,4-benzothiazine-3(4*H*)-one **210** through the cyclocondensation of 2-aminothiophenol (**208**). Subsequently, in situ-generated nitrilimine from the hydrazonyl chloride undergoes a 1,3-dipolar cycloaddition, resulting in the formation of thiophenol **211** after ring opening. This thiophenol **211** then reacts with another equivalent of hydrazonyl chloride to furnish pyrazole **209** (Scheme 72) [198]. The products could be additionally corroborated by X-ray structure analysis.

Sydnones **214** are mesomerically stabilized compounds that represent synthetic equivalents to diazomethinimes. In a copper-catalyzed sydnone-alkyne cycloaddition (CuSAC), they can be converted to pyrazoles with high efficiency and chemoselectivity [199]. Specklin et al. used this strategy for the consecutive three-component synthesis of 1,4-substituted pyrazoles **213** (Scheme 73) [200]. Sydnones are generated in situ by nitrosylation of arylglycines **212** with *t*-BuONO, followed by cyclization with trifluoroacetic anhydride. After adding terminal alkynes, the corresponding pyrazoles are formed via CuSAC reaction with subsequent decarboxylation. Notably, the process tolerates both electron-poor and electron-rich aryls, as well as numerous functional groups. It is noteworthy that the solvent THF leads to reduced yields, while *t*-BuOH/water proves to work well.

Other useful 1,3-dipoles utilized in cycloaddition reactions are diazomethinimines **217**. In some reactions, they are formed from hydrazones, which are generated from the condensation of aldehydes and hydrazines. In a sequential three-component reaction, diazomethinimines undergo 1,3-dipolar cycloaddition with nitroolefins **215**, forming pyrazolines. Under aerobic conditions, these pyrazolines undergo gradual oxidation and are subsequently transformed into the corresponding pyrazoles **216** through rapid nitrite elimination (Scheme 74) [201].

During the reaction, the pyrazoline intermediate exists in equilibrium with its Michael adduct, which is incapable of cyclization. Using polar solvents, the equilibrium can be shifted towards the formation of pyrazoline due to the stabilization of the dipolar diazomethinimines. However, a limitation of this method arises with strongly electron-withdrawing aldehydes, as they lead only to Michael adducts. The present concept can also be used to synthesize 3-(pyrazol-5-yl)chromones if 3-nitrovinylchromones are chosen as a starting material [202].

Furthermore, this method was also applied to 1,1-bis(methylsulfanyl)-2-nitroethene (**218**) for the consecutive three-component synthesis of 3-methylthiopyrazoles **219** in boiling ethanol (Scheme 75) [203]. In a similar method, nitrilimines can also be

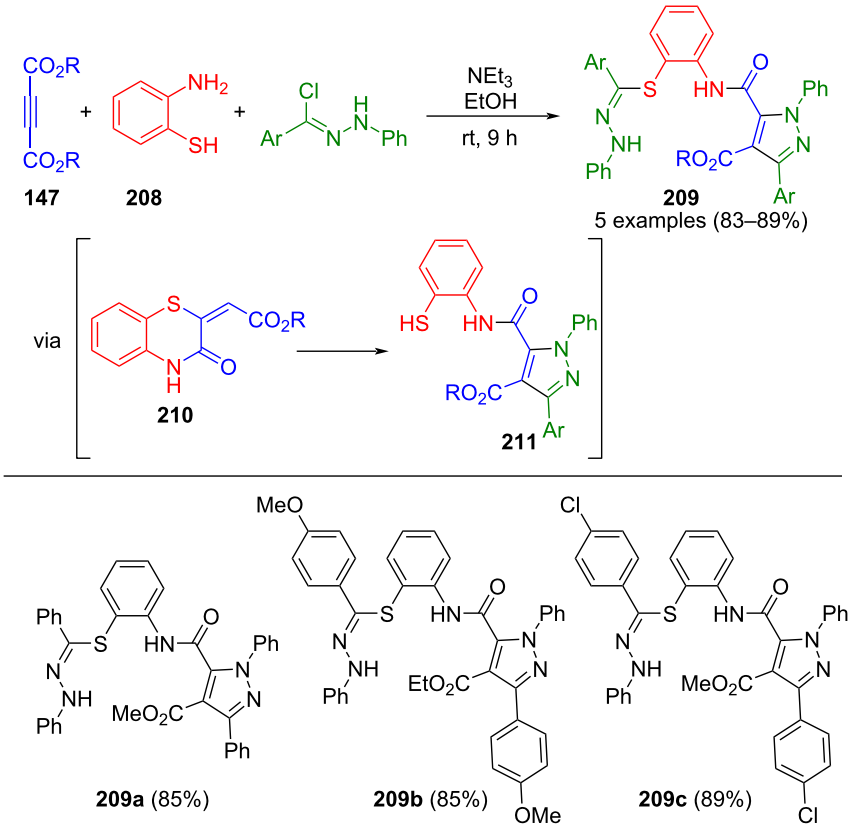

Scheme 72: Pseudo four-component synthesis of pyrazoles **209** from acetylene dicarboxylates **147**, hydrazonyl chloride, and 2-aminothiophenol (**208**) [198].

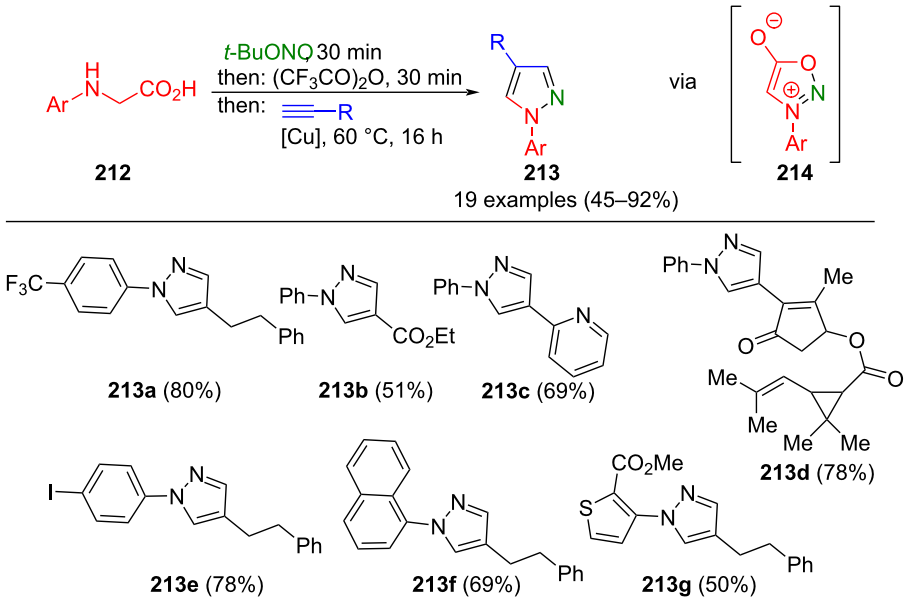

Scheme 73: Consecutive three-component synthesis of pyrazoles **213** via syndnones **214** [200].

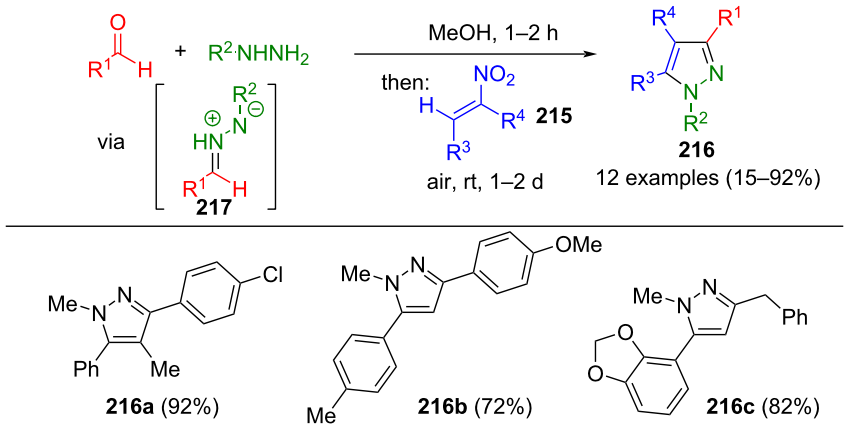

Scheme 74: Consecutive three-component synthesis of pyrazoles **216** via in situ-formed diazomethinimines **217** [201].

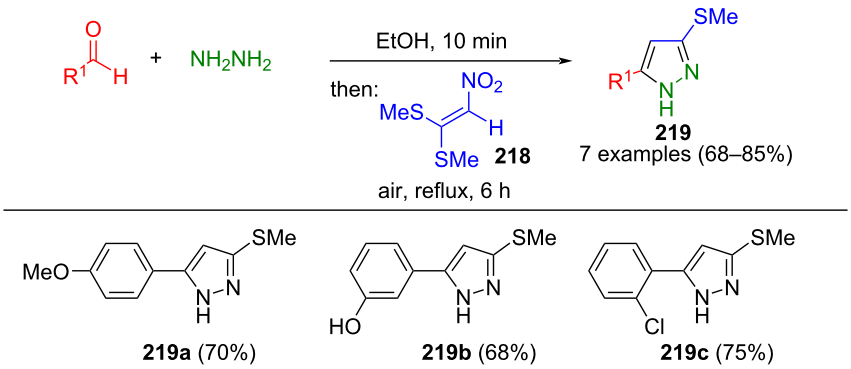

Scheme 75: Consecutive three-component synthesis of 3-methylthiopyrazoles **219** from aldehydes, hydrazine, and 1,1-bis(methylsulfanyl)-2-nitroethene (**218**) [203].

synthesized from aldehydes and hydrazines after treatment with $Hg(OAc)_2$ to react in a 1,3-dipolar cycloaddition with alkynes, affording the corresponding pyrazoles [204].

Hydrazones as key intermediates

The cyclization of hydrazones is similar to the 1,3-dipolar cycloaddition. Here, too, CN_2 building blocks are formed first, which are then converted to pyrazoles. However, hydrazones preferably react with β-ketoesters or ketones. Alternatively, they can undergo cyclization with alkynes. However, no dipolar intermediates are involved in these reactions.

For example, 1,3,5-substituted pyrazoles **220** can be synthesized via a domino Mannich/cyclization/oxidation reaction of terminal alkynes and hydrazones **221**, which are in situ generated from aromatic hydrazines and aldehydes (Scheme 76) [205]. This method tolerates a broad spectrum of functional groups, and using of electron-rich alkynes and aldehydes increases the yields. Multifunctional catalysts such as PTSA [205] and molecular iodine are viable options for catalyzing this sequence [206]. In addition, the process can be carried out with tosylhydrazine under copper catalysis [207].

Internal alkynes must be used to access fully substituted pyrazoles from hydrazones. Dimethyl acetylenedicarboxylate (DMAD) is a useful building block for this purpose. In the ionic liquid $[n\text{-}Bu_4P][CuBr_3]$, DMAD reacts strictly chemoselectively with hydrazones **223** formed in situ to give intermediary pyrazolines via radical cyclization. These are subsequently oxidized under an aerobic atmosphere to furnish 1,3,4,5-substituted pyrazoles **222** (Scheme 77) [208]. Since oxidation does not occur when very electron-rich aldehydes are used, these cannot be employed in this sequence. Besides simple aromatic aldehydes, 3-formylchromones are also tolerated in the reaction. The latter react with hydrazine in a one-pot process and form the corresponding pyrazoles with DMAD under $Yb(OTf)_3$ catalysis [209].

The research team led by Hao introduced a straightforward and novel approach for synthesizing pyrazoles **224** utilizing benzene

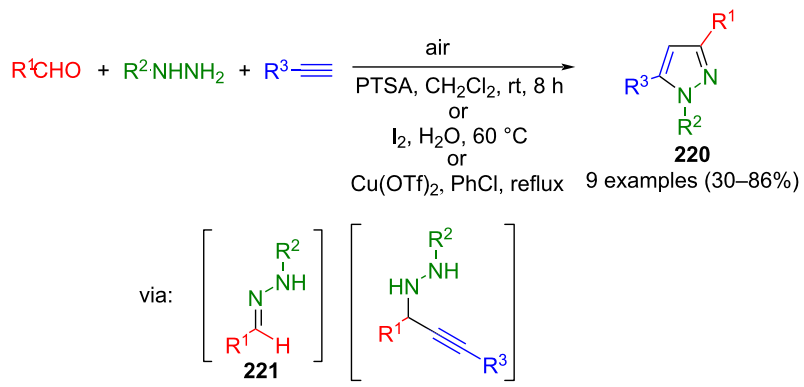

Scheme 76: Three-component synthesis of 1,3,5-substituted pyrazoles **220** from aldehydes, hydrazines, and terminal alkynes [205-207].

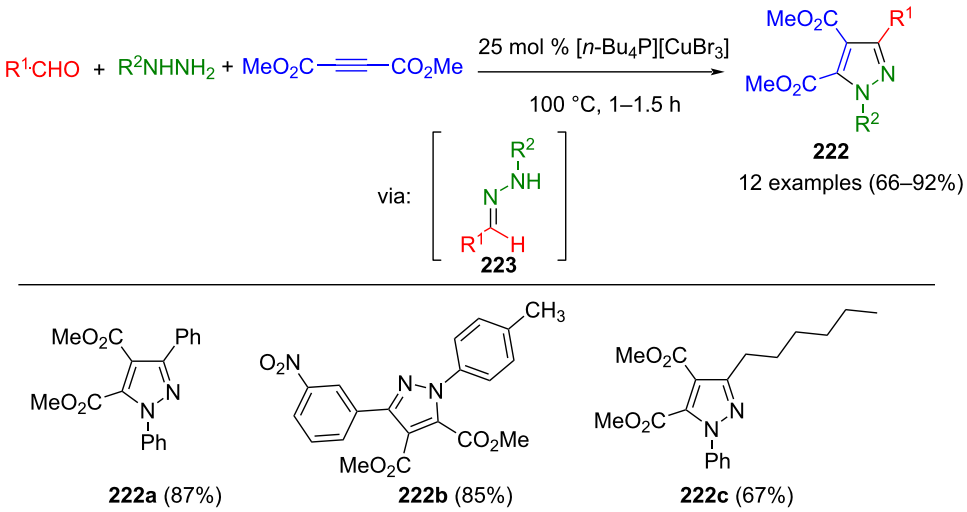

Scheme 77: Three-component synthesis of 1,3,4,5-substituted pyrazoles **222** from aldehydes, hydrazines, and DMAD [208].

sulfonylhydrazone and benzyl acrylate. This (3 + 2)-cycloaddition reaction simultaneously constructed two new C–N bonds and one C–C bond under transition-metal-free conditions (Scheme 78) [210]. The introduction of diverse electron-donating or -withdrawing groups at the *ortho*-, *para*- and *meta*-positions of benzene sulfonyl hydrazone demonstrates excellent compatibility within this transformation.

Miscellaneous processes

In addition to the methods discussed above, there have also been proposed several miscellaneous methods that do not fit into the framework of (3 + 2)-cyclocondensations or cycloadditions. In pyrazole synthesis, C–N bonds can also be formed by titanium catalysis. Majumder et al. developed a protocol for the consecutive four-component synthesis of 4,5-substituted pyra-

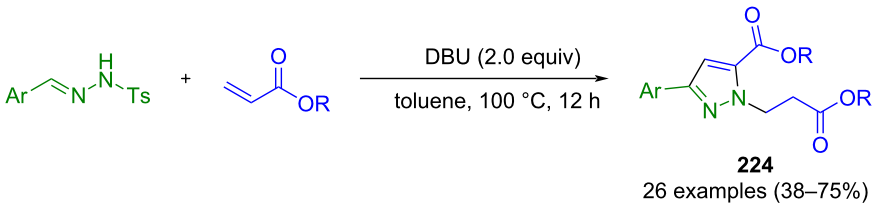

Scheme 78: Pseudo three-component synthesis of pyrazoles **224** from sulfonyl hydrazone and benzyl acrylate under transition-metal-free conditions [210].

zoles, as only a few methods are known for this. Initially, 3-aminoimines **226** are synthesized from alkynes, primary amines, and *tert*-butyl isocyanide using titanium catalysis. Subsequently, these intermediates are cyclized in a consecutive multicomponent reaction with hydrazines to give 4,5-substituted pyrazoles **225** (Scheme 79) [211]. Notably, both terminal and internal alkynes are tolerated in the reaction, with the more active catalyst Ti(dpm)$(NMe_2)_2$ typically used for the latter. One limitation, however, is that a mixture of regioisomers is obtained when utilizing these alkynes, even if one is preferentially formed.

Using hydrazines instead of amines in the above reaction enables the synthesis of pyrazoles via a domino reaction. This involves a (2 + 2)-cycloaddition with terminal alkynes, followed by the α-insertion of isonitriles, and protonolysis of another equivalent of hydrazine with the metal, leading to six-membered intermediates **228**. Subsequent intramolecular cyclization leads to the formation of a pyrazoline, which, upon elimination of cyclohexylamine, forms the corresponding pyrazole **227** (Scheme 80) [212]. The (2 + 2)-cycloaddition exhibits regioselectivity due to steric effects. However, unlike the previously mentioned method, this approach yields 3-substituted pyrazoles.

The copper-catalyzed Glaser coupling of alkynes enables concise access to symmetrical diynes **230** [213]. Concatenation via cyclization with hydrazines enables the pseudo-three-component synthesis of pyrazoles **229**, employing photoredox catalysis with blue LED lamps and ruthenium complexes as a catalyst system (Scheme 81) [214].

Interestingly, UV light is indispensable for both reaction steps of the sequence, while the ruthenium catalyst additionally accelerates the Glaser coupling. The reaction tolerates a broad spectrum of functional groups, and electron-withdrawing aryl substituents lead to increased yields. In addition, both methylhydrazine and phenylhydrazine can be used, while sterically demanding aliphatic hydrazines fail to yield the desired product.

In addition to C–C and C–N bond formation, transition metal catalysis can also form N–N bonds. In their investigations into the intramolecular cyclization of enaminoates, Neumann et al. uncovered an interesting phenomenon. When the reaction was carried out in acetonitrile, enaminoates coupled with the nitrile solvent in an intramolecular oxidation, leading to pyrazoles [215]. Remarkably, this N–N bond formation is copper-mediated, where copper acts both as a Lewis acid activator of the nitrile and an oxidizing agent. Under similar conditions, primary amines, nitriles, and 2,3-allenoates **231** engage in a three-component reaction via enamino-imine complexes **233** to afford pyrazoles **232** (Scheme 82) [216]. The nitrile is present in excess as a solvent in this domino reaction. Furthermore, in addition to allenoates, 2-alkynoates can also be used as starting substrates.

Tang et al. developed a catalytic variant for forming N–N bonds, as stoichiometric quantities of copper were used in the previously mentioned method. Imines **235** are generated from oxime acetates through copper(I)-mediated N–O bond scission, followed by nucleophilic addition of paraformaldehyde. Subsequent coupling with aniline and reductive elimination produces pyrazolines, which aromatize under aerobic conditions, to give

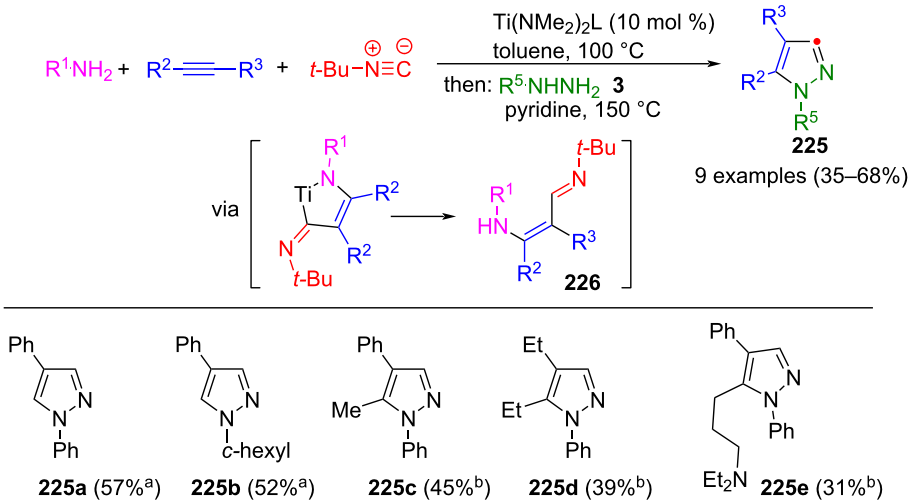

Scheme 79: Titanium-catalyzed consecutive four-component synthesis of pyrazoles **225** via enamino imines **226** [211]. [a]10 mol% Ti$(NMe_2)_2$(dpma); [b]20 mol % Ti(dpm)$(NMe_2)_2$.

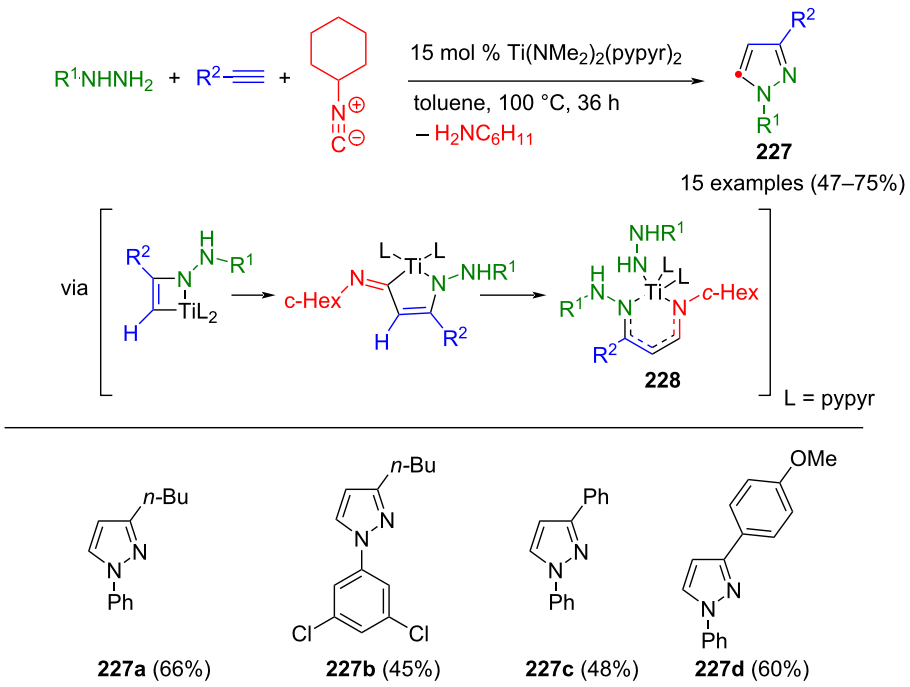

Scheme 80: Titanium-catalyzed three-component synthesis of pyrazoles **227** via enhydrazino imine complex intermediates [212].

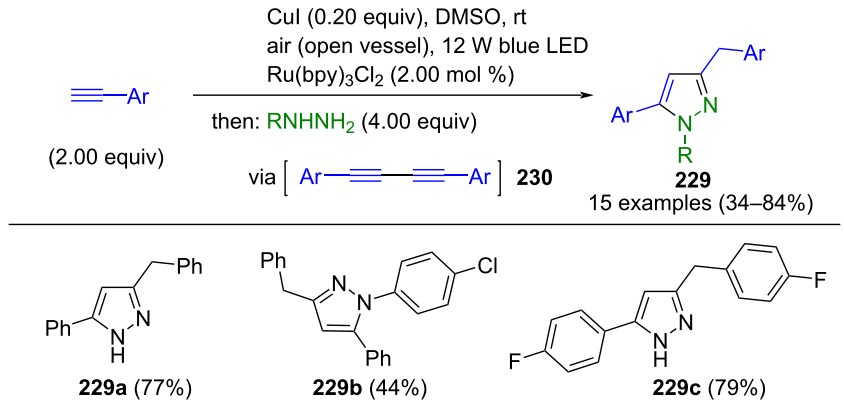

Scheme 81: Pseudo-three-component synthesis of pyrazoles **229** via Glaser coupling of terminal alkynes and photocatalytic cyclization with hydrazines [214].

pyrazoles **234** in a three-component reaction (Scheme 83) [217]. The introduction of caesium carbonate serves to enhance the reaction's conversion, although elevated base concentration leads to the deactivation of the oxime acetates. The method demonstrates tolerance towards both aliphatic and aromatic oxime acetates, with electron-rich substituents giving higher yields. A complementary observation is that anilines bearing electron-withdrawing substituents increase overall yields, whereas aliphatic amines are not tolerated in this method. A further limitation of the method is that the aldehyde reaction partner is restricted to paraformaldehyde.

Pyrazoles can be prepared via a radical-mediated one-pot process. For example, 2,2,2-trifluoroethyl groups can be introduced to the pyrazole core. In a notable three-component synthesis (Scheme 84), enones **236** undergo a reaction with hydrogen peroxide, silver nitrate, CF_3SO_2Na (**237**), and aryldiazonium salts **238**, yielding pyrazole **239** [218]. After the addition of the trifluoromethyl radical and the diazonium salt, hydrazones **240** are formed, which subsequently undergo intramolecular cyclocondensation, giving the corresponding pyrazole **239**. Remarkably, the process tolerates various substituents on both the aryl and the arylallyl ketone. Furthermore, its regioselectivi-

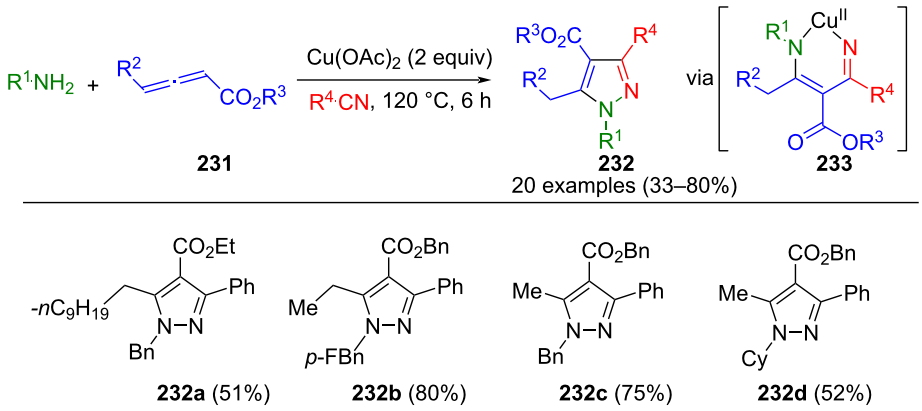

Scheme 82: Copper(II)acetate-mediated three-component synthesis of pyrazoles **232** [216].

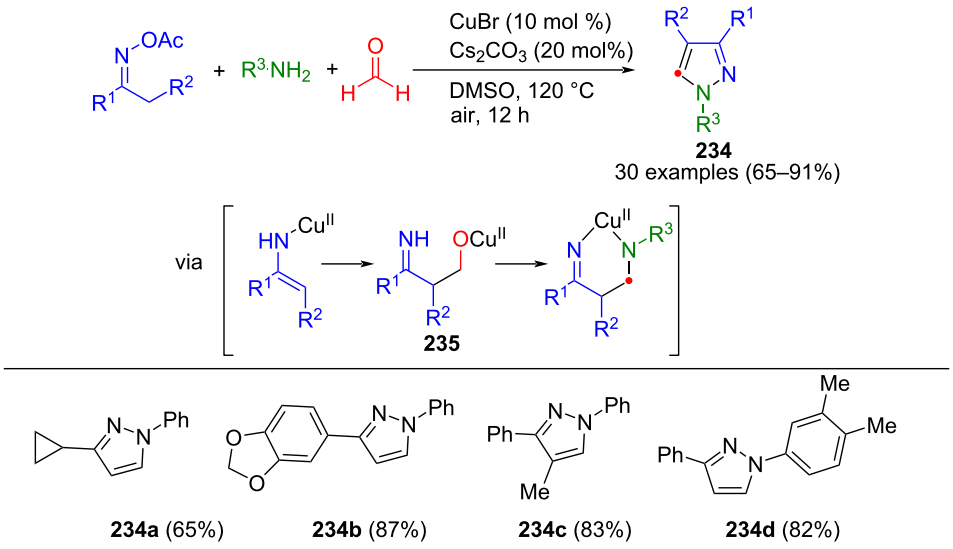

Scheme 83: Copper-catalyzed three-component synthesis of 1,3,4-substituted pyrazole **234** from oxime acetates, anilines, and paraformaldehyde [217].

ty represents an additional advantage. Notably, indoles and pyridazinones can be produced in a one-pot process using this concept.

In the synthesis of fully substituted pyrazoles by radical reactions, sulfonylhydrazines **241** can adopt a dual role. In a pseudo-three-component reaction involving 1,3-dicarbonyl compounds, along with tetra-*n*-butylammonium iodide (TBAI) as a catalyst and *tert*-butyl hydroperoxide (TBHP) as an oxidizing agent, these hydrazines serve both as a ring-forming component and as a sulfonyl precursor, to furnish 1,4-bisulfonyl substituted pyrazoles **242** (Scheme 85) [219]. Iodide causes the formation of *t*-BuO or *t*-BuOO radicals, which subsequently react with tosylhydrazine, liberating nitrogen nitrogen and generating a tosyl radical. H-Abstraction at the α-position of the resulting tosylhydrazone intermediate produces a further radical **243**. These radicals finally undergo cyclocondensation, resulting in the formation of the corresponding pyrazole **242**. Notably, this method tolerates many functional groups and can be scaled up to 16 grams. Only sterically demanding 1,3-dicarbonyl compounds and tosylhydrazines containing aliphatic residues do not lead to the desired product. Moreover, the reaction can be extended to enaminones [220].

In an attempt to synthesize 2*H*-[1,4,5]thiadiazocin-7-ones **247** from thietanones **244** and 1,2,4,5-tetrazines **245**, Suen et al. made an interesting discovery. Although the desired product is formed in situ in this three-component sequence, the presence

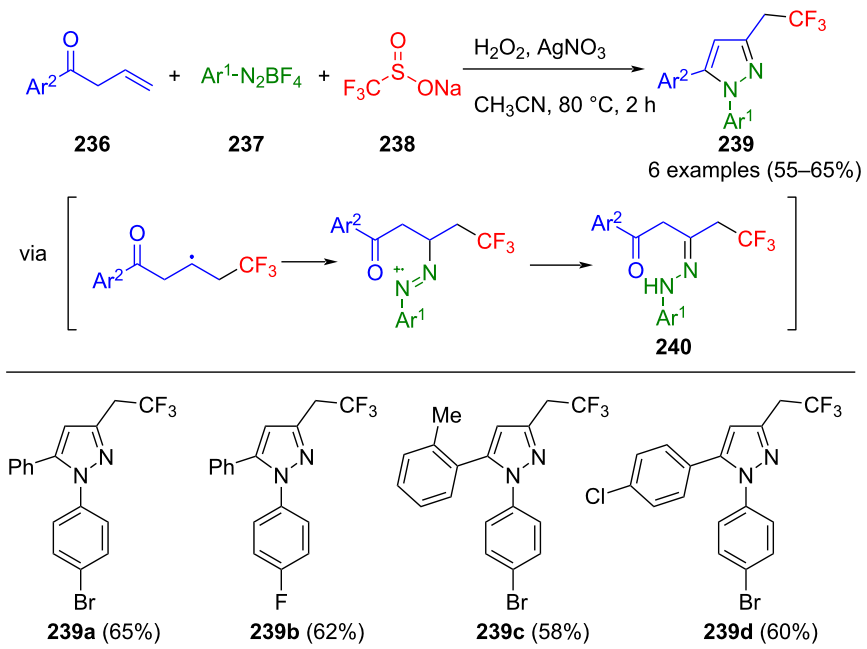

Scheme 84: Three-component synthesis of 3-trifluoroethylpyrazoles **239** [218].

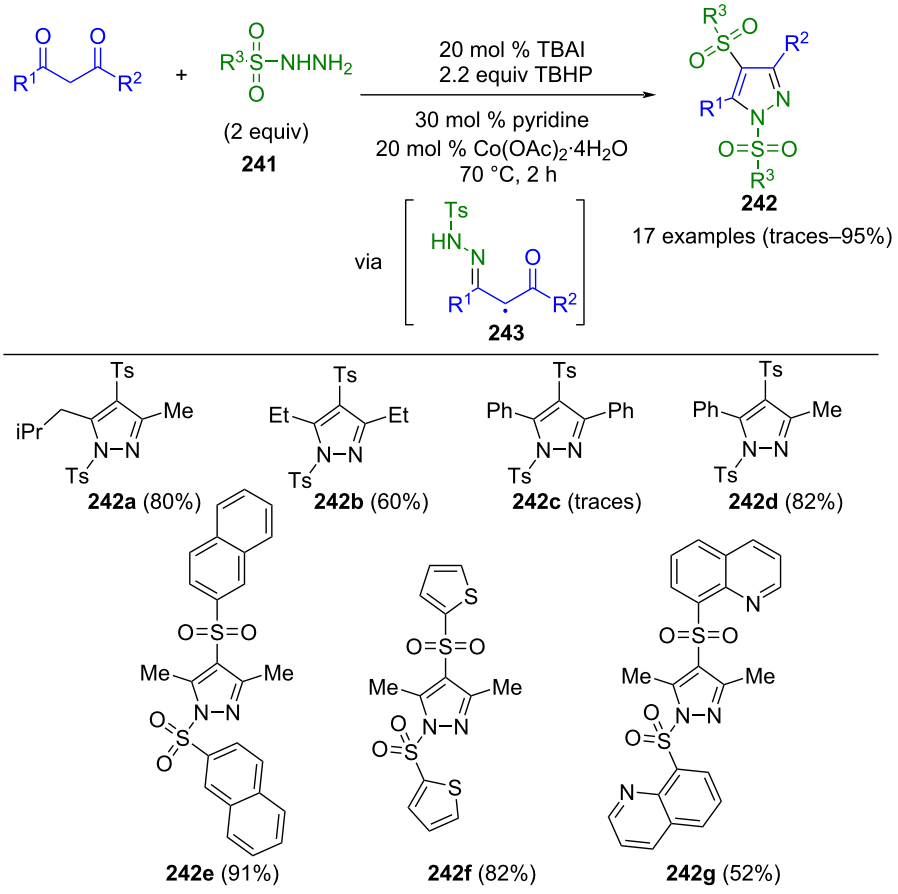

Scheme 85: Pseudo-three-component synthesis of 1,4-bisulfonyl-substituted pyrazoles **242** [219].

of alcohols under basic conditions triggers a condensation–fragmentation–cyclization–extrusion sequence to form fully substituted 4-hydroxypyrazoles **246** (Scheme 86) [221]. This allows for introducing an ether functionality. Notably, X-ray structural analysis shows that the isolated product is not the tautomeric pyrazolones.

Conclusion

Pyrazoles are evergreens in heterocyclic chemistry, and the multitude of applications still demands for novel synthetic concepts for their preparation, particularly in a modular and diversity-oriented fashion for exploring structural and functional space. Multicomponent reactions (MCR) per se fulfill the claim for modularity and diversity-orientation. According to the reactivity-based principle of MCR, functionalities are created and consumed en route, minimizing the number of necessary steps. For MCR synthesis of pyrazoles, there are two key transformations: (3 + 2)-cyclocondensations and (3 + 2)-cycloadditions. Although α,β-unsaturated acceptors are relevant in both cases, in the former case, they rather become the C_3 building block, while in the latter they serve as C2 blocks. This review delineates the major synthetic MCR strategies and highlights also the immediate potency of this approach, which is the concatenation of elementary organic and organometallic processes. The strategy not only allows extended modification but also exploiting reactivity patterns and establishing functional diversity for a variety of fields ranging from materials to life sciences. MCR establishes itself as a potent tool to uncover new properties of and propose new applications for pyrazoles due to the crucial synthetic expansion of the field.

Acknowledgements

We thank Ms. Anastasiia Pohorielova for her advice on the artwork of the graphical abstract.

Funding

We gratefully acknowledge the financial support provided by DAAD (scholarship for MMK), the Alexander von Humboldt Foundation (MSCA4Ukraine scholarship for MMK), and the Fonds der Chemischen Industrie.

Author Contributions

Ignaz Betcke: visualization; writing – original draft; writing – review & editing. Alissa C. Götzinger: conceptualization; visualization; writing – review & editing. Maryna M. Kornet: visualization; writing – original draft; writing – review & editing. Thomas J. J. Müller: conceptualization; funding acquisition; project administration; supervision; writing – original draft; writing – review & editing.

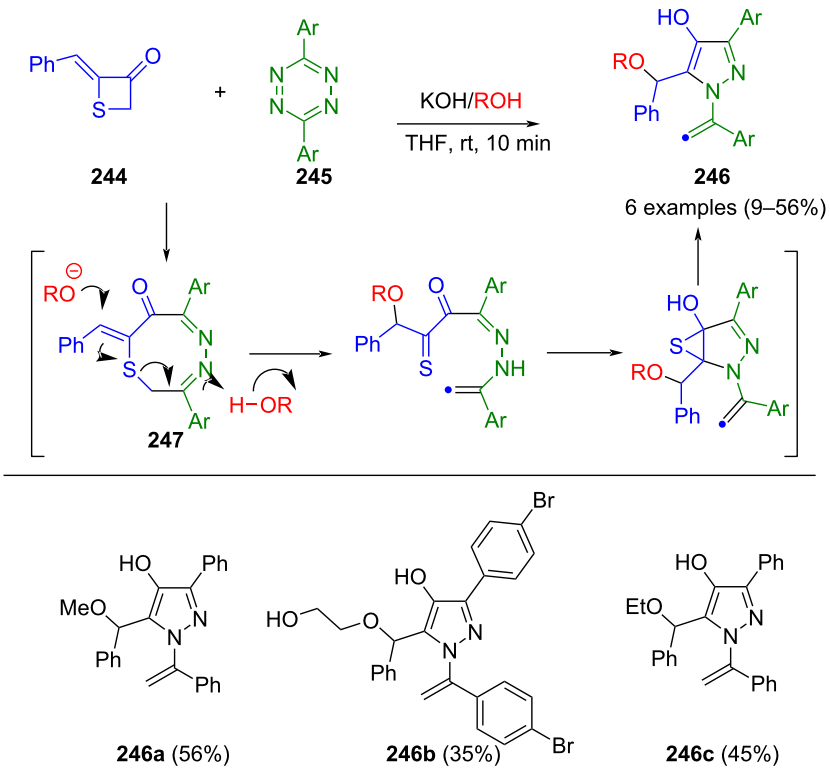

Scheme 86: Three-component synthesis of 4-hydroxypyrazole **246** [221].

ORCID® iDs

Alissa C. Götzinger - https://orcid.org/0009-0003-6509-7966
Maryna M. Kornet - https://orcid.org/0000-0002-9251-5700
Thomas J. J. Müller - https://orcid.org/0000-0001-9809-724X

Data Availability Statement

Data sharing is not applicable as no new data was generated or analyzed in this study.

References

1. Ehrlich, H. W. W. *Acta Crystallogr.* **1960,** *13,* 946–952. doi:10.1107/s0365110x60002296
2. Kumar, V.; Kaur, K.; Gupta, G. K.; Sharma, A. K. *Eur. J. Med. Chem.* **2013,** *69,* 735–753. doi:10.1016/j.ejmech.2013.08.053
3. Pérez-Fernández, R.; Goya, P.; Elguero, J. *ARKIVOC* **2014,** No. ii, 233–293. doi:10.3998/ark.5550190.p008.131
4. Bekhit, A. A.; Hymete, A.; Bekhit, A. E.-D. A.; Damtew, A.; Aboul-Enein, H. Y. *Mini-Rev. Med. Chem.* **2010,** *10,* 1014–1033. doi:10.2174/1389557511009011014
5. Karrouchi, K.; Radi, S.; Ramli, Y.; Taoufik, J.; Mabkhot, Y. N.; Al-aizari, F. A.; Ansar, M. *Molecules* **2018,** *23,* 134. doi:10.3390/molecules23010134
6. Becerra, D.; Abonia, R.; Castillo, J.-C. *Molecules* **2022,** *27,* 4723. doi:10.3390/molecules27154723
7. Chimenti, F.; Fioravanti, R.; Bolasco, A.; Manna, F.; Chimenti, P.; Secci, D.; Befani, O.; Turini, P.; Ortuso, F.; Alcaro, S. *J. Med. Chem.* **2007,** *50,* 425–428. doi:10.1021/jm060868l
8. Organ, M. G.; Mayer, S. *J. Comb. Chem.* **2003,** *5,* 118–124. doi:10.1021/cc020045r
9. Menozzi, G.; Mosti, L.; Fossa, P.; Mattioli, F.; Ghia, M. *J. Heterocycl. Chem.* **1997,** *34,* 963–968. doi:10.1002/jhet.5570340339
10. Terrett, N. K.; Bell, A. S.; Brown, D.; Ellis, P. *Bioorg. Med. Chem. Lett.* **1996,** *6,* 1819–1824. doi:10.1016/0960-894x(96)00323-x
11. Penning, T. D.; Talley, J. J.; Bertenshaw, S. R.; Carter, J. S.; Collins, P. W.; Docter, S.; Graneto, M. J.; Lee, L. F.; Malecha, J. W.; Miyashiro, J. M.; Rogers, R. S.; Rogier, D. J.; Yu, S. S.; Anderson, G. D.; Burton, E. G.; Cogburn, J. N.; Gregory, S. A.; Koboldt, C. M.; Perkins, W. E.; Seibert, K.; Veenhuizen, A. W.; Zhang, Y. Y.; Isakson, P. C. *J. Med. Chem.* **1997,** *40,* 1347–1365. doi:10.1021/jm960803q
12. Boyd, S. T.; Fremming, B. A. *Ann. Pharmacother.* **2005,** *39,* 684–690. doi:10.1345/aph.1e499
13. Motoba, K.; Nishizawa, H.; Suzuki, T.; Hamaguchi, H.; Uchida, M.; Funayama, S. *Pestic. Biochem. Physiol.* **2000,** *67,* 73–84. doi:10.1006/pest.2000.2477
14. Mohamed, F.; Senarathna, L.; Percy, A.; Abeyewardene, M.; Eaglesham, G.; Cheng, R.; Azher, S.; Hittarage, A.; Dissanayake, W.; Sheriff, M. H. R.; Davies, W.; Buckley, N. A.; Eddleston, M. *J. Toxicol., Clin. Toxicol.* **2004,** *42,* 955–963. doi:10.1081/clt-200041784
15. Sherman, T. D.; Duke, M. V.; Clark, R. D.; Sanders, E. F.; Matsumoto, H.; Duke, S. O. *Pestic. Biochem. Physiol.* **1991,** *40,* 236–245. doi:10.1016/0048-3575(91)90095-4
16. Liu, X.-H.; Tan, C.-X.; Weng, J.-Q. *Phosphorus, Sulfur Silicon Relat. Elem.* **2011,** *186,* 558–564. doi:10.1080/10426507.2010.508060
17. Maeda, H.; Ito, Y.; Kusunose, Y.; Nakanishi, T. *Chem. Commun.* **2007,** 1136–1138. doi:10.1039/b615787d
18. Catalán, J.; Fabero, F.; Claramunt, R. M.; Santa Maria, M. D.; de la Concepción Foces-Foces, M.; Hernández Cano, F.; Martinez-Ripoll, M.; Elguero, J.; Sastre, R. *J. Am. Chem. Soc.* **1992,** *114,* 5039–5048. doi:10.1021/ja00039a014
19. Sarkar, A.; Chakravorti, S. *Chem. Phys. Lett.* **1995,** *235,* 195–201. doi:10.1016/0009-2614(95)00111-g
20. Chen, X.-L.; Yu, R.; Zhang, Q.-K.; Zhou, L.-J.; Wu, X.-Y.; Zhang, Q.; Lu, C.-Z. *Chem. Mater.* **2013,** *25,* 3910–3920. doi:10.1021/cm4024309
21. Dorlars, A.; Schellhammer, C.-W.; Schroeder, J. *Angew. Chem., Int. Ed. Engl.* **1975,** *14,* 665–679. doi:10.1002/anie.197506651
22. Hendrickson, J. B. *J. Am. Chem. Soc.* **1975,** *97,* 5784–5800. doi:10.1021/ja00853a023
23. Gaich, T.; Baran, P. S. *J. Org. Chem.* **2010,** *75,* 4657–4673. doi:10.1021/jo1006812
24. Müller, T. J. J. Relative Reactivities of Functional Groups as the Key to Multicomponent Reactions. In *Multicomponent Reactions;* Müller, T. J. J., Ed.; Thieme: Stuttgart, Germany, 2014; Vol. 1, pp 5–27. doi:10.1055/sos-sd-210-00002
25. Elguero, J. Pyrazoles and their Benzo Derivatives. In *Comprehensive Heterocyclic Chemistry;* Katritzky, A. R.; Rees, C. W., Eds.; Pergamon Press, 1984; pp 167–303. doi:10.1016/b978-008096519-2.00072-2
26. Elguero, J. Pyrazoles. In *Comprehensive Heterocyclic Chemistry II;* Katritzky, A. R.; Rees, C. W.; Scriven, E. F. V., Eds.; Pergamon Press, 1996; Vol. 3, pp 1–75. doi:10.1016/b978-008096518-5.00059-9
27. Yet, L. Pyrazoles. In *Comprehensive Heterocyclic Chemistry III;* Katritzky, A. R.; Ramsden, C. A.; Scriven, E. F. V.; Taylor, R. J. K., Eds.; Elsevier: Amsterdam, Netherlands, 2008; Vol. 4, pp 1–141. doi:10.1016/b978-008044992-0.00401-6
28. Fustero, S.; Sánchez-Roselló, M.; Barrio, P.; Simón-Fuentes, A. *Chem. Rev.* **2011,** *111,* 6984–7034. doi:10.1021/cr2000459
29. Fustero, S.; Simón-Fuentes, A.; Sanz-Cervera, J. F. *Org. Prep. Proced. Int.* **2009,** *41,* 253–290. doi:10.1080/00304940903077832
30. Götzinger, A. C.; Müller, T. J. J. *Pyrazoles*. *Science of Synthesis Knowledge Updates;* Thieme: Stuttgart, Germany, 2017; Vol. 3, pp 1–229. doi:10.1055/sos-sd-112-00112
31. Aggarwal, R.; Kumar, V.; Kumar, R.; Singh, S. P. *Beilstein J. Org. Chem.* **2011,** *7,* 179–197. doi:10.3762/bjoc.7.25
32. Molteni, G. *ARKIVOC* **2007,** No. ii, 224–246. doi:10.3998/ark.5550190.0008.207
33. Schmidt, A.; Dreger, A. *Curr. Org. Chem.* **2011,** *15,* 1423–1463. doi:10.2174/138527211795378263
34. Anwar, H. F.; Elnagdi, M. H. *ARKIVOC* **2009,** No. i, 198–250. doi:10.3998/ark.5550190.0010.107
35. Santos, C. M. M.; Silva, V. L. M.; Silva, A. M. S. *Molecules* **2017,** *22,* 1665. doi:10.3390/molecules22101665
36. Castillo, J.-C.; Portilla, J. *Targets Heterocycl. Syst.* **2019,** *22,* 194–223. doi:10.17374/targets.2019.22.194
37. Neto, J. S. S.; Zeni, G. *Chem. – Eur. J.* **2020,** *26,* 8175–8189. doi:10.1002/chem.201905276
38. Ameziane El Hassani, I.; Rouzi, K.; Assila, H.; Karrouchi, K.; Ansar, M. *Reactions* **2023,** *4,* 478–504. doi:10.3390/reactions4030029
39. Maddila, S.; Jonnalagadda, S. B.; Gangu, K. K.; Maddila, S. N. *Curr. Org. Synth.* **2017,** *14,* 634–653. doi:10.2174/1570179414666161208164731

40. Bhaskaruni, S. V. H. S.; Maddila, S.; Gangu, K. K.; Jonnalagadda, S. B. *Arabian J. Chem.* **2020,** *13,* 1142–1178. doi:10.1016/j.arabjc.2017.09.016
41. Mamaghani, M.; Hossein Nia, R. *Polycyclic Aromat. Compd.* **2021,** *41,* 223–291. doi:10.1080/10406638.2019.1584576
42. Stanovnik, B.; Svete, J. Product Class 1: Pyrazoles. In *Science of Synthesis;* Neier, R., Ed.; Thieme: Stuttgart, Germany; Vol. 12, pp 15–225. doi:10.1055/sos-sd-012-00002
43. Kirschke, K. 1*H*-Pyrazole. In *Houben-Weyl, Methoden der organischen Chemie;* Schaumann, E., Ed.; Thieme: Stuttgart, Germany, 1994; Vol. E8b, pp 399–763. doi:10.1055/b-0035-110475
44. Heller, S. T.; Natarajan, S. R. *Org. Lett.* **2006,** *8,* 2675–2678. doi:10.1021/ol060570p
45. Shen, Q.; Huang, W.; Wang, J.; Zhou, X. *Org. Lett.* **2007,** *9,* 4491–4494. doi:10.1021/ol701961z
46. Jiang, J.-A.; Du, C.-Y.; Gu, C.-H.; Ji, Y.-F. *Synlett* **2012,** *23,* 2965–2968. doi:10.1055/s-0032-1317668
47. Jiang, J.-A.; Huang, W.-B.; Zhai, J.-J.; Liu, H.-W.; Cai, Q.; Xu, L.-X.; Wang, W.; Ji, Y.-F. *Tetrahedron* **2013,** *69,* 627–635. doi:10.1016/j.tet.2012.11.012
48. Xie, Y.-S.; Pan, X.-H.; Zhao, B.-X.; Liu, J.-T.; Shin, D.-S.; Zhang, J.-H.; Zheng, L.-W.; Zhao, J.; Miao, J.-Y. *J. Organomet. Chem.* **2008,** *693,* 1367–1374. doi:10.1016/j.jorganchem.2008.01.043
49. Zhai, J.; Gu, C.; Jiang, J.; Zhang, S.; Liao, D.; Wang, L.; Zhu, D.; Ji, Y. *Chin. J. Chem.* **2013,** *31,* 1526–1538. doi:10.1002/cjoc.201300776
50. Meng, L.; Lorsbach, B. A.; Sparks, T. C.; Fettinger, J. C.; Kurth, M. J. *J. Comb. Chem.* **2010,** *12,* 129–136. doi:10.1021/cc900133k
51. Gu, C.; Zhai, J.; Jiang, J.; Liu, H.; Wang, L.; Zhu, D.; Ji, Y. *Chin. J. Chem.* **2014,** *32,* 179–190. doi:10.1002/cjoc.201300878
52. Velpula, R.; Deshineni, R.; Gali, R.; Bavantula, R. *Res. Chem. Intermed.* **2016,** *42,* 1729–1740. doi:10.1007/s11164-015-2114-2
53. Degorce, S.; Jung, F. H.; Harris, C. S.; Koza, P.; Lecoq, J.; Stevenin, A. *Tetrahedron Lett.* **2011,** *52,* 6719–6722. doi:10.1016/j.tetlet.2011.09.150
54. Beveridge, R. E.; Fernando, D.; Gerstenberger, B. S. *Tetrahedron Lett.* **2010,** *51,* 5005–5008. doi:10.1016/j.tetlet.2010.07.077
55. Demers, J. P.; Klaubert, D. H. *Tetrahedron Lett.* **1987,** *28,* 4933–4934. doi:10.1016/s0040-4039(00)96662-0
56. Gerstenberger, B. S.; Rauckhorst, M. R.; Starr, J. T. *Org. Lett.* **2009,** *11,* 2097–2100. doi:10.1021/ol900515a
57. Cheng, B.; Bao, B.; Chen, Y.; Wang, N.; Li, Y.; Wang, R.; Zhai, H. *Org. Chem. Front.* **2017,** *4,* 1636–1639. doi:10.1039/c7qo00238f
58. Raw, S. A.; Turner, A. T. *Tetrahedron Lett.* **2009,** *50,* 696–699. doi:10.1016/j.tetlet.2008.11.099
59. Devery, J. J., III; Mohanta, P. K.; Casey, B. M.; Flowers, R. A., II. *Synlett* **2009,** 1490–1494. doi:10.1055/s-0029-1217163
60. Akula, R.; Xiong, Y.; Ibrahim, H. *RSC Adv.* **2013,** *3,* 10731–10735. doi:10.1039/c3ra41376d
61. Beyrati, M.; Hasaninejad, A. *Org. Prep. Proced. Int.* **2016,** *48,* 393–400. doi:10.1080/00304948.2016.1206426
62. Kamble, S. S.; Shankarling, G. S. *ChemistrySelect* **2018,** *3,* 2032–2036. doi:10.1002/slct.201702898
63. Fatahpour, M.; Noori Sadeh, F.; Hazeri, N.; Maghsoodlou, M. T.; Hadavi, M. S.; Mahnaei, S. *J. Saudi Chem. Soc.* **2017,** *21,* 998–1006. doi:10.1016/j.jscs.2017.05.009
64. Kim, S. H.; Lee, S.; Kim, S. H.; Kim, K. H.; Kim, J. N. *Bull. Korean Chem. Soc.* **2013,** *34,* 3415–3419. doi:10.5012/bkcs.2013.34.11.3415
65. Ben Mohamed, S.; Rachedi, Y.; Hamdi, M.; Le Bideau, F.; Dejean, C.; Dumas, F. *Eur. J. Org. Chem.* **2016,** 2628–2636. doi:10.1002/ejoc.201600173
66. Penta, S.; Vedula, R. R. *Org. Commun.* **2012,** *5,* 143–149.
67. Sujatha, K.; Deshpande, R. P.; Kesharwani, R. K.; Babu, P. P.; Rao Vedula, R. *Synth. Commun.* **2019,** *49,* 49–55. doi:10.1080/00397911.2018.1537398
68. Nandi, G. C.; Singh, M. S.; Ila, H.; Junjappa, H. *Eur. J. Org. Chem.* **2012,** 967–974. doi:10.1002/ejoc.201101397
69. Kruppa, M.; Müller, T. J. J. *Catalysts* **2023,** *13,* 350. doi:10.3390/catal13020350
70. Tasch, B. O. A.; Bensch, L.; Antovic, D.; Müller, T. J. J. *Org. Biomol. Chem.* **2013,** *11,* 6113–6118. doi:10.1039/c3ob41249k
71. Zapf, A.; Ehrentraut, A.; Beller, M. *Angew. Chem., Int. Ed.* **2000,** *39,* 4153–4155. doi:10.1002/1521-3773(20001117)39:22<4153::aid-anie4153>3.0.co;2-t
72. Xie, F.; Cheng, G.; Hu, Y. *J. Comb. Chem.* **2006,** *8,* 286–288. doi:10.1021/cc050159d
73. Bishop, B. C.; Brands, K. M. J.; Gibb, A. D.; Kennedy, D. J. *Synthesis* **2004,** 43–52. doi:10.1055/s-2003-44376
74. Fehér, C.; Kuik, Á.; Márk, L.; Kollár, L.; Skoda-Földes, R. *J. Organomet. Chem.* **2009,** *694,* 4036–4041. doi:10.1016/j.jorganchem.2009.08.029
75. Kirkham, J. D.; Edeson, S. J.; Stokes, S.; Harrity, J. P. A. *Org. Lett.* **2012,** *14,* 5354–5357. doi:10.1021/ol302418b
76. Lévai, A.; Silva, A. M. S.; Pinto, D. C. G. A.; Cavaleiro, J. A. S.; Alkorta, I.; Elguero, J.; Jekö, J. *Eur. J. Org. Chem.* **2004,** 4672–4679. doi:10.1002/ejoc.200400465
77. Tang, M.; Zhang, F.-M. *Tetrahedron* **2013,** *69,* 1427–1433. doi:10.1016/j.tet.2012.12.038
78. Hasaninejad, A.; Firoozi, S. *Mol. Diversity* **2013,** *17,* 459–469. doi:10.1007/s11030-013-9445-y
79. Nemati, F.; Nikkhah, S. H.; Elhampour, A. *Chin. Chem. Lett.* **2015,** *26,* 1397–1399. doi:10.1016/j.cclet.2015.07.009
80. Srivastava, M.; Rai, P.; Singh, J.; Singh, J. *RSC Adv.* **2013,** *3,* 16994–16998. doi:10.1039/c3ra42493f
81. Zolfigol, M. A.; Afsharnadery, F.; Baghery, S.; Salehzadeh, S.; Maleki, F. *RSC Adv.* **2015,** *5,* 75555–75568. doi:10.1039/c5ra16289k
82. Kolsepatil, S. R.; Pahade, N. V.; Deshmukh, S. U.; Netankar, P. D.; Lingampalle, D. L. *Heterocycl. Lett.* **2018,** *8,* 105–110.
83. Aryan, R.; Beyzaei, H.; Nojavan, M.; Rezaei, M. *Res. Chem. Intermed.* **2017,** *43,* 4731–4744. doi:10.1007/s11164-017-2908-5
84. Srivastava, M.; Rai, P.; Singh, J.; Singh, J. *New J. Chem.* **2014,** *38,* 302–307. doi:10.1039/c3nj01149f
85. Mishra, D.; Singh, R.; Rout, C. *J. Chem. Pharm. Res.* **2017,** *9,* 16–19.
86. Kiyani, H.; Bamdad, M. *Res. Chem. Intermed.* **2018,** *44,* 2761–2778. doi:10.1007/s11164-018-3260-0
87. Maddila, S.; Rana, S.; Pagadala, R.; Kankala, S.; Maddila, S.; Jonnalagadda, S. B. *Catal. Commun.* **2015,** *61,* 26–30. doi:10.1016/j.catcom.2014.12.005
88. Rakhtshah, J.; Salehzadeh, S.; Gowdini, E.; Maleki, F.; Baghery, S.; Zolfigol, M. A. *RSC Adv.* **2016,** *6,* 104875–104885. doi:10.1039/c6ra20988b
89. Arora, P.; Rajput, J. K. *J. Mater. Sci.* **2017,** *52,* 11413–11427. doi:10.1007/s10853-017-1304-2
90. Badhe, K.; Dabholkar, V.; Kurade, S. *Curr. Organocatal.* **2018,** *5,* 3–12. doi:10.2174/2213337205666180516094624
91. Vasuki, G.; Kumaravel, K. *Tetrahedron Lett.* **2008,** *49,* 5636–5638. doi:10.1016/j.tetlet.2008.07.055

92. Safaei-Ghomi, J.; Shahbazi-Alavi, H.; Heidari-Baghbahadorani, E. *J. Chem. Res.* **2015,** *39,* 410–413. doi:10.3184/174751915x14358475706316
93. Myrboh, B.; Mecadon, H.; Rohman, M. R.; Rajbangshi, M.; Kharkongor, I.; Laloo, B. M.; Kharbangar, I.; Kshiar, B. *Org. Prep. Proced. Int.* **2013,** *45,* 253–303. doi:10.1080/00304948.2013.798566
94. Wang, L.; Han, J.; Sheng, J.; Tian, H.; Fan, Z. *Catal. Commun.* **2005,** *6,* 201–204. doi:10.1016/j.catcom.2004.12.009
95. Shen, L.; Cao, S.; Liu, N.; Wu, J.; Zhu, L.; Qian, X. *Synlett* **2008,** 1341–1344. doi:10.1055/s-2008-1072766
96. Shen, L.; Zhang, J.; Cao, S.; Yu, J.; Liu, N.; Wu, J.; Qian, X. *Synlett* **2008,** 3058–3062. doi:10.1055/s-0028-1087348
97. Safaei, S.; Mohammadpoor-Baltork, I.; Khosropour, A. R.; Moghadam, M.; Tangestaninejad, S.; Mirkhani, V. *Synlett* **2011,** 2214–2222. doi:10.1055/s-0030-1261202
98. Jawale, D. V.; Pratap, U. R.; Mali, J. R.; Mane, R. A. *Chin. Chem. Lett.* **2011,** *22,* 1187–1190. doi:10.1016/j.cclet.2011.05.016
99. Kumari, K.; Raghuvanshi, D. S.; Jouikov, V.; Singh, K. N. *Tetrahedron Lett.* **2012,** *53,* 1130–1133. doi:10.1016/j.tetlet.2011.12.094
100. Khan, A. T.; Ghosh, A.; Basha R, S.; Mir, M. H. *Asian J. Org. Chem.* **2013,** *2,* 126–129. doi:10.1002/ajoc.201200148
101. Safaei, S.; Mohammadpoor-Baltork, I.; Khosropour, A. R.; Moghadam, M.; Tangestaninejad, S.; Mirkhani, V.; Khavasi, H. R. *Synlett* **2013,** *24,* 1086–1090. doi:10.1055/s-0032-1316900
102. Lellek, V.; Chen, C.-y.; Yang, W.; Liu, J.; Ji, X.; Faessler, R. *Synlett* **2018,** *29,* 1071–1075. doi:10.1055/s-0036-1591941
103. Gonçalves, H. A.; Pereira, B. A.; Teixeira, W. K. O.; Moura, S.; Flores, D. C.; Flores, A. F. C. *J. Fluorine Chem.* **2016,** *187,* 40–45. doi:10.1016/j.jfluchem.2016.05.009
104. Schranck, J.; Wu, X.-F.; Neumann, H.; Beller, M. *Chem. – Eur. J.* **2012,** *18,* 4827–4831. doi:10.1002/chem.201103643
105. Raghunadh, A.; Meruva, S. B.; Mekala, R.; Raghavendra Rao, K.; Krishna, T.; Gangadhara Chary, R.; Vaikunta Rao, L.; Syam Kumar, U. K. *Tetrahedron Lett.* **2014,** *55,* 2986–2990. doi:10.1016/j.tetlet.2014.03.125
106. Bisenieks, E.; Uldrikis, J.; Duburs, G. *Chem. Heterocycl. Compd.* **2004,** *40,* 869–875. doi:10.1023/b:cohc.0000044569.14048.79
107. Alinezhad, H.; Tajbakhsh, M.; Zare, M. *J. Fluorine Chem.* **2011,** *132,* 995–1000. doi:10.1016/j.jfluchem.2011.07.014
108. Alinezhad, H.; Tajbakhsh, M.; Zare, M. *Monatsh. Chem.* **2012,** *143,* 947–950. doi:10.1007/s00706-012-0721-9
109. Molteni, V.; Hamilton, M. M.; Mao, L.; Crane, C. M.; Termin, A. P.; Wilson, D. M. *Synthesis* **2002,** 1669–1674. doi:10.1055/s-2002-33650
110. Kendre, B. V.; Landge, M. G.; Bhusare, S. R. *Arabian J. Chem.* **2019,** *12,* 2091–2097. doi:10.1016/j.arabjc.2015.01.007
111. Pazenok, S.; Giornal, F.; Landelle, G.; Lui, N.; Vors, J.-P.; Leroux, F. R. *Eur. J. Org. Chem.* **2013,** 4249–4253. doi:10.1002/ejoc.201300561
112. Giornal, F.; Landelle, G.; Lui, N.; Vors, J.-P.; Pazenok, S.; Leroux, F. R. *Org. Process Res. Dev.* **2014,** *18,* 1002–1009. doi:10.1021/op500102h
113. Pazenok, S.; Lui, N.; Neeff, A. Process for preparing 3-dihalomethylpyrazole-4-carboxylic acid derivatives. WO Patent WO2008022777, Feb 28, 2008.
114. Arimori, S.; Matsubara, O.; Takada, M.; Shiro, M.; Shibata, N. *R. Soc. Open Sci.* **2016,** *3,* 160102. doi:10.1098/rsos.160102
115. Bouillon, J.-P.; Didier, B.; Dondy, B.; Doussot, P.; Plantier-Royon, R.; Portella, C. *Eur. J. Org. Chem.* **2001,** 187–192. doi:10.1002/1099-0690(200101)2001:1<187::aid-ejoc187>3.0.co;2-g
116. Kumar, S. V.; Yadav, S. K.; Raghava, B.; Saraiah, B.; Ila, H.; Rangappa, K. S.; Hazra, A. *J. Org. Chem.* **2013,** *78,* 4960–4973. doi:10.1021/jo400599e
117. Alizadeh, A.; Firuzyar, T.; Zhu, L.-G. *Tetrahedron* **2010,** *66,* 9835–9839. doi:10.1016/j.tet.2010.10.070
118. Jin, W.; Yu, H.; Yu, Z. *Tetrahedron Lett.* **2011,** *52,* 5884–5887. doi:10.1016/j.tetlet.2011.08.168
119. Beltrán-Rodil, S.; Edwards, M. G.; Pugh, D. S.; Reid, M.; Taylor, R. J. K. *Synlett* **2010,** 602–604. doi:10.1055/s-0029-1218521
120. Claisen, L. *Ber. Dtsch. Chem. Ges.* **1903,** *36,* 3664–3673. doi:10.1002/cber.190303603168
121. Whittaker, R. E.; Dermenci, A.; Dong, G. *Synthesis* **2016,** *48,* 161–183. doi:10.1055/s-0035-1560515
122. Nájera, C.; Sydnes, L. K.; Yus, M. *Chem. Rev.* **2019,** *119,* 11110–11244. doi:10.1021/acs.chemrev.9b00277
123. Gers-Panther, C. F.; Müller, T. J. J. *Adv. Heterocycl. Chem.* **2016,** *120,* 67–98. doi:10.1016/bs.aihch.2016.04.007
124. Willy, B.; Müller, T. J. J. *ARKIVOC* **2008,** No. i, 195–208. doi:10.3998/ark.5550190.0009.107
125. Niedballa, J.; Müller, T. J. J. *Catalysts* **2022,** *12,* 90. doi:10.3390/catal12010090
126. Liu, H.-L.; Jiang, H.-F.; Zhang, M.; Yao, W.-J.; Zhu, Q.-H.; Tang, Z. *Tetrahedron Lett.* **2008,** *49,* 3805–3809. doi:10.1016/j.tetlet.2008.03.153
127. Willy, B.; Müller, T. J. J. *Eur. J. Org. Chem.* **2008,** 4157–4168. doi:10.1002/ejoc.200800444
128. Liu, H.; Liang, Y.; Jia, T.-T.; Han, F.; Zhang, F.; Zhao, Y. *Eur. J. Org. Chem.* **2017,** 1443–1449. doi:10.1002/ejoc.201601506
129. Baxendale, I. R.; Schou, S. C.; Sedelmeier, J.; Ley, S. V. *Chem. – Eur. J.* **2010,** *16,* 89–94. doi:10.1002/chem.200902906
130. Chen, Q.; Yao, F.; Yin, L.; Cai, M. *J. Organomet. Chem.* **2016,** *804,* 108–113. doi:10.1016/j.jorganchem.2015.12.037
131. Hossain, S.; Park, J.-H.; Park, M.-K.; Jin, M.-J. *J. Korean Chem. Soc.* **2013,** *57,* 411–415. doi:10.5012/jkcs.2013.57.3.411
132. Tang, X.; Zheng, C.; Chen, Y.; Zhao, Z.; Qin, A.; Hu, R.; Tang, B. Z. *Macromolecules* **2016,** *49,* 9291–9300. doi:10.1021/acs.macromol.6b02192
133. Tamao, K.; Sumitani, K.; Kumada, M. *J. Am. Chem. Soc.* **1972,** *94,* 4374–4376. doi:10.1021/ja00767a075
134. Negishi, E.-i.; Kotora, M.; Xu, C. *J. Org. Chem.* **1997,** *62,* 8957–8960. doi:10.1021/jo971552b
135. Götzinger, A. C.; Müller, T. J. J. *Org. Biomol. Chem.* **2016,** *14,* 3498–3500. doi:10.1039/c6ob00483k
136. Götzinger, A. C.; Theßeling, F. A.; Hoppe, C.; Müller, T. J. J. *J. Org. Chem.* **2016,** *81,* 10328–10338. doi:10.1021/acs.joc.6b01326
137. Willy, B.; Müller, T. J. J. *Org. Lett.* **2011,** *13,* 2082–2085. doi:10.1021/ol2004947
138. Denißen, M.; Nordmann, J.; Dziambor, J.; Mayer, B.; Frank, W.; Müller, T. J. J. *RSC Adv.* **2015,** *5,* 33838–33854. doi:10.1039/c5ra03104d
139. Niesobski, P.; Klukas, F.; Berens, H.; Makhloufi, G.; Janiak, C.; Müller, T. J. J. *J. Org. Chem.* **2018,** *83,* 4851–4858. doi:10.1021/acs.joc.8b00430
140. Mohamed Ahmed, M. S.; Kobayashi, K.; Mori, A. *Org. Lett.* **2005,** *7,* 4487–4489. doi:10.1021/ol051841j
141. Mohamed Ahmed, M. S.; Mori, A. *Org. Lett.* **2003,** *5,* 3057–3060. doi:10.1021/ol035007a

142. Shi, L.; Xue, L.; Lang, R.; Xia, C.; Li, F. *ChemCatChem* **2014,** *6,* 2560–2566. doi:10.1002/cctc.201402277
143. Iizuka, M.; Kondo, Y. *Eur. J. Org. Chem.* **2007,** 5180–5182. doi:10.1002/ejoc.200700700
144. Tu, Y.; Zhang, Z.; Wang, T.; Ke, J.; Zhao, J. *Org. Lett.* **2017,** *19,* 3466–3469. doi:10.1021/acs.orglett.7b01447
145. Merkul, E.; Oeser, T.; Müller, T. J. J. *Chem. – Eur. J.* **2009,** *15,* 5006–5011. doi:10.1002/chem.200900119
146. Gers, C. F.; Rosellen, J.; Merkul, E.; Müller, T. J. J. *Beilstein J. Org. Chem.* **2011,** *7,* 1173–1181. doi:10.3762/bjoc.7.136
147. Merkul, E.; Dohe, J.; Gers, C.; Rominger, F.; Müller, T. J. J. *Angew. Chem., Int. Ed.* **2011,** *50,* 2966–2969. doi:10.1002/anie.201007194
148. Boersch, C.; Merkul, E.; Müller, T. J. J. *Angew. Chem., Int. Ed.* **2011,** *50,* 10448–10452. doi:10.1002/anie.201103296
149. Görgen, C.; Boden, K.; Reiss, G. J.; Frank, W.; Müller, T. J. J. *Beilstein J. Org. Chem.* **2019,** *15,* 1360–1370. doi:10.3762/bjoc.15.136
150. Kovács, S.; Novák, Z. *Tetrahedron* **2013,** *69,* 8987–8993. doi:10.1016/j.tet.2013.08.047
151. Levi, L.; Boersch, C.; Gers, C. F.; Merkul, E.; Müller, T. J. J. *Molecules* **2011,** *16,* 9340–9356. doi:10.3390/molecules16119340
152. Schreiner, E.; Braun, S.; Kwasnitschka, C.; Frank, W.; Müller, T. J. J. *Adv. Synth. Catal.* **2014,** *356,* 3135–3147. doi:10.1002/adsc.201400411
153. Chang, K.-T.; Choi, Y. H.; Kim, S.-H.; Yoon, Y.-J.; Lee, W. S. *J. Chem. Soc., Perkin Trans. 1* **2002,** 207–210. doi:10.1039/b108485m
154. Choi, Y. H.; Kim, K. S.; Lee, S.; Jeong, T.-S.; Lee, H.-Y.; Kim, Y. H.; Lee, W. S. *Heterocycles* **2003,** *60,* 2499–2510. doi:10.3987/com-03-9869
155. Harigae, R.; Moriyama, K.; Togo, H. *J. Org. Chem.* **2014,** *79,* 2049–2058. doi:10.1021/jo4027116
156. Zohreh, N.; Alizadeh, A. *Tetrahedron* **2011,** *67,* 4595–4600. doi:10.1016/j.tet.2011.04.076
157. Khan, I.; White, J. M. *Crystals* **2012,** *2,* 967–973. doi:10.3390/cryst2030967
158. Alizadeh, A.; Zarei, A.; Rezvanian, A. *Helv. Chim. Acta* **2012,** *95,* 278–281. doi:10.1002/hlca.201100317
159. Tu, X.-C.; Fan, W.; Jiang, B.; Wang, S.-L.; Tu, S.-J. *Tetrahedron* **2013,** *69,* 6100–6107. doi:10.1016/j.tet.2013.05.063
160. Adib, M.; Mohammadi, B.; Bijanzadeh, H. R. *Synlett* **2008,** 3180–3182. doi:10.1055/s-0028-1087365
161. Mohammadia, B.; Rahmani, M. *Iran. Chem. Commun.* **2016,** *4,* 226–235.
162. Jackowski, O.; Lecourt, T.; Micouin, L. *Org. Lett.* **2011,** *13,* 5664–5667. doi:10.1021/ol202389u
163. Padwa, A. *1,3-Dipolar Cycloaddition Chemistry;* John Wiley & Sons: New York, NY, USA, 1984; Vol. 1. doi:10.1002/0471221902
164. Hashimoto, T.; Maruoka, K. *Chem. Rev.* **2015,** *115,* 5366–5412. doi:10.1021/cr5007182
165. Chandrasekharan, S. P.; Dhami, A.; Kumar, S.; Mohanan, K. *Org. Biomol. Chem.* **2022,** *20,* 8787–8817. doi:10.1039/d2ob01918c
166. Molteni, G. *Heterocycles* **2005,** *65,* 2513–2537. doi:10.3987/rev-05-600
167. Hladíková, V.; Váňa, J.; Hanusek, J. *Beilstein J. Org. Chem.* **2018,** *14,* 1317–1348. doi:10.3762/bjoc.14.113
168. Požgan, F.; Al Mamari, H.; Grošelj, U.; Svete, J.; Štefane, B. *Molecules* **2018,** *23,* 3. doi:10.3390/molecules23010003
169. Abdulla Afsina, C. M.; Aneeja, T.; Neetha, M.; Anilkumar, G. *Curr. Org. Synth.* **2021,** *18,* 197–213. doi:10.2174/1570179417666201109151036
170. National Research Council (US) Committee on Prudent Practices in the Laboratory. *Prudent Practices in the Laboratory: Handling and Management of Chemical Hazards:* Updated Version. Washington (DC): National Academies Press (US); 2011. doi:10.17226/12654
171. Bamford, W. R.; Stevens, T. S. *J. Chem. Soc.* **1952,** 4735–4740. doi:10.1039/jr9520004735
172. Aggarwal, V. K.; de Vicente, J.; Bonnert, R. V. *J. Org. Chem.* **2003,** *68,* 5381–5383. doi:10.1021/jo0268409
173. Wu, L.-L.; Ge, Y.-C.; He, T.; Zhang, L.; Fu, X.-L.; Fu, H.-Y.; Chen, H.; Li, R.-X. *Synthesis* **2012,** *44,* 1577–1583. doi:10.1055/s-0031-1290772
174. Zhang, G.; Ni, H.; Chen, W.; Shao, J.; Liu, H.; Chen, B.; Yu, Y. *Org. Lett.* **2013,** *15,* 5967–5969. doi:10.1021/ol402810f
175. Haouas, A.; Hamadi, N. B.; Nsira, A.; Msadek, M. *J. Chem. Res.* **2013,** *37,* 435–437. doi:10.3184/174751913x13726128889197
176. Wu, L.; Shi, M. *J. Org. Chem.* **2010,** *75,* 2296–2301. doi:10.1021/jo100105k
177. Shu, W.-M.; Ma, J.-R.; Zheng, K.-L.; Sun, H.-Y.; Wang, M.; Yang, Y.; Wu, A.-X. *Tetrahedron* **2014,** *70,* 9321–9329. doi:10.1016/j.tet.2014.10.044
178. Shu, W.-M.; Zheng, K.-L.; Ma, J.-R.; Sun, H.-Y.; Wang, M.; Wu, A.-X. *Org. Lett.* **2015,** *17,* 1914–1917. doi:10.1021/acs.orglett.5b00605
179. Kamal, A.; Sastry, K. N. V.; Chandrasekhar, D.; Mani, G. S.; Adiyala, P. R.; Nanubolu, J. B.; Singarapu, K. K.; Maurya, R. A. *J. Org. Chem.* **2015,** *80,* 4325–4335. doi:10.1021/jo502946g
180. Mohanan, K.; Martin, A. R.; Toupet, L.; Smietana, M.; Vasseur, J.-J. *Angew. Chem., Int. Ed.* **2010,** *49,* 3196–3199. doi:10.1002/anie.200906781
181. Martin, A. R.; Mohanan, K.; Toupet, L.; Vasseur, J.-J.; Smietana, M. *Eur. J. Org. Chem.* **2011,** 3184–3190. doi:10.1002/ejoc.201100167
182. Ahamad, S.; Kant, R.; Mohanan, K. *ChemistrySelect* **2016,** *1,* 5276–5280. doi:10.1002/slct.201601113
183. Ahamad, S.; Patidar, R. K.; Kumar, A.; Kant, R.; Mohanan, K. *ChemistrySelect* **2017,** *2,* 11995–11998. doi:10.1002/slct.201702384
184. Kumar, R.; Verma, D.; Mobin, S. M.; Namboothiri, I. N. N. *Org. Lett.* **2012,** *14,* 4070–4073. doi:10.1021/ol301695e
185. Ahamad, S.; Gupta, A. K.; Kant, R.; Mohanan, K. *Org. Biomol. Chem.* **2015,** *13,* 1492–1499. doi:10.1039/c4ob02365j
186. Slobodyanyuk, E. Y.; Artamonov, O. S.; Shishkin, O. V.; Mykhailiuk, P. K. *Eur. J. Org. Chem.* **2014,** 2487–2495. doi:10.1002/ejoc.201301852
187. Li, F.; Nie, J.; Sun, L.; Zheng, Y.; Ma, J.-A. *Angew. Chem., Int. Ed.* **2013,** *52,* 6255–6258. doi:10.1002/anie.201301870
188. Li, F.; Wang, J.; Pei, W.; Li, H.; Zhang, H.; Song, M.; Guo, L.; Zhang, A.; Liu, L. *Tetrahedron Lett.* **2017,** *58,* 4344–4347. doi:10.1016/j.tetlet.2017.09.086
189. Britton, J.; Jamison, T. F. *Eur. J. Org. Chem.* **2017,** 6566–6574. doi:10.1002/ejoc.201700992
190. Britton, J.; Jamison, T. F. *Angew. Chem., Int. Ed.* **2017,** *56,* 8823–8827. doi:10.1002/anie.201704529
191. Hanamoto, T.; Koga, Y.; Kido, E.; Kawanami, T.; Furuno, H.; Inanaga, J. *Chem. Commun.* **2005,** 2041–2043. doi:10.1039/b419329f
192. Hanamoto, T.; Suetake, T.; Koga, Y.; Kawanami, T.; Furuno, H.; Inanaga, J. *Tetrahedron* **2007,** *63,* 5062–5070. doi:10.1016/j.tet.2007.03.117
193. Hanamoto, T.; Iwamoto, Y.; Yamada, K.; Anno, R. *J. Fluorine Chem.* **2007,** *128,* 1126–1130. doi:10.1016/j.jfluchem.2007.04.019

194. Hanamoto, T.; Egashira, M.; Ishizuka, K.; Furuno, H.; Inanaga, J. *Tetrahedron* **2006,** *62,* 6332–6338. doi:10.1016/j.tet.2006.04.043
195. Zhang, J.; Chen, W.; Huang, D.; Zeng, X.; Wang, X.; Hu, Y. *Tetrahedron Lett.* **2017,** *58,* 4133–4136. doi:10.1016/j.tetlet.2017.09.050
196. Gomha, S. M.; Edrees, M. M.; Faty, R. A. M.; Muhammad, Z. A.; Mabkhot, Y. N. *Chem. Cent. J.* **2017,** *11,* 37. doi:10.1186/s13065-017-0266-4
197. Alizadeh, A.; Roosta, A. *Synlett* **2016,** *27,* 2455–2458. doi:10.1055/s-0035-1562464
198. Alizadeh, A.; Moafi, L.; Zhu, L.-G. *J. Iran. Chem. Soc.* **2018,** *15,* 1255–1259. doi:10.1007/s13738-018-1323-1
199. Kolodych, S.; Rasolofonjatovo, E.; Chaumontet, M.; Nevers, M.-C.; Créminon, C.; Taran, F. *Angew. Chem., Int. Ed.* **2013,** *52,* 12056–12060. doi:10.1002/anie.201305645
200. Specklin, S.; Decuypere, E.; Plougastel, L.; Aliani, S.; Taran, F. *J. Org. Chem.* **2014,** *79,* 7772–7777. doi:10.1021/jo501420r
201. Deng, X.; Mani, N. S. *Org. Lett.* **2006,** *8,* 3505–3508. doi:10.1021/ol061226v
202. Soengas, R. G.; Silva, V. L. M.; Ide, D.; Kato, A.; Cardoso, S. M.; Almeida Paz, F. A.; Silva, A. M. S. *Tetrahedron* **2016,** *72,* 3198–3203. doi:10.1016/j.tet.2016.04.042
203. Alizadeh, A.; Esmaili zand, H. R.; Saberi, V.; Mokhtari, J. *Helv. Chim. Acta* **2013,** *96,* 2240–2244. doi:10.1002/hlca.201300070
204. Ningaiah, S.; Doddaramappa, S. D.; Chandra; Madegowda, M.; Keshavamurthy, S.; Bhadraiah, U. K. *Synth. Commun.* **2014,** *44,* 2222–2231. doi:10.1080/00397911.2014.891744
205. Liu, P.; Pan, Y.-M.; Xu, Y.-L.; Wang, H.-S. *Org. Biomol. Chem.* **2012,** *10,* 4696–4698. doi:10.1039/c2ob25487e
206. Rai, P.; Srivastava, M.; Singh, J.; Singh, J. *RSC Adv.* **2014,** *4,* 779–783. doi:10.1039/c3ra44315a
207. Wu, F.; Hao, L.; Zhan, Z.-p. *Heterocycles* **2013,** *87,* 657–663. doi:10.3987/com-12-12646
208. Safaei, S.; Mohammadpoor-Baltork, I.; Khosropour, A. R.; Moghadam, M.; Tangestaninejad, S.; Mirkhani, V. *New J. Chem.* **2013,** *37,* 2037–2042. doi:10.1039/c3nj40756j
209. Kasapidou, P. M.; Zarganes-Tzitzikas, T.; Tsoleridis, C. A.; Stephanidou-Stephanatou, J.; Neochoritis, C. G. *Synthesis* **2017,** *49,* 3619–3632. doi:10.1055/s-0036-1589013
210. Hao, L.; Wang, Z.; Wang, Y.; Yang, Z.; Liu, X.; Xu, X.; Ji, Y. *Org. Biomol. Chem.* **2023,** *21,* 7611–7615. doi:10.1039/d3ob01172k
211. Majumder, S.; Gipson, K. R.; Staples, R. J.; Odom, A. L. *Adv. Synth. Catal.* **2009,** *351,* 2013–2023. doi:10.1002/adsc.200900293
212. Dissanayake, A. A.; Odom, A. L. *Chem. Commun.* **2012,** *48,* 440–442. doi:10.1039/c1cc15809k
213. Glaser, C. *Ber. Dtsch. Chem. Ges.* **1869,** *2,* 422–424. doi:10.1002/cber.186900201183
214. Meng, Y.; Zhang, T.; Gong, X.; Zhang, M.; Zhu, C. *Tetrahedron Lett.* **2019,** *60,* 171–174. doi:10.1016/j.tetlet.2018.12.009
215. Neumann, J. J.; Suri, M.; Glorius, F. *Angew. Chem., Int. Ed.* **2010,** *49,* 7790–7794. doi:10.1002/anie.201002389
216. Chen, B.; Zhu, C.; Tang, Y.; Ma, S. *Chem. Commun.* **2014,** *50,* 7677–7679. doi:10.1039/c4cc02856b
217. Tang, X.; Huang, L.; Yang, J.; Xu, Y.; Wu, W.; Jiang, H. *Chem. Commun.* **2014,** *50,* 14793–14796. doi:10.1039/c4cc06747a
218. Matcha, K.; Antonchick, A. P. *Angew. Chem., Int. Ed.* **2014,** *53,* 11960–11964. doi:10.1002/anie.201406464
219. Zhang, J.; Shao, Y.; Wang, H.; Luo, Q.; Chen, J.; Xu, D.; Wan, X. *Org. Lett.* **2014,** *16,* 3312–3315. doi:10.1021/ol501312s
220. Guo, Y.; Wang, G.; Wei, L.; Wan, J.-P. *J. Org. Chem.* **2019,** *84,* 2984–2990. doi:10.1021/acs.joc.8b02897
221. Suen, Y. F.; Hope, H.; Nantz, M. H.; Haddadin, M. J.; Kurth, M. J. *J. Org. Chem.* **2005,** *70,* 8468–8471. doi:10.1021/jo051319a

License and Terms

This is an open access article licensed under the terms of the Beilstein-Institut Open Access License Agreement (https://www.beilstein-journals.org/bjoc/terms), which is identical to the Creative Commons Attribution 4.0 International License (https://creativecommons.org/licenses/by/4.0). The reuse of material under this license requires that the author(s), source and license are credited. Third-party material in this article could be subject to other licenses (typically indicated in the credit line), and in this case, users are required to obtain permission from the license holder to reuse the material.

The definitive version of this article is the electronic one which can be found at:
https://doi.org/10.3762/bjoc.20.178

BEILSTEIN JOURNAL OF ORGANIC CHEMISTRY

Cage-like microstructures via sequential Ugi reactions in aqueous emulsions

Rita S. Alqubelat, Yaroslava A. Menzorova and Maxim A. Mironov*

Letter

Open Access

Address:
Department of Technology for Organic Synthesis, Ural Federal University, Mira St. 19, Ekaterinburg, 620002, Russian Federation

Email:
Maxim A. Mironov* - m.a.mironov@urfu.ru

* Corresponding author

Keywords:
carboxymethylcellulose; chitosan; colloidosomes; Pickering emulsions; Ugi reaction

Beilstein J. Org. Chem. **2024,** *20,* 2078–2083.
https://doi.org/10.3762/bjoc.20.179

Received: 14 May 2024
Accepted: 06 August 2024
Published: 22 August 2024

This article is part of the thematic issue "Multicomponent reactions IV".

Associate Editor: T. J. J. Müller

© 2024 Alqubelat et al.; licensee Beilstein-Institut.
License and terms: see end of document.

Abstract

Cage-like microstructures were obtained in two steps by sequential Ugi reactions. At the first stage, submicron colloidal particles based on carboxymethylcellulose and chitosan with a domain structure were obtained in an aqueous suspension. In the second stage, the Ugi reaction was carried out on the surface of the Pickering emulsions with toluene. Removal of toluene and redissolution in water resulted in colloidosomes with large holes on the surface. Varying the cross-link density during the Ugi reaction made it possible to obtain structures with different hole sizes.

Introduction

Colloidosomes are microcapsules built on the basis of colloidal particles [1]. In the past 20 years, many methods have been proposed for the synthesis based on different particle types (inorganic, polymer, and composite) [2-4] and shape [5] (spheres, discs, and fibers). A distinctive feature of colloidosomes is the presence of pores, the sizes of which depend on the parameters of the original colloidal particles and the synthetic method [6]. Pores provide controlled permeability of these structures and open up rich opportunities for practical uses as catalysts, sorbents, and carriers of medicinal substances [7]. A particularly interesting area is the use of colloidosomes to model processes in living cells and produce artificial protocells [8,9]. The enlargement of pores on the surface of colloidosomes leads to structures that resemble microscopic cages [10]. Obtaining such cage-like structures is usually more complex than conventional colloidosomes and involves several stages. Pickering emulsions or polymer spheres coated with a monolayer of colloidal particles are used as initial templates for synthesis [11].

Thus, cage-like structures have been obtained using phase inversion in Pickering emulsions. The polystyrene particles were treated with sulfuric acid to form a surface layer of sulfonated polystyrene. These particles were then used to produce Pickering emulsions, which were transformed into large-pore structures when treated with an alcohol/water mixture [12]. Another method involves the formation of a double Pickering

emulsion using a microfluidic technique. Solidification of this structure and removal of the template resulted in the formation of nonspherical capsules with large openings [13]. The use of a polymer matrix that can swell in an organic solvent made it possible to obtain colloidosomes covered with fissures of a controlled size [10]. A simpler method recently proposed involves the self-assembly of starch granules on the surface of emulsion droplets. However, this approach did not allow the pore size to be controlled [14]. Thus, the currently available methods for obtaining cage-like structures are characterized by technical complexity, a multi-stage nature, and low yield of target structures.

To develop a one-step method for the synthesis of cage-like structures, it is necessary to control the deposition process of colloidal particles on the surface of emulsion droplets. As a rule, spherical particles of the same size form a uniform layer, one particle thick [5]. The soft microgel particles can deform when adsorbed onto the droplet surface and form a shield-like surface [15]. Nonspherical particles can form more complex 2D structures at the interface [16]. However, the relationship between the structure of the initial particles and the surface morphology of colloidosomes is not yet understood clearly enough. Quite often, there are cases where the number of colloidal particles is clearly insufficient to cover the surface of the droplets observed in stable Pickering emulsions. We also recently encountered this problem when we obtained Pickering emulsions stabilized by cellulose particles with an extremely low concentration, which would not have been enough to form a monolayer at the interface [17]. We assumed that in this case, a cage-like structure was formed on the surface of the oil droplets, such that the material was consumed more economically.

In this study, we present preliminary data that supports this assumption. Nonspherical particles with a raspberry-like domain structure spontaneously formed a cage-like structure on the surface of emulsion droplets. Fixing this structure with a cross-linker opened the way to the one-step synthesis of colloidosomes with large pores on the surface.

Results and Discussion

Previously, we have obtained stable colloidal particles by ionic gelation of carboxymethylcellulose (CMC) and low-molecular-weight chitosan in dilute aqueous solutions [17]. The use of this method led to the formation of particles with an average diameter in the range of 200–350 nm and with a domain structure. Domains of about 40 nm in size, consisting of CMC, were connected to each other by a soft material based on chitosan. Such structures existed only within a narrow pH range: when the pH value dropped below 5.5, the chitosan easily dissolved, and when the pH value was above 7, the CMC domains swelled and lost their properties. It is known that the Ugi reaction can be successfully used to obtain cross-linked gels based on polysaccharides [18]. Therefore, to stabilize such structures, the Ugi reaction in water was chosen, for which this particular pH value range is optimal [19]. The amino groups of chitosan and the carboxy groups of CMC reacted with each other and formed a stable structure that was no longer sensitive to changes in pH value. According to atomic force microscopy (AFM) data, the resulting particles had a domain structure and were similar in appearance to raspberries [20]. An interesting feature of the resulting particles was the high efficiency as Pickering emulsifiers: even at a concentration below 0.3 g/L, stable emulsions with linseed oil were obtained [17].

Analyzing the results obtained, we came to the conclusion that at a concentration of 0.3 g/L and with an average size of emulsion droplets of about 5 μm, the number of particles was insufficient to completely cover the surface of the droplets. In principle, two possible mechanisms were considered: (1) Soft CMC/chitosan gel particles interacted with the surface and flattened to form discs. (2) When particles were deposited on the surface, they did not completely cover it, forming a network. In this work, we tested these hypotheses and found arguments in favor of the second mechanism.

To identify the structure obtained on the surface of the droplets during the formation of the Pickering emulsion, we used fluorescent labels. Aminofluorescein was introduced into the CMC composition with a ratio of 3 mg per 1 g of cellulose using condensation in the presence of dicyclohexylcarbodiimide in dimethylformamide. The resulting product was precipitated with acetonitrile, dried, and redissolved in water. Fluorescein-labelled cellulose was used to produce submicron particles according to our previously described method via the Ugi reaction in water (Scheme 1) [17].

As before, depending on the CMC concentration, we obtained submicron particles with an average diameter from 200–600 nm, which were visible under an optical microscope in the form of luminous points. Next, Pickering emulsions were obtained by emulsifying toluene in an aqueous suspension of particles with a concentration of 0.3 g/L and a water/toluene ratio of 3:1. However, it was not possible to distinguish any details on the surface of the droplets using conventional and confocal microscopy (Figure 1). To do this, it was necessary to remove the solvent that interfered with obtaining a contrast image. In turn, removal of the solvent was possible only after cross-linking since otherwise, the structure would have collapsed upon drying.

Therefore, a second Ugi reaction was carried out after the particles had been deposited on the surface of the toluene droplets.

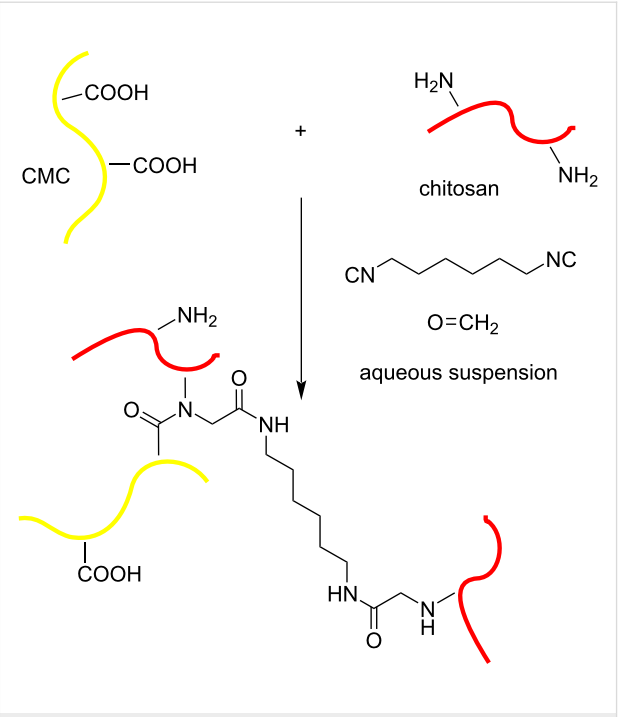

Scheme 1: Synthesis of cross-linked microgel labelled with aminofluorescein.

Thus, we carried out sequential Ugi reactions, the first to form colloidal particles and the second to consolidate the Pickering emulsion structure. In both cases, the same technique was used: a mixture of hexamethylene diisocyanide and formalin in acetonitrile was added dropwise into an aqueous suspension or emulsion at a ratio of 1:10 relative to the number of moles of amino groups in the chitosan. For the Ugi reaction to proceed to completion in water, it was ensured that the pH value did rise above 5.5. It should be noted that the reaction proceeded very quickly under these conditions, being completed within 2–3 min, which was monitored through the disappearance of isocyanide in the reaction medium using a color reaction [19]. Then the emulsion was applied to the glass surface and evaporated at a temperature of 50 °C. The resulting samples were analyzed using fluorescence microscopy at a wavelength of 490 nm.

After removing the solvent, the resulting structure could be easily identified using optical microscopy. They were cage-like microspheres with an average diameter corresponding to the diameter of droplets in the Pickering emulsion (Figure 2). The surface of the droplets was covered with a network of individual particles with holes of different diameter. It was likely that when deposited on the surface of the droplets, the particles stuck to each other, forming branched chains that gradually occupied all the available space.

This analysis confirmed incomplete coverage of the surface of droplets in the Pickering emulsions, which created a cage-like structure with a large distance between individual elements. At the same time, such a structure reliably protected against coalescence of individual droplets since Pickering emulsions obtained in this way were stable for a long time (more than one month). The formation of such structures opened up opportunities for the design of effective particle-based emulsifiers. The particles themselves consisted of 95–99% water. In addition, they did not completely cover the surface of the emulsion droplets. Therefore, the emulsifier consumption in terms of dry weight approached low-molecular-weight substances.

We used AFM to identify the structural features of the original colloidal particles. For this, colloidal particles were adsorbed on

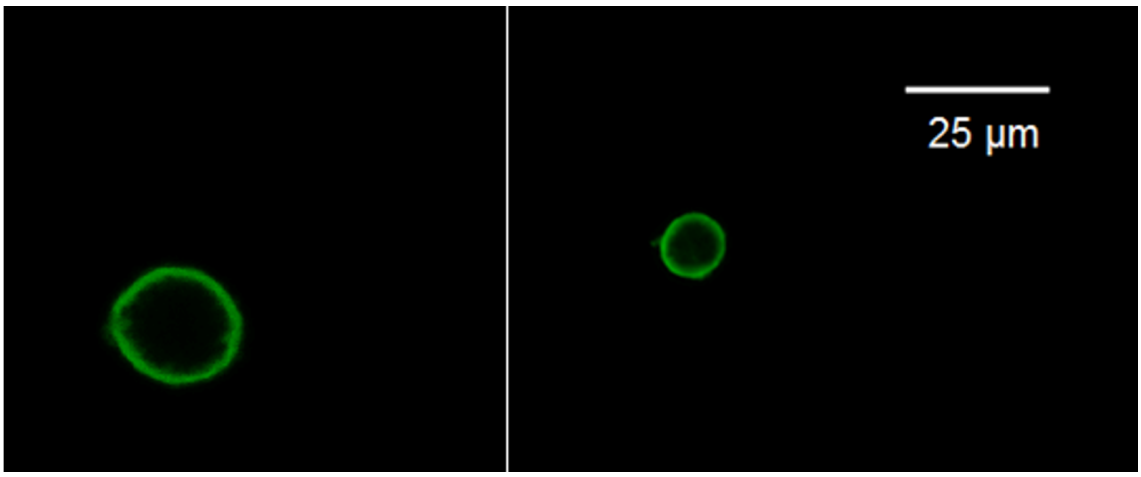

Figure 1: Single droplets of the Pickering emulsion attached to a glass surface.

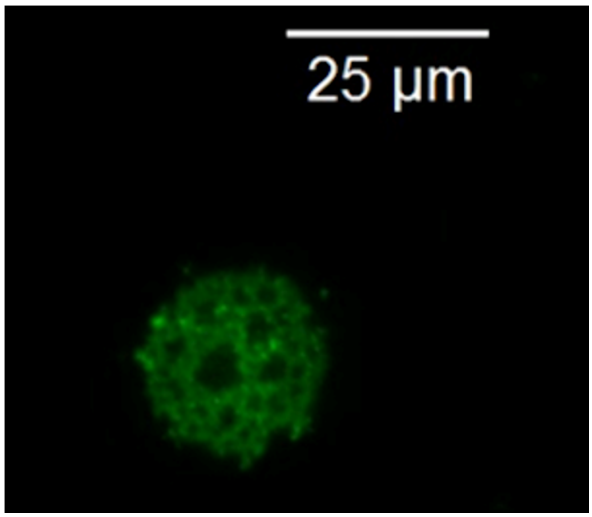

Figure 2: Cage-like microstructure obtained via sequential Ugi reactions.

the substrate surface and then analyzed without complete drying, which made it possible to reveal the initial microgel structure. Titration of CMC with hydrochloric acid, followed by treatment with a mixture of hexamethylene diisocyanide and formalin led to the formation of compact particles with an average diameter of 40–80 nm (Figure 3A). These particles were the main building blocks for the construction of cage-like structures. Following titration with a solution of low-molecular-weight chitosan and subsequent Ugi reaction, they formed agglomerates with a size of more than 500 nm that had a characteristic domain structure (Figure 3B).

These particles further interacted with each other on the surface of the droplets, forming a network. The repeated Ugi reaction resulted in the formation of a strong cage-like structure that was not destroyed upon removal of the solvent. We noticed a connection between the structure of the colloidal particles and their behavior at the interface. The developed surface of the particles, consisting of domains, promoted adhesion to each other and the formation of a network on the surface of the emulsion droplets. At the same time, the smooth surface of the particles contributed to the formation of a homogeneous monolayer at the phase interface.

To prove the influence of the structure of the colloidal particles on the formation of the surface in Pickering emulsions, we varied the conditions for their preparation. Specifically, we increased or decreased the cross-linking density using the Ugi reaction at the first (formation of colloidal particles) and second stages of the process (formation of a cage-like structure on the surface of emulsion droplets). Thus, when the amount of cross-linking agent at the second stage was halved to 5 mol % relative to chitosan, less durable microspheres were obtained. When the solvent was removed, they opened up, forming a cap-like structure (Figure 4A). An increase in the cross-linking density to 20 mol % at the first stage led to the formation of a denser packing of particles at the second stage of the process (Figure 4B). Supposedly, this was due to the large steric repulsion between the particles, which prevented the formation of chains on the surface of the emulsion droplets.

We also discovered that chitosan could be replaced by another polyamine in this synthesis, for example, polyvinylamine. In addition, the cellulose could be replaced by another polymer with carboxy groups, such as pectin. Thus, the scope of this synthesis can be significantly expanded in the future. These are the first examples showing how structure formation on the surface of emulsion droplets can be controlled by varying the

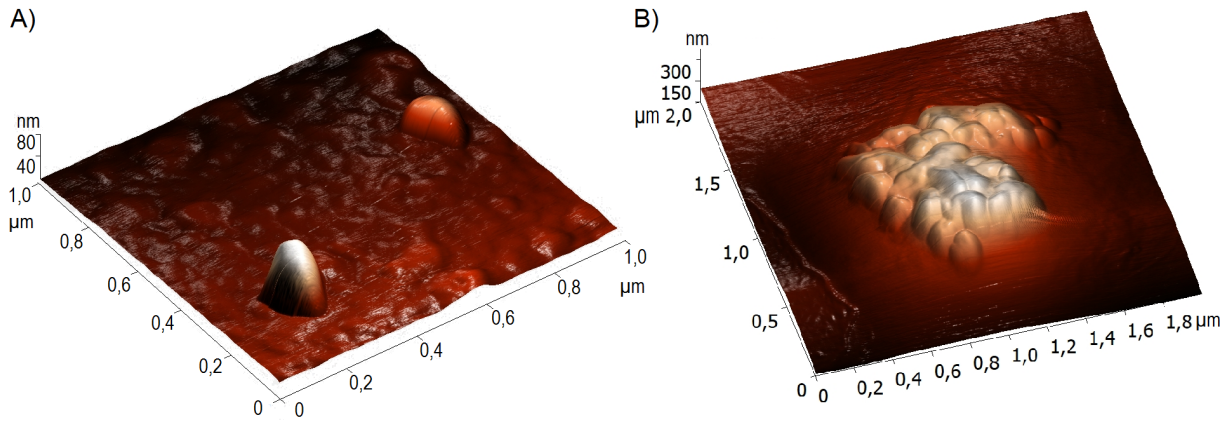

Figure 3: AFM images of A) single domains and B) cross-linked CMC/chitosan polymer particles.

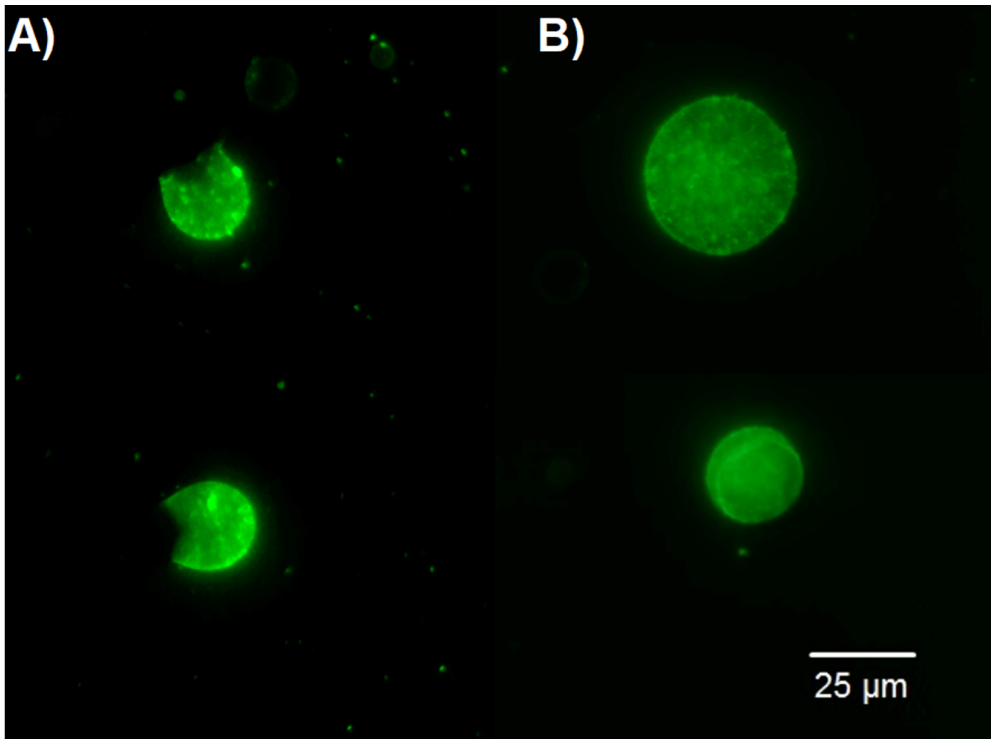

Figure 4: Variations of microstructures obtained via sequential Ugi reactions. A) Cap-like structures at 5 mol % cross-linking agent relative to chitosan at the second stage. B) Denser packing of particles at 20 mol % cross-linking density at the first stage.

conditions of the Ugi reaction. We are currently working to identify such dependencies and plan to publish the results of this work in the form of a full article.

Conclusion

In summary, we have proposed a convenient approach for the synthesis of cage-like structures from carboxymethylcellulose and chitosan using the Ugi reaction. At the first stage, colloidal particles with a characteristic domain structure reminiscent of raspberries were created. At the second stage of the synthesis, a network of these particles was formed on the surface of the Pickering emulsion droplets. Removal of the solvent and redissolution in water led to the target structures. The Ugi reaction in water was an ideal choice because it was characterized by high reaction rates over a narrow pH value range. This allowed to control the process of cage-like-structure formation. Changing the conditions of the Ugi reaction made it possible to obtain various structures, including cage- and cap-like structures, as well as hollow microspheres. Due to the developed surface, these materials have potential to be used as catalysts and sorbents. Further, these materials may be obtained in significant quantities since the method for the production is simple and does not include stages that are difficult to scale up. Thus, the method we have proposed has good prospects for practical application.

Supporting Information

Supporting Information File 1

Experimental data and optical microscopy data of the starting Pickering emulsions.
[https://www.beilstein-journals.org/bjoc/content/supplementary/1860-5397-20-179-S1.pdf]

Acknowledgements

The equipment of the Ural Center for Shared Use “Modern nanotechnology” Ural Federal University (Reg. No. 2968), which is supported by the Ministry of Science and Higher Education RF (Project No. 075-15-2021-677), was used for AFM investigations.

Funding

The authors thank the Russian Science Foundation for financial support (Grant 23-23-00125).

Author Contributions

Rita S. Alqubelat: conceptualization; data curation; investigation. Yaroslava A. Menzorova: formal analysis; investigation; project administration. Maxim A. Mironov: conceptualization;

data curation; formal analysis; funding acquisition; investigation; methodology; supervision; writing – original draft; writing – review & editing.

ORCID® iDs

Rita S. Alqubelat - https://orcid.org/0009-0008-2280-2190
Yaroslava A. Menzorova - https://orcid.org/0009-0000-7947-1806
Maxim A. Mironov - https://orcid.org/0009-0005-1851-0169

Data Availability Statement

The data that supports the findings of this study is available from the corresponding author upon reasonable request.

References

1. Dinsmore, A. D.; Hsu, M. F.; Nikolaides, M. G.; Marquez, M.; Bausch, A. R.; Weitz, D. A. *Science* **2002,** *298,* 1006–1009. doi:10.1126/science.1074868
2. Bollhorst, T.; Rezwan, K.; Maas, M. *Chem. Soc. Rev.* **2017,** *46,* 2091–2126. doi:10.1039/c6cs00632a
3. Thompson, K. L.; Williams, M.; Armes, S. P. *J. Colloid Interface Sci.* **2015,** *447,* 217–228. doi:10.1016/j.jcis.2014.11.058
4. Koroleva, M. Y.; Yurtov, E. V. *Russ. Chem. Rev.* **2022,** *91,* RCR5024. doi:10.1070/rcr5024
5. Ortiz, D. G.; Pochat-Bohatier, C.; Cambedouzou, J.; Bechelany, M.; Miele, P. *Engineering (Beijing, China)* **2020,** *6,* 468–482. doi:10.1016/j.eng.2019.08.017
6. Hsu, M. F.; Nikolaides, M. G.; Dinsmore, A. D.; Bausch, A. R.; Gordon, V. D.; Chen, X.; Hutchinson, J. W.; Weitz, D. A.; Marquez, M. *Langmuir* **2005,** *21,* 2963–2970. doi:10.1021/la0472394
7. Sun, Q.; Chen, J.-F.; Routh, A. F. *Expert Opin. Drug Delivery* **2019,** *16,* 903–906. doi:10.1080/17425247.2019.1652594
8. Park, J. H.; Galanti, A.; Ayling, I.; Rochat, S.; Workentin, M. S.; Gobbo, P. *Eur. J. Org. Chem.* **2022,** e202200968. doi:10.1002/ejoc.202200968
9. Wei, M.; Lin, Y.; Qiao, Y. *Giant* **2023,** *13,* 100143. doi:10.1016/j.giant.2023.100143
10. Xu, Z.; Hueckel, T.; Irvine, W. T. M.; Sacanna, S. *Chem. Mater.* **2023,** *35,* 6357–6363. doi:10.1021/acs.chemmater.3c01053
11. Rozynek, Z.; Józefczak, A. *Eur. Phys. J.: Spec. Top.* **2016,** *225,* 741–756. doi:10.1140/epjst/e2015-50267-7
12. Ge, X.; Ge, X.; Wang, M.; Liu, H.; Fang, B.; Li, Z.; Yang, C.; Li, G. *Colloid Polym. Sci.* **2012,** *290,* 1749–1757. doi:10.1007/s00396-012-2709-8
13. Lee, D.; Weitz, D. A. *Small* **2009,** *5,* 1932–1935. doi:10.1002/smll.200900357
14. Kierulf, A.; Mosleh, I.; Li, J.; Li, P.; Zarei, A.; Khazdooz, L.; Smoot, J.; Abbaspourrad, A. *Sci. Adv.* **2024,** *10,* eadi7069. doi:10.1126/sciadv.adi7069
15. Destribats, M.; Lapeyre, V.; Wolfs, M.; Sellier, E.; Leal-Calderon, F.; Ravaine, V.; Schmitt, V. *Soft Matter* **2011,** *7,* 7689–7698. doi:10.1039/c1sm05240c
16. Reynaert, S.; Moldenaers, P.; Vermant, J. *Langmuir* **2006,** *22,* 4936–4945. doi:10.1021/la060052n
17. Mensah, E. O.; Alqubelat, R. S.; Menzorova, Y. A.; Minin, A. S.; Mironov, M. A. *Colloids Surf., B* **2024,** *236,* 113827. doi:10.1016/j.colsurfb.2024.113827
18. Crescenzi, V.; Francescangeli, A.; Capitani, D.; Mannina, L.; Renier, D.; Bellini, D. *Carbohydr. Polym.* **2003,** *53,* 311–316. doi:10.1016/s0144-8617(03)00079-1
19. Shulepov, I. D.; Kozhikhova, K. V.; Panfilova, Y. S.; Ivantsova, M. N.; Mironov, M. A. *Cellulose* **2016,** *23,* 2549–2559. doi:10.1007/s10570-016-0957-3
20. Eren, E. D.; Moradi, M.-A.; Friedrich, H.; de With, G. *Nano Lett.* **2021,** *21,* 2232–2239. doi:10.1021/acs.nanolett.0c05059

License and Terms

This is an open access article licensed under the terms of the Beilstein-Institut Open Access License Agreement (https://www.beilstein-journals.org/bjoc/terms), which is identical to the Creative Commons Attribution 4.0 International License (https://creativecommons.org/licenses/by/4.0). The reuse of material under this license requires that the author(s), source and license are credited. Third-party material in this article could be subject to other licenses (typically indicated in the credit line), and in this case, users are required to obtain permission from the license holder to reuse the material.

The definitive version of this article is the electronic one which can be found at:
https://doi.org/10.3762/bjoc.20.179

BEILSTEIN JOURNAL OF ORGANIC CHEMISTRY

O,S,Se-containing Biginelli products based on cyclic β-ketosulfone and their postfunctionalization

Kateryna V. Dil[1,2] and Vitalii A. Palchykov*[1,§]

Full Research Paper

Open Access

Address:
[1]Research Institute of Chemistry and Geology, Oles Honchar Dnipro National University, Nauky Av. 72, Dnipro, 49045, Ukraine and [2]Enamine Ltd. (www.enamine.net), Winston Churchill Str. 78, Kyiv, 02094, Ukraine

Email:
Vitalii A. Palchykov* - palchikoff82@gmail.com

* Corresponding author
§ Web: https://palchykovchem.vercel.app

Keywords:
dihydropyrimidinone/thione/selenone; green chemistry; in silico biological profile; multicomponent reaction (MCR); thiopyrandioxide

Beilstein J. Org. Chem. **2024,** *20,* 2143–2151.
https://doi.org/10.3762/bjoc.20.184

Received: 14 May 2024
Accepted: 13 August 2024
Published: 27 August 2024

This article is part of the thematic issue "Multicomponent reactions IV".

Associate Editor: T. J. J. Müller

© 2024 Dil and Palchykov; licensee Beilstein-Institut.
License and terms: see end of document.

Abstract

A one-pot three-component Biginelli synthesis of dihydropyrimidinones/thiones/selenones via acetic acid or solvent-free $Yb(OTf)_3$-catalyzed tandem reaction of β-ketosulfone (dihydro-2*H*-thiopyran-3(4*H*)-one-1,1-dioxide), an appropriate urea, and arylaldehyde has been developed. The reaction proceeds with high chemo- and regioselectivity to give diverse DHPMs in reasonable yields up to 95%. Moreover, an SO_2-containing analogue of anticancer drug-candidate enastron (SO_2 vs C=O) was obtained by using the here reported method in gram scale. We also demonstrate the reactivity of the Biginelli product in various directions – synthesis of condensed thiazoles and tetrazoles. In silico assessment of ADMET parameters shows that most compounds meet the lead-likeness requirements. The biological profiles of new compounds demonstrate high probability levels of activity against the following pathogens/diseases: *Candida albicans, Alphis gossypii, Tripomastigote Chagas, Tcruzi amastigota, Tcruzi epimastigota, Leishmania amazonensis,* and *Dengue larvicida.*

Introduction

Multicomponent reactions (MCRs) are the key methodology to access valuable heterocycles for medicinal chemistry projects. The classical Biginelli reaction (1893) is an acid-catalyzed, three-component reaction between an aldehyde, β-ketoester, and urea that produces 3,4-dihydropyrimidin-2(1*H*)-ones, also known as DHPMs (Scheme 1A). This reaction is believed to be one of the most famous MCRs with >2000 papers published in the last 20 years (according to Scopus database). These MCRs allow the direct synthesis of known DHMP drugs such as monastrol, piperastrol, enastron, fluorastrol etc. (Scheme 1B) and dozens of highly bioactive compounds with anticancer, antihypertensive, antiinflammatory, antioxidant, antimicrobial, antifungal, antimalarial, antitubercular, antidiabetic, antifilarial, anti-Alzheimer, antiepileptics and other activities [1-11]. The

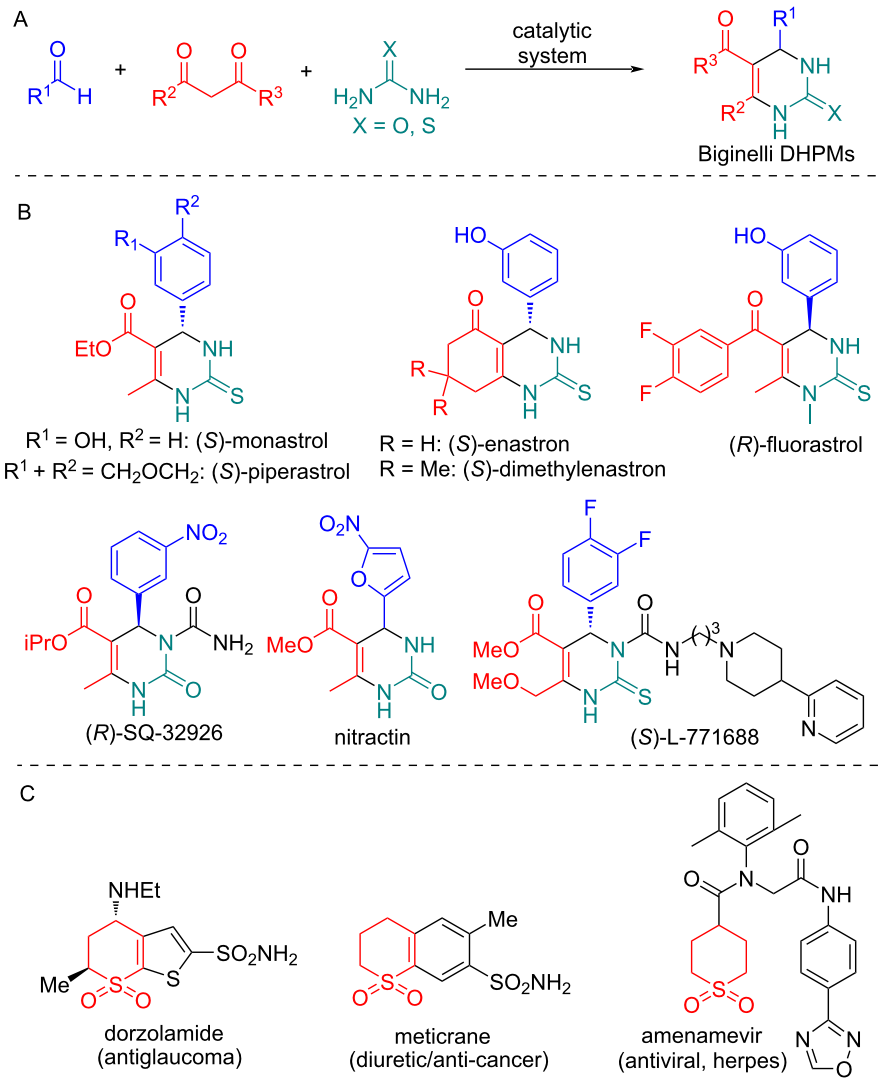

Scheme 1: The general Biginelli reaction (A) and examples of DHMP (B) and thiopyran-1,1-dioxide (C) containing drugs.

concept of "privileged structures" in medicinal chemistry highlights derivatives capable of interacting with multiple receptors or enzymes, making them ideal candidates for drug discovery. Dihydropyrimidinones (DHPMs) and their derivatives are particularly noteworthy within this category. Accordingly, their synthesis is of significant interest for organic and medicinal chemists. DHPMs are found in a variety of marine-sourced alkaloids, which are essential for creating biologically active natural products [10]. Some of the DHPM derivatives are also known as functional polymers, adhesives, and fabric dyes [8,12].

In recent decades, the scope of the original Biginelli reaction shown in Scheme 1A was significantly extended by variation of the 1,3-dicarbonyl-containing building blocks. Many groups have elegantly demonstrated the synthetic versatility of numerous enolizable carbonyl components, including β-keto esters, cyclic/acyclic β-diketones, β-keto amides, coumarins, alicyclic ketones, β-ketophosphonates, α-nitroketones, curcumin, and barbituric acid derivatives [1,2,8,9]. We analyzed a number of Biginelli-type products and publications and concluded that Se-containing DHPMs among the rarest examples and, in addition to this, ketosulfones have never been used as enolizable carbonyl component in this chemistry. To the best of our knowledge only one compound from the target group was published (2003) [13] before this work, however, without any spectral evidence (Figure 1).

Considering our constant interest in the development of methods for the synthesis of new S-heterocyclic systems we tried to combine the broad synthetic potential of Biginelli condensation and high reactivity β-ketosulfone **1** (dihydro-2*H*-

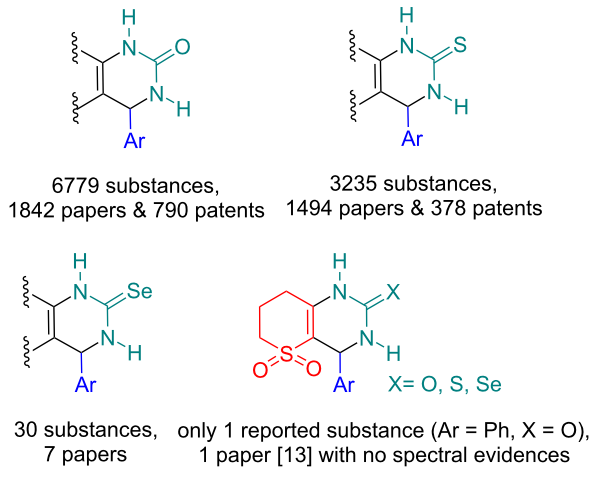

Figure 1: Number of aryl-substituted Biginelli-type products and publications as analyzed by Reaxys database. The search was performed using depicted substructures "on all atoms" (May 2024).

thiopyran-3(4*H*)-one-1,1-dioxide) in various condensation reactions [14-20]. It was also worth mentioning that the thiopyran-1,1-dioxide motif is presented in a number of biologically active compounds including important market drugs as antiglaucoma agent dorzolamide [21], diuretic/anticancer meticrane [22] and antiherpesvirus agent amenamevir (ASP-2151) [23] which was recently synthesized by Ugi-4CR [24] (Scheme 1C).

Results and Discussion

Reaction optimization

Over the past two decades more than 300 various catalytic systems have been proposed for Biginelli chemistry, e.g., simple inorganic and organic acids, metal salts, metal oxides, ionic liquids, phosphines, nanocatalysts, organocatalysts, ion exchange resins [1,4,9] or even visible light-driven methods [25-28].

We started our study from the optimization of the reaction conditions using β-ketosulfone **1**, benzaldehyde and thiourea as model reaction. According to the literature, the reaction has been shown to work best and most efficiently under acidic conditions since such conditions enhance the selectivity, so various catalysts, mainly acidic, were tested for the model Biginelli reaction and the results are shown in Table 1.

Table 1: Optimization of reaction.

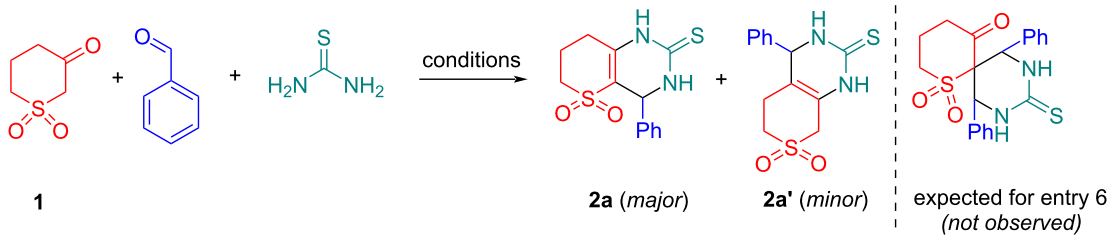

1 | **2a** (*major*) | **2a'** (*minor*) | expected for entry 6 (*not observed*)

Entry	Conditions[a]	Isolated yield **2a** + **2a'**, %	Isomer ratio, **2a:2a'**
1	0.8 equiv NaI, 0.8 equiv TMSCl, MeCN, 22 °C, 4 h	traces	n.d.
2	4 equiv TMSCl, DMF, 60 °C, 14 h	traces	n.d.
3	4 equiv TMSCl, DMF, –20 °C, 5 days	23	2:1
4	4 equiv TMSCl, DMF, 22 °C, 3 days	59	2:1.2
5	4 equiv TMSCl, DMF/MeCN (1:1), 22 °C, 2 days	51	3:1
6[b]	3 equiv TMSCl, DMF, 22 °C, 5 days	72	2:1
7	3 equiv HCl, EtOH, 82 °C, 6 h	23	1:0
8	10 mol % *p*-TsOH, MeOH, 82 °C, 36 h	35	1:0
9	10 mol % CAN, EtOH, 82 °C, 18 h	32	1:0
10	10 mol % $SrCl_2 \cdot 6H_2O$, EtOH, 82 °C, 18 h	8	1:0
11	10 mol % $La(NO_2)_3 \cdot 6H_2O$, solvent-free, 82 °C, 18 h	61	1:0
12[c]	**10 mol % $Yb(OTf)_3$, solvent-free, 140 °C, 6 h**	**65**	**1:0**
13[c]	AcOH, 110 °C, 14 h	68	1:0
14	AcOH, 82 °C, 14 h	40	1:0
15	AcOH, 110 °C, 4 h	71	1:0

Table 1: Optimization of reaction. (continued)

16[c]	**AcOH, 110 °C, 4 h**	**74**	**1:0**
17[d]	TFA, 110 °C, 14 h	45	1:0
18[c]	AcOH, MW (300 W), 120 °C, 20 min	36	1:0

[a]Unless specifically stated the ratio of ketosulfone/benzaldehyde/thiourea 1:1:1 (1 mmol scale); [b]ketosulfone (1 mmol, 1 equiv), benzaldehyde (2 mmol, 2 equiv), thiourea (1 mmol, 1 equiv); [c]ketosulfone (1 mmol, 1 equiv), benzaldehyde (1 mmol, 1 equiv), thiourea (1.2 mmol, 1.2 equiv); [d]ketosulfone (1 mmol, 1 equiv), benzaldehyde (1 mmol, 1 equiv), thiourea (3 mmol, 3 equiv).

One of the most effective promoters for this type of reaction is TMSCl [29-31] and we also tried to involve TMSCl in our study (Table 1, entries 1–6), but in any case, we received a mixture of regioisomeric products **2a**/**2a'** (3:1 to 2:1) confirmed by 2D NMR spectroscopy (see Supporting Information File 1, Figures S1–S6). Classical conditions for Biginelli reaction (reflux in ethanolic HCl) gave only 23% yield (Table 1, entry 7). Reflux in alcoholic media in the presence of *p*-toluenesulfonic acid or CAN (ceric ammonium nitrate) was also not particularly successful (Table 1, entries 8 and 9, yield 32–35%). We subsequently explored a range of reaction conditions to improve overall yield and selectivity. We experimented with Lewis acids (Table 1, entries 10–12) to catalyze the reaction and observe low conversion with $SrCl_2$. The reaction was significantly better with both $La(NO_2)_3$ and $Yb(OTf)_3$ under solvent-free conditions (Table 1, entries 11 and 12, yield 61–65%). The most promising results were obtained by using simplest heating in acetic acid (Table 1, entries 13–16). After some playing with temperature, reaction time, and ratio of starting reagents we ultimately found conditions (AcOH, 110 °C, 4 h) suitable best for our chemistry and leading to the yield of the target product **2a** 74% (Table 1, entry 16). However, increasing acidity and using trifluoroacetic acid (Table 1, entry 17) did not improve the overall yield. We also tried microwave activation conditions since this is a known technique for reactions of this type [32], but unfortunately, we did not find any improvement in the yield (Table 1, entry 18).

Reaction scope

We then used optimized reaction conditions from Table 1, entry 16 (method A) and 12 (method B) to further explore the scope of the reaction (Scheme 2). By employing various EWG/EDG-substituted benzaldehydes and urea/thiourea/selenourea we synthesized novel Biginelli products **2a**–**q** with up to 95% yield. The use of selenourea has been shown to give low yields of products (up to 33%). In fact, we have thus expanded the range of available selenium-containing DHPMs in addition to the work of other authors [33-35].

We also attempted to replace urea/thiourea/selenourea with *N*-alkyl/aryl-substituted analogues, and aldehyde component switch to heteroaromatic (2-pyridinaldehyde) and aliphatic (iPrCHO, cinnamaldehyde). Unfortunately, we failed in both replacements and were unable to obtain any reasonable products. The list of unsuccessful reagents is shown in Figure S7 (see Supporting Information File 1).

Next, we paid attention to testing the conditions we developed for the synthesis of the SO_2-containing analogue **2r** of potent anticancer drug enastron in gram scale (Scheme 3). Enastron is a novel dihydropyrimidine-based mitotic kinesin spindle protein KSP/Eg5 inhibitor [36]. We hope that compound **2r** and its analogues obtained in this work can be further deeply studied by in silico and in vitro methods to discover the compound most suitable for clinical trials.

The structures of the synthesized compounds **2a**–**r** were confirmed by spectral data. The ^{1}H NMR spectra of the obtained products are characterized by the following signals: aromatic ring protons (6.25–8.23 ppm), Ar–CH group proton singlet (5.13–5.44 ppm), broadened NH singlets (7.78–10.89 ppm), as well as the corresponding signals of successive 3 × CH_2 groups of the sulfone fragment (2.18–3.34 ppm). Such a set of signals clearly corresponds to the heterocycles depicted above. Figure S8 (see Supporting Information File 1) shows ^{1}H NMR spectra for Ph-substituted O,S,Se-DHPMs **2a,h,o**. It can be seen from them that when going from oxygen to selenium (**2h**→**2a**→**2o**), the signals of both NH groups shift to down field (7.87/9.26→9.75/10.50→10.26/10.85 ppm) and become more equivalent (Δδ = 1.39→0.75→0.59 ppm accordingly). The key signal in the ^{13}C NMR spectra is located in the regions 174.04–174.69 ppm (C=S), 151.44–151.86 ppm (C=O), and 170.15–170.91 ppm (C=Se) accordingly.

Utilization of reaction products

The Biginelli reaction is the traditional method for synthesizing DHPM scaffolds, but it faces limitations in product diversity. To overcome these challenges, two main strategies have been developed. The first strategy involves modifying the conventional components of the Biginelli chemistry, while the second focuses on the postmodification of the Biginelli products [2]. Both approaches were tested in this work. We used Hantzsch-

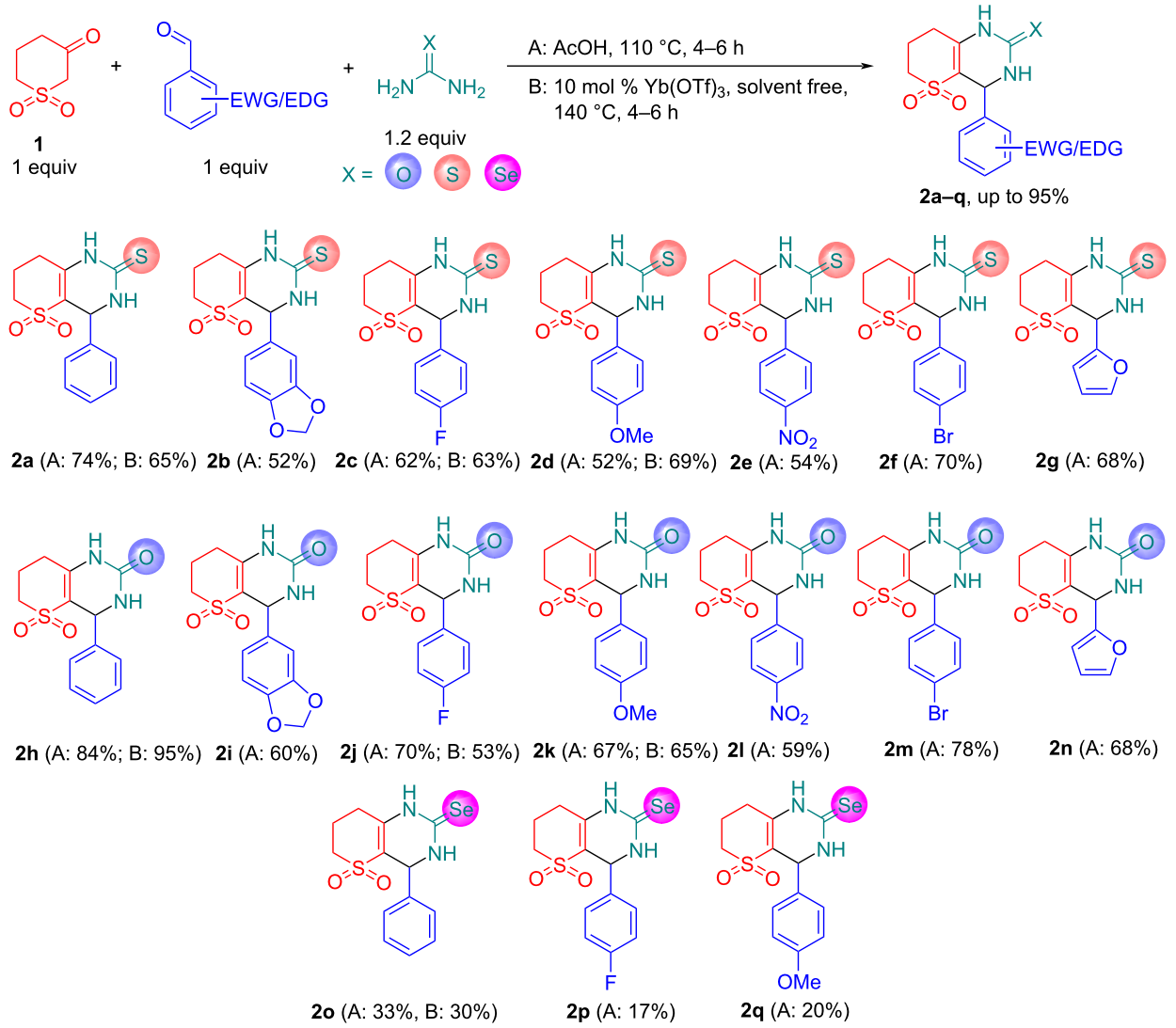

Scheme 2: Scope of the obtained Biginelli products **2a–q**.

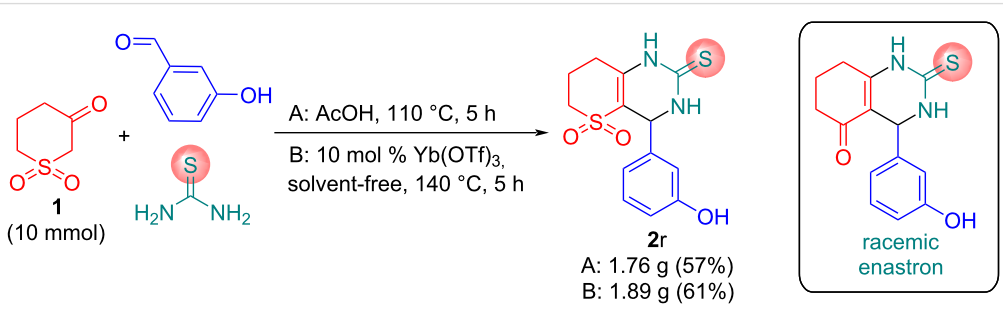

Scheme 3: Synthesis of SO_2-containing enastron analogue **2r**.

type thiazole synthesis for postmodification of product **2a**. By employing 2-bromoacetophenone, bromomalononitrile and 2-bromo-1-tetralone we obtained condensed thiazoles **3**–**5** in 67–88% yields using slightly modified methods described [37-39]. We also applied desulfurization to obtain products **6** and **7** [40,41] (Scheme 4).

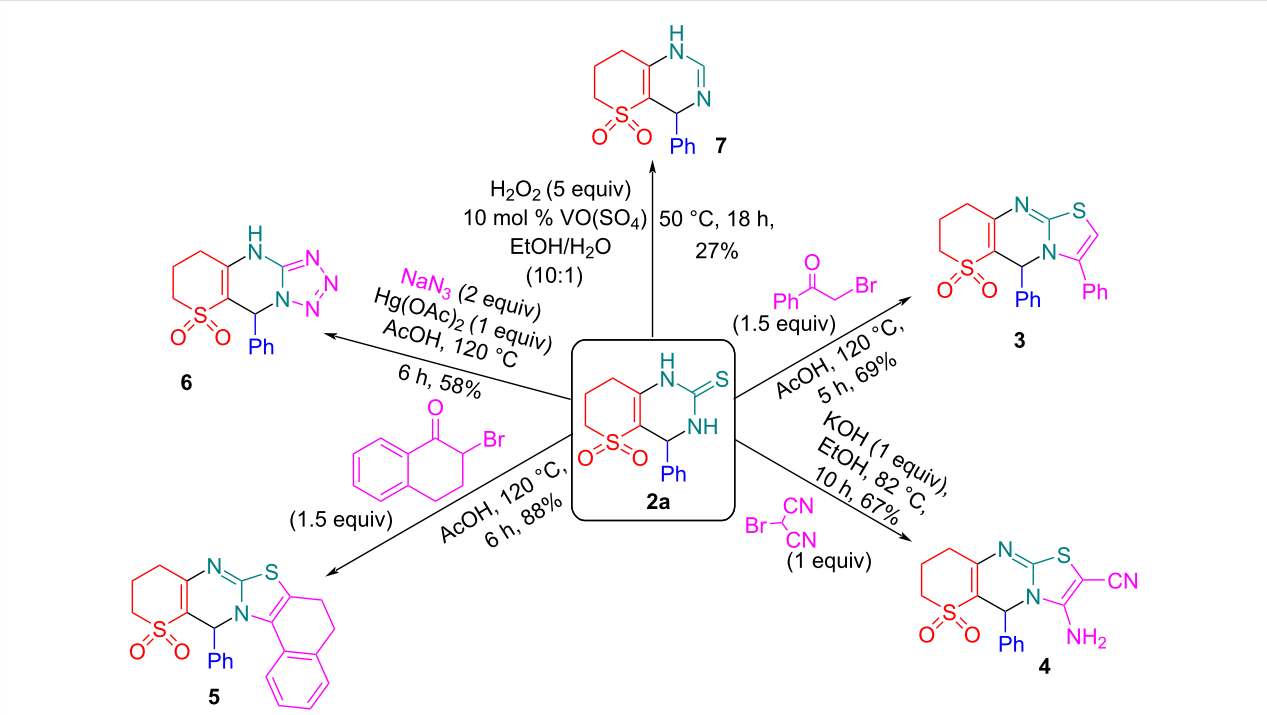

Scheme 4: Postmodification of the Biginelli product **2a**.

While the Hantzsch thiazole synthesis is well documented from a synthetic and mechanistic point [42,43] and do not need discussion, more desulfurizations and oxidations of rare Biginelli products are discussed in Supporting Information File 1 using compound **2a** as an example.

In silico evaluation of ADMET parameters and biological profile

We performed in silico screening of the biological properties of Biginelli products **2a**–**r** and their postfunctionalized derivatives **3**–**7** using SwissADME (http://www.swissadme.ch) [44], ProTox 3.0 (https://tox-new.charite.de) [45], and MolPredictX (https://www.molpredictx.ufpb.br) [46] free online software. Considering ADMET [47] and other crucial properties, we found that all compounds (except for the nitro derivative **2e**) do not violate the Lipinski, Ghose, Veber, Egan, and Muegge rules and PAINS filter [48-52]. The lipophilicity (estimated as log $P_{o/w}$) for all compounds was shown to be in a wide range from 0.43 to 4.11. The topological polar surface area (TPSA), which is important for oral bioavailability, was found to be 67–129 Å^2 for all compounds except products **4** and **2e**. None of the compounds penetrate the BBB (blood–brain barrier) except for seleno-**2p** and desulfurized product **7**. Regarding water solubility, we can conclude that all compounds are either soluble or moderately soluble. For more details, see Supporting Information File 1 (Table S1). To visualize the lead-likeness of compounds **2a**–**r**, **3**–**7**, we utilized the free online software LLAMA (https://llama.leeds.ac.uk) [53], which showed that 70% of the products (16 of 23) fall within the specific lead-like space (Figure 2).

We then used the free online software ProTox 3.0 for computational toxicity assessment of the products as their LD_{50} values. The tested compounds mainly belong to the 4th class of acute oral toxicity with 300 < LD_{50} ≤ 2000 mg/kg. In addition, we used MolPredictX (https://www.molpredictx.ufpb.br) [46] to evaluate potential biotargets (pathogens, species, diseases) for new synthesized compounds. If we focus on high levels of biological activity probability (80% and above), the following pathogens and diseases may be potential areas of interest: *Alphis gossypii, Tripomastigote Chagas, Candida albicans, Tcruzi amastigota, Leishmania amazonensis, Tcruzi epimastigota, Dengue larvicida,* and for selected cases *Alzheimer* and *Sars-COVID.* For more details, see Table S1 (Supporting Information File 1).

Conclusion

In summary, we have demonstrated the catalytic regioselective Biginelli synthesis of new S-heterocyclic systems – 4-aryl-4,6,7,8-tetrahydro-1*H*-thiopyrano[3,2-*d*]pyrimidine-2(3*H*)-one/thione/selenone 5,5-dioxides and some of their derivatives. Furthermore, this methodology was successfully applied for the synthesis of the SO_2-containing analogue of the anticancer drug-candidate enastron (SO_2 vs C=O), and we believe a multi-

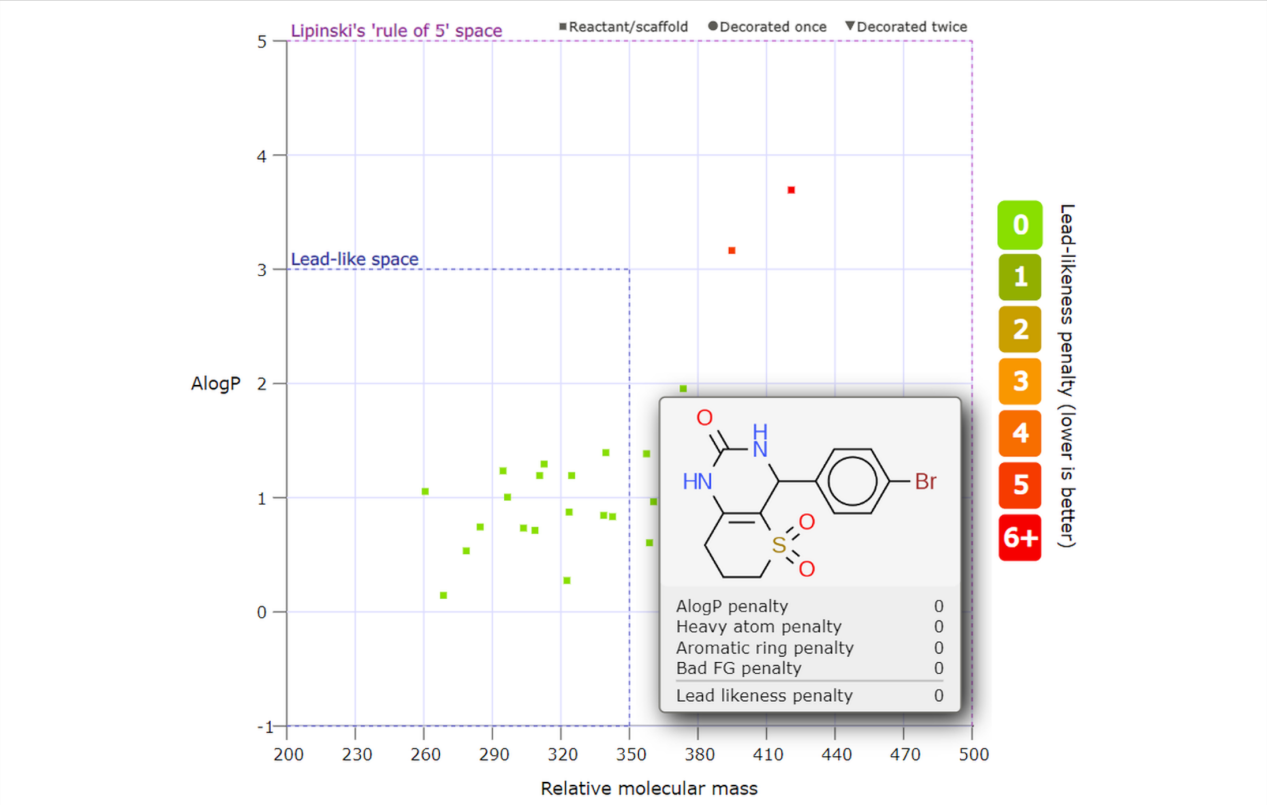

Figure 2: Distribution of compounds **2a–r**, **3–7** (log *P* (*y*)–MW (*x*)) through LLAMA software. The chemical structure of a representative compound **2m** is shown.

tude of other sulfones of both synthetic and biological importance can be obtained by using the in this work reported efficient, multicomponent and green protocol. We postfunctionalized the typical Biginelli product using Hantzsch-type thiazole chemistry and desulfurization. Assessing drug-likeness, we found that most of the synthesized compounds correspond to the parameters established by the Lipinski, Ghose, Veber, Egan, and Muegge rules. In silico screening of their biological profiles indicated that these new derivatives fall into the 4th class of acute toxicity. Additionally, they exhibit potential high activity against diseases associated with these species: *Alphis gossypii, Tripomastigote Chagas, Candida albicans, Tcruzi amastigota, Leishmania amazonensis, Tcruzi epimastigota, Dengue larvicida,* and for selected cases *Alzheimer* and *Sars-COVID.*

Supporting Information

Supporting Information File 1

Experimental procedures and characterization data of new compounds.
[https://www.beilstein-journals.org/bjoc/content/supplementary/1860-5397-20-184-S1.pdf]

Acknowledgements

The authors are grateful to Enamine Ltd. (Kyiv, Ukraine) for NMR/HRMS support. The authors also thank Charite University of Medicine, Germany (Institute for Physiology, Structural Bioinformatics Group), Federal University of Paraíba, Brazil (Laboratory of Cheminformatics), University of Lausanne, Switzerland (SIB Swiss Institute of Bioinformatics), and the University of Leeds, UK (School of Chemistry) for free online cheminformatics software. V.A.P. would like to express special thanks to the Matsumae International Foundation for financial support for the presentation of this work at the 15th International Kyoto Conference on New Aspects of Organic Chemistry (IKCOC-15, November 20–23, 2023, Kyoto, Japan). In addition, last but not least, we thank all brave defenders of Ukraine that made finalizing this work possible.

Funding

This work was partially supported by the Ministry of Education and Science of Ukraine (project 0122U001220).

Author Contributions

Kateryna V. Dil: investigation. Vitalii A. Palchykov: conceptualization; funding acquisition; methodology; supervision; writing – review & editing.

ORCID® iDs

Kateryna V. Dil - https://orcid.org/0000-0001-6659-6298
Vitalii A. Palchykov - https://orcid.org/0000-0003-3748-4566

Data Availability Statement

The data that supports the findings of this study is available from the corresponding author upon reasonable request.

References

1. Faizan, S.; Roohi, T. F.; Raju, R. M.; Sivamani, Y.; BR, P. K. *J. Mol. Struct.* **2023,** *1291,* 136020. doi:10.1016/j.molstruc.2023.136020
2. Sánchez-Sancho, F.; Escolano, M.; Gaviña, D.; Csáky, A. G.; Sánchez-Roselló, M.; Díaz-Oltra, S.; del Pozo, C. *Pharmaceuticals* **2022,** *15,* 948. doi:10.3390/ph15080948
3. Marinescu, M. *Molecules* **2021,** *26,* 6022. doi:10.3390/molecules26196022
4. Chopda, L. V.; Dave, P. N. *ChemistrySelect* **2020,** *5,* 5552–5572. doi:10.1002/slct.202000742
5. Costanzo, P.; Nardi, M.; Oliverio, M. *Eur. J. Org. Chem.* **2020,** 3954–3964. doi:10.1002/ejoc.201901923
6. Mohammadi, B.; Behbahani, F. K. *Mol. Diversity* **2018,** *22,* 405–446. doi:10.1007/s11030-017-9806-z
7. Kaur, R.; Chaudhary, S.; Kumar, K.; Gupta, M. K.; Rawal, R. K. *Eur. J. Med. Chem.* **2017,** *132,* 108–134. doi:10.1016/j.ejmech.2017.03.025
8. Nagarajaiah, H.; Mukhopadhyay, A.; Moorthy, J. N. *Tetrahedron Lett.* **2016,** *57,* 5135–5149. doi:10.1016/j.tetlet.2016.09.047
9. Suresh; Sandhu, J. S. *ARKIVOC* **2012,** No. i, 66–133. doi:10.3998/ark.5550190.0013.103
10. Matos, L. H. S.; Masson, F. T.; Simeoni, L. A.; Homem-de-Mello, M. *Eur. J. Med. Chem.* **2018,** *143,* 1779–1789. doi:10.1016/j.ejmech.2017.10.073
11. Palchykov, V.; Manko, N.; Finiuk, N.; Pokhodylo, N. *Ukr. Biochem. Zh.* **2022,** *94,* 64–74. doi:10.15407/ubj94.01.064
12. Zhao, Y.; Wu, H.; Wang, Z.; Wei, Y.; Wang, Z.; Tao, L. *Sci. China: Chem.* **2016,** *59,* 1541–1547. doi:10.1007/s11426-016-0219-4
13. Abelman, M. M.; Smith, S. C.; James, D. R. *Tetrahedron Lett.* **2003,** *44,* 4559–4562. doi:10.1016/s0040-4039(03)00985-7
14. Palchykov, V. A.; Dil, K. V.; Okovytyy, S. I. *J. Chem. Technol.* **2023,** *31,* 411–418. doi:10.15421/jchemtech.v31i2.126304
15. Dil, K. V.; Kozyriev, Y. K.; Palchykov, V. A. *Chem. Pap.* **2023,** *77,* 7249–7254. doi:10.1007/s11696-023-03006-9
16. Pokhodylo, N. T.; Tupychak, M. A.; Palchykov, V. A. *Synth. Commun.* **2020,** *50,* 1835–1844. doi:10.1080/00397911.2020.1757113
17. Shyyka, O. Y.; Pokhodylo, N. T.; Palchykov, V. A.; Finiuk, N. S.; Stoika, R. S.; Obushak, M. D. *Chem. Heterocycl. Compd.* **2020,** *56,* 793–799. doi:10.1007/s10593-020-02732-2
18. Kozirev, E. K.; Palchykov, V. A. *Chem. Heterocycl. Compd.* **2019,** *55,* 349–351. doi:10.1007/s10593-019-02463-z
19. Chabanenko, R. M.; Mykolenko, S. Yu.; Kozirev, E. K.; Palchykov, V. A. *Synth. Commun.* **2018,** *48,* 2198–2205. doi:10.1080/00397911.2018.1486427
20. Palchykov, V. A.; Chabanenko, R. M.; Konshin, V. V.; Dotsenko, V. V.; Krivokolysko, S. G.; Chigorina, E. A.; Horak, Y. I.; Lytvyn, R. Z.; Vakhula, A. A.; Obushak, M. D.; Mazepa, A. V. *New J. Chem.* **2018,** *42,* 1403–1412. doi:10.1039/c7nj03846a
21. Fekri, S.; Rabiei, A.; Hooshmandi, S.; Nouri, H.; Abtahi, S.-H. *Int. Ophthalmol.* **2024,** *44,* 101. doi:10.1007/s10792-024-03005-z
22. Wang, Y.; Sharma, A.; Ge, F.; Chen, P.; Yang, Y.; Liu, H.; Liu, H.; Zhao, C.; Mittal, L.; Asthana, S.; Schmidt-Wolf, I. G. H. *Front. Oncol.* **2023,** *13,* 1157366. doi:10.3389/fonc.2023.1157366
23. Kawashima, M.; Watanabe, D.; Fujio, K.; Komazaki, H. *J. Dermatol.* **2023,** *50,* 311–318. doi:10.1111/1346-8138.16608
24. Li, X.; Zarganes-Tzitzikas, T.; Kurpiewska, K.; Dömling, A. *Green Chem.* **2023,** *25,* 1322–1325. doi:10.1039/d2gc04869h
25. Mohamadpour, F. *Sci. Rep.* **2023,** *13,* 10262. doi:10.1038/s41598-023-37526-x
26. Mohamadpour, F. *ACS Omega* **2022,** *7,* 8429–8436. doi:10.1021/acsomega.1c05808
27. Gadkari, Y. U.; Hatvate, N. T.; Takale, B. S.; Telvekar, V. N. *New J. Chem.* **2020,** *44,* 8167–8170. doi:10.1039/d0nj01351j
28. Devthade, V.; Kamble, G.; Ghugal, S. G.; Chikhalia, K. H.; Umare, S. S. *ChemistrySelect* **2018,** *3,* 4009–4014. doi:10.1002/slct.201800591
29. Zhu, Y.; Pan, Y.; Huang, S. *Synth. Commun.* **2004,** *34,* 3167–3174. doi:10.1081/scc-200028607
30. Ryabukhin, S. V.; Plaskon, A. S.; Ostapchuk, E. N.; Volochnyuk, D. M.; Tolmachev, A. A. *Synthesis* **2007,** 417–427. doi:10.1055/s-2007-965881
31. Zhu, Y.-l.; Huang, S.-l.; Pan, Y.-j. *Eur. J. Org. Chem.* **2005,** 2354–2367. doi:10.1002/ejoc.200400845
32. Heravi, M. M.; Ghavidel, M.; Heidari, B. *Curr. Org. Synth.* **2016,** *13,* 569–600. doi:10.2174/1570179413666151218202307
33. Fouda, A. M.; Assiri, M. A.; Ali, T. E. *Phosphorus, Sulfur Silicon Relat. Elem.* **2020,** *195,* 324–330. doi:10.1080/10426507.2019.1694023
34. Mohammadi, B.; Behbahani, F. K.; Marandi, G. B.; Mirza, B. *Phosphorus, Sulfur Silicon Relat. Elem.* **2021,** *196,* 54–60. doi:10.1080/10426507.2020.1800702
35. Chen, P.; Tu, M. *Tetrahedron Lett.* **2018,** *59,* 987–990. doi:10.1016/j.tetlet.2018.01.070
36. Bouzina, A.; Bouone, Y. O.; Sekiou, O.; Aissaoui, M.; Ouk, T.-S.; Djemel, A.; Mansouri, R.; Ibrahim-Ouali, M.; Bouslama, Z.; Aouf, N.-E. *RSC Adv.* **2023,** *13,* 19567–19584. doi:10.1039/d3ra02904b
37. Nemr, M. T. M.; Teleb, M.; AboulMagd, A. M.; El-Naggar, M. E.; Gouda, N.; Abdel-Ghany, A. A.; Elshaier, Y. A. M. M. *J. Mol. Struct.* **2023,** *1272,* 134216. doi:10.1016/j.molstruc.2022.134216
38. Nagarajaiah, H. M.; Khazi, I. A.; Begum, N. S. *J. Chem. Sci.* **2015,** *127,* 467–479. doi:10.1007/s12039-015-0797-y
39. Banothu, J.; Khanapur, M.; Basavoju, S.; Bavantula, R.; Narra, M.; Abbagani, S. *RSC Adv.* **2014,** *4,* 22866–22874. doi:10.1039/c4ra02514h
40. Wang, X.-C.; Wei, Y.; Da, Y.-X.; Zhang, Z.; Quan, Z.-J. *Heterocycles* **2011,** *83,* 2811–2822. doi:10.3987/com-11-12351
41. Kim, S. S.; Choi, B. S.; Lee, J. H.; Lee, K. K.; Lee, T. H.; Kim, Y. H.; Shin, H. *Synlett* **2009,** 599–602. doi:10.1055/s-0028-1087920
42. Ali, S. H.; Sayed, A. R. *Synth. Commun.* **2021,** *51,* 670–700. doi:10.1080/00397911.2020.1854787
43. Duc, D. X.; Chung, N. T. *Curr. Org. Synth.* **2022,** *19,* 702–730. doi:10.2174/1570179419666220216122637
44. Daina, A.; Michielin, O.; Zoete, V. *Sci. Rep.* **2017,** *7,* 42717. doi:10.1038/srep42717
45. Banerjee, P.; Eckert, A. O.; Schrey, A. K.; Preissner, R. *Nucleic Acids Res.* **2018,** *46,* W257–W263. doi:10.1093/nar/gky318

46. Tullius Scotti, M.; Herrera-Acevedo, C.; Barros de Menezes, R. P.; Martin, H.-J.; Muratov, E. N.; Ítalo de Souza Silva, Á.; Faustino Albuquerque, E.; Ferreira Calado, L.; Coy-Barrera, E.; Scotti., L. *Mol. Inf.* **2022,** *41,* 10.1002/minf.202200133. doi:10.1002/minf.202200133
47. Guan, L.; Yang, H.; Cai, Y.; Sun, L.; Di, P.; Li, W.; Liu, G.; Tang, Y. *Med. Chem. Commun.* **2019,** *10,* 148–157. doi:10.1039/c8md00472b
48. Lipinski, C. A.; Lombardo, F.; Dominy, B. W.; Feeney, P. J. *Adv. Drug Delivery Rev.* **2001,** *46,* 3–26. doi:10.1016/s0169-409x(00)00129-0
49. Ghose, A. K.; Viswanadhan, V. N.; Wendoloski, J. J. *J. Comb. Chem.* **1999,** *1,* 55–68. doi:10.1021/cc9800071
50. Veber, D. F.; Johnson, S. R.; Cheng, H.-Y.; Smith, B. R.; Ward, K. W.; Kopple, K. D. *J. Med. Chem.* **2002,** *45,* 2615–2623. doi:10.1021/jm020017n
51. Egan, W. J.; Merz, K. M.; Baldwin, J. J. *J. Med. Chem.* **2000,** *43,* 3867–3877. doi:10.1021/jm000292e
52. Muegge, I.; Heald, S. L.; Brittelli, D. *J. Med. Chem.* **2001,** *44,* 1841–1846. doi:10.1021/jm015507e
53. Colomer, I.; Empson, C. J.; Craven, P.; Owen, Z.; Doveston, R. G.; Churcher, I.; Marsden, S. P.; Nelson, A. *Chem. Commun.* **2016,** *52,* 7209–7212. doi:10.1039/c6cc03244c

License and Terms

This is an open access article licensed under the terms of the Beilstein-Institut Open Access License Agreement (https://www.beilstein-journals.org/bjoc/terms), which is identical to the Creative Commons Attribution 4.0 International License (https://creativecommons.org/licenses/by/4.0). The reuse of material under this license requires that the author(s), source and license are credited. Third-party material in this article could be subject to other licenses (typically indicated in the credit line), and in this case, users are required to obtain permission from the license holder to reuse the material.

The definitive version of this article is the electronic one which can be found at:
https://doi.org/10.3762/bjoc.20.184

BEILSTEIN JOURNAL OF ORGANIC CHEMISTRY

Deuterated reagents in multicomponent reactions to afford deuterium-labeled products

Kevin Schofield[1], Shayna Maddern[1], Yueteng Zhang[2], Grace E. Mastin[2], Rachel Knight[2], Wei Wang[1,2], James Galligan[2] and Christopher Hulme[*1,2]

Full Research Paper

Open Access

Address:
[1]Department of Chemistry and Biochemistry, College of Science, University of Arizona, Tucson, Arizona, 85721, USA and [2]Department of Pharmacology and Toxicology, University of Arizona, Tucson, Arizona, 85721, USA

Email:
Christopher Hulme[*] - hulme@pharmacy.arizona.edu

* Corresponding author

Keywords:
deuterated aldehydes; deuterated formamides; deuterated isocyanides; DHPs; kinetic isotope effect; Leuckart–Wallach; microsomal stability; multicomponent reactions

Beilstein J. Org. Chem. **2024,** *20,* 2270–2279.
https://doi.org/10.3762/bjoc.20.195

Received: 07 June 2024
Accepted: 29 August 2024
Published: 06 September 2024

This article is part of the thematic issue "Multicomponent reactions IV".

Associate Editor: T. J. J. Müller

© 2024 Schofield et al.; licensee Beilstein-Institut.
License and terms: see end of document.

Abstract

The utility of bio-isosteres is broad in drug discovery and methodology herein enables the preparation of deuterium-labeled products is the most fundamental of known bio-isosteric replacements. As such we report the use of both [D_1]-aldehydes and [D_2]-isonitriles across 8 multicomponent reactions (MCRs) to give diverse arrays of deuterated products. A highlight is the synthesis of several FDA-approved calcium channel blockers, selectively deuterated at a $t_{1/2}$ limiting metabolic soft-spot via use of [D_1]-aldehydes. Surrogate pharmacokinetic analyses of microsomal stability confirm prolongation of $t_{1/2}$ of the new deuterated analogs. We also report the first preparation of [D_2]-isonitriles from [D_3]-formamides via a modified Leuckart–Wallach reaction and their use in an MCR to afford products with [D_2]-benzylic positions and likely significantly enhanced metabolic stability, a key parameter for property-based design efforts.

Introduction

Multicomponent reactions (MCRs) are one-pot reactions that utilize three or more readily available starting materials [1-4]. Typically, MCRs use reactive functional groups such as ketones or aldehydes, carboxylic acids, amines, and isocyanides where these simple building blocks can be utilized to form large libraries of drug-like compounds with synthetic ease [5,6]. In recent years use of deuterium in drug discovery has expanded beyond mechanistic and tracer studies to deuterium incorporation in small molecules in attempts to hijack the deuterium kinetic isotope effect to induce longer drug $t_{1/2}$ and greater systemic exposure [7-9]. Herein, we describe applications of deuterium-labeled reagents with MCRs through use of deuter-

ated aldehydes and deuterated isocyanides, an area of study with sparingly few examples.

One example by Srivastava obtained a 65% deuterated Passerini product starting from a 65% deuterated aldehyde [10]. Latterly, Yamamoto utilized a 90% deuterated [D_2]-isocyanide in a copper catalyzed [3 + 2] cycloaddition to afford a 60% deuterated [D_2]-pyrrole [11]. The utility of the Leuckart–Wallach reaction towards the generation of isocyanides was first explored by Dömling [12], yet the use of such reagents in MCRs and determination of discrepancies in deuterium retention with MCRs has yet to be explored, although one would expect scrambling to be limited. Thus, we began by gathering highly deuterated aldehydes (>95% D) prepared via NHC catalysis [13] and developed a route to deuterated [D_2]-benzylic isocyanides with a goal to apply them to the field of isocyanide multicomponent reaction (IMCR) chemistry which enables rapid access to arrays of biologically relevant chemotypes or secondary reactions thereafter [14,15]. Many of these chemotypes have populated corporate collections through in-house production or external purchase and have progressed along the value chain to the clinic and full approval [5]. Literature inspection reveals that an established common method to prepare deuterated benzylic isonitriles is reduction of a nitrile in the presence of a deuterium source (Scheme 1) [16-18].

Results and Discussion

We hypothesized that [D_1]-aldehydes could be converted to [D_2]-benzylic isocyanides using [D_2]-formic acid via Leuckart–Wallach reaction followed by dehydration. Surprisingly, the Leuckart–Wallach reaction gave [D_3]-formamides which are scarce in the primary literature. The common method to prepare [D_1]-formamides (D–C=O) is through a Leuckart–Wallach reaction with an amine and [D_1]-methyl/ethyl formate or [D_1]-dimethylformamide [19,20]. Stockmann and co-workers produced [D_2]-formamides (N–D, D–C=O) via acid-catalyzed nitrile hydrolysis with HCl and D_2O [21]. Thus, using the Leuckart–Wallach methodology developed herein, deuterated aldehydes can be converted into [D_2]-isocyanides. The optimized conditions for this reaction are summarized below (Table 1).

It is important to note that 1 equivalent of formamide and excess [D_2]-formic acid (Table 1, entry 2) leads to increased deuteration of formamide product while increasing formamide equivalents increases the yield at the cost of deuterated %. Excess reaction time increases side product formation and thermal degradation of the aldehyde starting material. To combat this, microwave irradiation was employed which dramatically increased the overall yield of the reaction (Table 1, entry 5). In summary, minimal formamide (1–2 equiv), excess [D_2]-formic acid, and heating to 170 °C in a microwave reactor for 5 minutes is expected to give excellent yields in good deuteration %.

A tentative mechanism to [D_3]-formamides is shown in Scheme 2 but is open to debate. Thus, formamide adds to the [D_1]-aldehyde **A** to form hemiaminal **B** which eliminates D_2O to give imine **D**. Deprotonation of formamide **D** forms the resonance and zwitterion-stabilized isocyanate **E** [22]. We then

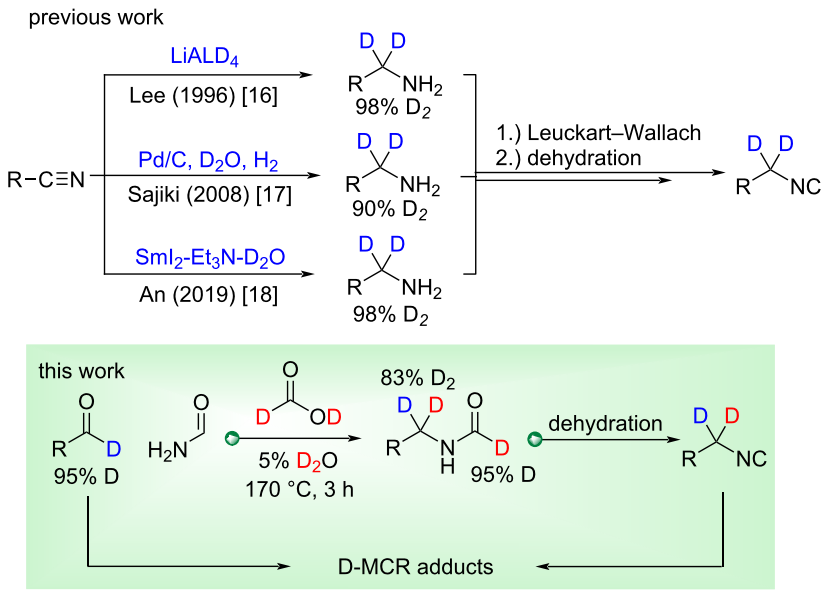

Scheme 1: Competitive examples of D_2-benzylamine formation via phenyl-nitriles.

Table 1: Optimization of deuterated Leuckart–Wallach reaction[a].

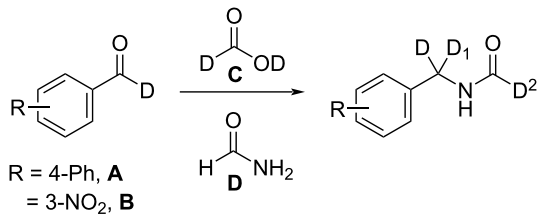

Entry	Aldehyde	C equiv	D equiv	Yield %	Deuteration % D^1, D^2
1	**A**	7.2	12	61	51, 42
2	**A**	6	1	24	70, 88
3	**A**	20	1	27	83, 94
4	**A**	12	10	80	27, 61
5[b]	**B**	**20**	**2**	**83**	**78, 40**

[a]Standard conditions: 170 °C, 3 h. [b]Reaction was heated to 180 °C for 5 minutes in a microwave reactor. D installed in product from D-aldehyde (**A or B**), D_1 and D_2 come from **C**. % Deuteration was determined via ^{1}H NMR.

hypothesize that zwitterion **E** rearranges with loss of CO_2 to form [D_3]-formamide.

The ability to deuterate at benzylic positions is particularly relevant as benzylic C–H bonds are common in biologically relevant chemotypes and moreover appear in approximately 25% of the top selling 200 pharmaceuticals [23]. Benzyl cation stability is a driver of metabolism at these sites where benzylic C–H bonds readily undergo metabolism driven by cytochrome P450 oxidases via single-electron oxidation [24]. This metabolic lability may be tempered by hydrogen replacement with deuterium, an almost perfect bio-isosteric replacement (C–H to C–D) which maintains 3D surface, shape and flexibility [8]. Indeed, early incorporation of deuterium during hit generation may negate the need for late-stage C–H functionalization which often requires strong external oxidants or affords products with significantly lower biological activity [25-27]. Thus, eight MCRs were evaluated for D-reagent scope of reactivity and determination of deuterium retention using a combination of deuterated aldehydes, [D_1]-, and/or [D_2]-isocyanides.

We began with the venerable Ugi 4-component reaction (Ugi-4CR), first reported by Ivar Ugi in 1959 [28]. The Ugi-4CR utilizes an amine, carbonyl, carboxylic acid, and isocyanide component to afford α-aminoacyl amide derivatives **1a**–**g** in good yield (Scheme 3). A [D_1]-aldehyde and [D_1]-isocyanide were independently used in conjunction with supporting reagents to afford **1b**–**d** and **1e** and **1f**, respectively, with no observation of deuterium scrambling. A post-condensation modification of **1d**, representative of the large swath of chemical space accessible by Ugi-deprotect-cyclize (UDC) methodology, gave the dihydroquinoxaline **1g** in good yield with high deuterium retention [29-32].

The catalytic three-component Ugi reaction was first reported by List in 2008 [33,34] and is comprised of reaction of an isonitrile, amine, and aldehyde/ketone, in the presence of phenylphosphinic acid (PPA), to give α-amino amides [35]. Examples of deuterated Ugi-3CR products are represented in Scheme 4. Like the Ugi 4-CR reaction, there was no deuterium scrambling in the Ugi 3-CR. Using a >95% deuterated aldehyde gave a >95% deuterated product. The low yield in **2c** is likely due to the difficult preparation of aliphatic deuterated aldehydes which led us to believe that the starting material was partially decomposed. Nonetheless, both aliphatic and aromatic deuterated aldehydes have been demonstrated to work without loss of deuterium in the Ugi-3CR.

First reported in 1961, the Ugi-azide reaction differs from the classical Ugi 4-CR in that an azide anion traps out the intermediate nitrilium ion, leading to formation of α-aminotetrazoles [36-39]. Thus, it comprises reaction of an isocyanide, carbonyl,

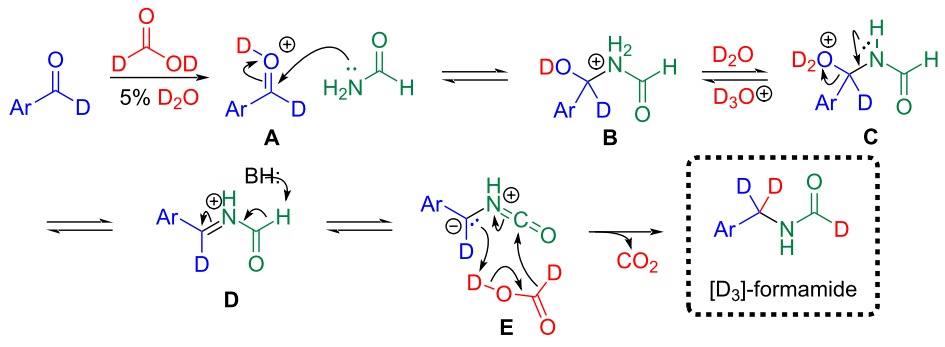

Scheme 2: Proposed tentative mechanism of [D_3]-formamide formation via modified Leuckart–Wallach reaction with [D_2]-formic acid.

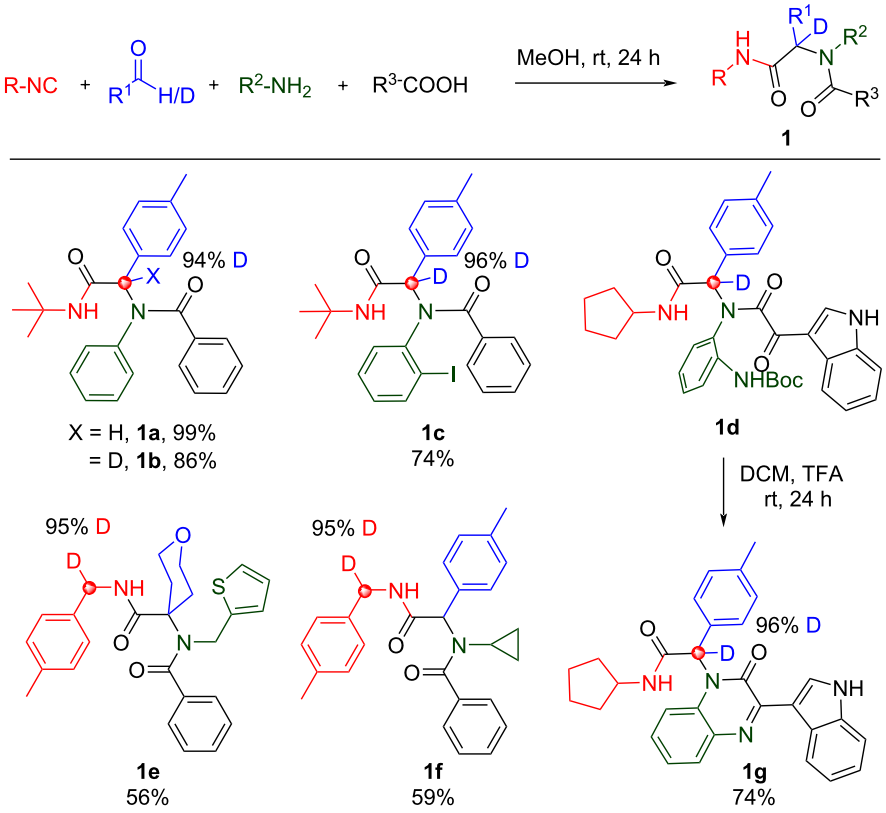

Scheme 3: Ugi-4CR products: no deuterium scrambling observed.

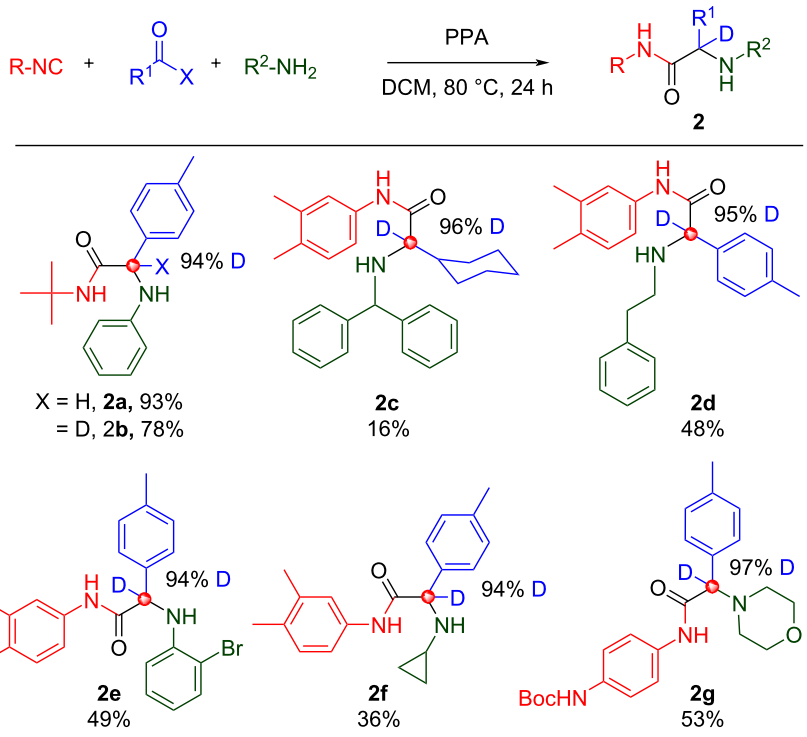

Scheme 4: Ugi-3CR products. No deuterium scrambling observed.

amine and $TMSN_3$ to give tetrazole containing products. Isolated yields for eight analogs are reported with excellent retention of the deuterium label (Scheme 5). Of note, **3i** was prepared from combination of a [D_2]-isocyanide and a [D_1]-aldehyde.

Another versatile IMCR is the Passerini reaction [40-43] discovered 60 years prior to the Ugi reaction. It uses the reactivity of isocyanides, aldehydes, and carboxylic acids to yield α-acyloxy amides (Scheme 6). Six deuterated analogs are reported in good yield with no observation of deuterium scrambling. For the preparation of **4d**, a deuterated isocyanide was solely employed and for **4a**,**b** and **4e**,**f**, water was used as solvent. For the latter, product precipitates from the aqueous solution which deters undesirable side-reactions whilst also aiding rate of the reaction.

The fifth MCR employed herein is the ubiquitous Strecker reaction [44,45] where a cyanide, aldehyde, and amine react to afford α-aminonitriles. Compound **5c** was converted to the deuterated amino acid **5d** under acidic conditions. This finding opens up the possibility of scale-production of deuterium-labeled α-amino acids. Deuterated Strecker products are presented in Scheme 7 in good yield with no observed deuterium scrambling.

The 19th century Biginelli reaction utilizes an arylaldehyde, urea, and acetoacetate component to give 3,4-dihydropyrimidin-2(1*H*)-ones [46]. Such molecules are widely used as calcium channel blockers and antihypertensive agents (Scheme 8) [47].

The Groebke–Blackburn–Bienaymé (GBB) reaction is an intramolecular variant of the Ugi reaction where the intermediate nitrilium ion is intercepted by heteroatoms from the amino-heterocyclic input. Discovered in 1998, and reported independently by three different research groups, it is a three-component reaction of α-amino-heterocycles, aldehydes, and isocyanides which affords various aza-bicyclic molecules [48-52]. The methodology has been widely used for file enhancement purposes. Three deuterated GBB products are presented, Scheme 9. Unlike the previous MCRs, labeling via a deuterated aldehyde is not feasible as deuterium is removed in favor of the aromatic bicyclic product. Both [D_2]- and [D_1]-isocyanides are exemplified in **7a**–**c**.

Finally, we studied the compatibility of the Hantzsch dihydropyridine synthesis with [D_1]-aldehydes. The reaction is a condensation of ethyl acetoacetate with aldehyde and ammonia to give 1,4-dihydropyridine [53]. Such scaffolds are seen in several FDA-approved calcium channel blockers including

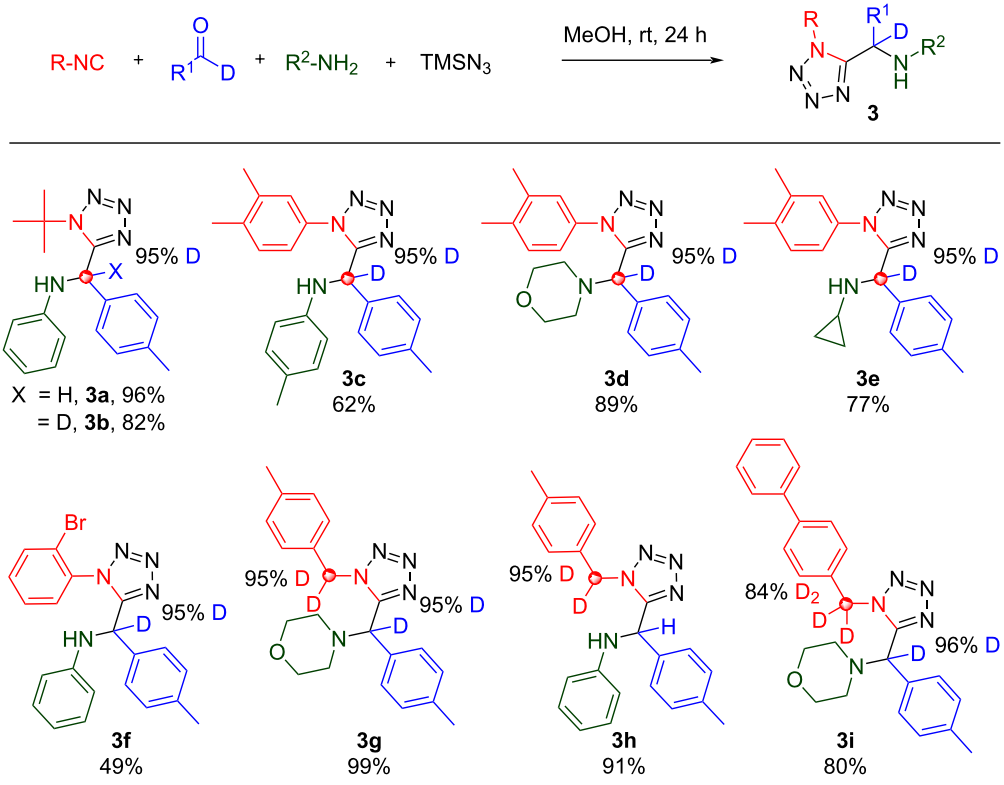

Scheme 5: Ugi-azide reaction products, no deuterium scrambling observed.

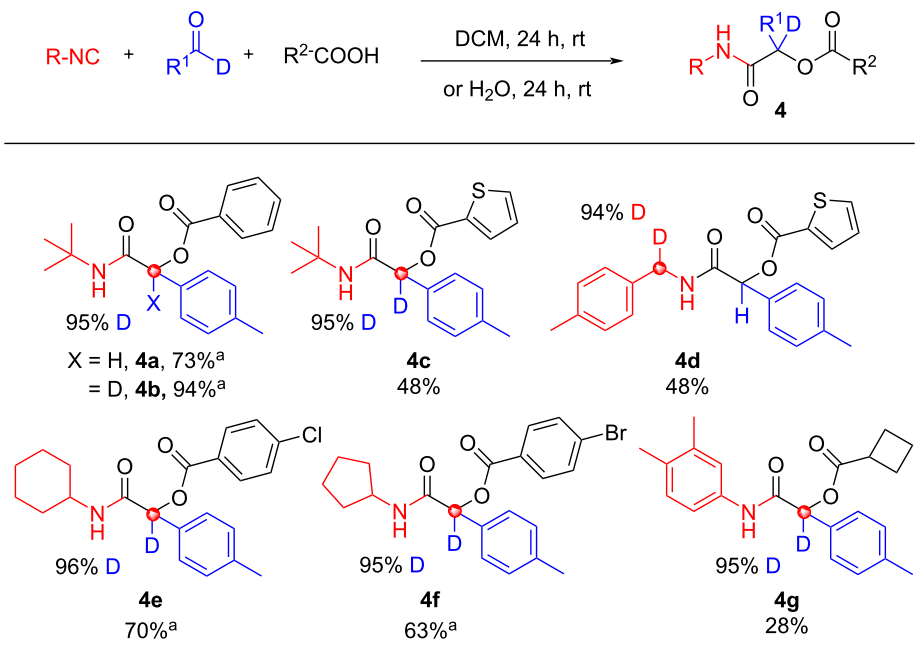

Scheme 6: Passerini products, no deuterium scrambling observed. [a]Water was used as solvent.

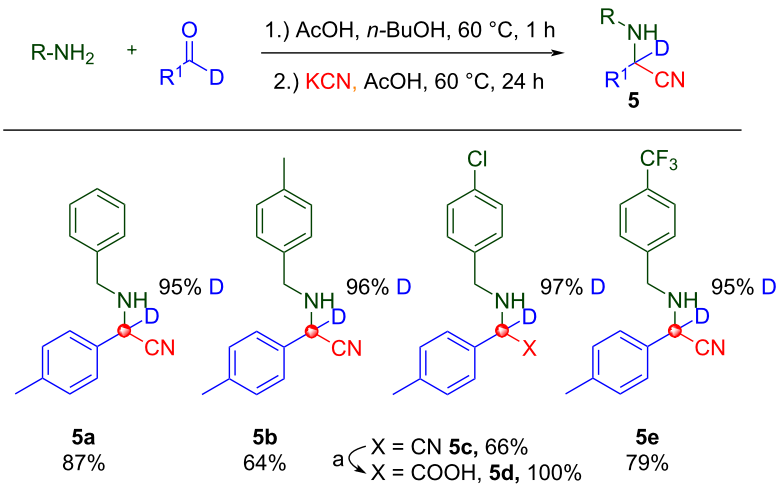

Scheme 7: Strecker reaction products (precursors to [D_1]-α-amino acids), no deuterium scrambling was observed. [a]The cyano-group was converted to a carboxylic acid via typical saponification conditions without loss of deuterium (See Supporting Information File 1 for conditions).

nifedipine, nicardipine and nimodipine and three site-specific deuterated analogs of approved 1,4-dihydropyridines (DHPs) are presented, Scheme 10. In line with all prior MCRs, good yields were observed with no deuterium scrambling.

Calcium channel blockers derived from this methodology are heavily metabolized by CYP3A4 via dehydrogenation to afford inactive pyridines, Scheme 11 [54]. As such, bio-isosteric deuterium–hydrogen exchange at this position was thought a reasonable approach to extend drug $t_{1/2}$ through exploitation of the kinetic isotope effect underpinned by the C–D bond being slightly shorter and stronger than a C–H bond. Such site-specific labeling was hypothesized to slow CYP3A4 metabolism.

To evaluate the hypothesis, surrogate studies were conducted in mouse liver microsomes to compare deuterated DHPs with their non-deuterated counterparts (Table 2).

D-Nicardipine saw a marginal increase in stability when compared to its non-deuterated counterpart H-nicardipine

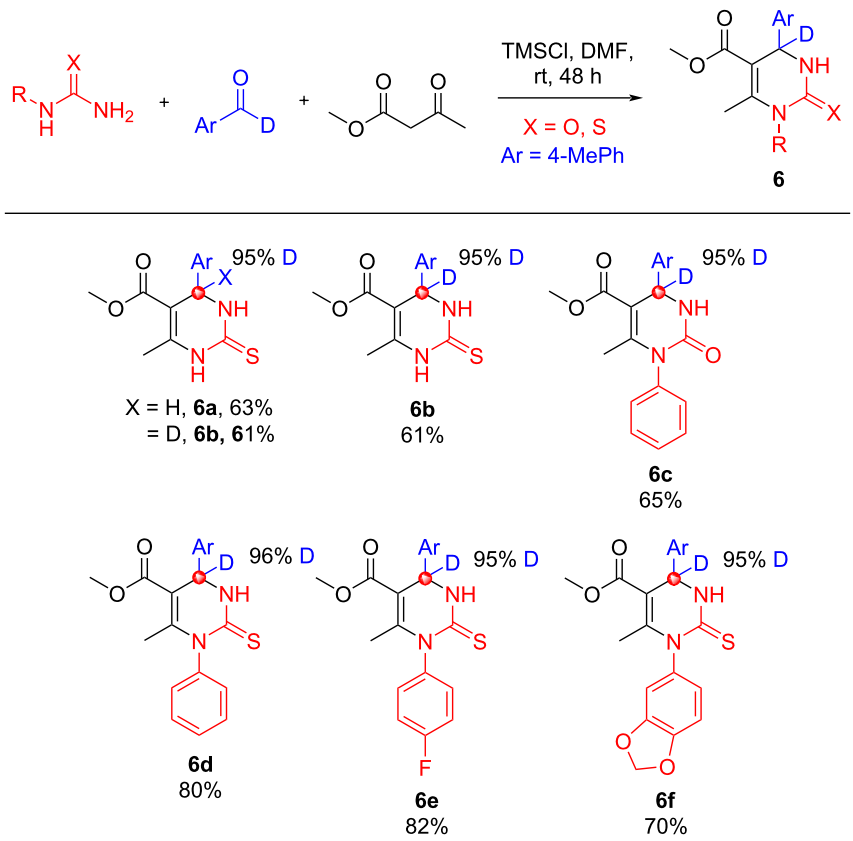

Scheme 8: Biginelli reaction products, no deuterium scrambling was observed. Six site-specific deuterated Biginelli products are revealed in good yield with no deuterium scrambling.

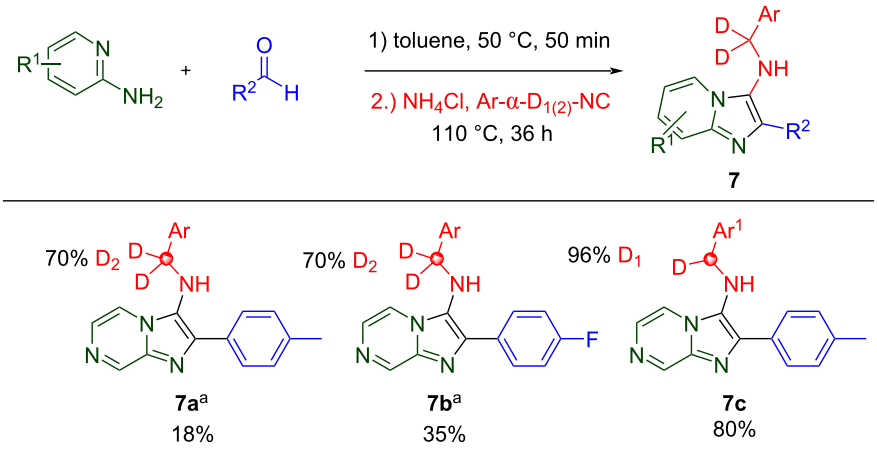

Scheme 9: GBB reaction products, no deuterium scrambling was observed. [a]A 70% [D_2]-isocyanide was used in **7a** and **7b**. Ar = 4-PhPh, Ar^1 = 4-MePh.

(3.0 vs 2.8 min) with both molecules being rapidly metabolized. D-Nimodipine witnessed a 23% improvement in $t_{1/2}$ over its non-deuterated counterpart although both molecules were quickly metabolized. The most significant improvement was seen with D-iPr-nicardipine – a 77% increase in MLM stability compared to H-iPr-nicardipine. Note that baseline stability of H-iPr-nicardipine was higher (8 min) related to enhanced ester stability with an isopropyl group versus a methyl ester. Collec-

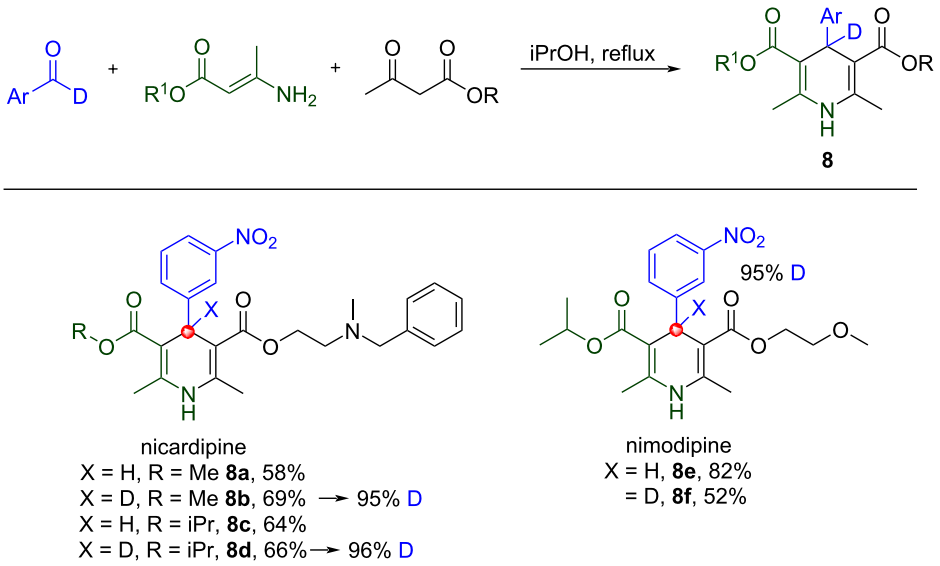

Scheme 10: Modified Hantzsch pyridine synthesis to afford 1,4-dihydropyridines. No deuterium scrambling was observed.

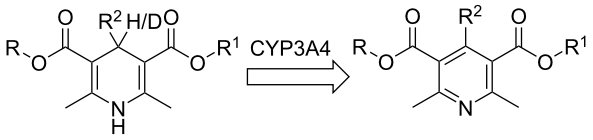

Scheme 11: CYP3A4 mediated dehydrogenation of dihydropyridines.

Table 2: Microsomal stability package of deuterated and non-deuterated dihydropyridines.

Sample ID	MLM $t_{1/2}$	MLM Cl[a]
H-nicardipine	2.8 min	1968.2
D-nicardipine	3.0 min	1860.8
H-nimodipine	2.1 min	2572.3
D-nimodipine	2.6 min	2098.5
H-iPr-nicardipine	8.0 min	687.0
D-iPr-nicardipine	14.2 min	386.6

[a]Mouse liver microsomes clearance (MLM Cl), unit: mL/min/kg.

tively these results point to high potential for translation in vivo where novel deuterated analogs exhibit longer $t_{1/2}$ and by extension oral bioavailability.

Conclusion

In summary we have presented the first method to prepare highly deuterated [D_3]-formamides and [D_2]-isocyanides from deuterated aldehydes. Furthermore, we have demonstrated that large libraries of deuterated drug-like molecules can be produced rapidly with MCR technology, with particular value for site selective deuteration of often metabolically soft benzylic C–H sites. Lastly and most importantly, preliminary surrogate metabolic stability studies on site selective [D_1]-DHPs suggest these novel deuterated analogs may afford increased exposure in an in vivo setting. The methodology is likely to have wide utility for the drug-hunting community at large.

Supporting Information

Supporting Information File 1

Experimental and analytical data and copies of NMR spectra.
[https://www.beilstein-journals.org/bjoc/content/supplementary/1860-5397-20-195-S1.pdf]

Acknowledgements

We thank the UA mass spectrometry and NMR facilities.

Funding

The Office of the Director, NIH, is thanked for funding (1RC2MH090878-01 and 1R01AG067926-01A1 to CH).

Author Contributions

Kevin Schofield: conceptualization; investigation; methodology; writing – original draft. Shayna Maddern: investigation. Yueteng Zhang: resources. Grace E. Mastin: methodology. Rachel Knight: methodology. Wei Wang: supervision. James Galligan: supervision. Christopher Hulme: conceptualization; writing – review & editing.

ORCID® iDs

Rachel Knight - https://orcid.org/0009-0006-1750-9120
James Galligan - https://orcid.org/0000-0002-5612-0680
Christopher Hulme - https://orcid.org/0000-0001-6602-9613

Data Availability Statement

All data that supports the findings of this study is available in the published article and/or the supporting information to this article.

Preprint

A non-peer-reviewed version of this article has been previously published as a preprint: https://doi.org/10.3762/bxiv.2024.38.v1

References

1. Dömling, A.; Wang, W.; Wang, K. *Chem. Rev.* **2012,** *112,* 3083–3135. doi:10.1021/cr100233r
2. Zhu, J.; Wang, Q.; Wang, M.-X. *Multicomponent Reactions in Organic Synthesis;* Wiley-VCH: Weinheim, Germany, 2014. doi:10.1002/9783527678174
3. Rotstein, B. H.; Zaretsky, S.; Rai, V.; Yudin, A. K. *Chem. Rev.* **2014,** *114,* 8323–8359. doi:10.1021/cr400615v
4. Brauch, S.; van Berkel, S. S.; Westermann, B. *Chem. Soc. Rev.* **2013,** *42,* 4948–4962. doi:10.1039/c3cs35505e
5. Hulme, C.; Ayaz, M.; Martinez-Ariza, G.; Medda, F.; Shaw, A. Recent Advances in Multicomponent Reaction Chemistry. In *Small Molecule Medicinal Chemistry: Strategies and Technologies;* Czechtizky, W.; Hamley, P., Eds.; John Wiley & Sons: Hoboken, NJ, USA, 2015; pp 145–187. doi:10.1002/9781118771723.ch6
6. Hulme, C.; Bienaymé, H.; Nixey, T.; Chenera, B.; Jones, W.; Tempest, P.; Smith, A. L. *Methods Enzymol.* **2003,** *369,* 469–496. doi:10.1016/s0076-6879(03)69024-5
7. Gant, T. G. *J. Med. Chem.* **2014,** *57,* 3595–3611. doi:10.1021/jm4007998
8. Pirali, T.; Serafini, M.; Cargnin, S.; Genazzani, A. A. *J. Med. Chem.* **2019,** *62,* 5276–5297. doi:10.1021/acs.jmedchem.8b01808
9. Meanwell, N. A. *J. Med. Chem.* **2011,** *54,* 2529–2591. doi:10.1021/jm1013693
10. Ghoshal, A.; Ambule, M. D.; Sravanthi, R.; Taneja, M.; Srivastava, A. K. *New J. Chem.* **2019,** *43,* 14459–14474. doi:10.1039/c9nj03533h
11. Kamijo, S.; Kanazawa, C.; Yamamoto, Y. *J. Am. Chem. Soc.* **2005,** *127,* 9260–9266. doi:10.1021/ja051875m
12. Neochoritis, C. G.; Zarganes-Tzitzikas, T.; Stotani, S.; Dömling, A.; Herdtweck, E.; Khoury, K.; Dömling, A. *ACS Comb. Sci.* **2015,** *17,* 493–499. doi:10.1021/acscombsci.5b00066
13. Geng, H.; Chen, X.; Gui, J.; Zhang, Y.; Shen, Z.; Qian, P.; Chen, J.; Zhang, S.; Wang, W. *Nat. Catal.* **2019,** *2,* 1071–1077. doi:10.1038/s41929-019-0370-z
14. Ayaz, M.; De Moliner, F.; Dietrich, J.; Hulme, C. Applications of Isocyanides in IMCRs for the Rapid Generation of Molecular Diversity. In *Isocyanide Chemistry: Applications in Synthesis and Material Science;* Nenajdenko, V. G., Ed.; Wiley-VCH: Weinheim, Germany, 2012; pp 335–384. doi:10.1002/9783527652532.ch10
15. Bedard, N.; Fistrovich, A.; Schofield, K.; Shaw, A.; Hulme, C. Recent Applications of Multicomponent Reactions Toward Heterocyclic Drug Discovery. In *Multicomponent Reactions towards Heterocycles: Concepts and Applications;* Van der Eycken, E. V.; Sharma, U. K., Eds.; Wiley-VCH: Weinheim, Germany, 2022; pp 339–409. doi:10.1002/9783527832439.ch9
16. Kim, S. S.; Yang, K. W.; Lee, C. S. *J. Org. Chem.* **1996,** *61,* 4827–4829. doi:10.1021/jo940292k
17. Kurita, T.; Aoki, F.; Mizumoto, T.; Maejima, T.; Esaki, H.; Maegawa, T.; Monguchi, Y.; Sajiki, H. *Chem. – Eur. J.* **2008,** *14,* 3371–3379. doi:10.1002/chem.200701245
18. Ding, Y.; Luo, S.; Weng, C.; An, J. *J. Org. Chem.* **2019,** *84,* 15098–15105. doi:10.1021/acs.joc.9b02056
19. Kesharwani, T.; Verma, A. K.; Emrich, D.; Ward, J. A.; Larock, R. C. *Org. Lett.* **2009,** *11,* 2591–2593. doi:10.1021/ol900940k
20. Suchý, M.; Elmehriki, A. A. H.; Hudson, R. H. E. *Org. Lett.* **2011,** *13,* 3952–3955. doi:10.1021/ol201475j
21. Stockmann, V.; Bakke, J. M.; Bruheim, P.; Fiksdahl, A. *Tetrahedron* **2009,** *65,* 3668–3672. doi:10.1016/j.tet.2009.02.072
22. Kende, A. S.; Brands, K. M. J.; Blass, B. *Tetrahedron Lett.* **1993,** *34,* 579–582. doi:10.1016/s0040-4039(00)61624-6
23. McGrath, N. A.; Brichacek, M.; Njardarson, J. T. *J. Chem. Educ.* **2010,** *87,* 1348–1349. doi:10.1021/ed1003806
24. Engst, W.; Landsiedel, R.; Hermersdörfer, H.; Doehmer, J.; Glatt, H. *Carcinogenesis* **1999,** *20,* 1777–1785. doi:10.1093/carcin/20.9.1777
25. Xu, W.; Wang, W.; Liu, T.; Xie, J.; Zhu, C. *Nat. Commun.* **2019,** *10,* 4867. doi:10.1038/s41467-019-12844-9
26. Guo, S.; AbuSalim, D. I.; Cook, S. P. *J. Am. Chem. Soc.* **2018,** *140,* 12378–12382. doi:10.1021/jacs.8b08547
27. Qin, Y.; Zhu, L.; Luo, S. *Chem. Rev.* **2017,** *117,* 9433–9520. doi:10.1021/acs.chemrev.6b00657
28. Ugi, I. *Angew. Chem.* **1959,** *71,* 373–388. doi:10.1002/ange.19590711110
29. Tempest, P.; Ma, V.; Thomas, S.; Hua, Z.; Kelly, M. G.; Hulme, C. *Tetrahedron Lett.* **2001,** *42,* 4959–4962. doi:10.1016/s0040-4039(01)00919-4
30. Dietrich, J.; Kaiser, C.; Meurice, N.; Hulme, C. *Tetrahedron Lett.* **2010,** *51,* 3951–3955. doi:10.1016/j.tetlet.2010.05.108
31. Hulme, C.; Gore, V. *Curr. Med. Chem.* **2003,** *10,* 51–80. doi:10.2174/0929867033368600
32. Xu, Z.; De Moliner, F.; Cappelli, A. P.; Ayaz, M.; Hulme, C. *Synlett* **2014,** *25,* 225–228. doi:10.1055/s-0033-1340219
33. Pan, S. C.; List, B. *Angew. Chem., Int. Ed.* **2008,** *47,* 3622–3625. doi:10.1002/anie.200800494
34. Ayaz, M.; Martinez-Ariza, G.; Hulme, C. *Synlett* **2014,** *25,* 1680–1684. doi:10.1055/s-0033-1339135
35. Tripolitsiotis, N. P.; Thomaidi, M.; Neochoritis, C. G. *Eur. J. Org. Chem.* **2020,** 6525–6554. doi:10.1002/ejoc.202001157
36. Ugi, I.; Steinbrückner, C. *Angew. Chem.* **1960,** *72,* 267–268. doi:10.1002/ange.19600720709
37. Ugi, I.; Steinbrückner, C. *Chem. Ber.* **1961,** *94,* 734–742. doi:10.1002/cber.19610940323
38. Gunawan, S.; Petit, J.; Hulme, C. *ACS Comb. Sci.* **2012,** *14,* 160–163. doi:10.1021/co200209a
39. Gunawan, S.; Hulme, C. *Org. Biomol. Chem.* **2013,** *11,* 6036–6046. doi:10.1039/c3ob40900g
40. Passerini, M.; Gazz, S. *Gazz. Chim. Ital.* **1921,** *51,* 126–129.
41. Banfi, L.; Basso, A.; Lambruschini, C.; Moni, L.; Riva, R. *Chem. Sci.* **2021,** *12,* 15445–15472. doi:10.1039/d1sc03810a

42. Banfi, L.; Basso, A.; Guanti, G.; Riva, R. *Mol. Diversity* **2003,** *6,* 227–235. doi:10.1023/b:modi.0000006778.42751.7f
43. Shaw, A. Y.; Medda, F.; Hulme, C. *Tetrahedron Lett.* **2012,** *53,* 1313–1315. doi:10.1016/j.tetlet.2011.12.073
44. Strecker, A. *Justus Liebigs Ann. Chem.* **1850,** *75,* 27–45. doi:10.1002/jlac.18500750103
45. Ayaz, M.; De Moliner, F.; Morales, G. A.; Hulme, C. *Sci. Synth.* **2014,** 99–122. doi:10.1055/sos-sd-210-00029
46. Biginelli, P. *Ber. Dtsch. Chem. Ges.* **1891,** *24,* 1317–1319. doi:10.1002/cber.189102401228
47. Rovnyak, G. C.; Atwal, K. S.; Hedberg, A.; Kimball, S. D.; Moreland, S.; Gougoutas, J. Z.; O'Reilly, B. C.; Schwartz, J.; Malley, M. F. *J. Med. Chem.* **1992,** *35,* 3254–3263. doi:10.1021/jm00095a023
48. Groebke, K.; Weber, L.; Mehlin, F. *Synlett* **1998,** 661–663. doi:10.1055/s-1998-1721
49. Blackburn, C.; Guan, B.; Fleming, P.; Shiosaki, K.; Tsai, S. *Tetrahedron Lett.* **1998,** *39,* 3635–3638. doi:10.1016/s0040-4039(98)00653-4
50. Bienaymé, H.; Bouzid, K. *Angew. Chem., Int. Ed.* **1998,** *37,* 2234–2237. doi:10.1002/(sici)1521-3773(19980904)37:16<2234::aid-anie2234>3.3.co;2-i
51. Hulme, C.; Lee, Y.-S. *Mol. Diversity* **2008,** *12,* 1–15. doi:10.1007/s11030-008-9072-1
52. Umkehrer, M.; Ross, G.; Jäger, N.; Burdack, C.; Kolb, J.; Hu, H.; Alvim-Gaston, M.; Hulme, C. *Tetrahedron Lett.* **2007,** *48,* 2213–2216. doi:10.1016/j.tetlet.2007.01.061
53. Hantzsch, A. *Ber. Dtsch. Chem. Ges.* **1881,** *14,* 1637–1638. doi:10.1002/cber.18810140214
54. Zhu, Y.; Wang, F.; Li, Q.; Zhu, M.; Du, A.; Tang, W.; Chen, W. *Drug Metab. Dispos.* **2014,** *42,* 245–249. doi:10.1124/dmd.113.055400

License and Terms

This is an open access article licensed under the terms of the Beilstein-Institut Open Access License Agreement (https://www.beilstein-journals.org/bjoc/terms), which is identical to the Creative Commons Attribution 4.0 International License (https://creativecommons.org/licenses/by/4.0). The reuse of material under this license requires that the author(s), source and license are credited. Third-party material in this article could be subject to other licenses (typically indicated in the credit line), and in this case, users are required to obtain permission from the license holder to reuse the material.

The definitive version of this article is the electronic one which can be found at:
https://doi.org/10.3762/bjoc.20.195

BEILSTEIN JOURNAL OF ORGANIC CHEMISTRY

Synthesis of benzo[*f*]quinazoline-1,3(2*H*,4*H*)-diones

Ruben Manuel Figueira de Abreu, Peter Ehlers and Peter Langer*§

Full Research Paper

Open Access

Address:
Universität Rostock, Institut für Chemie, Albert-Einstein-Str. 3a, 18059 Rostock, Germany

Email:
Peter Langer* - peter.langer@uni-rostock.de

* Corresponding author
§ Tel.: +49 381 498 6410, Fax: +49 381 498 6412

Keywords:
cross-coupling; cyclization; heterocycles; palladium

Beilstein J. Org. Chem. **2024,** *20,* 2708–2719.
https://doi.org/10.3762/bjoc.20.228

Received: 04 June 2024
Accepted: 09 October 2024
Published: 28 October 2024

This article is part of the thematic issue "Multicomponent reactions IV".

Associate Editor: T. J. J. Müller

© 2024 de Abreu et al.; licensee Beilstein-Institut.
License and terms: see end of document.

Abstract

We report the synthesis of polycyclic uracil derivatives. The method is based on palladium-catalysed Sonogashira–Hagihara and Suzuki–Miyaura cross-coupling reactions followed by Brønsted acid-mediated cycloisomerisation. The developed methodology tolerates various functional groups and leads to moderate up to quantitative yields of the final products. The impact of different functional groups on the optical properties was studied by UV–vis and fluorescence spectroscopy.

Introduction

Nucleobases contain the coded information and give DNA and RNA their typical structure. As a nucleobase, uracil is involved in numerous vital processes and is therefore a promising target and candidate for the development of new drugs against a wide range of diseases [1-4]. As it is not contained in the DNA, it could be used to distinguish between DNA and RNA-based pharmaceutical targets. In previous years, uracil has been successfully used in the development of several drugs that are still important and often used. Examples include 5-fluorouracil and brivudine. 5-Fluoruracil is an important anticancer drug, while brivudine is considered to be one of the most effective antiviral drugs against the HSV-1 virus [4-20]. Consequently, in recent years, new methods have been developed to introduce various functional groups at position 5 or 6 of uracil [19-50]. However, only a few methods are known which allow for an individual introduction of substituents at both positions [37,38,51-61]. In our previous work, we developed a new method which enables both positions to be independently functionalised by Sonogashira- and Suzuki–Miyaura cross-coupling reactions (Figure 1).

Polycondensed heterocycles containing a uracil moiety have also been studied in recent years. For example, compound **A** exhibits antitumor and antimicrobial properties (Figure 2) [66,67]. Compounds **A** and **B** are used as starting materials for the synthesis of polyaromatic derivatives of other compounds with medicinal or photophysical properties [52-55]. Compounds **A** are related to the class of natural products known as coumestans, while **B** resembles flavins. While the medical potential of coumestans is still the subject of current research, interesting

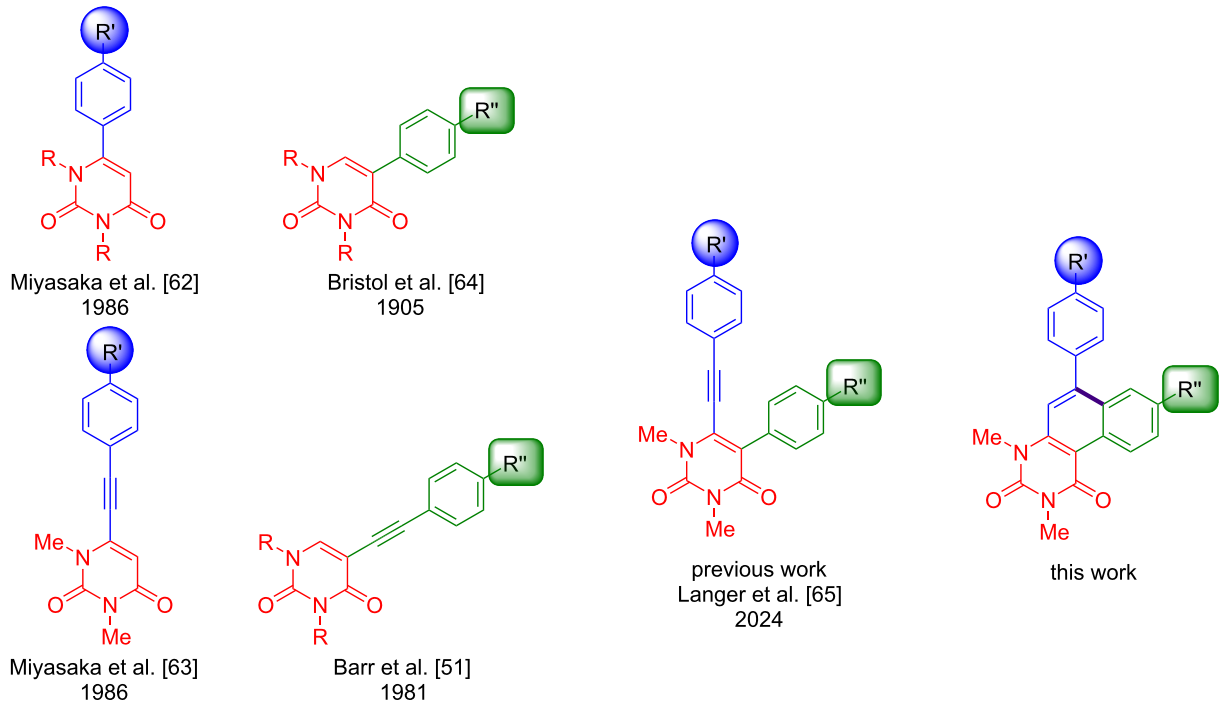

Figure 1: Synthesis of uracil-based alkynes and aryl structures [51,62-65].

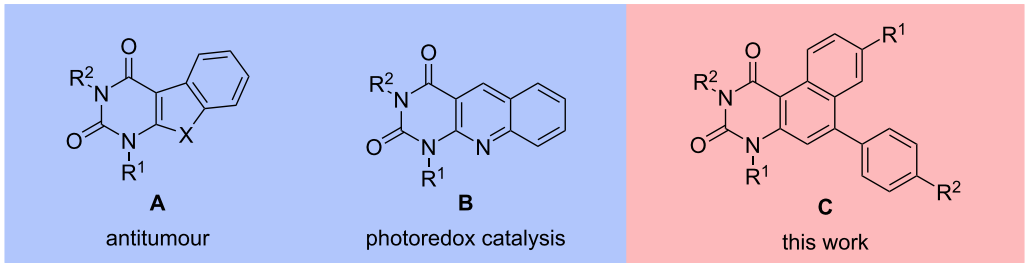

Figure 2: Structures of uracil derivatives **A**, **B**, and **C**.

photocatalytic properties have already been identified for flavins, making them interesting for photoredox catalysis [68,69]. Inspired by the current interest in the synthesis of novel uracil-derived cyclic compounds and our previous studies, we herein wish to report a new method for the synthesis of a series of novel uracil-based benzo[*f*]quinazoline-1,3(2*H*,4*H*)-diones **C** [65]. Furthermore, optical properties were analysed by UV–vis and fluorescence spectroscopy.

Results and Discussion

Synthesis

Our strategy for the synthesis of benzo[*f*]quinazoline-1,3(2*H*,4*H*)-diones is based on a four-step sequence and relies on a combination of palladium-catalysed Sonogashira–Hagihara and Suzuki–Miyaura cross-coupling reactions (Scheme 1). The final cyclisation step is accomplished by an acid-mediated cycloisomerisation. The synthesis of starting materials **4** was carried out by our previously reported protocol [65]. While compounds **4a–f** are known compounds, the synthesis of derivatives **4g–i** has not been previously reported (Scheme 2). Yields were generally lower in case of the presence of electron-withdrawing substituents.

Subsequently, the cyclisation of **4a–i** to **5a–i** by acid-mediated cycloisomerisation was studied. In our first attempt, we used platinum(II) chloride ($PtCl_2$) as the Lewis acid and **4a** as the model starting material. The reaction afforded a mixture of the desired product **5a** and the starting material. Separation of both compounds proved to be difficult and, hence, optimisation was carried out as depicted in Table 1. The employment of higher

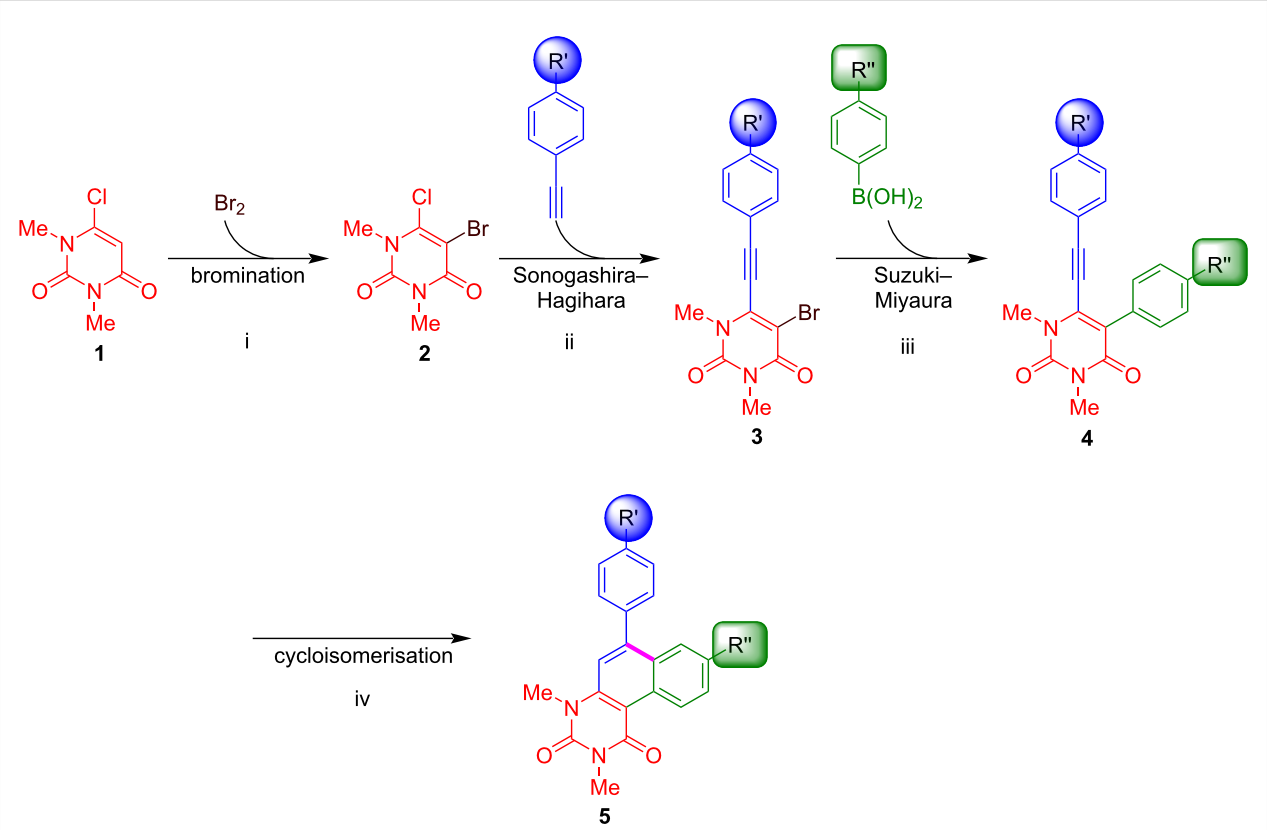

Scheme 1: Strategy for the synthesis of the cyclised product **5**. Conditions: i) Br_2 (2 equiv), Ac_2O (1.5 equiv), AcOH, 25 °C, 1 h [65]; ii) $Pd(PPh_3)Cl_2$ (5 mol %), CuI (5 mol %), NEt_3 (10 equiv), DMSO, 25 °C, 6 h; iii) $Pd(PPh_3)_4$ (10 mol %), NaOH (3 equiv), 1,4-dioxane/water 5:1, 100 °C, 1 h; iv) *p*-TsOH (20 equiv), toluene, 100 °C, 4 h.

temperatures resulted again in a mixture of **4a** and **5a** (Table 1, entry 2). Next, *p*-toluenesulfonic acid (*p*-TsOH·H_2O) was chosen as the Brønsted acid. To our delight, product **5a** was obtained in a yield of 59% after 2 hours (Table 1, entry 3). Further investigation showed that the yield could be improved to 99% by increasing the reaction time to 4 hours (Table 1, entry 4), while reduction of the amount of acid resulted in a drop of the yield to 85%.

With the optimised conditions in hand, the scope of the cycloisomerisation was studied and the products **5a**, **5d**, and **5f–i** were isolated in moderate to excellent yields (Scheme 3). The best yield was obtained for **5a** with 99%. Several functional groups, such as methyl, *N,N*-dimethylamino, and trifluoromethyl, are tolerated by the developed procedure. However, a fluorine group was converted to a hydroxy functional group (**5h**), most likely by nucleophilic aromatic substitution during aqueous workup. Interestingly, electron-donor groups, such as *N,N*-dimethylamino, proved to be beneficial in terms of yield when they are located at the alkyne-linked aryl group (Scheme 4a). In contrast, the *N,N*-dimethylanilino group is disadvantageous when located at position 5 of the uracil ring, which might be due to the protonation of the amine under the employed reaction conditions, making the aryl ring less feasible for the S_EAr reaction (Scheme 4b). The same effects may explain the cyclisation of **4f** to **5f**, while **4c** is not converted to the respective cyclisation product. Hence, the application of the reaction conditions to starting materials **4b**, **4c** and **4e** resulted in the decomposition of the starting materials and no product could be isolated. The employment of heterocyclic benzothiophene gave a very good yield of 80% for product **5i**.

Optical properties

All synthesized compounds exhibit photoluminescence by excitation with UV light. Hence, we studied the photophysical properties of all obtained derivatives **5** by steady-state absorption and fluorescence spectroscopy. The influence of the substitution pattern on the photophysical properties is displayed in Figure 3. The corresponding photophysical data and quantum yields are described in Table 2.

The analysis of the absorption spectra revealed well-resolved bands for derivatives **5a**, **5d**, **5f**, **5g**, and **5i** for short wavelengths (250–300 nm). At higher wavelength (300–450 nm)

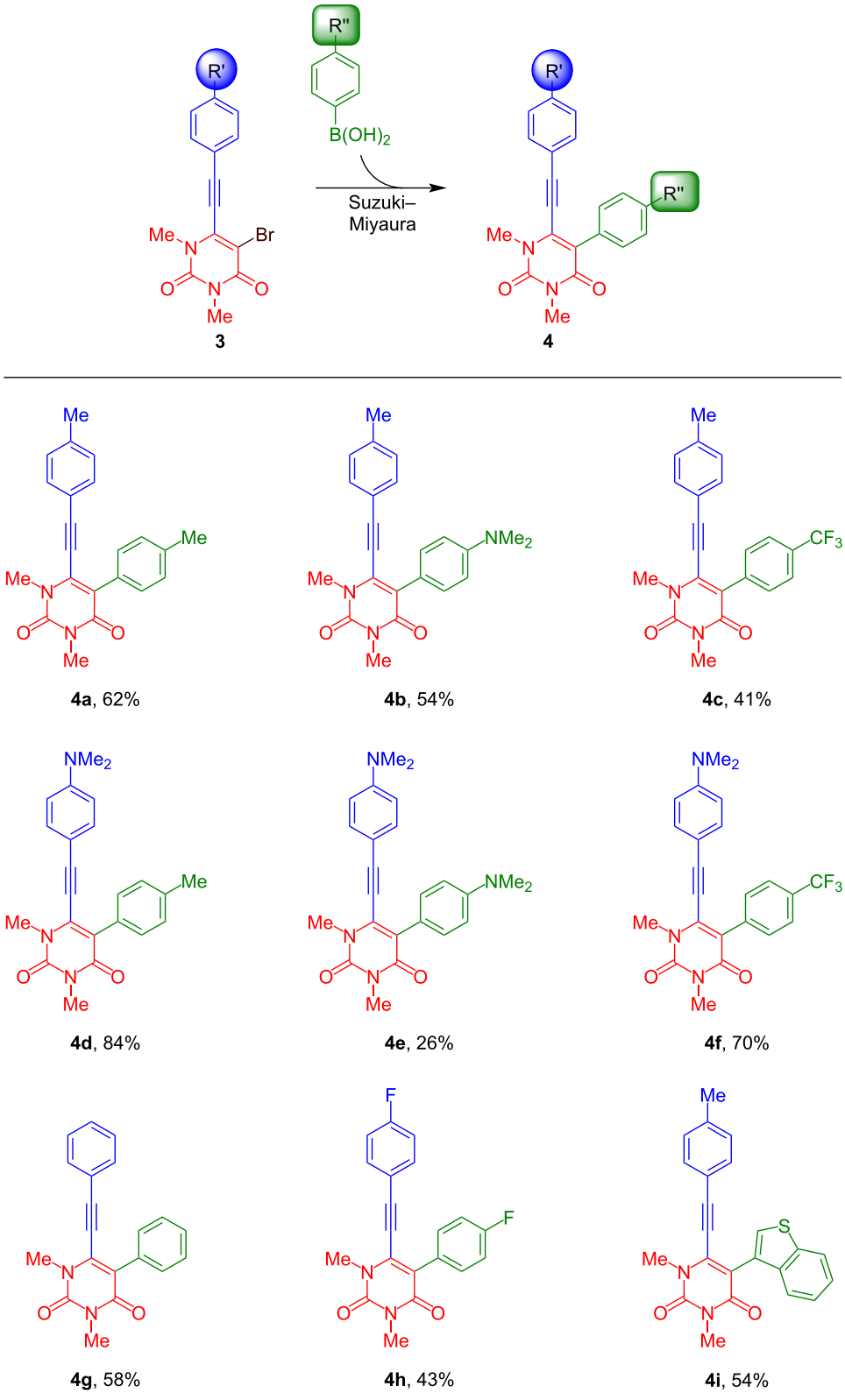

Scheme 2: Synthesis and isolated yields of 1,3-dimethyl-5-aryl-6-[2-(aryl)ethynyl]uracils **4a–i**. Reaction conditions: **3** (1 equiv), boronic acid (1.2 equiv), $Pd(PPh_3)_4$ (5 mol %), NaOH (3 equiv), 1,4-dioxane/water 5:1, 100 °C, 1 h.

Table 1: Optimization of the synthesis of **5a**.

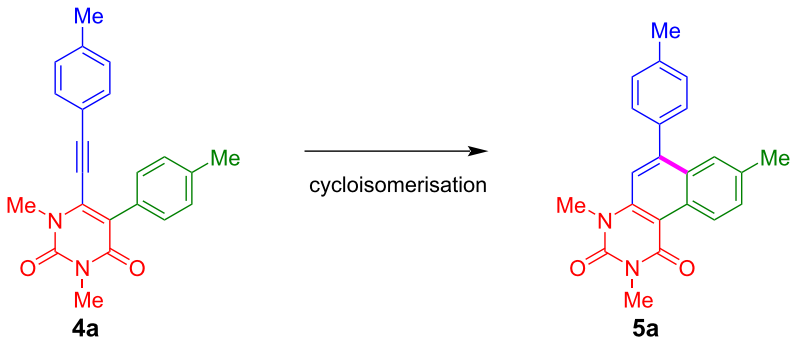

4a **5a**

Entry	Acid (equiv)	Solvent	Temperature (°C)	Time (h)	Yield (%)
1	$PtCl_2$ (0.1)	toluene	80	15	mixture
2	$PtCl_2$ (0.1)	toluene	100	15	mixture
3	*p*-TsOH·H_2O (20)	toluene	100	2	59
4	*p*-TsOH·H_2O (20)	toluene	100	4	99
5	*p*-TsOH·H_2O (15)	toluene	100	4	85

broad absorption bands with a certain fine-structure for compounds **5a**, **5g**, and **5i** and structure-less absorption features for compounds **5d**, **5f**, and **5h** containing electron-donating functional groups are observed. In addition, the presence of strongly electron-donating *N*,*N*-dimethylamino groups leads to increased extinction coefficients and bathochromically shifted absorption bands which might be a result of a certain intramolecular charge transfer between the donating *N*,*N*-dimethylamino group and the electron-deficient uracil moiety. Similar effects are observed for the emission spectra. The emission maxima of *N*,*N*-dimethylamino-group-containing compounds **5d** and **5f** are bathochromically shifted by ≈80 nm and ≈100 nm, respectively. The other compounds show similar emission maxima at ≈405 nm, hinting to a limited impact of the aryl substituents and their functional groups on the emission properties for these compounds. Moreover, the presence of *N*,*N*-dimethylamino groups leads to strongly enhanced quantum yields up to 71%.

The highest quantum yield is observed for **5d** (71%), followed by **5f** with 51%. However, the presence of a pair of donor and acceptor groups appears to be disadvantageous in terms of quantum yield and the presence of only one donor group is advantageous. Interestingly, the quantum yields of **5a** (12%), **5g** (13%), **5h** (8%), and **5i** (3%) are comparatively lower than in case of **5g** and **5f**. It is reasonable to assume that this large difference is caused by the chosen substitution pattern and can be used for further investigation or modulation of desired properties.

Conclusion

In summary, we have developed the synthesis of novel polycyclic uracil-based compounds. Careful optimisation of the reaction conditions led to the isolation of the desired products in excellent to moderate yields. The developed methodology tolerates various functional groups. The optical properties of as-prepared derivatives were investigated by steady-state absorption and photoluminescence spectroscopy. The photophysical properties are strongly altered by the presence *N*,*N*-dimethylaniline functional groups on the scaffold, which leads to strongly, bathochromically shifted absorption and emission spectra with elevated extinction coefficients and quantum yields up to 71%. Further studies will be directed to the synthesis to polycyclic, π-conjugated uracil derivatives.

Experimental

General information

Nuclear magnetic resonance spectra ($^1H/^{13}C/^{19}F$ NMR) were recorded on Bruker AVANCE 300 III, 250II, or 500 spectrometers. The analysed chemical shifts δ are referenced to the residual solvent signals of the deuterated solvents $CDCl_3$ (δ = 7.26 ppm/77.16 ppm). Multiplicities due to spin–spin correlation are reported as follows: s = singlet, d = doublet, dd = double doublet, m = multiplet; they are further described by their coupling constants *J*. Infrared spectra (IR) were measured as attenuated total reflection (ATR) experiments using a Nicolet 380 FT-IR spectrometer. The signals were characterised by their wavenumbers and corresponding absorption as very strong (vs), strong (s), medium (m), weak (w) or very weak (vw).

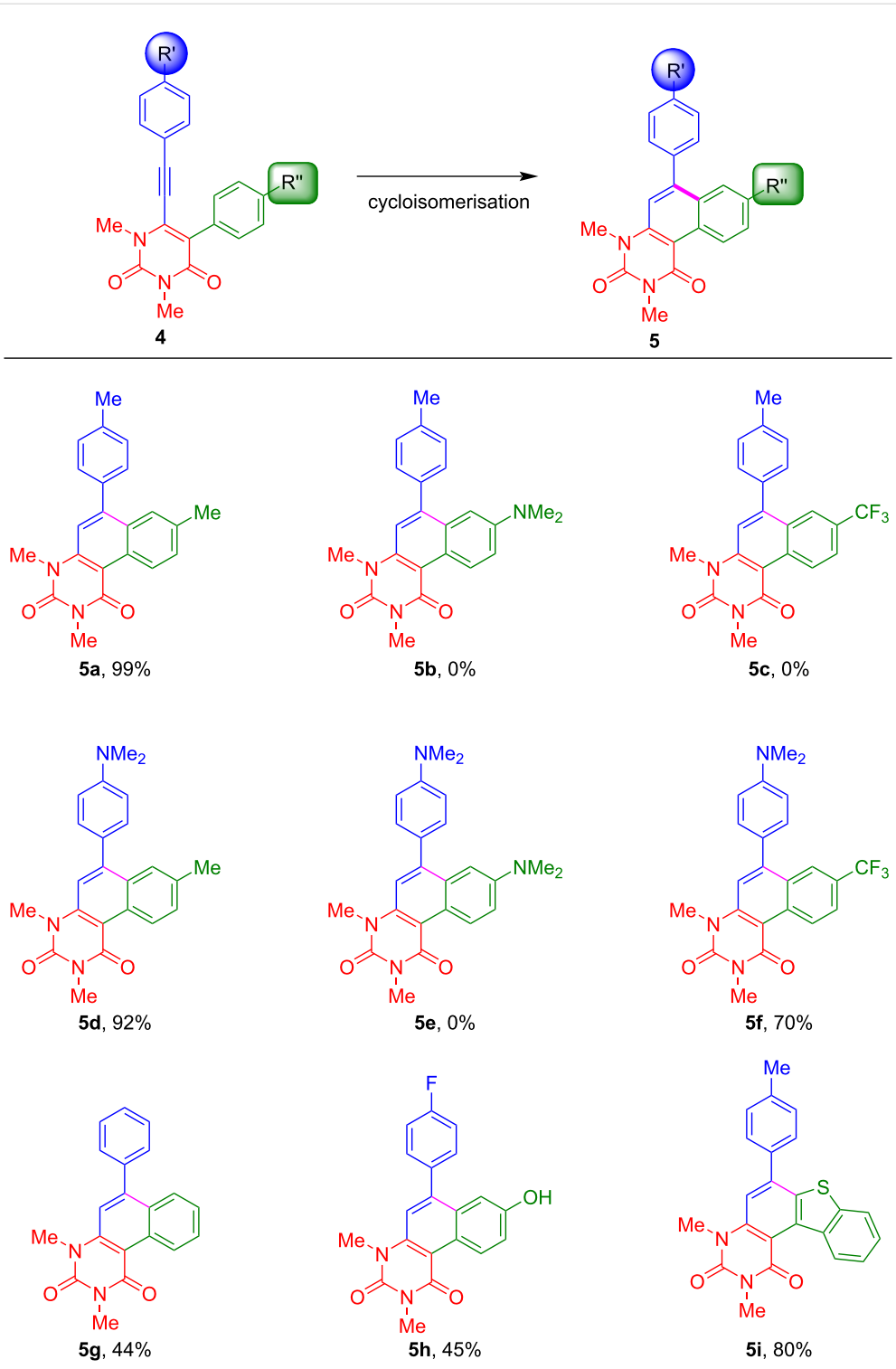

Scheme 3: Scope and isolated yields of the synthesis of **5**. Reaction conditions: **4** (1 equiv), *p*-TsOH·H_2O (20 equiv), toluene, 100 °C, 4 h.

UV–vis spectra were recorded on a Cary 60 UV–vis spectrophotometer and emission spectra were recorded on an Agilent Cary Eclipse fluorescence spectrophotometer. Basic and high-resolution mass spectra (MS/HRMS) were measured on instruments coupled to a preceding gas chromatograph (GC) or liquid chromatograph (LC). Samples were ionised by electron impact ionisation (EI) on an Agilent 6890/5973 or Agilent 7890/5977 GC–MS equipped with an HP-5 capillary column

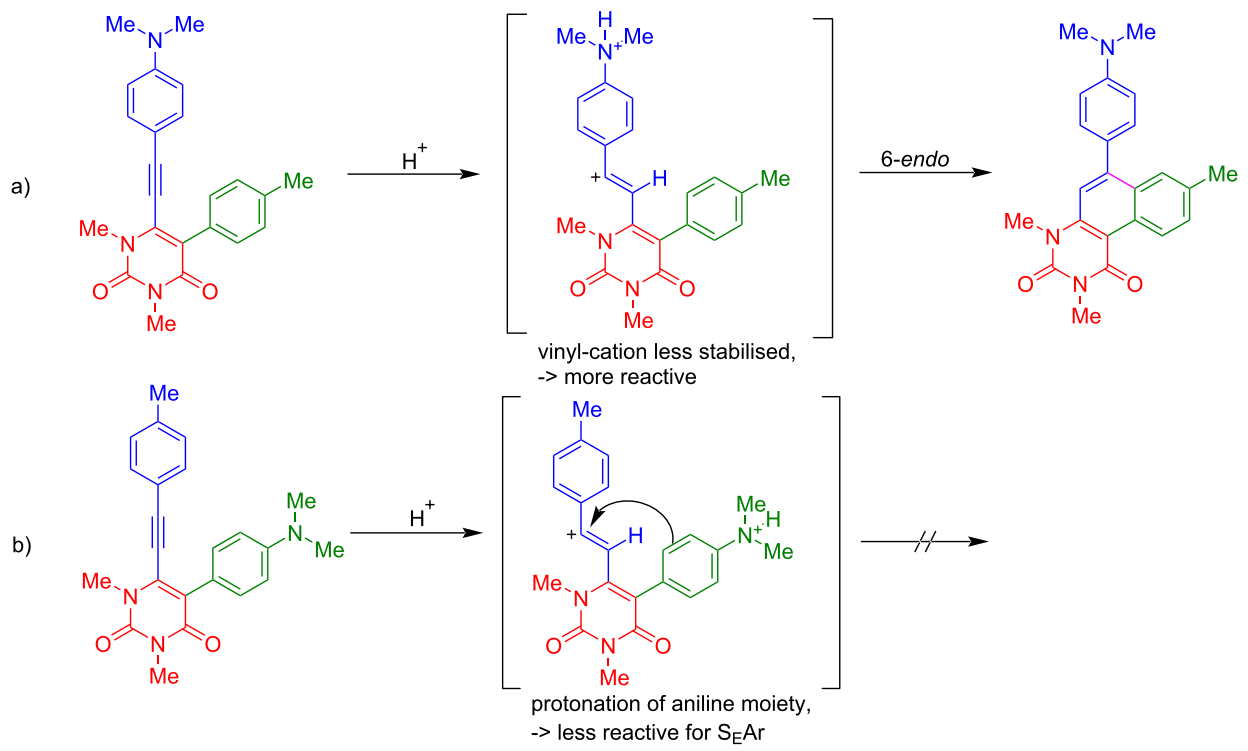

Scheme 4: Proposed reaction mechanism of the cyclisation with *N,N*-dimethylanilino functional groups.

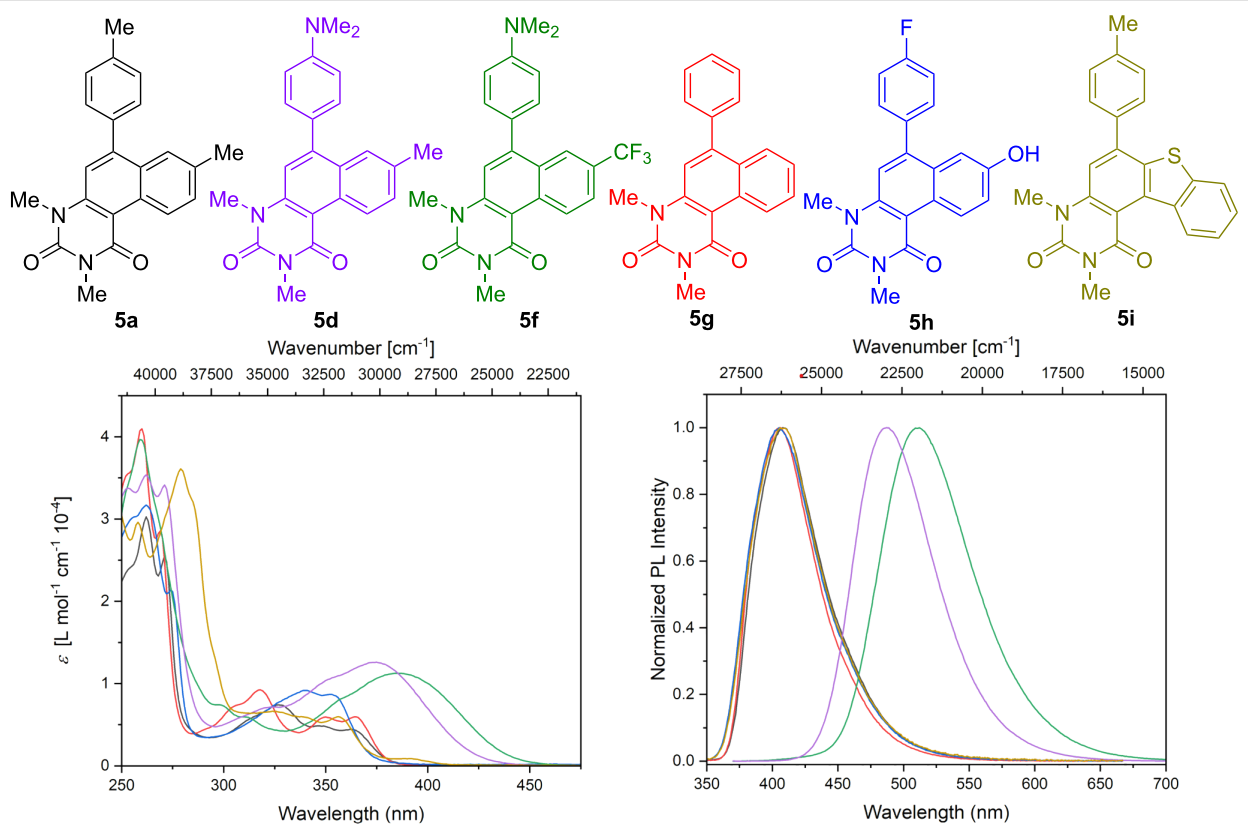

Figure 3: UV–vis absorption (left) and emission (right, λ_{ex} = 400 nm) spectra of **5a**, **5d**, **5f**, **5g**, **5h**, and **5i** in dichloromethane (c = 1·10^{-5} M).

Table 2: Photophysical data of 1,3-dimethyl-5-phenyl-6-[2-(phenyl)ethynyl]uracil derivatives **5a**, **5d**, **5f**, **5g**, **5h**, and **5i** in dichloromethane (c = 1·10^{-5} M) at 20 °C.

	5a	5d	5f	5g	5h	5i
$\lambda_{1,abs}$ (nm)	262	253	258	260	262	258
$\varepsilon_{\lambda1}$·10^4 (M^{-1} cm^{-1})	3.1	3.4	4.0	4.1	3.2	3.0
$\lambda_{2,abs}$ (nm)	271	262	387	269	274	278
$\varepsilon_{\lambda2}$·10^4 (M^{-1} cm^{-1})	2.6	3.5	1.1	2.9	2.1	3.6
$\lambda_{3,abs}$ (nm)	327	271		317	339	356
$\varepsilon_{\lambda3}$·10^4 (M^{-1} cm^{-1})	0.8	3.4		0.9	0.9	0.6
$\lambda_{4,abs}$ (nm)	347	322		349	353	
$\varepsilon_{\lambda4}$·10^4 (M^{-1} cm^{-1})	0.5	0.7		0.6	0.9	
$\lambda_{5,abs}$ (nm)	363	374		364		
$\varepsilon_{\lambda5}$·10^4 (M^{-1} cm^{-1})	0.5	1.3		0.6		
λ_{em}^{335} (nm)	408			406	405	408
λ_{em}^{355} (nm)		487	512			
Φ[a]	12[b]	71[c]	51[c]	13[b]	8[b]	3[b]

[a]Fluorescence standard: quinine hemisulfate in H_2SO_4 (0.05 M) (Φ = 0.52) [70,71]; [b]excitation at λ_{ex} = 335 nm; [c]excitation at λ_{ex} = 355 nm.

using helium carrier gas or by electron spray ionisation (ESI) on an Agilent 1200/6210 Time-of-Flight (TOF) LC–MS. The solvent, toluene, was purchased as dry solvent and applied without further purification. Other reagents, catalysts, ligands, acids, and bases were used as purchased from commercial suppliers. Column chromatography was performed on Merck Silica gel 60 (particle size 63–200 µm). Solvents for extraction and column chromatography were distilled prior employment.

Synthesis of 4a–i

The synthesis of **4a**–**f** has been previously reported. Novel derivatives **4g**–**i** were prepared according to our previously reported procedure [65].

1,3-Dimethyl-5-phenyl-6-(phenylethynyl)pyrimidine-2,4(1*H*,3*H*)-dione (4g). Compound **4g** was obtained as a brown solid in 58% yield (58.3 mg, 184 µmol, R_f 0.19 (heptane/ethyl acetate 3:2)); mp 152–154 °C; IR (ATR) ṽ: 1695 (s), 1642 (vs), 1582 (s), 1493 (s), 1440 (s), 1421 (s), 1176 (m), 1079 (m), 756 (s) cm^{-1}; ^{1}H NMR (500 MHz, chloroform-*d*) δ 7.51–7.48 (m, 2H), 7.45–7.41 (m, 2H), 7.41–7.36 (m, 2H), 7.34–7.29 (m, 2H), 7.24–7.21 (m, 2H), 3.71 (s, 3H), 3.45 (s, 3H); ^{13}C {^{1}H} NMR (126 MHz, chloroform-*d*) δ 162.1, 151.6, 134.3, 133.2, 131.9, 130.9, 130.5, 128.7, 128.3, 128.0, 120.7, 119.0, 104.2, 81.0, 34.6, 28.7; EIMS (70 eV) *m*/*z* (%): 315 (100, M$^+$), 258 (26), 230 (67), 215 (17), 202 (23), 189 (13); HRESIMS-TOF (*m*/*z*): [M + H]$^+$ calcd for $C_{20}H_{17}N_2O_2$, 317.1290; found, 317.1282.

5-(4-Fluorophenyl)-6-((4-fluorophenyl)ethynyl)-1,3-dimethylpyrimidine-2,4(1*H*,3*H*)-dione (4h). Compound **4h** was obtained as a brown solid in 43% yield (46.2 mg, 131 µmol, R_f 0.17 (heptane/ethyl acetate 3:2)); mp 187–189 °C; IR (ATR) ṽ: 1708 (s), 1654 (vs), 1574 (s), 1514 (s), 1506 (s), 1446 (s), 1423 (s), 1232 (s), 1158 (s) cm^{-1}; ^{1}H NMR (500 MHz, chloroform-*d*) δ 7.48–7.44 (m, 2H), 7.26–7.22 (m, 2H), 7.15–7.10 (m, 2H), 7.06–7.02 (m, 2H), 3.70 (s, 3H), 3.44 (s, 3H); ^{19}F NMR (471 MHz, chloroform-*d*) δ −113.3, −106.3; ^{13}C {^{1}H} NMR (126 MHz, chloroform-*d*) δ 163.9 (d, *J* = 253.7 Hz), 162.7 (d, *J* = 247.8 Hz), 162.0, 151.5, 134.3, 134.1 (d, *J* = 9.0 Hz), 132.8 (d, *J* = 8.2 Hz), 129.1 (d, *J* = 3.3 Hz), 117.9, 116.6 (d, *J* = 3.6 Hz), 116.4 (d, *J* = 22.4 Hz), 115.1 (d, *J* = 21.6 Hz), 103.3, 80.7, 34.7, 28.7; EIMS (70 eV) *m*/*z* (%): 352 (96, M$^+$), 294 (28), 266 (67), 251 (14), 238 (30), 160 (100); HRESIMS-TOF(*m*/*z*): [M + H]$^+$ calcd for $C_{20}H_{15}F_2N_2O_2$, 353.1101; found, 353.1100.

5-(Benzo[*b*]thiophen-3-yl)-1,3-dimethyl-6-(*p*-tolylethynyl)pyrimidine-2,4(1*H*,3*H*)-dione (4i). Compound **4i** was obtained as a brownish solid in 54% yield (189 mg, 488 µmol, R_f 0.21 (heptane/ethyl acetate 3:2)); mp 162–164 °C; IR (ATR) ṽ: 1695 (s), 1640 (vs), 1582 (s), 1510 (s), 1446 (s), 1428 (s), 1219 (m), 813 (s) cm^{-1}; ^{1}H NMR (300 MHz, chloroform-*d*) δ 7.94–7.87 (m, 1H), 7.65–7.59 (m, 1H), 7.58 (s, 1H), 7.39–7.31 (m, 2H), 7.06–7.01 (m, 2H), 6.86–6.80 (m, 2H), 3.73 (s, 3H), 3.48 (s, 3H), 2.30 (s, 3H); ^{13}C {^{1}H} NMR (75 MHz, chloroform-*d*) δ 161.7, 151.7, 141.2, 139.7, 138.3, 135.9, 131.9, 129.4, 128.5, 128.2, 124.3, 124.2, 123.4, 122.8, 117.2, 112.6, 106.2, 80.4, 34.7, 28.7, 21; EIMS (70 eV) *m*/*z* (%): 386 (58, M$^+$), 371 (100), 300 (68), 286 (51), 271 (18), 268 (26); HRESIMS-TOF (*m*/*z*): [M + H]$^+$ calcd for $C_{23}H_{19}N_2O_2S$, 387.1167; found, 387.1171.

General procedure for the preparation of 5

A mixture of the corresponding starting material **4** (0.145 mmol) and *p*-TsOH·H_2O (20 equiv; 2.94 mmol; 559 mg) was dissolved in dry toluene (2 mL) and stirred for 4 hours

under argon atmosphere at 100 °C. The reaction was monitored by TLC until completion. The reaction was neutralised with a saturated $NaHCO_3$ solution and diluted with water (40 mL). The phases were separated, and the aqueous layer was extracted with dichloromethane (3 × 30 mL). The combined organic layers were dried over Na_2SO_4, concentrated under reduced pressure, and purified by column chromatography (heptane/ethyl acetate).

2,4,8-Trimethyl-6-(*p*-tolyl)benzo[*f*]quinazoline-1,3(2*H*,4H)-dione (5a). According to general procedure, compound **5a** was obtained as a brown solid in 99% yield (49.3 mg, 143 µmol, R_f 0.29 (heptane/ethyl acetate 3:2)); mp 185–187 °C; IR (ATR) ṽ: 1685 (s), 1640 (vs), 1508 (s), 1421 (s), 1306 (m), 1121 (m), 1022 (m), 820 (s), 748 (s) cm^{-1}; ^1H NMR (500 MHz, chloroform-*d*) δ 9.82–9.78 (m, 1H), 7.76 (d, *J* = 8.5 Hz, 1H), 7.39–7.34 (m, 4H), 7.30 (dd, *J* = 8.6, 1.8 Hz, 1H), 7.27 (s, 1H), 3.72 (s, 3H), 3.59 (s, 3H), 2.60 (d, *J* = 0.8 Hz, 3H), 2.48 (s, 3H); ^{13}C {^1H} NMR (126 MHz, chloroform-*d*) δ 162.7, 151.5, 149.0, 141.4, 140.0, 138.5, 136.9, 132.6, 129.7, 129.3, 127.7, 126.8, 126.7, 125.5, 113.5, 106.4, 31.8, 28.8, 22.6, 21.4; EIMS (70 eV) *m*/*z* (%): 344 (M^+, 100), 258 (9), 232 (9), 215 (10), 202 (8); HREIMS (*m*/*z*): $[M]^+$ calcd for $C_{22}H_{20}N_2O_2$, 344.15173; found, 344.15193.

6-(4-(*N*,*N*-Dimethylamino)phenyl)-2,4,8-trimethylbenzo[*f*]quinazoline-1,3(2*H*,4*H*)-dione (5d). According to general procedure, compound **5d** was obtained as a brown solid in 92% yield (70 mg, 187 µmol, R_f 0.24 (heptane/ethyl acetate 3:2)); mp: 207–209 °C; IR (ATR) ṽ: 1697 (vs), 1642 (vs), 1512 (s), 1423 (s), 1201 (s), 1129 (s), 1036 (m), 820 (vs), 745 (s) cm^{-1}; ^1H NMR (300 MHz, chloroform-*d*) δ 9.81–9.74 (m, 1H), 7.90 (d, *J* = 8.6 Hz, 1H), 7.44–7.33 (m, 2H), 7.30 (dd, *J* = 8.5, 1.7 Hz, 1H), 7.24 (s, 1H), 6.92–6.80 (m, 2H), 3.70 (s, 3H), 3.57 (s, 3H), 3.06 (s, 6H), 2.59 (s, 3H); ^{13}C {^1H} NMR (75 MHz, chloroform-*d*) δ 162.7, 151.5, 150.6, 149.3, 141.5, 139.7, 132.7, 130.8, 127.4, 127.3, 127.0, 126.8, 125.5, 113.2, 112.1, 105.7, 40.6, 31.8, 28.8, 22.5; EIMS (70 eV) *m*/*z* (%): 373 (M^+, 100), 246 (22), 281 (7), 207 (15), 202 (8); HRESIMS-TOF (*m*/*z*): $[M + H]^+$ calcd for $C_{23}H_{24}N_3O_2$, 374.1868; found, 374.1859.

6-(4-(*N*,*N*-Dimethylamino)phenyl)-2,4-dimethyl-8-(trifluoromethyl)benzo[*f*]quinazoline-1,3-(2*H*,4*H*)-dione (5f). According to general procedure, compound **5f** was obtained as a brown solid in 70% yield (45.8 mg, 107 µmol, R_f 0.21 (heptane/ethyl acetate 3:2)); mp 259–261 °C; IR (ATR) ṽ: 1691 (s), 1596 (s), 1473 (s), 1314 (vs), 1147 (s), 1116 (vs), 1075 (vs), 818 (vs), 754 (m) cm^{-1}; ^1H NMR (300 MHz, chloroform-*d*) δ 10.10 (d, *J* = 9.2 Hz, 1H), 8.32 (s, 1H), 7.86 (dd, *J* = 9.2, 2.1 Hz, 1H), 7.44–7.35 (m, 3H), 6.92–6.84 (m, 2H), 3.75 (s, 3H), 3.59 (s, 3H), 3.09 (s, 6H); ^{19}F NMR (282 MHz, chloroform-*d*) δ −62.2; ^{13}C {^1H} NMR (75 MHz, chloroform-*d*) δ 162.3, 151.4, 150.9, 150.2, 142.6, 134.4, 130.8, 127.7, 127.3, 127.1 (q, *J* = 32.6 Hz), 126.0, 124.9 (q, *J* = 2.8 Hz), 124.7 (q, *J* = 4.7 Hz), 124.4 (q, *J* = 272.1 Hz), 115.3, 112.3, 106.0, 40.5, 31.9, 28.9; EIMS (70 eV) *m*/*z* (%): 427 (M^+, 100), 369 (5), 270 (4); HRESIMS-TOF (*m*/*z*): $[M + H]^+$ calcd for $C_{23}H_{21}F_3N_3O_2$, 428.1586; found, 428.1577.

2,4-Dimethyl-6-phenylbenzo[*f*]quinazoline-1,3(2*H*,4*H*)-dione (5g). According to general procedure, compound **5g** was obtained as a brown solid in 44% yield (22.2 mg, 70.2 µmol, R_f 0.26 (heptane/ethyl acetate 3:2)); mp 193–195 °C; IR (ATR) ṽ: 1693 (s), 1572 (s), 1423 (s), 1341 (s), 1125 (m), 1030 (m), 853 (m), 776 (vs), 766 (s) cm^{-1}; ^1H NMR (500 MHz, chloroform-*d*) δ 10.0–9.9 (m, 1H), 7.8 (dd, *J* = 8.4, 1.4 Hz, 1H), 7.7 (ddd, *J* = 8.6, 6.8, 1.5 Hz, 1H), 7.6–7.5 (m, 3H), 7.5–7.4 (m, 3H), 7.4 (s, 1H), 3.7 (s, 3H), 3.6 (s, 3H); ^{13}C {^1H} NMR (126 MHz, chloroform-*d*) δ 162.5, 151.4, 149.0, 141.2, 139.7, 132.3, 129.8, 129.7, 128.7, 128.6, 128.4, 126.9, 126.2, 125.7, 114.6, 107.0, 31.8, 28.9 (signals of two carbons are absent, which may relate to signal overlap); EIMS (70 eV) *m*/*z* (%): 316 (M^+, 100), 259 (16), 230 (16), 202 (9), 189 (5); HREIMS (*m*/*z*): $[M]^+$ calcd for $C_{20}H_{16}N_2O_2$, 316.12063; found, 316.12044.

6-(4-Fluorophenyl)-8-hydroxy-2,4-dimethylbenzo[*f*]quinazoline-1,3(2*H*,4*H*)-dione (5h). According to general procedure, compound **5h** was obtained as a brown solid in 45% yield (21.7 mg, 61.9 µmol, R_f 0.13 (heptane/ethyl acetate 3:2)); mp 317–319 °C; IR (ATR) ṽ: 1607 (vs), 1506 (s), 1423 (s), 1355 (s), 1230 (vs), 1224 (vs), 1090 (m), 832 (s), 748 (s) cm^{-1}; ^1H NMR (300 MHz, chloroform-*d*) δ 10.2 (s, 1H), 9.3 (d, *J* = 2.5 Hz, 1H), 7.6–7.5 (m, 3H), 7.4–7.4 (m, 2H), 7.3 (s, 1H), 7.1 (dd, *J* = 9.1, 2.6 Hz, 1H), 3.6 (s, 3H), 3.4 (s, 3H); ^{19}F NMR (282 MHz, chloroform-*d*) δ −113.9; ^{13}C {^1H} NMR (75 MHz, chloroform-*d*) δ 162.6 (d, *J* = 245.3 Hz), 162.3, 159.1, 151.0, 146.9, 142.2, 136.1 (d, *J* = 3.3 Hz), 134.1, 132.2 (d, *J* = 8.3 Hz), 128.5, 122.2, 117.7, 115.9 (d, *J* = 21.4 Hz), 112.6, 108.8, 105.0, 31.9, 28.8; EIMS (70 eV) *m*/*z* (%): 350 (M^+, 100), 295 (14), 267 (16), 164 (13), 238 (23), 160 (21); HREIMS (*m*/*z*): $[M]^+$ calcd for $C_{20}H_{15}FN_2O_3$, 350.1062; found, 350.10584.

2,4-Dimethyl-6-(*p*-tolyl)benzo[4,5]thieno[3,2-*f*]quinazoline-1,3(2*H*,4*H*)-dione (5i). According to general procedure, compound **5i** was obtained as a brown solid in 80% yield (60.1 mg, 155 µmol, R_f 0.22 (heptane/ethyl acetate 3:2)); mp 255–257 °C; IR (ATR) ṽ: 1648 (vs), 1483 (s), 1419 (s), 1333 (m), 1158 (m), 1030 (m), 914 (m), 820 (s), 743 (vs) cm^{-1}; ^1H NMR (300 MHz, chloroform-*d*) δ 7.89 (d, *J* = 7.9 Hz, 1H), 7.39–7.34 (m, 5H), 7.15–7.08 (m, 2H), 7.05 (s, 1H), 3.64 (s, 3H), 3.56 (s, 3H), 2.53 (s, 3H); ^{13}C {^1H} NMR (75 MHz, chloroform-*d*) δ 161.8, 151.2, 145.7, 141.7, 141.7, 139.2, 138.7, 137.3, 133.8, 129.7,

129.5, 128.6, 126.1, 124.2, 124.1, 122.6, 113.0, 108.3, 31.5, 28.7, 21.6; EIMS (70 eV) *m*/*z* (%): 386 (M^+, 100), 300 (13), 258 (14); HRESIMS-TOF (*m*/*z*): $[M + H]^+$ calcd for $C_{23}H_{19}N_2O_2S$, 387.1167; found, 387.1169.

Supporting Information

Supporting Information File 1

Copies of NMR spectra.
[https://www.beilstein-journals.org/bjoc/content/supplementary/1860-5397-20-228-S1.pdf]

Acknowledgements

We are grateful for the technical and analytical support of the University of Rostock (Germany) and Leibniz Institute for Catalysis (Germany).

Funding

We are grateful for the financial support of the State of Mecklenburg-Western Pomerania (Germany).

Conflict of Interest

There are no conflicts or financial interests to declare.

Author Contributions

Ruben Manuel Figueira de Abreu: investigation; writing – original draft. Peter Ehlers: conceptualization; formal analysis; methodology; writing – review & editing. Peter Langer: conceptualization; funding acquisition; resources; supervision; writing – review & editing.

Data Availability Statement

All data that supports the findings of this study is available in the published article and/or the supporting information to this article.

References

1. Myers, R. L. *The 100 Most Important Chemical Compounds,* 1st ed.; Greenwood Publishing Group: London, UK, 2007. doi:10.5040/9798400605284
2. Casy, A. F.; D'Arcy, P. F.; Scott, E. M.; Kuemmerle, H. P.; Oswald, I.; Schier, O.; Marxer, A.; Sternbach, L. H.; Swallow, D. L.; Venulet, J. *Progress in Drug Research;* Birkhäuser Verlag: Basel, Switzerland, 2013; Vol. 22. doi:10.1007/978-3-0348-7102-0
3. Silverman, R. B.; Holladay, M. W. *The Organic Chemistry of Drug Design and Drug Action,* 3rd ed.; Academic Press: San Diego, CA, USA, 2015. doi:10.1016/c2009-0-64537-2
4. Ramesh, D.; Vijayakumar, B. G.; Kannan, T. *Eur. J. Med. Chem.* **2020,** *207,* 112801. doi:10.1016/j.ejmech.2020.112801
5. Hitchings, G. H.; Falco, E. A.; Sherwood, M. B. *Science* **1945,** *102,* 251–252. doi:10.1126/science.102.2645.251
6. Prusoff, W. H.; Holmes, W. L.; Welch, A. D. *Cancer Res.* **1953,** *13,* 221–225.
7. Fischl, M. A.; Richman, D. D.; Grieco, M. H.; Gottlieb, M. S.; Volberding, P. A.; Laskin, O. L.; Leedom, J. M.; Groopman, J. E.; Mildvan, D.; Schooley, R. T.; Jackson, G. G.; Durack, D. T.; King, D.; The AZT Collaborative Working Group. *N. Engl. J. Med.* **1987,** *317,* 185–191. doi:10.1056/nejm198707233170401
8. Horwitz, J. P.; Chua, J.; Noel, M. *J. Org. Chem.* **1964,** *29,* 2076–2078. doi:10.1021/jo01030a546
9. Bergmann, W.; Burke, D. C. *J. Org. Chem.* **1956,** *21,* 226–228. doi:10.1021/jo01108a020
10. Bergmann, W.; Feeney, R. J. *J. Am. Chem. Soc.* **1950,** *72,* 2809–2810. doi:10.1021/ja01162a543
11. Prusoff, W. H. *Biochim. Biophys. Acta* **1959,** *32,* 295–296. doi:10.1016/0006-3002(59)90597-9
12. Geisman, A. N.; Valuev-Elliston, V. T.; Ozerov, A. A.; Khandazhinskaya, A. L.; Chizhov, A. O.; Kochetkov, S. N.; Pannecouque, C.; Naesens, L.; Seley-Radtke, K. L.; Novikov, M. S. *Bioorg. Med. Chem.* **2016,** *24,* 2476–2485. doi:10.1016/j.bmc.2016.04.010
13. Tănase, C. I.; Drăghici, C.; Cojocaru, A.; Galochkina, A. V.; Orshanskaya, J. R.; Zarubaev, V. V.; Shova, S.; Enache, C.; Maganu, M. *Bioorg. Med. Chem.* **2015,** *23,* 6346–6354. doi:10.1016/j.bmc.2015.08.033
14. Sneader, W. *Drug Discovery: A History,* 1st ed.; John Wiley & Sons: Chichester, UK, 2005. doi:10.1002/0470015535
15. de Clercq, E. *Acta Pharm. Sin. B* **2012,** *2,* 535–548. doi:10.1016/j.apsb.2012.10.001
16. De Clercq, E. *Adv. Virus Res.* **2009,** *73,* 1–53. doi:10.1016/s0065-3527(09)73001-5
17. Sidwell, R. W.; Allen, L. B.; Huffman, J. H.; Witkowski, J. T.; Cook, P. D.; Tolman, R. L.; Revankar, G. R.; Simon, L. N.; Robins, R. K. The Potential of Nucleosides as Antiviral Agents. In *Chemotherapy;* Williams, J. D.; Geddes, A. M., Eds.; Springer: New York, NY, USA, 1976; Vol. 6, pp 279–294. doi:10.1007/978-1-4684-3129-2_41
18. Ghorani-Azam, A.; Balali-Mood, M. Clinical Pharmacology and Toxicology of Mustard Compounds. In *Basic and Clinical Toxicology of Mustard Compounds;* Balali-Mood, M.; Abdollahi, M., Eds.; Springer International Publishing: Cham, Switzerland, 2015; Vol. 1, pp 63–99. doi:10.1007/978-3-319-23874-6_4
19. De Clercq, E.; Desgranges, C.; Herdewijn, P.; Sim, I. S.; Jones, A. S.; McLean, M. J.; Walker, R. T. *J. Med. Chem.* **1986,** *29,* 213–217. doi:10.1021/jm00152a008
20. De Clercq, E.; Descamps, J.; De Somer, P.; Barr, P. J.; Jones, A. S.; Walker, R. T. *Proc. Natl. Acad. Sci. U. S. A.* **1979,** *76,* 2947–2951. doi:10.1073/pnas.76.6.2947
21. Roh, K. R.; Kim, J. Y.; Kim, Y. H. *Tetrahedron Lett.* **1999,** *40,* 1903–1906. doi:10.1016/s0040-4039(98)02491-5
22. Lin, T. S.; Guo, J. Y.; Schinazi, R. F.; Chu, C. K.; Xiang, J. N.; Prusoff, W. H. *J. Med. Chem.* **1988,** *31,* 336–340. doi:10.1021/jm00397a011
23. Rahim, S. G.; Trivedi, N.; Bogunovic-Batchelor, M. V.; Hardy, G. W.; Mills, G.; Selway, J. W. T.; Snowden, W.; Littler, E.; Coe, P. L.; Basnak, I.; Whale, R. F.; Walker, R. T. *J. Med. Chem.* **1996,** *39,* 789–795. doi:10.1021/jm950029r
24. Perman, J.; Sharma, R. A.; Bobek, M. *Tetrahedron Lett.* **1976,** *17,* 2427–2430. doi:10.1016/0040-4039(76)90010-1
25. Farina, V.; Hauck, S. I. *Synlett* **1991,** 157–159. doi:10.1055/s-1991-20661

26. Hudson, R. H. E.; Li, G.; Tse, J. *Tetrahedron Lett.* **2002,** *43,* 1381–1386. doi:10.1016/s0040-4039(02)00024-2
27. Hirota, K.; Kitade, Y.; Isobe, Y.; Maki, Y. *Heterocycles* **1987,** *26,* 355–358. doi:10.3987/r-1987-02-0355
28. Stevenson, T. M.; Crouse, B. A.; Thieu, T. V.; Gebreysus, C.; Finkelstein, B. L.; Sethuraman, M. R.; Dubas-Cordery, C. M.; Piotrowski, D. L. *J. Heterocycl. Chem.* **2005,** *42,* 427–435. doi:10.1002/jhet.5570420310
29. Platonova, Y. B.; Volov, A. N.; Tomilova, L. G. *Bioorg. Med. Chem. Lett.* **2020,** *30,* 127351. doi:10.1016/j.bmcl.2020.127351
30. Sharma, R. A.; Bobek, M. *J. Org. Chem.* **1975,** *40,* 2377–2379. doi:10.1021/jo00904a025
31. Shih, Y.-C.; Chien, T.-C. *Tetrahedron* **2011,** *67,* 3915–3923. doi:10.1016/j.tet.2011.03.051
32. Fang, W.-P.; Cheng, Y.-T.; Cheng, Y.-R.; Cherng, Y.-J. *Tetrahedron* **2005,** *61,* 3107–3113. doi:10.1016/j.tet.2005.01.085
33. Cho, Y.-M.; Johnson, F. *Tetrahedron Lett.* **1994,** *35,* 1149–1152. doi:10.1016/0040-4039(94)88009-3
34. Tanaka, H.; Hayakawa, H.; Shibata, S.; Haraguchi, K.; Miyasaka, T.; Hirota, K. *Nucleosides Nucleotides* **1992,** *11,* 319–328. doi:10.1080/07328319208021706
35. Palmisano, G.; Santagostino, M. *Tetrahedron* **1993,** *49,* 2533–2542. doi:10.1016/s0040-4020(01)86332-8
36. Nencka, R.; Sinnaeve, D.; Karalic, I.; Martins, J. C.; Van Calenbergh, S. *Org. Biomol. Chem.* **2010,** *8,* 5234–5246. doi:10.1039/c0ob00061b
37. Hudson, R. H. E.; Moszynski, J. M. *Synlett* **2006,** 2997–3000. doi:10.1055/s-2006-948176
38. Kraljević, T. G.; Bistrović, A.; Dedić, M.; Pavelić, S. K.; Sedić, M.; Raić-Malić, S. *Tetrahedron Lett.* **2012,** *53,* 5144–5147. doi:10.1016/j.tetlet.2012.07.068
39. Janeba, Z.; Balzarini, J.; Andrei, G.; Snoeck, R.; De Clercq, E.; Robins, M. J. *Can. J. Chem.* **2006,** *84,* 580–586. doi:10.1139/v06-041
40. Park, G.; Ettles, C.; Charles, M.; Hudson, R. H. E. *J. Photochem. Photobiol., A* **2023,** *441,* 114653. doi:10.1016/j.jphotochem.2023.114653
41. Teppang, K. L.; Lee, R. W.; Burns, D. D.; Turner, M. B.; Lokensgard, M. E.; Cooksy, A. L.; Purse, B. W. *Chem. – Eur. J.* **2019,** *25,* 1249–1259. doi:10.1002/chem.201803653
42. Heidari, A.; Ghorbani-Choghamarani, A.; Hajjami, M.; Hudson, R. H. E. *Molecules* **2020,** *25,* 1995. doi:10.3390/molecules25081995
43. Freeman, N. S.; Moore, C. E.; Wilhelmsson, L. M.; Tor, Y. *J. Org. Chem.* **2016,** *81,* 4530–4539. doi:10.1021/acs.joc.6b00310
44. Suchý, M.; Hudson, R. H. E. *J. Org. Chem.* **2014,** *79,* 3336–3347. doi:10.1021/jo402873e
45. Kaczmarek, R.; Twardy, D. J.; Olson, T. L.; Korczyński, D.; Andrei, G.; Snoeck, R.; Dolot, R.; Wheeler, K. A.; Dembinski, R. *Eur. J. Med. Chem.* **2021,** *209,* 112884. doi:10.1016/j.ejmech.2020.112884
46. Bollu, A.; Sharma, N. K. *ChemBioChem* **2019,** *20,* 1467–1475. doi:10.1002/cbic.201800822
47. Meher, S.; Gade, C. R.; Sharma, N. K. *ChemBioChem* **2023,** *24,* e202200732. doi:10.1002/cbic.202200732
48. Mikami, A.; Mori, S.; Osawa, T.; Obika, S. *Chem. – Eur. J.* **2023,** *29,* e202301928. doi:10.1002/chem.202301928
49. Romero-Pérez, S.; López-Martín, I.; Martos-Maldonado, M. C.; Somoza, Á.; González-Rodríguez, D. *Org. Lett.* **2020,** *22,* 41–45. doi:10.1021/acs.orglett.9b03801
50. Zeng, Y.; Wang, Z.; Zeng, L.; Xiong, H. *Anal. Chem. (Washington, DC, U. S.)* **2023,** *95,* 18880–18888. doi:10.1021/acs.analchem.3c04415
51. Robins, M. J.; Barr, P. J. *Tetrahedron Lett.* **1981,** *22,* 421–424. doi:10.1016/0040-4039(81)80115-3
52. Youssefyeh, R. D.; Weisz, M. *Tetrahedron Lett.* **1973,** *14,* 4317–4318. doi:10.1016/s0040-4039(01)87209-9
53. Senda, S.; Hirota, K.; Takahashi, M. *J. Chem. Soc., Perkin Trans. 1* **1975,** 503–507. doi:10.1039/p19750000503
54. Dudkin, S.; Iaroshenko, V. O.; Sosnovskikh, V. Y.; Tolmachev, A. A.; Villinger, A.; Langer, P. *Org. Biomol. Chem.* **2013,** *11,* 5351–5361. doi:10.1039/c3ob26837c
55. Nishigaki, S.; Sato, J.; Shimizu, K.; Furukawa, K.; Senga, K.; Yoneda, F. *Chem. Pharm. Bull.* **1980,** *28,* 142–149. doi:10.1248/cpb.28.142
56. Majumdar, K. C.; Sinha, B.; Maji, P. K.; Chattopadhyay, S. K. *Tetrahedron* **2009,** *65,* 2751–2756. doi:10.1016/j.tet.2009.01.107
57. Sun, G.; Fecko, C. J.; Nicewonger, R. B.; Webb, W. W.; Begley, T. P. *Org. Lett.* **2006,** *8,* 681–683. doi:10.1021/ol052876m
58. Van Tinh, D.; Fischer, M.; Stadlbauer, W. *J. Heterocycl. Chem.* **1996,** *33,* 905–910. doi:10.1002/jhet.5570330358
59. Sako, M.; Ichioka, T.; Totani, R.; Hirota, K. *J. Org. Chem.* **1995,** *60,* 8115–8116. doi:10.1021/jo00129a068
60. Srivastav, N. C.; Rai, D.; Tse, C.; Agrawal, B.; Kunimoto, D. Y.; Kumar, R. *J. Med. Chem.* **2010,** *53,* 6180–6187. doi:10.1021/jm100568q
61. Petricci, E.; Radi, M.; Corelli, F.; Botta, M. *Tetrahedron Lett.* **2003,** *44,* 9181–9184. doi:10.1016/j.tetlet.2003.10.028
62. Satoh, K.; Tanaka, H.; Andoh, A.; Miyasaka, T. *Nucleosides, Nucleotides Nucleic Acids* **1986,** *5,* 461–469. doi:10.1080/07328318608068688
63. Tanaka, H.; Haraguchi, K.; Koizumi, Y.; Fukui, M.; Miyasaka, T. *Can. J. Chem.* **1986,** *64,* 1560–1563. doi:10.1139/v86-257
64. Wheeler, H. L.; Bristol, H. S. *Am. Chem. J.* **1905,** *33,* 437–447.
65. de Abreu, R. M. F.; Brockmann, T.; Villinger, A.; Ehlers, P.; Langer, P. *Beilstein J. Org. Chem.* **2024,** *20,* 898–911. doi:10.3762/bjoc.20.80
66. Hu, Y.-G.; Wang, Y.; Du, S.-M.; Chen, X.-B.; Ding, M.-W. *Bioorg. Med. Chem. Lett.* **2010,** *20,* 6188–6190. doi:10.1016/j.bmcl.2010.08.122
67. Hossain, M. I.; Bhuiyan, M. M. H. *J. Sci. Res. (Rajshahi, Bangladesh)* **2009,** *1,* 317–325. doi:10.3329/jsr.v1i2.2299
68. König, B.; Kümmel, S.; Svobodová, E.; Cibulka, R. *Phys. Sci. Rev.* **2018,** *3,* 20170168. doi:10.1515/psr-2017-0168
69. Tu, Y.; Yang, Y.; Li, Y.; He, C. *Pharmacol. Res.* **2021,** *169,* 105615. doi:10.1016/j.phrs.2021.105615
70. Brouwer, A. M. *Pure Appl. Chem.* **2011,** *83,* 2213–2228. doi:10.1351/pac-rep-10-09-31
71. Meech, S. R.; Phillips, D. *J. Photochem.* **1983,** *23,* 193–217. doi:10.1016/0047-2670(83)80061-6

License and Terms

This is an open access article licensed under the terms of the Beilstein-Institut Open Access License Agreement (https://www.beilstein-journals.org/bjoc/terms), which is identical to the Creative Commons Attribution 4.0 International License (https://creativecommons.org/licenses/by/4.0). The reuse of material under this license requires that the author(s), source and license are credited. Third-party material in this article could be subject to other licenses (typically indicated in the credit line), and in this case, users are required to obtain permission from the license holder to reuse the material.

The definitive version of this article is the electronic one which can be found at:
https://doi.org/10.3762/bjoc.20.228

BEILSTEIN JOURNAL OF ORGANIC CHEMISTRY

Synthesis of spiroindolenines through a one-pot multistep process mediated by visible light

Francesco Gambuti‡, Jacopo Pizzorno‡, Chiara Lambruschini, Renata Riva and Lisa Moni*

Full Research Paper

Open Access

Address:
Department of Chemistry and Industrial Chemistry, University of Genoa, Via Dodecaneso 31, 1646 Genova, Italy

Email:
Lisa Moni* - lisa.moni@unige.it

* Corresponding author ‡ Equal contributors

Keywords:
isocyanide; multicomponent reactions; one-pot reaction; oxidation; spiroindolenine; Ugi reaction; visible light

Beilstein J. Org. Chem. **2024,** *20,* 2722–2731.
https://doi.org/10.3762/bjoc.20.230

Received: 16 July 2024
Accepted: 11 October 2024
Published: 29 October 2024

This article is part of the thematic issue "Multicomponent reactions IV".

Associate Editor: T. J. J. Müller

© 2024 Gambuti et al.; licensee Beilstein-Institut.
License and terms: see end of document.

Abstract

Spiro-heterocyclic indolenines are privileged scaffolds widely present in numerous indole alkaloids. Here, we develop a novel approach for the one-pot multistep synthesis of different spiro[indole-isoquinolines]. The protocol proposed involves the visible light mediated oxidation of *N*-aryl tertiary amines using bromochloroform with the generation of a reactive iminium species, which reacts with an isocyanide and an electron-rich aniline in a three-component Ugi-type reaction to give an α-aminoamidine. This compound might undergo an additional visible light-mediated oxidation to furnish a second iminium intermediate, which acts as electrophile in an intramolecular electrophilic aromatic substitution giving the final spiro-indolenine. The scope of the process has been investigated with respect to all three components. Simple operations, mild conditions, and good yields make this strategy a convenient and sustainable way to obtain novel spiro-indolenine derivatives.

Introduction

Diversity-oriented synthesis (DOS) is a successful approach to biologically active scaffolds directed to create an enormous exploratory space in pharmaceutical hit discovery [1,2]. Among the common compound collections for drug discovery, the introduction of spirocyclic elements presents an attractive strategy for increasing molecular complexity without increasing molecular weight, and at the same time, for introducing structural novelty for patentability [3]. However, the construction of spirocyclic motifs is often associated with increased synthetic effort and number of synthetic steps. Hence, developing efficient strategies to access spirocyclic targets with structural diversity is highly desirable and valuable. Among the bioactive compounds containing spiro atoms, the spiro-indolenines, specially the spiro-heterocyclic indolenines, can be considered as a privileged scaffold, present in several natural products with interesting biological activities, as depicted in Figure 1 [4-7].

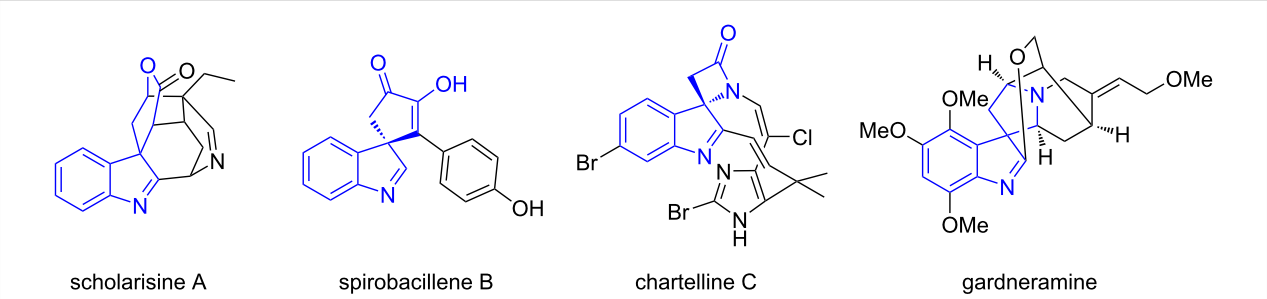

Figure 1: Selected natural products containing spiro-indolenines.

Among the known methods of synthesizing spiro-heterocyclic indolenines, the dearomative cyclization of the indole derivatives is the most popular (Scheme 1a). For instance, the efficient synthesis of spiro[indoline-3,2′-pyrrolidines] [8-10] or spiro-isoxazoles [11] through different dearomatization processes has been reported. Recently, Ramana and Dothe have proposed an elegant gold-catalyzed protocol to obtain spiro[benzo[*e*][1,3]oxazine-2,3'-indoles] starting from 2-alkynylphenyl azides and 1,2-benzisoxazoles [12] (Scheme 1b). However, all these processes generally involve the preparation of starting materials, often not trivial. On the other hand, in 2018 Aksenov and Rubin reported the acid-catalyzed [4 + 1] cycloaddition of commercially available substrates, as indoles and nitroalkenes to give spiro-isoxazoles (Scheme 1c), but acceptable yields were obtained just using nitrostyrenes [13,14].

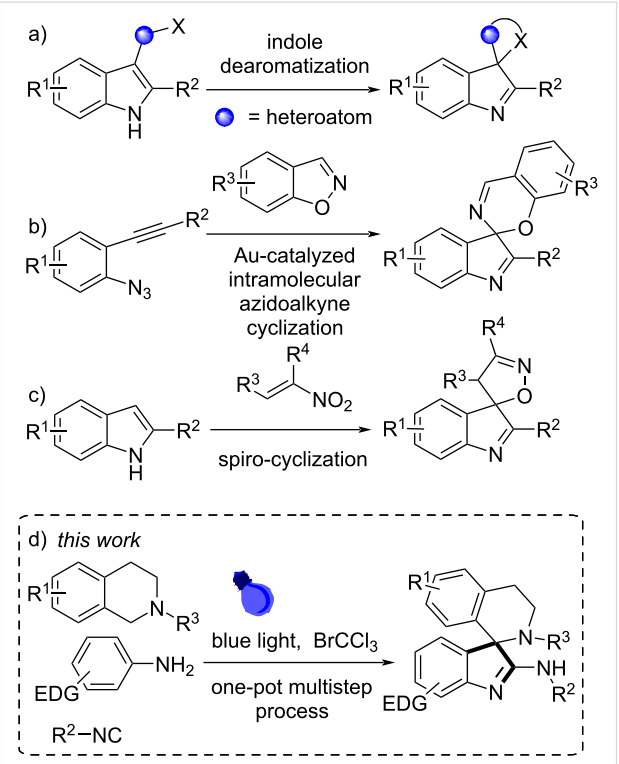

Scheme 1: Synthesis of spiro[indole-heterocycles].

Despite these examples, the highly efficient construction of structurally diverse spiro-heterocyclic indolenines from readily available starting materials under mild conditions and in a diversity-oriented fashion remains desirable.

In this contest, oxidative isocyanide-based multicomponent reactions (oxidative IMCRs) can be considered as a convenient tool [15]. Actually, the use of an external oxidant in combination with a multicomponent process allows to improve the scope of known MCRs by broadening the diversity and availability of starting materials, or by transforming unstable multicomponent adducts into stable compounds.

Following our research interest in developing new efficient methods for the synthesis of heterocycles by multicomponent processes and domino reactions [16-20], here we disclosed the oxidative one-pot four-step synthesis of 2-amino-3,3'-spiroindolenines using readily available tertiary amines, electron-rich anilines and isocyanides as starting materials (Scheme 1d). The synthetic procedure is achieved using blue light irradiation and bromotrichloromethane ($BrCCl_3$), as a one-pot procedure, minimizing chemical wastes, avoiding purification of intermediates, and simplifying practical aspects.

Results and Discussion

We have recently published the one-pot multistep synthesis of unprecedent 2,3-diaminoindolenines using graphene oxide (GO) as heterogeneous catalyst [21]. The protocol involves the three-component Ugi (3C-Ugi) reaction between aldehydes, isocyanides and 2 equivalents of electron-rich anilines to give α-aminoamidines, which undergo a C–N bond oxidation to generate α-iminoamidines and then a final cyclization takes place (Scheme 2a). Although the synthetic procedure allowed the preparation of highly substituted complex structures under mild reaction conditions and on gram scale, it suffers from a limited structural diversity. Since two anilines are incorporated

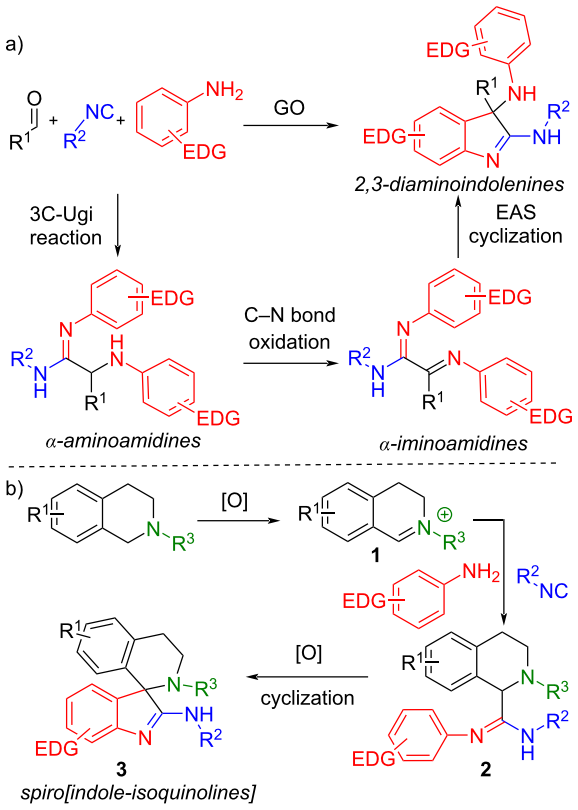

Scheme 2: Synthetic strategy for the new synthesis of 2,3-diaminoindolenines [21] and spiro[indole-isoquinolines].

in the final product, we speculated that the diversification of them could lead to different products.

Anyway, first attempts to use two different anilines in the reaction failed, giving complex mixtures of α-aminoamidines even using sequential or slow addition of reactants. Therefore, based on the previous studies on the oxidative 3-component Ugi–Joullié reaction [22-24] and our precedent experience [25-27], we speculated that cyclic imines could be good substrates for our reaction, thanks to their higher rigidity and stability.

As depicted in Scheme 2b, our plan provides: the oxidation of *N*-aryltetrahydroisoquinolines (*N*-Ar-THIQs) generating in situ the iminium ions **1**, the 3C Ugi-type reaction of an electron-rich aniline, an isocyanide and **1**; the subsequent oxidation of the Ugi-type product **2**; and the final cyclization to give the spiro[indole-THIQs] **3**.

Based on our experience on the use of graphene oxide (GO) as heterogeneous catalyst to promote MCRs and subsequent C–N bond oxidation [16,21], we first investigated the GO-promoted oxidation of *N*-Ph-THIQ and the subsequent 3C Ugi reaction to give α-aminoamidine **2a**. Applying the previously optimized reaction conditions, we observed good conversion of the starting material, but the desired compound was isolated in very poor yield, as the α-aminoamide **4a** resulted the main product (Table 1, entry 1). We were surprised about that, as, even if

Table 1: Initial investigation of the GO-promoted oxidation/3C-Ugi reaction process.

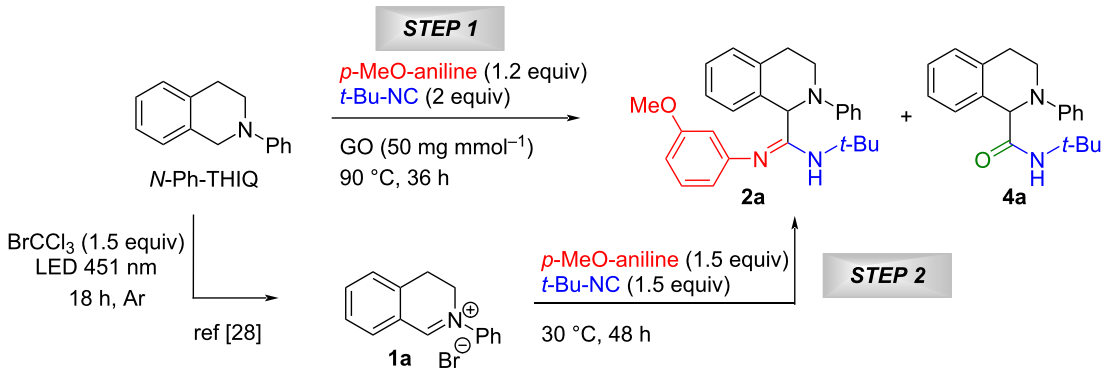

Entry	Step 1	Step 2	Yield **2a**[a]	Yield **4a**[a]
1	CH_3CN/H_2O (4:1)	–	12%	26%
2[b]	CH_3CN[b]	–	22%	–
3[b]	–	GO (30 mg $mmol^{-1}$) MeOH	64%	–
4[b]	–	MeOH	54%	–
5[b]	–	CF_3CH_2OH	43%	–
6[b]	–	CH_3CN	63%	–

[a]Isolated yield after column chromatography; [b]reactions were carried out under argon atmosphere with dry solvents.

water is present as co-solvent in the reaction mixture, we have never noted the formation of the α-aminoamide in our previous work. Repeating the reaction in the absence of water suppressed the **4a** formation but with a concomitant drop of the conversion, resulting again in a poor yield of **2a** (Table 1, entry 2).

Thus, we demonstrated that GO was able to oxidize the substrate, which reacted with the 3-methoxyaniline and *tert*-butyl isocyanide affording the α-aminoamidine, albeit inefficiently. Besides, the role of GO in the 3C Ugi reaction remained unclear. Actually, the iminium ion formed after the oxidation is already quite activated to react with isocyanide without the presence of a catalyst. In order to establish the role of GO we carried out the 3C Ugi-type reaction starting from iminium ion **1a**, freshly prepared by visible light irradiation in the presence of bromochloroform [28]. This protocol resulted quite convenient as can be conducted under argon atmosphere to prevent the interaction of oxygen or reactive oxygen intermediates, which are not always compatible with the substrates, as well as the key intermediates. Moreover, $BrCCl_3$ and its reduced form (chloroform) can be easily removed from the reaction mixture thanks to their low boiling point, allowing the easy purification of the products.

As expected, the reaction conducted in the absence of the carbocatalyst led to the obtainment of **2a** with comparable yield (Table 1, entries 3 and 4), demonstrating that **1a** is a sufficiently activated substrate for the 3C Ugi-type reaction to occur. Interestingly, different solvents, such as trifluoroethanol or acetonitrile (Table 1, entries 5 and 6), had a low impact, affording **2a** in acceptable yield.

The possibility of conducting the MCR in acetonitrile, the same solvent in which the oxidation of the C–N bond is performed, pushed us to perform the synthetic process in a one-pot manner, adding all the components from the very beginning. So, the blue-light-promoted reaction between *N*-Ph-THIQ, 3-methoxyaniline and *tert*-butyl isocyanide in the presence of $BrCCl_3$ was extensively optimized by varying several parameters, such as solvent, relative quantity of components and temperature (Table 2). We firstly irradiated with blue LEDs (451 nm) the mixture of the three components in the presence of 1.5 equiv of $BrCCl_3$ for 18 h at room temperature under argon atmosphere (Table 2, entry 1).

To our surprise, the reaction provided only traces of the expected α-aminoamidines **2a**, while the spiro-compound **3a** was the main product. **3a** was the result of a four-step one-pot process where an oxidation of *N*-Ph-THIQ, a 3C Ugi-type reaction, a second oxidation of the Ugi-type product **2a** and a final cyclization took place, as we had initially planned. Excited by this result, we optimized the reaction conditions to make the process more efficient.

Increasing the amount of isocyanide (Table 2, entry 2) and $BrCCl_3$ (Table 2, entry 3) influenced the yield, obtaining **3a** up to a yield of 56% using a double quantity of polyhalomethane. Different solvents were detrimental (Table 2, entries 4, 5 and 7), while higher temperature improved the efficiency of the process (Table 2, entry 6). Under the optimized conditions we were able to obtain **3a** with a 61% isolated yield, which can be considered an excellent result, as it is related to a four-step process (an average yield of 88% each step).

Table 2: Investigation of the one-pot four-step synthesis of spiro[indole-THIQ] **3a**.

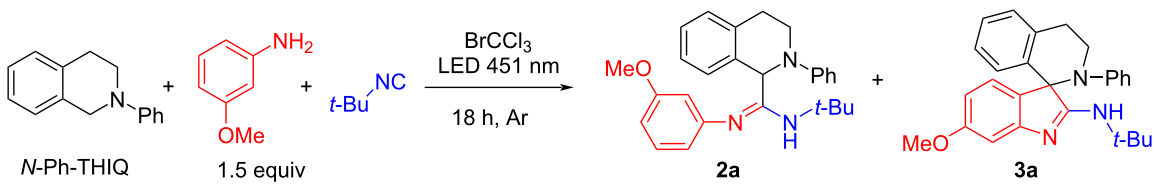

Entry	*t*-Bu-NC	$BrCCl_3$	Solvent (0.2 M)	Temp.	Yield **3a**[a]	Yield **2a**[a]
1	1.5 equiv	1.5 equiv	CH_3CN	20 °C	43%	3%
2	2.2 equiv	2.2 equiv	CH_3CN	20 °C	51%	–%
3	2.2 equiv	3 equiv	CH_3CN	20 °C	56%	2%
4	2.2 equiv	3 equiv	EtOH	20 °C	40%	18%
5	2.2 equiv	3 equiv	EtOAc	20 °C	2%	13%
6[b]	**2.2 equiv**	**3 equiv**	**CH_3CN**	**30 °C**	**61%**	**3%**
7	2.2 equiv	3 equiv	EtOH	30 °C	53%	5%

[a]Isolated yield after column chromatography with alumina; [b]optimized reaction conditions: *N*-Ph-THIQ (1 equiv), 3-methoxyaniline (1.5 equiv), $BrCCl_3$ (3 equiv) in CH_3CN (0.2 M), *tert*-butyl isocyanide (2.2 equiv), argon atmosphere, 451 nm (blue LEDs), 30 °C, 24 h.

Since, during the optimization of the reaction conditions, we have noticed a certain instability of the spiro-compounds through chromatography on silica gel, we have initially carried out the purifications using alumina as the stationary phase. However, during the scope studies, alumina proved to be ineffective as chromatographic stationary phase, providing the final products with insufficient purity, or not separating efficiently the side products. For this reason, we implemented the synthetic process treating the reaction mixture with 3 equivalents of Et_3N before evaporating the solvent and using Et_3N as additive for the eluent of the chromatography on silica gel. With these improvements, we have demonstrated that the yields are comparable to those obtained with purification on alumina but reaching significantly higher degrees of purity of the final products (see Supporting Information File 1).

Having the optimized conditions in our hands, we moved on to establish the scope (Scheme 3).

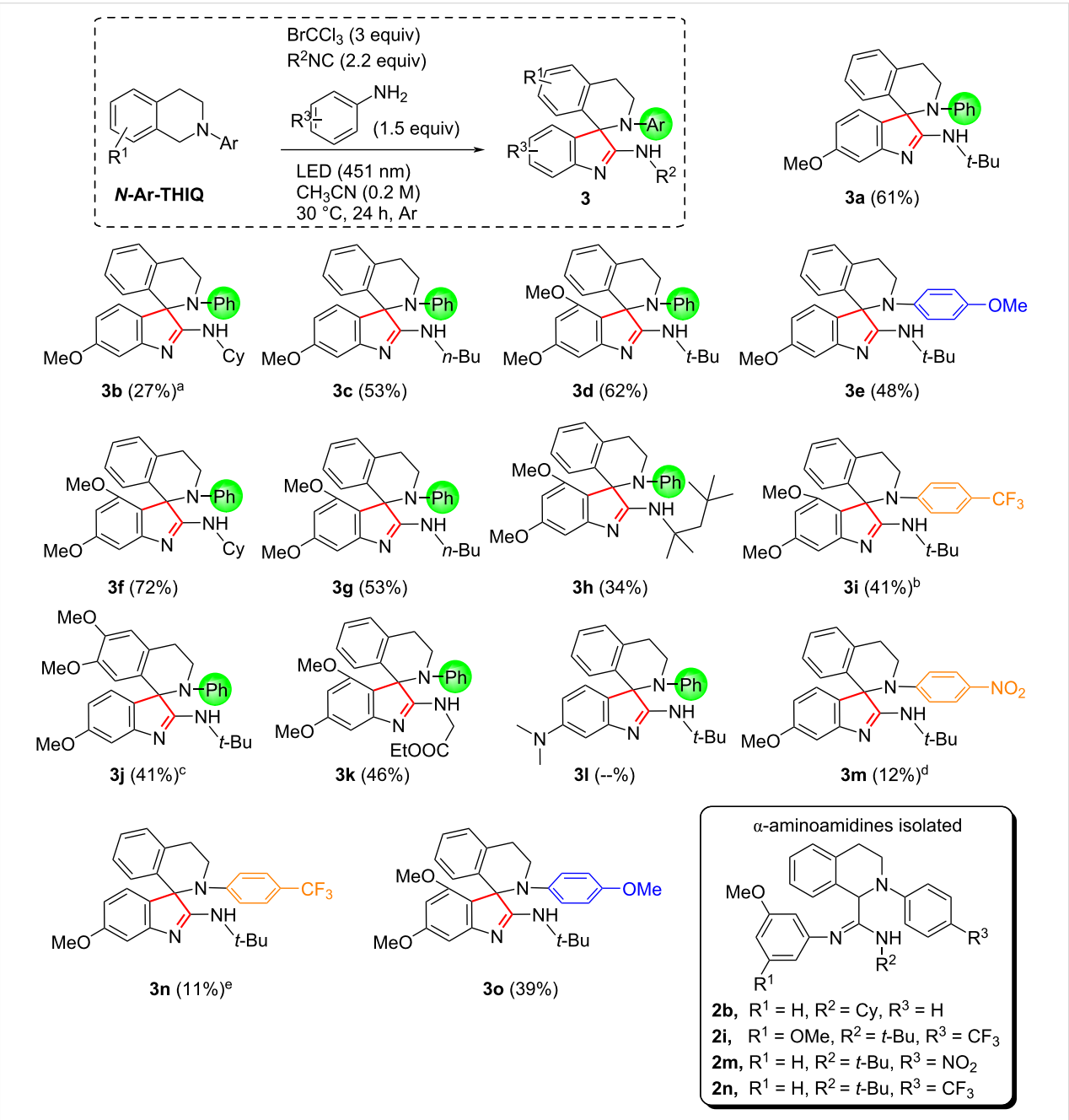

Scheme 3: Scope of the synthesis of spiro[indole-THIQs]. [a]α-aminoamidine **2b** has been isolated (54%) too; [b]α-aminoamidine **2i** has been isolated (16%) too; [c]white LEDs were used; [d]α-aminoamidine **2m** has been isolated (28%) too; [e]α-aminoamidine **2n** has been isolated (20%) too.

Different *N*-arylated-THIQs, isocyanides and electron-rich anilines have been combined. The overall yields of the protocol are good considering its multistep behavior.

Very good results were obtained when performing the reaction with a combination of *N*-Ph-THIQ and 3-methoxyaniline (**3a** and **3c**) or 3,5-dimethoxyanaline (**3d**, **3f** and **3g**). When a THIQ with electron-rich aryl group was employed, the final spiroindolenines **3e** and **3o** were isolated in good yield.

On the other hand, when *p*-CF_3-phenyl-THIQ or *p*-NO_2-phenyl-THIQ were reacted, the conversion was not complete and the spiroindolenines (**3i**, **3m** and **3n**) were obtained in poor yield together with the corresponding α-aminoamidines **2i**, **2m** and **2n** (16%, 28% and 20%, respectively). Different isocyanides, such as linear, branched, or functionalized (**3k**) can be used. Surprisingly, the use of cyclohexyl isocyanide does not lead to the complete conversion of the α-aminoamidine **2b** into the corresponding spiro compound **3b**, which were isolated in 54% and 27% yields, respectively. Employing electron-rich *N*-Ar-THIQ, no reaction occurred using optimized conditions. Based on the literature [28], the formation of an electron donor–acceptor complex between bromochloroform and *N*-Ar-THIQ seems essential for the reaction to occur. Since we did not observe the formation of any color during the irradiation of the solution of $BrCCl_3$ and this specific THIQ, we postulated that blue light was not the optimal one. Since, the absorption spectrum of the mixture showed better absorption at higher wavelengths (see Supporting Information File 1), we repeated the synthesis by irradiating with white LEDs, succeeding in isolating product **3j** in acceptable yield.

However, the synthetic protocol presents some limitations: employing non-electron-rich anilines (such as aniline or *p*-methylaniline) the reaction was unsuccessful, and the desired spiro-compounds were not obtained. To deeply investigate this point, we carried out the synthetic procedure with *p*-methylaniline step by step (Scheme 4).

While the 3C Ugi-type reaction between iminium ion **1a**, *p*-methylaniline and *tert*-butyl isocyanide gave product **2p** in good yield, when the α-aminoamidine was subjected to the oxidation–cyclization step, the starting material was completely converted, but **3p** was not isolated. Thus, we supposed that the second visible light-mediated oxidation properly occurred generating the iminium ion which underwent decomposition. Even using 3-(*N*,*N*-dimethylamino)aniline, the corresponding spiro compound **3l** was not obtained. In this case, it is assumed that the highly acidic environment of the reaction protonates the amino group, making the final cyclization less efficient.

Finally, we have tried to extend the synthetic protocol to other benzo-fused *N*-heterocycles. We investigated the benzo-fused 7-membered nitrogen heterocycles, both for our previous experience in applying them in MCRs [25,27] and for their known interest in medicinal chemistry.

Towards this goal, *N*-phenylbenzoxazepine **5** was synthesized and subjected to the one-pot protocol within *tert*-butyl isocyanide and 3,5-dimethoxyaniline (Scheme 5). Unfortunately, the reaction mixture appeared very complex and the desired product **6** was not observed. Instead, among the several side-products formed, we were able to isolate α-aminoamidine **7**, as the result of a 3C Ugi-type reaction between an aldehyde obtained from an oxidation–hydrolysis process of compound **5**, *tert*-butyl isocyanide and 2 equivalents of aniline, and the simultaneous insertion of an isocyanide into the N–H bond. This evidence shows that **5** was able to be oxidized but the iminium ion formed was not stable enough to take part in the subsequent reaction, preferring to hydrolytically open.

In order to test the synthetic utility of this procedure we also carried out a gram scale reaction. First, the suitability of the one-pot protocol toward the synthesis of spiro-derivative **3d** was verified by applying optimized conditions (Table 3, entry 1). To do this a different photoreactor has been used (see Supporting Information File 1 for details) [29].

While the overall yield resulted even better (76% starting from 1 g of *N*-Ph-THIQ), a slight decrease of the conversion of α-aminoamidine **2d** into the spiro[indole-THIQ] **3d** was observed. As expected, the use of a larger-diameter reactor caused

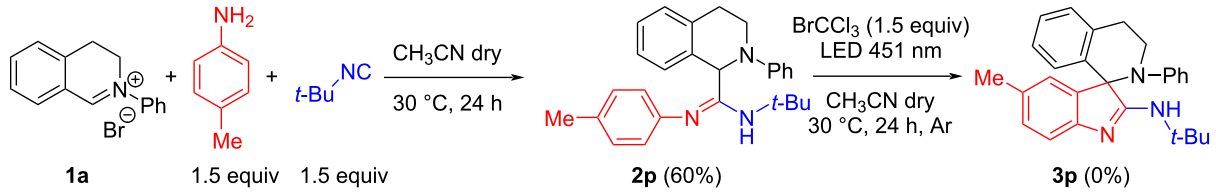

1a 1.5 equiv 1.5 equiv **2p** (60%) **3p** (0%)

Scheme 4: Two-step synthesis using *p*-methylaniline.

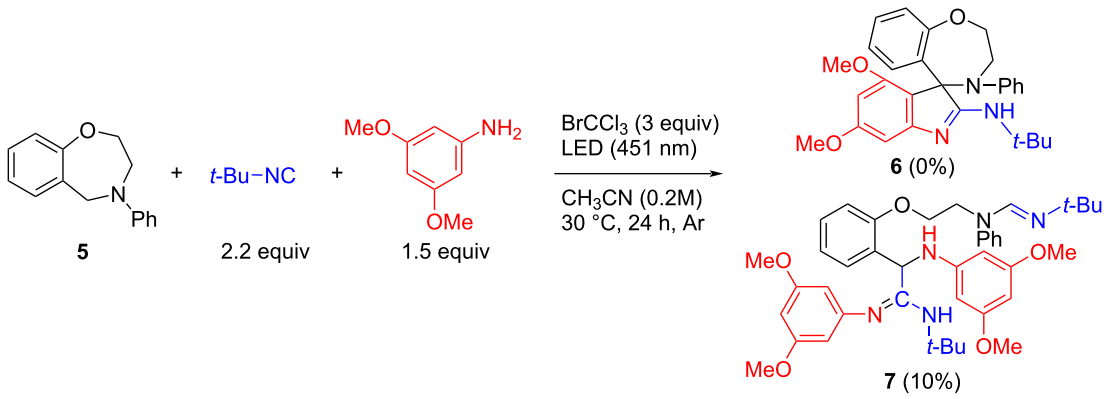

Scheme 5: Investigation of the one-pot four-step synthetic protocol employing *N*-Ph-benzoxazepine **5**.

Table 3: Gram scale reaction for the synthesis of spiro[indole-THIQs] **3**.

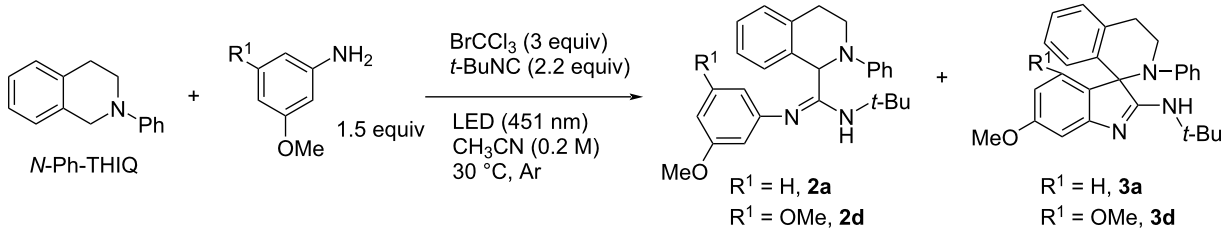

Entry	*N*-Ph THIQ (g)	R^1	Time (h)	Yield **3**[a]	Yield **2**[a]
1	1.00	OCH_3	24	48% (**3d**)	28% (**2d**)
2	0.50	OCH_3	48	68% (**3d**)	3% (**2d**)
3	1.00	H	48	51% (**3a**)	19% (**2a**)

[a]Isolated yield after column chromatography.

a low penetration of the irradiation, thus leading to lower efficiency.

Repeating the reaction on 500 mg for a longer reaction time a notable 68% isolated yield of **3d** was obtained (Table 3, entry 2). These slightly different conditions were applied to the gram scale synthesis of **3a** obtaining good results (Table 3, entry 3).

To obtain some information of the reaction mechanism and the intermediates involved, the relationship between the product conversions and the reaction time was investigated in the reaction between *N*-Ph-THIQ, 3,5-dimethoxyaniline and *t*-BuNC in the presence of $BrCCl_3$ under light irradiation (Figure 2). This time profile shows that, as soon as the *N*-Ph-THIQ is transformed into iminium ion **1a**, this compound instantly takes part in the Ugi-type reaction with 3,5-dimethoxyaniline and *t*-BuNC giving the α-aminoamidine **2d**. After 4 h, **2d** starts to be converted slowly into the final product **3d**, thanks to a second oxidation and a final cyclization. This study indicates that the second oxidation is faster than the multicomponent reaction, as intermediate **2d** is not accumulated in the reaction mixture, but easily undergoes the C–N bond oxidation and the subsequent cyclization.

A probable mechanistic pathway for the formation of spiroindolenine is outlined in Scheme 6. Based on the results reported by Zeitler [28], several mechanisms are involved in the oxidation of *N*-Ph-THIQ. The most probable involves the photoexcitation of the EDA (Electron Donor-Acceptor) complex promoting an electron transfer from *N*-Ph-THIQ to $BrCCl_3$ to afford the amine radical cation and highly reactive $BrCCl_3$ radical anion. Anyway, the *N*-Ph-THIQ can undergo numerous pathways towards the iminium ion **1a** (see reference [28] for details). The oxidation of compound **2d** may occur according to the same mechanism. However, alternative mechanisms, such as the direct hydride transfer from compound **2** to the iminium ion **1a**, cannot be ruled out (see Supporting Information File 1).

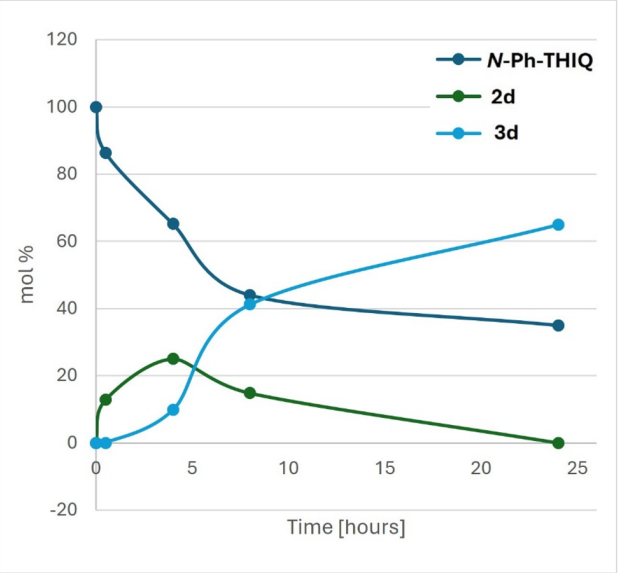

Figure 2: Time profile of the reaction of *N*-Ph-THIQ, 3,5-dimethoxyaniline and *t*-BuNC conducted under optimized conditions.

Conclusion

In conclusion, we have developed a novel visible light-promoted synthesis of spiro[indole-isoquinolines] employing simple and readily available starting materials. Our one-pot four-step synthesis allows the preparation of complex structures without using catalysts, and purification of intermediates. Remarkably, the reaction can be performed even on gram scale without loss of efficiency. Studies directed toward evaluating the biological activities of the spiroindolenines are currently underway in our laboratory, and the results will be reported in due course.

Experimental

General methods

^{1}H, ^{13}C and ^{19}F NMR spectra were recorded on a JEOL 400 spectrometer (at 400 MHz, 101 MHz and 376 MHz, respectively). Unless otherwise stated, NMR spectra were recorded using residual solvent as the internal standard; ^{1}H NMR: TMS = 0.00; $(CD_3)_2SO$ = 2.50; and ^{13}C NMR: $CDCl_3$ = 77.16; $(CD_3)_2SO$ = 39.52. Data for ^{1}H NMR spectra are reported as follows: chemical shift (δ ppm), multiplicity, coupling constants (Hz) and integration. Data for ^{13}C NMR spectra are reported in terms of chemical shift (δ ppm). Interpretation of spectra has been made also with the aid of gCOSY, gHSQC and gHMBC experiments. The following abbreviations are used to indicate the multiplicity in NMR spectra: s, singlet; d, doublet; t, triplet; q, quartet; m, multiplet. For some compounds the extra peaks are due to residual of the starting material (<5%) due to difficulties in the purification. IR spectra were recorded as solid, oil, or foamy samples, with the ATR (attenuated total reflectance) method. TLC analyses were carried out on pre-coated Merck silica gel 60 F254 plates or Aluminum oxide on TLC-plates and

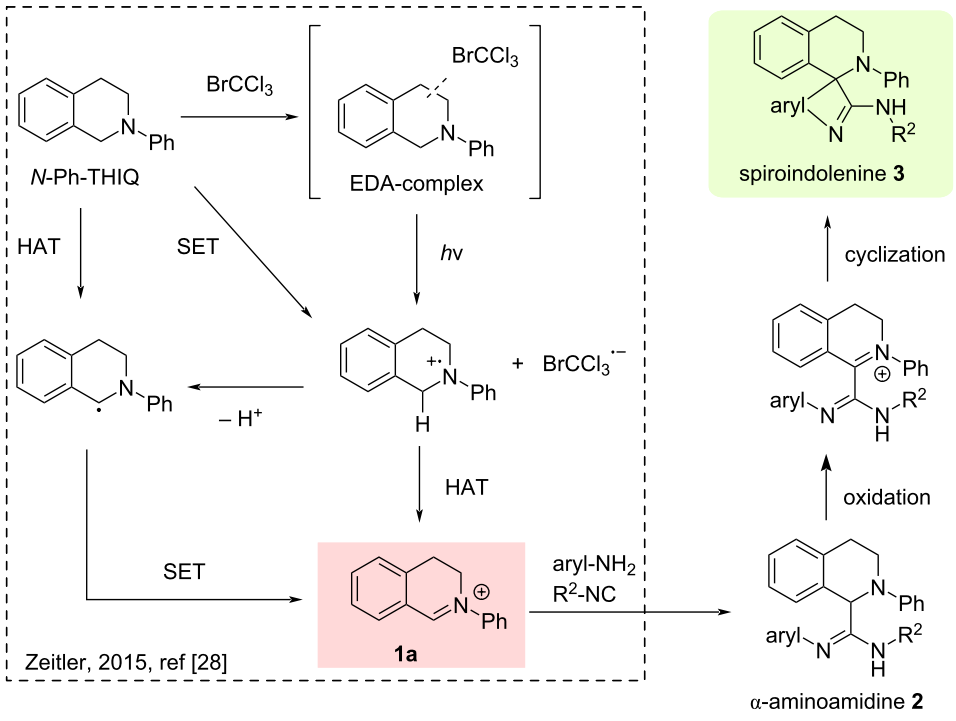

Scheme 6: Proposed mechanism.

viewed at UV (254 nm) and developed with Hanessian stain (dipping into a solution of $(NH_4)_4MoO_4{\cdot}4H_2O$ (21 g) and $Ce(SO_4)_2{\cdot}4H_2O$ (1 g) in H_2SO_4 (31 mL) and H_2O (469 mL) and warming). R_f were measured after an elution of 7–9 cm. Column chromatographies were done with the "flash" methodology using 220–400 mesh silica or 150 mesh aluminum oxide, activated, neutral, Brockmann I. Petroleum ether (40–60 °C) is abbreviated as PE. HPLC analysis was performed on Agilent HP 1100 equipped with a DAD detector (220 nm) and column ACE Excel 3 C18-AR (3 μm, 3 × 150 mm^2). Mass analysis was performed on a Microsaic 4000 MiD® mass spectrometer. HRMS analyses were performed by using the ionization method ESI+ with a 6230 TOF LC/MS, Agilent Technologies. Unless otherwise noted, analytical grade solvents and commercially available reactants were used without further purification. Common reagents were purchased from commercial sources and were used without further purification. Graphene oxide (GO) was purchased from Graphenea. All products were characterized by ^1H,^{13}C, ^{19}F (when fluorine is present) NMR, IR and HRMS.

General procedure for the one-pot synthesis of spiro[indole-isoquinoline] 3a: A solution of *N*-phenyltetrahydroisoquinoline (1 equiv, 0.48 mmol, 100 mg), 3-methoxyaniline (1.5 equiv, 0.72 mmol, 81 μL) and $BrCCl_3$ (3 equiv, 1.44 mmol, 140 μL) in CH_3CN (2.4 mL, 0.2 M) in a vial was degassed with argon for 2 minutes, then *tert*-butyl isocyanide (2.2 equiv, 1.06 mmol, 120 μL) was added and the vial sealed. The mixture was irradiated at 30 °C at 451 nm (blue LEDs) under magnetic stirring for 24 h. The reaction mixture was treated with Et_3N (3 equiv, 1.44 mmol, 200 μL), concentrated and the residue was purified by column chromatography on silica gel with PE/Et_2O (from 85:15 to 75:25) to give **3a** (121 mg, 61%), as yellow oil; IR (ATR) $\tilde{\nu}$ (cm^{-1}): 3393, 3367, 3051, 2995, 2967, 2923, 2860, 2828, 1916, 1851, 1706, 1623, 1598, 1562, 1525, 1491, 1472, 1464, 1451, 1437, 1422, 1387, 1359, 1327, 1296, 1274, 1250, 1222, 1207, 1186, 1176, 1151, 1119, 1096, 1080, 1057, 1040, 1026, 1009, 972, 964, 951, 943, 929, 909, 898, 854, 818, 810, 805, 782, 761, 744, 716, 695, 663, 655, 640, 624, 607; ^1H NMR (400 MHz, $CDCl_3$) δ 7.19 (dd, *J* = 7.9, 1.6 Hz, 1H, H Ar), 7.14 (td, *J* = 7.3, 1.3 Hz, 1H, H Ar), 7.11–7.04 (m, 2H, 2H Ar), 7.03–6.96 (m, 2H, 2H Ar), 6.93–6.86 (m, 3H, 3H Ar), 6.81 (d, *J* = 2.4 Hz, 1H, H Ar), 6.66 (dd, *J* = 8.0, 1.3 Hz, 1H, H Ar), 6.31 (dd, *J* = 8.1, 2.4 Hz, 1H, H Ar), 4.73 (s, 1H, NH), 3.98 (ddd, *J* = 11.9, 10.7, 3.5 Hz, 1H, 1H of CH_2 THIQ), 3.76 (s, 3H, OCH_3), 3.58 (ddd, *J* = 12.4, 5.7, 3.4 Hz, 1H, 1H of CH_2 THIQ), 3.31 (ddd, *J* = 16.1, 10.7, 5.5 Hz, 1H, 1H of CH_2 THIQ), 3.03 (dt, *J* = 15.9, 3.4 Hz, 1H, 1H of CH_2 THIQ), 1.25 (s, 9H, $3CH_3$ of *t*-Bu); ^{13}C NMR (101 MHz, $CDCl_3$) δ 175.3 (Cq amidine), 160.9 (Cq near O), 158.0 (Cq near N), 149.7 (Cq near N), 136.8 (Cq Ar), 133.9 (Cq Ar), 132.7 (Cq Ar), 129.0 (CH Ar), 128.5 (2 CH Ar), 126.9 (CH Ar), 126.9 (CH Ar), 126.5 (CH Ar), 123.5 (CH Ar), 123.3 (CH Ar), 123.2 (2 CH Ar), 107.1 (CH Ar), 103.5 (CH Ar), 75.9 (Cq spiro), 55.4 (OCH_3), 52.1 (Cq *t*-Bu), 47.9 (CH_2), 30.9 (CH_2), 28.5 (3 CH_3 of *t*-Bu); HRMS (ESI^+) (*m*/*z*) $[M + H]^+$: calcd for $C_{27}H_{30}N_3O$, 412.238; found, 412.2395.

Supporting Information

Supporting Information File 1

Additional optimization studies; description of photochemical equipment; characterization data of compounds (^1H, ^{13}C and ^{19}F NMR spectra, IR and UV–vis spectra).
[https://www.beilstein-journals.org/bjoc/content/supplementary/1860-5397-20-230-S1.pdf]

Acknowledgements

The University of Genova is kindly acknowledged for the contribution to the acquisition of an NMR instrument (D.R. 3404 19/7/2018). We thank Mr. Walter Sgroi for his collaboration for IR spectra, Valeria Rocca for HPLC-MS analysis and Lorenzo Esposito for practical collaboration to this work.

Author Contributions

Francesco Gambuti: investigation; validation; writing – review & editing. Jacopo Pizzorno: data curation; investigation; validation; writing – review & editing. Chiara Lambruschini: writing – review & editing. Renata Riva: writing – review & editing. Lisa Moni: conceptualization; data curation; investigation; project administration; resources; supervision; validation; visualization; writing – original draft.

ORCID® iDs

Francesco Gambuti - https://orcid.org/0009-0006-4449-5991
Jacopo Pizzorno - https://orcid.org/0009-0000-2708-9955
Chiara Lambruschini - https://orcid.org/0000-0003-1447-2650
Renata Riva - https://orcid.org/0000-0002-0829-9444
Lisa Moni - https://orcid.org/0000-0001-5149-2963

Data Availability Statement

All data that supports the findings of this study is available in the published article and/or the supporting information to this article.

References

1. Galloway, W. R. J. D.; Isidro-Llobet, A.; Spring, D. R. *Nat. Commun.* **2010,** *1,* 80. doi:10.1038/ncomms1081
2. Zheng, Y.; Tice, C. M.; Singh, S. B. *Bioorg. Med. Chem. Lett.* **2014,** *24,* 3673–3682. doi:10.1016/j.bmcl.2014.06.081

3. Batista, V. F.; Pinto, D. C. G. A.; Silva, A. M. S. *Expert Opin. Drug Discovery* **2022,** *17,* 603–618. doi:10.1080/17460441.2022.2055544
4. Cai, X.-H.; Tan, Q.-G.; Liu, Y.-P.; Feng, T.; Du, Z.-Z.; Li, W.-Q.; Luo, X.-D. *Org. Lett.* **2008,** *10,* 577–580. doi:10.1021/ol702682h
5. Park, H. B.; Kim, Y.-J.; Lee, J. K.; Lee, K. R.; Kwon, H. C. *Org. Lett.* **2012,** *14,* 5002–5005. doi:10.1021/ol302115z
6. Li, X.-N.; Cai, X.-H.; Feng, T.; Li, Y.; Liu, Y.-P.; Luo, X.-D. *J. Nat. Prod.* **2011,** *74,* 1073–1078. doi:10.1021/np2000254
7. Rosales, P. F.; Bordin, G. S.; Gower, A. E.; Moura, S. *Fitoterapia* **2020,** *143,* 104558. doi:10.1016/j.fitote.2020.104558
8. Tanaka, K.; Mori, Y.; Narasaka, K. *Chem. Lett.* **2004,** *33,* 26–27. doi:10.1246/cl.2004.26
9. Wang, P.-F.; Chen, C.; Chen, H.; Han, L.-S.; Liu, L.; Sun, H.; Wen, X.; Xu, Q.-L. *Adv. Synth. Catal.* **2017,** *359,* 2339–2344. doi:10.1002/adsc.201700073
10. Zhou, Y.; Li, D.; Tang, S.; Sun, H.; Huang, J.; Zhu, Q. *Org. Biomol. Chem.* **2018,** *16,* 2039–2042. doi:10.1039/c8ob00343b
11. Aksenov, A. V.; Aksenov, D. A.; Aksenov, N. A.; Skomorokhov, A. A.; Aleksandrova, E. V.; Rubin, M. *RSC Adv.* **2021,** *11,* 1783–1793. doi:10.1039/d0ra10219a
12. Dhote, P. S.; Ramana, C. V. *Adv. Synth. Catal.* **2022,** *364,* 1122–1133. doi:10.1002/adsc.202101412
13. Aksenov, A. V.; Aksenov, N. A.; Aksenov, D. A.; Khamraev, V. F.; Rubin, M. *Chem. Commun.* **2018,** *54,* 13260–13263. doi:10.1039/c8cc07451h
14. Aksenov, A. V.; Aksenov, D. A.; Arutiunov, N. A.; Aksenov, N. A.; Aleksandrova, E. V.; Zhao, Z.; Du, L.; Kornienko, A.; Rubin, M. *J. Org. Chem.* **2019,** *84,* 7123–7137. doi:10.1021/acs.joc.9b00808
15. Basso, A.; Moni, L.; Banfi, L.; Riva, R. *Synthesis* **2016,** *48,* 4050–4059. doi:10.1055/s-0035-1562527
16. Caputo, S.; Kovtun, A.; Bruno, F.; Ravera, E.; Lambruschini, C.; Melucci, M.; Moni, L. *RSC Adv.* **2022,** *12,* 15834–15847. doi:10.1039/d2ra01752k
17. Lambruschini, C.; Basso, A.; Moni, L.; Pinna, A.; Riva, R.; Banfi, L. *Eur. J. Org. Chem.* **2018,** 5445–5455. doi:10.1002/ejoc.201801129
18. Moni, L.; De Moliner, F.; Garbarino, S.; Saupe, J.; Mang, C.; Basso, A. *Front. Chem. (Lausanne, Switz.)* **2018,** *6,* 369. doi:10.3389/fchem.2018.00369
19. Spallarossa, M.; Banfi, L.; Basso, A.; Moni, L.; Riva, R. *Adv. Synth. Catal.* **2016,** *358,* 2940–2948. doi:10.1002/adsc.201600638
20. Moni, L.; Gers-Panther, C. F.; Anselmo, M.; Müller, T. J. J.; Riva, R. *Chem. – Eur. J.* **2016,** *22,* 2020–2031. doi:10.1002/chem.201504335
21. Caputo, S.; Donoso, S.; Banfi, L.; Basso, A.; Lambruschini, C.; Riva, R.; Kovtun, A.; Moni, L. *Eur. J. Org. Chem.* **2024,** *27,* e202400070. doi:10.1002/ejoc.202400070
22. Ngouansavanh, T.; Zhu, J. *Angew. Chem., Int. Ed.* **2007,** *46,* 5775–5778. doi:10.1002/anie.200701603
23. González-Zamora, E.; Islas-Jácome, A.; Gutiérrez-Carrillo, A.; García-Garibay, M. *Synlett* **2013,** *25,* 403–406. doi:10.1055/s-0033-1340218
24. Chen, Y.; Feng, G. *Org. Biomol. Chem.* **2015,** *13,* 4260–4265. doi:10.1039/c5ob00201j
25. Pinna, A.; Basso, A.; Lambruschini, C.; Moni, L.; Riva, R.; Rocca, V.; Banfi, L. *RSC Adv.* **2020,** *10,* 965–972. doi:10.1039/c9ra10689h
26. Speich, E.; Banfi, L.; Moni, L.; Riva, R.; Rocca, V.; Basso, A. *Chem. Heterocycl. Compd.* **2018,** *54,* 329–333. doi:10.1007/s10593-018-2268-0
27. Moni, L.; Banfi, L.; Basso, A.; Galatini, A.; Spallarossa, M.; Riva, R. *J. Org. Chem.* **2014,** *79,* 339–351. doi:10.1021/jo402527w
28. Franz, J. F.; Kraus, W. B.; Zeitler, K. *Chem. Commun.* **2015,** *51,* 8280–8283. doi:10.1039/c4cc10270c
29. Capurro, P.; Lambruschini, C.; Lova, P.; Moni, L.; Basso, A. *J. Org. Chem.* **2021,** *86,* 5845–5851. doi:10.1021/acs.joc.1c00278

License and Terms

This is an open access article licensed under the terms of the Beilstein-Institut Open Access License Agreement (https://www.beilstein-journals.org/bjoc/terms), which is identical to the Creative Commons Attribution 4.0 International License (https://creativecommons.org/licenses/by/4.0). The reuse of material under this license requires that the author(s), source and license are credited. Third-party material in this article could be subject to other licenses (typically indicated in the credit line), and in this case, users are required to obtain permission from the license holder to reuse the material.

The definitive version of this article is the electronic one which can be found at:
https://doi.org/10.3762/bjoc.20.230

BEILSTEIN JOURNAL OF ORGANIC CHEMISTRY

Multicomponent synthesis of α-branched amines using organozinc reagents generated from alkyl bromides

Baptiste Leroux[1], Alexis Beaufils[1], Federico Banchini[2], Olivier Jackowski[2], Alejandro Perez-Luna[2], Fabrice Chemla[2], Marc Presset[*1] and Erwan Le Gall[*1]

Full Research Paper

Open Access

Address:
[1]Univ Paris-Est Créteil, CNRS, ICMPE, UMR 7182, 2 rue Henri Dunant, 94320 Thiais, France and [2]Sorbonne Université, CNRS, Institut Parisien de Chimie Moléculaire, IPCM, 75005 Paris, France

Email:
Marc Presset[*] - marc.presset@cnrs.fr; Erwan Le Gall[*] - erwan.le-gall@cnrs.fr

* Corresponding author

Keywords:
alkyl bromides; branched amines; Mannich reaction; multicomponent reaction; zinc

Beilstein J. Org. Chem. **2024,** *20,* 2834–2839.
https://doi.org/10.3762/bjoc.20.239

Received: 22 July 2024
Accepted: 22 October 2024
Published: 07 November 2024

This article is part of the thematic issue "Multicomponent reactions IV".

Associate Editor: T. J. J. Müller

© 2024 Leroux et al.; licensee Beilstein-Institut.
License and terms: see end of document.

Abstract

The use of alkylzinc bromides in the multicomponent Mannich reaction is described. Heteroleptic organozinc compounds were obtained in THF or 2-MeTHF by direct insertion of zinc dust into the C–Br bond of alkyl bromides. It was found that the presence of a stoichiometric amount of LiCl was essential for the efficiency of the subsequent three-component coupling with aldehydes and amines. A variety of primary, secondary, and tertiary organozinc reagents as well as secondary amines and aromatic aldehydes could be used for the straightforward preparation of α-branched amines. Interestingly, whereas previously reported work describing the preparation and reaction of organozinc iodides in acetonitrile showed higher reactivity of secondary organozinc reagents over primary ones, reactions in THF in the presence of LiCl led to opposite results, with higher reactivity of primary organozinc reagents.

Introduction

The multicomponent Mannich reaction is one of the most powerful tools available in organic synthesis for the straightforward generation of α-branched amines [1-3]. Since its discovery in 1912, the reaction has benefitted from regular improvements over the years and recent developments, such as the use of organometallic species as nucleophiles in the so-called "organometallic Mannich reaction", which have helped to expand the boundaries of the original process [4]. In this context, while significant contributions have highlighted the reliable use of diverse organometallic species in the three-component coupling, most examples of sp^3-hybridized compounds have remained restricted to allyl [5] or benzyl [5,6] organometallic reagents. Conversely, examples of organometallic Mannich couplings involving nonstabilized organometallics are uncommon and mostly limited to dialkylzinc reagents, likely due to their commercial availability, their significant reactivity,

and their functional-group tolerance [7-10]. However, the molecular diversity accessible with these reagents is rather limited. Indeed, most examples involve dimethyl- or diethylzinc compounds as more elaborated dialkylzinc reagents represent a considerable synthetic challenge. Indeed, dialkylzinc reagents are accessible essentially through nucleophilic displacement of $ZnCl_2$ by Grignard reagents or organolithium reagents, thus limiting functional-group tolerance [11-13]. By contrast, heteroleptic (mixed) alkylzinc species (i.e., RZnX) are readily available and can typically be prepared from alkyl halides by direct insertion of metallic zinc into the carbon–halogen bond [14-21]. Thus, whereas Rieke et al. reported the insertion of activated zinc into alkyl bromides in THF at room temperature [16,17], Knochel et al. described the direct metalation of alkyl iodides in THF at 30 °C [18]. More recently, Knochel et al. improved their original method by the use of zinc dust in the presence of LiCl in THF for the metalation of alkyl bromides at room temperature [19]. Besides, Huo described the insertion of zinc dust into alkyl bromides at 80 °C in DMA or DMF [20].

Despite the high synthetic interest in mixed organozinc compounds, their use in the preparation of α-branched amines remains tenuous. Indeed, until recently, mixed alkylzinc species were only employed by Carretero and co-workers in related nucleophilic additions to activated imines under Cu catalysis [22]. In 2022, our group demonstrated that alkyl iodides offer a reliable source of heteroleptic organozinc compounds through the direct insertion of zinc dust into the C–I bond in acetonitrile at 50 °C [23]. Secondary as well as tertiary organozinc iodides were found to be more reactive than primary ones. Recently, Gaunt and co-workers confirmed this tendency in a related reductive multicomponent procedure involving alkyl iodides [24]. It was indeed noticed that the reactivity of primary iodides in the multicomponent carbonyl alkylative amination (CAA) reaction was quite sluggish compared to the secondary counterparts. In addition, primary alkyl bromides were found to be almost inactive in the process. Therefore, we reasoned that replacing alkyl iodides by alkyl bromides could be relevant to the field due to interesting assets such as better availability and lower cost of the parent alkyl halides.

Results and Discussion

We investigated new conditions that would allow for the synthesis of mixed alkylzinc bromides in order to explore their consecutive use in multicomponent Mannich reactions (Table 1).

While our experience in the development of multicomponent reactions involving organozinc compounds prompted us to initially consider acetonitrile as probably the most adapted solvent for the whole process [26-28], we observed that this solvent was not well-suited for the preparation of the organozinc species from the corresponding bromides, with no metalation being observed after 16 h at 80 °C (Table 1, entry 1). Conversely, the organozinc compound was formed in THF in nearly quantitative yield after 16 h at 80 °C (Table 1, entry 2). However, its suitability in the multicomponent coupling with an amine and an aldehyde still had to be demonstrated as there was no precedent for such a Mannich multicomponent coupling involving nonstabilized organozinc halides using THF or 2-MeTHF as solvent. To our delight, we found that the subsequent multicomponent coupling of the organozinc bromide with piperidine and benzaldehyde was possible, although it required the additional presence of lithium chloride to furnish a satisfactory result. We attributed the beneficial role of LiCl to the formation of more nucleophilic organozincate complexes (e.g., LiBuZnBrCl), which is a well-established process in THF [29,30]. Due to the hygroscopic character of LiCl and the necessity to determine the amount of organozinc by iodolysis [20] in order to adjust the stoichiometry of the reagents for the multicomponent coupling step, this salt was more conveniently introduced to the medium at the stage of organozinc preparation. We observed that the presence of LiCl was not deleterious for the metalation, although the organozinc yield decreased to 71% (Table 1, entry 3), probably due to the initial presence of water traces in the reaction medium. With these results in hands, we tried to determine whether LiCl could be replaced by other common lithium

Table 1: Optimization of the organozinc synthesis.[a]

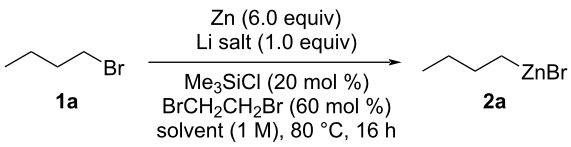

1a 2a

entry	Li salt	solvent	yield[b]
1	—	CH_3CN	0%
2	—	THF	95%
3	LiCl	THF	71%
4	LiBr	THF	10%
5	LiF	THF	52%
6	$LiClO_4$	THF	0%
7	LiCl	THF[c]	73%
8	LiCl	2-MeTHF	66%

[a]Reaction conditions: Zn dust (6.0 equiv) in bulk solvent (*c* = 1.0 M) activated by chlorotrimethylsilane (20 mol %) and 1,2-dibromoethane (60 mol %), then alkyl bromide (10 mmol), 80 °C, 16 h. [b]Titration by I_2: A 5 mL round-bottom flask was charged with accurately weighed I_2 (between 20 and 30 mg) and THF (2.5 mL). After the iodine was completely dissolved, the solution of organometallic reagent was added dropwise via a 1.00 mL syringe (0.01 mL graduations) until the brown color disappeared (see also [25] for details). [c]THF was distilled over Na and benzophenone prior to use.

salts that could lead to improved metalation (Table 1, entries 4–6). These experiments revealed that LiCl gave the best results, as a significant drop of the zincation yield was obtained with both LiBr (Table 1, entry 4) and $LiClO_4$ (Table 1, entry 6), whereas LiF gave an acceptable yield of organozinc reagent (Table 1, entry 5). Therefore, additional experiments were carried out with LiCl. We first tried to determine whether the use of distilled (Table 1, entry 7) instead of commercial THF (Table 1, entry 3) could have a significant impact on the zincation step and observed that this was not the case, with a comparable yield obtained under both conditions. Finally, we evaluated the influence of another ethereal solvent on the metalation and, notably, found that the use of biosourced 2-MeTHF led to a comparable result (Table 1, entry 8).

With these results in hands, we evaluated the scope of the zincation. The results are presented in Scheme 1.

The zincation conditions proved to be general, with a good yield of the organozinc compounds being obtained after 16 h at 80 °C in THF. It could be noted that comparable results were obtained in both THF and 2-MeTHF (i.e., organozinc compounds **2a** and **2d**). Interestingly, whereas simple primary (i.e., compounds **2a**–**g**) and secondary (i.e., compounds **2h**–**j**) aliphatic organozinc species could be obtained efficiently, a tertiary bromide furnished deceiving zincation results (i.e., compound **2k**). However, we were delighted to notice that functionalized organozinc species could be accessed from the corresponding bromides (i.e., organozinc compounds **2c**–**g**). After reaction and centrifugation, the solutions of the organozinc species **2** were collected using a syringe and allowed to react with an amine **3** and an aldehyde **4** under moderate heating (Scheme 2).

The multicomponent couplings proceeded smoothly, with an acceptable yield of the α-branched amine being obtained after 3 h at 50 °C. A range of secondary amines as well as various aromatic aldehydes could be used in the multicomponent coupling. Interestingly, functionalized organozinc reagents gave the multicomponent coupling product, except for the cyanated organozinc compound **2d**, which only provided traces of the expected α-branched amine. It can be noted that in sharp contrast to our previous reports on the related multicomponent reaction involving organozinc iodides in acetonitrile, for which secondary organozinc compounds provided better results than primary ones, primary organozinc bromides reacted more efficiently than secondary ones in THF in the presence of LiCl. In addition, whereas *tert*-butylzinc iodide was efficient in the multicomponent coupling (99% yield), *tert*-butylzinc bromide led to a very low yield (16% **5kaa**). The coupling presented some other limitations. It was not possible to carry out the reaction when a primary amine was employed. In addition, a secondary aniline only furnished traces of the expected product. Aliphatic aldehydes also failed to deliver the multicomponent adduct.

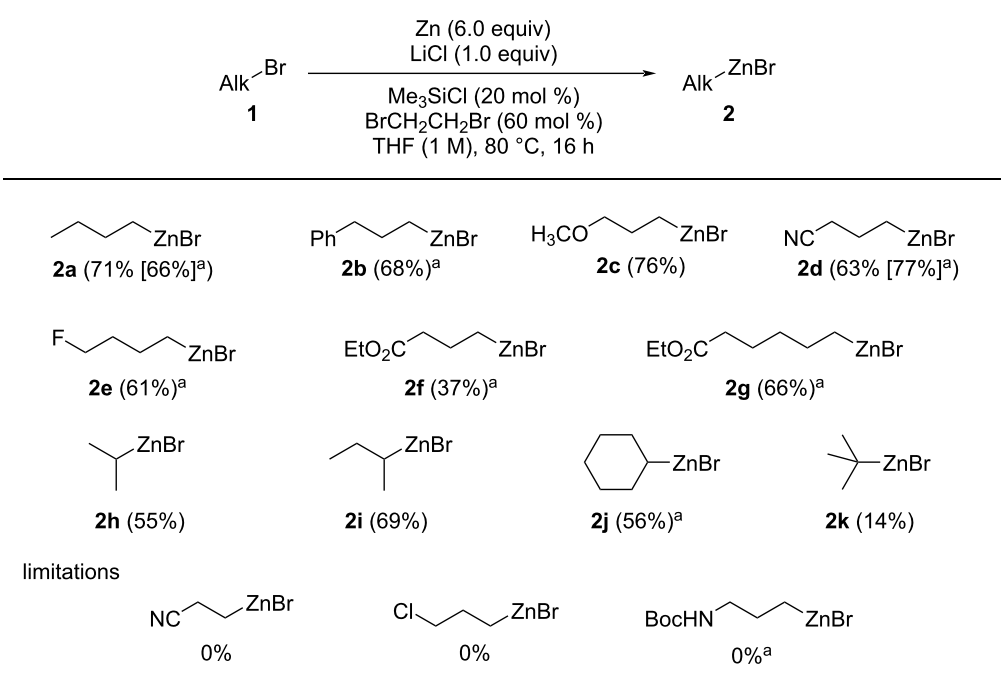

Scheme 1: Scope of organozinc reagents. Yield was determined by titration with I_2. Reaction conditions: Zn dust (6.0 equiv) in bulk THF (*c* = 1.0 M) activated by chlorotrimethylsilane (20 mol %) and 1,2-dibromoethane (60 mol %), then alkyl bromide (10 mmol), 80 °C, 16 h. [a]2-MeTHF was used as solvent.

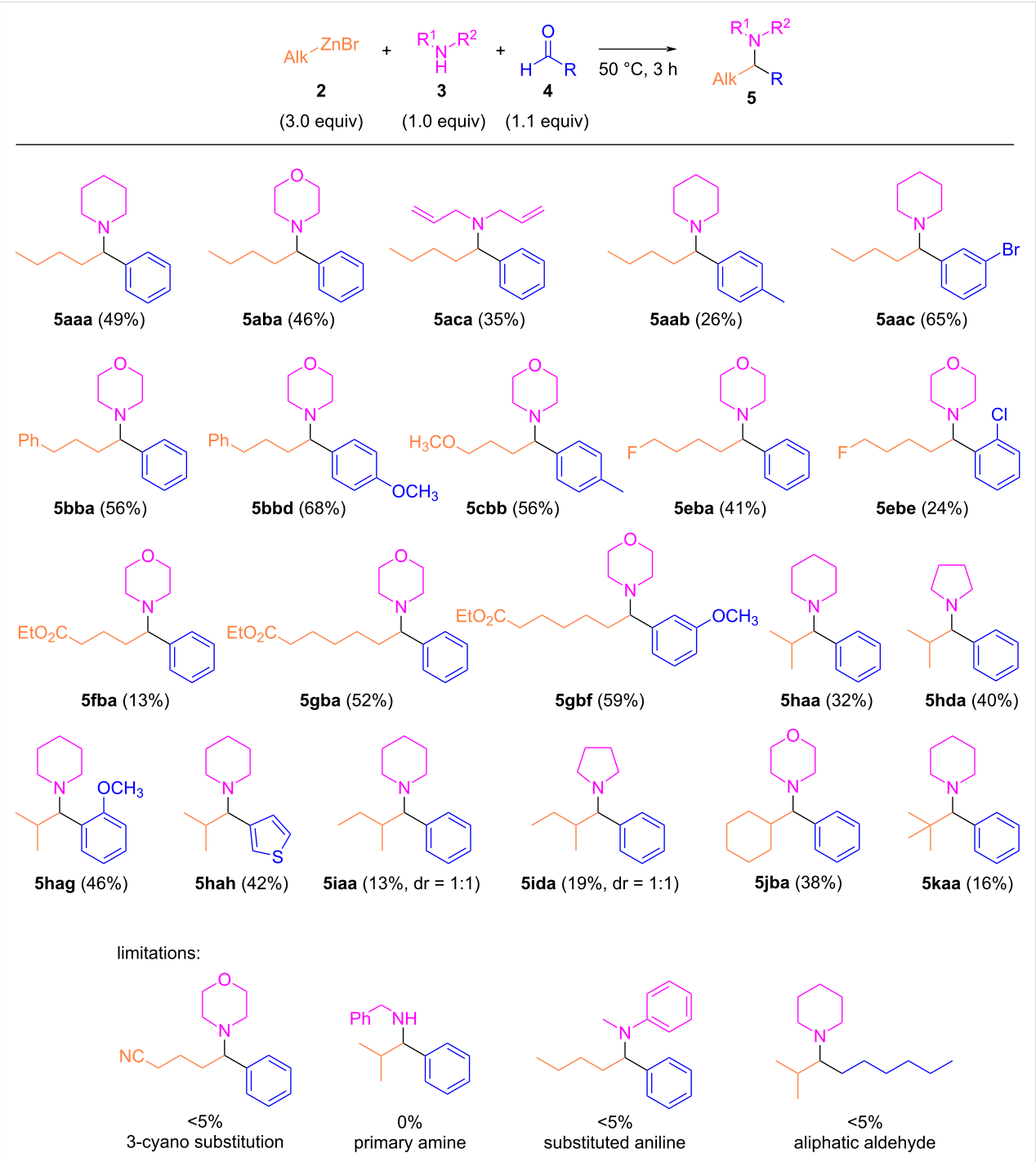

Scheme 2: Scope of the reaction. Yield of isolated product is given.

Conclusion

In conclusion, we have shown in this work that alkyl bromides can be used instead of alkyl iodides in a direct zincation–multicomponent organometallic Mannich reaction sequence to furnish α-branched amines in an acceptable yield. The reaction sequence is conducted in THF or 2-MeTHF, and the presence of LiCl is essential. Although the scope of the reaction is narrower than the analogous process relying on organozinc iodides, the reaction offers significant assets associated to the use of alkyl bromides, which are more easily prepared (or commercially available), less costly, and more stable than the corresponding alkyl iodides. In addition, the reaction can be conducted in commercial THF or 2-MeTHF and without special precautions. We also found a reversed reactivity order of primary and secondary

organozinc bromides in comparison to that of organozinc iodides. Herein, primary organozinc compounds reacted better than secondary ones.

Supporting Information

Supporting Information File 1

Experimental procedures, compound characterization data, and NMR spectra for all compounds.
[https://www.beilstein-journals.org/bjoc/content/supplementary/1860-5397-20-239-S1.pdf]

Funding

The authors acknowledge the support of the French Agence Nationale de la Recherche (ANR) under reference ANR-20-CE07-0003 (BILIOMAR project).

Author Contributions

Baptiste Leroux: conceptualization; investigation. Alexis Beaufils: investigation. Federico Banchini: validation; visualization; writing – review & editing. Olivier Jackowski: validation; visualization; writing – review & editing. Alejandro Perez-Luna: validation; visualization; writing – review & editing. Fabrice Chemla: validation; visualization; writing – review & editing. Marc Presset: conceptualization; investigation; supervision. Erwan Le Gall: conceptualization; funding acquisition; project administration; validation; writing – original draft.

ORCID® iDs

Olivier Jackowski - https://orcid.org/0000-0001-9162-3294
Alejandro Perez-Luna - https://orcid.org/0000-0002-5578-9024
Fabrice Chemla - https://orcid.org/0000-0001-6172-1504
Marc Presset - https://orcid.org/0000-0003-0994-5572
Erwan Le Gall - https://orcid.org/0000-0002-8972-3971

Data Availability Statement

All data that supports the findings of this study is available in the published article and/or the supporting information of this article.

References

1. Mannich, C.; Krösche, W. *Arch. Pharm. (Weinheim, Ger.)* **1912,** *250,* 647–667. doi:10.1002/ardp.19122500151
2. Mannich, C. *Arch. Pharm. (Weinheim, Ger.)* **1917,** *255,* 261–276. doi:10.1002/ardp.19172550217
3. Arend, M.; Westermann, B.; Risch, N. *Angew. Chem., Int. Ed.* **1998,** *37,* 1044–1070. doi:10.1002/(sici)1521-3773(19980504)37:8<1044::aid-anie1044>3.0.co;2-e
4. Paul, J.; Presset, M.; Le Gall, E. *Eur. J. Org. Chem.* **2017,** 2386–2406. doi:10.1002/ejoc.201700038
5. Fan, R.; Pu, D.; Qin, L.; Wen, F.; Yao, G.; Wu, J. *J. Org. Chem.* **2007,** *72,* 3149–3151. doi:10.1021/jo062616y
6. Haurena, C.; Le Gall, E.; Sengmany, S.; Martens, T.; Troupel, M. *J. Org. Chem.* **2010,** *75,* 2645–2650. doi:10.1021/jo1002328
7. Porter, J. R.; Traverse, J. F.; Hoveyda, A. H.; Snapper, M. L. *J. Am. Chem. Soc.* **2001,** *123,* 10409–10410. doi:10.1021/ja0118744
8. Akullian, L. C.; Snapper, M. L.; Hoveyda, A. H. *Angew. Chem., Int. Ed.* **2003,** *42,* 4244–4247. doi:10.1002/anie.200352081
9. Akullian, L. C.; Porter, J. R.; Traverse, J. F.; Snapper, M. L.; Hoveyda, A. H. *Adv. Synth. Catal.* **2005,** *347,* 417–425. doi:10.1002/adsc.200404319
10. Côté, A.; Charette, A. B. *J. Org. Chem.* **2005,** *70,* 10864–10867. doi:10.1021/jo0516483
11. Thiele, K.-H.; Wilcke, S.; Ehrhardt, M. *J. Organomet. Chem.* **1968,** *14,* 13–19. doi:10.1016/s0022-328x(00)92634-2
12. Mori, Y.; Mori, T.; Onodera, G.; Kimura, M. *Synthesis* **2014,** 2287–2292. doi:10.1055/s-0033-1339024
13. Takimoto, M.; Gholap, S. S.; Hou, Z. *Chem. – Eur. J.* **2015,** *21,* 15218–15223. doi:10.1002/chem.201502774
14. Knochel, P.; Singer, R. D. *Chem. Rev.* **1993,** *93,* 2117–2188. doi:10.1021/cr00022a008
15. Boudier, A.; Bromm, L. O.; Lotz, M.; Knochel, P. *Angew. Chem., Int. Ed.* **2000,** *39,* 4414–4435. doi:10.1002/1521-3773(20001215)39:24<4414::aid-anie4414>3.0.co;2-c
16. Zhu, L.; Wehmeyer, R. M.; Rieke, R. D. *J. Org. Chem.* **1991,** *56,* 1445–1453. doi:10.1021/jo00004a021
17. Rieke, R. D.; Hanson, M. V.; Brown, J. D.; Niu, Q. J. *J. Org. Chem.* **1996,** *61,* 2726–2730. doi:10.1021/jo952104b
18. Knochel, P.; Yeh, M. C. P.; Berk, S. C.; Talbert, J. *J. Org. Chem.* **1988,** *53,* 2390–2392. doi:10.1021/jo00245a057
19. Krasovskiy, A.; Malakhov, V.; Gavryushin, A.; Knochel, P. *Angew. Chem., Int. Ed.* **2006,** *45,* 6040–6044. doi:10.1002/anie.200601450
20. Huo, S. *Org. Lett.* **2003,** *5,* 423–425. doi:10.1021/ol0272693
21. Blümke, T. D.; Piller, F. M.; Knochel, P. *Chem. Commun.* **2010,** *46,* 4082–4084. doi:10.1039/c001845g
22. Esquivias, J.; Gómez Arrayás, R.; Carretero, J. C. *Angew. Chem., Int. Ed.* **2007,** *46,* 9257–9260. doi:10.1002/anie.200703239
23. Pinaud, M.; Le Gall, E.; Presset, M. *J. Org. Chem.* **2022,** *87,* 4961–4964. doi:10.1021/acs.joc.1c02996
24. Phelps, J. M.; Kumar, R.; Robinson, J. D.; Chu, J. C. K.; Flodén, N. J.; Beaton, S.; Gaunt, M. J. *J. Am. Chem. Soc.* **2024,** *146,* 9045–9062. doi:10.1021/jacs.3c14037
25. Krasovskiy, A.; Knochel, P. *Synthesis* **2006,** 890–891. doi:10.1055/s-2006-926345
26. Le Gall, E.; Haurena, C.; Sengmany, S.; Martens, T.; Troupel, M. *J. Org. Chem.* **2009,** *74,* 7970–7973. doi:10.1021/jo901704s
27. Le Gall, E.; Troupel, M.; Nédélec, J.-Y. *Tetrahedron Lett.* **2006,** *47,* 2497–2500. doi:10.1016/j.tetlet.2006.02.056
28. Le Gall, E.; Troupel, M.; Nédélec, J.-Y. *Tetrahedron* **2006,** *62,* 9953–9965. doi:10.1016/j.tet.2006.08.008
29. Fleckenstein, J. E.; Koszinowski, K. *Organometallics* **2011,** *30,* 5018–5026. doi:10.1021/om200637s
30. Koszinowski, K.; Böhrer, P. *Organometallics* **2009,** *28,* 771–779. doi:10.1021/om800947t

License and Terms

This is an open access article licensed under the terms of the Beilstein-Institut Open Access License Agreement (https://www.beilstein-journals.org/bjoc/terms), which is identical to the Creative Commons Attribution 4.0 International License (https://creativecommons.org/licenses/by/4.0). The reuse of material under this license requires that the author(s), source and license are credited. Third-party material in this article could be subject to other licenses (typically indicated in the credit line), and in this case, users are required to obtain permission from the license holder to reuse the material.

The definitive version of this article is the electronic one which can be found at:
https://doi.org/10.3762/bjoc.20.239

BEILSTEIN JOURNAL OF ORGANIC CHEMISTRY

N-Glycosides of indigo, indirubin, and isoindigo: blue, red, and yellow sugars and their cancerostatic activity

Peter Langer§

Review

Open Access

Address:
Institut für Chemie, Universität Rostock, Albert-Einstein-Str. 3a, 18059 Rostock, Germany

Email:
Peter Langer - peter.langer@uni-rostock.de

§ Fax: +49 381 4986412

Keywords:
cancerostatic activity; carbohydrates; heterocycles; *N*-glycosides; indirubin

Beilstein J. Org. Chem. **2024,** *20,* 2840–2869.
https://doi.org/10.3762/bjoc.20.240

Received: 05 June 2024
Accepted: 01 November 2024
Published: 08 November 2024

This article is part of the thematic issue "Multicomponent reactions IV" and is dedicated to Dr. Martin Hein.

Associate Editor: T. J. J. Müller

© 2024 Langer; licensee Beilstein-Institut.
License and terms: see end of document.

Abstract

Indigo, indirubin, and isoindigo derivatives have been used for centuries as pigments. Since the 1990s, a new aspect of the chemistry of this type of compounds is their activity against various types of cancer. *N*-Glycosides of indigo, indirubin, and isoindigo, blue, red, and yellow sugars, turned out to be of special interest because of their high cancerostatic activity and structural novelty. The present article provides an account on the synthesis and anticancer activity of these compounds.

Introduction

Indigo (**1a**), known for more than 6000 years and originally produced from indigo plants in India, represents a famous traditional blue pigment which was an expensive material in Europe (Scheme 1). It is obtained by extraction and isolation of the colorless indole-*O*-glycoside indicane which is then hydrolyzed to give indoxyl. The latter undergoes oxidative dimerization to provide indigo. In the 19th century, syntheses of indigo were developed which made the pigment readily available and cheap. Since then, indigo was produced in large scale. The synthesis, derivatization, and application of indigo derivatives have been widely studied [1-3]. Besides their application as dyes, indigo derivatives represent versatile tools for the development of innovative photophysical materials. While unsubstituted (parent) indigo (**1a**) is not a natural product, Tyrian purple (also known as Shellfish purple) is present in nature and represents, besides indigo, an important indigo derivative used as a dye for thousands of years [4].

Several types of cancers, Alzheimer's disease, and Parkinson's disease, cardiovascular diseases, inflammation, AIDS and others have their origin in context with the activities of protein kinases, such as glycogen synthase kinase-3 (GSK-3β) and cyclin-dependent kinases (CDK's). The phosphorylation of the amino acid moieties of several enzymes is controlled by such

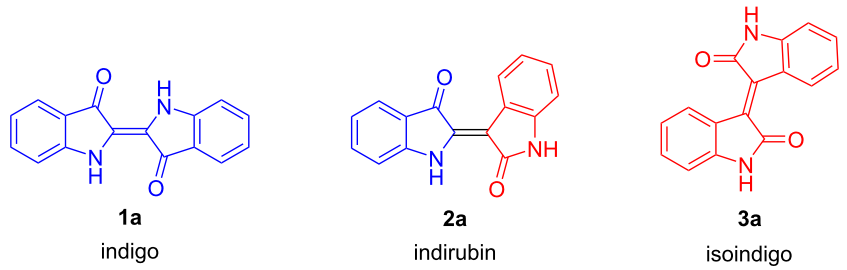

Scheme 1: Structures of indigo (**1a**), indirubin (**2a**) and isoindigo (**3a**).

protein kinases. Therefore, the investigation of the influence of drugs on protein kinases plays an important role in current medicinal chemistry. Indigo naturalis is a traditional drug, derived from indigo plants, which has been used in China for centuries and also more recently against myelocytic leukemia [5-7]. Indirubin, a red isomer of indigo, is an ingredient of indigo naturalis active against various cancers. Since the 1990s, we are witnessing a renaissance of the chemistry of indirubins because of their activity as potent inhibitors of several kinases, such as GSK-3β and CDK's [8-10]. In this context, the best CDK2 inhibitory activities were observed for indirubin-derived oximes [11].

Yellow colored isoindigo received a lot of attention as constituent of polymers applied as semi-conducting materials, organic light emitting materials (OLED), and for related applications [12,13]. In addition, there are more and more applications in the field of medicinal chemistry, especially for the treatment of cancer [14,15].

In the course of the renewed interest in the chemistry of indigo, indirubin, and isoindigo in the field of cancer research, *N*-glycosides of these compounds represent promising candidates for drug discovery, because of their improved water solubility, membrane permeability, and improved recognition by the respective receptors [16]. The present article aims to provide an updated review of the chemistry and biological applications of *N*-glycosides of indigo, indirubin, and isoindigo which can be regarded as blue, red, and yellow sugars, respectively.

Review

Indigo-*N*-glycosides (blue sugars)

In 2002, Laatsch and Maskey reported the isolation of the akashins A, B and C, indigo-*N*-glycosides, from terrestric *Streptomyces* (Scheme 2) [17,18]. These natural products exhibit an absorption at 618 nm and show a blue color. In contrast to biologically inactive indigo, akashines A–C are active against various human tumor cell lines (CNCL SF268, LCL H460, MACL, colon carcinoma CCL HT29, melanoma MEXF 514L, lung carcinoma LXFA 526L and LXFL 529L, breast cancer MCF-7, kidney tumors PRCL PC3M and RXF 631L) with IC_{50} values of about 2.8 mg mL^{-1} and IC_{70} values of >3 mg mL^{-1}.

In 2005, our group developed a synthesis of indigo-*N*-glycosides (Scheme 3) [19]. The TMSOTf-mediated reaction of readily available *N*-benzylindigo (**1b**) with tri-*O*-pivaloyl-α-L-rhamnosyl trichloroacetimidate (**4a**) initially resulted in the glycosylation of the oxygen atom to give intermediate **A** (−20 °C, 1.5 h). Extension of the reaction time (20 °C, 12 h) afforded *N*-indigoglycoside **5a** which was isolated in 35% yield. The product contained an α-rhamnosyl moiety with $^4C_1$ conformation. The formation of the product can be explained by rear-

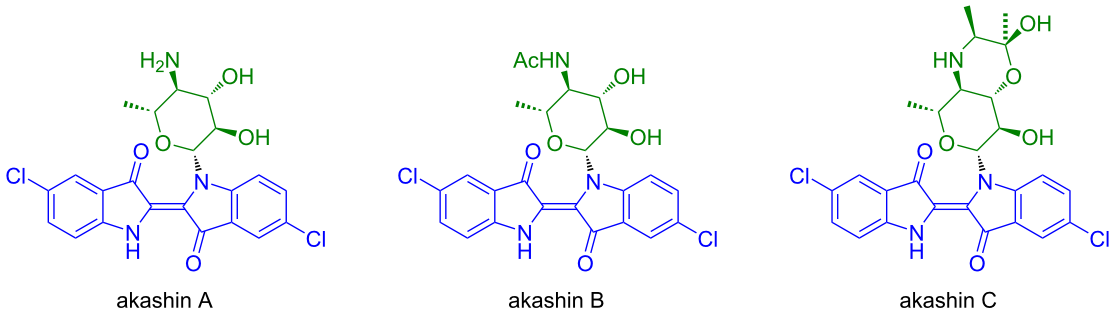

Scheme 2: Structures of akashins A–C.

rangement of the rhamnosyl group from the oxygen to the nitrogen atom. Oxidative debenzylation of **5a** afforded **5b** in high yield. Unfortunately, all attempts to remove the pivaloyl protective groups failed. On the other hand, employment of tri-*O*-acetyl-α-L-rhamnosyl trichloroacetimidate failed, due to competing formation of orthoester-like amide acetals during the reaction with **1b**. We then focused our work on an alternative synthetic approach (vide infra).

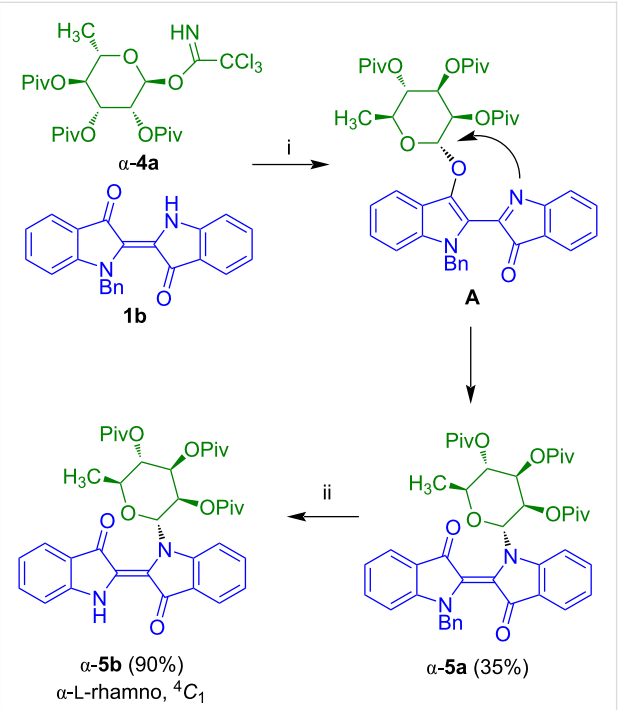

Scheme 3: Synthesis of **5b**. Reagents and conditions: i) TMSOTf, 4 Å MS, CH_2Cl_2, –20 °C, 1.5 h, then 20 °C, 8–12 h; ii) O_2, AcOH, 100 °C, 2 h.

In 2021, Pfretzschner and Unverzagt reported the application of our methodology to the synthesis of indigo-*N*-glucoside **7c** (Scheme 4) [20]. The reaction of **1b** with 3,4,6-tri-*O*-acetyl-2-*O*-benzoyl-α-D-glucosyl trichloroacetimidate (**6a**) afforded indigo-*N*-glycoside **7a**. The benzoyl group located at OH-2 seemed to be unreactive enough to avoid formation of orthoester-like amide acetals during the *N*-glycosylation with **1b**. Oxidative debenzylation of **7a** gave product **7b** which was transformed to the desired product **7c** by reaction with sodium methoxide and subsequent treatment with acidic ion exchange resin Amberlyst 15.

The synthesis of akashins A–C was studied next. This required the synthesis of the corresponding indigo and carbohydrate precursors. The base-mediated reaction of 5-chloroanthranilic acid (**8a**) with chloroacetic acid afforded **8b** (Scheme 5) [20]. Acetylation and base-mediated cyclization gave indoxyl **9a** which

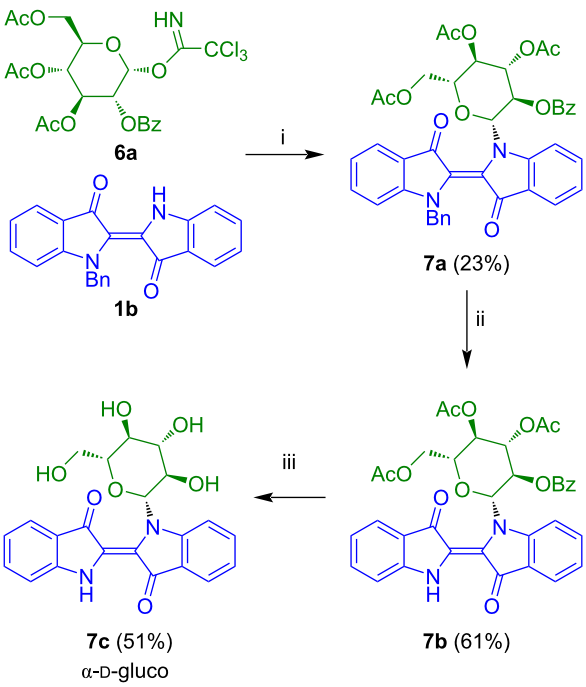

Scheme 4: Synthesis of **7c**. Reagents and conditions: i) TMSOTf, 4 Å MS, CH_2Cl_2, –18 °C, 3 h; then: TMSOTf, 4 Å MS, CH_2Cl_2, 20 °C, 10–12 h; ii) toluene/HOAc 1:1, 50 °C, air, 12–18 h; iii) 1) NaOMe/MeOH, 11 h; 2) Amberlyst 15 (H^+).

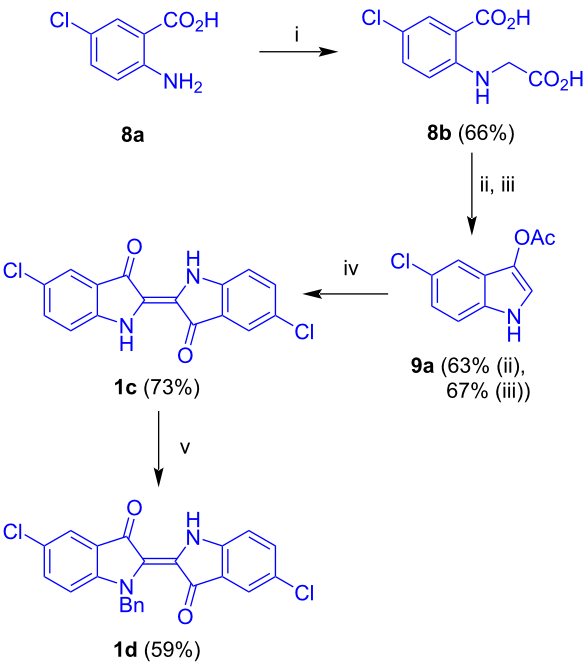

Scheme 5: Synthesis of **1d**. Reagents and conditions: i) chloroacetic acid, Na_2CO_3, reflux, 6 h; ii) Ac_2O, NaOAc, reflux, 3 h, 63%; iii) 1) NaOH, reflux, argon, 30 min; 2) Ac_2O, 0 °C, argon, 45 min, 67% over two steps; iv) NaOH, MeOH, air; v) NaH, DMF, BnBr, 2 h.

was transformed to indigo **1c** by oxidative dimerization. Benzylation finally afforded **1d**.

4,6-Benzylidenation of D-galactose and subsequent perbenzoylation afforded an anomeric mixture (α:β = 87:13) of tribenzoyl-4,6-benzylidene-D-galactose from which the pure α-anomer **10a** was separated (Scheme 6) [20]. Cleavage of the acetal and subsequent regioselective replacement of the hydroxy group OH-6 with an iodide by application of the Mukaiyama redox condensation using *N*-iodosuccinic imide (NIS) afforded **10b**. Hydrogenation resulted in defunctionalization to give **10c**. Transformation of OH-4 to a triflate and subsequent reaction with sodium azide afforded gluco-configured product **10d**. The latter was transformed to trichloroacetimidate **10e** by reaction with hydrazine and subsequent treatment with trichloroacetonitrile. The same synthesis was carried out also with the β-configured analogue of **10a**. However, employment of the α-anomer **10a** proved to be advantageous in terms of yield.

The reaction of **1d** with **10e** afforded indigo-*N*-glycoside **11a** (Scheme 7) [20]. Debenzylation gave product **11b** which was transformed to akashin A (**11c**) by reduction of the azide to the amine in the presence of propane-1,3-dithiol and subsequent debenzoylation. Akashin A was transformed to akashins B and C by acetylation and reaction with diacetyl, respectively.

Because of our difficulties to remove the pivaloyl protective groups of rhamnoside **5b** (Scheme 3), our group developed an alternative synthesis of indigo-*N*-glycosides based on the employment of dehydroindigo (**13**) instead of *N*-benzylindigo (**1b**) (Scheme 8) [21]. Known compound **13** was prepared in two steps from indigo (**1a**). The reaction of **1a** with potassium permanganate afforded product **12** which was transformed to dehydroindigo (**13**) by pyridine-mediated elimination of acetic acid. The reaction of **13** with tetra-*O*-trimethylsilyl-L-rhamnopyranose (**4b**) in the presence of trimethylsilyl iodide, addition of *n*-propyl mercaptane with subsequent addition of acetic anhydride, pyridine and KHF_2 afforded indigo-*N*-rhamnoside **5c** as a 2:1 mixture of α/β-anomers. The relatively low yield is a result of side reactions and decomposition, due to the rather unstable nature of the product. The reaction of **5c** with sodium *tert*-butanolate afforded the desired deprotected indigo-*N*-rhamnoside **5d** (α/β = 2:1). In contrast to the antiproliferative properties of the akashins, **5d** showed no significant activity against human cancer cell lines.

The glycosylation of **13** can be explained as follows (Scheme 9): Reaction of tetra-*O*-trimethylsilyl-L-rhamnopyranose (**4b**) with TMSI gave intermediate **A** containing an anomeric iodide. Electrophilic addition of rhamnosyl iodide **A** to one of the two imino groups of **13** gave intermediate **B**. Another electrophilic addition of *n*-propyl mercaptane to the second imino group afforded intermediate **C** which underwent extrusion of iodine and dipropyl disulfide to give intermediate **D**. Subsequent reaction with acetic anhydride, pyridine and KHF_2 resulted in the replacement of the TMS by acetyl groups which was important for practical reasons (stability during chromatography).

The reaction of **13** with TMS-protected D-glucosyl iodide, generated in situ by reaction of penta-*O*-trimethylsilyl-D-glucose (**6b**) afforded indigo-*N*-α-D-glucoside **7d**, albeit, in low yield (Scheme 10) [21].

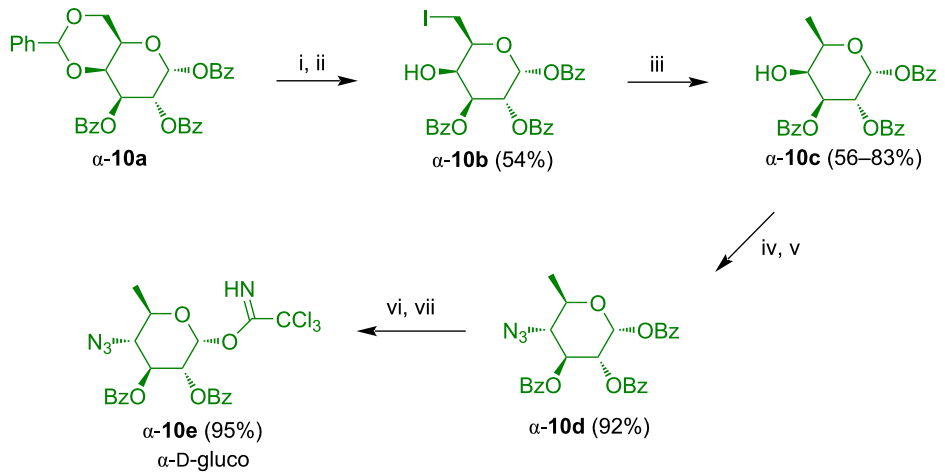

Scheme 6: Synthesis of **10e**. Reagents and conditions: i) *p*-TsOH·H_2O, acetonitrile, MeOH, 1 d; ii) NIS, PPh_3, DMF, 0–50 °C, 1 d; iii) H_2, Pd/C (10%), MeOH/HOAc 10:1; iv) Tf_2O, pyridine, CH_2Cl_2, −18 °C, 2 h; v) NaN_3, DMF, 30 min; vi) hydrazinium acetate, DMF, 20 °C, 3–6 h; vii) Cl_3CCN, DBU, CH_2Cl_2, 0 °C, 2 h.

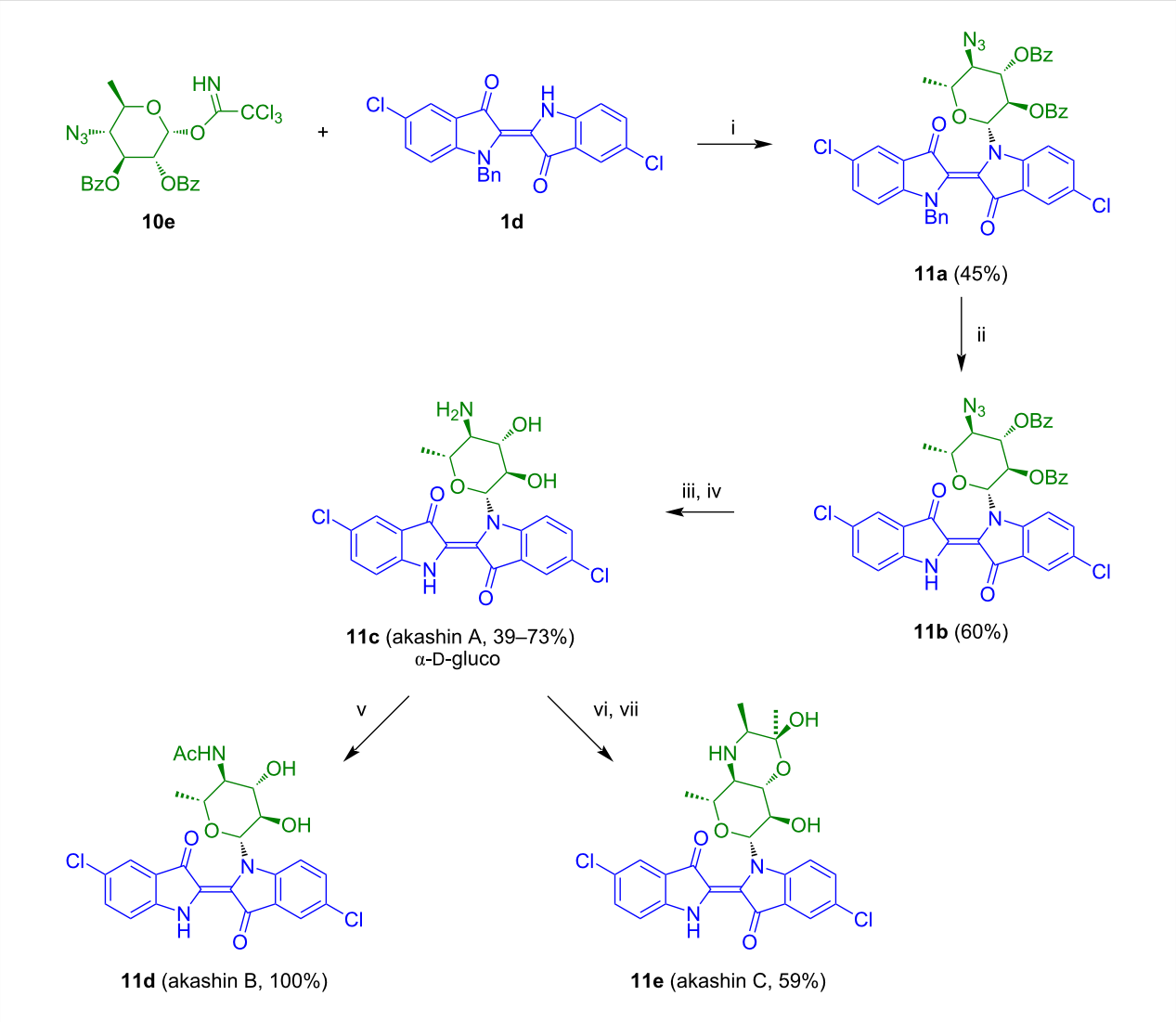

Scheme 7: Synthesis of akashins A–C. Reagents and conditions: i) TMSOTf, 4 Å MS, CH_2Cl_2, −18 to 20 °C, 15 h; ii) toluene/HOAc 1:1, 60 °C, air, 12–18 h; iii) propanedithiol, DIPEA, MeOH, exclusion of light, 3–4 d, argon; iv) CH_2Cl_2/AcOH 99:1, air, 60–90 min; v) Ac_2O, MeOH, H_2O, 30–90 min; vi) diacetyl, camphorsulfonic acid (CSA), trimethyl orthoformate, MeOH, 20 °C, 2–3 h; vii) $NaCNBH_3$; MeOH, 20 °C, 20–30 min.

The reaction of **13** with TMS-protected D-mannosyl iodide, generated in situ by reaction of penta-*O*-trimethylsilyl-D-mannose (**14**) afforded indigo-*N*-mannoside α-**15a**, albeit, in low yield (Scheme 11) [21]. Deacetylation afforded product α-**15b**.

Indirubin-*N*-glycosides (red sugars)

In contrast to indigo, indirubin is a non-symmetrical compound containing an amine- and an amide-type nitrogen atom. In our group, we developed a synthesis of indirubin-*N*-glycosides containing the carbohydrate moiety located at the amide-type nitrogen. Isatin-*N*-glycosides **16** were used as key building blocks. The reaction of L-rhamnose (**4c**) with aniline afforded *N*-glycosyl aniline **4d** which was acetylated to give **4e** (Scheme 12) [22]. The $AlCl_3$-mediated cyclization of **4e** with oxalyl chloride afforded yellow isatin-*N*-glycoside **16a** as an anomeric mixture from which the pure α- and β-anomer could be separated by chromatography. Likewise, isatin-*N*-glycosides **16b–f** were prepared which were all isolated (except from rhamnoside **16b**) as the pure β-anomers.

The condensation of anomerically pure β-configured β-**16a** with indoxyl acetate, in the presence of an excess of sodium carbonate, afforded β-configured indirubin-*N*-rhamnoside β-**17a** in very good yield as the pure *Z*-configured isomer (Scheme 13) [22]. Gratifyingly, the product, which showed the characteristic red color of indirubin, was directly obtained in its deprotected form. Indirubin-*N*-rhamnoside β-**17a** is significantly more stable than indigo-*N*-rhamnoside **5c**. Likewise, starting with 3,5-dimethylaniline, the β-configured indirubin-*N*-rhamnoside

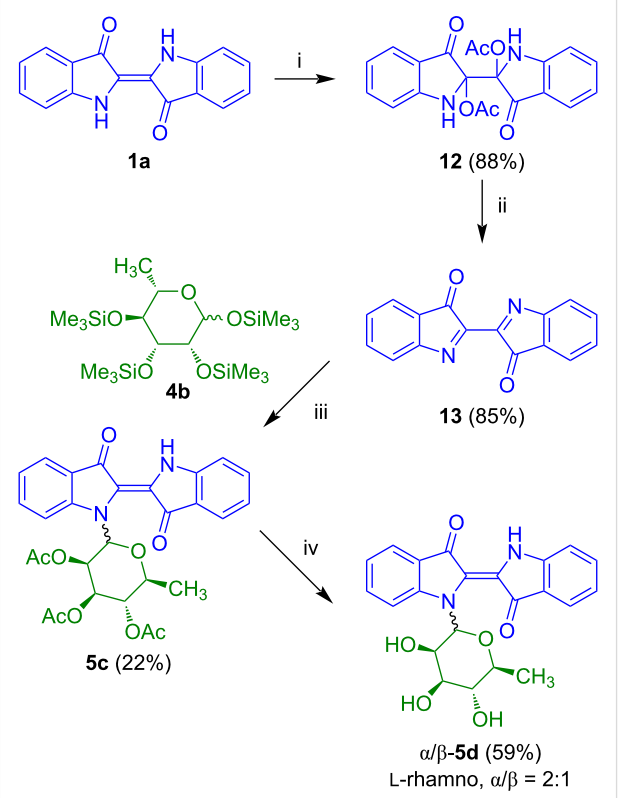

Scheme 8: Synthesis of **5d**. Reagents and conditions: i) $KMnO_4$, AcOH, high-power-stirring (12.000 rot/min), 20 °C, 3–4 h; ii) pyridine/toluene 1:2, 70 °C, 1 h; iii) 1) CH_2Cl_2, 2) Me_3SiI, 20 °C, 30 min, 3) 0 °C, 30 min; 4) *n*-PrSH, 0→20 °C, 1 h, 5) Ac_2O/pyridine 3:1, KHF_2, 70 °C, 3 h; iv) NaO*t*-Bu (15 mol %), MeOH, 20 °C, 4 h.

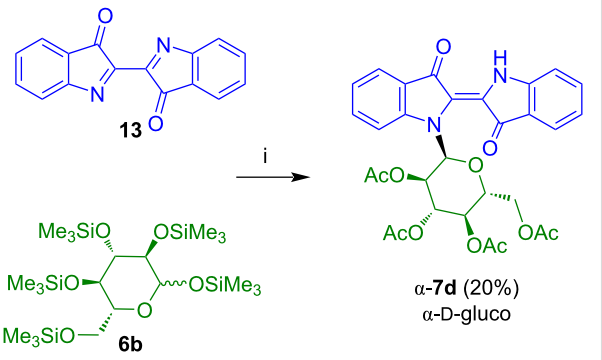

Scheme 10: Synthesis of **7d**. Reagents and conditions: i) 1) CH_2Cl_2, 2) Me_3SiI, 20 °C, 30 min, 3) 0 °C, 30 min, 4) *n*-PrSH, 0→20 °C, 1 h, 5) Ac_2O/pyridine 3:1, KHF_2, 70 °C, 3 h.

β-**17b** was prepared. Rhamnoside **17c** was prepared by condensation of β-**16a** with 3-acetoxy-5-chloroindole. Anomerically pure indirubin-*N*-glucoside β-**18a**, indirubin-*N*-riboside β-**19a**, indirubin-*N*-galactoside β-**20a**, and indirubin-*N*-mannoside β-**21a** were prepared in good yields starting from the corresponding sugars and anilines [12,13]. In case of the indoxyl moiety, both electron-donating and -withdrawing substituents were tolerated. In contrast, isatin-*N*-glycosides containing electron-withdrawing groups and, thus, the corresponding indirubin-*N*-glycosides could not be successfully prepared at this point (vide infra). In general, anomerically pure isatin-*N*-glycosides had to be employed in order to obtain anomerically pure indirubin-*N*-glycosides. As expected, no epimerization was observed during the base-mediated condensation as no aqueous acid was employed. All products were isolated as the pure *Z*-configured isomers (determination by NMR, the other isomer was not visible, *E*/*Z* < 2:98). The configurations were determined by comparison of chemical shifts of our products with those of non-glycosylated indirubin, by the presence of an intra-

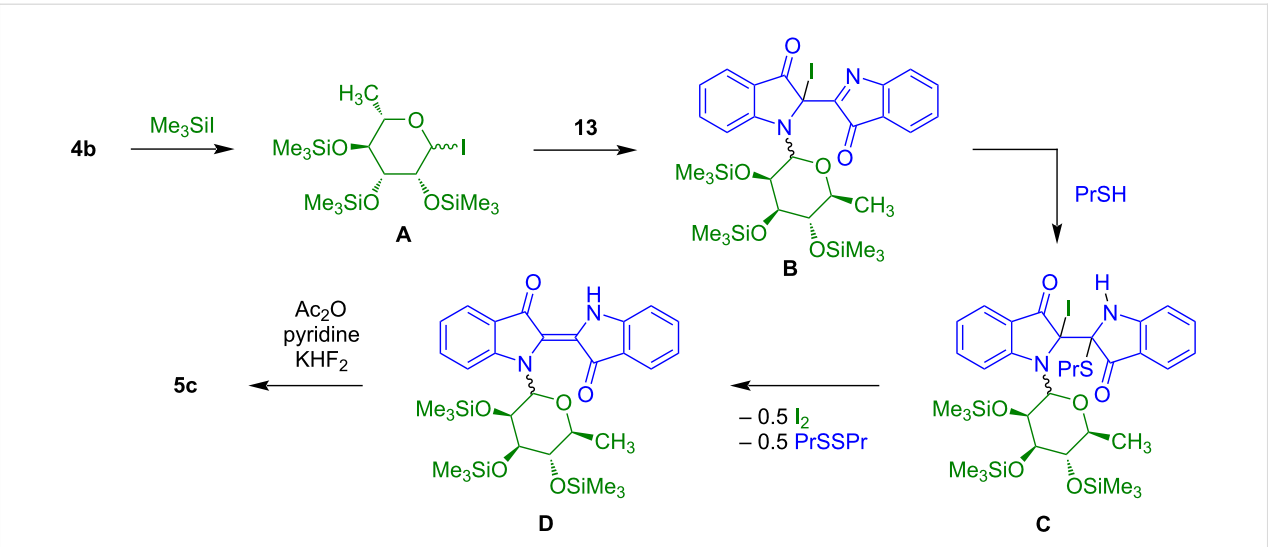

Scheme 9: Possible mechanism of the formation of **5c**.

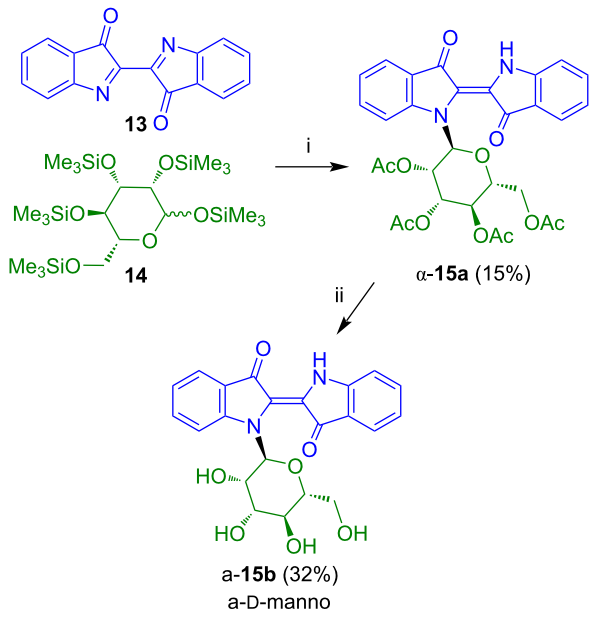

Scheme 11: Synthesis of α-**15b**. Reagents and conditions: i) 1) CH_2Cl_2, 2) Me_3SiI, 20 °C, 30 min, 3) 0 °C, 30 min, 4) *n*-PrSH, 0→20 °C, 1 h, 5) Ac_2O/pyridine 3:1, KHF_2, 70 °C, 3 h; ii) NaO*t*-Bu (15 mol %), MeOH, 20 °C, 4 h.

molecular hydrogen bond N–H···O and by crystal structure analysis. In fact, the chemical shifts of the H-4 proton signals are strongly influenced by the anisotropic effect of the indoxyl carbonyl group resulting in a downfield shift in case of the *Z*-isomers.

The reaction of anomerically pure α-configured isatin-*N*-rhamnoside α-**16a** with 3-acetoxyindole and 3-acetoxy-5-chloroindole afforded α-configured indirubin-*N*-rhamnosides α-**17a** and α-**17c**, respectively (Scheme 14) [23].

Water solubility plays an important role with regard to the pharmacological activity. It was previously shown that the water solubility and anticancer activity of non-glycosylated indirubins can be improved by conversion of the keto to an oxime group [8-11]. Therefore, we studied the synthesis of oximes of indirubin-*N*-glycosides. The reaction of isatin-*N*-rhamnoside β-**16a** with 3-acetoxyindole and subsequent acetylation afforded indirubin-*N*-rhamnoside β-**17e** which was subsequently deprotected to give oxime β-**17f** (Scheme 15) [23].

In collaboration with Michael Lalk and Patrick Bednarski (University of Greifswald), the antiproliferative activities of indirubin-*N*-rhamnosides **17a–c**,**f**, indirubin-*N*-glucoside β-**18a**, indirubin-*N*-galactoside β-**20a**, and indirubin-*N*-mannoside β-**21a** were studied. In this context, four human cancer cell lines were employed, namely, bladder (5637), small cell lung

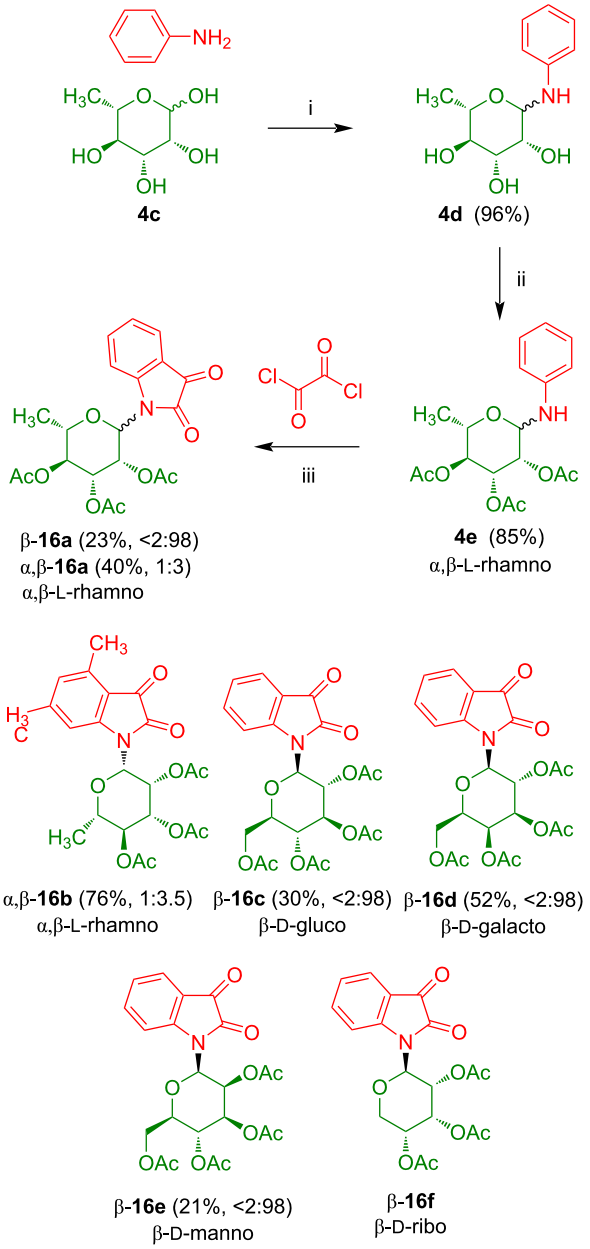

Scheme 12: Synthesis of isatin-*N*-glycosides **16a–f**. Reagents and conditions: i) $PhNH_2$, EtOH, 20 °C, 12 h; ii) Ac_2O, pyridine, 0 °C, 8–12 h; iii) oxalyl chloride, $AlCl_3$, 55 °C, 1.5 h.

(A-427), esophageal (Kyse-70), and breast (MCF-7) [23]. Rhamnosides α-**17a** and β-**17b** showed excellent activities against the human breast cancer cell line MCF-7. In general, the best activities were observed for indirubins containing no additional substituent. The carbohydrate moiety also has an influence on the antiproliferative activity. The best activities were observed for rhamnosides, while the lowest activity was observed for galactoside β-**20a**. The configuration of the anomeric carbon atom of the rhamnoside did not show a major influence as very good activities were observed for both α-**17a** and β-**17a**.

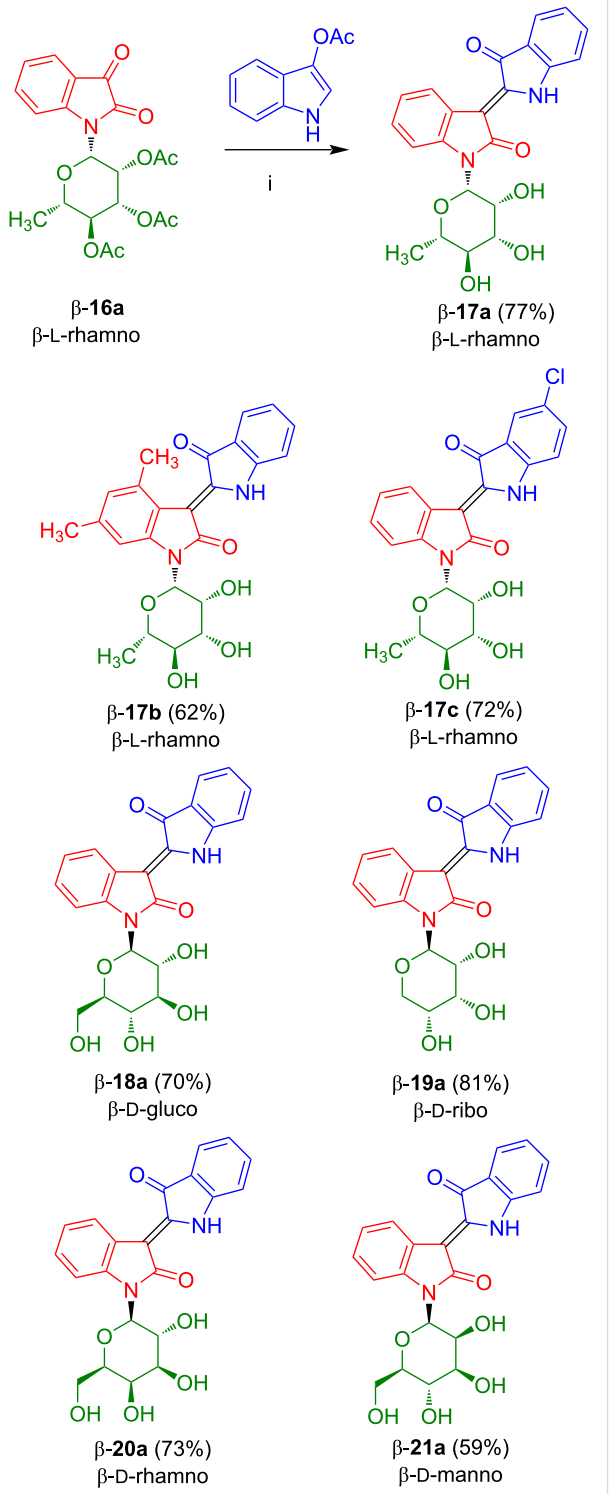

Scheme 13: Synthesis of **17**–**21**. Reagents and conditions: i) Na_2CO_3, MeOH, 20 °C, 4 h.

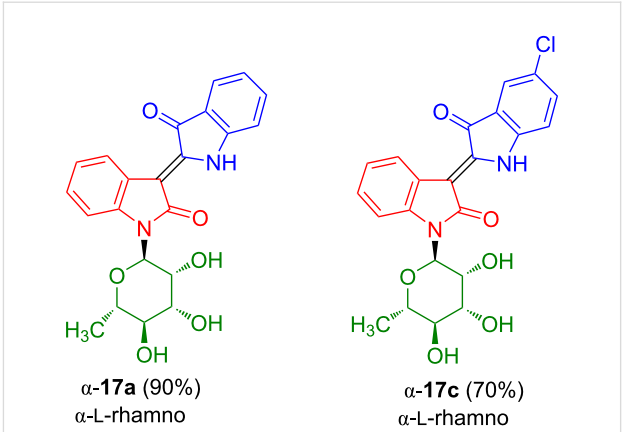

Scheme 14: Synthesis of indirubin-*N*-glycosides α-**17a** and α-**17b**.

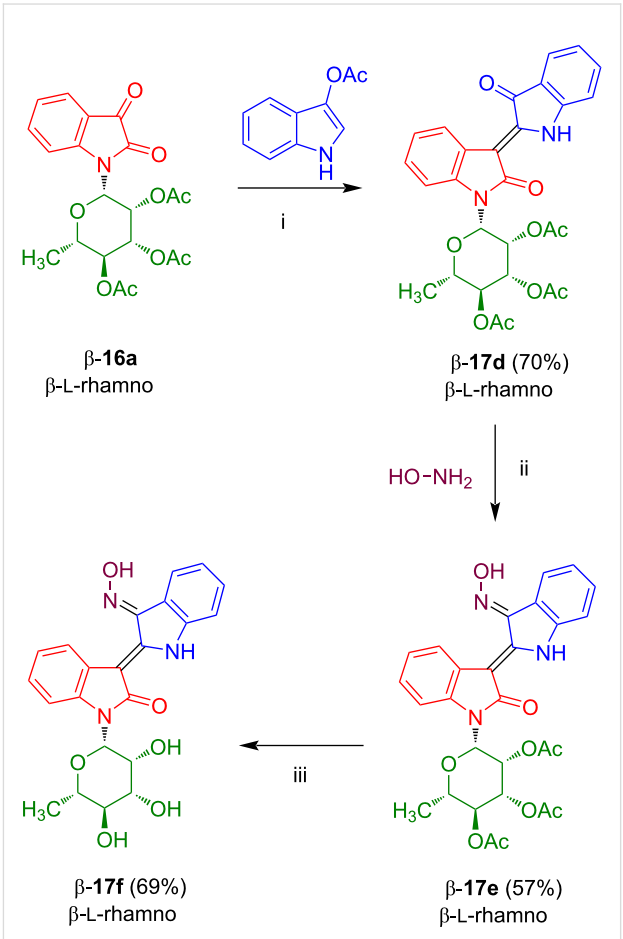

Scheme 15: Synthesis of β-**17f**. Reagents and conditions: i) 1) Na_2CO_3, MeOH, 20 °C, 4 h, 2) Ac_2O/pyridine 1:1, 0 °C, 12 h; ii) H_2NOH·HCl, pyridine, 90 °C, 7 h; iii) KO*t*-Bu, MeOH, 20 °C, 12 h.

It is important to note that the anticancer activity of all indirubin-*N*-glycosides, in particular of rhamnosides **α-17a** and β-**17a**, was considerably higher as compared to the activities of previously reported non-glycosylated indirubins [23,24]. A low activity was observed for oxime β-**17f** which is surprising, as good activities were previously reported for indirubin oximes as compared to other non-glycosylated indirubins.

As mentioned above, the synthesis of acceptor-substituted isatin-*N*-glycosides by Lewis acid-mediated cyclization of the corresponding acetyl-protected *N*-glycosyl anilines with oxalyl chloride was not possible. The failure of this reaction can be explained by electronic deactivation of the aromatic ring and steric hindrance which resulted in competing Claisen-type side-reactions of the acetyl groups. However, reactions of pivaloyl-protected *N*-glycosyl anilines also proved to be unsuccessful, which pointed to steric reasons. Therefore, we studied in our group the use of the less sterically hindered formyl instead of acetyl or pivaloyl protective groups. The reaction of glucose (**22a**) with aniline afforded anomerically pure *N*-glycosyl aniline β-**22b** which was formylated to give **22c** in 74% yield (Scheme 16) [24]. Product **22c** resides as a mixture of α- and β-anomers, because an anomeric equilibrium was activated during the acid-mediated formylation. The cyclization of **22c** with oxalyl chloride, carried out under forcing conditions ($TiCl_4$, chlorobenzene, 85 °C), afforded anomerically pure β-configured isatin-*N*-glucoside β-**23a** in 80% yield. The product was formed as the pure β-anomer, because the anomeric equilibrium was again active in the presence of the Lewis acid and the β-anomer is thermodynamically favored because of the steric demand of the isatin moiety and the α-anomeric form would result in a disfavorable 1,3-diaxial interaction between the isatin and the formyl group located at carbons C-1 and C-3, respectively. Deprotection with ammonia afforded the deprotected glucoside β-**24a** in anomerically pure form.

Following the methodology described above, acceptor-substituted isatin-*N*-glucosides **23b–f** and xyloside **23g** were prepared in 25–83% yields (Scheme 17) [24]. All products were formed as the β-anomers. The yield of product **23e** derived from *m*-fluoroaniline was significantly higher as compared to product **23c** derived from *p*-fluoroaniline which can be explained by the π-donating effect of fluorine which facilitates the cyclization via the *ortho*-position in case of *m*-, but not of *p*-fluoroaniline. It is worth to be noted that the formation of **23d** proceeded with excellent regioselectivity via carbon C-6 rather than C-2 of the 3-fluoroaniline moiety, presumably due to steric reasons. Deprotection of the isatin-*N*-glucosides **23b–f** and xyloside **23g** proceeded uneventfully and afforded products **24b–g** in 50–85% yields. All products were isolated as the β-anomers.

In our group, we also studied the synthesis of indirubin-*N*-glycosides containing the carbohydrate moiety located at the amine-type nitrogen atom (Scheme 18) [25]. For this purpose, we decided to react isatins with *N*-glycosylated indoxyls which were entirely unknown at that time. The reaction of L-rhamnose α/β-**4c** with indoline afforded α/β-**25a** (β:α ≈ 4:1). Dehydrogenation of the latter with DDQ afforded the anomerically pure indol-*N*-glycoside β-**26a** which upon benzylation and methylation gave products β-**27a** and β-**27b**, respectively. Iodination gave products β-**28a** and β-**28b**, however, due to the basic reaction conditions (I_2, NaOH, DMF), ether rather than ester protective groups had to be employed. The reaction of the 3-iodoindoles β-**28a** and β-**28b** with an excess of silver acetate under mild acidic conditions afforded 3-acetoxyindol-*N*-rhamnosides β-**29a** and β-**29b**, respectively.

The application of the conditions used for the synthesis of indirubin-*N*-glycoside **17a** (Scheme 13) failed for the reaction

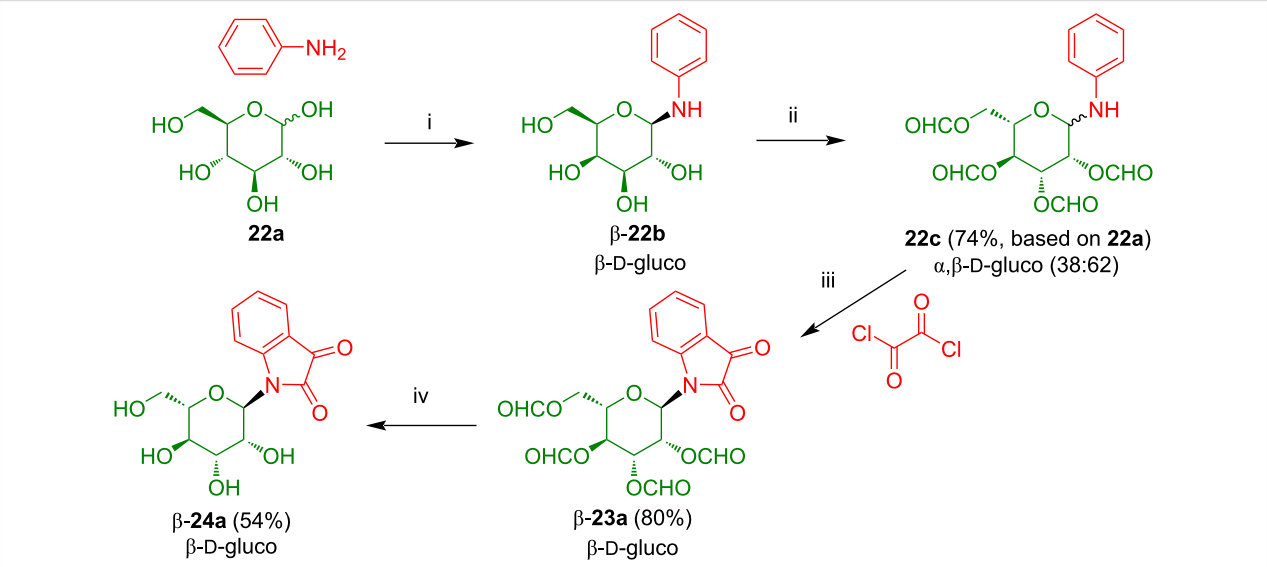

Scheme 16: Synthesis of β-**24a**. Reagents and conditions: i) *n*-PrOH, H_2O, formic acid (buffer, 100 mM), 2 h, 65 °C; ii) pyridine, DMF, formic acid, Ac_2O, ethyl formiate, 4 h, −40 °C; iii) 1) CH_2Cl_2, oxalyl chloride, 4 h, −20 °C, 2) ClC_6H_5, $TiCl_4$, 5 h, 85 °C; iv) THF, MeOH, NH_3, 30 min, 20 °C.

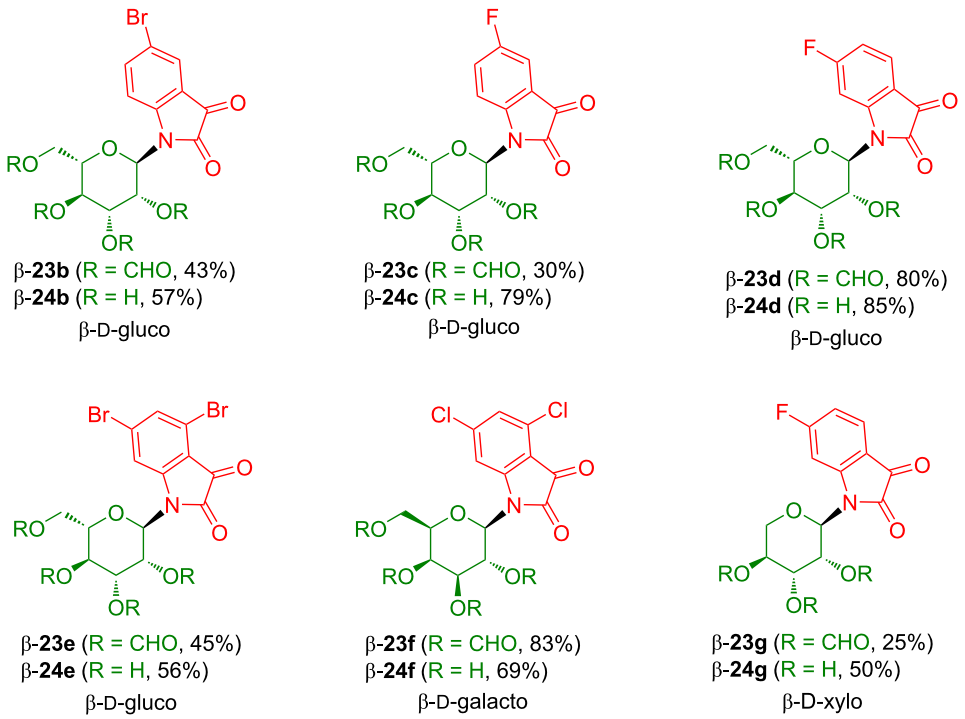

Scheme 17: Synthesis of isatin-*N*-glycosides **23b–g** and **24b–g**.

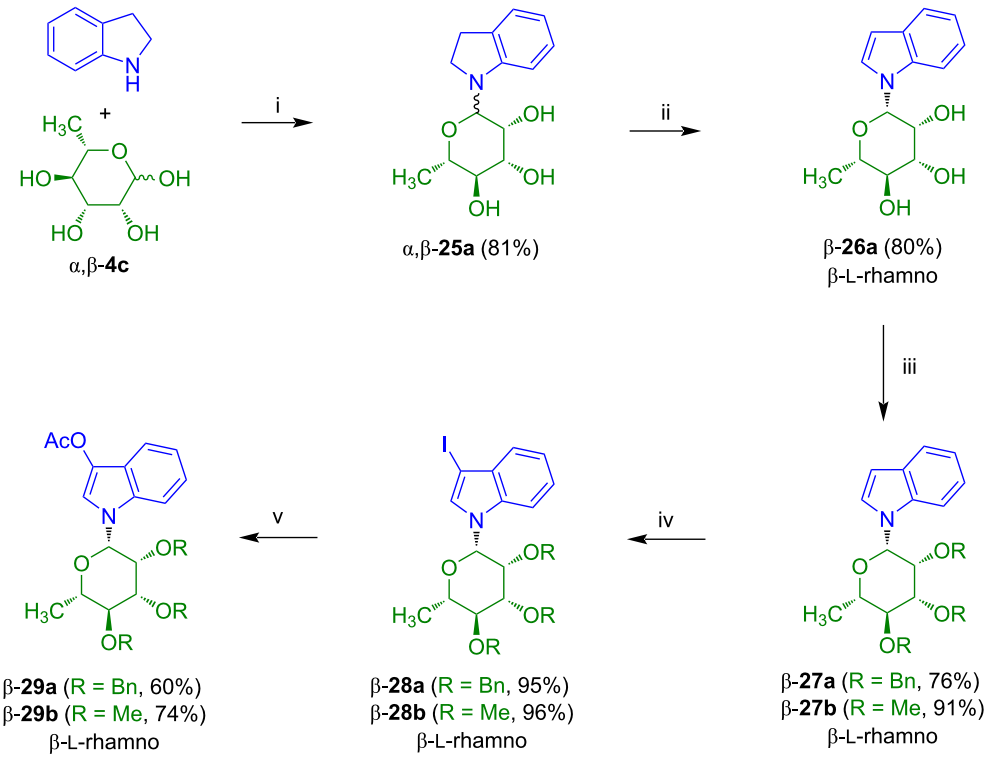

Scheme 18: Synthesis of β-**29a**,**b**. Reagents and conditions: i) EtOH, 20 °C, 12 h; ii) DDQ, dioxane, 20 °C, 12 h; iii) BnBr (for β-**27a**) or MeI (for β-**27b**), NaH, DMF, 0→4 °C, 12 h; iv) I_2, NaOH, DMF, 20 °C, 1 h; v) AgOAc, AcOH, 80 °C, 4 h.

of β-**29a** and β-**29b** with isatin. Likewise, various other conditions for base- or acid-mediated deacetylation and aldol-type condensation, typically used for the synthesis of non-glycosylated indirubins, proved to be unsuccessful. However, the acetyl group of β-**29a** could be selectively removed under slightly basic and reductive conditions (Na_2SO_3, dioxane, H_2O) to give the desired free indoxyl-*N*-glycoside. Due to its instability in the presence of air, the crude material was directly used for the reaction with isatin to give the desired indirubin-*N*-rhamnoside β-**30a**, albeit, in low yield (Scheme 19) [25]. Cleavage of the benzyl groups using boron tribromide afforded β-**31a**. In contrast to indirubin-*N*-rhamnoside **17a**, its isomer β-**31a** proved to be rather unstable. This fact was already earlier observed for indigo-*N*-rhamnoside **5d** and again suggests that compounds containing the sugar moiety attached to the amine-type nitrogen are less stable than the corresponding compounds containing the sugar moiety attached to the amide-type nitrogen atom. Unfortunately, the synthesis of β-**31a** was not a general method for the synthesis of indirubin-*N*-glycosides.

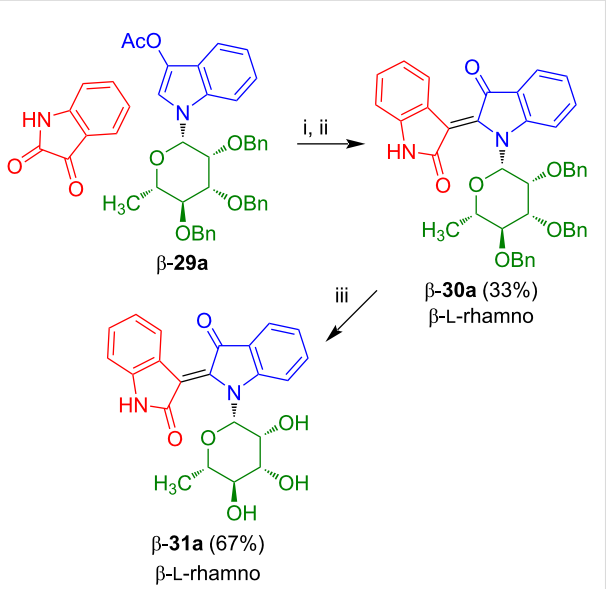

Scheme 19: Synthesis of β-**31a**. Reagents and conditions: i) Na_2SO_3, dioxane, H_2O, 110 °C, 2 d; ii) piperidine, benzene, 80 °C, 2 h; iii) BBr_3, CH_2Cl_2, –78 °C, 3.5 h.

Analogues of indirubin-*N*-glycosides

Thioindirubin-*N*-glycososides

In our group, we studied the reaction of isatin-*N*-glycoside **16a** with thiaindan-3-one which afforded red colored thioindirubin-*N*-rhamnoside β-**32a** in very good yield and with excellent *Z*-selectivity (Scheme 20) [26]. Deprotection of β-**32a** afforded β-**33a** in very good yield. Likewise, glucoside β-**33b**, galactoside β-**33c**, and mannoside β-**33d** were prepared. All products

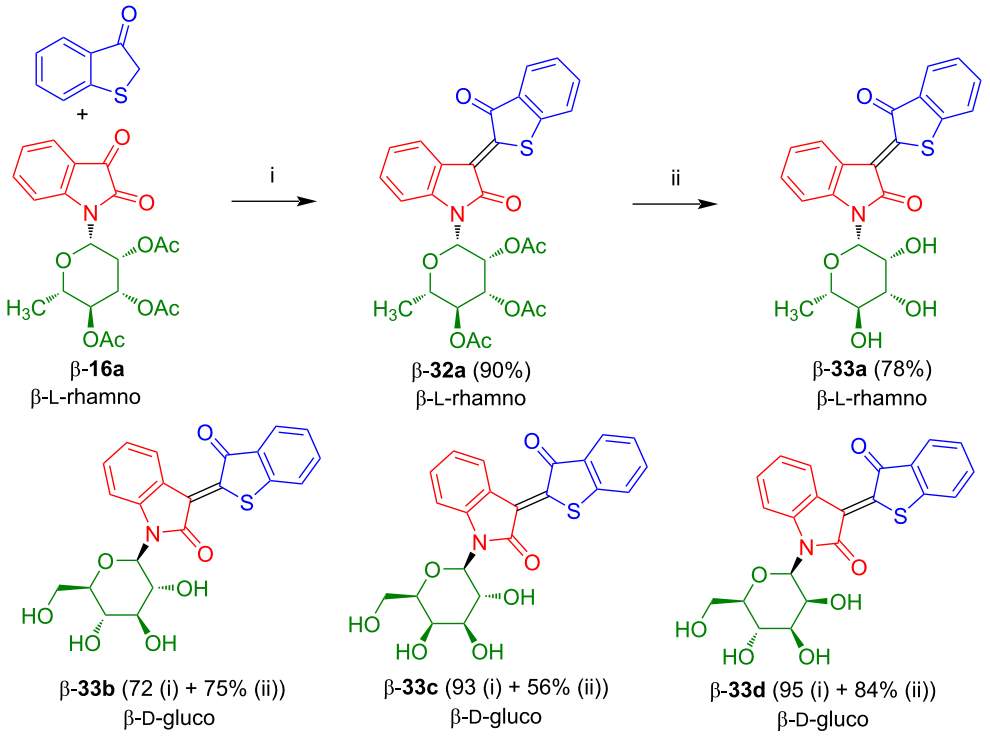

Scheme 20: Synthesis of **33a–d**. Reagents and conditions: i) Ac_2O, AcOH, NaOAc, 80 °C, 1 h; ii) 1) NaOMe, anhydrous MeOH, 20 °C, 2) 1% HCl in anhydrous MeOH, 20 °C. The yields of **33b–d** refer to the yields of the condensation and the deprotection step for each compound.

were isolated as the pure *Z*-configured isomers (determination by NMR, the other isomer was not visible, *E*/*Z* < 2:98). The configurations were determined by comparison of chemical shifts of our products with those of non-glycosylated thioindirubin and by crystal structure analysis. As mentioned above for the indirubins, the chemical shifts of the H-4 proton signals are strongly influenced by the anisotropic effect of the carbonyl group resulting in a downfield shift in case of the *Z*-isomers.

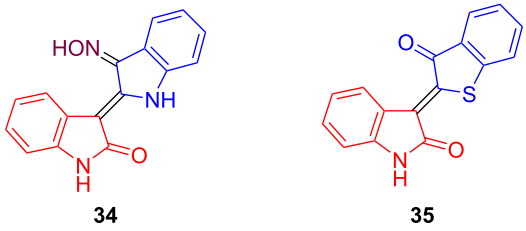

Scheme 21: Indirubins **34** and **35**.

In collaboration with Manfred Kunz (University of Leipzig), it was shown that all four compounds exhibit excellent antiproliferative activity against the malignant melanoma cell lines MeI-19, SK-MeI-29, SK-MeI-103, and SK-MeI-147. The compounds also induce apoptosis of the cancer cell lines which was investigated in collaboration with Jürgen Eberle (Charité Berlin) [27]. In fact, melanoma is a dangerous type of skin cancer which can be life threatening. Excellent IC_{50} values were observed for β-**33d** and other thioindirubin-*N*-glycosides. In contrast, indirubin-*N*-rhamnoside β-**17a**, lacking the sulfur atom, proved to be inactive against melanoma cell lines. In the future, it will be interesting to study the synthesis of acceptor-substituted thioindirubin-*N*-glycosides by reaction of thiaindan-3-one with acceptor-substituted isatin-*N*-glycosides **23b–g**. Indirubin- and thioindirubin-*N*-rhamnosides played an important role in an interdisciplinary project to understand the generation, development, and action of melanoma with the goal to develop new ways of clinical treatment of this dangerous disease. In this context, special emphasis was given to cell lines A-375 and SK-Mel-28 [27].

As mentioned above, non-glycosylated indirubins act as a ligand for the aryl hydrocarbon receptor (AhR) and also directly inhibit several cyclin-dependent kinases (CDK). A problem is generally the low water solubility of these compounds. The commercially available indirubin-3'-monoxime (**34**) shows a better solubility, due to the presence of the oxime group (Scheme 21). In fact, it represents one of the most active non-glycosylated indirubin derivatives against cancer [11,28]. It has been reported that the free NH function of the indirubin is crucial for CDK inhibition. The reaction of isatin with thiaindan-3-one has been reported to give thioindirubin **35** in very good yield as the pure *Z*-configured isomer [29]. For reasons of comparison, non-glycosylated indirubins **34** and **35** were prepared in our group.

Cutaneous squamous cell carcinoma (CSCC) is the second most common non-melanoma skin cancer (NMSC) after basal cell carcinoma (BCC). CSCC is responsible for 20% of cutaneous diseases and about 75% of all deaths are due to skin cancer, excluding melanoma. Due to the high incidence of CSCC and of actinic keratosis, there is a need of new therapeutic interventions. Thioindirubin-*N*-glycosides β-**33b** and β-**33d** show an excellent cytotoxic activity against melanoma and squamous cell carcinoma cells, lung cancer and glioblastoma cells [30]. It was shown in a WST-1 assay that these compounds exhibit a concentration-dependent inhibition of the metabolic activity of A375 and A431 cells, while the non-glycosylated derivative **34** proved to be inactive. The activities of β-**33b** and **34** on the cell viability was independently studied by using crystal violet as a dye for viable cells following a 48 h incubation of A375 melanoma cells and A431 squamous carcinoma cells. Interestingly, a concentration-dependent cytotoxicity was again observed for β-**33b**, but not for **35** in both cell lines. The IC_{50} values of β-**33b** were similar to those obtained by the WST-1 assay. A related proapoptotic effect was not observed for **35** in A375 cells. However, in case of A431 cells, a significant increase in caspase activity was observed for **35**, but at a much lower level as compared to β-**33b**.

For compound β-**33b**, the mitochondrial properties and cell viability of melanoma (A375) and squamous cell carcinoma cells (A431) of the skin were studied [31]. Glucoside β-**33b** resulted in a decrease of the cell viability. In addition, activation of caspases-3 and -7 and inhibition of colony formation were observed. Likewise, a concentration-dependent decrease of both the basal and ATP-linked oxygen consumption rate and of the capacity of oxidative respiration were observed at the mitochondrial level in the presence of compound β-**33b**. In addition, the morphology of the mitochondria was changed. The presence of β-**33b** provoked a significant upregulation of the enzyme heme oxygenase-1. In conclusion, mitochondria are attacked by compound β-**33b** in the context of its cytotoxic activity against skin cancer cells. Aglycon **35** again proved to be inactive in all assays.

It was mentioned above, that the free NH function of indirubin is important for CDK inhibition. We have shown in our group by enzyme studies that glycoside β-**33b**, lacking the free NH-function, does not act as a CDK inhibitor, despite its high

activity against melanoma cells and other cancers [32]. These results point to a completely different mode of action. In fact, the exact function of glycosylation is not clear. However, it might be assumed that the carbohydrate moiety increases the water solubility of the indirubin which results in a higher bioavailability of the drug. It might be speculated that the carbohydrate moiety is later hydrolytically cleaved in the cell to release the indirubin which then acts as a CDK inhibitor.

A synergistic effect of plasma-activated medium (PAM) and β-**33b** on human skin cancer cells was observed [32,33]. With regard to viability, adhesion capacity, apoptosis and G2/M cell cycle arrest, especially in A375 cells, glycoside β-**33b** alone showed a stronger anticancer effect as compared to oxime **34**. PAM significantly increased these effects in skin cancer cells. In contrast, no effect was observed for non-glycosylated thioindirubin **35** alone or in combination with PAM. It is anticipated that PAM activates channels of the membrane of melanoma cells to allow the antiproliferative compound (β-**33b**) to enter the cell. Thus, β-**33b** combined with PAM might be developed to a new and promising method of therapeutic intervention. This concept of combination of PAM with drugs could also be applied to other small compounds developed in our laboratory [34].

Selenoindirubin-*N*-glycososides

3-Acetoxybenzo[*b*]selenophene (**36f**) was prepared in our group according to a literature procedure (Scheme 22) [35-37]. The synthesis is based on the reaction of disodium diselenide with the diazonium salt derived from anthranilic acid (**36a**) to give diselenide **36b**, followed by reaction with the sodium salt of bromoactic acid, cyclization, and acetylation.

In our group, we investigated the reaction of isatin-*N*-rhamnoside **16a** with **36f** which afforded selenoindirubin-*N*-rhamnoside β-**37a** in good yield and with excellent *Z*-selectivity (Scheme 23) [38]. Deprotection of β-**37a** gave β-**38a** in very good yield. Likewise, rhamnosides β-**38b**–**d**, mannosides β-**33e**–**g**, and glucoside β-**38h** were prepared.

The reaction of **36f** with isatins **39a**–**h** afforded novel non-glycosylated selenoindirubins **40a**–**h** (Scheme 24) [38].

In collaboration with Jürgen Eberle and his team it was shown that selenoindirubin-*N*-glycosides β-**38a**–**h** showed antiproliferative activity against lung cancer cell lines H157 [38]. The antiproliferative activity against melanoma cells was accompanied by induced apoptosis in combination with the death ligand TRAIL (TNF-related apoptosis-inducing ligand). The death ligand TRAIL is a promising strategy for cancer treatment. In contrast to non-glycosylated thioindirubin **35**, a significant activity was observed also for non-glycosylated selenoindirubin **40h**. This might be due to the fact that selenoindirubin-*N*-glycosides show a considerably better solubility during the biological assays. Although the activities were, in general, only moderate, the results were promising in the sense that the activity was (again) concentration-dependent. It is important to note, however, that the results of the antiproliferative activities of selenoindirubin-*N*-glycosides β-**38a**–**h** were not directly comparable with those of thioindirubin-*N*-glycosides β-**33a**–**d**, because different cell lines were employed.

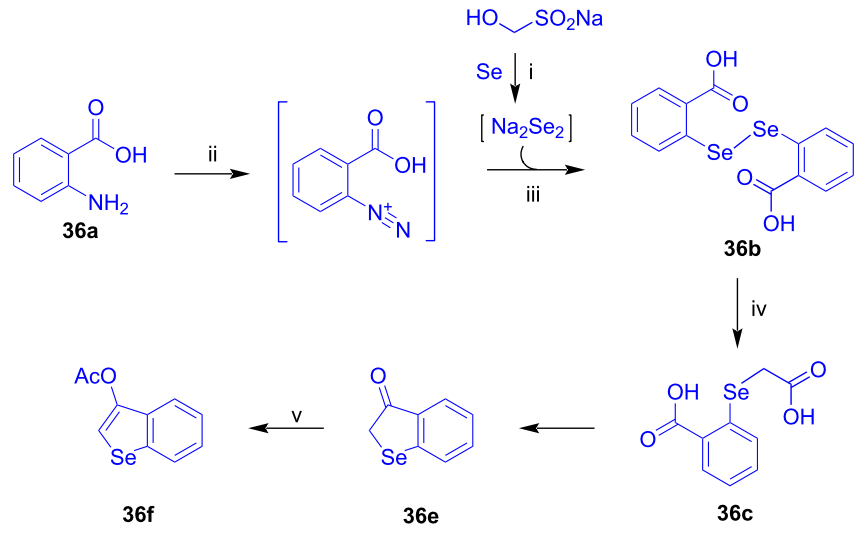

Scheme 22: Synthesis of **36f**. Reagents and conditions: i) NaOH, H_2O, 20 °C, 5 h; ii) HCl, $NaNO_2$, H_2O, −14 °C; iii) 1) Na_2Se_2, K_2CO_3, H_2O, 0→100 °C, 2) HCl; iv) 1) Zn, NaOH, H_2O, 100 °C, 0.5 h, 2) $BrCH_2COONa$, 100 °C, 0.5 h, 3) HCl; v) Ac_2O, pyridine, 90 °C, 6 h.

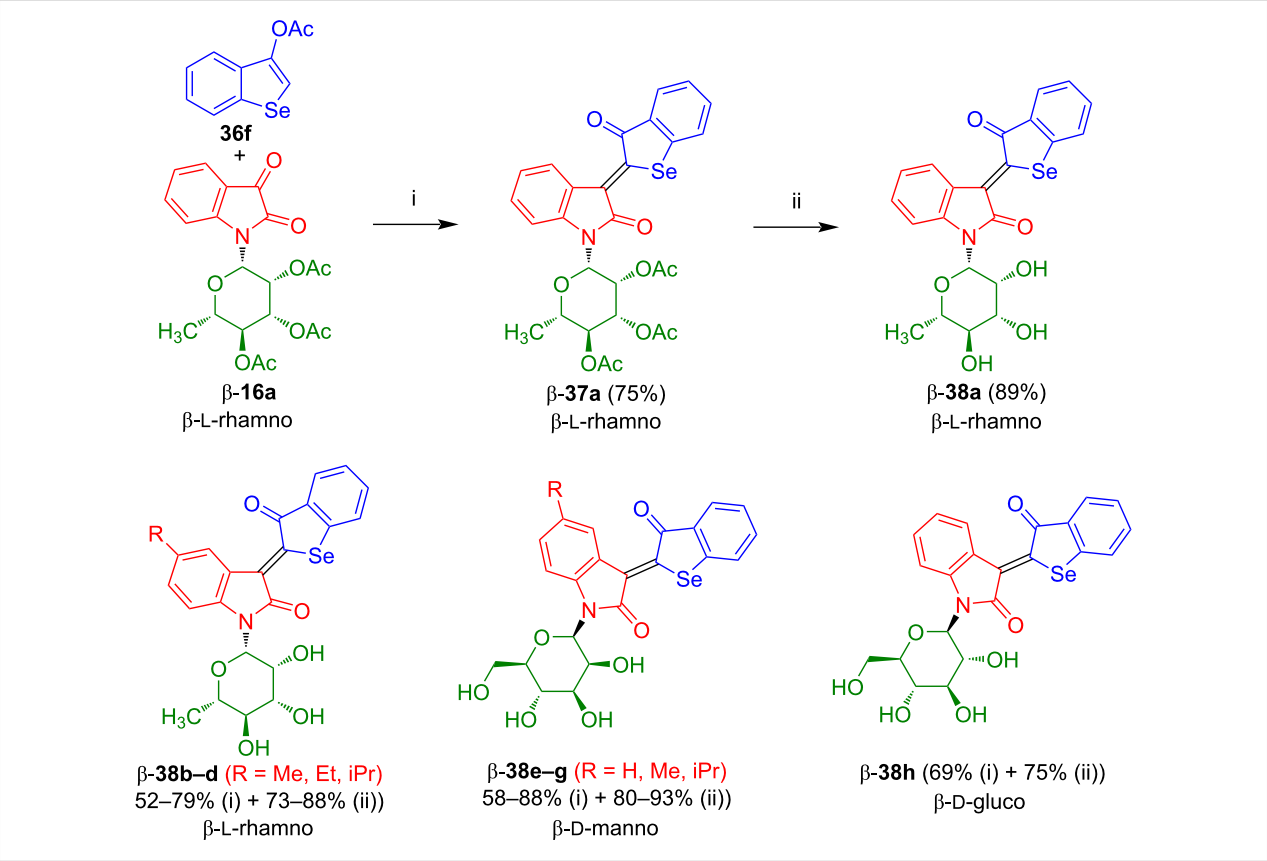

Scheme 23: Synthesis of **38a–h**. Reagents and conditions: i) 1) 0.1 equiv NaOMe, MeOH, 20 °C, 15–20 min, 2) HOAc, NaOAc, Ac_2O, 80 °C, 3–4 h; ii) NaOMe (cat.), MeOH/THF 2:1, 20 °C, 7 h. The yields of **38b–h** refer to the yields of the condensation and the deprotection step for each compound.

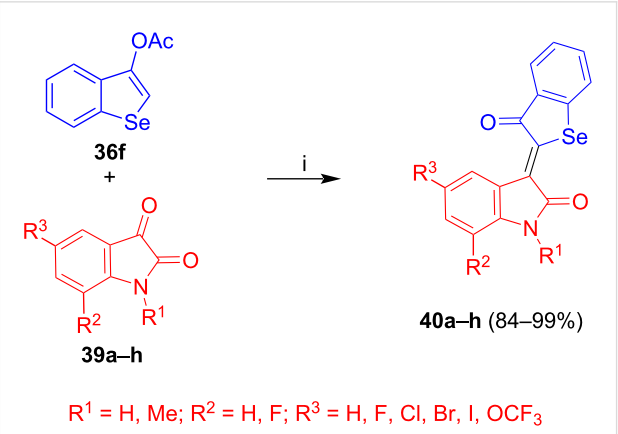

Scheme 24: Synthesis of **40a–h**. Reagents and conditions: i) method A: EtOH/THF, cat. KO*t*-Bu, 20 °C, 3–4.5 h; method B: 1) MeOH, NaOMe (0.1 equiv), 20 °C, 15–20 min, 2) HOAc (0.1 equiv); 3) cat. piperidine, EtOH, 1.5 h.

Oxoindirubin-*N*-glycososides

We studied in our group the reaction of isatin-*N*-rhamnoside **16a** with cumaran-3-one which afforded the desired oxoindirubin-*N*-rhamnoside as a separable mixture of *Z*-β-**41a** (55%) and *E*-β-**41a** (41%) (Scheme 25) [39]. Likewise, glucoside β-**41b**, galactoside β-**41c**, and mannoside β-**41d** were prepared and the two geometric isomers of each product were separated and isolated in pure form. However, the deprotection failed under various conditions, due to decomposition by retro-aldol reaction. Interestingly, while indirubin-*N*-glycosides **17**, thio- and selenoindirubin-*N*-glycosides **33** and **38** were formed as pure *Z*-isomers, oxoindirubin-*N*-glycosides **41** were formed as mixtures of *E*- and *Z*-isomers. The isolated yields of *Z*-β-**41a** (55%) and *E*-β-**41a** (41%) are in accordance with the relative thermodynamic stability of the two geometric isomers. According to DFT calculations, the Z-isomer is slightly energetically favored by 14.88 kJ/mol. The configurations were determined by comparison of chemical shifts of our products with those of non-glycosylated indirubin, by the presence of an intramolecular hydrogen bond N–H···O and by crystal structure analysis. As mentioned above for the indirubins and thioindirubins, the chemical shifts of the H-4 proton signals are strongly influenced by the anisotropic effect of the coumaranone carbonyl group resulting in a downfield shift in case of the *Z*-isomers. The different *E*/*Z*-selectivity in case of oxoindirubins as compared to other indirubin derivatives can be explained, on the one

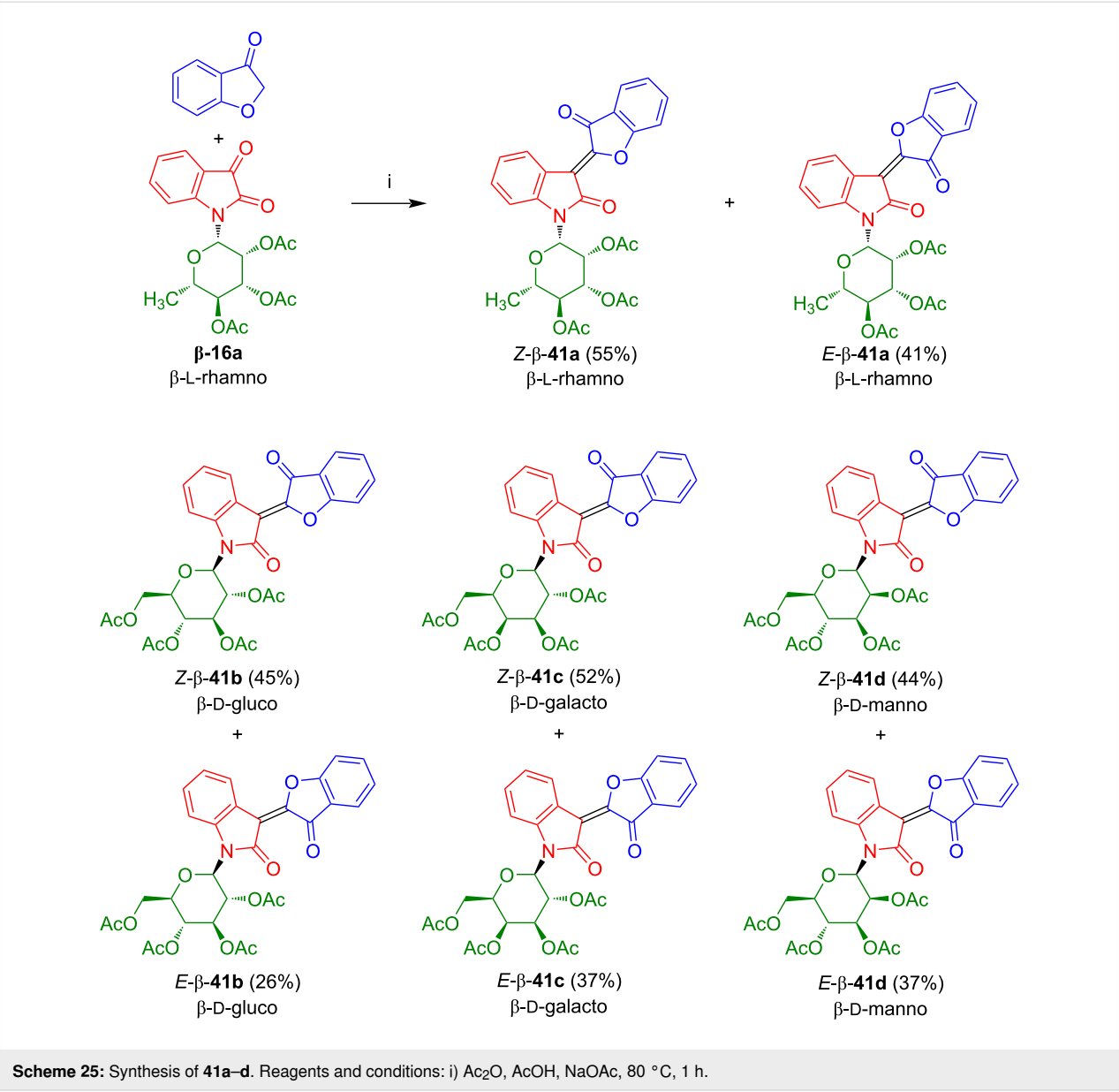

Scheme 25: Synthesis of **41a–d**. Reagents and conditions: i) Ac_2O, AcOH, NaOAc, 80 °C, 1 h.

hand, by the absence of the favorable intramolecular hydrogen bond which is present in case of indirubins **17**. However, this does not explain the difference to thio- and selenoindirubins **33** and **38**. In general, the isomer containing the two carbonyl groups on opposite sides of the central double bond is thermodynamically favored, due to electrostatic repulsion. However, the presence of the ring oxygen in case of the oxoindirubins **41** seems to decrease this unfavorable dipol situation in case of the *E*-configured isomers. It is likely, that an *E*/*Z* isomerization takes place under acidic conditions. The barrier of this equilibrium is most likely lowered by the presence of the ring oxygen as it represents a π-donor. Although nitrogen, as present in indirubins **17**, is an even better donor than oxygen, the stability of the intramolecular hydrogen bond overrules this effect. Sulfur and selenium are very weak π-donors. It was not studied so far whether the *E*/*Z* ratio of indirubin derivatives can be influenced by UV irradiation.

Kornienko et al. reported the synthesis and antiproliferative activity of non-glycosylated oxoindirubin *Z*-**41e** in 54% yield by reaction of cumaran-3-one with isatin under conditions similar to those employed by us (Scheme 26) [40]. However, the reaction time was much longer (24 instead of 1 h). Interestingly, in contrast to *N*-glycosides **41a–d**, only one geometrical isomer was formed. This result is surprising, as the carbohydrate moiety is located far away from the double bond and unlikely exerts a stereochemical effect. As the aldol condensation is irreversible once the double bond is formed, a thermodynamic

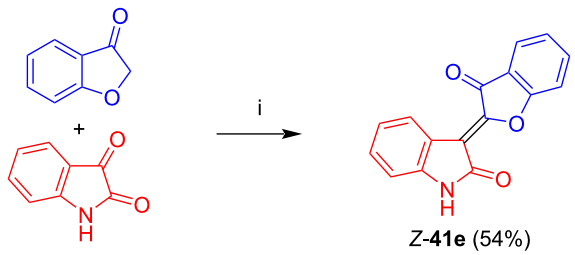

Scheme 26: Synthesis of **41e**. Reagents and conditions: i) AcOH, NaOAc, 110 °C, 24 h.

control of the *E*/*Z*-ratio and influence of the reaction time is unlikely. However, the reported formation of **41e** as a single isomer has to be treated with some care. In the publication, no supporting information and compound characterization was given. In addition, the yield of **41e** (54%) is in a range which does not really exclude the formation of the *E*-configured isomer as a side-product. In fact, we observed for the formation of *Z*-configured *N*-glycosides **41a**–**d** yields in the range of 44–55%, while the corresponding *E*-configured isomers were isolated in 26–41% yields. In any case, compound *Z*-**41e** was reported to exhibit a strong in vitro antiproliferative activity against breast cancer cells MCF-7 and melanoma mouse cells B16F10. In contrast, the activity against melanoma cells SKMEL-28 was only moderate.

Carboindirubin-*N*-glycososides

The reaction of isatin-*N*-rhamnoside **16a** with indan-1-ones **42a**,**b**, carried out in our group, afforded *E*-configured carboindirubin-*N*-rhamnosides *E*-β-**43a**,**b** in very good yields (Scheme 27) [39,41]. In this reaction, a solution (EtOH) of the starting materials and NEt_3 was stirred at 20 °C to give the corresponding aldol products. The latter were treated, without chromatographic purification, with MsCl (methanesulfonyl chloride), NEt_3, and DMAP to give the desired products *E*-β-**43a**,**b**. Similarly, glucosides *E*-β-**43c**,**d** and galactoside *E*-β-**43e** were obtained. In contrast to oxoindirubin-*N*-rhamnoside β-**41a**, all glycosides were obtained as pure *Z*-configured isomers (determination by NMR, the other isomer was not visible, *E*/*Z* > 98:2). Deprotection of *E*-β-**43a**,**b** under acidic conditions gave rhamnosides *E*-β-**44a**,**b** in good yields. However, deprotection of *E*-β-**43c**–**e** failed.

Kornienko et al. reported the synthesis and antiproliferative activity of non-glycosylated carboindirubin *E*-**43f** in 86% yield by

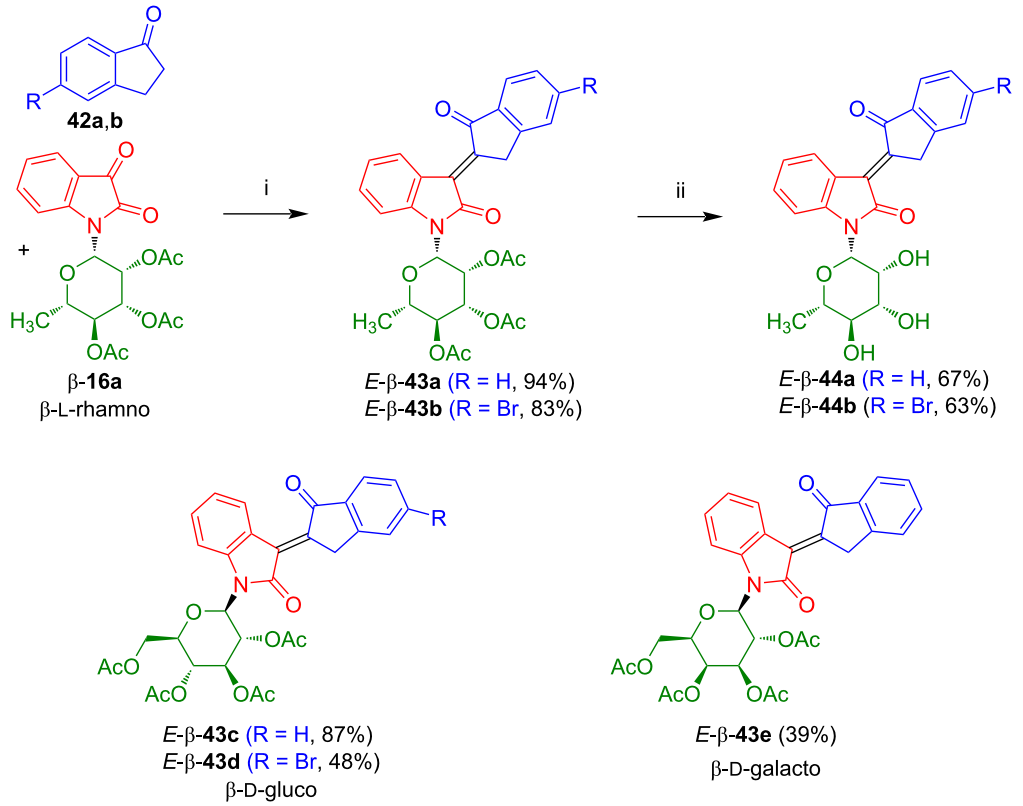

Scheme 27: Synthesis of *E*-β-**43a**–**e** and *E*-β-**44a**,**b**. Reagents and conditions: i) 1) NEt_3, EtOH, 20 °C, 12 h, 2) DMAP, NEt_3, MsCl, CH_2Cl_2, 0 to 20 °C, 20 h; ii) HCl in MeOH (1%), 20 °C, 12 h.

reaction of indan-1-one (**42a**) with isatin using sodium carbonate in methanol (Scheme 28) [40]. For this compound, only moderate or no antiproliferative activities were observed against various cancer cell lines.

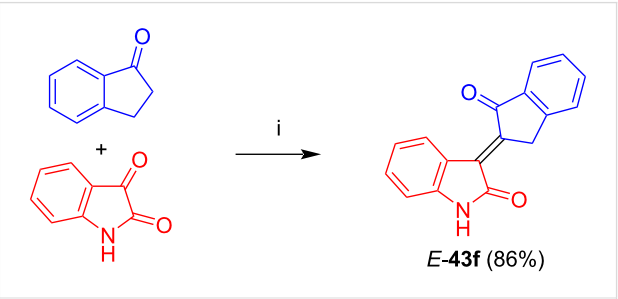

Scheme 28: Synthesis of *E*-**43f**. Reagents and conditions: i) Na_2CO_3, MeOH, 20 °C, 6–24 h.

3-Alkylideneoxindole-*N*-glycososides

3-Alkylideneoxindoles are of considerable pharmacological relevance and occur in a variety of clinically used drugs and natural products [42-45]. The reaction of isatin-*N*-rhamnoside **16a** with acetophenone (**45a**) afforded the desired 3-alkylideneoxindole-*N*-rhamnoside *E*-β-**46a** in good yield as an orange solid (Scheme 29) [46]. In the first step, a base-mediated aldol reaction was carried out. The corresponding alcohol was directly used as the crude product and treated with tosyl chloride, NEt_3, and DMAP (stirring for 2 h at 20 °C) to give the corresponding tosylate which was further stirred for 6 h at 20 °C to give *E*-β-**46a**. Likewise, rhamnosides *E*-β-**46b**–**e**, mannosides *E*-β-**46f**–**i**, glucosides *E*-β-**46j**,**k**, and galactosides *E*-β-**46l**,**m** were prepared. 3-Alkylideneoxindole-*N*-glycososides **46** can be regarded as analogues of indirubin-*N*-glycosides completely missing the nitrogen atom of the indoxyl moiety.

It was demonstrated that 3-alkylideneoxindole-*N*-glycosides **46** show a significant antitumor activity against melanoma human cell lines SK-Mel-147 and A-375 [46]. As mentioned above, the death ligand TRAIL is a promising strategy for cancer treatment. Unfortunately, melanoma cells show both preexisting and inducible TRAIL resistance. Similarly, as in case of the activity of selenoindirubin-*N*-glycosides **38** against lung cell carcinoma (Scheme 23), inhibition of melanoma cell proliferation and loss of cell viability were significantly increased by the presence of the death ligand TRAIL. The antitumor effects were related to the inhibition of the survival pathway of c-Jun and JNK2 (Jun N-terminal kinase).

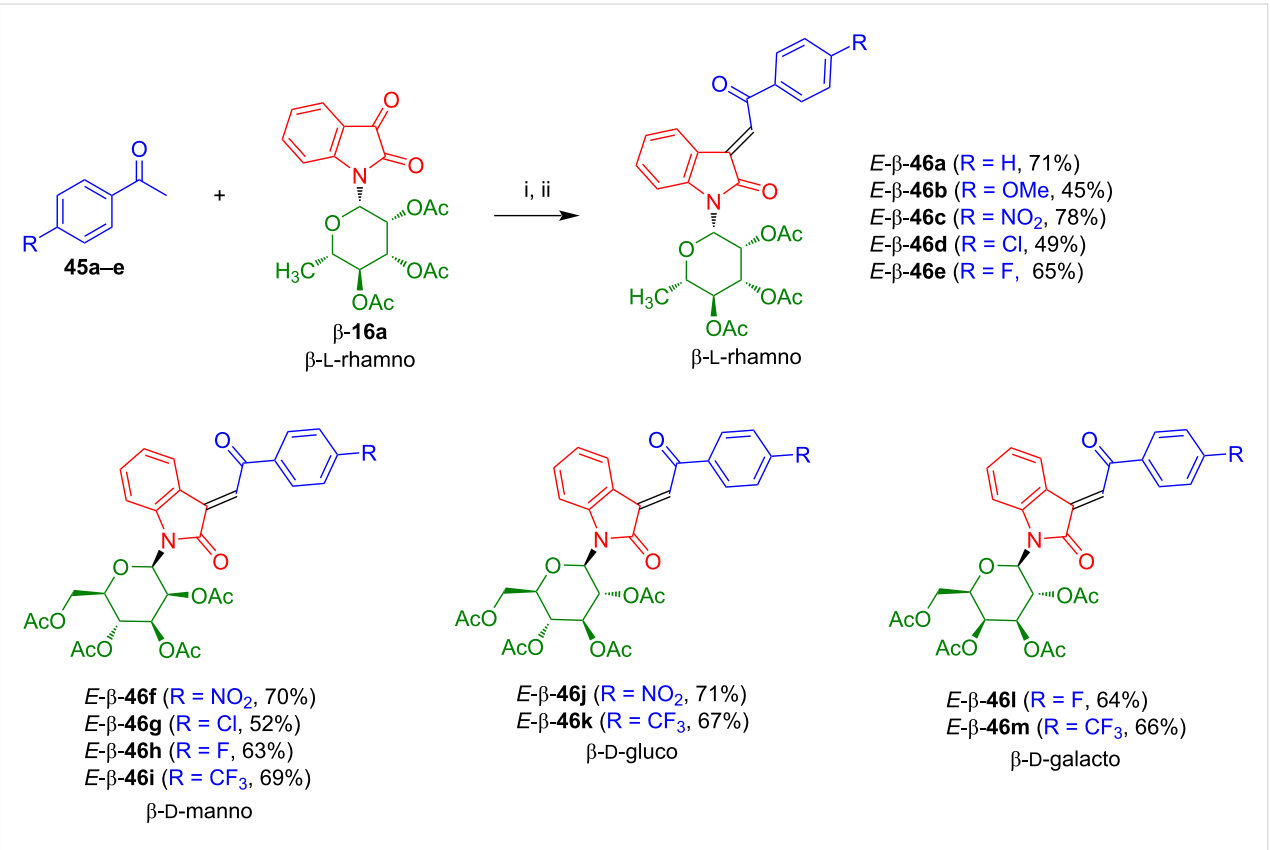

Scheme 29: Synthesis of **46a**–**m**. Reagents and conditions: i) NEt_3 (1 equiv), EtOH, 20 °C, 6–10 h; ii) MsCl, NEt_3, DMAP, CH_2Cl_2, 0–20 °C, 2 h, 20 °C, 6–8 h.

In an additional study, it was shown that treatment with derivative *E*-β-**46b** results in an increase of melanoma cell sensitivity for death ligands and allows to overcome resistance against TRAIL and CD95 agonists [47]. A detailed investigation of apoptotic signaling pathways revealed that TRAIL resulted, based on a negative feed-back loop, in a rapid downregulation of both agonistic TRAIL receptors DR4 and DR5. However, the presence of compound *E*-β-**46b** resulted in a compensation of this negative feed-back loop by TRAIL and an upregulation of both receptors. In addition, a loss of mitochondrial membrane potential and release of cytochrome c was observed which gave rise to an activation of intrinsic apoptosis pathways. The mitochondrial response seems to be related to an upregulation of Bax and Bad and to downregulation of Mcl-1. In fact, the presence of compound *E*-β-**46b** in combination with TRAIL was also able to overcome apoptosis resistance, due to overexpression of ectopic Bcl-2.

The proapoptotic effects of compound *E*-β-**46e** in melanoma cells were investigated in more detail. In fact, the downstream signaling pathways seem to be based on the production of reactive oxygen species [48]. Like *E*-β-**46b**, the presence of derivative *E*-β-**46e** appears to control apoptosis in melanoma cells which is (again) increased by the presence of TRAIL and results in complete loss of cell viability. As in case of compound *E*-β-**46b**, the signaling cascade was investigated also for derivative *E*-β-**46e**. Important biochemical steps were again activation of caspase-3, downregulation of XIAP, upregulation of p53 and TRAIL receptor 2, STAT-3 dephosphorylation, and loss of mitochondrial membrane potential. The most important biomolecular step, however, was the early production (already after one hour) of reactive oxygen species (ROS). This was demonstrated by pretreatment with antioxidants which completely stopped induction of apoptosis and of the loss of cell viability and resulted in disappearance of the signaling effects mentioned above. In fact, ROS were shown to be upstream of all proapoptotic signaling and to play a decisive role in apoptosis regulation which might lead to new strategies for the therapy of melanoma.

As mentioned above, cutaneous squamous cell carcinoma (CSCC) is the second most common non-melanoma skin cancer. In collaboration with Jürgen Eberle and his team, the activity of *E*-β-**46b**, *E*-β-**46e**, and *E*-β-**46k** in four CSCC cell lines were investigated [49]. High activities were observed for SCL-I, SCL-II, SCC-12, and SCC-13 cell lines with up to 80% reduction of cell proliferation, 60% reduction of cell viability and 30% induced apoptosis at a 10 μM level. Like in case of the studies mentioned above, apoptosis was further increased in combination with TRAIL. Induction of reactive oxygen species were again mandatory for these effects to be observed. In fact, apoptosis was entirely cancelled by antioxidative pretreatment and cancer cell viability and proliferation were fully regenerated. Complete activation of cascades of caspases-3, -4, -6, -7, -8, and -9, loss of mitochondrial membrane potential, activation of proapoptotic PKCδ (protein kinase C delta), and inhibition of STAT3 (signal transducer and activator of transcription 3) were observed as biochemical pathways, along with downregulation of antiapoptotic XIAP (X-linked inhibitor of apoptosis protein) and surviving as well as upregulation of the proapoptotic Bcl-2 protein Puma and the cell cycle inhibitor p21. It is worth to be noted that all these activation steps were stopped by the presence of antioxidants which indicates that ROS act as key regulators of the antitumor effects of 3-alkylideneoxindole-*N*-glycosides **48**.

In the last decades, we have witnessed an increasing incidence of cutaneous T-cell lymphoma (CTCL) which is, in fact, a dangerous form of non-Hodgkin's lymphomas (NHL) and there is a need for innovative therapies. In collaboration with Jürgen Eberle and his team it was shown that the action of 3-alkylideneoxindole-*N*-glycoside *E*-β-**46d** results in a strong decrease of CTCL proliferation and viability and in induction of apoptosis [50]. The presence of this compound results in downregulation of the caspase antagonistic proteins c-FLIP and XIAP via caspase-8 and caspase-3 in the (extrinsic) apoptosis cascade. Similarly as discussed above for the activity of 3-alkylideneoxindole-*N*-glycosides against melanoma and CSCC, a strong increase of the concentration of reactive oxygen species (ROS) as a rapid effect is observed in response of the treatment with *E*-β-**46d**.

3-(5-Oxo-2-thioxoimidazolidin-4-ylidene)indolin-2-one-*N*-glycosides

The reaction of isatin-*N*-rhamnoside β-**16a** with thiohydantoin (**47a**), carried out in our group, afforded red colored β- and *Z*-configured 3-(5-oxo-2-thioxoimidazolidin-4-ylidene)indolin-2-one-*N*-rhamnoside β-**48a** in 54% yield (Scheme 30) [51]. Likewise, rhamnoside β-**48b** and mannosides β-**48c** and β-**48d** were prepared. However, all attempts to achieve a deprotection failed. Compounds **48a**–**d** were investigated with regard to their antiproliferative activities against lung carcinoma cells (H157) and human corneal epithelial cells (HCEC). All compounds showed a moderate and selective activity against H157 with 60% inhibition for compound **48b** at a concentration of 100 μM. No activity was observed against HCEC. The activities were higher as compared to those observed for selenoindirubin-*N*-glycosides β-**38a**–**h** employed in the same assay.

Kornienko et al. reported the reaction of isatin with thiohydantoin (**47a**) to give condensation product **48e** (Scheme 31) [40].

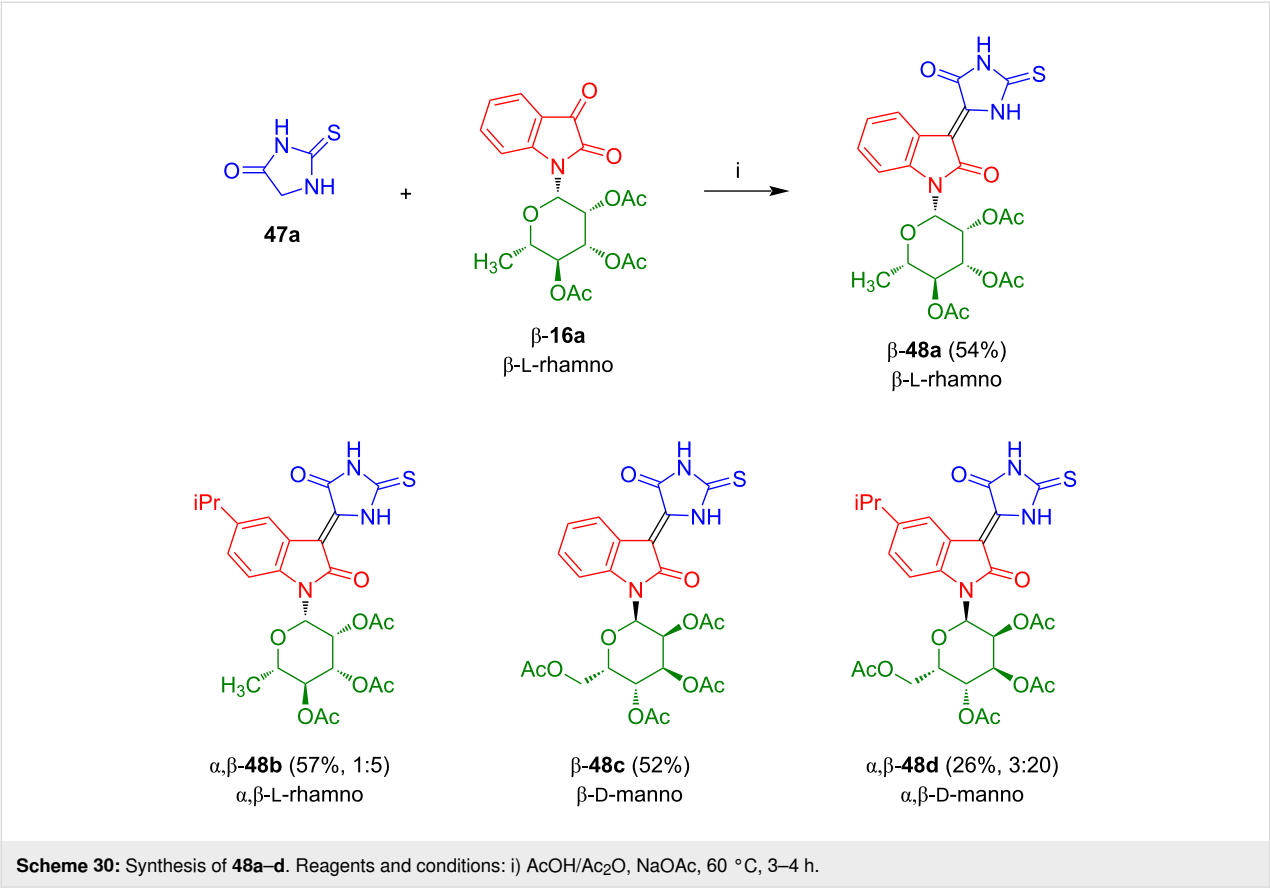

Scheme 30: Synthesis of **48a–d**. Reagents and conditions: i) AcOH/Ac_2O, NaOAc, 60 °C, 3–4 h.

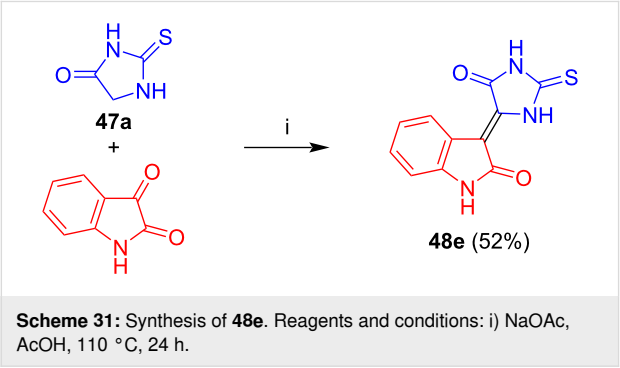

Scheme 31: Synthesis of **48e**. Reagents and conditions: i) NaOAc, AcOH, 110 °C, 24 h.

This compound only showed moderate or low antiproliferative activity against various cancer cell lines.

3-(2-Acetamido-4-oxo-4,5-dihydrothiazol-5-ylidene)indolin-2-one-*N*-glycosides

The reaction of isatin-*N*-glycosides β-**16a** and β-**16e** with pseudo-thiohydantoin (**47b**) afforded β- and *Z*-configured 3-(2-acetamido-4-oxo-4,5-dihydrothiazol-5-ylidene)indolin-2-one-*N*-glycosides β-**49a** and β-**49b**, respectively (Scheme 32) [51]. Again, a deprotection was not possible under various conditions. Compounds **49a**,**b** showed a moderate and selective activity against lung cancer cells H157 [52].

3-(4-Oxo-4,5-dihydrothiazol-5-ylidene)indolin-2-one-*N*-glycosides

The reaction of rhodanine (**50**) with glucosyl bromide β-**51a** afforded the acetyl-protected thiazolone-*S*-glucoside β-**52a** in 47% yield (Scheme 33) [51]. Condensation of the latter with isatin (**53a**) afforded 3-(4-oxo-4,5-dihydrothiazol-5-ylidene)indolin-2-one-*S*-glucoside β-**54a** in 62% yield and with very good *Z*-selectivity. Employment of the pivaloyl instead of the acetyl protective group resulted in an improved yield for both steps to give *S*-glucoside β-**54b**. All attempts to deprotect compounds **54a**,**b** failed. Compound **54a** shows a moderate and selective activity against lung cancer cells H157 [52].

The reaction of **50** with glucosyl and xylosyl bromides β-**51a**,**b** and isatins **53a**,**b** afforded pivaloyl-protected 3-(4-oxo-4,5-dihydrothiazol-5-ylidene)indolin-2-one-*S*-glycosides β-**54c–l** which, unfortunately, again could not be deprotected (Scheme 34) [51].

Isoindigo-*N*-glycosides (yellow sugars)

Isoindigo-*N*-glycosides

Sassatelli et al. reported the synthesis of isoindigo-*N*-glycosides β-**57a–c** by reaction of benzyl-protected isatin-*N*-glycosides β-**56a–c** with oxindole (**55**) (Scheme 35) [53-55]. Depro-

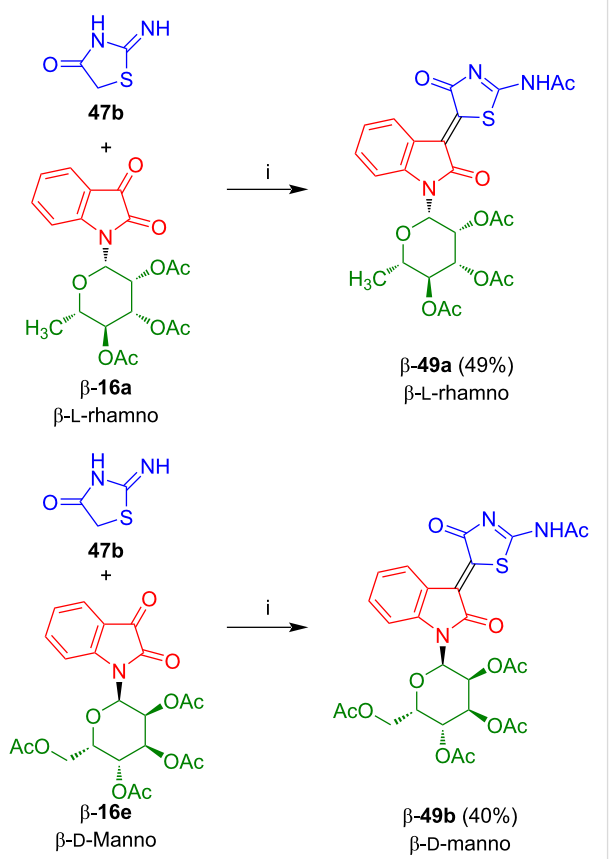

Scheme 32: Synthesis of β-**49a**,**b**. Reagents and conditions: i) AcOH/Ac_2O, NaOAc, 60 °C, 3–4 h.

tection by BBr_3 afforded β-**58a**–**c**. Isatins **56** were prepared by glycosylation of indoline, benzylation, and oxidation with CrO_3. Although this approach allowed for the synthesis of acceptor-substituted isatin-*N*-glycosides, it proved to be tedious and the yields were low. In a similar way, acetyl-protected isoindigo-*N*-glycosides were prepared. In addition, benzyl-protected isoindigo-*N*-glycoside β-**58d**, containing a 4-oxobutanoic acid side chain at the 5'-position, was prepared by reaction of the corresponding oxindole with isatin-*N*-glycoside **56a**. The in vitro antiproliferative activities of compounds β-**57a**–**c** and β-**58a**–**d** were studied toward a panel of human solid cancer cell lines (PC 3, DLD-1, MCF-7, M4Beu, A549, PA 1), a murine cell line (L929), and a human fibroblast primary culture. The most potent compound was β-**58d**.

Bouchikhi et al. reported the synthesis, kinase inhibitory potencies, and in vitro antiproliferative activities of acetylated 7'-azaisoindigo-*N*-glycosides, such as β-**58d** (Scheme 35) [56,57]. The presence of an additional nitrogen atom in the isoindigo moiety proved to be important for an improved antitumor activity. In vitro antiproliferative activities of these compounds were tested against the human buccal carcinoma cell line (KB) and human myeloid leukaemia cell lines (K562, HL60). While isoindigo-*N*-glycosides did not show cytotoxicity, two azaisoindigo-*N*-glycosides exhibited significant antiproliferative activities with cell proliferation inhibition of all the cell lines tested in a 75–80% range. The best activity was observed, in fact, for compound β-**58d**.

Isoindigo-*N,N'*-diglycosides

In our group, the synthesis of *N,N'*-diglycosylated isoindigos was studied. In contrast to isatin-*N*-glycosides, oxindole-*N*-glycosides are not readily available. Therefore, reductive dimerization of isatin-*N*-glycosides was considered as a strategy for the synthesis of the target compounds. Isatin-*N*-rhamnosides β-**16g**–**j** were prepared from the corresponding anilines as exemplified above for the synthesis of β-**16a**. Treatment of β-**16a**,**g**–**j** with tris(diethylamino)phosphine resulted in formation of dimers β-**59a**–**e** in good yields (Scheme 36) [58]. Deprotection afforded the desired isoindigo-*N,N'*-dirhamnosides β-**60a**–**e** as orange to brown solids.

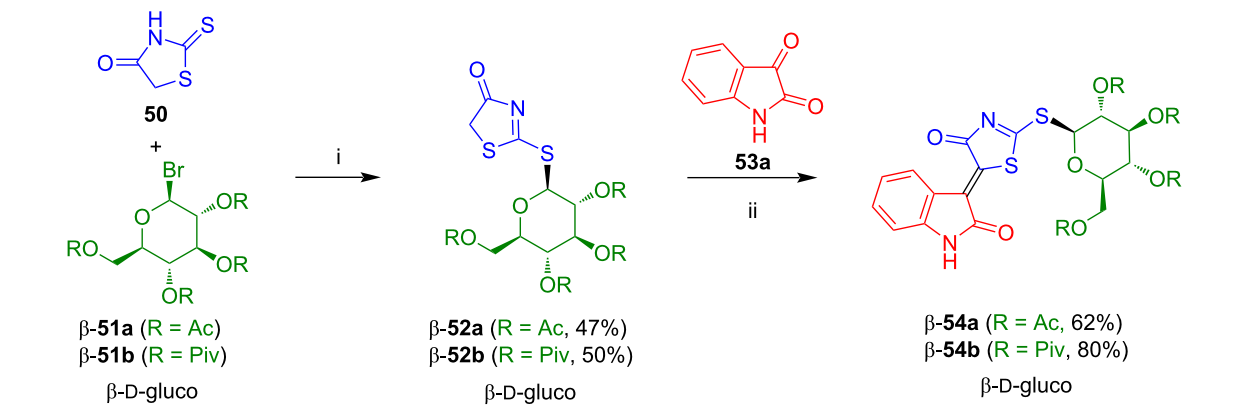

Scheme 33: Synthesis of β-**54a**,**b**. Reagents and conditions: i) 1) NaH, DMF, 0 °C, 15 min, 2) β-**51a**,**b**, 20 °C, 3 h; ii) EtOH or MeOH/THF, cat. piperidine, 20 °C, 1–2 h.

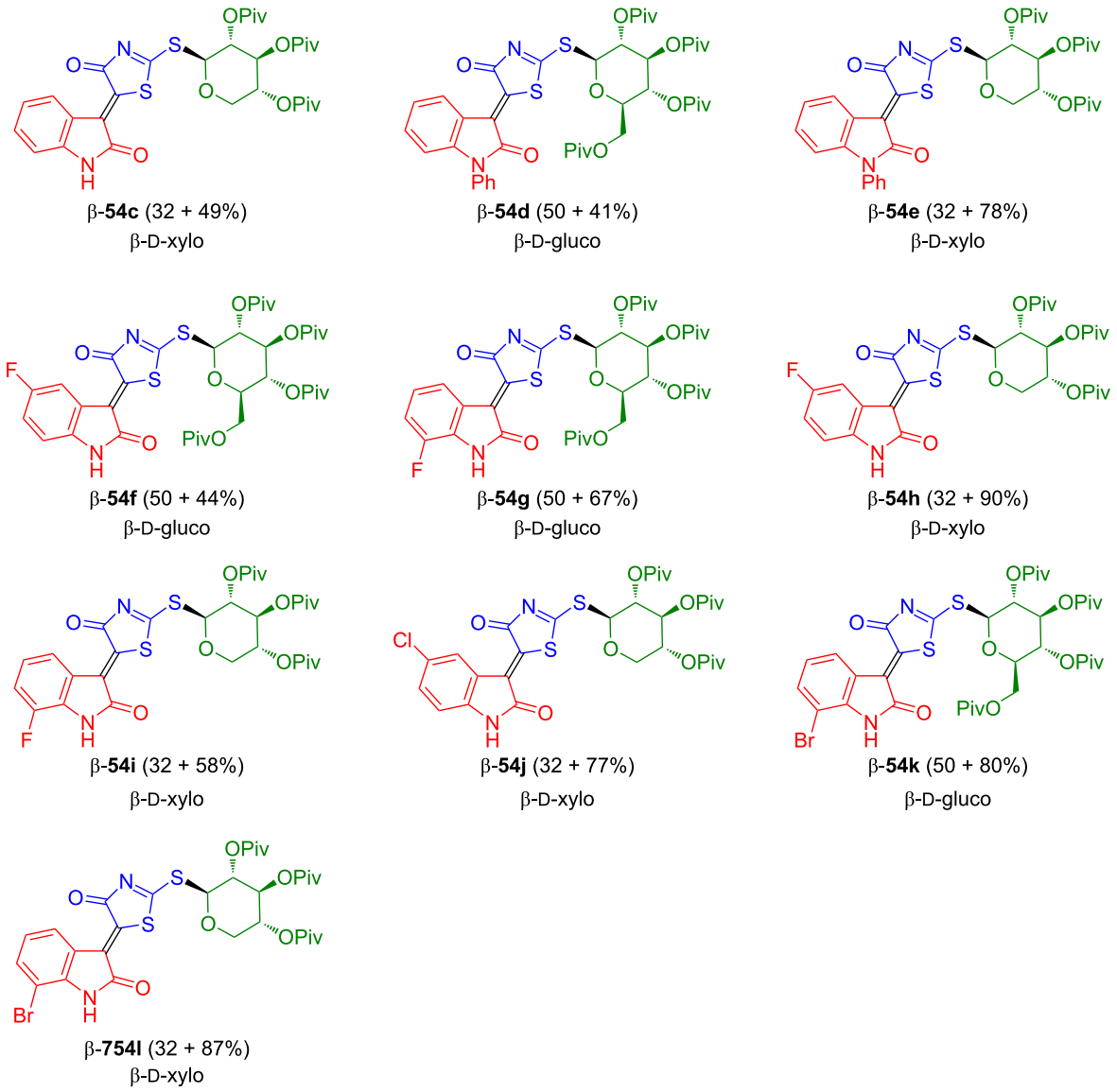

Scheme 34: Synthesis of **54c–l**. The yields refer to the yields of the first and second condensation step for each compound.

Similarly to the synthesis of rhamnosides **59**, the dimerization of isatin-*N*-mannosides β-**16e** and β-**16k–m** afforded isoindigo-*N,N*'-mannosides β-**61a–d** which were subsequently deprotected to give products β-**62a–d** in good yields (Scheme 37) [58]. The dimerization failed for isatin-*N*-glycosides derived from β-D-galactose, β-D-glucose, and β-D-xylose which might be due to their 1,2-*trans* configuration. An identical relative configuration (1,2-*trans*; 1,3-*cis*) is observed for the first three carbon atoms of β-D-galactose, β-D-glucose, and β-D-xylose. In contrast, for β-D-mannose and β-L-rhamnose, the first three C-atoms possess a different relative configuration (1,2-*cis*; 1,3-*cis*). This difference cannot be explained at the moment. A possible explanation is based on the assumption that, during dimerization, the acetate group of the 1,2-*trans*-configured sugars interacts with the carbenoid intermediate of the isatin and, thus, exerts an unfavorable influence.

Oxoisoindigo-*N*-glycosides

The reaction of isatin-*N*-rhamnoside β-**16a** with 2-coumaranone (**63**), carried out in our group, afforded the acetyl-protected oxoisoindigo-*N*-rhamnoside β-**64a** as an orange to red solid in 44% yield (Scheme 38) [59]. Unfortunately, all attempts to achieve a deprotection failed, due to cleavage of the lactone moiety. Starting with α-configured isatin-*N*-rhamnoside α-**16a**, anomerically pure α-**64a** could be prepared in 43% yield. Likewise, *N*-rhamnoside β-**64b**, *N*-glucoside β-**64c**, *N*-mannoside β-**64d,** and *N*-galactoside β-**64e** were prepared from the corresponding isatin-*N*-glycosides β-**16b–e** [60].

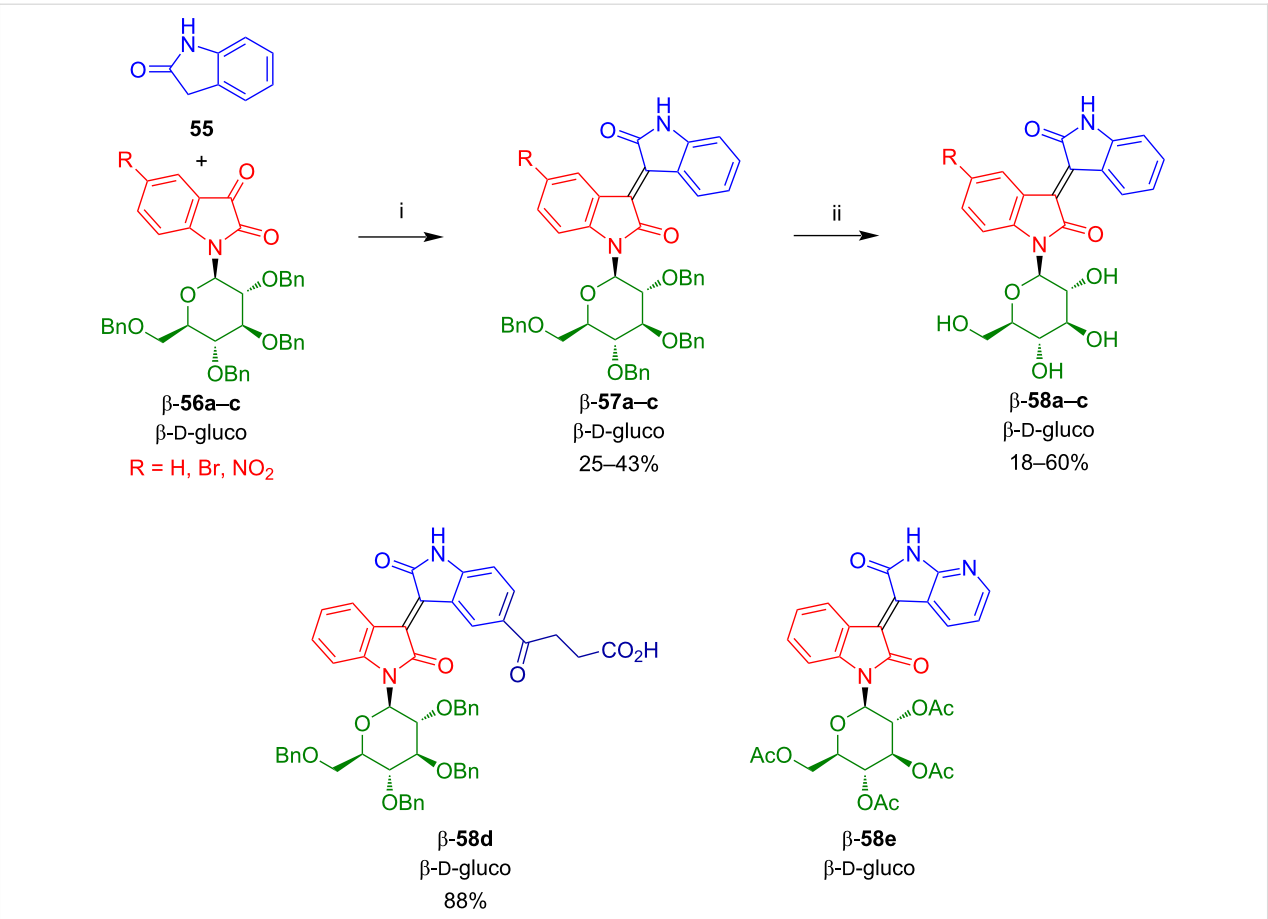

Scheme 35: Synthesis of **57a–c** and **58a–d**. Reagents and conditions: i) HCl (conc.), AcOH, reflux, 24 h; ii) 1) BBr_3, CH_2Cl_2, 20 °C, 2 h, 2) H_2O, −78 °C.

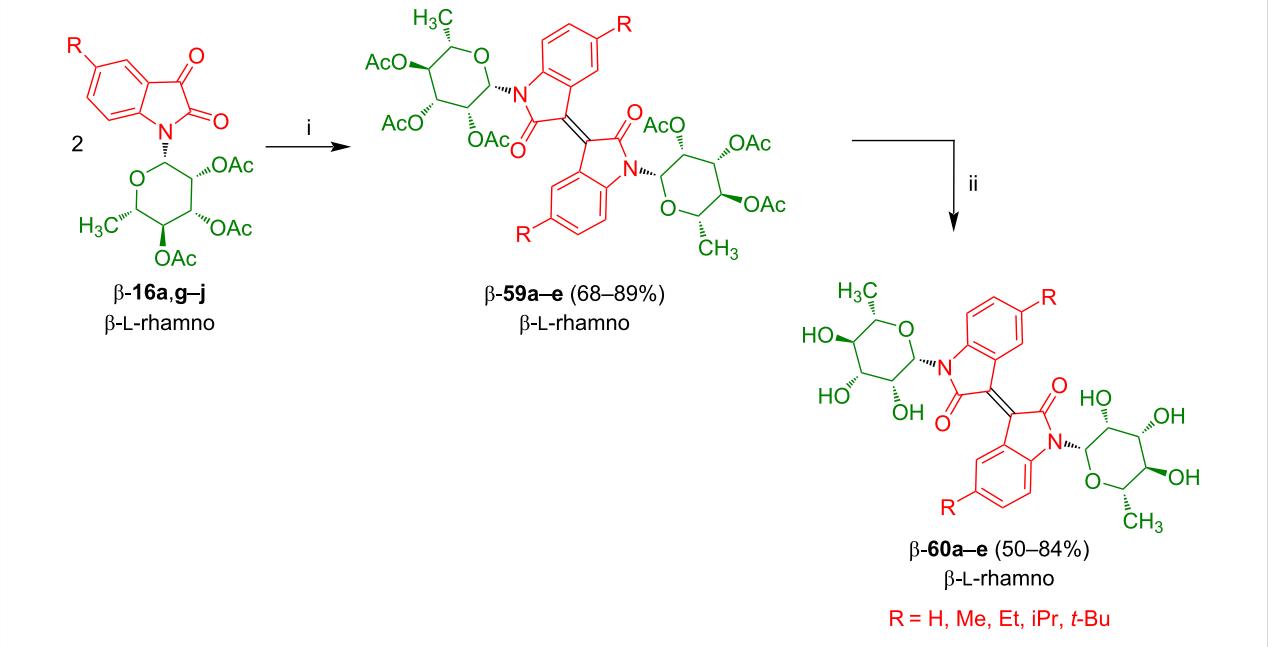

Scheme 36: Synthesis of **59a–e** and **60a–e**. Reagents and conditions: i) $P(NEt_2)_3$ (1.1 equiv), CH_2Cl_2, −78 °C to 25 °C; ii) NaOMe, MeOH (abs).

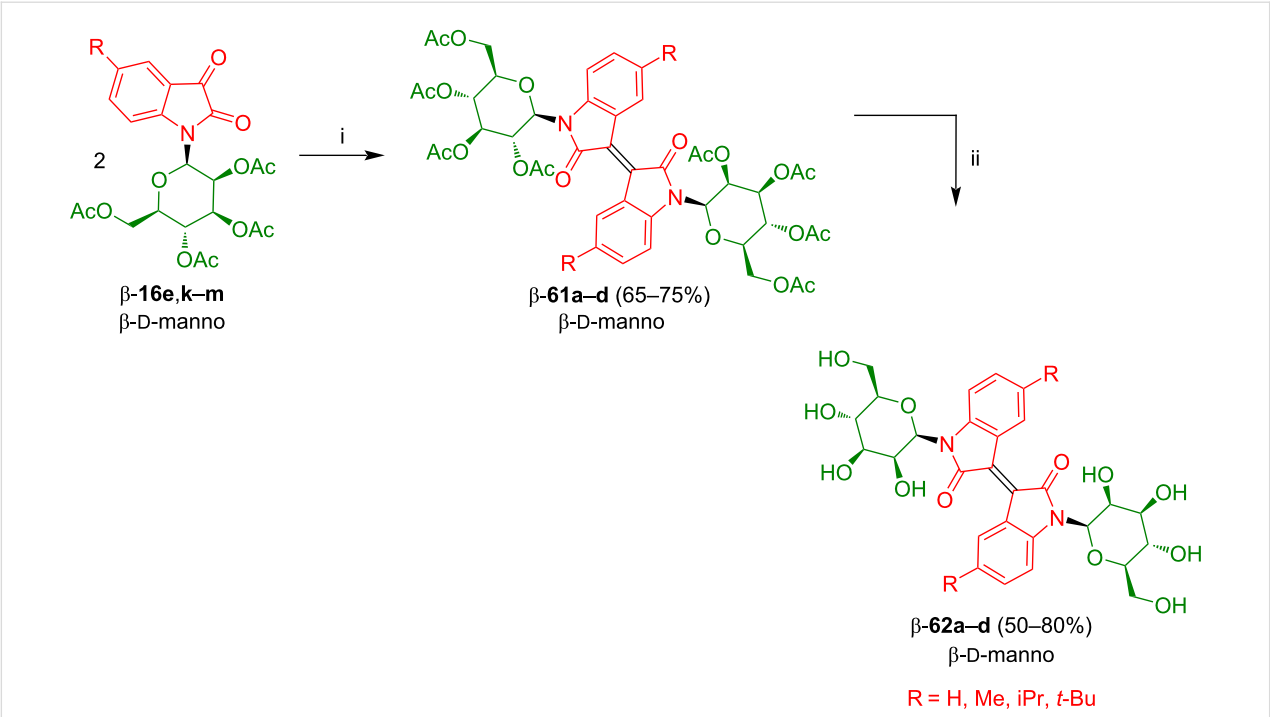

Scheme 37: Synthesis of **61a–d** and **62a–d**. Reagents and conditions: i) $P(NEt_2)_3$ (1.1 equiv), CH_2Cl_2, –78 °C to 25 °C; ii) NaOMe, MeOH (abs).

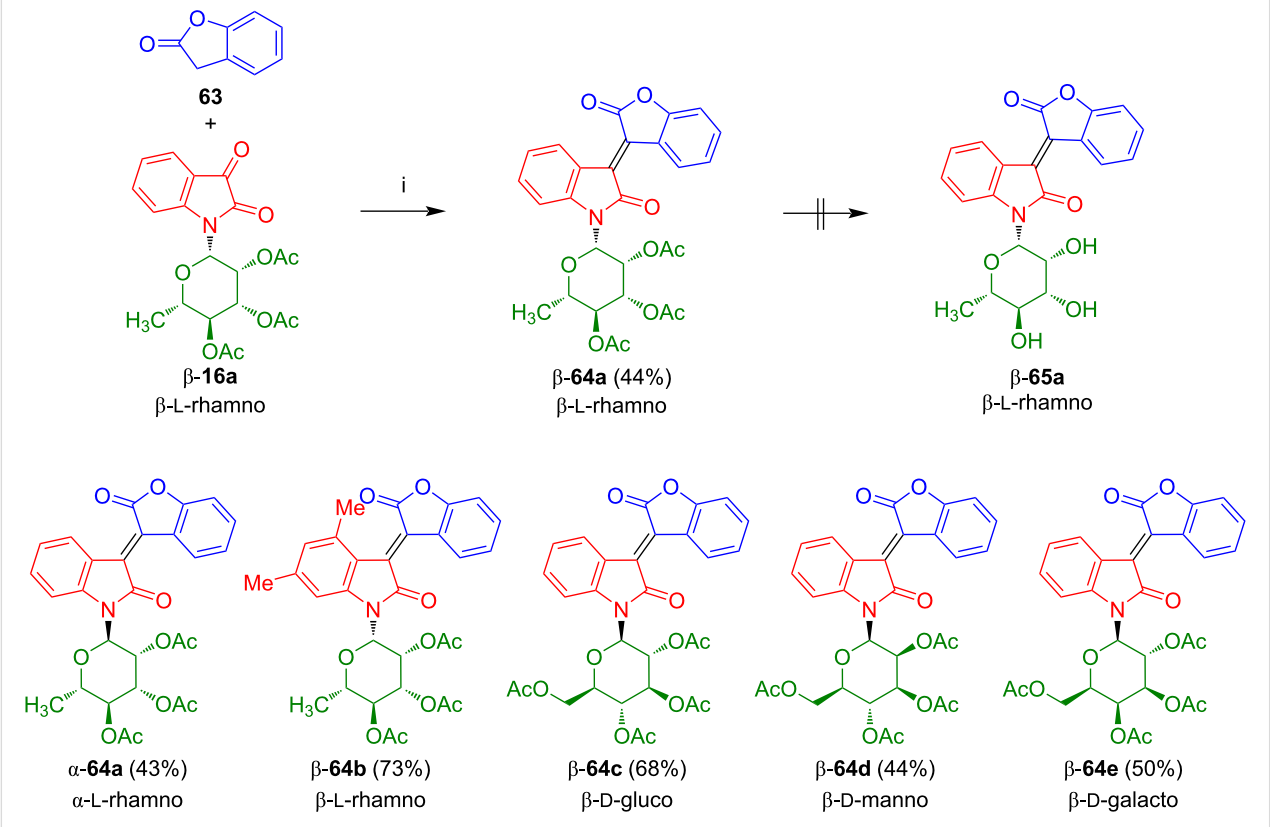

Scheme 38: Synthesis of β-**64a–e** and α-**64a**. Reagents and conditions: i) AcOH, Ac_2O, NaOAc, 90 °C, 6 h.

As a consequence, we decided to employ benzyl-protected isatin-*N*-rhamnoside β-**70** which was prepared in analogy to the method of Sassatelli reported for related isatin-*N*-glycosides [53-55]. The reaction of rhamnose with indoline (**66**) afforded β-**67a** which was transformed to indol-*N*-rhamnoside β-**68a** (Scheme 39) [59]. Benzylation and subsequent oxidation gave isatin-*N*-rhamnoside β-**70a**, albeit, in low yield. Condensation with 2-coumaranone (**63**) afforded the benzylated oxoisoindigo-*N*-rhamnoside β-**71a** which was successfully deprotected to give the desired product β-**72a**. It is worth to be noted that isatin-*N*-rhamnoside β-**70a** is not available by cyclization of the corresponding benzyl-protected aniline-*N*-rhamnoside with oxalyl chloride or by deacetylation of β-**16a** and subsequent benzylation.

Benzylation of indol-*N*-galactoside β-**68b** afforded β-**69b** which was oxidized to β-**70b** (Scheme 40) [60]. Condensation of the latter with 2-coumaranone (**63**) afforded oxoisoindigo-*N*-galactoside β-**71b** which was deprotected to give β-**72b**. The yields were comparable to those obtained for the corresponding rhamnosides.

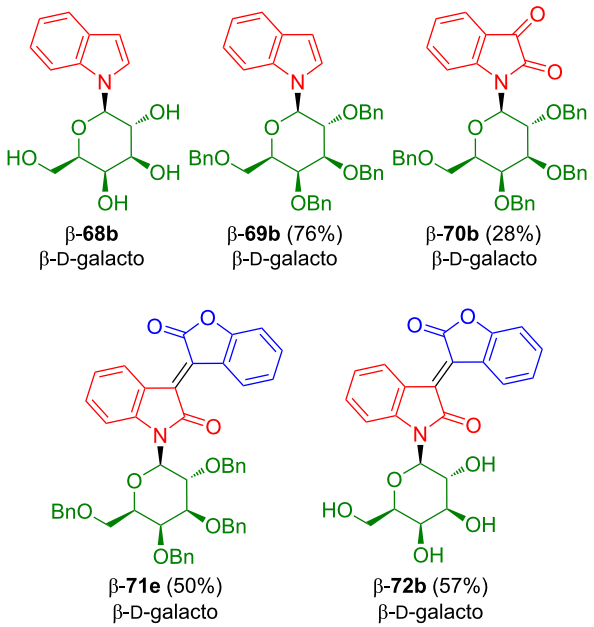

Scheme 40: Synthesis of β-**72b**.

Thioisoindigo-*N*-glycosides

The condensation of isatin-*N*-rhamnoside β-**16a** with 2,3-dihydrobenzo[*b*]thiophen-2-one (**73**), available in two steps from benzo[*b*]thiophene [61], afforded thioisoindigo-*N*-rhamnoside β-**74a** in 45% yield (Scheme 41) [60]. Like in the case of β-**64a**, deprotection proved to be unsuccessful, due to cleavage of the

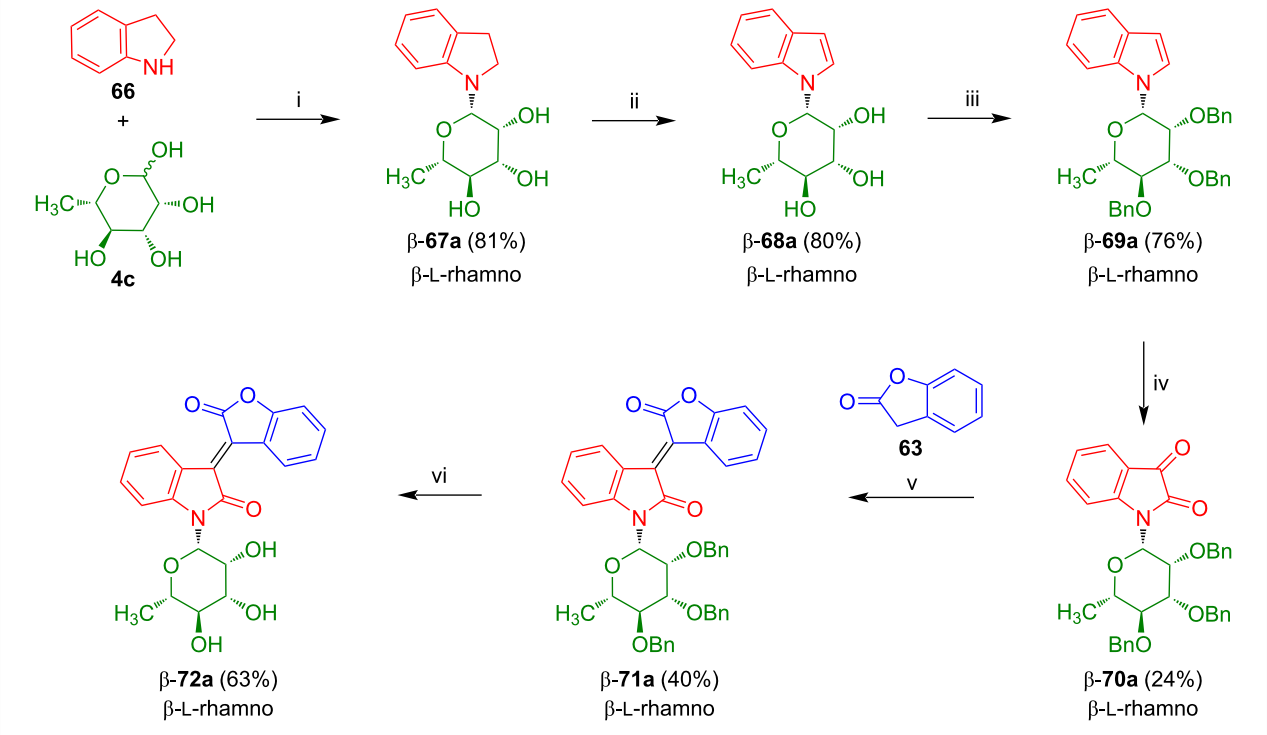

Scheme 39: Synthesis of β-**72a**. Reagents and conditions: i) **66**, EtOH, 20 °C, 12 h; ii) DDQ, dioxane, 20 °C, 12 h; iii) NaH, BnBr, DMF, 0 °C to 4 °C, 12 h; iv) CrO_3, acetone, AcOH, H_2O, 20 °C, 1.5 h; v) AcOH, Ac_2O, NaOAc, 90 °C, 2 h; vi) BBr_3, CH_2Cl_2, −78 °C, 2 h.

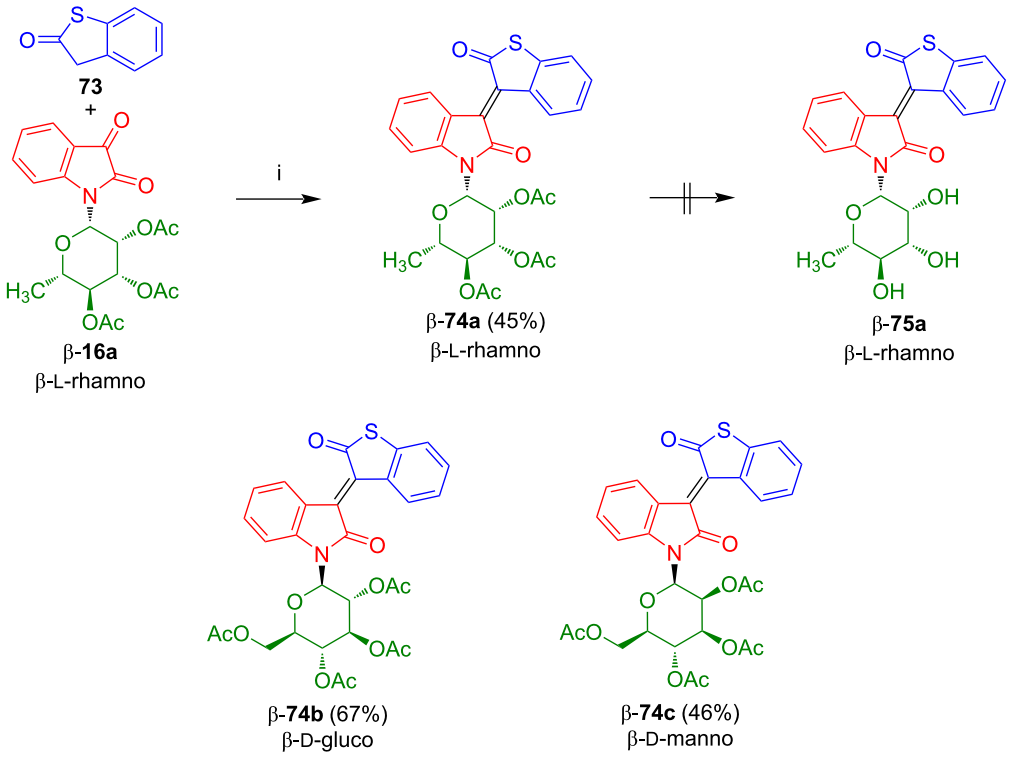

Scheme 41: Synthesis of β-**74a–c**. Reagents and conditions: i) AcOH, Ac_2O, NaOAc, 130 °C, 2 d.

lactone moiety. Starting from the respective isatin-*N*-glycosides, *N*-glucoside β-**74b** and *N*-mannoside β-**74c** were prepared.

Carboisoindigo-*N*-glycosides

The condensation of isatin-*N*-rhamnoside β-**16a** with indan-2-one (**76**) afforded carboisoindigo-*N*-rhamnoside β-**77** in 39% yield (Scheme 42) [60]. Despite the absence of a lactone moiety, deprotection proved to be unsuccessful, due to decomposition.

Miscelleaneous

6*H*-Indolo-[2,3-*b*]quinoxaline-*N*-glycosides

The cyclization of isatin-*N*-rhamnoside β-**16a** with 1,2-diaminobenzene (**79a**) afforded 6*H*-indolo-[2,3-*b*]quinoxaline-*N*-glycoside β-**80a** in 72% yield (Scheme 43) [62]. The first step, the condensation of the amine with the (more reactive) keto group of β-1**6a**, was carried out in glacial acetic acid (80 °C). Subsequent treatment with with *p*-toluenesulfonic acid (PTSA) resulted in cyclization via the lactam to give β-**80a**

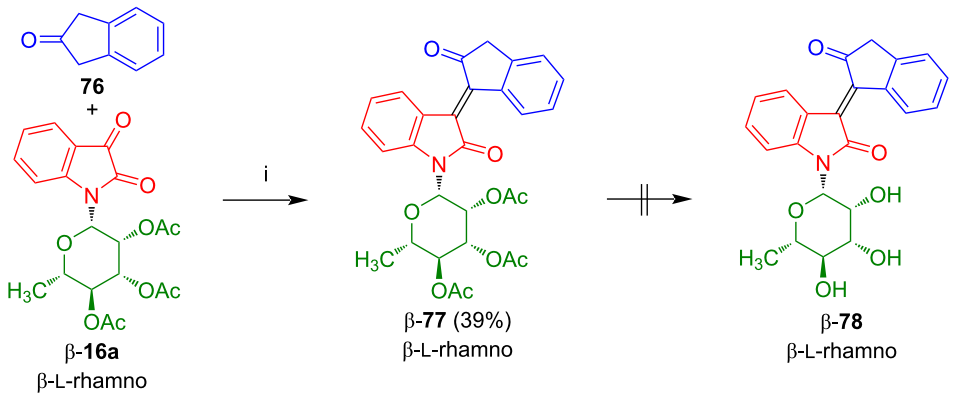

Scheme 42: Synthesis of β-**77**. Reagents and conditions: i) 1) NEt_3, EtOH, 20 °C, 12 h, 2) DMAP, NEt_3, MsCl, 0 °C to 20 °C, 20 h.

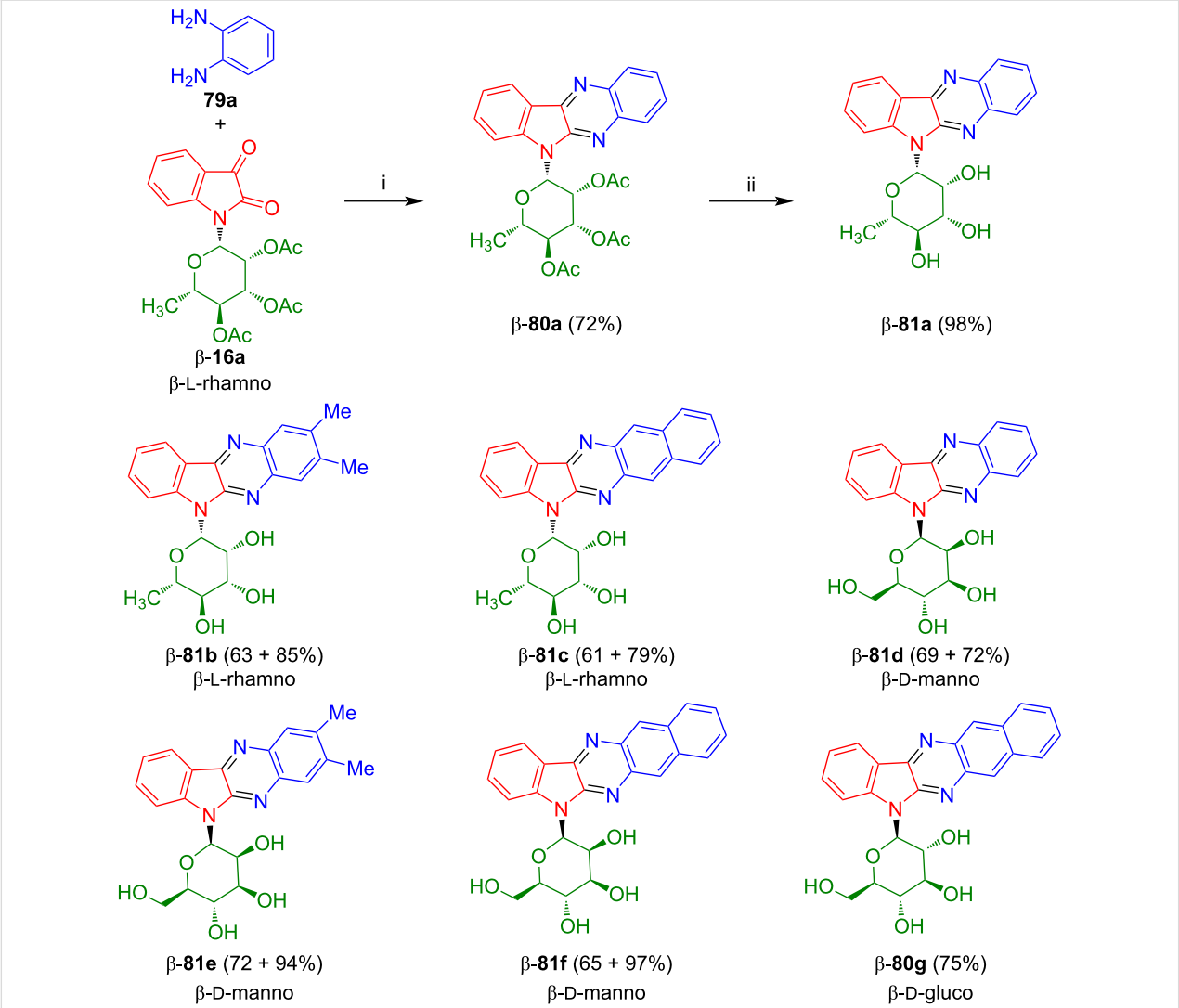

Scheme 43: Synthesis of β-**81a–f** and β-**80g**. Reagents and conditions: i) AcOH, 80 °C, 1–3 h; ii) benzene, PTSA, 80 °C, 1–3 h; iii) NaOMe, MeOH, 7 h, 20 °C. The yields of **81b–f** refer to the yields of the cyclocondensation and the deprotection step for each compound.

which upon deprotection with NaOMe afforded β-**81a** in 98% yield. Likewise, rhamnosides β-**81b**,**c** mannosides β-**81d–f**, and glucoside **β-80g** were obtained in good yields. Some products exhibited weak cytotoxic activity against human ceratinocytes (HaCaT). However, in contrast to many indirubin-*N*-glycosides and their analogues described above, glycosides **81** were inactive against cancer and melanoma cell lines.

3,3-Diaryloxindole-*N*-glycosides

The Friedel–Crafts acylation of isatin-*N*-rhamnoside β-**16a** with benzene (**82a**) afforded 3,3-diphenyloxindole-*N*-rhamnoside β-**83a** in 94% yield (Scheme 44) [63]. Deprotection of the latter afforded β-**84a** in 88% yield.

Friedel–Crafts acylation of isatin-*N*-glycosides β-**16c–e** with benzene, toluene, anisole, and *N*,*N*-dimethylaniline and subsequent deprotection afforded 3,3-diaryloxindole-*N*-glycosides β-**84b–l** (Scheme 45) [63]. Some of the products showed antiproliferative activity against malignant cutaneous melanoma cells HT-144 (ATCC HTB-63) and lung carcinoma (H157) cell line (ATCC CRL-5802).

Conclusion

Since the 1990s, we are witnessing a renaissance of the chemistry of the old pigment dyes indigo, indirubin, and isoindigo, due to their anticancer activity which dates back to early observations made in the context of ethno-pharmacy. The present article provides an account on the synthesis and cancerostatic activity of *N*-glycosides of indigo, indirubin, and isoindigo which can be, in fact, regarded as blue, red, and yellow sugars. While specific non-glycosylated indirubin derivatives, such as indirubin-3'-monoxime, already show a good activity against

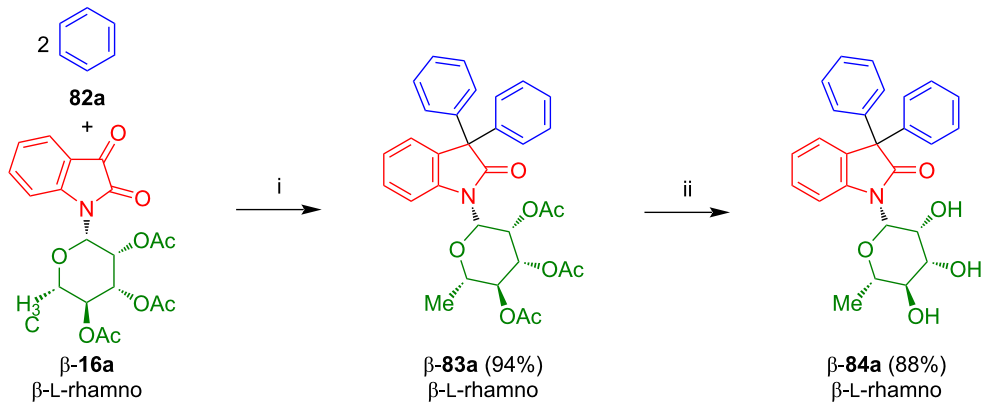

Scheme 44: Synthesis of **84a**. Reagents and conditions: i) benzene, $AlCl_3$, 20 °C, 10 min; ii) MeOH, NaOMe, 12 h, 20 °C.

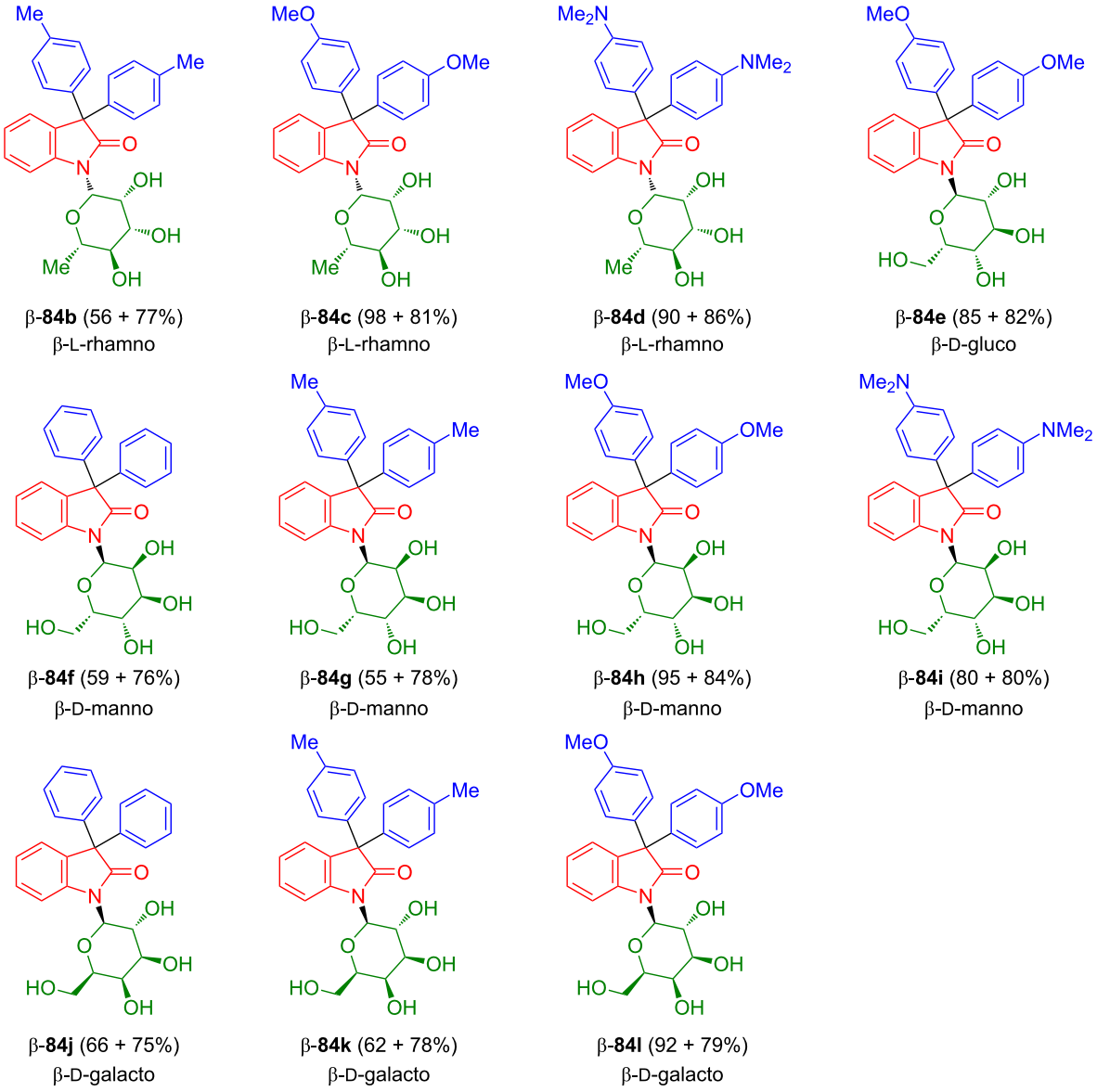

Scheme 45: Synthesis of **84b–l**. The yields refer to the yields of the condensation and the deprotection step for each compound.

various human cancer cell lines, the presence of a carbohydrate unit attached to the amide-type nitrogen atom of the indirubin moiety results in a dramatic increase of the activity. This might be due to an improved bioavailability by an improved water solubility or ability to pass the cell membrane or by an improved recognition of the drug in the active site of the receptor. In contrast to indirubin-*N*-glycosides, indigo-*N*-glycosides are relatively unstable and not highly active against cancer, except for the natural products akashins A–C. The best activity, especially against melanoma cells, was observed for thioindigo-*N*-glycosides. The activity is improved by the action of cold plasma. 3-Alkylideneoxindole-*N*-glycososides, structurally related to indirubin-*N*-glycosides, trigger apoptosis in melanoma cells, which is enhanced by the combination with TRAIL. In conclusion, indirubin-*N*-glycosides and their analogues exhibit the highest anticancer activity observed so far for indirubin derivatives. Future studies are directed to a modification of the isatin moiety of the products for which improved syntheses have been recently developed.

Acknowledgements

I am very grateful to my co-workers who contributed to the work included in this account article. These are (in alphabetical order): Drs Martin Becker, Christoph Cordes, Katrin Dyballa (née Driller), Friedrich Erben, Martin Hein, Dennis Kleeblatt, Philipp Lebrenz, Stefanie Libnow. I am also very grateful to my colleagues Profs. Patrick Bednarski, Jürgen Eberle, Steffen Emmert, Burkhard Hinz, Jamshed Iqbal, Manfred Kunz, Michael Lalk for the excellent collaboration with regard to the pharmacological studies.

Funding

I am grateful to the joint research project "ONKOTHER-H" which is supported by the European Social Fund (ESF), reference: ESF/14-BM-A55-0001/18, ESF/14-BM-A55-0002/18, ESF/14-BM-A55-0003/18, ESF/14-BMA55-0004/18, ESF/14-BM-A55-0005/18, ESF/14-BM-A55-0006/18, and the Ministry of Education, Science and Culture of Mecklenburg-Vorpommern, Germany.

Data Availability Statement

Data sharing is not applicable as no new data was generated or analyzed in this study.

References

1. Kaplan, G.; Seferoğlu, Z.; Berdnikova, D. V. *Beilstein J. Org. Chem.* **2024,** *20,* 228–242. doi:10.3762/bjoc.20.23
2. Kaplan, G.; Seferoğlu, Z. *Curr. Org. Synth.* **2023,** *20,* 361–364. doi:10.2174/1570179419666220830091956
3. Huang, C.-Y.; Hecht, S. *Chem. – Eur. J.* **2023,** *29,* e202300981. doi:10.1002/chem.202301808
4. Karapanagiotis, I. *Sustainability* **2019,** *11,* 3595. doi:10.3390/su11133595
5. Sun, Q.; Leng, J.; Tang, L.; Wang, L.; Fu, C. *Front. Pharmacol.* **2021,** *12,* 664022. doi:10.3389/fphar.2021.664022
6. Xiao, Z.; Hao, Y.; Liu, B.; Qian, L. *Leuk. Lymphoma* **2002,** *43,* 1763–1768. doi:10.1080/1042819021000006295
7. Iwaki, K.; Kurimoto, M. *Recent Res. Dev. Cancer* **2002,** *4,* 429–437.
8. Yang, L.; Li, X.; Huang, W.; Rao, X.; Lai, Y. *Biomed. Pharmacother.* **2022,** *151,* 113112. doi:10.1016/j.biopha.2022.113112
9. Wang, H.; Wang, Z.; Wei, C.; Wang, J.; Xu, Y.; Bai, G.; Yao, Q.; Zhang, L.; Chen, Y. *Eur. J. Med. Chem.* **2021,** *223,* 113652. doi:10.1016/j.ejmech.2021.113652
10. Schäfer, M.; Semmler, M. L.; Bernhardt, T.; Fischer, T.; Kakkassery, V.; Ramer, R.; Hein, M.; Bekeschus, S.; Langer, P.; Hinz, B.; Emmert, S.; Boeckmann, L. *Cancers* **2021,** *13,* 1770. doi:10.3390/cancers13081770
11. Moon, M. J.; Lee, S. K.; Lee, J.-W.; Song, W. K.; Kim, S. W.; Kim, J. I.; Cho, C.; Choi, S. J.; Kim, Y.-C. *Bioorg. Med. Chem.* **2006,** *14,* 237–246. doi:10.1016/j.bmc.2005.08.008
12. Bogdanov, A. V.; Mironov, V. F. *Beilstein J. Org. Chem.* **2021,** *17,* 1533–1564. doi:10.3762/bjoc.17.111
13. Deng, P.; Zhang, Q. *Polym. Chem.* **2014,** *5,* 3298–3305. doi:10.1039/c3py01598j
14. Huang, M.; Lin, H.-S.; Lee, Y. S.; Ho, P. C. *Int. J. Oncol.* **2014,** *45,* 1724–1734. doi:10.3892/ijo.2014.2548
15. Bogdanov, A. V.; Musin, L. I.; Mironov, V. F. *ARKIVOC* **2015,** No. vi, 362–392. doi:10.3998/ark.5550190.p009.090
16. Karapetyan, G.; Chakrabarty, K.; Hein, M.; Langer, P. *ChemMedChem* **2011,** *6,* 25–37. doi:10.1002/cmdc.201000374
17. Maskey, R. P.; Grün-Wollny, I.; Fiebig, H. H.; Laatsch, H. *Angew. Chem., Int. Ed.* **2002,** *41,* 597–599. doi:10.1002/1521-3773(20020215)41:4<597::aid-anie597>3.0.co;2-z *Angew. Chem.* **2002,** *114,* 623–625. doi:10.1002/1521-3757(20020215)114:4<623::AID-ANGE623>3.0.CO;2-M
18. Maskey, R. P.; Grün-Wollny, I.; Laatsch, H. *Nat. Prod. Res.* **2005,** *19,* 137–142. doi:10.1080/14786410410001704741
19. Hein, M.; Michalik, D.; Langer, P. *Synthesis* **2005,** 3531–3534. doi:10.1055/s-2005-918489
20. Pfretzschner, A. T.; Unverzagt, C. *ARKIVOC* **2021,** No. iv, 206–229. doi:10.24820/ark.5550190.p011.380
21. Hein, M.; Phuong, N. T. B.; Michalik, D.; Görls, H.; Lalk, M.; Langer, P. *Tetrahedron Lett.* **2006,** *47,* 5741–5745. doi:10.1016/j.tetlet.2006.06.021
22. Libnow, S.; Hein, M.; Michalik, D.; Langer, P. *Tetrahedron Lett.* **2006,** *47,* 6907–6909. doi:10.1016/j.tetlet.2006.07.024
23. Libnow, S.; Methling, K.; Hein, M.; Michalik, D.; Harms, M.; Wende, K.; Flemming, A.; Köckerling, M.; Reinke, H.; Bednarski, P. J.; Lalk, M.; Langer, P. *Bioorg. Med. Chem.* **2008,** *16,* 5570–5583. doi:10.1016/j.bmc.2008.04.003
24. Stiller, T.; Hein, M.; Langer, P., unpublished results.
25. Libnow, S.; Hein, M.; Langer, P. *Synlett* **2009,** 221–224. doi:10.1055/s-0028-1087394
26. Kunz, M.; Driller, K. M.; Hein, M.; Libnow, S.; Hohensee, I.; Ramer, R.; Hinz, B.; Berger, A.; Eberle, J.; Langer, P. *ChemMedChem* **2010,** *5,* 534–539. doi:10.1002/cmdc.200900506

27. Eberle, J.; Spangler, B.; Becker, J. C.; Heinemann, S. H.; Klein, C. A.; Kunz, M.; Kuphal, S.; Langer, P.; Mauch, C.; Meierjohann, S.; Paschen, A.; Schadendorf, D.; Schartl, M.; Schittek, B.; Schönherr, R.; Tüting, T.; Zigrino, P.; Bosserhoff, A. K. *Pigm. Cell Melanoma Res.* **2010,** *23,* 296–298. doi:10.1111/j.1755-148x.2010.00684.x
28. Lo, W.-Y.; Chang, N.-W. *PLoS One* **2013,** *8,* e70198. doi:10.1371/journal.pone.0070198
29. Shishkin, O. V.; Omelchenko, I. V.; Kalyuzhny, A. L.; Paponov, B. V. *Struct. Chem.* **2010,** *21,* 1005–1011. doi:10.1007/s11224-010-9638-2
30. Fischle, A.; Schwarz, R.; Wendt, F.; Kordt, M.; Ramer, R.; Boeckmann, L.; Hein, M.; Langer, P.; Emmert, S.; Vollmar, B.; Hinz, B. *Molecules* **2022,** *27,* 3031. doi:10.3390/molecules27093031
31. Wendt, F.; Wittig, F.; Rupprecht, A.; Ramer, R.; Langer, P.; Emmert, S.; Frank, M.; Hinz, B. *Cells* **2023,** *12,* 2409. doi:10.3390/cells12192409
32. Rebl, H.; Sawade, M.; Hein, M.; Bergemann, C.; Wende, M.; Lalk, M.; Langer, P.; Emmert, S.; Nebe, B. *Sci. Rep.* **2022,** *12,* 2528. doi:10.1038/s41598-022-06523-x
33. Berner, J.; Bekeschus, S.; Langer, P.; Hein, M. *Jpn. J. Appl. Phys.* **2023,** *62,* SA1006. doi:10.35848/1347-4065/ac78c0
34. Boeckmann, L.; Berner, J.; Kordt, M.; Lenz, E.; Schäfer, M.; Semmler, M.-L.; Frey, A.; Sagwal, S.; Rebl, H.; Miebach, L.; Niessner, F.; Sawade, M.; Hein, M.; Ramer, R.; Grambow, E.; Seebauer, C.; von Woedtke, T.; Nebe, B.; Metelmann, H.-R.; Langer, P.; Hinz, B.; Vollmar, B.; Emmert, S.; Bekeschus, S. *J. Adv. Res.* **2024,** *57,* 181–196. doi:10.1016/j.jare.2023.06.014
35. Magdesieva, N. N.; Vdovin, V. A. *Chem. Heterocycl. Compd.* **1970,** *6,* 1375–1379. doi:10.1007/bf00476776
36. Lohner, W.; Praefcke, K. *J. Organomet. Chem.* **1980,** *194,* 173–178. doi:10.1016/s0022-328x(00)86666-8
37. Muth, B. R.; Kiss, A. I. *J. Org. Chem.* **1956,** *21,* 576–578. doi:10.1021/jo01111a600
38. Erben, F.; Kleeblatt, D.; Sonneck, M.; Hein, M.; Feist, H.; Fahrenwaldt, T.; Fischer, C.; Matin, A.; Iqbal, J.; Plötz, M.; Eberle, J.; Langer, P. *Org. Biomol. Chem.* **2013,** *11,* 3963–3978. doi:10.1039/c3ob40603b
39. Dyballa, K. M.; Libnow, S.; Hein, M.; Langer, P. *Tetrahedron Lett.* **2024,** *144,* 155151. doi:10.1016/j.tetlet.2024.155151
40. Evdokimov, N. M.; Magedov, I. V.; McBrayer, D.; Kornienko, A. *Bioorg. Med. Chem. Lett.* **2016,** *26,* 1558–1560. doi:10.1016/j.bmcl.2016.02.015
41. Libnow, S.; Hein, M.; Langer, P., to be submitted.
42. Millemaggi, A.; Taylor, R. J. K. *Eur. J. Org. Chem.* **2010,** 4527–4547. doi:10.1002/ejoc.201000643
43. Dhokne, P.; Sakla, A. P.; Shankaraiah, N. *Eur. J. Med. Chem.* **2021,** *216,* 113334. doi:10.1016/j.ejmech.2021.113334
44. Soam, P.; Mandal, D.; Tyagi, V. *J. Org. Chem.* **2023,** *88,* 11023–11035. doi:10.1021/acs.joc.3c00994
And references cited therein.
45. Lin, W.-J.; Shia, K.-S.; Song, J.-S.; Wu, M.-H.; Li, W.-T. *Org. Biomol. Chem.* **2016,** *14,* 220–228. doi:10.1039/c5ob01863c
46. Girgis, A. S.; Panda, S. S.; Srour, A. M.; Abdelnaser, A.; Nasr, S.; Moatasim, Y.; Kutkat, O.; El Taweel, A.; Kandeil, A.; Mostafa, A.; Ali, M. A.; Fawzy, N. G.; Bekheit, M. S.; Shalaby, E. M.; Gigli, L.; Fayad, W.; Soliman, A. A. F. *Bioorg. Chem.* **2021,** *114,* 105131. doi:10.1016/j.bioorg.2021.105131
47. Kleeblatt, D.; Becker, M.; Plötz, M.; Schönherr, M.; Villinger, A.; Hein, M.; Eberle, J.; Kunz, M.; Rahman, Q.; Langer, P. *RSC Adv.* **2015,** *5,* 20769–20782. doi:10.1039/c4ra14301a
48. Berger, A.; Quast, S.-A.; Plötz, M.; Hein, M.; Kunz, M.; Langer, P.; Eberle, J. *Biochem. Pharmacol.* **2011,** *81,* 71–81. doi:10.1016/j.bcp.2010.09.010
49. Zhivkova, V.; Kiecker, F.; Langer, P.; Eberle, J. *Mol. Carcinog.* **2019,** *58,* 258–269. doi:10.1002/mc.22924
50. Zhu, J.; Langer, P.; Ulrich, C.; Eberle, J. *Antioxidants* **2021,** *10,* 1514. doi:10.3390/antiox10101514
51. Erben, F.; Michalik, D.; Feist, H.; Kleeblatt, D.; Hein, M.; Matin, A.; Iqbal, J.; Langer, P. *RSC Adv.* **2014,** *4,* 10879–10893. doi:10.1039/c3ra44362k
52. Soltan, M. Y.; Sumarni, U.; Assaf, C.; Langer, P.; Reidel, U.; Eberle, J. *Int. J. Mol. Sci.* **2019,** *20,* 1158. doi:10.3390/ijms20051158
53. Sassatelli, M.; Saab, E.; Anizon, F.; Prudhomme, M.; Moreau, P. *Tetrahedron Lett.* **2004,** *45,* 4827–4830. doi:10.1016/j.tetlet.2004.04.167
54. Sassatelli, M.; Bouchikhi, F.; Messaoudi, S.; Anizon, F.; Debiton, E.; Barthomeuf, C.; Prudhomme, M.; Moreau, P. *Eur. J. Med. Chem.* **2006,** *41,* 88–100. doi:10.1016/j.ejmech.2005.10.004
55. Sassatelli, M.; Bouchikhi, F.; Aboab, B.; Anizon, F.; Fabbro, D.; Prudhomme, M.; Moreau, P. *Anti-Cancer Drugs* **2007,** *18,* 1069–1074. doi:10.1097/cad.0b013e328182d281
56. Bouchikhi, F.; Anizon, F.; Moreau, P. *Eur. J. Med. Chem.* **2008,** *43,* 755–762. doi:10.1016/j.ejmech.2007.05.012
57. Bouchikhi, F.; Anizon, F.; Moreau, P. *Eur. J. Med. Chem.* **2009,** *44,* 2705–2710. doi:10.1016/j.ejmech.2009.01.027
58. Kleeblatt, D.; Siyo, B.; Hein, M.; Iaroshenko, V. O.; Iqbal, J.; Villinger, A.; Langer, P. *Org. Biomol. Chem.* **2013,** *11,* 886–895. doi:10.1039/c2ob25866h
59. Libnow, S.; Hein, M.; Langer, P. *Tetrahedron Lett.* **2008,** *49,* 289–291. doi:10.1016/j.tetlet.2007.11.057
60. Libnow, S.; Becker, M.; Hein, M.; Langer, P., unpublished results.
61. Bordwell, F. G.; Fried, H. E. *J. Org. Chem.* **1991,** *56,* 4218–4223. doi:10.1021/jo00013a027
62. Driller, K. M.; Libnow, S.; Hein, M.; Harms, M.; Wende, K.; Lalk, M.; Michalik, D.; Reinke, H.; Langer, P. *Org. Biomol. Chem.* **2008,** *6,* 4218–4223. doi:10.1039/b812308j
63. Kleeblatt, D.; Cordes, C. A.; Lebrenz, P.; Hein, M.; Feist, H.; Matin, A.; Raza, R.; Iqbal, J.; Munshi, O.; Rahman, Q.; Villinger, A.; Langer, P. *RSC Adv.* **2014,** *4,* 22828–22839. doi:10.1039/c4ra02627f

License and Terms

This is an open access article licensed under the terms of the Beilstein-Institut Open Access License Agreement (https://www.beilstein-journals.org/bjoc/terms), which is identical to the Creative Commons Attribution 4.0 International License (https://creativecommons.org/licenses/by/4.0). The reuse of material under this license requires that the author(s), source and license are credited. Third-party material in this article could be subject to other licenses (typically indicated in the credit line), and in this case, users are required to obtain permission from the license holder to reuse the material.

The definitive version of this article is the electronic one which can be found at:
https://doi.org/10.3762/bjoc.20.240

BEILSTEIN JOURNAL OF ORGANIC CHEMISTRY

Synthesis of pyrrole-fused dibenzoxazepine/dibenzothiazepine/triazolobenzodiazepine derivatives via isocyanide-based multicomponent reactions

Marzieh Norouzi[1], Mohammad Taghi Nazeri[*1], Ahmad Shaabani[*1,§] and Behrouz Notash[2]

Full Research Paper

Open Access

Address:
[1]Department of Organic Chemistry, Shahid Beheshti University, Daneshjou Boulevard, Tehran, 1983969411, Iran and [2]Department of Inorganic Chemistry, Shahid Beheshti University, Daneshjou Boulevard, Tehran, 1983969411, Iran

Email:
Mohammad Taghi Nazeri[*] - mt_nazeri@sbu.ac.ir; Ahmad Shaabani[*] - a-shaabani@sbu.ac.ir

* Corresponding author
§ Phone: +982129902800

Keywords:
cyclic imines; dibenzothiazepine; dibenzoxazepine; isocyanides; multicomponent reactions; pyrrole; triazolobenzodiazepine

Beilstein J. Org. Chem. **2024,** *20,* 2870–2882.
https://doi.org/10.3762/bjoc.20.241

Received: 05 August 2024
Accepted: 22 October 2024
Published: 11 November 2024

This article is part of the thematic issue "Multicomponent reactions IV".

Associate Editor: T. J. J. Müller

© 2024 Norouzi et al.; licensee Beilstein-Institut.
License and terms: see end of document.

Abstract

An efficient and facile synthesis of pyrrole-fused dibenzoxazepine/dibenzothiazepine/triazolobenzodiazepine derivatives was developed through the isocyanide-based multicomponent reaction of isocyanides, *gem*-diactivated olefins, and cyclic imines such as dibenzoxazepine, dibenzothiazepine, and triazolobenzodiazepine under solvent- and catalyst-free conditions. Purposefully, this approach produced various bioactive scaffolds using environmentally friendly, mild, and simple conditions. Due to their bioactive moieties, these compounds with exclusive fluorescence properties may attract great attention in biomedical applications, clinical diagnostics, and conjugate materials.

Introduction

Pyrroles and their derivatives are important *N*-heterocyclic compounds with antibiotic, antiviral, and anticancer properties that are found in many drugs and natural products [1-6]. Pyrroles' biological properties manifest when they are fused to other heterocycles [7-12]. Among them, seven-membered heterocycles of the benzodiazepine, benzoxazepine, and benzothiazepine derivatives are especially important. These consitute the central core of many natural and biological compounds and commercial drugs, including diazepam, clonazepam, lorazepam, telenzepine, chlordiazepoxide, loxapine,

and amoxapine [13-21]. Pyrrole-fused benzodiazepines, benzoxazepines, or benzothiazepines exhibit unique biological and pharmacological properties [22,23]. For example, midazolam is a hypnotic-sedative drug with anxiolytic, muscle relaxant, and anticonvulsant properties [24], flumazenil is made to induce general anesthesia for diagnostic and therapeutic procedures [25] or PBOX-6 is a drug for the treatment of depression [26]. Benzothiazepines are known as antidepressants and are molecules with interesting electronic properties (Figure 1) [27]. Accordingly, the synthesis of new derivatives of pyrrole-fused benzodiazepine/benzoxazepine/benzothiazepine is very important.

Due to the wide applications of pyrrole-fused heterocycles, very diverse approaches have been developed for their synthesis [28-32]. In recent years, multicomponent reactions (MCRs) have emerged as one of the most efficient and powerful methods to achieve this goal [7,33]. Among them, isocyanide-based multicomponent reactions (I-MCRs) are one of the well-known strategies in this field due to their operational simplicity, one-pot, convergent properties and atom economy, high efficiency, and high levels of chemical selectivity [34-36]. In addition to the application of isocyanides in a variety of MCRs, one of the unique reactions involves the formation of zwitterions from isocyanides upon reaction with acetylene and active olefin compounds such as alkyl acetylenedicarboxylates and *gem*-diactivated olefins. Due to having nucleophilic and electrophilic sites simultaneously in their structure, these zwitterions are able to participate in various cyclization processes, especially for the synthesis of pyrroles [37-40]. For example, Li et al. developed a one-pot four-component reaction (4-CR) of malononitrile, aldehydes, and isocyanides with 1,10-phenanthroline as cyclic imine under solvent-free conditions for the synthesis of pyrrole-fused phenanthroline. This reaction proceeds via in situ formation of zwitterion **I** through reaction of the aldehyde and malononitrile followed by 1,3-dipolar cycloaddition (Scheme 1a) [41]. Chen and co-workers reported a one-pot three-component reaction (3-CR) of sulfamate-derived cyclic imine, isocyanide, and acetylenedicarboxylate. In this reaction too, the pyrrole-fused sulfamate is synthesized through intermediacy of the in situ-formed zwitterion **II** and [1 + 2 + 2] annulation reaction (Scheme 1b) [42,43]. Another I-MCR for forming pyrroles is the in situ formation reaction of the zwitterion **III**, known as Huisgens 1,4-dipole. The latter is formed by the reaction of imines with acetylenedicarboxylates and can be trapped by an isocyanide through a [4 + 1] cyclization reaction to synthesize pyrroles. In our recent studies, we prepared pyrrole-fused dibenzoxazepines via an Ugi reaction. Here, the reaction of benzoxazepine imine and acetylenedicarboxylate leads to the Huisgens 1,4-dipole zwitterion in situ, which is trapped by an isocyanide through the cyclization process (Scheme 1c) [44,45].

Here, we report an efficient and facile approach for the synthesis of pyrrole-fused dibenzoxazepine, dibenzothiazepine, and triazolobenzodiazepine derivatives via I-MCRs of *gem*-diactivated olefins, isocyanides, and cyclic imines (dibenzoxazepines, benzothiazepine, and triazolobenzodiazepine) under solvent- and catalyst-free conditions (Scheme 1d).

Results and Discussion

Synthesis

Dibenzoxazepine as imine component, cyclohexyl isocyanide, and the *gem*-diactivated olefin (2-benzylidenemalononitrile) were selected as the starting materials to screen the reaction conditions (Scheme 2, Table 1). First, we investigated the reaction in dichloromethane at room temperature and at 40 °C (Table 1, entries 1 and 2) and we found that the reaction progressed slightly at 40 °C. This promising result prompet us to examine the reaction in multiple anhydrous solvents such as CH_3CN, toluene, EtOH, THF, EtOAc, and DMF at different temperatures (Table 1, entries 3–9). The result obtained from the study of solvents showed that pyrrole-fused dibenzoxazepine **4a** was obtained with a yield of 56% in ethanol as solvent at a temperature of 78 °C (Table 1, entry 4). To achieve a higher yield of product **4a**, the reaction was also attempted under solvent-free conditions at different temperatures (Table 1,

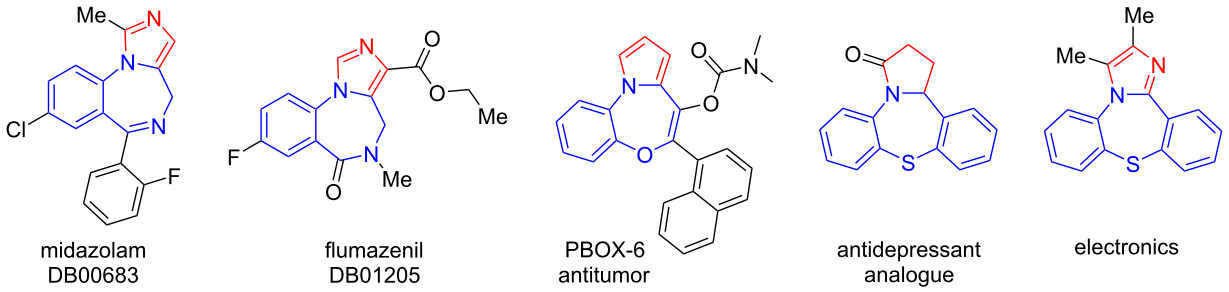

Figure 1: Representation of distinguished structures of benzodiazepine/benzoxazepine/benzothiazepine with pharmaceutical to electronic applications.

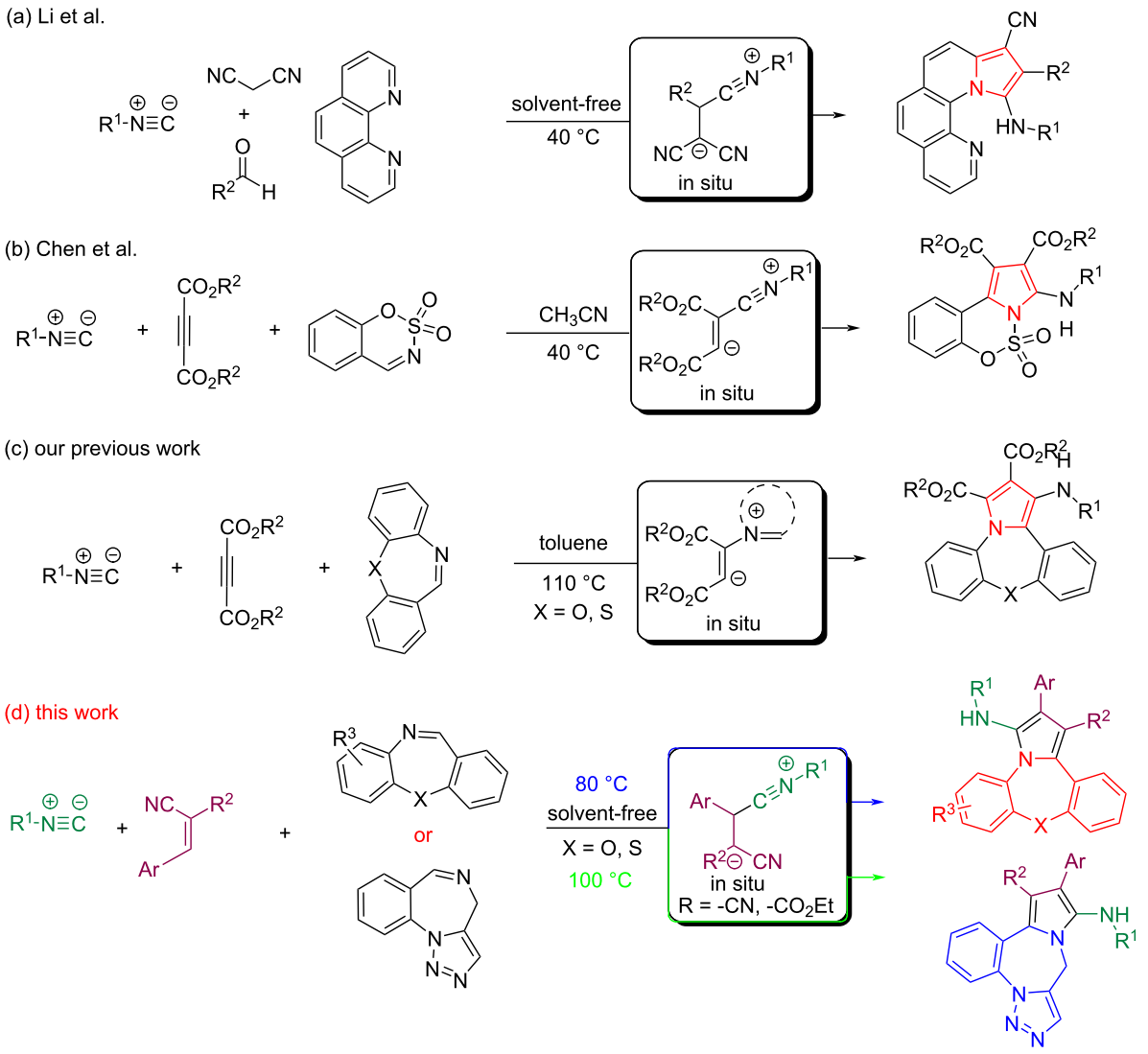

Scheme 1: Methods for the construction of pyrrole-fused heterocycles through I-MCR reactions.

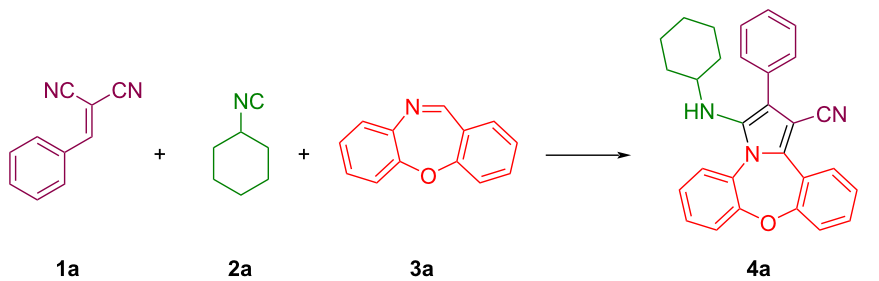

Scheme 2: The model reaction of dibenzoxazepine, *gem*-diactivated olefin (2-benzylidenemalononitrile), and cyclohexyl isocyanide.

entries 10–13). Interestingly, the highest yield of 70% of the desired product was achieved by conducting the reaction at 100 °C without using any solvent (Table 1, entry 12).

After having identified the optimal conditions, we next studied the scope of this reaction with substituted benzoxazepines, *gem*-diactivated olefins, and isocyanide derivatives (Scheme 3). As

Table 1: Optimization of the reaction conditions.[a]

Entry	Solvent	Temperature (°C)	Time (h)	Yield[b] (%)
1	CH_2Cl_2	25	24	0
2	CH_2Cl_2	40	24	23
3	CH_3CN	82	24	36
4	EtOH	78	24	56
5	toluene	110	24	33
6	THF	66	24	41
7	H_2O	100	24	trace
8	EtOAc	77	24	22
9	DMF	140	24	38
10	solvent-free	25	24	0
11	solvent-free	80	2	61
12	solvent-free	100	2	70
13	solvent-free	120	2	70

[a]Reaction conditions: **1a** (0.55 mmol), **2a** (0.55 mmol), and **3a** (0.50 mmol) were stirred in 2 mL of solvent in an oil bath at different temperatures and times. [b]Isolated yields.

illustrated in Scheme 3, both electron-donating (-Me, -OMe) and electron-withdrawing (-NO_2, Cl, and Br) groups were well tolerated under the optimal reaction conditions giving the products **4** in yields ranging from 68% to 87% (Scheme 3, **4a–l**). In this reaction, the presence of electron-withdrawing substituents in the aromatic rings of the *gem*-diactivated olefins led to slightly better yields of the products **4** when compared to the substrates having electron-donating substituents (Scheme 3). The cause of this phenomenon is probably related to the electron-widthdawing effect of these substitution groups in olefin, which affects the nucleophilic attack of the isocyanides. When a carboxylate substituent was present instead of the carbonitrile in the *gem*-diactivated olefins, the desired products were also obtained in good yields (Scheme 3, **4k** and **4l**). On the other hand, the presence of electron-donating and electron-withdrawing substitutions in the dibenzoxazepine core were also investigated and it was observed, that electron-withdrawing substituent led to an increase and the electron-donating substituents led to a decrease in the reaction efficiency (Scheme 3, **4a**–**k**). In addition, benzothiazepine was used in this protocol and the corresponding pyrrole-fused benzothiazepine was obtained with a yield of 73% (Scheme 3, **4l**). Also, various isocyanides were suitable for this reaction. By replacing cyclohexyl isocyanide with *tert*-butyl- and isopropyl isocyanide, the corresponding products were obtained with similar yields.

To investigate the reactivity of other cyclic imines in this protocol, we performed the reaction of triazolobenzodiazepine with *gem*-diactivated olefins and isocyanides (Scheme 4). As expected, under almost the same conditions as described in Scheme 3 (only at 80 °C), a new type of heterocyclic compounds, pyrrole-fused triazolobenzodiazepines, was obtained in high yield. As summarized in Scheme 4, a variety of *gem*-diactivated olefins with electron-donating (-Me, -OMe), electron-withdrawing (-NO_2), and halogen (-Cl and -Br) substitutions on the aromatic ring were well tolerated under the reaction conditions. Pyrrole-fused triazolobenzodiazepines **6** were obtained in yields ranging from 72% to 91% (Scheme 4, **6a–h**). Similar to the reaction of benzoxazepine, the presence of an electron-withdrawing group leads to an increase in the yield of pyrrole-fused triazolobenzodiazepines whereas electron-donating groups led to a decrease in its yield. Also, the substitution of naphthyl used in *gem*-diactivated olefins increased the efficiency of the desired product compared to the substitution of phenyl (Scheme 4, **6c**). Furthermore, *n*-butyl isocyanide was used to increase the variety of products and the *n*-butyl-substituted products **6f–h** were obtained with 72–78% yield .

All the products were characterized by ^{1}H NMR, ^{13}C NMR, and infrared spectroscopy, and mass spectrometry. Taking **4h** as an example for the analysis of its structure, in its ^{1}H NMR spectrum, one singlet signal appears at δ = 0.67 (9H) corresponding to the three methyl groups in the *tert*-butyl substituent. A singlet at δ = 2.39 (3H) is assigned to the protons of the CH_3-group on the phenyl. The signal at δ = 3.42 is the NH group. All the protons of the aromatic rings are located from δ = 7.10 to 7.99. In its ^{13}C NMR spectrum, all of the carbon signals appear at δ = 158.3, 152.5, 134.7, 134.2, 133.9, 133.2, 130.8, 130.4, 129.2, 129.1, 129.0 128.9, 128.4, 127.4, 125.8, 122.6, 121.1, 120.6, 117.1 (C_{Ar}), 91.1 (CN), 56.8, 29.4, 20.9 ($C_{Aliphatic}$), respectively. In its mass spectrum, the calculated value matched the found

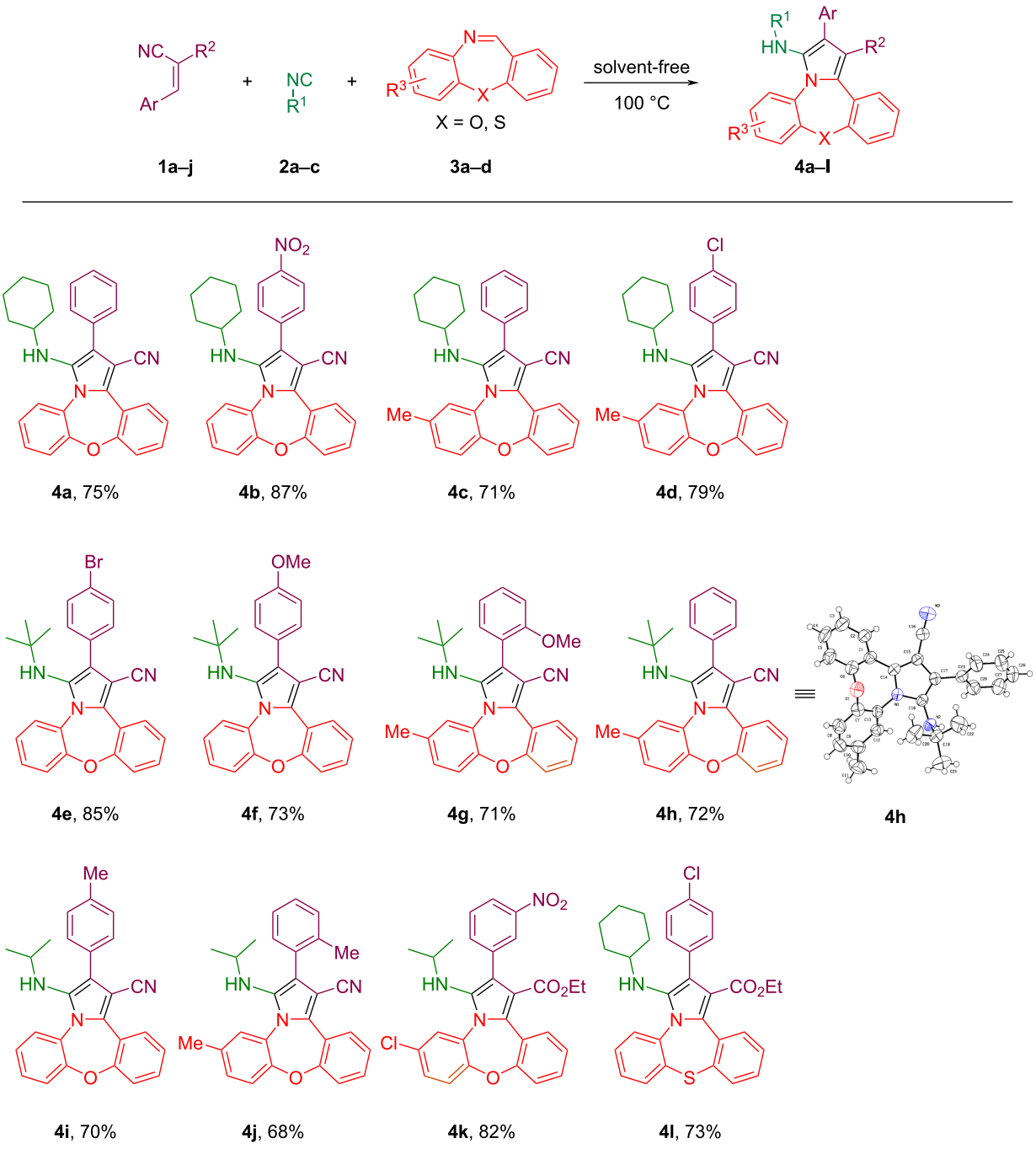

Scheme 3: Substrate scope. Conditions: Reactions were carried out using **1** (0.55 mmol), **2** (0.55 mmol), and **3** (0.50 mmol) under solvent-free conditions, stirring in an oil bath at 100 °C for 2 h (monitored by TLC).

value *m*/*z* 419 calculated for $[M]^+$ $C_{28}H_{25}N_3O$. In the IR spectrum, the absorption peak index in 2213 is related to the CN group. For final confirmation, the derivative **4h** was studied by X-ray diffraction analysis, and the crystal structure is illustrated in Figure 2 (detailed information can be found in the Supporting Information File 1).

The ^{1}H NMR spectrum of product **6f** obtained through the I-MCR was investigated and some unexpected chemical shifts were observed at room temperature (Figure 3A) [46]. Therefore, dynamic NMR measurements were performed for compound **6f** at various temperatures (25, 35, 45, 55, 65, 75, and 85 °C). As illustrated in Figure 3, all peaks in the spectrum correspond to

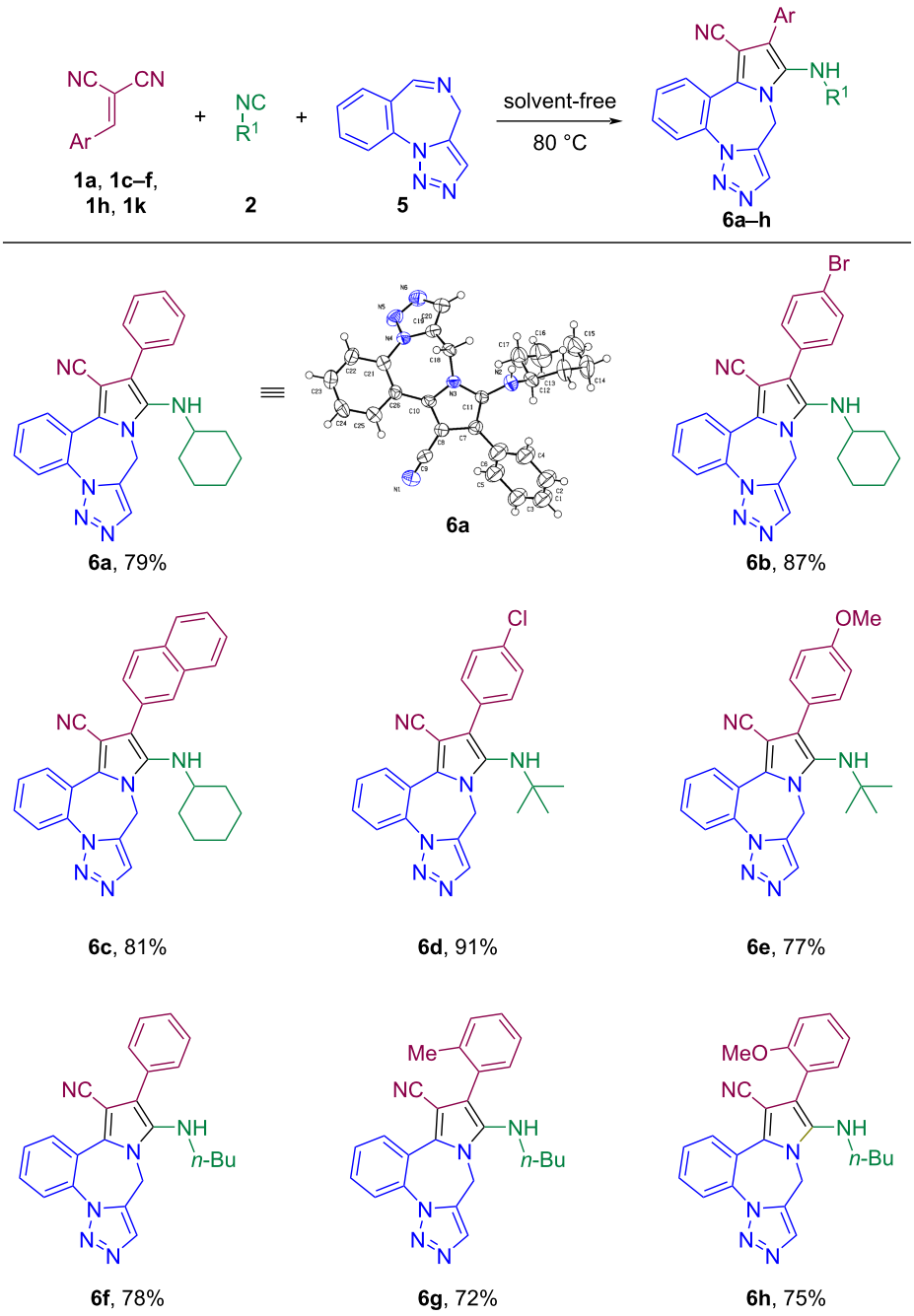

Scheme 4: Substrate scope. Conditions: reactions were carried out using **1** (0.55 mmol), **2** (0.55 mmol), and **5** (0.50 mmol) under solvent-free conditions, stirring in an oil bath at 80 °C for 2 h (monitored by TLC).

the structure of **6f**. Spectrum A recoreded at 25 °C has two broad singulet signals at δ = 4.65 and δ = 5.84 ppm corresponding to hydrogen I and hydrogen II. Remarkably, at higher temperatures (85 °C), the rapid inversion of the seven-membered ring results in it being observed as a single structure on the ^{1}H NMR time scale (see Figure 3, spectrum F) [19,47,48].

Furthermore, ^{13}C NMR analysis, mass spectrum, and IR are consistent with the structure (for details see Supporting Information File 1). Finally, a single crystal X-ray analysis of compound **6a** was performed, confirming the structure (Figure 4).

The proposed mechanism for an isocyanide-based multicomponent domino reaction for synthesizing pyrrole-fused dibenzox-

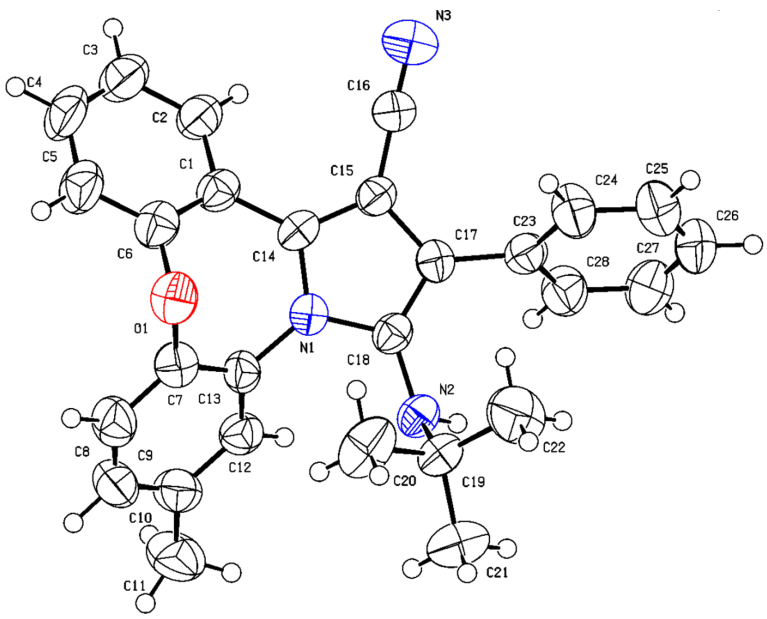

Figure 2: The crystal structure of **4h** (CCDC 2365305).

azepine is illustrated in Scheme 5. The reaction is initiated by the nucleophilic attack of the isocyanide **2** on the *gem*-diactivated olefin **1** to give the zwitterion intermediate **7**. The reaction proceeds with the nucleophilic attack of the zwitterion intermediate **8** on the cyclic imine **3** until intermediate **9** is formed. Then, with the cyclization process intermediate **10** is obtained. Finally, pyrrole-fused benzoxazepine is synthesized by successive processes involving the loss of HCN and the tautomeric enamine imine formation.

The successful synthesis of pyrrole-fused benzoxazepine/triazolobenzodiazepine derivatives via a 3-CR prompted us to investigate the synthesis of these compounds as a 4-CR. Fortunately, the pyrrole-fused benzoxazepine/triazolobenzodiazepines **4a** and **6a** could also be obtianed through a one-pot 4-CR from benzaldehyde, malononitrile, cyclohexyl isocyanide, and benzoxazepine/triazolobenzodiazepine imine (Scheme 6). However, the yield of the products based on the four-component method was lower compared to those obtained via the three-component strategy.

After the efficient and straightforward synthesis of the pyrrole-fused dibenzoxazepine/triazolobenzodiazepine derivatives on a submillimolar scale, two reactions were conducted on a gram scale to validate the protocol's efficacy (Scheme 7). Reacting each of the cyclic imines at a 3 mmol scale led to the pyrrole-fused dibenzoxazepine/triazolobenzodiazepine **4a** and **6a** in 80 and 87% yields, respectively. In general, a significant increase in the yield of the products was observed compared to the submillimole state.

Physical properties

The compounds such as benzoxazepines, benzothiazepines, benzodiazepines, and pyrrole have shown promising applications in optoelectronics, biophotonics, and cell imaging due to their suitable fluorophores [49-51]. The UV–vis absorption and emission spectra of products **4** and **6** were studied in ethanol at 298 K. The absorption range (λ_{abs}) was 400–225 nm, and the emission range (λ_{em}) was 560–400 nm. These findings are shown in Figure S3 in Supporting Information File 1. An interesting trend for the absorption of the synthesized derivatives **4** and **6** was observed when electron-donating substituents were present in the phenyl ring, which led to an increase in the intensity of the absorption and emission wavelengths (Supporting Information File 1, Figure S3). As is evident in numerous reports, quantum yield is one of the most important photophysical parameters for describing luminescent molecules and materials since high quantum efficiency is important for a wide range of applications, including displays, lasers, bio-imaging, solar cells, and accurate measurement of the quantum yield is therefore important [52-54]. Therefore, the quantum yield was determined using the standard of quinine sulfate for all the products (**4a–l** and **6a–h**). Products **4a** and **6c**, which had the highest intensity of absorption and emission from derivatives of benzoxazepines and triazolobenzodiazepines, respectively, their quantum yield was calculated and **4a** was obtained with 48.35%

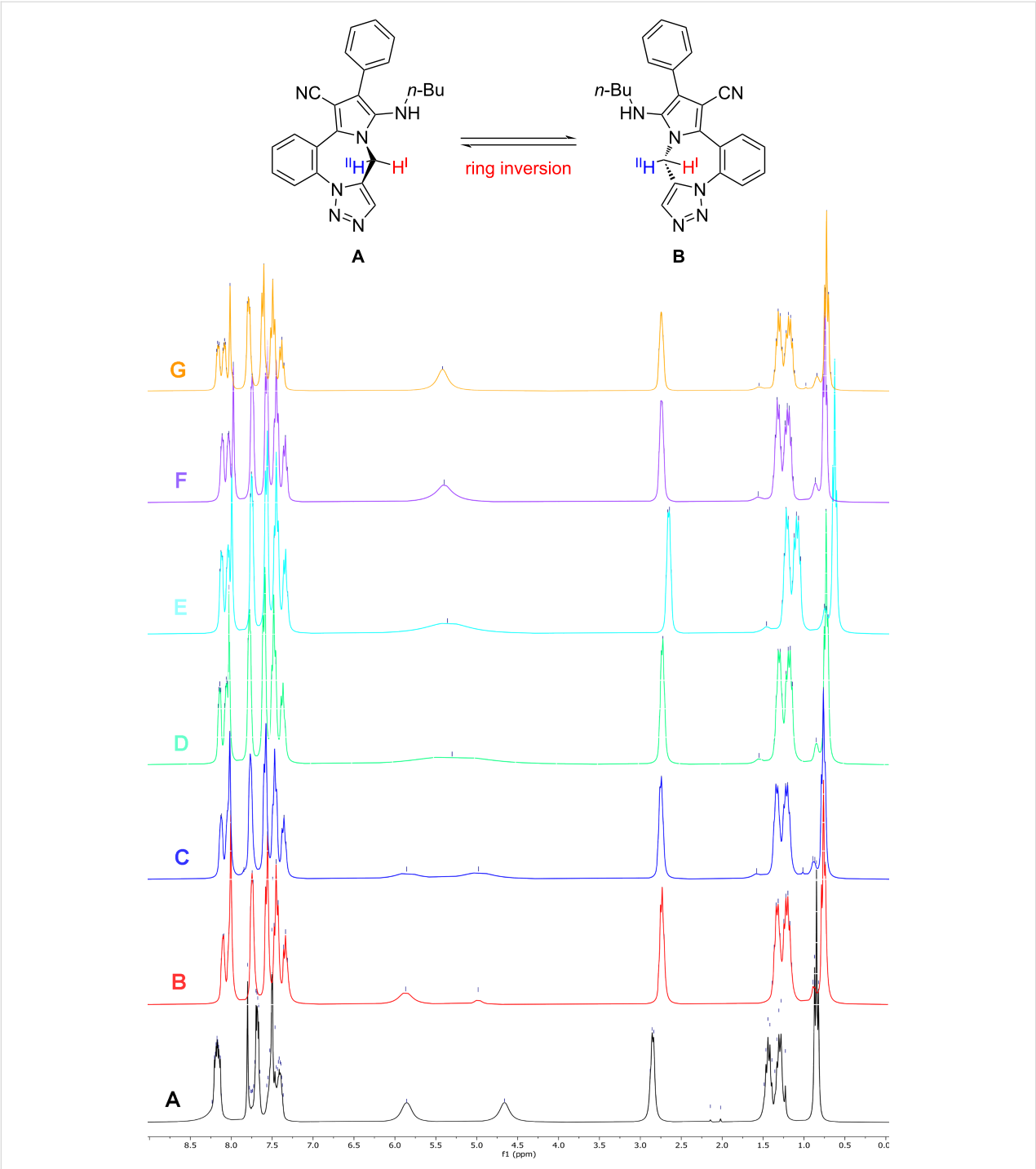

Figure 3: The DNMR (dynamic nuclear magnetic resonance) spectra of compound **6f** (DMSO-d_6, 300 MHz) at 25–85 °C; spectrum A: 25 °C, spectrum B: 35 °C, spectrum C: 45 °C, spectrum D: 55 °C, spectrum E: 65 °C, spectrum F: 75 °C and spectrum E: 85 °C.

and **6c** with 1.04% (Figure 5A and 5B) [55]. According to the results obtained from the quantum yield, we can claim that these synthesized derivatives pyrrole-fused dibenzoxazepine/dibenzothiazepine/triazolobenzodiazepine derivatives could serve as potential candidates for optoelectronic conjugate materials [56].

Conclusion

In summary, we have designed a simple and novel procedure for synthesizing pyrrole-fused dibenzoxazepine/dibenzothiazepine/triazolobenzodiazepine derivatives in high yields. This one-pot 3-CR includes isocyanides, *gem*-diactivated olefins, and cyclic imines (dibenzoxazepines, dibenzo-

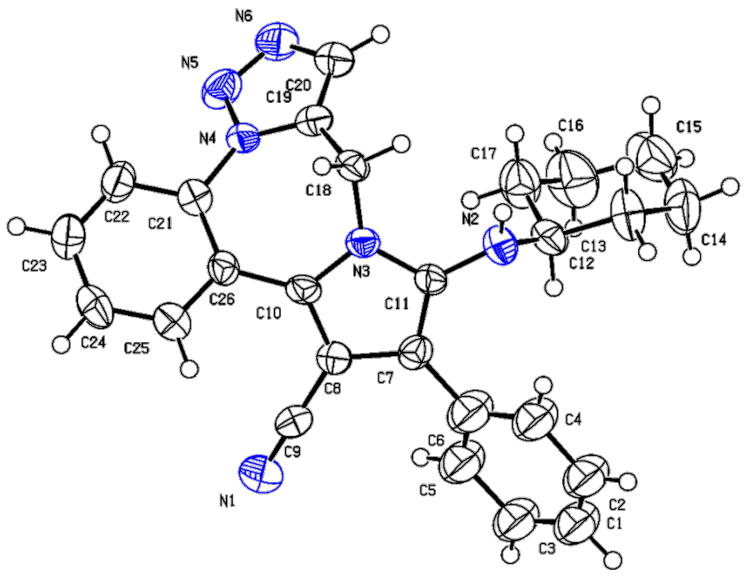

Figure 4: The crystal structure of **6a** (CCDC2365306).

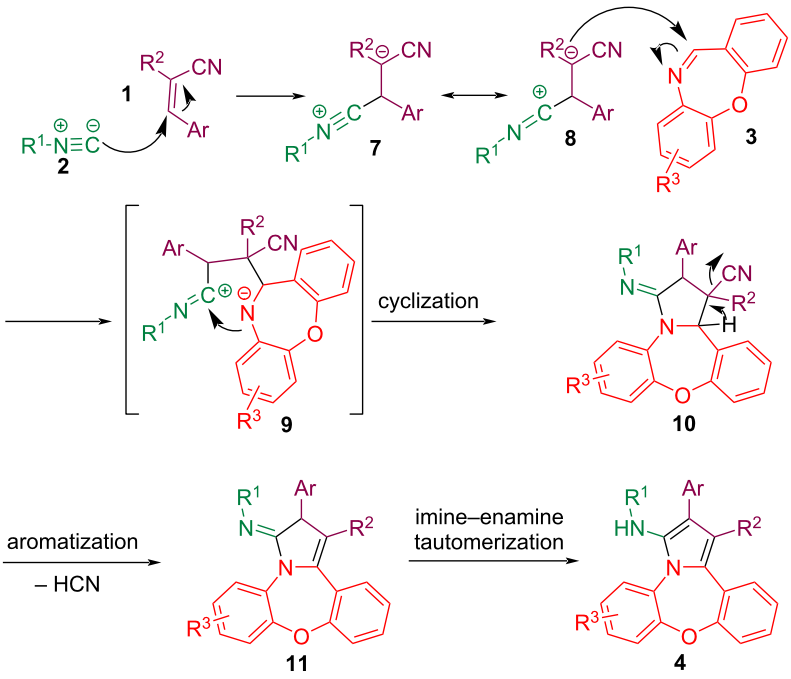

Scheme 5: A suggested mechanism for compounds **4**.

thiazepine, and triazolobenzodiazepine) under catalyst- and solvent-free conditions. Furthermore, the other advantages of this reaction include the manufacturing premium pharmaceutical scaffolds, a wide range of substrates, short reaction times, and simple operation. According to quantum efficiency calculations, all pyrrole-fused dibenzoxazepine/dibenzothiazepine/triazolobenzodiazepine derivatives with excellent emission could serve as potential candidates for optoelectronic conjugate materials.

Experimental

General information

All commercially available reagents and chemicals were bought from Merck & Co. and utilized without extra purification. The melting points of all synthesized compounds were measured utilizing an Electrothermal 9200 apparatus. ^{1}H and ^{13}C NMR and spectra in $CDCl_3$ and DMSO-d_6 solvents were recorded on a Bruker Avance spectrometer at 300.13 MHz and 75.47 MHz,

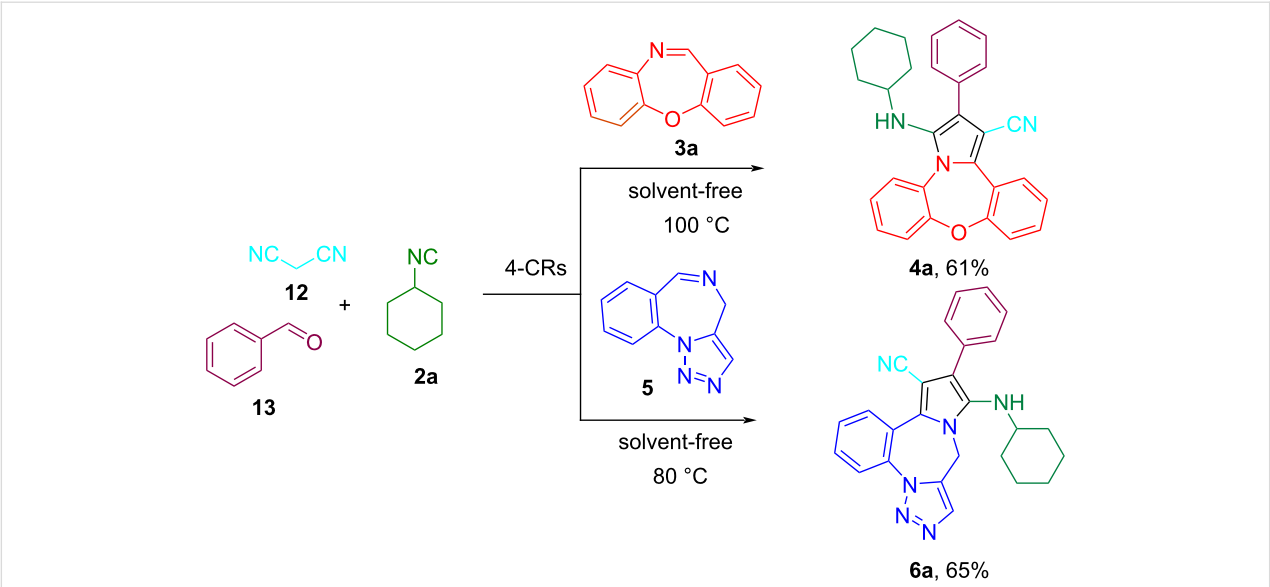

Scheme 6: Synthesis of pyrrole-fused dibenzoxazepine/triazolobenzodiazepine through a 4-CR.

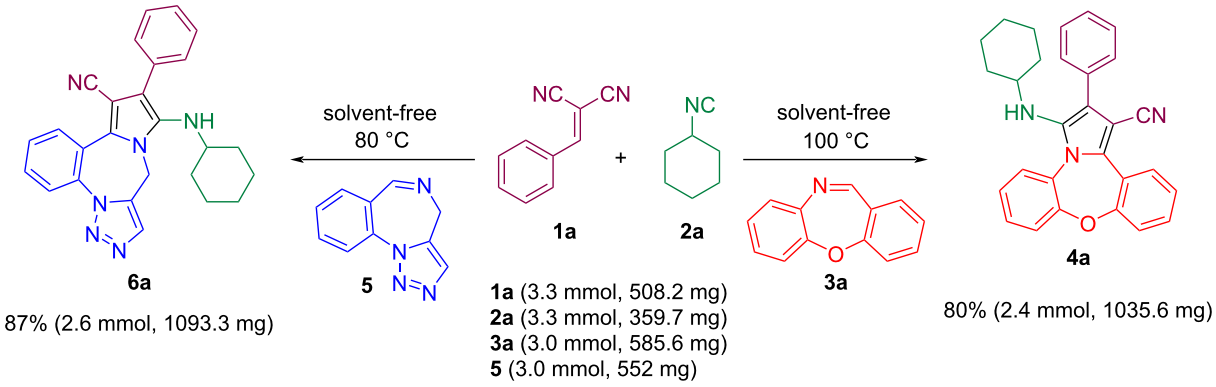

Scheme 7: Gram-scale synthesis of pyrrole-fused dibenzoxazepine/triazolobenzodiazepine **4a** and **6a** via 3-CRs.

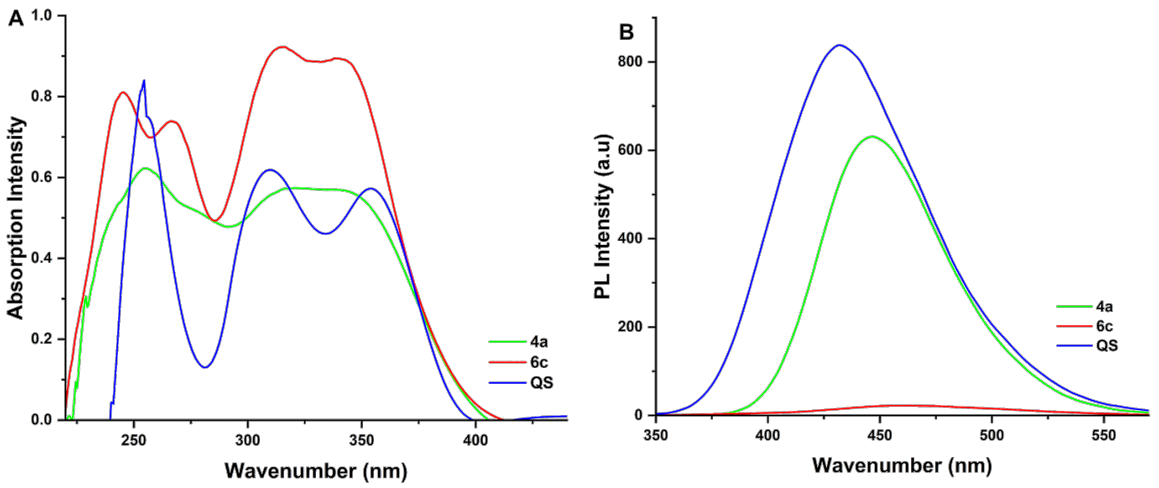

Figure 5: UV–vis absorption for compounds **4a**, **6c** and QS (quinine sulfate) (a); emission for **4a**, **6c** and QS (b); c = 75 ppm in ethanol and T = 298 K.

respectively. IR spectra were created on a Thermo Nicolet Nexus 470 FT-IR spectrometer in cm^{-1}. Mass spectra with an HP (Agile Technologies) 5975C Mass Selective Detector were used to confirm the mass of the synthesized products. The PL spectra of the products were obtained using an LS45 spectrometer from PerkinElmer. Elemental analyses were conducted using an Vario El CHN mode system from Elementar GmbH. The PL and the UV–vis spectra were obtained using a spectrofluorometer (LS45, PerkinElmer) and a Specord S 600 (Analytik Jena), respectively.

Preventive education for synthesizing triazolobenzodiazepine **6a–h**

Azides are highly reactive, toxic, explosive, and shock-sensitive chemicals that can be used under certain conditions. Special safety procedures must be followed during preparation, storage, handling, and disposal. $TMSN_3$ is an organic azide that is very sensitive to external factors such as light, heat, friction, and pressure and should be stored in amber plastic containers without light and at a temperature below zero degree Celsius. Exposure to azide occurs through skin absorption, inhalation, or ingestion through the respiratory tract. Which leads to skin and eye irritation, blurred vision, dizziness, weakness/fatigue, hypotension, seizures, and respiratory failure. The following instructions are required to work with $TMSN_3$. It is necessary to have a silver shield apron, breathing mask, safety glasses, lab coat, and gloves with high chemical resistance. The reactions should be carried out in a hood with a strong suction and with a protective explosion shield, which in this test should be as low as possible. Since exposure to water and strong acids leads to the formation of hydrazoic acid, which is very toxic, volatile, and explosive, the reaction containers must be completely dry and clean. When consuming $TMSN_3$, it should be done cold (below zero degree Celsius) in a container insulated from light. The reaction must be completely closed under the hood and the lid of the reaction container, and the product purification process must be carried out under the mentioned personal protective equipment. The reaction on a larger scale is carried out under special safety conditions [57-59].

3-(Cyclohexylamino)-2-phenyldibenzo[*b*,*f*]pyrrolo[1,2-*d*][1,4]oxazepine-1-carbonitrile (4a); ethyl 2-(4-chlorophenyl)-3-(cyclohexylamino)dibenzo[*b*,*f*]pyrrolo[1,2-*d*][1,4]thiazepine-1-carboxylate (4l) and 11-(cyclohexylamino)-12-phenyl-9*H*-benzo[*f*]pyrrolo[1,2-*d*][1,2,3]triazolo[1,5-*a*][1,4]diazepine-13-carbonitrile (6a); typical procedure: Cyclic imines of dibenzo[*b*,*f*][1,4]oxazepine **3a–c**, dibenzo[*b*,*f*][1,4]thiazepine **3d**, and 4*H*-benzo[*f*][1,2,3]triazolo[1,5-*a*][1,4]diazepine **5** were prepared according to the procedure in the previous report [44,45] and 0.50 mmol (**3a**, 98 mg; **3d**, 105 mg; **5**, 92 mg) of each was added separately along with 2-benzylidenemalononitrile (**1a**, 0.55 mmol, 85 mg), cyclohexyl isocyanide (**2a**, 0.55 mmol, 60 mg). The reaction mixture was stirred at temperatures of 100 or 80 °C for 2 h using a magnetic stirrer. After making sure that the reactions were completed (monitored by TLC), the reaction mixture was cooled to ambient temperature. Then, the crude mixture was purified using a silica gel chromatography column and washed with *n*-hexane and ethyl acetate solvent mixtures (1:3 for **3a** and **3d**; 2:1 for compounds **5**).

Supporting Information

Supporting Information File 1

General synthetic procedures and characterization and copies of ^1H NMR, ^{13}C NMR, FTIR and mass spectra.
[https://www.beilstein-journals.org/bjoc/content/supplementary/1860-5397-20-241-S1.pdf]

Funding

We gratefully acknowledge financial support from the Research Council of Shahid Beheshti University.

Author Contributions

Marzieh Norouzi: data curation; formal analysis; investigation; software. Mohammad Taghi Nazeri: conceptualization; formal analysis; methodology; resources; supervision; writing – original draft; writing – review & editing. Ahmad Shaabani: funding acquisition; project administration; supervision; writing – review & editing. Behrouz Notash: software.

ORCID® iDs

Mohammad Taghi Nazeri - https://orcid.org/0000-0002-4511-0890
Ahmad Shaabani - https://orcid.org/0000-0002-0304-4434
Behrouz Notash - https://orcid.org/0000-0003-4873-5770

Data Availability Statement

Data generated and analyzed during this study is available from the corresponding author upon reasonable request.

Preprint

A non-peer-reviewed version of this article has been previously published as a preprint: https://doi.org/10.3762/bxiv.2024.56.v1

References

1. Wei, L.; Shen, C.; Hu, Y.-Z.; Tao, H.-Y.; Wang, C.-J. *Chem. Commun.* **2019,** *55,* 6672–6684. doi:10.1039/c9cc02371b
2. Fang, W.-Y.; Ravindar, L.; Rakesh, K. P.; Manukumar, H. M.; Shantharam, C. S.; Alharbi, N. S.; Qin, H.-L. *Eur. J. Med. Chem.* **2019,** *173,* 117–153. doi:10.1016/j.ejmech.2019.03.063

3. Lamberth, C.; Jeanmart, S.; Luksch, T.; Plant, A. *Science* **2013,** *341,* 742–746. doi:10.1126/science.1237227
4. Vitaku, E.; Smith, D. T.; Njardarson, J. T. *J. Med. Chem.* **2014,** *57,* 10257–10274. doi:10.1021/jm501100b
5. Ahmad, S.; Alam, O.; Naim, M. J.; Shaquiquzzaman, M.; Alam, M. M.; Iqbal, M. *Eur. J. Med. Chem.* **2018,** *157,* 527–561. doi:10.1016/j.ejmech.2018.08.002
6. Nazeri, M. T.; Farhid, H.; Javanbakht, S.; Shaabani, A.; Notash, B. *Synlett* **2020,** *31,* 965–971. doi:10.1055/s-0039-1690887
7. Nazeri, M. T.; Shaabani, A. *New J. Chem.* **2021,** *45,* 21967–22011. doi:10.1039/d1nj04514h
8. Pramanik, C.; Barik, P.; Ali, S. A.; Nayak, D. S.; Ikbal, M.; Mandal, A.; Jana, R.; Giri, S.; Samanta, S. *New J. Chem.* **2023,** *47,* 6476–6527. doi:10.1039/d2nj05797b
9. Di Santo, R.; Tafi, A.; Costi, R.; Botta, M.; Artico, M.; Corelli, F.; Forte, M.; Caporuscio, F.; Angiolella, L.; Palamara, A. T. *J. Med. Chem.* **2005,** *48,* 5140–5153. doi:10.1021/jm048997u
10. Dubovtsev, A. Yu.; Dmitriev, M. V.; Silaichev, P. S.; Antonov, D. I.; Maslivets, A. N. *Synthesis* **2017,** *49,* 2223–2230. doi:10.1055/s-0036-1588407
11. Dai, L.; Shu, P.; Wang, Z.; Li, Q.; Yu, Q.; Shi, Y.; Rong, L. *Synthesis* **2017,** *49,* 637–646. doi:10.1055/s-0036-1588605
12. Chen, X.-Y.; Han, Y.; Sun, J.; Yan, C.-G. *Beilstein J. Org. Chem.* **2024,** *20,* 1436–1443. doi:10.3762/bjoc.20.126
13. Farhid, H.; Khodkari, V.; Nazeri, M. T.; Javanbakht, S.; Shaabani, A. *Org. Biomol. Chem.* **2021,** *19,* 3318–3358. doi:10.1039/d0ob02600j
14. Mandelli, M.; Tognoni, G.; Garattini, S. *Clin. Pharmacokinet.* **1978,** *3,* 72–91. doi:10.2165/00003088-197803010-00005
15. Browne, T. R. *N. Engl. J. Med.* **1978,** *299,* 812–816. doi:10.1056/nejm197810122991505
16. Rutgers, J. G.; Shearer, C. M. Lorazepam. In *Analytical profiles of drug substances;* Florey, K., Ed.; Academic Press, 1981; Vol. 9, pp 397–426. doi:10.1016/s0099-5428(08)60148-3
17. Galvan, M.; Boer, R.; Schudt, C. *Eur. J. Pharmacol.* **1989,** *167,* 1–10. doi:10.1016/0014-2999(89)90741-3
18. López-Muñoz, F.; Álamo, C.; García-García, P. J. *Anxiety Disord.* **2011,** *25,* 554–562. doi:10.1016/j.janxdis.2011.01.002
19. Mazumdar, W.; Driver, T. G. *Synthesis* **2021,** *53,* 1734–1748. doi:10.1055/s-0040-1705995
20. Bhattacharya, D.; Mitra, S.; Chattopadhyay, P. *Synthesis* **2015,** *47,* 2294–2298. doi:10.1055/s-0034-1379916
21. Gómez-Ayuso, J.; Pertejo, P.; Hermosilla, T.; Carreira-Barral, I.; Quesada, R.; García-Valverde, M. *Beilstein J. Org. Chem.* **2024,** *20,* 1758–1766. doi:10.3762/bjoc.20.154
22. Avendaño, C.; Menéndez, J. C. *Medicinal chemistry of anticancer drugs;* Elsevier: Amsterdam, Netherlands, 2015.
23. Kaufmann, C. N.; Spira, A. P.; Depp, C. A.; Mojtabai, R. *Psychiatr. Serv.* **2018,** *69,* 235–238. doi:10.1176/appi.ps.201700095
24. Nordt, S. P.; Clark, R. F. *J. Emerg. Med.* **1997,** *15,* 357–365. doi:10.1016/s0736-4679(97)00022-x
25. Whitwam, J.; Amrein, R. *Acta Anaesthesiol. Scand.* **1995,** *39* (Suppl. 108), 3–14. doi:10.1111/j.1399-6576.1995.tb04374.x
26. Sangshetti, J. N.; Altamash Shakeel Ahmad, A.; Kalam Khan, F. A.; Zaheer, Z. *Mini-Rev. Org. Chem.* **2015,** *12,* 345–354. doi:10.2174/1570193x12666150930224315
27. Lei, X.; Angeli, G.; Dömling, A.; Neochoritis, C. G. *Eur. J. Org. Chem.* **2022,** e202200220. doi:10.1002/ejoc.202200220
28. Lee, T.; Christov, P. P.; Shaw, S.; Tarr, J. C.; Zhao, B.; Veerasamy, N.; Jeon, K. O.; Mills, J. J.; Bian, Z.; Sensintaffar, J. L.; Arnold, A. L.; Fogarty, S. A.; Perry, E.; Ramsey, H. E.; Cook, R. S.; Hollingshead, M.; Davis Millin, M.; Lee, K.-m.; Koss, B.; Budhraja, A.; Opferman, J. T.; Kim, K.; Arteaga, C. L.; Moore, W. J.; Olejniczak, E. T.; Savona, M. R.; Fesik, S. W. *J. Med. Chem.* **2019,** *62,* 3971–3988. doi:10.1021/acs.jmedchem.8b01991
29. Boyer, S. J.; Burke, J.; Guo, X.; Kirrane, T. M.; Snow, R. J.; Zhang, Y.; Sarko, C.; Soleymanzadeh, L.; Swinamer, A.; Westbrook, J.; DiCapua, F.; Padyana, A.; Cogan, D.; Gao, A.; Xiong, Z.; Madwed, J. B.; Kashem, M.; Kugler, S.; O'Neill, M. M. *Bioorg. Med. Chem. Lett.* **2012,** *22,* 733–737. doi:10.1016/j.bmcl.2011.10.030
30. De Lucca, G. V.; Otto, M. J. *Bioorg. Med. Chem. Lett.* **1992,** *2,* 1639–1644. doi:10.1016/s0960-894x(00)80447-3
31. Shaabani, A.; Hezarkhani, Z.; Mofakham, H.; Ng, S. W. *Synlett* **2013,** *24,* 1485–1492. doi:10.1055/s-0033-1338953
32. Donald, J. R.; Martin, S. F. *Org. Lett.* **2011,** *13,* 852–855. doi:10.1021/ol1028404
33. Nenajdenko, V. G. *Russ. Chem. Rev.* **2020,** *89,* 1274–1336. doi:10.1070/rcr5010
34. Zlotin, S. G.; Egorova, K. S.; Ananikov, V. P.; Akulov, A. A.; Varaksin, M. V.; Chupakhin, O. N.; Charushin, V. N.; Bryliakov, K. P.; Averin, A. D.; Beletskaya, I. P.; Dolengovski, E. L.; Budnikova, Y. H.; Sinyashin, O. G.; Gafurov, Z. N.; Kantyukov, A. O.; Yakhvarov, D. G.; Aksenov, A. V.; Elinson, M. N.; Nenajdenko, V. G.; Chibiryaev, A. M.; Nesterov, N. S.; Kozlova, E. A.; Martyanov, O. N.; Balova, I. A.; Sorokoumov, V. N.; Guk, D. A.; Beloglazkina, E. K.; Lemenovskii, D. A.; Chukicheva, I. Y.; Frolova, L. L.; Izmest'ev, E. S.; Dvornikova, I. A.; Popov, A. V.; Kutchin, A. V.; Borisova, D. M.; Kalinina, A. A.; Muzafarov, A. M.; Kuchurov, I. V.; Maximov, A. L.; Zolotukhina, A. V. *Russ. Chem. Rev.* **2023,** *92,* RCR5104. doi:10.59761/rcr5104
35. Nazeri, M. T.; Nasiriani, T.; Farhid, H.; Javanbakht, S.; Bahri, F.; Shadi, M.; Shaabani, A. *ACS Sustainable Chem. Eng.* **2022,** *10,* 8115–8134. doi:10.1021/acssuschemeng.2c01030
36. Jiang, M.; Hu, K.; Zhou, Y.; Xiong, Q.; Cao, W.; Feng, X. *Org. Lett.* **2021,** *23,* 5261–5265. doi:10.1021/acs.orglett.1c01792
37. Nair, V.; Rajesh, C.; Vinod, A. U.; Bindu, S.; Sreekanth, A. R.; Mathen, J. S.; Balagopal, L. *Acc. Chem. Res.* **2003,** *36,* 899–907. doi:10.1021/ar020258p
38. Li, M.; Qiu, Z.-X.; Wen, L.-R.; Zhou, Z.-M. *Tetrahedron* **2011,** *67,* 3638–3648. doi:10.1016/j.tet.2011.03.085
39. Mironov, M. A.; Shulepov, I. D.; Kozhikhova, K. V.; Ivantsova, M. N.; Tokareva, M. I. *Chem. Heterocycl. Compd. (N. Y., NY, U. S.)* **2017,** *53,* 430–433. doi:10.1007/s10593-017-2071-3
40. Müller, T. J. J. *Multicomponent Reactions; Science of Synthesis*, Vol. 2; Thieme: Stuttgart, Germany, 2014. doi:10.1055/b-003-125831
41. Li, M.; Lv, X.-L.; Wen, L.-R.; Hu, Z.-Q. *Org. Lett.* **2013,** *15,* 1262–1265. doi:10.1021/ol400191b
42. Wang, C.-C.; Ma, Z.-W.; Qu, Y.-L.; Liu, Z.-J.; Chen, X.-P.; Zhou, J.; Chen, Y.-J. *Chem. – Asian J.* **2020,** *15,* 560–563. doi:10.1002/asia.201901780
43. Nazeri, M. T.; Shaabani, A.; Notash, B. *Org. Biomol. Chem.* **2021,** *19,* 3722–3734. doi:10.1039/d0ob02339f
44. Nazeri, M. T.; Ahmadi, M.; Ghasemi, M.; Shaabani, A.; Notash, B. *Org. Biomol. Chem.* **2023,** *21,* 4095–4108. doi:10.1039/d3ob00250k
45. Nazeri, M. T.; Ghasemi, M.; Ahmadi, M.; Shaabani, A.; Notash, B. *J. Org. Chem.* **2023,** *88,* 13504–13519. doi:10.1021/acs.joc.3c01013

46. Donald, J. R.; Wood, R. R.; Martin, S. F. *ACS Comb. Sci.* **2012,** *14,* 135–143. doi:10.1021/co2002087
47. Newkome, G. R. Eight-membered and larger rings. *Progress in Heterocyclic Chemistry;* Pergamon Press, 1996; Vol. 8, pp 320–336. doi:10.1016/s0959-6380(96)80019-5
48. Anet, F. A. L. *J. Am. Chem. Soc.* **1964,** *86,* 458–460. doi:10.1021/ja01057a034
49. Taliani, S.; Simorini, F.; Sergianni, V.; La Motta, C.; Da Settimo, F.; Cosimelli, B.; Abignente, E.; Greco, G.; Novellino, E.; Rossi, L.; Gremigni, V.; Spinetti, F.; Chelli, B.; Martini, C. *J. Med. Chem.* **2007,** *50,* 404–407. doi:10.1021/jm061137o
50. Chen, D.; Shan, Y.; Li, J.; You, J.; Sun, X.; Qiu, G. *Org. Lett.* **2019,** *21,* 4044–4048. doi:10.1021/acs.orglett.9b01220
51. Meyer, A. G.; Bissember, A. C.; Hyland, C. J. T.; Williams, C. C.; Szabo, M.; Pearsall, M. A.; Hyland, I. K.; Olivier, W. J. Seven-membered rings. *Progress in Heterocyclic Chemistry;* Elsevier: Amsterdam, Netherlands, 2020; Vol. 31, pp 597–647. doi:10.1016/b978-0-12-819962-6.00016-6
52. Levitus, M. *Methods Appl. Fluoresc.* **2020,** *8,* 033001. doi:10.1088/2050-6120/ab7e10
53. Rubin, M. B.; Braslavsky, S. E. *Photochem. Photobiol. Sci.* **2010,** *9,* 670–674. doi:10.1039/b9pp00182d
54. Würth, C.; Grabolle, M.; Pauli, J.; Spieles, M.; Resch-Genger, U. *Nat. Protoc.* **2013,** *8,* 1535–1550. doi:10.1038/nprot.2013.087
55. Sreejith, S.; Divya, K. P.; Ajayaghosh, A. *Chem. Commun.* **2008,** 2903–2905. doi:10.1039/b802958j
56. Ghosh, S.; Mandal, S.; Banerjee, C.; Rao, V. G.; Sarkar, N. *J. Phys. Chem. B* **2012,** *116,* 9482–9491. doi:10.1021/jp305095n
57. Keicher, T.; Löbbecke, S. Lab-Scale synthesis of azido compounds: safety measures and analysis. In *Organic Azides: Syntheses and Applications;* Bräse, S.; Banert, K., Eds.; John Wiley & Sons: Chichester, UK, 2009; pp 1–27. doi:10.1002/9780470682517.ch1
58. González-Bobes, F.; Kopp, N.; Li, L.; Deerberg, J.; Sharma, P.; Leung, S.; Davies, M.; Bush, J.; Hamm, J.; Hrytsak, M. *Org. Process Res. Dev.* **2012,** *16,* 2051–2057. doi:10.1021/op3002646
59. Bräse, S.; Gil, C.; Knepper, K.; Zimmermann, V. *Angew. Chem., Int. Ed.* **2005,** *44,* 5188–5240. doi:10.1002/anie.200400657

License and Terms

This is an open access article licensed under the terms of the Beilstein-Institut Open Access License Agreement (https://www.beilstein-journals.org/bjoc/terms), which is identical to the Creative Commons Attribution 4.0 International License (https://creativecommons.org/licenses/by/4.0). The reuse of material under this license requires that the author(s), source and license are credited. Third-party material in this article could be subject to other licenses (typically indicated in the credit line), and in this case, users are required to obtain permission from the license holder to reuse the material.

The definitive version of this article is the electronic one which can be found at:
https://doi.org/10.3762/bjoc.20.241

BEILSTEIN JOURNAL OF ORGANIC CHEMISTRY

Synthesis of the 1,5-disubstituted tetrazole-methanesulfonyl-indole hybrid system via high-order multicomponent reaction

Cesia M. Aguilar-Morales[‡1], América A. Frías-López[‡1], Nadia V. Emilio-Velázquez[1], Alejandro Islas-Jácome[2], Angelica Judith Granados-López[3], Jorge Gustavo Araujo-Huitrado[3], Yamilé López-Hernández[4], Hiram Hernández-López[5], Luis Chacón-García[*1], Jesús Adrián López[*3] and Carlos J. Cortés-García[*1]

Full Research Paper

Open Access

Address:
[1]Laboratorio de Diseño Molecular, Instituto de Investigaciones Químico-Biológicas, Universidad Michoacana de San Nicolás de Hidalgo. Ciudad Universitaria, C.P. 58030, Morelia, Michoacán, Mexico, [2]Departamento de Química, Universidad Autónoma Metropolitana-Iztapalapa, Av. Ferrocarril San Rafael Atlixco 186, Col. Leyes de Reforma 1A Sección, Iztapalapa, 09310, Ciudad de México, Mexico, [3]Laboratorio de microRNAs y Cáncer, Universidad Autónoma de Zacatecas, Av. Preparatoria S/N, Agronómica, Campus II, Zacatecas 98066, Zacatecas, Mexico, [4]Laboratorio de Metabolómica y Proteómica, Cátedra CONACYT, Unidad Académica de Ciencias Biológicas, Universidad Autónoma de Zacatecas, Av. Preparatoria S/N, Agronómica, Campus II, Zacatecas 98066, Zacatecas, Mexico and [5]Laboratorio de síntesis y modificación química, Unidad Académica de Ciencias Químicas, Universidad Autónoma de Zacatecas, Campus UAZ siglo XXI, carretera Zacatecas-Guadalajara km 6, Zacatecas, Zacatecas, 98160, México

Email:
Luis Chacón-García[*] - lchacon@umich.mx; Jesús Adrián López[*] - jalopez@uaz.edu.mx; Carlos J. Cortés-García[*] - ccortes@umich.mx

* Corresponding author ‡ Equal contributors

Keywords:
1,5-disubstituted tetrazoles; high-order multicomponent reaction; isocyanides; MCF-7 cell line; methanesulfonylindoles; Ugi-azide reaction

Beilstein J. Org. Chem. **2024,** *20,* 3077–3084.
https://doi.org/10.3762/bjoc.20.256

Received: 09 August 2024
Accepted: 11 November 2024
Published: 26 November 2024

This article is part of the thematic issue "Multicomponent reactions IV".

Associate Editor: T. J. J. Müller

© 2024 Aguilar-Morales et al.; licensee Beilstein-Institut.
License and terms: see end of document.

Abstract

A series of 1,5-disubstituted tetrazole-indole hybrids were synthesized via a high-order multicomponent reaction consisting of an Ugi-azide/Pd/Cu-catalyzed hetero-annulation cascade sequence. This operationally simple one-pot protocol allowed high bond-forming efficiency and creating six new bonds (two C–C, three C–N, and one N–N). Additionally, the products were evaluated against breast cancer MCF-7 cells, finding moderate activity in the compounds substituted with fluorine and chlorine.

Introduction

Nitrogen-containing heterocyclic moieties, such as 1,5-disubstituted tetrazoles and indoles, are considered pharmacophoric fragments due to their pivotal interactions with several targets involved in many diseases. They are found in a plethora of compounds with significant biological and pharmacological relevance [1-4]. These moieties are indispensable in the design and synthesis of novel drugs aimed at overcoming drug resistance, which is a global health threat [5-7]. To date, a strategy to access novel highly bioactive compounds that can be converted into drug candidates in a fast and efficient manner containing these moieties is the molecular hybridization [8-10]. It consists of covalently joining of two or more pharmacophoric fragments to provide new hybrid compounds with improved efficacy and affinity compared to their drug parents and by using powerful synthetic tools such as multicomponent reactions (MCRs) [11-13]. Among these, isocyanide-based multicomponent reactions (I-MCRs), such as the Ugi-azide reaction, have demonstrated the highest biological-synthetic relevance [1,14-16]. In this regard, a relatively unexplored field within MCRs comprises high-order multicomponent reactions, which involve reacting at least five or even more components in a single operational step. These reactions are highly convergent, efficient, and have superior atom economy, producing high structural diversity and complexity compared to classical 3- or 4-CRs [17-19].

In the same context, the hybridization of 1,5-disubstituted tetrazoles with an indole moiety using I-MCRs such as the Ugi-azide reaction as a key step, is very limited. To our knowledge, only three reactions have been described (Scheme 1a–c). In 2021, Dömling's research group synthesized a series of 1,5-disubstituted tetrazole-indoles **6** in good to excellent yields via an Ugi-azide/acidic ring-closure sequence [20]. Balalaie described an efficient method in 2018 for the synthesis of a new 1,5-disubstituted tetrazole-indole system **10**, in a two-step reaction: Ugi-azide followed by a cyclization reaction catalyzed by $AuCl_3$, in good to high yields [21]. In 2019, Salahi et al. synthesized the series of tetrazole-indoles **15** via an Ugi-azide reaction in moderate to high yields [22]. It is noteworthy that none of the previously described strategies involved the use of higher-order multicomponent reactions (HO-MCRs).

As part of our ongoing research program towards the synthesis of novel hybrid compounds based on the 1,5-disubstituted tetrazole moiety [23-27], we developed a synthetic strategy for the synthesis of a novel bis-heterocyclic hybrid, 1,5-disubstituted-tetrazole-indoles. The compounds were achieved through a high-order multicomponent reaction consisting of two sequential processes: an Ugi-azide reaction and a further Pd/Cu-catalyzed heteroannulation (Scheme 1d).

Results and Discussion

Our study commenced with synthesizing a series of 1,5-disubstituted tetrazole-methanesulfonylindoles **18a**–**n**, achieved through a high-order multicomponent approach. This strategy, similar to that previously reported by our research group for synthesizing the 1,5-disubstituted tetrazole-benzofuran bis-heterocyclic system [23], involves a two-step sequence starting with an Ugi-azide multicomponent reaction, followed by a Pd/Cu-catalyzed heteroannulation process, as depicted in Scheme 2. Conditions for the Ugi-azide reaction were optimized based on our recent findings, i.e., the reaction was performed in trifluoroethanol as the solvent and at room temperature [23-26]. In the initial reaction, propargylamine served as a bifunctional reagent, with the primary amine group participating in the first step and the terminal alkyne promoting the subsequent heteroannulation. (Scheme 2). As observed in our previous studies, we employed benzaldehyde derivatives with various stereoelectronic decoration, excluding aliphatic ones due to their decreased reactivity resulting in failures to proceed [24-27]. Commercially available isocyanides utilized were cyclohexyl and *tert*-butyl isocyanide. Notably, an isolation of the 1,5-disubstituted tetrazole-alkyne intermediates was unnecessary; we previously reported this heterocyclic system [24-26]. The heteroannulation reaction was then investigated under the most common conditions, utilizing a catalytic system comprising $PdCl_2(PPh_3)_2$, Et_3N and CuI [23,28]. Therefore, the key component for this reaction was methanesulfonyl 2-iodoaniline **17**, as it has been reported that the use of 2-iodoaniline results in the formation of only the Sonogashira coupling product [29,30]. Moreover, as shown in Scheme 2, this high-order multicomponent protocol yielded fourteen 1,5-disubstituted tetrazole-methanesulfonylindole derivatives, with yields ranging from 16% to 55% after purification by column chromatography. Despite some yields being modest, they are deemed reasonable considering the reaction's structural complexity, atom economy, and the efficiency achieved in terms of time and resource optimization. In addition, all the target compounds were fully characterized using ^1H and ^{13}C NMR spectroscopy and HRMS. It is important to mention that this protocol cannot be considered a true one-pot synthesis, as it requires a solvent exchange between reaction steps (e.g., from trifluoroethanol to Et_3N for the subsequent catalysis). Thus, this protocol enabled a straightforward and rapid synthesis of highly 2-substituted indoles under mild reaction conditions, highlighting the versatility of propargylamine as a bifunctional reagent in post-Ugi-azide transformations. Our group pioneered the application of this reagent as a central building block in the synthesis of hybrid systems via Ugi-azide reactions, including structures based on triazoles-tetrazoles [24,26,27], benzofuran-tetrazoles [23] and indolizines-tetrazoles [25], all of which have

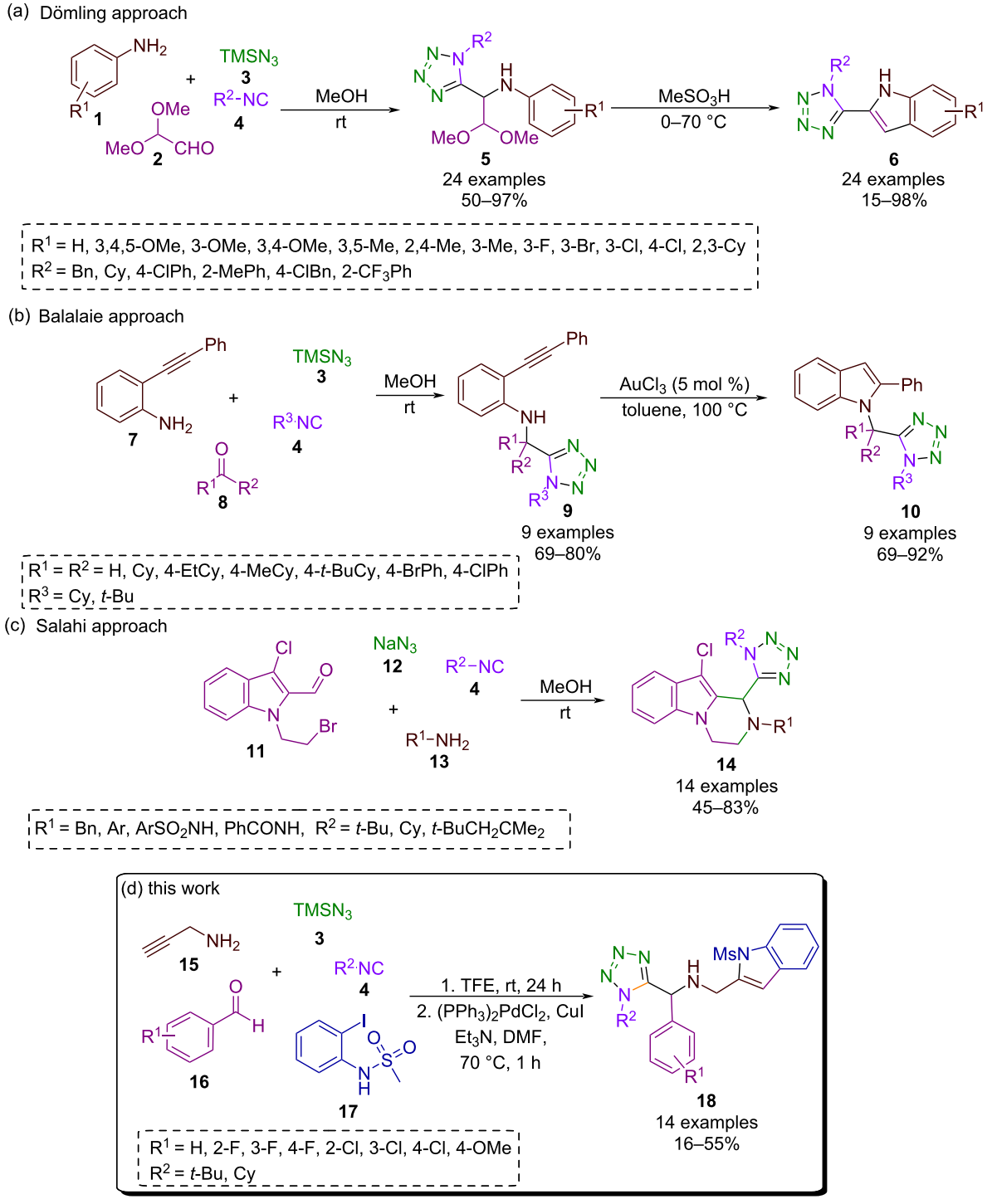

Scheme 1: Synthetic approaches to obtain the 1,5-disubstituted tetrazole-indole system and our synthetic approach.

significant relevance in medicinal chemistry and optical science.

A plausible reaction mechanism for the formation of the target molecules **18a**–**n** via a high-order multicomponent reaction is shown in Scheme 3 and consists of two processes: an Ugi-azide reaction and a Pd/Cu-catalyzed heteroannulation reaction. The Ugi-azide reaction mechanism to obtain the 1,5-disubstituted tetrazole-alkyne **19** is well-documented and hence, it is not herein described in detail [1,26,31]. Thus, based on Pal and

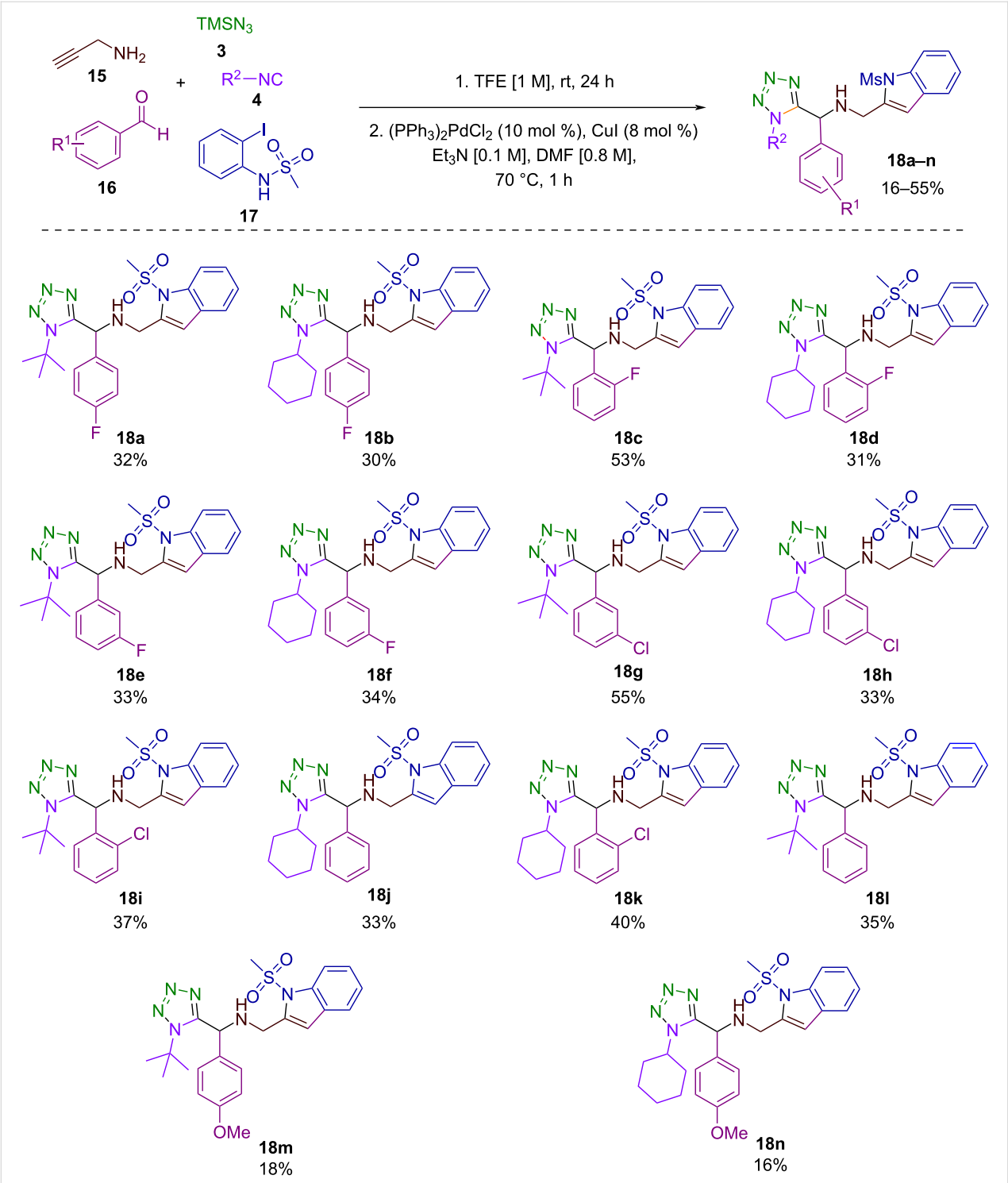

Scheme 2: High-order multicomponent reaction for the synthesis of 1,5-disubstituted tetrazol-methanesulfonylindole hybrids.

co-workers' proposal [32,33], the second process involves two catalytic cycles: 1) a Sonogashira coupling, and 2) a 5-*endo-dig* cyclization. The first catalytic cycle begins with the coupling of 1,5-disubstituted tetrazole-alkyne **19** and methanesulfonyl-2-iodoaniline **17** forming the intermediate **23**. Following a reductive elimination, the Sonogashira-like product **24** is produced, which then progresses into the second catalytic cycle. In this cycle, an intramolecular cyclization takes place, facilitated by CuI. This step involves a 5-*endo-dig* cyclization, where the negatively nitrogen atom of the sulfonamide **25** attacks intramo-

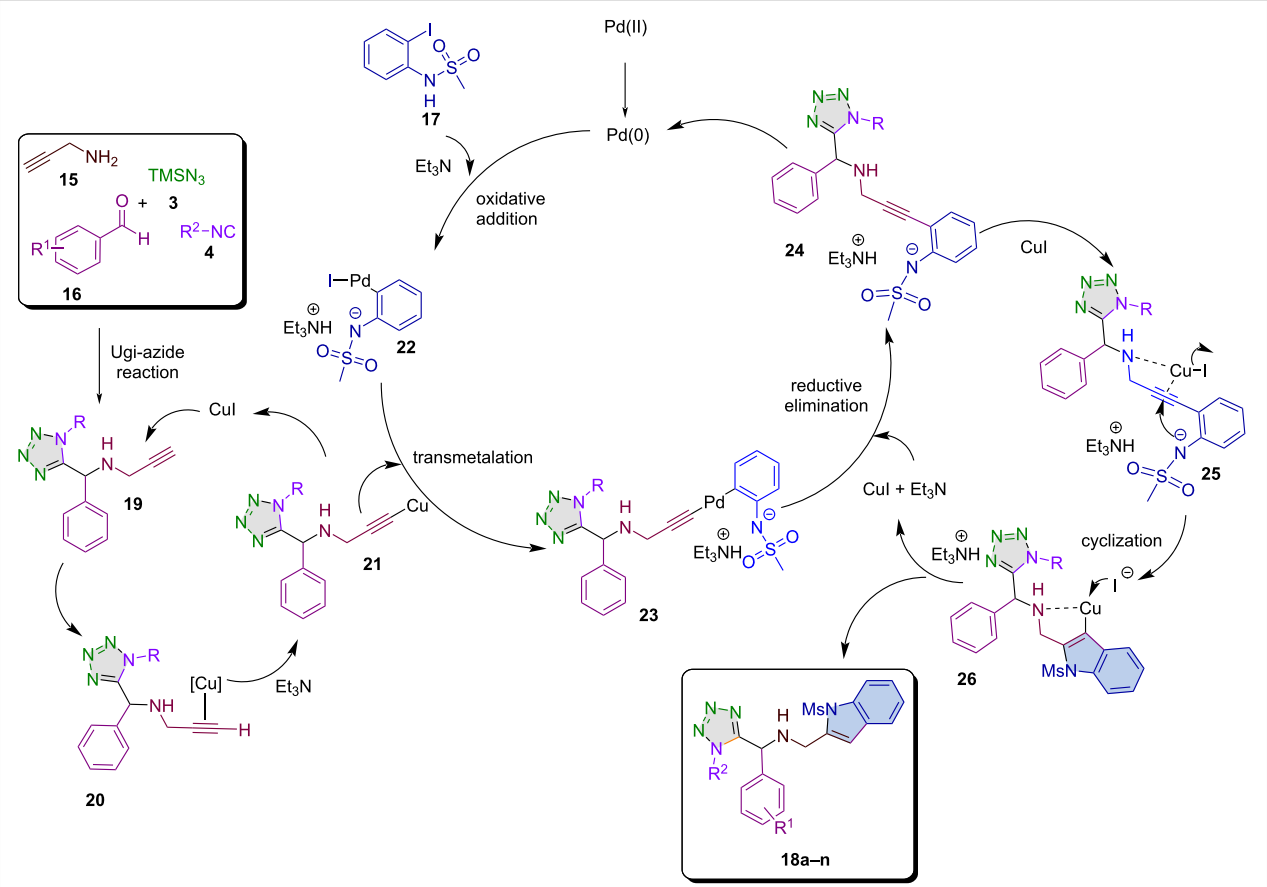

Scheme 3: Plausible reaction mechanism for the synthesis of target molecules **18a–n**.

lecularly to yield the intermediate **26**. The final product is formed when iodide is regenerated as CuI, allowing it to re-enter into the catalytic cycle.

On the other hand, the sulfonyl group in its sulfonamide form is typically associated with antibacterial activity. However, it has been little studied the sulfonyl group regarding biological activity when attached to the indole nitrogen. Although scarce, some recent representative studies include antibacterial, anti-inflammatory, antioxidant, selective inhibitor of COX-2 [34], and anti-HIV activity [35]. In this context, even though indole is considered a privileged scaffold present in some anticancer agents [36], a few examples of methanesulfonylindoles are studied as cytotoxic compounds. For example, a cytotoxic effect was found in CAL 27 cells, presumably through a mechanism of TNF-α inhibition in vitro, which could be related to the anti-inflammatory effect identified in several studies of NSAIDs that inhibit cancer cell viability in vitro [37,38]. In another study aimed at inhibiting tubulin assembly, *N*-mesyl-2-(1-phenylvinyl)indoles were active against HCT-116 cells on the order of a GI_{50} of 10 mM, although the mechanism originally sought was not demonstrated [39].

Therefore, in this work, the cytotoxic activity of methanesulfonylindoles **18a–j** was explored against MCF-7 cell line, which has been used as a model for breast cancer (BC), a public health issue very common and a deadly pathology worldwide, where women between 45 and 55 years of age are the most vulnerable population. In 2020, 684,996 deaths were recorded [40-43]. This in vitro bioactivity study was proposed based on observations that indole-coumarin-thiadiazole hybrid compounds described by Kamath et al. [44], as well as indole-benzimidazole hybrids reported by Singla et al. [45] have shown potential as therapeutic agents for breast cancer treatment. Thereby, we hypothesized that combining the indole moiety with the 1,5-disusbtituted tetrazole pharmacophore could increase the non-covalent interactions, including π–π stacking, hydrogen bonding, and hydrophobic interactions. This combination may improve the pharmacodynamic profile, providing a solid foundation for developing compounds with greater efficacy and selectivity against targets related to BC. Thus, the 1,5-disubstituted tetrazole-indole hybrids, presented different effects on cell proliferation inhibition in MCF-7 cells (Figure 1) that could be attributable to the molecular background of cells [46-49]. The compounds that elicited proliferation inhibition are

ordered below from the highest to lowest effect on MCF-7 cell line: **18d**, **18j**, **18h**, **18i**, **18b**, **18f**, **18a**, **18g**, **18c**, and **18e**. Compounds **18c**, and **18e** did not affect MCF-7 cell proliferation inhibition. Regarding the structure–activity relationship, the importance of the *tert*-butyl and cyclohexyl substituents in the imidazole can be deduced. According to the IC_{50} results presented in Figure 1, it can be seen that all cyclohexyl-substituted derivatives tested show activity. In contrast, those carrying the *tert*-butyl group are inactive, except for **18i** and **18a**, which show moderate and low activity, respectively. The modification of this substituent is seen when comparing the analogous derivatives **18d** and **18c**; **18h** and **18g**; **18b** and **18a**; **18f** and **18e**, where the replacement of cyclohexyl by *tert*-butyl leads to a loss of activity in each case. Concerning the substituent on the phenyl group, it is interesting to note that the most active compound of the whole series is the fluorinated derivative **18d**, followed in order of inhibition by **18j**, which has no substituents. The position of this halogen is also relevant since the activity decreases when it is in the 4' position (**18b**) and is almost lost when it is in the 3' position (**18a**). Interestingly, compound **18i**, which contains chlorine at the 2'-position, is the only derivative with significant activity in the series of *tert*-butyl derivatives. This suggests that a chloro or fluoro substituent at this position is relevant for the cytotoxic activity.

The 1,5-disubstituted tetrazole-1,2,3-triazole hybrids synthesized by our group [26] had similar effects to the present compounds, suggesting that 1,5-disubstituted tetrazole and indole are pharmacophoric fragments with significant biological and pharmacological potential in anticancer drug design. However, it should be taken into account that the sulfonyl group can radically change the pharmacokinetic properties of a drug, so the effect it may have on its ADMET properties should be determined in an additional study.

Conclusion

A novel synthetic strategy has been developed for synthesizing a small series of 1,5-disubstituted tetrazole-methanesulfonyl-indole hybrid compounds under mild reaction conditions. This strategy employs a cascade process consisting of a sequential Ugi-azide and Pd/Cu-catalyzed heteroannulation reactions, achieving low to moderate yields. Significantly, this protocol

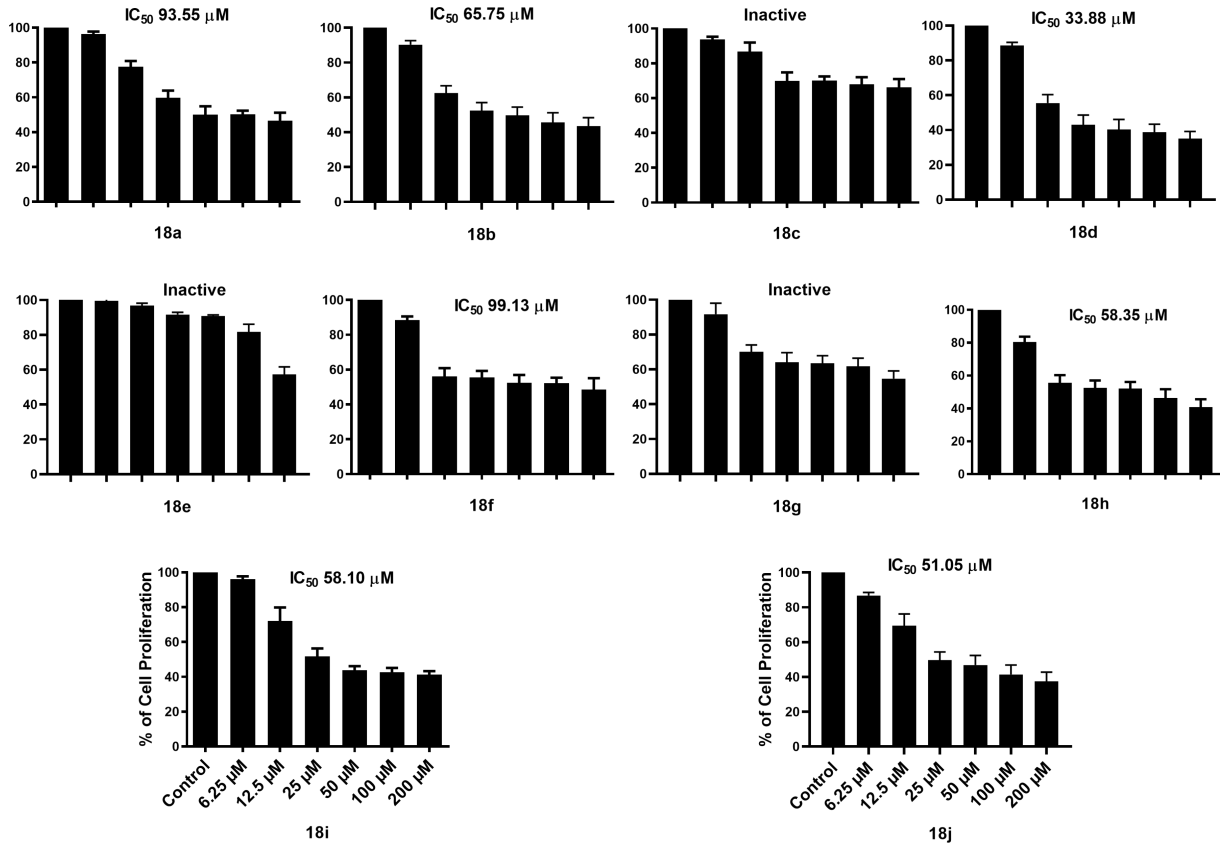

Figure 1: Differential effect of the 1,5-disubstituted tetrazole-indole hybrid compounds **18a–j** on proliferation of MCF-7 cell line. MCF-7 cells were treated with increasing doses of compounds **18a–j**. Controls were cells treated with DMSO.

enables the rapid and straightforward synthesis of highly 2-substituted indoles with high bond-forming efficiency, creating six new bonds (two C–C, three C–N, and one N–N). Our synthetic strategy would represent the second report in which the Pd/Cu-catalyzed heteroannulation reaction is utilized as a post-Ugi-azide reaction, using propargylamine as a key bifunctional reagent. The results of cytotoxic activity were moderate. However, the information obtained from this study, together with that obtained with previously described analogs, provide important information for proposing new structures with improved activity.

Supporting Information

Supporting Information File 1

Experimental procedures, compound characterization data, and copies of NMR spectra.
[https://www.beilstein-journals.org/bjoc/content/supplementary/1860-5397-20-256-S1.pdf]

Funding

C.M. A-M. (756225) and América A. Frías-López (833463) acknowledges the support of CONACHYT through a graduate scholarship. This work was financially supported by Instituto De Ciencia, Tecnología e Innovación del Estado de Michoacán de Ocampo (ICTI-PICIR23-024) and CIC-UMSNH (18104).

Author Contributions

Cesia M. Aguilar-Morales: data curation; methodology. América A. Frías-López: methodology; visualization. Nadia V. Emilio-Velázquez: methodology. Alejandro Islas-Jácome: data curation; formal analysis. Angelica Judith Granados-López: data curation; formal analysis. Jorge Gustavo Araujo-Huitrado: methodology. Yamilé López-Hernández: data curation; methodology. Hiram Hernández-López: software; validation. Luis Chacón-García: conceptualization; funding acquisition; writing – review & editing. Jesús Adrián López: data curation; writing – original draft; writing – review & editing. Carlos J. Cortés-García: conceptualization; project administration; writing – original draft.

ORCID® iDs

Hiram Hernández-López - https://orcid.org/0000-0002-4286-163X
Jesús Adrián López - https://orcid.org/0000-0001-8012-7041
Carlos J. Cortés-García - https://orcid.org/0000-0003-4632-6316

Data Availability Statement

All data that supports the findings of this study is available in the published article and/or the supporting information of this article.

References

1. Neochoritis, C. G.; Zhao, T.; Dömling, A. *Chem. Rev.* **2019,** *119,* 1970–2042. doi:10.1021/acs.chemrev.8b00564
2. Zhang, J.; Wang, S.; Ba, Y.; Xu, Z. *Eur. J. Med. Chem.* **2019,** *178,* 341–351. doi:10.1016/j.ejmech.2019.05.071
3. Kumari, A.; Singh, R. K. *Bioorg. Chem.* **2019,** *89,* 103021. doi:10.1016/j.bioorg.2019.103021
4. Thanikachalam, P. V.; Maurya, R. K.; Garg, V.; Monga, V. *Eur. J. Med. Chem.* **2019,** *180,* 562–612. doi:10.1016/j.ejmech.2019.07.019
5. Salam, M. A.; Al-Amin, M. Y.; Salam, M. T.; Pawar, J. S.; Akhter, N.; Rabaan, A. A.; Alqumber, M. A. A. *Healthcare* **2023,** *11,* 1946. doi:10.3390/healthcare11131946
6. Bergkessel, M.; Forte, B.; Gilbert, I. H. *ACS Infect. Dis.* **2023,** *9,* 2062–2071. doi:10.1021/acsinfecdis.3c00189
7. Szumilak, M.; Wiktorowska-Owczarek, A.; Stanczak, A. *Molecules* **2021,** *26,* 2601. doi:10.3390/molecules26092601
8. Singh, A. K.; Kumar, A.; Singh, H.; Sonawane, P.; Paliwal, H.; Thareja, S.; Pathak, P.; Grishina, M.; Jaremko, M.; Emwas, A.-H.; Yadav, J. P.; Verma, A.; Khalilullah, H.; Kumar, P. *Pharmaceuticals* **2022,** *15,* 1071. doi:10.3390/ph15091071
9. Alkhzem, A. H.; Woodman, T. J.; Blagbrough, I. S. *RSC Adv.* **2022,** *12,* 19470–19484. doi:10.1039/d2ra03281c
10. Ivasiv, V.; Albertini, C.; Gonçalves, A. E.; Rossi, M.; Bolognesi, M. L. *Curr. Top. Med. Chem.* **2019,** *19,* 1694–1711. doi:10.2174/1568026619666190619115735
11. Graziano, G.; Stefanachi, A.; Contino, M.; Prieto-Díaz, R.; Ligresti, A.; Kumar, P.; Scilimati, A.; Sotelo, E.; Leonetti, F. *Int. J. Mol. Sci.* **2023,** *24,* 6581. doi:10.3390/ijms24076581
12. Brandão, P.; Marques, C. S.; Carreiro, E. P.; Pineiro, M.; Burke, A. J. *Chem. Rec.* **2021,** *21,* 924–1037. doi:10.1002/tcr.202000167
13. Ibarra, I. A.; Islas-Jácome, A.; González-Zamora, E. *Org. Biomol. Chem.* **2018,** *16,* 1402–1418. doi:10.1039/c7ob02305g
14. Mohammadkhani, L.; Heravi, M. M. *Mol. Diversity* **2020,** *24,* 841–853. doi:10.1007/s11030-019-09972-1
15. Fouad, M. A.; Abdel-Hamid, H.; Ayoup, M. S. *RSC Adv.* **2020,** *10,* 42644–42681. doi:10.1039/d0ra07501a
16. Dömling, A.; Wang, W.; Wang, K. *Chem. Rev.* **2012,** *112,* 3083–3135. doi:10.1021/cr100233r
17. Nikoofar, K.; Yielzoleh, F. M. *Curr. Org. Synth.* **2022,** *19,* 115–147. doi:10.2174/1570179418666210910111208
18. Ma, X.; Zhi, S.; Zhang, W. *Molecules* **2021,** *26,* 1986. doi:10.3390/molecules26071986
19. Brauch, S.; van Berkel, S. S.; Westermann, B. *Chem. Soc. Rev.* **2013,** *42,* 4948–4962. doi:10.1039/c3cs35505e
20. Lei, X.; Lampiri, P.; Patil, P.; Angeli, G.; Neochoritis, C. G.; Dömling, A. *Chem. Commun.* **2021,** *57,* 6652–6655. doi:10.1039/d1cc02384e
21. Nikbakht, A.; Balalaie, S.; Baghestani, F.; Rominger, F. *Synlett* **2018,** *29,* 1892–1896. doi:10.1055/s-0037-1610502
22. Salahi, S.; Ghandi, M.; Abbasi, A. *J. Heterocycl. Chem.* **2019,** *56,* 1296–1305. doi:10.1002/jhet.3499
23. Aguilar-Morales, C. M.; Alejandre-Castañeda, V.; Contreras-Celedón, C.; Ramírez-Díaz, M. I.; Islas-Jácome, A.; Meza-Carmen, V.; Chacón-García, L.; Cortés-García, C. J. *Org. Biomol. Chem.* **2024,** *22,* 7240–7244. doi:10.1039/d4ob00995a
24. Aguilar-Morales, C. M.; Servín-García, G.; del Río, R. E.; Islas-Jácome, A.; Gámez-Montaño, R.; Chacón-García, L.; Cortés-García, C. J. *Synth. Commun.* **2023,** *53,* 127–134. doi:10.1080/00397911.2022.2154165

25. Niño-Pantoja, I.; GallardoAlfonzo, A.; SolisSantos, M.; Ordoñez, M.; ContrerasCeledón, C.; IslasJácome, A.; ChacónGarcía, L.; CortésGarcía, C. J. *Eur. J. Org. Chem.* **2022,** e202200230. doi:10.1002/ejoc.202200230
26. Aguilar-Morales, C. M.; Araujo-Huitrado, J. G.; López-Hernández, Y.; Contreras-Celedón, C.; Islas-Jácome, A.; Granados-López, A. J.; Solorio-Alvarado, C. R.; López, J. A.; Chacón-García, L.; Cortés-García, C. J. *Molecules* **2021,** *26,* 6104. doi:10.3390/molecules26206104
27. Aguilar-Morales, C. M.; de Loera, D.; Contreras-Celedón, C.; Cortés-García, C. J.; Chacón-García, L. *Synth. Commun.* **2019,** *49,* 2086–2095. doi:10.1080/00397911.2019.1616301
28. Debnath, S.; Mondal, S. *Tetrahedron Lett.* **2018,** *59,* 2260–2263. doi:10.1016/j.tetlet.2018.04.081
29. Bruneau, A.; Gustafson, K. P. J.; Yuan, N.; Tai, C.-W.; Persson, I.; Zou, X.; Bäckvall, J.-E. *Chem. – Eur. J.* **2017,** *23,* 12886–12891. doi:10.1002/chem.201702614
30. Zhang, H.-C.; Brumfield, K. K.; Jaroskova, L.; Maryanoff, B. E. *Tetrahedron Lett.* **1998,** *39,* 4449–4452. doi:10.1016/s0040-4039(98)00844-2
31. Pharande, S. G.; Corrales Escobosa, A. R.; Gámez-Montaño, R. *Green Chem.* **2017,** *19,* 1259–1262. doi:10.1039/c6gc03324e
32. Reddy, G. S.; Hossain, K. A.; Kumar, J. S.; Thirupataiah, B.; Edwin, R. K.; Giliyaru, V. B.; Chandrashekhar Hariharapura, R.; Shenoy, G. G.; Misra, P.; Pal, M. *RSC Adv.* **2020,** *10,* 289–297. doi:10.1039/c9ra09236f
33. Sujeevan Reddy, G.; Babu Nallapati, S.; Sri Saranya, P. S. V. K.; Sridhar, B.; Bhat Giliyaru, V.; Chandrashekhar Hariharapura, R.; Gautham Shenoy, G.; Pal, M. *Tetrahedron Lett.* **2018,** *59,* 4587–4592. doi:10.1016/j.tetlet.2018.11.037
34. Philoppes, J. N.; Abdelgawad, M. A.; Abourehab, M. A. S.; Sebak, M.; Darwish, M. A.; Lamie, P. F. *J. Enzyme Inhib. Med. Chem.* **2023,** *38,* 246–266. doi:10.1080/14756366.2022.2145283
35. Ran, J.-Q.; Huang, N.; Xu, H.; Yang, L.-M.; Lv, M.; Zheng, Y.-T. *Bioorg. Med. Chem. Lett.* **2010,** *20,* 3534–3536. doi:10.1016/j.bmcl.2010.04.132
36. Wan, Y.; Li, Y.; Yan, C.; Yan, M.; Tang, Z. *Eur. J. Med. Chem.* **2019,** *183,* 111691. doi:10.1016/j.ejmech.2019.111691
37. Venkateshwarlu, R.; Nath Singh, S.; Siddaiah, V.; Ramamohan, H.; Dandela, R.; Amirul Hossain, K.; Vijaya Babu, P.; Pal, M. *Bioorg. Med. Chem. Lett.* **2020,** *30,* 127112. doi:10.1016/j.bmcl.2020.127112
38. Vijaya Babu, P.; Ashfaq, M. A.; Shiva Kumar, K.; Mukkanti, K.; Pal, M. *Arabian J. Chem.* **2019,** *12,* 2749–2759. doi:10.1016/j.arabjc.2015.05.018
39. Tréguier, B.; Rasolofonjatovo, E.; Hamze, A.; Provot, O.; Wdzieczak-Bakala, J.; Dubois, J.; Brion, J.-D.; Alami, M. *Eur. J. Org. Chem.* **2011,** 4868–4876. doi:10.1002/ejoc.201100540
40. Ataollahi, M. R.; Sharifi, J.; Paknahad, M. R.; Paknahad, A. *J. Med. Life* **2015,** *8* (Suppl. 4), 6–11.
41. Sharma, G. N.; Dave, R.; Sanadya, J.; Sharma, P.; Sharma, K. K. *J. Adv. Pharm. Technol. Res.* **2010,** *1,* 109–126.
42. Ferlay, J.; Colombet, M.; Soerjomataram, I.; Mathers, C.; Parkin, D. M.; Piñeros, M.; Znaor, A.; Bray, F. *Int. J. Cancer* **2019,** *144,* 1941–1953. doi:10.1002/ijc.31937
43. Akram, M.; Iqbal, M.; Daniyal, M.; Khan, A. U. *Biol. Res.* **2017,** *50,* 33. doi:10.1186/s40659-017-0140-9
44. Kamath, P. R.; Sunil, D.; Joseph, M. M.; Abdul Salam, A. A.; T.T., S. *Eur. J. Med. Chem.* **2017,** *136,* 442–451. doi:10.1016/j.ejmech.2017.05.032
45. Singla, R.; Gupta, K. B.; Upadhyay, S.; Dhiman, M.; Jaitak, V. *Eur. J. Med. Chem.* **2018,** *146,* 206–219. doi:10.1016/j.ejmech.2018.01.051
46. Mato, M.; Franchino, A.; Garcıa-Morales, C.; Echavarren, A. M. *Chem. Rev.* **2021,** *121,* 8613–8684. doi:10.1021/acs.chemrev.0c00697
47. Gazdar, A. F.; Kurvari, V.; Virmani, A.; Gollahon, L.; Sakaguchi, M.; Westerfield, M.; Kodagoda, D.; Stasny, V.; Cunningham, H. T.; Wistuba, I. I.; Tomlinson, G.; Tonk, V.; Ashfaq, R.; Leitch, A. M.; Minna, J. D.; Shay, J. W. *Int. J. Cancer* **1998,** *78,* 766–774. doi:10.1002/(sici)1097-0215(19981209)78:6<766::aid-ijc15>3.0.co;2-l
48. Brandes, L. J.; Hermonat, M. W. *Cancer Res.* **1983,** *43,* 2831–2835.
49. Fogh, J.; Wright, W. C.; Loveless, J. D. *J. Natl. Cancer Inst.* **1977,** *58,* 209–214. doi:10.1093/jnci/58.2.209

License and Terms

This is an open access article licensed under the terms of the Beilstein-Institut Open Access License Agreement (https://www.beilstein-journals.org/bjoc/terms), which is identical to the Creative Commons Attribution 4.0 International License (https://creativecommons.org/licenses/by/4.0). The reuse of material under this license requires that the author(s), source and license are credited. Third-party material in this article could be subject to other licenses (typically indicated in the credit line), and in this case, users are required to obtain permission from the license holder to reuse the material.

The definitive version of this article is the electronic one which can be found at:
https://doi.org/10.3762/bjoc.20.256

BEILSTEIN JOURNAL OF ORGANIC CHEMISTRY

Multicomponent reactions driving the discovery and optimization of agents targeting central nervous system pathologies

Lucía Campos-Prieto[‡1,2], Aitor García-Rey[‡1,2], Eddy Sotelo[1,2] and Ana Mallo-Abreu[*3,4]

Review

Open Access

Address:
[1]Centro Singular de Investigación en Química Biolóxica e Materiais Moleculares (CIQUS), Universidade de Santiago de Compostela, 15782 Santiago de Compostela, Spain, [2]Departamento de Química Orgánica, Facultade de Farmacia, Universidade de Santiago de Compostela, 15782 Santiago de Compostela, Spain, [3]Laboratory of Medicinal Chemistry (CSIC Associated Unit), Faculty of Pharmacy and Food Sciences, University of Barcelona, Av. Joan XXIII, 27-31, E-08028 Barcelona, Spain and [4]Institute of Biomedicine of the University of Barcelona (IBUB), Av. Diagonal 643, E-08028 Barcelona, Spain

Email:
Ana Mallo-Abreu[*] - ana.mallo.abreu@ub.edu

* Corresponding author ‡ Equal contributors

Keywords:
Alzheimer; depression; epilepsy; multicomponent reactions; Parkinson; schizophrenia

Beilstein J. Org. Chem. **2024,** *20,* 3151–3173.
https://doi.org/10.3762/bjoc.20.261

Received: 08 August 2024
Accepted: 19 November 2024
Published: 03 December 2024

This article is part of the thematic issue "Multicomponent reactions IV".

Associate Editor: T. J. J. Müller

© 2024 Campos-Prieto et al.; licensee Beilstein-Institut.
License and terms: see end of document.

Abstract

The ongoing quest to discover effective treatments for diseases remains a significant challenge for the scientific community. Multicomponent reactions (MCRs) have emerged as powerful tools in accelerating drug discovery, enabling the rapid generation of chemical libraries with high diversity in a time-efficient and environmentally sustainable manner. In this review, we focus on central nervous system (CNS) disorders, particularly Alzheimer's disease, Parkinson's disease, schizophrenia, depression, and epilepsy, where MCRs have contributed to the development of promising ligands in recent years. Rather than providing an exhaustive overview, this review aims to highlight key studies that address major CNS pathologies, relevant drug targets, and various MCR approaches. We have carefully selected representative articles and apologize to the authors whose important contributions may not be included. By concentrating on these pivotal studies, we strive to offer a clear and concise perspective on current research trends and breakthroughs in this field.

Introduction

Multicomponent reactions

Due to efforts to develop new drug arsenals faster to overcome the difficulties of medicinal chemistry (multistage and highly wasteful processes), multicomponent reactions (MCRs) have emerged as a plausible solution. MCRs are convergent reactions in which three or more reagents are combined in one step to yield a single product that contains most of the atoms from

the starting materials [1,2]. Among the advantages of MCRs are their high atom economy and efficiency in bond formation, along with the cost-effectiveness of separating and purifying products [3]. These aspects are aligned with the goal of addressing concerns related to the generation of environmentally hazardous waste [4]. In addition, this type of reaction allows for the efficient discovery of low molecular weight compounds. As a result, most of these compounds are drug-like according to Lipinski's rule of five (Ro5) [5].

Classical examples of MCRs include Ugi [6], Passerini [7], Hantzsch [8], Bucherer-Bergs [9], Gewald [10], and Petasis reactions [11], among others (Figure 1). Additionally, recent advancements have been seen in the discovery of novel MCRs by combination with other approaches such as visible light, microwaves, heterogeneous catalysis, and ultrasound [12-15].

Due to its versatility, one of the most prevalent of these MCRs is the Ugi reaction [16]. This reaction generally combines an isocyanide with an acid, an amine, and an aldehyde or ketone to obtain α-acylaminoamides. Innovation in recent years with alternative reagents, like *N*-hydroxyimides or nitric acid in place of an acid, *N*-alkylated hydrazines, or nitrobenzene derivatives (reduced in situ to anilines) instead of amines, and in situ-prepared isocyanides, makes it a versatile method for synthesizing diverse scaffolds [6].

Furthermore, the Ugi reaction exhibits versatility in forming both fused and unfused heterocyclic compounds, involving 4-, 5-, 6-, and 7-membered rings [17]. This capability is exploited by various approaches, including the Ugi–Deprotection–Cyclization strategy (UDC) and post-modification reactions. Examples of these reactions include the Ugi/Dieckmann reactions, Ugi/Robinson–Gabriel reactions, Ugi/Buchwald–Hartwig reactions, Ugi reaction followed by a catalytic aza-Wittig cyclization, Ugi reaction followed by SNAr strategy, Ugi/Heck reactions, Ugi/Huisgen cycloaddition, and Ugi reactions followed by Mitsunobu cyclization, among other strategies (Figure 2) [16].

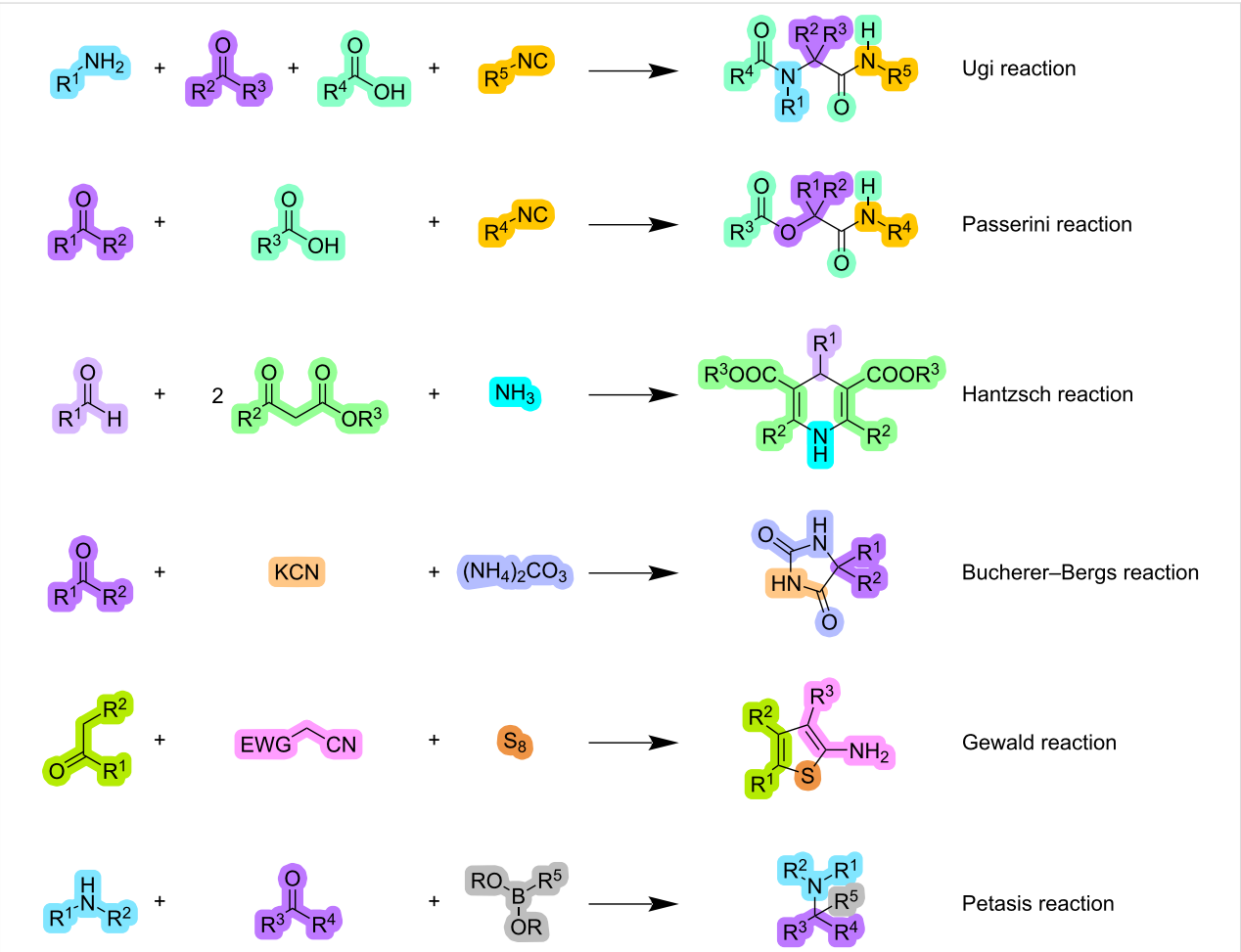

Figure 1: Classical MCRs.

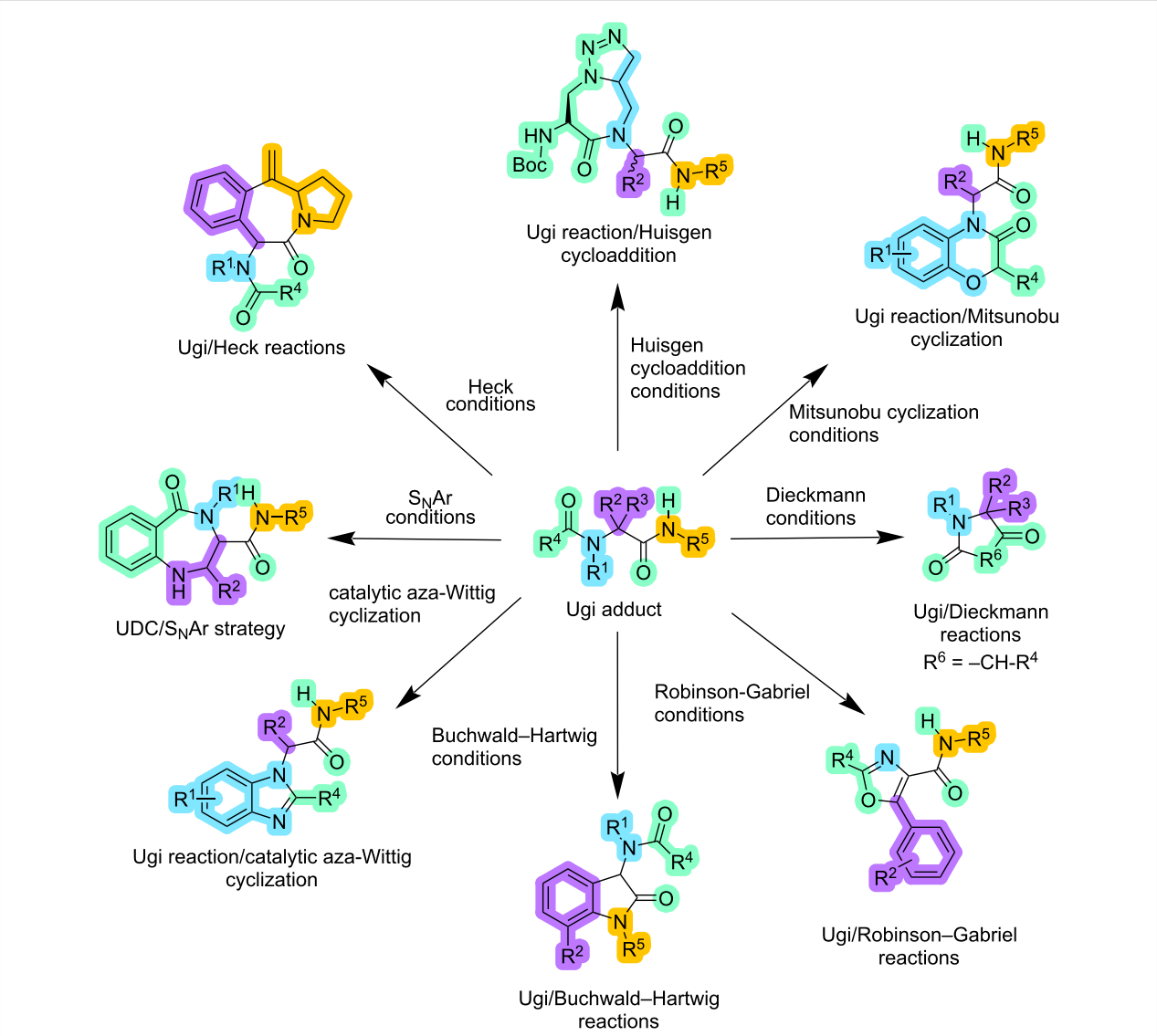

Figure 2: Different scaffolds that can be formed with the Ugi adduct.

Central nervous system diseases

Central nervous system (CNS) diseases are the main cause of disability and the second cause of mortality worldwide, indeed, according to the 2019 World Health Organization report stroke ranked second among the leading causes of disease globally, followed by Alzheimer's disease (AD), and other dementias [18,19]. CNS diseases can be classified according to the etiological and pathological features into traumatic diseases, such as spinal cord and traumatic brain injuries, neurodegenerative diseases, such as AD and Parkinson's disease (PD), demyelinating diseases such as multiple sclerosis (MS), etc. [20].

However, despite advances in the etiology of psychosis indicating both polygenetic and environmental factors, significant gaps remain [21]. Psychosis is a subgroup of severe mental illnesses characterized by delusions, hallucinations, and disorganized behavior. This illness can manifest itself across a spectrum of conditions such as major depressive disorder (MDD), bipolar disorder, delusional and schizophreniform disorder. The prototypical psychotic disorder is schizophrenia, which is a chronic and debilitating condition whose etiology is unclear and about which there are many different hypotheses [20,21]. In the case of MDD, even though the etiology is unknown, there are several models that have focused on genes, environmental factors, and gene–environment interactions [22]. In relation to epilepsy, the etiology of seizures depends on age. In children, seizures are frequently originated by genetic factors, malformations of cortical evolution, and injuries from perinatal events. In adults lacking an inherited tendency, typical causes include encephalitis or meningitis, traumatic brain injuries, and brain

tumors. Finally, in elderhood, seizures are often linked to primary craniocephalic trauma, brain tumors, and neurodegenerative disorders [23].

This review centers on five neurological disorders where ligands obtained using multicomponent reactions (MCRs) have been identified: Alzheimer's disease, Parkinson's disease, depression, schizophrenia, and epilepsy. Our goal is not to provide a comprehensive survey but rather to spotlight key studies that address significant CNS disorders, pertinent drug targets, and various MCR methodologies. We have thoughtfully selected representative articles and extend our apologies to authors whose important works may not be included. By focusing on these studies, we aim to present a clear and concise view of current research directions and significant advancements in the field.

Review

Ligands targeting CNS diseases obtained from MCR approaches

Alzheimer's disease (AD)

The pathogenesis of AD is still not clear but is marked as a multifactorial disease [24], including a good deal of hypotheses involving the cholinergic hypothesis, glutamate excitotoxicity, tau aggregation, abnormal extracellular accumulation of Aβ peptides, and oxidative stress (OS) [25].

Alzheimer's disease (AD) is commonly thought to emerge from a deficiency of the neurotransmitter acetylcholine (ACh) in neuronal and neuromuscular regions, according to the most recognized theory. This deficit may be caused by reduced synthesis or enzymatic function of acetylcholinesterase (AChE) on ACh. Among the five drugs prescribed for AD, four (donepezil, rivastigmine, galantamine, and tacrine) are built upon the cholinergic hypothesis [26]. In contrast, memantine emerges as the only drug available that targets the glutamatergic system for AD, functioning as a non-competitive antagonist of the *N*-methyl-D-aspartate (NMDA) receptor to regulate excessive glutamate stimulation [27]. The β-amyloid hypothesis for AD is based on the formation of senile plaques, which are formed after the accumulation of insoluble aggregates of β-amyloid protein, primarily Aβ-42, in the brain. The gene for amyloid precursor protein (APP), found on chromosome 21, undergoes a mutation that causes the production of Aβ-42 instead of Aβ-40. APP, a transmembrane protein, is typically cleaved by α-secretase and γ-secretase, which leads to the formation of soluble Aβ-40. However, when cleaved by β-secretase and γ-secretase, it produces Aβ-42. This form misfolds, leading to the formation of insoluble protein aggregates known as senile plaques, causing toxicity [28,29]. Oxidative stress occurs when there is an imbalance between prooxidants and antioxidants in the body, leading to damage in various biomolecules like DNA and lipids. Lipid peroxidation and membrane disruption can cause random cross-linking, resulting in cell death and the fragmentation of proteins and enzymes. Elevated concentrations of reactive oxygen species (ROS) from various molecular processes contribute to the oxidation of proteins, nucleic acids, polysaccharides, and lipids. These modifications can impact the structure and biological functions of these molecules, ultimately leading to neuronal death, as observed in conditions like AD [30,31].

Recent studies highlight OS as an early event in AD pathogenesis, and mitochondria-directed and metabolic antioxidants have shown efficacy in AD mouse models, with ongoing trials for vitamin E and selenium [32].

Ugi reaction: As already mentioned, one of the main targets in AD treatment are cholinesterase ligands. In recent years, butyrylcholinesterase, an enzyme present in high concentrations in the later stages of this pathology, has been gaining attention for the treatment of this disease. In 2021, Brandão et al. [33] developed a series of molecules inspired by the oxoindole-β-lactam core, a structural motif, present in many acetylcholinesterase inhibitor drugs, through the Ugi reaction (Scheme 1). A wide variety of isatins were suitable for performing the 4-center 3-component Ugi reaction (U4C-3CR), as well as isocyanides. Using 3-aminopropanoic acid (or β-alanine) and 4-aminobutanoic acid (or γ-aminobutyric acid), the corresponding β- and γ-lactam derivatives were obtained, respectively.

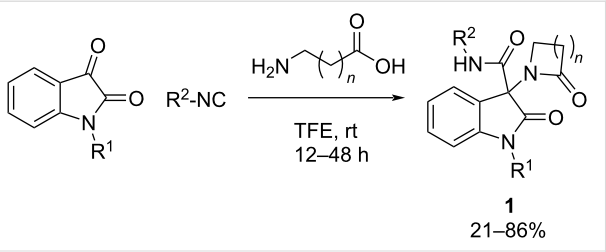

Scheme 1: Oxoindole-β-lactam core produced in a U4C-3CR.

For the evaluation of the inhibitory activity of the compounds, model cholinesterases type VI-S, purified from *Electrophorus electricus* (EeAChE) and butyrylcholinesterase, purified from equine serum (eqBuChE) were employed. Only one compound showed moderate inhibitory activity (IC_{50} = 45 μM) on EeAChE. On the other hand, the inhibitory activity on eqBuChE was more promising, with the best scoring compounds being **1a**, **1b**, and **1c** (Figure 3). These compounds have mixed inhibitory activity (they can bind both the free enzyme and the enzyme–substrate complex, E–S complex). Additional-

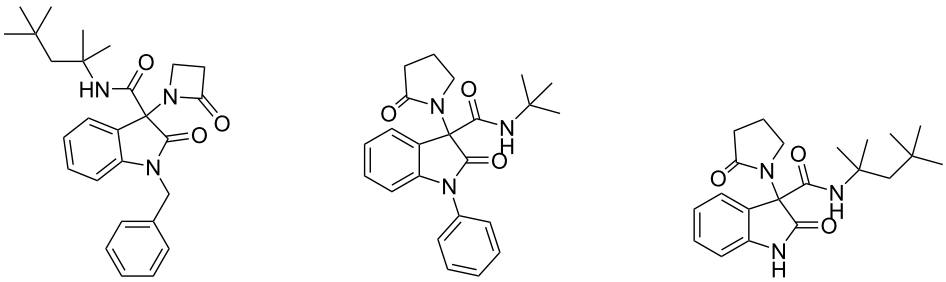

Figure 3: Most active oxoindole-β-lactam compounds developed by Brăndao et al. [33].

ly, compound **1a** showed more potency than galantamine (IC_{50} = 3.9 μM), a cholinesterase inhibitor in clinical use against AD.

In the search for novel ligands for Alzheimer's treatment, a common strategy involves the combination of structural fragments from different molecules. This concept often yields new compounds with improved biological activities. Employing this approach, Kushwaha et al. [34] synthesized a series of compounds containing benzofuran, tetrazole, and pyrazole within a single structure (Scheme 2). Benzofurans and tetrazole pharmacophores have demonstrated potential anti-Alzheimer activity by inhibiting AChE, while pyrazole scaffolds possess the ability to reduce the tau and β-amyloid dual aggregation. Benzofuran-pyrazole aldehydes were employed in the Ugi azide reaction to give the desired hybrids.

From the screened compounds, **2a**, **2b**, **2c**, **2d**, **2e**, and **2f** demonstrated notable efficacy in regulating the paralysis rate of worms (Figure 4). Specifically, they exhibited a percentage of paralysis inhibition of 67%, 47%, 57%, 42%, 45%, and 64%, respectively, which indicates their potential in inhibiting β-amyloid toxicity in AD. These compounds were selected to assess their potential as acetylcholinesterase inhibitors, and their effects were investigated using the Amplex-Red® kit in *C. elegans*. Individuals exposed to compounds **2a**, **2b**, **2c**, **2d**, **2e**, and **2f** at a concentration of 1 mM were analyzed for AChE activity in their extracts. The results revealed significant inhibition of AChE levels, with compound **2e** demonstrating the highest potential among the tested compounds against acetylcholinesterase.

Furthermore, Pachón-Angona et al. [35] synthesized hybrid molecules using the Ugi reaction (Scheme 3), with antioxidant compounds as starting substrates, pursuing the aim of developing more powerful antioxidants.

The antioxidant properties were determined by oxygen radical absorbance capacity assay (ORAC-FL), expressed as Trolox equivalents (TE) and using fluorescein as probe. Additionally, the study investigated the ability of the compounds to activate the nuclear factor (erythroid-derived 2)-like 2 (Nrf2) pathway in cells containing the Nrf2/antioxidant response element (ARE).

The melatonin–lipoic acid (LA) hybrids **3a** and **3b** emerged as potent antioxidants, successfully inducing the Nrf2 transcrip-

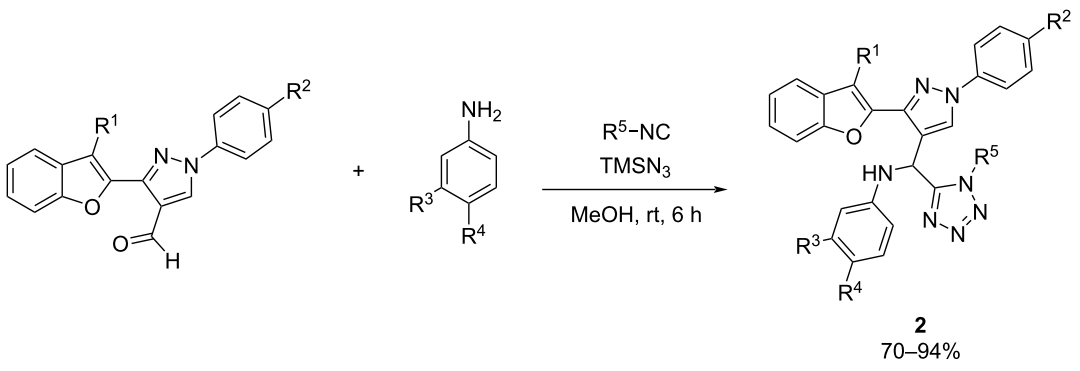

Scheme 2: Ugi-azide synthesis of benzofuran, pyrazole and tetrazole hybrids.

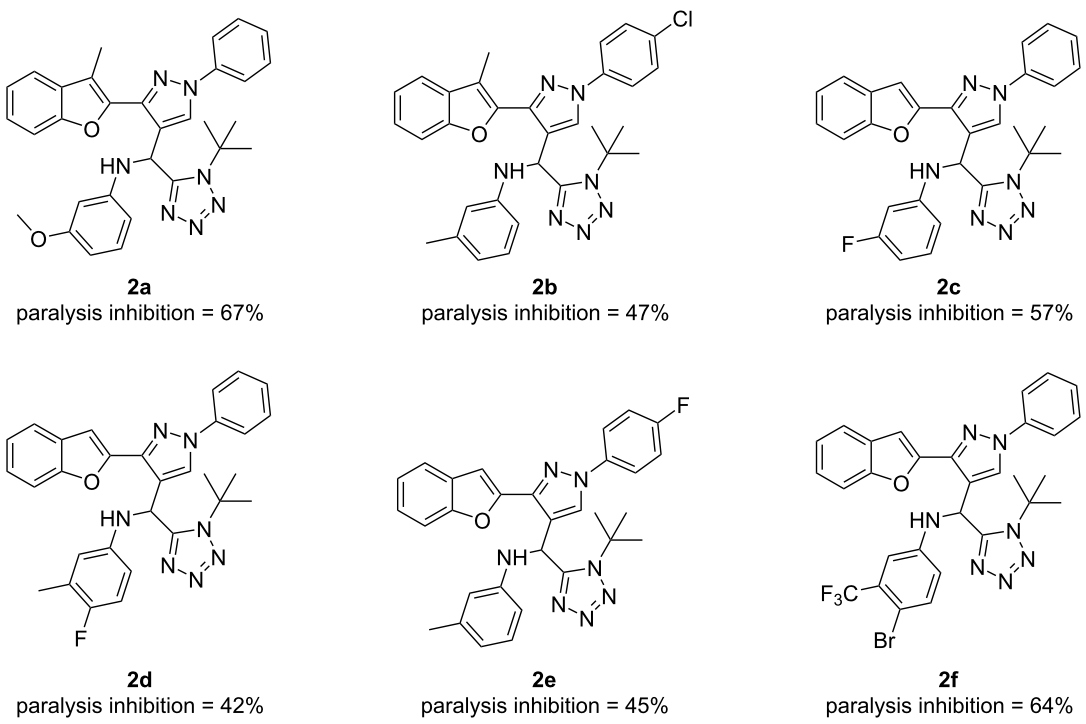

Figure 4: The most promising hybrids synthesized via the Ugi-azide multicomponent reaction reported by Kushwaha et al. [34].

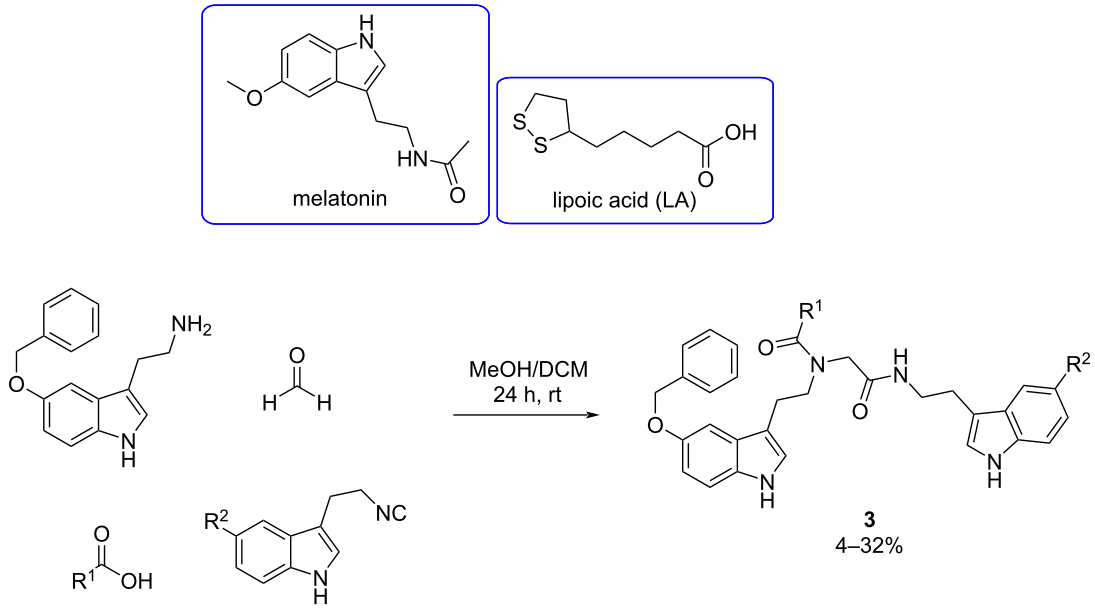

Scheme 3: Four-component Ugi reaction for the synthesis of novel antioxidant compounds.

tional pathway at concentrations of 10, 30, and 100 μM (Figure 5). Notably, these hybrids exhibited lower CD values (28.1 and 31.6 μM, respectively), which is the concentration required to double the specific luciferase reporter activity, compared to melatonin (CD = 66.4 μM). The results suggest that compounds **3a** and **3b** are promising as potent antioxidant ther-

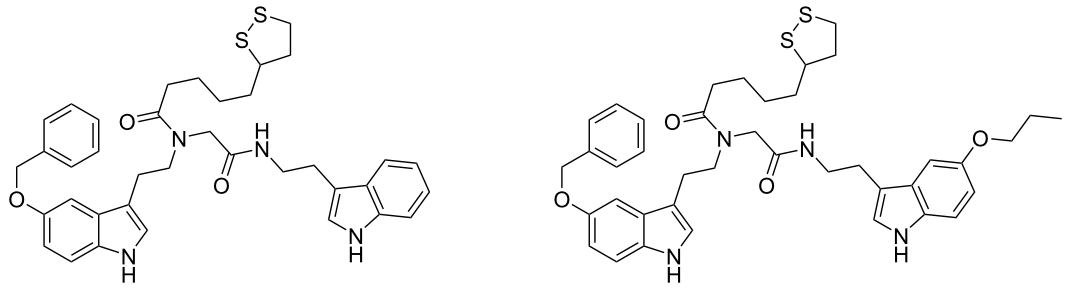

Figure 5: Most potent antioxidant compounds obtained through the Ugi four-component reaction developed by Pachón-Angona et al. [35].

apeutic agents. Furthermore, the results of the ORAC-FL assay were also remarkable, yielding a value 2-fold higher than melatonin (ORAC = 2.45 TE).

Natural polyphenols have shown promising potential in inhibiting β-amyloid aggregation and also antioxidant properties, suggesting their effectiveness in preventing AD. To address this, Lambruschini et al. [36] developed artificial, 'natural-like' polyphenols, using the Ugi reaction, since it leads to mixed polyphenol–peptidomimetic structures (Scheme 4).

The procedure involved an Ugi reaction using phenolic building blocks protected as allyl ethers, followed by deprotection, acetylation, and high-yielding solvolysis of the polyacetates. Also, the Ugi reaction gave the best results when imine preformation was implemented. In this preliminary paper, it was observed that the ferulic derived part was highly significant and for this reason, further experiments were conducted by Galante et al. [37] maintaining the carboxylic building block.

The obtained molecules were evaluated for their ability to inhibit β-amyloid aggregation by the interaction with two β-amyloid peptides, Aβ1-42 and AβpE3-42. The aggregation inhibition experiment, which measures the decrease of fluorescence, was carried out with the thioflavin T methodology highlighting compounds **4a** (Aβ1-42 = 65% and AβpE3-42 = 53% of fluorescence) and **4b** (Aβ1-42 = 50% and AβpE3-42 = 90% of fluorescence) from the first publication and compound **4c**

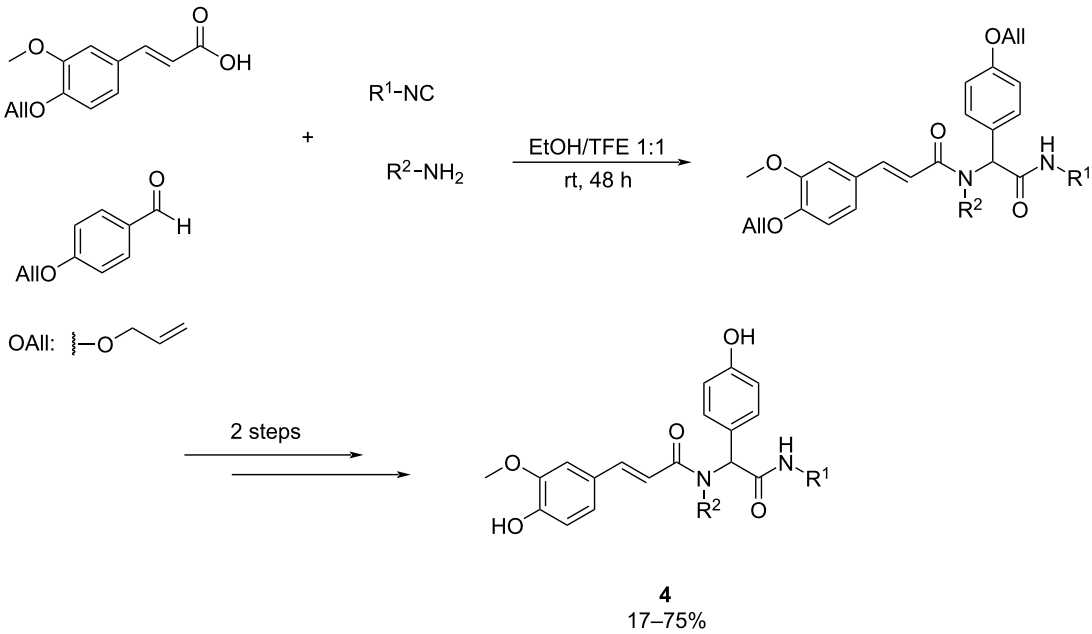

Scheme 4: Four-component Ugi reaction to synthesize β-amiloyd aggregation inhibitors.

(Aβ1-42 = 74% and AβpE3-42 = 51% of fluorescence) from the second one (Figure 6). The latter was able to slightly improve activity towards AβpE3-42 but accomplishing increased solubility.

Due to the multifactorial pathogenesis of AD, one of the current drug discovery approaches is the so-called multitarget-directed ligands (MTDLs). In 2015, Benchekroun et al. [38] reported the design, synthesis, and biological evaluation of a new family of ferulic acid–tacrine hybrids (FATHs), using the Ugi reaction. FATHs were selected because tacrine is a well-known cholinesterase (ChE) inhibitor, although it is hepatotoxic, and ferulic acid is a potent antioxidant.

Fourteen FATH were synthesized and tested for hepatotoxicity, cholinesterase inhibition (human BuChE, hBuChE), Aβ1-42 self-aggregation inhibition, and antioxidant activity. FATH **5a** (Scheme 5) emerged as a promising candidate, showing lower

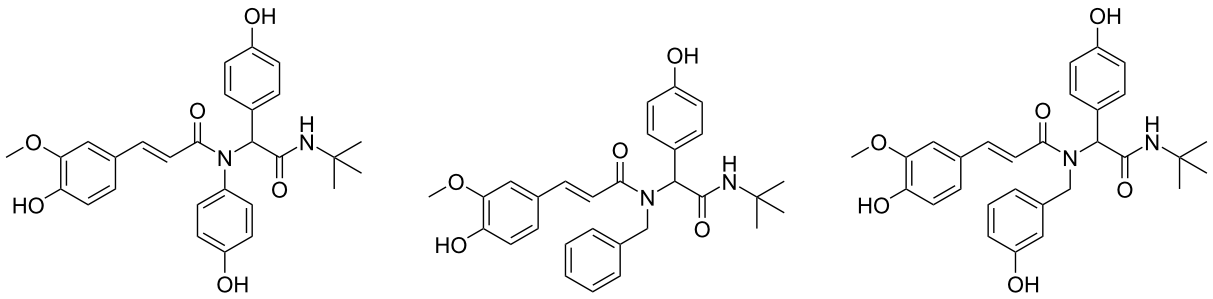

Figure 6: The most potential β-amiloyd aggregation inhibitors generated by Galante et al. [37].

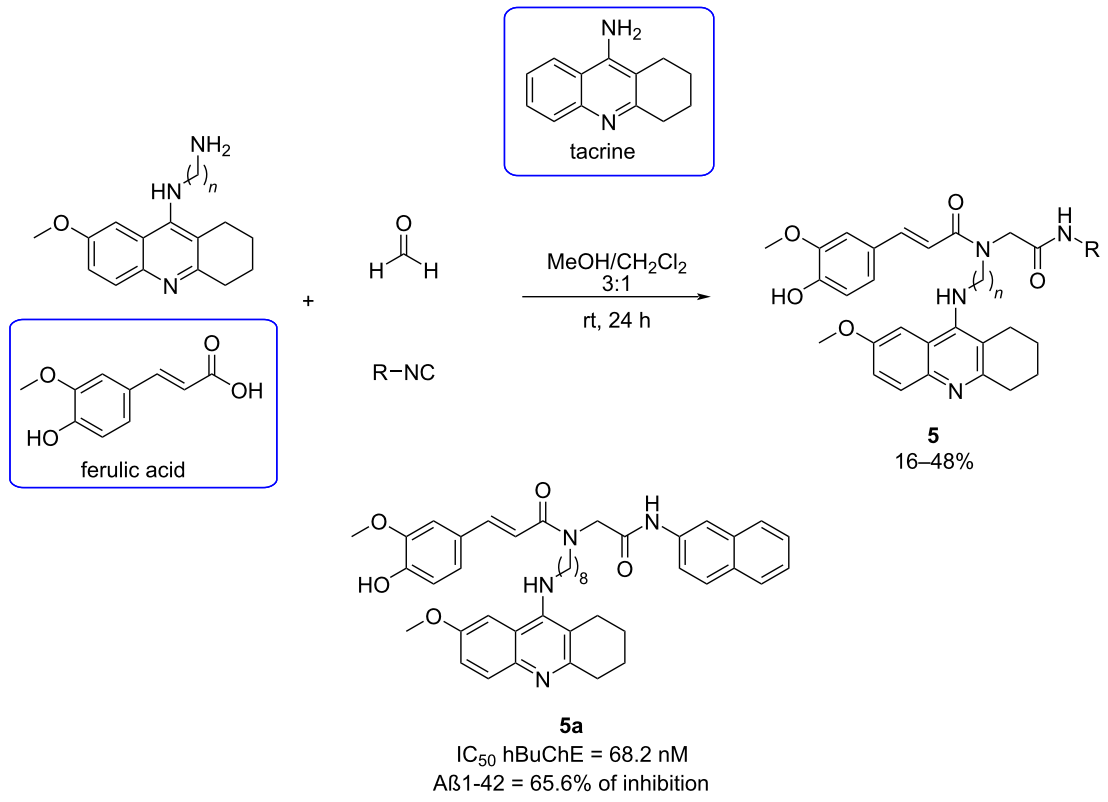

Scheme 5: Four-component Ugi reaction to obtain FATH hybrids and the best candidate synthesized.

hepatotoxicity at 1000 μM (59.4%, 1.72-fold less toxic than tacrine), moderate and selective hBuChE inhibition (IC_{50} = 68.2 nM), strong antioxidant properties and notable inhibition of Aβ1-42 self-aggregation (65.6% of inhibition). These findings suggest FATH **5a** as a potential lead compound for further investigation in AD therapy.

In 2016, the same group developed ferulic acid–tacrine–melatonin hybrids (FATMHs) and lipoic acid–tacrine–melatonin hybrids (LATMHs), deciding to incorporate melatonin as a new target for the MTDL [39]. Melatonin has the ability to combat OS, which is a crucial factor in the pathogenesis of AD. Moreover, it plays a neuroprotective role against Aβ-peptides and easily crosses the blood–brain barrier (BBB). Finally, recent research has implicated melatonin in modulating the Nrf2/ARE pathway, a crucial defense mechanism against OS and inflammation.

In this study, FATMHs and LATMHs were synthesized through Ugi reaction and evaluated for their therapeutic potential in AD. Among these compounds, FATMH **6a** emerged as a remarkable candidate, demonstrating strong antioxidant properties (9.11 TE), potent cholinesterases inhibition, particularly BuChE [IC_{50} (hAChE) = 1290 nM; IC_{50} (hBuChE) = 234 nM], positive non-hepatotoxic profile (at 100, 300, and 1000 μM) compared to tacrine, and favorable neuroprotective effects against toxic insults such as H_2O_2 and Aβ-peptides (Scheme 6). Additionally, compound **6a** showed promising activity in activating the Nrf2 signaling pathway, indicating its potential to mitigate OS and inflammation in AD. These findings highlight FATMH **6a** as a promising lead compound for further development as a therapeutic agent for AD.

Petasis reaction: Continuing in the context of the development of MTDLs, in 2023 Madhav et al. [40] reported the synthesis of pyrazine-based MTDLs using the Petasis reaction, which involves a secondary amine, a suitable aldehyde, and a substituted boronic acid in the presence of MeCN, under inert atmospheric conditions at 90 ºC for 14 h (Scheme 7).

The efficacy of these MTDLs was assessed in terms of their ability to inhibit AChE and tau aggregation, along with their neuroprotective effects on the SH-SY5Y cell line. The evaluation of hAChE inhibitory action was conducted at a concentration of 10 μM, with donepezil serving as a positive control. To measure their impact on cellular tau oligomerization, the fluorescence resonance energy transfer (FRET) signal intensity was quantified in a cellular tau FRET assay at the same 10 μM concentration, using MK-886, a known tau-oligomerization inhibitor, as the positive control. Two compounds (**7a** and **7b**,

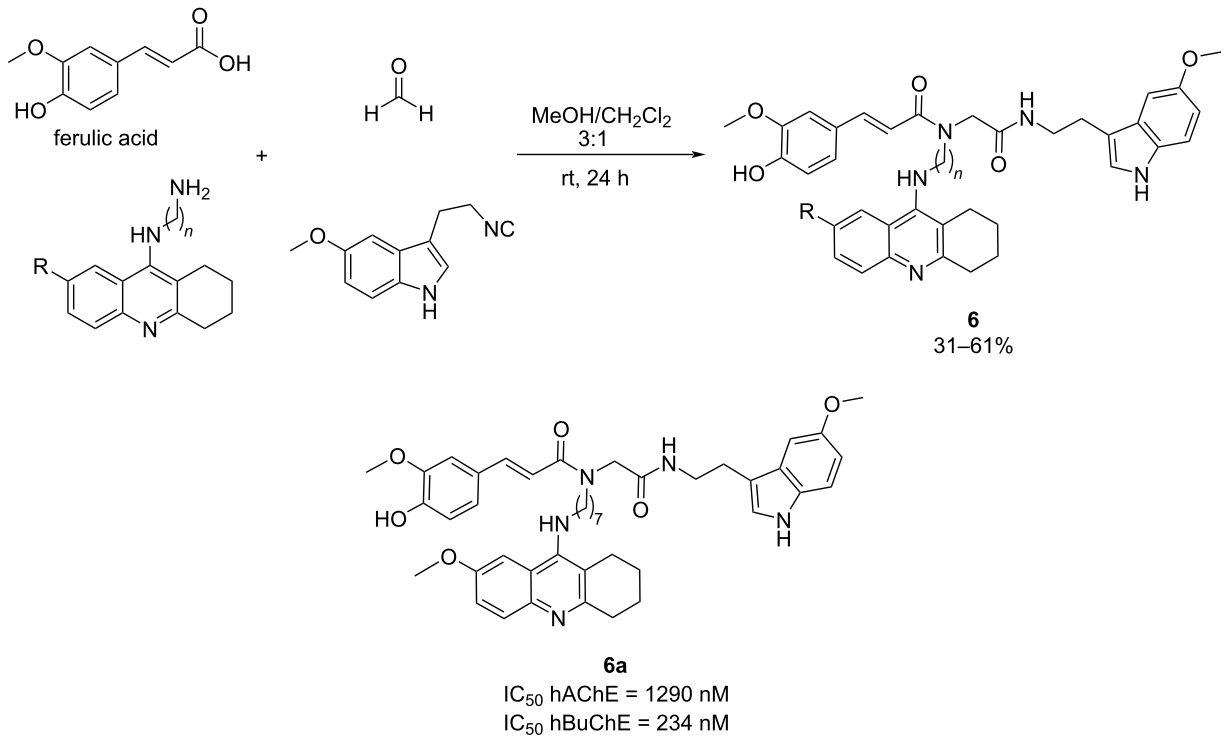

Scheme 6: Four-component Ugi reaction for the synthesis of FATMH hybrids and the best candidate synthesized.

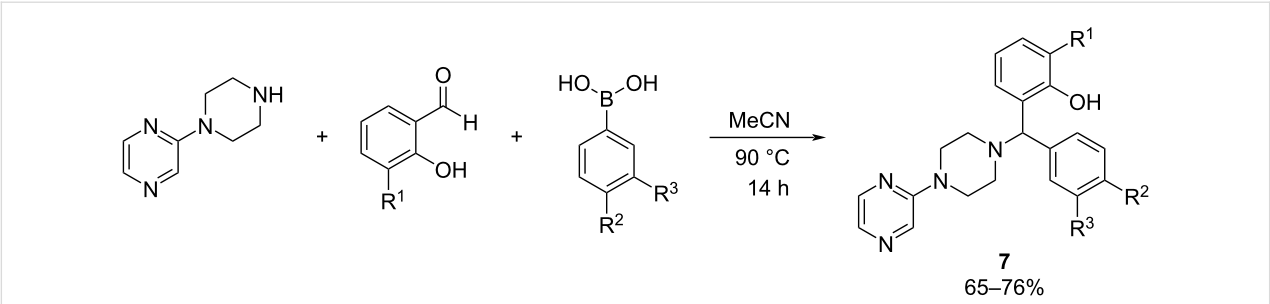

Scheme 7: Petasis multicomponent reaction to produce pyrazine-based MTDLs.

Figure 7) demonstrated a high inhibitory activity against AChE and tau-oligomerization, which were selected for further exploration.

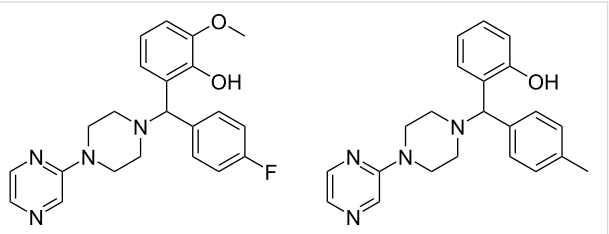

Figure 7: Best pyrazine-based MTDLs synthesized by Madhav et al. [40].

The neuroprotective effects of the compounds were assessed in comparison to MK-886 and donepezil, employing a widely accepted tauopathy model in SH-SY5Y cells. Notably, compound **7a** was identified as the most promising multitarget-directed ligand in the study, exhibiting superior neuroprotection compared to both MK-886 and the commercial drug donepezil in a cell viability MTT assay. These findings reinforced the theory that developing MTDLs could provide a more effective approach for addressing complex neurodegenerative disorders than conventional single-target strategies.

Knoevenagel-based multicomponent reactions: Several quinazolinone derivatives have already been developed as MTDLs, inspired by natural alkaloids such as deoxyvasicinone and evodiamine with promising inhibition of ChEs and antioxidant and neuroprotective effects against glutamate-induced OS in HT-22 cells [41].

In 2016, Dgachi et al. [42] applied a Knoevenagel-based multicomponent approach to further explore the quinazolinone scaffold. They have obtained new benzochromenopyrimidinones, abbreviated as BCPOs, whose synthesis has been accomplished in two steps. First, a microwave-assisted reaction of ethyl cyanoacetate, selected aromatic aldehydes, and 2-naphthol was performed. The second step was the condensation of the obtained intermediates with the appropriate commercial lactams, under microwave irradiation (Scheme 8).

As a result, compound **8a** has been identified as a promising derivative potentially useful in further AD drug discovery for its antioxidant activity (4.7 TE in ORAC-FL assay), moderate hAChE inhibition (IC_{50} = 1.28 μM), and non-toxicity in liver HepG2 cells.

Hantzsch-based strategies: As mentioned before, in response to the challenges posed by the multifactorial nature of AD, the MTDL approach has emerged as a promising strategy. This approach involves designing drugs capable of binding simultaneously to various enzymatic systems or receptors implicated in AD pathology. In 2019, Malek et al. [43] designed and obtained a new family of 1,4-dihydropyridines (DHPs), as a series of MTDLs, which were prepared using a multicomponent reaction, particularly the Hantzsch reaction (Scheme 9).

The synthesized DHPs result from the juxtaposition of nimodipine, a well-known calcium channel blocker and melatonin, a reputed antioxidant agent. This approach lies in the known association between increased cytosolic calcium levels and the formation of Aβ peptides, which are implicated in AD pathology. Calcium also regulates kinases involved in the hyperphosphorylation of tau, contributing to neurofibrillary tangles. Meanwhile, melatonin is known for its neuroprotective properties, countering oxidative stress by scavenging radical oxygenated species and exhibiting potent antioxidant capacity [44,45].

The calcium channel blockade was determined by the measure of Ca^{2+} influx induced by K^{+}-depolarization in SH-SY5Y neuroblastoma cells, previously loaded with the fluorescent dye Fluo-4AM. On the other hand, the antioxidant activity of the DHPs was evaluated using the ORAC-FL method.

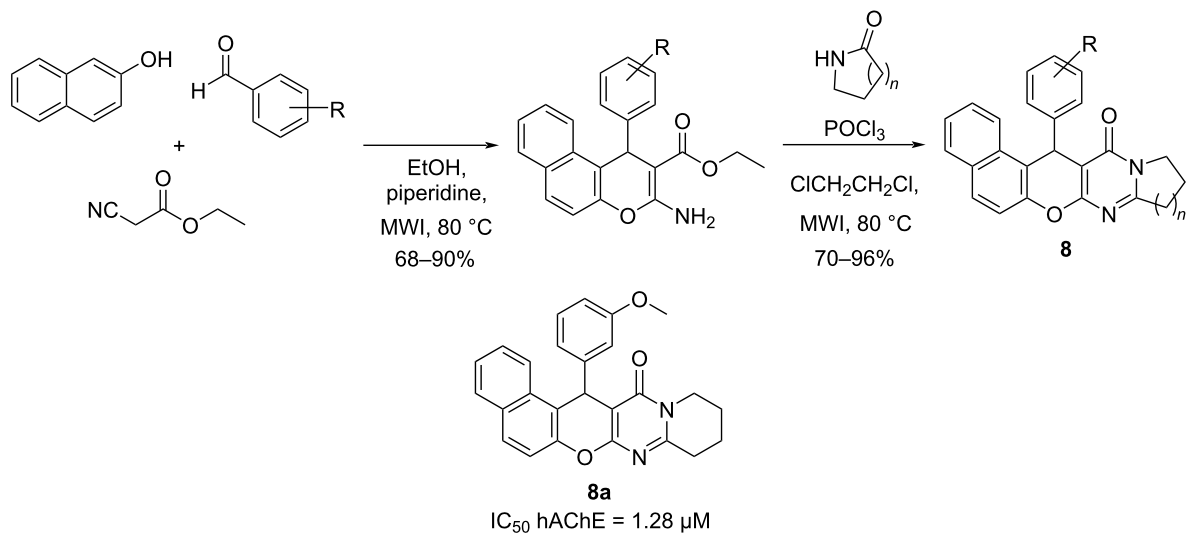

Scheme 8: Synthesis of BCPOs employing a Knoevenagel-based multicomponent reaction and the best candidate synthesized.

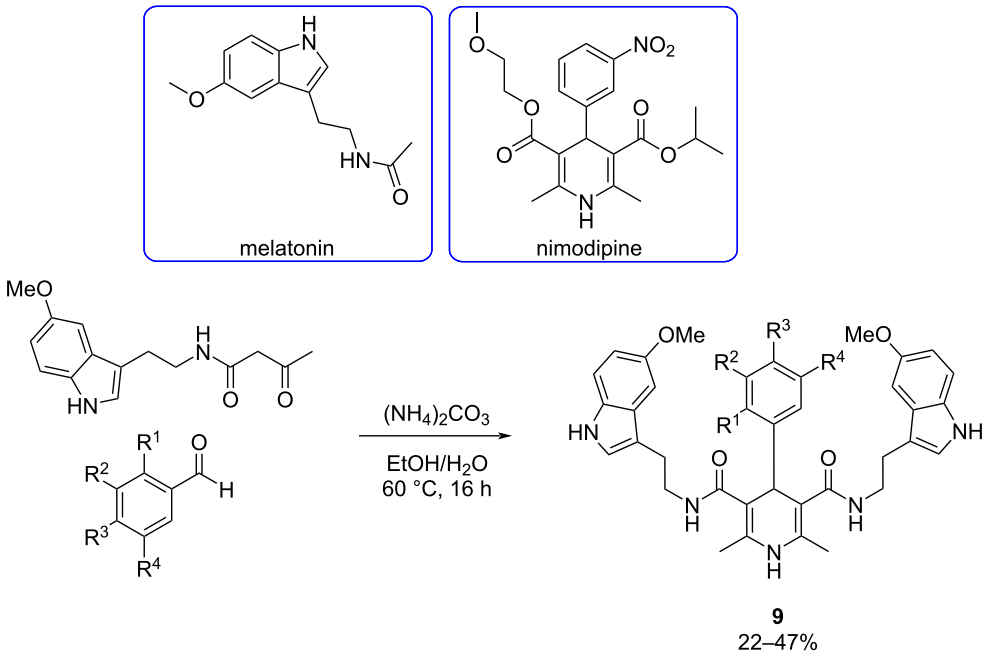

Scheme 9: Hantzsch multicomponent reaction for the synthesis of DHPs as novel MTDLs.

The most potent compounds, particularly DHPs **9a**, **9b**, and **9c**, demonstrated significant efficacy (Figure 8). DHP **9c** emerged as the most balanced MTDLs, being the most potent antioxidant and showing equipotency with nimodipine as a calcium channel blocker, which suggests that DHP **9c** may be promising for potential AD treatment.

Passerini reaction: Based on the power of multicomponent reactions to afford rapidly and efficiently chemical diversity and continuing with an effort to develop new MTDL, Malek et al. [46] described in 2019 the design, synthesis, and the biological evaluation of new racemic chromone donepezil hybrids (CDHs) via Passerini reaction (Scheme 10), combining the antioxidant properties of chromone with the cholinesterase inhibitor (ChEI) donepezil.

The antioxidant activity of the synthesized compounds was evaluated using the ORAC-FL method and the anti-

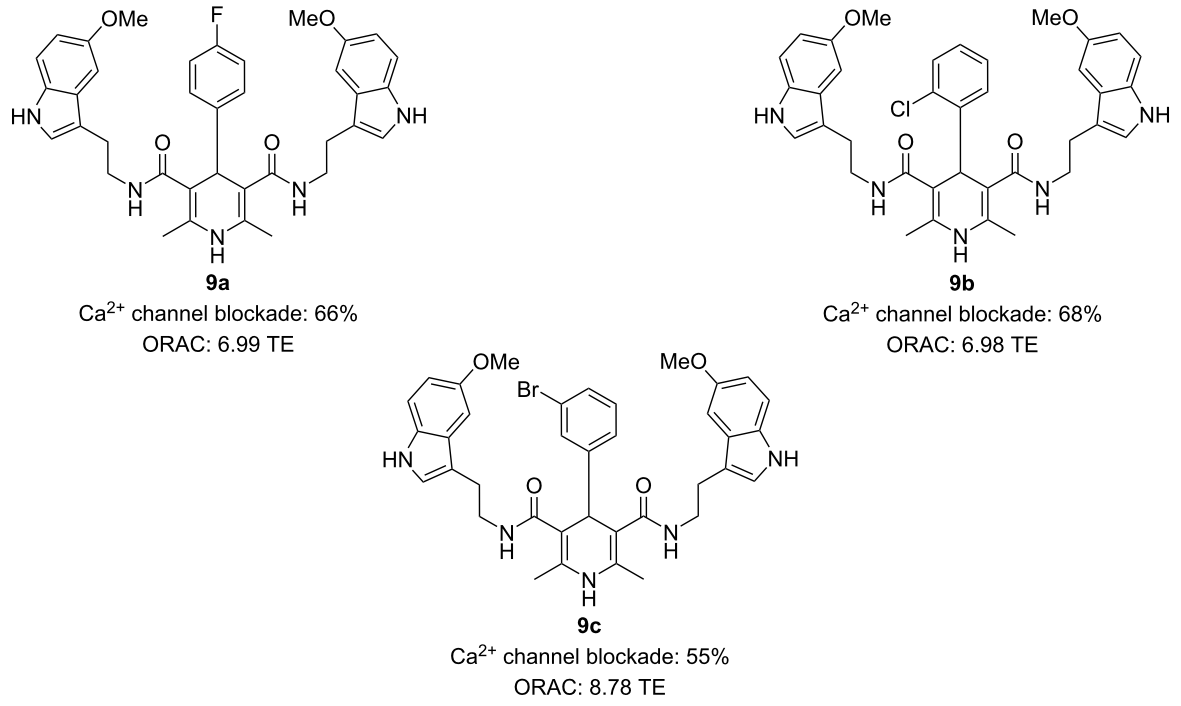

Figure 8: Most active 1,4-dihydropyridines developed by Malek et al. [43].

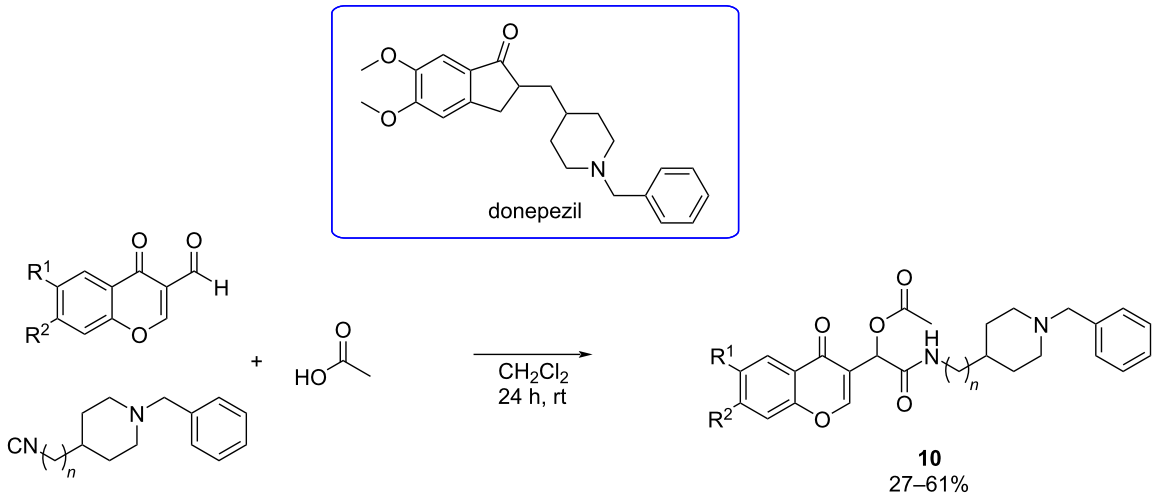

Scheme 10: Chromone–donepezil hybrid MTDLs obtained via the Passerini reaction.

cholinesterase activity against EeAChE and eqBuChE using Ellman's protocol (Figure 9). CDH **10b** emerged as a potent EeAChEI (IC_{50} = 0.30 μM) and CDH **10c** as a strong eqBuChEI (IC_{50} = 0.03 μM), both showing promising activity compared to tacrine and donepezil. A SAR analysis indicated the linker length's crucial role in CDH inhibition activity, as all the compounds with n = 2 were more potent. All compounds were very modest antioxidants compared to ferulic acid, showing values ranging between 0.42–1.27 TE with derivative **10a** being the most potent antioxidant.

The amyloid hypothesis, which states that β-amyloid (Aβ) aggregates cause the onset and progression of AD, is a leading proposal to explain AD etiology. Based on this hypothesis,

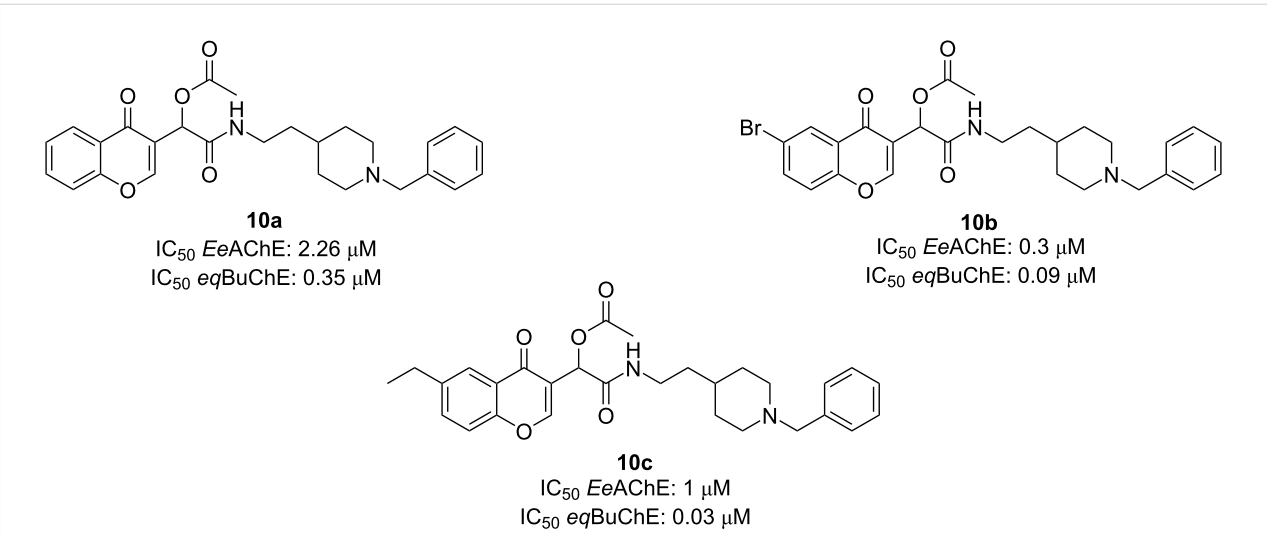

Figure 9: Best CDH-based MTDLs as AChE inhibitors synthesized by Malek et al. [46].

compounds that inhibit γ-secretase, one of the enzymes responsible for forming Aβ, are potential therapeutics for AD.

In 2024, Fragkiadakis et al. [47] developed a rapid synthesis of benzodioxepinones. The attention was focused on the oxazepane scaffold **11** (Scheme 11). Replacing the nitrogen in the bioactive lactam **11** (γ-secretase inhibitor in AD therapy) with an oxygen should reduce the hydrogen bond donating (HBD) ability of the compounds.

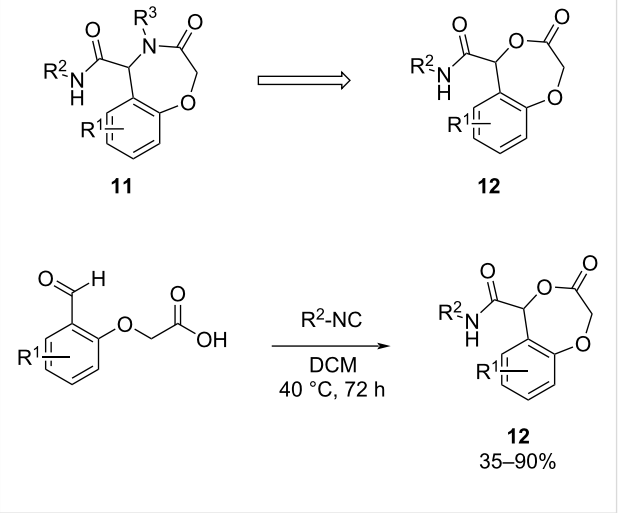

Scheme 11: Replacement of the nitrogen in lactams **11** with an oxygen in **12** to influence hydrogen-bond donating properties and synthesis of the benzodioxepinone derivatives via Passerini reaction.

The method employs readily available starting materials, resulting in the desired compounds in a single step. The oxazepine scaffold can be easily accessed using the Ugi four-component reaction. By modifying this scaffold, the researchers aimed to reduce the hydrogen-bond donating properties. The Passerini reaction, employing bifunctional salicylaldehydes and isocyanides successfully yielded benzodioxepinones **12** in all cases (Scheme 11). The synthesized compounds demonstrated excellent drug-like features.

Parkinson disease (PD)

Knoevenagel–Michael addition/cyclization (MCR 3 + 2): Sirtuins, a group of enzymes that rely on NAD^+ to function as protein deacetylases, have garnered attention across multiple areas, including lifespan extension, obesity, age-associated diseases, neurological function, cardiovascular disorders, and cancer. Notably, the inhibition of sirtuin 2 (SIRT2) has demonstrated protective effects in both primary neuronal cultures and invertebrate models of PD [48]. SIRT2 is present in various tissues, with a prominent expression in the adult brain, where it contributes to metabolic processes, aging, and epigenetic regulation. In this context, the group of Hasaninejad et al. (2017) [49] described the synthesis of spirooxindole, spiroacenaphthylene, and bisbenzo[*b*]pyran derivatives using a multicomponent reaction to obtain SIRT2 inhibitors (Scheme 12). The authors suggest a Knoevenagel condensation approach between isatin derivatives and ethyl cyanoacetate, followed by a Michael addition with C–H activated carbonyl compounds and intramolecular cyclization [50]. They synthesized 45 compounds with high yields (84–92%). The three most promising compounds of the library (**13a**, **13b**, and **13c**) were selected for further detailed characterization. In vitro evaluation was performed employing a high-performance liquid chromatography (HPLC)-based methodology, using the fluorogenic histone deacetylase substrate

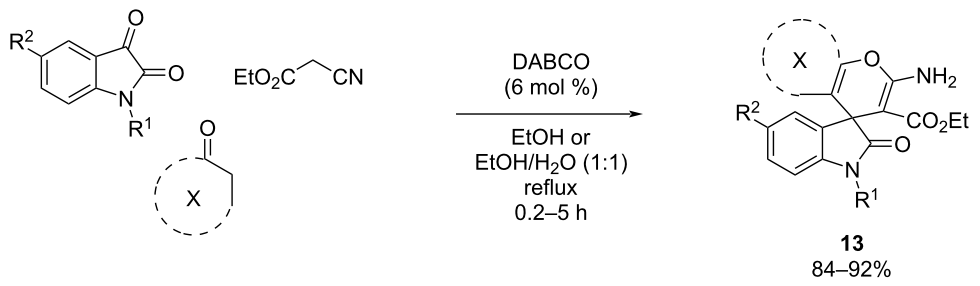

Scheme 12: MCR 3 + 2 reaction to develop spirooxindole, spiroacenaphthylene, and bisbenzo[*b*]pyran compounds.

MAL to determine the inhibitory activity, and using sirtinol as positive control.

When compared to sirtinol (IC_{50} = 67 μM), selected compounds showed moderate affinity towards SIRT2, with IC_{50} values ranging from 118 to 126 μM (Figure 10).

Gewald reaction: Cannabinoid receptors have been proposed as promising neuroprotective targets in several chronic progressive disorders such as AD and PD [51]. Recently, in 2023, Figuerola-Asencio et al. [52] synthesized a series of novel compounds derived from ML192, an antagonist ligand for GRP55. This receptor responds to certain cannabinoids, suggesting it can be part of the endocannabinoid system. GRP55 is extensively distributed throughout the CNS, notably in regions such as peripheral tissues, hippocampus, thalamus, and cerebellum, and in the basal ganglia. The therapeutic potential of GRP55 receptor modulators makes it necessary to search for new selective non-cannabinoid ligands due to the important motor impairment found in mice lacking GPR55 [51].

In this context, ML192 analogs were synthesized employing a divergent synthetic route starting with a multicomponent reaction, the Gewald reaction (Scheme 13). This reaction allows to easily build the principal heterocycle of the compounds. Good reaction yields (70–87%) made it possible to obtain the aminothiophene carboxylates necessary for the following steps of the route [52].

Some of the intermediates of the Gewald reaction were oxidized to provide further exploration of the heterocyclic core. The novel compounds were first evaluated using β-arrestin recruitment assays in CHO (chinese hamster ovary) cells overexpressing human GPR55. These new compounds have been evaluated in competitive binding assays for cannabinoid receptors, but all of them showed to be selective for GPR55 (>4 μM for cannabinoid receptors). Then, the most promising antagonist (**14a**; IC_{50} = 0.28 μM) was selected for a G-protein-dependent functional assay, where **14a** acted as a weak GPR55 inverse agonist (EC_{50} = 0.9 μM).

Depression and anxiety

Benzodiazepines are widely used in treating a range of CNS disorders, including epilepsy, muscle relaxation, insomnia, anesthesia, anxiety, and depression [53]. The common coexistence of depression and anxiety may indicate the simultaneous presence of mood and anxiety disorders. Clinical observations imply that benzodiazepines may have utility in treating depres-

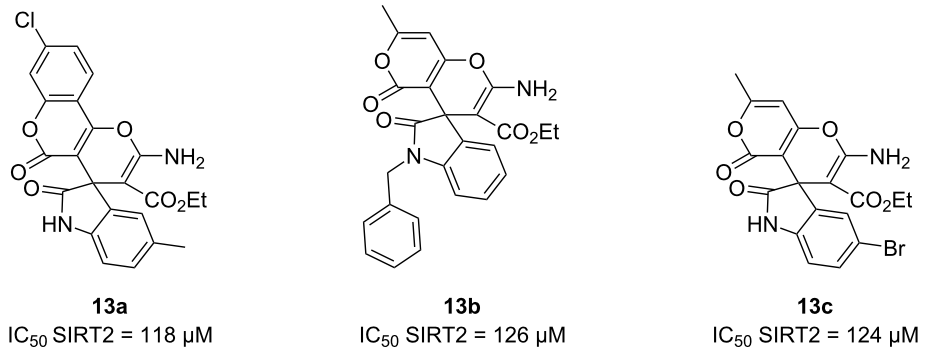

Figure 10: SIRT2 activity of best derivatives obtained by Hasaninejad et al. [49].

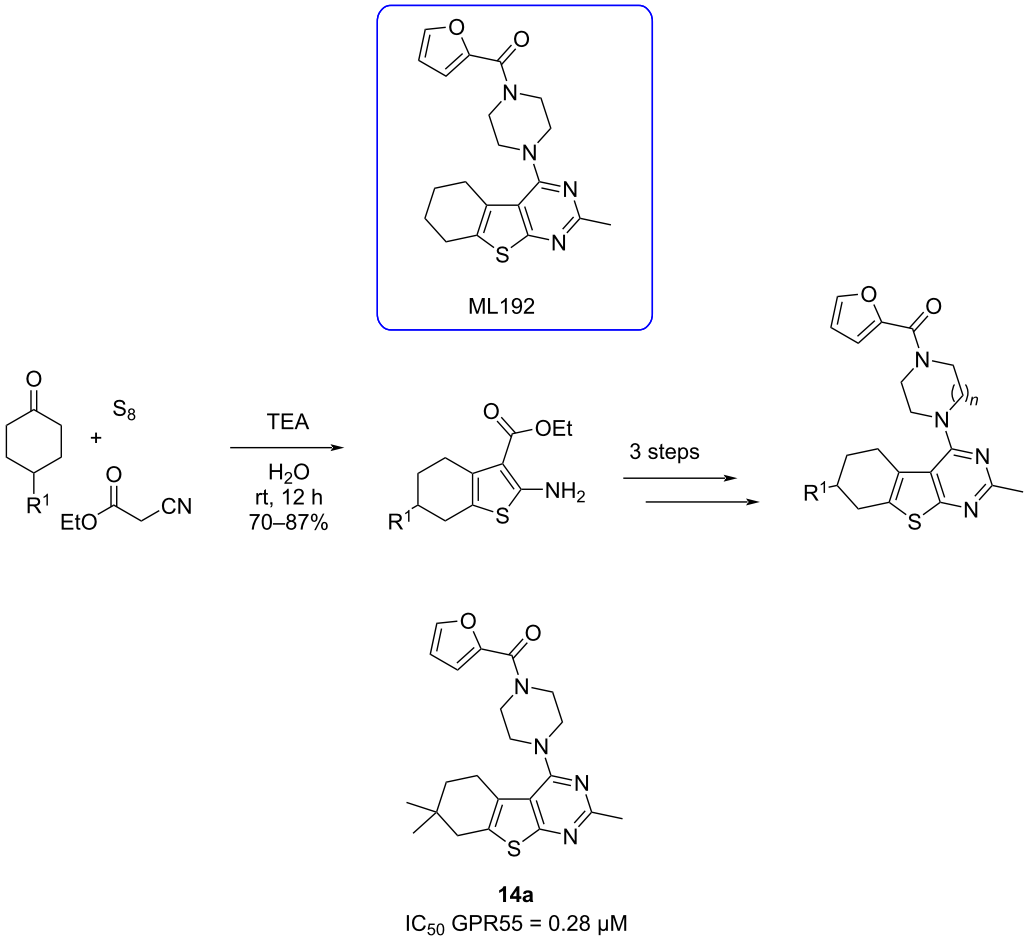

Scheme 13: Synthesis of ML192 analogs using the Gewald multicomponent reaction and the best candidate synthesized.

sion, particularly when accompanied by anxiety. In the initial four weeks of treatment, combining medications proved more effective in reducing depressive symptoms and achieving response and remission of major depression, while showing comparable results in reducing anxiety [54].

Recent advancements in organic synthesis, particularly through MCRs, have streamlined the synthesis of benzodiazepines, making it more efficient and environmentally friendly [55]. For example, olanzapine as a benzodiazepine-based clinical drug was appropriately and concisely synthesized via MCR [56,57].

Over the last twenty years, the Ugi reaction has emerged as a highly considered reaction due to its mild conditions, broad applications, and product diversity. It enables the selective assembly of precursors, facilitating various post-reaction transformations such as deprotection cyclization, 1,3-dipolar cycloaddition, and intramolecular SNAr reactions.

Ugi-4CR/deprotection/cyclization (UDC) strategy: In the UDC approach a protected amine and an electrophilic functional group like esters or ketones are used. Convertible isocyanides can also be employed. Once the Ugi reaction is completed, the protecting group is removed, and the heterocyclic scaffold is subsequently formed [58].

In 2015, Xu et al. [59] reported the synthesis of 1,5-benzodiazepines using the UDC approach. The process begins with Ugi-4CRs, incorporating amines, glyoxaldehydes, 2-(*N*-Boc-amino)phenylisocyanide, and carboxylic acids. Following this, the Boc group is eliminated through microwave-assisted treatment under acidic conditions, resulting in the intramolecular cyclization of the amine onto the ketone derived from glyoxaldehyde (Scheme 14).

Vézina-Dawod and co-workers [60] introduced a strategy, which consists of two reactions, for synthesizing highly substituted 1,4-benzodiazepin-3-ones using the UDC method. This

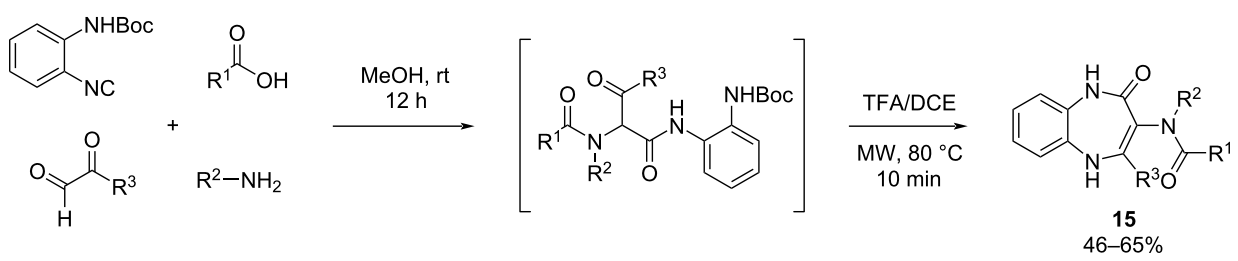

Scheme 14: Development of 1,5-benzodiazepines via Ugi/deprotection/cyclization (UDC) approach by Xu et al. [59].

process involves *N*-Fmoc-amino acids, isocyanides, amines, and derivatives of 2-fluorobenzaldehyde (Scheme 15).

Ugi-4CR/reduction/cyclization (URC) strategy: The URC pathway enables the synthesis of benzodiazepines by using amine surrogates, such as nitro or azide groups, rather than protected amines. Following the Ugi-4CR, the nitro or azide group is reduced to form the amine, leading to a condensation reaction that results in the formation of the benzodiazepine ring [55].

Pertejo et al. [61] described the diastereselective synthesis of 3-carboxamide-1,4-benzodiazepin-5-ones when enantiopure (*S*)-(−)-α-methylbenzylamine and arylglyoxals were used. Thus, a reversal of diastereoselectivity was observed depending on the cyclization methodology employed, the reduction of a nitro group or the Staudinger/aza-Wittig on azide derivatives. This strategic approach allows precise control of the stereogenic centers at the C3-position during cyclization (Scheme 16).

Ugi-4CR/metal-catalyzed reaction: The fusion of MCRs with cross-coupling reactions represents an attractive approach as a result of the increased intricacy and effectiveness [62]. Moreover, this strategy may offer a broad selection of compounds with biological interest. Asgari et al. [63] described an efficient two-step approach for the synthesis of triazolobenzodiazepines in good to excellent yields (Scheme 17). The protocol is initiated by Ugi-4CRs followed by sequential click/intramolecular Ullmann-type C–N coupling reactions.

Azido-Ugi 4CR/cyclization (AU-4CR) strategy: The azido-Ugi four-component reaction (AU-4CR) is an elegant and atom economical approach for obtaining substituted tetrazoles, which are very relevant in medicinal chemistry [64]. When combined with suitable post-Ugi transformations, it is possible to obtain diverse heterocyclic compounds with tetrazole moieties [65]. In this context, Medda et al. [66] developed a three-step process to access biologically active imidazotetrazolodiazepinones. The first one is the AU-4CRs among ethyl glyoxalate, amines, isocyanide, and $TMSN_3$, after which the Ugi adduct is treated with an excess of different isocyanates resulting in the corresponding hydantoin derivatives. Finally, under microwave irradiation, the Boc group is removed under acid conditions and the benzodiazepine core is formed after ring closure (Scheme 18).

Ugi-3CR/deprotection/cyclization strategy: Kröger and colleagues [67] reported a novel synthetic pathway for synthesizing a series of thiazolo- and oxazolo[1,4]benzodiazepine-2,5-diones employing combinatorial MCRs. The first step is the Asinger-4CR, which involves a ketone, α-chloroaldehyde, ammonia, and either sodium hydroxide or sodium hydrogen sulfide to obtain a cyclic imine. Subsequently, the U-3CR is

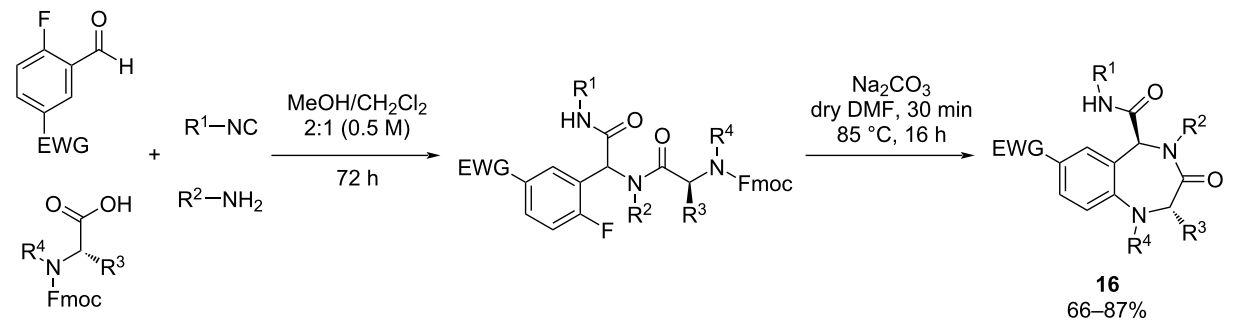

Scheme 15: Synthesis of polysubstituted 1,4-benzodiazepin-3-ones using UDC strategy.

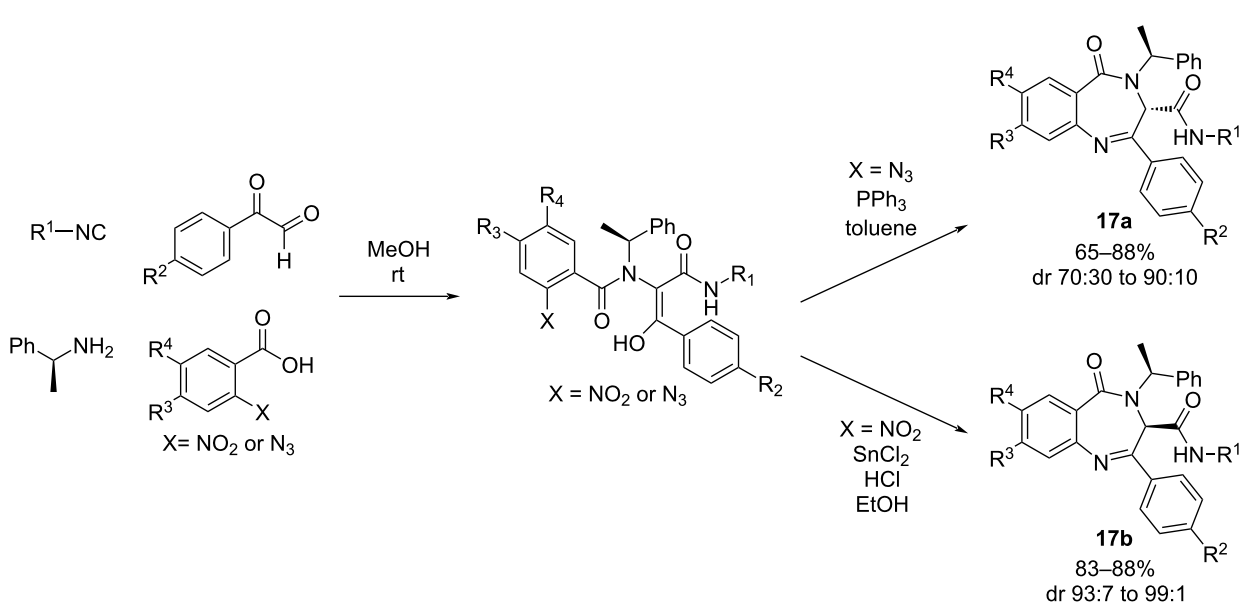

Scheme 16: Synthetic procedure to obtain 3-carboxamide-1,4-benzodiazepin-5-ones employing Ugi–reduction–cyclization (URC) approach.

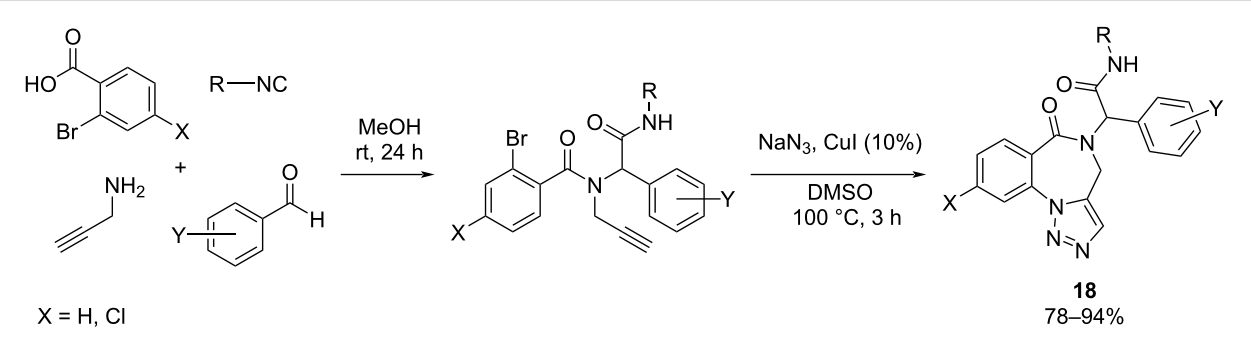

Scheme 17: Ugi cross-coupling (U-4CRs) to synthesize triazolobenzodiazepines.

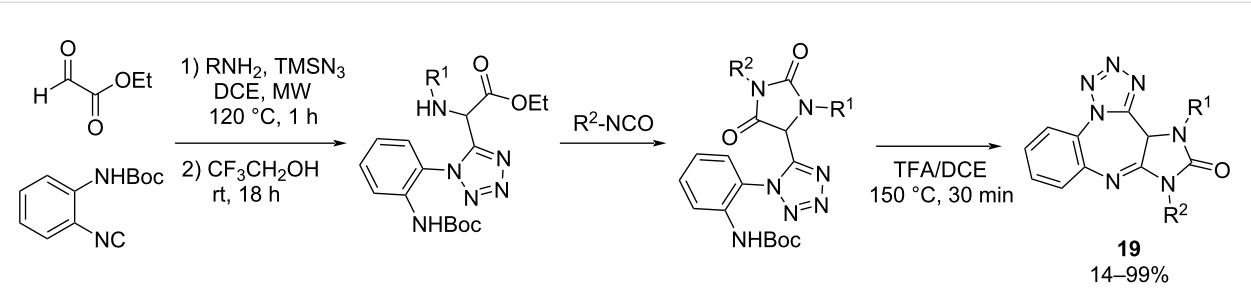

Scheme 18: Azido-Ugi four component reaction cyclization to obtain imidazotetrazolodiazepinones.

performed, where the cyclic imine reacts with an electron-deficient 2-fluorobenzoic acid and an isocyanide to yield a bisamide. Then, the bisamide undergoes an intramolecular SNAr reaction to form the oxazolo- and thiazolo-fused benzodiazepinediones (Scheme 19).

Schizophrenia

As previously mentioned in the introduction, the pathophysiology of schizophrenia remains unclear, and therefore, there are numerous hypotheses to explain it, including the dopaminergic and glutamatergic pathways, among others.

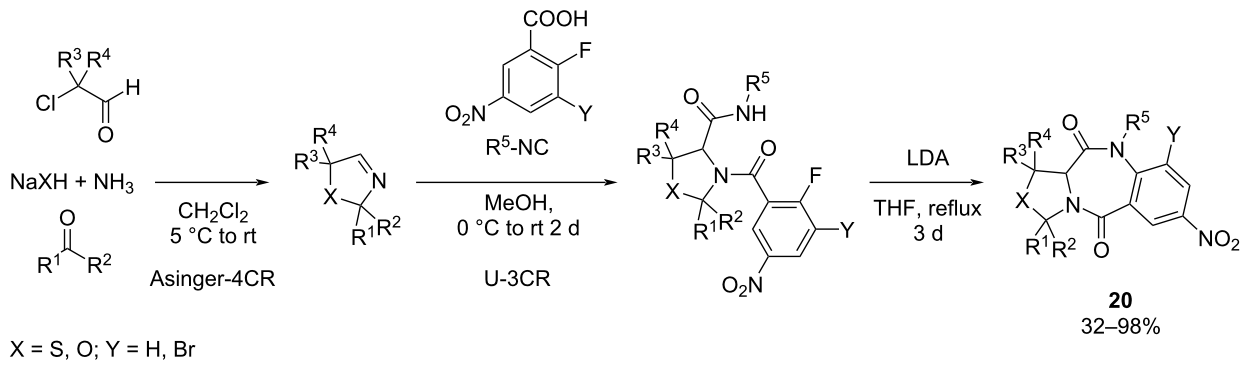

Scheme 19: Synthesis of oxazolo- and thiazolo[1,4]benzodiazepine-2,5-diones via Ugi/deprotection/cyclization approach.

Ugi reaction: The D_2 dopamine receptor (DRD2) is the target of different drugs, including antipsychotics, antiparkinsonian agents, and addiction-related disorders. Aripiprazole and cariprazine are prototypes of newer antipsychotic drugs with a bitopic ligand structure, which includes both primary and secondary pharmacophores. Inspired by the structure and bioactivity profile of aripiprazole, a novel series of DRD2-biased agonists have been developed. The study involves the design, synthesis, and pharmacological characterization of DRD2 partial agonists [68].

Employing Ugi and Ugi post-cyclization reactions, 21 novel 2,3-dichlorophenylpiperazine-derived compounds were synthesized (Scheme 20). These novel compounds were evaluated for their activity on the DRD2 receptor through cAMP functional assays. Furthermore, the most promising ligands were selected for further investigation using β-arrestin-2 recruitment assays. Ligands **21a** and **26a** showed a significant bias towards the cAMP pathway, while ligands **25a** and **26b** exhibited β-arrestin biased agonism (Figure 11). These findings demonstrate the potential for developing functionally selective DRD2 ligands with diverse signaling profiles using a multicomponent approach.

Bucherer–Bergs reaction: The dense presence of mGlu2/3 receptors in regions associated with psychiatric disorders suggests them as potential drug targets. One clinical candidate to treat psychiatric disorders was the mGluR2/3 agonist pomaglumetad methionil (POM). This drug was withdrawn from phase III clinical trials due to insufficient efficacy compared to current antipsychotic drugs (APDs). However, POM demonstrated to be effective to treat certain populations [69].

The large-scale synthesis of a key intermediate of POM was described by Waser et al. [70] in 2011. In this study, they employed the Bucherer–Bergs reaction, a versatile multicomponent reaction which enables the formation of a hydantoin that represents a masked amino acid functionality (Scheme 21). After subsequent saponification and acidification, the desired compound crystallizes along with impurities from other isomers. The undesired isomers were removed in later steps.

In 2020, Sonnenschein et al. [69] studied the effects of POM on dopaminergic neuron activity in states of increased ventral hippocampus (vHPC) activity, measuring the electrical activity of neurons in the brain of rats. Their findings illustrated that POM has the capability to restore normal dopamine neuron activity in situations of increased hippocampal activity. These results showed that a deep understanding of the mechanistic function of mGlu2/3, and particularly the agonist POM, is needed.

Epilepsy

Epilepsy is a disease caused by several biological causes, such as uncontrolled inflammation, neurodegeneration, and aberrant neurogenesis. Levetiracetam is the first member of a new class of anti-epileptic drugs, which selectively accumulates rapidly firing neurons and inhibits their activity. This drug binds to SV2A, a synaptic vesicle protein that is required for normal synaptic function, interfering with the release of the neurotransmitter [71,72].

Ugi reaction: Cioc et al. [73] recognized the 2-oxo-1-pyrrolidino acetamide structure of levetiracetam as a potential Ugi scaffold and aimed to construct racetam derivatives through a multicomponent condensation. While previous Ugi approaches toward racetam derivatives existed, they typically involved indirect grafting of the pyrrolidone core. In this study, the authors synthesized the 2-oxo-1-pyrrolidino acetamide scaffold directly from γ-aminobutyric acid, a carbonyl compound, and an isocyanide in a single operation. The reaction proved to be effective using different isocyanides, both aromatic and aliphatic ones. Additionally, the transformation worked with the convertible isocyanide. This opened the possibility of synthe-

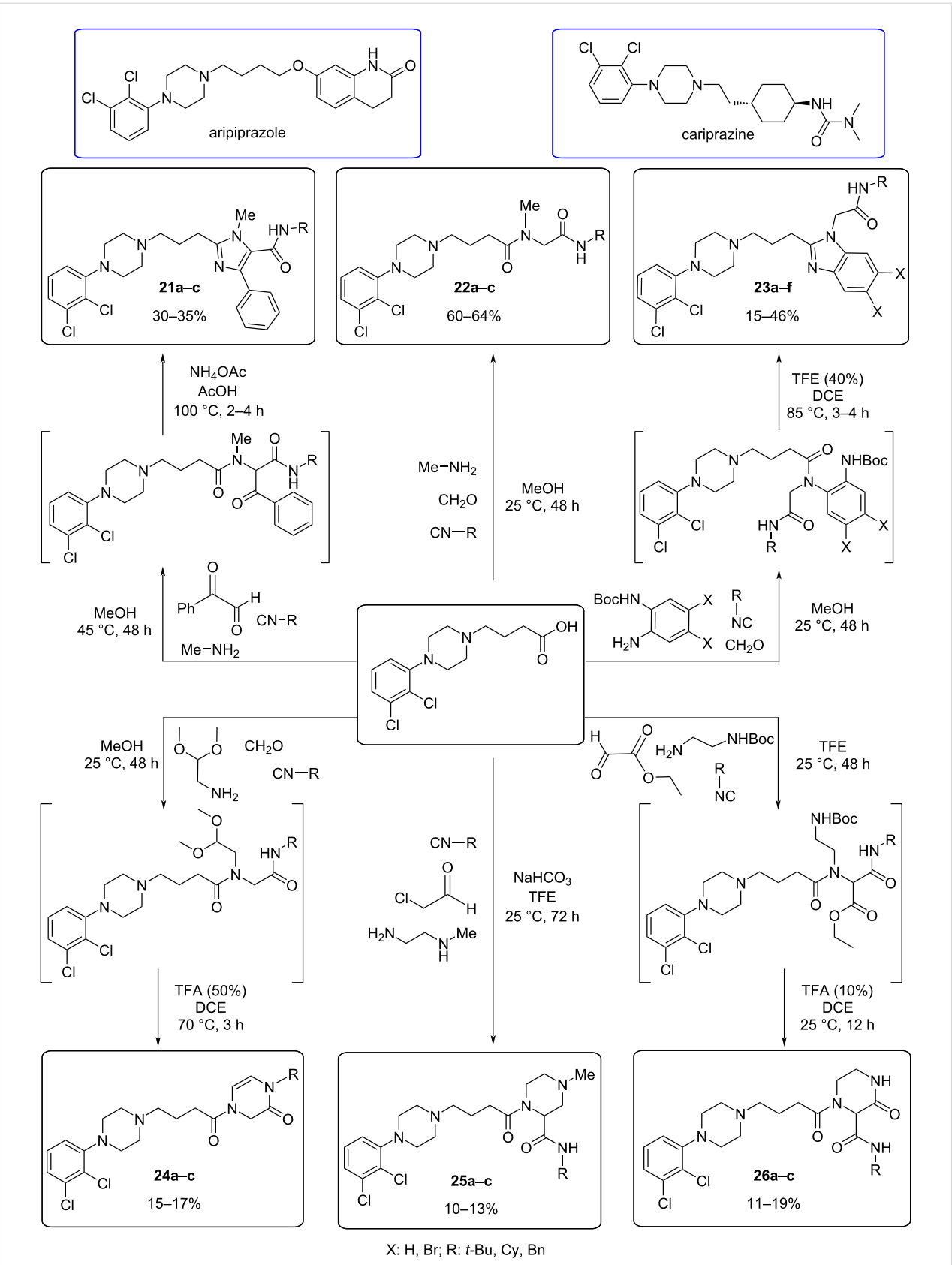

Scheme 20: General synthesis of 2,3-dichlorophenylpiperazine-derived compounds by the Ugi reaction and Ugi/deprotection/cyclization approach.

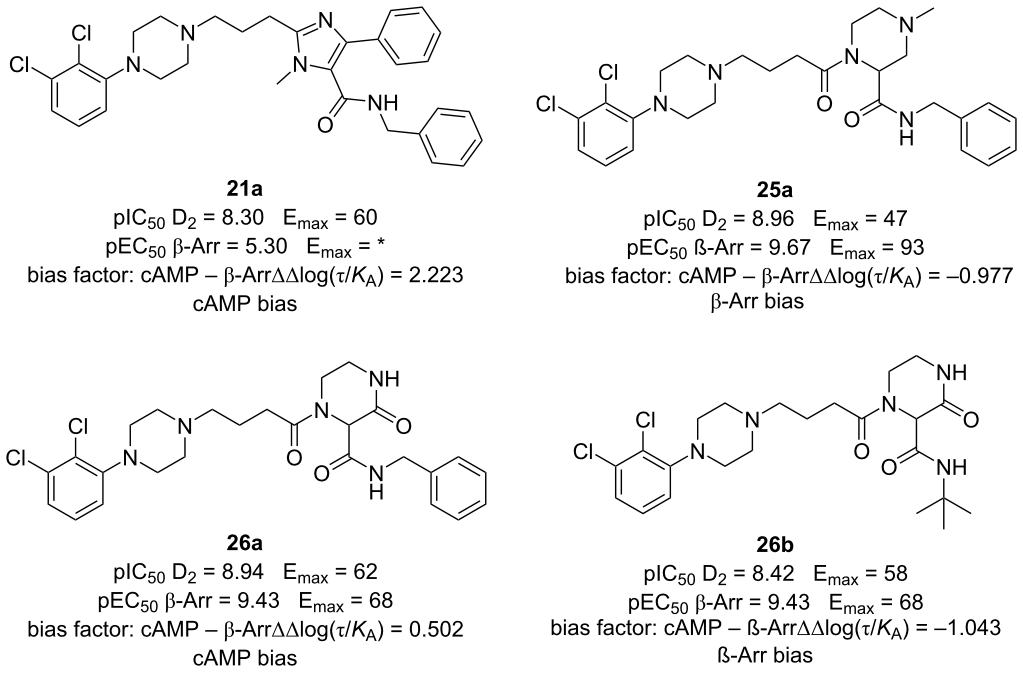

Figure 11: Best DRD2 compounds synthesized using a multicomponent strategy.

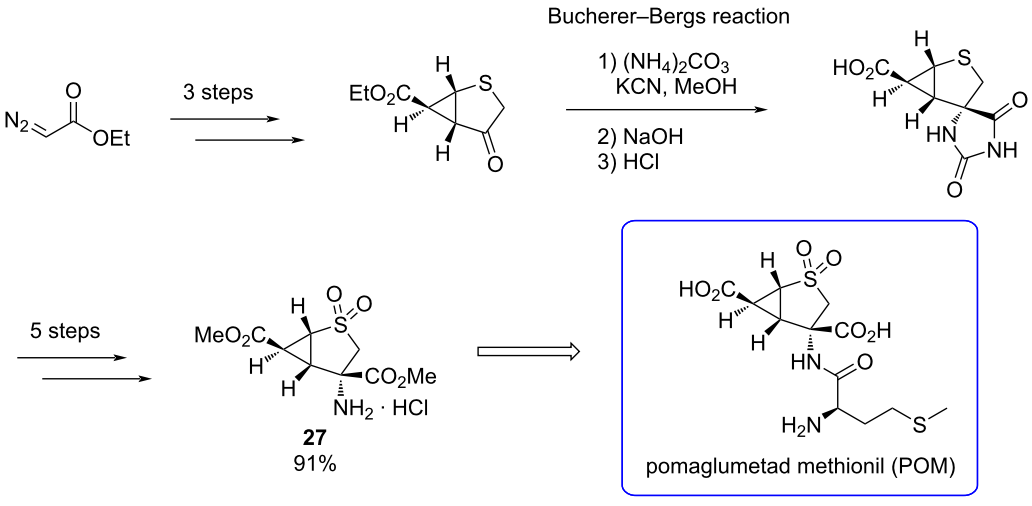

Scheme 21: Bucherer–Bergs multicomponent reaction to obtain a key intermediate in the synthesis of pomaglumetad methionil (POM).

sizing various derivatives of racetams (Scheme 22). On the other hand, they demonstrated the feasibility of the reaction for the synthesis of different racetams useful in the clinic, such as etiracetam (racemic form of (*S*)-levetiracetam) and nefiracetam, another antiepileptic with racetam structure and similar properties [74].

Conclusion

This review highlights the remarkable advantages of multicomponent reactions (MCRs) as a powerful tool in the rapid development of pharmacologically active compounds, particularly for addressing critical nervous system disorders. The ability of MCRs to generate diverse chemical libraries in a short time frame makes them invaluable in accelerating drug discovery processes. The synergy between multicomponent chemistry and medicinal chemistry offers a highly attractive and competitive approach to accelerate drug discovery and development, facilitating the identification and the optimization of novel therapeutic agents for central nervous system pathologies. This combination not only enhances the pace of discovery but also

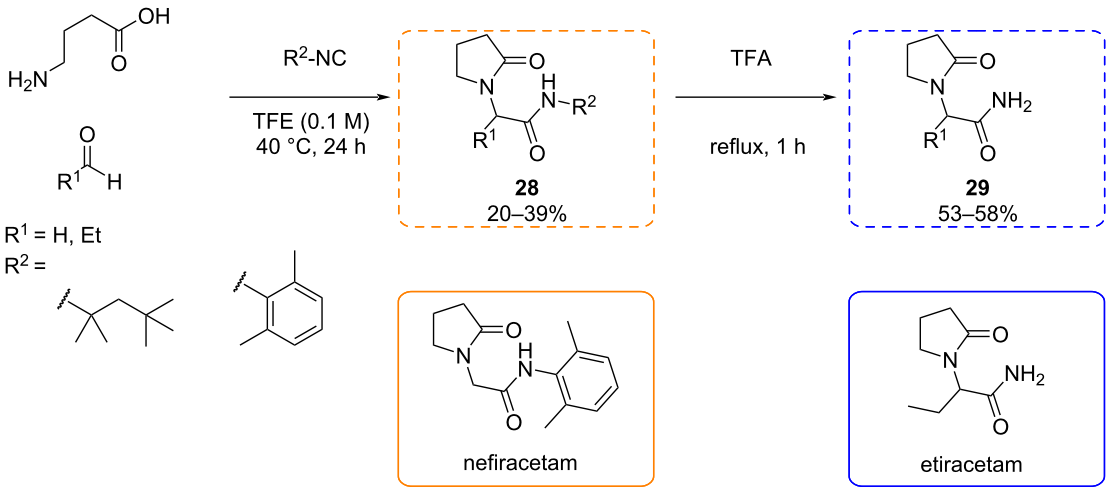

Scheme 22: Ugi reaction to synthesize racetam derivatives and example of two racetams synthesized by Cioc et al. [73].

broadens the scope of potential treatments, underscoring the significant impact of MCRs in medicinal chemistry.

Funding

This work was financially supported by grant FJC2021-047571-I funded by MICIU/AEI/ 10.13039/501100011033 and European Union NextGenerationEU/PRTR, grant FPU21/01359 funded by MICIU/AEI/10.13039/501100011033 and ESF+, Consellería de Cultura, Educación e Ordenación Universitaria of the Galician Government (ED431B 2020/43), Centro Singular de Investigación de Galicia accreditation 2019-2022 (ED431G 2019/03), Ministerio de Ciencia, Innovación y Universidades (PID2020-118511RB-I00 and PID2021-124010OB-100).

ORCID® iDs

Lucía Campos-Prieto - https://orcid.org/0000-0002-2332-8100
Aitor García-Rey - https://orcid.org/0000-0003-1633-872X
Ana Mallo-Abreu - https://orcid.org/0000-0002-5092-3538

Data Availability Statement

Data sharing is not applicable as no new data was generated or analyzed in this study.

References

1. Ghashghaei, O.; Pedrola, M.; Seghetti, F.; Martin, V. V.; Zavarce, R.; Babiak, M.; Novacek, J.; Hartung, F.; Rolfes, K. M.; Haarmann-Stemmann, T.; Lavilla, R. *Angew. Chem., Int. Ed.* **2021,** *60,* 2603–2608. doi:10.1002/anie.202011253
2. Ma, X.; Zhi, S.; Zhang, W. *Molecules* **2021,** *26,* 1986. doi:10.3390/molecules26071986
3. Cimarelli, C. *Molecules* **2019,** *24,* 2372. doi:10.3390/molecules24132372
4. Müller, T. J. J. *Beilstein J. Org. Chem.* **2019,** *15,* 1974–1975. doi:10.3762/bjoc.15.192
5. Rainoldi, G.; Begnini, F.; de Munnik, M.; Lo Presti, L.; Vande Velde, C. M. L.; Orru, R.; Lesma, G.; Ruijter, E.; Silvani, A. *ACS Comb. Sci.* **2018,** *20,* 98–105. doi:10.1021/acscombsci.7b00179
6. Hooshmand, S. E.; Zhang, W. *Molecules* **2023,** *28,* 1642. doi:10.3390/molecules28041642
7. Wu, Y.; Cheng, H.; Li, J.; Liu, J.; Sun, J. *J. Org. Chem.* **2023,** *88,* 11186–11196. doi:10.1021/acs.joc.3c01206
8. Pachón-Angona, I.; Bernard, P. J.; Simakov, A.; Maj, M.; Jozwiak, K.; Novotna, A.; Lemke, C.; Gütschow, M.; Martin, H.; Oset-Gasque, M.-J.; Contelles, J.-M.; Ismaili, L. *Pharmaceutics* **2024,** *16,* 121. doi:10.3390/pharmaceutics16010121
9. Kalník, M.; Gabko, P.; Bella, M.; Kóoš, M. *Molecules* **2021,** *26,* 4024. doi:10.3390/molecules26134024
10. Duvauchelle, V.; Meffre, P.; Benfodda, Z. *Environ. Chem. Lett.* **2023,** *21,* 597–621. doi:10.1007/s10311-022-01482-1
11. Ricardo, M. G.; Llanes, D.; Wessjohann, L. A.; Rivera, D. G. *Angew. Chem., Int. Ed.* **2019,** *58,* 2700–2704. doi:10.1002/anie.201812620
12. Machado, I. V.; dos Santos, J. R. N.; Januario, M. A. P.; Corrêa, A. G. *Ultrason. Sonochem.* **2021,** *78,* 105704. doi:10.1016/j.ultsonch.2021.105704
13. Zhu, F.; Yin, P. *Chem. – Eur. J.* **2023,** *29,* e202301826. doi:10.1002/chem.202301826
14. Gulati, S.; John, S. E.; Shankaraiah, N. *Beilstein J. Org. Chem.* **2021,** *17,* 819–865. doi:10.3762/bjoc.17.71
15. Tuten, B. T.; De Keer, L.; Wiedbrauk, S.; Van Steenberge, P. H. M.; D'hooge, D. R.; Barner-Kowollik, C. *Angew. Chem., Int. Ed.* **2019,** *58,* 5672–5676. doi:10.1002/anie.201901506
16. Fouad, M. A.; Abdel-Hamid, H.; Ayoup, M. S. *RSC Adv.* **2020,** *10,* 42644–42681. doi:10.1039/d0ra07501a
17. Bariwal, J.; Kaur, R.; Voskressensky, L. G.; Van der Eycken, E. V. *Front. Chem. (Lausanne, Switz.)* **2018,** *6,* 557. doi:10.3389/fchem.2018.00557
18. Waris, A.; Ali, A.; Khan, A. U.; Asim, M.; Zamel, D.; Fatima, K.; Raziq, A.; Khan, M. A.; Akbar, N.; Baset, A.; Abourehab, M. A. S. *Nanomaterials* **2022,** *12,* 2140. doi:10.3390/nano12132140

19. Luo, M.; Lee, L. K. C.; Peng, B.; Choi, C. H. J.; Tong, W. Y.; Voelcker, N. H. *Adv. Sci.* **2022,** *9,* 2201740. doi:10.1002/advs.202201740
20. Chen, Z.; Wu, H.; Zhang, M. *Neurochem. Int.* **2021,** *148,* 105101. doi:10.1016/j.neuint.2021.105101
21. Zwicker, A.; Denovan-Wright, E. M.; Uher, R. *Psychol. Med.* **2018,** *48,* 1925–1936. doi:10.1017/s003329171700383x
22. Pitsillou, E.; Bresnehan, S. M.; Kagarakis, E. A.; Wijoyo, S. J.; Liang, J.; Hung, A.; Karagiannis, T. C. *Mol. Biol. Rep.* **2020,** *47,* 753–770. doi:10.1007/s11033-019-05129-3
23. Falco-Walter, J. *Semin. Neurol.* **2020,** *40,* 617–623. doi:10.1055/s-0040-1718719
24. Sampietro, A.; Pérez-Areales, F. J.; Martínez, P.; Arce, E. M.; Galdeano, C.; Muñoz-Torrero, D. *Pharmaceuticals* **2022,** *15,* 545. doi:10.3390/ph15050545
25. Scheltens, P.; De Strooper, B.; Kivipelto, M.; Holstege, H.; Chételat, G.; Teunissen, C. E.; Cummings, J.; van der Flier, W. M. *Lancet* **2021,** *397,* 1577–1590. doi:10.1016/s0140-6736(20)32205-4
26. Colvee-Martin, H.; Parra, J. R.; Gonzalez, G. A.; Barker, W.; Duara, R. *Diagnostics* **2024,** *14,* 704. doi:10.3390/diagnostics14070704
27. Kaur, A.; Nigam, K.; Srivastava, S.; Tyagi, A.; Dang, S. *J. Microencapsulation* **2020,** *37,* 355–365. doi:10.1080/02652048.2020.1756971
28. Srivastava, S.; Ahmad, R.; Khare, S. K. *Eur. J. Med. Chem.* **2021,** *216,* 113320. doi:10.1016/j.ejmech.2021.113320
29. Griffiths, J.; Grant, S. G. N. *Semin. Cell Dev. Biol.* **2023,** *139,* 13–23. doi:10.1016/j.semcdb.2022.05.028
30. Cioffi, F.; Adam, R. H. I.; Broersen, K. *J. Alzheimer's Dis.* **2019,** *72,* 981–1017. doi:10.3233/jad-190863
31. Tönnies, E.; Trushina, E. *J. Alzheimer's Dis.* **2017,** *57,* 1105–1121. doi:10.3233/jad-161088
32. Forman, H. J.; Zhang, H. *Nat. Rev. Drug Discovery* **2021,** *20,* 689–709. doi:10.1038/s41573-021-00233-1
33. Brandão, P.; López, Ó.; Leitzbach, L.; Stark, H.; Fernández-Bolaños, J. G.; Burke, A. J.; Pineiro, M. *ACS Med. Chem. Lett.* **2021,** *12,* 1718–1725. doi:10.1021/acsmedchemlett.1c00344
34. Kushwaha, P.; Fatima, S.; Upadhyay, A.; Gupta, S.; Bhagwati, S.; Baghel, T.; Siddiqi, M. I.; Nazir, A.; Sashidhara, K. V. *Bioorg. Med. Chem. Lett.* **2019,** *29,* 66–72. doi:10.1016/j.bmcl.2018.11.005
35. Pachón-Angona, I.; Martin, H.; Chhor, S.; Oset-Gasque, M.-J.; Refouvelet, B.; Marco-Contelles, J.; Ismaili, L. *Future Med. Chem.* **2019,** *11,* 3097–3108. doi:10.4155/fmc-2019-0191
36. Lambruschini, C.; Galante, D.; Moni, L.; Ferraro, F.; Gancia, G.; Riva, R.; Traverso, A.; Banfi, L.; D'Arrigo, C. *Org. Biomol. Chem.* **2017,** *15,* 9331–9351. doi:10.1039/c7ob02182h
37. Galante, D.; Banfi, L.; Baruzzo, G.; Basso, A.; D'Arrigo, C.; Lunaccio, D.; Moni, L.; Riva, R.; Lambruschini, C. *Molecules* **2019,** *24,* 2636. doi:10.3390/molecules24142636
38. Benchekroun, M.; Bartolini, M.; Egea, J.; Romero, A.; Soriano, E.; Pudlo, M.; Luzet, V.; Andrisano, V.; Jimeno, M.-L.; López, M. G.; Wehle, S.; Gharbi, T.; Refouvelet, B.; de Andrés, L.; Herrera-Arozamena, C.; Monti, B.; Bolognesi, M. L.; Rodríguez-Franco, M. I.; Decker, M.; Marco-Contelles, J.; Ismaili, L. *ChemMedChem* **2015,** *10,* 523–539. doi:10.1002/cmdc.201402409
39. Benchekroun, M.; Romero, A.; Egea, J.; León, R.; Michalska, P.; Buendía, I.; Jimeno, M. L.; Jun, D.; Janockova, J.; Sepsova, V.; Soukup, O.; Bautista-Aguilera, O. M.; Refouvelet, B.; Ouari, O.; Marco-Contelles, J.; Ismaili, L. *J. Med. Chem.* **2016,** *59,* 9967–9973. doi:10.1021/acs.jmedchem.6b01178
40. Madhav, H.; Abdel-Rahman, S. A.; Hashmi, M. A.; Rahman, M. A.; Rehan, M.; Pal, K.; Nayeem, S. M.; Gabr, M. T.; Hoda, N. *Eur. J. Med. Chem.* **2023,** *254,* 115354. doi:10.1016/j.ejmech.2023.115354
41. Huang, G.; Kling, B.; Darras, F. H.; Heilmann, J.; Decker, M. *Eur. J. Med. Chem.* **2014,** *81,* 15–21. doi:10.1016/j.ejmech.2014.05.002
42. Dgachi, Y.; Bautista-Aguilera, O. M.; Benchekroun, M.; Martin, H.; Bonet, A.; Knez, D.; Godyń, J.; Malawska, B.; Gobec, S.; Chioua, M.; Janockova, J.; Soukup, O.; Chabchoub, F.; Marco-Contelles, J.; Ismaili, L. *Molecules* **2016,** *21,* 634. doi:10.3390/molecules21050634
43. Malek, R.; Maj, M.; Wnorowski, A.; Jóźwiak, K.; Martin, H.; Iriepa, I.; Moraleda, I.; Chabchoub, F.; Marco-Contelles, J.; Ismaili, L. *Bioorg. Chem.* **2019,** *91,* 103205. doi:10.1016/j.bioorg.2019.103205
44. Manchester, L. C.; Coto-Montes, A.; Boga, J. A.; Andersen, L. P. H.; Zhou, Z.; Galano, A.; Vriend, J.; Tan, D.-X.; Reiter, R. J. *J. Pineal Res.* **2015,** *59,* 403–419. doi:10.1111/jpi.12267
45. Chen, C.-H.; Zhou, W.; Liu, S.; Deng, Y.; Cai, F.; Tone, M.; Tone, Y.; Tong, Y.; Song, W. *Int. J. Neuropsychopharmacol.* **2012,** *15,* 77–90. doi:10.1017/s1461145711000149
46. Malek, R.; Refouvelet, B.; Benchekroun, M.; Iriepa, I.; Moraleda, I.; Andrys, R.; Musilek, K.; Marco-Contelles, J.; Ismaili, L. *Curr. Alzheimer Res.* **2019,** *16,* 815–820. doi:10.2174/1567205016666191011112624
47. Fragkiadakis, M.; Zingiridis, M.; Loukopoulos, E.; Neochoritis, C. G. *Mol. Diversity* **2024,** *28,* 29–35. doi:10.1007/s11030-022-10502-9
48. Chen, X.; Lu, W.; Wu, D. *Front. Neurosci.* **2021,** *15,* 614107. doi:10.3389/fnins.2021.614107
49. Hasaninejad, A.; Mandegani, F.; Beyrati, M.; Maryamabadi, A.; Mohebbi, G. *ChemistrySelect* **2017,** *2,* 6784–6796. doi:10.1002/slct.201701364
50. Könning, D.; Swatschek, J. Essential Multicomponent Reactions II. *Multicomponent Reactions;* John Wiley & Sons: Hoboken, NJ, USA, 2015; pp 416–495. doi:10.1002/9781118863992.ch13
51. Burgaz, S.; García, C.; Gonzalo-Consuegra, C.; Gómez-Almería, M.; Ruiz-Pino, F.; Unciti, J. D.; Gómez-Cañas, M.; Alcalde, J.; Morales, P.; Jagerovic, N.; Rodríguez-Cueto, C.; de Lago, E.; Muñoz, E.; Fernández-Ruiz, J. *Molecules* **2021,** *26,* 7643. doi:10.3390/molecules26247643
52. Figuerola-Asencio, L.; Morales, P.; Zhao, P.; Hurst, D. P.; Sayed, S. S.; Colón, K. L.; Gómez-Cañas, M.; Fernández-Ruiz, J.; Croatt, M. P.; Reggio, P. H.; Abood, M. E.; Jagerovic, N. *ACS Med. Chem. Lett.* **2023,** *14,* 18–25. doi:10.1021/acsmedchemlett.2c00325
53. Dubovsky, S. L.; Marshall, D. *Psychother. Psychosom.* **2022,** *91,* 307–334. doi:10.1159/000524400
54. Ogawa, Y.; Takeshima, N.; Hayasaka, Y.; Tajika, A.; Watanabe, N.; Streiner, D.; Furukawa, T. A. *Cochrane Database Syst. Rev.* **2019,** *6,* CD001026. doi:10.1002/14651858.cd001026.pub2
55. Farhid, H.; Khodkari, V.; Nazeri, M. T.; Javanbakht, S.; Shaabani, A. *Org. Biomol. Chem.* **2021,** *19,* 3318–3358. doi:10.1039/d0ob02600j
56. Cores, Á.; Clerigué, J.; Orocio-Rodríguez, E.; Menéndez, J. C. *Pharmaceuticals* **2022,** *15,* 1009. doi:10.3390/ph15081009
57. Chakrabarti, J. K.; Hotten, T. M.; Tupper, D. E. Method For Preparing A Derivative Of Tienobenzodiazepin, Used As A Pharmaceutical Product. Portuguese Patent PT97446B, July 31, 1997.

58. Banfi, L.; Basso, A.; Lambruschini, C.; Moni, L.; Riva, R. *Chem. Heterocycl. Compd.* **2017,** *53,* 382–408. doi:10.1007/s10593-017-2065-1
59. Xu, Z.; Martinez-Ariza, G.; Cappelli, A. P.; Roberts, S. A.; Hulme, C. *J. Org. Chem.* **2015,** *80,* 9007–9015. doi:10.1021/acs.joc.5b00955
60. Vézina-Dawod, S.; Gerber, N.; Liang, X.; Biron, E. *Tetrahedron* **2017,** *73,* 6347–6355. doi:10.1016/j.tet.2017.09.028
61. Pertejo, P.; Corres, N.; Torroba, T.; García-Valverde, M. *Org. Lett.* **2015,** *17,* 612–615. doi:10.1021/ol503628r
62. Li, J.; Yang, S.; Wu, W.; Jiang, H. *Eur. J. Org. Chem.* **2018,** 1284–1306. doi:10.1002/ejoc.201701509
63. Asgari, M. S.; Soheilizad, M.; Ranjbar, P. R.; Larijani, B.; Rahimi, R.; Mahdavi, M. *Tetrahedron Lett.* **2019,** *60,* 583–585. doi:10.1016/j.tetlet.2019.01.009
64. Neochoritis, C. G.; Zhao, T.; Dömling, A. *Chem. Rev.* **2019,** *119,* 1970–2042. doi:10.1021/acs.chemrev.8b00564
65. Mohammadkhani, L.; Heravi, M. M. *Mol. Diversity* **2020,** *24,* 841–853. doi:10.1007/s11030-019-09972-1
66. Medda, F.; Martinez-Ariza, G.; Hulme, C. *Tetrahedron Lett.* **2015,** *56,* 5295–5298. doi:10.1016/j.tetlet.2015.07.083
67. Kröger, D.; Stalling, T.; Martens, J. *Synthesis* **2016,** *48,* 4189–4198. doi:10.1055/s-0035-1562457
68. Mallo-Abreu, A.; Reyes-Resina, I.; Azuaje, J.; Franco, R.; García-Rey, A.; Majellaro, M.; Miranda-Pastoriza, D.; García-Mera, X.; Jespers, W.; Gutiérrez-de-Terán, H.; Navarro, G.; Sotelo, E. *J. Med. Chem.* **2021,** *64,* 8710–8726. doi:10.1021/acs.jmedchem.1c00704
69. Sonnenschein, S. F.; Grace, A. A. *Neuropsychopharmacology* **2020,** *45,* 2106–2113. doi:10.1038/s41386-020-0764-2
70. Waser, M.; Moher, E. D.; Borders, S. S. K.; Hansen, M. M.; Hoard, D. W.; Laurila, M. E.; LeTourneau, M. E.; Miller, R. D.; Phillips, M. L.; Sullivan, K. A.; Ward, J. A.; Xie, C.; Bye, C. A.; Leitner, T.; Herzog-Krimbacher, B.; Kordian, M.; Müllner, M. *Org. Process Res. Dev.* **2011,** *15,* 1266–1274. doi:10.1021/op100325h
71. Ciruelas, K.; Marcotulli, D.; Bajjalieh, S. M. *Semin. Cell Dev. Biol.* **2019,** *95,* 130–141. doi:10.1016/j.semcdb.2019.02.003
72. Howard, P.; Remi, J.; Remi, C.; Charlesworth, S.; Whalley, H.; Bhatia, R.; Hitchens, M.; Mihalyo, M.; Wilcock, A. *J. Pain Symptom Manage.* **2018,** *56,* 645–649. doi:10.1016/j.jpainsymman.2018.07.012
73. Cioc, R. C.; Schaepkens van Riempst, L.; Schuckman, P.; Ruijter, E.; Orru, R. V. A. *Synthesis* **2016,** *49,* 1664–1674. doi:10.1055/s-0036-1588672
74. Kitano, Y.; Komiyama, C.; Makino, M.; Takasuna, K.; Takazawa, A.; Sakurada, S. *Epilepsia* **2005,** *46,* 811–818. doi:10.1111/j.1528-1167.2005.66504.x

License and Terms

This is an open access article licensed under the terms of the Beilstein-Institut Open Access License Agreement (https://www.beilstein-journals.org/bjoc/terms), which is identical to the Creative Commons Attribution 4.0 International License (https://creativecommons.org/licenses/by/4.0). The reuse of material under this license requires that the author(s), source and license are credited. Third-party material in this article could be subject to other licenses (typically indicated in the credit line), and in this case, users are required to obtain permission from the license holder to reuse the material.

The definitive version of this article is the electronic one which can be found at:
https://doi.org/10.3762/bjoc.20.261

BEILSTEIN JOURNAL OF ORGANIC CHEMISTRY

Heteroannulations of cyanoacetamide-based MCR scaffolds utilizing formamide

Marios Zingiridis, Danae Papachristodoulou, Despoina Menegaki, Konstantinos G. Froudas and Constantinos G. Neochoritis*

Full Research Paper

Open Access

Address:
Department of Chemistry, University of Crete, Voutes, 71003 Heraklion, Greece

Email:
Constantinos G. Neochoritis* - kneochor@uoc.gr

* Corresponding author

Keywords:
2-amino-substituted heterocycles; cyanoacetamide; Gewald reaction; multicomponent reaction (MCR); pyrimidine

Beilstein J. Org. Chem. **2025,** *21,* 217–225.
https://doi.org/10.3762/bjoc.21.13

Received: 21 October 2024
Accepted: 14 January 2025
Published: 24 January 2025

This article is part of the thematic issue "Multicomponent reactions IV".

Associate Editor: T. J. J. Müller

© 2025 Zingiridis et al.; licensee Beilstein-Institut.
License and terms: see end of document.

Abstract

C1 chemistry has a central role in the efficient utilization of single-carbon molecules, contributing significantly to sustainability, innovation and economic growth across various sectors. In this study, we present an efficient and rapid method for synthesizing a variety of heteroannulated pyrimidones using cyanoacetamide-based multicomponent reaction (MCR) chemistry. By utilizing specific MCR-based scaffolds as precursors and employing the abundant and inexpensive formamide as a C1 feedstock under neat conditions, we were able to efficiently access substituted thieno-, quinolino- and indolopyrimidones without the need of column chromatography. Further, a single-crystal X-ray structure was obtained, revealing certain geometrical features.

Introduction

The term “net-zero carbon” is becoming increasingly common as we consider a future marked by a rising global temperature and severe weather patterns – a result of human-induced greenhouse gas emissions. The principle of net-zero revolves around the idea of using Earth’s carbon resources at a rate that does not exceed their natural replenishment. In 2015, the United Nations introduced the Sustainable Development Goals (SDGs), wherein the 7th goal focuses on ensuring access to affordable, renewable and clean energy [1]. Moreover, the European Union has committed to ambitious environmental targets as part of the European Green Deal [2].

Advancements in C1 chemistry are pivotal to achieving this equilibrium. As such, it is becoming increasingly essential for synthetic methods to align with a net-zero carbon future [2,3]. Therefore, advancing C1 chemistry remains a crucial endeavor for our group [4]. In synthetic organic chemistry, C1 compounds are usually installed using CO, CO_2, HCO_2H, CH_3OH

and CH_4, which is mostly due to their presence in greenhouse emissions [5,6]. Although abundant and inexpensive, their valorization still remains problematic due to their thermodynamic stability and chemical inertness [7-15]. Multicomponent reaction (MCR) chemistry is a type of convergent chemistry characterized by diversity, complexity and efficiency. MCRs are compatible with C1 chemistry due to the generally great tolerance of different functional groups. They have been mostly employed in the synthesis of oxazolidinones and oxazinanones utilizing CO_2 and CO [4,16-20]. In addition, carbonyldiimidazole-based heteroannulations via MCRs have been reported, giving access to drug like scaffolds [21-24]. However, their employment in C1 chemistry should and could be advanced.

Herein, we point out formamide as an alternative relevant building block for C1 chemistry by using specific, suitably functionalized MCR scaffolds. This positions formamides as versatile, synthetic hubs towards privileged scaffolds and high-end chemicals. Over the years, the reactivity of formamide has been widely explored in heterocyclic chemistry, but it has only recently started to be established as a C1 feedstock. [25]. Its high polarity and dielectric constant (it is miscible with water) [26], with the ability to solubilize a wide range of reagents, from salts to polymers, proteins and saccharides, renders formamide an excellent C1 building block [25,27]. Thus, our target under the umbrella of C1 chemistry was to provide a straightforward access to the privileged scaffold of fused heteroannulated pyrimidones, which demonstrate a broad range of biological activities [28-35], including use as emissive nucleoside analogues [36-38]. Moreover, they are used in a variety of commercially available drugs (Figure 1).

Results and Discussion

Design and strategy

We envisioned applying the Niementowski quinazoline synthesis [25,39-41] (Scheme 1A) by employing three different heterocyclic systems as precursors, which have both an orthogonally installed amino group and a disubstituted amide group at the 2- and 3-positions, respectively, and reacting them with formamide (Scheme 1B). Those synthetic hubs can be rapidly accessed by cyanoacetamide-based MCRs, which is an interesting reaction type that gives access to privileged cores and has been utilized numerous times in medicinal chemistry campaigns as hits, leads and eventually even drugs, such as 2-aminothiophenes, -quinolines and -indoles [42-45].

Synthetic exploitation

The synthesis of the key cyanoacetamide building blocks was our primary objective. In a parallel setup, a variety of primary amines was reacted with methyl cyanoacetate [46], giving rise to the corresponding cyanoacetamides **1** (Scheme 2). Subsequently, they were reacted accordingly to yield a variety of the targeted precursors, 2-aminothiophenes **2** [42], 2-aminoquinolines **3** [45] and 2-aminoindoles **4** [44], via Gewald three-component reactions. Our focus was to create a representative, diverse and structurally complex library of building blocks, covering a range of shapes and chemical spaces, to facilitate formamide-based heteroannulation for the synthesis of the desired adducts. Thus, we employed aliphatic and (hetero)aro-

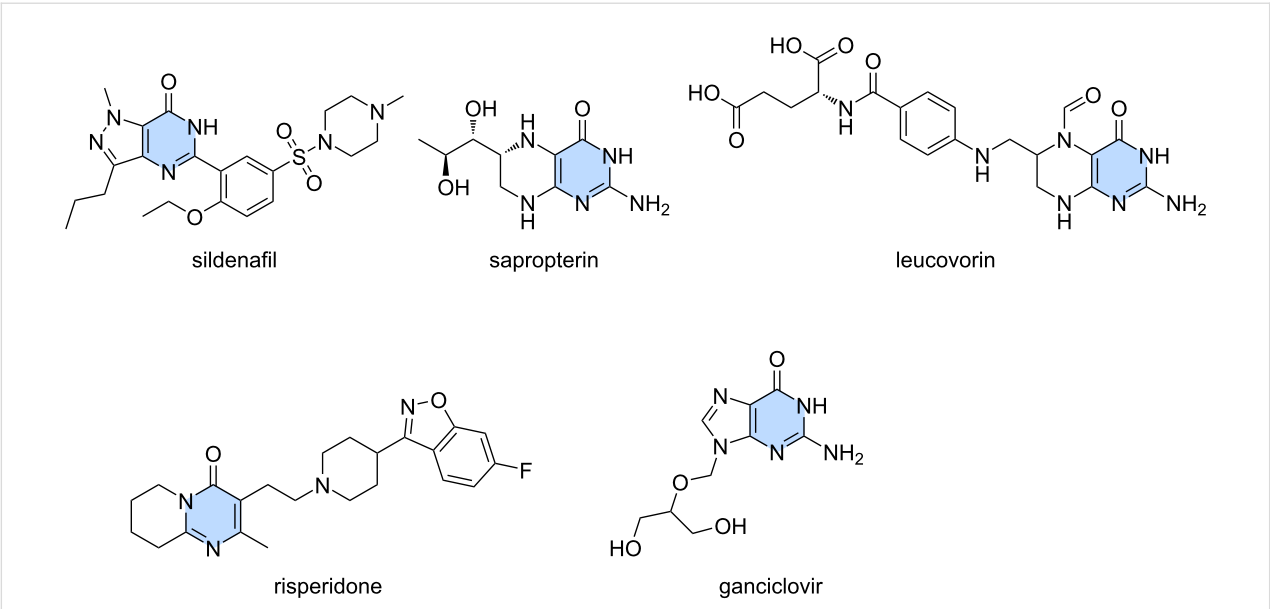

Figure 1: Heteroannulated pyrimidones in drug discovery: blockbuster drugs that are based on the privileged pyrimidine scaffold.

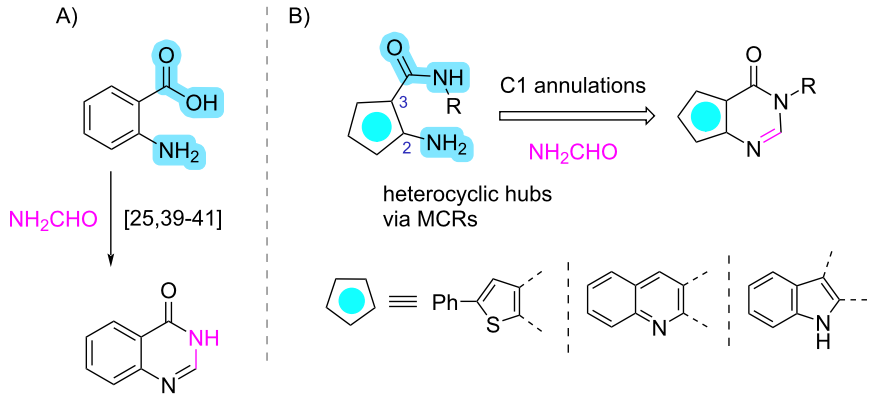

Scheme 1: Strategies towards targeted adducts: A) Niementowski quinazoline synthesis utilizing anthranilic acid and B) access to heteroannulated pyrimidones by MCRs of suitably substituted heterocycles and formamide as C1 source.

matic, bulky and linear amines with different substitution patterns. The compounds **2**–**4** were purified by recrystallization and employed as such (Scheme 2).

To our great delight, the heterocycles **2**–**4** could successfully be subjected to refluxing formamide under neat conditions, instantly yielding the desired thienopyrimidones **5a**–**e**, quinolinopyrimidones **6a**–**e** and indolopyrimidones **7a**–**e**, respectively, as reported in the literature [42,44]. In accordance with the reported mechanism, after the initial formylation of the amino group at position 2, an intramolecular nucleophilic attack by the NH moiety of the amide group resulted in pyrimidone annulation [41]. This was observed for the first time and completed the reported heteroannulation landscape utilizing the Niementowski reaction [25]. In general, the reactions had a rather broad scope as a great range of cyanoacetamides was compatible. The synthesis was efficient and rapid as the final adducts could be isolated only by precipitation. In addition, the reactions were performed in a parallel setup using custom-made metal blocks.

Specifically, thienopyrimidine and thienopyrimidone derivatives exhibit a range of biological activities, i.e., analgesia, anti-inflammation, antihypertension and many more (DB06889, DB07397, DB08777) [47-56]. Thienopyrimidone derivatives have also been used in the context of other Gewald-based MCRs in the past, but the reported diversity has been rather low [57-60]. The reaction of **2** with formamide was performed within only 3 h (Scheme 3), yielding the N-substituted thienopyrimidones **5a**–**e** in 30–99% total yield (2 steps), as well with aliphatic and (hetero)aromatic substituents.

Quinoline derivatives are prevalent in nature, and many exhibit a range of biological activities, including antimalarial, antitumor, anthelmintic, antibacterial, antiasthmatic, and antiplatelet effects [61-63]. In particular, quinolinopyrimidine and pyrimidone derivatives have attracted a great interest due to their biological profile [64-69]. After some optimization, we determined that harsher reaction conditions than for the synthesis of **5** were required for the targeted adducts **6** to form. Additional treatment with DIPEA/DMF afforded the corresponding substituted quinolinopyrimidones **6a**–**e** in 47–65% total yield (2 steps) within 12–16 h. Notably, the products carried a series of aliphatic and aromatic substituents (Scheme 4).

Pyrimidines and pyrimidone-bearing indole derivatives are crucial in organic chemistry because of their extensive use as bioactive compounds with a wide array of significant biological activities (DB03074, DB03304, DB08131) [70-72]. In a similar fashion, substituted indolopyrimidone derivatives **7a**–**e** were obtained within 3 h in 31–90% total yield (2 steps) upon heating with formamide (Scheme 5).

Next, we characterized certain physicochemical properties of the newly synthesized compounds. The absorbance and emission spectra of **5**–**7** were obtained, showing similar profiles across all the different scaffolds (Figure 2 and Supporting Information File 1). The compounds **5**–**7** exhibited a maximum absorbance (λ_{max}) at 330 nm, 284 nm and 310 nm, respectively, which also corresponded to their excitation wavelength (λ_{ex}). Upon excitation, fluorescence emission was observed at an average wavelength of 384 nm for **5a**–**e**, 439 nm for **6a**–**e** and 430 nm for **7a**–**e** (see Supporting Information File 1 for detailed information).

In support of the proposed scaffold **7b**, we were able to solve its crystal structure (Figure 3). An intermolecular bifurcated hydrogen bond network of 2.0 Å was revealed, demonstrating potential of these derivatives in drug and material discovery.

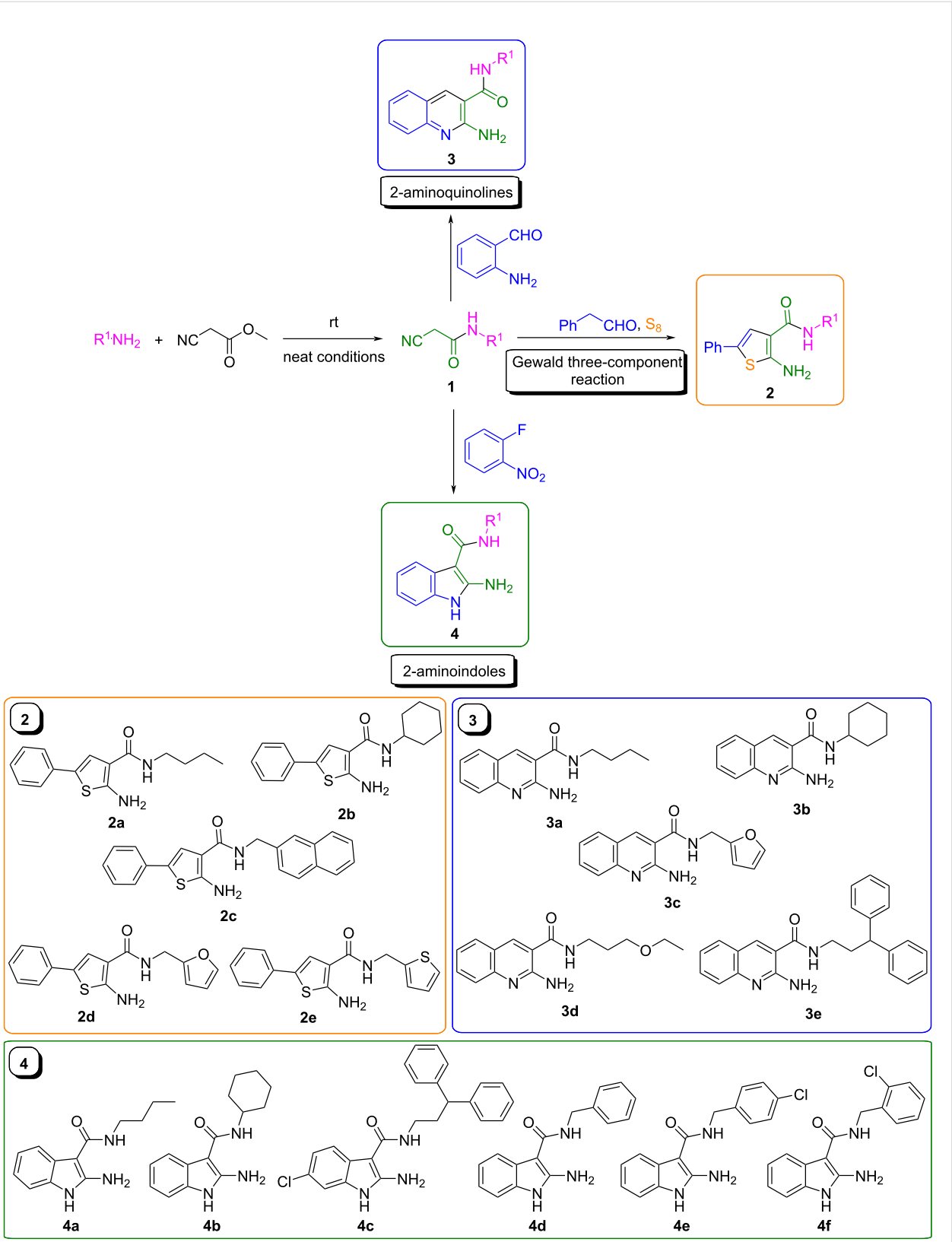

Scheme 2: Access to the key building blocks **2**–**4** by employing three different nonisocyanide-based MCRs. Diversity and complexity were the essential features of our library of starting materials. The colored frames indicate the different scaffold types.

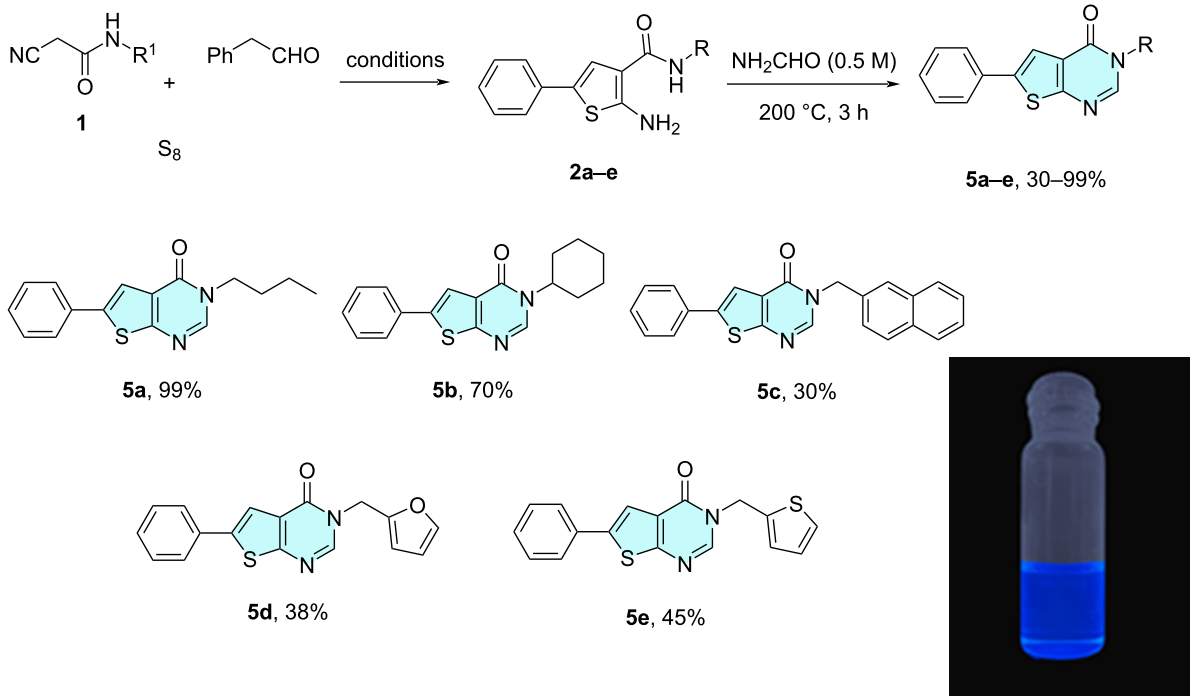

Scheme 3: Synthesis of N-substituted thienopyrimidones **5a–e** by a Gewald three-component reaction employing 2-aminothiophenes **2a–e** and formamide as C1 source. A characteristic fluorescence for compound **5a** was reported (365 nm in DMSO). The reported yield refers to the overall two-step synthesis.

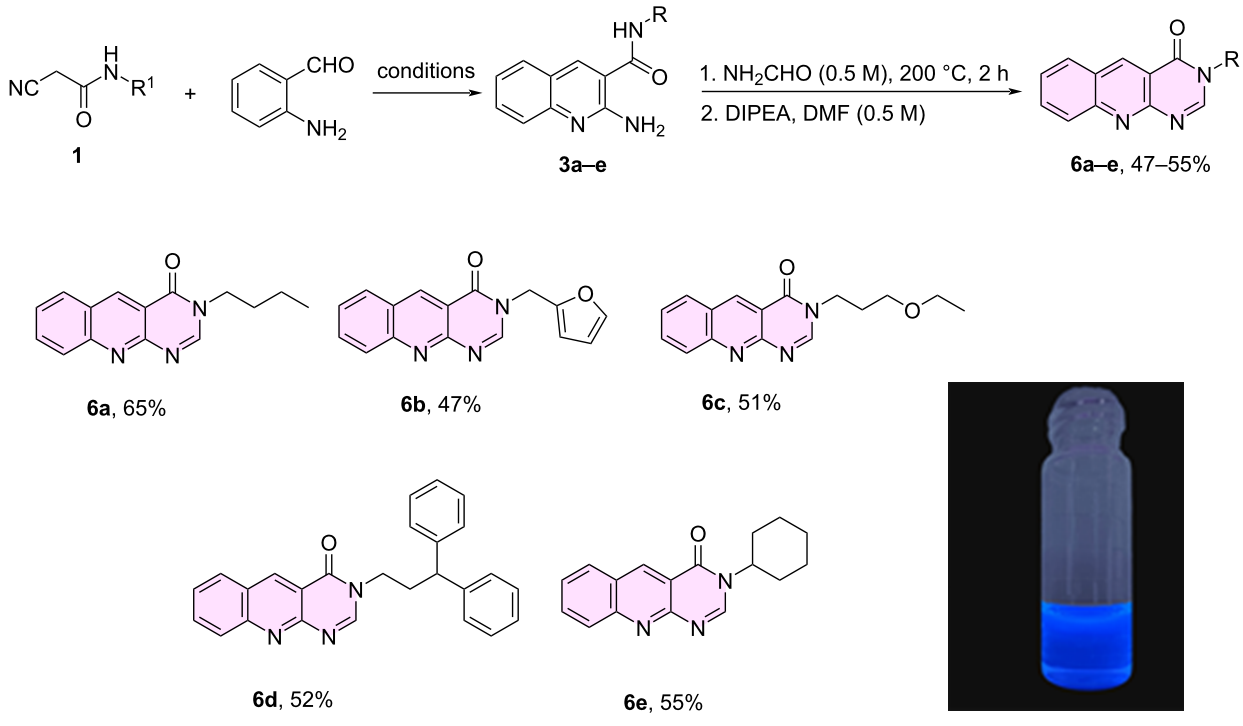

Scheme 4: Synthesis of N-substituted quinolinopyrimidones **6a–e** from 2-aminoindoles **3a–e** and formamide as C1 source. A characteristic fluorescence for compound **6c** was reported (365 nm in DMSO). The reported yields refer to the overall two-step synthesis.

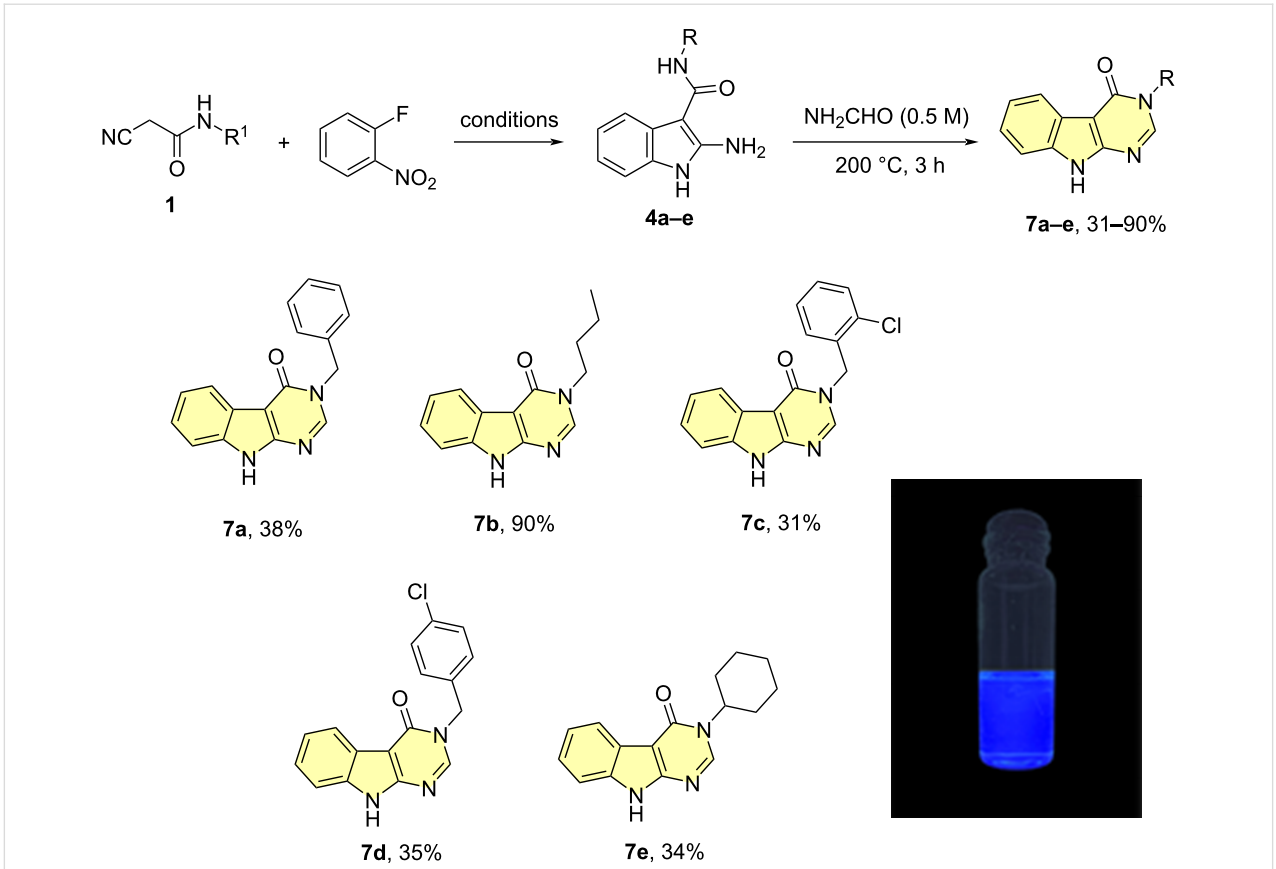

Scheme 5: Synthesis of N-substituted indolopyrimidones **7a–e** from 2-aminoindoles **4a–e** and formamide as C1 source. A characteristic fluorescence for compound **7b** was reported (365 nm in DMSO). The reported yield refers to the overall two-step synthesis.

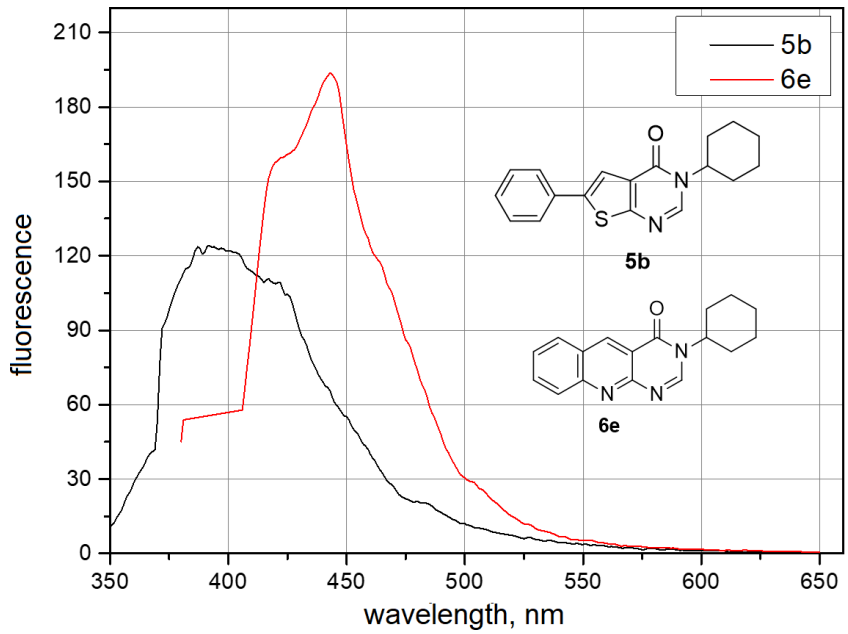

Figure 2: Representative fluorescence spectrum of compounds **5b** (λ_{ex} = 330 nm) and **6e** (λ_{ex} = 430 nm) at 0.2 M in DMSO.

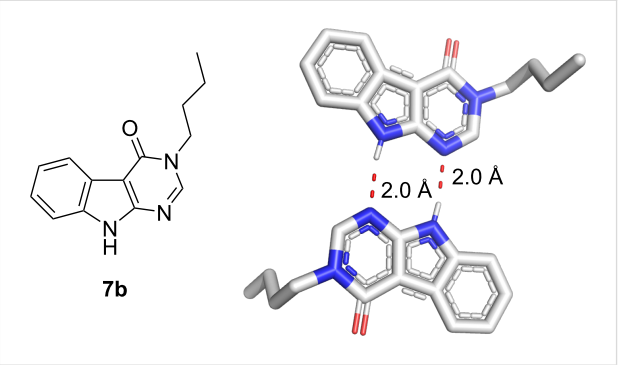

Figure 3: Molecular geometry observed within the crystal structure of compound **7b** (CCDC 2376493).

Conclusion

In conclusion, we successfully combined the Niementowski quinazoline synthesis with nonisocyanide-based chemistry, thereby expanding and enhancing the scope of C1 MCR chemistry. That way, we obtained 15 diversely substituted heteroannulated pyrimidones, employing privileged thiophene, quinoline and indole scaffolds in a rapid fashion, without the need of column chromatography, in a parallel setup.

Supporting Information

Supporting Information File 1

Experimental methods, synthetic procedures, analytical data and exemplary copies of NMR spectra of novel compounds.
[https://www.beilstein-journals.org/bjoc/content/supplementary/1860-5397-21-13-S1.pdf]

Supporting Information File 2

CheckCIF report for **7b**.
[https://www.beilstein-journals.org/bjoc/content/supplementary/1860-5397-21-13-S2.pdf]

Supporting Information File 3

CIF file for **7b**.
[https://www.beilstein-journals.org/bjoc/content/supplementary/1860-5397-21-13-S3.cif]

Acknowledgements

We acknowledge the mass spectrometry facility of the University of Crete.

Funding

The research project was supported by Empeirikion Idryma and University of Crete (ELKE) funding to C.G.N.

Author Contributions

Marios Zingiridis: data curation; formal analysis; investigation; methodology; project administration; validation. Danae Papachristodoulou: investigation; validation; visualization. Despoina Menegaki: investigation; methodology. Konstantinos G. Froudas: investigation; methodology. Constantinos G. Neochoritis: funding acquisition; investigation; project administration; supervision; writing – original draft; writing – review & editing.

ORCID® iDs

Marios Zingiridis - https://orcid.org/0009-0008-1150-2926
Danae Papachristodoulou - https://orcid.org/0009-0007-0615-4018
Constantinos G. Neochoritis - https://orcid.org/0000-0001-5098-5504

Data Availability Statement

Data generated and analyzed during this study is available from the corresponding author upon reasonable request.

References

1. United Nations Department of Economic and Social Affairs (UNDESA) and the Secretariat of the United Nations Framework Convention on Climate Change (UNFCCC). Third Global Conference on Strengthening Synergies Between the Paris Agreement and the 2030 Agenda For Sustainable Development, 2022.
2. Wu, X.-F.; Dyson, P. J.; Arndtsen, B. A. *J. Org. Chem.* **2023,** *88,* 4891–4893. doi:10.1021/acs.joc.3c00626
3. Trost, B. *Science* **1991,** *254,* 1471–1477. doi:10.1126/science.1962206
4. Fragkiadakis, M.; Anastasiou, P.-K.; Volyrakis, I.; Pantousas, A.; Stoumpos, C. C.; Neochoritis, C. G. *Chem. Commun.* **2023,** *59,* 14411–14414. doi:10.1039/d3cc04597h
5. Kerdphon, S.; Sanghong, P.; Chatwichien, J.; Choommongkol, V.; Rithchumpon, P.; Singh, T.; Meepowpan, P. *Eur. J. Org. Chem.* **2020,** 2730–2734. doi:10.1002/ejoc.202000257
6. Jacquet, O.; Das Neves Gomes, C.; Ephritikhine, M.; Cantat, T. *ChemCatChem* **2013,** *5,* 117–120. doi:10.1002/cctc.201200732
7. Dabral, S.; Schaub, T. *Adv. Synth. Catal.* **2019,** *361,* 223–246. doi:10.1002/adsc.201801215
8. Liu, Q.; Wu, L.; Jackstell, R.; Beller, M. *Nat. Commun.* **2015,** *6,* 5933. doi:10.1038/ncomms6933
9. Sakakura, T.; Choi, J.-C.; Yasuda, H. *Chem. Rev.* **2007,** *107,* 2365–2387. doi:10.1021/cr068357u
10. Mikkelsen, M.; Jørgensen, M.; Krebs, F. C. *Energy Environ. Sci.* **2010,** *3,* 43–81. doi:10.1039/b912904a
11. Pinaka, A.; Vougioukalakis, G. C. *Coord. Chem. Rev.* **2015,** *288,* 69–97. doi:10.1016/j.ccr.2015.01.010
12. Aresta, M.; Dibenedetto, A.; Angelini, A. *Chem. Rev.* **2014,** *114,* 1709–1742. doi:10.1021/cr4002758
13. Wang, S.; Xi, C. *Chem. Soc. Rev.* **2019,** *48,* 382–404. doi:10.1039/c8cs00281a
14. Pradhan, S.; Roy, S.; Sahoo, B.; Chatterjee, I. *Chem. – Eur. J.* **2021,** *27,* 2254–2269. doi:10.1002/chem.202003685
15. Hang, W.; Li, D.; Zou, S.; Xi, C. *J. Org. Chem.* **2023,** *88,* 5007–5014. doi:10.1021/acs.joc.2c01840

16. Niemi, T.; Perea-Buceta, J. E.; Fernández, I.; Hiltunen, O.-M.; Salo, V.; Rautiainen, S.; Räisänen, M. T.; Repo, T. *Chem. – Eur. J.* **2016,** *22,* 10355–10359. doi:10.1002/chem.201602338
17. Mei, C.; Zhao, Y.; Chen, Q.; Cao, C.; Pang, G.; Shi, Y. *ChemCatChem* **2018,** *10,* 3057–3068. doi:10.1002/cctc.201800142
18. Wang, B.; Elageed, E. H. M.; Zhang, D.; Yang, S.; Wu, S.; Zhang, G.; Gao, G. *ChemCatChem* **2014,** *6,* 278–283. doi:10.1002/cctc.201300801
19. Feng, L.; Li, X.; Xu, C.; Sadeghzadeh, S. M. *Catal. Lett.* **2020,** *150,* 1729–1740. doi:10.1007/s10562-019-03073-2
20. Wang, L.; Qi, C.; Xiong, W.; Jiang, H. *Chin. J. Catal.* **2022,** *43,* 1598–1617. doi:10.1016/s1872-2067(21)64029-9
21. Li, J.; Di Lorenzo, V.; Patil, P.; Ruiz-Moreno, A. J.; Kurpiewska, K.; Kalinowska-Tłuścik, J.; Velasco-Velázquez, M. A.; Dömling, A. *ACS Comb. Sci.* **2020,** *22,* 356–360. doi:10.1021/acscombsci.0c00072
22. Eleftheriadis, N.; Poelman, H.; Leus, N. G. J.; Honrath, B.; Neochoritis, C. G.; Dolga, A.; Dömling, A.; Dekker, F. J. *Eur. J. Med. Chem.* **2016,** *122,* 786–801. doi:10.1016/j.ejmech.2016.07.010
23. Xiao, Z.; Osipyan, A.; Song, S.; Chen, D.; Schut, R. A.; van Merkerk, R.; van der Wouden, P. E.; Cool, R. H.; Quax, W. J.; Melgert, B. N.; Poelarends, G. J.; Dekker, F. J. *J. Med. Chem.* **2022,** *65,* 2059–2077. doi:10.1021/acs.jmedchem.1c01598
24. Xiao, Z.; Dekker, F. Substituted Thiophene Compounds as D-Dopachrome Tautomerase Inhibitors. WO Patent WO2023031246, March 9, 2023.
25. Sacchelli, B. A. L.; Rocha, B. C.; Fantinel, M.; Andrade, L. H. *Eur. J. Org. Chem.* **2024,** *27,* e202300930. doi:10.1002/ejoc.202300930
26. Jiang, L.; Li, K.; Porter, W. N.; Wang, H.; Li, G.; Chen, J. G. *J. Am. Chem. Soc.* **2024,** *146,* 2857–2875. doi:10.1021/jacs.3c13374
27. Xu, L.; Jiang, Y.; Ma, D. *Org. Lett.* **2012,** *14,* 1150–1153. doi:10.1021/ol300084v
28. Abdellatif, K. R. A.; Bakr, R. B. *Med. Chem. Res.* **2021,** *30,* 31–49. doi:10.1007/s00044-020-02656-8
29. Vyas, A.; Sahu, B.; Pathania, S.; Nandi, N. K.; Chauhan, G.; Asati, V.; Kumar, B. *J. Heterocycl. Chem.* **2023,** *60,* 1081–1121. doi:10.1002/jhet.4593
30. Thakur, S.; Ansari, A. J.; Joshi, G. FDA approved fused pyrimidine-based drugs. In *Fused Pyrimidine-Based Drug Discovery;* Raj, K., Ed.; Elsevier: Amsterdam, Netherlands, 2023; pp 13–38. doi:10.1016/b978-0-443-18616-5.00004-1
31. Xu, G.-F.; Song, B.-A.; Bhadury, P. S.; Yang, S.; Zhang, P.-Q.; Jin, L.-H.; Xue, W.; Hu, D.-Y.; Lu, P. *Bioorg. Med. Chem.* **2007,** *15,* 3768–3774. doi:10.1016/j.bmc.2007.03.037
32. Long, C.; Li, P.; Chen, M.; Dong, L.; Hu, D.; Song, B. *Eur. J. Med. Chem.* **2015,** *102,* 639–647. doi:10.1016/j.ejmech.2015.08.029
33. Kulkarni, S. S.; Singh, S.; Shah, J. R.; Low, W.-K.; Talele, T. T. *Eur. J. Med. Chem.* **2012,** *50,* 264–273. doi:10.1016/j.ejmech.2012.02.001
34. Kargbo, R. B. *ACS Med. Chem. Lett.* **2024,** *15,* 1193–1195. doi:10.1021/acsmedchemlett.4c00327
35. Cline, S. J.; Hodgson, D. J. *J. Am. Chem. Soc.* **1980,** *102,* 6285–6288. doi:10.1021/ja00540a018
36. Sinkeldam, R. W.; McCoy, L. S.; Shin, D.; Tor, Y. *Angew. Chem., Int. Ed.* **2013,** *52,* 14026–14030. doi:10.1002/anie.201307064
37. Ludford, P. T., III; Yang, S.; Bucardo, M. S.; Tor, Y. *Chem. – Eur. J.* **2022,** *28,* e202104472. doi:10.1002/chem.202104472
38. Shin, D.; Sinkeldam, R. W.; Tor, Y. *J. Am. Chem. Soc.* **2011,** *133,* 14912–14915. doi:10.1021/ja206095a
39. Bogert, M. T.; Gotthelf, A. H. *J. Am. Chem. Soc.* **1900,** *22,* 522–535. doi:10.1021/ja02046a008
40. Von Niementowski, S. *J. Prakt. Chem.* **1895,** *51,* 564–572. doi:10.1002/prac.18950510150
41. Meyer, J.; Wagner, E. C. *J. Org. Chem.* **1943,** *08,* 239–252. doi:10.1021/jo01191a005
42. Wang, K.; Kim, D.; Dömling, A. *J. Comb. Chem.* **2010,** *12,* 111–118. doi:10.1021/cc9001586
43. Kok, T.; Wapenaar, H.; Wang, K.; Neochoritis, C. G.; Zarganes-Tzitzikas, T.; Proietti, G.; Eleftheriadis, N.; Kurpiewska, K.; Kalinowska-Tłuścik, J.; Cool, R. H.; Poelarends, G. J.; Dömling, A.; Dekker, F. J. *Bioorg. Med. Chem.* **2018,** *26,* 999–1005. doi:10.1016/j.bmc.2017.12.032
44. Wang, K.; Herdtweck, E.; Dömling, A. *ACS Comb. Sci.* **2011,** *13,* 140–146. doi:10.1021/co100040z
45. Wang, K.; Herdtweck, E.; Dömling, A. *ACS Comb. Sci.* **2012,** *14,* 316–322. doi:10.1021/co3000133
46. Wang, K.; Nguyen, K.; Huang, Y.; Dömling, A. *J. Comb. Chem.* **2009,** *11,* 920–927. doi:10.1021/cc9000778
47. Ali, E. M. H.; Abdel-Maksoud, M. S.; Oh, C.-H. *Bioorg. Med. Chem.* **2019,** *27,* 1159–1194. doi:10.1016/j.bmc.2019.02.044
48. Eissa, K. I.; Kamel, M. M.; Mohamed, L. W.; Doghish, A. S.; Alnajjar, R.; Al-Karmalawy, A. A.; Kassab, A. E. *Drug Dev. Res.* **2023,** *84,* 937–961. doi:10.1002/ddr.22064
49. Zhong, W.; Pasunooti, K. K.; Balamkundu, S.; Wong, Y. H.; Nah, Q.; Gadi, V.; Gnanakalai, S.; Chionh, Y. H.; McBee, M. E.; Gopal, P.; Lim, S. H.; Olivier, N.; Buurman, E. T.; Dick, T.; Liu, C. F.; Lescar, J.; Dedon, P. C. *J. Med. Chem.* **2019,** *62,* 7788–7805. doi:10.1021/acs.jmedchem.9b00582
50. Tinney, F. J.; Cetenko, W. A.; Kerbleski, J. J.; Connor, D. T.; Sorenson, R. J.; Herzig, D. J. *J. Med. Chem.* **1981,** *24,* 878–882. doi:10.1021/jm00139a021
51. Russo, F.; Romeo, G.; Santagati, N.; Caruso, A.; Cutuli, V.; Amore, D. *Eur. J. Med. Chem.* **1994,** *29,* 569–578. doi:10.1016/0223-5234(94)90149-x
52. Modica, M.; Santagati, M.; Santagati, A.; Russo, F.; Cagnotto, A.; Goegan, M.; Mennini, T. *Bioorg. Med. Chem. Lett.* **2000,** *10,* 1089–1092. doi:10.1016/s0960-894x(00)00165-7
53. Duval, E.; Case, A.; Stein, R. L.; Cuny, G. D. *Bioorg. Med. Chem. Lett.* **2005,** *15,* 1885–1889. doi:10.1016/j.bmcl.2005.02.005
54. Miao, Z.; Sun, Y.-m.; Zhao, L.-y.; Li, Y.-s.; Wang, Y.-f.; Nan, J.-s.; Qiao, Z.-e.; Li, L.-l.; Yang, S.-y. *Bioorg. Med. Chem. Lett.* **2020,** *30,* 126966. doi:10.1016/j.bmcl.2020.126966
55. Basile, L.; Álvarez, S.; Blanco, A.; Santagati, A.; Granata, G.; Di Pietro, P.; Guccione, S.; Muñoz-Fernández, M. Á. *Eur. J. Med. Chem.* **2012,** *57,* 149–161. doi:10.1016/j.ejmech.2012.09.005
56. Zhu, W.; Chen, H.; Wang, Y.; Wang, J.; Peng, X.; Chen, X.; Gao, Y.; Li, C.; He, Y.; Ai, J.; Geng, M.; Zheng, M.; Liu, H. *J. Med. Chem.* **2017,** *60,* 6018–6035. doi:10.1021/acs.jmedchem.7b00076
57. Bassetto, M.; Leyssen, P.; Neyts, J.; Yerukhimovich, M. M.; Frick, D. N.; Brancale, A. *Eur. J. Med. Chem.* **2016,** *123,* 31–47. doi:10.1016/j.ejmech.2016.07.035
58. Salahuddin, M.; Kakad, S.; Shantakumar, S. M. *E-J. Chem.* **2009,** *6,* 801–808. doi:10.1155/2009/361282

59. Pédeboscq, S.; Gravier, D.; Casadebaig, F.; Hou, G.; Gissot, A.; Rey, C.; Ichas, F.; De Giorgi, F.; Lartigue, L.; Pometan, J.-P. *Bioorg. Med. Chem.* **2012,** *20,* 6724–6731. doi:10.1016/j.bmc.2012.09.034
60. Spooner, R. A.; Watson, P.; Smith, D. C.; Boal, F.; Amessou, M.; Johannes, L.; Clarkson, G. J.; Lord, J. M.; Stephens, D. J.; Roberts, L. M. *Biochem. J.* **2008,** *414,* 471–484. doi:10.1042/bj20080149
61. Zishiri, V. K.; Joshi, M. C.; Hunter, R.; Chibale, K.; Smith, P. J.; Summers, R. L.; Martin, R. E.; Egan, T. J. *J. Med. Chem.* **2011,** *54,* 6956–6968. doi:10.1021/jm2009698
62. Lilienkampf, A.; Mao, J.; Wan, B.; Wang, Y.; Franzblau, S. G.; Kozikowski, A. P. *J. Med. Chem.* **2009,** *52,* 2109–2118. doi:10.1021/jm900003c
63. Swain, S. S.; Pati, S.; Hussain, T. *Eur. J. Med. Chem.* **2022,** *232,* 114173. doi:10.1016/j.ejmech.2022.114173
64. El-Gazzar, A. B. A.; Hafez, H. N.; Nawwar, G. A. M. *Eur. J. Med. Chem.* **2009,** *44,* 1427–1436. doi:10.1016/j.ejmech.2008.09.030
65. Ali, H. I.; Ashida, N.; Nagamatsu, T. *Bioorg. Med. Chem.* **2008,** *16,* 922–940. doi:10.1016/j.bmc.2007.10.014
66. Joshi, A. A.; Viswanathan, C. L. *Bioorg. Med. Chem. Lett.* **2006,** *16,* 2613–2617. doi:10.1016/j.bmcl.2006.02.038
67. Ibrahim, N. S. M.; Kadry, H. H.; Zaher, A. F.; Mohamed, K. O. *Chem. Biol. Drug Des.* **2023,** *102,* 996–1013. doi:10.1111/cbdd.14307
68. Karthikeyan, C.; Lee, C.; Moore, J.; Mittal, R.; Suswam, E. A.; Abbott, K. L.; Pondugula, S. R.; Manne, U.; Narayanan, N. K.; Trivedi, P.; Tiwari, A. K. *Bioorg. Med. Chem.* **2015,** *23,* 602–611. doi:10.1016/j.bmc.2014.11.043
69. Eleftheriadis, N.; Neochoritis, C. G.; Leus, N. G. J.; van der Wouden, P. E.; Dömling, A.; Dekker, F. J. *J. Med. Chem.* **2015,** *58,* 7850–7862. doi:10.1021/acs.jmedchem.5b01121
70. Sayed, M.; Kamal El-Dean, A. M.; Ahmed, M.; Hassanien, R. *J. Chin. Chem. Soc.* **2019,** *66,* 218–225. doi:10.1002/jccs.201800115
71. Yang, Y.; Wu, S.; Zhao, C.; He, H.; Wu, Z.; Zhang, J.; Song, R. *J. Agric. Food Chem.* **2024,** *72,* 11331–11340. doi:10.1021/acs.jafc.3c08950
72. Enriz, R. D.; Tosso, R. D.; Andújar, S. A.; Cabedo, N.; Cortés, D.; Nogueras, M.; Cobo, J.; Vargas, D. F.; Trilleras, J. *Tetrahedron* **2018,** *74,* 7047–7057. doi:10.1016/j.tet.2018.10.038

License and Terms

This is an open access article licensed under the terms of the Beilstein-Institut Open Access License Agreement (https://www.beilstein-journals.org/bjoc/terms), which is identical to the Creative Commons Attribution 4.0 International License (https://creativecommons.org/licenses/by/4.0). The reuse of material under this license requires that the author(s), source and license are credited. Third-party material in this article could be subject to other licenses (typically indicated in the credit line), and in this case, users are required to obtain permission from the license holder to reuse the material.

The definitive version of this article is the electronic one which can be found at:
https://doi.org/10.3762/bjoc.21.13

BEILSTEIN JOURNAL OF ORGANIC CHEMISTRY

New tandem Ugi/intramolecular Diels–Alder reaction based on vinylfuran and 1,3-butadienylfuran derivatives

Yuriy I. Horak, Roman Z. Lytvyn, Andrii R. Vakhula, Yuriy V. Homza, Nazariy T. Pokhodylo* and Mykola D. Obushak*

Full Research Paper

Open Access

Address:
Department of Organic Chemistry, Ivan Franko National University of Lviv, 6 Kyryla i Mefodiya St., Lviv 79005, Ukraine

Email:
Nazariy T. Pokhodylo* - nazariy.pokhodylo@lnu.edu.ua;
Mykola D. Obushak* - mykola.obushak@lnu.edu.ua

* Corresponding author

Keywords:
1,3-butadienylfuran; furo[2,3-*f*]isoindole; intramolecular Diels–Alder reaction; isoindole; one-pot; Ugi reaction; vinylfuran

Beilstein J. Org. Chem. **2025,** *21,* 444–450.
https://doi.org/10.3762/bjoc.21.31

Received: 07 September 2024
Accepted: 10 February 2025
Published: 26 February 2025

This article is part of the thematic issue "Multicomponent reactions IV".

Associate Editor: T. J. J. Müller

© 2025 Horak et al.; licensee Beilstein-Institut.
License and terms: see end of document.

Abstract

A new tandem sequence involving the Ugi reaction and Diels–Alder [4 + 2] cycloaddition based on vinylfuran and 1,3-butadienylfuran derivatives was designed and studied. It was found that in the case of 3-(furan-2-yl)acrylaldehyde, a one-pot Ugi reaction and intramolecular Diels–Alder vinylarene (IMDAV) reaction leads to the formation of the insufficiently studied furo[2,3-*f*]isoindole derivatives. Ugi adducts formed from (*E*)-3-(furan-2-yl)acrylaldehyde, maleic acid monoanilide, isonitrile, and an amine spontaneously underwent the IMDAV reaction with a high level of stereoselectivity, leading to single pairs of enantiomers of 4,4a,5,6,7,7a-hexahydro-3a*H*-furo[2,3-*f*]isoindole core in excellent yields. Under the same conditions, the (2*E*,4*E*)-5-(furan-2-yl)penta-2,4-dienal gives an Ugi adduct that undergoes the IMDA reaction without involving the furan core. The cycloaddition leads to the formation of 2,3,3a,4,5,7a-hexahydro-1*H*-isoindoles in high yields. The studied tandem Ugi and intramolecular Diels–Alder reactions allow high substituent variation in the named isoindoles.

Introduction

Energy-saving and environmentally friendly synthetic strategies, especially one-pot multicomponent and tandem reactions, are key to modern organic and medicinal chemistry [1-7] and have proven to be successful in generating diverse heterocyclic scaffolds, as highlighted in a recent book [8]. Multicomponent reactions, for instance, have contributed to high-throughput screening for drug discovery, facilitating the identification of new therapeutic compounds. [9,10]. A notable example is ivosidenib, approved in 2018, which was synthesized using the Ugi reaction to target mutated IDH1 in acute myeloid leukemia [11-13]. Advancements in one-pot syntheses, like combining the Ugi reaction with other methods [14-18], for example, the Huisgen cycloaddition, have led to the creation of unique [1,2,3]triazolo[1,5-*a*]pyrazine derivatives [19]. Tandem

reactions are particularly valued for their atom and step-economy, making them promising for future commercial applications.

Partly hydrogenated isoindoles and their derivatives exhibit broad biological activities and are considered privileged motifs in medicinal chemistry [20,21]. These compounds, when condensed with aromatics or heterocycles, form heterolignans, which are synthetic derivatives of naturally occurring lignans [22-25]. This has gained significant attention in drug discovery [26].

Several synthetic routes, such as tandem Pummerer/Diels–Alder or Wittig/Diels–Alder approaches, have been developed for heterolignan construction [27,28]. For instance, the intramolecular Diels–Alder reactions of vinylarenes (IMDAV) strategy [29,30] has been used to synthesize annulated isoindoles, including thieno[2,3-*f*]isoindoles [31,32] and furo[2,3-*f*]isoindoles [33,34], from thienyl- or furylallylamines and unsaturated acid derivatives. Also, benzoisoindoles have been synthesized via the pseudo-four-component reaction of 3-phenylallylamines with maleic anhydride [35]. Finally, furfural was utilized in the Ugi reactions with unsaturated acids leading to the intramolecular Diels–Alder furan (IMDAF) reaction (Figure 1) [36].

In the present work, the new tandem sequence involving an Ugi reaction and Diels–Alder [4 + 2] cycloaddition based on vinylfuran, 1,3-butadienylfuran derivatives was designed and studied.

Results and Discussion

To carry out an intramolecular Diels–Alder reaction, we tested (*E*)-3-(furan-2-yl)acrylaldehyde (**1a**) in the Ugi reaction with a maleic acid to form adducts containing both, diene and dienophilic fragments. It was found that aldehyde **1a** reacted with amines **2**, isonitriles **3**, and maleic acid monoanilide (**4a**) to form an adduct that spontaneously underwent a [4 + 2] cycloaddition giving furoisoindoles **5a**–**h** under the Ugi reaction conditions (Scheme 1). A furan double bond and an exocyclic double bond, forming the diene, enter the intramolecular cyclization, and a residue formed by the monoanilide of maleic acid acts as a dienophile. Notably, non-cyclized Ugi adducts **A1** were not found in the products. The products were identified via NMR as 4,4a,5,6,7,7a-hexahydro-3a*H*-furo[2,3-*f*]isoindoles.

The structures of compounds **5** were confirmed by NMR spectroscopy data (for details and discussion see Supporting Information File 1). The NMR data for the obtained furoindole skeleton signals and spin-coupling constants agree with our

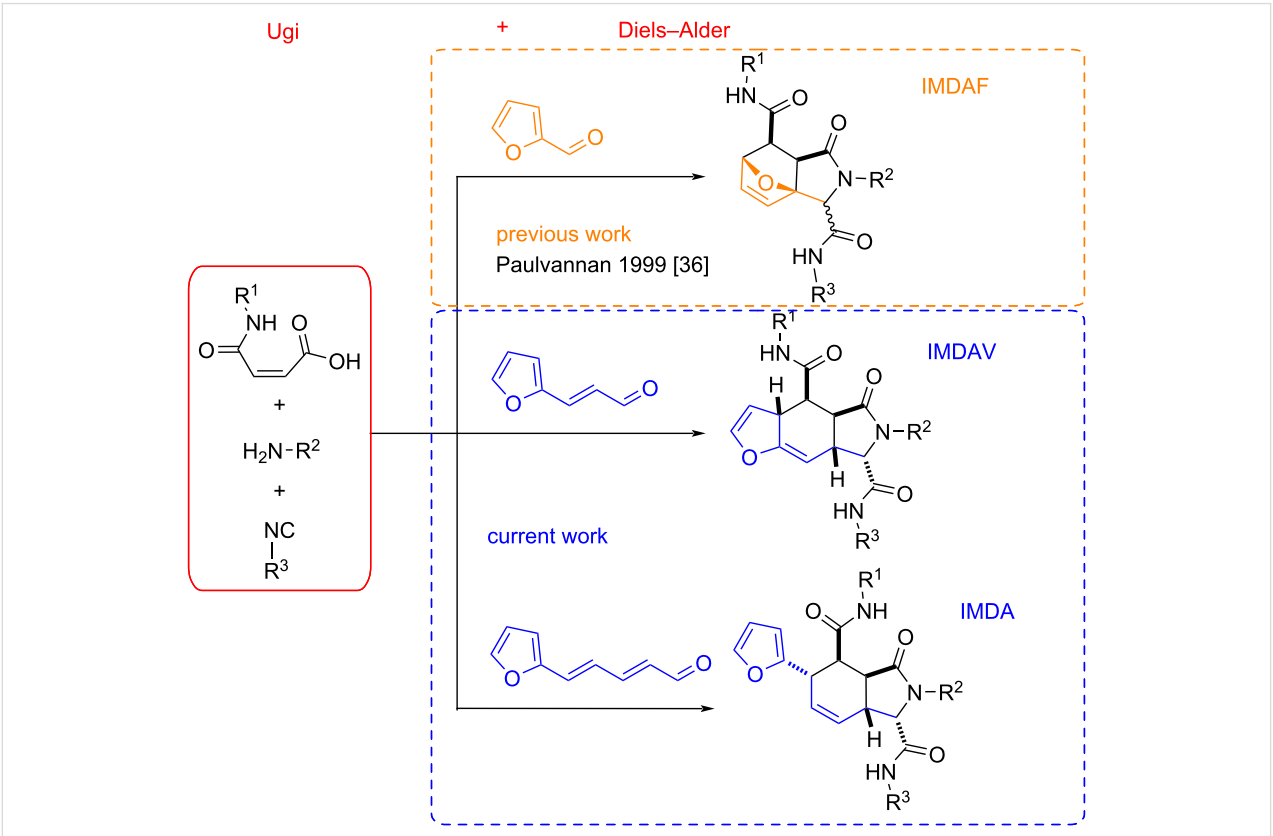

Figure 1: State of the art of Ugi/Diels–Alder reaction based on furan.

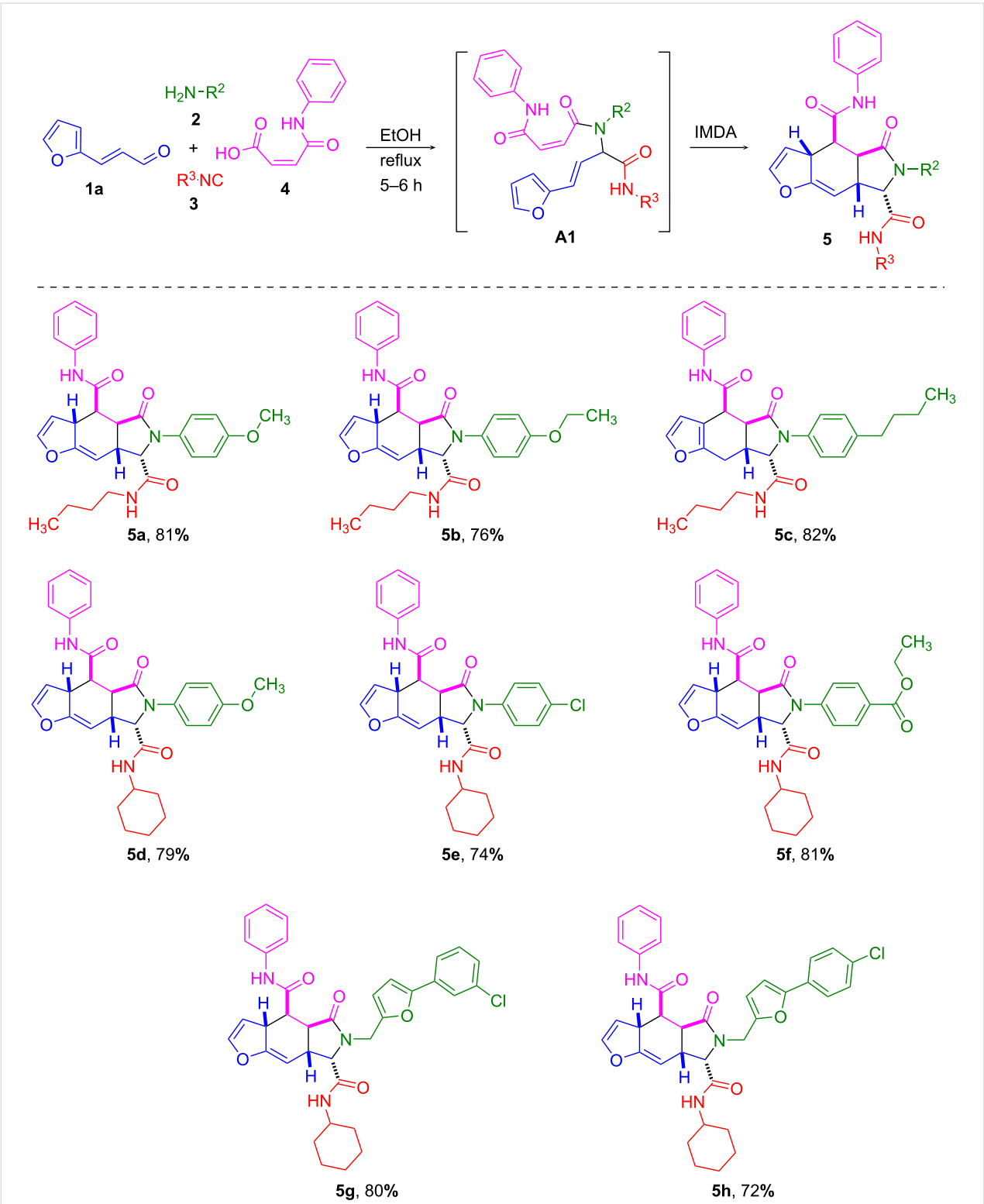

Scheme 1: Preparation of 4,4a,5,6,7,7a-hexahydro-3a*H*-furo[2,3-*f*]isoindoles via Ugi/IMDAV tandem reaction.

previous results on tandem acylation/Diels–Alder reactions [31-33] and lead us to conclude that the final Diels–Alder reaction products are formed as the *exo*-adducts. Moreover, since we do not observe other stereoisomers we speculate that the Ugi and Diels–Alder reactions occur under a coordinated mechanism.

Noteworthy, the primary kinetic product of the cycloaddition reaction **5** is not transformed into the thermodynamic product **6** via a H-shift at the last stage. The expected aromatization with the formation of a furan ring, as happens in similar reactions, does not occur (Scheme 2).

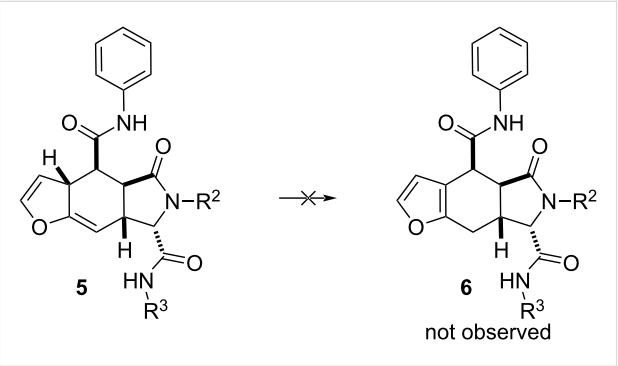

Scheme 2: Kinetic product **5** does not transform into thermodynamic product **6**.

However, if maleic acid was used instead of its monoanilide, then an aromatic furan product was obtained (Scheme 3). Most likely, the presence of a carboxyl group near the hydrogen in the 3-position of the furan ring contributes to its shift and isomerization to a more thermodynamically beneficial aromatic product.

Since we previously studied the reaction of 3-(thien-2-yl)allylamines with maleic anhydride [30], followed by a domino sequence involving successive acylation/[4 + 2] cycloaddition steps, that leads to the formation of the thieno[2,3-*f*]isoindole core, it was interesting to investigate the possibility of obtaining related compounds in the Ugi/IMDAV reaction. It was found that the reaction of (*E*)-3-(thiophen-2-yl)acrylaldehyde proceeds similarly to furylacrylaldehyde and with a high level of stereoselectivity, forms a single pair of enantiomers of 4,4a,5,6,7,7a-hexahydro-3a*H*-thieno[2,3-*f*]isoindoles in excellent yield (Scheme 4). The H-shift does not take place at the last stage, which correlates with the results obtained earlier. This shows the possibility of replacing the furan ring with a thiophene one, which significantly expands the possibilities of this approach for achieving molecular diversity of derivatives for creating libraries of compounds for bioscreening.

Finally, in such a tandem Ugi/IMDA reaction, furyl-2-pentadienal was studied. It was found, that the Ugi adduct formed from (2*E*,4*E*)-5-(furan-2-yl)penta-2,4-dienal (**8**) underwent the IMDA reaction, without involving the furan core in the cycloaddition, thus leading to the 2,3,3a,4,5,7a-hexahydro-1*H*-isoindole core **9**. In the IMDA stage, the exocyclic diene system is involved (Scheme 5). The yields of the products listed below for the Ugi/Diels–Alder tandem reactions were 73% (**9a**) and 70% (**9b**). The structures of these compounds were confirmed by NMR spectroscopy (see Supporting Information File 1).

Conclusion

In summary, we showed the practical usage of 3-(furan-2-yl)acrylaldehyde in the four-component Ugi reaction with the prospect of further intramolecular [4 + 2] cycloaddition of the Ugi reaction product. We managed to carry out these two tandem reactions in one-pot, and, thus, proposed a new variant of the Ugi/Diels–Alder tandem reaction, which is highly vari-

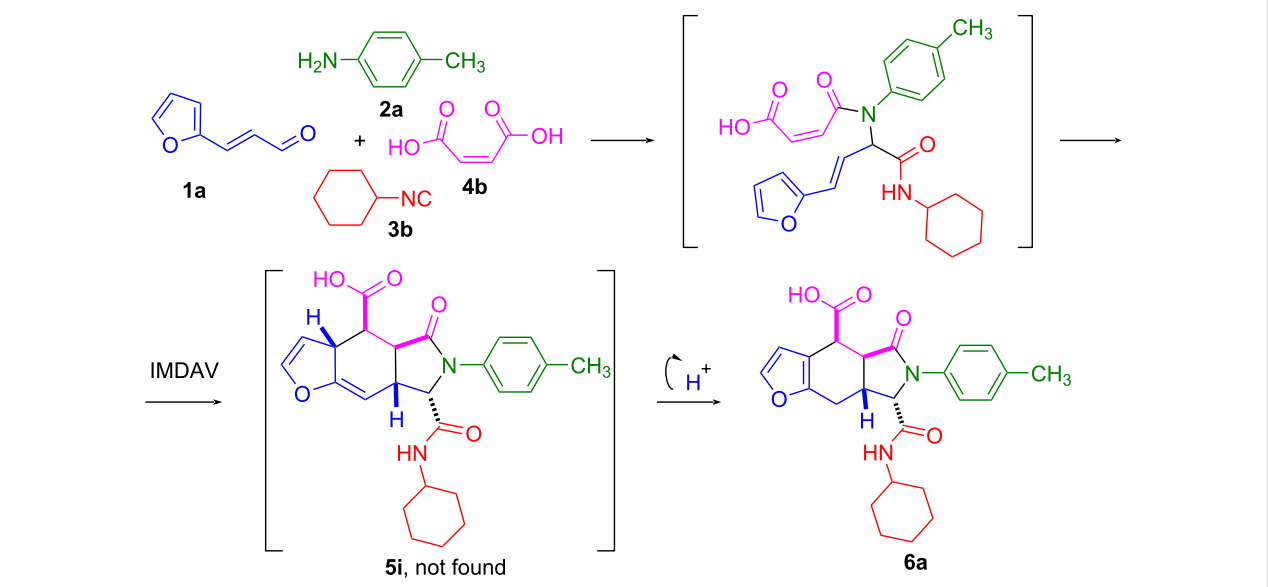

Scheme 3: Synthesis of compounds **6a**.

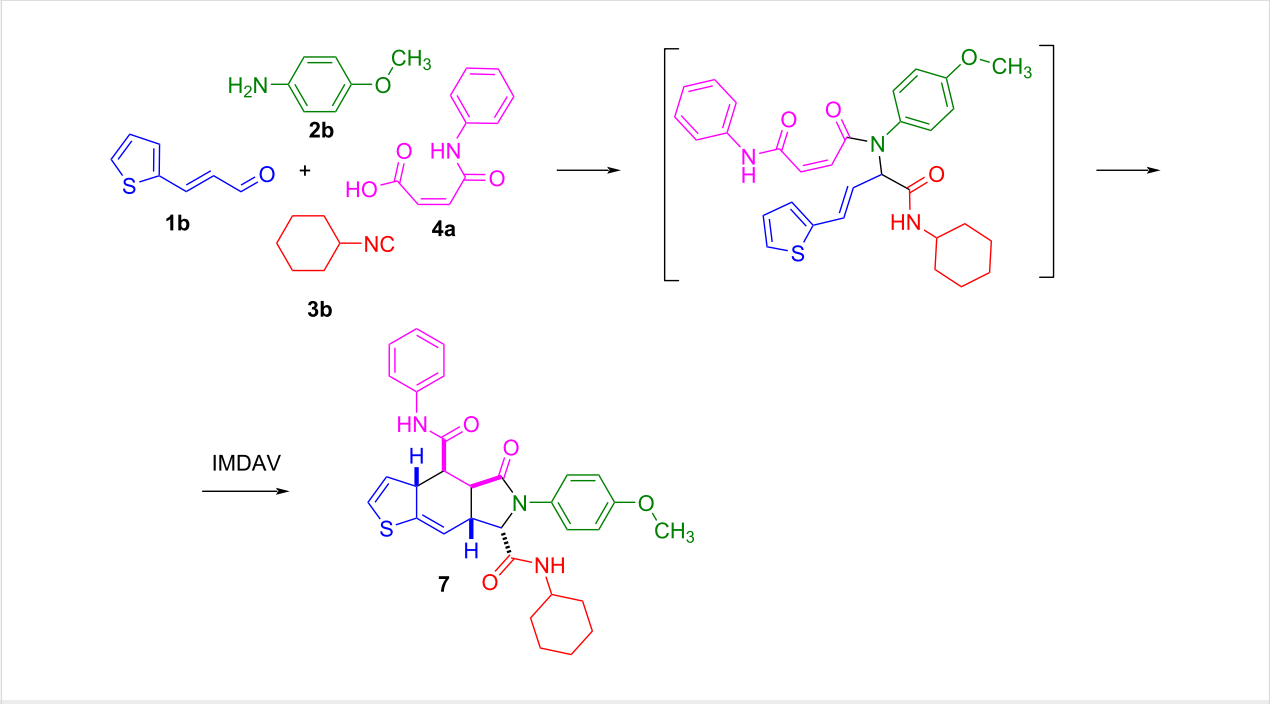

Scheme 4: Synthesis of compound **7**.

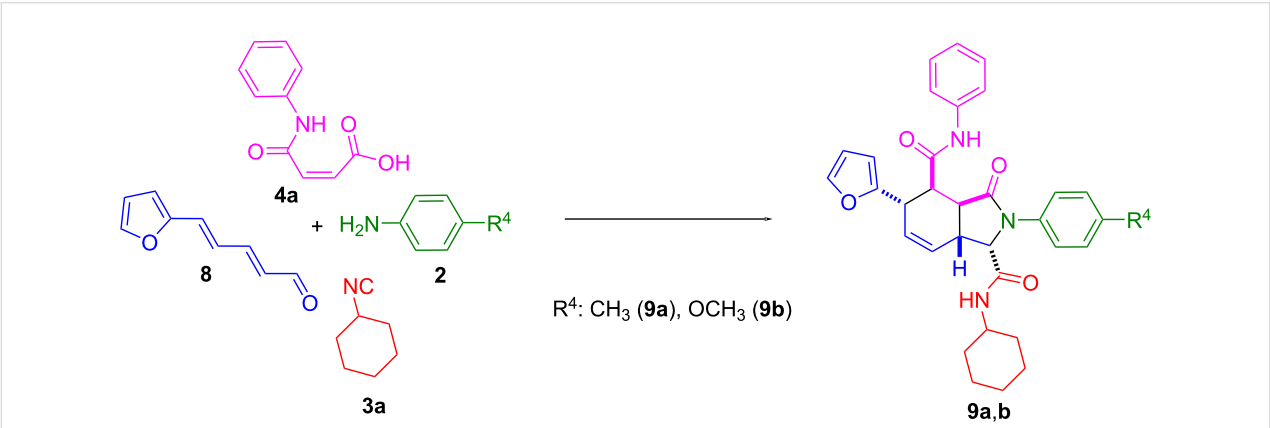

Scheme 5: Synthesis of compounds **9**.

able and promising for implementation in combinatorial synthesis.

Supporting Information

Supporting Information File 1

Experimental procedures, compound characterizations, and NMR spectra.
[https://www.beilstein-journals.org/bjoc/content/supplementary/1860-5397-21-31-S1.pdf]

Funding

The authors are thankful to the Ministry of Education and Science of Ukraine and Simons Foundation (Award Numbers: 1290588) for financial support.

Author Contributions

Yuriy I. Horak: investigation; methodology. Roman Z. Lytvyn: methodology; validation; writing – original draft. Andrii R. Vakhula: investigation. Yuriy V. Homza: investigation. Nazariy T. Pokhodylo: validation; visualization; writing – original draft; writing – review & editing. Mykola D. Obushak: conceptualization; project administration; supervision; validation.

ORCID® iDs

Yuriy I. Horak - https://orcid.org/0000-0002-3195-2325
Roman Z. Lytvyn - https://orcid.org/0000-0001-7086-9703
Andrii R. Vakhula - https://orcid.org/0009-0006-1979-8974
Yuriy V. Homza - https://orcid.org/0009-0001-9598-7631
Nazariy T. Pokhodylo - https://orcid.org/0000-0001-8222-5008
Mykola D. Obushak - https://orcid.org/0000-0001-8146-9529

Data Availability Statement

All data that supports the findings of this study is available in the published article and/or the supporting information of this article.

References

1. Herrera, R. P.; Marqués-López, E., Eds. *Multicomponent Reactions: Concepts and Applications for Design and Synthesis;* Wiley-VCH: Weinheim, Germany, 2015. doi:10.1002/9781118863992
2. Zhu, J.; Bienaymé, H., Eds. *Multicomponent Reactions;* Wiley-VCH: Weinheim, Germany, 2005. doi:10.1002/3527605118
3. Langer, P. *Eur. J. Org. Chem.* **2024,** *27,* e202400153. doi:10.1002/ejoc.202400153
4. Müller, T. J. J.; D'Souza, D. M. *Pure Appl. Chem.* **2008,** *80,* 609–620. doi:10.1351/pac200880030609
5. Gers, C. F.; Rosellen, J.; Merkul, E.; Müller, T. J. J. *Beilstein J. Org. Chem.* **2011,** *7,* 1173–1181. doi:10.3762/bjoc.7.136
6. John, S. E.; Gulati, S.; Shankaraiah, N. *Org. Chem. Front.* **2021,** *8,* 4237–4287. doi:10.1039/d0qo01480j
7. Levi, L.; Müller, T. J. J. *Chem. Soc. Rev.* **2016,** *45,* 2825–2846. doi:10.1039/c5cs00805k
8. Ameta, K. L.; Dandia, A., Eds. *Multicomponent Reactions: Synthesis of Bioactive Heterocycles;* CRC Press: Boca Raton, FL, USA, 2017. doi:10.1201/9781315369754
9. Graebin, C. S.; Ribeiro, F. V.; Rogério, K. R.; Kümmerle, A. E. *Curr. Org. Synth.* **2019,** *16,* 855–899. doi:10.2174/1570179416666190718153703
10. Fouad, M. A.; Abdel-Hamid, H.; Ayoup, M. S. *RSC Adv.* **2020,** *10,* 42644–42681. doi:10.1039/d0ra07501a
11. Dömling, A.; Ugi, I. *Angew. Chem., Int. Ed.* **2000,** *39,* 3168–3210. doi:10.1002/1521-3773(20000915)39:18<3168::aid-anie3168>3.0.co;2-u
12. Mason, K. M.; Meyers, M. S.; Fox, A. M.; Luesse, S. B. *Beilstein J. Org. Chem.* **2016,** *12,* 2032–2037. doi:10.3762/bjoc.12.191
13. Rocha, R. O.; Rodrigues, M. O.; Neto, B. A. D. *ACS Omega* **2020,** *5,* 972–979. doi:10.1021/acsomega.9b03684
14. Rudick, J. G.; Shaabani, S.; Dömling, A. *Front. Chem. (Lausanne, Switz.)* **2020,** *7,* 918. doi:10.3389/fchem.2019.00918
15. Nazeri, M. T.; Farhid, H.; Mohammadian, R.; Shaabani, A. *ACS Comb. Sci.* **2020,** *22,* 361–400. doi:10.1021/acscombsci.0c00046
16. Ojeda, G. M.; Ranjan, P.; Fedoseev, P.; Amable, L.; Sharma, U. K.; Rivera, D. G.; Van der Eycken, E. V. *Beilstein J. Org. Chem.* **2019,** *15,* 2447–2457. doi:10.3762/bjoc.15.237
17. Niu, J.; Wang, Y.; Yan, S.; Zhang, Y.; Ma, X.; Zhang, Q.; Zhang, W. *Beilstein J. Org. Chem.* **2024,** *20,* 912–920. doi:10.3762/bjoc.20.81
18. Ilyin, A.; Kysil, V.; Krasavin, M.; Kurashvili, I.; Ivachtchenko, A. V. *J. Org. Chem.* **2006,** *71,* 9544–9547. doi:10.1021/jo061825f
19. Pokhodylo, N. T.; Tupychak, M. A.; Goreshnik, E. A.; Obushak, M. D. *Synthesis* **2023,** *55,* 977–988. doi:10.1055/s-0042-1751382
20. Pemberton, N.; Mogemark, M.; Arlbrandt, S.; Bold, P.; Cox, R. J.; Gardelli, C.; Holden, N. S.; Karabelas, K.; Karlsson, J.; Lever, S.; Li, X.; Lindmark, H.; Norberg, M.; Perry, M. W. D.; Petersen, J.; Blomqvist, S. R.; Thomas, M.; Tyrchan, C.; Eriksson, A. W.; Zlatoidsky, P.; Öster, L. *J. Med. Chem.* **2018,** *61,* 5435–5441. doi:10.1021/acs.jmedchem.8b00447
21. Mariaule, G.; De Cesco, S.; Airaghi, F.; Kurian, J.; Schiavini, P.; Rocheleau, S.; Huskić, I.; Auclair, K.; Mittermaier, A.; Moitessier, N. *J. Med. Chem.* **2016,** *59,* 4221–4234. doi:10.1021/acs.jmedchem.5b01296
22. Mishra, R.; Sachan, N.; Kumar, N.; Mishra, I.; Chand, P. *J. Heterocycl. Chem.* **2018,** *55,* 2019–2034. doi:10.1002/jhet.3249
23. Tilve, S. G.; Torney, P. S.; Patre, R. E.; Kamat, D. P.; Srinivasan, B. R.; Zubkov, F. I. *Tetrahedron Lett.* **2016,** *57,* 2266–2268. doi:10.1016/j.tetlet.2016.04.038
24. Huang, L.; Ye, L.; Li, X.-H.; Li, Z.-L.; Lin, J.-S.; Liu, X.-Y. *Org. Lett.* **2016,** *18,* 5284–5287. doi:10.1021/acs.orglett.6b02599
25. Li, J.; Zhang, X.; Renata, H. *Angew. Chem., Int. Ed.* **2019,** *58,* 11657–11660. doi:10.1002/anie.201904102
26. Rifai, Y.; Tani, H. B.; Nur, M.; Aswad, M.; Lallo, S.; Wahyudin, E. *Arch. Pharm. (Weinheim, Ger.)* **2016,** *349,* 848–852. doi:10.1002/ardp.201600069
27. Sarkar, T. K.; Panda, N.; Basak, S. *J. Org. Chem.* **2003,** *68,* 6919–6927. doi:10.1021/jo0344081
28. Huang, J.; Du, X.; Van Hecke, K.; Van der Eycken, E. V.; Pereshivko, O. P.; Peshkov, V. A. *Eur. J. Org. Chem.* **2017,** 4379–4388. doi:10.1002/ejoc.201700747
29. Krishna, G.; Grudinin, D. G.; Nikitina, E. V.; Zubkov, F. I. *Synthesis* **2022,** *54,* 797–863. doi:10.1055/s-0040-1705983
30. Yakovleva, E. D.; Shelukho, E. R.; Nadirova, M. A.; Erokhin, P. P.; Simakova, D. N.; Khrustalev, V. N.; Grigoriev, M. S.; Novikov, A. P.; Romanycheva, A. A.; Shetnev, A. A.; Bychkova, O. P.; Trenin, A. S.; Zubkov, F. I.; Zaytsev, V. P. *Org. Biomol. Chem.* **2024,** *22,* 2643–2653. doi:10.1039/d3ob01933k
31. Nadirova, M. A.; Laba, Y.-O. V.; Zaytsev, V. P.; Sokolova, J. S.; Pokazeev, K. M.; Anokhina, V. A.; Khrustalev, V. N.; Horak, Y. I.; Lytvyn, R. Z.; Siczek, M.; Kinzhybalo, V.; Zubavichus, Y. V.; Kuznetsov, M. L.; Obushak, M. D.; Zubkov, F. I. *Synthesis* **2020,** *52,* 2196–2223. doi:10.1055/s-0039-1690833
32. Horak, Y. I.; Lytvyn, R. Z.; Laba, Y.-O. V.; Homza, Y. V.; Zaytsev, V. P.; Nadirova, M. A.; Nikanorova, T. V.; Zubkov, F. I.; Varlamov, A. V.; Obushak, M. D. *Tetrahedron Lett.* **2017,** *58,* 4103–4106. doi:10.1016/j.tetlet.2017.09.038
33. Horak, Y. I.; Lytvyn, R. Z.; Homza, Y. V.; Zaytsev, V. P.; Mertsalov, D. F.; Babkina, M. N.; Nikitina, E. V.; Lis, T.; Kinzhybalo, V.; Matiychuk, V. S.; Zubkov, F. I.; Varlamov, A. V.; Obushak, M. D. *Tetrahedron Lett.* **2015,** *56,* 4499–4501. doi:10.1016/j.tetlet.2015.05.115
34. Zubkov, F. I.; Zaytsev, V. P.; Mertsalov, D. F.; Nikitina, E. V.; Horak, Y. I.; Lytvyn, R. Z.; Homza, Y. V.; Obushak, M. D.; Dorovatovskii, P. V.; Khrustalev, V. N.; Varlamov, A. V. *Tetrahedron* **2016,** *72,* 2239–2253. doi:10.1016/j.tet.2016.03.023
35. Voronov, A. A.; Alekseeva, K. A.; Ryzhkova, E. A.; Zarubaev, V. V.; Galochkina, A. V.; Zaytsev, V. P.; Majik, M. S.; Tilve, S. G.; Gurbanov, A. V.; Zubkov, F. I. *Tetrahedron Lett.* **2018,** *59,* 1108–1111. doi:10.1016/j.tetlet.2018.02.015
36. Paulvannan, K. *Tetrahedron Lett.* **1999,** *40,* 1851–1854. doi:10.1016/s0040-4039(99)00072-6

License and Terms

This is an open access article licensed under the terms of the Beilstein-Institut Open Access License Agreement (https://www.beilstein-journals.org/bjoc/terms), which is identical to the Creative Commons Attribution 4.0 International License (https://creativecommons.org/licenses/by/4.0). The reuse of material under this license requires that the author(s), source and license are credited. Third-party material in this article could be subject to other licenses (typically indicated in the credit line), and in this case, users are required to obtain permission from the license holder to reuse the material.

The definitive version of this article is the electronic one which can be found at:
https://doi.org/10.3762/bjoc.21.31

BEILSTEIN JOURNAL OF ORGANIC CHEMISTRY

Formaldehyde surrogates in multicomponent reactions

Cecilia I. Attorresi[‡1,2,3], Javier A. Ramírez[‡1,2] and Bernhard Westermann[*3]

Review

Open Access

Address:
[1]CONICET - Universidad de Buenos Aires, Unidad de Microanálisis y Métodos Físicos en Química Orgánica (UMYMFOR), Ciudad Universitaria, Intendente Güiraldes 2160, Pabellón 2, 3° Piso, Ciudad Autónoma de Buenos Aires, C1428EGA, Argentina, [2]Departamento de Química Orgánica, Facultad de Ciencias Exactas y Naturales, Universidad de Buenos Aires, Ciudad Universitaria, Ciudad Autónoma de Buenos Aires, C1428EGA, Argentina and [3]Department of Bioorganic Chemistry, Leibniz Institute of Plant Biochemistry, Weinberg 3, D-06120 Halle (Saale), Germany

Email:
Bernhard Westermann[*] - Bernhard.Westermann@ipb-halle.de

* Corresponding author ‡ Equal contributors

Keywords:
cascade reactions; formaldehyde surrogates; green chemistry; heterocycles; multicomponent reactions

Beilstein J. Org. Chem. **2025,** *21,* 564–595.
https://doi.org/10.3762/bjoc.21.45

Received: 27 May 2024
Accepted: 18 February 2025
Published: 13 March 2025

This article is part of the thematic issue "Multicomponent reactions IV" and is dedicated to Prof. H.-U. Reißig on the occasion of his 75th birthday.

Associate Editor: T. J. J. Müller

© 2025 Attorresi et al.; licensee Beilstein-Institut.
License and terms: see end of document.

Abstract

Formaldehyde emerges as a cornerstone in multicomponent reactions, mainly prized for its robust reactivity. Yet, alongside these beneficial traits, this highly reactive C1-building block raises concerns, primarily regarding its toxicity. One notable issue is the challenge of controlling the formation of undesired byproducts during its reactions. This review explores alternative C1-building blocks that serve as surrogates for formaldehyde, aiming to mitigate some of the challenges associated with its use in multicomponent reactions. By identifying these alternatives, toxicity concerns and improved reaction control can be addressed, paving the way for more efficient and sustainable synthetic methodologies.

Introduction

Organic chemistry is a mature discipline that has undergone significant changes since the term was first coined. Since its inception, organic chemistry has straddled the boundaries between art, creativity, and industrial applications. It is a science that is needed to solve complex retrosynthetic problems and develop molecules in gram to kilogram scales for commercialization. Although numerous challenges still need to be addressed, many are not trivial, and solutions thereof lie beyond known approaches. One of them is still the search for the ideal reaction.

Scheme 1 exemplifies the ideal reaction, featuring simple reaction conditions (e.g., ambient temperatures, no specifically prepared solvents), one-pot, batch processes leading to tandem or cascade reactions, resource efficiency through the application of the 12 principles of Green Chemistry, and readily available

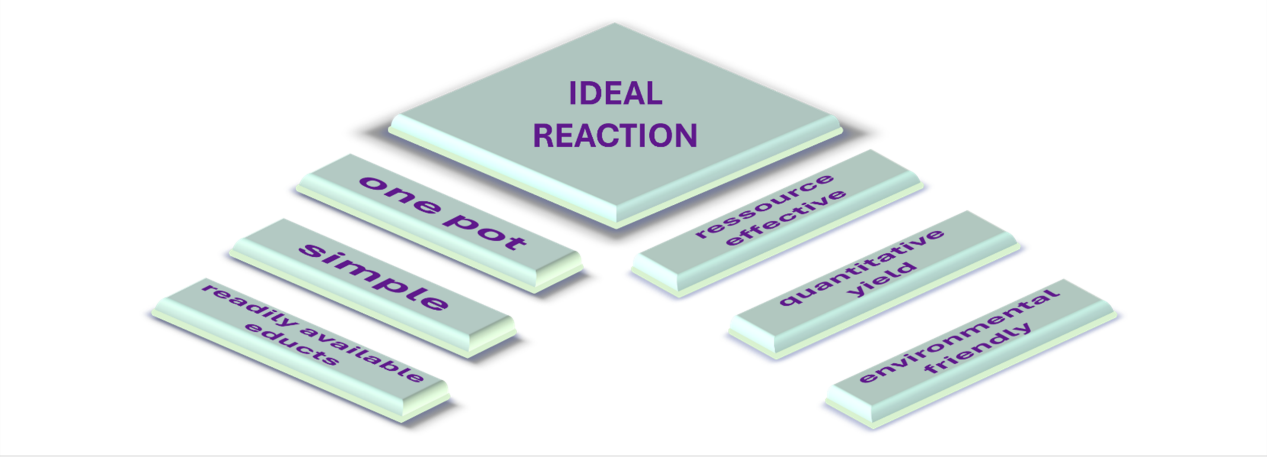

Scheme 1: Features of the ideal reaction (redrawn from P. A. Wender et al. [1]).

starting materials such as waste materials from food production processes [1-3].

In recent years, multicomponent reactions (MCRs) have become one of the most important synthetic tools coming close to fulfilling the requirements of ideal reactions. They are ideally suited also for the generation of high chemical diversity compounds from simple reagents, either through scaffold diversification or scaffold decoration [4]. In these reactions, three or more compounds react together in one single reaction step to generate a more complex product where most of the atoms of starting materials are present [5]. This high atom economy positions MCRs as ecofriendly (green) reactions because their implementation often implies fewer purification steps to achieve the target molecules, leading to a reduction of waste, when compared to traditional "step by step" synthesis. Another advantage of MCRs is that by selecting appropriate starting materials, follow-up functionalization by, e.g., post-cyclization of the MCR product is possible thus increasing the versatility of these reactions in terms of structural diversity and molecular complexity. In this context, a wide variety of heterocycles and macrocycles as important biological scaffolds have been synthesized [6].

One of the most important components used in MCRs is formaldehyde, which acts as a highly reactive electrophilic C1 building block in central MCRs reactions such as the Mannich, Biginelli, Ugi, and Passerini reactions (Scheme 2) [7]. In these reactions, formaldehyde undergoes formally the consecutive attack of two other reactants on the carbon atom, due to the readiness for losing a water molecule.

Formaldehyde is commonly used in its polymeric form (paraformaldehyde) or in a 37% aqueous solution (formalin). The exceptional solubility of formaldehyde in water or biobased solvents, such as ethanol and glycerol, enhances the feasibility of green MCRs due to its high reactivity under these conditions [7]. However, this reactivity also increases the potential for the formation of byproducts. Furthermore, formaldehyde is widely recognized to be toxic and is considered carcinogenic by the World Health Organization (WHO) both in solution and in solid forms [8,9].

Given the limitations mentioned above, there has been a critical impetus in recent years to identify formaldehyde substitutes, such as C1 synthons, in MCR. Various efforts have been made to explore alternative reagents that may act as a source of formaldehyde in the reaction medium or lead to the formation of the same final product as that achieved with formaldehyde, but through different reaction mechanisms. Due to the importance of this research, this review aims to summarize and analyze the significant efforts made in this regard in recent years. Major emphasis will be devoted to dimethyl sulfoxide, dihalomethanes, hexamethylene tetramine, and glyoxylates as C1-building blocks, substituting formaldehyde.

Review

Methanol as a source of formaldehyde

There are several reports on the use of alcohols under oxidative conditions as aldehyde surrogates in Ugi and Passerini reactions [10]. Oxidation of the alcohol is done in situ to avoid problems regarding the isolation and instability of the aldehyde produced, although undesirable reactions, such as oxidation of the amines or isocyanides or overoxidation of the alcohol, could also be problematic [11,12]. In this regard, several efforts have been made to improve the chemoselectivity of the oxidation step. Among the most relevant examples, *o*-iodoxybenzoic acid (IBX) has been used in Ugi and Passerini reactions to oxidize the suitable alcohol to the desired aldehyde [13]. Alternatively, catalytic amounts of a ternary system ($CuCl_2$, $NaNO_2$, TEMPO)

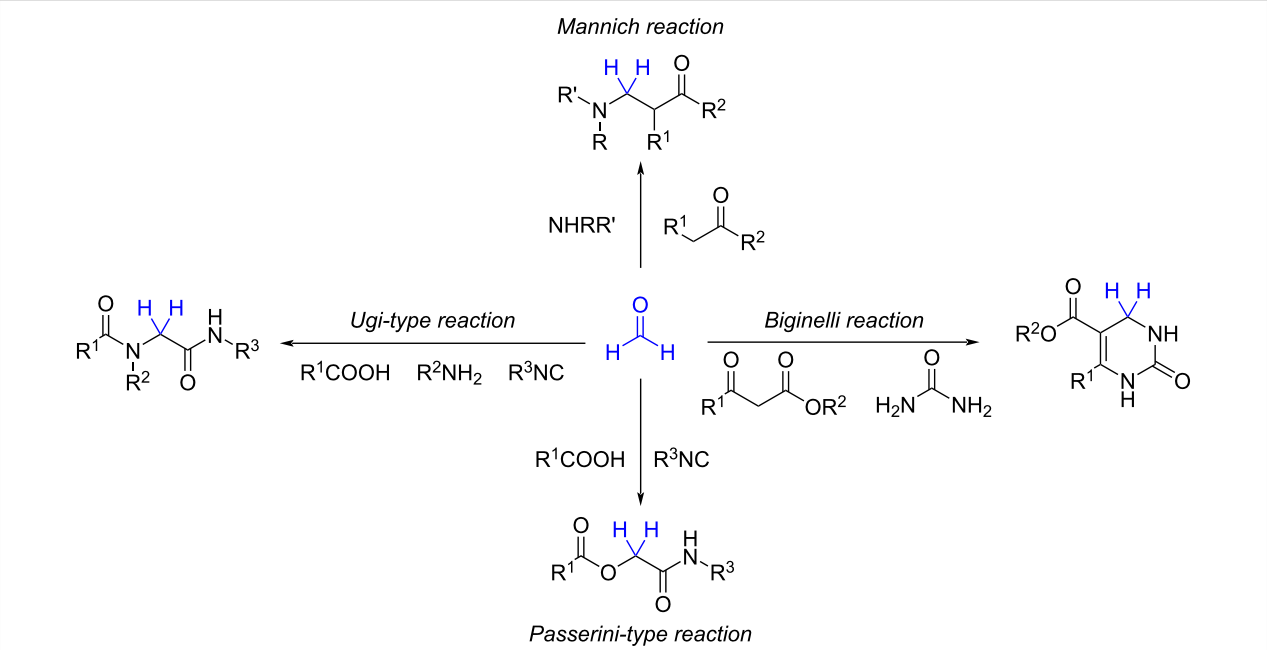

Scheme 2: Some of the most popular MCRs with formaldehyde as the carbonyl component.

using molecular oxygen as a terminal oxidant have also been used [12].

Nevertheless, neither of these conditions was successful when they were applied to methanol to generate formaldehyde, because overoxidation is an important side reaction in these cases [12-15]. However, in a recent work, Pan et al. could chemoselectively oxidize methanol using a TEMPO-catalyzed electro-oxidation process, even in the presence of oxidizable amines, such as benzylamine, paving the way for the use of methanol as a formaldehyde surrogate in these isocyanide-based MCRs (Scheme 3) and, eventually, in other MCRs where formaldehyde acts as a C1 building block [16]. As can be seen in Scheme 3, under this strategy a wide variety of diamide com-

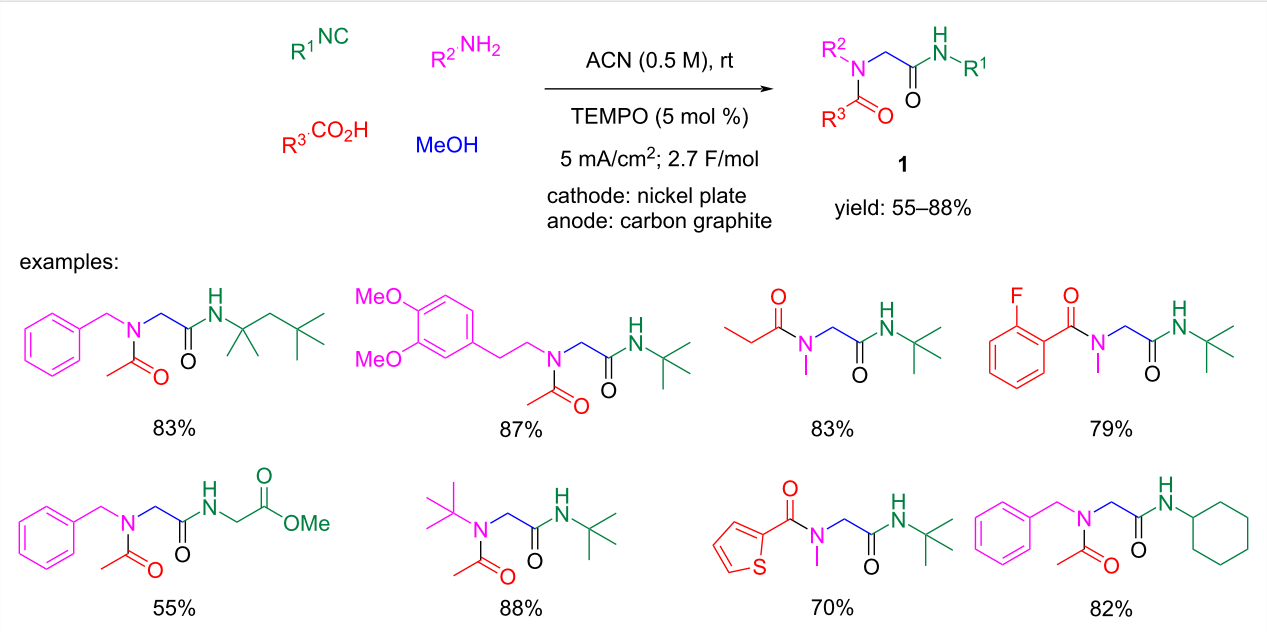

Scheme 3: Ugi reaction under a catalyzed electro-oxidation process using TEMPO (2,2,6,6-tetramethyl-1-piperidinyloxyl) as the redox mediator in the oxidation of methanol to formaldehyde.

pounds **1** could be afforded with very good yields applying MeOH as a formaldehyde source in a traditional Ugi reaction.

Dimethyl sulfoxide (DMSO) as surrogate and source of formaldehyde

Dimethyl sulfoxide is a well-known polar-aprotic solvent with high boiling point that is used in several organic synthetic reactions because of affordable cost and relatively low toxicity. There are numerous examples that show the use of DMSO as a C1 or C2 building block [17,18]. An important drawback of this solvent is the difficulty of its removal from the reaction crude, and extractions with water are commonly employed before purification.

Depending on the reaction conditions, DMSO can be transformed into different products, e.g., under redox conditions, DMSO can decompose into DMS (dimethyl sulfide), which then can act as a nucleophile in several MCRs (Scheme 4) [19-22]. In this context, DMSO can be used as a source of the methylsulfanyl (-SCH_3) group after DMS follows a nucleophilic addition or substitution, allowing one to obtain different types of products (products **2** to **5**, Scheme 4).

In other cases, under acidic and thermal conditions, DMSO can undergo a Pummerer-type process in which, upon activation of the sulfoxide oxygen, a reactive methyl(methylene)sulfonium ion (MMS) is formed (Scheme 5) that acts as an active electrophile. Depending on the nucleophilic species present in the reaction medium, MMS can act as a methylene source. Under hydrolysis conditions, it can be a source of formaldehyde (Scheme 5a), but with other nucleophiles, after nucleophilic addition, the sulfide group can work as a leaving group, allowing for a sequential domino process such as an aza-Prins cyclization [23] and aza-Diels–Alder reaction [24], where MMS serves as direct source of the methylene (-CH_2-) group (Scheme 5b).

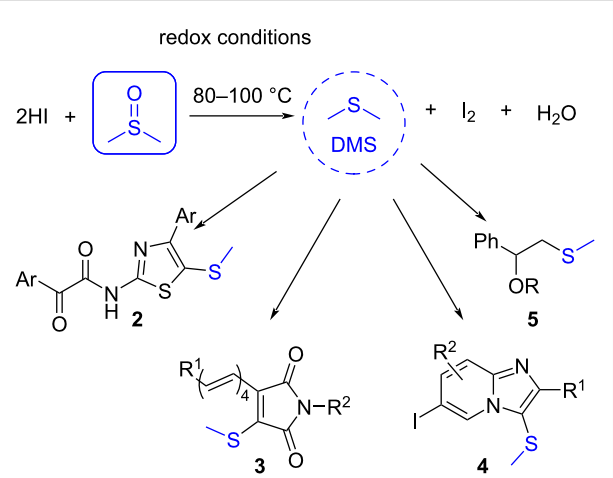

Scheme 4: Examples of different products obtained by MCRs in which DMSO serves as -SCH_3 source.

In both cases, the resulting reactive species (MMS or formaldehyde) can participate as electrophilic component in several MCRs as C1 building block.

Synthesis of heteroaromatic systems

One of the most powerful applications of MCRs is the synthesis of heterocyclic compounds and several reports in recent years showed the advantages of using this tool as a synthetic strategy to generate complex molecular scaffolds with medicinal relevance [25-27].

In this context, quinoline and its derivatives are privileged structures in several natural products and biologically active compounds, rendering this scaffold an important synthetic target. An attractive strategy to afford tetrahydroquinolines and quinolines is the Povarov reaction, a type of aza-Diels–Alder reaction between an imine and an alkene (Scheme 6). Very suc-

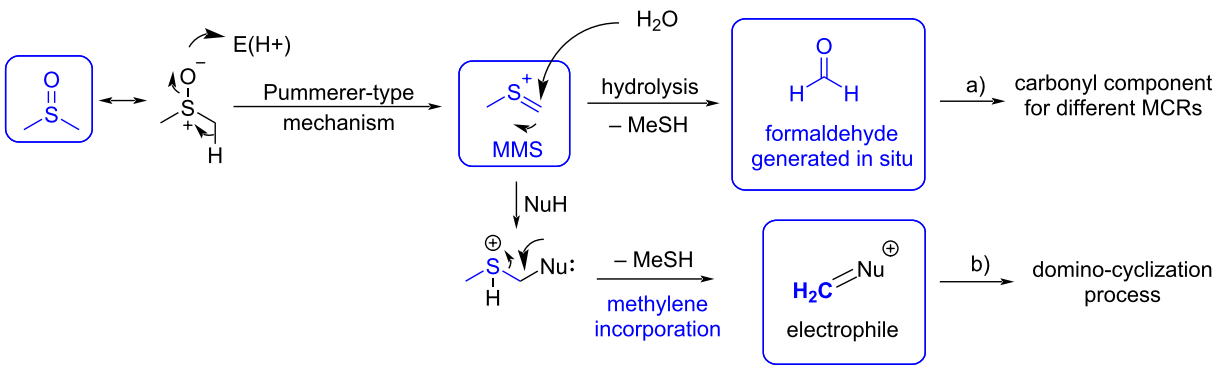

Scheme 5: Mechanism of the decomposition of DMSO under acidic or thermal conditions. a) In situ generation of formaldehyde after hydrolysis of MMS. b) Reaction with other nucleophiles (Nu^-).

cessfully, the multicomponent version of the Povarov reaction using aldehydes, anilines, and alkenes has been explored in a three-component cascade reaction to quinolines [28-31] (Scheme 6). Furthermore, protocols have been developed in which the alkene compound has been replaced with other surrogates for electrophilic addition, such as ketones [32-34]. In the case of the carbonyl component, it is generally an aromatic aldehyde [30,33,34] and there are not many reports on using formaldehyde in the Povarov reaction.

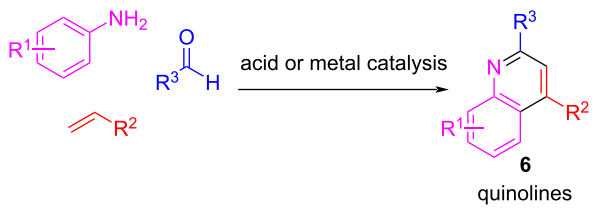

Scheme 6: Povarov multicomponent reaction to quinolines.

In a remarkable example, when formaldehyde was used, the reaction did not provide the desired quinoline **6** as the main product but rather julolidines **7** (Scheme 7) [31].

However, the use of paraformaldehyde and glycine can produce the desired products with low yields, but very expensive catalysts and complex separation processes are required [32,35,36].

In this context, DMSO has been used as an alternative to formaldehyde for the MCR synthesis of a wide variety of quinolines and related compounds. For example, Zhang et al. showed that starting from anilines and substituted styrenes while using $K_2S_2O_8$ for the conversion of DMSO to MMS, a wide range of 4-arylquinolines can be synthesized (Scheme 8, path I) [24]. In this reaction, the persulfate ion generates the thionium ion (MMS), which is trapped by a nucleophilic aniline. The loss of methyl sulfide generates an imine intermediate **B**, which, in turn, reacts with substituted styrene under copper(I) catalysis to give the target compounds via a Povarov reaction. A further aromatization process yields product **I** (Scheme 8, path I). In a closely related approach, the same group reported on the synthesis of quinolines from anilines and alkynes [37]. In this case, the alkyne first reacts with the aniline under cobalt(III) catalysis, and the resulting intermediate **C** then attacks the thionium ion **A**. Quinolines of general structure **II** are formed after the loss of methyl sulfide from intermediate **D**, followed by final cyclization of intermediate **E** (Scheme 8, path II).

Additionally, the Tiwari group developed a metal-free protocol using only $K_2S_2O_8$ as an oxidant for the activation of DMSO to MMS (Scheme 8, path II) [38]. Under these conditions, an alternative mechanism arises in which the imine intermediate **B**, formed as previously stated through reaction between the aniline compound and MMS, undergoes an aza-Diels–Alder cyclization with the alkyne, and after oxidation and aromatization steps generates quinoline **II**. Unfortunately, under these gentle and greener conditions, aliphatic alkynes remain unreacted, compared to the metal-catalyzed version developed by Xu et al. [37] with which a wide range of aromatic and aliphatic disubstituted alkynes were reactive, resulting in a greater diversity of quinolines **II**.

In both cases, regardless of the catalyst used, the MCR tolerates a wide variety of anilines that have either electron-donating or electron-withdrawing groups with various substitution patterns in the aromatic ring, allowing a high variety of quinolines of general structure **I** and **II**.

In a related work, quinolines of structure **I** (Scheme 8) could be obtained by similar reaction pathways. Jadhav et al. proposed a three-component cascade reaction between anilines, methyl aryl ketones, and DMSO under iron(III) catalysis and using $K_2S_2O_8$ for its activation [39]. The proposed mechanism is very close to those described above, with the methyl aryl ketone taking part of the reaction in place of the styrene component in the Povarov cyclization. In this case, the imine reacts with the enolate of the ketone, which is stabilized by coordination with Fe(III), resulting in the formation of the C–C bond. A further oxidative arom-

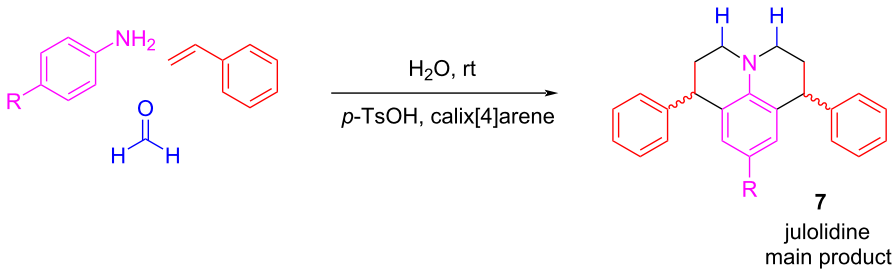

Scheme 7: Example of the Povarov reaction with formaldehyde with a julolidine derivative as main product.

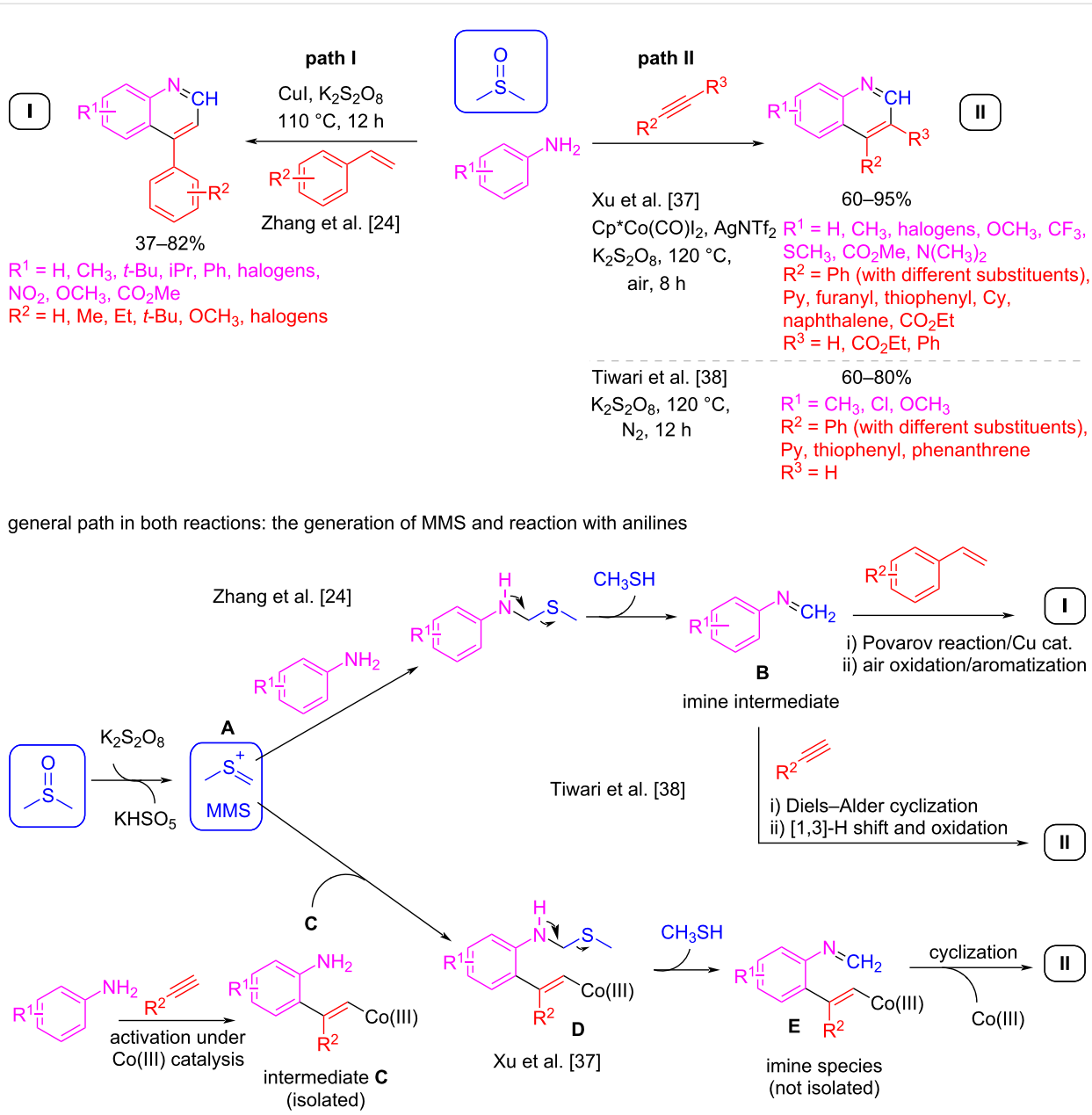

Scheme 8: Povarov multicomponent reaction to quinoline derivatives **I** and **II** using DMSO as formaldehyde surrogate.

atization process affords compound **I**. Compared to the protocol developed by Zhang et al. [24], the reaction is less regioselective, as Troger's base derivatives are isolated as side-products. Interestingly, when Liu et al. [40] modified this reaction by using a copper(II) catalyst under aerobic oxidative conditions, the regioisomers **III** (2-arylquinolines) were obtained (Scheme 9).

To rationalize this singular result, the authors proposed a mechanism in which, after MMS formation, this reactive species is subsequently captured by the stabilized Cu(II) enolate of the ketone, to provide an α,β-unsaturated ketone intermediate **F**. This compound condenses with the aniline component to give an imine **G** that follows a cyclization and aromatization cascade reaction, affording 2-arylquinolines **III**.

All of these examples showed the versatility of DMSO as a methylene source in the synthesis of substituted quinoline compounds (structures **I**, **II**, and **III**; Scheme 8 and Scheme 9), using different substrates (such as styrenes, alkynes, and methyl aryl ketones) and consequently, different catalytic strategies to afford the electrophilic addition on the final cyclization step.

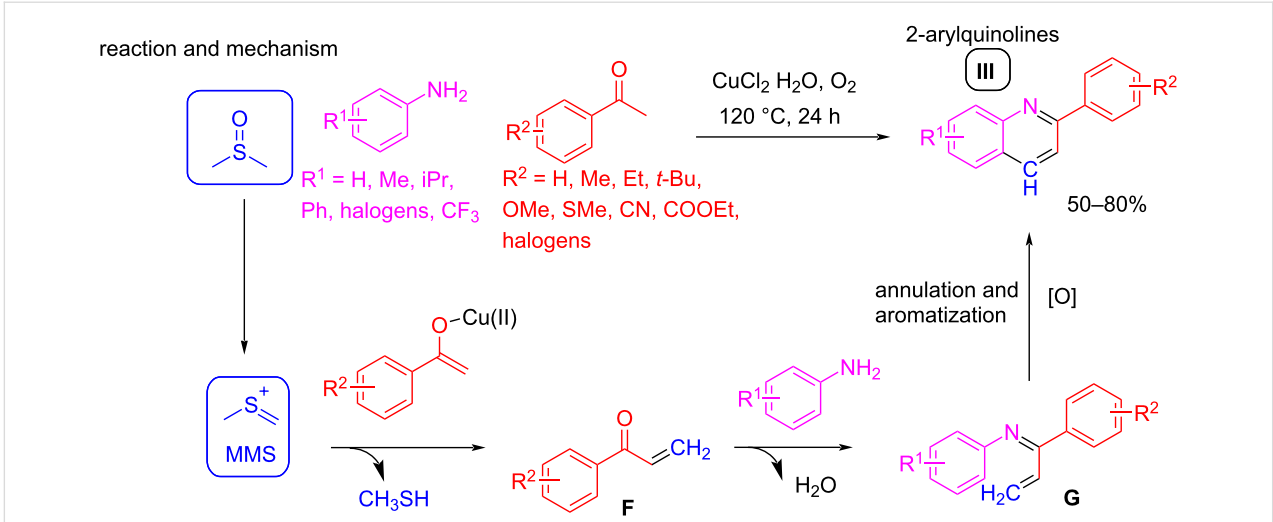

Scheme 9: Example of a Povarov three-component reaction with change of catalyst, yielding regioisomer **III**. In this case, the methylene group is assembled at the C4 position.

Finally, other examples show the synthesis of 3-aryl and alkyl quinoline-3-carboxylate derivatives under acid catalysis for the activation of DMSO via the Pummerer reaction (Scheme 10). In these cases, phenylalanine and aspartate derivatives react with aniline compounds to provide quinoline regioisomers **IV** and **V**, respectively [41]. These reactions are suited for a broad range of reactants with both electron-donating and electron-withdrawing groups.

DMSO activation through a Pummerer reaction (as exemplified in Scheme 10 above) and its use in heterocycle multicomponent synthesis is not limited to quinolines, as the reaction to diarylpyridines [42,43], quinazolinones [44], and pyrazoles [45] is also described by this approach (Scheme 11). These examples deserve further discussion.

Quinazolinones **10** can be synthesized from substituted acetophenones and aromatic amines (Scheme 11) [44]. On the other hand, diarylpyridines **8**, **9**, and **11** can be obtained from acetophenones, but using aliphatic amines or ammonium formate as the nitrogen source [42,43]. In all these cases, the activation of DMSO was carried out via copper catalysis or iodine–acid ca-

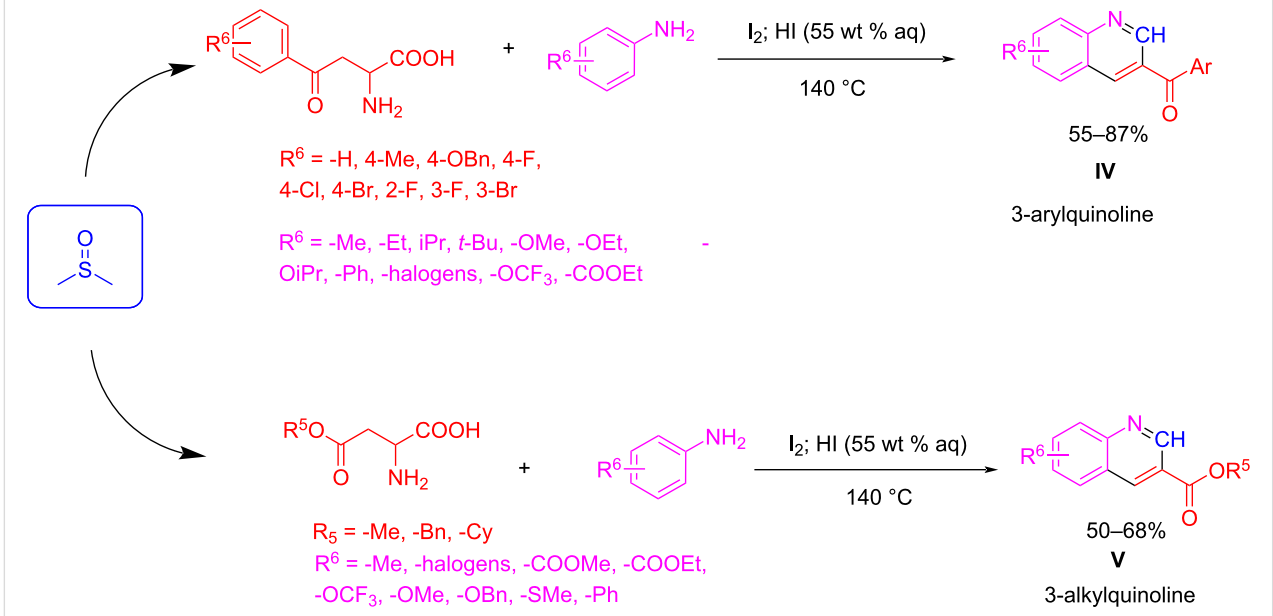

Scheme 10: The Povarov three-component reactions carried out under acidic catalysis to afford quinoline regiosomers **IV** and **V**.

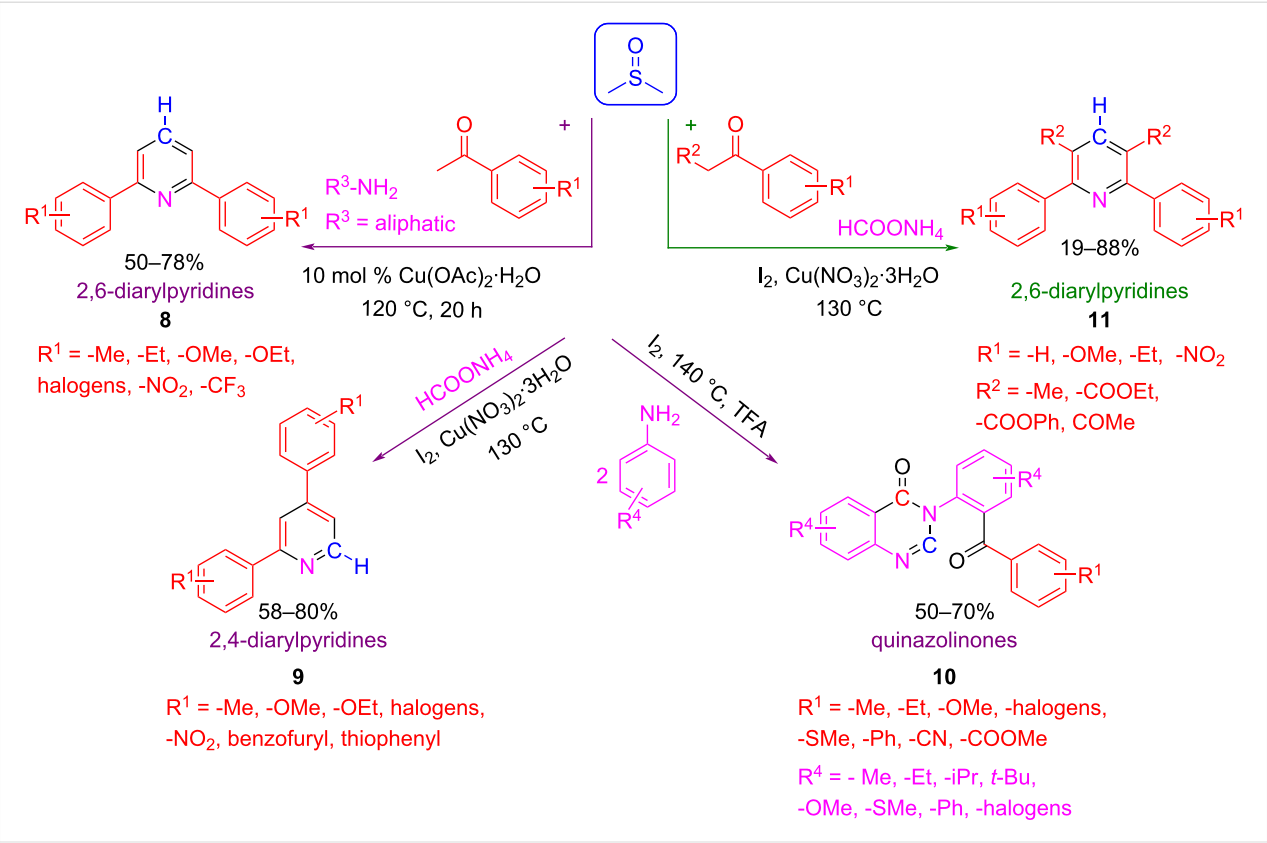

Scheme 11: Different MCR routes involving DMSO to synthesize complex heterocycles such as diarylpyridines and quinazolinones.

talysis. Interestingly, when aliphatic amines are employed (R^3 = *n*-Pr, *n*-Bu, product **8**) only the N atoms are incorporated in the structure of the final product, probably because the high temperature favors the elimination of the alkyl group. The reaction works very well for a wide variety of functional groups and substitution patterns in the aryl methyl ketone substrate, affording the desired heterocycle with good yields. Even heteroaryl methyl ketone and 1,3-dicarbonyl compounds work very well under these reaction conditions, leading to more complex heterocycle products of general structure **9** and **11**. Interestingly, Wu et al. demonstrated that the reaction did not proceed when paraformaldehyde is used as the C1 synthon, indicating that formaldehyde is not involved in the reaction [43]. Furthermore, in isotope labelling studies using DMSO-d_6 all of these authors confirmed, after analyzing the position of the deuterium atoms in the final compound, that the methylene unit incorporated into the heterocycle came from DMSO.

In the case of pyrazole synthesis, Guo et al. proposed a three-component cascade reaction of enaminones, hydrazines, and DMSO (Scheme 12) [45]. In this case, the reaction works well under metal-free conditions using iodine as the catalyst. Remarkably, the activation of DMSO was accomplished using Selectfluor, and in this case, DMSO is the source of a C-1 unit.

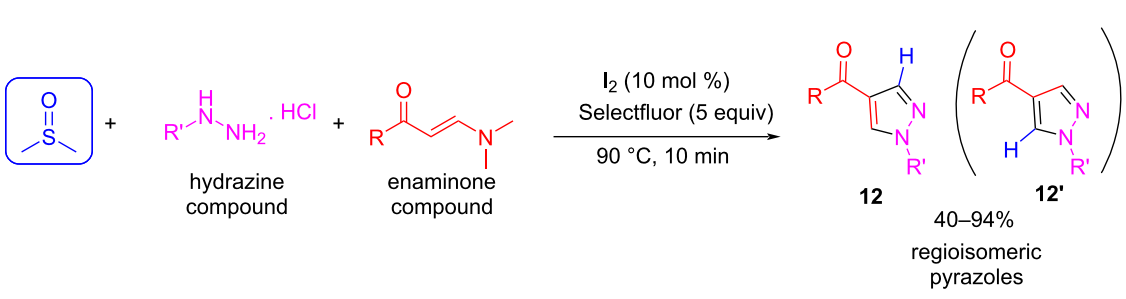

Scheme 12: Pyrazole synthesis by a three-component reaction using DMSO as a source of a C-1 unit.

It is important to note that the reaction could be performed using formaldehyde in only minor yields. This can be explained in terms of the regiospecificity of the reaction: when DMSO is used as the C1 synthon, two different ways of transferring the CH group at different positions in the pyrazole ring (**12** and **12'**) are allowed. However, this cannot be accomplished in the case of formaldehyde, making the reaction more regioselective.

In the cases shown above, we discussed different ways to activate DMSO. In almost all of them, MMS appears as the reactive species due to its high electrophilicity, which allows for an efficient nucleophilic addition, and the presence of an excellent leaving group (methyl sulfide) which permits further transformations during the domino sequences. This dual effect of MMS makes DMSO an interesting C1 synthon that works not only as a source of a methylene unit (-CH_2-) in terms of formaldehyde surrogate, but also as a promotor of the cyclization process producing various highly diverse nitrogen-containing heterocycles, which are valuable scaffolds in medicinal chemistry [46].

Synthesis of non-aromatic heterocycles

As stated above, DMSO can also hydrolytically decompose to formaldehyde. There are many examples of reactions in which DMSO is used as a formaldehyde surrogate, which have been summarized in recent reviews [17,18,47]. We would like to highlight those examples where MCR reactions are involved. In this context, Zhong's group developed the synthesis of sulfenylated 1,3-oxazinanes **13** and oxazolidines **14** via a thia-aza-Prins cyclization reaction of homoallylic amines with disulfides and DMSO under copper catalysis, where DMSO acts as a solvent and a formaldehyde source at the same time (Scheme 13) [48]. This protocol represents a versatile method for the construction of oxygen-containing heterocycles, in which the oxazinane skeleton is an interesting scaffold for the design of synthetic routes for drug targets.

The reaction works very well with a broad range of aromatic disulfides. *Ortho, meta,* and *para*-substituents with different electronic properties afford moderate to excellent yields. The reaction fails only when aliphatic disulfides are used because of the higher Lewis basicity of the alkylated sulfur atom, which poisons the copper catalyst. When the reaction was carried out with paraformaldehyde and other solvents (such as DMF, 1,4-dioxane, toluene, and DCE) the yield was very low (between 0–34%), but when DMSO is used as solvent and reagent, the yield was greatly improved.

The proposed mechanism involves the activation of the disulfide component by $CuBr_2$ as the Lewis acid (Scheme 14). The copper(II) center coordinates the sulfur atom of the disulfide allowing for the electrophilic addition to the alkene moiety of the amine. The resulting stabilized carbocation **15** is then captured by formaldehyde (generated in situ from DMSO) leading to an intermediate oxocarbenium **16** that undergoes a cyclization to obtain the sulfenylated oxazinane derivative **13**.

In isotope labelling experiments using DMSO-d_6 the expected deuterated product **17** is obtained, confirming the in situ generation of formaldehyde from DMSO as the source of the methylene group. Interestingly, the reaction gives better yields under these conditions than that observed when paraformaldehyde is used.

DMSO in Mannich-type MCRs

Sun et al. developed a three-component Mannich-type reaction under oxidative and catalytic conditions that allows the coupling of aryl ketones **18** and saccharine (**19**) using DMSO as the solvent and the source for a methylene bridge linking the two building blocks (Scheme 15) [49]. Following this strategy, they synthesized a large library of compounds of general structure **20**. Furthermore, they extended the reaction to heteroaryl ketones to obtain a heterocycle containing β-amino ketones **21a–f**

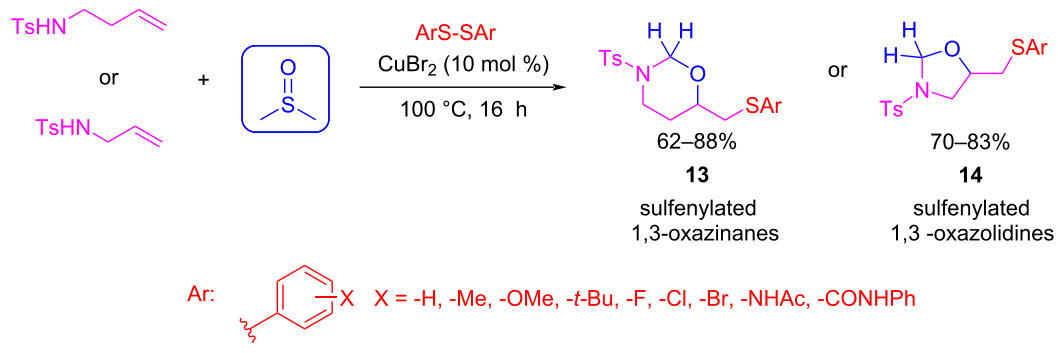

Scheme 13: Three-component reactions for the synthesis of aliphatic heterocycles **13** and **14** using DMSO as a formaldehyde surrogate.

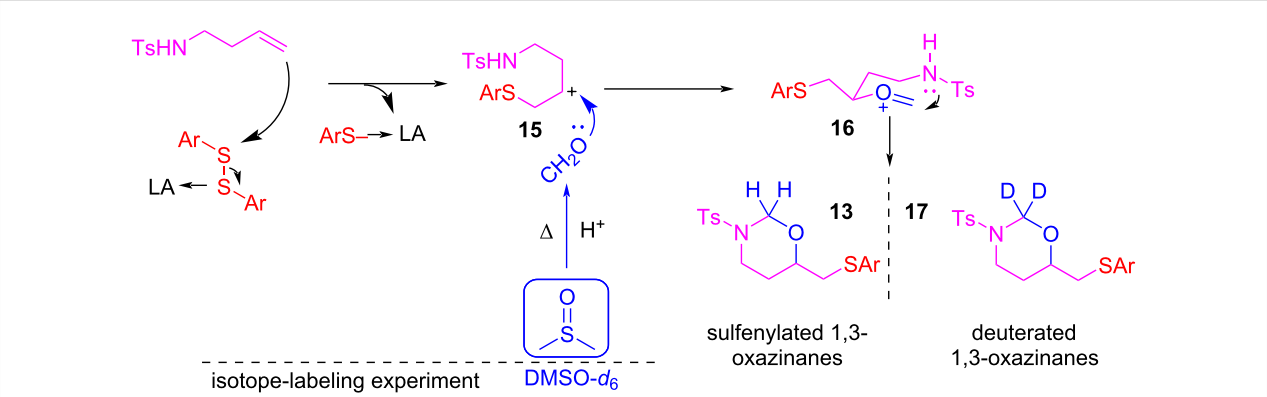

Scheme 14: Proposed mechanism for the 3CR between homoallylic amines, disulfides, and DMSO.

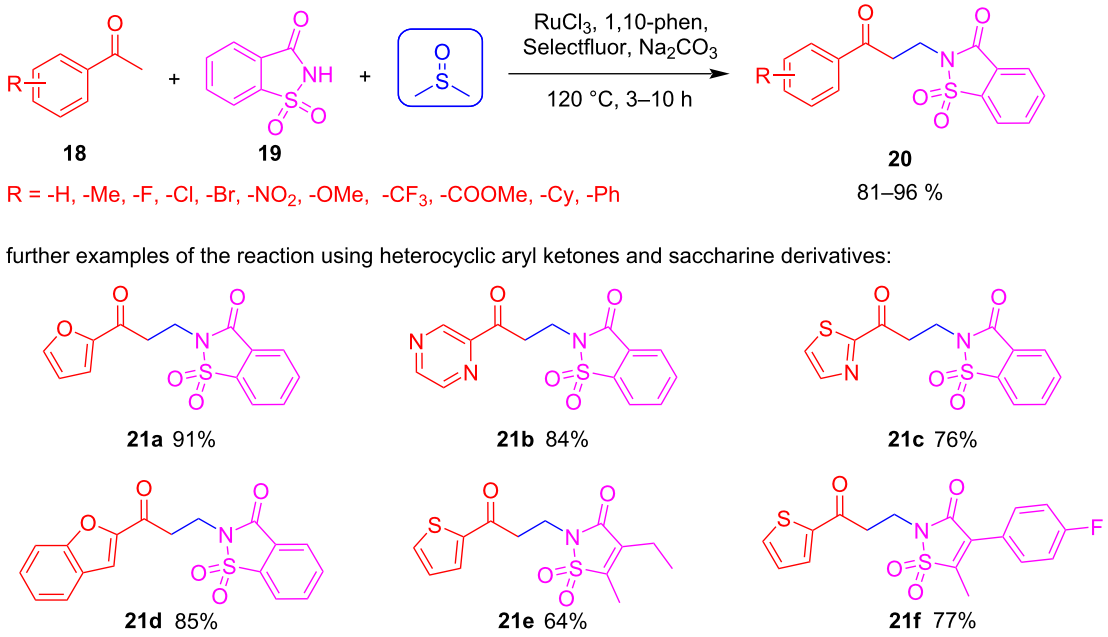

Scheme 15: Mannich-type reaction using DMSO as formaldehyde surrogate.

[50]. The reaction tolerates a wide range of functional groups at the substrates, giving a wide structural scope to the resulting compounds.

Once again, DMSO was confirmed as the origin of the methylene bridge by isotope labelling experiments using DMSO-d_6. The proposed mechanism comprises the activation of DMSO by a Ru(III) catalyst and the role of Selectfluor working as the oxidant that allows the "activation" of the methyl sulfur group in intermediate **22** for the cleavage of the C–S bond. In the end, the C–C bond is formed between intermediate **23** and the enol form from the methyl ketone **18**. Sodium carbonate is added to prevent too much acidification of the reaction medium and to deprotonate the NH that traps the sulfonium ylide (Scheme 16).

In an independent work, Mhaske et al. proposed an alternative methodology to furnish β-amino ketone **20a** (Scheme 17), using DMSO as a formaldehyde surrogate but with activation via ammonium persulfate (APS), avoiding the use of transition-metal catalysis [51]. In this case, the mechanism appears to proceed through the formation of free radical species, where APS plays the role of oxidant and radical activator of DMSO, generating reactive radical species of DMSO or dimethyl sulfone that react with the nitrogen of saccharine compound **19** without the need for a catalyst.

Another recent example for the use of DMSO as C1 synthon was reported by Bhattacharjee et al. They used DMSO in a 3CR to install a methylene unit between an indazole **24** and a

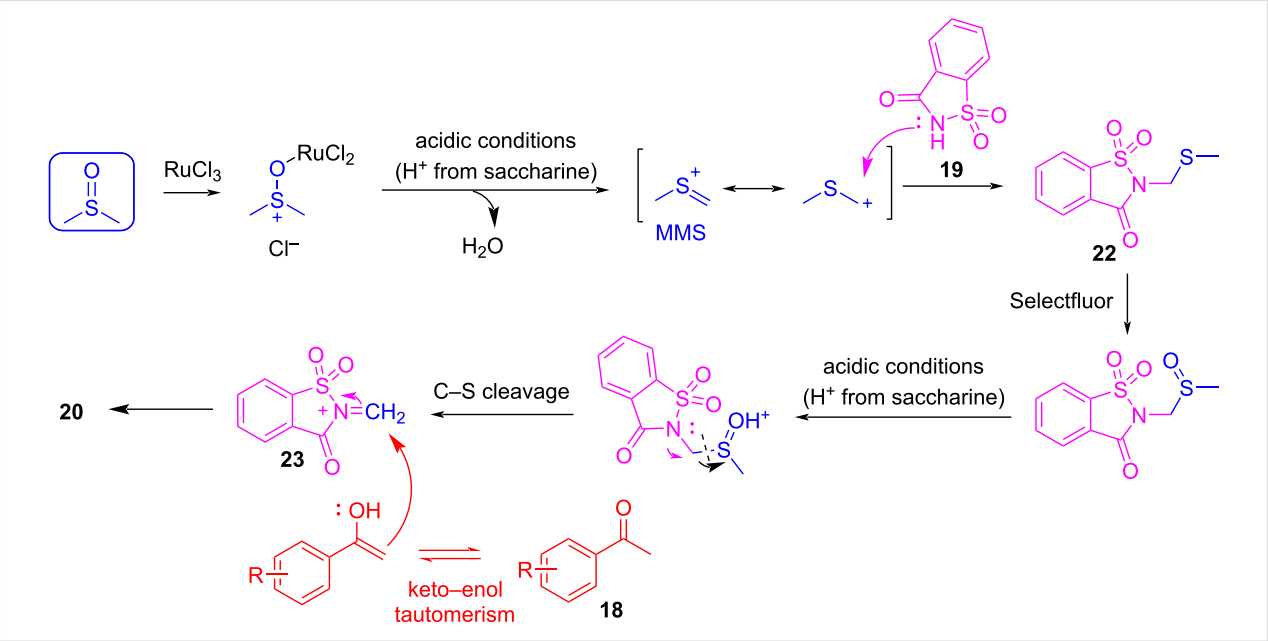

Scheme 16: Mechanism for the 3CR-Mannich-type reaction between aryl ketone **18**, saccharine (**19**), and DMSO. The generation of C-1 unit MMS arises from the decomposition of DMSO under acidic and catalytic conditions.

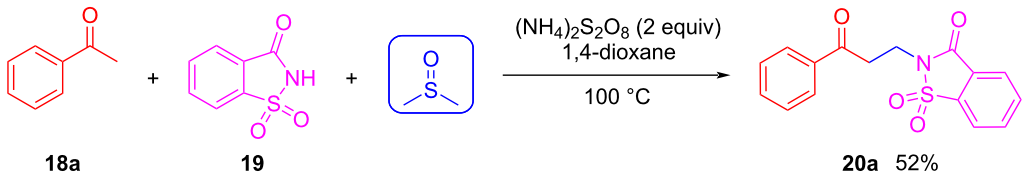

Scheme 17: Mannich-type reaction using DMSO as formaldehyde surrogate and under oxidative activation.

carboxylic acid **25** (Scheme 18) [52]. Under radical conditions using $K_2S_2O_8$, they obtained a series of carboxylic acid esters of indazoles **26**.

In all these multicomponent reactions DMSO was applied to install a C1-bridge between two structural units that already have a heterocycle moiety incorporated.

Dihalomethanes

Dihalomethanes are good solvents for several organic syntheses. Their low boiling points and polar non-protic nature make them suitable dissolving agents for a wide range of reagents. Furthermore, the polar bond C–X can be activated by different chemical procedures (metal or acid catalysis, for example) and serves as a reactive center. In this regard, dihalomethanes can

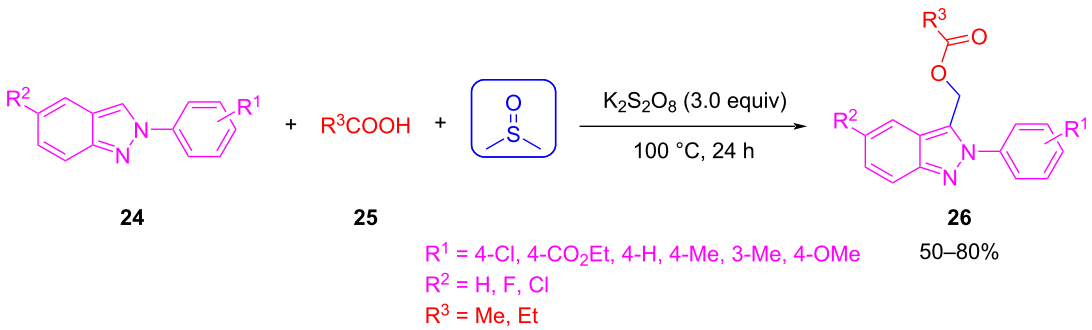

Scheme 18: Three-component reaction between an indazole, a carboxylic acid, and DMSO.

act as halogen donors in nucleophilic reactions or as methylene sources in electrophilic reactions [53-57]. In the latter case, they are employed as C1 building blocks, with abundant examples in the literature [55-57]. This section will focus on the most important uses of dihalomethanes as formaldehyde alternatives in MCR reactions applied to the synthesis of propargylamines and aminophosphonates. We will discuss the reaction conditions, mechanisms, and scope.

Synthesis of propargylamines

Propargylamines are essential building blocks for the synthesis of natural products or biologically active compounds in medicinal chemistry [58]. One of the most effective strategies for their synthesis is the addition of alkynes to imines or enamines, which is typically carried out under metal catalysis and elevated temperatures. This process requires the use of high boiling point solvents such as toluene, dimethylformamide (DMF), dimethyl sulfoxide (DMSO), or dioxane to achieve high yields. The assumed mechanism is initiated by activation of the C–H bond of the terminal alkyne by a metal catalyst. The resulting metal acetylide reacts with the imine/enamine through a nucleophilic addition. Because imines/enamines are available from the reaction between aldehydes and amines (primary or secondary), the reaction is called AAA coupling: amine–aldehyde–alkyne coupling (Scheme 19).

In this context, the use of formaldehyde as a C1 building block is suitable despite the unstable aminol intermediate. There are several examples showing how formaldehyde or paraformaldehyde can be used in the AAA coupling of three components for the synthesis of propargylamines [58-61]. However, the problems associated with the stability of the imine/enamine intermediate generated from formaldehyde must still be addressed.

Several attempts have been made to replace formaldehyde with dihalomethanes. These can react with certain secondary amines to generate stable aminals, which increase the rate of reaction at higher temperatures or pressures. This gives rise to products derived from iminium ions and therefore, dihalomethanes can function as aldehyde equivalent in reactions where iminium species are involved. In this case, the C–X bond of the dihaloalkanes can be activated by metal catalysis, allowing the incorporation of the C1 building block by a mechanism that does not involve the preformation of an imine/enamine intermediate. These are the basis for the AHA coupling: amine–haloalkane–alkyne coupling for the synthesis of propargylamines by the activation of both C–H and C–X bonds by metal catalysis (Scheme 20).

In general, the activation of both CH and CX bonds is accomplished by homogeneous metal catalysis with CuCl being the most used one. This is usually done at a load of 5 mol % in CH_3CN as solvent and CH_2Cl_2 as a C1 synthon, under moderate reaction conditions (60 °C). Consequently, this synthetic strategy is less dependent on temperature compared to AAA coupling [62].

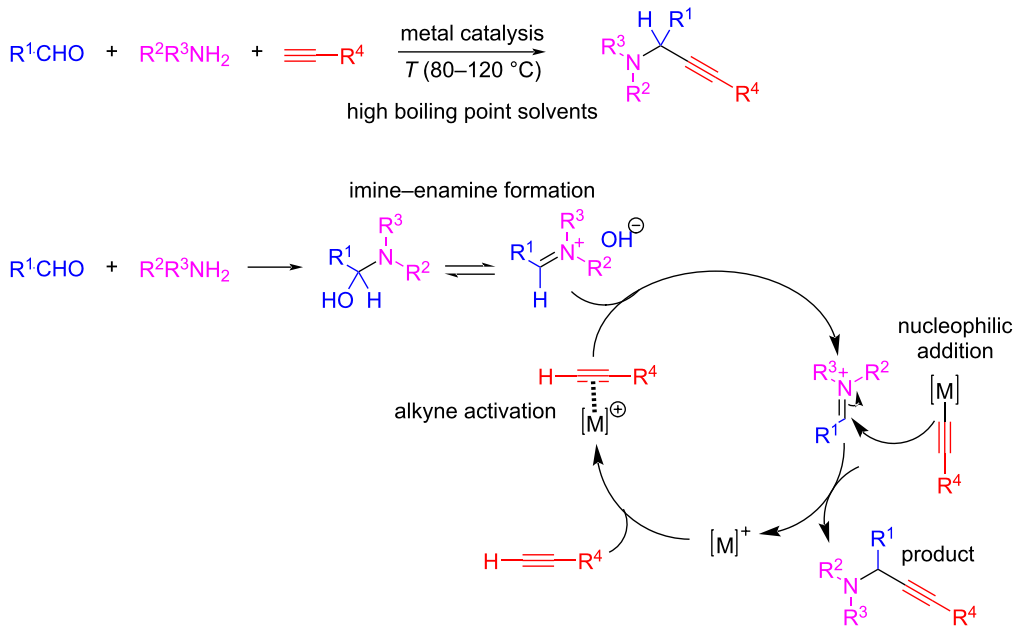

Scheme 19: Amine–aldehyde–alkyne (AAA) coupling reaction and plausible mechanism.

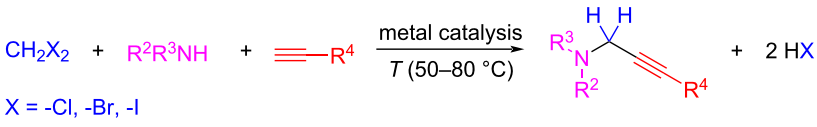

Scheme 20: AHA coupling for the synthesis of propargylamines using dihalomethanes as C1 building blocks.

Several reports also showed that gold (as $AuCl_3$, 5 mol %) [63], indium (as In_2O_3 nanoparticles, 5 mol %) [64], iron (as $FeCl_3$, 20 mol %) [65], cobalt (as $CoBr_2$, 10 mol %) [66], and nickel (as $Ni(py)_4Cl_2$, 15 mol %) [67] can act as metal catalyst for the 3CC reaction. In all these cases, the temperature was lower (usually between 60–80 °C) compared to the AAA coupling, except for iron, where the temperature must be increased to 100 °C. This can be explained in terms of the activation of both the C–H and C–X bonds by metal catalysis, which is not the case in AAA couplings, where only the C–H bond is activated, making the last step (nucleophilic addition) more temperature dependent. However, in the case of nickel catalysis, during AHA coupling, a suitable ligand, such as bipyridine, is needed for the in situ formation of a metal complex that activates the C–H and C–X bond [67].

The solvents used most in the AHA coupling are CH_3CN [62,65-67], DMSO [64], water, and even neat conditions [62]. In some cases, the same dihalomethane can be used as both the reactant and solvent. For example, Aguilar et al., proved that when using CH_2Cl_2 as both a solvent and a C1 source, they could obtain propargylamines **29** with good yields from secondary amines **27** and alkynes **28** (Scheme 21) [63]. In this case, the catalysis was accomplished by a gold(III) catalyst.

In general, CH_2Cl_2 is preferentially chosen as the dihalomethane compound due to economic reasons and ease of access, but some reports also used CH_2Br_2 and CH_2I_2 with good results [62,66,67].

In some cases, the addition of a non-nucleophilic base is needed to neutralize the HCl generated during the reaction (Scheme 20). For example, Yu et al. demonstrated that the reaction yield could be significantly increased when the reaction was performed in the presence of one equivalent of DBU [62]. They argued that organic bases such as DBU are superior than inorganic bases in improving the yields, probably because of the low solubility of the last ones in the reaction system. In the same way, other bases such as DABCO [64], DBU [66], and TMG (1,1,3,3-tetramethylguanidine) [65,67] were shown to be useful for metal activation of the C–H alkyne deprotonation.

The use of dihalomethanes in these reactions provides a wide scope in terms of the type of alkyne and amine that can be employed (Scheme 22) [62-68]. In general, aromatic and aliphatic alkynes, even with electron-donating or electron-withdrawing groups, work well under these conditions. However, the amine component does not react when primary or aromatic secondary amines are used. It works very well with cyclic or acyclic aliphatic secondary amines, such as piperidine or dibutylamine. In all cases, the yields are between 60–95% for all metal catalysis conditions.

The most widely accepted mechanism is as follows: the alkynyl C–H bond is activated by the metal catalyst (Scheme 23). The metal can be added in its proper oxidation state (such as Cu(I)) or generated in situ (as in the case of Au(I), Co(I), Fe(II) and Ni(I)) by reducing the suitable salts (containing Au(III), Co(II), Fe(III), and Ni(II), respectively) at the beginning of the catalytic cycle. The metal in its reduced species (depicted in Scheme 23) activates the C–H bond of the alkyne. After this activation step, a weak base (like DBU, TMG, or even the same amine component) deprotonates the terminal alkyne, generating the metal acetylide derivative **A**, which is the active nucleophilic species in the reaction. Intermediate **A** undergoes an oxidative addition by the dihaloalkane, generating intermediate **B**. This undergoes reductive elimination to afford propargyl halide **C**. Finally, intermediate **C** reacts with the secondary amine to give the propargylamine product **D**.

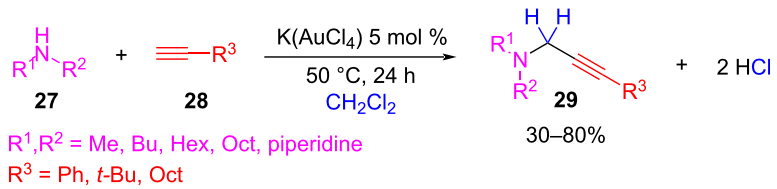

Scheme 21: AHA coupling using CH_2Cl_2 as both solvent and methylene source.

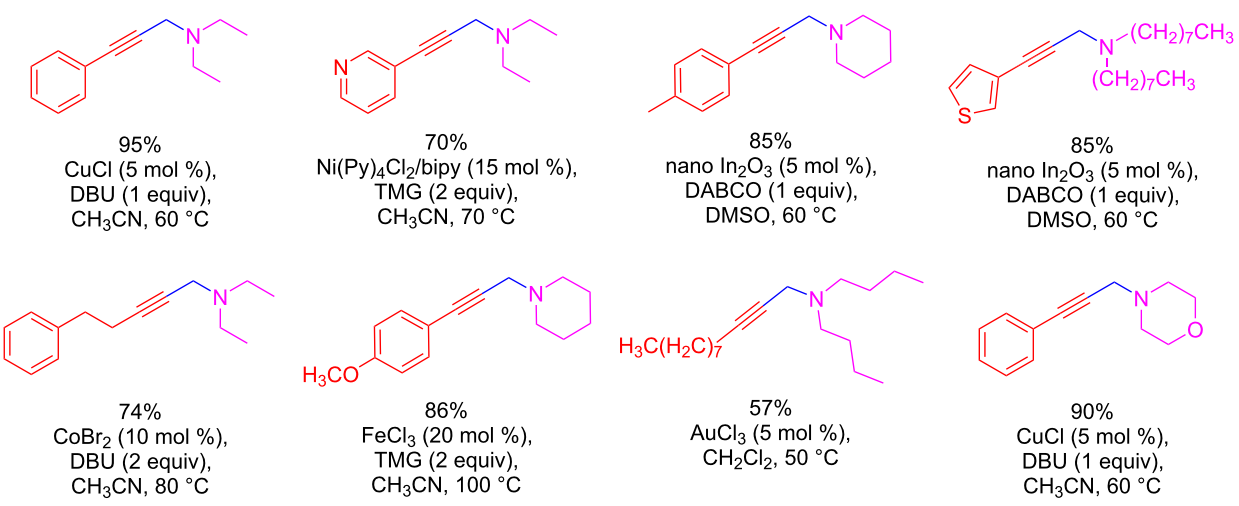

Scheme 22: Examples of propargylamines synthesized under catalytic AHA protocols.

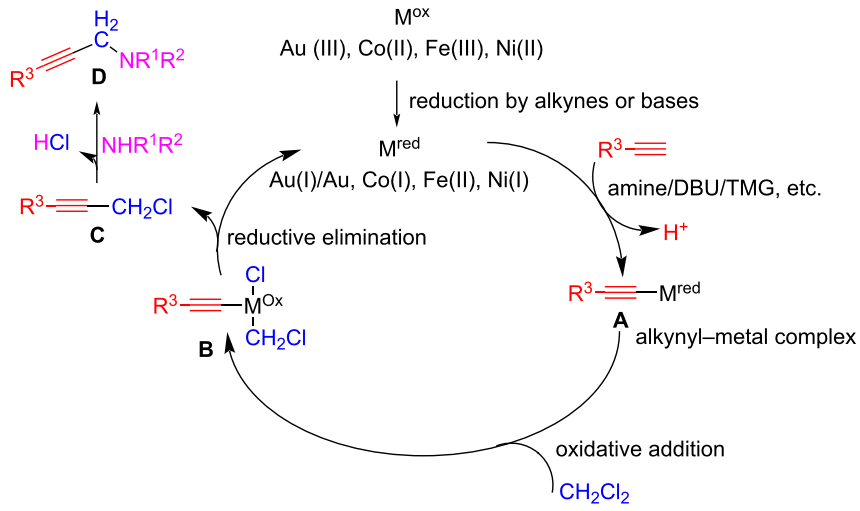

Scheme 23: Proposed mechanism for the synthesis of propargylamines using dichloromethane as a C1 source.

As outlined in the catalytic cycle, the presence of a base plays a dual role: co-activation of the alkynyl C–H bond through deprotonation and trapping of the HCl produced during the last step (nucleophilic substitution in intermediate **C** by the amine compound). Depending on the conditions, the role of the base can be fulfilled by the amine itself [63] or by the addition of another base such as DBU [66], DABCO [64], or TMG [65].

This mechanism is supported by experimental evidence for the formation of intermediates. Gao et al. studied the generation of metal acetylide **A** by IR spectroscopy [65]. When subsequent additions of 1 equiv $FeCl_3$ were made in a solution of alkyne and TMG, the C–H stretch peak at 3277 cm^{-1} started to decrease as the temperature increased from 30 to 100 °C. This result suggests the generation of the Fe acetylide intermediate type **A**. On the other hand, Tang et al. prepared a derivative of intermediate **C** and subjected it to reaction with piperidine under optimized reaction conditions (DBU in MeOH at 80 °C) and obtained the propargylamine product **D** [66]. Based on this result, the implication of intermediate **C** in the reaction mechanism was demonstrated.

However, an alternative pathway from intermediate **A** to the propargylamine product has been proposed when copper is used as the catalyst. In this case, the activation of the C–X bond of the dihaloalkane requires not only the metal catalyst but also the amine compound for the reaction to proceed [62]. It was suggested that the propargylamine product is formed directly from

the activated intermediate **B** by the amine. This can be deduced from experiments performed starting from an alkyne and dichloromethane under these catalytic conditions (CuCl, 5 mol % and 1 equiv of DBU), in which intermediate **C** is not produced if the amine compound is absent, thus suggesting that the amine is necessary for the activation of the C–X bond. Besides, an alternative mechanism has been proposed similar to the AAA coupling, in which the copper catalyst (CuCl, 15 mol %) only activates the C–H bond of the terminal alkyne, and the resulting nucleophile **A** reacts with the iminium ion **F** generated from CH_2Cl_2 and the secondary amine via an aminal intermediate **E** (Scheme 24) [68].

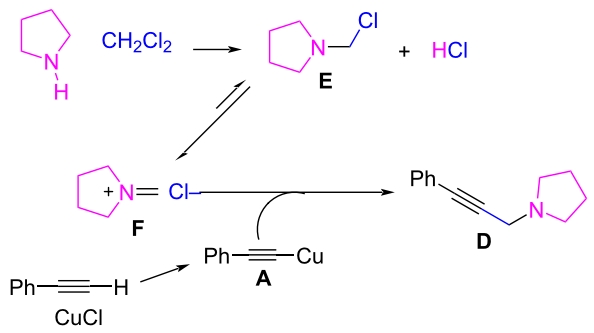

Scheme 24: Mechanism proposed for the generation of the aminal intermediate **E** by Buckley et al. [68].

However, Yu et al. found no evidence for the formation of an aminal intermediate **E** or the enamine derivative when they tried to obtain it from the reaction of CH_2Cl_2 and diethylamine in the absence of alkyne under suitable conditions (CuCl, 5 mol %, DBU 1 equiv, CH_3CN, 60 °C) [62]. Only in some cases can the reaction of CH_2Cl_2 and certain cyclic secondary amines such as piperidine or pyrrolidine afford an aminal or an iminium ion, in general under high temperature or pressure conditions, which is not the case for the AHA coupling [69,70]. Despite these cases, the absence of evidence in terms of iminium ion generation confirms that the AHA coupling reaction by metal catalysis is an option to avoid the problems regarding iminium or aminal stability. This is an important issue in AAA coupling when formaldehyde is used as the C1 source.

Finally, a later work proposes a catalysis-free protocol for the synthesis of propargylamines by an AHA coupling reaction [71]. Here, the reaction is carried out under mild conditions (CH_2Cl_2, 70 °C) without the need for catalysis or additional base for the activation of C–H and C–X bonds of the alkyne and dihalomethane compounds, respectively. However, this strategy has a limited scope in terms of the alkyne compound as no reaction is observed with aliphatic alkynes. Furthermore, the yields are between 50–80%, which are slightly lower than those under metal-catalyzed conditions. Nevertheless, these results open the door to further studies aimed at developing more efficient, non-catalyzed synthetic procedures for obtaining propargylamines.

Synthesis of α-aminophosphonates

One of the most robust methods for the synthesis of α-aminophosphonates is the Pudovik reaction, along with its multicomponent version, the Kabachnik–Fields reaction (Scheme 25) [72,73].

In the Pudovik reaction, a dialkyl phosphite **31** containing a PH bond adds to the C=N bond of a preformed imine **30**, while in

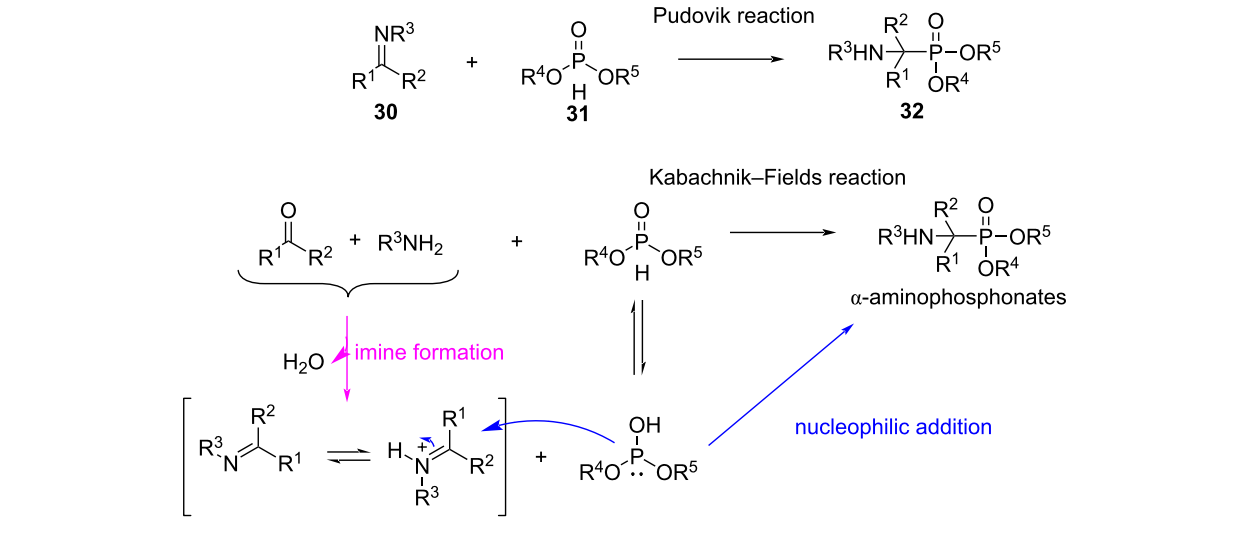

Scheme 25: Pudovic and Kabachnik–Fields reactions for the synthesis of α-aminophosphonates.

the three-component Kabachnik–Fields reaction, the imine, which is generated in situ from a carbonyl compound and an amine, reacts with the dialkyl phosphite to produce the desired α-aminophosphonates **32** (Scheme 25) [72,74]. This reaction has been reported to proceed with a wide variety of aliphatic aldehydes, in particular formaldehyde, under different reaction conditions with or without solvent or catalysis [72,74-76]. However, a significant problem with the Kabachnik–Fields reaction arises from the fact that dialkyl phosphites can also undergo an addition to the C=O bond of the carbonyl component (Abramov reaction) giving α-hydroxy phosphonates **33** as byproducts (Scheme 26a) [72]. Competition between the two nucleophiles for the electrophilic carbonyl compound depends on their relative reactivity [74,77] and this lack of chemoselectivity becomes important when formaldehyde is used. Moreover, primary amines (alkyl- and arylamines) can also react with two equivalents of both the formaldehyde and the P(O)H compound. In this case, a double Kabachnik–Fields condensation gives bis(phosphorylmethyl)amines **34** as possible byproducts (Scheme 26b) [76,78].

Because of the tendency of formaldehyde to generate these byproducts, several efforts have been made to optimize the chemoselectivity of the Kabachnik–Fields reaction. In this context, Zhao et al. proposed a more selective strategy for the synthesis of α-amino phosphorus compounds using dihalomethanes (Scheme 27) [79]. They developed a three-component reaction between amines (mainly tertiary amines), a

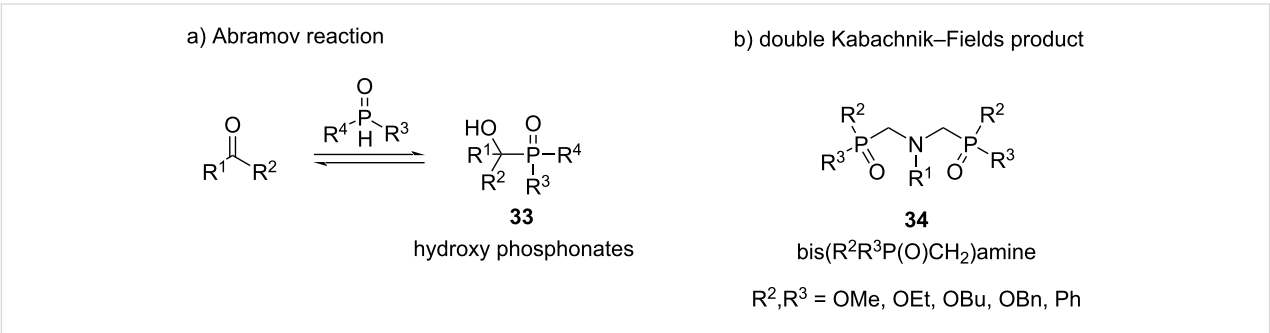

Scheme 26: a) Abramov side reaction that generates α-hydroxy phosphonate as a byproduct during the Kabachnik-Fields reaction. b) Bis(phosphorylmethyl)amine derivative product obtained from double Kabachnik–Fields reaction using formaldehyde.

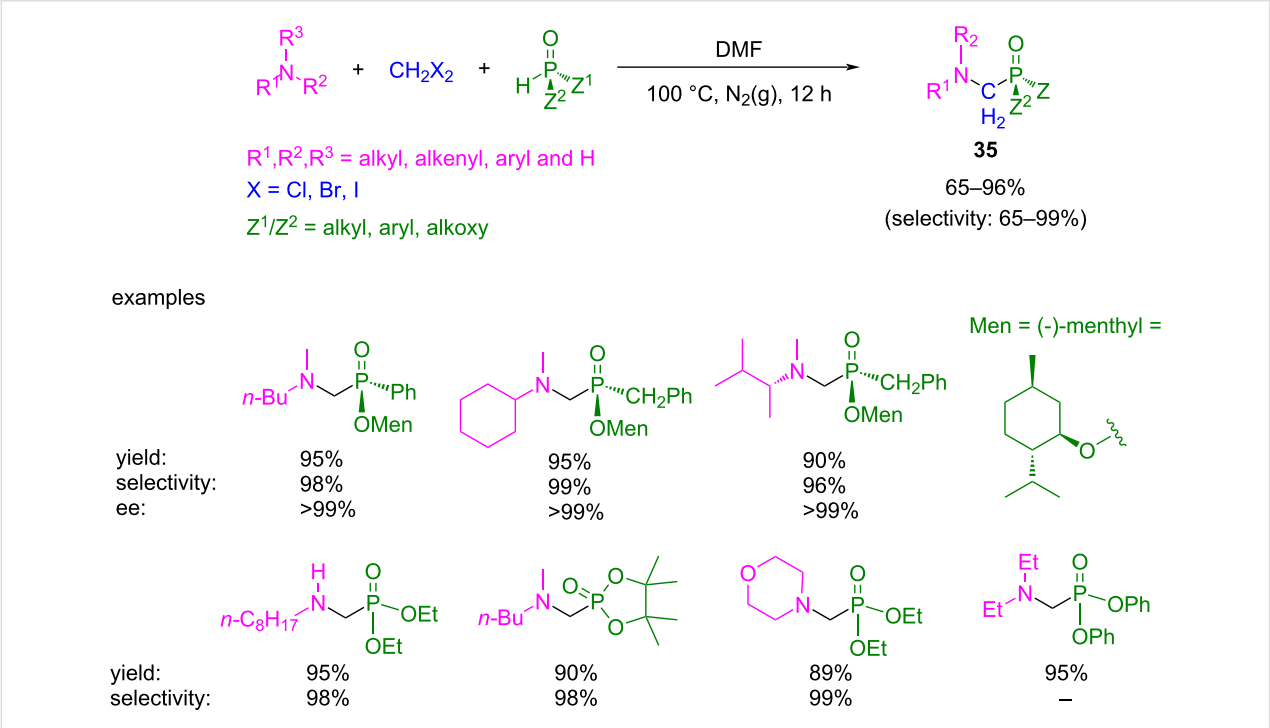

Scheme 27: Catalyst-free three component reaction to afford α-amino phosphorus product **35** using 1,1-dihaloalkanes as a C1 building source.

dihalomethane, and a P(OH) species (like phosphonate, phosphinate, or secondary phosphine oxide) under catalyst-free conditions to afford α-amino phosphorus compounds **35**. The products are very appealing biologically relevant scaffolds due to their structural similarity to aminocarboxylic acids [80]. Moreover, the stereochemistry at the phosphorus center is conserved during the reaction.

The reaction could also be performed with CH_2Br_2 and CH_2I_2 as the C1 building blocks and DMSO or MeCN as solvents. The reaction works very well with tertiary amines (both symmetrical and asymmetrical) and with some bulky primary and secondary amines (such as *n*-octyl-, dibutylamine, and *N*-methyl-*N*-butylamine). When applying primary or secondary amines are used, milder reaction conditions (75 °C) are needed.

The selectivity of the reaction shown in Scheme 27 could be explained according to the proposed mechanism (Scheme 28a).

The first step is the generation of the trialkyl(chloromethyl)ammonium chloride species **36** from the amine compound and CH_2Cl_2. Then, **36** decomposes by a cleavage of an N–C bond, where the stability of the leaving carbocation is the main factor that affects the rate of this step. Next, intermediate **37** is attacked by the phosphorus compound, giving product **35** with retention of the configuration. This mechanism was confirmed when compound **36a** was isolated as colorless crystals from the reaction between Et_3N and CH_2Cl_2 at 100 °C in DMF. Subsequently, the corresponding α-aminophosphonate **35a** was obtained by heating **36a** with an equal amount of diethyl phosphite (Scheme 28b). Furthermore, when the reaction was carried out with CD_2Cl_2, the corresponding deuterated product **35b** was obtained, confirming that the dihaloalkane compound is the source of the methylene unit (Scheme 28c).

Depending on the stability of the leaving carbocation, the selectivity of the R–N cleavage follows the decreasing order for the R groups: H, *t*-Bu, allyl, benzyl > methyl > primary, secondary alkyl group. Therefore, for primary and secondary amines, the N–H-bond cleavage takes place predominantly instead of the other two N–R cleavage possibilities. However, in the case of tertiary amines, the N–R cleavage depends on the stability of the carbocation generated. For example, when using an amine with two methyl groups and a benzyl or allyl group, the cleavage of the N–CH_2Ph and N–allyl bond takes place more selective (by 85% and 67%, respectively), instead of the cleavage of an N–Me bond. This explains the high selectivity observed for some examples in Scheme 27.

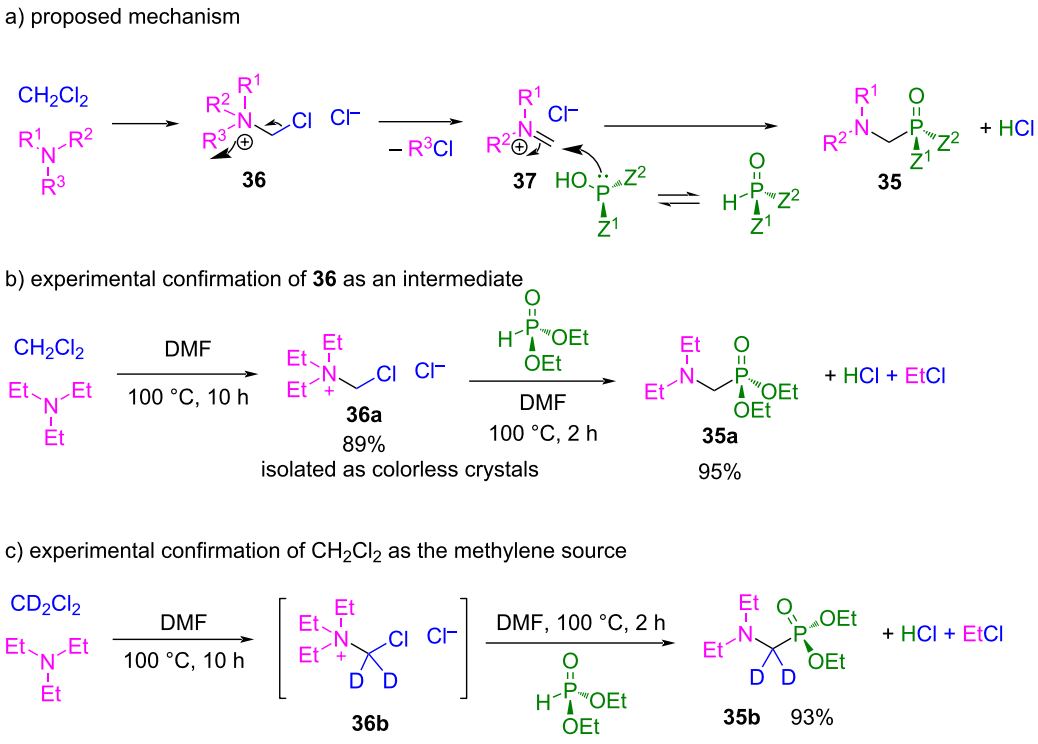

Scheme 28: a) Proposed mechanism for the three-component reaction of dichloromethane, amine and phosphorus compound to α-amino phosphorus products **35** with conserved phosphorus stereochemistry. b) Confirmation of **36** as a reaction intermediate. c) Isotope experiment for confirmation of the role of the dihaloalkane.

Finally, this methodology is a very interesting alternative for the synthesis of P-chiral α-aminophosphorous compounds without formaldehyde due to the straightforward procedure, the good yields observed, and the absence of byproducts compared to more conventional methods (Pudovik reaction or Kabachnik–Fields MCR reaction) [72,73].

Hexamethylenetetramine

In Ugi-type isocyanide-mediated reactions, the formation of an imine from the amine and the carbonyl component is a crucial step that, and when hampered, strongly affects the outcome of the entire process. In general, the imine readily forms when aliphatic or aromatic amines and carbonyl components are used. However, when ammonia and formaldehyde are employed, side reactions are favored leading to low yields or even to no Ugi product at all [81,82].

Rosalba et al. showed that HMTA (hexamethylene tetramine) can be used as a formaldehyde surrogate to generate formaldehyde and ammonia in situ by heating [83]. Under these conditions, the water present in hydrated HMTA is sufficient for this hydrothermal decomposition to occur. On the other hand, an excess of ammonia must be added to the reaction mixture to shift the equilibrium towards the imine. Using this procedure, a library of acylamino acetamide derivatives **38** was synthesized from aliphatic and aromatic isocyanides and carboxylic acids, with good yields. When ammonia is replaced by methylamine, the main product incorporates methylamine as the amine component. This result indicates that HMTA is the main source of formaldehyde but not for ammonia, so the methodology can be used with other amines, too (Scheme 29).

Glyoxylate derivatives

Due to its low toxicity and reactivity, glyoxylic acid and its glyoxylate derivatives are among the most interesting formaldehyde surrogates in multicomponent reactions (Scheme 30). As glyoxylates are C2 structures, their use as C1 building blocks in MCRs instead of formaldehyde, requires an extra path, usually a decarboxylation process, after the condensation reaction. However, by appropriately choosing the glyoxylate derivatives (for example, ethyl glyoxylate), post-cyclization of the MCR product can be achieved, extending the universe of molecule diversity in comparison to the use of formaldehyde.

Glyoxylic acid as a C1 building block

Glyoxylic acid has been applied as a greener alternative to formaldehyde but also as an option to incorporate a C1 building block in multicomponent reactions where formaldehyde per se cannot react.

For example, in the Groebke–Blackburn–Bienaymé (GBB) multicomponent reaction, a three-component reaction of hetero-

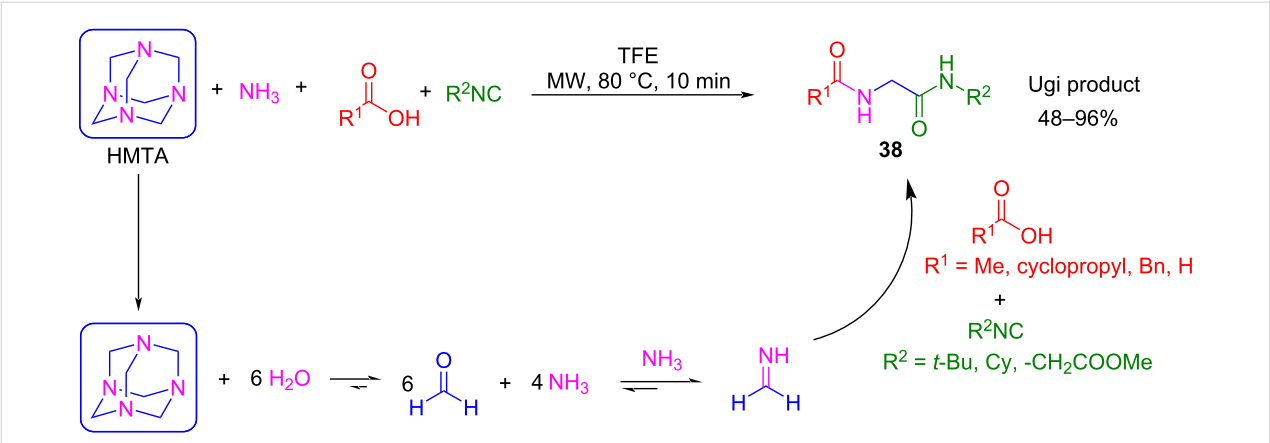

Scheme 29: Ugi-ammonia strategy using HMTA as a formaldehyde surrogate.

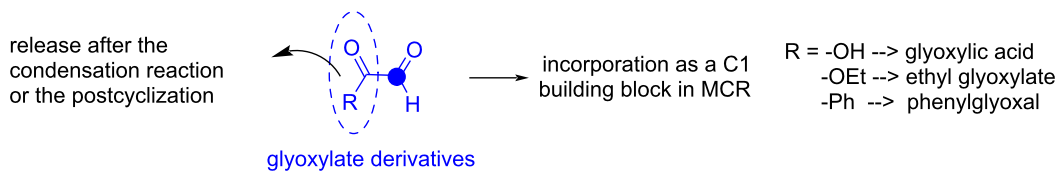

Scheme 30: Glyoxylate and its derivatives as C1 building blocks.

cyclic amidines **39**, aldehydes **40** and isocyanides **41** under acidic catalysis generates heterobicyclic products **42** through a [4 + 1] cycloaddition step that ends with aromatization through a 1,3-H shift (Scheme 31) [84,85]. These compounds are highly relevant biological scaffolds for drug discovery [84].

In general, this reaction works very well with a wide variety of Lewis acids (as $Sc(OTf)_3$ and $MgCl_2$) and Brønsted acids (e.g., NH_4Cl and acetic acid) and with a wide variety of isocyanides, aldehydes, and amidines. However, strikingly, the use of formaldehyde as the C1 building block is not always successful. In the few cases where the reaction proceeded as expected, low yields were obtained accompanied with several byproducts that are difficult to separate [86-88].

Probably, the high reactivity of the imines generated by formaldehyde leads to their polymerization [84] or even to the incorporation of other nucleophiles present in the reaction mixture, such as the solvent or a second molecule of the amidine component (Scheme 32) [84,89-91].

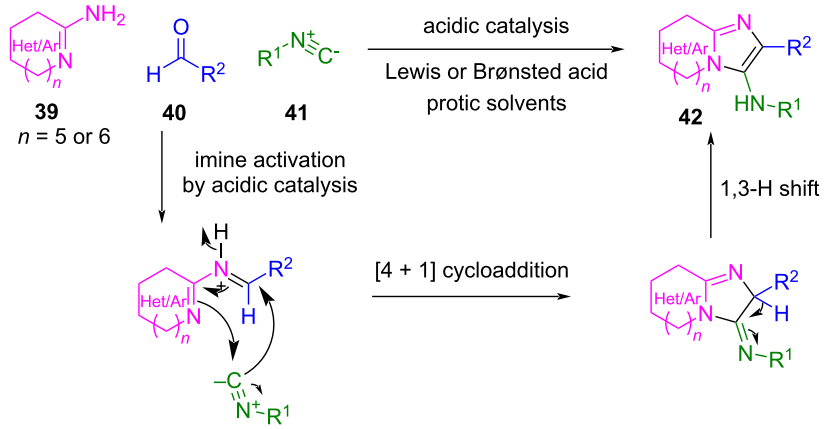

Scheme 31: The Groebke–Blackburn–Bienaymé multicomponent reaction (GBB) and its mechanism.

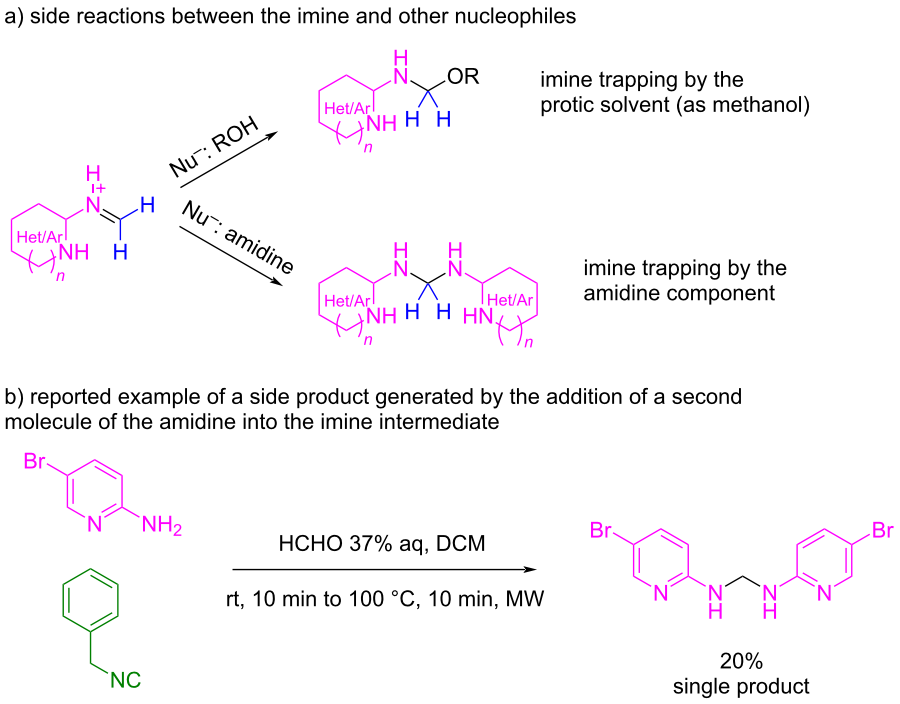

Scheme 32: a) Byproducts in the GBB multicomponent reaction (GBB) when formaldehyde is used as the carbonyl component and b) a reported example [91].

It is also known that two regioisomers can be generated during the GBB reaction depending on the nature of the amidine and the aldehyde used and, therefore, the type of imine formed [85,90]. As formaldehyde is a very reactive molecule, it will be more susceptible to form imines with either of the two nucleophilic nitrogen atoms present in the amidine component, thus leading to the production of both regioisomers **42a** and **42b** and therefore to a demanding purification process (Scheme 33).

To avoid these drawbacks, Lyon et al. optimized the reaction by using free monohydrated glyoxylic acid or MP-glyoxylate (glyoxylic acid immobilized on macroporous polystyrene resin, starting from MP-carbonate, MP-CO_3) instead of formaldehyde (Scheme 34) [88].

When glyoxylic acid ("free" or immobilized) is used, the reaction affords 2-unsubstituted 3-aminoimidazo heterocycles **42a** as the only regioisomer with very good yields. For the immobilized glyoxylic acid, the best conditions required the use of the methanol-compatible resin, MP-carbonate. After coupling of the three components, decarboxylation at 50 °C released the product, while, when working with 'free' glyoxylic acid, decarboxylation occurred at room temperature. The mild reaction conditions for both strategies ("free" or immobilized glyoxylic acid) allows for a broad scope in terms of 2-aminoazines and isocyanide components (some examples are shown in Scheme 34).

It is important to note that these imidazo heterocycles have been reported using an alternative synthetic strategy [92], but lower efficiency in terms of yields, number of steps, and scope compared to this multicomponent methodology.

Inspired by this previous work, Sharma et al. improved the reaction for free and immobilized glyoxylic acid, with and without acid catalysis, respectively [86,93]. They extended the scope of the reaction to a wider range of amidines and isocyanides using glyoxylic acid in 50% aqueous solution, with $HClO_4$ as acid catalyst (Scheme 35) [86]. Under these conditions, the yield, the scope, and the regioselectivity of the reaction increased notably.

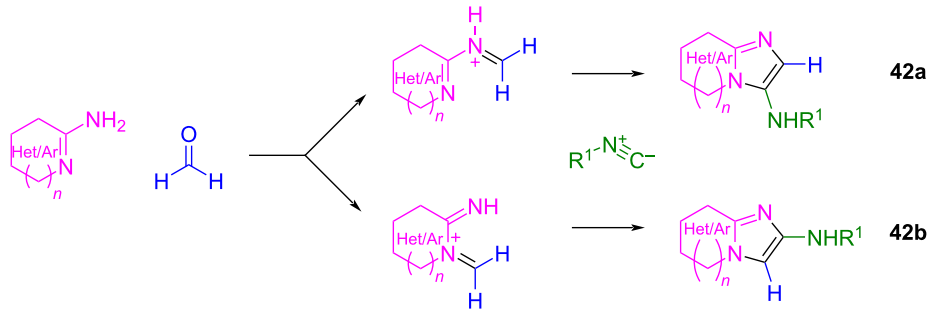

Scheme 33: Possible regioisomers in the GBB multicomponent reaction when formaldehyde is used as the carbonyl component.

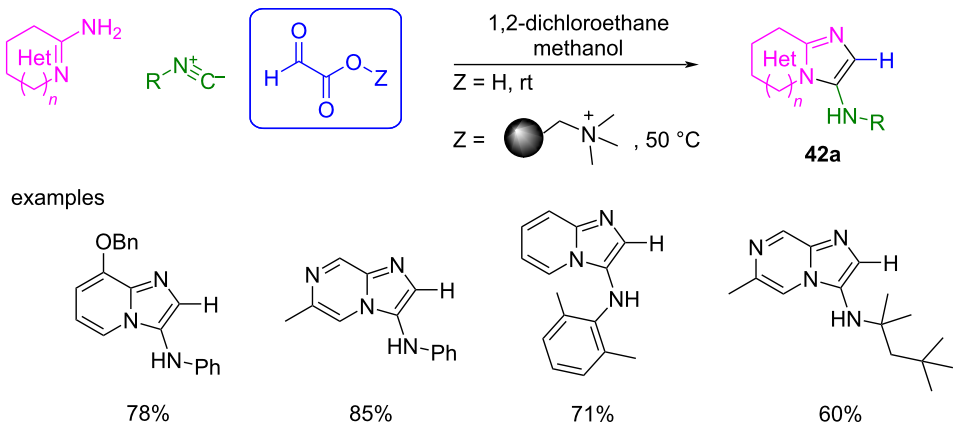

Scheme 34: The multicomponent GBB reaction yields 2-unsubstituted 3-aminoimidazo heterocycles **42a** using MP-glyoxylate as a formaldehyde equivalent without catalyst [88].

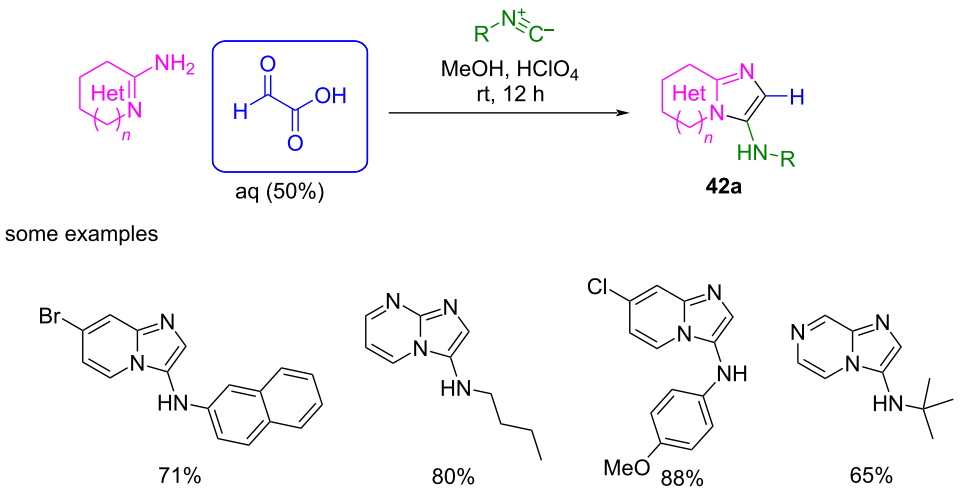

Scheme 35: GBB multicomponent reaction to 2-unsubstituted 3-amino imidazo heterocycles **42a** using glyoxylic acid under acid catalysis.

Later, the same group developed an alternative method by using glyoxylic acid immobilized on silica, and the reaction conditions were optimized using microwave irradiation and avoiding the use of solvent or additional catalysts [93]. In this way, derivatives of **42a** were obtained in good yields and within shorter reaction times (Scheme 36).

In recent years, several groups have applied these strategies to identify products with biological activity [94,95]. Representative examples are shown in Scheme 37.

On the other hand, the van Leusen three-component reaction of an aryl-substituted tosyl methyl isocyanide (TosMIC), an aldehyde, and an amine is a well-known procedure for synthesizing polysubstituted imidazoles **43** (Scheme 38). The reaction involves a cycloaddition between the isocyanide and the imine generated in situ, ending with the hydrolysis of the tosyl group.

This methodology works well for a wide variety of solvents and under mild basic conditions, since the solubility of the reagents and ease of product isolation are the factors that govern the choice. Sisko et al. used DMF/K_2CO_3 as the best conditions to carry out the cycloaddition of a wide variety of amines, aldehydes, and tosyl methyl isocyanides [96]. However, when the authors attempted the reaction with 37% aqueous formaldehyde, the reaction did not produce the 1,4-disustituted imidazole **43a** but instead the 2-aminooxazoline derivative **44** (Scheme 39). It was proposed that the cycloaddition between formaldehyde and the isocyanide component is preferred over the formation of the imine, probably because of the high reactivity of the carbonyl compound or the low stability of the imine. After cycloaddition, the tosyloxazoline derivative undergoes an addition at C-2 by the primary amine, followed by elimination of the toluenesulfinate moiety, producing the 2-aminooxazoline derivative **44** as the main product.

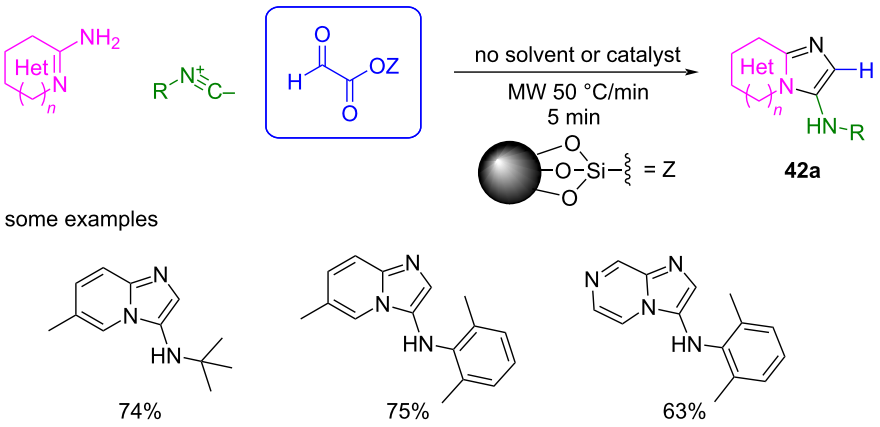

Scheme 36: GBB reaction using glyoxylic acid immobilized on silica as formaldehyde surrogate.

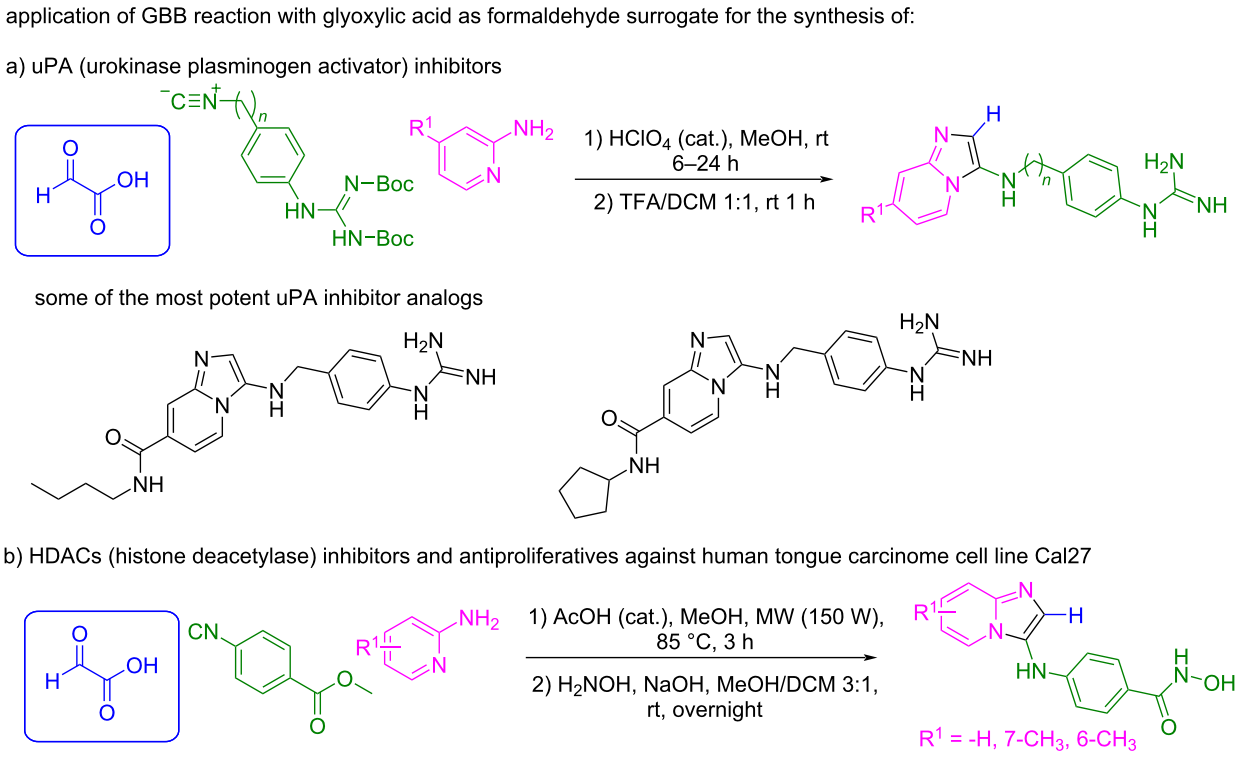

Scheme 37: Bioactive products synthesized by the GBB reaction using glyoxylic acid.

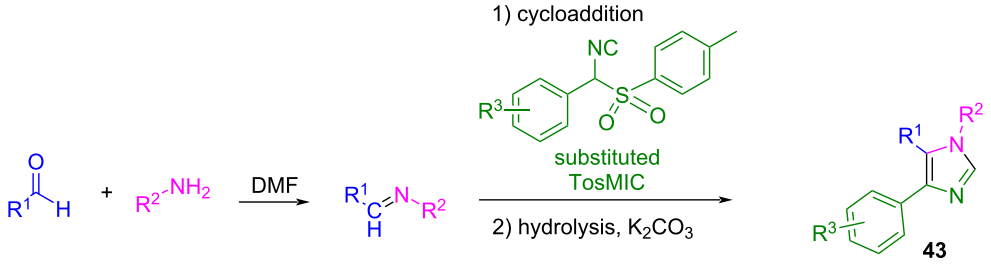

Scheme 38: van Leusen three-component reaction to imidazoles.

In this report, it was stated that this result can be avoided by replacing formaldehyde with glyoxylic acid (Scheme 40). Using similar reaction conditions, the authors obtained the desired 1,4-disubstituted imidazole derivatives **43** with very good yields and for a wide range of amines and tosyl methyl isocyanides, after a decarboxylation/elimination sequence of the putative intermediate **45**.

This procedure was the basis for the work by Dow et al. on the synthesis of a new series of CB1 receptor antagonists (cannabinoid-1) **46** (Scheme 41) [97].

Unfortunately, this procedure does not work properly when amino acids or ammonia are used as amine components. In the case of ammonia, the corresponding imine was not generated, but rather a byproduct that incorporated two molecules of isocyanide **47** (Scheme 42). It was suggested that the isocyanide component decomposes to an arylimine, which undergoes a cycloaddition with another isocyanide molecule to this byproduct. However, if an amino acid is exchanged for an amino ester, the reaction affords the corresponding product **43e** (Scheme 40) as an amino acid derivative.

Application of glyoxylate derivatives in post-cyclization reactions as a C1 building block

Glyoxylate derivatives have been used in Ugi- and Passerini-type reactions, since the adduct generated in both cases has two reactive centers for post-cyclization possibilities: the ester

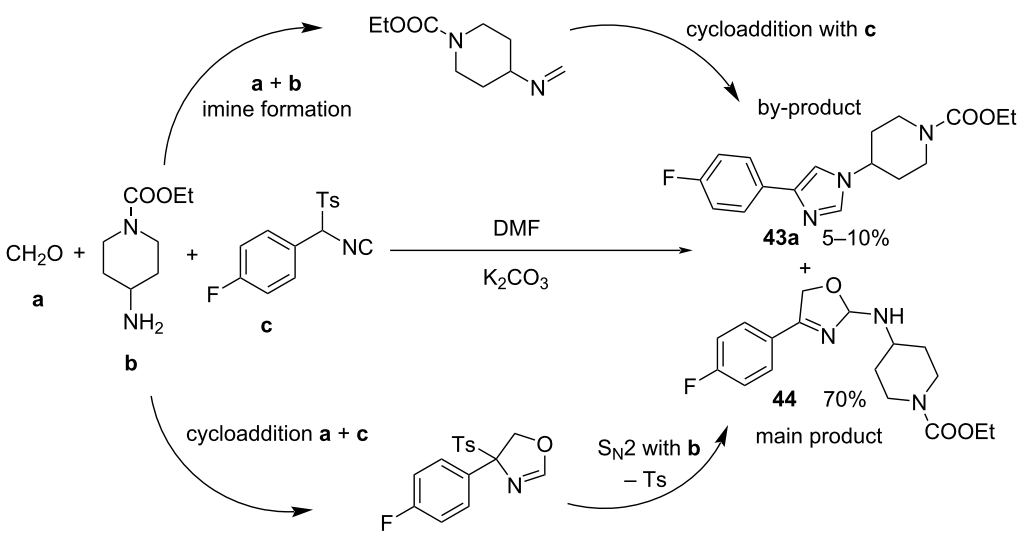

Scheme 39: Side reaction during the synthesis of imidazoles with formaldehyde as the carbonyl compound.

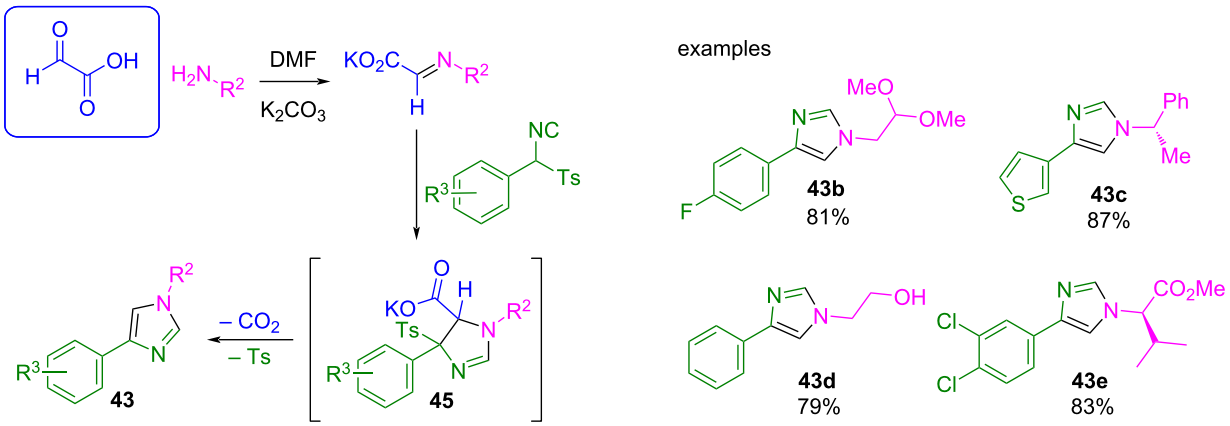

Scheme 40: Optimization of the van Leusen three component reaction to 1,4-disubstituted imidazoles **43** using glyoxylic acid as a formaldehyde surrogate.

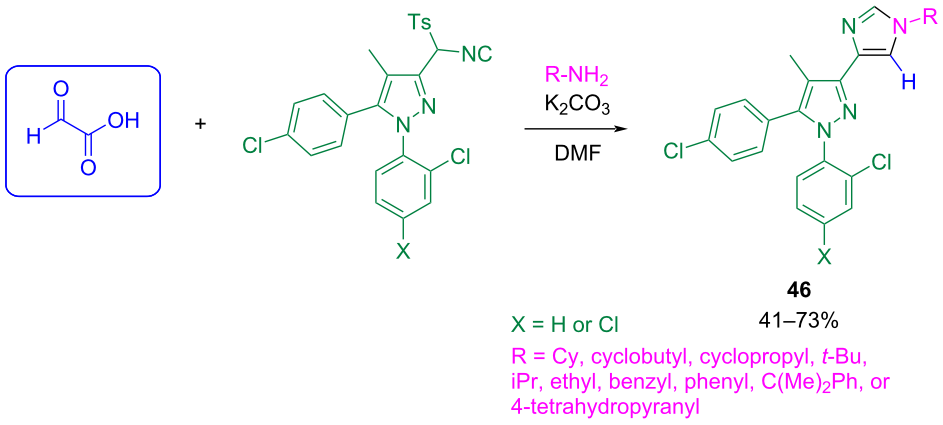

Scheme 41: Application of the Sisko strategy [96] for the synthesis of CB1 receptor antagonist compounds [97].

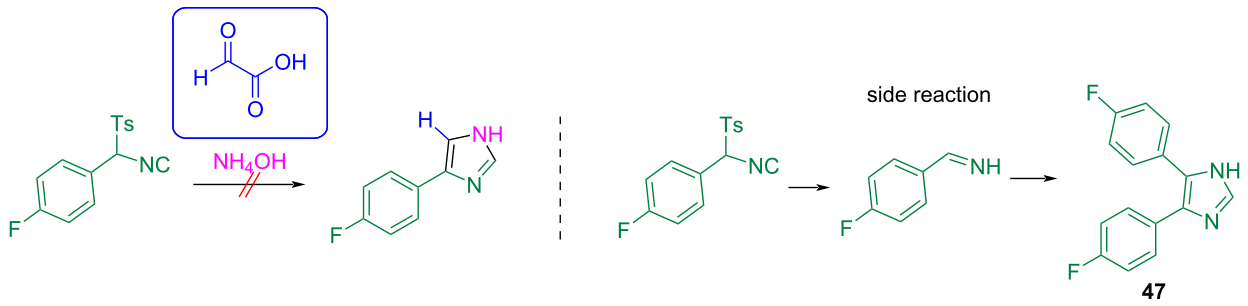

Scheme 42: Side reaction, when NH_4OH is used as amine component.

moiety and the α-carbon to the peptide carbonyl group. Both moieties result from the glyoxylate compound (Scheme 43).

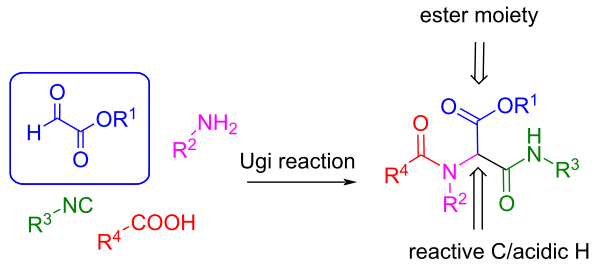

Scheme 43: Ugi-type adducts with the ester moiety and the acidic CH to be used for post-cyclization sequences.

There are many examples in which the ester moiety opens the possibility of a further intramolecular cyclization with a nucleophile (for example, a protected amine in an Ugi/deprotection/cyclization sequence [98-104]), or with a carbanion generated by a strong base in an Ugi/Dieckmann cyclization [105]. In all these cases, the glyoxylate derivative incorporates two carbon atoms into the final product, thus serving as a C2-building block.

Similarly, the ester group increases the acidity of the proton in the C-α position, which leads to a stable carbanion with even mild bases, that can promote intramolecular cyclization. For example, Flores-Constante et al. [106] and Nechaev et al. [107] synthesized Ugi adducts with a propargyl group that could be used as a Michael acceptor (**48**–**50**, Scheme 44). The alkyne reacts with the in situ-generated carbanion through a 5-*endo*-*dig*-cycloisomerization process to yield a nitrogen-containing five-membered heterocycle (Scheme 44). Examples in which the propargyl group is incorporated into the amine [106] or the carboxylic acid components [107] are known, leading to different cyclization products such as pyrrolines **53** and pyrrolones **51**, respectively. The procedure was also extended to Passerini adducts to afford butenolide structures **52** after the post-cyclization process [107].

In all the cases described above, the ester group of glyoxylate remains in the final products, however, it can be released after a decarboxylative or reductive reaction (β-position), allowing the use of ethyl glyoxylate as a C1 building block.

This strategy was explored by Miranda et al., who first obtained a series of γ-lactams **56** and isoindolinones **57** using ammonium persulfate salts and TEMPO as the radical initiator/oxidant couple that promoted the intramolecular radical cyclization of suitable 1,3-dicarbonyl Ugi adducts **54** and **55** (Scheme 45) [108,109]. The stabilization of the enol in the 1,3-dicarbonyl Ugi adduct allows single-electron transfer (SET) with the anion radical species of the ammonium persulfate salt. Subsequently, the radical delocalization process gives rise to the carbon-centered radical, which follows the intramolecular cyclization onto the double bond or onto the aromatic ring depending on the case.

The γ-lactams **56** and isoindolinones **57** can subsequently be subjected to a decarboxylation or reductive reaction after hydrolysis of the ester group to obtain final compounds **58** and **59** whose structures incorporate only one carbon atom of the ethyl glyoxylate, and which cannot be obtained using formaldehyde (Scheme 46).

It is important to note that, in these examples, even if the whole process is performed in one-pot, the reaction needs two steps: the generation of the Ugi (or Passerini) adduct and then the post-cyclization reaction. Interestingly, Peshkov et al. showed that when phenyl glyoxal is used instead of ethyl glyoxylate, a pyrrolone derivative **60** is obtained in one step under Ugi reaction conditions following an Ugi reaction/5-*endo*-*dig* carbocyclization/retro-Claisen fragmentation cascade reaction (Scheme 47) [110].

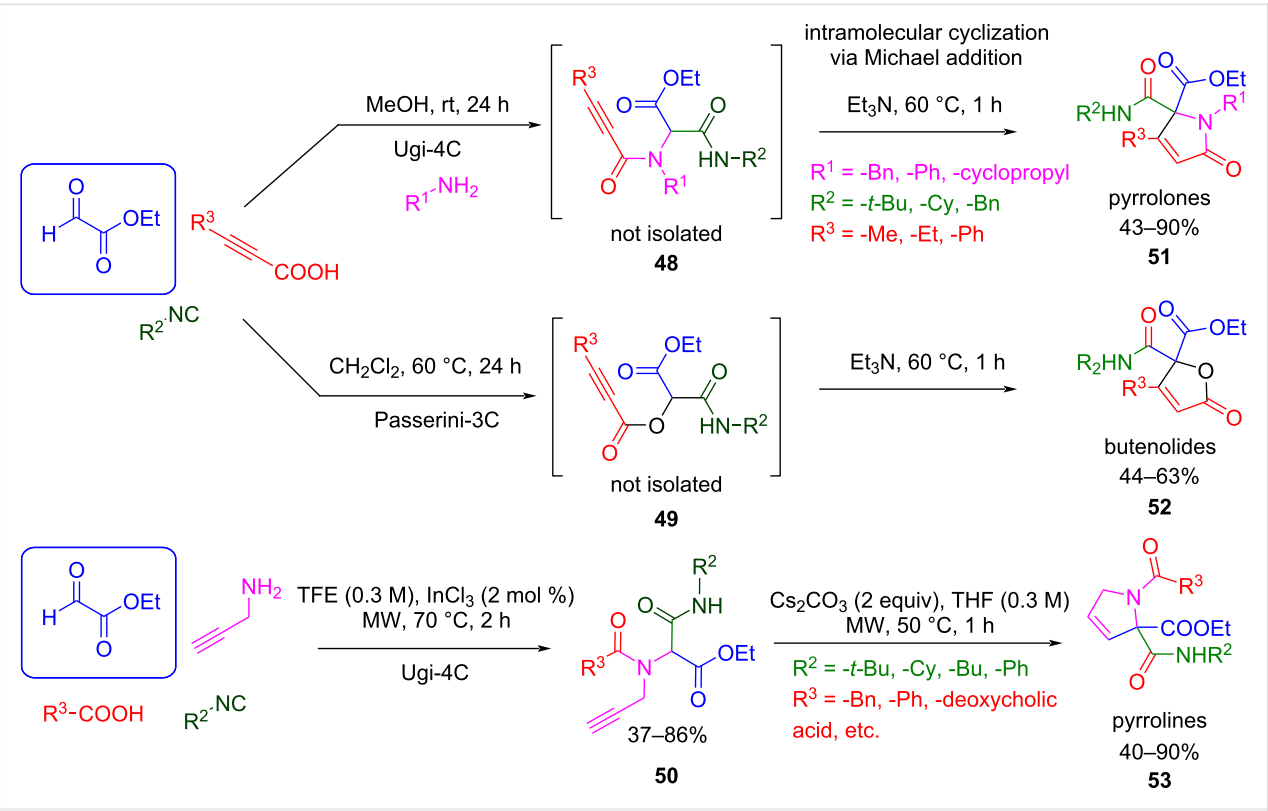

Scheme 44: Ugi/cycloisomerization process to pyrrolones **51**, butenolides **52**, and pyrroline **53**.

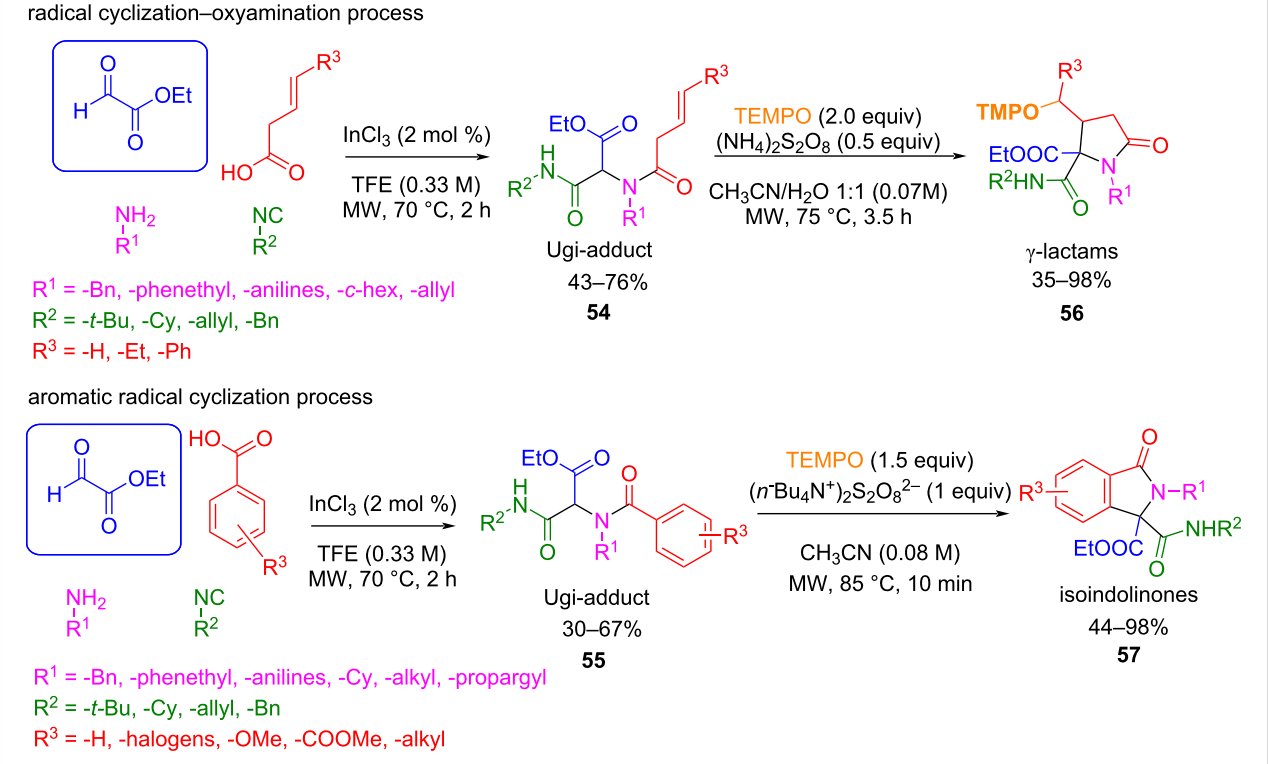

Scheme 45: Radical cyclization reactions from Ugi adducts promoted by TEMPO.

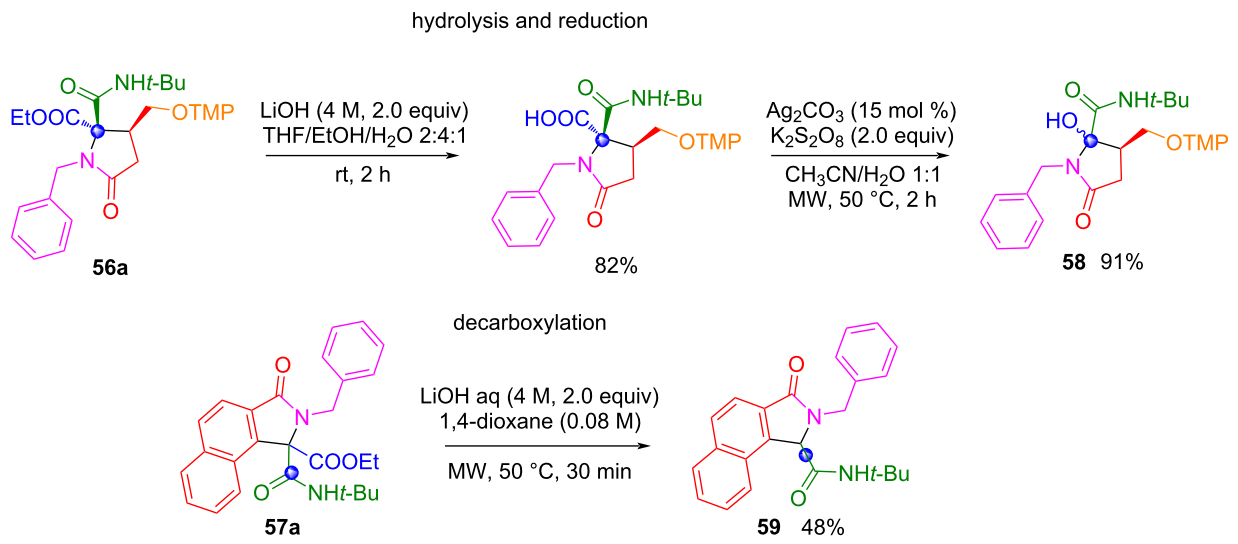

Scheme 46: Hydrolysis and decarboxylation reactions to products with incorporation of a C1 unit of ethyl glyoxylate.

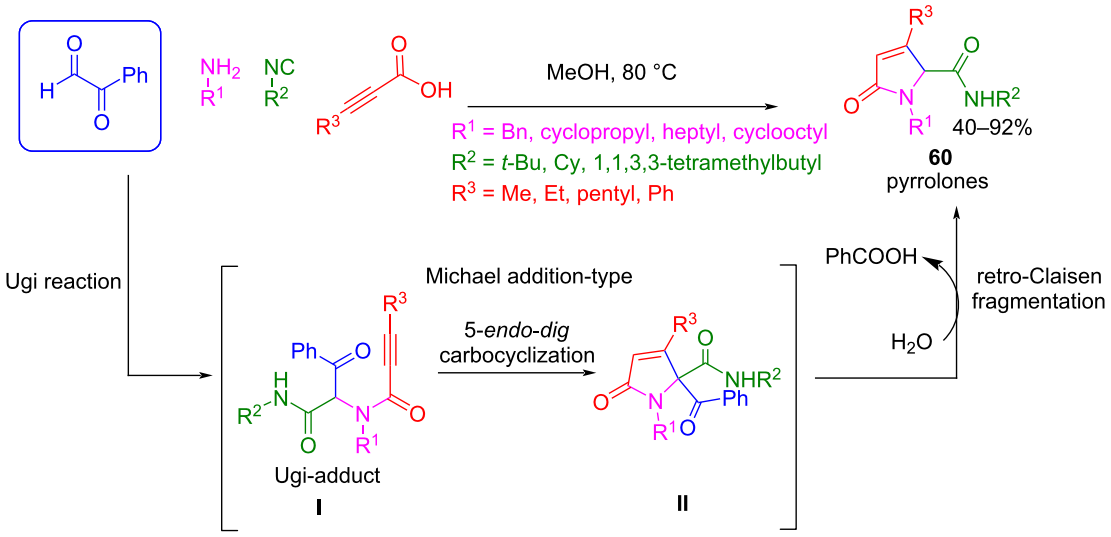

Scheme 47: One-step synthetic route to pyrrolones **60** using phenylglyoxal.

Although the reaction is performed under the conditions typically used in Ugi reactions (MeOH, 80 °C), in this case the outcome is determined by the presence of 3-substituted propargylic acid and phenylglyoxal as aldehyde component (Scheme 47). The Ugi adduct is not isolated, and pyrrolones **60** are spontaneously generated after cyclization of intermediate **I**, probably due to the presence of a propargyl group (conjugated with an amide) and the enolizable position favored by the presence of an additional withdrawing group (phenylcarboxy). It was proposed that, after the cyclization, intermediate **II** follows a retro-Claisen fragmentation to give the final product by releasing the phenyloxy group as benzoic acid.

It is important to note that when using paraformaldehyde instead of phenylglyoxal, only the Ugi adduct is obtained. This result suggests that the presence of the electron-withdrawing group in the carbonyl component is essential for the reaction to proceed through the cyclization step, making phenylglyoxal an excellent formaldehyde surrogate for obtaining heterocycles that could not be afforded directly.

In the same way, Xu's group extended the use of stable enolate at the α-carbon in Ugi adducts as a nucleophile in *pseudo*-Knoevenagel and *pseudo*-Dieckmann cascade reactions [111,112]. Using ethyl glyoxylate, benzoyl carboxylic acids, ar-

omatic amines having ester substituents, and a variety of aromatic and aliphatic isocyanides, these authors reported the synthesis of indoline-piperidinones fused heterocycles **61** via an Ugi/*pseudo*-Knoevenagel/ring expansion/*pseudo*-Dieckmann rearrangement cascade sequence in one pot (Scheme 48) [112].

After the completion of the Ugi reaction, the crude product was subjected without purification to basic conditions for the generation of a carbanion that attacks the carbonyl group of the ketone moiety, provoking a ring expansion that leads to intermediate **I**. Basic hydrolysis and decarboxylation at high temperature, yields a carbanionic intermediate **II** that undergoes a *pseudo*-Dieckmann reaction to give a spiro intermediate **III** which, in turn, undergoes a new rearrangement followed by water elimination to give the final product **61**.

It is important to note that, when ethyl glyoxylate was replaced by paraformaldehyde, the corresponding cyclization sequence

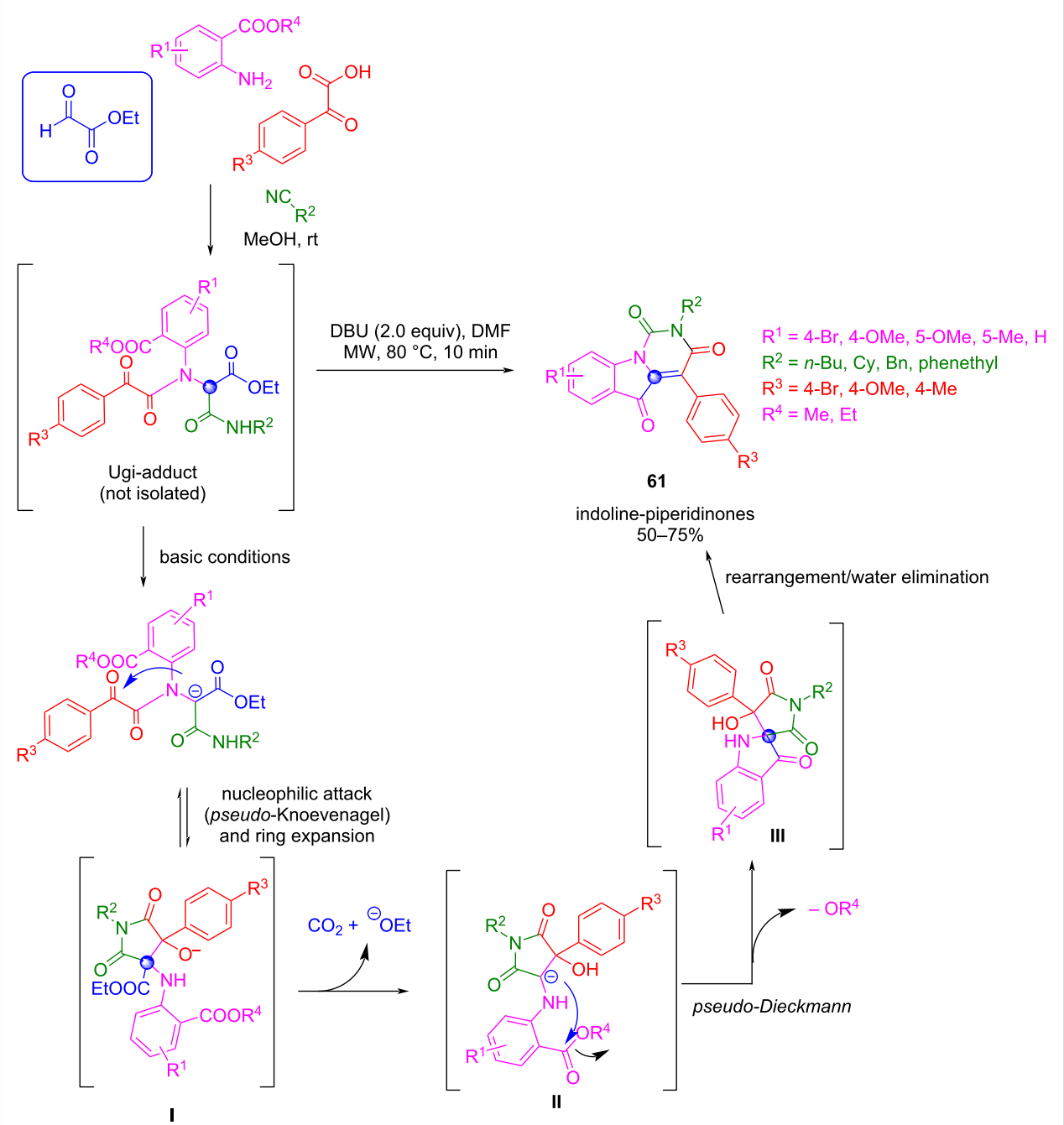

Scheme 48: Ugi-*pseudo*-Knoevenagel-*pseudo*-Dieckmann cascade sequence for the synthesis of fused heterocycles.

could not proceed because the ethyl ester group is necessary to form stable carbanion **II**, which follows the intramolecular *pseudo*-Dieckmann cyclization.

In a similar context, the same authors showed that by selecting the appropriate building blocks for the synthesis of the Ugi adduct, alternative cyclization cascade reactions can be developed [111]. For example, when an aromatic amine was used lacking an additional ester group, the *pseudo*-Dieckmann intramolecular cyclization could not proceed. In this case, after the *pseudo*-Knoevenagel reaction occurred, different pathways are possible depending on the nature of the base employed (Scheme 49). When triethanolamine (TEAO) is used in DMF at 130 °C, the final product is aziridine **62**, the *cis* stereoisomer being the sole stereoisomer observed. In contrast, when treatment of the aziridinyl succinimide **62** is performed under

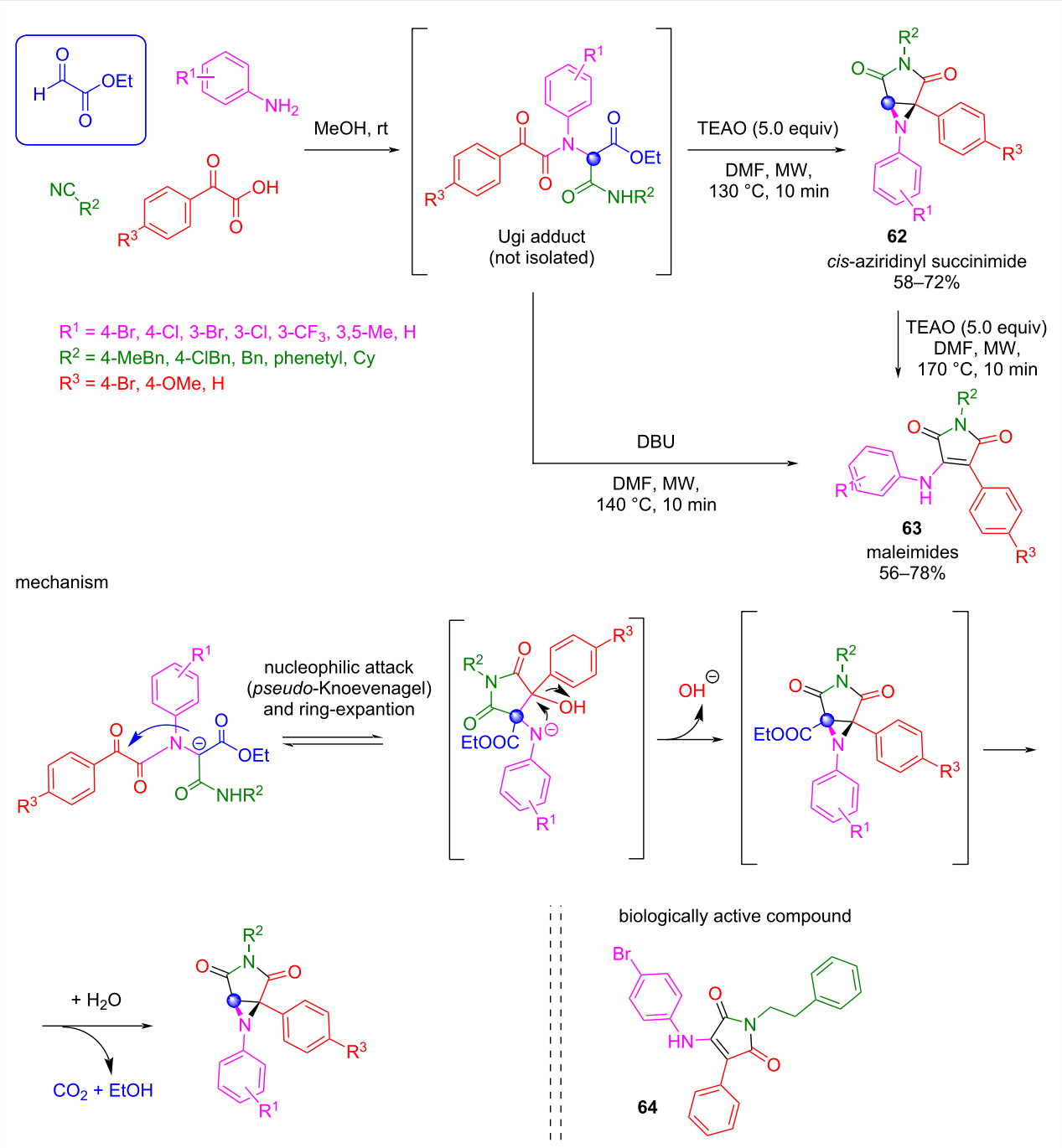

Scheme 49: Ugi-*pseudo*-Knoevenagel reaction from ethyl glyoxylate.

stronger basic conditions, a ring-opening reaction is favored and maleimides **63** are obtained.

These complex one-pot cascade reactions allowed the synthesis of biologically relevant heterocyclic scaffolds. For example, one of the compounds described by these authors showed an interesting in vitro antiproliferative activity against a hepatocarcinoma cell line (**64**, Scheme 49) [111].

Conclusion

This review summarizes the wide range of formaldehyde surrogates that can be used in MCR as a C1 building blocks to afford better reaction conditions in the synthesis of a variety of products, including imidazo compounds, pyrrolones, pyrrolines, indoline pyperidonones, propargylamines, and α-aminophosphorus compounds, among others. These products of biological relevance can be synthesized using traditional MCR reactions as GBB, Povarov, Mannich, Pudovic, Kabachnik–Fields, and isocyanide-based MCRs such as the Ugi reactions. Along with dihalomethanes, alcohols, imines, and dimethyl sulfoxide, glyoxylate and its derivatives are the most versatile formaldehyde surrogates, offering better yields, mild reaction conditions, and the potential for post-condensation reactions that are not possible with formaldehyde. In this context, Knoevenagel, Dieckmann, cyclo-isomerization, radical cyclization, and even hydrolysis and decarboxylation reactions can be implemented as post-condensation steps when glyoxylate is used in Ugi reactions. This expands the universe of possibilities to synthesize structurally more complex products via MCR.

However, despite the plethora of MCR applications wherein formaldehyde has been replaced with alternative C1 building blocks, there remain unexplored MCR reactions where this approach was not studied. This review will open new avenues for the MCR community, both in terms of applying novel formaldehyde surrogates and expanding the range of MCR reactions amenable to these substitutes.

Funding

This research was supported by the Universidad de Buenos Aires (UBACyT 20020220200151BA). Cecilia I. Attorresi would like to thank the financial support received from the following Ph.D. programs: DAAD-ALEARG Scholarship program (between the German Academic Exchange Service, DAAD, and the Ministry of Education of Argentina) and Doctoral fellowship program from CONICET (National Council for Scientific and Technical Research, Argentina)

Author Contributions

Cecilia I. Attorresi: conceptualization; investigation; writing – original draft. Javier A. Ramírez: funding acquisition; project administration; supervision; visualization; writing – original draft; writing – review & editing. Bernhard Westermann: conceptualization; funding acquisition; project administration; writing – original draft; writing – review & editing.

ORCID® iDs

Cecilia I. Attorresi - https://orcid.org/0009-0009-9303-0754
Javier A. Ramírez - https://orcid.org/0000-0002-2013-540X
Bernhard Westermann - https://orcid.org/0000-0002-6228-5991

Data Availability Statement

Data sharing is not applicable as no new data was generated or analyzed in this study.

References

1. Wender, P. A.; Handy, S. T.; Wright, D. L. *Chem. Ind.* **1997,** *19,* 765–768.
2. Anastas, P.; Eghbali, N. *Chem. Soc. Rev.* **2010,** *39,* 301–312. doi:10.1039/b918763b
3. Castiello, C.; Junghanns, P.; Mergel, A.; Jacob, C.; Ducho, C.; Valente, S.; Rotili, D.; Fioravanti, R.; Zwergel, C.; Mai, A. *Green Chem.* **2023,** *25,* 2109–2169. doi:10.1039/d2gc03772f
4. Cioc, R.; Ruijter, E.; Orru, R. V. A. Multicomponent Synthesis: Cohesive Integration of Green Chemistry Principles. In *Green Chemistry in Drug Discovery;* Richardson, P. F., Ed.; Methods in Pharmacology and Toxicology; Humana Press: New York, NY, USA, 2022; pp 237–267. doi:10.1007/978-1-0716-1579-9_8
5. Brauch, S.; van Berkel, S. S.; Westermann, B. *Chem. Soc. Rev.* **2013,** *42,* 4948–4962. doi:10.1039/c3cs35505e
6. Ceballos, L. G.; Pacheco, D. F.; Westermann, B.; Rivera, D. G. Solid-Phase Heterocycle Synthesis Using Multicomponent Reactions. In *Multicomponent Reactions towards Heterocycles: Concepts and Applications;* Van der Eycken, E.; Sharma, U. K., Eds.; John Wiley & Sons: Hoboken, NJ, USA, 2022; pp 139–162. doi:10.1002/9783527832439.ch4
7. Liu, C.; Huang, W.; Zhang, J.; Rao, Z.; Gu, Y.; Jérôme, F. *Green Chem.* **2021,** *23,* 1447–1465. doi:10.1039/d0gc04124f
8. Golden, R.; Valentini, M. *Regul. Toxicol. Pharmacol.* **2014,** *69,* 178–186. doi:10.1016/j.yrtph.2014.03.007
9. Zhang, B.; Hu, X.; Zhang, Y.; Gao, Y.; Wang, X.; Jiang, J.; He, G.; Chen, Y.; Zhang, C.; Sun, J.; Wu, F. *IOP Conf. Ser.: Earth Environ. Sci.* **2021,** *692,* 032050. doi:10.1088/1755-1315/692/3/032050
10. Moni, L.; Banfi, L.; Riva, R.; Basso, A. *Synthesis* **2016,** *48,* 4050–4059. doi:10.1055/s-0035-1562527
11. Ngouansavanh, T.; Zhu, J. *Angew. Chem., Int. Ed.* **2006,** *45,* 3495–3497. doi:10.1002/anie.200600588
12. Brioche, J.; Masson, G.; Zhu, J. *Org. Lett.* **2010,** *12,* 1432–1435. doi:10.1021/ol100012y
13. Zhdankin, V. V. *J. Org. Chem.* **2011,** *76,* 1185–1197. doi:10.1021/jo1024738
14. Drouet, F.; Masson, G.; Zhu, J. *Org. Lett.* **2013,** *15,* 2854–2857. doi:10.1021/ol401181a
15. Kan, X.-W.; Deng, X.-X.; Du, F.-S.; Li, Z.-C. *Macromol. Chem. Phys.* **2014,** *215,* 2221–2228. doi:10.1002/macp.201400264

16. Pan, N.; Xinen Lee, M.; Bunel, L.; Grimaud, L.; Vitale, M. R. *ACS Org. Inorg. Au* **2021,** *1,* 18–22. doi:10.1021/acsorginorgau.1c00003
17. Jones-Mensah, E.; Karki, M.; Magolan, J. *Synthesis* **2016,** *48,* 1421–1436. doi:10.1055/s-0035-1560429
18. Wu, X.-F.; Natte, K. *Adv. Synth. Catal.* **2016,** *358,* 336–352. doi:10.1002/adsc.201501007
19. Liu, S.; Gao, Q.; Wu, X.; Zhang, J.; Ding, K.; Wu, A. *Org. Biomol. Chem.* **2015,** *13,* 2239–2242. doi:10.1039/c4ob02591a
20. Xue, W.-j.; Zheng, K.-l.; Li, H.-z.; Gao, F.-f.; Wu, A.-x. *Tetrahedron Lett.* **2014,** *55,* 4212–4215. doi:10.1016/j.tetlet.2014.05.101
21. Gao, Q.; Wu, X.; Li, Y.; Liu, S.; Meng, X.; Wu, A. *Adv. Synth. Catal.* **2014,** *356,* 2924–2930. doi:10.1002/adsc.201400474
22. Gao, X.; Pan, X.; Gao, J.; Jiang, H.; Yuan, G.; Li, Y. *Org. Lett.* **2015,** *17,* 1038–1041. doi:10.1021/acs.orglett.5b00170
23. Ebule, R.; Mudshinge, S.; Nantz, M. H.; Mashuta, M. S.; Hammond, G. B.; Xu, B. *J. Org. Chem.* **2019,** *84,* 3249–3259. doi:10.1021/acs.joc.8b03162
24. Qin, F.; Tang, L.; Huang, F.; Li, X.; Zhang, W. *Chin. J. Org. Chem.* **2021,** *41,* 318–324. doi:10.6023/cjoc202007003
25. Hossein Nia, R.; Taati, Z.; Mamaghani, M. *Polycyclic Aromat. Compd.* **2024,** *44,* 671–706. doi:10.1080/10406638.2023.2173622
26. Gulati, S.; John, S. E.; Shankaraiah, N. *Beilstein J. Org. Chem.* **2021,** *17,* 819–865. doi:10.3762/bjoc.17.71
27. Cores, Á.; Clerigué, J.; Orocio-Rodríguez, E.; Menéndez, J. C. *Pharmaceuticals* **2022,** *15,* 1009. doi:10.3390/ph15081009
28. Ferreira de Paiva, W.; de Freitas Rego, Y.; de Fátima, Á.; Fernandes, S. A. *Synthesis* **2022,** *54,* 3162–3179. doi:10.1055/a-1794-8355
29. Vicente-García, E.; Ramón, R.; Preciado, S.; Lavilla, R. *Beilstein J. Org. Chem.* **2011,** *7,* 980–987. doi:10.3762/bjoc.7.110
30. Gao, Q.; Liu, S.; Wu, X.; Wu, A. *Org. Lett.* **2014,** *16,* 4582–4585. doi:10.1021/ol502134u
31. Simões, J. B.; de Fátima, Â.; Sabino, A. A.; de Aquino, F. J. T.; da Silva, D. L.; Barbosa, L. C. A.; Fernandes, S. A. *Org. Biomol. Chem.* **2013,** *11,* 5069–5073. doi:10.1039/c3ob40927a
32. Xu, X.; Yang, Y.; Chen, X.; Zhang, X.; Yi, W. *Org. Biomol. Chem.* **2017,** *15,* 9061–9065. doi:10.1039/c7ob02310c
33. Luo, Y.; Sun, H.; Zhang, W.; Wang, X.; Xu, S.; Zhang, G.; Jian, Y.; Gao, Z. *RSC Adv.* **2017,** *7,* 28616–28625. doi:10.1039/c7ra00870h
34. Geng, X.; Wu, X.; Zhao, P.; Zhang, J.; Wu, Y.-D.; Wu, A.-X. *Org. Lett.* **2017,** *19,* 4179–4182. doi:10.1021/acs.orglett.7b01686
35. Midya, S. P.; Sahoo, M. K.; Landge, V. G.; Rajamohanan, P. R.; Balaraman, E. *Nat. Commun.* **2015,** *6,* 8591. doi:10.1038/ncomms9591
36. Xiang, J.-C.; Wang, Z.-X.; Cheng, Y.; Xia, S.-Q.; Wang, M.; Tang, B.-C.; Wu, Y.-D.; Wu, A.-X. *J. Org. Chem.* **2017,** *82,* 9210–9216. doi:10.1021/acs.joc.7b01501
37. Xu, X.; Yang, Y.; Zhang, X.; Yi, W. *Org. Lett.* **2018,** *20,* 566–569. doi:10.1021/acs.orglett.7b03673
38. Phanindrudu, M.; Wakade, S. B.; Tiwari, D. K.; Likhar, P. R.; Tiwari, D. K. *J. Org. Chem.* **2018,** *83,* 9137–9143. doi:10.1021/acs.joc.8b01204
39. Jadhav, S. D.; Singh, A. *Org. Lett.* **2017,** *19,* 5673–5676. doi:10.1021/acs.orglett.7b02838
40. Liu, Y.; Hu, Y.; Cao, Z.; Zhan, X.; Luo, W.; Liu, Q.; Guo, C. *Adv. Synth. Catal.* **2018,** *360,* 2691–2695. doi:10.1002/adsc.201800373
41. Ma, J.-T.; Chen, T.; Tang, B.-C.; Chen, X.-L.; Yu, Z.-C.; Zhou, Y.; Zhuang, S.-Y.; Wu, Y.-D.; Xiang, J.-C.; Wu, A.-X. *J. Org. Chem.* **2023,** *88,* 3760–3771. doi:10.1021/acs.joc.2c03034
42. Vodnala, N.; Gujjarappa, R.; Satheesh, V.; Gupta, R.; Kaldhi, D.; Kabi, A. K.; Malakar, C. C. *ChemistrySelect* **2020,** *5,* 10144–10148. doi:10.1002/slct.202002968
43. Wu, X.; Zhang, J.; Liu, S.; Gao, Q.; Wu, A. *Adv. Synth. Catal.* **2016,** *358,* 218–225. doi:10.1002/adsc.201500683
44. Zhao, P.; Yu, X.-X.; Zhou, Y.; Geng, X.; Wang, C.; Huang, C.; Wu, Y.-D.; Zhu, Y.-P.; Wu, A.-X. *Org. Lett.* **2020,** *22,* 7103–7107. doi:10.1021/acs.orglett.0c02415
45. Guo, H.; Tian, L.; Liu, Y.; Wan, J.-P. *Org. Lett.* **2022,** *24,* 228–233. doi:10.1021/acs.orglett.1c03879
46. Weyesa, A.; Mulugeta, E. *RSC Adv.* **2020,** *10,* 20784–20793. doi:10.1039/d0ra03763j
47. Cuprova, L.; Dobbs, A. P. *Adv. Heterocycl. Chem.* **2020,** *130,* 251–278. doi:10.1016/bs.aihch.2019.10.006
48. Ni, Y.; Zuo, H.; Yu, H.; Wu, Y.; Zhong, F. *Org. Lett.* **2018,** *20,* 5899–5904. doi:10.1021/acs.orglett.8b02551
49. Sun, K.; Lv, Y.; Zhu, Z.; Zhang, L.; Wu, H.; Liu, L.; Jiang, Y.; Xiao, B.; Wang, X. *RSC Adv.* **2015,** *5,* 3094–3097. doi:10.1039/c4ra14249g
50. Sun, K.; Wang, X.; Jiang, Y.; Lv, Y.; Zhang, L.; Xiao, B.; Li, D.; Zhu, Z.; Liu, L. *Chem. – Asian J.* **2015,** *10,* 536–539. doi:10.1002/asia.201403358
51. Mahajan, P. S.; Tanpure, S. D.; More, N. A.; Gajbhiye, J. M.; Mhaske, S. B. *RSC Adv.* **2015,** *5,* 101641–101646. doi:10.1039/c5ra21801b
52. Bhattacharjee, S.; Laru, S.; Ghosh, P.; Hajra, A. *J. Org. Chem.* **2021,** *86,* 10866–10873. doi:10.1021/acs.joc.1c01188
53. Grounds, O.; Zeller, M.; Rosokha, S. V. *Crystals* **2024,** *14,* 124. doi:10.3390/cryst14020124
54. Roberts, A. L.; Sanborn, P. N.; Gschwend, P. M. *Environ. Sci. Technol.* **1992,** *26,* 2263–2274. doi:10.1021/es00035a027
55. Bull, J. A.; Mousseau, J. J.; Charette, A. B. *Org. Lett.* **2008,** *10,* 5485–5488. doi:10.1021/ol802315k
56. Rudine, A. B.; Walter, M. G.; Wamser, C. C. *J. Org. Chem.* **2010,** *75,* 4292–4295. doi:10.1021/jo100276m
57. Dunlap, L. E.; Olson, D. E. *ACS Omega* **2018,** *3,* 4968–4973. doi:10.1021/acsomega.8b00507
58. Ghosh, S.; Biswas, K. *RSC Adv.* **2021,** *11,* 2047–2065. doi:10.1039/d0ra09392k
59. Patil, M. K.; Keller, M.; Reddy, B. M.; Pale, P.; Sommer, J. *Eur. J. Org. Chem.* **2008,** 4440–4445. doi:10.1002/ejoc.200800359
60. Zhang, X.; Corma, A. *Angew. Chem.* **2008,** *120,* 4430–4433. doi:10.1002/ange.200800098
61. Zhang, Y.; Li, P.; Wang, M.; Wang, L. *J. Org. Chem.* **2009,** *74,* 4364–4367. doi:10.1021/jo900507v
62. Yu, D.; Zhang, Y. *Adv. Synth. Catal.* **2011,** *353,* 163–169. doi:10.1002/adsc.201000691
63. Aguilar, D.; Contel, M.; Urriolabeitia, E. P. *Chem. – Eur. J.* **2010,** *16,* 9287–9296. doi:10.1002/chem.201000587
64. Rahman, M.; Bagdi, A. K.; Majee, A.; Hajra, A. *Tetrahedron Lett.* **2011,** *52,* 4437–4439. doi:10.1016/j.tetlet.2011.06.067
65. Gao, J.; Song, Q.-W.; He, L.-N.; Yang, Z.-Z.; Dou, X.-Y. *Chem. Commun.* **2012,** *48,* 2024–2026. doi:10.1039/c2cc17616e
66. Tang, Y.; Xiao, T.; Zhou, L. *Tetrahedron Lett.* **2012,** *53,* 6199–6201. doi:10.1016/j.tetlet.2012.08.136
67. Lanke, S. R.; Bhanage, B. M. *Appl. Organomet. Chem.* **2013,** *27,* 729–733. doi:10.1002/aoc.3071

68. Buckley, B. R.; Khan, A. N.; Heaney, H. *Chem. – Eur. J.* **2012,** *18,* 3855–3858. doi:10.1002/chem.201103987
69. Holm, S. C.; Straub, B. F. *Org. Prep. Proced. Int.* **2011,** *43,* 319–347. doi:10.1080/00304948.2011.593999
70. Mills, J. E.; Maryanoff, C. A.; McComsey, D. F.; Stanzione, R. C.; Scott, L. *J. Org. Chem.* **1987,** *52,* 1857–1859. doi:10.1021/jo00385a038
71. Rawat, V. S.; Bathini, T.; Govardan, S.; Sreedhar, B. *Org. Biomol. Chem.* **2014,** *12,* 6725–6729. doi:10.1039/c4ob00986j
72. Zefirov, N. S.; Matveeva, E. D. *ARKIVOC* **2008,** No. i, 1–17. doi:10.3998/ark.5550190.0009.101
73. Haji, M. *Beilstein J. Org. Chem.* **2016,** *12,* 1269–1301. doi:10.3762/bjoc.12.121
74. Keglevich, G.; Bálint, E. *Molecules* **2012,** *17,* 12821–12835. doi:10.3390/molecules171112821
75. Fan, W.; Verrier, C.; Wang, L.; Ahmar, M.; Tan, J.-N.; Popowycz, F.; Queneau, Y. 5-(Hydroxymethyl)furfural and 5-(glucosyloxymethyl)furfural in multicomponent reactions. In *Recent Trends in Carbohydrate Chemistry;* Rauter, A. P.; Christensen, B. E.; Somsák, L.; Kosma, P.; Adamo, R., Eds.; Elsevier: Amsterdam, Netherlands, 2020; pp 73–100. doi:10.1016/b978-0-12-817467-8.00002-5
76. Keglevich, G.; Kiss, N. Z.; Bálint, E.; Henyecz, R.; Grün, A.; Mucsi, Z. *Phosphorus, Sulfur Silicon Relat. Elem.* **2019,** *194,* 391–395. doi:10.1080/10426507.2018.1521406
77. Gancarz, R.; Gancarz, I.; Masiowska, A. *Phosphorus, Sulfur Silicon Relat. Elem.* **1996,** *111,* 195. doi:10.1080/10426509608054824
78. Bálint, E.; Tajti, Á.; Ádám, A.; Csontos, I.; Karaghiosoff, K.; Czugler, M.; Ábrányi-Balogh, P.; Keglevich, G. *Beilstein J. Org. Chem.* **2017,** *13,* 76–86. doi:10.3762/bjoc.13.10
79. Zhao, Y.; Chen, X.; Chen, T.; Zhou, Y.; Yin, S.-F.; Han, L.-B. *J. Org. Chem.* **2015,** *80,* 62–69. doi:10.1021/jo501961h
80. Villemin, D.; Moreau, B.; Bar, N. *Organics* **2021,** *2,* 98–106. doi:10.3390/org2020009
81. Patil, P.; de Haan, M.; Kurpiewska, K.; Kalinowska-Tłuścik, J.; Dömling, A. *ACS Comb. Sci.* **2016,** *18,* 170–175. doi:10.1021/acscombsci.5b00189
82. Patil, P.; Kurpiewska, K.; Kalinowska-Tłuścik, J.; Dömling, A. *ACS Comb. Sci.* **2017,** *19,* 343–350. doi:10.1021/acscombsci.7b00033
83. Rosalba, T. P. F.; Kas, S. S. A.; Sampaio, A. B. S.; Salvador, C. E. M.; Andrade, C. K. Z. *Eur. J. Org. Chem.* **2021,** 2831–2842. doi:10.1002/ejoc.202001671
84. Boltjes, A.; Dömling, A. *Eur. J. Org. Chem.* **2019,** 7007–7049. doi:10.1002/ejoc.201901124
85. Shaaban, S.; Abdel-Wahab, B. F. *Mol. Diversity* **2016,** *20,* 233–254. doi:10.1007/s11030-015-9602-6
86. Sharma, A.; Li, H.-Y. *Synlett* **2011,** 1407–1412. doi:10.1055/s-0030-1260568
87. Chernyak, N.; Gevorgyan, V. *Angew. Chem., Int. Ed.* **2010,** *49,* 2743–2746. doi:10.1002/anie.200907291
88. Lyon, M. A.; Kercher, T. S. *Org. Lett.* **2004,** *6,* 4989–4992. doi:10.1021/ol0478234
89. Hulme, C.; Lee, Y.-S. *Mol. Diversity* **2008,** *12,* 1–15. doi:10.1007/s11030-008-9072-1
90. Mandair, G. S.; Light, M.; Russell, A.; Hursthouse, M.; Bradley, M. *Tetrahedron Lett.* **2002,** *43,* 4267–4269. doi:10.1016/s0040-4039(02)00709-8
91. Nichol, G. S.; Sharma, A.; Li, H.-Y. *Acta Crystallogr., Sect. E: Struct. Rep. Online* **2011,** *67,* o833. doi:10.1107/s160053681100821x
92. Katritzky, A. R.; Xu, Y.-J.; Tu, H. *J. Org. Chem.* **2003,** *68,* 4935–4937. doi:10.1021/jo026797p
93. Surkar, P.; Kaur, T.; Sharma, A. *Synlett* **2015,** *26,* 1403–1407. doi:10.1055/s-0034-1380653
94. Gladysz, R.; Adriaenssens, Y.; De Winter, H.; Joossens, J.; Lambeir, A.-M.; Augustyns, K.; Van der Veken, P. *J. Med. Chem.* **2015,** *58,* 9238–9257. doi:10.1021/acs.jmedchem.5b01171
95. Mackwitz, M. K. W.; Hamacher, A.; Osko, J. D.; Held, J.; Schöler, A.; Christianson, D. W.; Kassack, M. U.; Hansen, F. K. *Org. Lett.* **2018,** *20,* 3255–3258. doi:10.1021/acs.orglett.8b01118
96. Sisko, J.; Kassick, A. J.; Mellinger, M.; Filan, J. J.; Allen, A.; Olsen, M. A. *J. Org. Chem.* **2000,** *65,* 1516–1524. doi:10.1021/jo991782l
97. Dow, R. L.; Hadcock, J. R.; Scott, D. O.; Schneider, S. R.; Paight, E. S.; Iredale, P. A.; Carpino, P. A.; Griffith, D. A.; Hammond, M.; DaSilva-Jardine, P. *Bioorg. Med. Chem. Lett.* **2009,** *19,* 5351–5354. doi:10.1016/j.bmcl.2009.07.130
98. Huang, Y.; Wolf, S.; Bista, M.; Meireles, L.; Camacho, C.; Holak, T. A.; Dömling, A. *Chem. Biol. Drug Des.* **2010,** *76,* 116–129. doi:10.1111/j.1747-0285.2010.00989.x
99. Gunawan, S.; Ayaz, M.; De Moliner, F.; Frett, B.; Kaiser, C.; Patrick, N.; Xu, Z.; Hulme, C. *Tetrahedron* **2012,** *68,* 5606–5611. doi:10.1016/j.tet.2012.04.068
100. Gunawan, S.; Nichol, G.; Hulme, C. *Tetrahedron Lett.* **2012,** *53,* 1664–1667. doi:10.1016/j.tetlet.2012.01.080
101. Hulme, C.; Cherrier, M.-P. *Tetrahedron Lett.* **1999,** *40,* 5295–5299. doi:10.1016/s0040-4039(99)00960-0
102. Medda, F.; Hulme, C. *Tetrahedron Lett.* **2012,** *53,* 5593–5596. doi:10.1016/j.tetlet.2012.07.135
103. Xu, Z.; De Moliner, F.; Cappelli, A. P.; Ayaz, M.; Hulme, C. *Synlett* **2014,** *25,* 225–228. doi:10.1055/s-0033-1340219
104. Medda, F.; Martinez-Ariza, G.; Hulme, C. *Tetrahedron Lett.* **2015,** *56,* 5295–5298. doi:10.1016/j.tetlet.2015.07.083
105. Li, Y.; Huang, Z.; Xu, J.; Ding, Y.; Tang, D.-Y.; Lei, J.; Li, H.-y.; Chen, Z.-Z.; Xu, Z.-G. *Beilstein J. Org. Chem.* **2020,** *16,* 663–669. doi:10.3762/bjoc.16.63
106. Flores-Constante, G.; Sánchez-Chávez, A. C.; Polindara-García, L. A. *Eur. J. Org. Chem.* **2018,** 4586–4591. doi:10.1002/ejoc.201800756
107. Nechaev, A. A.; Peshkov, A. A.; Peshkov, V. A.; Van der Eycken, E. V. *Synthesis* **2016,** *48,* 2280–2286. doi:10.1055/s-0035-1561422
108. Borja-Miranda, A.; Sánchez-Chávez, A. C.; Polindara-García, L. A. *Eur. J. Org. Chem.* **2019,** 2453–2471. doi:10.1002/ejoc.201801871
109. Borja-Miranda, A.; Valencia-Villegas, F.; Lujan-Montelongo, J. A.; Polindara-García, L. A. *J. Org. Chem.* **2021,** *86,* 929–946. doi:10.1021/acs.joc.0c02441
110. Peshkov, A. A.; Peshkov, V. A.; Li, Z.; Pereshivko, O. P.; Van der Eycken, E. V. *Eur. J. Org. Chem.* **2014,** 6390–6393. doi:10.1002/ejoc.201402723
111. Lei, J.; Song, G.-T.; He, L.-J.; Luo, Y.-F.; Tang, D.-Y.; Lin, H.-K.; Frett, B.; Li, H.-y.; Chen, Z.-Z.; Xu, Z.-G. *Chem. Commun.* **2020,** *56,* 2194–2197. doi:10.1039/c9cc08220d
112. Lei, J.; Song, G.-T.; Luo, Y.-F.; Tang, D.-Y.; Yan, W.; Li, H.-y.; Chen, Z.-Z.; Xu, Z.-G. *Org. Chem. Front.* **2020,** *7,* 737–741. doi:10.1039/d0qo00028k

License and Terms

This is an open access article licensed under the terms of the Beilstein-Institut Open Access License Agreement (https://www.beilstein-journals.org/bjoc/terms), which is identical to the Creative Commons Attribution 4.0 International License (https://creativecommons.org/licenses/by/4.0). The reuse of material under this license requires that the author(s), source and license are credited. Third-party material in this article could be subject to other licenses (typically indicated in the credit line), and in this case, users are required to obtain permission from the license holder to reuse the material.

The definitive version of this article is the electronic one which can be found at:
https://doi.org/10.3762/bjoc.21.45

BEILSTEIN JOURNAL OF ORGANIC CHEMISTRY

α-Ketoglutaric acid in Ugi reactions and Ugi/aza-Wittig tandem reactions

Vladyslav O. Honcharov[1], Yana I. Sakhno*[1], Olena H. Shvets[1,2], Vyacheslav E. Saraev[1], Svitlana V. Shishkina[1,3], Tetyana V. Shcherbakova[1] and Valentyn A. Chebanov*[1,2]

Full Research Paper

Open Access

Address:
[1]Institute of Functional Materials Chemistry, State Scientific Institution "Institute for Single Crystals" of National Academy of Sciences of Ukraine, Nauky Ave., 60, 61072, Kharkiv, Ukraine, [2]Faculty of Chemistry, V. N. Karazin Kharkiv National University, Svobody sq., 4, 61022, Kharkiv, Ukraine and [3]Institute of Organic Chemistry, National Academy of Sciences of Ukraine, Akademika Kukharya Street, 5, 02660, Kyiv, Ukraine

Email:
Yana I. Sakhno* - sakhno@isc.kh.ua; Valentyn A. Chebanov* - chebanov@isc.kh.ua

* Corresponding author

Keywords:
α-ketoglutaric acid; aza-Wittig reaction; multicomponent reaction; quinoxalinone derivative; Ugi reaction

Beilstein J. Org. Chem. **2025,** *21,* 2021–2029.
https://doi.org/10.3762/bjoc.21.157

Received: 18 June 2025
Accepted: 22 September 2025
Published: 07 October 2025

This article is part of the thematic issue "Multicomponent reactions IV".

Associate Editor: M. Desage-El Murr

© 2025 Honcharov et al.; licensee Beilstein-Institut.
License and terms: see end of document.

Abstract

A small library of bis- and tetraamides was synthesized by the Ugi reaction with α-ketoglutaric acid, *tert*-butyl isocyanide, aromatic aldehydes, and aromatic amines. When *o*-azidoanilines were used, azidated peptidomimetics were obtained, the post-cyclization of which by the aza-Wittig reaction yielded a series of substituted 3-(3-oxo-3,4-dihydroquinoxalin-2-yl)propanoic acids containing a pharmacophore quinoxalinone moiety. The tandem Ugi/aza-Wittig combination was also carried out in a one-pot procedure without isolation of the intermediate.

Introduction

Multicomponent reactions are powerful tools in organic chemistry that enable the synthesis of structurally complex and multifunctional compounds from three or more starting materials in a single synthetic step. They are widely used in drug discovery because, unlike conventional linear synthesis strategies, they enable the preparation of libraries of organic compounds in higher yields and with significantly less time, resources, and chemical waste [1-5].

The Ugi reaction, discovered in 1959 by Ivar Karl Ugi [6], is one of the classic multicomponent reactions, widely used as a green alternative for the synthesis of active pharmaceutical ingredients [7] and opens up the possibility of creating new compounds from the class of peptidomimetics [8-10], which often exhibit diverse biological effects [11] including antidiabetic [12], antiviral [13], antibacterial [8,14,15], and anticancer [16,17] activities.

The use of the Ugi reaction followed by post-cyclization is an effective strategy that yields diverse heterocycle-containing peptidomimetics and requires a minimal number of steps [18]. For example, Mazur et al. [19] developed an efficient method for the preparation of benzodiazepinone derivatives, which showed promising psychotropic effects [20-24], using a tandem combination of Ugi/azide–alkyne cycloaddition reactions. From this point of view, azido amines are promising reagents for use in the Ugi reaction, opening up the possibility of synthesizing various heterocyclic systems such as quinazolines [25], diazepinones [25,26], quinoxalinones [27], diazocinones [28], and imidazolines [29] due to the exceptional reactivity of the azido group. However, the use of azido amines in the Ugi reaction together with oxoacids, which have an additional reaction center for post-cyclizations, is scarcely reported in the literature [25,30,31].

Among the numerous tandem synthetic approaches, the combination of Ugi/aza-Wittig reactions is of particular interest. In recent years, several works have been dedicated to the synthesis of nitrogen-containing heterocyclic compounds using various modifications of this sequence [32-36]. Among others, Yan et al. [31] described a facile way to quinoxalinone derivatives using an Ugi/Staudinger/aza-Wittig tandem combination with pyruvic acid or phenylglyoxylic acid.

Quinoxalinones are regarded as privileged heterocyclic moieties in the development of new pharmacologically active organic compounds (Figure 1) [37]. These structures are of great interest to chemists because of their broad spectrum of potential biological effects, including anticancer [38], antibacterial [39] and anti-HIV [40] activities. Furthermore, a quinoxaline-containing commercial drug, caroverine, has been proven effective in the treatment of tinnitus [41]. In addition, in vivo studies in mice and rats with various quinoxalinone derivatives have shown favorable analgesic and anti-inflammatory properties as well as low toxicity of these substances [42]. Biological activity screening also suggests that quinoxalinone-based compounds can inhibit aldose reductase [43], α-amylase and α-glucosidase [44], as well as key enzymes involved in the processes of saturated fatty acid conversion [45] and glycogenolysis [46]. Therefore, these molecules can be considered as potential antidiabetic agents.

α-Ketoglutaric acid (KGA) is an attractive precursor for medically oriented syntheses using multicomponent reactions due to its chemical structure as a dibasic keto acid and its role as an important component of numerous biochemical processes [47]. However, there are only a few studies in the literature on multicomponent reactions based on KGA. In 1992, Gein et al. [48] reported a multicomponent reaction involving KGA, aromatic aldehydes, and aromatic amines. This led to the formation of pyrrolone derivatives **I**, which showed anti-inflammatory activity [49,50] (Scheme 1, pathway A). In an earlier study by our research group, Sakhno et al. [51] described a three-component Doebner-type reaction involving KGA, aromatic aldehydes, and 3-amino-5-methylisoxazole, which led to the formation of [2-aryl-4-hydroxy-1-(5-methylisoxazol-3-yl)-5-oxo-2,5-dihydro-1*H*-pyrrol-3-yl]acetic acids **II** (Scheme 1, pathway B). Subsequently, a four-component Ugi reaction of compounds **II** with temperature-controlled formation of diastereomers of peptidomimetics **III** was also studied [52].

Taking into account all mentioned above, this work is dedicated to the synthesis of novel peptidomimetics using the four-component Ugi reaction and the study of a tandem Ugi/aza-Wittig combination based on α-ketoglutaric acid for the preparation of earlier unavailable quinoxalinone derivatives.

Results and Discussion

We began by studying the behavior of α-ketoglutaric acid in the four-component Ugi reaction with equimolar amounts of the reagents. It was found that stirring of aromatic aldehydes **2a**–**d**, aromatic amines **3a**–**d**, KGA (**1**) and *ter*t-butyl isocyanide (**4**) (in a 1:1:1:1 molar ratio) in methanol for 24 hours at 45 °C resulted in the formation of 5-((aryl)(1-aryl-2-(*tert*-butylamino)-

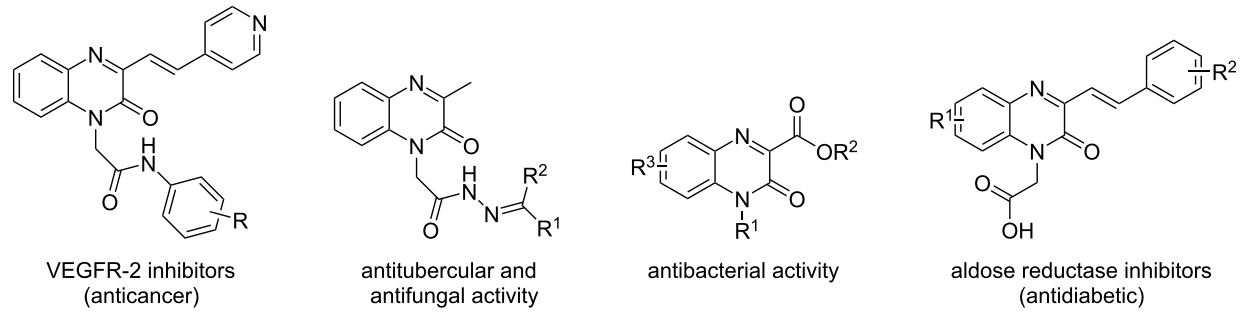

Figure 1: Some biologically active quinoxalinone derivatives.

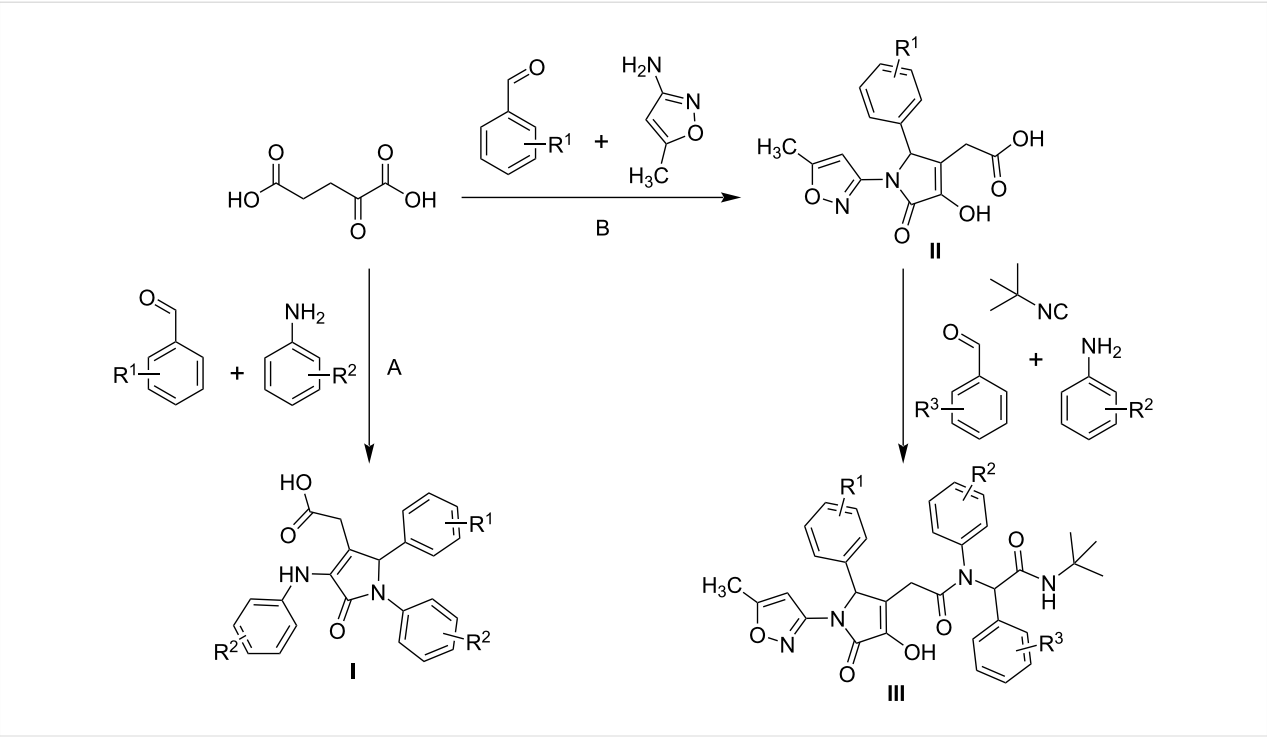

Scheme 1: Known multicomponent reactions of KGA.

2-oxoethyl)amino)-4,5-dioxopentanoic acids **5a–l** in 50–81% yields (Scheme 2, pathway A; Table 1). The compounds **5a–l** were isolated easily by adding water to the reaction mass until it became cloudy, whereupon a precipitate of the product was formed and isolated (all experimental procedures can be found in Supporting Information File 1).

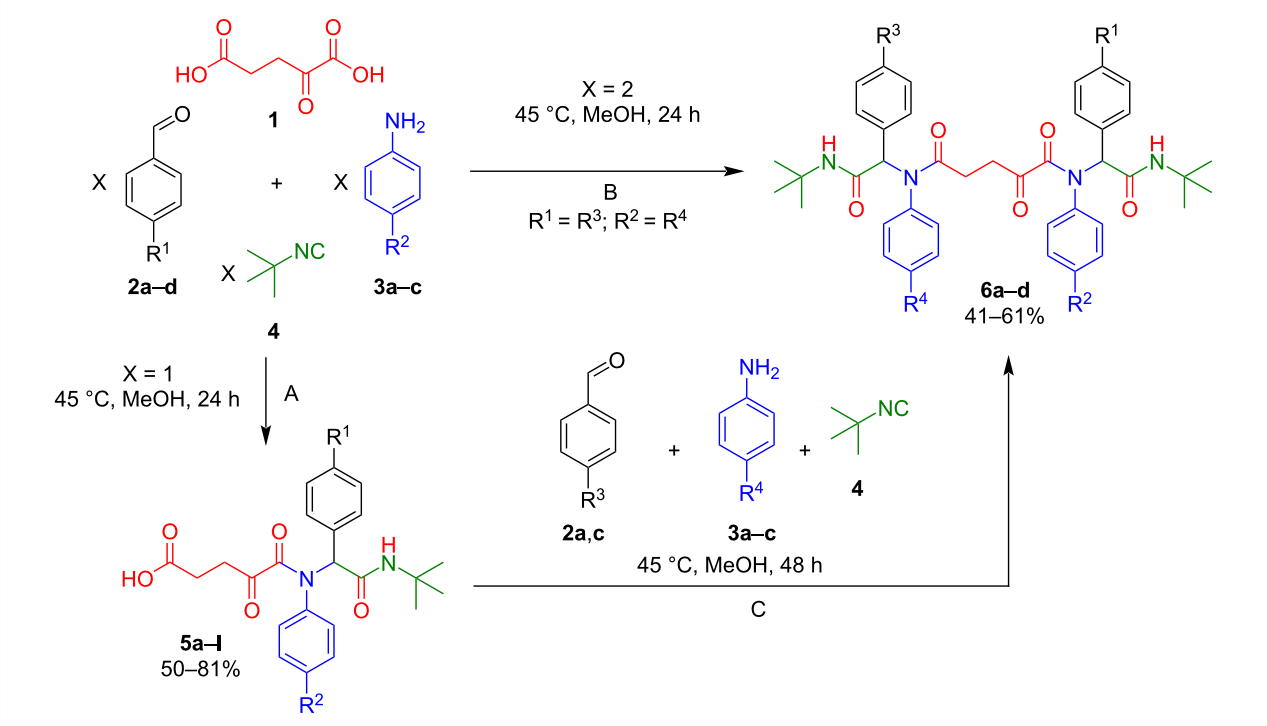

Scheme 2: Ugi reaction involving KGA.

Table 1: Yields of compounds **5a–l**.

Aldehyde	R^1	Amine	R^2	Compound	Yield, %
2a	4-Cl	**3a**	4-Cl	**5a**	81
2a	4-Cl	**3b**	4-CH_3	**5b**	64
2a	4-Cl	**3c**	4-OCH_3	**5c**	68
2b	4-OCH_3	**3a**	4-Cl	**5d**	50
2b	4-OCH_3	**3b**	4-CH_3	**5e**	54
2b	4-OCH_3	**3c**	4-OCH_3	**5f**	52
2c	4-$COOCH_3$	**3a**	4-Cl	**5g**	57
2c	4-$COOCH_3$	**3b**	4-CH_3	**5h**	72
2c	4-$COOCH_3$	**3c**	4-OCH_3	**5i**	54
2d	4-Br	**3a**	4-Cl	**5j**	77
2d	4-Br	**3b**	4-CH_3	**5k**	73
2d	4-Br	**3c**	4-OCH_3	**5l**	61

Since α-ketoglutaric acid is dibasic, increasing the stoichiometric amounts of the starting materials enables the Ugi reaction involving two carboxyl groups. Thus, mixing KGA (**1**), 4-chlorobenzaldehyde (**2a**), 4-chloroaniline (**3a**), and *tert*-butyl isocyanide (**4**) in a molar ratio of 1:2:2:2 in MeOH and subsequent stirring at a temperature of 45 °C for 24 hours led to the formation of N^1,N^5-bis(2-(*tert*-butylamino)-1-(4-chlorophenyl)-2-oxoethyl)-N^1,N^5-bis(4-chlorophenyl)-2-oxopentanediamide (**6a**) in 55% yield (Scheme 2, pathway B; Table 2).

Compounds **5** contain a free carboxyl group and thus can also be used as an acidic component in the Ugi reaction. Indeed, it was established that the reaction of 5-((2-(*tert*-butylamino)-1-(4-chlorophenyl)-2-oxoethyl)(4-chlorophenyl)amino)-4,5-dioxopentanoic acid (**5a**) with aldehydes **2a**,**c**, amines **3a**–**c**, and *tert*-butyl isocyanide (**4**) in a molar ratio of 1:1:1 at 45 °C for 48 hours gave N^1,N^5-diaryl-N^1,N^5-bis(1-aryl-2-(*tert*-butylamino)-2-oxoethyl)-2-oxopentanediamides **6a**–**d** in 41–61% yields (Scheme 2, pathway C; Table 2). It is important to note that compounds **6a**–**d** rapidly precipitated from the solution and did not require further purification after filtration.

The use of starting components containing highly reactive groups, for example, an azide group, in the Ugi reaction provides opportunities for various post-cyclizations to obtain nitrogen-containing heterocyclic systems with potential biological activity [18]. To prepare new quinoxalinone derivatives, we studied a tandem combination of Ugi/aza-Wittig reactions involving α-ketoglutaric acid and *o*-azidoanilines. First, 5-((2-arylazido)(1-aryl-2-(*tert*-butylamino)-2-oxoethyl)amino)-4,5-dioxopentanoic acids **8a**,**b**,**d**,**f**–**h** were synthesized by the reaction of KGA (**1**), aldehydes **2**, *o*-azidoanilines **7**, and *tert*-butyl isocyanide (**4**) for 24 hours at 45 °C in 35–78% yields (Scheme 3; Table 3).

To isolate compounds **8a**,**b**,**d**,**f**–**h**, the reaction mixture was poured onto ice and the resulting precipitate was filtered. These compounds also often had to be additionally purified by column chromatography.

Subsequently, the compounds **8a**,**b**,**d**,**f**–**h** were dissolved in DCM and stirred in the presence of a stoichiometric amount of triphenylphosphine at 20 °C for 12 hours, resulting in the formation of 3-(4-(1-aryl-2-(*tert*-butylamino)-2-oxoethyl)-3-oxo-3,4-dihydroquinoxalin-2-yl)propanoic acids **9a**,**b**,**d**,**f**–**h** in 33–93% yields (Scheme 3; Table 3). According to the literature [31,53], this reaction proceeds through the formation of an iminophosphorane intermediate (Scheme 3), the product of a

Table 2: Yields of compounds **6a–d**.

Acid	Aldehyde	R^3	Amine	R^4	Compound	Yield, %
5a	**2a**	4-Cl	**3a**	4-Cl	**6a**	45 (55)[a]
	2a	4-Cl	**3c**	4-OCH_3	**6b**	41
	2a	4-Cl	**3b**	4-CH_3	**6c**	61
	2c	4-$COOCH_3$	**3b**	4-CH_3	**6d**	42

[a]The yield for the Ugi reaction on two carboxyl groups of KGA is given in parentheses.

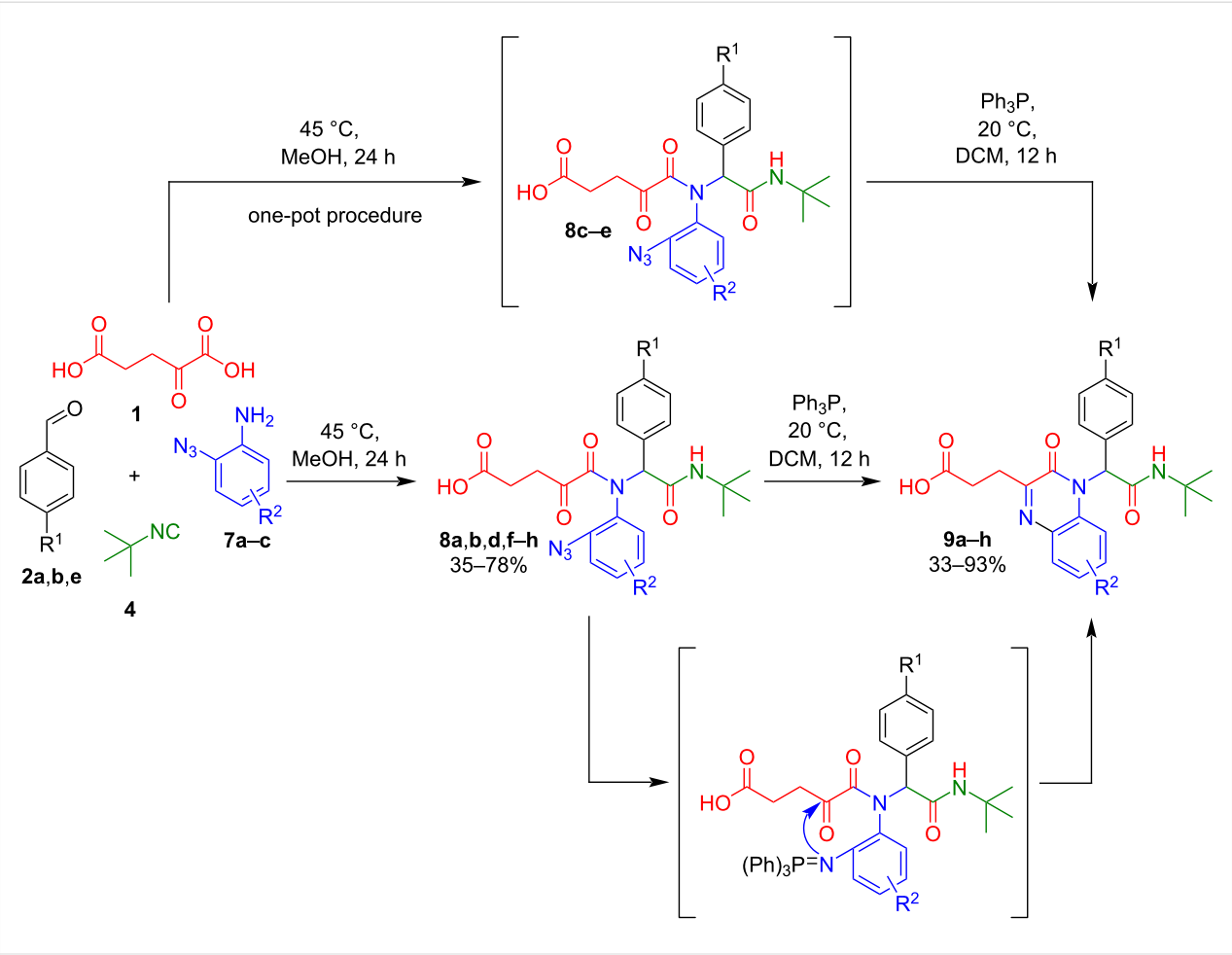

Scheme 3: Tandem Ugi/aza-Wittig combination involving KGA.

Table 3: Yields of compounds **8a**,**b**,**d**,**f–h** and **9a–h**.

Aldehyde	R^1	Azidoaniline	R^2	Compound	Yield, %
2a	4-Cl	**7a**	4-Cl	**8a**	57
2a	4-Cl	**7b**	H	**8b**	54
2b	4-OCH_3	**7b**	H	**8d**	35
2e	H	**7a**	4-Cl	**8f**	78
2e	H	**7b**	H	**8g**	71
2e	H	**7c**	4,6-CH_3	**8h**	64
2a	4-Cl	**7a**	4-Cl	**9a**	82
2a	4-Cl	**7b**	H	**9b**	93
2a	4-Cl	**7c**	4,6-CH_3	**9c**	46[a]
2b	4-OCH_3	**7b**	H	**9d**	75 (51)[a]
2b	4-OCH_3	**7c**	4,6-CH_3	**9e**	35[a]
2e	H	**7a**	4-Cl	**9f**	83
2e	H	**7b**	H	**9g**	59
2e	H	**7c**	4,6-CH_3	**9h**	47

[a]The yield for the one-pot Ugi/aza-Wittig combination in terms of KGA.

Staudinger reaction, which, however, was not isolated because it easily undergoes intramolecular cyclization on a sufficiently electrophilic carbonyl carbon atom with the elimination of triphenylphosphine oxide via the aza-Wittig reaction.

It should be noted that the best method for the isolation of quinoxalinones **9** was column chromatography using an elution gradient of hexane/ethyl acetate 3:1 to hexane/ethyl acetate 1:2 with the addition of 0.1% formic acid. The use of other eluents such as acetonitrile and different ratios of hexane/ethyl acetate, dichloromethane/methanol as well as the application of methods for the isolation of triphenylphosphine oxide by complexation with calcium and magnesium salts [54,55] or precipitation from non-polar solvents such as hexane and toluene did not lead to a complete separation of quinoxalinones **9** and Ph_3PO. We attribute this to the ability of Ph_3PO to form a strong hydrogen bond between the phosphoryl oxygen and a proton from the donor group of the second molecule [56-58], in this case a carboxyl proton.

In order to avoid the step of isolation of the intermediate azide derivatives **8**, we also studied a one-pot method for the synthesis of compounds **9**. For this KGA **1**, aldehydes **2a**,**b**, azidoanilines **7b**,**c**, and *tert*-butyl isocyanide (**4**) were stirred in methanol at 45 °C for 24 hours. The solvent was then evaporated, the residue dissolved in DCM, and stirred in the presence of Ph_3P for 12 hours at 20 °C to give compounds **9c–e** in 35–51% yields (Table 3).

Identification and structure determination of the compounds obtained was based on elemental analysis, mass spectrometry, ^{1}H and ^{13}C NMR spectroscopy, and by X-ray diffraction study (see Experimental part). The ^{1}H NMR spectra of compounds **5** are characterized by the following signals: a broad carboxyl group proton singlet at 12.10–12.17 ppm, an NH group proton singlet at 7.74–8.02 ppm, an aromatic protons multiplet at 6.52–8.15 ppm, a CH group singlet at 5.93–6.12 ppm, triplets for two CH_2 groups in the range of 2.04–2.89 ppm, a *tert*-butyl group singlet at 1.23–1.25 ppm, and signals for protons of the functional group. It should be noted that a doubling of the ^{1}H NMR signals is observed for the azide derivatives **8** compared to compounds **5**, which can be clearly seen in the spectrum of compound **8h** with both substituted *ortho*-positions of the amine moiety. In our opinion, this indicates the presence of rotamerism [59,60] caused by the restricted rotation of the sterically hindered amide group.

The ^{1}H NMR spectra of compounds **6** are marked by the following differences: the absence of the proton signal for the carboxyl group, the presence of two singlets for NH groups in the range of 7.61–7.96 ppm and two singlets for CH groups at 5.96–6.05 ppm, increased integral intensity of the aromatic multiplet in the range of 6.28–7.81 ppm, corresponding to 16 protons, multiplets for CH_2 groups at 1.78–2.96 ppm, and two signals for *tert*-butyl groups protons at 1.21–1.24 ppm. The increase in signal multiplicity compared to compounds **5** could indicate the presence of diastereomerism and restricted amide rotation in compounds **6**.

In the ^{1}H NMR spectra of quinoxalinones **9**, a shift of the methylene groups signal to a weaker field (2.90–3.14 ppm and 2.63–2.77 ppm) is observed in comparison to compounds **8** (2.60–3.06 ppm and 2.14–2.35 ppm). Furthermore, comparison of the ^{13}C NMR spectra of compounds **8** and **9** shows a characteristic shift of the signal in the 198 ppm region, corresponding to the carbonyl carbon of compounds **8**, to a stronger field in quinoxalinones **9**, where cyclization of the keto group has occurred. The structure of quinoxalinones of type **9** was finally assigned based on X-ray diffraction analysis made for 3-(4-(2-(*tert*-butylamino)-1-(4-methoxyphenyl)-2-oxoethyl)-5,7-dimethyl-3-oxo-3,4-dihydroquinoxalin-2-yl)propanoic acid (**9e**) (Figure 2).

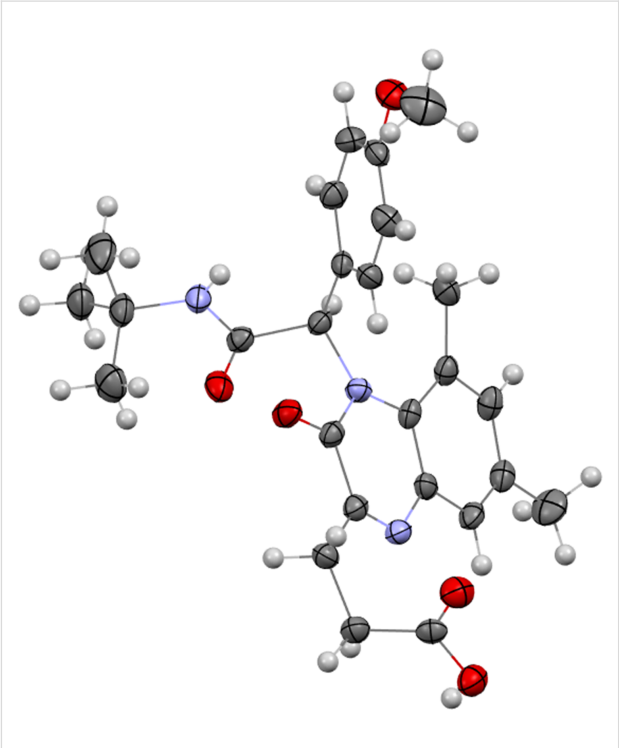

Figure 2: Molecular structure of 3-(4-(2-(*tert*-butylamino)-1-(4-methoxyphenyl)-2-oxoethyl)-5,7-dimethyl-3-oxo-3,4-dihydroquinoxalin-2-yl)propanoic acid (**9e**) according to X-ray diffraction data.

Conclusion

To summarize, we have studied the Ugi reaction and its tandem combination with aza-Wittig reactions involving α-ketoglutaric

acid. Depending on the stoichiometric ratio of the reagents, the Ugi reaction involves one or both carboxyl groups of KGA, leading to 5-((aryl)(1-aryl-2-(*tert*-butylamino)-2-oxoethyl)amino)-4,5-dioxopentanoic acids or N^1,N^5-diaryl-N^1,N^5-bis(1-aryl-2-(*tert*-butylamino)-2-oxoethyl)-2-oxopentanediamides, respectively. The tandem combination of Ugi and aza-Wittig reactions involving α-ketoglutaric acid and *o*-azidonanilines is an efficient method for the preparation of earlier unavailable quinoxalinone derivatives and can be carried out as a one-pot procedure without isolation of an intermediate azide-containing Ugi reaction product. Both quinoxalinones and Ugi reaction products may be valuable for organic synthesis and medicinal chemistry because the presence of a free carboxyl group makes them promising for use as building blocks for the construction of complex heterocyclic structures, including those using multicomponent reactions.

Supporting Information

Supporting Information File 1

General synthetic procedures, characterization of compounds, ^{1}H and ^{13}C NMR spectra and X-ray data.
[https://www.beilstein-journals.org/bjoc/content/supplementary/1860-5397-21-157-S1.pdf]

Acknowledgements

The authors thank all the brave defenders of Ukraine who allow us to continue our scientific work and complete this research.

Funding

The authors thank the National Research Foundation of Ukraine for financial support, the project of the National Research Foundation of Ukraine ‘Development of new materials based on supramolecular systems for biomedical and veterinary applications’ (2023.05/0003).

ORCID® iDs

Vladyslav O. Honcharov - https://orcid.org/0009-0008-2825-6995
Yana I. Sakhno - https://orcid.org/0000-0003-0561-635X
Olena H. Shvets - https://orcid.org/0000-0003-4791-2114
Vyacheslav E. Saraev - https://orcid.org/0000-0002-2312-8774
Svitlana V. Shishkina - https://orcid.org/0000-0002-3946-1061
Valentyn A. Chebanov - https://orcid.org/0000-0001-7564-778X

Data Availability Statement

Data generated and analyzed during this study is available from the corresponding author upon reasonable request.

References

1. Cores, Á.; Clerigué, J.; Orocio-Rodríguez, E.; Menéndez, J. C. *Pharmaceuticals* **2022,** *15,* 1009. doi:10.3390/ph15081009
2. dos Santos, J. A.; de Castro, P. P.; de Oliveira, K. T.; Brocksom, T. J.; Amarante, G. W. *Curr. Top. Med. Chem.* **2023,** *23,* 990–1003. doi:10.2174/1568026623666230403102437
3. Buskes, M. J.; Coffin, A.; Troast, D. M.; Stein, R.; Blanco, M.-J. *ACS Med. Chem. Lett.* **2023,** *14,* 376–385. doi:10.1021/acsmedchemlett.3c00012
4. Chebanov, V. A.; Desenko, S. M.; Lipson, V. V.; Gorobets, N. Y. Multicomponent-Switched Reactions in Synthesis of Heterocycles. *Multicomponent Reactions towards Heterocycles;* Wiley-VCH: Weinheim, Germany, 2022; pp 287–338. doi:10.1002/9783527832439.ch8
5. Desenko, S. M.; Gorobets, M. Y.; Lipson, V. V.; Sakhno, Y. I.; Chebanov, V. A. *Chem. Rec.* **2024,** *24,* e202300244. doi:10.1002/tcr.202300244
6. Ugi, I. *Angew. Chem.* **1959,** *71,* 386.
7. Fotopoulou, E.; Anastasiou, P. K.; Tomza, C.; Neochoritis, C. G. *Tetrahedron Green Chem* **2024,** *3,* 100044. doi:10.1016/j.tgchem.2024.100044
8. Murlykina, M. V.; Kolomiets, O. V.; Kornet, M. M.; Sakhno, Y. I.; Desenko, S. M.; Dyakonenko, V. V.; Shishkina, S. V.; Brazhko, O. A.; Musatov, V. I.; Tsygankov, A. V.; Van der Eycken, E. V.; Chebanov, V. A. *Beilstein J. Org. Chem.* **2019,** *15,* 1281–1288. doi:10.3762/bjoc.15.126
9. Kolomiiets, O. V.; Tsygankov, A. V.; Kornet, M. N.; Brazhko, A. A.; Musatov, V. I.; Chebanov, V. A. *Beilstein J. Org. Chem.* **2023,** *19,* 727–735. doi:10.3762/bjoc.19.53
10. Tsygankov, A. V.; Vereshchak, V. O.; Savluk, T. O.; Desenko, S. M.; Ananieva, V. V.; Buravov, O. V.; Sakhno, Y. I.; Shishkina, S. V.; Chebanov, V. A. *Beilstein J. Org. Chem.* **2024,** *20,* 1773–1784. doi:10.3762/bjoc.20.156
11. Liu, C.; Voskressensky, L. G.; Van der Eycken, E. V. *Chem. – Eur. J.* **2024,** *30,* e202303597. doi:10.1002/chem.202303597
12. Ahmadi Shourkaei, F.; Rashidi Ranjbar, P.; Taslimi, P.; Mahdavi, M. *Chem. Biodiversity* **2024,** *21,* e202301292. doi:10.1002/cbdv.202301292
13. Morales-Salazar, I.; Montes-Enríquez, F. P.; Garduño-Albino, C. E.; García-Sánchez, M. A.; Ibarra, I. A.; Rojas-Aguirre, Y.; García-Hernández, M. E.; Sarmiento-Silva, R. E.; Alcaraz-Estrada, S. L.; Díaz-Cervantes, E.; González-Zamora, E.; Islas-Jácome, A. *RSC Med. Chem.* **2023,** *14,* 154–165. doi:10.1039/d2md00350c
14. Zeng, Y.; Li, Y.; Liu, G.; Wei, Y.; Wu, Y.; Tao, L. *ACS Appl. Polym. Mater.* **2020,** *2,* 404–410. doi:10.1021/acsapm.9b00874
15. Valdes, O.; Ali, A.; Carrasco-Sánchez, V.; Cabrera-Barjas, G.; Duran-Lara, E.; Ibrahim, M.; Ahmad, S.; Moreno, R.; Concepción, O.; de la Torre, A. F.; Abrar, M.; Morales-Quintana, L.; Abril, D. *Comput. Biol. Chem.* **2023,** *106,* 107932. doi:10.1016/j.compbiolchem.2023.107932
16. Tomohara, K.; Maneenet, J.; Ohashi, N.; Nose, T.; Fujii, R.; Kim, M. J.; Sun, S.; Awale, S. *Biol. Pharm. Bull.* **2023,** *46,* 1412–1420. doi:10.1248/bpb.b23-00224
17. Li, Y.; He, L.; Qin, H.; Liu, Y.; Yang, B.; Xu, Z.; Yang, D. *Molecules* **2024,** *29,* 464. doi:10.3390/molecules29020464

18. Bariwal, J.; Kaur, R.; Voskressensky, L. G.; Van der Eycken, E. V. *Front. Chem. (Lausanne, Switz.)* **2018,** *6,* 557. doi:10.3389/fchem.2018.00557
19. Mazur, M. O.; Zhelavskyi, O. S.; Zviagin, E. M.; Shishkina, S. V.; Musatov, V. I.; Kolosov, M. A.; Shvets, E. H.; Andryushchenko, A. Y.; Chebanov, V. A. *Beilstein J. Org. Chem.* **2021,** *17,* 678–687. doi:10.3762/bjoc.17.57
20. Botsula, I.; Schavikin, J.; Heinämäki, J.; Laidmäe, I.; Mazur, M.; Raal, A.; Koshovyi, O.; Kireyev, I.; Chebanov, V. *Eur. J. Pharm. Sci.* **2024,** *195,* 106712. doi:10.1016/j.ejps.2024.106712
21. Botsula, I. V.; Kireyev, I. V.; Mazur, M. O.; Chebanov, V. A. *Visn. Farm.* **2024,** *107,* 136–143. doi:10.24959/nphj.24.144
22. Botsula, I. V.; Kireyev, I. V.; Koshovyi, O. M.; Chebanov, V. A. *Curr. Issues Pharm. Med.: Sci. Pract.* **2023,** *16,* 217–222. doi:10.14739/2409-2932.2023.3.287999
23. Botsula, I. V.; Kireyev, I. V.; Koshovyi, O. M.; Mazur, M. O.; Chebanov, V. A. *Farm. Chasopic* **2023,** 70–77. doi:10.11603/2312-0967.2023.4.14297
24. Botsula, I.; Kireyev, I.; Koshovyi, O.; Heinämäki, J.; Raal, A.; Mazur, M.; Chebanov, V. *ScienceRise: Pharm. Sci.* **2024,** *1,* 40–48. doi:10.15587/2519-4852.2024.299205
25. Xiong, J.; Wei, X.; Wan, Y.-C.; Ding, M.-W. *Tetrahedron* **2019,** *75,* 1072–1078. doi:10.1016/j.tet.2019.01.014
26. Hollanders, C.; Elsocht, M.; Van der Poorten, O.; Jida, M.; Renders, E.; Maes, B. U. W.; Ballet, S. *Chem. Commun.* **2021,** *57,* 6863–6866. doi:10.1039/d1cc01701b
27. Yan, Y.-M.; Li, H.-Y.; Zhang, M.; Wang, R.-X.; Zhou, C.-G.; Ren, Z.-X.; Ding, M.-W. *Synlett* **2020,** *31,* 73–76. doi:10.1055/s-0037-1610737
28. Barlow, T. M. A.; Jida, M.; Guillemyn, K.; Tourwé, D.; Caveliers, V.; Ballet, S. *Org. Biomol. Chem.* **2016,** *14,* 4669–4677. doi:10.1039/c6ob00438e
29. Welsch, S. J.; Umkehrer, M.; Kalinski, C.; Ross, G.; Burdack, C.; Kolb, J.; Wild, M.; Ehrlich, A.; Wessjohann, L. A. *Tetrahedron Lett.* **2015,** *56,* 1025–1029. doi:10.1016/j.tetlet.2015.01.043
30. Yan, Y.-M.; Li, H.-Y.; Ren, J.; Wang, S.; Ding, M.-W. *Synlett* **2018,** *29,* 1447–1450. doi:10.1055/s-0037-1609846
31. Yan, Y.-M.; Gao, Y.; Ding, M.-W. *Tetrahedron* **2016,** *72,* 5548–5557. doi:10.1016/j.tet.2016.07.048
32. Yang, M.-L.; Chen, H.-R.; Zhao, L.; Ding, M.-W. *Synthesis* **2023,** *55,* 465–472. doi:10.1055/a-1932-5811
33. Yang, M.-L.; Zhao, L.; Chen, H.-R.; Ding, M.-W. *J. Org. Chem.* **2023,** *88,* 16424–16434. doi:10.1021/acs.joc.3c01955
34. Yang, M.-L.; Zhao, L.; Chen, H.-R.; Ding, M.-W. *J. Org. Chem.* **2023,** *88,* 1898–1906. doi:10.1021/acs.joc.2c02621
35. Xu, Y.; Yuan, D.; Zhang, Y.; Zhang, Y.; He, P.; Ren, Z.-L. *Tetrahedron Lett.* **2024,** *140,* 155046. doi:10.1016/j.tetlet.2024.155046
36. Sun, M.; Zeng, C.-Y.; Zhang, E.-S.; Zhang, Q.; Chen, K.; Xu, Y.-G.; Fan, M.-X.; He, M.-R.; Shi, J.-H.; Ding, M.-W. *Asian J. Org. Chem.* **2024,** *13,* e202400036. doi:10.1002/ajoc.202400036
37. Jiang, X.; Wu, K.; Bai, R.; Zhang, P.; Zhang, Y. *Eur. J. Med. Chem.* **2022,** *229,* 114085. doi:10.1016/j.ejmech.2021.114085
38. Ayoup, M. S.; Rabee, A. R.; Abdel-Hamid, H.; Amer, A.; Abu-Serie, M. M.; Ashraf, S.; Ghareeb, D. A.; Ibrahim, R. S.; Hawsawi, M. B.; Negm, A.; Ismail, M. M. F. *ACS Omega* **2024,** *9,* 24643–24653. doi:10.1021/acsomega.4c01075
39. Odusami, J. A.; Ikhile, M. I.; Olasupo, I. A.; Fotsing, M. C. D.; Asekun, O. T.; Ndinteh, D. T.; Familoni, O. B. *Sci. Afr.* **2024,** *25,* e02317. doi:10.1016/j.sciaf.2024.e02317
40. El Bakri, Y.; Saravanan, K.; Ahmad, S.; Mague, J. T. *J. Biomol. Struct. Dyn.* **2023,** *41,* 5277–5290. doi:10.1080/07391102.2022.2084456
41. Suthar, S. K.; Chundawat, N. S.; Singh, G. P.; Padrón, J. M.; Jhala, Y. K. *Eur. J. Med. Chem. Rep.* **2022,** *5,* 100040. doi:10.1016/j.ejmcr.2022.100040
42. Meka, G.; Chintakunta, R. *Results Chem.* **2023,** *5,* 100783. doi:10.1016/j.rechem.2023.100783
43. Hussain, S.; Parveen, S.; Hao, X.; Zhang, S.; Wang, W.; Qin, X.; Yang, Y.; Chen, X.; Zhu, S.; Zhu, C.; Ma, B. *Eur. J. Med. Chem.* **2014,** *80,* 383–392. doi:10.1016/j.ejmech.2014.04.047
44. Missioui, M.; Mortada, S.; Guerrab, W.; Serdaroğlu, G.; Kaya, S.; Mague, J. T.; Essassi, E. M.; Faouzi, M. E. A.; Ramli, Y. *J. Mol. Struct.* **2021,** *1239,* 130484. doi:10.1016/j.molstruc.2021.130484
45. Koltun, D. O.; Parkhill, E. Q.; Vasilevich, N. I.; Glushkov, A. I.; Zilbershtein, T. M.; Ivanov, A. V.; Cole, A. G.; Henderson, I.; Zautke, N. A.; Brunn, S. A.; Mollova, N.; Leung, K.; Chisholm, J. W.; Zablocki, J. *Bioorg. Med. Chem. Lett.* **2009,** *19,* 2048–2052. doi:10.1016/j.bmcl.2009.02.019
46. Dudash, J., Jr.; Zhang, Y.; Moore, J. B.; Look, R.; Liang, Y.; Beavers, M. P.; Conway, B. R.; Rybczynski, P. J.; Demarest, K. T. *Bioorg. Med. Chem. Lett.* **2005,** *15,* 4790–4793. doi:10.1016/j.bmcl.2005.07.021
47. Bayliak, M. M.; Lushchak, V. I. *Ageing Res. Rev.* **2021,** *66,* 101237. doi:10.1016/j.arr.2020.101237
48. Gein, V. L.; Popov, A. V.; Andreichikov, Y. S. *J. Gen. Chem. USSR* **1992,** *62,* 1378.
49. Gein, V. L.; Popov, A. V.; Kolla, V. É.; Popova, N. A.; Potemkin, K. D. *Pharm. Chem. J.* **1993,** *27,* 343–346. doi:10.1007/bf00819965
50. Gein, V. L.; Popov, A. V.; Kolla, W. E.; Popova, N. A. *Pharmazie* **1993,** *48,* 107–109.
51. Sakhno, Y. I.; Radchenko, O. V.; Muravyova, E. A.; Sirko, S. M.; Shishkina, S. V.; Musatov, V. I.; Desenko, S. M.; Chebanov, V. A. *Chem. Heterocycl. Compd.* **2021,** *57,* 261–265. doi:10.1007/s10593-021-02902-w
52. Sakhno, Y.; Radchenko, O.; Saraev, V.; Shliapkina, Y.; Kaidash, M.; Shyshkina, M.; Shishkina, S.; Musatov, V.; Desenko, S.; Chebanov, V. *SynOpen* **2023,** *7,* 258–266. doi:10.1055/a-2091-7934
53. Pedrood, K.; Montazer, M. N.; Larijani, B.; Mahdavi, M. *Synthesis* **2021,** *53,* 2342–2366. doi:10.1055/a-1394-7511
54. Moschetta, E. G.; Cardinal-David, B.; Dunn, T. B.; Diwan, M. *Org. Process Res. Dev.* **2024,** *28,* 2677–2682. doi:10.1021/acs.oprd.4c00071
55. Hergueta, A. R. *Org. Process Res. Dev.* **2022,** *26,* 1845–1853. doi:10.1021/acs.oprd.2c00104
56. Smith, G.; Lynch, D. E.; Byriel, K. A.; Kennard, C. H. L. *Z. Kristallogr.* **1997,** *212,* 130–134. doi:10.1524/zkri.1997.212.2.130
57. Yenikaya, C.; Öğretir, C. *J. Mol. Struct.: THEOCHEM* **2005,** *731,* 1–5. doi:10.1016/j.theochem.2004.09.063
58. Etter, M. C.; Baures, P. W. *J. Am. Chem. Soc.* **1988,** *110,* 639–640. doi:10.1021/ja00210a076
59. Ototake, N.; Nakamura, M.; Dobashi, Y.; Fukaya, H.; Kitagawa, O. *Chem. – Eur. J.* **2009,** *15,* 5090–5095. doi:10.1002/chem.200802627
60. Watanabe, Y.; Take, U.; Senda, R.; Sato, A.; Kitagawa, O. *J. Org. Chem.* **2025,** *90,* 784–793. doi:10.1021/acs.joc.4c02772

License and Terms

This is an open access article licensed under the terms of the Beilstein-Institut Open Access License Agreement (https://www.beilstein-journals.org/bjoc/terms), which is identical to the Creative Commons Attribution 4.0 International License (https://creativecommons.org/licenses/by/4.0). The reuse of material under this license requires that the author(s), source and license are credited. Third-party material in this article could be subject to other licenses (typically indicated in the credit line), and in this case, users are required to obtain permission from the license holder to reuse the material.

The definitive version of this article is the electronic one which can be found at:
https://doi.org/10.3762/bjoc.21.157

BEILSTEIN JOURNAL OF ORGANIC CHEMISTRY

Switchable pathways of multicomponent heterocyclizations of 5-amino-1,2,4-triazoles with salicylaldehydes and pyruvic acid

Yana I. Sakhno*[1], Oleksander V. Buravov[1,2], Kostyantyn Yu. Yurkov[2], Anastasia Yu. Andryushchenko[1], Svitlana V. Shishkina[1] and Valentyn A. Chebanov*[1,3]

Full Research Paper

Open Access

Address:
[1]Institute of Functional Materials Chemistry, State Scientific Institution "Institute for Single Crystals" of National Academy of Sciences of Ukraine, Nauky Ave., 60, 61072, Kharkiv, Ukraine, [2]Enamine Ltd., Winston Churchill Street 78, Kyiv 02094, Ukraine and [3]Faculty of Chemistry, V. N. Karazin Kharkiv National University, Svobody sq., 4, 61022, Kharkiv, Ukraine

Email:
Yana I. Sakhno* - sakhno@isc.kh.ua; Valentyn A. Chebanov* - chebanov@isc.kh.ua

* Corresponding author

Keywords:
5-amino-1,2,4-triazole; heterocyclization; multicomponent reaction; salicylaldehyde; ultrasonication

Beilstein J. Org. Chem. **2025,** *21,* 2030–2035.
https://doi.org/10.3762/bjoc.21.158

Received: 16 June 2025
Accepted: 25 September 2025
Published: 08 October 2025

This article is part of the thematic issue "Multicomponent reactions IV".

Associate Editor: I. Baxendale

© 2025 Sakhno et al.; licensee Beilstein-Institut.
License and terms: see end of document.

Abstract

Switchable multicomponent reactions involving 3-substituted-5-amino-1,2,4-triazoles, pyruvic acid, and salicylaldehydes were studied under different conditions. Upon conventional heating, benzotriazolooxadiazocine-5-carboxylic acids were formed in the three-component reactions as single reaction products. Upon ultrasonic activation or mechanical stirring at room temperature, the multicomponent reaction of the same starting materials led to the formation of only tetrahydrotriazolopyrimidine derivatives.

Introduction

Multicomponent reactions (MCRs) are a powerful tool for the formation of heterocyclic systems in a minimal number of steps and offer several ways to vary substituents and they are widely used in drug discovery and development, as well as in diversity-oriented synthesis [1-4]. In addition, the application of condition-based divergence strategy [5] and the concept of multicomponent-switched reactions [6] allows to tune the selectivity of MCRs and direct them into several different pathways. That is why the study of multicomponent heterocyclizations of aromatic aldehydes, compounds with an active methylene group and aminoazoles, for example with 3-amino-1,2,4-triazoles, is important because the formation of different chemotypes of final heterocyclic compounds are possible depending on the structure of the reagents, the solvents and the catalysts, and type of activation methods [7-9].

MCRs of aminotriazoles, methylene-active compounds, and substituted salicylaldehydes are particularly interesting because of the possibility of additional reactions and post-cyclizations involving the *o*-hydroxy group. It was demonstrated [10-12]

that the multicomponent reaction of substituted 3-amino-1,2,4-triazoles, various salicylaldehydes, and acetone depending on the conditions, can either be limited to a Biginelli condensation with the formation of hydroxytetrahydropyrimidines or proceed with further post-cyclization to form oxygen-bridged triazolobenzoxadiazocine derivatives. Furthermore, a multicomponent synthesis of oxygen-bridged pyrimidine systems also was described in several other publications [13-15]. On the other hand, three-component reactions of aminoazoles, salicylaldehyde, and esters (or amides) of acetoacetic acid with isolation of other types of heterocylic compounds were described in some papers [16,17].

Our early works were devoted to the study of the reactions of aminoazoles, pyruvic acid and its derivatives with salicylaldehydes and it was found that depending on the conditions (reaction time, temperature, and method of process activation, in particular ultrasound and microwave irradiation), different types of heterocycles **I**–**VI** were formed (Scheme 1) [8,18,19].

It is known that substituents in aminoazoles can significantly influence their behavior in multicomponent heterocyclization reactions [4,8,20,21]. However, the reactions of 5-amino-1,2,4-triazoles containing substituents in position 3, which can also affect their chemical behaviour, with pyruvic acid, and salicylaldehydes remain undescribed. The present paper is intended to fill this gap and complete the description of this type of switchable multicomponent reactions.

Results and Discussion

Therefore, the MCRs between some 3-substituted 5-amino-1,2,4-triazoles, salicylaldehydes, and pyruvic acid were studied under different reaction conditions. In particular, it was found that the three-component reaction of an equimolar mixture of 5-amino-3-methylthio(methoxy)-1,2,4-triazole **1a,b**, salicylaldehydes **2a**–**f**, and pyruvic acid (**3**) under conventional heating at reflux in acetic acid for 3 h for aminotriazole **1a** or in *n*-BuOH for 7 h in case of aminotriazole **1b** led to the formation of oxygen-bridged 2-(methylthio or methoxy)-11,12-dihydro-5*H*-5,11-methanobenzo[*g*][1,2,4]triazolo[1,5-*c*][1,3,5]oxadiazocine-5-carboxylic acids **4a**–**j** (Scheme 2, Table 1). It should be noted that this MCR involving unsubstituted 5-amino-1*H*-1,2,4-triazole under various conditions never proceeds towards the formation of oxygen-bridged compounds

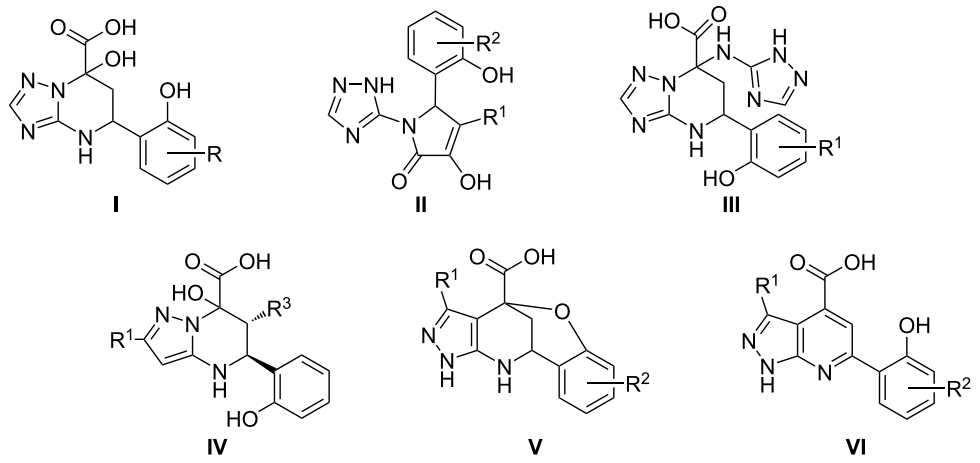

Scheme 1: Diversity of heterocyclization products from reaction of aminoazoles with salicylaldehydes, and pyruvic acids.

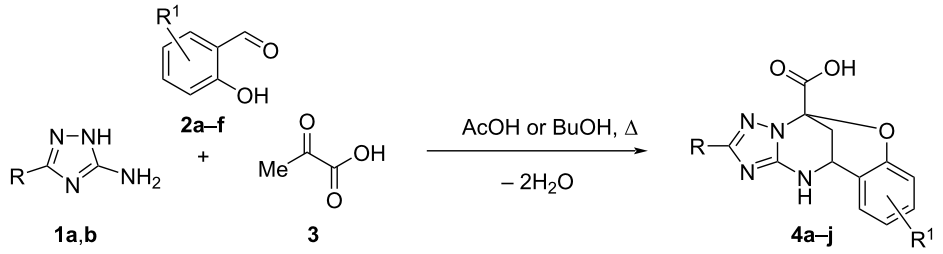

Scheme 2: MCRs of 3-amino-5-methylthio-1,2,4-triazole (**1a**) and 3-amino-5-methoxy-1,2,4-triazole (**1b**) with salicylaldehydes **2a**–**f**, and pyruvic acid (**3**).

Table 1: Synthesis of compounds **4a–j**.

Entry	Starting materials				Reaction time (hours)	Product	Yield (%)
	Compd.	R	Compd.	R^1			
1	**1a**	SCH_3	**2a**	H	3	**4a**	45
2	**1a**	SCH_3	**2b**	3-CH_3O	3	**4b**	60
3	**1a**	SCH_3	**2c**	5-Br	3	**4c**	42
4	**1a**	SCH_3	**2d**	5-NO_2	3	**4d**	35
5	**1a**	SCH_3	**2e**	5-F	3	**4e**	32
6	**1a**	SCH_3	**2f**	5-Cl	3	**4f**	42
7	**1b**	OCH_3	**2b**	3-CH_3O	7	**4g**	46
8	**1b**	OCH_3	**2c**	5-Br	7	**4h**	41
9	**1b**	OCH_3	**2e**	5-F	7	**4i**	35
10	**1b**	OCH_3	**2f**	5-Cl	7	**4j**	68

[18]. Thus, there is indeed a significant influence of the substituent in position 3 of 5-amino-1*H*-1,2,4-triazoles on their chemical behavior in this MCR.

In the case of 3-carbomethoxy- and 3-(trifluoromethyl)-5-amino-1,2,4-triazoles the treatment with pyruvic acid and salicylaldehydes under thermal heating in different solvents (AcOH, DMF, *n*-butanol), instead of oxygen-bridged compounds gave a mixture of unidentified products with trace amounts of Schiff bases between amino-1,2,4-triazole and salicylaldehyde as well as with impurities of the reagents. This is most likely due to the electron-withdrawing nature of the substituent at C(3) in these 5-amino-1,2,4-triazoles that do not favor the proceeding of the MCR in contrast to 5-aminotriazoles **1a,b** having pronounced electron-donating substituents (methylthio- and methoxy groups).

On the other hand, the MCR of the reagents **1a**, **2a–c** and **3** under ultrasonic irradiation for 2 h at room temperature (25 °C) (Scheme 3) afforded a mixture of 5-(2-hydroxyphenyl)-2-(methylthio)-7-((3-(methylthio)-4*H*-1,2,4-triazol-5-yl)amino)-4,5,6,7-tetrahydro[1,2,4]triazolo[1,5-*a*]pyrimidine-7-carboxylic acids **5a–d** and 5-(2-hydroxyphenyl)-7-hydroxy-2-(methylthio)-4,5,6,7-tetrahydro[1,2,4]triazolo[1,5-*a*]pyrimidine-7-carboxylic acids **6a–d** (in a ratio of ca. 80:20 for compounds **5a–c** and **6a–c**; and 15:85 for compounds **5d** and **6d**). Unfortunately, all attempts to separate these mixtures were unsuccessful.

However, repeating the reaction under mechanical stirring at room temperature for 72 h yielded tetrahydrotriazolopyrimidine-7-carboxylic acids **5a–c** as a mixture of two diastereomers (Scheme 3, Table 2). In the case of aldehyde **2b**, the MCR always led to the formation of a mixture of products **5d** and **6d**. Attempts to synthesize **5d** and **6d** as individual compounds under various conditions were unsuccessful.

In addition, it was found that compounds **5** can be converted into oxygen-bridged heterocycles **4** after 1 hour of conven-

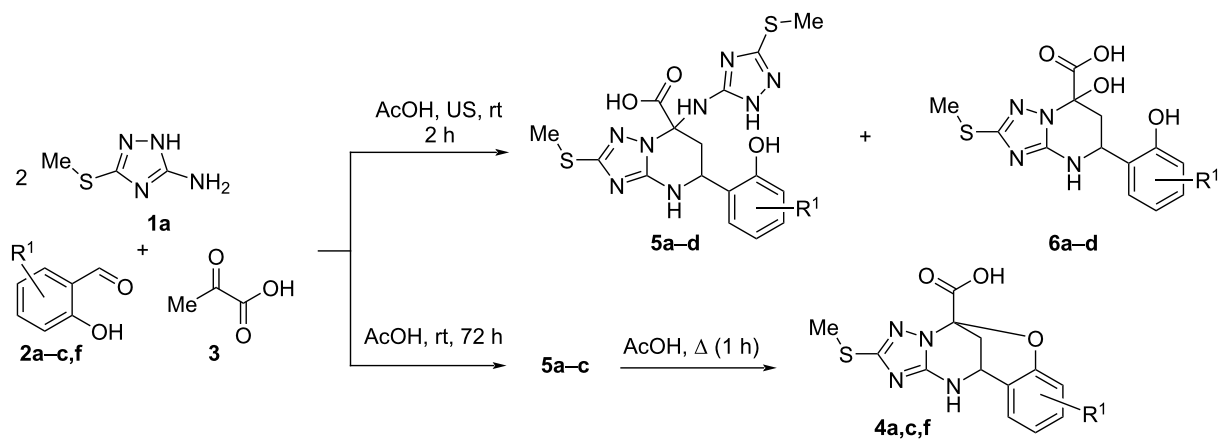

Scheme 3: MCRs of 3-amino-5-methylthio-1,2,4-triazole (**1a**), salicylaldehydes **2a–c**,**f**, and pyruvic acid (**3**) under different conditions.

Table 2: Synthesis of compounds **5a–c**.

Entry	Starting materials Compd.	R^1	Reaction time (hours)	Temperature regime Method	Product	Yield (%)
1	**2a**	H	72	mech. stir, rt	**5a**	58
2	**2c**	5-Br	72	mech. stir, rt	**5b**	69
3	**2f**	5-Cl	72	mech. stir, rt	**5c**	67

tional heating at reflux in acetic acid (Scheme 3). In contrast, all attempts to transform 7-triazolylamino derivatives of pyrimidinecarboxylic acids **5** into their 7-hydroxy derivatives **6** were unsuccessful. It also failed to perform the reverse conversion. The same situation was observed for similar compounds based on 5-amino-1*H*-pyrazole-4-carbonitrile [22].

It should be noted that diazocines **4** were stable and did not undergo transformations when heated or irradiated with ultrasound. This may indicate that pyrimidine-7-carboxylic acids **5** and **6** are formed in parallel processes under kinetic control of the reaction, while oxygen-bridged heterocycles **4** are formed under thermodynamic control.

The purity and structure of compounds **4** and **5** were established by elemental analysis, mass spectrometry, ^{1}H and ^{13}C NMR spectroscopy, and X-ray diffraction study (Figure 1).

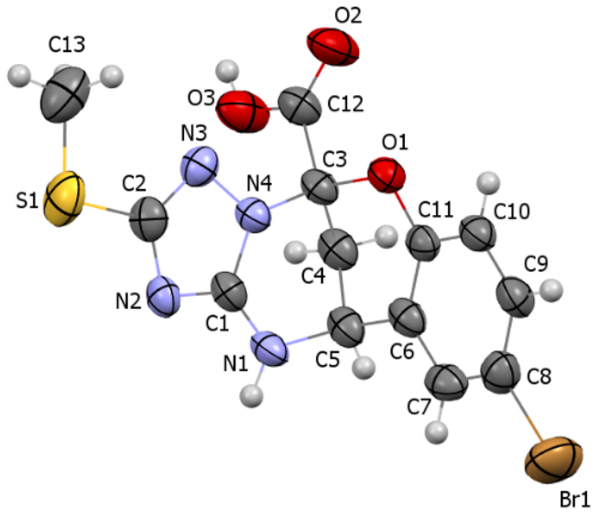

Figure 1: Molecular structure of compound **4c** according to X-ray diffraction data. Thermal ellipsoids are shown at 50% probability level.

For example, the ^{1}H NMR spectra of products **4a–f** exhibit signals for proton of the pyrimidine NH group (8.38–8.53 ppm), signals for aromatic protons (6.58–8.34 ppm), multiplet for the proton of the CH group at 4.64–4.92 ppm, a singlet for the protons for the triazole SCH_3 group at 2.37–2.38 ppm as well as signals for other substituents. The peaks of the proton of the carboxyl group is not recognized, probably due to exchange processes. The signals of the CH_2 group in the range around δ = 2.5 ppm are not always clearly identifiable, as they partially or completely overlap with the remaining DMSO signal. Compounds **4g–j** are characterized by the following signals in the ^{1}H NMR spectra: a proton singlet of the pyrimidine NH group at 8.30–8.31 ppm, a multiplet of aromatic protons in the region of 6.95–7.51 ppm, a proton multiplet of the CH group at 4.65–4.68 ppm and singlet for protons for the triazole CH_3O group at 3.7 ppm.

The ^{1}H NMR spectra of heterocyclic acids **5a–c** exhibited a broad singlet of proton of the carboxyl group at 11.88–14.02 ppm, a singlet of proton of the hydroxy group at 9.41–9.86 ppm, a singlet of proton of the pyrimidine NH group at 7.72–7.91 ppm, a singlet of proton of the triazolylamine NH group at 7.44–7.57 ppm, peaks for aromatic protons at 6.70–7.52 ppm, a multiplet of proton of the CH group at 5.0–5.19 ppm and two signals for diastereotopic protons of CH_2 group (about 2.89–3.11 and 2.28–2.35 ppm) and protons for the triazole SCH_3 group at 2.38–2.46 ppm. The doubling of some signals in the ^{1}H NMR spectra probably indicates the formation of both possible diastereomers. The structure of compounds **6a–d** was confirmed from the ^{1}H NMR spectra and the mass spectra of mixture by comparison with literature data for similar pyrimidines [17,18].

Conclusion

In summary, the multicomponent reaction of 3-amino-5-methylthio(methoxy)-1,2,4-triazoles with salicylaldehydes, and pyruvic acid can be switched between two different directions using conventional thermal heating, mechanical stirring at room temperature and ultrasonication at room temperature. The treatment under reflux conditions leads to the formation of oxygen-bridged benzo[*g*][1,2,4]triazolo[1,5-*c*][1,3,5]oxadiazocine-5-carboxylic acids exclusively while the reaction under mechanical stirring gives 5-(2-hydroxyphenyl)-2-(methylthio)-7-((3-(methylthio)-4*H*-1,2,4-triazol-5-yl)amino)-4,5,6,7-tetrahydro[1,2,4]triazolo[1,5-*a*]pyrimidine-7-carboxylic acids.

The reaction under ultrasonication at room temperature yields a mixture of the latter with 5-(2-hydroxyphenyl)-7-hydroxy-2-(methylthio)-4,5,6,7-tetrahydro[1,2,4]triazolo[1,5-*a*]pyrimidine-7-carboxylic acids.

Supporting Information

Supporting Information File 1

Experimental procedures, product characterization, and copies of NMR spectra.
[https://www.beilstein-journals.org/bjoc/content/supplementary/1860-5397-21-158-S1.pdf]

Acknowledgements

The authors thank the National Research Foundation of Ukraine for financial support. The authors also thank all the brave defenders of Ukraine who allow us to continue our scientific work and complete this research.

Funding

The project of National Research Foundation of Ukraine 'Development of new materials based on supramolecular systems for biomedical and veterinary applications' (2023.05/0003).

ORCID® iDs

Yana I. Sakhno - https://orcid.org/0000-0003-0561-635X
Oleksander V. Buravov - https://orcid.org/0009-0008-8433-5524
Kostyantyn Yu. Yurkov - https://orcid.org/0009-0005-2979-6238
Anastasia Yu. Andryushchenko - https://orcid.org/0009-0006-9166-0435
Svitlana V. Shishkina - https://orcid.org/0000-0002-3946-1061
Valentyn A. Chebanov - https://orcid.org/0000-0001-7564-778X

Data Availability Statement

Data generated and analyzed during this study is available from the corresponding author upon reasonable request.

References

1. Graebin, C. S.; Ribeiro, F. V.; Rogério, K. R.; Kümmerle, A. E. *Curr. Org. Synth.* **2019,** *16,* 855–899. doi:10.2174/1570179416666190718153703
2. John, S. E.; Gulati, S.; Shankaraiah, N. *Org. Chem. Front.* **2021,** *8,* 4237–4287. doi:10.1039/d0qo01480j
3. Graziano, G.; Stefanachi, A.; Contino, M.; Prieto-Díaz, R.; Ligresti, A.; Kumar, P.; Scilimati, A.; Sotelo, E.; Leonetti, F. *Int. J. Mol. Sci.* **2023,** *24,* 6581. doi:10.3390/ijms24076581
4. Murlykina, M. V.; Morozova, A. D.; Zviagin, I. M.; Sakhno, Y. I.; Desenko, S. M.; Chebanov, V. A. *Front. Chem. (Lausanne, Switz.)* **2018,** *6,* 527. doi:10.3389/fchem.2018.00527
5. Scheffelaar, R.; Ruijter, E.; Orru, R. V. A. *Top. Heterocycl. Chem.* **2010,** *25,* 95–126. doi:10.1007/7081_2010_44
6. Chebanov, V. A.; Desenko, S. M.; Lipson, V. V.; Gorobets, N. Y. Multicomponent-Switched Reactions in Synthesis of Heterocycles. In *Multicomponent Reactions towards Heterocycles;* Van der Eycken, E.; Sharma, U. K., Eds.; Wiley-VCH: Weinheim, Germany, 2022; pp 287–338. doi:10.1002/9783527832439.ch8
7. Damera, T.; Pagadala, R.; Rana, S.; Jonnalagadda, S. B. *Catalysts* **2023,** *13,* 1034. doi:10.3390/catal13071034
8. Desenko, S. M.; Gorobets, M. Y.; Lipson, V. V.; Sakhno, Y. I.; Chebanov, V. A. *Chem. Rec.* **2024,** *24,* e202300244. doi:10.1002/tcr.202300244
9. Sakhno, Y. I.; Mykhailenko, M. V.; Kolosov, M. A.; Shvets, E. H.; Musatov, V. I.; Chorna, N. V.; Desenko, S. M.; Chebanov, V. A. *Ukr. Bioorg. Acta* **2020,** *15,* 22–26. doi:10.15407/bioorganica2020.02.022
10. Doğan, İ. S.; Gümüş, M. K.; Gorobets, N. Y.; Reis, R.; Orak, D.; Sipahi, H.; Sari, S.; Chebanov, V. A. *Pharm. Chem. J.* **2022,** *56,* 769–776. doi:10.1007/s11094-022-02708-w
11. Zeng, M.; Xue, Y.; Qin, Y.; Peng, F.; Li, Q.; Zeng, M.-H. *Chin. Chem. Lett.* **2022,** *33,* 4891–4895. doi:10.1016/j.cclet.2022.02.075
12. Gorobets, N. Y.; Sedash, Y. V.; Ostras, K. S.; Zaremba, O. V.; Shishkina, S. V.; Baumer, V. N.; Shishkin, O. V.; Kovalenko, S. M.; Desenko, S. M.; Van der Eycken, E. V. *Tetrahedron Lett.* **2010,** *51,* 2095–2098. doi:10.1016/j.tetlet.2010.02.045
13. Jing, X.; Li, Z.; Pan, X.; Wang, Q.; Yan, C.; Zhu, H. *Synth. Commun.* **2009,** *39,* 3796–3803. doi:10.1080/00397910902838896
14. Cui, X.; Lin, J.-J.; Wang, S.; Li, J.-P.; Xia, X.-S.; Huang, C. *Tetrahedron Lett.* **2022,** *89,* 153603. doi:10.1016/j.tetlet.2021.153603
15. Světlík, J.; Veizerová, L. *Helv. Chim. Acta* **2011,** *94,* 199–205. doi:10.1002/hlca.201000193
16. Světlík, J.; Kettmann, V. *Tetrahedron Lett.* **2011,** *52,* 1062–1066. doi:10.1016/j.tetlet.2010.12.051
17. Tkachenko, V. V.; Muravyova, E. A.; Desenko, S. M.; Shishkin, O. V.; Shishkina, S. V.; Sysoiev, D. O.; Müller, T. J. J.; Chebanov, V. A. *Beilstein J. Org. Chem.* **2014,** *10,* 3019–3030. doi:10.3762/bjoc.10.320
18. Murlykina, M. V.; Sakhno, Y. I.; Desenko, S. M.; Shishkina, S. V.; Shishkin, O. V.; Sysoiev, D. O.; Kornet, M. N.; Schols, D.; Goeman, J. L.; Van der Eycken, J.; Van der Eycken, E. V.; Chebanov, V. A. *Eur. J. Org. Chem.* **2015,** 4481–4492. doi:10.1002/ejoc.201500469
19. Murlykina, M. V.; Sakhno, Y. I.; Desenko, S. M.; Konovalova, I. S.; Shishkin, O. V.; Sysoiev, D. A.; Kornet, M. N.; Chebanov, V. A. *Tetrahedron* **2013,** *69,* 9261–9269. doi:10.1016/j.tet.2013.08.055
20. Muravyova, E. A.; Desenko, S. M.; Rudenko, R. V.; Shishkina, S. V.; Shishkin, O. V.; Sen'ko, Y. V.; Vashchenko, E. V.; Chebanov, V. A. *Tetrahedron* **2011,** *67,* 9389–9400. doi:10.1016/j.tet.2011.09.138
21. Sakhno, Y.; Murlykina, M.; Morozova, A.; Kozyrev, A.; Chebanov, V. *Fr.-Ukr. J. Chem.* **2015,** *3,* 1–20. doi:10.17721/fujcv3i2p1-20
22. Sakhno, Y. I.; Murlykina, M. V.; Zbruyev, O. I.; Kozyryev, A. V.; Shishkina, S. V.; Sysoiev, D.; Musatov, V. I.; Desenko, S. M.; Chebanov, V. A. *Beilstein J. Org. Chem.* **2020,** *16,* 281–289. doi:10.3762/bjoc.16.27

License and Terms

This is an open access article licensed under the terms of the Beilstein-Institut Open Access License Agreement (https://www.beilstein-journals.org/bjoc/terms), which is identical to the Creative Commons Attribution 4.0 International License (https://creativecommons.org/licenses/by/4.0). The reuse of material under this license requires that the author(s), source and license are credited. Third-party material in this article could be subject to other licenses (typically indicated in the credit line), and in this case, users are required to obtain permission from the license holder to reuse the material.

The definitive version of this article is the electronic one which can be found at:
https://doi.org/10.3762/bjoc.21.158